

# EXTENDED ABSTRACTS

BRAZIL  
1991



FIFTH  
INTERNATIONAL  
KIMBERLITE  
CONFERENCE



Printed By  
Companhia de Pesquisa de Recursos Minerais - CPRM



Digitized by the Internet Archive  
in 2018 with funding from  
University of Alberta Libraries

<https://archive.org/details/fifthinternation05inte>

*FIFTH INTERNATIONAL  
KIMBERLITE CONFERENCE*

Araxá, June 1991

**EXTENDED ABSTRACTS**



CPRM—Special Publication 2/91

Brasília

Copyright © 1991 by CPRM. All rights reserved.

Additional copies and other volumes associated with the Conference  
may be purchased from:

Companhia de Pesquisa de Recursos Minerais – CPRM  
Centro de Documentação Técnica – CEDOT  
Av. Pasteur, 404 – Urca – 22.290  
Rio de Janeiro – RJ – Brazil.  
Tel.: (021) 295-0032 R. 389 – Fax.: (021) 542-3647

International Kimberlite Conference, 5. Araxá, 1991.

Extended abstracts. Brasília, CPRM, 1991.

584p. ilust. (CPRM – Special Publication, 2/91).

1. Kimberlito – Congressos. I. Companhia de Pesquisa de Recursos  
Minerais, ed. II. Série. III. Título.

CDD: 552.063  
CDU: 552.323.6

Abstracts were submitted by the authors in camera-ready form and, therefore, were not edited. The Organizing Committee of the *5<sup>th</sup> International Kimberlite Conference* takes no responsibility for author errors or omissions.

**FIFTH INTERNATIONAL KIMBERLITE CONFERENCE**

**ORGANIZING COMMITTEE**

**CHAIRMEN**

**H. O. A Meyer**  
Purdue University

**O. H. Leonardos**  
University of Brasília

**SECRETARIAT**

**J. C. Gaspar**  
University of Brasília

**L. A. Tompkins**  
University of Western Australia

**SPONSORSHIP**

---

The Organizing Committee of the *Fifth International Kimberlite Conference* generously acknowledges the help and sponsorship of the following organizations:

Academia Brasileira de Ciências (ABC)  
Companhia Brasileira de Metalurgia e Mineração (CBMM)  
Companhia de Pesquisa de Recursos Minerais (CPRM)  
Companhia Vale do Rio Doce (CVRD)  
Conselho Nacional de Desenvolvimento Científico e Tecnológico (CNPq)  
Departamento Nacional da Produção Mineral (DNPM)  
International Mineralogical Association (IMA)  
Mineralogical Society of America (MSA)  
National Science Foundation (NSF)  
Purdue University  
RTZ Mineração Ltda.  
Sociedade Brasileira de Geologia (SBG)  
SOPEMI – Pesquisa e Exploração de Minérios Ltda.  
Universidade de Brasília (UnB)

---

## Author Index

- Afanas'ev, V.P. . . . . 1  
Afanasiev, V.P. . . . . 391  
Allsopp, H.L. . . . . 76  
Almeida, F.F.M. de . . . . 3  
Ambroise, M. . . . . 6  
Amshinsky, A.N. . . . . 339  
Amstrong, R. . . . . 17  
Andi, Z. . . . . 10, 154,  
. . . . . 208, 285, 448  
Ashchepkov, I.V. . . . . 13  
Aspen, P. . . . . 241  
Bailey, D.K. . . . . 237  
Baker, N.R. . . . . 14  
Barankevich, V.G. . . . . 495, 556  
Barasckov, Yu. P. . . . . 565  
Baxter-Brown, R. . . . . 14  
Bezborodov, S.M. . . . . 391, 481  
Billington, F.R. . . . . 58  
Bizzi, L.A. . . . . 17  
Blacic, J.D. . . . . 20  
Blaine, J.L. . . . . 58  
Bodnier, J.L. . . . . 281  
Bodrov, V.A. . . . . 527  
Bogatikov, O.A. . . . . 484  
Bogdanov, G.V. . . . . 492,  
. . . . . 495, 498  
Boltenkov, A.V. . . . . 573  
Borch, R.S. . . . . 212  
Botelho, N.F. . . . . 60  
Botkunov, A.I. . . . . 391  
Botova, M.M. . . . . 579  
Boyd, S.R. . . . . 231  
Boyd, F.R. . . . . 323, 329  
Brandt, S.B. . . . . 558  
Brey, G.P. . . . . 23, 26,  
. . . . . 29, 92, 106  
Bristow, J.W. . . . . 46  
Brown, M.A. . . . . 76  
Brown, L. . . . . 329  
Browning, P. . . . . 405  
Bulanova, G.P. . . . . 486, 488  
Bulatov, V. . . . . 29  
Bush, M.D. . . . . 435  
Bushueva, E.B. . . . . 490, 530  
Caporuscio, F.A. . . . . 267, 385  
Carlson, R.W. . . . . 183, 329  
Castelo Branco, R.M.G. . . . 35  
Chappell, B.W. . . . . 344  
Chaves, M.L.S.C. . . . . 40  
Chen, Y.D. . . . . 42, 45, 316  
Chien-Lu, C. . . . . 38  
Clark, T.C. . . . . 46, 373  
Clarke, L.B. . . . . 49  
Clement, C.R. . . . . 361  
Colgan, E.A. . . . . 76  
Condliffe, E. . . . . 310  
Cooper, G.I. . . . . 279  
Coopersmith, H.G. . . . . 52  
Crozas, G. . . . . 410  
Cumming, B.C. . . . . 58  
Damarapurshad, A. . . . . 163, 383  
Daniels, L.R.M. . . . . 55, 58  
Danni, J.C. M. . . . . 60  
Dante, C. . . . . 32  
Davies, G.R. . . . . 63, 66,  
. . . . . 310, 326  
Dawson, J.B. . . . . 69  
De Wit, M.J. . . . . 17  
Deakin, A.S. . . . . 71  
Dehuan, X. . . . . 10  
Deines, P. . . . . 74  
Dhamelincourt, P. . . . . 448  
Dickin, A.P. . . . . 133, 136  
Dheprovskaya, L.V. . . . . 558, 573  
Dobbs, P.N. . . . . 76  
Doroshev, A. . . . . 26  
Downes, H. . . . . 281  
Duncan, D.J. . . . . 76, 160  
Duncan, R. . . . . 205  
Eckert, J.O. . . . . 410  
Edgar, A.D. . . . . 79  
Edwards, D. . . . . 82  
Eggler, D.H. . . . . 85, 88  
Egorov, K.N. . . . . 492,  
. . . . . 495, 498, 573  
Ermolaeva, L.A. . . . . 367  
Falk, R.W. . . . . 261  
Fengxiang, L. . . . . 248, 454  
Feoktistov, G.D. . . . . 501  
Fett, A. . . . . 92  
Field, S.W. . . . . 94, 323  
Fipke, C.E. . . . . 97  
Fodor, R.V. . . . . 101  
Fogel, R. . . . . 20  
Foley, S.F. . . . . 29  
Furlong, K.P. . . . . 103, 106, 109  
Foster, J.G. . . . . 112  
Fröhlich, G. . . . . 245  
Frantsesson, E.V. . . . . 516  
Furlong, K.P. . . . . 85  
Galimov, E.M. . . . . 502  
Gandhok, G.R. . . . . 101  
Garanin, V.K. . . . . 481, 484, 490,  
. . . . . 505, 508, 510, 525, 530  
Gaspar, J.C. . . . . 127  
Geach, C.L. . . . . 130  
Gerneke, D.A. . . . . 318  
Gibson, S.A. . . . . 133, 136, 420  
Girnir, A. . . . . 513, 564  
Gittins, J. . . . . 193  
Gobba, J.M. . . . . 116  
Green, D.H. . . . . 313, 417  
Green II, H.W. . . . . 212  
Grib, V.P. . . . . 367, 530  
Griffin, B.J. . . . . 82, 231  
Griffin, W.L. . . . . 42, 119,  
. . . . . 139, 142, 145, 148,  
. . . . . 310, 316, 332, 463, 475  
Griffin, B.W. . . . . 231  
Griffin, S.R. . . . . 463  
Grossi-Sad, J.H. . . . . 60  
Grubb, M.D. . . . . 151  
Guanliang, L. . . . . 234  
Günther, M. . . . . 122  
Guo, L. . . . . 154, 448  
Gurney, J.J. . . . . 119, 125, 142,  
. . . . . 167, 177, 224, 225, 264  
. . . . . 298, 318, 320, 322, 336  
Haebig, A.E. . . . . 376  
Haggerty, S.E. . . . . 157,  
. . . . . 323, 347  
Hall, A.E. . . . . 202, 376, 380  
Hamilton, R. . . . . 112  
Harris, J.W. . . . . 160, 318,  
. . . . . 336, 456, 459  
Hart, R.J. . . . . 163  
Harte, B. . . . . 167, 224,  
. . . . . 313, 318, 456, 459  
Hatton, C.J. . . . . 370, 383  
Hearn, B. C.Jr. . . . . 170  
Helmstaedt, H.H. . . . . 173, 224  
Hendry, G.L. . . . . 133, 136  
Hochella, M.F.Jr. . . . . 432  
Hoefler, H. . . . . 106  
Hollis, J.D. . . . . 398  
Hongfu, Z. . . . . 248  
Hops, J.J. . . . . 177  
Horsch, H. . . . . 383  
Hu, S. . . . . 76, 466  
Huntley, P.M. . . . . 261  
Hwang, P. . . . . 180  
Irving, A.J. . . . . 183, 186, 188  
Jacob, D. . . . . 190  
Jacques, A.L. . . . . 202,  
. . . . . 205, 392, 475  
Jago, B.C. . . . . 193  
Jagoutz, E. . . . . 122, 190  
Janse, A.J.A. . . . . 196, 199  
Jennings, C.M.H. . . . . 58  
Jianping, Z. . . . . 248  
Jianzong, Z. . . . . 10  
Jin, Z-M. . . . . 212  
Kaminsky, F.V. . . . . 214  
Kharkiv, A.D. . . . . 551,  
. . . . . 567, 579  
Keller, J. . . . . 217  
Kingston, M.J. . . . . 219  
Kinny, P.D. . . . . 45, 222  
Kirkley, M.B. . . . . 224, 225  
Kisel' S.I. . . . . 516  
Knutson, J. . . . . 205  
Koeber, C. . . . . 163  
Kogarko, L. . . . . 26, 513, 564  
Kolesnik, Yu.N. . . . . 514  
Kolod'ko, A.A. . . . . 516  
Komov . . . . . 518  
Kononova, K.A. . . . . 484  
Koptil, V.I. . . . . 391  
Kornilova, V.P. . . . . 521  
Kostrovitsky, S.I. . . . . 523  
. . . . . 525, 527  
Kudrjavitseva, G.P. . . . . 481,  
. . . . . 484, 490, 505,  
. . . . . 508, 510, 530  
Kulakova, I.I. . . . . 533, 547  
Kuligin, S. . . . . 391  
Kvasnitsa, V. N. . . . . 569  
Lasnier, B.M. . . . . 35  
Lashchenov, V.A. . . . . 543  
Laverova, T.N. . . . . 490,  
. . . . . 508, 530  
Laz'ko, E.E. . . . . 228, 581  
Le Bas, M.J. . . . . 49  
Leat, P.T. . . . . 133, 420  
Lee, J.E. . . . . 58  
Lee, D.C. . . . . 231  
Lei, Z. . . . . 248  
Leonardos, O.H. . . . . 408, 437  
Levin, V.I. . . . . 516  
Lihe, G. . . . . 10, 208  
Lipskaya, V.I. . . . . 495, 556  
Lloyd, F.E. . . . . 79, 237  
Logvinova, A.M. . . . . 240  
Long, A. . . . . 241

Lorand, J.P. . . . .	88	Otter, M.L. . . . .	261, 318,	Silva, N.B. da . . . . .	460	Towie, N.J. . . . .	435
Lorenz, V. . . . .	245, 392		320, 322	Sinitsyn, A.V. . . . .	367	Ukhanov, A.V. . . . .	567
Lucas, H. . . . .	380	Pasteris, J.D. . . . .	323	Skinner, E.M.W. . . . .	46,	Ulbrich, M.N.C. . . . .	437
Maggiore, C. . . . .	20	Pavlenko, T.A. . . . .	579		370, 373	Upton, B.G.J. . . . .	241
Makhin, A. I. . . . .	579	Pavlova, L.A. . . . .	488	Skipnichenko, V.A. . . . .	527	Valenca, J.G. . . . .	359
Makhotkin, I.L. . . . .	484	Pearson, N.J. . . . .	42, 332	Skvortsova, V.L. . . . .	533, 547	Valle, P. . . . .	460
Manning, E.R. . . . .	435	Pearson, D.G. . . . .	323,	Smelova, G.B. . . . .	549	Valley, J.W. . . . .	353
Mariano, A.N. . . . .	251		326, 329	Smirhov, G.I. . . . .	551	Valter, A.A. . . . .	569
Marshall, T.R. . . . .	254	Plusnin, G.S. . . . .	527	Smith, C.B. . . . .	17, 46,	Varlamov, D.A. . . . .	490
Marx, M.R. . . . .	435	Pokhilenko, N.P. . . . .	1,		76, 373, 383	Vasiljeva, E.R. . . . .	530
Maslovskaya, M.N. . . . .	558, 573		329, 339	Smith, Chris B. . . . .	202, 376,	Verichev, E.M. . . . .	530
Mathez, E.A. . . . .	20	Ponomarenko, A.I. . . . .	391, 581		380, 392	Viljoen, K.S. . . . .	46,
Matthews, M.B. . . . .	167	Posukhova, T.V. . . . .	530	Smith, J.V. . . . .	69		353, 373, 440
McCallum, M.E. . . . .	151, 163,	Preser, I.B. . . . .	334	Smyth, J.R. . . . .	267, 385	Vishnevsky, A.A. . . . .	571
	257, 261, 273, 276, 320, 443,	Ramos, Z.N. . . . .	383	Sobolev, N.V. . . . .	1, 119,	Vladimirov, B.M. . . . .	498,
McCandless, T.E. . . . .	264	Ramsey, R.R. . . . .	380, 429		142, 190, 240, 339, 391		501, 543, 560, 573
McCormick, T.C. . . . .	267, 385	Raynor, L.R. . . . .	398	Sobolev, E.V. . . . .	388	Vladykin, N.V. . . . .	576,
McDonough, W.F. . . . .	270, 344	Reddcliffe, T. . . . .	231	Sobolyev, V.K. . . . .	553		577, 578
Memmi, J.M. . . . .	273, 276	Rex, D.C. . . . .	63	Solovjeva, L.V. . . . .	495, 556,	Vos, W.P. . . . .	448
Mendelsohn, M.J. . . . .	279,	Rickard, R.S. . . . .	225, 336		558, 560, 562	Vukadinovic, D. . . . .	79
	285, 290	Robey, J.V. . . . .	460	Solovova, I. . . . .	513, 564	Waldman, M.A. . . . .	139, 264
Mendes, M.H. . . . .	66	Robinson, D.N. . . . .	440	Souza, J.C.F. . . . .	408	Wall, F. . . . .	446
Menshagin, Yu.V. . . . .	543	Robison, H.R. . . . .	463	Spetsius, Z.V. . . . .	391	Wang, W. . . . .	154, 448
Menzies, M.A. . . . .	186, 241, 281	Rock, N.M.S. . . . .	82, 112,	Spiczuzza, M. . . . .	353	Wang, A. . . . .	154, 448
Meyer, H.O.A. . . . .	17, 88,		80, 364, 414	Spiro, B. . . . .	49	Wedepohl, K.H. . . . .	451
	163, 279,	Rodionov, A.S. . . . .	339	Spriggs, A.J. . . . .	63	Weikun, Ye. . . . .	454
	285, 290, 408	Roksandic, Z. . . . .	202	Stachel, T. . . . .	392	White, S.H. . . . .	71
Mia, Q. . . . .	160	Rombouts, L. . . . .	342	Steele, I.M. . . . .	69	Wilding, M.C. . . . .	318,
Middleton, R.C. . . . .	287	Rudenko, A.P. . . . .	533, 547	Stern, C.R. . . . .	395		456, 459
Mikhailichenko, O.A. . . . .	484,	Rudnick, R.L. . . . .	344	Stock, C.F. . . . .	370	Williamson, P.A. . . . .	460
	510, 530	Ryabchikov, I. . . . .	513, 564	Suddaby, P. . . . .	339	Win, T.T. . . . .	142, 145, 475
Milledge, H.J. . . . .	279, 285, 290	Ryan, C.G. . . . .	119, 139, 142,	Sun, S-S. . . . .	82	Winterburn, P.A. . . . .	167
Mitchell, T.E. . . . .	20		145, 148, 475	Sutherland, F.L. . . . .	398	Wuyi, W. . . . .	10, 208
Mitchell, J.G. . . . .	136	Safronov, A.F. . . . .	541	Suvorov, V.D. . . . .	541	Wyatt, B.A. . . . .	463
Mitchell, R.H. . . . .	251,	Sautter, V. . . . .	347	Svisero, D.P. . . . .	3	Xilin, X. . . . .	208
	292, 295	Schepina, N.A. . . . .	481, 490, 530	Sworen, I.M. . . . .	565	Xiling, X. . . . .	10
Moore, R.O. . . . .	125, 177, 298	Schulze, D.J. . . . .	148, 350, 353	Swash, P.M. . . . .	440	Yefimova, E.S. . . . .	391
Morrison, M.A. . . . .	133, 136	Seal, M. . . . .	285	Szabó, C. . . . .	401	Zaitsev, A.I. . . . .	541
Muggeridge, M.T. . . . .	301	Seckerin, A.P. . . . .	543	Tainton, K.M. . . . .	405	Zavjalova, L.L. . . . .	562
Nadejdina, E. . . . .	535	Sellschop, J.P.F. . . . .	163	Tallarico, F.H.B. . . . .	408	Zhang, F. . . . .	160
Navon, O. . . . .	304, 307	Sen, G. . . . .	356	Tal'nikova, S.B. . . . .	565	Zhang, P. . . . .	466
Neal, C.R. . . . .	410	Serenko, V.P. . . . .	228	Taylor, W.R. . . . .	82, 180,	Zhenxin, D. . . . .	470, 473
Nenashev, N.I. . . . .	541	Sgarbi, P.B.A. . . . .	359		364, 414, 417	Zhiqiang, X. . . . .	234
Nixon, P.H. . . . .	63, 145, 310,	Shalashilina, T. . . . .	535	Taylor, L.A. . . . .	401, 410	Zhou, J. . . . .	208, 475
	323, 326, 329	Shcherbakova, Y.P. . . . .	541	Temby, P. . . . .	398	Zhu, Y. . . . .	160
Novgorodov, P.G. . . . .	537	Shee, S.R. . . . .	76, 361, 370, 463	Thirlwall, M. . . . .	241, 281	Zhuravlev, A.Z. . . . .	581
O'Brien, H.E. . . . .	188	Sheppard, S. . . . .	364	Thompson, R.N. . . . .	133,	Zimanowski, B. . . . .	245
O'Reilly, S.Y. . . . .	42, 45,	Sheraton, J. . . . .	202		136, 420	Zinchuk, N.N. . . . .	551
	139, 145, 316, 332	Shirey, S.B. . . . .	329	Thornber, C.R. . . . .	423	Zuev, V.M. . . . .	391
Odling, N.W.A. . . . .	313	Shpount, B.R. . . . .	545	Tingle, T.N. . . . .	212, 432	Zweistra, W.L. . . . .	463
Oleinikov, O.B. . . . .	539	Sial, A.N. . . . .	101	Tompkins, L.A. . . . .	426, 429		

## CONTENTS

Exogenous Changes of the Indicator Minerals at the Formation of Mineralogical Halos of Kimberlite Bodies . . . . .	1
Structural Setting and Tectonic Control of Kimberlite and Associated Rocks of Brazil . . . . .	3
Geology of the NE Angolan Kimberlite Region . . . . .	6
The Status and Future of Diamond Exploration in China . . . . .	10
Composite Garnet Peridotite Xenolith from Picrite-Basalt, Vitim Plateau (Trans Baikal): Implication for the Thermobarometry and Reconstructions of the Mantle Sections. . . . .	13
Discovery of Diamond Deposits in the Quebrada Grande Catchment, Venezuela. . . . .	14
Mesozoic Kimberlites and Related Alkalic Rocks in South-Western São Francisco Craton, Brazil: a Case for Local Mantle Reservoirs and their Interaction. . . . .	17
Oxygen in Diamond by the Nuclear Microprobe: Analytical Technique and Initial Results. . . . .	20
Fictive Conductive Geotherms Beneath the Kaapvaal Craton . . . . .	23
The Join Pyrope-Knorringite: Experimental Constraints for a New Geothermobarometer for Coexisting Garnet and Spinel. . . . .	26
Origin of Low-Ca, High-Cr Garnets by Recrystallization of Low-Pressure Harzburgites . . . . .	29
Experimental Evidence for the Exsolution Origin of Cratonic Peridotite. . . . .	32
Geology and Geophysics of the Redondão Kimberlite Diatreme, Northeastern Brazil. . . . .	35
Inclusions of Carbonatite Calcite from the Oka Complex, Quebec. . . . .	38
Palaeogeographic Studies on the Diamond-Bearing Sopa Conglomerate in the Diamantina Region (Minas Gerais), Brazil. . . . .	40
Applications of Olivine-Orthopyroxene-Spinel Oxygen Geobarometers to the Redox State of the Upper Mantle . . . . .	42
Dating the Cratonic Lower Crust by the Ion Microprobe Shrimp: An U-Th-Pb Isotopic Study on Zircons from Lower Crustal Xenoliths from Kimberlite Pipes . . . . .	45
Isotopic and Geochemical Variation in Kimberlites from the South Western Craton Margin, Prieska Area, South Africa. . . . .	46
Rare Earth, Trace Element and Stable Isotope Fractionation of Carbonatites at Kruidfontein, Transvaal. . . . .	49
Geology and Exploration of the Kelsey Lake Diamondiferous Kimberlites, Colorado, USA. . . . .	52
A Crystallization Model for Peridotitic Diamond Inclusion Spinels . . . . .	55
The Geology of the M1 Kimberlite, Southern Botswana. . . . .	58
Bulk and Mineral Chemistry of the Olivine Leucitite from Juana Vaz, Sacramento, Minas Gerais, Brazil. . . . .	60
A Non Cognate Origin for the Gibeon Kimberlite Megacryst Suite. . . . .	63

The Petrogenesis of Metasomatised Sub-Oceanic Mantle Beneath Santiago: Cape Verde Islands. . . . .	66
Peralkaline Plutonic Magmatic Rocks of the Carbonatite Volcano Oldoinyo Lengai. . . . .	69
Shear Zone Control of Alkali Intrusives – Examples from Argyle and West Africa. . . . .	71
Model Simulations of Carbon Isotope Variability in the Mantle. . . . .	74
The Geology of the Mengyin Kimberlites, Shandong, China. . . . .	76
Distribution of Fluorine between Minerals and Glass in Lamproites, Lamprophyres and Kamafugites: Implications for the Role of F in Deep Mantle-Derived Magmas. . . . .	79
The Aries Diamondiferous Kimberlite Pipe, Central Kimberley Block, Western Australia: Mineralogy, Petrology and Geochemistry of the Pipe Rock and Indicator Minerals. . . . .	82
Destruction of Subcratonic Mantle Keel: the Wyoming Province. . . . .	85
Sulfides, Diamonds, Mantle fO <sub>2</sub> , and Recycling. . . . .	88
Significance of Aluminium, Calcium, Chromium, Zirconium, Niobium and Iron Concentrations in Rutile from High Pressure Rocks . . . . .	92
Symplectites in Upper Mantle Harzburgites and Garnet Harzburgites . . . . .	94
Significance of Chromite, G5 Mg-Almandine Garnet, Zircon and Tourmaline in Heavy Mineral Detection of Diamond Bearing Lamproite . . . . .	97
Vertical Sampling of Mantle beneath Northeastern Brazil as Represented by Ultramafic Xenoliths and Megacrysts in Tertiary Basalts . . . . .	101
Experimental Studies of Olivine Lamproite at Pressures in the Diamond Stability Field . . . . .	103
The Stability of Priderite, Lindsleyite-Mathiasite and Yimengite- Hawthorneite under Lower Continental Lithosphere Conditions: Experiments at 35 to 50 Kbar . . . . .	106
The Origin of Kimberlite and Lamproite in Veined Lithospheric Mantle . . . . .	109
The Mineralogy, Petrology and Geochemistry of Ultramafic Lamprophyres of the Yilgarn Craton, Western Australia . . . . .	112
The Geology and Mineralogy of some Kimberlites in the Mwadui Area . . . . .	116
Comparative Geochemical Evolution of Cratonic Lithosphere: South Africa and Siberia . . . . .	119
Systematics of Isotopic Disequilibria between Minerals of Low Temperature Garnet Lherzolites . . . . .	122
Geochemical Correlations between Kimberlitic Indicator Minerals and Diamonds as Applied to Exploration . . . . .	125
The Magmatic Evolution of the Jacupiranga Complex, Brazil . . . . .	127
Byro Sub-Basin as a Potential Diamond-Bearing Province . . . . .	130
Ultrapotassic Magmas along the Flanks of the Oligo-Miocene Rio Grande Rift, USA: Monitors of the Zone of Lithospheric Mantle Extension and Thinning Beneath a Continental Rift . . . . .	133
Geochemical and Petrographic Evidence for High Mg-Ultrapotassic Magmas in SE Colorado, USA . . . . .	136
Indicator Minerals from Prairie Creek and Twin Knobs Lamproites: Relation to Diamond Grade. . . . .	139
Chromite Macrocysts in Kimberlites and Lamproites: Geochemistry and Origin. . . . .	142
Trace Elements in Garnets from Tanzanian Kimberlites: Relation to Diamond Content and Tectonic Setting. . . . .	145
Ilmenite and Silicate Megacrysts from Hamilton Branch: Trace Element Geochemistry and Fractional Crystallization. . . . .	148

Genesis of Diamond Placers on the Guiana Shield, South America. . . . .	151
IR Spectroscopic Characters Of Garnets and SpinelS – a Potential Discriminative Tool for Diamond Exploration. . . . .	154
Emplacement and Implications of Ultra-Deep Xenoliths and Diamonds from the Transition Zone. . . . .	157
The Physical Characteristics and Syngenetic Inclusion Geochemistry of Diamonds from Pipe 50, Liaoning Province, People’s Republic of China. . . . .	160
The Trace Element Analysis of Single Diamond Crystal by Neutron Activation Analysis. . . . .	163
Aspects of Melt Composition, Crystallization, Metasomatism and Distribution, Shown by Mantle Xenoliths from the Matsoku Kimberlite Pipe. . . . .	167
Composite Megacrysts and Megacryst Aggregates from the Williams Kimberlites, Montana, USA: Multiple Products of Mantle Melts. . . . .	170
Geotectonic Controls of Diamonds and Kimberlites and their Application to Diamond Exploration. . . . .	173
The Individuality of On and Off-Craton Megacryst Suites in Southern Africa. . . . .	177
Petrology, Mineralogy, and Geochemistry of the Metters Bore No. 1 Lamproite Pipe, West Kimberley Province, Western Australia. . . . .	180
Mantle Xenoliths in Potassic Magmas from Montana: Sr, Nd and Os Isotopic Constraints on the Evolution of the Wyoming Craton Lithosphere. . . . .	183
Isotopic Evidence for Variably Enriched Morb Lithospheric Mantle in Xenoliths from North Queensland, Australia. . . . .	186
Isotopic and Trace Element Remote Sensing of Montana Continental Lithosphere from Erupted Magmas. . . . .	188
A Diamond-graphite Bearing Eclogitic Xenolith from Roberts Victor – Indication for Petrogenesis from Pb, Nd, and Sr Isotopes. . . . .	190
The Role of Fluorine in the Crystallization of Niobium and Phosphorus Ores in Carbonatites. . . . .	193
Is Clifford’s Rule Still Valid? Affirmative Examples from Around the World. . . . .	196
Non-Kimberlitic Diamonds Source Rocks. . . . .	199
Peridotitic Paragenesis Planar Octahedral Diamonds from the Ellendale Lamproite Pipes, Western Australia. . . . .	202
A Review of the Carbonatites of Australia. . . . .	205
Spinel – As Indicator for Diamond. . . . .	208
Unusual Spinel-Garnet Lherzolite Xenoliths from Basalt in Eastern China: Constraints on the Late-Tertiary Thermal Structure of the Upper Mantle. . . . .	212
Carbonado and Yakutite: Properties and Possible Genesis. . . . .	214
Petrogenetic Carbonatite – Melilitite Relationships in the Kaiserstuhl Complex, Upper Rhinegraben. . . . .	217
Developments in Remote Sensing of Carbonatites; Airborne Imaging Spectrometry at Mountain Pass, California and Iron Hill, Colorado. . . . .	219
High-Resolution Ion-Probe Analyses of Rare Earth Elements in Kimberlitic Zircons. . . . .	222
Geochemical Correlations in Roberts Victor Eglotites. . . . .	224
Jwaneng Framesites – Inclusions and Carbon Isotopes. . . . .	225

Unequilibrated Ultramafic Xenoliths from Udachnaya Kimberlite Pipe, Western Yakutia. . . . .	228
Coanjula Diamonds, Northern Territory, Australia. . . . .	231
New Type Lamproite of the Dahongshan Area, Hubei Province, China. . . . .	234
The Genesis of Perovskite-Bearing Bebedourite and the Problems Posed by Clinopyroxenite-Carbonatite Complexes. . . . .	237
Crystalline Inclusions in Chromites from Kimberlites and Lamproites. . . . .	240
Geochemical Systematics in Mantle Megacrysts and their Host Basalts from the Archaean Craton and Post-Archaean Mobile Belts of Scotland. . . . .	241
Experiments on Explosive Basic and Ultrabasic, Ultramafic, and Carbonatitic Volcanism. . . . .	245
Palaeozoic Lithosphere Mantle Feature Beneath Fuxian, Liaoning Province, China: the Information from No. 50 Kimberlite Pipe. . . . .	248
Mineralogy and Geochemistry of Perovskite-Rich Pyroxenites. . . . .	251
The Diamondiferous Gravels of the Southwestern Transvaal, South Africa. . . . .	254
Lamproitic(?) Diatremes in the Golden Area of the Rocky Mountain Fold and Thrust Belt, British Columbia, Canada. . . . .	257
Morphological, Resorption and Etch Feature Trends of Diamonds from Kimberlites within the Colorado-Wyoming State Line District, USA. . . . .	261
Macro and Microdiamonds from Arkansas Lamproites: Morphology, Inclusions and Isotope Geochemistry. . . . .	264
Secondary Phases in Mantle Eclogites. . . . .	267
Chemical and Isotopic Systematics of Continental Mantle. . . . .	270
Enhancement of Geophysical Data for Kimberlite Exploration at Iron Mountain, Wyoming, USA. . . . .	273
Finite Element Modeling of Resistivity Data from Kimberlites in Colorado–Wyoming, USA. . . . .	276
Infrared Microspectroscopy of Diamond in Relation to Mantle Processes. . . . .	279
Asthenosphere–Lithosphere Relationships within Orogenic Massifs. . . . .	281
Comprehensive Investigations of Chinese Diamonds. . . . .	285
Middle Jequitinhonha Alluvial Diamonds. . . . .	287
Infrared and Cathodoluminescence Studies of Inclusion–Bearing Diamonds from Brazil. . . . .	290
Accessory Rare Earth, Strontium, Barium and Zirconium Minerals in the Benfontein and Wesselton Calcite Kimberlites. . . . .	292
What's in a Name? Suggestions for Revisions to the Terminology of Kimberlites and Lamprophyres from a Genetic Viewpoint. . . . .	295
Garnet Megacrysts from Group II Kimberlites in Southern Africa. . . . .	298
Distribution of Lamproite Pathfinders in Surface Soils. . . . .	301
Pressure – Temperature – Volume Path of Micro-Inclusion-Bearing Diamonds. . . . .	304
Radial Variation in the Composition of Micro-Inclusions and the Chemical Evolution of Fluids Trapped in Diamonds. . . . .	307
Cr Garnet – Diamond Relationships in Venezuela Kimberlites. . . . .	310

The Composition of Partial Melts in a Volatile Bearing, Reduced Mantle. . . . .	313
Geochemical and Geophysical Mantle Domains. . . . .	316
Diamond Growth Histories Revealed by Cathodoluminescence and Carbon Isotope Studies. . . . .	318
A Physical Characterization of the Sloan Diamonds. . . . .	320
Primary Diamond Subpopulations at Individual Localities. . . . .	322
Graphite-Bearing Peridotites from the Kaapvaal Craton their Carbon Isotopic Compositions and Implications for Peridotite Thermobarometry. . . . .	323
Diamond Facies Pyroxenites from the Beni Bousera Peridotite Massif and Implications for the Origin of Eclogite Xenoliths. . . . .	326
Rhenium-Osmium Isotope Systematics in Southern African and Siberian Peridotite Xenoliths and the Evolution of Subcontinental Lithospheric Mantle. . . . .	329
The Thermal Evolution of Cratonic Lower Crust/upper Mantle: Examples from Eastern Australia and Southern Africa. . . . .	332
Characterization of Lamproites from Paraguay (South America). . . . .	334
Mineral Inclusions in Diamonds from Jagersfontein Mine. . . . .	336
Ilmenite-Bearing Peridotites and Megacrysts from Dalnaya Kimberlite Pipe, Yakutia. . . . .	339
Statistical Distributions for Diamonds. . . . .	342
Cratonic and Oceanic Lithospheric Mantle beneath Northern Tanzania. . . . .	344
Ultra-Deep (> 300km), Ultramafic Xenoliths: Direct Petrological Evidence for the Transition Zone. . . . .	347
Low-Ca Garnet Harzburgite Xenoliths from Southern Africa: Abundance, Composition, and Bearing on the Structure and Evolution of the Subcratonic Lithosphere. . . . .	350
Carbon Isotope Composition of Graphite in Mantle Eclogites. . . . .	353
On the Scale of Heterogeneities in Clinopyroxenes of Spinel Lherzolite Xenoliths from Oahu, Hawaii: Implications for Non-Modal Advection-Diffusion Controlled Trace Element Enrichment. . . . .	356
Petrography and General Chemical Features of Potassic Mafic to Ultramafic Alkaline Volcanic Rocks of Mata da Corda Formation, Minas Gerais State, Brazil. . . . .	359
The Petrology of the Wesselton Kimberlite Sills, Kimberley, Cape Province, South Africa. . . . .	361
Barium-Rich, Olivine-Mica Lamprophyres with Affinities to Lamproites, from the Mt Bunday Area, Northern Territory, Australia. . . . .	364
The Arkhangelsk Diamond-Kimberlite Province – A Recent Discovery in the North of the East-European Platform. . . . .	367
Kimberlitic Olivine. . . . .	370
The Petrography, Tectonic Setting and Emplacement Ages of Kimberlites in the South Western Border Region of the Kaapvaal Craton, Prieska Area, RSA. . . . .	373
Patterns of Diamond and Kimberlite Indicator Mineral Dispersal in the Kimberley Region, Western Australia. . . . .	376
Diamond Prospectivity from Indicator Mineralogy: a Western Australian Perspective. . . . .	380
Eclogite Xenolith with Exsolved Sanidine from the Proterozoic Kuruman Kimberlite Province, Northern Cape, RSA. . . . .	383
Pyroxene Crystal Chemistry and the Evolution of Eclogites in the Mantle. . . . .	385
The Impurity Centers and Some Problems of Diamond Genesis. . . . .	388

Eclogite Pateogenesis of Diamonds from Udachnaya and Mir Pipes, Yakutia. . . . .	391
Volcanology and Geochemistry of the Ellendale Lamproite Field (Western Australia). . . . .	392
Mantle Xenoliths from the Quaternary Pali-aike Volcanic Field of Southernmost South America: Implications for the Accretion of Phanerozoic Continental Lithosphere. . . . .	395
Anomalous Hosts, Unusual Characters and the Role of Hot and Cool Geotherms for East Australian Diamond Sources. . . . .	398
Mantle Xenoliths from Alkali Basalts in the Nograd–Gomor Region of Hungary and Czechoslovakia. . . . .	401
The Group–2–Kimberlite – Lamproite Connection: Some Constraints from the Barkly-West District, Northern Cape Province, South Africa. . . . .	405
The Mata do Lenço Mica–Rich Kimberlite, Western Minas Gerais. . . . .	408
Crustal Signatures in Mantle Eclogites: REE Patterns of Clinopyroxene and Garnet by Sims and Inaa. . . . .	410
Major Element Systematics of Alkaline Volcanic and Lamprophyric Rocks – Toward a Geochemical and Petrogenetic Classification Scheme for the Potentially Diamondiferous Alkaline Rocks. . . . .	414
Mineral Chemistry of Silicate and Oxide Phases From Fertile Peridotite Equilibrated With A C-O-H Fluid Phase – a Low FO <sub>2</sub> Data Set for the Evaluation of Mineral Barometers, Thermometers and Oxygen Sensors. . . . .	417
Overt and Cryptic Strongly Potassic Mafic Liquids in the Neogene Magmatism of the Northernmost Part of the Rio Grande Rift, USA: A Lithospheric Drip-Feed into a Asthenospheric-source Magmas? . . . . .	420
Hot, Cold, Wet, and Dry Hutaymah Ultramafic Inclusions: a Record of Mantle Magmatism beneath the Arabian Shield and Flanking the Red Sea Rift. . . . .	423
Kimberlite Structural Environments and Diamonds in Brazil. . . . .	426
The Boa Esperança and Cana Verde Pipes; Córrego D’Anta, Minas Gerais, Brazil. . . . .	429
Reduced Carbonaceous Matter in Basalts and Mantle Xenoliths. . . . .	432
The Aries Diamondiferous Kimberlite Pipe Central Kimberley Block, Western Australia.. . . .	435
The Ultrabasic Potassic Rocks of Presidente Olegario, Serra da Mata da Corda, Minas Gerais, Brazil. . . .	437
Diamond- and Graphite-Peridotite Xenoliths from the Roberts Victor Mine. . . . .	440
Application of Simple Paramagnetic Susceptibility to Rapid Discrimination of Ilmenite Compositions in Exploration for Kimberlite in the Colorado – Wyoming Province, USA. . . . .	443
Comparison of Element Distribution in Rare Earth-Rich Rocks from the Kangankunde and Knombwa Carbonatite Complexes. . . . .	446
Micro-Structural Variations in Mantle Derived Garnets. . . . .	448
The Composition of the Primitive Upper Earth’s Mantle. . . . .	451
The Characteristics and Origins of Ultrabasic Volcanic Rocks and their Xenoliths from Lixian Area, Gansu Province, P.R. of China. . . . .	454
Evidence for a Deep Origin for São Luiz Diamonds. . . . .	456
Inclusion Chemistry, Carbon Isotopes and Nitrogen Distribution in Bultfontein Diamonds. . . . .	459
The Moana-Tinguis Mililitite Province, Piauí State, Northeastern Brazil. . . . .	460

The Petrology of the Cleve Kimberlite, Eyre Peninsula, South Australia. . . . .	463
Metallogenic Model of Kimberlite in North China Craton, China. . . . .	466
Micas in Kimberlites from China. . . . .	470
Olivines in Shandong Kimberlites. . . . .	473
Geochemistry of Indicator Minerals from Chinese Kimberlites and Lamproites. . . . .	475

### *Appendix*

The Peculiarities of the Mineral Composition of the Diamond Bearing Eclogites from the Udachnaja Kimberlite Pipe. . . . .	481
Ore Minerals from the Lamproite Ground Mass. . . . .	484
Natural Diamonds Growth Conditions According to the Mineral Inclusions Study. . . . .	486
The Evolution of Natural Diamond Growth Conditions. . . . .	488
Chemico-Genetic Classification of the Most Important Minerals-Satellites of the Diamond. . . . .	490
Mineralogical-Isotopic Dynamics, Physico-Chemical Conditions and Stages of Serpentinization Process of Kimberlites from Yakutia. . . . .	492
Evidence of Magmatism, Matasomatism and Deformation Processes Obtained from the Study of the Unique Compositionally Complex Nodule from the Udachnaya Kimberlite Pipe (Yakutia). . . . .	495
Geology, Petrology and Mineral Composition of the Udachnaya Kimberlite Ore Complex (Yakutia). . . . .	498
Trend of SiO <sub>2</sub> in Garnets from Kimberlite Pipes. . . . .	501
Isotope Fractionation Related to Kimberlite Magmatism and Diamond Formation. . . . .	502
New Technology of the Searching of the Diamond Bearing Kimberlites Methodological Basis and Fields of Applications. . . . .	505
The Comparative Characteristics of Ilmenite from the Kimberlite Provinces of the USSR. . . . .	508
Mineralogy of Oxides from the Ground Mass of Kimberlites of Jakutija and Northern European Part of the USSR. . . . .	510
Petrogenesis of Prairie Creek Lamproites: Constraints from Melt Inclusions and High-pressure Experiments. . . . .	513
Al-Solubility in Orthopyroxene in Equilibrium with Garnet: A Reinterpretation of Existing Experimental Data and the Petrogenetic Implications in Garnet Peridotite Xenolith. . . . .	514
Genetic Types of Kimberlite Pipe Craters of a New Diamond-Bearing Province of the USSR and some Aspects of their Development. . . . .	516
Traditional and New Types of Diamond-Bearing Rocks and Methods for their Estimation. . . . .	518
Composition of Groundmass Minerals from Petrographically Distinct Types of Kimberlites. . . . .	521
The Regularities of Variability of Kimberlite Compositions in Multi-Phase Pipes. . . . .	523
Chrome Titanate Inclusions of Unusual Composition in Pyropes from Lamprophyres and Kimberlites. . . . .	525
Sr, C, O Isotope Composition in Kimberlites of the North-russian Province (USSR). . . . .	527
Geological Structure and Mineralogy of the Kimberlites of the Archangelsk Kimberlite Province. . . . .	530
The Formation Kimberlite Diamonds Through Chemical Synthesis in Open Catalytic System. . . . .	533

Diamonds in Metamorphic Rocks. . . . .	535
Primary Melt Inclusions in Eclogite Diamonds and their Genetic Implication. . . . .	537
Native Metals in Kimberlites of Yakytia and their Genesis. . . . .	539
<b>Kimberlite-Controlling Zones in the Crust and Uppermost Mantle Of The West Yakutia: Their Composition And Evolution. . . . .</b>	<b>541</b>
Pre-Cambrian Diamond-Bearing Veined Bodies from South-West of the Siberian Platform. . . . .	543
Geodynamic Regime of Kimberlite Magmatism Manifestations on the Siberian Platform. . . . .	545
The Catalytic Function of Kimberlite Elements in the Formation of Natural Diamonds. . . . .	547
Mineral Inclusions in Bort from the Mir Pipe, Yakutia. . . . .	549
On the Problem of Vertical Zoning of Kimberlite Bodies. (on the Example of Lesotho). . . . .	551
The Problem of Primary Source of Brazil-Type Diamonds (the Case-History of Discovery of Diamond Deposits in the Arkhangelsk Region). . . . .	553
Metasomatic Processes in Subcontinental Lithospheric Mantle beneath the Siberian Platform. . . . .	556
O, C and Sr Isotopic Composition of Calcites in Garnet Megacrysts and Carbonatized Granulitic Xenoliths from the Udachnaya Kimberlite Pipe, Yakutia. . . . .	558
Cognate Suite of Garnet Clinopyroxenite-Olivine Websterite- Lherzolite from the Udachnaya Kimberlite Pipe, Yakutia. . . . .	560
Layered Structure of the Upper Mantle beneath the Siberian Platform: Petrological and Geophysical Data. . . . .	562
A Study of Microinclusions in Minerals of Spanish Lamproites. . . . .	564
Study of Gaseous Phase in Diamonds with Eclogitic and Ultrabasic Inclusions from Yakutian Kimberlite Pipes. . . . .	565
Upper Mantle Composition beneath Yakutian Kimberlite Province. . . . .	567
The Genetic Types of Natural Diamonds. . . . .	569
Kelyphites on Garnets in Mantle Xenoliths and Kimberlites: Composition, Genesis, Petrological Implication. . . . .	571
Basaltic and Mica Kimberlites of the Siberian Platform and their Time-Space and Genetic Relationships. . . . .	573
Carbonatites of K-Alkaline Complexes of the Aldan, North Pamir and South Mongolia. . . . .	576
Chemical Composition and Geochemical Features of Micras from Lamproites of the Aldan Schield, USSR. . . . .	577
Geological Position, Petrology and Geochemistry of Lamproites (Aldan Schield, Siberia). . . . .	578
Inclusions of Plutonic Minerals in Diamonds from Kimberlite Rocks of the Northern East-European Platform. . . . .	579
Ancient Depleted Subcontinental Lithosphere Under Siberian Platform: Nd-Sr Isotopic and REE Evidence from Garnet Peridotite Xenoliths of Mir Pipe (Western Yakutia). . . . .	581

## EXOGENOUS CHANGES OF THE INDICATOR MINERALS AT THE FORMATION OF MINERALOGICAL HALOS OF KIMBERLITE BODIES.

*Afanas'ev, V.P.; Sobolev, N.V. and Pokhilenko, N.P.*

During the mineralogical halos formation the kimberlite minerals are affected by the powerful exogenous factors changing both individual minerals and the composition of mineral associations. The main factors of exogenous changes are mineral transportation during the mineral halos formation and physical-chemical changes in the formed sediments.

The changes during the process of transportation are expressed in two forms - i.e. the hydraulic grading of the transportation of the minerals of different density and proportional to the value of their hydraulic fall diameter (the velocity of the free fall of the minerals in the aqueous medium, m/sec). The expressions for the fall diameter determination are obtained on the experimental basis: diamond -  $V = 62,3 \cdot p^{0,24}$ , pyrope -  $V = 61,6 \cdot p^{0,23}$ , picroilmenite -  $V = 69,2 \cdot p^{0,24}$ , chromespinel -  $V = 71,3 \cdot p^{0,23}$ . On their basis the coefficients of the mineral inertness for the plain rivers conditions (Yakultia) are calculated.

Another aspect of the mineral transportation is a decrease in their concentration with the removal from a kimberlite body. The hydraulic gradient and the distribution of the mineral concentration relative to the kimberlite body is expressed by the formulae in the idealized form:

$$P = P_0 - BX \quad P = P_0 e^{-BX},$$

where  $X$  - is the distance up to kimberlite body,  $B$  - the coefficient of the mineral inertness,  $P_0$  - the mineral concentration in kimberlite body elluvium,  $P$  - the mineral concentration at a distance  $X$ .

The mechanical wearing depends mainly on the landscape dynamic conditions. Under the alluvial conditions on the continent, the kimberlite minerals are weakly rounded, on minerals larger than 2mm, the signs of rounding appear at a distance of some dozens of kilometers. The smaller ones are transported with no rounding to many dozens of kilometers. The minerals assume the medium level of rounding at wearing under the conditions of littoral alluvial plains which could be periodically flooded by the shallow basin waters and the minerals could be rounded under the influence of waves. The minerals are rounded to the maximum extent under the littoral conditions in the process of forth/back moviments under the wave influence, the minerals of the medium and high level of rounding are widely spread in the ancient mineral halos at the different regions of the world. The alluvial conditions are unfavorable for the good hydraulic grading of minerals. The best grading takes place under littoral conditions. Here the formation of the diamond-pyrope association with the similar grain sizes occurs and the mineral concentration grows, therefore, the rich diamond placers could be formed under the given conditions. Besides, according to the calculations and experimental data, the picroilmenite mechanical stability is approximately twice lower than of pyrope. Therefore, whether pyrope ultimately rounded, than picroilmenite could be destroyed completely. Diamonds are also rounded under these conditions.

The physical-chemical changes occur after fixation of the minerals in the sediments. Four main types of changes are discovered, i.e. under the condition of hypergenesis, diagenesis, metagenesis and metasomatosis.

The hypergenous changes connected with the crust of weathering are widely spread in all parts of the world. The maximum changes are connected with the upper part of the crust of weathering profile, i.e. the hydrogenesis zone. According to the degree of stability the main deep-seated kimberlite minerals form series: diamond - zircon - chromespinel - picroilmenite - pyrope - clinopyroxene - olivine. Diamond and zircon are practically unchangeable. Olivine is completely destroyed, the grains of chromediopside are seldom preserved. Pyrope reveals specific features of the hypergen dissolution. It is poorly imperfect grains at dissolution acquire the form of cuboid with the prominent faces which represent the dissolution equilibrium form. The spontaneous corrosion cracking occurs. During the experiments and the study of the mineral halos has been discovered that the pyrope resistance to dissolution is greatly dependent on the chemical composition. The orange low chromous pyropes being the least stable, their fractions in the halos decreases and the fraction of the violet chromous pyrope increases under hypergenic conditions respectively.

Picroilmenite under the hypergenic conditions is dissolved or it is substituted by leucoxene.

Chromespinel is not dissolved, its changes are connected with the appearance of microcracks at the surface which are due to the effect of spontaneous corrosion cracking.

Diagenesis slightly influences the kimberlite minerals. The main form of changes is corrosion cracking, mainly of pyrope and picroilmenite.

The changes under metagenesis and metasomatism are not so widely spread as hypergenesis or diagenesis ones, but their influence on the minerals could be very significant. Metagenous changes in minerals occur during the orogeny processes. They are traced in the minerals from the triassic deposits of the Verkhoyansk folded zone along the right bank of the Lena river and in the Middle Devonian deposits in the Urals. In both cases pyrope cracks and it is substituted by chlorite. The pyramidal-tilted relief formed under the chlorite over the pyrope surface. In the Ural Devonian deposits the picroilmenite cracks and it is replaced by anatase. Chromespinel behaviour is not studied. Pyrope and picroilmenite could be completely destroyed under the given conditions replacing by the secondary minerals.

The metasomatic changes of the kimberlite minerals are connected with the influence of the intrusions of the differentiated traps. In the metasomatism zone pyrope is substituted by chlorite with the formation of pyramidal-tilted relief like at the metagenesis. Picroilmenite is substituted by the anatase crystals, chromespinel assumes cavernous relief. Diamond under such conditions is unstable and it oxidizes forming oxidizing dissolution-trigontrioctahedroid. In the zone of maximum metasomatic changes the kimberlite minerals, including diamond, could be completely destroyed.

Thus, the complex of the exogenous changes of the kimberlite minerals strongly influences the composition of the mineral association, mineral concentration and their habit. The specific character of both mechanical and physical-chemical changes permits to solve the inverse problem i.e. according to the mineral habit to determine the conditions under which they were and on this basis to clear up the history of the development of the mineral halos.

## STRUCTURAL SETTING AND TECTONIC CONTROL OF KIMBERLITE AND ASSOCIATED ROCKS OF BRAZIL.

Almeida, <sup>(1)</sup> F.F.M. de and Svisero, <sup>(2)</sup> D.P.

(1) Instituto de Pesquisas Tecnológicas do Estado de São Paulo, Caixa Postal 7141, CEP 01000, S. Paulo, SP, Brazil;

(2) Instituto de Geociências, Universidade de São Paulo, Caixa Postal 20899, CEP 01498, S. Paulo, SP, Brazil.

Although diamonds have been known in the Brazilian Platform since 1725, kimberlites were discovered only in the late 1960's. Presently, kimberlites occur in at least eleven different provinces: Alto Paranaíba (Coromandel) and Bambuí (Minas Gerais), Amarinópolis (Goiás), Paranatinga, Fontanillas-Juina and Pontes e Lacerda (Mato Grosso), Pimenta Bueno (Rondônia), Gilbués and Picos (Piauí), Lages (Santa Catarina) and Jaguari-Rosário do Sul (Rio Grande do Sul) (Svisero and Chierigati 1990).

The kimberlites of Alto Paranaíba are associated in space and possibly in time with carbonatites, basic-ultrabasic dykes trending NW-SE and several types of alkalic ultrabasic rocks, including lavas with lamproitic and kamafugitic affinities. Kimberlites and alkalic ultrabasic lavas occur mainly as diatremes intruding the Proterozoic Araxá and Brasília Fold Belts developed along the western margin of the São Francisco Craton. Geological field work has revealed that the intrusions comprise several distinct fields centered around Catalão, Coromandel, Presidente Olegário, Carmo do Paranaíba and Araxá as well. The tectonic pattern of the area resembles that of northwestern Australia where diamond-bearing lamproites and kimberlites intrude fold belts around the Kimberley Craton (Jaques, Lewis and Smith 1986). Therefore, we predict that new findings of lamproites will certainly be registered in the future. In addition, there is a distinct possibility that the detrital diamonds of western Minas Gerais, which have been mined for two centuries, may be related to lamproites rather than to kimberlitic sources. Moreover, the presence of mineral indicators such as chromium pyrope garnet, magnesium ilmenite and chromium spinel, among the heavies in the diamond-bearing conglomerates that presently cover large areas of Araxá and Bambuí Groups, points to local sources for the diamonds.

The Bambuí Province is located in southwest Minas Gerais and comprise intrusions scattered over the southwest border of the São Francisco Craton, which was stabilized around 2.0 Ga. At this stage, we admit that the huge fracture zones reflected by the lineaments of Alto Paranaíba controlled the emplacement of kimberlites and associated rocks in both Alto Paranaíba and Bambuí Provinces. Amarinópolis on the northern rim of Paraná Basin includes in addition to kimberlites several types of alkalic ultrabasic rocks intrusive into the Proterozoic

Araguaia Fold Belt. The Provinces of Paranatinga and Fontanillas-Juína are located in the Rio Negro-Juruena Mobile Belts made up of rocks of continental crust formed between 1.55 and 1.75 Ga. Pimenta Bueno lies on the border of the Rio Negro-Juruena and Rondoniense Mobile Belts, the latter having developed around 1.3 Ga. Pontes e Lacerda in remote southwest Mato Grosso is also intrusive in rocks of the Rondoniense Belt. Apparently, there is a remarkable regional trend joining the Provinces of Alto Paranaíba, Amarinópolis, Paranatinga, Fontanillas-Juína and Pimenta Bueno. This possible megalineament trends N35W and may have played an important role in kimberlite emplacement either via hot spots or through reactivation during the late Cretaceous (Almeida 1986).

Kimberlites of Gilbués (southern Brazil) and Picos (eastern Piauí) are intrusive in Paleozoic and Mesozoic sediments of the Paranaíba Basin. Intrusions in Picos were controlled by the magnetic lineament of Senador Pompeu or Serra Grande and those of Gilbués by the regional Transbrasiliiano lineament. These NE-SW structures converge in middle Brazil before disappearing beneath the sediments of the Paraná Basin in line with the lamproites and basanites of Asunción, Paraguay. Lages in central eastern Santa Catarina and Jaguari-Rosário do Sul in central southern Rio Grande do Sul are poorly known. The Lages diatremes are intrusive in Paleozoic sediments of the Paraná Basin and are associated with breccias, carbonatites, melilitites and other alkaline rocks. In spite of the lack of information on the basement in Lages it is thought to consist of rocks of the Proterozoic Itajaí Fold Belt. Kimberlites of Jaguari-Rosário do Sul are intrusive into basalt flows of the Paraná Basin, whose basement is supposed to be the Craton Rio de la Plata.

In summary, the majority of the kimberlites and associated rocks known in Brazil up to this moment are intrusive in fold belts or mobile belts of Proterozoic age. Notable exceptions include the Bambuí Province on the border of São Francisco Craton and Jaguari-Rosário do Sul probably on Rio de la Plata Craton. Nothing is known about Amazon Craton mainly due to the tropical covering forest. Finally, we mention the occurrences of detrital diamonds in metaconglomerates of Middle Proterozoic Espinaço and Roraima Belts whose sources are completely unknown.

#### REFERENCES

Almeida, F.F.M. de (1986) Regional distribution and tectonic relations of the post-paleozoic magmatism in Brazil. *Revista Brasileira de Geociências*, 16, 325-349 (in Portuguese).

Jaques, A.L., Lewis, J.D. and Smith, C.B. (1986) The kimberlites and lamproites of Western Australia. Geological Survey of Western Australia, Bulletin 132, 268p.

Svisero, D.P. and Chieregati, L.A. (1990) Geologic context of diamond and kimberlites in Brazil. Special Publication, Instituto de Geociências da Universidade de São Paulo, p. 132-138 (in Portuguese).

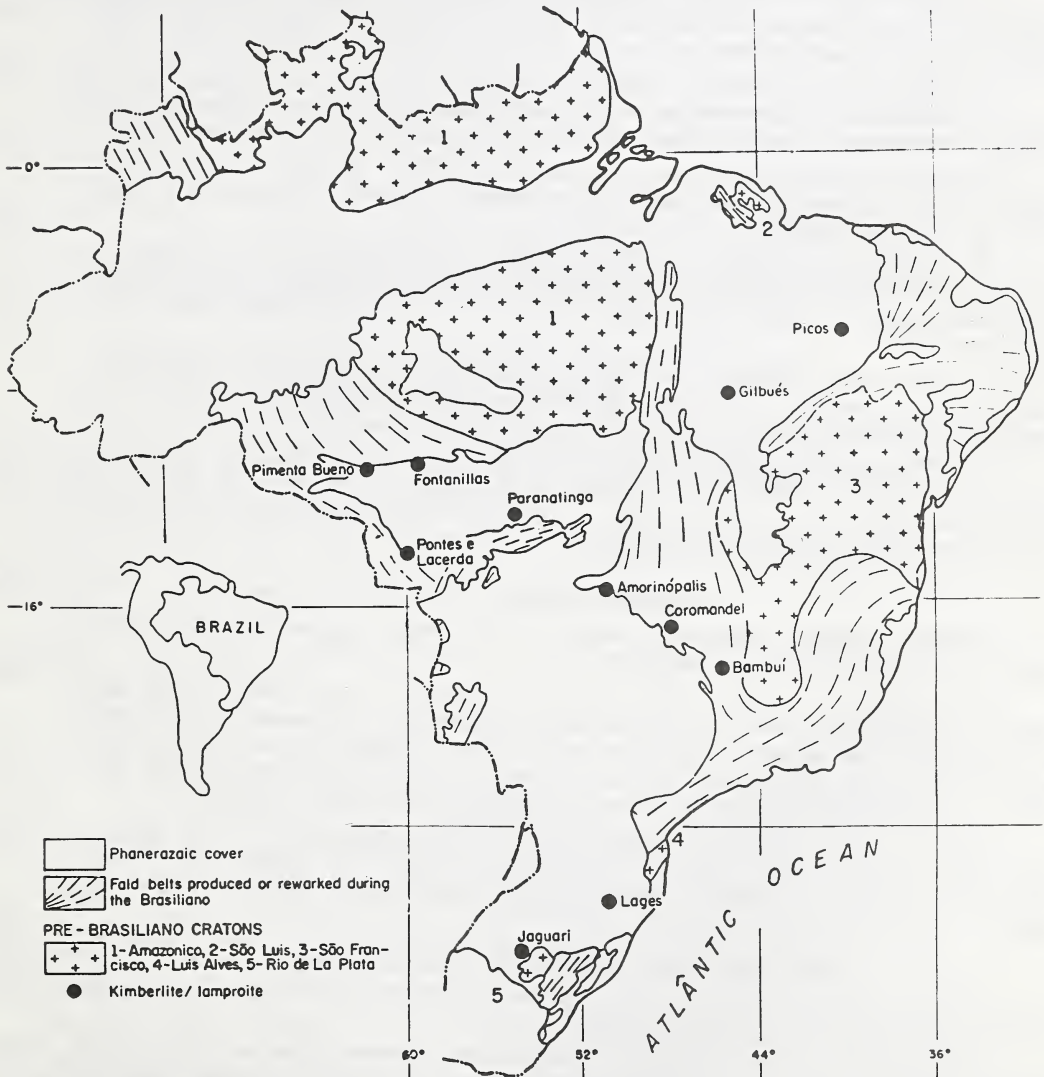


Fig.1- SIMPLIFIED TECTONIC FRAMEWORK OF BRAZIL AND SITES OF KIMBERLITE/ LAMPROITE OCCURRENCES

## GEOLOGY OF THE N.E ANGOLAN KIMBERLITE REGION.

*Mankenda Ambrose.*

*National Directorate of Mines, Luanda, Box 1260, Tx 3470, Angola.*

### ABSTRACT

The Northeast of Angola known as Lunda, is one of the greatest regions of the Diamond Provinces of Africa where gem diamonds have been exploited for almost a century .

In the late cretaceous a period of rapid erosion occurred, giving rise to piedmont conglomerates with sandstones and other sediments which formed a secondary type of diamond deposits known as "Calonda Formation".

The first kimberlites were discovered from the diamond satellite minerals ( chromdiopside, pyrope and ilmenite ) found in the heavy fraction of alluvial gravel .

The platform basement of the region is fractured by a number of faults of N.E and latitudinal directions. what can be seen from a sporadic development of the metamorphic rocks of the Luana group and karroo sediments .

In the region kimberlite intrusion occurred before the fundamental change of its general structure: up to the cretaceous time structural and facies zonation was determined by the latitudinal faults .

The first paleotectonic maps of Lunda region were made to establish criteria for more effective prospection and exploration works, and to assist those who devote to the study of Angolan diamond geology in discive-ry of new diamond primary deposits .

### INTRODUCTION

Corrent angolan diamond production is from river beds, alluvial flats, terrace and eluvial deposits.

Although the diamond exploitation was made in this area during many years, its geology is still little known. This fact has made it difficult to determine the general regularities of the primary and secondary diamond ore-bedding formation, as well as the choice of guidance and more suitable prospection methods of the kimberlite and other deposits .

Based on the research carried out in the kimberlite of this region, the paleotectonic conditions of cretaceous kimberlite magmatism indications and alluvial diamond formation are hereby examined for the first time .

### LUNDA GEOLOGICAL FRAMEWORK OF KIMBERLITES

The territory of Angola has complex geological structure. It belongs to the precambrian african platform .

Tectonically, Lunda region includes the western slope of the shield Cassai adjacent part of Cassanje depression. The gneiss-magmatites and granulites are the most represented precambrian rocks from the part of the shield in question.

The most recent pre-cambric rocks preserved in fragments, are detached in the Luana group represented by quartzic sandstones, quartzites and greywacke, with metabasaltic layers in some places .

From the phanerozoic coverage formations, locally preserved in the Cassai shield flank, the oldest are the continental deposits of the karroo system ( C<sub>3</sub> - T<sub>1</sub> ) .

More recent, the Calonda formation is represented by fragments in the shield flank preserved in the form of erosion witnesses in the precambrian rocks .

In the Cassai shield the deposits in question are characterized by the considerable facies lateral change that enable to determine the formation conditions of old fluvial valleys with placer deposit of cretaceous.

The above characterize rocks of the crystallin basement and covering ones are recovered by partial erosion by the red continental deposits of the paleogenic-neogenic kalahari group .

The accumulative quaternary terraces of the region were mostly formed in the weathering process of the Calonda formation deposits and of the cretaceous kimberlites, that is why there are rich diamond bearing placer deposits in some places.

In the Northeastern Angola, platform magmatism of cretaceous are well developed: kimberlites and complex of alkalic rocks.

The kimberlites are dated between 80-120 m.y. and are represented by the breccia and massive varieties. The most recent alkalic complexes are composed of sienites and phonolites .

It should be pointed out that the alkalic complexes are located within the granite - gneissic ovoids of the basement, whereas kimberlites area associated with the intra-ovoid zones. This witnesses the influence of the basement structures and corresponding old disuniformities in the platform magmatism process.

#### GEOLOGICAL EVOLUTION OF THE CASSAI SHIELD AND RELATED DIAMOND ORE-BED FORMATION

The geological development of the Lunda region ( Cassai shield ) can be followed from the upper proterozoic when the covering deposits of the Luana group were accumulate in the archaic consolidated basement, crossed by the lower proterozoic granites .

At the end of the lower proterozoic there was the uprising of the west flank of the shield followed by the intrusion of alkaline granitic and alkaline complexes and movement of embasement blocks.

In the lower and medium proterozoic, Lunda region was upraised and weathered, the first differentiated vertical movements appeared in the upper paleozoic-triassic .

At that time, two intra-continental depressions of the graben type were individualized perpendicularly oriented: one in the west- sub-meridional with which the formation of Cassanje depression started, and another of the N.E-SW direction along the lineation gabbro-noritic of archaic. In jurassic most of the Lunda region was expressed by the uprising of the shield, submitted to the planar erosion .

At the end of jurassic initiation cretaceous, the western edge of the Cassai shield suffered heavy tectonization according to the same fault systems of sub-meridional and NE-SW direction. The cataclasis was followed by the kimberlites intrusion which shows the connection of the faults with a very deep tectonomagmatic system .

The important changes in the geological development of the Lunda region occurred in the cretaceous. According to the distribution of the deposits of this age, it was possible to reconstitue the complex system of the graben type depressions on the boundaries of the Cassai shield (fig.1).

The greatest depression along the western edge of the shield coincided in general with the main area of the earlier kimberlitic magmatism

The thick granularity of the cretaceous continental deposits developed in the western part of the Cassai shield, indicates their formation in the valleys. According to the distribution of these sediments it is possible to reconstitue the old ramified river system of creta-

ceous falling into the north, running off to the close depression of lacustrine type of the Congo sineclise in which the sandy-clay deposits were greatly accumulated ( Fig. 1 ) .

The slope process and rivers falling into the north of the western edge of the Cassai shield, along the tectonic depressions weathered the lower cretaceous kimberlites which conditioned the formation of diamond bearing alluvial deposits of this age .

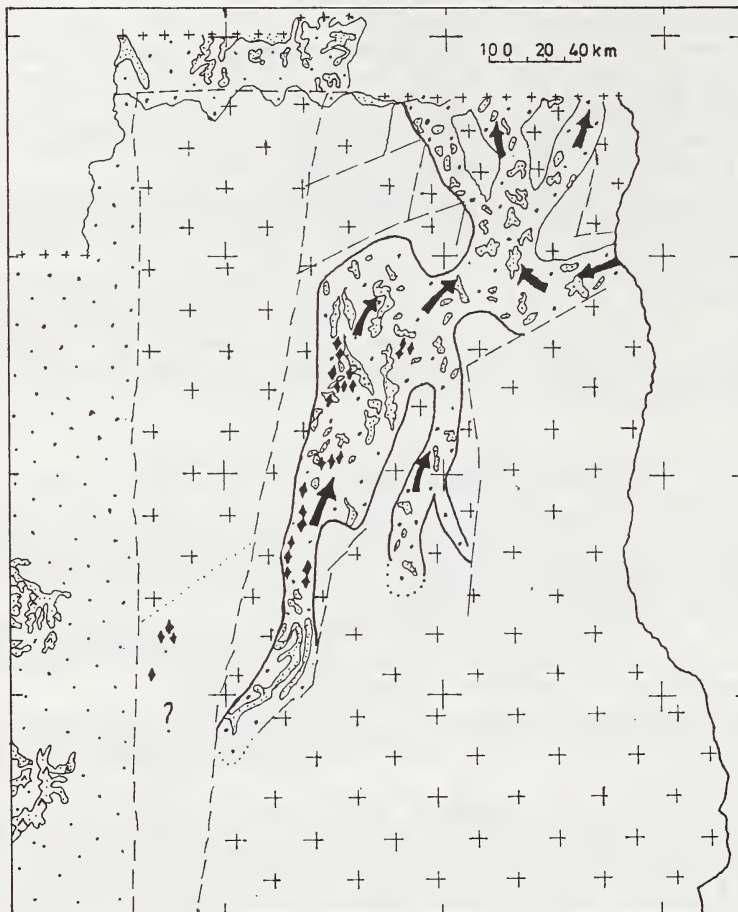
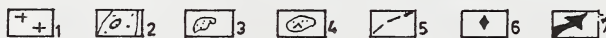


Fig. 1 - PALEOTECTONIC SCHEME DURING CRETACEOUS



- 1 - Basic Complex; 2 - Area of Cretaceous Deposits Development;  
 3 - Area of Present Cretaceous Outcrop; 4 - Complex of Alkalic Rocks;  
 5 - Faults; 6 - Kimberlites; 7 - Hydrographical Network Orientation

### CONCLUSIONS

1. The platform development of Lunda region, initiated in the upper proterozoic was guided by the deep faults of two main directions sub-meridional and NE-SW: the deepest were probably the faults of the last direction which inherited the archaic gabbro-noritic lineation. Precisely on the crossing with the meridional faults the lower cretaceous kimberlites introduced .

2. The assessment of data enabled to outline the old fluvial arteries from the development of which resulted the accumulation of the diamond bearing placer deposits.

3. The outlined sequence of the geological development of the Lunda region can be used as general scientific basis for drawing up the further study programmes of its diamond bearing potential. That sequence enables us to determine the likely location of the kimberlites and lamproites not yet detected, the ways of transport and its diamonds during the cretaceous and cenozoic .

#### REFERENCES

1. Beetz P.F.W. Geology of South West Angola, between Cunene and Lunda Axis. Trans. Geol. Soc. Afr., Johannesburg, 1933 v.36, p.137

2. Dawson J.B. the structural setting of African Kimberlite magmatism J.African magmatism and tectonics, 1970, p.326

3. Mankenda A. Geology of the diamond deposits of North-East ern Angola. Abstrat of PH. D thesis in Geology and mineralogy ( economic geology ). Moscow, 1989, p. 1- 19

4. Zuyev V.M., Kharkiv A.D., Zinchuk H.I., Mankenda A. Slightly eroded kimberlite pipes of Angola. Geology and Geophysics. SD AS USSR, Novosibirsk, Nauka, 1988, N 3, p. 56-63 ( in Russian ).

## THE STATUS AND FUTURE OF DIAMOND EXPLORATION IN CHINA

Zhang Andi; Xu Dehuan; Xie Xiling; Guo Lihe; Zhou Jianzong and Wang Wuyi.

*Institute of Mineral Deposits, Chinese Academy of Geological Sciences, Beijing 100037, China.*

Diamond exploration in China is discussed, based on the statistical study of the chemistry of macrocryst garnets and chrome-spinels from concentrates of 68 bodies of both Chinese and non-Chinese kimberlites, lamproites and lamprophyres, integrated with available chemical data for inclusions in diamonds from Chinese kimberlites, plus geological and tectonic information.

Diamonds occur in three major cratons of China, namely, Sinokorean, Yangtze and Tarim, but kimberlites are mainly found in the Sinokorean craton. Eight kimberlite fields have been recognized (Fig. 1). Only four are diamondiferous, i.e. Fuxian, Tieling and Huanren in Liaoning province and Mengyin in Shandong province, and all these are all restricted to the vicinity of the *Liaolu terrain* (Wu Jiashan et al.1990). These kimberlite occurrences are mainly small dykes and small pipes. Only two are mined, i.e. pipe no. 50 in Fuxian and Shengli no.1 in Mengyin, which are deeply eroded. In outcrop, either root zone hypabyssal facies or facies transitional between diatreme and root zone can be easily identified. Pipe no. 50 produces high quality gemstones at a grade of about 60-230 cts/100t, and has dimensions of 245x55 m, while the pipe of Shengli No. 1 yields a grade of 40-250 cts/100t and is 5000 m # in size. As to size and grade of these two pipes, it is difficult to compare them with pipes in Yakutia like Mir or Udachnaya and in South Africa like Finsch or others, but the Sobolev garnet CaO-Cr<sub>2</sub>O<sub>3</sub> diagrams of the two Chinese kimberlite pipes and the chemistries of their diamond inclusions are quite similar to those from kimberlites of Vilui in Yakutia and the Kaapvaal craton of South Africa (Fig. 2a-d). This shows that the constitutions of the upper mantle under the Sinokorean, Vilui and Kaapvaal cratons are the same, and characterized by four subparageneses of peridotites, i.e. harzburgite, dunite, lherzolite and wehrlite, with lherzolite always dominant as it is the major constituent of the upper mantle (Lucas et al.1989). In addition, the chemistry of subcalcic Cr-pyrope, Na-bearing pyrope-almandine and Cr-spinel from concentrates, together with diamond inclusions of Chinese and non-Chinese kimberlites, are also similar. A tectonic-magmatic arc, represented by a granite-greenstone belt, is recognized, which separated the Sinokorean Craton into two parts. So far all the diamondiferous kimberlites and placers occur only in the eastern part (the Liaolu terrain) which extends from Baishanzhen (Jilin province), through Qinyuan and Anshan (Liaoning province) to Taishan (Shandong province). This terrain is considered to be the most prospective target area for diamonds of kimberlitic type in China.

Another four kimberlite fields have been found in the western part of the craton. From North to South (Fig. 1), Yinxian, Shexian and Hebi occur along Taihang fault zone while Liulin

is located in Luliang mountain area. The kimberlites are well differentiated serpentine calcite types which contain relatively small amounts of olivine macrocrysts. The content of xenocrysts is low and they are invariable in composition, with pyrope low in Cr; no G10 pyrope, high Cr-spinel or diamonds have been found. The basement beneath the Taihang fault strand is a Pt<sub>1-2</sub> paleorift zone, thus explaining the occurrence of barren kimberlites in this area.

So far, lamproites have been found only in the Yangtze craton. This craton contains "Proton" basements situated in central Sichuan and on the western flange of the craton, both of them having 1850 Ma as the age of cratonization. That in central Sichuan is overlain by a Mesozoic basin, but the vast area to the south of it, including southeastern Sichuan, northeastern Guizhou and western Hubei (the Wuling mountain area) is worthy of attention for diamonds. High-Cr spinels (Cr<sub>2</sub>O<sub>3</sub> ≈67%) have been recovered from stream concentrates and >2.5 Ga basement ages have been obtained. The similarity of Cr<sub>2</sub>O<sub>3</sub>-Al<sub>2</sub>O<sub>3</sub> diagrams of lamproite Cr-spinels from the Yangtze and W. Australia Kimberley cratons suggests that the upper mantle is similar under these two areas. Logically therefore, Wuling mountain area is probably the most prospective area within the craton. Overall, the Yangtze craton is a prospective target area for diamonds of lamproitic type (Fig. 2e-h).

## References

- Lucas, H., Ramsay, R.R., Hall, A.E., Smith, C.B. and Sobolev, N.V. (1989). Garnets from Western Australian kimberlites and related rocks. In: Kimberlites and related rocks, 2, Geological Society of Australia, Special publication No. 14, 809-819.
- Wu Jiashan, Geng Yuansheng, Tang Lianjiang and Zhang Andi (1990). Relationship of diamondiferous kimberlites with tectonic setting of basement in Sino-Korean platform (in press).

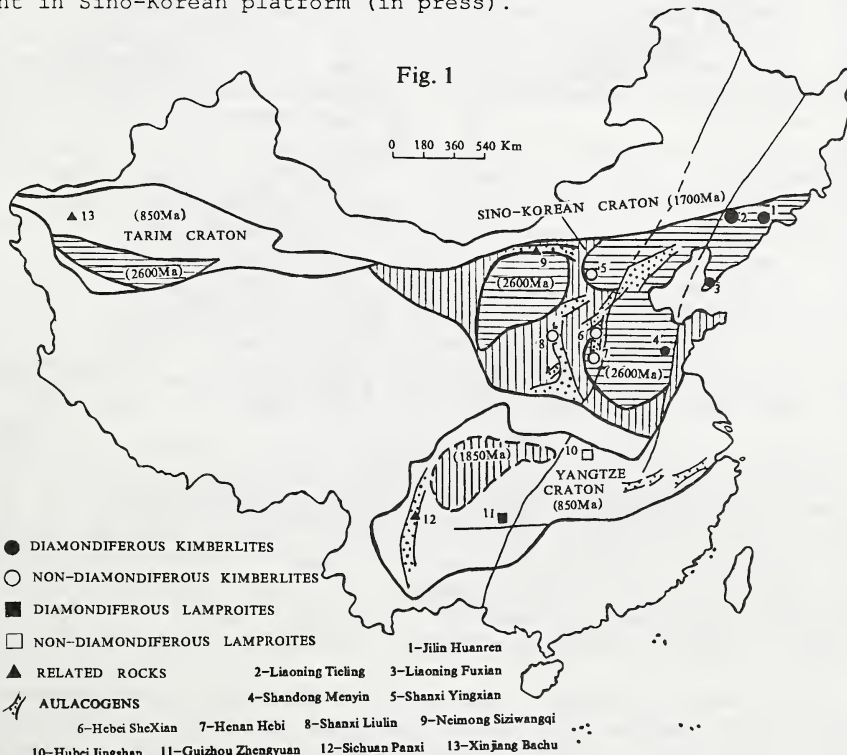


Fig.1. Principal lamproite and kimberlite occurrences in China

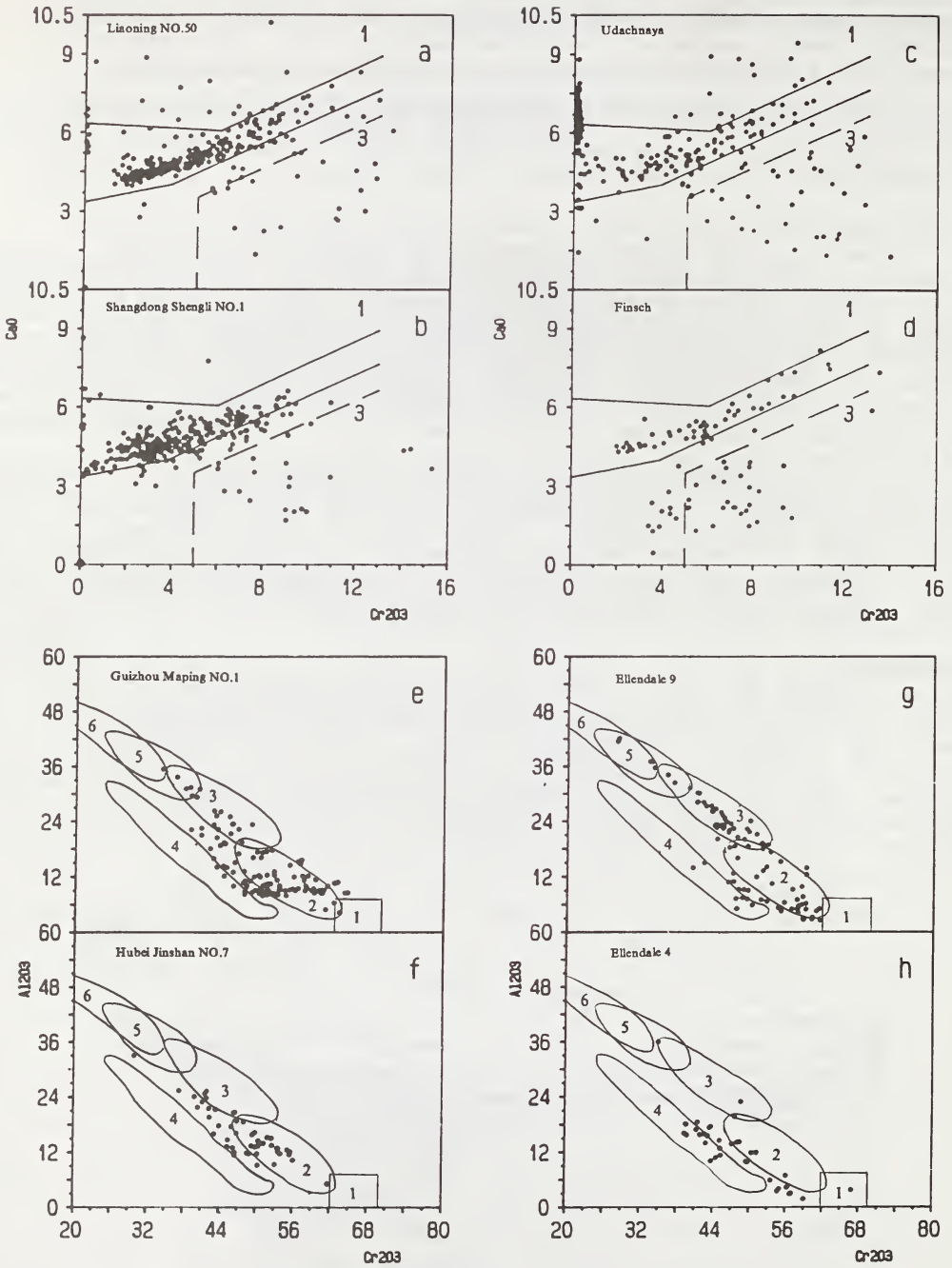


Fig. 2

e — h: 1—Diamond—Chromite facies; 2—Coesite facies; 3—Grospsydite facies;  
 4—Dunite facies; 5—Spinel—Pyrope facies; 6—Spinel—Pyroxen facies

COMPOSITE GARNET PERIDOTITE XENOLITH FROM PICRITE-BASALT, VITIM  
PLATEAU (TRANS BAIKAL): IMPLICATION FOR THE THERMOBAROMETRY  
AND RECONSTRUCTIONS OF THE MANTLE SECTIONS.

*I. V. Ashchepkov.*

*Institute of Geology and Geophysics, Siberian division USSR Academy of Sciences, Novosibirsk.*

In Vitim plateau garnet lherzolites were found in Oligocene picrite-basalt tuff (Ashchepkov et al 1988) and Pliocene hawaiite cones and flows. In first location composite nodules with contact zone of different pyroxenite types are divided in several types. Green Cr-diopside garnet websterites usually show an equilibrium with lherzolites. Their minerals are slightly enriched in Al, Na and Ti. Two pyroxene temperatures for this veins vary within usual for garnet lherzolite interval of 950 - 1050 C and 22 - 26 kbar. Dark-green Cr and more Ti-rich branched pyroxenites occurred at lower temperatures - 900 - 980 C as well as Cr-poor green clinopyroxenites containing exsolved garnet and orthopyroxene. Blue-green eclogite-like rocks forms visible reaction zones. Cr-diopside zone is changed by garnet websterite zone then substituted by garnet clinopyroxenite and then by clinopyroxenite. There is a relic trend of increasing temperature in this direction from 1020 to 1080 C. All this magmatic veins seems to be formed at the previous stages of mantle activity.

Hot pyroxenites are of two types. Green Cr-less cumulative poikilitic websterites in some cases containing rare garnet and having equilibrated temperatures about of 1200 - 1300 C and pressure 27-30 kbar. The next group are presented by Ti-rich clinopyroxenites containing interstitial garnet and orthopyroxene. They occurred at the same temperature interval but at slightly low pressure. This hot pyroxenites drop to the same field at TP diagram as highly deformed lherzolites which form the inflection on the estimated geotherm but direct contacts of this pyroxenite and deformed lherzolites were not found yet. The only one found contact of such type seems to be deformed after interaction of magma with wall rock peridotites.

Last vein group containing amphibole and phlogopite may have been formed during the percolation of water saturated melts trough garnet lherzolites. Small amphibole veinlets occurred only in spinel lherzolites but phlogopite ones may be found in all peridotite rocks. They show small diffusion zoning around them. Large veins found in garnet lherzolites contain hydrous minerals only at the central parts. The outer contacts composed by pyroxene aggregates. Their compositions suggest forming of veins in more high-temperature conditions then those of contact lherzolite associations. It is supported by break up of the garnet near the contacts.

Composite temperature equilibrated xenoliths with diffusion zonation of associated minerals allow to test the thermobarometric methods in different systems. All used thermometers (Wells, 1977; Bertrand & Mercier; 1985; Harley, 1984; O'Neil & Wood, 1981; Brey and Kohler, 1990 etc.) show the coincidence of obtained data for the all part of such type of composite xenoliths within the 45 C interval. The best of barometric methods appeared to be equation from Nickel & Green, 1985 and Webb & Wood, 1988 version of Wood barometer.

Reconstructed geotherm for the mantle under Vitim plateau using new data appeared several level of magma interaction with mantle wall rock lherzolites besides only one deep-seated level reported earlier (Ashchepkov et al, 1988). This points correspond to deformed and hot pyroxenites. Green types of pyroxenite xenoliths believed to be more high temperature.

## DISCOVERY OF DIAMOND DEPOSITS IN THE QUEBRADA GRANDE CATCHMENT, VENEZUELA.

*Baxter-Brown, <sup>(1)</sup> R.; Baker, <sup>(2)</sup> N.R*

*(1) 101 Walton Heath, 20 Jacobs Lane, Fairways 2196, South Africa; (2) 3 Upper Camden Place, Bath, Avon BA1 5HX, United Kingdom.*

A new field of diamondiferous kimberlites, containing at least two types and ages of kimberlite (Nixon et al., 1989) has been discovered during this decade in Venezuela. They are located near the village of La Salvacion in the Guaniamo drainage basin. (See map). These highly prospective diamond source rocks have been intruded into the stable Archaean-Proterozoic Guyana Shield.



Alluvial diamonds were first discovered in Venezuela in 1887 on the Caroni River, the principal drainage of southeastern Venezuela. Diamonds have since been extracted from placers over a wide area of the Caroni drainage basin by diggers or "mineros". Mining has been on a small scale, using hydraulic jets, or small dredges, with jigs to recover the diamond. Gold is also commonly recovered.

In 1968 a rich alluvial diamond deposit was discovered in the Quebrada Grande, a tributary of the Guaniamo River in the western shield of Venezuela. Between 1969 and 1970 Venezuela's diamond production increased by 158%, reflecting the impact of the Guaniamo discoveries. From 1970 to 1974 this production had expanded to the extent that it was 1.62 times more than the total weight of diamonds produced in Venezuela from 1937 to 1970. (Baptista et al 1978).

While a proximal source rock for Guaniamo's diamonds has been suspected by several experts, no systematic exploration for kimberlite was undertaken until 1982.

Until recently, all diamonds in northern South America were thought to be multi-cycle, latterly derived from conglomerate bands within the Roraima Formation. For almost a century diamond placers have been worked at localities near the foot of Roraima escarpments and in rivers draining remnants of this formation.

The coincidence was convincing and carried with it the implication that the original primary source rocks could be so remote in time as to have been long eroded below root level, and so remote in space as actually to be in West Africa. The nearest outlier of Roraima to the Quebrada Grande occurs 70 kilometres to the south and lies beyond the Guaniamo drainage. While the Roraima Formation must once have covered much of the western shield, it could not realistically be invoked as a secondary source for such rich, discrete and individually distinct diamond diggings as occur in the restricted area of the Quebrada Grande.

Following a 1982 study of Guaniamo diamonds it was apparent that local variations in diamond characteristics from virtually adjacent diggings could only be explained by there being a number of local source rocks to which different diggings were related. Kimberlite exploration was therefore justified and a six month programme of close-interval stream sediment sampling was started in June 1982. The programme included air photo interpretation supported by RADAM maps, and the construction of a 1:50 000 drainage map of the Quebrada Grande area. A laboratory in San Antonio, Texas, was contracted to treat the Guaniamo samples.

Sample size averaged 80kg of -2mm fraction; these were taken from the best stream trap sites available. Initial laboratory concentrates in the +400 micron size range gave no kimberlite indicator minerals and it was not until the -200 micron size fraction was examined that kimberlitic pyropes were recognised. Sample BBV17, taken from the upper Candado drainage - a richly diamondiferous tributary of the Quebrada Grande - yielded 10 micro-diamonds, 9 kimberlitic garnets and 1 chromite grain. A follow-up sample, JD10, composed of 18kg of highly weathered bedrock clay, yielded 2000 kimberlitic garnets and 4 micro-diamonds. This clay proved to be the first primary source rock discovered in Venezuela (August 1982).

Guaniamo kimberlites are extremely weathered so that olivine and pyroxenes are not liberated to the regolith. Ilmenite appears to be absent and the chrome spinels are indistinguishable from background species. The most distinctive and common indicator mineral is the high chrome, low calcium variety of pyrope, or G10 variety of Dawson and Stephens (1975). These are highly fractured and reduced to almost colourless -100 micron shards. Analysis of stream gravel samples is thus a painstaking process.

Since 1987 local diggers have learned to recognise weathered kimberlite and its economic significance. Mining has now exposed 15 kimberlite occurrences that extend over a distance of 12km by 5km. The original discovery is pipe-like in appearance, whereas the other exposures consist of horizontal to inclined sheets (up to 15°) that are commonly 2 metres thick. The inclined sheets are controlled by the dominant NNW structural trend of the area. Attitude and regional distribution support the view that the original kimberlite dykes have been subjected to post-emplacement folding and/or block-faulting.

Two varieties of diamond bearing mantle rock have been recognised. The older rock has returned a Sr whole rock age of 1.9 Ga  $\pm$  0.05 Ga, whereas Nd dating indicates 2.0 Ga  $\pm$  0.05 Ga. Argon dating of the younger rock gives an age of 850 Ma. Both varieties have been severely weathered so that precise bulk chemistry is difficult to determine. However, P.H.Nixon (paper in preparation) is inclined to classify the older rock as a Group 1

kimberlite. The younger rock tends towards lamproite, with  $K_2O$  around 5%. Narrow veins of the lamproitic rock cut through a horizontal sheet of kimberlite in the 039 Area. This rock is composed mainly of phlogopite with diamond and rare pyrope.

The Guaniamo kimberlites pre-date the deposition of the Roraima Formation (1.75 - 1.65 Ga), and are intruded into pre-Roraima Archaean-style Basement. The area has been affected by the Cuchivero-Pacaraima thermal event (1.8 - 1.9 Ga). It is proposed therefore that the folding and faulting of the kimberlites is related to this event and that the Sr & Nd age determinations reflect metamorphic adjustment. Thermal metamorphism may also partly explain the unusual chemistry and mineralogy of the kimberlite. This proposal implies a greater age for the emplacement of the kimberlite than has been determined. The lamproite occurrence post-dates the Roraima Formation. This fact has important implications for diamond exploration elsewhere in Venezuela, in particular in those areas where this massive sedimentary cover is widespread and exceeds 3 km in thickness. Here, lamproites (as well as younger kimberlites) can be expected to be preserved as large bodies and not eroded to root zones as is the case in Area 039.

The discovery of diamond bearing mantle rocks in Guaniamo is a benchmark event for source rock exploration in Venezuela and the Guyana Shield as a whole. Past myths as to the origin of the placer diamonds have as a result been dispelled and the door is open to a new era of diamond exploration in this prospective region. In addition, recent statements issued by the Venezuelan Government suggest that foreign investment is to be encouraged, and exploration for minerals promoted. To maximise its revenue and at the same time limit environmental and ethnographic damage, the Government must convert areas which are at present haphazard diggings, into long term concessions granted to responsible and accountable mining companies.

#### REFERENCES

- Baptista, J. & Svisero, D.P. (1978) Geologia de los depositos diamantiferos de la parte noroccidental de la Guayana Venezolana. Direccion General Sectorial de Minas y Geologia. 23 No 24.
- Dawson, J.B. & Stephens, W.E. (1975) Statistical classification of garnets from kimberlitic and associated xenoliths. *Journal of Geology*, 83, 589-607.
- Nixon, P.H., Davies, G.R., Condliffe, E., Baker, N.R., & Baxter-Brown, R. (1989) Discovery of ancient source rocks of Venezuela diamonds, 28th Geological Congress. Extended Abstracts. Workshop on diamonds, Washington DC.

MESOZOIC KIMBERLITES AND RELATED ALKALIC ROCKS IN SOUTH-WESTERN SÃO FRANCISCO CRATON, BRAZIL: A CASE FOR LOCAL MANTLE RESERVOIRS AND THEIR INTERACTION.

Bizzi,<sup>(1,2)</sup> L.A.; Smith,<sup>(3)</sup> C.B.; Meyer,<sup>(4)</sup> H.O.A.; Armstrong,<sup>(5)</sup> R. and De Wit,<sup>(1)</sup> M.J.

(1) *Geology Department, University of Cape Town. Cape Town, Rondebosch 7700. RSA;* (2) *Sopemi Pesq. Exploração de Minérios. SLA Trecho 2, 1591. Brasília, DF. Brazil;* (3) *Bernard Price Institute of Geophysical Research, University of the Witwatersrand. Johannesburg, Wits 2050. RSA;* (4) *Dept. of Earth and Atmos. Sciences, Purdue University. IN47907. USA;* (5) *Geochemistry Department, University of Cape Town. Cape Town, Rondebosch 7700. RSA.*

Proterozoic rocks which flank the late Archean Sao Francisco craton, and which were last deformed during the 800-450 my Brazilliano event, are intruded by upper Cretaceous kimberlites, olivine melilitites, tuffaceous diatremes and carbonatite complexes. The most important focii of alkalic magmatic activity occur in an area of late Jurassic to early Cretaceous continental extension (the Alto Paranaiba uplift) over a period of about 40 Ma concomitant with the deposition of the Cretaceous Mata da Corda Formation (Fig.1).

The studied kimberlites are hypabyssal calcite-monticellite types, with uniformly distributed groundmass minerals. Their mineralogy comprises macrocrysts and phenocrysts of olivine, phlogopite and scattered ilmenite set in a groundmass of serpentinized monticellite, phlogopite, opaque minerals, perovskite, serpentine and calcite. Mica Rb-Sr emplacement ages of 95 Ma were obtained for kimberlitic rocks from the Tres Ranchos and Indaia/Perdizes river localities.

Sediment and breccia-filled maars or diatremes of alkalic affinity contain sporadic olivine macrocrysts and abundant phenocrysts set in a groundmass of serpentinized monticellite, phlogopite, clinopyroxene, pseudo-leucite, opaque spinel and perovskite. Some of the occurrences contain rare sodium-rich or potassium-rich glass phases which are assumed to be representative of more evolved melt components which crystallized under supercooled conditions. Mica Rb-Sr emplacement ages ranging from 85 to 109 Ma were obtained from alkaline rock samples from Carmo do Paranaiba, Presidente Olegario and the Pantano peridotite.

In the carbonatite complexes of Catalao, metasomatized magnetite and mica-peridotites and pyroxenites of an early stage are associated with five other late-stage magmatic carbonatites and late hydrothermal activity represented by foscrite, sovite, cryptocrystalline berforsite, glimmerite and lamprophyre. Enrichment of incompatible elements observed in the carbonatitic rocks is represented to some extent in the studied kimberlites within 20 km distance of the carbonatite complexes. A Rb-Sr emplacement age of 119 Ma was obtained on micas from the late-stage phases, which contrasts with the 83 Ma K/Ar age obtained previously (Hassui and Cordani, 1968).

One locality of basalt breccia and composite lava flows near Patos de Minas was also studied. Angular to rounded xenoliths, mineralogically similar to matrix material, with clinopyroxene, opaque minerals, perovskite, altered olivine, ghost relicts of feldspar and rare leucite, phlogopite and apatite are set in a groundmass of secondary clay, chlorite and serpentine. A mica Rb-Sr emplacement age of 118 Ma was obtained.

Xenoliths of spinel lherzolite, harzburgite and dunite, with evidence of spinel and phlogopite metasomatism, are common in some kimberlites from the

Coromandel area. In the Presidente Olegario and Patos de Minas areas cognate nodules with cumulus perovskite and olivine are fairly common, suggesting sampling of temperature-zoned reservoirs within the lithosphere.

Geothermobarometric calculations and the lack of high-pressure xenolith populations (i.e. garnet peridotites and diamonds) in these rocks compared to other kimberlites elsewhere in the world, point to a shallow lithospheric source for the xenoliths and possibly the alkalic rocks.

Figure 2 shows that the studied rocks have a relatively restricted range of Sr-Nd isotopic compositions approximated as a single component with average present-day  $^{143}\text{Nd}/^{144}\text{Nd} = 0.51228$  and  $^{87}\text{Sr}/^{86}\text{Sr} = 0.7058$ . Nd model ages (CHUR) average 478 Ma. Present-day Pb signatures range as follows:  $^{206}\text{Pb}/^{204}\text{Pb} = 17.066$  to  $20.957$ ;  $^{207}\text{Pb}/^{204}\text{Pb} = 15.309$  to  $15.679$  and  $^{208}\text{Pb}/^{204}\text{Pb} = 30.157$  to  $40.149$ . These are the first documented examples of kimberlites and related rocks with such isotopic compositions falling between those of Group I and II South African kimberlites (Smith, 1983). The source character of these Brazilian kimberlites is thus dissimilar to kimberlites in general worldwide, whereas their petrography and mineralogy are similar to South African Group I kimberlites.

The studied alkalic rocks have Sr and Nd isotopic signatures like those of the kimberlites although their Pb/Pb signatures show slight differences. A common source character can, therefore, be postulated for the kimberlites, para-kimberlites, carbonatites and alkali basalts. Increasing alkalinity and exceptionally high incompatible element concentrations (eg La, Ce, Th, Nb and Nd) in some of the kimberlites may be inherited from heterogeneously enriched portions of the lithosphere. In the more evolved rocks interelement ratios of incompatible elements suggest that differentiation processes were dominated by assimilation and fractional crystallization (AFC) rather than different degrees of partial melting.

Heterogeneities in the U/Pb and Pb/Pb isotopic ratios correlate with different enrichment styles, suggesting involvement of different magma reservoirs within the same source region and/or successive interactions of different source regions at different times. Negative correlation between U/Pb and K/Nb suggests that U/Pb fractionation was strongly influenced by a potassic phase, probably phlogopite. It is therefore likely that the trace element enrichment events, in which phlogopite had a key role, have taken place at relatively shallow depths (<250 km) in the upper-mantle.

Derivation of the different rock types by crustal contamination alone seems unlikely, given the clustering of Sr-Nd isotopic signatures, low Rb/Sr, low Ba/La and the relatively high Ti/K<sub>2</sub>O contents. However, a case can possibly be made for some recycling of metasomatized lithosphere in view of the higher Ba/Nb, Ba/La and Sr/Nd ratios observed in samples from Presidente Olegario and Carmo do Paranaíba. The relatively higher assimilation of continental crust and the nature of the nodules in these occurrences could possibly be pointing to a major discontinuity (the Western limits of the Sao Francisco craton) in the sub-continental lithospheric mantle in this area as delineated at the surface by the rocks of the Mata da Corda Formation preserved within a NE-SW system of grabens (Fig.1).

Isotopic and chemical similarities of the studied volcanics with those of the high-Ti Continental Flood Basalts of the Northern Parana Basin (within approximately 200 km of the study area) and with those of the Oceanic Basalts at the Walvis Ridge in the South Atlantic, suggest that their sources are closely related and were all affected by the "Dupal type" mantle enrichment. The relative input of mantle plumes, asthenospheric and lithospheric sources in the generation of the Minas Gerais rocks is under investigation. At this stage of the study, the preferred petrogenic model for the studied rocks assumes their derivation by partial melting

of upper-mantle similar to an enriched (E-type) source which had become heterogeneous on a small scale due to introduction of small volume melts and metasomatic fluids.

**References:**

Hassui and Cordani (1968). Cong. Bras. Geol. XXII-B. Horizonte.  
 Smith, C.B. (1983). Nature 304, 51-54.

Fig.1 - Location map (after Thompkins and Gonzaga, 1989)

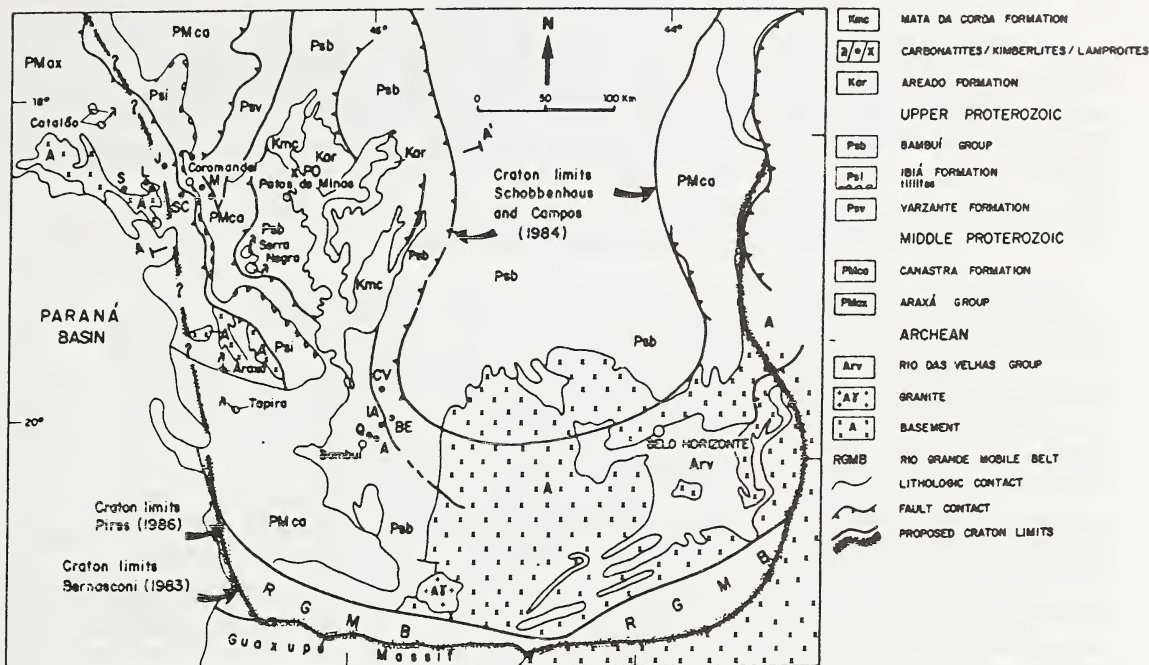
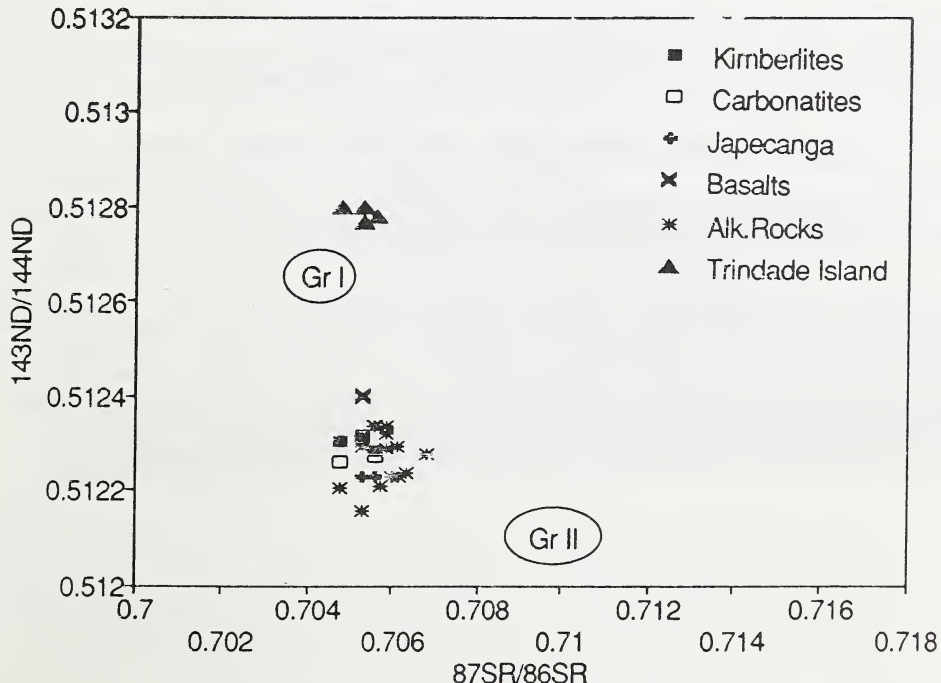


Fig.2 - Present-day isotopic signatures (Group I and II kimberlites after C. Smith, 1983).



## OXYGEN IN DIAMOND BY THE NUCLEAR MICROPROBE: ANALYTICAL TECHNIQUE AND INITIAL RESULTS.

(1) J.D. Blacic; (2) E.A. Mathez; (3) C. Maggiore; (3) T.E. Mitchell and (2) R. Fogel.

(1) Geophysics Group, Earth and Space Sciences Division, Los Alamos National Laboratory, Los Alamos NM 87545 USA; (2) Department of Mineral Sciences, American Museum of Natural History, New York, NY 10024, USA; (3) Center for Materials Sciences, Los Alamos National Laboratory, Los Alamos, NM 87545 USA.

Investigations of diamonds indicate that oxygen, along with light volatile elements, is a major impurity in diamond (Sellschop, 1979), suggesting that the oxygen content of diamond may be used to qualitatively characterize the oxidation state of its source region. This is of interest because some diamonds contain reduced mineral inclusions such as moissanite (SiC) and iron metal (e.g., Moore and Gurney, 1989; Meyer and McCallum, 1986), implying that some parts of the upper mantle are reduced and that its oxidation state is variable.

The analysis of oxygen in diamond has been accomplished by an *in situ* microactivation technique. Diamonds were bombarded with a 4.5 MeV beam of  $^3\text{He}$  ions. The beam was focused to a spot 200-300  $\mu\text{m}$  across with a superconducting solenoid, which provided for relatively high beam currents and short activation times (1.5-2 hrs.). The analytical depth extends to  $\approx 8 \mu\text{m}$ . The incident ions interact with carbon and oxygen in the diamonds according to the reactions  $^{12}\text{C}(^3\text{He},\alpha)^{11}\text{C}$  and  $^{16}\text{O}(^3\text{He},p)^{18}\text{F}$ . Both reaction products are radioactive and decay by positron emission. However, because the half lives of  $^{11}\text{C}$  and  $^{18}\text{F}$  are 20.9 and 109.7 minutes, respectively, their decay activities, which are determined by coincidence counting with NaI detectors, are easily distinguished on a plot of decay activity vs. time (Fig. 1). The theoretical detection limit of the technique is  $<10$  ppm atomic oxygen, but in practice it is limited by the amount of oxygen adsorbed on the diamond surface. The precision, which is limited by precision in measurement of the  $^3\text{He}$  beam current, is  $\approx 15\%$  relative.

Two problems are associated with the analytical surface. The first involves adsorbed atmospheric oxygen and arises because there is no facility in the sample chamber to remove (e.g., by sputtering) the adsorbed layer. The amount of oxygen adsorbed on nominally clean, polished diamond surfaces exposed to atmosphere was determined by Rutherford backscattering spectrometry (RBS). Surface oxygen concentrations are typically  $\approx 1 \times 10^{15}$  at/cm<sup>2</sup> (detection limit  $\approx 0.4 \times 10^{15}$  at/cm<sup>2</sup>), in agreement with previous estimates (Sellschop, 1979). This amount, representing  $\approx 15$  ppm in the bulk analysis, is equivalent to a continuous monolayer of surface oxygen and, since diamond surfaces are not known to oxidize, is taken to be the maximum amount that can be adsorbed. A more serious problem is due to the build-up of an oxygen-rich contaminant on the analytical surface during activation. Elimination of this contamination, which is apparently due to a sealant in the sample chamber, was necessary because it adds significant oxygen to the analysis. The  $^{18}\text{F}$  nuclei produced by reaction (2) possess an energy of 2.2 MeV; thus most  $^{18}\text{F}$  generated in the contaminant is implanted in the diamond and cannot be removed.

The problem was circumvented by coating nominally clean diamonds before activation with a 2  $\mu\text{m}$  thick layer of gold, which serves to trap the  $^{18}\text{F}$  from the contaminant. The configuration is illustrated in Fig. 2. After activation and before counting, the gold coat and trapped contaminants were removed by polishing. After the diamonds were counted, their surfaces were reexamined by RBS to confirm that all gold had been removed.

We examined nine type IIA (verified by IR) and five type I diamonds. The former are doubly polished 1 mm plates purchased commercially. Oxygen contents were found to range from 16 to 102 ppm at. (ave. = 67 ppm). The type I diamonds are fragments each with a single polished face. Their oxygen contents range from 49 to 116 ppm (ave. = 81 ppm). The ranges are similar to those reported by Bibby and Sellschop (1974) determined by fast neutron activation.

There are several potential sources of oxygen. One possibility is that oxygen exists in the gold coats and the analyses are artifacts. However, there is no indication that the gold layers contain oxygen, and the variability in the analyses cannot obviously be accounted for by this possibility. Experiments are presently underway to confirm this. A second possibility is that oxygen is contained in inclusions. Although the regions analyzed in all samples are free of inclusions or other defects visible by optical microscopy, submicroscopic inclusions are possible. To test this, two type IIA diamonds were examined by TEM and were found to be inclusion free. Type IIA diamonds are known to possess relatively high concentrations of dislocations, so a third possibility is that oxygen exists in such structures. The average dislocation density, which was determined by counting the number of intersections with the diamond surface, was found to be  $\approx 2 \times 10^{13}/\text{m}^2$ . Only  $\approx 1$  ppm oxygen can be accommodated in dislocations assuming that their cores are undissociated and saturated with an oxygen atom at every atomic position along the dislocation. If the dislocation cores are dissociation in saturated stacking faults 40  $\text{\AA}$  wide, concentrations as high as 10 ppm are possible. However, higher concentrations must be in solution.

#### References Cited

- Bibby, D.M., and Sellschop, J.P.F. (1974) The determination of oxygen and silicon in diamond by 14 MeV neutron activation analysis. *J. Radioanalytical Chemistry*, 22, 103-111.
- Meyer, H.O.A., and McCallum, M.E. (1986) Mineral inclusions in diamonds from the Sloan kimberlites. *J. Geology*, 94, 600-612.
- Moore, R.O., and Gurney, J.J. (1989) Mineral inclusions in diamond from the Monastery kimberlite, South Africa. In *Geological Society of Australia Sp. Publ.*, 12, 1029-1041.
- Sellschop, J.P.F. (1979) Nuclear probes in physical and geochemical studies of natural diamonds. In J.E. Field, Ed., *Properties of diamonds*, p. 107-163, Academic Press, London.
- Sellschop, J.P.F., Mandiba, C.C.P., and Annegarn, H.J. (1980) Light volatiles in diamond: Physical interpretation and genetic significance. *Nuclear Instr. Methods*, 168, 529-534.

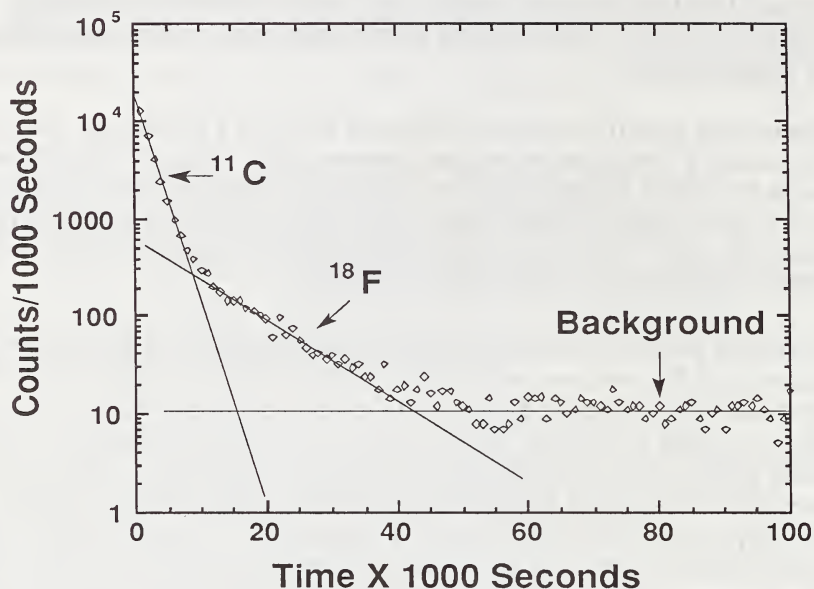


Fig. 1. Decay activity of diamonds activated by  $^3\text{He}$ . The activity is composed of three components representing decay of  $^{11}\text{C}$  ( $t_{1/2} = 20.9$  min.),  $^{18}\text{F}$  ( $t_{1/2} = 109.7$  min.) and a background, which is constant with time.

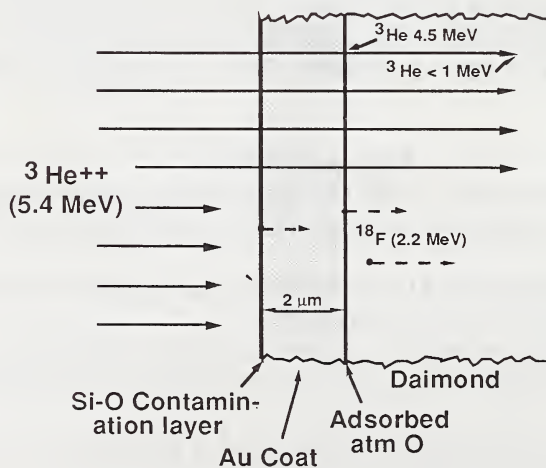


Fig. 2. Configuration of a gold coated diamond being activated by  $^3\text{He}$ .  $^{18}\text{F}$  is generated from a layer of contamination on the gold, from the diamond surface (which had been exposed previously to the atmosphere), and from within the diamond itself.

## FICTIVE CONDUCTIVE GEOTHERMS BENEATH THE KAAPVAAL CRATON.

Brey, G.

Max-Planck-Institut für Chemie, D-6500 Mainz, F.R.G.

Garnet peridotite xenoliths from kimberlites, lamproites, minette and rarely alkali basalts are the major source of information on the chemistry and physical state of the continental lithosphere and possibly the underlying asthenosphere. Pressures and temperatures of crystallisation may be calculated for these xenoliths with various geothermobarometers. These pressures and temperatures are usually aligned along conductive continental geotherms as calculated from heat flow measurements at the Earth's surface. While the major issue of debate was and is the existence or non-existence of an inflected geotherm (Boyd, 1973; Nickel and Green, 1985; Bertrand et al., 1986; Carswell and Gibb, 1987), opinions also existed which simply questioned the reality and validity of calculated conductive geotherms beneath the Kaapvaal craton (Fraser and Lawless, 1978; Harte and FreÛr, 1982).

Based on experiments in natural and simple systems from 2-60 kb and 900-1400 °C Brey and Köhler (1990) calibrated new versions of the two-pyroxene thermometer ( $T_{BKN}$ ) and the Al-in-opx barometer ( $P_{BKN}$ ). Tests of published geothermobarometers with their experiments in natural systems indicate that the Fe-Mg exchange thermometers of O'Neill and Wood (1979; grt-ol;  $T_{O'NEILL}$ ) and of Krogh (1988; grt-cpx;  $T_{KROGH}$ ) and a Ca-in-olivine barometer (Köhler and Brey, 1990;  $P_{KB}$ ) can be used to reliably calculate pressures and temperatures of crystallisation. All these geothermobarometers should yield identical results (within their mutual errors) if the samples were in internal mineral equilibrium.

P,T-conditions calculated with the potentially most accurate combination of the two-pyroxene thermometer with the Al-in-opx barometer are aligned along a conductive geotherm of about 44 mW/m<sup>2</sup> for mostly granular (low-T) nodules from the Kaapvaal craton (examples are shown in Fig. 1 for Bultfontein, Thaba Putsoa and Matsoku) while sheared (high-T) nodules form arrays at higher temperatures and subparallel to conductive geotherms. No kink (inflection) appears in our calculated geotherms (Fig. 1).

**Tests for internal mineral equilibrium:**

In general, all thermometers and barometers yield consistent results when applied to the *high-T* suite of nodules indicating internal mineral equilibrium.

In contrast, temperatures calculated with  $T_{O'NEILL}$  are systematically underestimated compared to results from the two-pyroxene thermometer with increasing  $T_{BKN}$ ;  $T_{KROGH}$  gives similar results and  $P_{KB}$  systematically overestimates pressures compared to  $P_{BKN}$  for granular (low-T) nodules indicating disequilibrium between the various minerals. These inconsistencies may be the result of different blocking

temperatures of elements in the different minerals. In the absence of apparent zoning this should be reflected as inconsistencies in mineral chemistry as demonstrated in Figs. 2-4.

Fig. 2 is a diagram of Ca<sup>opx</sup> vs Ca<sup>cpx</sup>. Ca in the two pyroxenes should show a negative correlation if the samples under consideration are derived from a range of temperatures. This is the case for the suite of high-T nodules. Orthopyroxenes from low-T nodules have constant Ca at individual localities, but differ between localities indicating a low and constant temperature, whereas Ca in cpx varies widely indicating variable temperatures. The two minerals cannot be in equilibrium at least with respect to Ca and in the higher temperature range. Ca in olivine is similarly constant as Ca in opx and Ca in cpx is also not in equilibrium with Ca in olivine.

Al in opx varies concomitantly with Ca in cpx (compare Figs. 2 and 3); it may be argued that these two elements reflect peak metamorphic conditions of the samples, whereas Ca in opx and Ca in olivine had adjusted to lower temperatures. It must then be shown, however, that garnet was in equilibrium with opx and cpx at the peak metamorphic conditions. It can be demonstrated, however, from Ca-Cr relationships of garnets (Fig. 4), that garnet was never in equilibrium with clinopyroxene except if the nodules experienced very high temperatures at one stage of their history (higher than calculated here from the two-pyroxene thermometer), and that the garnet compositions were frozen in at these conditions. Much lower temperatures calculated with <sup>T</sup>O'Neill argue against this possibility. I must therefore concur with the conclusions of Fraser and Lawless (1978) and of Harte and Freer (1982) that it is not possible to deduce pressures and temperatures of crystallisation for the low-T nodule suite from the Kaapvaal craton and that we do not know the thermal state of its lithospheric mantle. If any estimates are to be made it can only be that the mantle is cooler than a conductive geotherm of 44 mW/m<sup>2</sup>.

The Kaapvaal craton nodule suite is unique in that nodules from other localities worldwide (and also from Namibia) generally appear to be in internal mineral equilibrium and realistic geothermal gradients may be determined from the nodule suites. This further demonstrates that the Kaapvaal craton is an inappropriate place to make general models of cratonic parts of the upper mantle.

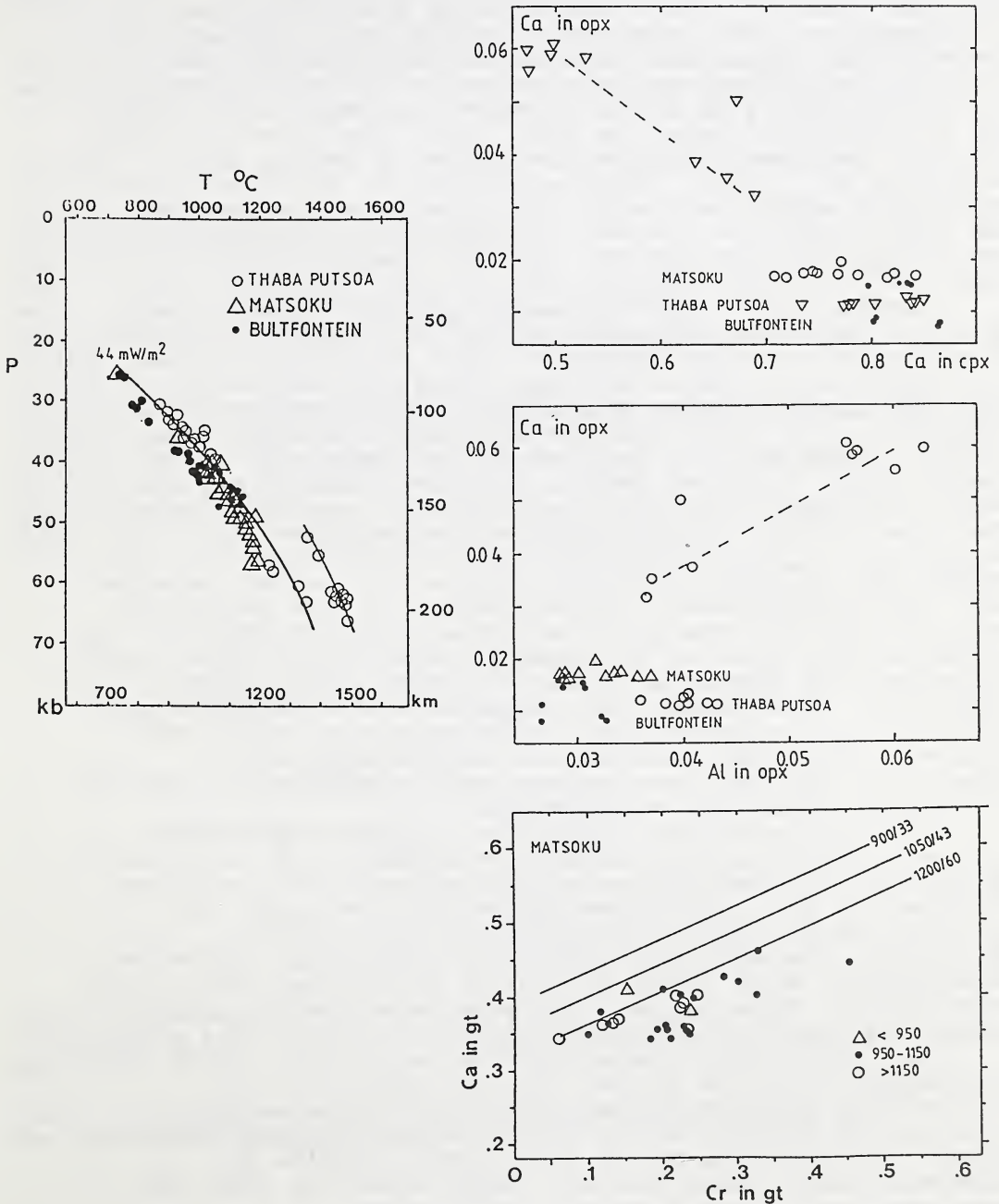
- Bertrand, P., Sotin, C., Mercier, J.-C.C. and Takahashi, E. (1986). *Contrib. Mineral. Petrol.*, 93, 168-178  
 Boyd, F.R. (1973). *Geochim. Cosmochim. Acta*, 37, 2533-2546  
 Brey, G. and Köhler, T. (1990). *J. Petrol.*, 31, 1353-1378  
 Carswell, D.A. and Gibb, F.G.F. (1987), 97, 473-487  
 Fraser, D. and Lawless, (1978)  
 Harte, B. and Freer, R. (1982). *Terra Cognita*, 2, 273-275  
 Hervig, R.L., Smith, J.B. and Dawson, J.B. (1986). *Trans. Royal Soc. Edinbg.: Earth Sci.*, 77, 181-201  
 Köhler, T. and Brey, G. (1990). *Geochim. Cosmochim. Acta*, 54, 2375-2388  
 Krogh, E.J. (1988). *Contrib. Mineral. Petrol.*, 99, 44-48  
 Nickel, K.G. and Green, D.H. (1985), *Earth Planet. Sci. Lett.*, 73, 158-170  
 O'Neill, H.St.C. and Wood, B.J. (1979). *Contrib. Mineral. Petrol.*, 70, 59-70

Fig. 1: Calculated P,T-conditions ( $T_{BKN} + P_{BKN}$ ) for garnet peridotites from Matsoku, Bultfontein and Thaba Putsoa (KAAPVAAL craton; mineral data from various sources).

Fig. 2: Ca in opx vs Ca in cpx for nodules suites from the Kaapvaal craton (only data from Hervig et al., 1986)

Fig. 3: Ca in opx vs Al in opx for nodules suites from the Kaapvaal craton (only data from Hervig et al., 1986)

Fig. 4: Ca-Cr relationships for garnets from peridotites from Matsoku. Isolines for constant P,T conditions are derived from experiments in natural systems. Garnet compositions should plot along these lines in case of equilibrium between garnet and clinopyroxene. They plot, however, at too low Ca contents.



THE JOIN PYROPE-KNORRINGITE: EXPERIMENTAL CONSTRAINTS FOR A NEW  
GEOTHERMOBAROMETER FOR COEXISTING GARNET AND SPINEL.

Brey, <sup>(1)</sup>G.; Doroshev, <sup>(2)</sup>A. and Kogarko, <sup>(3)</sup>L.

(1) *Max-Planck-Institut für Chemie, D-6500 Mainz, F.R.G.*; (2) *Inst. Geol. USSR Academy of Sciences, Novosibirsk*;  
(3) *Vernadsky Inst. USSR Academy of Sciences, Moscow.*

Pyropic garnets in lherzolites and harzburgites from diamond-bearing pipes contain significant amounts of chromium. Similar garnets also occur as disseminated grains in kimberlites. Such garnets are usually low in calcium and chromium must be present mostly as the  $Mg_3Cr_2Si_3O_{12}$  end member knorringite. Garnets found as inclusions in diamonds are particularly rich in this component, commonly with 30-40 mol % knorringite (Meyer and Boyd, 1969; Sobolev et al. 1969) and in a few cases with more than 60 mol-% (Meyer, 1975; Sobolev et al., 1973). Experimental work on the join pyrope-knorringite was already undertaken more than three decades ago (Coes, 1955) but, because of experimental problems, there remains serious disagreement about the pressure stability limit of knorringite (Fig. 1).

Ringwood (1977) synthesized pure knorringite and solid solutions between pyrope and knorringite at pressures between 60 and 80 kb and temperatures of 1400 - 1500 °C. Irifune et al. (1982) and Irifune and Hariya (1983) synthesized pure knorringite at pressures greater than 105 kb and described a stability limit with a positive dP/dT slope. Turkin et al. (1983) brought down the position of the knorringite stability field to 80 - 90 kb and found a negative dP/dT slope. The same group investigated the composition of coexisting garnet and spinel in the 4-mineral harzburgite paragenesis  $Gar_{ss} + Opx_{ss} + Sp_{ss} + Fo$  in the system MASCr from 30 to 70 kb and showed that (i) the knorringite component in garnet increases with increasing pressure and temperature in this paragenesis (negative dP/dT slopes of Cr-isopleths) and (ii) the microchromite component in spinel increases with pressure and decreases with temperature (positive dP/dT slopes of Cr-isopleths). Thus pressure and temperature of crystallisation can be defined uniquely from coexisting garnet and spinel. Moreover, estimated pressures and temperatures are potentially very accurate because the Cr-isopleths for garnet and spinel cut at very steep angles.

These prospects for application to geothermobarometry led us to try to clarify the present situation by reversibly determining the compositions of coexisting phases in piston cylinder and belt apparatuses in the pressure range from 27 to 60 kb and at temperatures from 1200 to 1500 °C. Equilibrium composition of coexisting phases were determined reversibly by using mixes of minerals with either high or low Cr/Al ratios. Phase compositions were determined from X-ray properties and by electron microprobe.

In a first step we determined the solubility limits of knorringite in pyrope garnets and the composition of coexisting orthopyroxene and corundum-escolaitite solid solution and derived thermodynamic mixing parameters for all phases. Extrapolation of our experimental results is consistent with Turkin's et al. (1983) stability limit for pure knorringite with a negative dP/dT slope.

We also determined the composition of coexisting phases for the 4-phase harzburgitic assembly. Compositions determined for coexisting garnet<sub>ss</sub> and spinel<sub>ss</sub> are presented in Fig. 2 as a function of pressure and temperature. Based on Fig. 2 we have derived Cr/(Cr+Al) isopleths and plotted them in a pressure-temperature-diagram (Fig. 3). There is qualitative agreement with the results of Malinovsky et al. (1975), although position and slopes of Cr-isopleths differ. Straightforward application of the isopleths presented in Fig. 3 to garnet inclusions in diamonds yields a narrow range of pressures of origin for most of these diamonds between 52 and 60 kb. This assumes that these garnets were in equilibrium with spinel; the estimated pressures are minimum values if this was not the case.

The presence of Fe and Ca will influence the Cr contents of the phases and appropriate corrections are needed for a more precise application to natural rock samples. Experiments to determine this influence of Fe and Ca are in progress.

Irifune, T. and Hariya, Y. (1983). *Mineralogical Journal*, 11, 269-281

Irifune, T., Ohtani, E. and Kumazawa, M. (1982). *Phys. Earth Planet. Interiors*, 27, 263-272

Malinovsky, I.Y., Doroshev, A.M. and Ran, E.N. (1975). *Bull. Inst. Geol. Geophysics, Novosibirsk*, 110-115

Meyer, H.O.A. (1975). *Geochim. Cosmochim. Acta*, 39, 929-936

Meyer, H.O.A. and Boyd, F.R. (1969). *Carnegie Inst. Wash. Yearbk.*, 68, 315-324

Ringwood, A.E. (1977). *Earth Planet. Sci. Lett.*, 36, 443-448

Sobolev, N.V., Lavrent'ev, Y., Pospelova, L. and Sobolev, E. (1969). *Dokl. Acad. Sci. USSR*, 189, p. 162

Sobolev, N.V., Lavrent'ev, Y., Pokhilenko, N.P. and Usova, L. (1973). *Contrib. Mineral. Petrol.*, 40, 39-

Turkin, A.I., Doroshev, A.M. and Malinovsky, I.Y. (1983). *Bull. Inst. Geol. Geophysics, Novosibirsk*, 5-24

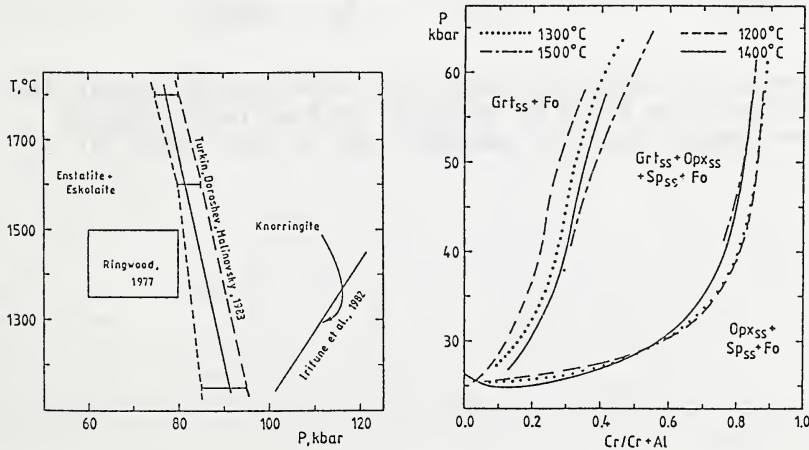


Fig. 1: Pressure stability limits for synthesis of knorringite from enstatite and Eskolaite after various authors

Fig. 2.: Compositions of coexisting garnet and spinel as derived from our experiments

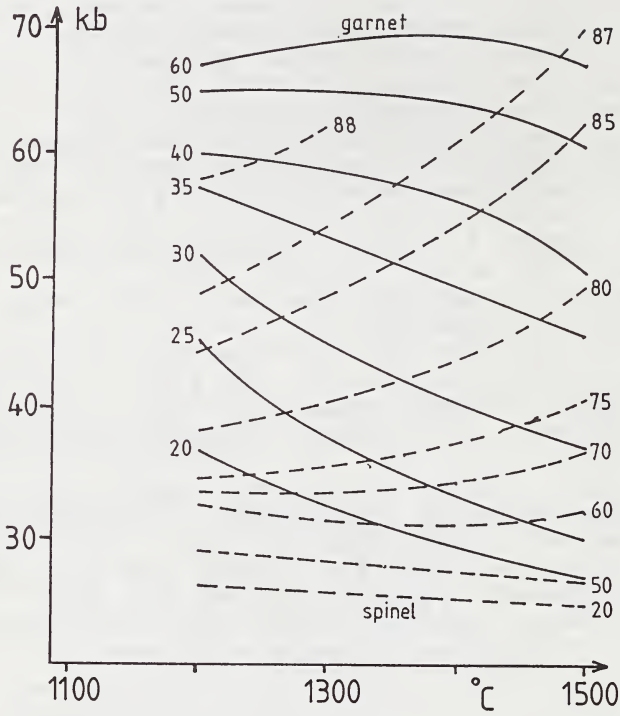


Fig. 3: Isopleths of  $100 \times \text{Cr}/(\text{Cr} + \text{Al})$  for coexisting garnet and spinel as derived from Fig. 2. Numbers on the left side of the lines give composition of garnets and on the right of spinels.

## ORIGIN OF LOW-CA, HIGH-CR GARNETS BY RECRYSTALLIZATION OF LOW-PRESSURE HARZBURGITES.

*Bulatov, <sup>(1)</sup> V.; Brey, <sup>(2)</sup> G.P. and Foley, <sup>(3)</sup> S.F.*

*(1) Institute of Lithosphere, Moscow, USSR.; (2) Max-Planck-Institut für Chemie, Saarstrasse 23, 6500 Mainz, Germany; (3) Mineralogisch-Petrologisches Institut, Universität Göttingen, Goldschmidtstrasse 1, 3400 Göttingen, Germany.*

Garnets with exceptionally low CaO (0.5-4 wt%) and high Cr<sub>2</sub>O<sub>3</sub> (1-13 wt%) contents are commonly found as inclusions in diamonds as part of the peridotitic inclusion suite, but up to date there is no clear consensus as to their origin. Any hypothesis for their origin must account for both the low CaO and the high Cr<sub>2</sub>O<sub>3</sub> contents, in a process which operated in, but may not have been restricted to, the earliest tectonic regimes applicable to the Earth's mantle.

Explanations of their formation have been principally of three types, of which the first two appeal to formation of the garnet in equilibrium with a melt phase, whereas the third explains the garnets as metamorphic products from garnet-free rocks:

(i) The garnets are part of a restitic garnet peridotite suite formed by the loss of a considerable "basaltic" melt fraction, probably komatiitic; the exceptionally low Ca contents are thus a measure of the extreme depletion of the restite.

(ii) The low Ca-garnets crystallized from a melt which was itself derived as a "second-stage" melt from an extremely depleted peridotite type such as harzburgite. Such a melt would be enriched in MgO and poor in Ca, Al and Na amongst the major elements.

(iii) The garnets are metamorphic products formed from re-equilibration of subducted oceanic crustal material, either serpentinite or harzburgite.

Here we summarize experimental results of three types which have bearing on the above hypotheses: (i) Partial melting experiments on an anhydrous pyrolite composition with analyses of restitic garnets, (ii) sandwich experiments on the equilibrium between basaltic melt and spinel peridotite, which catalogue the composition of spinels in equilibrium with basaltic melt over a range of pressure and temperature, and (iii) near-solidus experiments on an olivine lamproite composition, which documents the composition of garnets crystallized in a very CaO-poor melt at high pressures. These studies lead us to the conclusion that low-CaO, high-Cr<sub>2</sub>O<sub>3</sub> garnets most probably originate by metamorphic re-equilibration of Cr-spinel harzburgite, and that the Cr-spinel originally formed at pressures below 10 Kbar.

### I. MORB-Pyrolite melting experiments

Experiments on dry melting were carried out at 50 and 60 kb on MORB-Pyrolite (Green et al., 1986) and experiments below the solidus on a similar primitive mantle composition (Brey et al., 1990). The Cr contents of garnets produced in these experiments are low and constant (even 200 °C above the

solidus) over a range of temperatures from 900 - 1800 °C, whereas CaO decreases from 6 wt% to 3.5 wt% (Fig. 1). The experimentally produced garnets do not overlap in composition with natural Cr-rich subcalcic garnets. These garnets therefore do not originate from residues of partial melting at high pressures.

## II. Spinel-peridotite/basalt sandwich experiments

Sandwich-type experiments on partial melting of a primitive mantle composition were carried out from 5 to 20 kb. Mineral separates from a primitive spinel lherzolite were recombined such that the centre of the sandwich consisted of spinel and clinopyroxene (the low-melting components) surrounded by olivine, orthopyroxene and spinel and clinopyroxene less the amount placed in the centre. The bulk corresponded to the original composition. Large melt pools are created at temperatures above the solidus and melt composition and restite mineral phases can be measured very easily with the electron microprobe. Restite spinels become enriched in Cr with increasing temperature and depleted in Al (Fig. 2). Spinels with the highest Cr/Al ratios are produced at lowest pressures and highest temperatures. Such Cr-rich spinel harzburgites will transform at high pressures to garnet harzburgites with garnets having low Ca and high Cr. Subduction or another type of removal to high pressure may be the process to bring the spinel harzburgites to great depth.

## III. Olivine lamproite melting experiments

Experiments on lamproites may serve to model a very depleted mantle source in terms of major elements. No garnet is found near the liquidus up to pressures of 55 kb (Foley, 1989 and unpublished results), but experiments close to the solidus yield ol, phlog, opx and garnet. These garnets are always rich in CaO (5.8 - 7.4 wt%) and poor in Cr<sub>2</sub>O<sub>3</sub> (< 1%) and are not counterparts of the Cr-rich subcalcic garnets found in kimberlites.

From the presentation of experimental data above it appears that the only reasonable process to generate Cr-rich subcalcic garnets is that of metamorphic recrystallization of a Cr-spinel harzburgite. We envision harzburgite because the Ca-poor nature of the garnets does not allow cpx to be present and we favour Cr-spinel because the high Cr in garnet must come from there. Cr-spinel harzburgites are the residues of high degrees of partial melting at low pressures of plagioclase or spinel peridotite. These protoliths were subsequently transferred to high pressures.

Brey, G.P., Köhler, T. and Nickel, K.G. (1990), *J. Petrol.* 31, 1313-1352

Foley, S.F. (1989), In: Jaques, A.L., Ferguson, J. and Green, D.H., "Kimberlites and Related Rocks." Blackwells, Melbourne, 616-631

Green, D.H., Falloon, T.J., Brey, G.P. and Nickel, K.G. (1986), Fourth International Kimberlite Conference. Extended Abstracts, 181-183

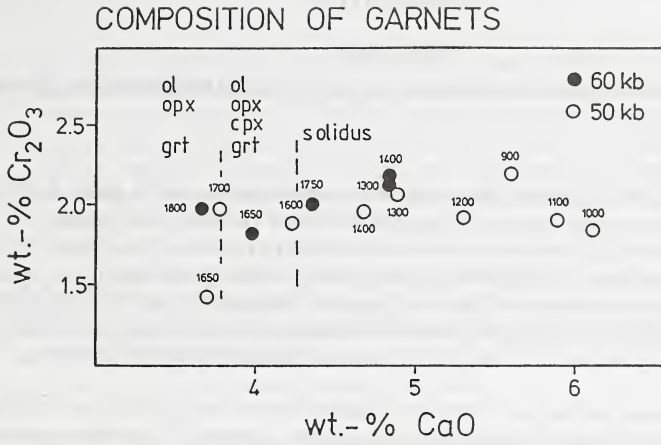


Fig. 1: Ca-Cr relationship of experimentally produced garnets in a pyrolite composition. Small numbers are temperatures in °C.

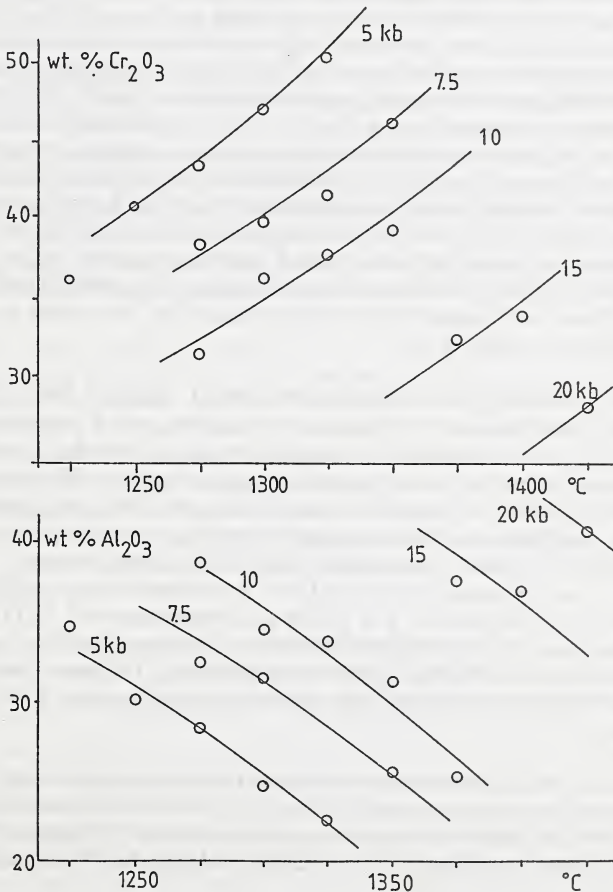


Fig. 2: Composition of spinel from partial melting experiments on a natural primitive upper mantle composition

## EXPERIMENTAL EVIDENCE FOR THE EXOLUTION ORIGIN OF CRATONIC PERIDOTITE.

*Canil, Dante.*

*Bayerisches Geoinstitut, Universität Bayreuth, Postfach 10 12 51, D-8580 Bayreuth, Germany.*

Geochemical analyses of several large peridotite xenoliths hosted in south African kimberlites indicate a clear compositional distinction between 'oceanic' and 'cratonic' lithosphere (1,2). The petrologic processes which contributed to the compositional spectrum of relatively young 'oceanic' type lithosphere are fairly well understood, but those which have led to the compositional spectrum of ancient 'cratonic' lithosphere are still the subject of debate (1,3-5). Understanding the origin of cratonic lithosphere is important for models on mantle evolution, cratonization, and the origin of diamond within mantle lithosphere.

Coarse-grained garnet peridotites hosted in kimberlites erupted within the Archean Kaapvaal craton of southern Africa comprise the bulk of the 'cratonic' lithosphere beneath this region (1). Recent detailed petrographical analysis of coarse grained peridotites from southern Africa have noted a statistically significant spatial association of garnet and clinopyroxene with orthopyroxene (6). These observations have led to the hypothesis that all garnet and clinopyroxene in these rocks may have at one time been dissolved in orthopyroxene at temperatures higher than those now recorded by the xenoliths (800 - 1200 °C). The probable compositions of these 'precursor' high temperature orthopyroxenes have been estimated by recombining the compositions of spatially associated orthopyroxene-clinopyroxene-garnet assemblages in the coarse grained peridotites studied. The resulting Ca, Al-rich high temperature orthopyroxenes are thought to have equilibrated with ultramafic melts at high pressures in the Archean mantle, but upon cooling to ambient temperatures, exsolved clinopyroxene and garnet to become the common low temperature coarse-grained garnet lherzolites recognized in many kimberlites emplaced within the Kaapvaal craton (6,7). This exsolution process was enhanced by deformation in the mantle (7) and it has been further proposed that many garnet lherzolites could have had a similar high temperature origin (6). Isotopic and bulk chemical considerations of garnet lherzolite samples from southern Africa are consistent with this proposal (1,8), but there are as yet no experimental constraints on its credibility.

Phase equilibrium experiments in the system CaO - MgO - Al<sub>2</sub>O<sub>3</sub> - SiO<sub>2</sub> - FeO - Cr<sub>2</sub>O<sub>3</sub> on typical 'oceanic' and 'cratonic' peridotite compositions, and a 'precursor' Ca, Al-rich high temperature orthopyroxene composition were undertaken to test the feasibility of a high temperature 'exsolution' origin for garnet peridotites, and to provide further constraints on models for the origin of 'cratonic' lithosphere beneath southern Africa and possibly other Archean cratons. Starting compositions were estimates of average 'oceanic' and 'cratonic' peridotite, as given in Boyd (1) and a hypothetical Ca,Al-rich high temperature orthopyroxene similar to those presented in Cox et al (6). Experiments were performed on all three starting materials from pressures of 5 to 8 GPa and temperatures of 1300 to 1600 °C using a multi-anvil apparatus at the Bayerisches Geoinstitut. Sectioned graphite heaters were used for all experiments to minimize thermal gradients to less than 20 °C/mm. Starting materials were contained in graphite capsules. Run durations varied between 1 and 11 hours depending on temperature.

Equilibrium in the experiments was assumed based on the convergence of orthopyroxene, garnet and clinopyroxene compositions in all runs at the same pressure and temperature on two different peridotite starting compositions; 'oceanic' peridotite with high Ca/Al, low Mg/Fe and 'cratonic' peridotite with low Ca/Al and high Mg/Fe. In addition,

reversals were performed at the lowest temperature (1300 °C) and therefore, 'worst case', of all experiments.

'Oceanic' peridotite crystallizes a garnet harzburgite assemblage at pressures and temperatures above 5 GPa and 1450°C, respectively, but at lower temperatures crystallizes clinopyroxene to become true lherzolite. 'Cratonic' peridotite crystallizes a garnet harzburgite assemblage at pressures above 5 GPa and temperatures below 1450 °C. Garnet-free harzburgite crystallizes from both 'cratonic' and 'oceanic' peridotite at temperatures above 1500 °C and pressures at or below 5 GPa. Phase relations for the Ca,Al-rich orthopyroxene mimic those of 'oceanic' peridotite.

Phase equilibria for all three starting compositions confirm predictions (6,7,9) that lherzolititic compositions actually become harzburgitic at high temperatures and/or pressures. At conditions of very high temperature and lower pressure near or above the peridotite solidus, both 'cratonic' and 'oceanic' peridotite would be biminerally harzburgites consisting of only olivine and Ca, Al-rich orthopyroxene.

The comparison of experimental orthopyroxene compositions from this and other experimental studies on ultramafic compositions, with orthopyroxenes from natural south African lherzolite and harzburgite nodules (2,6,10) and 'precursor' high temperature orthopyroxenes calculated from south African garnet lherzolites (6), provide some constraints on the probable conditions at which biminerally harzburgites could have formed during the Archean, and how such rocks cooled (and exsolved) to become lherzolites.

In the 'cratonic' peridotite and Ca,Al-rich orthopyroxene starting compositions, orthopyroxenes not in equilibrium with garnet and/or clinopyroxene are similar to the high-temperature 'precursor' orthopyroxenes from which garnet and clinopyroxene are thought to have exsolved in the common low-temperature, coarse-textured garnet lherzolites from south African kimberlites. Thus, 'precursor' orthopyroxenes in these latter xenoliths could have equilibrated at maximum pressures of 5 GPa near or slightly above the fertile mantle solidus (1500 - 1600°C). At pressures above or temperatures below such conditions, the Al- and Ca-solubilities of these orthopyroxenes are exceeded, forming garnet and shifting their compositions more towards those typical of natural garnet harzburgites and lherzolites.

None of the orthopyroxenes produced in experiments reported herein have the high Ca and Al contents of the proposed 'precursor' orthopyroxenes for high temperature, porphyroclastic garnet peridotites. Calculated 'precursor' orthopyroxenes for the latter samples are too Ca- and Al-rich to have equilibrated with either typical 'cratonic' or 'oceanic' lherzolite bulk compositions under any P-T condition investigated (> 5 GPa). Samples from which these high Ca, Al 'precursor' orthopyroxenes were constructed all have compositions characteristic of 'oceanic' lithosphere, whereas low temperature coarse-grained peridotites with calculated 'precursor' orthopyroxenes which match fairly well those observed in the experiments (discussed above), all have bulk compositions typical of 'cratonic' lithosphere.

In contrast, orthopyroxenes generated at lower pressure (< 3 GPa) above the peridotite solidus have compositions similar to the predicted 'precursor' high temperature orthopyroxenes for sheared 'oceanic' peridotites. Orthopyroxenes coexisting with ol+cpx+gt+liq at 3 GPa and 1550 °C (11) or at 2.5 GPa and 1470°C (12), have the high Ca and Al contents predicted for the 'precursor' orthopyroxenes of 'oceanic' peridotite compositions. Using these constraints, orthopyroxenes parental to garnet and/or clinopyroxene in high temperature, porphyroclastic lherzolites having 'oceanic' compositions are predicted to have equilibrated above the peridotite solidus (1400 and 1600 °C) at pressures less than 3 GPa. These conditions of formation for porphyroclastic samples with 'oceanic' compositions are remarkably similar to those predicted by Cox et al (6).

Thus, the apparent cooling path for the presumed original high-temperature harzburgite protoliths of garnet lherzolites differs depending on bulk composition. The cooling history of high-temperature harzburgite protoliths parental to porphyroclastic 'oceanic' garnet lherzolite samples is complicated by the fact that such rocks originally formed at pressures less than 3 GPa, as indicated by their 'precursor' orthopyroxene compositions, but were sampled by their host kimberlite at pressures in excess of 6 GPa. The equilibration of the 'oceanic' lherzolites at pressures higher than those at which they are thought to have formed requires that mantle represented by these rocks was transported from shallower to deeper levels. It is speculated that such transport could have been accomplished by convective circulation of oceanic lithosphere, but that the convected mantle represented by these samples is ancient, because isotopic studies of these rocks indicate they were removed from the asthenosphere about 2.5 to 3.0 Ga ago (8).

Compared to the porphyroclastic 'oceanic' lherzolites, the coarse textured 'cratonic' lherzolites have undergone a much simpler cooling history since their original formation. Parental orthopyroxenes from which clinopyroxene and garnet exsolved in 'cratonic' lherzolites appear to have formed at pressures near 5 GPa and temperatures near or above the fertile peridotite solidus (1500 to 1800 °C). At these P - T conditions along the fertile peridotite solidus, melts would have been ultramafic in composition (10,13). The bulk compositions and isotopic characteristics of typical 'cratonic' lherzolites are best explained by Archean ultramafic liquid extraction from primitive mantle compositions such as pyrolite (1,5,8). The compositional overlap between orthopyroxenes in equilibrium with olivine and melt along the liquidus of aluminum undepleted komatiite (14) and 'precursor' orthopyroxenes for 'cratonic' coarse grained peridotites, is strong evidence for this scenario. Therefore, the P-T history of 'cratonic' lherzolite was probably one of simple isobaric cooling from formation temperatures near the peridotite solidus (5 GPa, > 1500 °C) to those at which they were sampled in the mantle root of the Kaapvaal craton (< 1200 °C).

In summary, phase equilibria from this and other experimental studies on ultramafic systems are consistent with an origin for 'cratonic' peridotite as a residue of Archean ultramafic liquid extraction, which has since cooled and exsolved clinopyroxene and garnet to become the common low temperature coarse-grained peridotite comprising the bulk of the Kaapvaal craton. This model may indeed apply to cratonic lithosphere underlying other less well studied (or well sampled) Archean cratons such as the Wyoming and/or Superior provinces in North America.

1. F.R. Boyd, *Earth Planet. Sci. Lett.*, 96, 15-26, 1989.
2. F.R. Boyd and P.H. Nixon, *Contrib. Mineral. Petrol.*, submitted
3. C. Herzberg, M. Feigenson, C. Skuba and E. Ohtani, *Nature* 332, 823-826, 1988.
4. S. E. Kesson and A.E. Ringwood, *Chem. Geol.*, 78, 97-118, 1989.
5. E. Takahashi, *J. Geophys. Res.*, 95, 15941-15954, 1990.
6. K.G. Cox, M.R. Smith and S. Beswetherick, in: *Mantle Xenoliths*, P.H. Nixon, ed., pp. 537-550, John Wiley and Sons, New York, N.Y., 1987.
7. J.B. Dawson, J.V. Smith and R.L. Hervig, *Phil. Trans. R. Soc. Lond.*, A297, 323-331, 1980.
8. R.J. Walker, R.W. Carlson, S.B. Shirey and F.R. Boyd, *Geochim Cosmo Acta* 53, 1583-1595, 1989.
9. M.J. O'Hara, M.J. Saunders, and E.L.P. Mercy, *Phys. Chem. Earth*, 9, 571-604, 1975.
10. P.H. Nixon, P.W.C. van Calsteren, F.R. Boyd and C.J. Hawkesworth, in: *Mantle Xenoliths*, P.H. Nixon, ed., pp. 523-533, John Wiley and Sons, New York, N.Y., 1987.
11. E. Takahashi, *J. Geophys. Res.*, 91, 9367-9382, 1986.
12. D. Elthon and C.M. Scarfe, *Am. Miner.*, 69, 1-15, 1984.
13. E. Takahashi and C.M. Scarfe, *Nature*, 315, 566-568, 1985.
14. K. Wei, R.G. Tronnes and C.M. Scarfe, *J. Geophys. Res.*, 95, 15817-15827, 1990.

# GEOLOGY AND GEOPHYSICS OF THE REDONDÃO KIMBERLITE DIATREME, NORTHEASTERN BRAZIL.

Castelo Branco, <sup>(1)</sup>R.M.G and Lasnier, <sup>(2)</sup>B.M.

(1) Depto. de Geologia, Univ. Federal do Ceará, Brasil; (2) Université de Nantes, Lab. Pétrologie et Minéralogie, France.

## INTRODUCTION

Over the past three decades several kimberlite bodies have been recognized in Brazil, mostly in the south-eastern part of the country. They occur mainly in the state of Minas Gerais, generally as small, rounded or elliptical, weathered diatremes. However, other occurrences in the Mato Grosso, Goiás, Rondônia, Santa Catarina and Piauí states are less well documented.

Investigations of the Brazilian kimberlites were first made by mining and prospecting companies. Svisero et al. (1984) made a synthesis of the geology of some bodies known at that time. Castelo Branco (1986a) documented several diatremes in the Parnaíba basin, northeastern Brazil.

## THE REDONDÃO DIATREME: GENERAL GEOLOGY

The Redondão diatreme was the first kimberlite body discovered in Brazil during a regional geological survey carried out by PETROBRAS (Brazilian Oil Company) in 1962, but unpublished. Figure 1 shows the localization of the studied area and figure 1b shows the geology of Redondão and adjacent area.

The Redondão diatreme consists of a semi-square structure, with a diameter lengthened around 1100 meters in the NNW direction. Depths may reach up to 60 meters in the center of the structure relative to the Guaribas plateau, which has an average altitude of 600 meters above sea level. The well-shaped structure occurs in the Carboniferous and Permian rocks of the Parnaíba basin (Piauí and Pedra de Fogo sedimentary formations). These rocks are represented mainly by sandstones, siltstones and shales of various colors and grain size. In addition, there are thin, localized deposits of recent sediments such as sands and clays scattered over the Guaribas plateau. In this region, the total thickness of the Paleozoic sediments (Serra Grande, Pimenteiras, Cabeças, Longá, Poti, Piauí, Pedra de Fogo formations) can reach 2000 meters over the Precambrian crystalline rocks (Lodoño 1958, Mesner & Wooldridge 1964).

Photogeologic interpretation with processed remote sensing and associated field geology studies provides detailed information on the geology inside the diatreme, as well as on the regional interpretation of lineaments (Castelo Branco 1986b).

Inside the Redondão structure, the outcrops are formed by weathered kimberlitic breccia surrounded, in most cases, by soil formations. Yellow ground is, therefore, frequent and forms slight depressions; this material forms 60% of the structure. On the other hand, near several elevations, there are floating reefs of sandstone (Piauí Formation) and others of recent lateritic formations as well as small alluvial and colluvial deposits (40% of the structure).

The typical kimberlite outcrops comprise soft, yellowish rocks enclosing numerous fragments (0,5 - 20 mm) of various shapes. The whole assemblage forms a volcanic breccia. There are fragments of an "accidental" and "cognate" nature as well. In thin section, the Redondão kimberlite breccia consists essentially of 40% argillaceous minerals, 10% carbonates, 12% chlorites, 10% talc, 10% quartz, 10% serpentines, 5% phlogopites, and 3% opaques.

The Redondão diatreme also contain xenoliths of mantle origin which Svisero et al. (1977) has been reported as a garnet-serpentine xenoliths composed of pyrope garnet, serpentine, clinopyroxene, phlogopite, chromite and spinel.

The garnets of Redondão breccia were analysed using an electron microprobe with a TRACOR system. They occur as red rounded isolated crystals (<2.5mm) within the breccia matrix. The microprobe analysis showed them to be pyrope with CaO 4.49-5.67 weight per cent and Cr<sub>2</sub>O<sub>3</sub> 1.77-4.54 weight per cent. The Cr-pyrope of Redondão diatreme have an average composition (mol. per cent end-members) of pyrope 66.51-67.41, almandine 17.76-19.08, grossular 10.23-10.86, uvarovite 1.83-4.67. Figure 2 displays a diagram with the composition of Redondão garnets compared with those of worldwide kimberlite localities and those of garnets from other Brazilian occurrences.

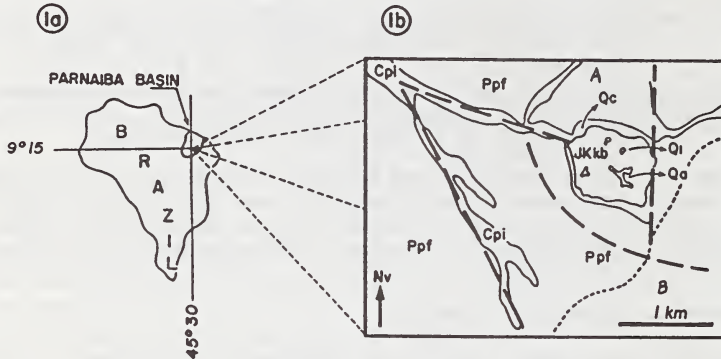


Figure 1a shows the geographic localization of the Redondão area in the Brazilian shield. Figure 1b displays the geology of Redondão diatreme and adjacent areas: Q (Quaternary a-alluvium, c-colluvium, l-laterites), P (Permian pf-Pedra de Fogo), C (Carboniferous pi-Piauí), JK (Juro/Cretacic kb-kimberlite breccias), Ppf and Cpi essentially sandstone and siltstone. Heavy lines-lineaments, fine lines-geological contacts, trace lines-road, A-B geophysical profile orientation.

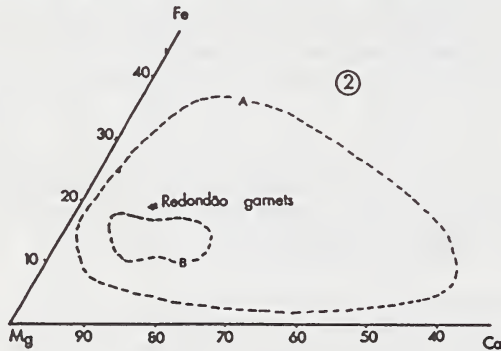


Figure 2 Diagram (mol. per cent end-members) of Redondão garnets. A-Kimberlite garnets worldwide occurrences, B-Kimberlites garnets from Brazilian occurrences.

## GEOPHYSICAL SURVEYING AND ITS INTERPRETATION

Magnetometric profiles, electrical resistivity soundings, as well as gamma ray spectrometry exploration, were used in conjunction with geological mapping crossing the diatreme in the NS direction. The best adjustment obtained to compare the field curve with a theoretical one is presented in figure 3 as a result of 2-D computing treatment of the geophysical and dimensional parameters as well as the geological evidence and models of kimberlite diatreme generation. The geophysical parameters used are also visible in the caption. The draft roughly presents the model adopted here.

The diatreme has a funnel shape which extends downwards vertically to 2 Km under the actual surface (1,1 to 1,3 Km in diameter). At depth, there is 2-5 Km thick feeder dike, of kimberlitic nature, oriented in NE direction and dipping 70 - 80° SE. This dike, responsible for 80% of the magnetic anomaly, is set in the cataclastic zone of the

"Transbrasiliiano" lineament and can reach 20 Km in length, as shown by aeromagnetic anomaly. Other, well-defined profiles

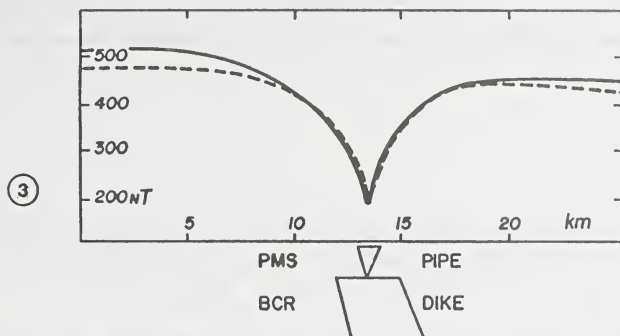


Figure 3 presents the results of the best adjustment between the field and theoretical curves. Geophysical parameters were MSC for dike 0.0055emu, for the pipe MSC 0.0022emu, anomaly due to induced magnetisation, MI 7°, MD -19°, MTF 25700nT, Transverse azimuth of the profile 133°, Total field. PMS-Paleomesozoic sediments, BCR-basement crystalline rocks. Heavy line-field curve, trace line-theoretical. Dimensional parameters-see text.

extending out of the diatreme confirm the presence of this dike. The diatreme was formed by explosive activity at an intersection of a NNW lineament (Serra do Boqueirão). This indicates that the formation of kimberlite diatremes is a localized geological process.

Vertical electrical profiles of apparent resistivity versus Schlumberger array electrode spacing have been applied over the Redondão diatreme. They indicate 4 altered layers with an increasing apparent resistivity at depth around 200 meters. The bottom layer showed resistivities greater than 300 ohm.m, corresponding to a less weathered layer of breccias.

The gamma ray spectrometric results supplied limited geological information over the diatreme surface and were useful for determining the contacts between the kimberlite rocks as a whole and the sedimentary adjacent rocks.

#### ACKNOWLEDGMENTS

Castelo Branco would like to acknowledge CNPq - Conselho Nacional de Pesquisa e Desenvolvimento Científico that was provided a part of financial support and wish to extend sincere appreciation to Prof. José Marcio Lins Marinho and to Prof. Benjamin Bley de Brito Neves. I am also indebted to Dr. Frances Westall who carefully reviewed the final manuscript and to Dr. G.Cornen and Dr.G.Bossière for help in chemical analysis.

#### REFERENCES

- Castelo Branco, R.M.G. (1986a) Geological aspects of Brazilian kimberlites with emphasis of the occurrences of SW Piauí state. *Rev. Esc. Minas Ouro Preto*, 39(2), 21-26 (in Portuguese).
- Castelo Branco, R.M.G. (1986b) Fracture trend analyse of Santa Filomena and Gilbues region, south border of Parnaíba basin, Piauí. *Brazilian Geological Society-NE*, 12, 127-137 (in Portuguese).
- Lodoño, D.H. (1958) Basement depth of the Maranhão basin as obtained from airborne magnetometer data. *Petrobras, int. Report*.
- Mesner, J.C. & Wooldridge, L.C.P. (1964) Maranhão Paleozoic basin and Cretaceous coastal basins, north Brazil. *Bull. Assoc. Petr. Geol.*, 48(9), 1475-1512.
- Svisero, D.P.; Meyer, H.O.A. & Tsai, H.M. Kimberlite minerals from Vargem (Minas Gerais) and Redondão (Piauí) diatremes, and garnet lherzolite xenoliths from Redondão diatreme. *Rev. Bras. Geoc.*, 7(1), 1-13.
- Svisero, D.P., Meyer, H.O.A., Haralyi, N.L.E. & Hasui, Y. (1984) A note on the geology of some Brazilian kimberlites. *Journal of Petrology*, 92(3), 331-338.

## INCLUSIONS OF CARBONATITE CALCITE FROM THE OKA COMPLEX, QUEBEC.

*Chan, Chien-Lu.*

*Department of Geology and Geophysics, University of Minnesota, Minneapolis, Minnesota 55455, USA.*

Mineral inclusions in carbonatite calcite from the Oka complex, Quebec, Canada were examined. Samples include coarse-grained calcite from carbonatite, alnöite and glimmerite.

An isolated phlogopite was found in a calcite in coarse-grained sövite (Bond Zone). The phlogopite is prismatic, near 90  $\mu\text{m}$  length-wise, titaniferous and sodic (Table 1). Two smaller phlogopite inclusions (< 50  $\mu\text{m}$ ) were found in a glimmerite calcite.

A totally enclosed euhedral calcite crystal, in a calcite from the very coarse-grained sövite (VCGS), approximately 110  $\mu\text{m}$  in the longest dimension is close to but not epitaxially related to the host calcite. Lamellar twins and a set of fractures radiating from the inclusion can be interpreted by the thermal expansion coefficients of calcite,  $\alpha_a$  and  $\alpha_c$ , which differ in sign and magnitude, and interfacial stress. The calcite is not fluorescent.

A discrete magnetite was found in a calcite from pyroxene sövite. The magnetite is magnesian (5.8 wt.% MgO), approximately 80  $\mu\text{m}$  in dimension. The magnetite in the sövite is less magnesian (up to approximately 5%) than the magnetite inclusion.

One zircon was recovered from an alnöite calcite (Bond Zone). Its composition is near stoichiometric zirconium silicate, with minor iron, and poor in heavy elements.

Alkali halides (NaCl and KCl) were identified in some calcites in the VCGS. Where inclusions are aligned, it is possible they are located in a healed fracture possibly extending to the surface, and secondary in origin. One VCGS calcite contains over 40 crowded halide inclusions.

Twinned calcites examined contain inclusions more frequently than single crystals. Contact twins defined by a c-axis twin law and {0112} twin law are common. Penetration twins are also present. Etched sections across composition planes reveal association of some inclusions with twinning. Doubly twinned and multiply twinned calcites examined, however, are not more inclusion-rich than single twins. Therefore inclusions are not necessarily promoted by twinning.

Origins of these inclusions are uncertain. Hydrothermal is a likely origin for some of the inclusions. The calcite inclusion can be magmatic in origin.

Table 1. Compositions of inclusions.

	Magnetite MT4	Calcite CC1a	Phlogopite PH2
SiO <sub>2</sub>			35.53
TiO <sub>2</sub>	2.42		2.01
Al <sub>2</sub> O <sub>3</sub>	0.45	0.02	19.18
FeO + Fe <sub>2</sub> O <sub>3</sub>	84.04	0.69	5.63
MnO	2.21	0.12	0.12
CaO	0.11	52.06	0.22
MgO	5.84	2.14	23.27
Na <sub>2</sub> O	0.00	0.10	0.86
K <sub>2</sub> O	0.01	0.08	9.48
P <sub>2</sub> O <sub>5</sub>	0.09	0.12	0.16
Total	95.17	55.33	96.46

**PALAEOGEOGRAPHIC STUDIES ON THE DIAMOND-BEARING SOPA CONGLOMERATE  
IN THE DIAMANTINA REGION (MINAS GERAIS), BRAZIL.**

*Chaves, M.L.S.C.*

*Instituto de Geociências, Univ. Fed. Minas Gerais, C.P. 2608, Belo Horizonte-MG, Brazil.*

Since 1985 the author realizes studies on the diamondiferous conglomerate and breccia of the Sopa Formation (Espinhaço Supergroup) in the Diamantina District, State of Minas Gerais, Brazil. These deposits are exploited since the last century by "garimpos" and small washing plants.

The Espinhaço belt is a long chain of mountains with about one thousand kilometers crossing the States of Minas Gerais and Bahia. The Mid-Proterozoic Espinhaço Supergroup is a 5000 meters thick metasedimentary section, predominantly composed by quartzites and phyllites. The regional trend of the Espinhaço Supergroup is N-S.

The Sopa Formation consists of quartzites, phyllites, conglomerates and breccias. The polymictic conglomerates occur as lenses and channels deposits up to 150 meters thick. Regional studies allow five main diamondiferous fields to be recognized in the Diamantina District: Campo Sampaio-São João da Chapada, Sopa-Guinda, Extração, Datas and Presidente Kubitschek (Chaves, 1988). The present contribution describes the palaeogeographic arrangements of Sopa-Guinda, Extração and Datas fields.

In the studied fields detailed geological mapping, sedimentary environments and facies analysis, with data on the attitude of the cross-bedding in the sequences enable us to draw the following conclusions:

(1) In the Diamantina District general transport of sediments was to the east and south into a coastal region,

(2) The diamond-bearing sediments were deposited mainly on alluvial fans and fan deltas, but diamond-rich sandstone deposits of braided river type also occur,

(3) In the Sopa-Guinda and Datas fields the deposition occurred in alluvial fans, but only at Datas the sediments reached the ocean where they were reworked by strong waves developed during stormy weather,

(4) In the Extração field the fan delta sedimentation resulted from vertical movements with uplift of continental areas (the Volcanic-Sedimentary Complexes) and of blocks with small sedimentation load (the basal portion of the Espinhaço Supergroup), forming large islands parallel to the coast (Abreu, 1984),

(5) In the Extração field the proximal fan facies crop out, while in the Datas and Sopa-Guinda fields mainly the meddium to distal deposits are exposed,

(6) As a result, the diamond concentration in the three studied fields was controled by the distance to the source area.

#### AKNOWLEDGEMENTS

A careful review by Prof. Dr. E.A. Ladeira helped to improve the exposition of the manuscript.

#### REFERENCES

- ABREU, P.A.A. (1984) The influence of tectonic activities in the formation of deltas, spatial compartment and the evolution of the Lower Proterozoic sedimentary environment in the Espinhaço Range, Minas Gerais, Brazil. *Anais da Academia Brasileira de Ciências*, 56 (1): 109.
- CHAVES, M.L.S.C. (1988) Metaconglomerados diamantíferos da Serra do Espinhaço Meridional (Minas Gerais). *Revista de Geologia*, 1 (2): 71-82.

## APPLICATIONS OF OLIVINE-ORTHOPYROXENE-SPINEL OXYGEN GEOBAROMETERS TO THE REDOX STATE OF THE UPPER MANTLE.

*Chen, <sup>(1)</sup> Y.D.; Pearson, <sup>(1)</sup> N.J.; O'Reilly, <sup>(1)</sup> S.Y. and Griffin, <sup>(2)</sup> W.L.*

*(1) School of Earth Sciences, Macquarie University, Sydney, N.S.W., 2109, Australia. (2) Division of Exploration Geosciences, CSIRO, North Ryde, N.S.W., 2113, Australia.*

### INTRODUCTION

Early oxygen-specific electrochemical measurements of the "intrinsic oxygen fugacity" (e.g., Arculus and Delano, 1981; Arculus et al., 1984) on mantle xenoliths indicated that the Cr-diopside group xenoliths (Wilshire and Shervais, 1975) were characterized by oxygen fugacities close to the iron-wustite (IW) buffer, while Al-augite group xenoliths were found to be more oxidized, with oxygen fugacities between QFM and the nickel-nickel oxide (NNO) buffer. More recently, O'Neill and Wall (1987), Mattioli and Wood (1988), Nell and Wood (in Wood et al., 1990) and Ballhaus et al. (1990) have calibrated the reaction  $2\text{Fe}_3\text{O}_4$  (in spinel) +  $6\text{FeSiO}_3$  (in orthopyroxene) =  $6\text{Fe}_2\text{SiO}_4$  (in olivine) +  $\text{O}_2$  to calculate  $f\text{O}_2$  from the mineral chemistry of xenoliths, and applied these calibrations to upper mantle xenolith suites from a number of localities around the world. The results indicate a relative uniformity of  $f\text{O}_2$  values from the upper mantle with most values lying between the QFM and MW buffers. In the present study, we have calculated oxygen fugacities of more mantle xenolith suites using several calibrations of the olivine-orthopyroxene-spinel oxygen geobarometer.

### DATA SOURCES AND XENOLITH SUITES

The mineral analyses we used in the calculation of oxygen fugacities are from mantle xenoliths from eastern Australia, eastern China and southern Africa. The eastern Australia's xenoliths include those from western Victoria and from northeastern and southeastern Queensland and cover both the Cr-diopside suite and the Al-augite suite. Many of western Victorian xenoliths have been cryptically or modally metasomatised (containing amphibole  $\pm$  mica  $\pm$  apatite) (Griffin et al., 1984; O'Reilly and Griffin, 1988; Griffin et al., 1988; O'Reilly et al., unpublished data). Modally-metasomatised (amphibole-bearing) xenoliths are also present in Queensland xenolith suite (Ewart and Grenfell, 1985; Chen et al., unpublished data) but are much less common than in the western Victorian suite. Eastern China's mantle xenoliths included in this study are exclusively Cr-diopside suite and these are from seventeen localities spread over a distance of 5000 km of eastern China. In addition to our unpublished data, mineral analyses are taken from the literature (Fan and Hooper, 1989; Song and Frey, 1989). Two of the lherzolites contain garnet in addition to spinel. Several lherzolite xenoliths from Nushan, Anhui province, contain minor amount of amphibole. African xenoliths are mostly from kimberlites in southern Africa. Also included are some amphibole and/or mica-bearing spinel lherzolite xenoliths from basalts of the Rift Valley of northern Tanzania (Dawson and Smith, 1988). The mineral analyses of the southern African xenoliths are mainly from an unpublished data base of the Anglo American Research Laboratories with those in Carswell et al. (1984) included. Xenolith types include garnet-spinel harzburgite, garnet-spinel lherzolite, spinel harzburgite, spinel lherzolite, amphibole-bearing spinel harzburgite and amphibole-bearing spinel lherzolite. The xenolith localities can be grouped into (1) on-craton; (2) craton margin; and (3) off-craton settings.

### RESULTS AND DISCUSSIONS

*The ranges of calculated oxygen fugacities.* Among the four calibrations of the oxygen barometer we used in our calculation (O'Neill and Wall, 1987; Mattioli and Wood, 1988; Nell and Wood, 1990; Ballhaus et al., 1990), the results calculated by using the latter two calibrations agree better than those calculated by others. The ranges of oxygen fugacities summarized here refer only to those calculated by Ballhaus et al.'s calibration. The xenoliths from western Victoria, Australia, range from about 3 log units below to 0.5 log units above the QFM buffer with most being within 2 log units of QFM. The xenoliths from Queensland, Australia, and from various localities of eastern China have oxygen fugacities in general

comparable to those of the western Victoria xenoliths. Both the temperature and the calculated oxygen fugacities for xenoliths from Africa cover wider ranges than are seen in the basalt-borne xenoliths from China and Australia, but the majority of samples still have oxygen fugacities between the QFM and MW buffers. These observations are consistent with the previous conclusions (e.g., O'Neill and Wall, 1987) that the Cr-diopside suite xenoliths record oxygen fugacities more oxidized than predicted by intrinsic oxygen fugacity measurements (e.g., Arculus and Delano, 1981; Arculus et al., 1984).

*Cr-diopside series versus Al-augite series* The Al-augite xenoliths from western Victoria and Queensland have oxygen fugacity values falling within the range defined by the Cr-diopside xenoliths. This observation confirms those of O'Neill and Wall (1987) and Wood and Virgo (1989), and is in contrast with the finding from intrinsic oxygen fugacity studies that the Al-augite suite xenoliths are distinctly more oxidized than the Cr-diopside suite xenoliths (e.g., Arculus et al., 1984).

*Garnet-absent versus garnet-bearing xenoliths* There is not a clear-cut distinction in terms of calculated oxygen fugacities between the the garnet-bearing and the garnet-absent xenoliths in the southern African xenolith suite, but the oxygen fugacities of garnet-bearing xenoliths are in general higher than those of most garnet-absent samples. The two garnet-bearing xenoliths from eastern China have oxygen fugacities falling within the range defined by other garnet-absent xenoliths. In addition, there is also no systematic difference in oxygen fugacities for southern African xenoliths from on-craton, craton-margin and off-craton localities.

*Effect of mantle metasomatism* Mattioli et al. (1989) and Ballhaus et al. (1990) found that modally-metasomatised upper mantle xenoliths record higher oxygen fugacity than those without obvious evidence of metasomatism. In the the western Victorian xenolith suite, there is no general distinction on the basis of calculated oxygen fugacities between hydrous and anhydrous xenoliths. It is known that the cryptic and modal metasomatism of xenoliths is accompanied by elevated  $^{87}\text{Sr}/^{86}\text{Sr}$  and lowered  $\epsilon_{\text{Nd}}$  (O'Reilly and Griffin, 1988; Griffin et al., 1988); a plot of the calculated oxygen fugacities versus  $^{87}\text{Sr}/^{86}\text{Sr}$  and  $\epsilon_{\text{Nd}}$  shows a rough trend of increasing  $^{87}\text{Sr}/^{86}\text{Sr}$  and decreasing  $\epsilon_{\text{Nd}}$  with decreasing oxygen fugacity. In addition, the overall western Victorian xenolith suite is highly reduced although heavily metasomatised. This suggests that this particular type of mantle metasomatism is coupled with reduced oxygen fugacity. The metasomatising fluids beneath western Victoria have been speculated to be derived from a subducting slab. If this is correct, then the relatively low  $f\text{O}_2$  fluid derived from the slab might have been buffered by graphitic sediments in the slab cover (Shaw and Flood, 1981).

Mica- ( $\pm$ amphibole)-bearing xenoliths in the African suite have relatively high  $f\text{O}_2$ . Many high-T sheared garnet peridotite xenoliths of southern Africa suite, although they contain no hydrous phases, have been shown to be extensively metasomatised by infiltrating melts resulting in the addition of large amounts of garnet and clinopyroxene, as well as Zr, Y, Na and Ti (Smith and Boyd, 1987; Griffin et al., 1989). Griffin et al (1989) have suggested that the metasomatising melt is asthenosphere-derived. The highest oxygen fugacities among the African xenoliths are seen in some high-T garnet peridotites. This suggests that, in the African xenolith suite, metasomatism is coupled with increasing oxygen fugacities.

A combination of our data from the western Victoria and the African xenolith suites as well as the observation made by previous workers (e.g., Mattioli et al., 1989; Ballhaus et al., 1990), it is suggested that there is no consistent worldwide relation between mantle metasomatism and the oxygen fugacity of mantle xenoliths; the direction of change of oxygen fugacity probably depends on the source of the metasomatising fluids.

#### REFERENCES

- Arculus, R. J., and Delano, J. W. (1981) Intrinsic oxygen fugacity measurements: Techniques and results for spinels from upper mantle peridotite and megacryst assemblages. *Geochimica et Cosmochimica Acta*, 45, 899-913.
- Arculus, R. J., Dawson, J. B., Mitchell, R. H., Gust, D. A., and Holmes, R. D. (1984) Oxidation states of the upper mantle recorded by megacryst ilmenites in kimberlites and type A and B spinel lherzolites. *Contributions to Mineralogy and Petrology*, 85, 85-94.

- Ballhaus, C., Berry, R. F., and Green, D. H. (1990) High pressure experimental calibration of the olivine-orthopyroxene-spinel oxygen barometer - implications for redox conditions in the upper mantle. *Contributions to Mineralogy and Petrology*, in press.
- Carswell, D. A., Griffin, W. L., and Kresten, P. (1984) Peridotite nodules from Ngopetsoe and Lipelaneng kimberlites, Lesotho: A crustal or mantle origin. In J. Kornprobst, Ed., *Kimberlites II: the mantle and crust-mantle relationships*, p.229-43, Elsevier, Amsterdam.
- Dawson, J. B., and Smith, J. V. (1988) Metasomatized and veined upper-mantle xenoliths from Pello Hill, Tanzania: Evidence for anomalously-light mantle beneath the Tanzanian sector of the East African Rift Valley. *Contributions to Mineralogy and Petrology*, 100, 510-527.
- Ewart, A., and Grenfell, A. (1985) Cainozoic volcanic centers of southeastern Queensland with special reference to the Main Range, Bunya Mountains and the volcanic centers of the northern Brisbane coastal region. Paper of the Geology Department of Queensland University, 11, 1-57.
- Fan, Q. C., and Hooper, P. R. (1989) The mineral chemistry of ultramafic xenoliths of eastern China: Implications for upper mantle composition and the paleogeotherm. *Journal of Petrology*, 30, 1117-1158.
- Griffin, W. L., Wass, S. Y., and Hollis, J. D. (1984) Ultramafic xenoliths from Bullenmerri and Gnotuk Maars, Victoria, Australia: Petrology of a sub-continental crust-mantle transition. *Journal of Petrology*, 25, 53-87.
- Griffin, W. L., O'Reilly, S. Y. and Stabel, A. (1988) Mantle metasomatism beneath western Victoria, Australia: II Isotopic geochemistry of Cr-diopside lherzolites and Al-augite pyroxenites. *Geochimica et Cosmochimica Acta*, 52, 449-459.
- Griffin, W.L., Smith, D., Boyd, F.R., Cousens, D.R., Ryan, C.G., Sie, S.H., and Suter, G.F. (1989) Trace-element zoning in garnets from sheared mantle xenoliths. *Geochimica et Cosmochimica Acta*, 53, 561-567.
- Mattioli, G. S., and Wood, B. J. (1988) Magnetite activities across the  $MgAl_2O_4$ - $Fe_3O_4$  spinel join, with application to thermobarometric estimates of upper mantle oxygen fugacity. *Contributions to Mineralogy and Petrology*, 98, 148-162.
- Mattioli, G. M., Baker, M. B., Rutter, M.J., and Stolper, E. M. (1989) Upper mantle oxygen fugacity and its relationship to metasomatism. *Journal of Geology*, 97, 521-536.
- O'Neill, H. St. C., and Wall, V. J. (1987) The olivine-orthopyroxene-spinel oxygen geobarometer, the nickel precipitation curve, and the oxygen fugacity of the Earth's upper mantle. *Journal of Petrology*, 28, 1169-1191.
- O'Reilly, S.Y., and Griffin, W. L. (1988) Mantle metasomatism beneath western Victoria: I. Metasomatic processes in Cr-diopside lherzolite. *Geochimica et Cosmochimica Acta*, 52, 433-447.
- Shaw, S. E., and Flood, R. H. (1981) The New England Batholith, eastern Australia: geochemical variation in time and space. *Journal of Geophysical Research*, 86, B11, 10530-10544.
- Smith, D., and Boyd, F. R. (1987) Compositional heterogeneities in a high-temperature lherzolite nodule and implications for mantle processes. In P. H. Nixon, Ed., *Mantle xenoliths*, p.551-561, Wiley, New York.
- Song, Y., and Frey, F. A. (1989) Geochemistry of peridotite xenoliths in basalt from Hannuoba, eastern China: Implications for subcontinental mantle heterogeneity. *Geochimica et Cosmochimica Acta*, 53, 97-113.
- Wilshire, H. G., and Shervais, J. W. (1975) Al-augite and Cr-diopside ultramafic xenoliths in basaltic rocks from Western United States. *Physics and Chemistry of the Earth*, 9, 257-272.
- Wood, B. J., Bryndzia, L. T., and Johnson, K. E. (1990) Mantle oxidation state and its relationship to tectonic environment and fluid speciation. *Science*, 248, 337-345.

DATING THE CRATONIC LOWER CRUST BY THE ION MICROPROBE SHRIMP:  
AN U-Th-Pb ISOTOPIC STUDY ON ZIRCONS FROM LOWER CRUSTAL  
XENOLITHS FROM KIMBERLITE PIPES.

Chen, <sup>(1)</sup> Y. D.; O'Reilly, <sup>(1)</sup> S.Y. and Kinny <sup>(2)</sup> P.D.

(1) School of Earth Sciences, Macquarie University, Sydney, NSW, 2109, Australia. (2) Research School of Earth Sciences, The Australian National University, Canberra, ACT, 2601, Australia.

We here report an U-Th-Pb isotopic study of zircons from a suite of lower crustal (probably also upper mantle) xenoliths from some kimberlitic pipes at Calcutteroo, South Australia by using the ion microprobe SHRIMP at Research School of Earth Sciences of The Australian National University. In particular, zircons from a xenolith of eclogitic composition were first time found and dated.

Xenoliths found from the Calcutteroo kimberlitic pipes include spinel lherzolite, eclogite, mafic and quartzo-feldspathic granulites with the mafic granulite predominant. The importance of these xenoliths is that they are extremely rare occurrence of samples of lower crust and upper mantle from a tectonic environment of eastern margin of the Australian Craton. Petrological, geothermobarometric and geochemical studies on these xenoliths (Pearson et al., 1991) have resulted in information on the composition and stratigraphy of the lower crust and upper mantle of the region but not the timing. Seven mafic to felsic granulite xenoliths were previously dated by whole-rock Rb/Sr and Sm/Nd techniques (McCulloch et al., 1982). On the assumption that these xenoliths were petrogenetically coherent and recorded a major intracrustal differentiation event, an age of 2400 Ma was suggested from the whole-rock isochron. In the present study, we separated and dated zircons from three xenolith types: eclogite (1 xenolith), mafic (1 xenolith) and quartzo-feldspathic (3 xenoliths) granulites.

Zircons from the three quartzo-feldspathic granulite xenoliths gave bimodal age distribution: 1700-1500 Ma and 600-350 Ma. Zircons from the mafic granulite xenolith have ages mostly clustered between 800 and 700 Ma with subordinate number of spot analyses being younger (530-480 Ma). Zircons from the eclogite xenolith range in age from 600 to 300 Ma. The immediate significance of these zircon growth ages is that they invalidate the previous Rb/Sr and Sm/Nd isochron ages. It is shown that the different types of xenoliths were not co-genetic and therefore a whole-rock isochron age is not meaningful.

More importantly, the zircon data indicate that the formation of lower crust (also upper mantle) of the region is the result of multiple-episodes. The 1700-1500 Ma age of the zircons found from the quartzo-feldspathic granulite xenoliths broadly coincides with the development duration of the Willyama metamorphic complex occurring in South Australia and New South Wales; this indicates that the distribution of Willyama complex is more extensive than presently exposed and is southwards extended to beneath the region of Calcutteroo. The different, younger ages found in all xenolith types indicate that several later episodes of mantle-derived magma intrusion and regional metamorphism have occurred in the region and significantly contributed to the growth and evolution of the lower crust.

#### REFERENCES

- McCulloch, M.T., Arculus, R.J., Chappell, B.W., and Ferguson, J. (1982) Lower continental crust: inference from isotopic and geochemical studies on nodules in kimberlites. *Nature*, 300, 166-169.
- Pearson, N.J., O'Reilly, S.Y., and Griffin, W.L. (1991) The granulite to eclogite transition beneath the eastern margin of the Australian craton. *European Journal of Mineralogy*, in press.

## ISOTOPIC AND GEOCHEMICAL VARIATION IN KIMBERLITES FROM THE SOUTH WESTERN CRATON MARGIN, PRIESKA AREA, SOUTH AFRICA.

Clark, <sup>(1,2)</sup> T.C.; Smith, <sup>(1)</sup> C.B.; Bristow, <sup>(3)</sup> J.W.; Skinner, <sup>(3)</sup> E.M.W and Viljoen, <sup>(3)</sup> K.S.

(1) *Bernard Price Institute for Geophysical Research, U. Witwatersrand, Johannesburg 2050, R.S.A.*; (2) *GENMIN Laboratories, Springs 1560, R.S.A.*; (3) *Anglo American Research Laboratories, Box 106, Crown Mines 2025, R.S.A.*

Approximately 130 known kimberlite bodies occur in a broad belt from northwest of Prieska to Sutherland in the northern part of the Cape Province (see location map in Skinner et al., this volume). Being situated peripherally to the Kaapvaal Craton, the kimberlites generally lack diamond, comprise both micaceous and non-micaceous types as defined by Skinner (1989), and were emplaced during at least five separate periods between 74 and 140 Ma (Skinner et al., this volume).

Age-corrected Nd and Sr whole-rock isotopic ratios indicate that both Group I and Group II varieties as defined by Smith (1983) are present, as well as an additional, probably subsidiary variety with transitional isotopic character (Fig. 1). Group I kimberlites include Uintjiesberg, Britstown, Violkraal West, and Hartebeesfontein, and have initial  $^{87}\text{Sr}/^{86}\text{Sr}$  and  $^{143}\text{Nd}/^{144}\text{Nd}$  ratios of .7035 to .7045 and about .51265, respectively, very typical of other Group I kimberlites. The Pampoenpoort kimberlite has a significantly lower initial Nd isotopic ratio near bulk earth in composition, and in this regard is very similar to the Frank Smith kimberlite from the Barkly West district near Kimberley. Emplacement events for the Group I bodies occurred at about 74, 100 and 114 Ma., and the kimberlites occur dominantly in domains I, II and IV of the Prieska area as defined by Skinner et al. (this volume).

Group II kimberlite emplacement occurred dominantly between 114 and 120 Ma with a possible earlier event at 126 Ma, and include Markt, Middlewater, Jonkerwater, Brandewynskuil, Eendekuil, Slypsteen, Welgevonden, Witberg East dyke, Silvery Home and Sandrift. Initial Sr isotope ratios range from .7075 to .7090, and initial Nd isotope ratios range from .5119 to nearly .5122 (Fig. 1). These kimberlites are situated in domains I, II and III (Skinner et al., this volume), with the majority apparently in III, an area bounded by the Brakbos and Dornberg faults. Insofar as the latter is generally taken to be the Kaapvaal Craton boundary, those kimberlites may be defined as off-craton. However, domain III is underlain by crust of apparent Archaean age of uncertain relation to the Kaapvaal (Cornell et al., 1986). The Group II kimberlites in this domain tend to have somewhat less radiogenic Nd isotopic compositions for a given Sr isotopic composition compared to other Group II localities, but are otherwise not isotopically distinctive compared to occurrences from within the bounds of the Kaapvaal Craton.

Several occurrences of micaceous kimberlite have isotopic, petrographic and geochemical features transitional between Group I and Group II types. The kimberlites include Skietkop, Sweetput-Soutput, Droogfontein and Melton Wold and apparently occur largely in domain V of the area except for Sweetput-Soutput (domain II). Emplacement ages are not well constrained (Skinner et al., this volume); Sweetput-Soutput is about 115 Ma in age, but the others could be significantly older according to perovskite dating. Initial Sr and Nd isotopic ratios respectively vary from .7055 to .707 and from .51215 to .51235, with two Melton Wold samples having the most radiogenic Nd and highly variable Sr isotopic compositions (Fig. 1). Previous studies of cratonic kimberlites have indicated that samples with transitional Sr isotopic features were altered and/or contaminated, but the samples analyzed in this study are fresh and the transitional features are a primary component that therefore reflects source composition.

Whole-rock geochemical analyses of the kimberlites show similar major, minor and trace element patterns to their cratonic counterparts (e.g. Smith et al., 1985). Group I kimberlites contain (on average) less  $\text{SiO}_2$ ,  $\text{Al}_2\text{O}_3$ ,  $\text{Na}_2\text{O}$ , Ba, Rb, Sr, Cr, Ni and REE contents than Group II rocks.  $\text{K}_2\text{O}$  and  $\text{TiO}_2$  contents are particularly good discriminators (Fig. 2), being a function of the mineralogical differences between the types, and showing the group distinctions very similar to those noted by Smith et al. (1985). There are few apparent and significant differences between on- and off-craton kimberlites of either Group I or Group II, although cratonic Group I kimberlites tend to have higher Th/U than off-craton Group I, and off-craton Group II kimberlites have significantly greater LREE enrichment compared to off-craton Group I. The distinction in REE patterns between Groups I and II is not apparent in the on-craton setting.

The isotopically defined transitional kimberlites also have transitional geochemical features. In Fig. 2 the transitional kimberlites plot in the Group II field in keeping with their micaceous character, but they also have somewhat elevated  $\text{TiO}_2$  in keeping with abundant perovskite (not generally present in on-craton Group II). As regards REE abundances, the transitional rocks are similar to Group II for the LREE, but more akin to Group I for Yb.

The isotopic and geochemical characteristics of these kimberlites are consistent with derivation of Group I rocks from sub-lithospheric plume sources, while Group II sources could reside in ancient enriched lithosphere, or could also occur in DUPAL-like asthenospheric plume sources. The transitional kimberlites are apparently derived from mixed source regions, a process possibly enhanced in areas of thinner lithosphere presumably corresponding with the craton margin. While this does not preclude plume sources for either Group I or II kimberlites, the presence of the transitional rocks may also be consistent with the creation of their sources from mixed asthenospheric and ancient lithospheric domains during Proterozoic crust/lithosphere formation represented by the Namaqua Province.

## REFERENCES

- Cornell, D., Hawkesworth, C.J., van Calsteren, P., and Scott, W.D. (1986) Sm-Nd study of Precambrian crustal development in the Prieska-Copperton region, Cape Province. *Trans. Geol. Soc. S. Africa* 89, 17-28.
- Fraser, K.J. (1987) Petrogenesis of kimberlites from South Africa and lamproites from Western Australia and North America, PhD thesis, Open University.
- Skinner, E.M.W. (1989) Contrasting group I and Group II kimberlite petrology: towards a genetic model for kimberlites. In J. Ross, Man. ed., *Kimberlites and Related Rocks, Their Composition, Occurrence, Origin and Emplacement*, Geol. Soc. Australia Spec. Publ. 14, p. 528-544.
- Skinner, E.M.W., Viljoen, K.S., Clark, T.C., Smith, C.B., and Bristow, J.W. (this volume) The geology of kimberlites in the south western border region of the Kaapvaal Craton, Prieska area, South Africa.
- Smith, C.B. (1983) Pb, Sr and Nd isotopic evidence for sources of southern African Cretaceous kimberlites. *Nature* 304, 51-54.
- Smith, C.B., Gurney, J.J., Skinner, E.M.W., Clement, C.R., and Ebrahim, N. (1985) Geochemical character of southern African kimberlites: A new approach based on isotopic constraints. *Trans. Geol. Soc. S. Africa* 88, 267-280.
- Spriggs, A.J. (1988) An isotopic and geochemical study of kimberlite and associated alkaline rocks from Namibia, PhD thesis, University of Leeds.

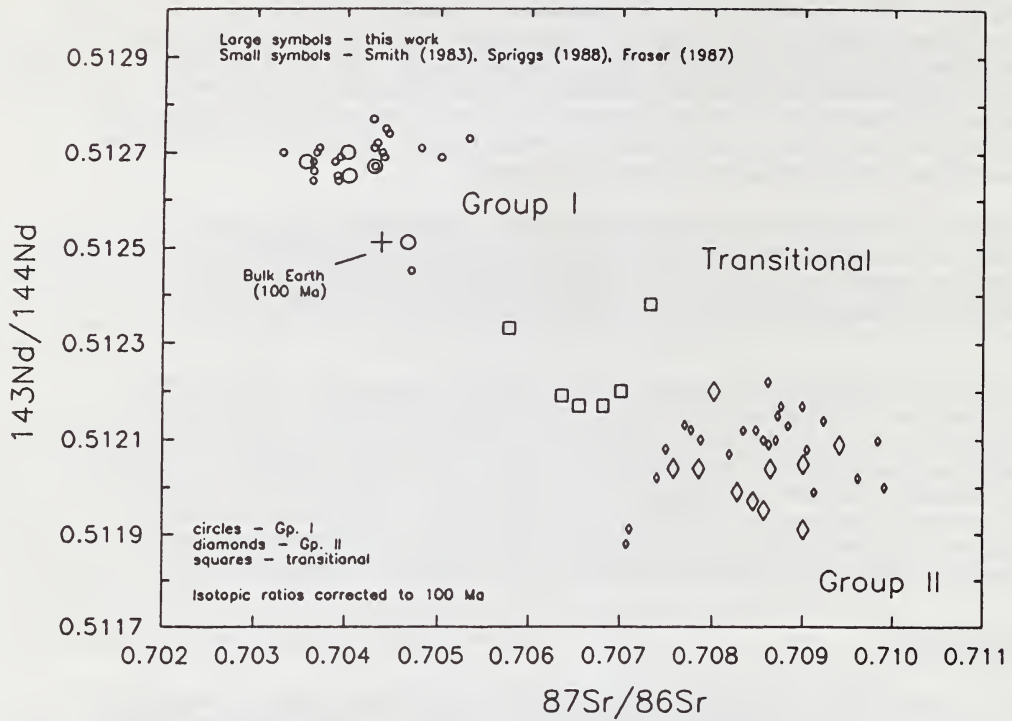


Figure 1. Nd-Sr isotope correlation diagram for Prieska kimberlites.

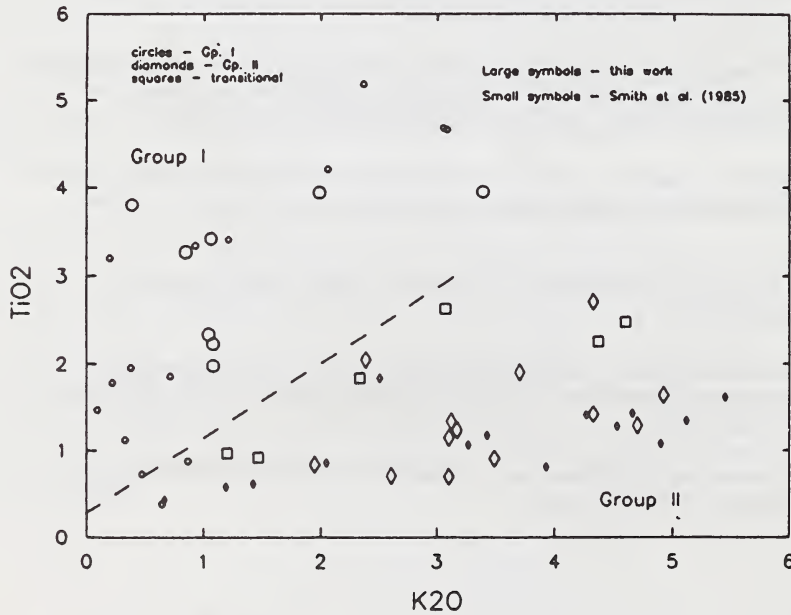


Figure 2. TiO<sub>2</sub> vs. K<sub>2</sub>O for Prieska kimberlites.

## RARE EARTH, TRACE ELEMENT AND STABLE ISOTOPE FRACTIONATION OF CARBONATITES AT KRUIDFONTEIN, TRANSVAAL.

Clarke, <sup>(1)</sup> L.B.; Le Bas, <sup>(1)</sup> M.J. and Spiro <sup>(2)</sup> B.

(1) Department of Geology, University of Leicester, LE1 7RH, UK; (2) Isotope Geosciences Laboratory, British Geological Survey, Keyworth, Nottingham, NG12 5GG, UK.

The intrusive sequence of calcite carbonatites in the Proterozoic collapsed carbonatitic caldera at Kruidfontein shows fractionation of the trace and Rare Earth elements. The inclusion of two sovites from the immediately adjacent (4 km away) plutonic carbonatitic complex at Nootgedacht extends this sequence. This fractionation can be correlated with Rayleigh fractionation of  $\delta^{18}\text{O}$  and  $\delta^{13}\text{C}$  such as is produced by a  $\text{H}_2\text{O}/\text{CO}_2$  molar ratio of  $<0.5$  in a co-existing ( $\text{H}_2\text{O} + \text{CO}_2$ ) vapour phase (Fig. 1). It is less well correlated with contamination by ground waters although some is likely to have taken place. It does not correlate with loss of isotopically light water during pressure reduction at the time of emplacement. For comparable values of  $\delta^{18}\text{O}$  in the intrusive carbonatites, the extrusive calcitic carbonatitic tuffs have lower  $\delta^{13}\text{C}$  values, which may be attributed to the loss of  $^{13}\text{C}$  to the vapour phase. The unmineralized extrusive dolomitized carbonatitic tuffs have higher  $\delta^{13}\text{C}$  values. Contamination of the carbonatite by the Transvaal Sequence dolomite, which is the country rock, is not the prime cause for the dolomitization.

The carbonatitic fractionation from sovite to alvikite, taking only un-recrystallized samples, is best revealed by the Rare Earth elements, which show a three-fold overall increase (Fig. 2). This increase can be correlated with the increase in  $\delta^{18}\text{O}$  (Fig. 3). The early precipitation of pyrochlore caused La to act as a compatible element at first, but after the pyrochlore ceased to be precipitated, La became incompatible and the content remaining in the carbonatitic melt rose (Fig. 3). Other elements which behaved incompatibly are Ba, Zn and Mn.

Like Nb, Sr behaved as a compatible element. Sr was strongly partitioned into apatite and calcite, both of which crystallized throughout the sequence. As a result, Sr steadily decreased with fractionation of the carbonatitic melt (Fig. 4). Recrystallization of carbonatite, usually marked by increase of  $\delta^{18}\text{O}$ , caused mobility particularly of the incompatible elements, with only lesser effects on elements such as Sr.

A major late-stage event was the fluorite mineralization, and the progressive mineralization of both intrusive and extrusive carbonatites correlates with increasing values of  $\delta^{18}\text{O}$ , but with  $\delta^{13}\text{C}$  remaining constant (Fig. 1). This also correlates well with hydrothermal alteration during equilibration with ground waters at low temperatures (c. 200°C), and is taken to indicate that late-stage F-bearing fluids from the carbonatite mixed with ground water during the fluoritization.

The mineralization process, which affected the extensive carbonatitic tuffs preserved in the caldera and to a lesser extent the intrusive carbonatites, was accompanied by recrystallization of the carbonatites. The dolomitization and the mineralization are thought to be independent processes.

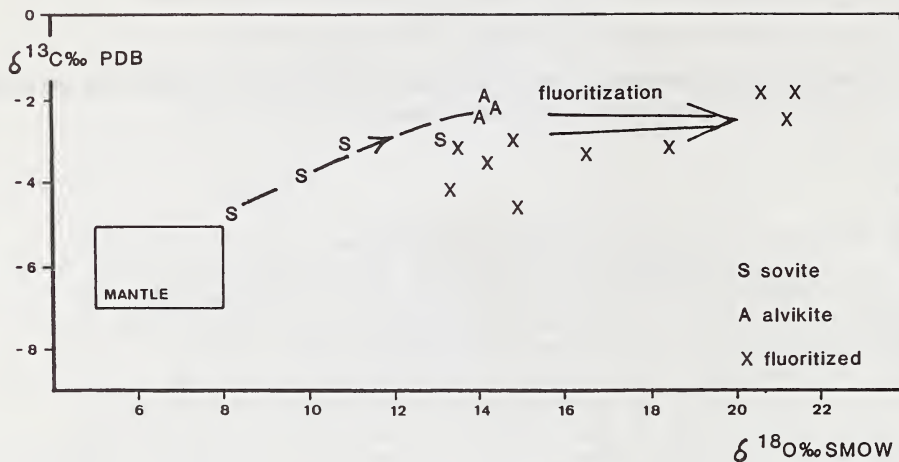


Fig. 1. Plot showing the fractionation of O and C isotopes with progressive crystallization from sovitic to alvikitic carbonatites. Arrow shows direction of increasing fluoritization in samples, all recrystallized, containing from zero to 50% fluorite.

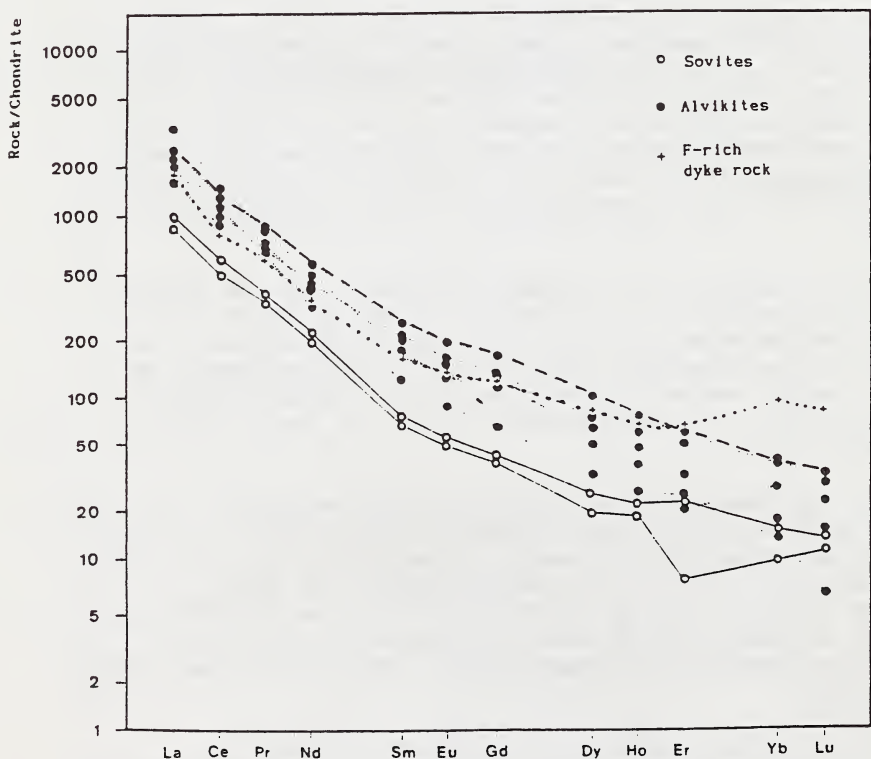


Fig. 2. Chondrite-normalized REE variation diagram showing the progressive increase in total REEs from sovite to alvikite. Fluoritization caused a lowering of the LREE/HREE<sub>n</sub> ratio. (ICP data)

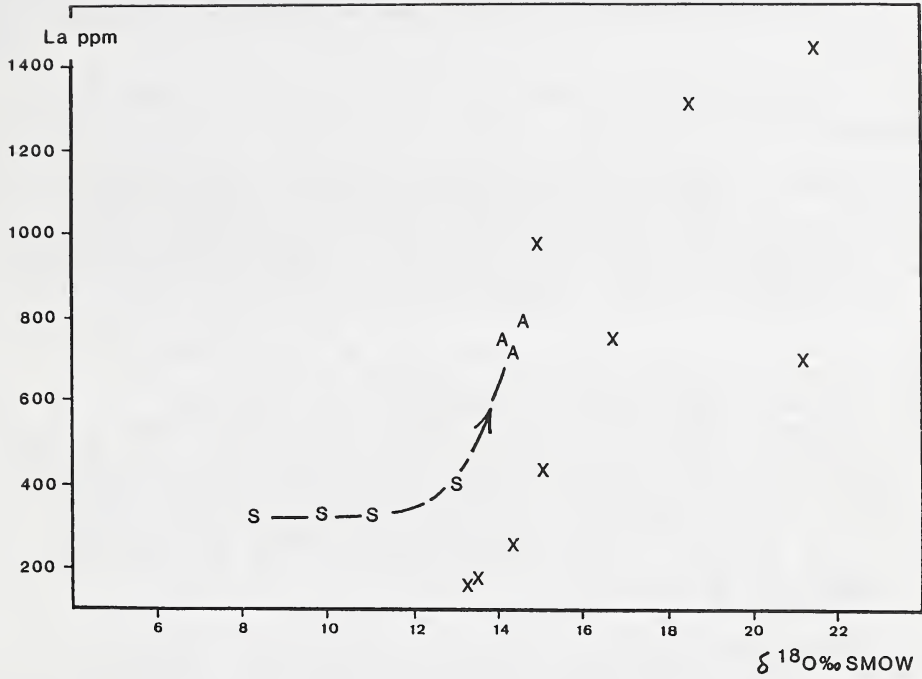


Fig. 3. Oxygen isotope - La plot showing the fractionation in the carbonatites (S and A) and the scatter caused by the fluoritization and recrystallization.

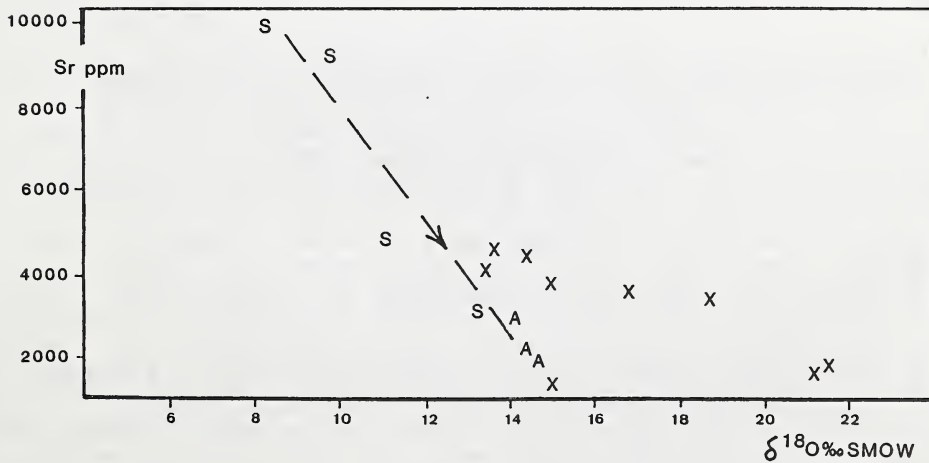


Fig. 4. Oxygen isotope - Sr plot showing the compatible behaviour of Sr during fractionation, and the dilution of Sr during late-stage fluoritization that is marked by the increase from c. 14 up to 22 per mille  $\delta^{18}\text{O}$

## GEOLOGY AND EXPLORATION OF THE KELSEY LAKE DIAMONDFEROUS KIMBERLITES, COLORADO, U.S.A.

*Coopersmith, Howard G.*

*Ashton Mining Limited, P.O. Box 1916, Fort Collins, Colorado 80522 U.S.A.*

### Introduction

A cluster of several kimberlites comprise the Kelsey Lake Project, a Joint Venture between Diamond Company NL (a Member Company of the Ashton Mining Group) and Moonstone Diamond Corporation (a private Company). These are currently being evaluated for their commercial diamond potential.

The cluster is in the northern State Line Kimberlite District of the Colorado/Wyoming Diamond Province. The cluster comprises the Schaffer, Maxwell, and Aultman kimberlite pipes. Two relatively large pipes and a few smaller bodies, termed the Kelsey Lake kimberlites, are being investigated. Various other properties in the District have been evaluated for diamond, with results ranging from zero diamonds to close to 1 carat per hundred tonne. No deposits have yet been recognized as economically viable. A location map is presented as Figure 1.

The Kelsey Lake kimberlites are depicted on Figure 2. These were in part previously referred to as the Schaffer 8 group (McCallum and co-workers). This project concentrated on the evaluation of the two largest pipes, KL-1 and KL-2. These were mapped, and sampled for kimberlite minerals and microdiamonds. Mineral chemistry was favorable for diamond occurrence. Microdiamonds and small diamonds were recovered from weathered surface samples. The bodies were drilled for delineation and mapping.

### Geology

The Kelsey Lake kimberlites form a small group of irregular shaped pipes and fissures (Figure 2). The pipes intrude Proterozoic granitic rocks of the Sherman and Log Cabin Batholiths. Shape is largely controlled by jointing in the country rock. The kimberlite intrudes 1400 my granite, contains sedimentary xenoliths of Cambrian to Early Devonian age, and is presently overlain by Pennsylvanian-Permian sedimentary formations. Isotopic ages of other kimberlites in the district are in the 390 my, or Early Devonian, range, which fit well with geological ages seen at Kelsey Lake.

The KL-1 pipe was shown to be a multiphase pipe of diatreme facies and crater facies kimberlite, with a surface area of approximately 12 acres. Pellet-rich tuffisitic serpentine kimberlite breccia occupies the southern fissure appendage of the main pipe. This was extremely rich in mantle xenocrysts, megacrysts and xenoliths. The south-central portion of the pipe contains pellet- and autolith-rich layered pyroclastic kimberlite, generally of a sandy tuff. This is significant as crater facies kimberlite had not previously been observed in State Line District kimberlites. Quantity of quartz sand and sedimentary xenolith material varied between and within layers. Very large (to 3 m)

sedimentary xenolith blocks were locally present. This zone had a moderate amount of mantle xenocrystal and xenolithic material. The main pipe, comprising the northern blow, was not sampled (or drilled) due to difficult access. The very northern edge of the main pipe contains tuffisitic serpentine kimberlite breccia with a moderate amount of mantle component.

The KL-2 pipe is a multiphase diatreme facies complex, with a surface area in excess of 8 acres. No crater facies material was noted. At least four distinct phases of tuffisitic serpentine kimberlite breccia are present. These are locally rich in mantle xenocrysts and xenoliths. Sedimentary xenolith content, size and preservation varies considerably between phases. Alteration and carbonatization is also variable. The northern part of the pipe contains abundant crustal xenoliths in excess of 1 m. Occurrence of contact breccia is indicated.

Late stage alteration and surface weathering has destroyed much of the primary mineralogy of both bodies of kimberlite. Ubiquitous phenocrystal and macrocrystal olivine is totally replaced by serpophitic or lizardite serpentine, and often later carbonatized. Groundmass diopside, perovskite, apatite and opaques are generally preserved. Groundmass serpentine and calcite may be either primary or secondary. Macrocrysts and xenocrysts of Mg-ilmenite, pyrope, spinels, phlogopite and Cr-diopside are generally preserved, as are megacrysts of Mg-ilmenite, Cr-poor titanian pyrope and sub-calcic diopside. Groundmass in autoliths and pellets is relatively fresh, and generally phlogopite-rich. Petrographically these rocks are Group 1 kimberlites.

Xenolithic material in the pipes includes upper mantle garnet peridotite, spinel peridotite, eclogite, lower crustal granulite, and crustal granitic, metamorphic and sedimentary rocks. Content and size ranges of xenolithic and megacrystal material varies widely within the pipes.

### Bulk Sample Testing

Approximately 1000 tonnes of in situ kimberlite was bulk sampled for diamond processing, roughly 500 tonnes each from the KL-1 and KL-2 pipes. Sample sites were chosen to be representative of the pipe. Sample was excavated only from definite in situ kimberlite rock below the zone of most intense surface weathering.

Sample was trucked to a contract Diamond Test Plant. The plant generally consisted of crushing, scrubbing, screening, recrushing, Heavy Media Separation, Sortex X-ray sorting and grease table circuits. Basically all 2mm to 25mm material was tested for diamond. Recovery efficiency was continually monitored. Near 100 per cent recovery was obtained.

### Diamonds

The diamonds are generally colorless. Some stones have a faint to strong brownish-pink color. The industrial stones are only partly translucent, due primarily to their multicrystalline aspect. In general, the larger stones are of better color. Diamond sizes ranged from under 0.05 carat to greater than 1 carat.

Diamond morphology is dominated by primary octahedral forms. Multicrystalline aggregates are common. Some macles are present, along with other minor forms. Resorption has modified most octahedra to tetrahedral forms, ranging from pristine octahedra to various rounded stages. Surface etching is weak to moderate. Deformation features are common, dominated by lamination lines. Broken stones are common. Differential resorption and preserved primary surface features suggest a prolonged xenolithic transport and protection.

Results and Conclusions

The Kelsey Lake kimberlites were shown to be complex pipes of diatreme facies and locally crater facies material. This is the first known occurrence of crater facies kimberlite in the province. Several phases of kimberlite are present; all represent classical Group 1 kimberlites. The pipes are typical of other State Line District occurrences, with the mantle components and diamonds being more similar to other pipes in the northern part of the District.

A first pass bulk sample diamond test was completed on the Kelsey Lake 1 and 2 kimberlite pipes. Encouraging diamonds were recovered but overall grades were low. Size, color and clarity of the diamonds are considered good. Alluvial diamond potential of the property has not yet been assessed.

Acknowledgements

Ashton Mining Limited and Moonstone Diamond Corporation are thanked for permission to perform and present this work. M.E. McCallum, G.P. Gregory and R. Baxter-Brown provided useful discussions in the field. R. Falk painstakingly described the diamonds. M.B. Burrell ably managed the field and plant operations.

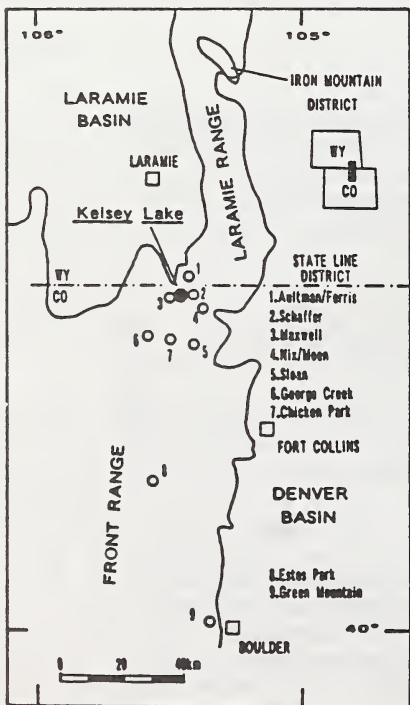


Figure 1.

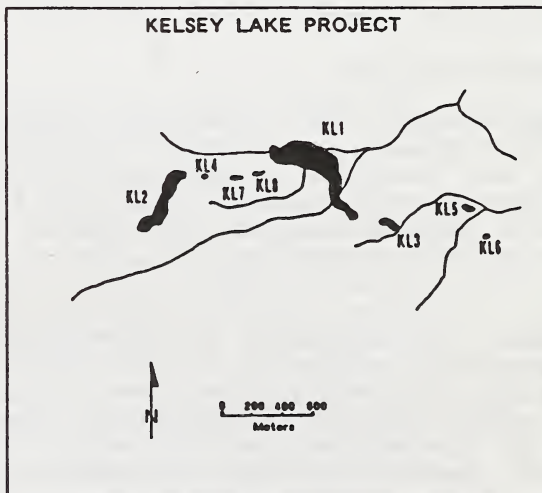


Figure 2.

## A CRYSTALLIZATION MODEL FOR PERIDOTITIC DIAMOND INCLUSION SPINELS.

Daniels, Leon R.M.\*

Dept. Geochemistry, University of Cape Town, Rondebosch 7700, South Africa.

\*Present address: Geocontracts Botswana (Pty) Ltd, Private Bag 00140, Gaborone, Botswana.

Spinel, together with olivine, is the most common diamond inclusion in Yakutia<sup>(1)</sup> and at some southern African occurrences (e.g. Dokolwayo). It has been commonly found to coexist in diamondiferous xenoliths<sup>(2)</sup> and diamonds with olivine, orthopyroxene, G10 garnets and rarely with diopside, zircon and graphite<sup>(1-5)</sup>. In both southern Africa and Yakutia similar compositional characteristics have been observed within the spinels (Table 1).

TABLE 1 - DIAMOND INCLUSION SPINELS

OXIDE (wt%)	YAKUTIA <sup>(1)</sup> (n=720)	S. AFRICA (n=134)
TiO <sub>2</sub>	< 0.7	< 0.7
Al <sub>2</sub> O <sub>3</sub>	3.5 - 7.5	2.77 - 13.9
Cr <sub>2</sub> O <sub>3</sub>	62 - 67	57.9 - 68.5
FeO	12 - 19*	4.17 - 16.4
MgO	11 - 15.5	11.1 - 18.7

\* Total Fe as FeO

Calculated equilibrium temperatures at 50 kbar for the southern African diamonds with spinel inclusions suggest subsolidus temperatures which is consistent with the temperatures calculated for diamonds from this sub-region containing silicate phases. Calculated  $fO_2$ 's at 50 kbar suggest oxygen fugacities between WM and IW.

The coexistence of the diamond inclusion-type spinels with G10 garnets suggest a common paragenesis within a subcalcic chromium-rich harzburgitic environment. It is suggested that the key to determining the paragenesis of the spinels lies in establishing the origin of the G10 garnets. In addition to the subsolidus equilibrium temperatures calculated for diamonds containing G10 garnets, the most significant characteristic of these garnets is a depletion in Ti, Fe, Ca, Y, Zr, Ga and Zn which is accompanied by an enrichment in Cr, Mg and LREE's<sup>(6)</sup>. A model of subsolidus crystallization is proposed.

The extraction of komatiitic or basaltic melts from a chondritic mantle at 2000 °C and 50-70 kbar leaves a dry spinel-harzburgite residue depleted in Ca, Ti, Y, Zr, Ca and Zn, and which is resistant to large scale melting. The olivines in the residue are forsteritic. At these temperatures and pressures the residual orthopyroxenes are Al<sub>2</sub>O<sub>3</sub> and Cr<sub>2</sub>O<sub>3</sub> enriched with low Al<sub>2</sub>O<sub>3</sub>/Cr<sub>2</sub>O<sub>3</sub> ratios (Cr<sup>\*</sup>, ± 1), Ti and Ca-depleted and contain a significant component

of dissolved garnet. Based on the behaviour of chromium and titanium in silicate melts, the spinels may be  $\text{Cr}_2\text{O}_3$  (> 55wt%) and  $\text{TiO}_2$  (average >.07 wt%) rich. Vertical subduction, driven by the stacking of successive extrusions of komatiites and Archaean ocean floor basalts<sup>(7)</sup>, results in advective thickening. LREE's, alkalis and carbon volatiles fluxing from the base of the descending slab, consisting of an undepleted sub-tectospheric mantle, metasomatizes the harzburgitic residue<sup>(8)</sup>. In the absence of garnet the LREE's will, in preference to olivine and spinel, partition into the residual orthopyroxene. The carbon volatiles remain in solution.

On cooling from 2000 °C at which the komatiite melts are extracted to a steady state geothermal temperature of 1200 °C the orthopyroxene exsolves its garnet component. The major element composition of the exsolved garnet will be dependent on the composition of the residual orthopyroxene immediately after the extraction of the komatiite melts. The Cr- and Mg-enriched nature of the unexsolved orthopyroxene will favour the formation of  $\text{Mg}_3\text{Cr}_2\text{Si}_3\text{O}_{12}$  in the exsolving garnet which, together with the depletion of the FeO, CaO and  $\text{TiO}_2$ , is consistent with major element compositional characteristics of G10 garnets. The LREE's partition from the orthopyroxenes preferentially into the garnet and consequently enrich the G10's in LREE's.

The exsolution of G10 garnets from residual orthopyroxenes will progressively deplete  $\text{Al}_2\text{O}_3$  in the pyroxene and the Cr in the exsolving garnet will gradually increase. Although the knorringite molecule in the garnet allows for greater solubility of the Cr in the garnet, the exsolution of spinels will be favoured at low  $\text{Cr}^*$  in the orthopyroxene. The predicted low  $\text{Cr}^*$  and  $\text{TiO}_2$ -depleted composition of the residual komatiite orthopyroxenes will favour the exsolution of  $\text{TiO}_2$ -poor Cr-rich spinels together with the exsolution of G10 garnets. The presence of both G10 garnets and Cr-rich spinels, depleted in  $\text{TiO}_2$ , in diamonds, xenoliths and the concentrate of diamondiferous kimberlites is consistent with the model above.

Subcalcic G10 garnets at Dokolwayo have  $\text{Cr}^* > 1.00$ . The exsolution of these garnets from the residual orthopyroxenes would deplete Al in the residual pyroxene while Cr-enrichment occurs. Spinel exsolving from the orthopyroxene will therefore become increasingly Cr-rich. This may result in zonation patterns within the spinels exhibiting increasing  $\text{Cr}_2\text{O}_3$  contents from centre to edge. Approximately fifty percent of the Dokolwayo concentrate spinels are compositionally similar to the diamond inclusion spinels and are characterized by  $\text{TiO}_2/\text{Al}_2\text{O}_3 < 0.2$ . These spinels commonly exhibit zonation patterns consistent with the model above. It should be noted that the Dokolwayo concentrate spinels with  $\text{Al}_2\text{O}_3/\text{TiO}_2 > 0.2$  show no significant evidence of  $\text{Cr}_2\text{O}_3$  zoning.

Calculated  $f\text{O}_2$  conditions suggest that the dominant carbon volatile species is  $\text{CH}_4$ . At the reigning T, P and  $f\text{O}_2$  conditions diamond crystallizes from the  $\text{CH}_4$  either through fractionation or oxidation of  $\text{CH}_4$ . Mass balancing exercises show that olivine and a small amount of orthopyroxene, depleted of garnet component, also exsolves from original Al,Cr-enriched orthopyroxene. Because diamond crystallization and the process of exsolution occur simultaneously, the

diamonds may occlude the exsolved minerals. The syngenetic relationship between diamonds and their primary inclusions suggests that the processes of exsolution and diamond crystallization occur simultaneously.

## References

- (1) Sobolev, N.V. et al. (1989). Chrome spinels coexisting with Yakutian diamonds. 28th Int. Geol. Cong. Wash., Ext. Abstr., Workshop on Diamonds, 105-108.
- (2) Sobolev, N.V. et al. (1984). Xenoliths of diamond-bearing peridotites in kimberlites and the problem of diamond origin. *Geol. Geofiz.*, 25, 63-80.
- (3) Daniels, L.R.M. and Gurney, J.J. (1989). The chemistry of the garnets, chromites and diamond inclusions of the Dokolwayo kimberlite, Kingdom of Swaziland. In: Ross, J., Jaques, A.L., Ferguson, J., Green D.H., O'Reilly, S.Y., Danchin, R.V., Janse, A.J.A., Eds., *Kimberlites and Related Rocks, Volume 2: Their Mantle/Crust Setting, Diamonds and Diamond Exploration*, GSA Spec. Publ. No 14, Blackwell Scientific Publications, 1012-1021.
- (4) Gurney J.J. et al. (1979). Silicate and oxide inclusions in diamonds from the Finsch kimberlite pipe. In: Boyd, F.R. and Meyer, H.O.A., Eds., *Kimberlites, Diatremes and Diamonds, Their Geology, Petrology and Geochemistry*. A.G.U., Washington, 1-15.
- (5) Gurney, J.J. et al. (1984). Minerals associated with diamonds from the Roberts Victor Mine. In: Kornprobst, J., Ed., *Kimberlites II: Their Mantle and Crust-mantle relationships*. Develop. in Petrology 11B, Elsevier, Amsterdam, 25-32.
- (6) Richardson, S.H. et al. (1984). Origin of diamonds in old enriched mantle. *Nature*, 310, 198-202.
- (7) De Wit, M.J. and Tredoux, M. (1988). PGE in the 3.5 Ga Jamestown Ophiolite Complex, Barberton Greenstone Belt, with implications for PGE distribution in simatic lithosphere. In: Pritchard, H.M., Potts, P.J., Bowles, J.F.W. and Cribb, S.J., Eds., *Geo-Platinum 87*, 319-341.
- (8) Jordan, T.H. (1988). Structure and formation of the continental tectosphere. *J. Petrol.* 29, 11-37.

## THE GEOLOGY OF THE M1 KIMBERLITE, SOUTHERN BOTSWANA.

*Daniels, \*L.R.M.; Jennings, \*\*C.M.H.; Lee, J.E.; Blaine, J.L.; Billington F.R.; and Cumming B.C.*

*Falconbridge Explorations (Botswana) (Pty) Limited, P.O. Box 1463, Gaborone, Botswana.*

*\*Present address: Dept. of Geochemistry, University of Cape Town, Rondebosch 7700, South Africa.*

*\*\*Present address: Repadre Capital Corporation, Suite 1900, 120 Adelaide Street West, Toronto MSH 1T1, Canada.*

The M1 kimberlite, 40 km southwest of Tshabong in southern Botswana, is the largest in a field of 37 kimberlites. With a surface area of 180 hectares it may be the largest kimberlite discovered to date. It has a U-Pb zircon age of 77.5 My which was determined from several fragments of a single zircon.

The kimberlite is covered by approximately 80 m of Kalahari sediments and was initially detected from an aeromagnetic survey with 500 m line spacing. The aeromagnetic anomaly produced by the kimberlite is a broad feature approximately 2000 x 1000 m in plan with an amplitude of 70 nTesla. A gravity survey over the aeromagnetic target produced a gravity low anomaly which flattened across the centre, suggesting the presence of crater-fill epiclastics.

Seven different lithologies were identified in the M1 kimberlite:

- g) Ablation Facies
- f) Epiclastic Mudstone Facies
- e) Gravel-Grit-Mudstone Facies
- d) Mudstone-Phlogopite Siltstone Facies
- c) Breccia-Mudstone Facies
- b) Tuffaceous Facies
- a) Intrusive Facies

A model for the geological history of the kimberlite has been reconstructed from an interpretation of the different facies, their igneous or sedimentary features and their distribution within the pipe. The model is summarised as follows:

- 1) No root zone material was intersected. The features of this zone are therefore unknown.
- 2) The crater was formed by explosive breakthrough from a depth in excess of 500 m. Repeated intrusive/eruptive cycles continued for an unspecified period of time giving rise to a thick pile of tuffisitic kimberlite breccias and the building of an extensive tuff cone on the perimeter of the crater.
- 3) A late stage kimberlite sill, characterised by abundant olivine, calcite and ilmenite with minor perovskite was emplaced within the tuff beds in the southeast of the crater after the cessation of the main igneous activities.
- 4) The crater gradually filled with water. Destabilisation of the tuff cone together with slope failure occurred resulting in gravity slumps of tuff cone material into the water-filled basin which gave rise to debris flows and turbidite-like deposits.

5) The tuff cone was eventually eroded into stabilised tuff hills surrounding the crater. In a generally moist climate, as indicated by the fern and podocarp pollen spores in the mudstone-phlogopite siltstone facies, small streams removed the fine and the light fractions from the tuff hill, leaving behind the coarser and heavier fraction of material. The fine sediment was deposited in the lake as varved mudstone-phlogopite siltstone couplets.

6) A shallowing of the basin and a change in the climate to a more arid period, probably characterised by thunderstorms and flash floods, occurred. The resultant high energy streams deposited the coarser and heavier material from the remaining tuff hills in alluvial fan-type deposits characterised by poorly-sorted immature gravels and grits showing moderately developed stratification. The crater sediments in the upper 40 m exhibit a facies change from an alluvial fan association to a proximal association and finally to a distal association from the southeast to the northwest of the crater.

7) A continued change in climate to a dry environment occurred. Fine mudstones were deposited in a few shallow, localised pans.

8) With the onset of a very dry climate the wind winnowed out light material from the surface while heavy material was deposited as an eluvial concentration on the ablation surface.

9) The Kalahari Formation covers the kimberlite crater and associated sediments.

10) Bioturbation transports kimberlite indicator minerals to the surface.

**BULK AND MINERAL CHEMISTRY OF THE OLIVINE LEUCITITE FROM JUANA VAZ,  
SACRAMENTO, MINAS GERAIS, BRAZIL.**

*José Caruso Moresco Danni<sup>(1)</sup>; Nilson Francisquini Botelho<sup>(1)</sup>; João H. Grossi Sad<sup>(2)</sup>.*

*(1) Depto. Mineral and Petrol. – Univ. Brasília; (2) Inst. Geoc., Univ. Fed. Minas Gerais.*

The olivine leucitite from Juana Vaz, Sacramento, Minas Gerais State, Brazil, is the first occurrence of leucitite bearing volcanic rock recognized in continental Brazil (Murta, 1965, 1966; Guimarães, 1966). The occurrence was discovered during a prospection program for bentonitic clay. It is located 40 km southeasterly of the town of Sacramento, at the border of a plateau named "Chapadão dos Bugres."

The rock occurs on a deep clayey soil (up to 60 meters) originated by weathering of tuffs and pyroclastic breccias of the Mata da Corda Formation. The rock occurrence may represent a lava flow unit situated at the base of pyroclastic rocks.

The olivine leucitite is black, aphanitic, and presents a micro-prophiritic texture. It is essentially composed by olivine (33% in volume), leucite (20,4%), diopside (24,1%), phlogopite (7,0%), magnetite + ilmenite (9,7%), perowskite (1,7%), apatite (1,0%), and interstitial glass (3,1%).

Diopside forms prismatic crystals arranged around sub-circular crystals of leucite (0.2 mm), which shows multiple complex twins. Ilmenite, magnetite and perowskite have tendency to form skeletal crystals (0,1 - 0,05 mm). The interstitial glass is brown in color and have acicular inclusions (apatite?).

The crystallization order is: olivine, leucite, diopside, apatite + oxides + perowskite, phlogopite, and glass. This is in agreement with the sequence of crystallization experimentally obtained by Foley, (1985) to perpotassic liquids (lamproitic) on low fO<sub>2</sub> condition (MW buffer).

Olivine xenocrystals are zoned with Mg richer cores (Mg/Mg+Fe=0,90) than borders (0,86). Euhedral and corroded phenocrysts present very constant Mg/Mg+Fe ratios (0,86), and relatively high values of CaO (0,4 to 0,6 wt%). Clinopyroxenes have very constant Mg:Fe:Ca ratios corresponding to diopside with Mg/Mg+Fe = 0.89. Characteristically they are Si and Al deficient, needing Fe<sup>3+</sup> to complete the tetrahedral positions. The TiO<sub>2</sub> content (2,3 to 2,6 wt%) is distinct from diopsides from other ultrapotassic rocks (0,7 to 2,4 wt%) (Barton, 1979; Mitchell, 1985). Their Al and Na contents are closer to clinopyroxenes from the Leucite Hills rocks than the Toro Ankole diopsides. Leucite has a composition very similar to the ideal formula, except by a little deficiency in silicon (0,03 cation/unit), that is compensated by the entry of Fe<sup>3+</sup> in tetrahedral site. Contrary to leucites from Toro Ankole, they are very poor in sodium, i.e. without kalsilite exsolutions. Phlogopites have high contents in BaO (2,3 to 3,4 wt%) and present Si and Al deficiency (0,55 to 0,48 atoms per formula unit). They have compositions similar to the kamafugitic phlogopites and are very distinct from the lamproitic and kimberlitic phlogopites (Mitchell, 1985). In a MgTiO<sub>3</sub>, FeTiO<sub>3</sub>, and Fe<sub>2</sub>O<sub>3</sub> plot, the ilmenites fall in the kimberlitic field and present MgO values (8,5wt%), higher than the lamproitic ones. Apatites are fluor, Ba, and REE bearing, and present a P<sup>4+</sup> deficiency, due probably to a substitution of the type: Ca+P = REE + Si. Perowskite shows high contents of BaO (2,7 - 4,0wt%), La, Nd,

and Sm oxides (2,5wt%), and carry 0,9 wt% of Na<sub>2</sub>O. The brown interstitial glass is very poor in SiO<sub>2</sub>, Na, and K (leucite depleted), rich in Al and probably H<sub>2</sub>O. Fe, Mg and Ti are relatively concentrated in it. A CIPW norm composition results in olivine, hypersthene, orthoclase, anorthite and corindon. This leucitite is an ultrabasic (SiO<sub>2</sub> - 40wt%), perpotassic (K<sub>2</sub>O/Na<sub>2</sub>O > 2,5), sub-aluminous rock, with MgO/MgO+FeO (moleculas proportion) of 75. It presents simultaneously high concentration in transitions elements (Ti, Ni, Cr, Co) and in LIL elements (K, Rb, Ba, Sr, Nb, Zr). These features, common to others kamafugitic rocks, are characteristic of primary liquids, probably derived from low grade partial fusion of an enriched peridotitic mantle with phlogopite and K-richterite, (Foley et al., 1987). In view of the above features and due to the abundance of olivine leucitites in the volcanic pile of the Mata da Corda Formation (Seer and Moraes, 1988), this rock can represent one of the primary magmas that originated the volcanic alkaline Alto Paranaíba Province.

**Rock chemistry (1 and 2), CIPW norm and Interstitial glass composition (3)**

Oxides	1	2	3	1ppm	1	2
SiO <sub>2</sub>	40.89	39.37	37.25	Sc - 17.1	or 7.4	-
TiO <sub>2</sub>	4.06	4.20	2.90	V - 208	an -	3.5
Al <sub>2</sub> O <sub>3</sub>	4.56	5.36	11.50	Cr -1366	le 6.9	12.5
FeO <sup>T</sup>	12.69	12.38	10.58	Co - 69	ne 4.4	3.2
MnO	0.16	0.37	0.07	Ni -1034	di 19.4	11.9
MgO	22.23	25.70	20.27	Pb - 8.7	hd 5.2	2.7
CaO	7.01	6.55	0.76	Th - 9.4	fo 32.5	41.0
BaO	0.12	-	-	Ga - 12.2	fa 10.9	11.6
SrO	0.12	-	-	Sr - 944	cs -	2.2
Na <sub>2</sub> O	1.01	0.71	0.19	Ba -1481	il 7.7	8.0
K <sub>2</sub> O	2.74	2.70	2.45	Rb - 167	ap 1.7	1.3
P <sub>2</sub> O <sub>5</sub>	0.70	0.56	-	Nb - 77	DI 18.7	15.7
LOI	1.93	2.10	13.8*	Zr - 384		
TOT	98.22	98.00	100.00	Ce - 97		
				Y - 17.2		
				Yb - 2.55		
				La - 88		

(2) after Murta, 1966. \* Calculated by difference.

**Bibliography**

- Barton, M., 1979 - A comparative study of some minerals occurring in the potassium-rich alkaline rocks of the leucite Hills, Wyoming, the Vico volcano, Western Italy, and the Toro Ankole region, Uganda, N.Jb. Min. Abh. 137. 113-134.
- Foley, S.F., 1985 - The oxidation state of Lamproitic Magmas, IMPM Tschermaks Min. Petr. Mitt. 34, 217-238.
- Foley, S.F., Venturelli, G., Green, D.H., Toscani L., 1987 - The ultrapotassic rocks: characteristics, classifications, and contrants for Petrogenetic models, Earth Sci. Rev. 24, 81-134.
- Guimarães, D. 1966 - Idade do Ugandito de Sacramento, M.G., pelo método da birrefringência, Bol. Inst. Geol. EFMOP, V.1 no. 3,4, 107-159, Ouro Preto, MG.

- Ladeira, E.A., Brito, O.E.A., 1968 - Contribuição à geologia do Planalto da Mata da Corda, An. XXII Cong. Bras. Geol., v.2, p. 181-199, Belo Horizonte, MG.
- Mitchell, R.H., 1985 a Review of the mineralogy of lamproites. Trans. Geol. Soc. Africa, 88, 411-437.
- Murta, L.L.R. 1965 - Nota sobre a rocha leucitítica de Sacramento, Minas Gerais, Rev. Cienc. Cult. V. 17, no. 2, p. 135, São Paulo, SP.
- Murta, L.L. R. 1966 - O vulcanito leucitítico de Sacramento, Minas Gerais, Bol. Inst. Geol., EFMOP, v. 1 no. .. 13-20, Ouro Preto, MG.
- Seer, HJ.J., Moraes, L.C., 1988 - Estudo Petrografico das rochas ígneas alcalinas da região de Lagoa Formosa, MG., REV. Bras. Geoc., v. 18, nO. 2, 134-140, São Paulo, SP.

## A NON COGNATE ORIGIN FOR THE GIBEON KIMBERLITE MEGACRYST SUITE.

G.R. Davies<sup>(1)</sup>; A.J. Spriggs<sup>(2)</sup>; P.H. Nixon<sup>(2)</sup> and D.C. Rex<sup>(2)</sup>.*(1) Department of Geological Sciences, The University of Michigan, Ann. Arbor, MI 48109; (2) Department of Earth Sciences, University of Leeds LS2 9JT, U.K.*

The Gibeon kimberlite province, Namibia, occupies an area 100 by 80 km centered at 25°30'S and 18°E. In excess of 60 kimberlite pipes are known, and they tend to occur in NNE-SSW trending clusters. The kimberlite province is underlain by circum cratonic basement stabilized circa 2.1 Ga. Undersaturated volcanism in Namibia defines an approximate SW-NE lineament. Several workers have proposed that post-Karoo igneous activity in Namibia results from the migration of the Discovery and Vema hotspots beneath Namibia from 85 to 60 and 60 to 40 Ma respectively (e.g. Hartnady and Le Roex 1985). However, age determinations of the magmatic events have until now been poor precluding a rigorous assessment of this hypothesis.

Petrographically unaltered kimberlite samples were obtained from four drill cores that penetrated kimberlite pipes of hyperbyssal facies. Core samples were coarsely crushed and crustal and mantle xenolithic material removed. The petrology of each pipe is variable implying either a heterogeneous magma or that each pipe contains several different intrusions. Garnet and clinopyroxene megacrysts were collected from 7 diatreme facies kimberlites. Samples for isotope analysis were selected on the basis of their unaltered nature. The aim is to ensure that alteration has not disrupted parent-daughter relationships and that the megacrysts have not interacted with the host kimberlite which has trace element contents several orders of magnitude higher than the megacrysts. All megacrysts were crushed, sieved and washed prior to hand picking under liquids and subsequently ultrasonically leached in 6M HCl. Sr isotope analyses were not performed on garnet megacrysts due to their extremely low Rb and Sr contents (<0.1 ppm) which makes them susceptible to alteration.

Previous workers (e.g. Mitchell, 1987) have established that Namibian diopside and garnet megacrysts have large compositional ranges and concluded that as a whole the megacryst suite is generated by cumulate processes during the fractional crystallization of several batches of magma. Each kimberlite pipe in the Gibeon Province has its own characteristic megacryst suite which may form two or more populations indicating a non-genetic origin.

In order to compare the Sr-Nd-Pb isotope systematics of the kimberlite and megacrysts the time of kimberlite eruption must be known to  $\pm 10$  Ma. Macrocystic phlogopites were separated from the kimberlite and leached in 2M HCl for 10 minutes to remove any carbonate and have  $^{87}\text{Rb}/^{86}\text{Sr}$  ratios that range from 6.7 to 92.7 and  $^{87}\text{Sr}/^{86}\text{Sr}$  from 0.7106 to 0.7879. Three Rb-Sr mica-whole-rock ages range from 71.2 to 71.6 Ma (one sample from an altered kimberlite yields an age of 64 Ma). Reid et al. (1990) recently reported a K-Ar age for the adjacent Gross Brukkaros alkaline complex of  $77 \pm 2$  Ma and a Rb-Sr mica age of  $68 \pm 2$  Ma, ages that bracket our proposed kimberlite eruption age of 71.5 Ma.

The four kimberlite pipes have considerable variation in initial Sr and Nd isotope ratios;  $\epsilon_{\text{Nd}}$  + 1.6 to +4.0;  $\epsilon_{\text{Sr}}$  -14 to +10. These data are comparable to group I kimberlites (e.g. Smith, 1983) to which the Namibian kimberlites have strong whole-rock chemical affinities. Pipe K2 has comparable Nd isotope ratios but higher  $^{87}\text{Sr}/^{86}\text{Sr}$  ratios that trend to values more radiogenic than Group I kimberlites. Compared to other Namibian kimberlites and Group I kimberlites K2 is characterized by higher Ba, Rb, Sr, K and P concentrations. These characteristics are not a consequence of crustal interaction, a process that would produce lower concentrations of Sr, Nb, P and LREE. The style of trace element enrichment (e.g., higher K/Nb, K/Ti and Ba/Nb) is similar to, although less extreme than, Group II kimberlites which are also generally characterized by relatively radiogenic  $^{87}\text{Sr}/^{86}\text{Sr}$  (Fraser et al., 1985).

Present day and initial Pb isotope ratios of Namibian kimberlites are characterized by relatively high  $^{207}\text{Pb}/^{204}\text{Pb}$  and  $^{208}\text{Pb}/^{204}\text{Pb}$  ratios comparable to Group I kimberlites. Pipe K2 is again transitional towards Group II kimberlite compositions in having less radiogenic

$^{206}\text{Pb}/^{204}\text{Pb}$ . All Namibian kimberlites have high  $\mu$  and  $\kappa$  values (50 to 80, 220 to 310). On a  $^{207}\text{Pb}/^{204}\text{Pb}$  vs  $^{206}\text{Pb}/^{204}\text{Pb}$  diagram initial Pb isotope ratios of all the kimberlites define an array with a slope sub-parallel to some S. Atlantic ocean islands (e.g. Bouvet). As a whole the initial Pb data of the kimberlites plots between the fields of S. Atlantic islands. Clinopyroxene megacrysts have a restricted range in initial Sr and Nd isotope ratios ( $\epsilon_{\text{Nd}}$  2.8 to 4.7,  $\epsilon_{\text{Sr}}$  -10 to -18).  $\epsilon_{\text{Nd}}$  values are generally higher and  $\epsilon_{\text{Sr}}$  lower than the host kimberlites. On a Sr-Nd isotope covariation diagram the megacrysts plot close to, or slightly below, the 'mantle array'. Only a clinopyroxene megacryst from the Deutsch Erde pipe plots within the field of Namibian kimberlites. The clinopyroxene megacrysts define three distinct groups; 1) Mukarob, ii) Hanaus and Koherab, iii) Deutsch Erde. Clinopyroxenes from these three regions show significant inter-group REE variation implying geographic variations in the source of the megacrysts.

The clinopyroxene megacrysts have large variations in Pb isotope ratios (e.g.  $^{206}\text{Pb}/^{204}\text{Pb}$  18-19.5) and are characterized by relatively elevated  $^{207}\text{Pb}/^{204}\text{Pb}$  and  $^{208}\text{Pb}/^{204}\text{Pb}$  such that they plot above the NHRL. These data define approximate linear arrays with a relatively restricted range in  $^{207}\text{Pb}/^{204}\text{Pb}$  but large variations in  $^{206}\text{Pb}/^{204}\text{Pb}$  and  $^{208}\text{Pb}/^{204}\text{Pb}$ . Measured U/Pb ratios of the clinopyroxene megacrysts are low compared to the host kimberlite ( $\mu=1$  to 22). Initial  $^{207}\text{Pb}/^{204}\text{Pb}$  and  $^{206}\text{Pb}/^{204}\text{Pb}$  are distinct from the kimberlites but are comparable with continental flood basalts from Namibia and Brazil (Hawkesworth et al., 1986).

The Sr-Nd-Pb isotope disequilibrium between the megacrysts and host kimberlites palpably rules out a simple cogenetic relationship. Previous workers have noted apparent Sr-Nd isotope disequilibrium but have either ascribed the isotopic differences to minor alteration or erected models that invoke the early precipitation of the megacryst suite from a 'proto-kimberlitic' melt followed by compositional change in the melt due to fractional crystallisation and assimilation (e.g. Jones 1987).

These models are very difficult to reconcile with several aspects of kimberlite chemical and isotopic compositions. First the chemical compositions of kimberlites record little evidence of the extraction of the megacryst suite. Fractionation of olivine would rapidly deplete the magma in MgO and Ni, spinels Ni and Cr, clinopyroxene fractionation deplete Sc, garnet fractionation deplete Sc and HREE. The LREE concentration of liquids calculated to be in equilibrium with the megacryst suite are at least a factor of 2 lower than the host kimberlite. In order to produce a two-fold increase in LREE concentrations requires the fractionation of 50% of the melt assuming that La is perfectly incompatible. Even if fractional crystallisation was coupled with significant assimilation of peridotite, the calculated degrees of fractionation appear too high to produce a liquid with a kimberlitic composition.

The topology of the Sr-Nd-Pb isotope diagrams helps to constrain possible source components in megacryst and kimberlite genesis. Sr/Nd ratios of most mantle derived magmas are within the range 10 to 20 (excluding subduction related volcanism) such that mixing lines between components on a Sr-Nd isotope diagram are close to straight lines. In terms of their Sr-Nd isotopes the kimberlites and megacrysts could be explained through some form of mixing process that involves a relatively depleted source (MORB or OIB component) and an enriched component (DUPAL-OIB). The Mukarob megacryst samples have relatively unradiogenic Sr isotope ratios such that they have characteristics transitional toward HIMU and EM1 ocean islands (e.g. St Helena and Cape Verde). On Pb/Pb diagrams the megacryst suite forms arrays sub-parallel to some Atlantic ocean islands and has relatively high  $^{207}\text{Pb}/^{204}\text{Pb}$  and  $^{208}\text{Pb}/^{204}\text{Pb}$  ratios that are more extreme than Atlantic ocean islands with the 'DUPAL' isotope signature (e.g. Gough, Walvis Ridge and Cape Verde). In contrast HIMU islands generally have radiogenic  $^{206}\text{Pb}/^{204}\text{Pb}$  and relatively low  $^{207}\text{Pb}/^{204}\text{Pb}$  and  $^{208}\text{Pb}/^{204}\text{Pb}$ . Consequently the Sr-Nd-Pb isotope systematics of the megacryst suite are only comparable to continental flood basalts from the Parana and Karoo.

The Gibeon kimberlite volcanism occurred between 7 and 10 Ma after the passage of the Discovery hotspot (Hartnady and Le Roex, 1985). The kimberlites contain coarse garnet lherzolite xenoliths that, on the basis of geobarometry, were derived from the base of the lithosphere at 150 km. If kimberlite volcanism were the product of a plume it would occur as the plume past beneath the region not 7 to 10 Ma later. Initial Sr-Nd-Pb ratios of the kimberlites are different from Discovery and not simply related by the incorporation of MORB-like mantle into the plume suggesting there is no simple genetic relationship. The

similar ages do, however, suggest some form of relationship and we propose that heat transfer from the hotspot has caused melting of the asthenosphere-lithosphere boundary layer. This boundary layer which is in contact with the convecting asthenosphere will have a Sr-Nd-Pb isotope composition typical of the ambient regional mantle. The kimberlites have initial Sr-Nd-Pb ratios similar to an average composition of the S. Atlantic ocean islands whose hotspot traces have passed beneath southern Africa (Gough, Bouvet, Shona and Tristan) compatible with melting of the asthenosphere-lithosphere boundary layer that has been modified by periodic hotspot related magmas.

The megacryst suite crystallised in the lithosphere from an alkali basalt derived from an asthenospheric source with isotope characteristics comparable to S. Atlantic islands such as Bouvet and Ascension. Due to the low trace element contents of the 'cumulates' they record evidence of variable equilibration with 'DUPAL-like' sub-continental lithosphere that was the source of Karoo volcanism. The product has relatively high Sm/Nd and low m and Rb/Sr so that with time the suite records growth in radiogenic  $^{143}\text{Nd}$  but little change in Sr and Pb isotope ratios. The megacryst suite was probably formed by the hotspot related activity that is thought to produce the Karoo-Parana flood basalts. The Gibeon Group 1 kimberlites were produced later and their higher trace element contents record less evidence of interaction with the lithosphere and consequently have less 'DUPAL' signature. The exception being K2 which assimilated lithosphere with a 'DUPAL' signature and fractionated to produce kimberlites with a more evolved major element composition.

Sr-Nd-Pb isotope analyses were also performed on unaltered material from three non-kimberlite localities; Dikker Willem carbonatite ( $49 \pm 1$  Ma, Reid et al., 1990), Schwarzeberg nephelinite ( $30 \pm 1$  Ma) and the Blue Hills monticellite peridotite associated with the Gross Brukkaros carbonatite (68-77 Ma, Reid et al., 1990). All samples plot below the mantle array on a Sr-Nd isotope diagram, the Dikker Willem carbonatite being the most divergent. The Blue hills and Schwarzeberg samples have Sr-Nd isotope systematics comparable to the group 1 Namibian kimberlites. All the alkaline volcanics have very radiogenic initial  $^{208}\text{Pb}/^{204}\text{Pb}$  and  $^{207}\text{Pb}/^{204}\text{Pb}$  ratios so that they plot above the NHRL and the Gibeon kimberlites and megacrysts on Pb-Pb diagrams. The alkaline volcanism is characterised by  $\mu$  values higher than the kimberlites (125-150). The Pb isotope signatures are more radiogenic than the Etendeka volcanism. However, age correction to 121 Ma, the time of Etendeka volcanism, lowers  $^{208}\text{Pb}/^{204}\text{Pb}$  and  $^{207}\text{Pb}/^{204}\text{Pb}$  ratios to values comparable to Etendeka-Parana volcanism. Alkaline volcanism occurred between 5 and 30 My after the passage of the Vema and Discovery hotspots. The large apparent SCL signature recorded by the volcanism is consistent with conduction of heat from the plumes into the lithosphere causing melting. Preliminary conduction modelling suggests that following the passage of a plume the bottom 10 to 20 km of the lithosphere will be heated by circa  $50^\circ\text{C}$  within 10 My consistent with Namibian alkaline volcanism being derived from the lithosphere.

Fraser K.J., Hawkesworth C.J., Erlank A.J., Mitchell R.H. and Scott-Smith B.H. 1985. Sr,Nd and Pb isotopes and trace elements of lamproites and kimberlites. *Earth Planet. Sci. Lett.* 76, 57-70.

Hartnady C.J. and Le Roex A.P. 1983. Southern Ocean hotspot tracks and the Cenozoic absolute motions of the African, Antarctic and South American plates. *Earth Planet. Sci. Lett.* 75, 245-57.

Hawkesworth C.J., Mantovani M.S.M., Taylor P.N. and Palacz Z. 1986. Evidence from the Parana of south Brazil for a continental contribution to Dupal islands. *Nature* 322, 356-59.

Jones R.A. 1987. Sr and Nd isotopic and REE evidence for the genesis of megacrysts in kimberlites of southern Africa. In Nixon P.H. *Mantle Xenoliths*.

Mitchell R.H. 1987. Megacrysts in kimberlites from the Gibeon field, Namibia. *Neues Jahrbuch Miner.* 157, 267-283.

Reid D.L., Cooper A.F., Rex D.C. and Harmer R.E. 1990. Timing of post-Karoo alkaline volcanism in southern Namibia. *Geol. Mag.* 127, 427-433.

Smith C.B. 1983. Pb, Sr and Nd isotopic evidence for sources of southern African Cretaceous kimberlites. *Nature* 304, 51-54.

## THE PETROGENESIS OF METASOMATISED SUB-OCEANIC MANTLE BENEATH SANTIAGO: CAPE VERDE ISLANDS.

*Davies, <sup>(1)</sup>G.R. and Mendes, <sup>(2)</sup>M.H.*

*(1)Department of Geological Sciences, University of Michigan, Ann Arbor, MI 48109; (2)Centro de Geologia, Inst. Investigação Científica Tropical Alameda D. Alfonso Henriques, 41 Lisbon, Portugal.*

The Cape Verde Islands are the surface manifestation of a large oceanic plateau and are situated approximately 500 km west of the Senegalese coast of Africa. All nine major islands include highly undersaturated volcanic rocks including larnite normative melilites. Carbonatites are reported from 6 islands, including Santiago. The islands are situated near the pole of rotation of the African plate which has resulted in semi-continuous volcanism since the early Tertiary. Ultramafic xenoliths are common in volcanics on several Cape Verde Islands. This study is confined to Santiago where abundant xenoliths, up to 30 cm across, occur in Cenozoic olivine nephelinite, basanite and olivine basalt. The xenoliths comprise three lithological groups; 1) spinel lherzolite; 2) dunite; 3) wehrlite. The spinel lherzolite suite has allotriomorphic-granular textures. Olivine (Fo88-91) and orthopyroxene (Wo 0.5 En 91.4 Fs 8.1 to Wo 3.4 En 85.0 Fs 11.6) are anhedral deformed grains (up to 1 cm). Clinopyroxene (Wo 39.8 En 53.1 Fs 7.1 - Wo 48.5 En 46.7 Fs 4.8) up to 3 mm, is anhedral chrome-diopside and contains exsolved spinel blebs and orthopyroxene. Intergranular domains consisting of glass and euhedral to subhedral fine-grained olivine (0.4 mm), diopside and chrome spinel are relatively common. In addition some glassy zones which contain phlogopite and carbonate are interpreted as local partial melts probably formed by decompression.

The dunite suite has allotriomorphic-granular textures with anhedral and deformed olivine grains. Olivines have more Fe-rich compositions than the lherzolite-harzburgite suite (Fo 84-89). Wehrlites typically possess igneous textures with poikilitic clinopyroxene enclosing olivine and spinel. Deformed olivine has similar composition to the dunite suite. Clinopyroxene compositions are more iron-rich than those of the dunitic and harzburgite-lherzolite suites.

The Cape Verde lherzolite xenoliths show little petrological or chemical evidence of secondary alteration ( $H_2O < 1\%$ ). The lherzolites define an inverse relationship between CaO,  $Al_2O_3$ ,  $TiO_2$  and  $Na_2O$  with MgO content comparable to trends defined by other xenolith assemblages (e.g., Maaloe and Aoki, 1977). These chemical variations are accompanied by systematic changes in mineral compositions (e.g. Fo in olivine). Therefore, despite petrological evidence of metasomatism the lherzolites retain chemical evidence of melt extraction. Several trace elements (Co, Cr, V, Ni, Sc) show systematic variations as a function of MgO. By utilizing the known partitioning of Fe/Mg and Ni between peridotite residuals and melts it is possible to calculate the degree of melt extracted from a peridotite. The least metasomatized lherzolites require the extraction of between 15 and 28% melt. Calculated melt compositions are comparable to picritic compositions proposed as primary MORB compositions (e.g., Elthon, 1979).

The lherzolite xenoliths that have undergone the greatest apparent metasomatism have lower MgO and higher CaO and  $Na_2O$ . Notably there appears little increase in  $Al_2O_3$  content with modal metasomatism which implies that either the fluid had low  $Al_2O_3$ , or that no  $Al_2O_3$  bearing phases were produced. The presence of metasomatic amphibole, phlogopite, spinel and carbonate, indicates that the metasomatic fluid was highly silica undersaturated possibly melilititic or carbonatitic in composition. The dunite and wehrlite xenoliths have suffered minor metasomatism. Compared to the lherzolites xenoliths the dunites have higher Cr, FeO, Co and  $TiO_2$  and lower Ni,  $Al_2O_3$ , Sc and V contents consistent with a cumulate origin. The major and trace element variations of the dunite-wehrlite suite establish they represent the cumulate products of a fractionating magma involving the precipitation of spinel, olivine and clinopyroxene.

The dunites have low REE contents,  $(Yb)_n = 0.5$ , that are characterized by slight LREE enrichment  $(Ce/Yb)_n = 4$ . The wehrlites have higher REE abundances than the dunites  $(Yb)_n = 1-3$ . Wehrlite REE patterns are characteristic of many other pyroxene-rich xenoliths (Irving, 1980) being characterized by MREE enrichment with a maximum at Nd and relative depletion in La and Ce. This REE distribution is compatible with precipitation of a clinopyroxene-rich cumulate from LREE enriched magma (e.g., Irving, 1980). Using published REE partition coefficients it is possible to calculate the REE content of the magma parental to the pyroxenites. These calculations indicate  $(Ce/Yb)_n$  ratios of parental magmas between 8 and 12 comparable to the least undersaturated Cape Verde magmas.

The lherzolite xenoliths have highly variable REE abundances ( $Yb$ )<sub>n</sub> 0.8-2, ( $Ce$ )<sub>n</sub> 0.9-19. Xenoliths depleted in terms of their major element abundances have the lowest HREE contents and are characterized by MREE depletion. Despite the major and trace element evidence for a residual origin the LREE are markedly enriched, ( $Ce/Sm$ )<sub>n</sub> 3.5-7.3 defining a "v" shaped pattern. In contrast the four xenoliths that show petrographic evidence for the greatest metasomatism have relatively simple LREE enriched patterns. As with the wehrlite samples, La and Ce enrichment is less marked than expected from the slope of the middle REE. The "v" shaped REE patterns of the lherzolites requires the involvement of two processes in their petrogenesis. HREE depletion and lower MREE abundances implies that the xenoliths originated as residues following partial melting. Subsequent LREE enrichment was superimposed on a LREE depleted pattern. Assuming that the lherzolite xenoliths were initially LREE depleted comparable to a MORB-like source it is possible to calculate the approximate REE composition of the material added to each xenolith. The calculated fluids have ( $Ce/Yb$ )<sub>n</sub> ratios greater than 50. This extremely high degree of LREE enrichment is only found in the most undersaturated melilitites and carbonatites among the Cape Verde volcanics. Xenoliths that have suffered the greatest degree of metasomatism record increased HREE abundances. If we again assume derivation from a MORB-like source, it is possible to estimate the nature of the metasomatic fluid. In contrast to the "depleted" lherzolite, the addition of melilitites or carbonatites would result in greater LREE enrichment than observed. Approximately 10% basanite addition is required to explain the REE patterns. The metasomatic fluids are less LREE enriched than those that produced the "depleted" xenoliths.

In order to fully evaluate the petrogenesis of Santiago ultramafic xenoliths the isotopic variations of the host volcanism must be known (see Davies et al. (1989) plus refs therein). Sr-Nd isotope ratios of the northern islands are less depleted than Atlantic MORB (0.7029-0.7032; 0.5130-0.5129) and on a Sr-Nd isotope diagram plot below the "mantle array" between MORB and HIMU islands. On a Sr-Nd isotope diagram the southern islands define a slope that is steeper than the "mantle array" extending from the field of the northern islands (0.7032-0.7039; 0.5129-0.5126). Rocks from Santiago have significant Sr-Nd isotope heterogeneity and encompass almost the entire range defined by the southern islands. Pb isotope ratios also form two geographically controlled groups. The northern islands define arrays that plot on the NHRL on both  $^{207}Pb/^{204}Pb$  v  $^{206}Pb/^{204}Pb$  and  $^{208}Pb/^{204}Pb$  v  $^{206}Pb/^{204}Pb$  diagrams with  $^{206}Pb/^{204}Pb$  between 19.14 and 19.77. The youngest volcanism in the northern islands generally has the most depleted Sr-Nd-Pb isotope ratios. The southern islands have generally less radiogenic Pb isotope ratios ( $^{206}Pb/^{204}Pb$  19.44 to 18.74) and are characterized by relatively high  $^{207}Pb$  and  $^{208}Pb$  such that they plot above the NHRL. Although less extreme, the southern islands are characterized by Sr, Nd and Pb isotope ratios similar to Hawaii and Walvis Ridge (EMI).

The Cape Verde xenolith suite records significant Sr-Nd isotope variation. On a Sr-Nd covariation diagram samples plot below the 'mantle array' with Nd isotope values ranging from close to Bulk Earth to almost MORB, 0.51269-0.5130. These data plot within the field defined by Cape Verde volcanism. The Santiago xenoliths most depleted in terms of major elements plot within the field of the northern Cape Verde Islands. The xenoliths have significant Pb isotope variation ( $^{206}Pb/^{204}Pb$ , 18.7-19.3) that extends to  $^{206}Pb/^{204}Pb$  values less radiogenic than Cape Verde volcanism. In terms of a  $^{207}Pb/^{204}Pb$  v  $^{206}Pb/^{204}Pb$  diagram there is considerable overlap with the field defined by the southern islands. However, on a  $^{208}Pb/^{204}Pb$  v  $^{206}Pb/^{204}Pb$  diagram only the four xenoliths that have the greatest trace element enrichment plot in the field of the southern islands. The two "depleted" samples with the most extreme "v" shaped REE patterns plot on the NHRL with values close to or within the field defined by the northern islands.

An important conclusion to be made from the Sr-Nd-Pb isotope ratios of the xenoliths is that they are different to the Santiago volcanics proving that the xenoliths are not simply the product of, or the source to the volcanism. Mixing relationships on Sr-Nd-Pb diagrams establish that at least three isotopically distinct components are involved in the petrogenesis of the xenoliths; components from the northern and southern islands and a MORB-like component. Sr-Pb and Nd-Pb isotope variation diagrams show that over half of the xenoliths have isotope systematics distinct from the host lavas of Santiago. The two wehrlite xenoliths have Sr-Nd-Pb isotope systematics compatible with formation from the lavas of Santiago. Coupled with the major and trace element relationships, these isotope relationships prove that the wehrlites are products of Santiago volcanism. Lherzolite xenoliths with the greatest trace element enrichment (28,27) also have Sr-Nd-Pb systematics that are indistinguishable from Santiago volcanism suggesting that the trace elements of the lherzolites dominated by a metasomatic component derived from Santiago volcanism. Four xenoliths (29,42,41 and 34) represent mixtures between a MORB residue and Santiago volcanism. The mixing relationships on Pb-Pb and Pb-Sr isotope diagrams imply that both the precursor MORB source and the metasomatic component are isotopically heterogeneous such that no single mixing lines are evident. Two "depleted" xenoliths with the most LREE enrichment (30,39) appear to represent mixtures between MORB-like and northern island

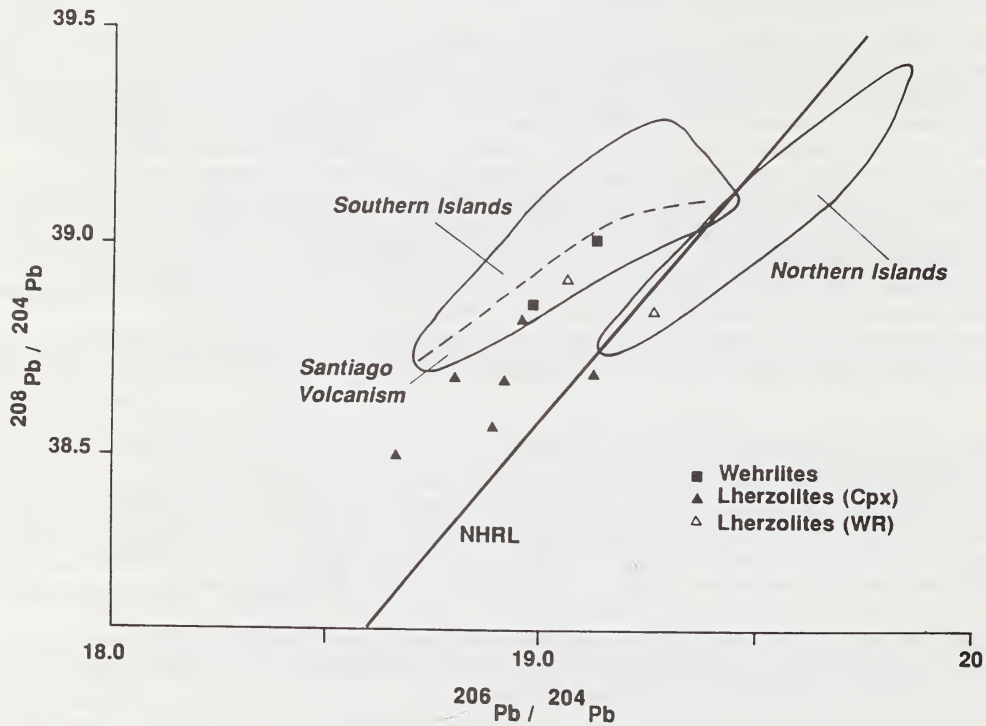
components. The extreme LREE enrichment and relatively high CaO imply that the metasomatic fluid was a carbonatite. No isotope data are available for carbonatites from the southern island. However, we expect that all Cape Verde carbonatites come from a similar source and hence have isotope systematics comparable to the northern Cape Verde islands.

Davies, G.R., Norry, M.J., Gerlach, D.C. and Cliff, R.A. (1989) A combined Pb-Sr-Nd isotope study of the Azores and Cape Verde hot-spots: the geodynamic implications. In Saunders and Norry M.J., Eds., *Magmatism in the Ocean Basins*. Geol. Soc. Lond. Spec. Pub. 42, 231-255.

Elthon, D. (1979) High magnesia liquids as the parental magma for ocean floor basalts. *Nature* 570, 514-18.

Irving, A.J. (1980) Petrology and geochemistry of composite ultramafic xenoliths in alkalic basalts and implications for magmatic processes within the mantle. *Amer. J. Sci.* 280, 349-426.

Maaloe, S and Aoki, K. (1977) The major element composition of of the upper mantle estimated from the composition of lherzolites. *Contrib. Mineral. Petrol.* 63, 161-73.



PERALKALINE PLUTONIC MAGMATIC ROCKS OF THE CARBONATITE VOLCANO  
OLDOINGYO LENGAI.

Dawson, <sup>(1)</sup>J.B.; Smith, <sup>(2)</sup>J.V; and Steele, <sup>(2)</sup>I.M.

(1)Dept. Geology and Geophysics, Univ. Edinburgh, Edinburgh EH9 3JM, UK; (2)Dept. Geophysical Sciences, Univ. Chicago, I11 60637, USA.

Coarse-grained blocks in the nephelinitic and phonolitic tuffs and agglomerates of the active carbonatite volcano Oldoinyo Lengai, Tanzania, include xenoliths of metasomatic crustal and mantle rocks (felses and olivine-mica-pyroxenites) and igneous cumulates (Dawson, 1989). The igneous suite comprises jacupirangites, alkali pyroxenites, ijolites and nepheline syenites; there are also blocks of sovite, sanidine-calcite rock and nepheline wollastonite. Most rocks have cumulate textures, though a few nepheline syenite, ijolite and wollastonite specimens have a resorbed texture suggesting derivation from dykes or contacts; with the exception of the jacupirangites, many specimens are cellular and cemented by vesicular intergranular glass.

Mineralogically, the suite consists of clinopyroxene, nepheline, titanomagnetite, pyrrhotite (all rock types), Ti-andradite and wollastonite (in ijolites), perovskite and phlogopite (in ijolites and jacupirangites), sanidine, euclite and titanite (in nepheline syenites). The pyroxenes have resorbed cores, and oscillatory-zoned overgrowths, indicating a complex crystallisation history but overall show a trend from diopsides in jacupirangites and resorbed cores in ijolites, to aegerine- and hedenbergite-rich types in nepheline syenites and overgrowths in ijolites; the trend indicates increasing  $Fe^{2+}/(Fe^{2+}+Mg)$  and increasing  $Fe^{3+}/(Fe^{2+}+Fe^{3+})$  in the more alkali-rich syenites. Nephelines are in the range Ne<sub>70-80</sub> Ks<sub>14-22</sub> Qz<sub>2-12</sub>, the only noticeable differences between rocks being higher Qz in syenite nephelines; Fe<sub>2</sub>O<sub>3</sub> concentrations are mainly in the range 1-2 wt% but 5.2 wt% is found in nepheline in a nepheline-wollastonite-glass vein. Garnets are Ti-andradites (schorlomite+andradite = ~90% of total), containing <1% MgO and <0.1 wt% Cr<sub>2</sub>O<sub>3</sub>, and many have light-coloured rims containing less TiO<sub>2</sub>, FeO, and MgO, but higher SiO<sub>2</sub>, Fe<sub>2</sub>O<sub>3</sub> and MnO than dark coloured cores; Na<sub>2</sub>O is present in small but persistent amounts (0.20-0.37 wt%). The micas are Ti-phlogopites; the most magnesian (mg .86) occurs in reaction rims around xenocrystal olivine, whereas the most iron-rich (mg .58) is groundmass mica in ijolite. Wollastonite is CaSiO<sub>3</sub> except for around 1 wt% FeO. The "magnetite" is magnesian magnetite-ulvospinel with around 20% Fe<sub>2</sub>O<sub>3</sub> molecule in solid solution; the phase in jacupirangite is more magnesian and aluminous than that in ijolite or nepheline syenite. The syenite feldspars are mainly sanidine (Ab<sub>15-32</sub>, Or<sub>67-85</sub>) though almost pure albite (Ab<sub>99</sub> Or<sub>1</sub>) occurs in one specimen; the sanidines contain up to 0.83 wt% Fe<sub>2</sub>O<sub>3</sub>. Intergranular glasses are enriched in SiO<sub>2</sub>, total FeO, MnO, Na<sub>2</sub>O and K<sub>2</sub>O relative to bulk rocks. Perovskites have significant concentrations of FeO (up to 1 wt%), Na<sub>2</sub>O (up to 1.2 wt%) and Nb<sub>2</sub>O<sub>5</sub> (up to 2.2wt.%) LREE (up to 5 wt% in jacupirangite perovskite). The apatites contain up to 0.5 wt% REE. Titanite contains up to 0.3 wt% REE,

significant  $ZrO_2$  (up to 1.2 wt.% and  $Na_2O$  up to 2.2 wt.%. REE partitioning is perovskite >apatite >titanite. Compared with corresponding phases occurring as phenocrysts in the nephelinite-phonolite lava suite (Donaldson et al. 1987) those in the plutonic suite show some differences, e.g. the volcanic feldspars are  $Or_{43-57}Ab_{39-53}$ , nepheline extends to more potassic compositions ( $Ks_{26}$ ) but most are compositionally similar, in particular the zoning in pyroxenes and garnets.

Bulk chemical analyses show that the overall suite is silica-undersaturated and highly evolved with agpaitic indices ( $Na + K/Al$ ) ranging from 0.50 (jacupirangite) to ~ 1 (ijolite) and 1.78 (eucolite nepheline syenite). They contain high concentrations of LILE, and the light REE concentrations are high both absolutely and relative to heavy REE, particularly in perovskite-apatite-rich jacupirangite. Calcite carbonatite is enriched in Sr (6200 ppm) and Ba (9000 ppm). Chemically the ijolites and nepheline syenites are richer in  $CaO$ ,  $TiO_2$ , total Fe and  $MgO$  but lower in  $Al_2O_3$ ,  $K_2O$  and  $Na_2O$  than nephelinites and phonolites of equivalent  $SiO_2$  content, reflecting the higher modal contents of perovskite, pyroxene and apatite relative to nepheline and feldspar in the plutonic rocks. Perovskite-magnetite-pyroxene fractionation of parental ijolite can give rise to jacupirangite and nepheline syenite.

Analytical work has been supported by N.S.F. and N.E.R.C., and our inter-institutional cooperation has been made possible by travel grants from N.A.T.O.

Dawson, J.B. (1989 ) Sodium carbonatite extrusions from Oldoinyo Lengai Tanzania: implications for carbonatite complex genesis. In K. Bell, Ed., Carbonatites: genesis and evolution, p. 255-277, Unwin Hyman, London.

Donaldson C.H., Dawson, J.B., Kanaris-Sotiriou, R., Batchelor, R.A. and Walsh, J.N. (1987). The silicate lavas of Oldoinyo Lengae, Tanzania. Neues Jhb. Mineral. Abh., 156, 247-279.

## SHEAR ZONE CONTROL OF ALKALI INTRUSIVES – EXAMPLES FROM ARGYLE AND WEST AFRICA.

Deakin, <sup>(1)</sup>A.S.; and White, <sup>(2)</sup>S.H.

(1)Argyle Diamond Mines, P.O. Box 508, Kununurra, Western Australia, 6743; (2)Dept. Geology, Univ. Utrecht, P.O. Box 80.021, 3508 TA Utrecht, Netherlands.

### Introduction

The large scale regional controls of alkali intrusions have been given spasmodic attention in the literature. There is a tendency to associate the kimberlite pipes in West Africa with the landward extension of oceanic transform systems (Williams and Williams, 1977; Sykes, 1978). The argument is that the transforms first formed during the initiation of rifting by the reactivation of old major continental structures which were then mimicked within the developing oceanic crust. The resultant transforms may change direction during the formation of the oceanic crust as the rift direction changes. As a consequence there need not be parallelism between the oceanic transform and its continental parent. The corollary of the above is that there is an association between major continental shear or fault zones that form fundamental zones of weakness in the continental crust and alkali intrusives. This can also be illustrated by the lamproites in the Kimberley area of Western Australia (Jaques et al., 1986). The Argyle pipes located within the Halls Creek Mobile Zone, another major zone of continental weakness. A question that remains is, what are the local structural controls for the emplacement of diamondiferous alkali intrusives. We have selected two areas where there is a clear local structural control to emplacement, viz. Argyle, Western Australia and Yengema, Sierra Leone, and show that at a local scale these intrusions are located by second or third order structures within major first order planes of weakness in the continental crust.

### Proposed Structural Controls of the Argyle Pipe Emplacement

The Argyle pipe occurs within the Halls Creek Mobile Zone. This mobile zone along with the King Leopold Zone form the two major tectonic entities bordering the Kimberley Block in north-western Australia. White and Muir (1989) have recently argued that they formed a coupled, orthogonal tectonic system since the Early Proterozoic. They produce evidence that the King Leopold Zone mainly acted as a zone of vertical tectonics (extensional and compressional) which has been supported by additional observations by Tyler and Griffith (1990) and that the Halls Creek Mobile Zone mainly acted as a strike slip transfer zone to the vertical movements in the King Leopold Mobile Zone. It was during a phase of sinistral transfer movement during the late Proterozoic that local basin formation and the emplacement of the Argyle pipe occurred.

The individual faults (second order structures) in the Halls Creek Mobile Zone form a Reidel geometrical shear array based on the Halls Creek Fault and the Greenvale Fault as the main D-shears. Their geometries and kinematics are consistent with a late Proterozoic sinistral movement (Plumb, 1968; White and Muir, 1989). The Argyle pipe occurs in an area which was dominated by normal and Reidel faults and a dilational bend in the adjacent Halls Creek Fault. The fault interactions resulted in a local pull-apart type basin in which late Proterozoic sediments were deposited and the pipe emplaced.

At the local scale, the pipe is situated adjacent to the dilational intersection of the northerly trending Gap Fault, a dilational R-shear within the sinistral Reidel scheme, and the Razor Ridge Fault. The latter

is a dextral X-shear or conjugate shear within the Halls Creek Mobile Zone. A swarm of lamproitic dykes, the Lissadell Road dykes, are associated with it in the exposed basement. The dykes were emplaced along tension and R-shear gashes. Neither the Gap Fault nor the Razor Ridge Fault is a major fault, both are third order faults or shears. However, the area in which the dykes and pipe has been intruded is a major dilational area created by second order shears within a fundamental continental shear zone.

#### Proposed Structural Controls of Kimberlite Emplacement; Yengema

The Yengema field, centred on the town of Koidu in Sierra Leone, has been the main diamond mining centre in West Africa. The region contains swarms of kimberlite dykes and several small pipes.

A strong north-south foliation is present in the migmatitic Archaean basement. Prominent lineaments occur trending at  $010^\circ$ . The kimberlite dykes are confined between two such lineaments, the Oyie-Shongbo Fault in the west and the Yaamba fault in the east, and strike at  $070^\circ$ . They occupy a zone some 22km long by 10km wide. Other minor kimberlite dykes occur aligned at  $030^\circ$  and  $045^\circ$ . Only rarely are kimberlite dykes located on the main  $010^\circ$  lineaments.

The  $070^\circ$  trending dykes are discontinuous, lensic and often occur en-echelon. Horizontal slickensides are occasionally apparent on the walls of the dykes but measurable displacement of structures across the dykes is minimal. Movement must therefore have been limited. The  $070^\circ$  structures are minor structures. A substantial zone of joints trends in this direction. Outside of the fault-bounded Shongbo-Yaamba fault block these joints do not contain kimberlite.

The orientation of these structures conform to a Reidel array corresponding to movement in a dextral sense along the main  $010^\circ$  bounding faults. The principal  $070^\circ$  dyke direction is an antithetic strike-slip ( $R_1$ ) structure with sinistral movement. The  $030^\circ$  and  $045^\circ$  dykes are related to synthetic (R) shears and tension gashes respectively. Both of these structures are poorly-developed compared to the main dyke direction.

Lineaments trending at  $130^\circ$  and  $160^\circ$  are also evident and indistinct  $115^\circ$  structures occur. Dolerite dykes of probable Early Mesozoic age intrude these structures and are cut by the Upper Cretaceous kimberlite dykes.

The main stress field operating as a result of dextral movement along the regional  $010^\circ$  faults caused structures with strikes in the  $030^\circ$ - $070^\circ$  direction to be in extension and these structures were filled with kimberlite to varying degrees. Structures in the  $130^\circ$ - $160^\circ$  direction were in compression and thus did not provide avenues for the intrusion of kimberlite.

Under a simple dextral shear stress regime, the most favourable sites for kimberlite emplacement are theoretically at the extensional intersections of the  $010^\circ$ ,  $030^\circ$ ,  $045^\circ$  and  $070^\circ$  structures. However, the situation is complicated by the presence of other pre-existing lines of weakness oriented at  $115^\circ$ ,  $130^\circ$  and  $160^\circ$ . In the field, pipe location is broadly related to intersections of  $010^\circ$  and  $130^\circ$  structures with the  $070^\circ$  kimberlite dyke orientation.

#### Conclusions

The controls of kimberlite/lamproite emplacement at Argyle and Yengema show similar characteristics. In both areas, ancient, prominent lineaments were reactivated. Diamondiferous primary orebodies are locally governed by extensional lower order structures which form part of a regional Reidel shear array, rather than the main bounding faults of the array.

References

- Jaques, A.L., Lewis, J.D. and Smith, C.B. The kimberlites and lamproites of Western Australia. Geol. Surv. Western Australia, Bull. 132, 268 pp. (1986).
- Plumb, K.A., Lissadell, W.A. 1:250,000 Geological Series Bur. Miner. Resour. Aust. Sheet SE/52-2 (1968).
- Sykes, L.R. Intraplate seismicity, reactivation of pre-existing zones of weakness, alkaline magmatism and other tectonism postdating continental fragmentation. Revs. Geophysics and Space Physics, 16, 621-689 (1978).
- Tyler, I.M. and Griffin, T.J. Structural development of the King Leopold Orogen, Western Australia. J. Struct. Geol. 12, 703-714 (1990).
- White, S.H. and Muir, M.D. Multiple reactivation of coupled orthogonal fault systems: an example from the Kimberley region in northern Western Australia. Geology, 17, 618-621 (1989).
- Williams, H.R. and Williams, R.A. Kimberlites and plate tectonics in West Africa. Nature 270, 501-508 (1977).

## MODEL SIMULATIONS OF CARBON ISOTOPE VARIABILITY IN THE MANTLE.

*Deines, P.**Department of Geosciences The Pennsylvania State University, University Park, PA 16802.*

The  $\delta^{13}\text{C}$  sampling frequency distributions of kimberlitic diamonds from southern Africa and Russia are indistinguishable. The summary distribution for the two continents may have thus broader significance and has been used to test geochemical models that can be proposed to explain carbon isotope variations in the mantle. The distribution has a weighted mean of -7 ‰, a major mode at -5.5 ‰, is highly skewed towards negative  $\delta^{13}\text{C}$  values, and may have a minor second mode between -15 and -19 ‰. Hence it differs significantly from the normal  $\delta^{13}\text{C}$  distributions of carbonatite and kimberlite carbonates whose means and modes all coincide at -5.5 ‰.

Chemical fractionation models which allow for changes in pressure, temperature, oxygen fugacity, and depletion of a carbon reservoir can explain systematic variations of  $\delta^{13}\text{C}$  of a few ‰. However, they are not capable to account for the very high negative skewness of the diamond  $\delta^{13}\text{C}$  distribution.

Subduction of sedimentary, organic carbon has been considered as a cause for the existence of  $^{13}\text{C}$  depleted diamonds. The consequences of such a process have been examined with the aid of models simulating isotope exchange and mixing. Because at this time no evidence has been presented for an isotopic composition difference between the crustal and mantle carbon reservoir the mean isotopic composition of the subducted carbon is assumed to be -7 ‰. The extent to which the carbon isotopic composition of the sedimentary end members (organic carbon  $\delta^{13}\text{C} = -25$  ‰, limestones  $\delta^{13}\text{C} = 0$  ‰) are preserved or altered through isotope exchange and homogenization during subduction is unknown. It has been assumed in the model that the retention of the endmember isotopic compositions is as probable as the establishment of any intermediate isotopic composition through isotopic exchange. The only restriction assumed is that the weighted mean isotopic composition of the carbon compounds remained -7 ‰. The volume over which the carbon isotopic composition is homogenized during subduction is also important for the resulting  $\delta^{13}\text{C}$  sampling distribution. If the volume is very small it is more likely that the extreme sedimentary carbon isotopic compositions are retained in the mantle, if the volume is very large the weighted mean value of -7 ‰ must be attained. The model was set up so that varying degrees of homogenization over a variable range of volumes could be examined.

Over 100 different combinations of exchange and homogenization scales have been studied. Emphasis was placed on an examination of those models which would most closely simulate the relative abundance of the low  $\delta^{13}\text{C}$  diamonds which have been proposed as indicators of subducted carbon. The results have been compared with the summary diamond  $\delta^{13}\text{C}$  distribution.

Those model  $\delta^{13}\text{C}$  distributions which have the highest abundance of low  $\delta^{13}\text{C}$  diamonds and at the same time an abundance at the major mode which matches that of the observed diamond distribution, predict lower relative abundances of  $^{13}\text{C}$  depleted diamonds than actually observed. Models which predict correctly the observed relative abundance of low  $\delta^{13}\text{C}$  diamonds predict, however, also that there should be 50% fewer diamonds with the isotopic composition of the major mode, and a very much higher abundance of diamonds of isotopic compositions between 0 and -3 ‰ than is actually found.

In all cases the mode of the model distribution occurs at -7 ‰, rather than at -5.5 ‰. The success to match more than one feature of the model distribution with the observed

diamond distribution has been limited. The model computations suggest that if the low  $\delta^{13}\text{C}$  diamonds were to be the result of subduction of reduced sedimentary carbon that this carbon would be subducted in preference to carbonate carbon. Consequently a difference in the carbon isotopic composition between crustal and mantle carbon reservoirs would have to be postulated.

Models simulating the effect of the removal of  $^{13}\text{C}$  enriched  $\text{CO}_2$  from the mantle as a result of degassing have also been constructed. The fractionation factor for such a process can be deduced from the skewness of the diamond  $\delta^{13}\text{C}$  distribution. The estimate ( $\alpha = 1.0038$ ) is much larger than expected on the basis of known isotope effects and recent experiments. A large number of model frequency distributions were investigated, using different assumptions for the initial reservoir isotopic composition, reservoir variability, and fractionation factor. It was found to be impossible to match all major features of any of the model distributions with those of the observed diamond  $\delta^{13}\text{C}$  distribution.

The  $\delta^{13}\text{C}$  variability of diamonds has probably multiple causes which may include: 1. chemical isotope effects related to temperature, pressure, and oxygen fugacity; 2. reservoir depletion effects; 3. existence of carbon isotope reservoirs of differing isotopic composition which could remain from accretion or be introduced by subduction. It is unlikely that any one of these causes alone can produce the observed diamond carbon isotopic composition distribution. The relative importance of the various causes remains to be established.

If the limited data we have accumulated to date on the  $^{13}\text{C}$  depletion of asthenospheric South African diamonds would reflect a general mantle feature, one could propose that the mantle is for several reasons heterogeneous in  $\delta^{13}\text{C}$ , and that with increasing depth the relative abundance of low  $\delta^{13}\text{C}$  carbon increases. This concept could explain: 1. the common mode in  $\delta^{13}\text{C}$  of carbonatite and diamond carbon isotopic compositions; 2. the significant difference in mean  $\delta^{13}\text{C}$  between carbonatites (-5.5) and diamonds (-7 ‰); 3. a higher relative abundance of  $^{13}\text{C}$  depleted asthenospheric diamonds; 4. the common features of diamond and meteorite  $\delta^{13}\text{C}$  distribution; and 5. the apparent difference in the mean carbon isotopic composition of meteorite and mantle carbon. The proof of this type carbon isotope distribution within the mantle - which would have to be established through further work - would significantly alter our concepts of the geochemical cycle of carbon.

## THE GEOLOGY OF THE MENGYIN KIMBERLITES, SHANDONG, CHINA.

*P.N. Dobbs<sup>(1)</sup>; D.J. Duncan<sup>(1)</sup>; S. HU<sup>(2)</sup>; S.R. Shee<sup>(3)</sup>; E.A. Colgan<sup>(4)</sup>; M.A. Brown<sup>(4)</sup>; C.B. Smith<sup>(5)</sup> and H.L. Allsopp<sup>(5)</sup> (deceased).*

*(1)Sino-British Cooperation, Dalian, China; (2)7th Geological Brigade, Linyi, Shandong, China; (3)Stockdale Prospecting, South Yarra, Australia; (4)Chichester Diamond Services, London; (5)Bernard Price Institute of Geophysical Research, University of the Witwatersrand, Johannesburg, RSA.*

The Mengyin kimberlite province was discovered in 1965 by geologists of the Shandong Bureau of Geology. Kimberlites Shengli 1 and 2 and Hongqi 1 were subsequently mined for diamonds. Further detailed prospecting between 1986 and 1988, including re-analysis of some of the historical data, shed new light on the mineralogical and petrological nature of the kimberlites, their age and structural setting and also found unusual features in the diamond population.

The kimberlites are located within the He-Huai block of the North China sub-plate, 80 to 100km west of the Tanlu fault, a major NNE-trending fracture that separates Archaean granite-gneiss of the 2 500Ma Taishan Formation in the west of Shandong from the Jiaodong Group, of early Proterozoic age, in the east. Between 520km and 740km of sinistral displacement is indicated for the Tanlu fault, with significant episodes of movement occurring in the Middle Proterozoic and Mesozoic. There are three zones of kimberlites (Changma, Xiyu and Poli) within a NNE-trending belt some 50 km long and 17.5 km wide. Their present structural setting is on the SE flank of a major NE-trending arch, which has been subjected to SSW reverse faulting along listric structures. The tectonic regime that prevailed in the Ordovician is less clear, but the Tanlu fault must by then have formed the eastern margin of the western Shandong terrain.

Each zone consists of many small en echelon dykes, with a dextral orientation. The maximum recorded width for a dyke is 3m at Hongqi 1, while average widths are usually 20 to 40cms. Hongqi 1 is also the longest dyke, at 1.4km. The Poli zone contains only very narrow dykes of limited extent. Clusters of small pipes of irregular shape occur in the central parts of the Changma and Xiyu zones. Drilling to 600m by 7th Brigade showed that the pipes coalesce below the present surface and become more dyke-like, with strong NNE strikes and NW-trending apophyses. Dip angles for pipes and dykes are usually steeper than 70°. An internal dyke is exposed in the open pit at Shengli 1, but the ages of the other dykes, relative to the age of the pipes, are unknown. A kimberlite sill occurs at the southern end of the Xiyu zone, Hongqi 23, and dips approximately 45° to the WNW. Most kimberlites intrude the Archaean gneiss, but the dykes in the Poli zone and those at the southern end of the Xiyu zone have Cambrian to Middle Ordovician limestone wall rock.

Hongqi 1 dyke was mined in an underground operation to a maximum depth of 90m along a strike length of 900m and an average width of 0.7m. Between 20 000 and 30 000 carats were recovered at an approximate mining grade of 80 carats per 100 tons. Shengli 1 has been mined since 1975 in an open-cast operation at a rate of approximately 30 000 tons per year. The grade of this deposit varies between 80 and 120

carats per 100 tons. The largest stone recovered from the Mengyin mine was a yellowish octahedron, weighing 119.01 carats, although three stones of 96.04, 124.27 and 158.97 carats were recovered from alluvial deposits, 130km to the southeast of Mengyin, that may have been derived from the Mengyin kimberlites.

Evaluation sampling of the kimberlites showed that, within each kimberlite zone, the diamond grade varies by between one and two orders of magnitude. There is an overall decline in grade from south to north within both the Changma and Xiyu zones, with a tendency for the central pipe clusters to contain the highest values of 10 carats per cubic metre.

The intrusions are root zone hypabyssal facies Group I kimberlites. Rare examples of tuffisitic kimberlite breccia are found, but these are thought to represent sub-surface fluidisation in the early stages of pipe formation. Kimberlite wall rock breccia, containing Archaean gneiss xenoliths up to 1m across occurs at Shengli 1 and Hongqi 6 and 8. Dykes contain more aphanitic kimberlite than the pipes and show much less mineralogical and textural variation. Present evidence suggests erosion is within the deep root zone.

Hypabyssal kimberlites are predominantly macrocrystic with a fine grained, uniform, granular to felty interlocking groundmass. They consist of abundant altered olivine macrocrysts and phenocrysts set in a groundmass of monticellite, phlogopite, opaque minerals, perovskite, apatite, serpentine and carbonate. Phlogopite and apatite are notably more abundant than in most southern African kimberlites and monticellite in Hongqi 6 reaches 0.1mm in size, while in southern African localities this mineral is typically 0.02mm

Hongqi 6 contains an unusual rock type with a globular texture which may be produced by mechanical rounding during emplacement of a partially consolidated magma. This differs from the globular-segregatory texture that occurs in southern African kimberlites.

Unusual rock types include a clinopyroxene and phlogopite-rich kimberlite breccia and volatile-rich cross-cutting veins. The former variety occurs in Hongqi 6 and Shengli 1 and is thought to be produced by extensive resorption of country rock fragments. Late stage volatile-rich veins of apatite and serpentine occur in Hongqi 6. These infiltrate the kimberlite groundmass and modify the original mineralogy, suggesting volatiles were trapped in deep-seated intrusions.

Systematic heavy mineral sampling of 26 of the kimberlites showed that pyrope and chromite abundances vary substantially over the kimberlite province and also within the Changma and Xiyu zones. The Changma zone contains pyrope and chromite in similar quantities and grain counts decline from south to north. In the Xiyu zone these two minerals are both less abundant than at Changma, but chromite is an order of magnitude more abundant than pyrope. Too few samples were collected from the Poli zone for trends to emerge but chromite is abundant while pyrope is rare.

Clinopyroxene is rare in the +0.5mm concentrates, although smaller grains are commonly seen in thin section. Ilmenite is present in most samples, but is unusually rare for Group I kimberlites. A crichtonite group mineral of the lindsleyite - mathiasite (LIMA) suite occurs in abundance at Hongqi 27, but such grains are not sufficiently widespread for use as prospecting indicators.

The mineral chemistries of the main heavy minerals are consistent with the diamondiferous nature of the province. Pyrope is mainly the low-TiO<sub>2</sub> peridotitic variety, with some discrete and high-TiO<sub>2</sub> types. Subcalcic peridotitic pyrope is common. Both low and high-TiO<sub>2</sub> chromite is present and diamond inclusion compositions are found.

Radiometric dating of macrocrystic mica from the Shengli 1 and Hongqi 1 kimberlites using the Rb-Sr technique gave an age range of 450 to 500 Ma with a current best estimate of 475 Ma. This result is supported by additional age determinations, made by J W Bristow, using the U-Pb ion-probe method on perovskite from the Shengli 1 kimberlite. This gave a mean age of 456 +/- 8 Ma. There appeared to be no detectable difference in the ages of Shengli 1 and Hongqi 1.

A production parcel of diamonds mined from the Shengli 1 open pit were examined by J W Harris in 1986. A total of 1200 diamonds in six sieve classes were classified. A distinctive feature is an increase in the proportion of octahedral shapes in the smaller size ranges, being the reverse of the trend found in other studies. Octahedra, dodecahedra and flattened dodecahedra together form a relatively constant 20% in each sieve class, which may indicate a single diamond population. This implies also that the larger stones have been preferentially released and resorbed by the kimberlite magma. Macles make up 30%, on average, of each sieve class and brown stones constitute 80% of the population; both these features are unique. Syngenetic inclusions in diamonds from Shengli 1 are predominantly peridotitic.

The Mengyin kimberlites are petrographically and mineralogically similar to the kimberlites at Fuxian in Liaoning Province, 550km to the northeast. The latter were dated using the Rb-Sr technique on macrocrystic phlogopites, which produced a reliable isochron age of 461.7 +/- 4.8 Ma. The two kimberlite provinces are therefore coeval.

However, the Fuxian bodies intrude Proterozoic sediments, which are rare at Mengyin, and they occur on the opposite side of the Tanlu fault. It seems that the blocks on either side of the Tanlu fault had substantially different histories from some time during the Proterozoic to at least the early Palaeozoic and may therefore have been widely separated during this period. Similarities in stratigraphy, lithofacies and thickness of the Sinian, Cambrian and Ordovician formations of northern Jiangsu-Anhui provinces and southern Liaoning Province suggest that the Fuxian kimberlites may have been to the south of Mengyin at the time of kimberlite intrusion. The possibility that the scattered alluvial diamonds and associated kimberlitic minerals of northern Jiangsu-Anhui could be derived from the Fuxian kimberlites therefore needs to be considered. Present evidence does not point to the Mengyin and Fuxian kimberlites being contiguous at the time of their emplacement, although it seems that they were closer together than they are today.

**DISTRIBUTION OF FLUORINE BETWEEN MINERALS AND GLASS IN LAMPROITES,  
LAMPROPHYRES AND KAMAFUGITES: IMPLICATIONS FOR THE ROLE OF F IN DEEP  
MANTLE-DERIVED MAGMAS.**

*Edgar, <sup>(1)</sup>A.D.; Vukadinovic, <sup>(1)</sup>D. and Lloyd, <sup>(2)</sup>F.E.*

*(1)Department of Geology, University of Western Ontario, London, Ontario, Canada, N6A 5B7.; (2)Department of Geology, University of Reading, Reading, U.K. RG6 2AB..*

Lamproites, lamprophyres and kamafugites are among the most F-rich igneous rocks. With increasing K<sub>2</sub>O contents (>1 wt.% K<sub>2</sub>O) the average F contents in kamafugites, type 1 kimberlites, olivine lamproites, lamprophyres and leucite lamproites are 0.1, 0.2, 0.25, 0.3 and 0.5 wt.% respectively.

The higher abundances of F in these deep mantle-derived magmas relative to magmas originating at shallower levels, suggests that F may be very important in ultrapotassic magma genesis. Among the roles proposed for F is that the speciation and amount of F may affect fO<sub>2</sub> buffering in the mantle that consequently controls differentiation and other important petrogenetic hypotheses (e.g. Foley et al., 1986). These hypotheses depend on the availability of F in mantle reservoirs and whether on partial melting F is partitioned into melt or solid phases. Data on the F contents of likely mineral reservoirs (phlogopite, apatite and amphibole) in mantle-derived xenoliths (Aoki et al., 1981; Smith et al., 1981) are limited and where available indicate that F is not particularly abundant in these minerals. Experiments to determine partitioning of F under mantle conditions are also few (Edgar and Arima, 1985) and time consuming. In the present study the distribution of F between minerals and glass in lamproitic, lamprophyric and kamafugitic rocks was determined and compared to the abundance and distribution of F with similar data from mantle-derived xenoliths from the kamafugitic provinces of south-west Uganda and the West Eifel of Germany.

Distribution of F between phlogopite, amphibole, apatite and glass in 26 lamproites from Leucite Hills, West Kimberly, Smoky Butte, Prairie Creek and Gaussberg is very complex both within and between lamproite localities, with some mineral reservoirs showing distinctly different trends in different localities, e.g. phlogopite in Leucite Hills and West Kimberly lamproites has increasing and decreasing F from core to rim respectively. Generally F is most abundant in phlogopite and apatite relative to amphibole and glass. In evolved glasses F may be absent. With increasing evolution, F decreases in the rocks and in its amphibole and glass. Fluorine appears to be related to the Ba contents in apatite and glass in some lamproites.

Fluorine in minerals and glass in kamafugitic rocks from south-west Uganda and West Eifel, Germany, is only slightly lower than in lamproites and shows similar trends. Phlogopites in the West Eifel kamafugites have high F and BaO contents whereas the phlogopites from Ugandan kamafugites

have lower F and BaO. Glass in kamafugites from West Eifel and Uganda has low F contents and shows no trend in F with evolution as determined by MG no., unlike that of glass in lamproites from Leucite Hills in which F decreases with decreasing MG no. The F in amphibole in the Ugandan rocks is higher than that of amphibole in most lamproites.

In West Eifel mantle xenoliths F in phlogopite is very low (<0.5 wt.%) whereas apatite in a Ugandan xenolith averages 1.3 wt.% fluorine. Fluorine in glass in both West Eifel and Ugandan xenoliths is low (<0.5 wt.%). This suggests that if glass represents metasomatizing agents (Edgar et al., 1989) that these agents did not have sufficient F to provide the levels of abundance observed in the lava. Also, the very low F contents of the mineral reservoirs in the xenoliths implies that observed abundances of F in these kamafugites could not have been derived solely by partial melting of the mantle source.

The distribution of F between phases in kamafugitic lavas is similar to that observed in lamproites. Analyses from individual rocks indicate that F is richest in phlogopite followed by apatite, amphibole and glass. This is generally true for both lamproites and kamafugites. Fluorine contents in glass from kamafugites are usually less than 1 wt.% and approximately an order of magnitude smaller than F abundances in volatile-bearing phases within the same rock, suggesting that F is a compatible element.

Fluorine contents in apatite and phlogopite in minettes from Hopi-Navajo, U.S.A., are generally lower relative to those in kamafugitic rocks and show no significant trends.

The complex distribution of F between phlogopite, apatite, amphibole and glass in lamproites, lamprophyres and kamafugites does not allow determination of partition coefficients because of the inability to clearly establish mutual chemical equilibrium between F-bearing phases, possibly due to changes in parameters such as  $fO_2$  during evolution, or other variables. This study suggests that F preferentially enters solid rather than liquid phases in these magmas and that F is not abundant in minerals of mantle xenoliths in kamafugitic hosts. Fluorine in mantle mineral reservoirs is likely to be insufficient to provide the high F contents for these ultrapotassic magmas. The possibility that these magmas derive their high F contents during degassing on ascent rather than during partial melting is considered.

#### REFERENCES

- AOKI, K., ISHIWAKA, K. and KANISAWA, S. (1981) Fluorine geochemistry of basaltic rocks from continental and oceanic regions and their petrogenetic applications. *Contributions Mineralogy Petrology* 76, 53-59.

- EDGAR, A.D. and ARIMA, M. (1985) Fluorine and chlorine contents of phlogopites crystallizing from ultrapotassic rock compositions in high pressure experiments: implications for halogen reservoirs in source regions. *American Mineralogist* 70, 529-536.
- EDGAR, A.D., LLOYD, F.E., FORSYTH, D.M. and BARNETT, R.L. (1989) Origin of glass in upper mantle xenoliths from the Quaternary volcanics of Gees, West Eifel, Germany. *Contributions Mineralogy Petrology* 103, 277-286.
- FOLEY, S.F, TAYLOR, W.R. and GREEN, D.H. (1986) The role of fluorine and oxygen fugacity in the genesis of the ultrapotassic rocks. *Contributions Mineralogy Petrology* 94, 183-192.
- SMITH, J.V., DELANEY, J.S., HERVIG, R.L and DAWSON, J.B. (1981) Storage of F and Cl in the upper mantle: geochemical implications. *Lithos* 14, 133-147.

THE ARIES DIAMONDIFEROUS KIMBERLITE PIPE, CENTRAL KIMBERLEY BLOCK,  
WESTERN AUSTRALIA: MINERALOGY, PETROLOGY AND GEOCHEMISTRY OF THE  
PIPE ROCK AND INDICATOR MINERALS.

D. Edwards<sup>(1)</sup>, N.M.S. Rock<sup>(1)</sup>, W.R. Taylor<sup>(1)</sup>, B.J. Griffin<sup>(2)</sup> & S-S. Sun<sup>(3)</sup>.

(1)Geology Dept., University of Western Australia, Nedlands 6009, WA; (2)Electron Microscopy Centre, University of Western Australia, WA; (3)Bureau of Mineral Resources, Canberra 2601, ACT.

The mineralogy of the Aries pipe is very similar to that of S.African Group II (micaceous) kimberlites, but differs from that of typical lamproites, not least in the abundance of carbonate and absence of diagnostic lamproitic minerals such as priderite and richterite (Table 1). Three textural varieties of Aries magmatic kimberlite can be recognized in pipe rock from available drillcore: (1) macrocrystal medium-grained; (2) aphanitic ( $\leq 5$  vol% olivine macrocrysts); and (3) macrocrystal segregated. Autoclastic breccias are also abundant. The kimberlites contain two generations of olivine pseudomorphs (30-40 vol%), and two of phlogopite (up to 60 vol%), in a groundmass of apatite, calcite, diopside, sphene, spinels, serpentine, talc, and accessory groundmass minerals such as aeschynite [(Ce,Ca)(Ti,Nb)<sub>2</sub>O<sub>6</sub>], barite, ilmenite, monazite, rutile, siderite, and unidentified Nb-Fe-titanates.

Phlogopite is complexly zoned, with somewhat distinct compositional trends among the pipe's four lobes, but follows kimberlitic compositions and trends on Al-Ti plots (TiO<sub>2</sub> 0.5-4 wt%, Al<sub>2</sub>O<sub>3</sub> 9-16wt%); Cr<sub>2</sub>O<sub>3</sub> and BaO both range up to 1.5wt% and F up to 1.8wt%; local tetraferriphlogopite substitution is indicated. Diopside is low in Cr, Al, Na and Ti with high Mg# (Mg/[Mg+Fe<sup>2+</sup>]  $\approx 93$ ). Apatite contains variable SrO (up to 17.5wt%). Sphene contains significant Nb<sub>2</sub>O<sub>5</sub> ( $\leq 1.5$ wt%) and FeO ( $\leq 2$ wt%). Rare ilmenite contains 2.6wt% Nb<sub>2</sub>O<sub>5</sub> and 16wt% MnO but no detectable MgO. Calcite is virtually Mg-Fe-free but has up to 1.7wt% SrO and 0.5wt% MnO.

TABLE 1

Mineralogical summary comparison of Aries rocks with lamproites, Group I and Group II kimberlites

	Olivine	Cpx	Calcite	Amphi-bole	Phlogopite	Monticellite	Leucite, sanidine	Ilmenite	Priderite etc.	Zircon, perovsk.
Olivine-lamproite	abundant	common	rare	minor	abundant	absent	minor	rare	present	present
Leucite-lamproite	minor	common	rare	present	abundant	absent	present	present	common	absent
Group I kimberlite	dominant	absent	abundant	absent	minor	common	absent	common	absent	present
Group II kimberlite	dominant	common	abundant	v.rare	abundant	absent	absent	rare	absent	absent
Aries	dominant	present	abundant	absent	abundant	absent	absent	v.rare	absent	absent

common = commonly present but only in small amounts

present = commonly present but in variable amounts

Data summarized from Jaques *et al.*(1986), Mitchell (1986), Skinner (1989) and Mitchell & Bergman (1991)

Complex morphological, textural and compositional variations are present in drillcore spinels. They can be divided into five main textural-genetic types: (1) cognate groundmass chrome spinels; (2) chrome spinels included in olivine macrocrysts, probably representing either early phenocrysts or mantle xenocrysts; (3) macrocryst chrome spinels, probably representing xenocrysts; (4) late-stage groundmass ferric spinels, probably derived from serpentinization of olivine; (5) alteration ferric spinels, found as inclusions associated with siliceous melt inclusions in other spinels, and probably representing interaction of types (2) and (3) with late-stage melts. Some of these show further textural sub-types with no recognized genetic significance.

The Aries pipe is rich in country-rock (basalt, quartzite) xenoliths, but the only mantle-type materials so far yielded have been two diamond indicator minerals – spinel and rare garnet – recovered as isolated grains via heavy-mineral concentrate (HMC) programmes. Aries HMC chrome spinels can be easily distinguished, texturally and compositionally, from basaltic spinels derived from the local country-rocks. Like chrome spinels from the drillcore, they show complex textural, morphological and compositional variations, but six distinct textural types can be combined into two broader textural-compositional classes. *Class 1 spinels* show replacement textures, are non-stoichiometric, Cr-rich (up to 67wt%), apparently free of  $\text{Fe}^{3+}$ , and may carry  $\text{Cr}^{2+}$ ; they probably originated from metasomatised, depleted harzburgitic mantle within the diamond stability field at the base of the lithosphere. Central and South Lobes have abundant Class 1 spinels but North Lobe and North Extension virtually lack them. All four lobes contain texturally diverse *Class 2 spinels*, which show 'fractured, interlocking, pockmarked, symplectic or uniform' textures; these are more oxidized, poorer in  $\text{Cr}_2\text{O}_3$ , and higher in MgO than Class 1, and may have originated from shallower mantle sources.

Garnets are relatively rare in Aries heavy-mineral concentrates and have not been identified at all in drillcore. The few analyzed to date are 'G9' and 'G11' compositions under Dawson & Stephens' classification (55-60mol% pyrope, 7-10wt% CaO, 8-11wt%  $\text{Cr}_2\text{O}_3$ , 16-18% MgO), indicating lherzolithic and/or wehrlitic sources on the Sobolev et al. scheme. Despite the known diamond potential of the pipe, none of the 'G10' (subcalcic chrome pyrope) garnets regarded in southern Africa as a hallmark of diamondiferous pipes have yet been identified. This is however consistent with data from other Australian pipes, suggesting 'G10' garnets to be a less reliable diamond indicator in Australia than in southern Africa.

Several magma-pulses were involved in the formation of the Aries pipe. All four lobes probably contain at least one magma-pulse in common; this sampled one class of HMC spinels and is characterized by similar phlogopite zoning trends. However, Central and South Lobes contain magma(s) which sampled another

whilst North Lobe and North Extension contain magma(s) which may have been generated at higher levels in the mantle, yielded comparatively evolved phlogopite trends, and probably reduced their diamond prospectivity relative to the other lobes.

Geochemically Aries is again most like S.African Group II kimberlites. Certain incompatible element abundances and ratios (e.g. very high Nb/Zr) are unusual, but are shared with at least two other contemporaneous ( $\approx 820$  Ma) lamprophyric intrusions of the east Kimberley (at Maude Creek and Bow Hill), suggesting a regionally anomalous mantle source (Fig.1). Isotopically, however, Aries had  $\epsilon_{\text{Nd}} \approx -1$  when it was emplaced,  $\approx 820$  Ma ago ( $\approx -14$  present-day  $\epsilon_{\text{Nd}}$ ); this tends to suggest that unlike Argyle, the W.Kimberley lamproites, or Group II kimberlites of S.Africa, any contribution to Aries from an ancient, LREE-enriched lithospheric component is minor.

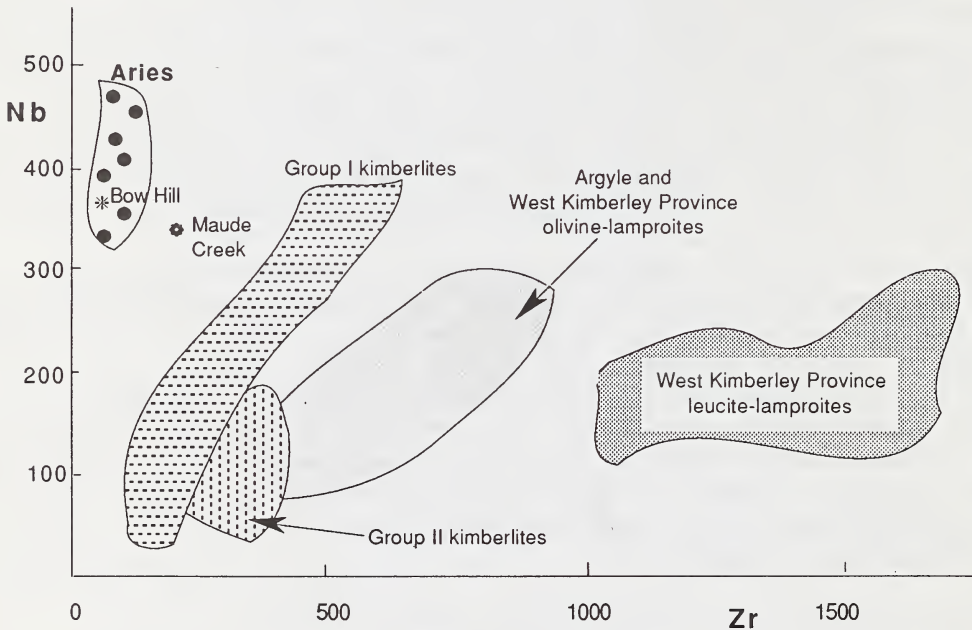


FIG.1. Nb versus Zr plot (ppm). Aries whole-rocks are compared with West Australian lamproites and the two global groups of kimberlites

The regional distribution of Aries and other lamprophyric bodies in and around the Australian Kimberley craton has two implications. (1) There exists a scattered magmatic province in the Kimberley, resulting from an  $\approx 800$  Ma lamprophyric intrusive event; as well as Aries in the central Kimberley, this includes all dated bodies from the currently named North Kimberley Province (e.g. Skerring kimberlite), and some from the East Kimberley 'province' (Bow Hill lamprophyres, but not the Argyle lamproite). (2) The traditional S.African model of diamond occurrence (Clifford's rule) requires modification if it is to be applied in the Australian Kimberley.

## DESTRUCTION OF SUBCRATONIC MANTLE KEEL: THE WYOMING PROVINCE.

Egglar, <sup>(1)</sup>David H.; Furlong, <sup>(1)</sup>Kevin P.<sup>(1)</sup>Geosciences Dept., The Pennsylvania State University, University Park, PA 16802 USA.

**Evidence of Keel.** Kimberlite diatremes in the Front Range of Colorado-Wyoming (e.g. Egglar *et al.* 1987) and in the Missouri Breaks area of Montana (e.g. Hearn and McGee 1984) contain mantle, lower-crustal, and upper-crustal xenoliths. Geothermobarometry of these xenoliths yields fossil geotherms that are cool (Fig. 1) and indicative of mantle that transfers heat by conduction, not convection. Thus in at least two places, one within the Wyoming Craton and one at its southern boundary, mantle lithosphere existed in the past that was at least 175 km thick. By the southern Africa model (e.g. Boyd 1973), such a lithosphere or keel had been welded to the Archean crust since the time of crustal formation. Also, by the southern Africa model, somewhat thinner mantle lithosphere underlay Proterozoic terranes around the old cratonic nucleus.

Cretaceous-to-Pleistocene magmas within the Wyoming Province, including the Absarokas, Crazy Mountains, Highwood and BearPaw Mountains, Smoky Butte, and Leucite Hills, are quite disparate in major-element chemistry, ranging from calc-alkaline and high-K rocks in the Absarokas to highly alkaline and from sodic series to potassic series. Yet the magmas share a number of trace-element and heavy-isotope similarities (review by Egglar *et al.* 1988). In particular, in a  $^{143}\text{Nd}/^{144}\text{Nd}$  -  $^{87}\text{Sr}/^{86}\text{Sr}$  diagram, they plot distinctly below the "mantle array", implying that they have been derived from ancient LREE-enriched sources. O'Brien *et al.* (1991) interpret that array as a mixing line between asthenosphere and a single LREE-enriched source. We interpret the array as heterogeneous sources and attach significance to Nd model ages. Those ages and Pb secondary isochrons can be interpreted as ages of separation of those sources from asthenospheric mantle, ranging from 3.8 Ga to 0.8 Ga, clustering around 1.8 Ga. The 1.8 Ga cluster in turn can be interpreted to represent metasomites added to the Archean mantle keel during accretional and collisional tectonics about the old continental core.

**Heat-Flow Evidence for Destruction.** Egglar *et al.* (1988) modeled the regional heat-flow data of Decker *et al.* (1980, 1984) and Sass *et al.* (1981) utilizing a best-guess model of the petrology of the crust and mantle lithosphere. Geotherms were calculated by solving equations for heat production and conduction. Fig 1 was produced by assuming a 1200°C isotherm for the lithosphere-asthenosphere boundary. In this simplified approach, variations in surface heat flow are attributed almost entirely to variations in thickness of the conductive layer (lithosphere). Decker *et al.* (1988) arrive at a quite different interpretation of the heat-flow data using an assumption that most surface heat-flow variation is a result of upper-crust heterogeneities in heat production. Although our approach is based on petrology observed at the surface or from xenoliths, we freely admit that the

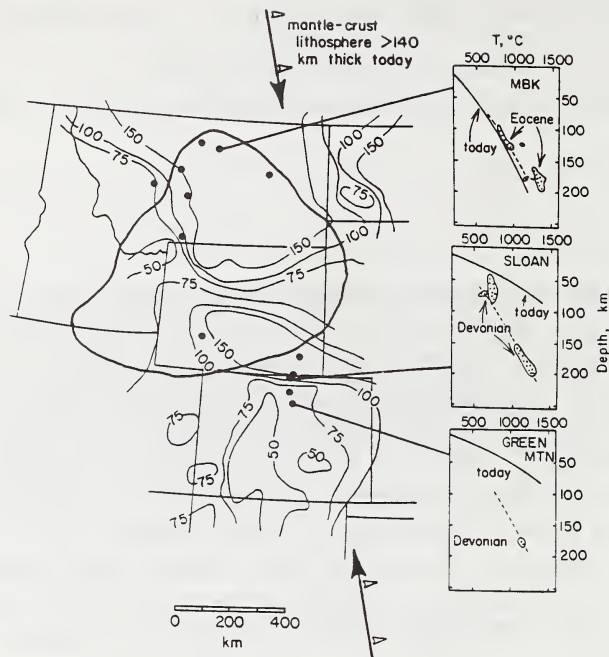


Figure 1. Minimum thickness of lithosphere, in km, calculated from heat-flow data. The lithosphere-asthenosphere boundary was taken as the  $1200^{\circ}\text{C}$  isotherm. Heavy arrows show the regional edge of thick ( $> 140$  km) mantle lithosphere that presently exists beneath the Great Plains (Grand 1987). The heavy line encircles the Wyoming Craton; dots are magmatic centers or kimberlite pipes. Windows show fossil geotherms from xenolith localities together with computed present-day geotherms. Interpolated present-day heat flows: Missouri Breaks (MBK),  $52 \text{ mW/m}^2$ ; Sloan, 73; Green Mountain, 80. The reference fossil geotherm (dashed line) is from southern Africa (Boyd 1973). An interpretation of this diagram is that thick mantle lithosphere that once was present throughout the Rocky Mountains now exists only in central Montana and southeastern Wyoming.

most probable shortcoming in the approach is an oversimplification of upper crust, the most heterogeneous unit and the greatest heat producer. Boundary depths of 50 km or less in Fig 1 undoubtedly represent upper-crust anomalies, because the temperatures imply partial melting that is not observed either by geophysics or by recent volcanism. The anomalies probably represent active or recently active magma bodies because they coincide with late Cenozoic volcanism, but they may also represent upper crust that is very high in K-U-Th and therefore in heat production. On either count, the calculated  $1200^{\circ}\text{C}$  isotherm would be too shallow, and the depths shown are minima.

Heat-flow modeling must be added to paleogeothermobarometry discussed above. The calculated geotherm in central Montana today (Fig. 1) is essentially the same as the conductive portion of the Eocene geotherm -- mantle lithosphere is at least as thick now as it was then and, presumably, as thick as it had been since the Archean. In northern Colorado-southern Wyoming, calculated geotherms today are much hotter than Devonian fossil geotherms -- mantle lithosphere is much thinner and has been destroyed. Regionally (Fig. 1), only two remnants of thick mantle lithosphere remain, one in central Montana and one in southeastern Wyoming.

**Seismologic Evidence for Destruction.** Egger *et al.* (1988) discuss several geophysical surveys that indicate that mantle beneath the Great Plains is

significantly different from that beneath most of the Rocky Mountains. The most definitive survey is a tomographic inversion for shear velocity (Grand 1987). Fig 2 is a simplified portion of Grand's cross-section B-B' that crosses the portion of Montana identified from heat-flow as underlain by thick mantle lithosphere. Block size for the velocity study was 500 km (horizontally), allowing the west-to-east transition from low to high velocities, above 400 km depth, to be up to several hundred km in width, although it may in fact be an extremely sharp feature. Because of the large block size, Fig 2 should not be overinterpreted. It does show, however, a high-velocity structure beneath the Great Plains that extends into Montana and that coincides with the old mantle lithosphere identified from xenoliths and heat-flow. Such structure is absent in Colorado, where the low-to-high velocity transition is east, not west, of the Front Range.

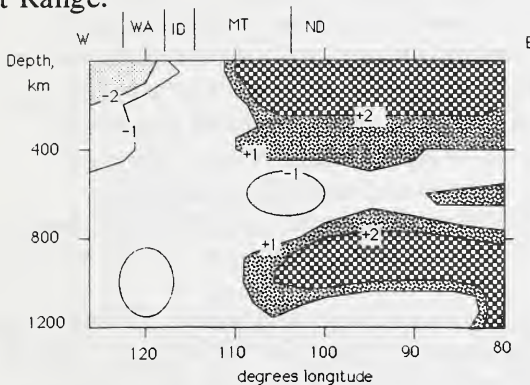


Figure 2. A simplified cross-section, after Grand (1987), of shear velocity across Montana and adjacent states. The line of section is approximately 46° latitude. Velocity changes are contoured with a unit that represents about 1.25% change above 320 km, about 0.62% from 320 to 405 km depth, and about 0.4% below 405 km depth.

**Tectonic Implications.** We believe that much of the central and northern Rocky Mountains was underlain by a keel of mantle lithosphere prior to Cretaceous time. The keel was tectonically stable and welded to old crust because it was buoyant -- although colder than asthenosphere, it was more magnesian (Jordan 1975). Cretaceous-to-Eocene tectonomagmatism destroyed much of that lithosphere eastward to the Great Plains, so that remnants exist today only in central Montana and southeastern Wyoming. That lithosphere was a clear impediment to low-angle subduction and the massive transport of lower crust and mantle lithosphere from southwest to northeast argued by Bird (1984, 1989). At the same time, some connection between subduction and tectonomagmatism cannot be denied. That connection began in the late Jurassic and continued into the mid-Tertiary. Egger *et al.* (1988) and Meen *et al.* (1988) argue for a back-arc rather than arc setting for Montana magmatism; the main role of the plate was to induce back-arc asthenospheric upflow that accounts for a minor component of magmatism and for a major component of lithospheric thinning and partial melting. Other schemes may emphasize tears or rifts in lithosphere through which asthenosphere or slab-derived melts ascend.

Bird, P. 1984 *Tectonics* 3:741. Bird, P. 1988 *Science* 239:1501. Boyd, F.R. 1973 *Geochim Cosmo Acta* 37:2533. Decker, E.R. *et al.* 1980 *J. Geophys Res* 85:311. Decker, E.R. *et al.* 1984 *New Mexico Geol Soc Guidebook*, 45-50. Decker, E.R. *et al.* 1988 *Geol Soc Amer Bull* 100:1851. Egger, D.H. *et al.* 1987 *Geol Soc Amer Sp Paper* 215:77. Egger, D.H. *et al.* 1988 *Colo Sch Mines Quar* 83:25. Grand, S.P. 1987 *J. Geophys Res* 92:14065. Hearn, B.C. Jr. & E.S. McGee 1984 in Kornprobst, J., ed., *Kimberlites II: The Mantle and Crust-Mantle Relationships*; Elsevier, 57-70. Jordan, T.H. 1975 *Rev Geophys* 13:1. Meen, J.K. & D.H. Egger 1987 *Geol Soc Amer Bulletin* 98:238. Meen, J.K. *et al.* 1988 *Geol Soc Amer Abstr* 20:432. O'Brien, H.E. *et al.* 1988 *EOS Trans Amer Geophys Union* 69:519. O'Brien, H.E. *et al.* 1991 *J Geophys Res* in press. Sass, J.H. *et al.* 1981 in Touloukian, Y.S. *et al.*, eds., *Physical Properties of Rocks and Minerals*, McGraw-Hill, 503-548.

SULFIDES, DIAMONDS, MANTLE fO<sub>2</sub>, AND RECYCLING.Eggler, <sup>(1)</sup>David H., Lorand, <sup>(2)</sup>J.P.; and Meyer, <sup>(3)</sup>H.O.A.

(1)Geosciences Dept., Penn State Univ., Univ. Park, PA 16802 USA; (2)Museum National d'Histoire Naturelle, Unite Associee au CNRS 736, 61 Rue Buffon, 7500 Paris FRANCE; (3)Dept. Earth Atmos. Sci., Purdue Univ., West Lafayette, IN 47907 USA

Oxidation state (fO<sub>2</sub>) of the mantle bears upon fluid speciation, partial melting, electrical conductivity, ductile flow, early Earth history, and recycling. Opinion of the early 1980's that much of the mantle is 'reduced', based on intrinsic fO<sub>2</sub> measurements of single-phase xenolithic olivines and spinels (e.g. Arculus and Delano 1981), is now in question because intrinsic measurements can perturb samples by carbon-induced reduction-exsolution or auto-oxidation (Virgo *et al.* 1988). Thermodynamic calculations on multi-phase ilmenite-bearing (Eggler 1983) or spinel-bearing (Mattioli and Wood 1986) peridotite xenoliths reestablished an older 'oxidized' view. Here we establish a new oxybarometer based on sulfides and apply it to peridotite xenoliths in alkali basalts (modern mantle) and peridotitic diamond inclusions (Archean mantle).

**THERMODYNAMICS OF MSS.** Monosulfide solid solution (MSS) is (Fe,Ni)<sub>1-x</sub>S or, following Toulmin and Barton (1964), (Fe,Ni)S-S<sub>2</sub>. A high P-T standard state for S<sub>2,xt</sub> is achieved by reintegrating T&B eqn (8) with new boundary conditions, arriving at:

$$\log a_{S_{2,xt}} = -85.83 (1000/T-1) N_{MS} + 39.30 u - 39.30$$

where  $u = (1 - 0.9981N_{MS})^{0.5}$  and  $N_{MS} = N_{FeS} + N_{NiS} + N_{CuS} + N_{CoS}$  (1)

$$\log f_{S_{2,g}} = 70030/T - 42.64 + \log a_{S_{2,xt}} + 0.0522/T \int_1^P V_{S_{2,xt}} dP \quad (2)$$

Gibbs-Duhem integration in the ternary FeS-NiS-S<sub>2</sub> gives  $a_{FeS}$ . Scott *et al.* (1974) indicate that that Fe<sub>1-x</sub>S and Ni<sub>1-x</sub>S mix ideally at a given mol% S, equivalent to saying that  $a_{S_{2,xt}}$  depends only on the number of cation holes in the (Fe,Ni)<sub>1-x</sub>S structure, not on the cation species. Then

$$\log a_{FeS} = \log N_{FeS} + 85.83 (1000/T - 1) (\ln N_{MS} - N_{MS}) + 19.61 \ln ((1-u)/(1+u)) + 39.30 u - 0.434 \ln N_{MS} - 0.002 \quad (3)$$



Equilibrium (4) represents the assemblage olivine - orthopyroxene - MSS. For the pure phases S,  $\Delta H_f$ , V,  $\alpha$ , and  $\beta$  were taken largely from Robie *et al.* (1978) and Wood (1987). Olivine and orthopyroxene activity-composition relations are from Wood (1987). Uncertainties entirely reflect errors in analysis of phase compositions. For each trial of the Monte Carlo method a random number technique returned metal or oxide values whose overall distribution functions have standard deviations equal to 1% of the amount present in each phase. For sulfide compositions computed by a combination of phase and modal analysis, the 1% error was doubled.

**ALKALI BASALT XENOLITHS.** Sulfides in spinel peridotite xenoliths (e.g. Lorand and Conquere 1983; Lorand 1987; Dromgoole and Pasteris 1987) undergo: (1) Formation as cogenetic immiscible melt blebs

enclosed within silicates or interstitial to silicates; (1a) contamination with nongenetic sulfide liquid or with sulfur-bearing metasomatic fluids;

(2) Crystallization/ reequilibration to MSS-olivine-pyroxene-spinel assemblages, losing the Fe<sub>3</sub>O<sub>4</sub> component of sulfide melt; (3) during ascent of host basalt, separation of Ni-Cu-rich sulfide partial melt; (4) reequilibration at ~600°C to two or more monosulfide solid solutions; (5) reequilibration/

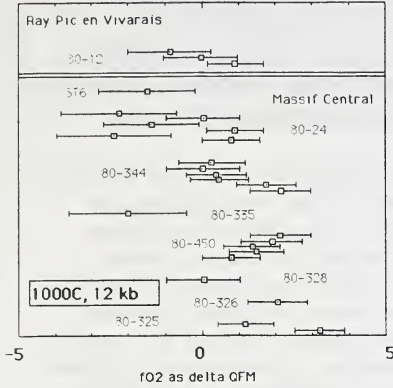


Fig. 1. Sulfide oxybarometry of spinel peridotite xenoliths in Massif Central alkali basalts, in log units relative to QFM. Groups of points indicate multiple sulfide inclusions within a single sample. Within-sample variability shows that sulfide oxybarometry is not as precise as spinel oxybarometry, but if samples are averaged it appears that fO<sub>2</sub>'s are within one log unit of QFM. Similar results have been obtained on similar modern subcontinental mantle lithosphere, using spinel oxybarometry, by Mattioli and Wood (1986) and Wood and Virgo (1989).

exsolution to PO/MSS ± PN ± CPY or PO/MSS ± PN ± CB at T < 300°C; (5a) Interstitial sulfides may undergo reduction/ desulfidation attendant to serpentinization. Stage (2) represents typical mantle equilibration conditions (1000°C, 12 kb), for which sulfides included in silicates and free of magnetite are the best candidates. Their high-temperature compositions (Fig. 1) are reconstructed from modes and analyses of the low-temperature assemblages.

**DIAMOND INCLUSIONS.** Sulfides in the peridotitic diamond suite omit steps (1), (1a), (3), and (5a) above (Meyer 1987). Equilibrium (4) was applied to a suite of peridotitic sulfide inclusions analyzed by Yefimova *et al.* (1983) (Fig. 2). Although only one diamond contained both olivine and opx, all were assumed to have been in equilibrium with both, and the olivine was assumed to be Fo<sub>93</sub>, the mean of diamond olivines (Meyer 1987). The P&T

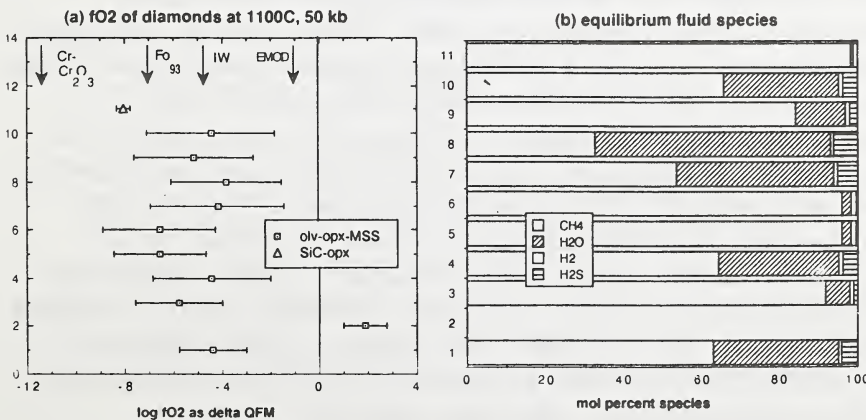


Fig. 2. (a) Sulfide oxybarometry of peridotitic sulfide inclusions in Siberian diamonds, in log units relative to QFM. Also shown is one moissanite (SiC)-bearing diamond from Colorado. Reference buffers are at P&T. Diamond itself is stable to fO<sub>2</sub> just above EMOD. (b) Species of high P&T fluids calculated from the fO<sub>2</sub> and fS<sub>2</sub> of (a) and an MRK EOS; ordinate numbers correspond to ordinate numbers of (a).

are typical of peridotitic diamonds (Meyer 1987). Despite wide error brackets, reflecting uncertainty in  $a_{S_2}$  at low contents of  $NS_2$ , the means of nine diamonds are surprisingly well-grouped near the IW buffer. Clearly, sulfides in diamonds formed under more reduced conditions than the sulfides calculated by the same method in Fig.1.

**STABILITY OF SiC AND (Fe,Mg)O.** Thermodynamic functions for moissanite, SiC (JANAF 1985) and an activity model for magnesiowustite (ferropericlase) (Hahn and Muan 1962) were added (Fig. 3) to show stability of these peridotite suite (Moore et al. 1986; Otter and Gurney 1989) minerals. If the assemblage of moissanite-Cr-diopside reported by Otter and Gurney

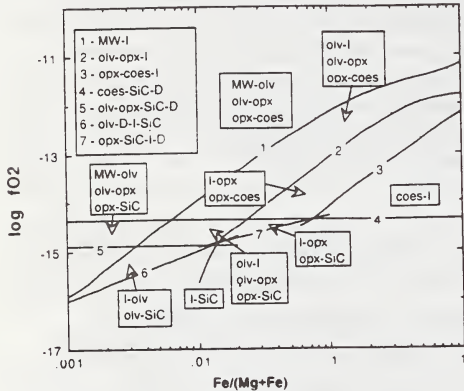


Fig. 3. Stability relations in the system  $MgO-Si-Fe-C-O$  at  $1100^{\circ}C$ , 50 kb. Ferromagnesian phases of univariant assemblages (numbered lines) have the  $Fe/(Mg+Fe)$  shown. Where olivine and opx coexist, the olivine composition is shown. Boxes show the various divariant assemblages. Calculations for pure iron metal; if metal is nickel-bearing, relevant curves will rise somewhat in  $fO_2$ . Ferropericlase must form above curve 1 and so does not indicate particularly reduced conditions. It may coexist with olivine but should not coexist with opx. Moissanite may exist 3.5 log  $fO_2$  units below IW; it may coexist with opx but not with olivine.

(1989) at Sloan kimberlite, Colorado also included opx, then  $fO_2$  is bracketed between curves 4 and 7 (Fig. 3 and Fig. 2).

**IMPLICATIONS.** Modern subcontinental mantle lithosphere has  $fO_2$  near QFM in the spinel peridotite facies (e.g. Wood and Virgo 1989). Deeper lithosphere may be more reduced (Luth *et al.*, 1990; Jaques *et al.*, 1990) in part, but the ilmenite-bearing peridotites (Eggler 1983) and carbonated mantle (EMOD) that melts to produce kimberlites certainly is not. Suboceanic asthenosphere  $fO_2$ 's range from QFM to about 3 log units below QFM (Bryndzia and Wood, 1990; Christie *et al.* 1986). Some, if not all, peridotitic diamonds formed beneath both the Kaapvaal and Siberian cratons about 3.3 Ga ago (Richardson *et al.*, 1984; Richardson 1986) at  $fO_2$  near IW (Fig. 2). A simple interpretation is that most mantle 3.3 Ga ago was more reduced than average mantle today. Mantle gases (Fig. 2) and volcanic gases and therefore the atmosphere were reduced ( $CH_4-H_2O-H_2S$  rather than  $CO_2-H_2O-SO_2$ ). Hydrogen loss to space and rapid recycling of crustal  $O_2$  created, by the Proterozoic, a more oxidized mantle- crust- atmosphere system. Some deep subcontinental mantle may be a relict of Archean conditions, as may be regions of today's asthenosphere. By this model, few regions of today's mantle are  $fO_2$ -buffered. Sliding equilibria such as diamond-COHS fluids, olivine-opx-spinel, and eqn (4) all reflect  $fO_2$  rather than control it.

Arculus, R.J. & J.W. Delano 1981 *Geoch Cosm Acta* 45:899. Bryndzia, T. & B.J. Wood 1990 *Amer J Sci* 290:1093. Christie, D.M. *et al.* 1986 *Earth Plan Sci Lett* 79:397. Dromgoole, E.L. & J.D. Pasteris 1987 *Geol Soc Am Sp Pap* 215:25. Eggler, D.H 1983 *Geophy Res Lett* 10: 365. Hahn, W.C. Jr. & A. Muan 1962 *Trans Metal Soc AIME* 224:416. JANAF Thermo. Tables 1985. Jaques, A.L. *et al.* 1990 *Contrib Min Petr* 104:255. Lorand, J.P 1987 *Bull Soc Geo France* 8.t.III:643. Lorand, J.P. & F. Conquere 1983 *Bull Mineral* 106:585. Luth, R. *et al.* 1990 *Contrib Min Petr* 104:56. Mattioli, G.S. & B.J. Wood 1986 *Nature* 322:626. Meyer, H.O.A. 1987 in P.H. Nixon, ed. *Mantle Xenoliths*, 501. Moore *et al.* 1986 *Abstr Geol Soc Aust* 16:409. Otter, M. & J. Gurney 1987 *Geol Soc Aust Sp Pub* 14:1042. Richardson, S.H. 1986 *Abstr Geol Soc Aust* 16:418. Richardson S.H. *et al.* 1984 *Nature* 310:198. Robie, R.A. *et al.* 1978 *USGS Bull* 1452. Scott, S.D. *et al.* 1974 *Econ Geol* 67:1010. Wood, B.J. 1987 *Rev Min* 17:71. Wood, B.J. & D. Virgo 1989 *Geoch Cosm Acta* 53:1277. Yefimova, E.S. *et al.* 1983 *Zap Vses Mineral Obsch* 112:300.

## SIGNIFICANCE OF ALUMINIUM, CALCIUM, CHROMIUM, ZIRCONIUM, NIOBIUM AND IRON CONCENTRATIONS IN RUTILE FROM HIGH PRESSURE ROCKS

*Fett, A. & Brey, G.**Max-Planck-Institut für Chemie, 6500 Mainz, Germany*

Natural rutile from medium to high pressure and temperature rocks is an ubiquitous minor mineral phase. Electron microprobe analyses have been made on rutiles from different eclogitic parageneses and also from granulites and amphibolites.

Beam current was set at 50 nA at 15 kV and a PAP correction procedure was applied to the raw intensities. Count times were 100 s (Ca, Cr), 120 s (Al) and 150 s (Zr, Nb, Fe).

Trace element contents range from 30 - 2500 ppm (Al), 30 - 3000 ppm (Ca), 250 - 4000 ppm (Cr), 180 - 7500 ppm (Zr), 200 - 3400 ppm (Nb) and 170 - 10000 ppm (Fe). Variations in concentrations appear to depend on pressure, temperature and whole rock chemistry.

Fig.1 and 2 are diagrams of Cr and Al respectively against temperature. Both Cr and Al appear to increase with temperature whereas Ca (Fig.3) appears to decrease with temperature.

In diagrams of element against element e.g. Zr against Al (Fig. 4) samples from different localities can be distinguished very clearly.

Pressures and temperatures are inferred from literature data which are based on geothermobarometers and circumstantial geological arguments.

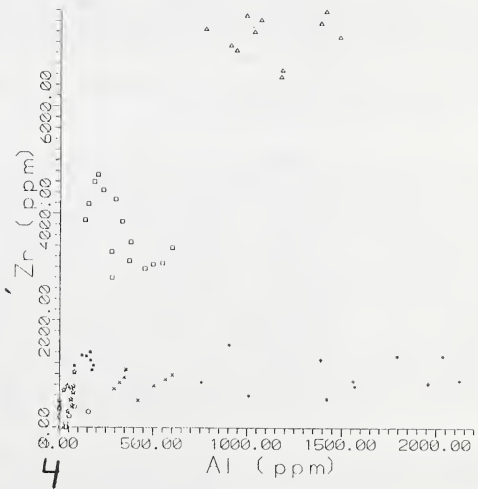
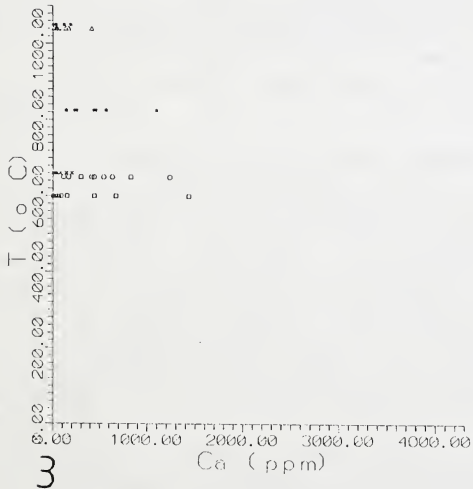
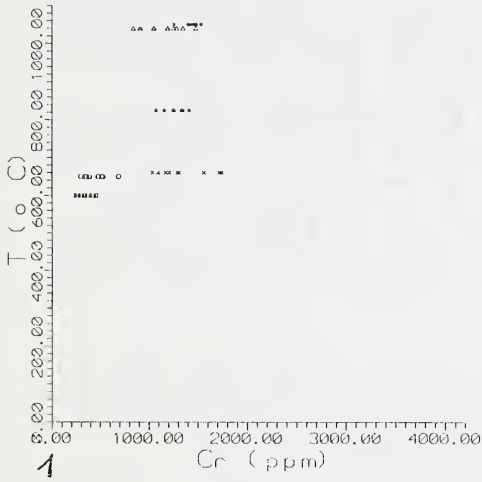
For samples from these localities different p,T conditions of origin are inferred and trace element contents in rutile may be the basis for functioning geothermobarometers for eclogites.

Sobolev et al. (1972) were the first to suggest that the Al content of rutile could be an indicator for pressure and/or temperature and our extended data base may provide a better foundation for this and further elements to design experiments aimed at calibrating on eclogite barometer.

Ref.:

N. Sobolev, J. G. Lavrent'ev & L. W. Usowa (1972), *Geologiya i Geofizika*, 11, (108 - 112)

□	S305	granulite	(Matsoku, Lesotho)
×	S308	eclogit	(Matsoku, Lesotho)
○	Mg1	amphibolite	(Münchb. Gneism., Germany)
◇	U30	eclogite	(Moldefjord, Norway)
★	Sk1	eclogite	(Steiermark, Austria)
★	1	eclogite	(Alpe Arami, Switzerland)
△	BD1934	eclogite	(Vissuri, Tanzania)
*	S470	eclogite	(Roberts Victor Mine, South Africa)



## SYMPLECTITES IN UPPER MANTLE HARZBURGITES AND GARNET HARZBURGITES

*Field, S.W.**Stockton State College, Pomona New Jersey, 08240*

Symplectites are complex mineral intergrowths commonly found in upper mantle peridotites recovered from kimberlite pipes (Exlev et.al., 1982; Dawson and Smith, 1975). Symplectites are abundant in harzburgites and garnet harzburgites found in the Cretaceous Jagersfontein kimberlite in South Africa. Symplectites in harzburgites are composed of either enstatite, diopside, and spinel or diopside and spinel. Symplectites in garnet harzburgites are composed of either diopside, garnet, and spinel or garnet and spinel. Amphibole is found in a few symplectites and is thought to be of metasomatic origin. Temperature estimates for the garnet harzburgites obtained from Lindsley and Andersons (1983) two pyroxene geothermometer range from 650 to 1300 c with most falling between 850 and 1000 c. Pressure estimates from garnet-diopside geobarometry (Brey et.al., 1986) range from 12 to 47 kilobars with most estimates falling between 20 and 35 kilobars. Temperature estimates for symplectite-bearing harzburgites range from a low of 775 c to a high of 1300 c.

Petrography: Harzburgites containing symplectites are composed dominantly of medium-grained olivines (0.5-2.0mm) surrounding cluster of enstatites. Symplectites, generally less than 0.5 mm in diameter, make up less than 1 modal percent of the peridotites. Symplectites are constructed of a single or small number of optically homogeneous pyroxene crystals embedded with tens to hundreds of small, wavy, spinel lamellae. The symplectites are located adjacent to discrete enstatite and are generally triangular or arcuate in shape. Spinel lamellae are crystallographically oriented in the pyroxene and radiate outward away from the enstatite.

Garnet harzburgites are composed of clusters of large discrete enstatites surrounded by olivines. Within the enstatite clusters are small interstitial garnets, spinels, and diopsides. Enstatites contain abundant planar lamellae of spinel, diopside and in some samples garnet. Symplectites are located within enstatite clusters adjacent to lamellae-bearing pyroxenes. Symplectite structure consists of either small spinel blebs within large garnets or commonly a central core of diopside crystals embedded with tens to hundreds of wavy spinel lamellae surrounded by a rim or partial rim of garnet.

Mineral Chemistry: Olivines in harzburgites and garnet harzburgites have identical chemistries and range from  $Fo_{92}$  to  $Fo_{94}$ . Diopsides in harzburgites, present dominantly in symplectites, have a lower Na content (.02-.08 cat./6 oxy) and slightly higher Mg content (.93-.96 cat./6 oxy) than diopsides in

garnet harzburgites (Na .03-.13, Mg .90-.96 cat./6 oxy). Discrete enstatite in harzburgites differ compositionally from enstatites in garnet harzburgites. Harzburgite enstatite Al contents (.03-.14 cat./6 oxy), Ca contents (.01-.04 cat./6 oxy) and Cr contents are higher than Al (.03-.05 cat./6 oxy), Ca (<.01 cat./6 oxy), and Cr contents in garnet harzburgite enstatites. Silicon and magnesium contents in harzburgite enstatites are distinctly lower than Si and Mg contents in garnet harzburgite enstatites. In addition discrete harzburgite enstatites are enriched in Ca, Al, and Cr contents with respect to enstatites in symplectites (Al .04-.09, Ca .01-.02 cat./6 oxy). Symplectite enstatites in harzburgites are intermediate in chemistry to discrete harzburgite enstatites and discrete garnet harzburgite enstatites.

Symplectite spinels in harzburgites are Mg (5.3-6.1 cat./32 oxy) and Al rich (6.8-11.2 cat./32 oxy) and Cr (4.8-8.5 cat./32 oxy) and Fe<sub>T</sub> poor (2.0-2.8 cat./32 oxy). Spinel in garnet harzburgites are found as lamellae in enstatite, as small discrete interstitial grains, and as lamellae in symplectites. All the garnet harzburgite spinels are rich in Fe<sub>T</sub> (3.2-4.4 cat./32 oxy) and Cr (9.7-10.9 cat./32 oxy) and poor in Mg (4.6-5.2 cat./32 oxy) and Al (4.1-6.2 cat./32 oxy). Although spinels in harzburgites and garnet harzburgites have generally different compositions the compositions form a continuous trend from Mg and Al rich to Fe and Cr poor. Garnets found only in garnet harzburgites, are found as lamellae in enstatites, discrete interstitial grains, and as rims or partial rims around symplectites. Garnets have a limited range in composition (Py 67-73 Alm 12-19 Sp 0.5-1.5) in all morphological forms.

Discussion: The petrography and chemistry of minerals in symplectites and symplectite-bearing peridotites indicate that intergrowth formation was complex and involved exsolution, diffusion, metamorphism, and in some cases metasomatism and that symplectites in harzburgites and garnet harzburgites may be genetically related. Lamellae in enstatite and the position of symplectites adjacent to lamellae-bearing enstatites indicates symplectite diopside diffused out of enstatite. The optical orientation of spinel in symplectites and the textural relationship of spinel to pyroxene suggest that spinel unmixed from diopside after the pyroxene diffused from enstatite. Garnet appears to have formed by a reaction between olivine or enstatite, spinel, and diopside after formation of the symplectite core. Metasomatic reactions formed amphibole by replacement of garnet, diopside, enstatite, and spinel in some peridotites. Harzburgites which contain high Al discrete enstatites and modally minor symplectites may be precursors to garnet harzburgites containing low Al enstatites and a modally higher percentage of spinel, diopside, and garnet.

Table 1. Mineral Chemistry

	1	2	3	4	5	6	7	8
Si	.996	2.992	1.977	1.926	1.935	1.993	0	0
Ti	0	0	.001	.001	0	0	0	0
Al	0	1.856	.076	.138	.097	.029	8.158	4.708
Cr	0	.170	.030	.020	.021	.005	7.548	10.575
Fe <sup>3+</sup>	0	-	-	-	-	-	.294	.717
Fe <sup>2+</sup>	.139	.490	.044	.129	.129	.139	2.404	2.817
Mn	0	.029	-	0	0	.004	.045	.051
Mg	1.860	2.080	.946	1.736	1.810	1.820	5.552	5.133
Ca	0	.389	.881	.027	.024	.006	-	-
Na	.006	-	.035	-	.001	0	.002	-
Total	3.001	8.006	3.990	3.978	4.016	3.998	24.001	24.001

1. Olivine - cat./4 oxv
2. Garnet - cat./12 oxv
3. Diopside cat./6 oxv
4. Enstatite (Discrete, Harzburgite) cat./6 oxv
5. Enstatite (symplectite, Harzburgite) cat./6 oxv.
6. Enstatite (Discrete, Garnet Harzburgite) cat./6 oxv.
7. Spinel (Symplectite, Harzburgite) cat./32 oxy.
8. Spinel (Symplectite, Garnet Harzburgite) cat./32 oxy.

Brey, G.P., Nickel, K.G., Kogarko, L., 1986, Garnet-pyroxene equilibria in the system CaO-MgO-Al<sub>2</sub>O<sub>3</sub>-SiO<sub>2</sub> (CMAS): prospects for simplified (T-independent) Iherzolite barometry and an eclogite barometer. *Contrib. Mineral. Petrol.*, V 92, p. 448-455.

Dawson, J.B., Smith, J.V., 1975, Chromite-silicate intergrowths in upper-mantle peridotites: In L.H. Ahrens, J.B. Dawson, A.R., Duncan, A.J. Erlank, Eds., *Physics and Chemistry of the Earth*, v.9, p. 339-350, Pergamon Press, New York.

Exley, R.A., Smith, J.V., Hervig, R.L., 1982, Cr-rich spinel and garnet in two peridotite xenoliths from the Frank Smith mine South Africa: Significance of Al and Cr distribution between spinel and garnet. *Min. Mag.*, Vol 45, p. 129-134.

Lindsley, D.H., Anderson, D.J., 1983, A two-pyroxene thermometer: Proceedings of the thirteenth Lunar and Planetary Science Conference. *Journal of Geophysical Research*, Vol. 88, p. A 887 - A906.

# SIGNIFICANCE OF CHROMITE, G5 Mg-ALMANDINE GARNET, ZIRCON AND TOURMALINE IN HEAVY MINERAL DETECTION OF DIAMOND BEARING LAMPROITE

*Fipke, Charles E.*

*C.F. Mineral Research Ltd., 263 Lake Ave., Kelowna, B.C., Canada V1Y 5W6*

A project, with the objective of identifying heavy minerals that could be utilized in heavy mineral prospecting programs to detect diamondiferous lamproite, was completed by the Geological Survey of Canada and C.F. Mineral Research Ltd. consultants in 1990.

The project involved ball milling, heavy mineral concentrating and S.E.M. micro analysing of all heavy mineral species from large (30 - 180 kg) rock samples from the Argyle (AT) Australia, the Prairie Creek (PC) Arkansas, and the Jack (JK) B.C., Canada, diamondiferous lamproites.

Potential abrasion resistant heavy indicator minerals identified in the foregoing samples were similarly concentrated and analyzed using bulk rock samples from the following diatremes: the Ellendale 4 (EL4) diamondiferous lamproite, Australia; the Smoky Butte (SB) lamproite, Montana, U.S.A.; the Sloan 1 (SL) diamondiferous kimberlite, Colorado, U.S.A.; the Presidente Olegario (PO2, PO3) and satellite (PO1) possible lamproitic diatremes, Brazil; the Sover (SV) and the New Elands kimberlites, South Africa; and from Canada - the Larry (LR), the Mark (MR) and the Mike (MK) lamproitic diatremes, B.C.; the Batty (BT), N.W.T., the Crossing Creek (CC), B.C., the Joff (JF), B.C., the Kirkland Lake (KL), Ont., the Sturgeon Lake (SK), Sask., barren and diamondiferous kimberlites; the Blackfoot (BF), B.C., the HP (HP), B.C., the Ile' Bizard (IB), Que., alkaline lamprophyres; and the Mountain (MD) olivine melilitic diatreme, N.W.T.

The indicator minerals recovered and analyzed from the foregoing diatremes as well as world wide diamond inclusion mineral compositions were computer classified. The classifications used were adapted from Dawson and Stephens (1975&1977) and R. Moore's (1990) methods of classifying garnets and clinopyroxenes ("Cpx") so that J. Gurney's (1985) method of classifying G10 composition garnets was included and minerals of regional "R" compositions excluded.

Table 1 illustrates that only three "E" eclogitic and three "P" peridotitic garnets were recovered from 32 kg. of the most diamondiferous sandy tuff phase of Argyle (AT); similarly, only two "E" and three "P" garnets were recovered from 42 kg. of the most diamondiferous phase of Prairie Creek (PC). Low counts were similar for the Jack (JK) but substantially higher for the Ellendale 4 (EL4) diamondiferous lamproite. Although significant quantities of Cpx were recovered from (PC) and (EL4) only three Cpx (classified according to Dawson's methods) were recovered from the (AT) sample and four Cpx from the (JK) sample. It is thus probable that the Argyle and Jack lamproites would be bypassed by prospecting surveys based only on results of "P" and "E" garnets and Cpx.

Table 1 illustrates that chromites, G5 garnets, zircons and tourmaline are the most abundant abrasion resistant heavy minerals present in concentrates from all diamondiferous lamproites sampled - ( AT, EL4, PC, JK ). A summary of characteristics of these minerals is as follows:

CHROMITES from diamondiferous lamproite tend to be euhedral to slightly rounded and/or broken, opaque black to translucent brown colored grains that commonly exhibit grey alteration frosting of outer rims. Table 1 illustrates that between 1.5% (for PC) and 12% (for AT) of the chromites analyzed have >60% Cr2O3. Most of these plot within the diamond inclusion and intergrowth fields of MgO-Cr2O3, Al2O3-Cr2O3, and Cr2O3-TiO2 (figure 1). Figure 1 illustrates that non-diamond inclusion chromites from diamondiferous lamproites (and kimberlites) have enriched Cr2O3 and TiO2 compared to a file of 821 chromite analyses from volcanic, ophiolite,

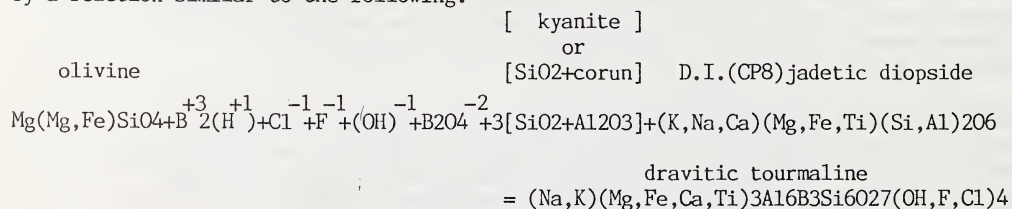
alpine and layered ultramafic sources. Some chromites from the PO1 diatreme situated near Presidente Olegario, Brazil, plot within the enriched Cr2O3-TiO2 field.

G5 Mg-ALMANDINE GARNETS recovered from diamondiferous lamproite exhibit pink to purple or pale brown coloration and tend to exhibit broken or anhedral form, thought to be a result from milling of megacrystic forms. Although these garnets typically classify as "R" regional garnets by R. Moore parameters, a search of publications did not identify any regional rocks as sources for these G5 garnets of FeO <29.94% other than kimberlite or lamproite. Table 1 (bottom) demonstrates that seven garnets, included in diamond, classified as G5. While such G5 garnets could be useful in some regional heavy mineral prospecting programs to locate lamproite and kimberlite they are non discriminating between barren and diamondiferous as illustrated in table 1 (note barren SB count).

DIATREME ZIRCONS appear to differ from round xenocystic zircons from sandstone wallrocks by the presence of glassy to frosted textures typical of "E" and "P" garnets and by the absence of abrasion textures characteristic of clastic rounded zircons. These tiny (<0.5mm) mostly round to spherical, purple to brown colored, non fluorescent zircons and pink to honey colored orange fluorescent (to UV) zircons were recovered from 22 of the 23 diatremes tested. Such zircons, in some cases, contain concentric overgrowths of dark purple or pink zircon on round light zircon cores. Lead isotopes dates to 1856 MY have been obtained from round zircons from the Prairie Creek and to 2685 MY from the Jack lamproites. Levels of up to 0.16 K2O and 1.7% MgO have been detected in zircons recovered from diamondiferous lamproite.

DIATREME TOURMALINES are characteristically unzoned, exhibit glassy to frosted textures typical of "E" and "P" garnets and typically lack abrasion surface textures. Minor to abundant quantities of round to rounded, light translucent brown to opaque brown dravitic tourmaline was recovered from all diamondiferous lamproite tested (AT, EL4, PC and JK) but was significantly absent from the Smoky Butte (SB) barren lamproite and most other diatremes tested (Table 1). Fifty four out of fifty nine (92%) diatreme tourmalines microprobe analyzed to date contain (33.7-37.4 %) SiO2, (28.1-35.3 %) Al2O3, <0.15% Cr2O3, <0.22% MnO, (2.9-13.0%) FeO, (>1.0-8.8%) Al2O3, <0.15% TiO2, (1.3-2.3%) Na2O, (>0.05-2.0%) CaO, <10.7% B2O3, <0.55%F and <0.3% Cl. Thirty nine out of a file of 164 regional tourmalines (from world wide literature sources) also classify within the foregoing compositional limits of diatreme tourmalines. Figure 2, a TiO2 - K2O compositional plot of the 54 diatreme and 39 regional tourmalines, demonstrates that 30 of 39 total tourmalines from diamondiferous lamproite (77%) and 7 of 164 total regional tourmalines (4%) plot in a field of elevated TiO2 - K2O. None of the diatreme tourmalines, from non-diamondiferous pipes, plot within the elevated TiO2 - K2O field.

The presence of dravitic tourmaline of elevated TiO2 - K2O in diamondiferous lamproite (and kimberlite(SK)), as well as the common presence of CP8 jadetic diopside included in worldwide diamond inclusions but absence of CP8 clinopyroxene in worldwide diamondiferous lamproite and kimberlite (refer to table 1) can be explained by a reaction similar to the following:



The above reaction would necessitate olivine-rich kimberlitic or lamproitic magmas charged with boron and weak acid gases to react on intrusive contact with jadetic diopside and kyanite or corundum (with excess SiO2) constitutes of diamond



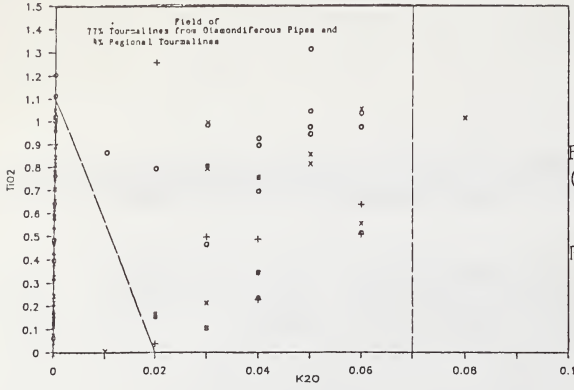


FIGURE 2: ALL TOURMALINES  
(AT,EL4,PC,):o JK:+ SK:s analy-  
zed by U. of Saskatchewan

Reg:x from many literature sources

DAWSON, J.B., and STEPHENS, W.E. (1975) Statistical Classification of Garnets from Kimberlite and Associated Xenoliths, *Journal of Geology*, vol. 83, p. 589-607

FIPKE, C.E., GURNEY, J.J., MOORE, R.O., NASSICHUK, W.W., et al (1990) The Development of Advanced Technology to Distinguish Between Productive Diamondiferous & Barren Diatremes, *Geological Survey of Canada, Open File Rep. 2124*, vol. 3, p. 518-550

GURNEY, J.J. (1985) A Correlation between Garnets and Diamonds in Kimberlites, Kimberlites Occurrence and Origin: A Basis for Conceptual Models in Exploration, *The University of Western Australia, Publication No. 8*, p. 143-166

MOORE, R.O. (1986) A Study of the Kimberlites, Diamonds & Associated Rocks & Minerals from the Monastery Mine, S.A., PhD Thesis, University of Cape Town, vol. 2, p. 22

STEPHENS, W.E., and DAWSON, J.B. (1977) Statistical Comparison Between Pyroxenes from Kimberlites and Their Associated Xenoliths, *Journal of Geology*, vol. 85, p. 433-449

VERTICAL SAMPLING OF MANTLE BENEATH NORTHEASTERN BRAZIL AS  
REPRESENTED BY ULTRAMAFIC XENOLITHS AND MEGACRYSTIS  
IN TERTIARY BASALTS

*Fodor, <sup>(1)</sup>R.V.; Gandhok; <sup>(1)</sup>G.R.; and Sial, <sup>(2)</sup>A.N.*

*(1)North Carolina State University, Raleigh, NC 27695, USA.; (2)Universidade Federal de Pernambuco, Recife, PE, Brazil*

Tertiary (13-31 Ma) alkalic basaltic centers in northeastern Brazil contain lherzolite and harzburgite xenoliths and pyroxene megacrysts. Plate reconstruction places these basaltic centers near the Fernando de Noronha hotspot during their times of eruption. We determined the compositions of basalts at four of these centers (three in Rio Grande do Norte state and one in Pernambuco state), and trace element and mineral compositions of their ultramafic xenoliths and xenocrysts. The geographic distances represented by these four sites spans about 200 km n-s.

Results: Basalts are olivine-phyric and have high Mg#s (68-73), K<sub>2</sub>O 1.2-1.3 wt.%, Ni 300-350 ppm, Sr 600-900 ppm, Zr 155-225 ppm, and La/Yb 19-27. Xenoliths have Fo 89-91, opx and cpx Mg#s of 88-92, and spinel Cr#s of 9-39. Notable is that pyroxene compositions define two groups of xenoliths: (i) coexisting low-Wo opx and high-Wo cpx (Wo<1 and Wo>45), and (ii) coexisting high-Wo opx and low-Wo cpx (Wo>2 and Wo<44). These compositions respectively describe two regimes of pyroxene equilibration temperatures, 750-950°C and 1050-1200°C (based on Wells, 1977). The three Rio Grande do Norte centers each have xenoliths of both types; only the low-T type was observed at the Pernambuco xenolith site. Pyroxene compositional characteristics associated with these two groups include: lower Cr and higher Na in cpx and lower Cr and Na in opx of the low-Wo opx (i.e. low-T) group when compared to cpx and opx in the high-Wo opx (i.e. high-T) group. Spinel Cr#s are lowest (9-18) in the low-T group and higher (26-39) in the high-T group. Also, CaO is lower in ol of the low-T group, ≤0.02 wt.%, compared to CaO in olivine of the high-T group, ≥0.09 wt.%. Finally, the low-T group has flat patterns for middle-to-heavy REE at 2-3 x chondrites, and LREE enrichment where La(n) is 5-15 (analyses of cpx also show LREE enrichment); patterns for the high-T group are either flat at M-H REE (~chondritic values) or U-shaped (MREE(n)~0.01), and with La(n) 2-3.

Orthopyroxene and clinopyroxene megacrysts have compositions consistent with the type II (high-A1, low-Cr augite) group of xenoliths in basalts. An opx-cpx pair provides 1260°C equilibrium temperature.

Conclusions: High MgO and Ni in the basalt hosts are consistent with near-primary melts from mantle peridotite; however, accurate assessment of MgO is complicated by the presence of olivine disaggregated from the xenoliths. Xenolith geothermometry and corresponding mineral compositions (e.g. high-T group has higher spinel Cr#, lower Na and higher Cr in cpx) suggest that the northeastern Brazil basalt centers contain samples of mantle that had a vertical gradient in terms of temperature and degree of melting, where the high-T xenoliths have mineral and trace-element compositions that reflect mantle more refractory than that represented by the low-T xenoliths. The megacrysts indentify metasomatic veining in this environment. Subsequent to (or associated with) the melting events that created distinct compositional (and equilibrium temperature) mantle zones, small-percent LREE-rich fluids infiltrated the environment. LREE abundances suggest that all mantle environments represented by the xenolith samples underwent enrichment; higher total REE concentrations now reside in members of the low-T group possibly because this material was not as depleted prior to fluid infiltration. These mantle samples from northeastern Brazil, therefore, offer an unusual perspective of vertical compositional "stratigraphy" related to temperature, melting, and the results of metasomatic events within subcontinental mantle.

## EXPERIMENTAL STUDIES OF OLIVINE LAMPROITE AT PRESSURES IN THE DIAMOND STABILITY FIELD

Foley, S.F.

*Mineralogisch-Petrologisches Institut, Universität Göttingen, Goldschmidtstrass 1, 3400 Göttingen, Germany*

At the last kimberlite conference, results of liquidus experiments at pressures up to a maximum of 40 Kbar on two lamproite compositions were presented (Foley, 1989a). The compositions studied were modelled on a leucite lamproite from Gaussberg, Antarctica, and an estimated primary magma composition for olivine lamproites from the West Kimberley lamproite field in Western Australia. The experiments on olivine lamproite are here extended to pressures up to 55 Kbar, and thus into the diamond stability field.

The new experiments were performed under the same volatile conditions as in the previous study, namely volatile saturated in the C-O-H system at oxygen fugacities one to two log units above the iron-wüstite buffer; the volatile phase consists principally of  $H_2O > CH_4$ .

These volatile conditions were chosen to test the hypothesis that a range of lamproite primary magmas with  $SiO_2$  contents from 42 wt% to about 53 wt% could be derived from a single source assemblage (phlogopite harzburgite) under reducing conditions ( $H_2O > CH_4$ ) by variation in the pressure of melting. In this scheme, the  $SiO_2$  contents of lamproites would be inversely proportional to their pressure of origin (Foley et al., 1986). The liquidus results up to 40 Kbar were consistent with this model; leucite lamproite could be reconciled with a mica harzburgite source mineralogy at pressures of 15-20 Kbar if allowance was made for there being too much fluid in the experiments, whereas olivine lamproite had olivine at its liquidus up to 40 Kbar as expected.

The higher pressure experiments were performed in a high temperature-calibrated belt apparatus at the Max-Planck-Institut für Chemie in Mainz. Natural polycrystalline  $CaF_2$  was used as the pressure-transmitting medium, with pressure controlled automatically to within 300 bar. The results are depicted in Figure 1, together with the lower pressure results from Foley (1989a). Olivine remains the only liquidus mineral to pressures above 50 Kbar, and is joined by mica and orthopyroxene and then ilmenite towards lower temperatures. At 55 Kbar, 1300°C Ol, Opx and Phl coexist, whereas at 55 Kbar, 1350°C no primary crystalline phase is observed. This is consistent with the mica harzburgite melting model with a pressure of origin of 55 Kbar for olivine lamproite. The olivine stability field has been extrapolated to pressures greater than 55 Kbar in Figure 1 since, as argued for leucite lamproite, the experiments contain an unrealistically large amount of fluid: this extra  $H_2O$  has the effect of shrinking the Ol phase volume, so that the true pressure of origin is more probably 60 Kar or slightly higher.

Partial melts of phlogopite harzburgite can be represented by the peritectic melting point  $Ol+Opx+Phl+Lq$  in the system kalsilite-forsterite-quartz. This simple system also expresses the main variation in the major element chemistry of lamproites, which is in  $K_2O$ ,  $Al_2O_3$ ,  $SiO_2$  and  $MgO$ . A combination of experimentally determined points for  $H_2O$ -saturated conditions (3 and 28 Kbar; Luth, 1967; Gupta and Green, 1988) and recast norms for leucite and olivine lamproite defines a trend representing the variation of composition of partial melts of phlogopite harzburgite with pressure (Figure 2). The low-pressure end of this trend lies at  $MgO$ -poor and thus  $K_2O$ ,  $Al_2O_3$  and  $SiO_2$ -richer compositions. The most extreme natural examples are probably leucite lamproites from Spain and the Leucite Hills, USA, which may originate at depths of 10-15 Kbar. At the other extreme, olivine lamproites from Western Australia originate at 60 Kbar or more. The persistence of olivine at subliquidus temperatures above 45 Kbar (not predicted by Foley, 1989a) can be explained by eutectic crystallization to the Fo-side of the Opx-Phl join.

The pressure trend depicted in Figure 2 applies to reduced,  $CO_2$ -free

conditions. Variation of  $f_{O_2}$  in the volatile system C-O-H causes the melt composition to follow a trend transverse to the pressure trend. Only in the presence of  $CO_2$ , and thus in more oxidizing conditions, will  $SiO_2$ -undersaturated melt compositions result. Such  $CO_2$ -bearing conditions are not possible for the main lamproite series, but may apply to the rarer madupitic lamproites, which are characterized by higher CaO and lower  $SiO_2$  contents than most lamproites.

The origin of most lamproites in reduced conditions, where  $CH_4$  rather than  $CO_2$  is the main carbon species, is supported by the following lines of evidence:

- (i) Leucite cores in the Gausberg lamproite have  $Fe^{3+}$  contents of ~0.3 wt% corresponding to  $f_{O_2} \ll (IW+3)$ . Rims and the main phenocryst population crystallized at marginally less than Ni-NiO (Foley, 1985). This indicates considerable near-surface oxidation of the lamproite magma.
- (ii) Spinel inclusions in lamproitic olivines indicate more reducing conditions than groundmass spinels using an experimental  $f_{O_2}$  calibration (Foley, 1985).
- (iii) Lamproites are typically rich in  $H_2O$  and poor in  $CO_2$ . The paucity of C is readily explained by its presence as  $CH_4$ , which is much less soluble in silicate melts than  $CO_2$ .
- (iv) Partial melting of a mica harzburgite in which the mica has  $K_2O/Al_2O_3 \approx 1$  provides a convincing explanation for the extremely high  $K_2O/Al_2O_3$  of lamproites. Such a mica can only crystallize in reduced conditions with  $f_{O_2}$  close to IW (Foley, 1989b); more oxidized micas have  $K_2O/Al_2O_3$  considerably less than 1.
- (v) Lamproites from Smoky Butte, USA, have micas which possess these same "reduced" characteristics, and also contain armalcolite phenocrysts which indicate  $f_{O_2} \approx IW$  to  $IW+2$  log units (Friel et al., 1977).

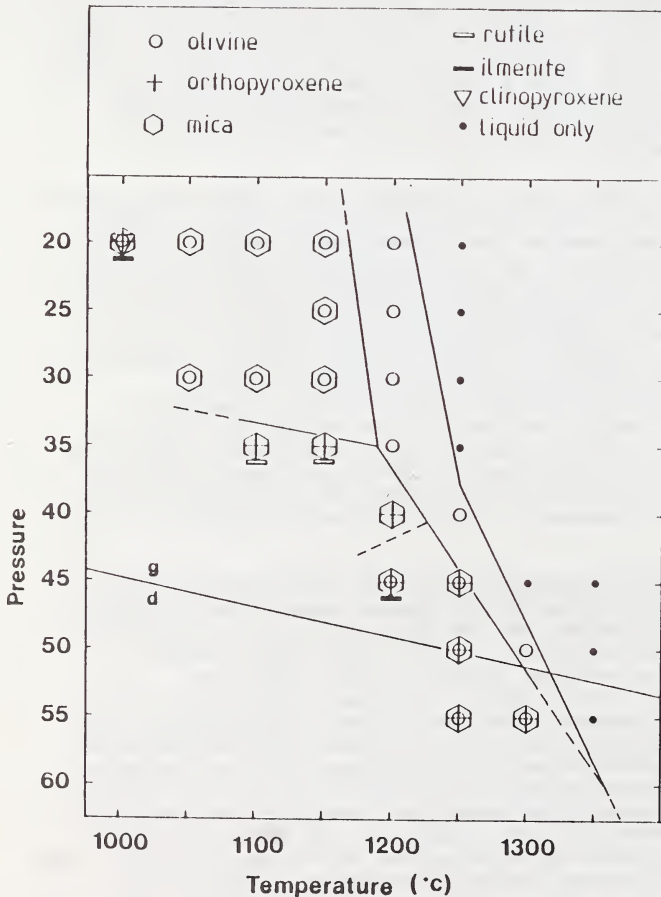
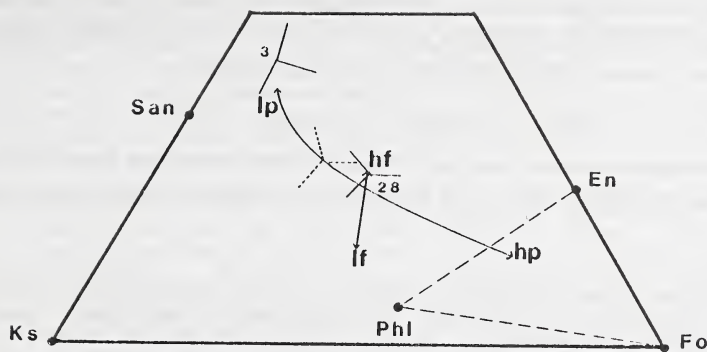


Figure 1

Experimental results for liquidus experiments on olivine lamproite.

Figure 2:



In addition to the liquidus study on the estimated primary olivine lamproite composition, a few experiments have been conducted using a natural olivine lamproite from dyke sample BMR 8321-1034 (kindly supplied by Lynton Jaques). This lamproite has a composition similar to the estimated primary magma, but with lower  $K_2O$  (3.4 wt%) and  $Na_2O$  contents (0.15 wt%); details of chemistry and petrography for this sample are given by Jaques et al. (1989).

The composition has been modified slightly by the addition of  $TiO_2$ , increasing the content from 3.44 to 5 wt%. These experiments form part of another experimental program aimed principally at studying  $TiO_2$  solubilities in mantle-derived magmas, and the possible role of titanate minerals in their sources. However, mention of them is relevant here because they include several runs at temperatures considerably below the liquidus. The experiments were conducted in the COH-fluid system using graphite capsules and a Co-CoO buffer mixture. This buffer defines the composition of the fluid phase as extremely  $H_2O$ -rich (>99.5 mol% - measured by mass spectrometer) at high pressures and relatively low temperatures. The  $fO_2$  lies slightly above that defined by the CWI technique used for the other lamproite experiments. Use of this buffer has not yet been perfected, so that some of the experiments were not fluid-saturated; the  $fO_2$  should nevertheless be very close to the Co-CoO buffer.

At subliquidus temperatures in the Argyle experiments, clinopyroxene appears at much higher temperatures than garnet. At 35 Kbar, Cpx is present in a run at 1200°C (together with Opx, Phl + Rut), whereas garnet is not present at 1050°C (Cpx, Opx, Phl + Rut present). Garnet is present at 43 Kbar, 1020°C in a run which also contains Opx, Cpx, Phl, rutile and apatite. The Cpx has Mg-number of 89, and low  $Al_2O_3$  contents (0.5-0.9 wt%). Garnet has much lower Mg-number ( $\approx 70$ ), and has low CaO (5.8-7.4 wt%) and high MnO (0.6-0.9 wt%) contents. Rutile shows similar characteristics to those analysed previously in lamproite experiments, with high Fe and Cr.

Since the phase volume of Cpx expands greatly with a small increase in  $fO_2$  (i.e. with  $CO_2$  present), madupitic lamproites leaving Cpx stable in the residuum could be generated from a similar source to other lamproites where slightly higher  $fO_2$  prevails.

Foley, S.F. (1985) *Tschermaks Min. Petr. Mitt.* 34, 217-238

Foley, S.F. (1989a) In: *Kimberlites and related rocks I* (eds. A.L.Jaques, J.Ferguson and D.H.Green) 616-632, Blackwells, Melbourne.

Foley, S.F. (1989b) *Eur. J. Mineral.* 1, 411-426

Foley, S.F., Taylor, W.R. and Green, D.H. (1986) *Contrib. Mineral. Petrol.* 93, 46-55

Friel, J.J., Harker, R.I and Ulmer, G.C. (1977) *Geochim. Cosmochim. Acta* 41, 403-410

Gupta, A.K. and Green, D.H. (1988) *Mineral. Petrol.* 39, 163-174

Jaques, A.L., Sun, S-S. and Chappell, B.W. (1989) In: *Kimberlites and related rocks I* (eds. A.L.Jaques, J.Ferguson and D.H.Green) 170-188, Blackwells, Melbourne.

Luth, W.C. (1967) *J.Petrol.* 8, 372-416

THE STABILITY OF PRIDERITE, LINDSLEYITE-MATHIASITE AND YIMENGITE-HAWTHORNEITE UNDER LOWER CONTINENTAL LITHOSPHERE CONDITIONS:  
EXPERIMENTS AT 35 TO 50 KBAR

Foley, <sup>(1)</sup>S.F.; Hoefler, <sup>(2)</sup>H.; and Brey, <sup>(2)</sup>G.P.

(1) *Mineralogisch-Petrologisches Institut, Universität Göttingen, Goldschmidtstrasse 1, 3400 Göttingen, Germany;*  
(2) *Max-Planck-Institut für Chemie, Abt. Kosmochemie, Saarstrasse 23, 6500 Mainz, Germany*

Members of the alkali-titanate mineral series Priderite, Lindsleyite-Mathiasite and Yimengite-Hawthorneite are potentially important reservoirs for silicate-incompatible elements in the source regions of alkaline magmas including kimberlites and lamproites. Particularly LIMA and YIHA can contain considerable abundances of Sr, LREE and HFSE (Haggerty et al. 1983).

Priderite occurs as a late-crystallizing phase in lamproites and is also known from nodules which are interpreted to represent the high-pressure crystallization products of lamproitic magmas. LIMA and YIHA occur in "metasomatized" xenoliths where an incompatible element-rich agent has infused a depleted peridotite wall-rock; the Cr-rich nature of spinels and other titanates in depleted peridotite appears to be crucial to the genesis of these minerals (Jones et al., 1982; Haggerty, 1983).

LIMA, YIHA and priderite have all been found as inclusions in diamonds from southern Africa, Siberia or Western Australia, indicating their possible stability in the source regions of kimberlites and lamproites. Mineral associations of YIHA have been used to suggest that hawthorneite in southern Africa crystallized at 70-100 km depth (Haggerty et al., 1989), whereas yimengites from Venezuela originate as deep as 150 km (Nixon and Condliffe, 1989). Only preliminary high-pressure experiments investigating the stability of these minerals have been undertaken, and to a maximum pressure of only 30 Kbar (Dubeau and Edgar, 1985).

Experiments investigating the stability of these minerals at 35 to 50 Kbar and temperatures of 1200-1550°C are reported here. The LIMA (AM<sub>21</sub>O<sub>38</sub>) and YIHA (AM<sub>12</sub>O<sub>19</sub>) compositions investigated are simplified with respect to natural minerals whilst retaining enough of their characteristics to allow application of the results to the Earth's mantle. The compositions were simplified in the following ways: (i) only K and Ba were included in the A-site, omitting such elements as Ca, Sr and LREE; (ii) for LIMA, the M-site contains > 12 cations Ti, and Cr is the second most abundant cation as in natural minerals; (iii) no cations with valency 5 are included. The formulae of the compositions investigated, in which all Fe is trivalent, are;

LIMA: (K<sub>0.5</sub>Ba<sub>0.5</sub>) (Ti<sub>13</sub>Cr<sub>3.5</sub>Fe<sub>1</sub>Zr<sub>1</sub>Mg<sub>2.5</sub>) O<sub>38</sub>

YIHA: (K<sub>0.5</sub>Ba<sub>0.5</sub>) (Ti<sub>3</sub>Cr<sub>4.5</sub>Fe<sub>2</sub>Mg<sub>2.5</sub>) O<sub>19</sub>

All experiments were synthesis runs using starting mixtures made up of oxides (Ti, Cr, Zr, Mg and Fe), titanates (K<sub>2</sub>Ti<sub>2</sub>O<sub>5</sub> and BaTiO<sub>3</sub>) and/or BaFe<sub>2</sub>O<sub>4</sub>. Since K<sub>2</sub>CO<sub>3</sub> and BaCO<sub>3</sub> were used as sources for potassium and barium, the titanates and ferrite were crystallized at 1 atm to avoid inclusion of CO<sub>2</sub> in the high pressure experiments.

Experiments were run in a high-temperature-calibrated belt apparatus at the Max-Planck-Institut für Chemie in Mainz, with pressure controlled automatically to within 300 bar. Samples were sealed in Pt capsules, and natural polycrystalline CaF<sub>2</sub> was used as the pressure-transmitting medium. Run times varied from 4.72 hours for priderite at 50 Kbar and 1550°C to 113 hours for YIHA at 50 Kbar and 1200°C.

Priderite was found to be stable at 50 Kbar and 1200 to 1500°C (runs were made at 100°C intervals); only at 1500°C was appreciable melt present. Lower temperature runs with small amounts of glass (<2%) are interpreted to

represent stable priderite whose composition is slightly removed from the arbitrarily chosen bulk charge composition. Two mixes differing in K/Ba and Ti/Fe were used for priderite in runs with Fe present as ferric iron; K/Ba ratios were 1.5 and 3.0 and Ti/Fe ratios 3.89 and 6.75 respectively. These showed that the stable high-pressure priderite has high K/Ba of between 3.85 and 4.05 even when K/Ba of the starting mix is only 1.5. Priderite forms large crystals (50-100 $\mu$ ) which are deeply coloured and pleochroic between purplish grey and greenish brown.

LIMA crystallized to form bright green crystals generally 30-50 $\mu$  in size under all conditions studied (35 Kbar, 1300°C; 50 Kbar, 1200-1350°C). LIMA formed a single phase with composition only very slightly different from the starting material, as can be seen by comparing the microprobe analysis of a run product in the table with the formula for the starting mix given above. The largest difference is the higher K/Ba of the stable mineral.

*Microprobe analyses and structural formulae of high-pressure phases*

	LIMA	Yimengite	Hawthorneite
	50Kbar, 1350°C	50Kbar, 1350°C	50Kbar, 1350°C
TiO <sub>2</sub>	60.94	25.23	24.31
Cr <sub>2</sub> O <sub>3</sub>	15.49	36.32	35.67
Fe <sub>2</sub> O <sub>3</sub>	4.78	14.09	17.00
MgO	6.09	16.82	10.43
ZrO <sub>2</sub>	7.74	0.00	0.00
K <sub>2</sub> O	1.47	7.24	1.78
BaO	3.49	0.29	10.80
<u>Cations</u>			
Ti	12.962	2.845	2.920
Cr	3.464	4.306	4.504
Fe	1.018	1.590	2.043
Mg	2.568	3.758	2.482
Zr	1.067	0.000	0.000
K	0.532	1.386	0.364
Ba	0.387	0.017	0.676
oxygens	38	19	19
A-total	0.92	1.40	1.04
M-total	21.08	12.50	11.95

YIHA was investigated at 43 Kbar, 1150-1250°C and 50 Kbar, 1200-1350°C. Under all these conditions yimengite and hawthorneite form separate phases, indicating the presence of a solvus between potassium- and barium-rich end-members. Yimengite forms large crystals (50-100 $\mu$ ), whereas hawthorneite crystals are extremely small (<10 $\mu$ ). Atomic ratios (K/Ba) on the A-site for these coexisting phases are > 45:1 for yimengite and approximately 1:2 for the hawthorneitic crystals. In spite of the yimengite being closer to the end-member composition in terms of K/Ba, the

stoichiometry of the hawthorneites is much closer to the ideal formula  $AM_{12}O_{19}$  (see table). The yimengites show consistent excess in cation totals on both A-site and M-site, although the cation charge total equals 38.004 with all Fe as  $Fe^{3+}$ ; the  $AM_{12}O_{19}$  "magnetoplumbite" structure was confirmed by x-ray diffraction. Large excesses of cations are known from natural LIMA crystals (Haggerty et al., 1983), but not from natural YIHA.

In separate experiments, end-members compositions of lindsleyite, mathiasite, yimengite and hawthorneite have been successfully synthesized at 50 Kbar and 1300°C. Crystallographic studies have confirmed the hawthorneite to be space group  $P6_3$ ; hexagonal unit cell parameters are (a) 5.862 (2) Å and (c) 22.91 (2) Å in comparison to the calculated values of (a) 5.871 (2) Å and (c) 23.06 (2) Å of Haggerty et al. (1989). Structural refinements of the other end-member phases are in progress; preliminary X-ray data are similar to published patterns, confirming the presence of the end-member minerals.

Both K-rich and Ba-rich natural examples of the yimengite-hawthorneite series are known from xenoliths in China and southern Africa respectively (Haggerty et al., 1989). Nixon and Condliffe (1989) have reported natural yimengites from Venezuela with up to 19% of A-sites occupied by Ba: this falls within the solvus region defined by the present experiments, indicating either that different conditions applied (e.g. higher temperatures leading to closure of the solvus) or that the solvus is more restricted in natural systems. Intermediate members of this series with K/Ba close to unity have not yet been reported, which may be due to the solvus, although exsolved examples are also lacking.

A second starting mix of priderite in which all iron is present in the ferrous state has been briefly studied. This modification was prompted by the cation totals of priderite inclusions in diamonds from Western Australia (Jaques et al. 1989); these are much closer to the expected stoichiometry if Fe is ferrous instead of ferric as often assumed. Also, it is unlikely that all iron could be present in the ferric state at  $fO_2$  low enough to allow diamond stability. In these extra experiments, a graphite sleeve was included inside the Pt capsule to prevent excessive alloying of Pt with Fe in the sample. Iron was included in the starting mix as a mixture of metallic Fe,  $Fe_2O_3$  and  $BaFe_2O_4$ . This priderite has been successfully synthesized at 35 Kbar, 1200°C and 50 Kbar, 1200-1300°C.

These experiments confirm the stability of priderite, LIMA, yimengite and hawthorneite at pressures corresponding to those of the diamond stability field, and thus underline their possible importance as reservoirs for silicate-incompatible elements in the source regions of kimberlites and/or olivine lamproites. Petrographic and mineral chemical studies, however, suggest that these minerals may be restricted to reaction zones between metasomatic enriching agents and depleted peridotite containing Cr-rich spinels (Jones et al., 1982; Haggerty 1983). Further experiments testing the stability of these alkali-titanates in assemblages such as Cr-spn + ol + opx + phl are needed to closely delineate the assemblages with which alkali-titanates could coexist in the mantle.

- Dubeau, M.L. and Edgar, A.D. (1985) *Min. Mag.* 49, 603-606  
 Haggerty, S.E. (1983) *Geochim. Cosmochim. Acta* 47, 1833-1854  
 Haggerty, S.E., Smyth, J.R., Erlank, A.J., Rickard, R.S. and Danchin, R.V. (1983) *Am. Mineral.* 68, 494-505  
 Haggerty, S.E., Grey, I.E., Madsen, I.C., Criddle, A.J., Stanley, C.J. and Erlank, A.J. (1989) *Am. Mineral.* 74, 668-675  
 Jaques, A.L., Hall, A.E., Sheraton, J.W., Smith, C.B., Sun, S-S., Drew, R.M., Foudoulis, C. and Ellingsen, K. (1989) In: *Kimberlites and related rocks Vol.2* (eds. S.Y. O'Reilly, R.V.Danchin and A.J.A.Janse) 966-989, Blackwell, Melbourne.  
 Jones, A.P., Smith, J.V. and Dawson, J.B. (1982) *J.Geol.* 90, 435-453  
 Nixon, P.H. and Condliffe, E. (1989) *Min. Mag.* 53, 305-309

## THE ORIGIN OF KIMBERLITE AND LAMPROITE IN VEINED LITHOSPHERIC MANTLE

Foley, S.F.

*Mineralogisch-Petrologisches Institut, Universität Göttingen, Goldschmidtstrasse 1, 3400 Göttingen, Germany*

Widely accepted models for the origin of alkaline magmas implicitly assume large-scale homogeneity and equilibrium in the mantle source regions by invoking partial melting of garnet lherzolite. A petrogenetic grid based on partial melting experiments on lherzolithic compositions works well for the voluminous basalt types from picrites to alkali basalts, but is less successful for more alkaline magma types. The presence of volatiles has been recognised as necessary for the genesis of e.g. basanites and nephelinites (H<sub>2</sub>O) and melilitites and kimberlites (CO<sub>2</sub>), but the action of volatiles has been consistently envisaged as being superimposed on the same underlying assumption of homogeneous lherzolite. Thus, carbonated garnet lherzolite and phlogopite lherzolite are normally considered as sources for kimberlites and ultrapotassic rocks (e.g. Wyllie, 1980; Wendlandt and Eggler, 1980)

Increasingly, the need for "heterogeneity" and different "domains", "components" or "reservoirs" is discussed, but without a clear picture of the physical structure of the upper mantle source being developed. Strongly alkaline melts are generally accepted to originate by very small degrees of partial melting, and the influence of incompatible element-enriched accessory minerals is often invoked to explain patterns of minor and trace elements. In some cases, e.g. calcite, dolomite and alkali titanates, these accessory minerals are either believed or known not to be stable in lherzolite at upper mantle pressures.

A more realistic scheme than the homogeneous lherzolite model invokes a veined source rock composed of veins derived by solidification of earlier magma batches and wall-rocks of variably depleted lithospheric peridotite. Melt source regions for alkaline magmas are thus minute windows centred on these veins; homogeneity and equilibrium, if present at all, are only very local.

Composite nodules have provided many dyke-margin samples from about 100 km depth, and geobarometric estimates indicate that veined nodules from southern African kimberlites originate from as deep as 170 km. Thus the brittle regime, characterised by flow through fractures as opposed to flow along grain boundaries, extends to at least 170 km beneath some cratons, and its persistence to depths in excess of 200 km, applicable to the source regions of kimberlites and olivine lamproites, is not unreasonable. The transition zone between this brittle zone and the underlying grain boundary flow (GBF) regime has been modelled by Sleep (1988) as a region in which veins collect melt from a restricted surrounding volume by grain boundary flow, and in which the proportion of veins increases upwards. A densely veined lower boundary to the brittle regime is thus a logical consequence of this scenario (McKenzie, 1989).

**Melting processes in veined source rocks**

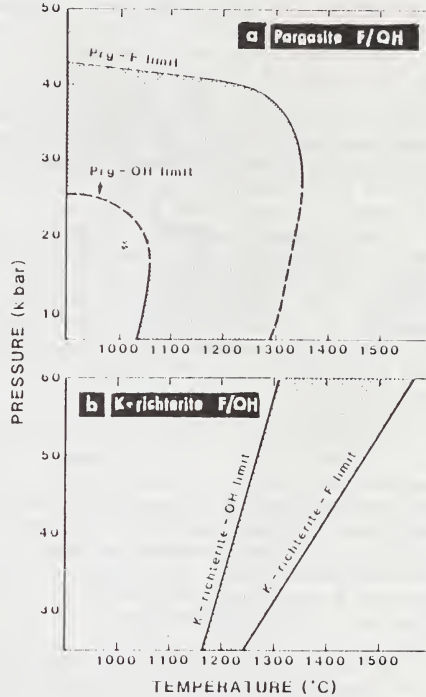
The initial stages of melting will be centred on the vein assemblage due to the concentration of carbonate and hydrous minerals, many of which are enriched in incompatible elements. Evidence from (i) the few available near-solidus high-pressure experiments on basaltic compositions, and (ii) the parageneses of composite mantle xenoliths, suggests that the veins will consist dominantly of clinopyroxene and mica or amphibole, and will be essentially olivine-free. Minerals which are present only as accessories in lherzolite may be common (e.g. apatite).

Partial melting experiments by Lloyd et al. (1985) showed that low-alumina ultrapotassic melts can be produced by 30% melting of mica-pyroxenite. Titanates remained stable in the residuum to in excess of 30% melting, apatite to >20% melting.

With continued melting of the vein-plus-wall-rock system, the veins and host peridotite do not behave as distinct systems, despite their

inherently different solidus temperatures, because of the operation of solid-solution melting reactions which bridge the gap between the melting temperatures of the different assemblages. A well-known example of the solid solution melting effect is the Cr/Al ratio of spinel: peridotites depleted by loss of a basaltic melt fraction retain a Cr-rich spinel, whereas the Al-component is lost preferentially to the melt.

Solid solution melting reactions occur wherever a mineral contains end-members with greatly differing thermal stabilities. For vein assemblages in the subcontinental lithosphere, amphibole and mica, and probably to a lesser extent apatite and titanates, will exhibit important solid solution melting behaviour. Recent experiments on the hydroxy- and fluor-end-members of pargasite and K-rich-richterite, which are the most likely amphiboles to be stable in lherzolite and harzburgite respectively, show that the fluor end-members are more stable by 150-250°C and 10-15 Kbar relative to the OH-end-members (Fig.1). Furthermore, the temperature difference for K-rich-richterite increases with increasing pressure towards lower lithosphere levels relevant to kimberlite and olivine lamproite genesis. In experiments in the system kalsilite-forsterite-quartz with H<sub>2</sub>O or F, the peritectic point  $Ol+Opx+Phl+Lq$ , which models partial melting of a mica-bearing ultramafic assemblage, indicates that the corresponding difference between F and OH end-members for phlogopite is 320°C at 28 Kbar.



The effect of the solid solution melting reactions is a smooth progression from vein melting to melting of the surrounding wall-rocks, so that an initial vein-derived strongly alkaline melt fraction becomes increasingly diluted by a more basaltic melt fraction from the wall-rocks.

Melting of veined lithosphere exhibits the following important general features:

- (i) Magmas seen at the Earth's surface are hybrids of melt components derived from veins (V-component) and surrounding peridotitic wall-rock (W-component). The alkalinity of the magma broadly reflects the V/W ratio.
- (ii) The carbonate and/or hydrous minerals in the source are already concentrated into veins; they may be rare (or absent) in the surrounding wall-rock. This contrasts with most petrogenetic models in which these minerals are homogeneously distributed.
- (iii) The chemistry of the V-component may be controlled by minerals which are *insignificant* or even *unstable* in spinel- or garnet lherzolite. Examples are K-rich-richterite and alkali-chrome-titanates which are almost certainly restricted to alkali-rich and alumina-poor environments.
- (iv) The composition of the hybrid magma will be dependent on variations in (a) the nature of the melt which solidifies to form the veins, (b) the wall-rock assemblage, and (c) the conditions of melting, such as pressure,  $fO_2$  and volatile speciation.
- (v) Solid-solution is of paramount importance, and cannot be neglected as in many peridotite melting models, especially those in simple systems. The stability of phlogopite and amphibole during a large melting

interval makes these important buffer phases for many incompatible trace elements.

- (vi) At larger degrees of melting than for strongly alkaline melts (*i.e.* lower V/W ratios), commoner basaltic melt types will result. The incompatible element patterns of these basaltic rocks may nevertheless be attributable to vein components, and thus may show similar characteristics, but different abundances, to strongly alkaline rocks. In zones of extension, these vein components may be further diluted by an asthenospheric basalt component.

#### Genesis of kimberlites

A veined source explains the well-known hybrid characteristics of kimberlite, namely its alkaline and carbonate-rich, but nevertheless very magnesian nature. The conditions in the source noted in (iv) above can be constrained: The V-component must be carbonate-rich and thus oxidized, whereas the wall-rock is in most cases garnet lherzolite, as indicated by the occurrence of Ol, Opx, Cpx and Gt together near the liquidus of an average kimberlite composition (Eggler and Wendlandt, 1979).

The carbonate-rich vein material may be produced by partial melting of peridotite in the presence of CO<sub>2</sub> and H<sub>2</sub>O; this has been shown to produce Na-carbonatitic melts at 20-30 Kbar (Wallace and Green, 1988), and may lead to Na-poorer, Ca-richer melts with very low silica contents at higher pressures due to the greater solution of Na<sub>2</sub>O in Cpx (Brey et al., 1991). This vein component would explain the correlation between CaO and CO<sub>2</sub> in kimberlites as being due to a melt and not a CO<sub>2</sub>-rich fluid (*cf.* Bailey, 1984). Partial melting of lherzolite at 50-70 Kbar produces very Mg-rich melts, which together with abundant xenolithic material, impart the 'peridotitic' character to kimberlite. The VW-model differs from that of McKenzie (1989) in that low-degree melts from the grain boundary flow regime are here seen as the source for only the first-stage vein assemblages, which eventually give rise to only the first of two components of the kimberlite magma; the GBF melts themselves are nowhere seen at the Earth's surface.

#### Genesis of lamproites

Mica is abundant in the vein assemblages of ultrapotassic rock sources, and remains stable in the residuum of at least the lamproites. The low CaO, Al<sub>2</sub>O<sub>3</sub> and Na<sub>2</sub>O of lamproites indicates a harzburgite or very depleted lherzolite wall-rock, since residual minerals of the source region as a whole are Phl, Ol and Opx (Foley, 1989a).

The vein paragenesis cannot be closely defined at present because of the dearth of experimental work on non-lherzolitic ultramafic assemblages. The stability of Cpx is extremely sensitive to fO<sub>2</sub> in lamproitic compositions, but is unlikely to be important in the source since fO<sub>2</sub> is very low: low fO<sub>2</sub> is indicated by the behaviour of mica chemistry, which can cause the extremely high K/Al of lamproites only in reduced conditions (Foley 1989b). Incompatible element-rich accessory phases such as priderite, apatite and wadeite may be present in the vein assemblage.

- Bailey, D.K. (1984) in *Kimberlites I: kimberlites and related rocks* (ed. J.Kornprobst) 323-333, Elsevier, Amsterdam.
- Brey, G.P., Ryabchikov, I.D. and Bulatov, V. (1991) *N.Jb.Min.Mh.*
- Eggler, D.H. and Wendlandt, R.F. (1979) in *Kimberlites, diatremes and diamonds* (eds. F.R.Boyd and H.O.A.Meyer) 330-338, Am. Geophys. Union, Washington.
- Foley, S.F. (1989a) in *Kimberlites and related rocks I* (eds. A.L.Jaques, J.Ferguson and D.H.Green) 616-632, Blackwells, Melbourne.
- Foley, S.F. (1989b) *Eur. J. Mineral.* 1, 411-426
- McKenzie, D. (1989) *Earth Planet.Sci.Lett.* 95, 53-72
- Sleep, N.H. (1988) *J.Geophys.Res.* 93, 10255-10272
- Wallace, M.E. and Green, D.H. (1988) *Nature* 335, 343-346
- Wendlandt R.F. and Eggler, D.H. (1980) *Am.J.Sci.* 280, 421-458
- Wyllie, P.J. (1980) *J.Geophys.Res.* 85, 6902-6910

THE MINERALOGY, PETROLOGY AND GEOCHEMISTRY OF ULTRAMAFIC  
LAMPROPHYRES OF THE YILGARN CRATON, WESTERN AUSTRALIA

Foster, <sup>(1)</sup>J.G.; Hamilton, <sup>(1)</sup>R. and Rock, <sup>(2)</sup>N.M.S.

(1)Western Mining Corporation, 55 MacDonal St, Kalgoorlie, WA, 6430, Australia; (2)Key Centre for Strategic Mineral Deposits, Department of Geology, University of Western Australia, WA, 6009. Australia

Four fields of ultramafic lamprophyres (UML) have so far been discovered in the Eastern Goldfields province of the Archæan (4.2–2.7 Ga) Yilgarn Craton (Figure 1). Bulljah, Lara, Melrose and Norseman. Melrose and Lara have not previously been reported whilst two hitherto unrecorded bodies are here reported from Norseman. The isotopic ages of the intrusives vary from  $849 \pm 9$  Ma (Rb–Sr) at Norseman (Robey et al., 1986) to  $305 \pm 7$  Ma at Bulljah (Hamilton and Rock, 1990). No isotopic ages are available for the bodies at Melrose or Lara. The UML at Melrose intrude Archæan granites and geological relationships indicate a pre-Permian post-Archæan age for Lara. These intrusives are significantly younger than the 2.1 Ga Mt Weld carbonatite and the 2.7 Ga Yilgarn calc-alkaline lamprophyre dyke swarms (Rock, 1990) which are also located in the Eastern Goldfields province. Peak metamorphism reflecting the last Archæan tectono-thermal event occurred at 2.7 Ga, therefore the UML represent the youngest post-cratonisation magmatic events so far recorded on the Yilgarn craton.

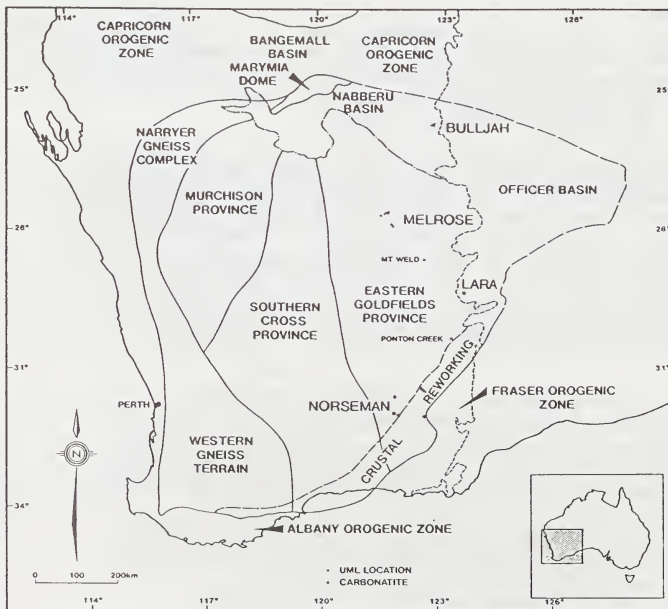


Fig. 1 Location of Yilgarn UML

The bodies typically form dykes which may be discontinuous over several kilometres. The Melrose dykes have widths up to 80cm and commonly exhibit flow differentiation on a centimetre scale. This feature has been reported from aillikites in Labrador (Malpas et al., 1986). Four pipe like bodies are also reported, two from Bulljah, one from Melrose

and one from Lara. The country rock of one Bulljah pipe has been metasomatised and magnetite alteration has occurred over a width of several metres.

The cognate mineralogy of the Yilgarn UML's comprise phenocryst phases of phlogopite and subhedral to euhedral olivines set in a matrix of varying abundances of phlogopite, cpx, calcite, spinel series, apatite, Mg-Mn ilmenite, serpentine, perovskite and Ti-bearing andradite schorlomite garnet; melilite and nepheline are absent. Late stage carbonate veining and segregation features are apparent. Irregular segregation structures often contain chlorite, pyrite and pyrrhotite inclusions (Archer, 1986).

Phlogopites evolve towards tetraferriphlogopite as a result of the replacement of  $Al^{3+}$  by  $Fe^{3+}$  in the tetrahedral site. Rare Ba-bearing phlogopites and feldspars are recorded at Bulljah, olivines are commonly serpentinised, the few fresh grains analysed carry up to 44 wt% MgO. Diopsides range from low Al-Ti diopside through to titaniferous salite. The presence of both high  $TiO_2$  and  $Al_2O_3$  in cpx is particularly diagnostic of ultramafic lamprophyres world-wide (Rock, 1987). The spinels describe a wide continuum from low  $Cr_2O_3$  aluminous magnesian chromite (AMC) to high  $Cr_2O_3$  titanian magnesian aluminous chromite (TMAC) to low  $Al_2O_3$  titanian magnesian chromite (TMC) to high  $FeO$ , titanomagnetite (TM). This trend corresponds to the trend 2' of kimberlite and lamproite spinels (Mitchell, 1986). At both Bulljah and Melrose early grains are often rimmed by later stage more evolved groundmass compositions. We suggest the spinel spectrum represented here is probably magmatic although AMC spinels overlap xenocrysts from garnet and spinel lherzolite. It is envisaged that the AMC trend results from the early Co-crystallisation with phlogopite which effectively reduces the amount of  $Al^{3+}$  for AMC spinel growth.

Xenocryst and macrocryst phases are common. Macrocrystal olivine is ubiquitous at Norseman, grains tend to be anhedral and contrast sharply with the subhedral to euhedral phenocrysts. Picroilmenite is also ubiquitous with compositions ranging from moderate MgO (6-12 wt%), high  $Cr_2O_3$  (0.5-2.5 wt%), moderate MnO (0.5-1 wt%) to low MgO (4 wt%) low  $Cr_2O_3$  (0.0-0.5 wt%). All picroilmenites have high  $FeO$ , possibly reflecting formation under relatively oxidising conditions. Mantle derived xenocrysts occur at Bulljah and Melrose. Bulljah concentrates yielded an array of garnets corresponding to Dawson and Stephens' (1975) G1, G3, G5, G9 and G10 categories plus two species of chrome diopsides and red-brown aluminous spinels. The garnets indicate that the UML sampled garnet lherzolite, garnet harzburgite, spinel lherzolite, eclogite and lower crustal material on its ascent. Ultramafic nodules are not apparent in surface exposures, but five well rounded spinel lherzolite nodules recovered from diamond drill core represent the only intact mantle sample recovered from beneath the Yilgarn craton. The largest nodule (6cm) comprises red-brown spinel, cpx, opx, calcite and serpentine and altered olivine. Analyses of cpx indicate equilibration at less than 1000°C (Jaques, 1989). G3, G5, G9 garnets and Cr-diopsides were recovered from Melrose. No ultramafic nodules were discernible at outcrop but abundant rounded crystal xenoliths exhibiting reaction rims were apparent at one locality.  $Na_2O$  levels in G3 garnets from both Bulljah and Melrose (<0.02 wt%), indicate relatively shallow origin.

Geochemically the Yilgarn UML's are potassic ( $K_2O/Na_2O \geq 1$ ), ultrabasic undersaturated ( $SiO_2 = 37.57\%$ ), primitive ( $MgO = 16.74\%$ ), titanian ( $TiO_2 = 4.25\%$ ) and iron rich ( $FeO_T = 14.2\%$ ). They can easily be discriminated from kimberlites on the basis of their  $MgO/CaO$  and  $SiO_2/Al_2O_3$  ratios (Figure 2a). One analysis in the kimberlite field represents an anomalously olivine rich portion of an ultramafic lamprophyre dyke from Melrose. The  $FeO_T$  of the UMLs are very high with respect to kimberlites and reflect high titanomagnetite content. Ni and Cr values are moderate, average 492 ppm and 457 ppm. Incompatible elements are typically enriched (average Ba 829 ppm, Rb 58 ppm, Sr 800 ppm, Nb 123 ppm, Zr 799 ppm, La 104 ppm and Ce 261 ppm). The enhanced light rare earth element (LREE) signature is typical for all members of the lamprophyre clan and is attributed to derivation from a partial melt of metasomatised mantle.

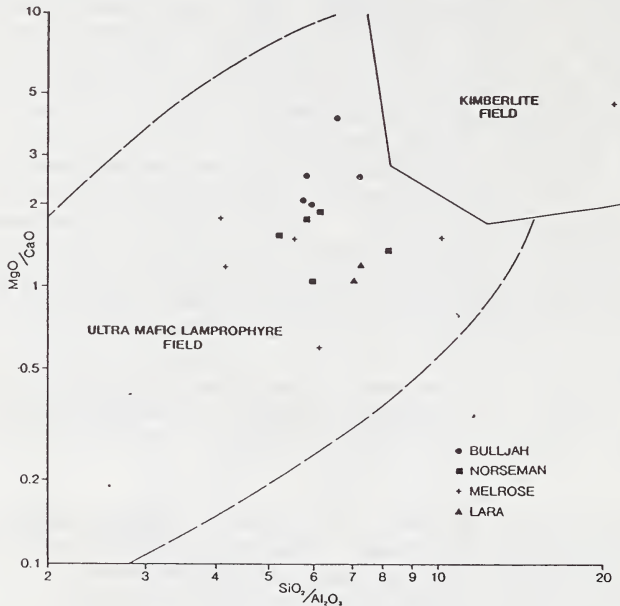


Fig. 2 Discrimination Diagram Based on Whole Rock Geochemistry

We conclude that the UMLs are the youngest member of the following spectrum of mantle-derived magmatic rocks within the Yilgarn craton. Komatiite (2.8 Ga) → basalt (2.7 Ga) → calc alkaline lamprophyre (2.7-2.6 Ga) → peralkaline granitoid (2.6 Ga) → dolerite (2.5-2.2 Ga) → carbonatite (2.1 Ga) → UML (0.8, 0.3 Ga). We suggest that widespread UML magmatism (coupled with the absence of true kimberlites) is the hallmark of intracratonic provinces with an early history of massive komatiite basalt extraction and subsequent tectonic stability. Cratonic provinces with a similar history of development such as the Superior Province may have few or no true kimberlites and low diamond potential.

Archer, N.R. (1986) : Ultramafic lamprophyres of the Yilgarn craton, Western Australia. MSc Thesis, Leicester University, England.

Dawson, J.B. and Stephens, W.F. (1975) : Statistical analysis of garnets from kimberlites and associated xenolith. *J. Geol.* 83:589-607.

Hamilton, R. and Rock, N.M.S. (1990) : Geochemistry, mineralogy and petrology of a new find of ultramafic lamprophyres from Bulljah Pool, Nabberu Basin, Yilgarn craton, Western Australia. *Lithos*, 24, 275-290.

Jaques, A.L. (1989) : Report on peridotite xenoliths from Bulljah Pool ultramafic lamprophyres. BMR Canberra, ACT.

Mitchell, R.H. (1986) : Kimberlites: Mineralogy, Geochemistry and Petrology. Plenum, New York, 442p.

Malpas, J., Foley, S.F. and King, A.F. (1986) : Alkaline mafic and ultramafic lamprophyres from the Aillik Bay area, Labrador. *Canadian Journal of Earth Sciences*, 23, 1902-1917.

Robey, J.V.A., Bristow, J.W., Marx, M.R., Joyce, J., Danchin, R.V. and Arnott, F. (1986) : Alkaline ultrabasic dikes near Norseman, Western Australia in J. Ross, Ed., Kimberlites and Related Rocks Volume 1, p382-391. Blackwell Scientific Australia.

Rock, N.M.S. (1991) : Lamprophyres: Blackie, Glasgow, 285p.

## THE GEOLOGY AND MINERALOGY OF SOME KIMBERLITES IN THE MWADUI AREA

*Gobba, J.M.**Williamson Diamonds Ltd., Mwadui Mine, Tanzania.*

The Mwadui kimberlite-bearing area is located in the Tanzania Archean Craton (2.5 - 3.0 Ma). The craton contains the oldest rocks known in Tanzania namely greenstones (basic and acid metavolcanics, banded ironstones and metasediments) and granitoids. The majority of the kimberlites lie within the craton and the Mwadui area is one with the highest number of fertile kimberlites. Out of the 67 known kimberlites in the latter area, 25 are diamondiferous, and only 3 have been economically exploited for diamonds. Among the three economic kimberlites is the Mwadui kimberlite pipe covering an area of about 146 ha making it the largest kimberlite in the world. Since its discovery (1940) the Mwadui pipe has produced 3.4 tons of diamonds valued at US\$1200 million.

The Mwadui area kimberlites were emplaced into the granitoids and greenstones during the Early Tertiary times (40-53 Ma; Davis, 1977; Raber, 1978; Shee, 1981). A considerably older age of Mid-Proterozoic (1097 Ma) has been obtained for one kimberlite in the Bubiki area (Bristow, 1986).

A preferred structural trend of the kimberlites is NE-SW which coincides with the trend of dolerite dyke swarms of Upper Proterozoic age. The Mwadui pipe lies at the intersection of the NE-trending dolerite dykes and a NW-striking shear zone. Close to the pipe is a major NNE-trending lineament. A structural trend between N and NNE appears to be associated with major kimberlitic intrusions e.g. Mwadui, Mhunze and Nyamigunga.

Macroscopic and microscopic study done recently has permitted in the mineralogical and textural classification of kimberlites in the Mwadui area. The mineralogical classification follows Skinner and Clement (1979) and is based on the predominant macrocrysts whereas the textural classification (Clement and Skinner, 1979) gives the facies (crater, diatrema and hypabyssal).

The study of the geology of the Mwadui pipe has shown that all the facies of a true kimberlite are preserved namely crater, diatrema, and hypabyssal (Gobba, 1989). In the crater facies are found both epiclastic and pyroclastic kimberlitic sediments (tuffs, shales, mudstones). The crater facies rocks are overlain by superficial deposits (gravels, silcretes, calcretes, and clays). Below the bedded crater facies rocks are the diatrema facies tuffisitic kimberlite breccias which are characterized by abundant unaltered xenoliths, discrete and fragmented autoliths of hypabyssal kimberlite and xenocrysts from deeper crustal/mantle sources. True hypabyssal facies within the main pipe has not been exposed. However, there are kimberlite dykes to the N and S of the main

pipe which show mineralogical and textural properties of hypabyssal kimberlite. The dyke to the north has a NE-SW orientation and is an altered serpentine-diopside kimberlite. The southern dyke has a SE trend and is an altered kimberlite containing serpentine and clay minerals.

A few other kimberlites show all the three facies (e.g. Mhunze and Nyamigunga) whilst most of the remaining are eroded to deeper levels removing some of the facies (mainly the crater facies).

Many Mwadui area kimberlitic intrusions are characterised by an absence of macrocrystal olivine and it is suggested that these could be related rocks here after called para-kimberlites, transitional between kimberlites and other ultramafic rocks (Gobba and Saxby, 1982; Gobba and Edwards, 1983). The criteria used in this study to classify a rock as a para-kimberlite is the morphology of olivine grains and the presence of groundmass minerals such as nepheline or analcime (Shee, 1980). Some kimberlitoids have been found in Mwadui area e.g. 65K34 kimberlite pipe. In this intrusion extensive mineral alteration to serpentine, carbonates and clay minerals are common. Pseudomorphs of olivine and monticellite are found, spinels and apatite are ubiquitous. At Bubiki (48K5 kimberlite pipe) olivines have unusual shapes and perovskites are unusually large. Overall the rock is considered to be a marginal kimberlite possibly transitional to an olivine melilite type rock association.

Some of the occurrences may represent aphanitic kimberlites and may have come about through filter pressing process. These however are not common and usually occur in specific geological settings such as dykes and sills. The fairly widespread occurrence with this texture is unusual for kimberlites. Several possibilities are given by Wyatt (1983) who suggested that they could be of relevance if these rocks are kimberlites. Firstly, they could have unusual structural control which could account for the removal of coarse constituents. Alternatively the absence of macrocrysts could be an intrinsic feature of the Mwadui area as a whole. It is therefore interesting to speculate that since the Mwadui kimberlite is almost completely preserved, we may be observing, in the Mwadui area, the terminal features of kimberlitic episodes that may not normally be observed in other areas. However considering combined evidence to date it seems probable that these occurrences are related rocks rather than aphanitic kimberlites. In regard to this it would seem that the presence of Mwadui true kimberlite in a province with fairly numerous occurrences of kimberlite-related rocks is unusual.

## REFERENCES

- BRISTOW, J.W. (1986) Ion probe U-Pb perovskite dating of the Bubiki kimberlite, Tanzania. Report on specimen CBE 5/25 Research School of Earth Sciences, Australian National University, Canberra.
- CLEMENT, C.R. and SKINNER, E.M.W. (1979) A textural genetic classification of kimberlite rocks. Poster session abstracts, De Beers kimberlite symposium, Cambridge, U.K.

- DAVIS, C.L. (1977) The ages and uranium contents of zircons from kimberlites and associated rocks. Carnegie Institute, Washington, Yearbook 76, p. 631-654.
- GOBBA, J.M. (1989) Kimberlite exploration in Tanzania. *Journal of African Earth Sciences*, 9, 3/4, 565-578.
- GOBBA, J.M. and SAXBY, P.B. (1982) Report on prospecting Licence 1/81 covering 104 square kilometers near Mhunze/Kishapu, Shinyanga Region. Unpublished Report Williamson Diamonds Limited.
- GOBBA, J.M. and EDWARDS, C.B. (1983) Report on prospecting Licence 1/81 covering 885 square kilometers near Mhunze/Kishapu area, Shinyanga Region. Unpublished Report, Williamson Diamonds Limited.
- RABER, E. (1978) Zircons from diamond-bearing kimberlites. Oxide reactions, fission track dating and mineral inclusions study. M.Sc. thesis, University of Massachusetts.
- SHEE, S.R. (1981) Dating of mineral and whole rock samples by U-Th-Pb method and application to kimberlites. Kimberly Petrographic Laboratory Report no. DBG/PI/81-88 of 47/11/81.
- SHEE, S.R. (1980) The petrography of some Tanzanian kimberlites and para-kimberlites. Unpublished Report no. DBG/PI/80, Williamson Diamonds Limited.
- SKINNER, E.M.W. and CLEMENT, C.R. (1979) Mineralogical classification of South African kimberlites. *Proceedings of 2nd International Conference*, 1, 129-135.
- WYATT, B.A. (1983) Petrography of assorted rock samples derived over aeromagnetic anomalies in the Mwadui area in Tanzania. Unpublished report no. AARI 475.WDS 1124 Williamson Diamonds Limited.

## COMPARATIVE GEOCHEMICAL EVOLUTION OF CRATONIC LITHOSPHERE: SOUTH AFRICA AND SIBERIA

W.L. Griffin<sup>(1)</sup>; J.J. Gurney<sup>(2)</sup>; N.V. Sobolev<sup>(3)</sup> and C.G. Ryan<sup>(1)</sup>

(1)CSIRO Div. of Exploration Geoscience, Box 136, N. Ryde, NSW 2113, Australia; (2)Dept. of Geochemistry, Univ. of Cape Town, Rondebosch 7700, RSA; (3)Inst. of Geology & Geophysics, USSR Acad. of Sciences, Novosibirsk, USSR

This paper compares geochemical data (trace elements by proton microprobe) on diamond-inclusion minerals (DI) and the corresponding phases in heavy-mineral concentrates, from kimberlites in Siberia (SIB) and southern Africa (SA). The SIB data are from Udachnaya, Aikhal, Sytykanskaya and Mir pipes; the SA concentrate data and most of the DI data are from kimberlites on the Kaapvaal craton, but the DI data include a few grains from Botswana. Published Nd model ages on garnets indicate Archean ages for peridotite-suite diamonds in both SIB and SA kimberlites. Comparison of major- and trace-element patterns in diamond-inclusion (DI) garnets and spinels from these two areas shows many similarities, and some important differences.

Garnet DI populations are dominated by subcalcic pyropes in both areas, but calcic (lherzolitic) garnets may be more common in SA. The Nickel Thermometer (Griffin et al, 1989) has been used to estimate temperature ( $T_{Ni}$ ) for individual garnet grains.  $T_{Ni}$  in South African DI garnets ranges from 950-1500 °C; in SIB garnets the range is 800-1500°C, but all DI with  $T < 950^\circ\text{C}$  are from the Mir pipe. The DI garnets from SA and SIB show similar patterns of depletion in Zr, Y, Ga and Ti, and enrichment in Sr, with decreasing Ca/Cr. However, SIB DI garnets have higher median Cr# values, and lower median Mg# values, than DI from South Africa. Chromite is an abundant DI phase in SIB kimberlites, and less common in SA. DI chromites from the two areas show similar ranges in Cr#, Ni and Ga, but those from SIB have lower median MgO and Mg#, and higher Cr/Mg, Fe and Zn. The differences in Mg# of garnet and chromite DI populations between the two areas, and the lower Zn in the SA chromites, would be consistent with a 150-200°C higher average T beneath SA at the time of diamond formation. However, this difference is not apparent in the  $T_{Ni}$  values of DI garnets, which show very similar mean and median temperatures for the two cratonic areas. In addition, the well-defined Fe-Zn correlations in the DI chromite populations (Fig. 1) are *en echelon*, rather than continuous with one another as would be expected if only a T difference was involved. It therefore appears that the deeper portions of the cratonic lithosphere beneath SA had lower Cr and higher Mg# than the Siberian mantle, at the time of diamond formation.

Comparison of garnet concentrates from diamondiferous kimberlites also shows several significant differences between SA (Kaapvaal craton) and SIB. Concentrates from both areas contain significant proportions of subcalcic garnets, but moderately subcalcic pyropes (3-5% CaO) appear to be more common in SIB concentrates, relative to extremely subcalcic and lherzolitic garnets. The concentrates show a similar range of  $T_{Ni}$ , but the SIB distribution is strongly weighted toward lower T relative to the SA distribution. Other factors being equal, this lower T distribution would imply a greater proportion of material from the graphite stability field in the Siberian pipes. This is not consistent with their high diamond grades; the favored alternate interpretation is that the geotherm at the time of emplacement of kimberlites was lower beneath Siberia than beneath the Kaapvaal craton. The existence of low-T (<950°C) DI garnets in SIB suggests that a similarly low geotherm may have existed in Archean time. The maximum Cr content of concentrate garnets shows a strong correlation with T (and presumably with P) in both sets of concentrates (Fig. 2). However, the SIB garnets show higher Cr (maximum and average values) at any T than those from SA. SIB concentrate garnets also have higher median Cr/Mg and lower median Mg# than those from SA, mirroring the differences seen in the DI garnet populations.

SA concentrate garnets are significantly enriched in Zr, Y and Ga relative to those from SIB. The median Zr and Y contents of calcic garnets (>4% CaO) in SA are 35 and 13 ppm, respectively, compared to 28 ppm Zr and 9 ppm Y for SIB garnets. 30% of such garnets in SIB concentrates have <10 ppm Zr, compared to 12% of SA garnets. The low-Ca garnets in both areas are very depleted in Y (median 2-3 ppm), but those in SA are considerably richer in Zr, with a median value of 24 ppm compared to 14 ppm in SIB. Significant levels (>5ppm) of

Sr, like those seen in DI garnets, are common in the subcalcic garnets of the SIB concentrates, but very rare in the SA concentrates.

Comparison of the DI and concentrate data suggests that the SA lithosphere is lower in Cr and Cr/Mg, and higher in Mg#, than the SIB lithosphere. The SA mantle is thus more refractory in terms of Mg#, but less refractory in terms of Cr#; this is inconsistent with a simple difference in degree of depletion through removal of basic melts. These differences existed at the time of Archean diamond formation, and have persisted since. The SA lithosphere is enriched in Zr and Y relative to the SIB lithosphere, and probably contains a lower proportion of highly depleted harzburgite. These differences in LIL elements and possibly in bulk Ca content were established after diamond formation.

These differences may be related to other significant differences in kimberlite mineralogy between the two cratons. The maximum, and perhaps mean, diamond grades of Siberian kimberlites are reported informally to be higher than those of kimberlites on the Kaapvaal craton. Siberian diamonds from the pipes considered here are typically octahedra with little evidence of resorption, while SA diamonds typically are dodecahedral, and have lost up to 50 % of their mass by resorption. K-richertite and other metasomatic minerals occur in many SA pipes, but apparently are rare in SIB ones. Finally, the garnets of sheared garnet peridotites from SA kimberlites show elevated Fe<sup>3+</sup> contents (Luth et al., 1990), suggesting that the melt metasomatism that affected these xenoliths (Griffin et al. 1989b) has involved an increase in the oxygen fugacity of the lithosphere.

We suggest that: (1) Early Archean processes were similar in the SA and SIB lithospheres, leading to depletion in most LIL and HFSE elements, a high proportion of harzburgite relative to lherzolite, and enrichment of very subcalcic garnets in Sr (and LREE). (2) The differences in major-element composition (Cr#, Mg#) were established in very early Archean time, and do not reflect simple differences in degree of depletion; they may reflect original heterogeneity. (3) the SA lithosphere was "refertilized" following diamond formation, by metasomatic processes which have affected the Siberian lithosphere little if at all. (4) Effects of these processes include introduction of Zr, Y and Ca (and probably K and Ti); reduction in the proportion of harzburgite to lherzolite, and stripping of Sr and LREE from subcalcic garnets. (5) The same process may have raised the oxygen fugacity of the SA lithosphere, leading to resorption of diamonds whether in the mantle wall rock, or in later kimberlites which have been buffered to the oxidation state of those wall rocks.

Griffin, W.L., Cousens, D.R., Ryan, C.G., Sie, S.H. and Suter, G.F. 1989a. *Contrib. Mineral. Petrol.* 103, 199-202.

Griffin, W.L., Smith, D., Boyd, F.R., Cousens, D.R., Ryan, C.G., Sie, S.H. and Suter, G.F. 1989b. *Geochim. Cosmochim. Acta* 53, 561-567.

Luth, R.W., Virgo, D., Boyd, F.R. and Wood, B.J. 1990. *Contrib. Mineral. Petrol.* 104, 56-72.

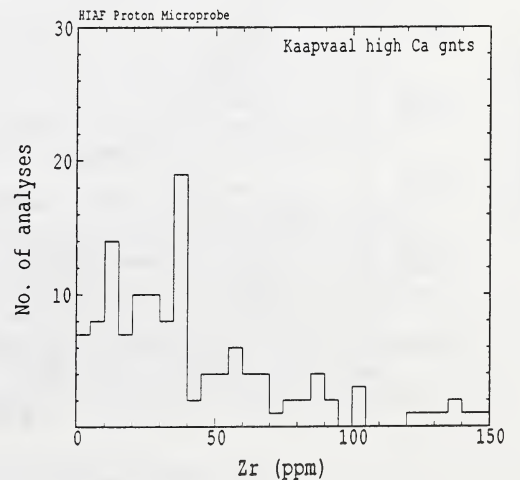
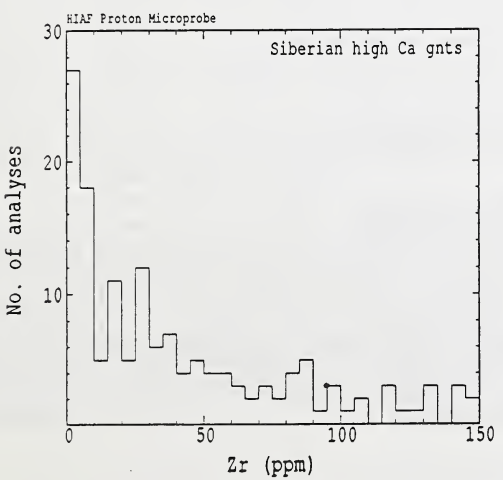
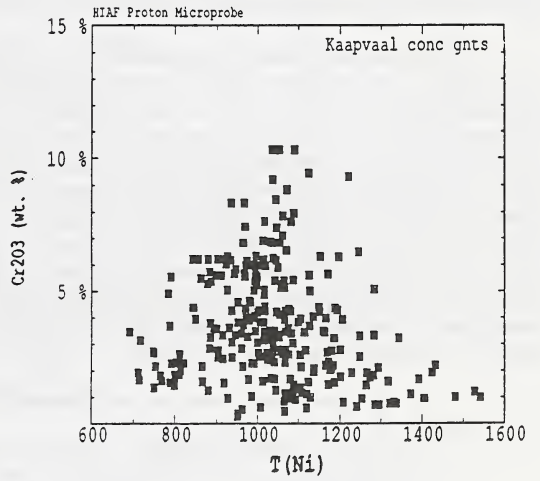
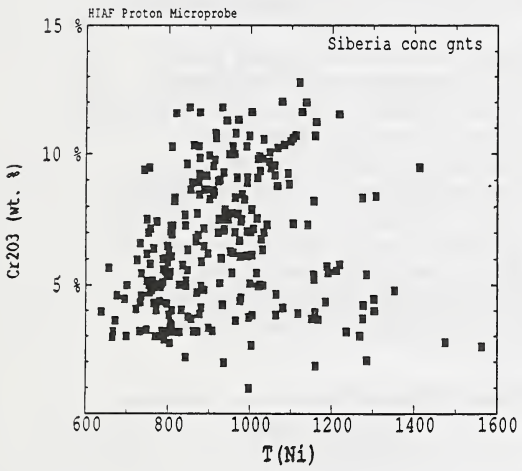
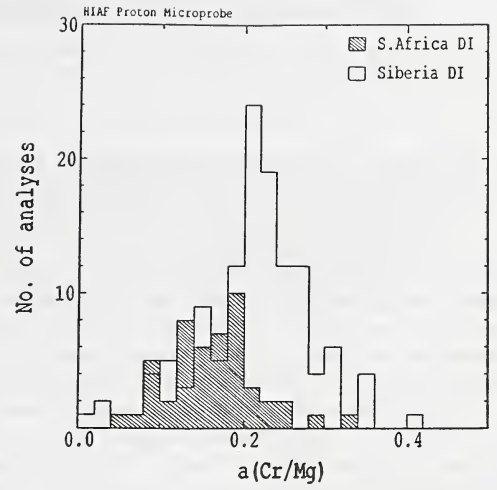
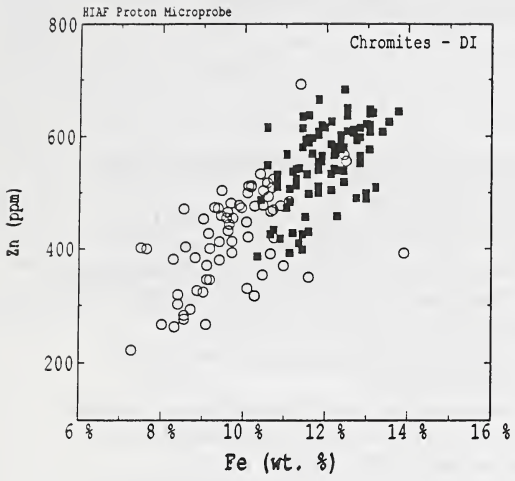
FIGURES (next page)

Fig. 1 (top left). Fe-Zn relations in DI chromites. Squares, SIB; circles, SA. The trends toward higher Fe and Zn in each group reflect cooling.

Fig. 2 (top right). Histograms of Cr/Mg for DI garnets. Hatched area: SA; clear, SIB.

Fig. 3 (middle). Cr-T relations in concentrate garnets from SIB and SA.

Fig. 4 (bottom). Histograms of Zr content in high-Ca (>4% CaO) concentrate garnets from SIB (n=147) and SA (n=128).



## SYSTEMATICS OF ISOTOPIC DISEQUILIBRA BETWEEN MINERALS OF LOW TEMPERATURE GARNET LHERZOLITES

M. Günther and E. Jagoutz

*Max-Planck-Istitut für Chemie, Abteilung Kosmochemie, Saarstrasse 23, 6500 Mainz, F.R.G.*

The garnet bearing lherzolites of the southern African craton can be divided into two types:

- 1.) High temperature deformed garnet lherzolites (1200-1400 °C)
- 2.) Lower temperature (900-1100 °C) coarse (and deformed) garnet lherzolites (1).

The chemical equilibration of minerals under mantle PT conditions is an unsolved problem. For petrographic PT estimations to reconstruct geothermal gradient, it is essential to assume chemical equilibrium between the minerals. Since the multidimensional chemical reactions are not quantitatively understood yet, only isotopic analysis can provide informations on chemical equilibrium between the minerals. Furthermore the isotopes are giving the only time information of the last chemical equilibration.

Spinell lherzolites from alkali basalts show a mineral Nd isotopic equilibrium between OPX and CPX (2) at the time of eruption. High temperature deformed garnet lherzolites are in Nd isotopic equilibrium between CPX and garnet, as they were sampled by the kimberlites, while the low temperature lherzolites are commonly not in isotopic equilibrium (3).

We investigated mineral separates of three coarse grain low temperature garnet harzburgites. Two of them contain some CPX (<5%). The samples were collected in Kimberley floors, S.A., in 1986, during a fieldtrip, by the courtesy of the Anglo American Company. The xenoliths were arranged according to their macroscopic appearance. Especially the texture of the garnets is striking. It is possible to classify the xenoliths in order of "increasing deformation" of the garnets: In one endmember (EJ 8601) the garnet occurs only in several cm large clusters, intergrown with OPX little CPX and phlogopite. With "increasing deformation" the clusters become disordered and gradually smeared out, ending in a homogenous distribution of garnet. EJ 8604 shows garnet intergrown with OPX/CPX and little phlogopite, still as clusters, whereas EJ 8631 displays a much more homogenous distribution of garnets. These clusters are suggesting to be the reaction products of a preexisting mineral phase.

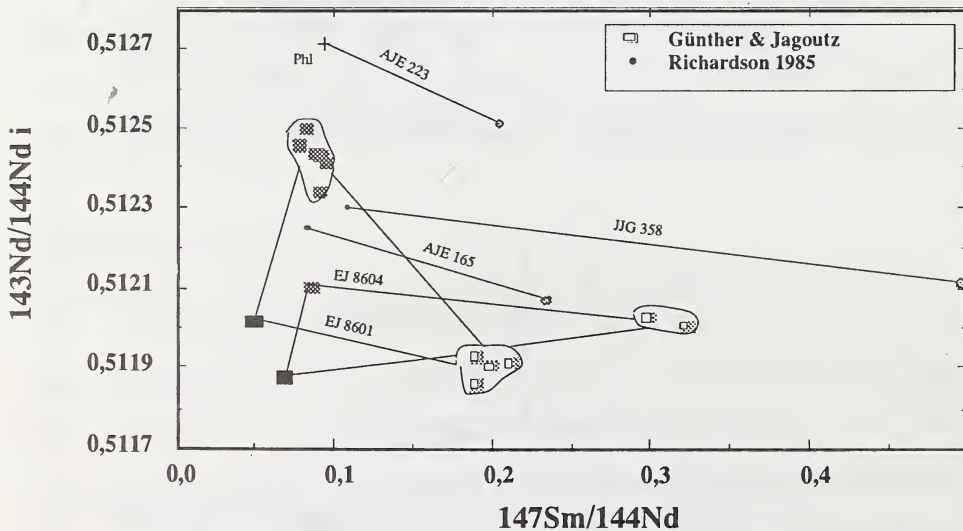


Fig. 1 Nd/Sm disequilibria (Symbols see Fig. 1)

We analysed mineral separates for Sr, Nd, and Pb isotopic systematics. Although the Sm/Nd ratios in garnets are about 5 to 10 times higher than in CPX and OPX, the Nd isotopic composition of garnet is less radiogenic, resulting in "future isochrones" with negative slopes. Similar results are reported by Richardson et al. (1985), as shown in Fig 1, while the sample EJ 8631, which contains the most deformed garnet cluster, is equilibrated in respect to the Nd isotopes, but their Sr isotopes are still recording a chemical disequilibrium. It seems that the Sr isotopes are more resistant to equilibration. While the Rb content of all these minerals is to little to explain a variation in the Sr isotopic composition, the measured isotopic composition of the minerals varies over a wide range. Garnets are always containing very radiogenic Sr (Fig. 2). The lead composition of EJ 8601, which contains the least deformed garnet clusters shows an extreme composition in garnet (206/204: 32,09, 207/204: 16,41, 208/204: 42,18), while its CPX plots above the enriched part of the oceanic basalt field. The other CPX's are laying near the field of unradiogenic depleted mantle, the OPX lies near above the enriched part of the oceanic basaltic field (after 4), while the garnets have consistantly the most radiogenic lead values (Fig. 3). The  $^{208}\text{Pb}$  systematics shows, that the Th/U ratio in the garnets is lower than in OPX, also indicating an isotopic disequilibrium between these mineral phases (Fig. 3).

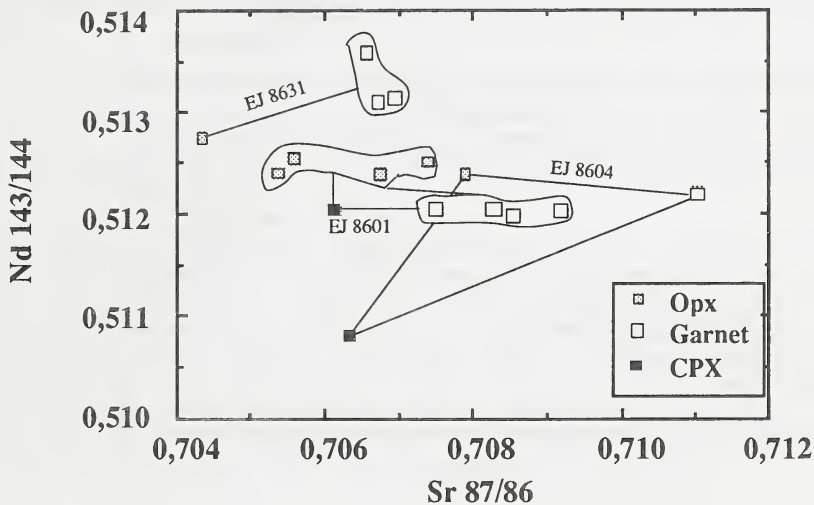


Fig. 2 Nd/Sr distribution plot

Since an information on the age can only be obtained in an equilibrated system, it is not possible to give an age estimate by using the above mentioned isotopic systematics. Only the U Pb system opens the possibility to look through the different metamorphic episodes. While the 206/204 versus  $\mu$  diagram is giving the eruption age, the Pb/U concordia diagram of EJ 8604 and EJ 8631 indicates a very old age of the protolith (more than 4 g.a.), and a young (200 ma) disturbance, which might be connected to the beginning of the eruption event. This young event might be the commonly referred metasomatic episode (5). The very early differentiation of harzburgites was also suggested by Boyd 1987 (6), according to their higher Si content.

The Nd and the Sr isotopic systematic proves that the minerals of garnet harzburgites, the comon low temperature or coarse granular xenolith from kimberlites, are not in chemical equilibrium. We suggest that the garnet had a precursor mineral phase. Compared to CPX this mineral phase had a low Sm/Nd and Th/U ratio but a high Rb/Sr and U/Pb ratio. We propose that an aqueous fluid invaded a depleted harzburgite and a hydrous phase (possibly an amphibole) was crystallized. Also the 208/204 versus 206/204 indicates an early disturbance of the protolith, which might also to be seen in the 207/204 versus 206/204, showing an "isochron" between OPX and garnet (EJ 8604) of about 1,4 g.a., which might be the age of hydration.

After a time of isotopic evolution this amphibole reacted to garnet+OPX +phlogopite+/-CPX, possibly caused by an episodic increase of pressure, about 200 m.a.ago. During this event the primary CPX and OPX was not isotopically equilibrated (EJ 8601, EJ 8604), while the garnet inherited the isotopic composition of the preexisting amphibole but lost some of its Nd U and Th. Since in the deformed sample (EJ 8631) the Nd was isotopically equilibrated at the time of sampling by the kimberlite 90 m.a. ago the deformation might be only as old as the eruption.

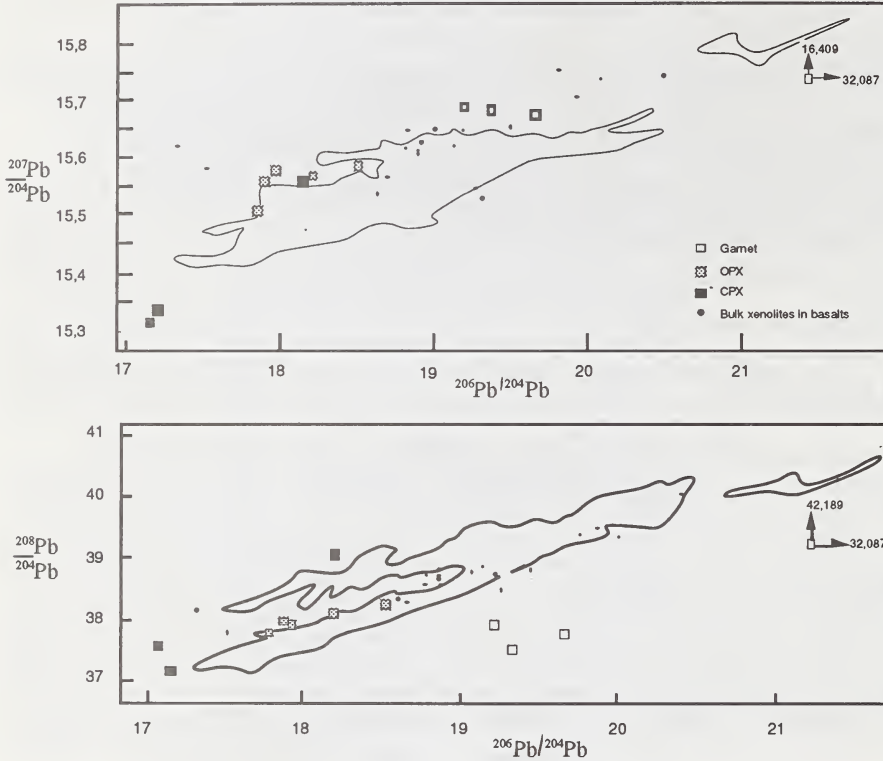


Fig. 3 Lead diagramm

### References

- (1) Boyd, F.R. and Nixon, P.H. (1978) Ultramafic nodules from the Kimberley pipes, South Africa. *Geochim. et Cosmochim. Acta*, 42, 1367-1382.
- (2) Jagoutz, E., Carlson, R.W. and Lugmair, G.W. (1980) Equilibrated Nd-unequilibrated Sr isotopes in mantle xenoliths. *Nature*, 286, 708-710.
- (3) Richardson, S.H., Erlank, A.J. and Hart, S.R. (1985) Kimberlite-borne garnet peridotite xenoliths from old enriched subcontinental lithosphere. *Earth Planet. Sci. Lett.*, 75, 116-128.
- (4) Hart, S.R. (1988) Heterogeneous mantle domains: signatures, genesis and mixing chronologies. *Earth Planet. Sci. Lett.*, 90, 273-296.
- (5) Dawson, J.B. (1980) *Kimberlites and their xenoliths*, Springer, Berlin.
- (6) Boyd, F.R. (1987) High- and low temperature garnet peridotite xenoliths and their possible relation to the lithosphere-asthenosphere boundary beneath southern Africa. In P.H. Nixon (ed.), *Mantle xenoliths*, p. 403-412. Elsevier, Amsterdam.

## GEOCHEMICAL CORRELATIONS BETWEEN KIMBERLITIC INDICATOR MINERALS AND DIAMONDS AS APPLIED TO EXPLORATION

Gurney, <sup>(1)</sup>J.J.; and Moore, <sup>(2)</sup>R.O.

(1)Dept. Geochemistry, Univ. Cape Town, Rondebosch 7700, South Africa; (2)P.O. Box 1372, Wangara, W. Australia 6065

Diamond Potential Based on the assumption that diamonds in kimberlite are derived from disaggregated xenoliths of peridotite and eclogite, the presence of diamond can frequently be successfully predicted by identifying the presence of the appropriate xenocrysts of two other resistant minerals, garnet and chromite. Since these are frequently sought in exploration programmes, such a predictive capability can be very useful in assigning priorities to prospective targets.

Both peridotitic and eclogitic diamonds are present in every well characterised kimberlite world-wide and in lamproites. Peridotitic diamonds predominate overall, but either paragenesis may dominate the diamond population at individual localities.

Peridotitic Diamonds The dominant source rocks of peridotitic diamonds are predicted to be harzburgites (probably carbonated) ± garnet and/or chromite. Lesser amounts of diamond are derived from garnet lherzolite. Garnet and chromite macrocrysts liberated from diamond harzburgite are in general more abundant than diamond itself and can be used as pathfinders to predict the presence of diamond. The garnets and chromites can be recognised by their compositions which are similar to some inclusions in diamonds.

Garnet and chromite macrocrysts from diamondiferous lherzolite cannot be similarly identified, and at present they are not useful in determining the economic potential of a kimberlite occurrence.

Eclogitic Diamonds Chrome-poor garnet macrocrysts liberated from potentially diamond-bearing eclogite (Group I eclogite) can also be identified on the basis of distinctive compositions. In some kimberlites, Group I eclogite has made a major contribution to the overall diamond content of the pipe.

Megacryst Minerals Many kimberlites contain megacryst suite minerals including abundant garnet similar in appearance to some eclogitic garnets, with which they may have overlapping major element compositions. Care must be taken to discriminate against these megacrysts since they are not related to diamond. Since megacryst garnets as a group show strong igneous trends they can be differentiated from eclogitic garnets on the basis of simple linear plots.

Preservation of Diamonds Resorption of diamonds after formation is an important process in southern Africa and some other diamond provinces. It is much less significant in the best known Siberian diamond populations and in places such as Angola. In southern Africa, highly oxidised ilmenite compositions with elevated inferred  $\text{Fe}_2\text{O}_3$  contents are not associated with high grade kimberlites. This is inferred to be correlated with the resorption process that has affected the diamonds.

Application Based on a sound database, indicator mineral compositions can be used to predict the diamond content of kimberlites in a semi-quantitative way with considerable success, providing diamond content is regarded as the sum of harzburgitic diamonds plus eclogitic diamonds modified by resorption.

Exceptions Exceptions can occur. These can often be detected by additional investigations that better define the petrogenetic history of the indicator minerals and their source rocks.

## THE MAGMATIC EVOLUTION OF THE JACUPIRANGA COMPLEX, BRAZIL

Gaspar, J.C.

*Departamento de Mineralogia e Petrologia, Instituto de Geociências, Universidade de Brasília, 70910 Brasília, Brazil.*

The Jacupiranga Complex is composed of two major rock bodies, dunite to the North and magnetite pyroxenite to the South. The magnetite pyroxenite body is intruded by:

a - pyroxenite and nepheline-bearing pyroxenite dykes. Many of them fenitized.

b - a crescent-shape ijolite intrusion composed of melilite ijolites and fenitized ijolites.

c - an elongated carbonatite intrusion consisting of five mainly phases: C1 - sovite, C2 - calcite-dolomite carbonatite, C3 - sovite, C4 - sovite, and C5 - beforosite. C1 is chemically different and C2 to C5 may represent four separate magma batches derived from an evolving parental carbonatite magma (Gaspar 1989).

d - phonolite dykes and pegmatitic nepheline syenite veins near the contacts of the complex.

A suite of Si-saturated rocks occurs as veins, dikes, and small intrusions in the borders of the Complex, displaying a large petrographic variety: gabbros, diorites, olivine monzonites, porphyritic and non-porphyritic monzonites and syenites, alkali syenites, quartz monzonites and syenites.

Microprobe analyses of minerals from the ultramafic and nepheline-bearing rocks showed that:

1 - spinels from pyroxene-bearing dunites are similar or more evolved than magnetites from the magnetite pyroxenites. The substitution mechanisms of the dunitic spinels present a magmatic evolution that is different from all other rocks of the complex.

2 - primary micas, olivines, and pyroxenes from the fenitized pyroxenites are less evolved than the same minerals from any other pyroxenite.

3 - spinels and pyroxenes from melilite ijolites are less evolved than spinels and pyroxenes from the metasomatized ijolites.

Mineral chemistry of the saturated suite indicated that there is no possible differentiation process that is able to explain the mineral composition of those rocks:

a - spinels, pyroxenes, and micas from syenites, monzonites, and gabbros and diorites present three parallel composition trends.

b - plagioclases from quartz monzonites are as calcic as those from olivine monzonites and mela-monzonites.

Plagioclases from quartz syenites are much more calcic than any other syenite plagioclase.

According to the above data a multi-stage magmatic system is required to explain the ultramafic and nepheline-bearing rocks (Figure 1):

1 - early crystallization and accumulation of olivine gave rise to dunites and wehrlites.

2 - just aside the dunites occurred the accumulation of clinopyroxene originating the magnetite pyroxenites. This new magma was compositionally different from the melt from which the olivines crystallized. Pyroxene crystal mushes were injected in country rocks forming the pyroxenite dikes found around the complex.

3 - dikes and sills of nepheline-bearing pyroxenites, with and without olivine, intruded the magnetite pyroxenites. A silicate melt possibly related to these nepheline-bearing pyroxenites split in two immiscible liquids and gave rise to C1 and melilite-free ijolites. This process occurred in a magma chamber underneath the magnetite pyroxenites.

4 - a second intrusive phase of dikes and sills of nepheline-bearing pyroxenites, with or without olivine. Once more a magma related to these nepheline-bearing pyroxenites split in two liquids originating a carbonatite magma and the melilite ijolites. Episodically upwards injection of this differentiating carbonatite magma resulted in the C2 to C5 carbonatite bodies. Fenitization produced by this carbonatitic activity affected early formed nepheline-bearing pyroxenites and melilite-free ijolites. Parent magmas for stages 2, 3, and 4 were certainly very similar in composition. Nepheline syenites and phonolites represent the closing stages of magmatic activity 3 and/or 4. Injections of pyroxene crystal mushes may have resulted in pyroxenite dikes intruding magnetite pyroxenites and country rocks. As seen above, gabbros and diorites, monzonites, and syenites, may represent each a different batch of magma. We suggest that the Jacupiranga plagioclase-bearing rocks were produced by different degrees of crustal contamination of the same magmas that originated the nepheline-bearing rocks and carbonatites. Three major factors could have contributed to this variety of plagioclase-bearing rocks that do not represent differentiation series: a) more than one magmatic stage occurred at the complex; b) liquids of different differentiation degrees may have been contaminated giving rise to melts of many particular compositions; c) different degrees of wall-rock assimilation could have occurred.

The history of the Jacupiranga complex is not the history of a magma chamber but rather that of a conduit.

#### References

- Gaspar, J. C. (1989) *Géologie et minéralogie du Complexe Carbonatitique de Jacupiranga, Brésil*. PhD Thesis. University of Orléans.



## BYRO SUB-BASIN AS A POTENTIAL DIAMOND-BEARING PROVINCE

*C.L. GEACH*

*Quicksilver Resources NL*

### Location and Regional Geology

The Byro prospect is located approximately 700 kilometres NNE of Perth, Western Australia.

The Western Gneiss terrain, a cratonised older component of the Yilgarn Block underlies the Permian aged Byro sub basin and an older Proterozoic sequence known as the Badgeradda Group.

The proximity of the Byro sub basin to the Yilgarn Block would suggest it lies as a Cratonic peripheral zone underlain by a cratonised, faulted basement of the same age as the Yilgarn Block (c.2.6-3.2 Ga).

### Exploration

In 1988 during follow up work by Quicksilver Holdings Pty Ltd and Hardman Resources NL to two previous microdiamond finds, abundant chromite concentrations were located; indicating an ultrabasic source for some of the chromites. Chromite morphology exhibited fresh to fractured octahedra indicating limited travel. Bevelled and frosted edges on some of the grains were indicative of the more magnesian (lamproitic) chromites identified by geochemical cation ratio plots  $Cr/Cr+Al$  vs  $Mg/Mg+Fe^{2+}$ .

The abundance of chromite, and the apparently fresh and often pristine chromite morphological characteristics suggests a provenance within the Byro sub basin. The near occurrence of a G-10 type pyrope, pyropic almandine as well as niobium (2%) enriched rutile and hafnium (5%) enriched zircon suggests a kimberlitic affinity. Chromites recovered from an initial 25 kg stream sediment sample programme over 53 sites produced a 78% chromite recovery rate.

### Geophysical Study

Aeromagnetics were at 200 metre line spacing and nominal sensor height of 60 metres. Colour 1:20,000 scale photographs were used for ground control and navigation. The data was also digitally processed. Several magnetic anomalies were recognised as immediate targets.

### Primary Magnetic Feature AN2

A localised, primary dipolar ground magnetic anomaly (AN2) was thought to be the source for chromites. AN2 can best be described as an EW trending tabloid. Subsequent pitting, aircore and diamond drilling around AN2 delineated an unexpected NE-SW trending palaeo-infill, part outcropping, consisting of fragmental and bouldery ingredients set in a clay bound silty matrix. The infill trends NE-SW and is

offset from the centre of AN2. Chromite has been recovered throughout the depth of the infill to 41 metres. Some of the chromites exhibit lamproitic cation ratios in the diamond inclusion field.

Trace element geochemistry detracts from a kimberlitic source for the infill.

### Petrography & Stratigraphy

Petrographic studies on 20 rock thin sections describe three major stratigraphic horizons.

**Uppermost Unit:** Two thin sections from surface rock samples at AN2 describe a superficial sediment, termed the Infill, of Miocene or younger age and composed of quartz fragments in a clay rock matrix, clastic in nature and slightly bedded.

Mineralogical study of Wilfley tabled concentrates from a 20kg+ specimen of infill produced six particles of gold which were mostly flakes of between 0.1 and 0.25mm. Heavy mineral observation of downhole samples of the infill recovered abundant (60+ grains) chromite and pyrope almandine out of 2-3 kg of air core sample to 27 metres. A diamond drill hole provided angular clay fragments one of which at 23.2 metres was indicative of a komatiitic type ultramafic origin.

**Middle Unit:** Claystone Grit Unit (regional exposed rock unit, considered part of a glacial Permian - Lyons Formation): described as a sandy siltstone with poor sorting containing lithic clasts to 2mm and a silt textured matrix. Clasts range from very coarse sand to coarse silt. The large diameter clasts are a mixture of quartz-rich rocks of igneous origin, both plutonic and volcanic textured examples.

The matrix stains very positively for K-feldspar, optically unresolvable. There is also extensive carbonate and some 0.1mm minerals, some of which have been determined as ilmenite, iron oxide, pyrite and a single grain of rounded chromite. This chromite has a very high Cr/Fe ratio and low Al and Si. It measures 62 microns.

SEM analysis identified various heavies, and garnet, of the almandine pyrope species. The opaques included iron oxides with a trace of Cr, Mn ilmenite and rare chromite. The chromite has Cr, Fe, significant Ti and very low Al and Mg.

**Lowermost bedded Siltstone Unit:** The description for this Upper Permian aged unit is a siltstone dominant in quartz and K-feldspar. Within the siltstone the feldspar content implies a tuff component. Quartz 30-40%, K-feldspar 30-40%, muscovite 5-20%, carbonate 2-3%. The accessories were identified by SEM. The opaques were all iron oxide with low Mn. The garnet was an almandine spessartite. The monazite is thorium bearing, less than 1%. Opaques were estimated to be 3-5%.

AN2 - Infill Age Determination

A palynological study was undertaken of drill core rock specimens from the AN2 area. Examined sample ARB-3 from the lower bedded unit described as a grey siltstone contained microfossil assemblages of Late Permian (230Ma) age, younger than the Upper Carboniferous - Lower Permian Lyons Formation (280Ma) thought to exist in the area. A second drill core sample ARB-1 from the infill deposit yielded microfossils of Miocene or younger age establishing a Miocene (25-7Ma) or younger age for the infill. The type of microfossils recovered supports a freshwater mode of deposition, however, the lower bedded unit may also have survived a brackish water environment.

Conclusions & Recommendations

The occurrence of many grains of fresh chromite exhibiting lamproitic cation ratios, together with a G-10 pyrope garnet from 25 kg stream sediment samples illustrates the opportunity for alkali and/or kimberlite style of intrusion to exist within the Byro sub basin. The results derived from this latest phase of diamond exploration goes far to verify that previous microdiamond finds made by another company in the Byro sub basin are real.

A younger Miocene aged unit termed the infill, contains abundant chromite, pyropic almandine and occasional gold and sulphides. The infill is a localised deposit and remnant of a previous larger palaeo-channel. It cross cuts all three stratigraphic units.

The highly potassic nature of the lower most bedded unit of Upper Permian age and the middle bedded unit of uncertain age cannot be explained wholly. Both units often resemble tuffaceous sediment derivatives probably from an acid - intermediate volcanic terrain. The source for pyropic almandine and non kimberlitic chromite in the middle unit has not been established. Furthermore, pyropic almandine in one drill hole of the middle unit is coincident with a linear NE magnetic trend cutting across the G-10 pyrope occurrence. The linear feature may have been a progenator for intrusives of alkali-kimberlitic magmatic type.

Magnetic anomaly AN2 has been drilled and as yet the source of the anomaly remains unexplained. A dyke or sill source for the chromite is not to be ruled out. Slightly elevated magnetic susceptibilities in the lower bedded unit at depths between 40-65 metres may be confirming the source of the AN2 anomaly as sedimentary in origin similar to many other magnetic targets previously drilled.

Anomalous, magnesian chromite occurring within a Miocene aged deposit over the Byro sub basin in conjunction with interpreted structural trends and past diamond finds suggests a tectonic inter-relationship prevails in the Byro sub basin.

ULTRAPOTASSIC MAGMAS ALONG THE FLANKS OF THE OLIGO-MIOCENE RIO GRANDE RIFT, U.S.A.: MONITORS OF THE ZONE OF LITHOSPHERIC MANTLE EXTENSION AND THINNING BENEATH A CONTINENTAL RIFT

Gibson, <sup>(1)</sup>S.A.; Thompson, <sup>(1)</sup>R.N.; Leat, <sup>(2)</sup>P.T.; Morrison, <sup>(3)</sup>M.A.; Hendry, <sup>(3)</sup>G.L. & Dickin, <sup>(4)</sup>A.P.

(1)Department of Geological Sciences, University of Durham, South Road, Durham, DH1 3LE (UK); (2)British Antarctic Survey, High Cross, Madingley Road, Cambridge, CB3 0ET (UK); (3)School of Earth Sciences, University of Birmingham, Edgbaston, Birmingham, B15 2TT (UK); (4)Department of Geology, McMaster University, 1280 Main Street West, Hamilton, L8S 4M1 (Canada)

Recent theoretical studies of rift tectonics have concluded that their observed geophysical features require that: (1) extension affects a much wider zone of the underlying lithospheric mantle than the crust; (2) early extension involves a comparatively wide zone, that narrows with time (e.g. Rowley & Sahagian, 1986; Buck et al., 1988). The Neogene evolution of the segment of the Rio Grande rift between the Great Plains and Colorado Plateau shows this theoretical pattern clearly. The width of the crustal extension zone narrowed from ~170km in the Oligo-Miocene to ~50km in the Pliocene (e.g. Aldrich et al., 1986; Fig.1). In contrast, both gravity and teleseismic studies (Parker et al., 1984) indicate that the current width of the zone of thinned lithospheric mantle ( $\beta=2-3$ ) beneath the rift is ~750km wide. This is presumably the aggregate result of all Neogene extension in the area, most of which took place in the Oligo-Miocene. We have sampled a diverse range of Oligo-Miocene magmatism (ranging from ultrapotassics to Hy- and Ne-normative basalts) extending ~650km across the thinned lithospheric mantle zone at 36-38°N, from the Navajo Igneous Province, Arizona, to Two Buttes, SE Colorado. The section is centered on the present day rift (Espanola Basin) and crosses L. Miocene hypabyssal intrusion complexes on the rift shoulders at Dulce and Riley, west of the rift, and Spanish Peaks to the east. A geochemical traverse along this section shows a spatially symmetrical variation in element and oxide ratios, such as  $\text{Na}_2\text{O}/\text{K}_2\text{O}$  (Fig. 2) and Ba/Nb, around the physiographic Rio Grande rift. Average  $\text{Na}_2\text{O}/\text{K}_2\text{O}$  ratios are as low as 0.4 in L. Miocene vents and intrusions above thick lithosphere (~150km) on the stable platforms flanking the rift. Examples of rock types from this tectonic setting are the "kimberlites" and minettes of the Navajo Province and minettes at Two Buttes. Average  $\text{Na}_2\text{O}/\text{K}_2\text{O}$  ratios increase towards the rift shoulders (1.2) and range from 1.4 to 8.66 in the centre of the rift where the lithosphere is ~75km thick. The large range in  $\text{Na}_2\text{O}/\text{K}_2\text{O}$  ratios in the Espanola Basin reflects the occurrence of both alkali and tholeiitic L. Miocene basalts in that area. A similar symmetrical spatial variation is apparent in Sr and Nd isotope ratios; average  $^{87}\text{Sr}/^{86}\text{Sr}$  ratios range from 0.70713 on the flanks to 0.70433 in the centre of the rift.

The variation in average  $\text{Na}_2\text{O}/\text{K}_2\text{O}$  ratios broadly parallels the corresponding teleseismic lithosphere thickness profile and is a mirror image of the gravity profile. Tectonic reconstructions show that the Farallon Plate was being subducted eastwards under the area at 24 Ma and the seismic tomographic study of Grand (1987) has provided direct evidence for this hypothesis. It has been suggested that the upward migration of volatiles from the sinking slab were responsible for mantle metasomatism and consequent ultrapotassic magmatism in the Navajo Province from 28-23 Ma (Laughlin et al., 1986; Rowell & Edgar, 1983). However the symmetrical ratio plots of incompatible elements,  $\text{Na}_2\text{O}/\text{K}_2\text{O}$  and isotopes of magmas in a 650km zone centered on the rift axis suggests that the ultrapotassic magmas on the stable flanks and shoulders of the rift are not directly related to the subduction of the Farallon plate; an asymmetric process. In the Espanola Basin,  $^{87}\text{Sr}/^{86}\text{Sr}$  and  $^{143}\text{Nd}/^{144}\text{Nd}$  isotope ratios and incompatible element concentrations are comparable to those of ocean island basalts (OIB's), e.g. Hawaii. This suggests that

the magmas in the rift axis, both tholeiitic and alkalic, were derived from an asthenospheric source. On the stable rift flanks almost all of the magmas are highly enriched in strongly incompatible elements and are depleted in high-field-strength elements such as Nb and Ta. These compositions are more typical of lithosphere-derived magmas (e.g. Thompson et al., 1990); a view concordant with the evidence of their radiogenic isotope ratios. The majority of dykes on the rift shoulders show similar elemental enrichments and depletions to the intrusions on the rift flanks but rare OIB-type magmas are also present. Our interpretations of magmatism across the rift zone are in agreement with those of Roden et al., (1990) who have recently suggested that the minettes of the Navajo Province are the a result of mixing melts from asthenospheric and lithospheric mantle sources. They suggest that the radiogenic Nd-isotope ratios of the peridotite xenoliths in the Navajo magmas reflects their long term isolation from mantle convection and that these inclusions are not samples of recently subducted lithosphere. The base of the lithosphere may be metasomatised by the percolation of small melt fractions from asthenosphere (McKenzie, 1989). Remelting of this underlying metasomatised lithosphere by stretching and decompression in the first phase of extension of the Rio Grande rift may explain the symmetrical occurrence of ultrapotassic magmatism in our sampled section. Such a model does not satisfactorily explain the lack of strongly potassic compositions amongst the Oligo-Miocene magmatism of the rift axis. However, this axis has a marked tendency to link sites of substantial Oligocene pre-rift magmatism along the Southern Rocky Mountains. These earlier liquids may have heated the sub-continental lithospheric mantle sufficiently to melt out any pre-existing fusible potassic fractions before rifting began.

#### References.

- Aldrich, M.J., Jr., Chapin, C.E. & Laughlin, A.W., 1986. Stress history and tectonic development of the Rio Grande rift, New Mexico. *Journal of Geophysical Research*, 91, 6199-6211.
- Buck, R.W., Martinez, F., Steckler, M.S. & Cochran, J.R., 1988. *Tectonics*, 7, 213-234.
- Cordell, L., 1982. Extension in the Rio Grande rift. *Journal of Geophysical Research*, 87, 8561-8569.
- Grand, S.P., 1987. Tomographic inversion for shear velocity beneath the North American Plate. *Journal of Geophysical Research*, 92, 14065-14090.
- Laughlin, A.W., Aldrich, M.J., Shafiqullah, M. & Husler, J., 1986. Tectonic implications of the age, composition and orientation of lamprophyre dikes, Navajo volcanic field, Arizona. *Earth and Planetary Science Letters*, 76, 361-374.
- McKenzie, D. P., 1989. Some remarks on the movement of small melt fractions in the mantle. *Earth and Planetary Science Letters*, 95, 53-72.
- Parker, E.C., Davis, P.M., Evans, J.R., Iyer, H.M. & Olsen, K.H., 1984. Upwarps of anomalous asthenosphere beneath the Rio Grande rift. *Nature*, 312, 354-356.
- Roden, M.F., Smith, D. & Murthy, V.R. 1990. Chemical constraints on lithosphere composition and evolution beneath the Colorado Plateau. *Journal of Geophysical Research*, 95, 2811-2831.
- Rowell, W.F. & Edgar, A.D., 1983. Cenozoic potassium-rich mafic volcanism in the western USA: its relationship to deep subduction. *Journal of Geology*, 91, 338-341.
- Rowley, D.B. & Sahagian, D., 1988. Depth dependent stretching: A different approach. *Geology*, 14, 32-35.
- Thompson, R.N., Leat, P.T., Dickin, A.P., Morrison, M.A., Hendry, G.L. & Gibson, S.A., 1990. Strongly potassic mafic magmas from lithospheric mantle sources during continental extension and heating: evidence from Miocene minettes of northwest Colorado, USA. *Earth and Planetary Science Letters*, 98, 139-153.

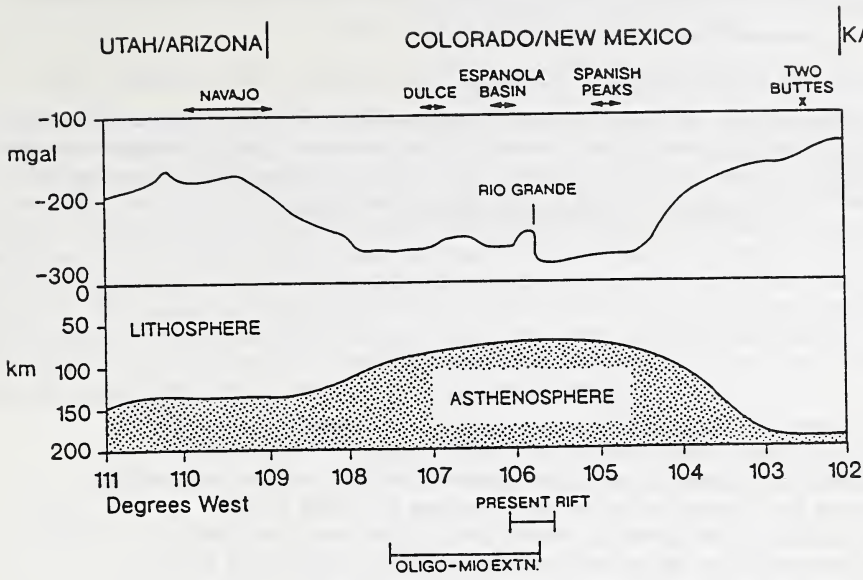


Fig. 1. Crustal structure at approximately 37°N beneath the Colorado Plateau, Rio Grande rift and Great Plains, from the gravity study of Cordell (1982) and the teleseismic study of Parker et al. (1984).

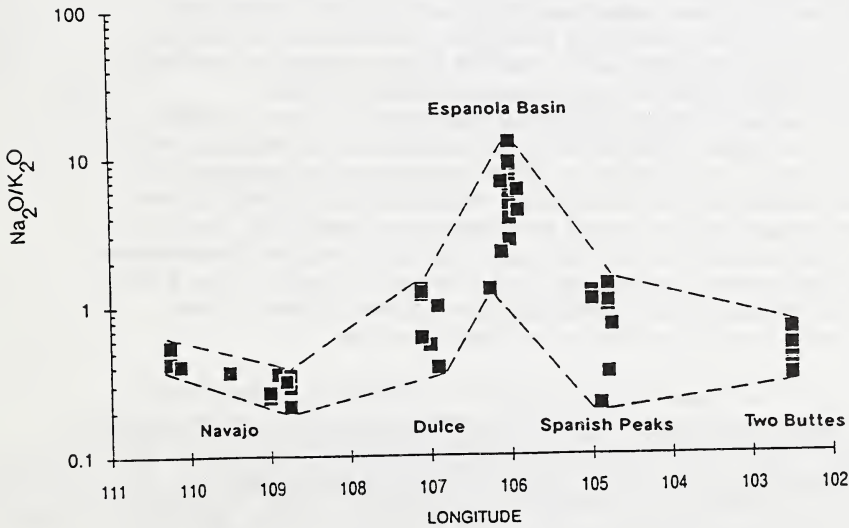


Fig. 2. Variation in alkali content of Oligo-Miocene magmas across the Rio Grande rift between 36° and 38° N.

## GEOCHEMICAL AND PETROGRAPHIC EVIDENCE FOR HIGH MG-ULTRAPOTASSIC MAGMAS IN SE COLORADO, USA

*Gibson, <sup>(1)</sup>S.A.; Thompson, <sup>(1)</sup>R.N.; Mitchell, <sup>(2)</sup>J.G.; Dickin, <sup>(3)</sup>A.P.; Morrison, <sup>(4)</sup>M.A. & Hendry, <sup>(4)</sup>G.L.*

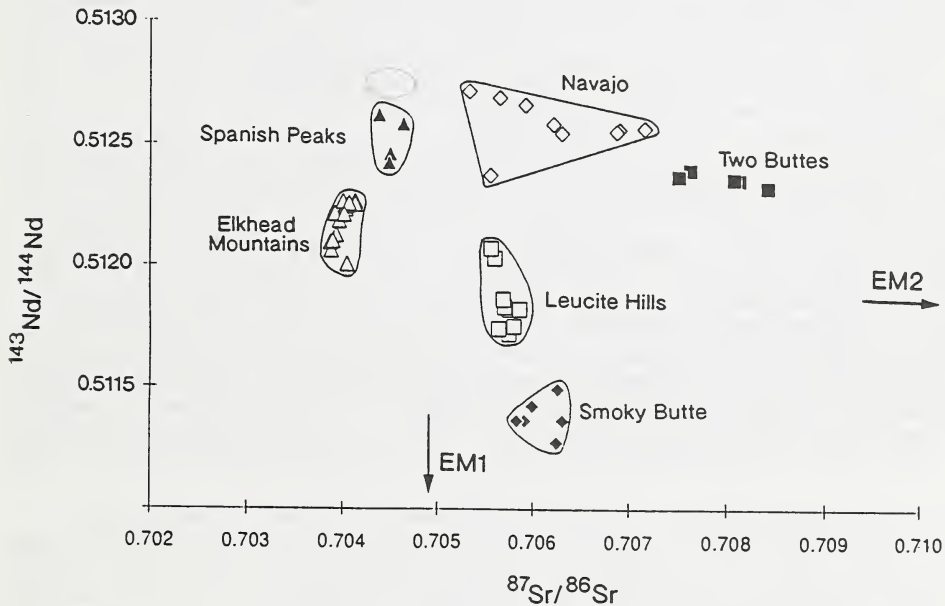
*(1)Department of Geological Sciences, University of Durham, South Road, Durham, DH1 3LE (UK); (2)Department of Physics, The University, Newcastle upon Tyne, NE1 7RU (UK); (3)Department of Geology, McMaster University, 1280 Main Street West, Hamilton, Ontario, L8S 4M1 (Canada); (4)School of Earth Sciences, University of Birmingham, Edgbaston, Birmingham, B15 2TT (UK).*

Two Buttes, Colorado (37°30'N 102°30'W) is situated on the stable plateau of the Great Plains, 300km east of the present-day axis of the Rio Grande rift. This complex consists of two laccoliths and numerous associated dykes which have intruded sediments of Triassic and Cretaceous age. The laccoliths are cut by sparse late-stage syenitic pegmatite veins and contain crustal xenoliths. Petrographically the rocks comprising the laccoliths consist of phenocrysts of clinopyroxene and phlogopite ± olivine that are set in a groundmass of feldspar, magnetite, clinopyroxene and phlogopite. Phlogopite mineral separates from these previously undated rocks yielded K/Ar ages of 27-35 Ma. The Oligocene age of these intrusions corresponds with the initiation of extension and magmatism in the Rio Grande rift and further west. The Two Buttes minettes therefore appear to represent the most easterly outcrop of rift-related magmatism.

The rocks were originally called powersites by Cross (1906) but have recently been classified as minettes (Bergman, 1987). The Two Buttes intrusions have an ultrapotassic geochemistry ( $K_2O/Na_2O=1.5-3.2$ ) but have concentrations of  $Al_2O_3$  that are too high (12.5-15.8 wt.%) for the rocks to be classified as lamproites. Concentrations of MgO vary from 4.0-9.6 wt.% and  $SiO_2$  from 50.3-56.8 wt.%. The Two Buttes minettes are enriched in light rare-earth elements (LREE) relative to heavy rare-earth elements (HREE;  $Ce/Yb_n=11-19$ ) and are enriched in large ion lithophile elements (LIL) relative to LREE's ( $Ba/La_n=1-2$ ). Chondrite-normalised incompatible element diagrams show troughs at Nb and Ta relative to LREE's ( $La/Nb_n=3-4$ ) and LIL's. In terms of whole-rock geochemistry, the Two Buttes minettes are similar to those in the Navajo Province which lies 200km to the west of the Rio Grande rift axis. The minettes at Two Buttes have lower  $Ce/Yb_n$  ratios than the minettes from the Navajo Province ( $Ce/Yb_n=36-79$ ) and have higher concentrations of HREE's for a given MgO content. We suggest that this variation in  $Ce/Yb_n$  ratios is due to partial melting, i.e. the minettes at Two Buttes represent a greater degree of partial melting of a garnet bearing mantle than those in the Navajo province.

$^{87}Sr/^{86}Sr$  ratios for the Two Buttes minettes range from 0.707512 to 0.70842. These are higher than those observed from other western USA ultrapotassics, such as the Leucite Hills and Smoky Butte.  $^{143}Nd/^{144}Nd$  isotope ratios range from 0.512321 to 0.512392 and show a negative correlation with Sr-isotopes.  $^{143}Nd/^{144}Nd$  ratios show a positive correlation with MgO, i.e. the most evolved minettes have the lowest  $^{143}Nd/^{144}Nd$  ratios.  $^{87}Sr/^{86}Sr$  ratios exhibit a corresponding negative correlation with MgO. We interpret this in terms of AFC style contamination. The minettes appear to have assimilated Sr-rich crust during fractionation. The absence of mantle xenoliths within the Two Buttes minettes is consistent with them fractionating in upper-crustal magma chambers. On an Sr, Nd isotope plot the Two Buttes minettes, like the Navajo minettes, trend towards EM2 (Zindler & Hart, 1986). It has been suggested that an EM2 component is typical of a circumcratonic lithospheric mantle domain, as opposed to the EM1 cratonic domain (Menzies, 1989). However potassic rocks in and around the Rio Grande rift e.g. Spanish Peaks, Elkhead Mountains, appear to have either EM1 or EM2 signatures, implying that the domains are localised. EM1 and EM2 reservoirs may contain a mixture of recycled subducted oceanic crust and sediments. The isotopic compositions of oceanic crust, with either pelagic sediments or terrigenous sediments, are thought to be responsible for the isotope

chemistry of EM1 and EM2 reservoirs, respectively (Chauvel & Hofmann, 1990). Relative depletions in Nb, Ta and Ti may: i) represent subduction related magmas or ii) result from the high crystal/liquid distribution coefficients of high-field-strength elements (HFSE) relative to LREE's and LIL's. Meen & Ayers (1989) and Kelemen et al. (1990) calculated that basaltic magma ascending relatively slowly through lithospheric mantle and reacting with it will develop HFSE depletions. Inversions of REE concentrations of other similar high-Mg K-rich magmas from the western United States (McKenzie & O'Nions, in press) show that the magma sources are preferentially enriched, relative to chondrite, in the LREE (i.e. La to Sm) rather than the MREE to HREE (i.e. Eu to Lu). They suggest that the magmas were in equilibrium with an amphibole-bearing peridotite and that the enrichment of the source regions was associated with subduction. During extension, enriched mantle regions bearing amphibole would be the first to melt. Unlike the Navajo Province, Two Buttes is situated 300km east of the projected limit of the zone effected by Mesozoic and early-Cenozoic eastward subduction of the Farallon Plate (Grand, 1987). Any subduction component within the Two Buttes minettes would have to have been inherited from the underlying accreted Proterozoic island arc-volcanics.



Sr-Nd isotope plot of high-Mg ultrapotassic magmas in the Western United States. Sources of data are as follows: Elkhead Mountains, Leat et al., 1988; Leucite Hills and Smoky Butte, Fraser, 1987; Navajo, Alibert et al., 1986 and our unpublished data; Spanish Peaks and Two Buttes, our unpublished data.

#### References.

- Alibert, C., Michard, A. & Albareda, F., 1986. Isotope and trace element geochemistry of Colorado Plateau volcanics. *Geochimica et Cosmochimica Acta*, 50, 2735-2750.
- Bergmann, S.C., 1987. Lamproites and other potassium-rich igneous rocks: a review of their occurrence, mineralogy and geochemistry. In Fitton, J.G & Upton, B J., (ed.s) *Alkaline Igneous Rocks*, Special Publication of the Geological Society of London, 30. .
- Cross, W. 1906. Prowersose (syenitic lamprophyre) from Two Buttes, Colorado. *Journal of Geology*, 1906, 165-172.

- Chauvel, C. & Hofmann, A.W., 1990. The HIMU-EM connection. International Volcanological Congress (Abstracts).
- Fraser, K. J., 1987. Petrogenesis of kimberlites from South Africa and lamproites from western Australia and North America. Unpublished Ph.D thesis, Open University.
- Grand, S.J., 1987. Tomographic inversion for shear velocity beneath the North American plate. *Journal of Geophysical Research*, 92, 14065-14090.
- Kelemen, P.B., Johnson, K.T.M., Kinzler, R.J., & Irving, A.J., 1990. High-field-strength element depletions in arc basalts due to mantle-magma interaction. *Nature*, 345, 521-524.
- Meen, J.K., & Ayers, J.C., 1989. Cryptic metasomatism and creation of melts with depleted contents of the high-field-strength elements: coupled effects due to infiltration of melt in harzburgite. In *Continental magmatism (abstracts)*. New Mexico Bureau of Mines and Mineral Resources Bulletin, 131, 185.
- McKenzie, D.P. & O'Nions, R.K., in press. Partial melt distributions from inversion of rare-earth element concentrations. *Journal of Petrology*.
- Leat, P.T., Thompson, R.N., Morrison, M.A., Hendry, G.L. & Dickin, A.P., 1988. Silicic magmas derived by fractional crystallisation from Miocene minette, Elkhead mountains, Colorado. *Mineralogical Magazine*, 52, 577-585.
- Zindler, A. & Hart, S., 1986. Chemical Geodynamics. *Annual Review Earth and Planetary Science Letters*, 14, 493-571.

## INDICATOR MINERALS FROM PRAIRIE CREEK AND TWIN KNOBS LAMPROITES: RELATION TO DIAMOND GRADE.

*W. L. Griffin<sup>(1)</sup>; S.Y. O'Reilly<sup>(2)</sup>; C.G. Ryan<sup>(1)</sup> and M.A. Waldman<sup>(3)</sup>.*

*(1) CSIRO Div. of Exploration Geoscience, Box 136, N. Ryde, NSW 2113, Australia; (2) School of Earth Sciences, Macquarie University, Sydney 2009, Australia; (3) Waldman Consulting, 6900 W. Quincy Ave., Littleton, CO 80123, USA.*

Prairie Creek (PC) and Twin Knobs #1 (TK1) are Late Cretaceous diatremes of olivine lamproite in the Murfreesboro field, Arkansas, and are separated by ca. 1 km. Prairie Creek has a historical grade of 13 carats/ 100 tonnes, whereas TK1 has a grade of <1 carat/100 tonnes (Waldman et al., 1987). We have used the proton microprobe to obtain rapid, non-destructive trace-element analyses of macrocryst (>0.5 mm) garnet, chromite and ilmenite in heavy-mineral concentrates from PC and TK1. The aim is to test the usefulness of such analyses in evaluation of diamond exploration targets, and to explain the difference in grade of these adjacent diatremes.

**Garnets:** Garnet concentrates from PC and TK1 show similar ranges of Ca and Cr, and both contain ca. 10% of mildly subcalcic "G10" pyropes (Fig. 1). PC contains a higher proportion of relatively low-Cr, high-Ca garnets. Both diatremes contain a population of relatively Zr-rich (>50 ppm Zr) garnets with Zr/Y ≈ 5 (Fig. 2), high TiO<sub>2</sub> (0.6-1%) and a strong Zr-Ti correlation. In PC this group has low Cr contents, whereas the high-Zr garnets in TK1 have >7% Cr<sub>2</sub>O<sub>3</sub>. Temperature has been estimated for each grain using the Nickel Thermometer of Griffin et al. (1989a). The garnet concentrates show markedly different temperature distributions (Fig. 3). The main population at PC lies in the range 850-1050 °C, with another peak at T>1250°C representing the highest-Cr grains. The main populations at TK1 lie from 700-900 °C and 1200-1500°C. On a cratonic geotherm, the diamond stability field extends from ca. 950°C (the intersection of the geotherm with the diamond-graphite curve) to ca. 1250°C (ca. 200 km, the probable base of the lithosphere). About 1/3 of the PC garnets, and 1/5 of the TK1 garnets, lie in this "diamond window". Temperature estimates for the "G10" garnets at both TK1 and PC show that the lower-Cr G10 grains are derived from the graphite stability field, while the high-Cr ones have unusually high temperatures. Similar high-Cr, high-T garnets are found at Sloan, where they have been described as high-Cr megacrysts (Eggler et al., 1979). The high-Zr,Ti garnets are interpreted as the result of interaction between magma and mantle wall rock, by analogy with the garnets of sheared garnet peridotite xenoliths (Griffin et al., 1989b; Smith et al., 1991). Most high-Cr garnets in TK1 have suffered such melt metasomatism, while most high-Cr garnets in PC are still depleted (<50 ppm Zr).

**Chromites:** PC and TK1 contain similar chromite macrocrysts; both show two populations (Fig. 4). The main population in both contains 30-55% Cr<sub>2</sub>O<sub>3</sub> and >1000 ppm Ni; it is similar to the main population in lamproites worldwide. The other population contains 50->60% Cr<sub>2</sub>O<sub>3</sub>, 10-15% MgO, < 0.5% TiO<sub>2</sub>, and <600 ppm Ni. The high-Ni population shows a trend to high Ti (>5% TiO<sub>2</sub>) at low Al and high Cr. It essentially follows Mitchell's (1987) "Trend 2", and is interpreted as magmatic; it may have crystallized from the (proto-)lamproite magma.

The low-Ni population is similar in all respects to spinels from garnet lherzolite xenoliths from kimberlites in South Africa and Siberia. These grains have Zn contents from 800-1700 ppm, negatively correlated with Ni. This implies equilibration temperatures of ca. 700-900 °C (Griffin et al., 1991), and indicates that these spinels, despite their high Cr# and Mg# and low Ti, are derived from the graphite stability field. Neither of the diatremes contains spinels equivalent to the main population in Group 1 kimberlites, which is derived largely from harzburgites and dunites (Griffin et al., 1991).

**Ilmenites:** PC contains few picroilmenites, whereas they are abundant at TK1. The ilmenites from TK1 show a large range in MgO (9%-15%) and Cr<sub>2</sub>O<sub>3</sub> (0.2-4.5%) and a very well-defined parabolic relation between Mg and Cr (Waldman et al., 1987). They also define smooth continuous curves on plots of Ni, Cr, Mg and Zr against Nb (Fig. 5). All of these features are consistent with extended fractional crystallization of a single batch of magma; similar patterns are seen in many kimberlites (Moore et al, 1991; Griffin et al, unpubl.). Many of the ilmenites at PC are low-Nb, Ni, Zr types of probable crustal derivation. However,

several grains fall near the trends defined by the TK1 ilmenites, and are probably derived from a similar, magma. The unusually high Cr content of the ilmenites suggests a relationship to the high-Cr garnet population.

**Discussion:** The garnet concentrate from TK1 contains a larger proportion of material from the graphite stability field than that from PC; it also contains a higher proportion of high-T, probably magmatic, garnets. The volume of mantle sampled by TK1 appears to have been more affected by melt metasomatism than that sampled by PC. Both of these factors are consistent with the lower diamond grade in TK1. The spinels in both diatremes consist of a magmatic population common to lamproites worldwide, and a smaller xenocryst population. The xenocrysts are all probably derived from lherzolites in the graphite stability field. Neither pipe has sampled typical depleted mantle in the diamond stability field; this may be related to the relatively low grade of both pipes. The ilmenites are all high-Mg types, of the type usually regarded as "good" indicators. However, the trace elements show that they represent an extended fractionation sequence, which may have allowed time for extensive metasomatism of the mantle wall rocks adjacent to the magma chamber. This study demonstrates the usefulness of trace-element data, especially on garnets, in evaluating the diamond potential of exploration targets. Whereas the major-element data on the garnets suggest similar potential for PC and TK1, the trace-element data clearly identify PC as the more attractive target. In addition, data on both garnets and spinels, when compared with our larger database, are consistent with a relatively low grade for PC.

Griffin, W.L., Cousens, D.R., Ryan, C.G., Sie, S.H. and Suter, G.F. 1989a. *Contrib. Mineral. Petrol.* 103, 199-202.

Griffin, W.L., Smith, D., Boyd, F.R., Cousens, D.R., Ryan, C.G., Sie, S.H. and Suter, G.F. 1989b. *Geochim. Cosmochim. Acta* 53, 561-567.

Eggler, D.H., McCallum, M.E. and Smith, C.B. 1979. in Boyd, F.R. and Meyer, H.O.A. (eds.) *The Mantle Sample: Inclusions in Kimberlites and Other Volcanics*. AGU, Washington D.C., pp. 213-226.

Mitchell, R.H. 1987. *Kimberlites: Mineralogy, Geochemistry and Petrology*. Plenum Press, New York, 442 pp.

Moore, R.O., Griffin, W.L., Gurney, J.J., Ryan, C.G., Cousens, D.R., Sie, S.H. and Suter, G.F., 1991. *Contrib. Mineral. Petrol.*, in press.

Smith, D., Griffin, W.L., Ryan, C.G. and Sie, S.H. 1991. *Contrib. Mineral. Petrol.*, in press.

Waldman, M.A., McCandless, T.E. and Dummett, H.T., 1987. *Geol. Soc. America Spec. Paper* 215, 205-216.

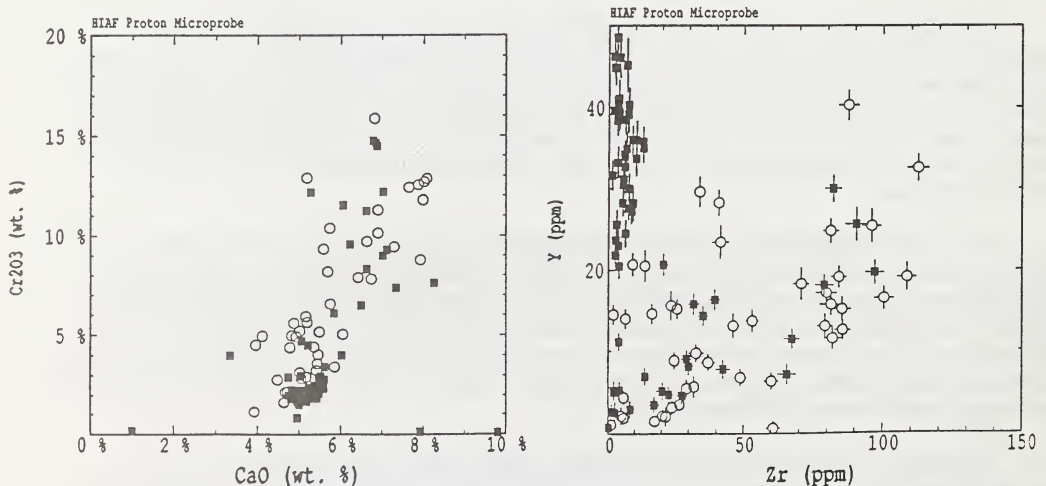


Fig. 1. Ca-Cr relations in garnets. Squares, PC; circles, TLK1.

Fig. 2. Zr-Y relations in garnets. Symbols as in Fig. 1.

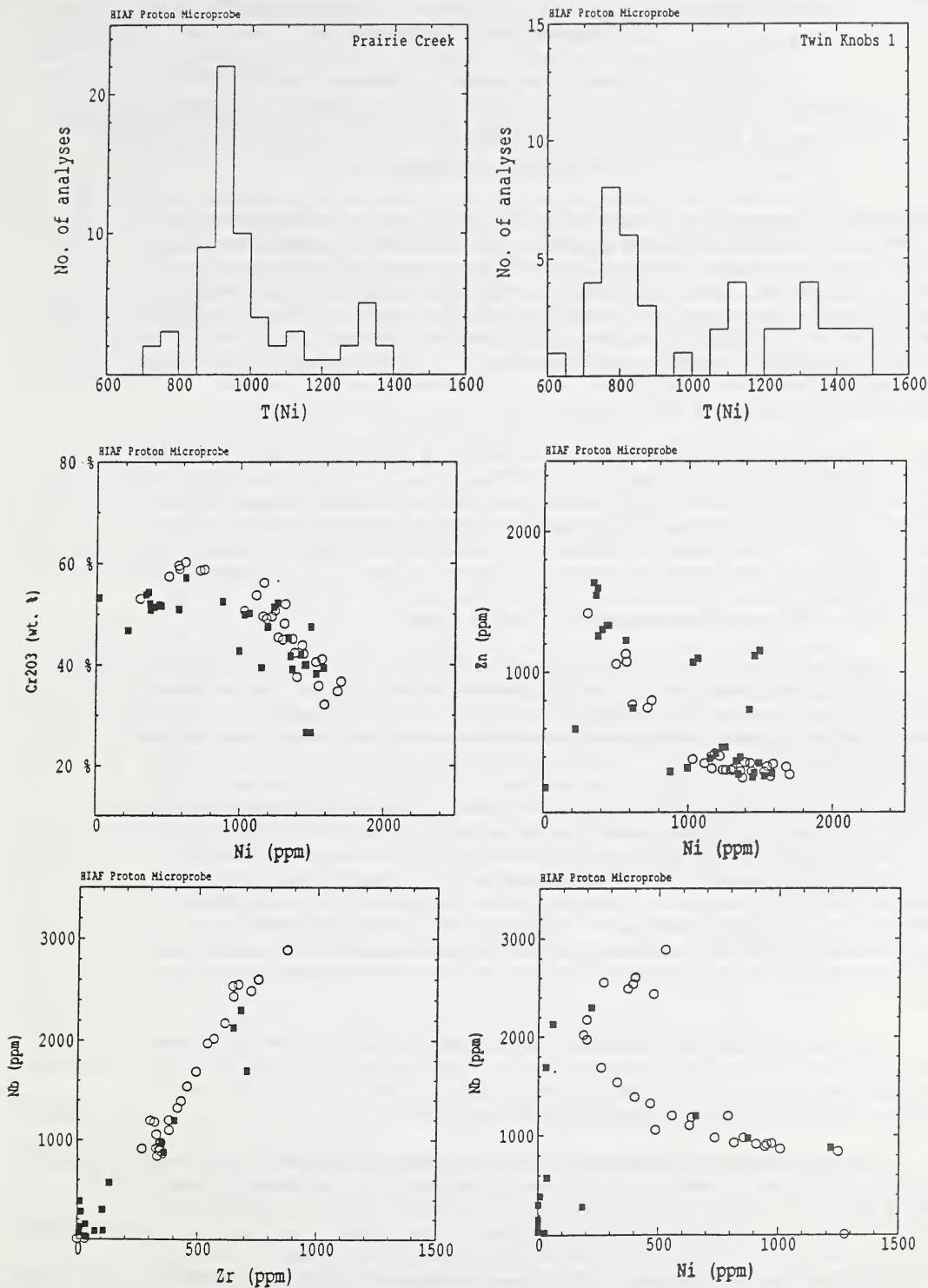


Fig. 3 (top).  $T_{Ni}$  histograms for PC and TK1.

Fig. 4 (middle). Cr-Ni and Zn-Ni relations in chromite macrocrysts. Symbols as in Fig. 1.

Fig. 5 (bottom). Nb-Zr and Nb-Ni relations in ilmenites. Symbols as in Fig. 1.

**CHROMITE MACROCRYSTS IN KIMBERLITES AND LAMPROITES:  
GEOCHEMISTRY AND ORIGIN.**

*W.L. Griffin<sup>(1)</sup>; C.G. Ryan<sup>(1)</sup>; J.J. Gurney<sup>(2)</sup>; N.V. Sobolev<sup>(3)</sup> and T.T. Win<sup>(1)</sup>.*

*(1) CSIRO Div. of Exploration Geoscience, Box 136, N. Ryde 2113, Australia; (2) Dept. of Geochemistry, Univ. Of Cape Town, Rondebosch 7700, Sout Africa; (3) Inst. of Geology & Geophysics, USSR Academy of Sciences, Novosibirsk, USSR.*

**Introduction:** Macrocrysts of chrome-spinel (CMs; 0.2-2mm, anhedral to euhedral) are common in many kimberlites and lamproites, and are important as indicator minerals during diamond exploration. However, the use of chromites in exploration is usually based on major-element criteria which may be ambiguous. Analysis of trace elements by proton microprobe can add another level of discrimination, and a program to this effect is in progress at the CSIRO. Here we discuss major- and trace-element data on >1000 chromites from kimberlites and lamproites worldwide, on >170 diamond-inclusion (DI) chromites from South Africa and Siberia, and on >70 garnet-chromite pairs from xenoliths and concentrates. Data for various elements are combined in Figure 1.

**Data:** CMs from kimberlites show limited ranges in Cr<sub>2</sub>O<sub>3</sub> (45-65%) and Al<sub>2</sub>O<sub>3</sub> (2%-12%); Cr# [Cr/(Cr+Al)] ranges from 0.7 to 0.95. Lamproite CMs show a much greater range to lower Cr and higher Al, with Cr# down to 0.2; there is little overlap in Al<sub>2</sub>O<sub>3</sub> between kimberlite and lamproite CM populations. Mg# [Mg/(Mg+Fe)] ranges mainly from 0.4 to 0.7. CMs from Group 2 kimberlites extend to lower Mg# than those from Group 1 kimberlites, and lamproites contain significant numbers of high-Mg#, low-Cr# spinels. In general there is no correlation between Mg# and Cr#; the low-Cr "tail" in Fig. 1 is defined by a small proportion (<10%) of the sample.

More than 1/3 of the analyzed CMs contain >1% TiO<sub>2</sub>, and many, especially in Group 2 kimberlites, contain 2-4%. Ti typically shows a broad negative correlation with Al and Mg#, and a weak positive correlation with Cr#, especially in lamproites. In general, therefore, chromite macrocrysts from kimberlites and lamproites follow the first part of Mitchell's (1987) "Trend 2", rather than the "AMC trend". Ni contents of CMs range from 300-2000 ppm; they show no correlation with Mg# or MgO, but are broadly anticorrelated with Cr. The highest Ni values are found in the low-Cr CM populations in lamproites. Group 2 kimberlites contain two major populations of CMs with Ni contents of ca. 400-700 ppm and 900-1200 ppm, respectively; Group 1 kimberlites have one major population with ca. 600-900 ppm. Zn contents of CMs in kimberlites are mainly in the range 400-900 ppm, with a few higher values. Lamproites, and some Siberian kimberlites, contain many CMs with Zn >1000 ppm; the high-Ni population in lamproites contains 200-500 ppm Zn and shows a negative correlation between Zn and Ni. Ga contents of CMs range from <2-100 ppm, and show a broad positive correlation with Ni.

DI chromites show narrow ranges of Cr# and Mg#, and for most trace elements as well. Siberian DI chromites show significantly lower Mg# and MgO, and higher Zn, than those from South Africa. Ti and Ga contents of DI chromites are typically low, but even lower values of Ga are found in CMs from kimberlites.

Harzburgite chromites typically lie in a very narrow range of Cr# and Mg#, while lherzolite spinels show a wider range of Cr# and a rough negative correlation between Cr# and Mg#. Only four xenolith spinels, all from lherzolites, contain >1000 ppm Ni. 10% of the analyzed xenolith spinels, divided equally between harzburgites and lherzolites, contain >1% TiO<sub>2</sub>. In general, lherzolite spinels contain less Ni, more Ga and more Zn than harzburgite spinels. The Nickel Thermometer (Griffin et al., 1989) allows calculation of a temperature for each garnet-chromite pair. Fig. 2 shows a good correlation between 1/T and the Zn content of the xenolith spinels, and probably reflects partitioning between chromite and olivine. The correlation between Ni and 1/T is not as good, which suggests bulk-composition effects on the partitioning of Ni.

**Discussion:**

(1) Origin of macrocryst chromites: Comparison of the CM populations with the data on xenolith spinels provides clues to the origin of chromite macrocrysts. The low-Ti

CMs in Group 1 kimberlites appear to be true xenocrysts, derived mainly from harzburgites. Very low-Ga CMs from these kimberlites may be derived from as garnet-free chromite harzburgites and dunites. Group 2 kimberlites contain two major populations, one of which is equivalent to the xenolith spinels. The minimum Zn content of this population is higher than the equivalent in Group 1 kimberlites, indicating a lower maximum temperature. The other population in Group 2 kimberlites is essentially identical to Mitchell's (1987) "Trend 2", and is considered to be magmatic (phenocrystal) in origin. CM concentrates from some Group 2 kimberlites are dominated by this magmatic population. CMs intermediate between the two major populations in Group 2 kimberlites may reflect reaction of xenocryst spinels with (proto-?)kimberlite magma; this may also be the origin of high-Ti CMs in Group 1 kimberlites. CM concentrates from lamproites typically contain relatively few xenocrystal spinels, and many of these are low-T lherzolite chromites. The major CM population in many lamproites has high Ti, Ni, Cr and lower Mg#. It also follows Trend 2, but at higher Mg#, MgO and Ni, and lower Zn, than the corresponding population in Group 2 kimberlites. It is interpreted as a magmatic population, reflecting a higher temperature of crystallization.

(2) Mantle stratigraphy and origin of host rocks: The general separation of the xenolith spinels with harzburgites at high T and lherzolites at lower T (Fig. 2) might reflect a general stratification of the cratonic lithosphere. Alternatively, it may reflect a general lack of spinel-bearing lherzolites at greater depth. The distribution of  $T_{Ni}$  in garnet concentrates from kimberlites strongly suggests that lherzolites and harzburgites are interleaved in the deeper parts of the lithosphere, and that lherzolites are volumetrically dominant.

The Mg and Zn distributions in their respective xenocryst populations suggest that Group 1 kimberlites have sampled the mantle from greater depths, on average, than Group 2 kimberlites. This is consistent with derivation of Group 1 kimberlites from the asthenosphere and Group 2 mainly from the lithosphere. Sr-Nd data suggest that both Group 2 kimberlites and lamproites are derived from enriched lithosphere; the differences in their magmatic CM populations suggest that the major difference between the two rock types is the higher temperature of lamproitic magmas.

(3) Implications for Exploration: The use of "diamond inclusion" compositions to evaluate exploration targets may be misleading, since MgO contents, in particular, will be affected by cooling following diamond formation. Also, many high-grade Group 2 kimberlites are dominated by the magmatic CM population, which should be recognized as a positive indication although it has lower Mg# and Cr# than DI chromites. The low-P limit of the diamond stability field corresponds to ca. 950°C on a cratonic geotherm; reference to Fig. 2 shows that only chromites with <ca.700 ppm Zn, and >ca. 600 ppm Ni, are likely to be derived from the diamond stability field. The Ga content of chromites appears to correlate broadly with degree of depletion; DI spinels and harzburgite spinels typically contain <30 ppm Ga. The proportion of chromites with low Zn and Ga, and high Ni, in a concentrate may serve as a rough guide to the diamond potential of an exploration target.

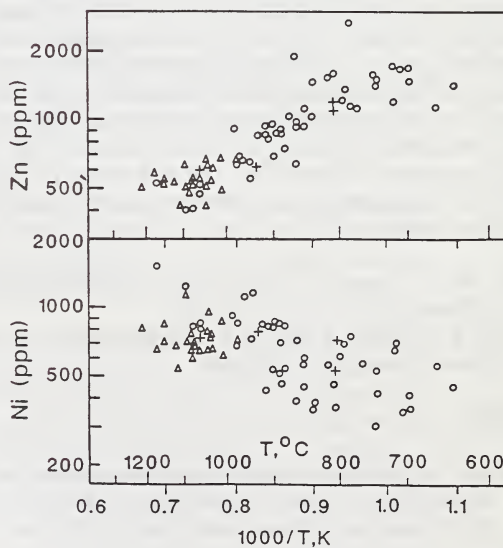
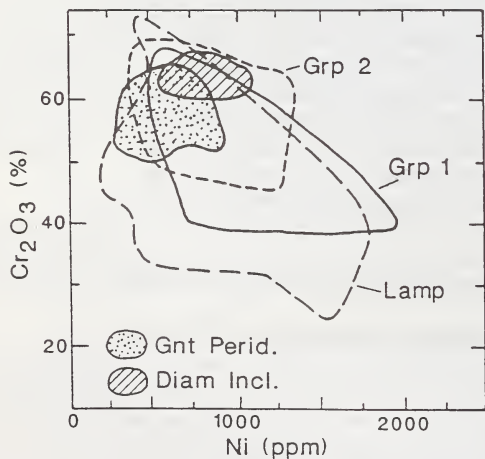
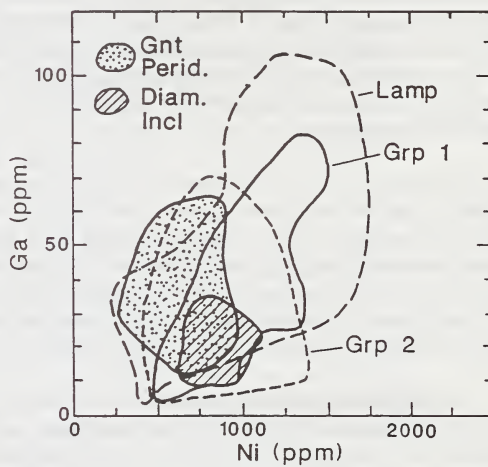
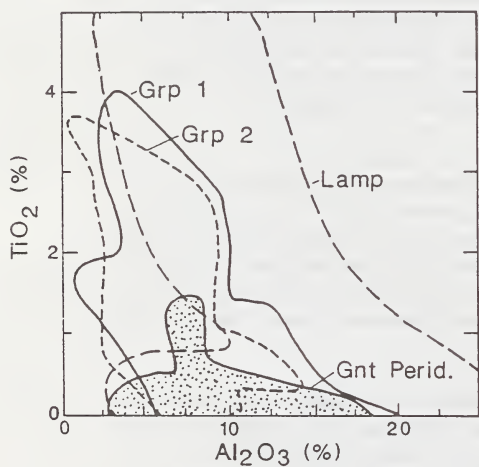
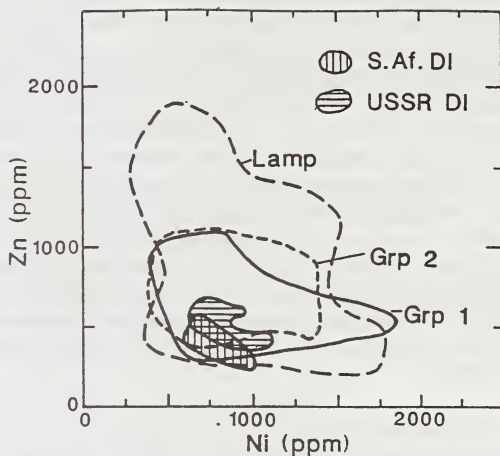
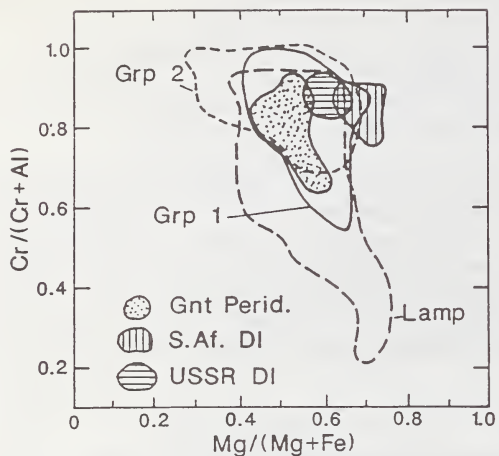
Griffin, W.L., Cousens, D.R., Ryan, C.G., Sie, S.H. and Suter, G.F. 1989. *Contrib. Mineral. Petrol.* 103, 199-202.

Mitchell, R.H. 1987. *Kimberlites: Mineralogy, Geochemistry and Petrology*. Plenum Press, New York, 442 pp.

FIGURES (next page)

Fig. 1 a-e. Interelement relations in chromite macrocrysts from Group 1 and 2 kimberlites (Southern Africa) and lamproites (Australia, China, USA), compared with data from diamond-inclusion chromites and chromite-garnet peridotites.

Fig. 2 (lower right). Zn and Ni contents of chromites, plotted against  $1/T$  as determined by nickel thermometry on coexisting chrome-pyrope garnets.



## TRACE ELEMENTS IN GARNETS FROM TANZANIAN KIMBERLITES: RELATION TO DIAMOND CONTENT AND TECTONIC SETTING.

W.L. Griffin<sup>(1)</sup>; C.G. Ryan<sup>(2)</sup>; S.Y. O'Reilly<sup>(2)</sup>; P.H. Nixon<sup>(3)</sup> and T.T. Win<sup>(1)</sup>.

(1) CSIRO Div. of Exploration Geoscience, Box 136, N. Ryde, NSW 2113, Australia; (2) School of Earth Sciences, Macquarie University, Sydney 2009, Australia; (3) Dept. of Earth Sciences, Univ. of Leeds, Leeds LS2 9JT, U.K.

**Introduction:** The Tanzanian craton contains >400 known kimberlite occurrences, divided geographically into an Eastern and a Western zone (Nixon & Condliffe, 1989). The Western Zone includes both diamondiferous pipes (including Mwadui) and barren ones. The kimberlites of the Eastern Zone, closer to the craton margin, apparently are all barren. Tanzania is therefore a good example of an area with abundant targets for exploration, in which rapid evaluation and ranking of targets is important in limiting the cost of exploration and testing. The major-element composition of concentrate garnets commonly plays an important role in such evaluation, but involves several levels of ambiguity. For example, subcalcic ("G10") pyropes are known from many barren deposits (Kuruman province; Sekameng), while some economic deposits (e.g. Argyle) contain few if any subcalcic pyropes.

In this work we have used trace-element data, obtained by proton microprobe, to add another level of discrimination to the use of garnets in target evaluation. The Ni content of garnet is strongly temperature-dependent (Griffin et al., 1989a), and this "Nickel Thermometer" provides key data for the more sophisticated interpretation of garnet concentrate data. In an area with a "cratonic" geotherm, the diamond stability field lies between ca. 950°C (the intersection of the geotherm with the diamond stability field) and ca. 1250°C (roughly the base of the lithosphere). The proportion of concentrate garnets within this "diamond window" is a measure of whether the kimberlite has sampled potentially diamond-bearing mantle. Other elements, such as Zr, Y, Ti and Ga, provide information on the degree of depletion, and on the nature and extent of metasomatic processes.

**Data:** Cr-pyrope garnets are abundant in most pipes in the area. There is a similar range of Ca and Cr contents, and a similar abundance of moderately subcalcic garnets, in the kimberlites of both zones. In the Western Zone, subcalcic pyropes occur in both diamond-bearing and barren pipes (Nixon & Condliffe, 1989). Fig. 1 compares the distribution of nickel temperatures in pipes from the Eastern Zone (mainly Makibulei) with those from barren (mainly 80K6, 99K2) and diamond-bearing pipes (mainly Mwadui, Sultan) in the Western Zone. There is a clear difference between the barren and diamondiferous pipes in the Western Zone; the diamondiferous ones contain a significant proportion of garnets in the "diamond window", whereas these garnets are almost absent in the barren pipes. Both barren and diamondiferous pipes also contain a population of garnets with  $T > 1250^\circ\text{C}$ . The garnets from the Eastern Zone kimberlites show a major peak lying on the low-T side of the diamond window, as well as the high-T population seen in the Western Zone pipes.

The high-T group in all three groups is similar in composition; Cr<sub>2</sub>O<sub>3</sub> is 1-3%, Zr is mainly >50 ppm, Zr/Y is nearly constant at 4 (Fig. 2), and TiO<sub>2</sub> is high (0.2-1%) and strongly correlated with Zr (Fig. 3). The garnets within the diamond window are mostly enriched, with 20-50 ppm Zr, Zr/Y = 2-4, and relatively high Y/Ga (Fig. 4). These values are typical of garnets from relatively fertile lherzolites. Some garnets show high Zr without corresponding Ti enrichment, and are similar to garnets from phlogopite-bearing peridotites, which are inferred to have experienced hydrous metasomatism.

The low-T garnets of the barren Western Zone kimberlites have generally low Zr (0-40 ppm, aver. ca. 20 ppm); many of these also have low Y contents, and probably are derived from depleted lherzolites. A separate population has high Y and Y/Ga, with Zr/Y < 1. These are typical of many low-T, P garnets, and reflect the partitioning of Y into garnet, and Zr into cpx, with decreasing T (O'Reilly & Griffin, 1989). The low-T garnets of the Eastern Zone show a wide range of Zr contents. Most higher-Zr ones (Zr > 50 ppm) also show Ti enrichment. The rest are either very depleted (low-Zr, Y) types, or those with high Y and low Zr/Y, as seen in the barren Western Zone pipes.

**Discussion:** The high-temperature garnet population in all the pipes is similar in composition to low-Cr megacryst garnets, and to the overgrowth rims on the garnets of sheared peridotite xenoliths in kimberlite (Griffin et al. 1989b). This is also consistent with their high temperatures of equilibration. This population, and other garnets with high and correlated values of Ti and Zr, are therefore interpreted as magmatic (megacrysts), and/or as peridotite garnets affected by melt metasomatism; these melts are inferred to be asthenosphere-derived (Smith et al., 1991).

There is essentially no difference in degree of depletion between the Eastern Zone and the Western Zone, in the sense of one having a higher proportion of harzburgitic garnets. The G10 garnets in both the barren pipes of the Eastern Zone and the diamond-bearing pipes of the western zone have relatively high Cr<sub>2</sub>O<sub>3</sub> (5-10%), and mostly lie in the T range 900-1050°C. This places them on the low-T boundary of the diamond stability field, assuming a 40 mW/m<sup>2</sup> geotherm, and shallower than similar garnets from the Kaapvaal craton. The G10 garnets in the barren Western Zone pipes contain 2-3% Cr<sub>2</sub>O<sub>3</sub>, and are all derived from the graphite stability field.

Garnet concentrates from most South African diamondiferous pipes have median Zr and Y contents of 20-30 and 5-10 ppm, respectively. The barren pipes of both zones in Tanzania contain a high proportion of such depleted lherzolite garnets. In contrast, the garnets from the diamondiferous pipes, including those in the "diamond window", are more fertile, with median Zr and Y ≈ 50 ppm and 15 ppm, respectively. There is therefore no clear correlation between diamond grade and the fertility of the sampled mantle in these pipes. The data raise the interesting possibility that the deeper parts of the Tanzanian lithosphere are more fertile than the shallower parts, and that this fertility is due to interaction with asthenospheric magmas. A similar process may have affected the Kaapvaal craton, but to a lesser degree (Griffin et al., 1991).

The main difference between the diamond-bearing and barren pipes of the Western Zone is in the depth range sampled by the kimberlites. The barren ones have only sampled quite shallow mantle (70-100 km), whereas the diamond-bearing ones contain material derived from 120-200 km deep. Assuming a cratonic geotherm, those in the Eastern Zone have sampled from 100-130 km, and should include some material from the diamond stability field. However, the geotherm in this zone, nearer the craton margin, may be slightly higher than 40mW/m<sup>2</sup>; this would move the intersection of the geotherm with the diamond-graphite stability field to greater depth, and place all of the low-T garnets from the Eastern Zone in the graphite stability field.

**Conclusions:** At the moment, this study is based on a limited number of pipes, with relatively few garnets from several. However, the results clearly indicate that depth of sampling is the primary control on the diamond potential of kimberlites in the area. The results also demonstrate the usefulness of trace-element analysis of concentrate garnets as a rapid and cost-effective tool for the evaluation of diamond exploration targets.

Griffin, W.L., Cousens, D.R., Ryan, C.G., Sie, S.H. and Suter, G.F. 1989a. *Contrib. Mineral. Petrol.* 103, 199-202.

Griffin, W.L., Smith, D., Boyd, F.R., Cousens, D.R., Ryan, C.G., Sie, S.H. and Suter, G.F. 1989b. *Geochim. Cosmochim. Acta* 53, 561-567.

Griffin, W.L., Gurney, J.J., Sobolev, N.V. and Ryan, C.G., 1991 (this vol.).

Nixon, P.H. and Condliffe, E. 1989. in *Kimberlites and Related Rocks*, Vol. 1. *Geol. Soc. Australia Spec. Publ.* 14. pp. 407-416.

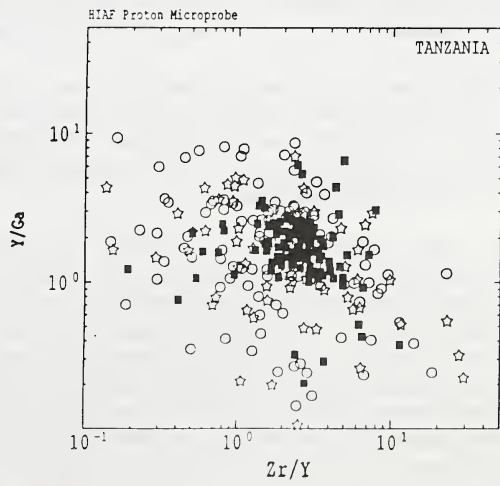
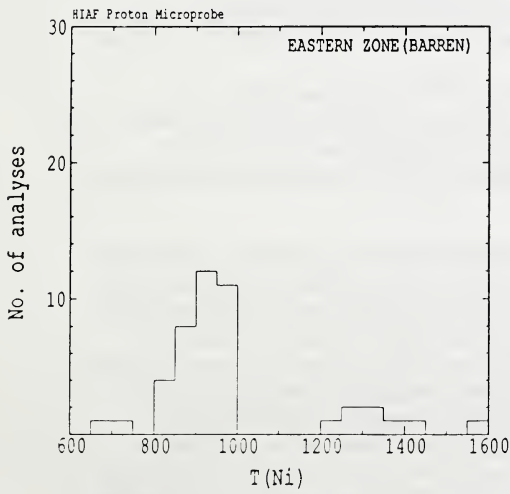
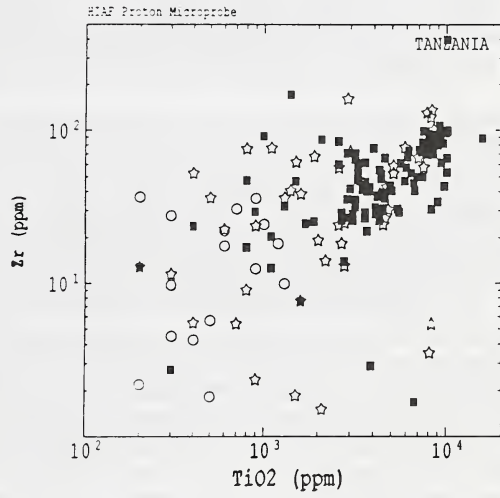
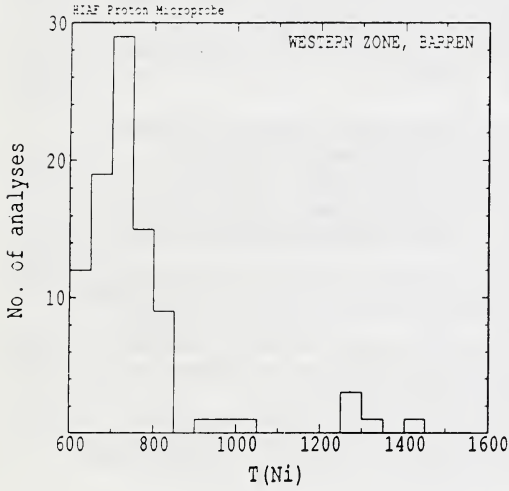
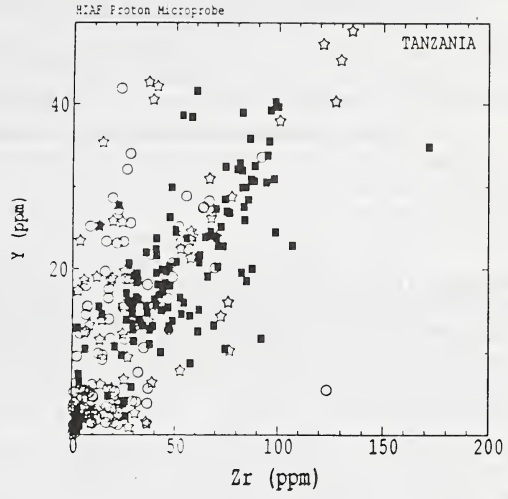
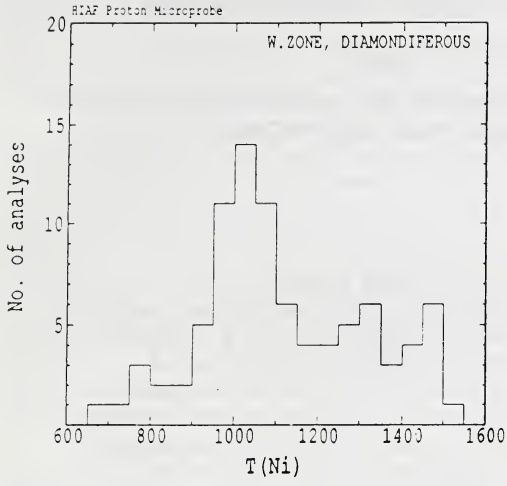
O'Reilly, S.Y. and Griffin, W.L. 1989. *Terra Abstracts* 1, 9-10.

Smith, D., Griffin, W.L., Ryan, C.G. and Sie, S.H. 1991. *Contrib. Mineral. Petrol.*, in press.

FIGURES (next page)

Fig. 1 (left). T<sub>Ni</sub> histograms for diamondiferous and barren pipes of the Western and Eastern Zones.

Figs. 2 (top right) to 4 (bottom right). Zr-Ti-Y-Ga relations. Squares, W. Zone diamondiferous pipes; circles, W. Zone barren pipes; stars, E. Zone pipes.



## ILMENITE AND SILICATE MEGACRYSTS FROM HAMILTON BRANCH: TRACE ELEMENT GEOCHEMISTRY AND FRACTIONAL CRYSTALLIZATION.

*W.L. Griffin<sup>(1)</sup>; C.G. Ryan<sup>(1)</sup> and D.J. Schulze<sup>2</sup>.*

*(1) CSIRO Div. of Exploration Geoscience, Box 136, North Ryde, NSW 2113, Australia; (2) Dept. of Geology, Univ. of Toronto, Erindale College, Mississauga, Ontario L5L1C6, Canada.*

**Introduction:** The Hamilton Branch kimberlite in eastern Kentucky contains a well-developed suite of ilmenite and silicate (cpx+opx+gnt) megacrysts. The ilmenites range in MgO from 15% to 9% and in Cr<sub>2</sub>O<sub>3</sub> from 5% to 0.2%, describing a rough parabola in a Cr-Mg plot (Fig. 1; Schulze, 1984). High-Cr, high-Mg ilmenites occur as inclusions in silicates, and lower-Cr, high-Mg ones in intergrowths with clinopyroxene; small silicate inclusions occur in low-Cr ilmenites with 12-14% MgO. No silicates are known to be associated with the ilmenites containing <12% MgO. This trend has been interpreted as the result of fractional crystallization; a continuous increase in Ca/(Ca+Mg) in clinopyroxene with decreasing Cr in silicates and ilmenite suggests that silicates and ilmenite crystallized together over a T range from ca. 1450-1200 °C. This study presents trace-element data, obtained by proton microprobe, on the ilmenites and associated clinopyroxene, and provides further information on the processes of fractional crystallization that have produced the ilmenite megacrysts.

**Data:** Schulze (1984) showed that Cr in cpx decreases as Ca/(Ca+Mg) increases, i.e. with declining T. Our data show that Ni in cpx also decreases, and Zr increases, as Cr and Mg decrease; these trends are consistent with the fractional crystallization model. Sr in cpx decreases slightly, from 180-140 ppm, as Ni drops from 350-110 ppm, then drops to 80 ppm at 60 ppm Ni. This trend suggests that clinopyroxene was a major fractionating phase, and is consistent with its abundance in the megacryst assemblage.

Nb in ilmenite ranges from 400-2600 ppm, and is positively correlated with Zr (250-900 ppm) (Fig. 2). Nb shows a strong negative correlation with Mg in ilmenite (Fig. 3), while the Mg content of the ilmenites is positively correlated with Mg in coexisting silicates. Nb and Zr appear to have behaved as incompatible elements during the entire crystallization process, and the Nb content of the ilmenites is therefore taken as an index of fractionation.

Most of the increase in the Nb content of ilmenite takes place after MgO has declined below 12%, i.e. after the point where coexisting silicates have not been recognized. The Cr and Ni contents of ilmenites decrease as Nb rises; Cr drops to its minimum value at a lower Nb content than does Ni (Figs. 4,5). The smooth covariation of Mg and Ni against Nb is interrupted by a major spike at ca. 1000 ppm Nb; Ni rises from 200-950 ppm, and MgO from 12.5-15%, at essentially constant Nb and Zr. Another possible spike is represented by 2 points near 2000 ppm Nb.

Al<sub>2</sub>O<sub>3</sub> in ilmenite decreases steadily ( from >1% to 0.25%) as Nb increases. Ga contents of ilmenites show a weak and irregular increase from ca. 12 ppm to ca. 20 ppm with increasing Nb. Zn contents also rise, from ca. 100-120 ppm, following the end of silicate crystallization, then fall slowly again. Nb/Ta varies irregularly at first, then rises from 6 to 8 as Nb increases from 1000-2600 ppm.

**Discussion:** The smooth covariance of Ni, Zr etc. against Nb is typical of ilmenite megacryst suites from kimberlites and some lamproites, worldwide (Moore et al., 1991; Griffin and Ryan, unpubl.). These smooth variations are generally consistent with the fractional crystallization of a single batch of magma. At Hamilton Branch, most of the rise in the Nb and Zr contents of ilmenite takes place after mafic silicates apparently stopped crystallizing; this corresponds to the late stages of crystallization, at T<1200°C. Simple calculations, treating Nb and Zr as perfectly incompatible elements, show that >60% of the liquid crystallized between the beginning of ilmenite precipitation and the end of cpx crystallization. Half of the remainder crystallized to produce the lowest-Mg, highest-Nb ilmenites. Since Nb and Zr were obviously not completely incompatible, these are minimum estimates of the degree of crystallization, and any pre-ilmenite crystallization of mafic silicates would raise these estimates. The rise in Nb/Ta of the ilmenites at high Nb is further evidence of extreme fractional crystallization.

The major spike in the Ni-Nb and Mg-Nb curves (Figs. 2-4) is interpreted as the result

of mixing between the main batch of magma and a similar, less-fractionated magma. This would have the most severe effects on the strongly depleted, compatible elements, but less on Nb and Zr. Similar magma-mixing episodes earlier in the sequence may have contributed to the scatter in the high-Mg limb of the Mg-Cr plot (Fig. 1); these would be difficult to recognize without the enrichment of Nb and Zr as benchmarks.

Schulze (1984) argued that other phases (olivine, phlogopite and/or carbonate) must have crystallized together with ilmenite in the late stages of fractionation, to prevent the magma from being enriched in Mg. However, the relatively gradual drop in Ni, and the fact that the Ni content of ilmenite does not drop below 100 ppm, suggest that olivine was not a coprecipitating phase. However, the fact that Ni appears to remain constant as Nb increases from 1000 to >2000 ppm argues for the crystallization of a Ni-bearing phase, perhaps sulfide. Cr is incompatible at this stage, rising from 0.2 to 0.4% (Fig. 1). The slow drop in Al during the fractionation may reflect the precipitation of phlogopite, but the rise in Ga during the late fractionation would appear to contradict this. The ilmenites from the Twin Knobs lamproite (Griffin et al, 1991) are quite similar to those from Hamilton Branch, but show a rise in Ni and Cr equivalent to the rise in Nb late in the fractionation, consistent with the absence of any mafic silicates in the cumulate assemblage.

The high Nb and Zr contents of the ilmenites, compared to the Nb and Zr contents of known magmatic rocks, suggest that ilmenite/magma  $K_D$  values for these elements are  $\gg 1$ . The apparently continuous rise in Nb and Zr during fractionation, despite the high Nb and Zr contents of ilmenite, therefore implies that ilmenite was never more than a minor phase in the cumulate assemblage. If olivine and phlogopite are ruled out as late cumulate phases, then carbonate may be required to buffer the Mg content of the liquid, as suggested by Schulze (1984).

The low-Mg, moderate-Cr ilmenites that define the low-Mg arm of the "parabola" in Fig. 1 may not be related to the main ilmenite assemblage. Both analyzed grains lie off the main Nb-Ni curve, and one has lower Zr than the main trend. While they appear on Fig. 1 to represent the latest stages of fractionation, they do not have the highest Nb contents. There is therefore no clear evidence that they represent a continuation of the main fractionation trend. However, their high Nb and Zr contents show that they are late-stage ilmenites, and they may be from a related but separate batch of cumulates, sampled by the ascending kimberlite.

Griffin, W.L., O'Reilly, S.Y., Ryan, C.G. and Waldman, M.A., 1991 (this vol).

Moore, R.O., Griffin, W.L., Gurney, J.J., Ryan, C.G., Cousens, D.R., Sie, S.H. and Suter, G.F., 1991. *Contrib. Mineral. Petrol.*, in press.

Schulze, D.J., 1984. in Kornprobst, J. (ed.) *Kimberlites II: the Mantle and Crust-Mantle Relationships*. Elsevier, Amsterdam. pp. 97-108.

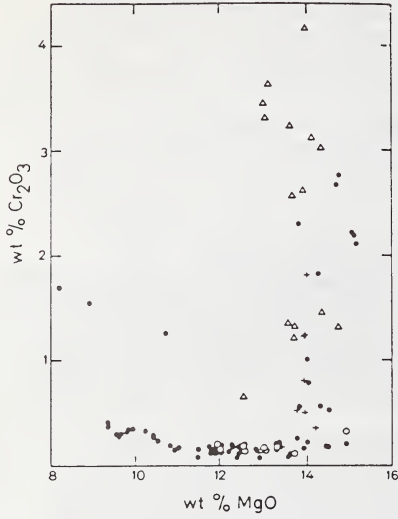


Fig. 1. Mg-Cr in Hamilton Branch ilmenites. Triangles: tiny ilmenites in silicate megacrysts; crosses, cpx-ilm intergrowths; open circles, ilmenites with silicate inclusions; dots, monomineralic ilmenites.

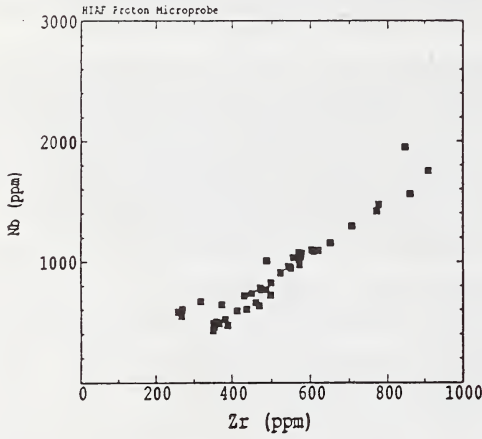


Fig. 2. Nb-Zr relations in ilmenites

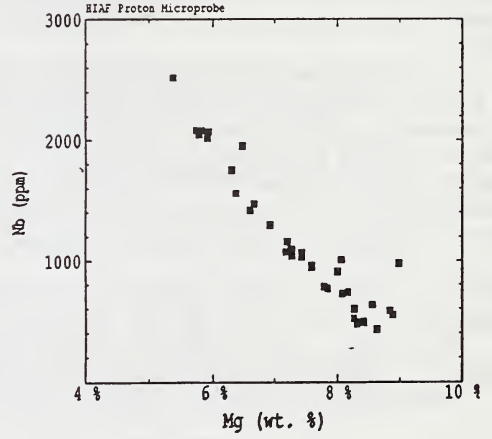


Fig. 3. Nb-MgO relations in ilmenites

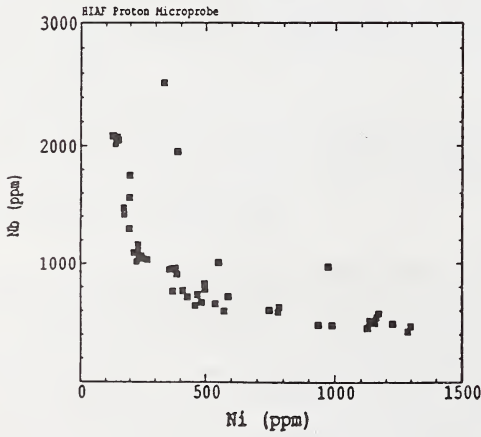


Fig. 4. Nb-Cr relations in ilmenites

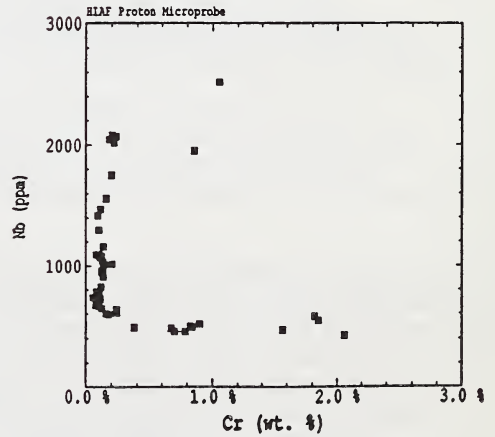


Fig. 5. Nb-Ni relations in ilmenites

## GENESIS OF DIAMOND PLACERS ON THE GUIANA SHIELD, SOUTH AMERICA.

Grubb, <sup>(1), (2)</sup>Mark D. and McCallum, <sup>(2)</sup>M.E.*(1) P.O. Box 725, Tehachapi, CA 93581; (2) Dept. Earth Resources, Colorado State Univ., Fort Collins, CO 80523.*

Detailed geological and geomorphological field investigations in the Issineru-Enachu mining district of Guyana were combined with analyses of the sedimentary sequence in the Guiana Basin and regional scale geomorphic analyses of the Guiana Shield to form a coherent placer genesis model for the region. Placer deposits are the result of interactions between three parameters: 1) source rock, 2) regional geologic setting, and 3) regional and local geomorphic evolution.

The principal source for diamond on the Guiana Shield is inferred to be fluvial deposits of the Proterozoic Roraima Group (Fig. 1). Although no diamonds have been found in these rocks, the spatial coincidence of diamonds and the Roraima Group offers strong evidence that this is their major source on the Shield. The Roraima Group is composed dominantly of orthoquartzite, quartz arenite, quartzose and polymictic conglomerate, and arkosic arenite. The depositional environment of these sediments is interpreted to be a series of coalescing wet-type alluvial fans that accumulated to more than 3000 m thick. Structural, sedimentological, and paleocurrent data suggest that the present northeastern escarpment of the Roraima Group closely approximates the Roraima sedimentary basin margin. Fan-head depositional sites of this type are well documented as sites of placer enrichment (Schumm, 1977; Minter, 1978).

The geomorphic mechanisms responsible for placer formation of diamonds on the Guiana Shield are eluvial concentration due to humid tropical climate weathering and fluvial transportation coupled with sorting and concentration in a semiarid climate. The latter mechanism is enhanced by two factors: 1) multiple rapid shifts between humid tropical rain-forest conditions and semiarid savannah type conditions that have been documented for at least the Pliocene to the Holocene and 2) low amplitude episodic epeirogenic uplift of the Guiana Shield (Table 1). Extensive sedimentological, palynological, geochronologic, and geomorphological evidence support the model (Pflug, 1969; Damuth and Fairbridge, 1970; Van der Hammen, 1972).

Fluvial system instability resulting from either climate change or uplift typically leads to a complex response, and, in the Guiana Shield region, this is reflected by evidence of repeated aggradation and incision of alluvial valleys as the system continually readjusted toward equilibrium. Such oscillations result in the repeated reworking of alluvium that is a requisite to placer formation (Schumm, 1977; Lampietti and Sutherland, 1978). The modern fluvial system on the Guiana Shield is entrenched into a stripped etchplain that is thinly veneered by regolith and alluvial sediments (Fig. 2). Consequently, location and grade of placer deposits are controlled mainly by bedrock structural fabric, a situation that is highly conducive to placer concentration.

Phanerozoic age low amplitude episodic uplift is evidenced by six major regional planation surfaces cut into the Shield. Crustal flexure of the trailing edge continental margin created profound bedrock nickpoints in trunk streams draining into the Atlantic Ocean and has isolated the

upland fluvial systems from sea level fluctuations associated with glacial-interglacial cycles (Fig. 2). This isolation prevented wholesale stripping and transportation of alluvium from the uplands and allowed repeated reworking of pre-existing and newly created sediments into high grade placers. The 1:1 ratio of gem to industrial diamonds recovered in much of Guyana reflects extensive reworking of the placer diamonds and contrasts strongly with the lower ratios associated with primary diamond sources such as kimberlite pipes.

Uplift of the Guiana Shield combined with episodic climatic shifts has resulted in the development of two widespread Pleistocene age terraces underlain by braided river alluvial deposits and a deep, Holocene age, gravel-rich valley fill in the Issineru-Enachu mining district. Placer grade and diamond quality increase in progressively younger terraces and ultimately in the valley fill. The valley fill underlying the modern fluvial system has undergone a minimum of four dramatic erosion-sedimentation cycles, resulting in a gem to industrial diamond ratio of greater than 2:1.

Reconnaissance sampling indicates that more than 100 million cubic yards of ore gravel occurs in the valley fill within the mining district, assuming an ore horizon of 1 m. This estimate includes well developed point bars associated with the trunk stream in the district, the Mazaruni river. Overburden beneath the floodplain of the Mazaruni River is inferred from seismic refraction measurements to be from 7 m to more than 18 m thick.

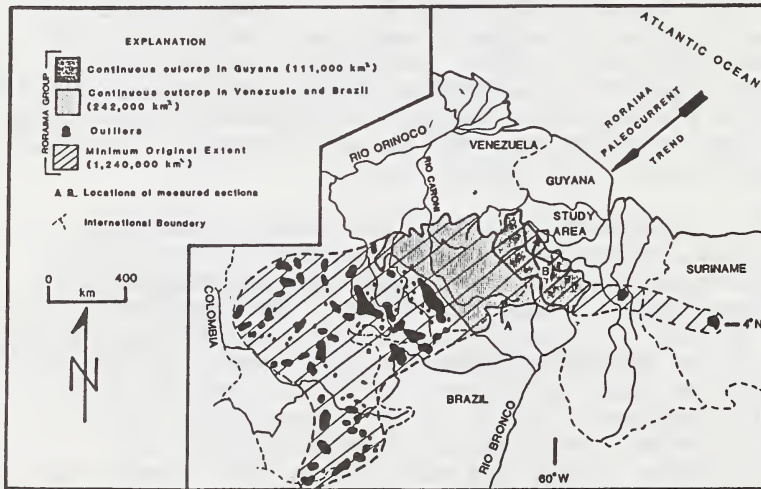


Figure 1. Map depicting the extent of Roraima Group rocks and their general paleo-current trend. Modified from Keats (1974).

#### REFERENCES

- Damuth, J.E. and Fairbridge, R.W. (1970) Equatorial Atlantic deep-sea arkosic sands and ice-age aridity in tropical South America. *Geological Society of America Bulletin*, 81, 189-206.
- Keats, W. (1974) The Roraima Formation of Guyana: a revised stratigraphy and a proposed environment of deposition. *Memoria 2nd. Congreso Latinamericano de Geologia, Caracas, 1973, Venezuela Ministerio de Minas e Hidrocarburos, Buletin de Geologia, Publicacion Especial, 2,7, 901-940.*
- Lampietti, F.J. and Sutherland, D. (1978) Prospecting for diamonds--some current aspects. *Mining Magazine*, 139, 117-123.
- Minter, W.E.L. (1978) A sedimentological synthesis of placer gold, uranium, and pyrite concentrations in Proterozoic Witwatersrand sediment. *Canadian Society of Petroleum Geology Memoir*, 5, 431-440.

Phlug, R. (1969) Quaternary lakes of eastern Brazil. *Photogrammetria*, 24, 29-35.  
 Schumm, S.A. (1977) *The Fluvial System*, 338p. John Wiley and Sons, New York.  
 Van der Hammen, T. (1972) Changes in vegetation and climate in the Amazon basin and surrounding areas during the Pleistocene. *Geol. Mijnbouw*, 51, 641-643.

Table 1. Pliocene to Holocene geologic and geomorphic history of northern Guyana proposed as a model for the Guiana Shield.

AGE	SEDIMENTARY DEPOSITS		GEOMORPHIC SURFACE ON THE GUIANA SHIELD (elevation, m above mean sea level)	INFERRED PALEOCLIMATE
	GUIANA BASIN	GUIANA SHIELD		
HOLOCENE	(D)	(D)		HUMID TROPICAL
PLEISTOCENE	(B)	(B)	Mazaruni (70 - 90)	SEMIARID
	(C)	(C)		HUMID TROPICAL
PLIOCENE	(M)	(M)	Llanos (100 - 170)	SEMIARID

(D) DEMERARA ALLOFORMATION. Well sorted coarse to fine sand and clay.

(C) COROPINA ALLOFORMATION. Silty loam, clay and pyrite bearing peat.

(B) BERBICE ALLOFORMATION. Coarse to fine, angular, poorly sorted sand that locally contains gravel and is locally arkosic. Includes a carbonate reef allomember.

(M) HACKENZIE ALLOFORMATION. Coarse to fine angular, poorly sorted, sand that locally contains gravel and is locally arkosic.

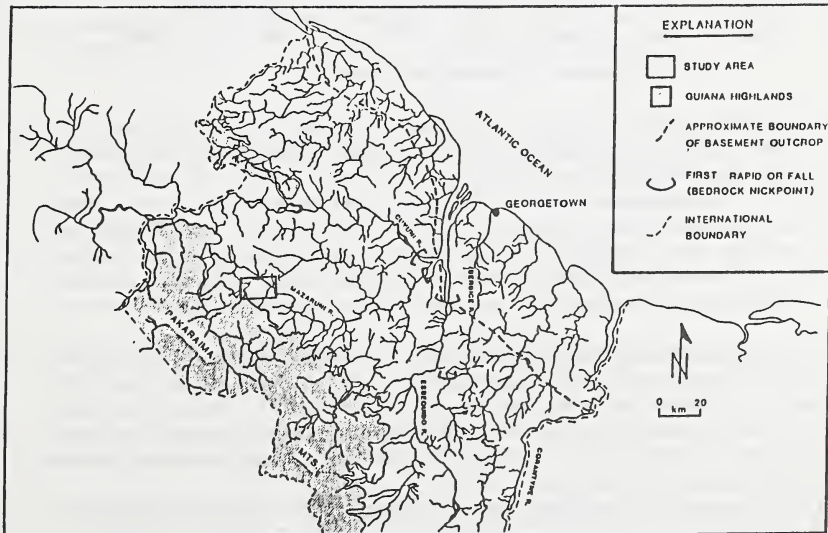


Figure 2. Map of Northern Guyana illustrating the bedrock nick-points and the approximate hingeline of crustal flexure as indicated by the trace of basement outcrop.

## IR SPECTROSCOPIC CHARACTERS OF GARNETS AND SPINELS – A POTENTIAL DISCRIMINATIVE TOOL FOR DIAMOND EXPLORATION.

*Lihe Guo; Wuyi Wang; Alian Wang and Andi Zhang.*

*Institute of Mineral Deposits, CAGS, Beijing 100037, China.*

Garnet and chromite are two important indicator minerals for diamond exploration. Most reported studies were focused on their compositional characters [1, 2, 3, 4, 5, 6, 7, 8] over the years. Although the structural refinement analysis [9, 10, 11], and spectroscopic studies [12, 13, 14] of garnet and spinel have been done in detail, but there is no one using the structural characters of garnet and chromite to discriminate primary diamond sources so far.

In recent years, the structure and spectroscopic features of above two minerals have been studied by the authors [15,16,17 for garnet and 18,19 for chromite]. It has been discovered that there are some peculiar garnets and chromites to diamondiferous kimberlitic rocks. An IR microanalysis method has been established [18]. In order to contrast the spectroscopic character with its chemical composition of these two minerals because the IR spectroscopic and compositional information could be obtained from the same grain.

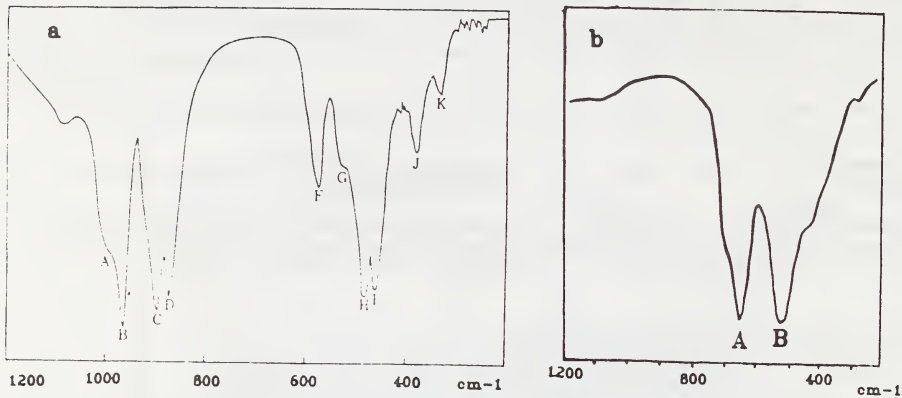


Fig. 1 IR spectra of Garnet(a) and chromite(b)

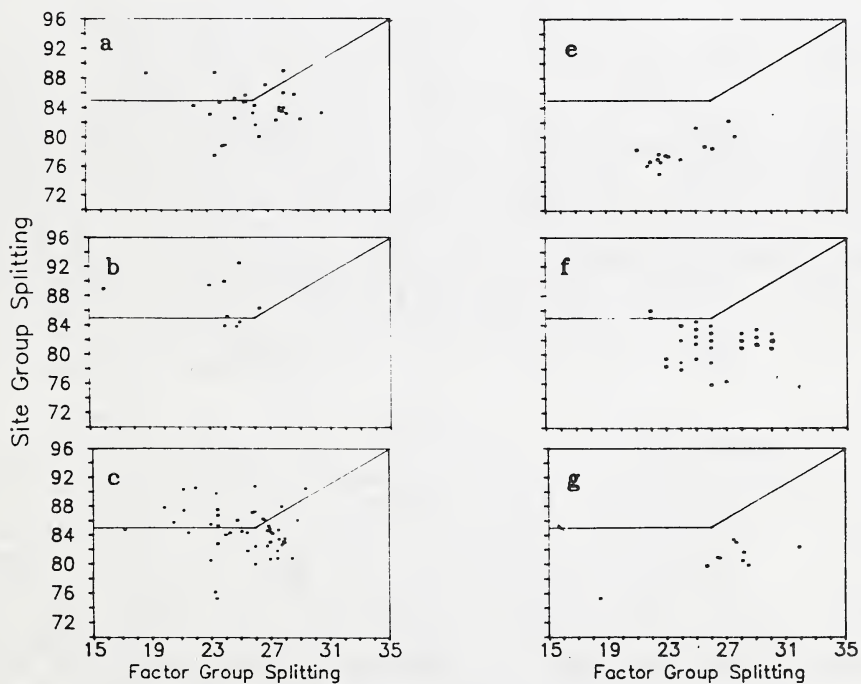
Figure 1a is a typical IR spectrum of garnet. The frequency differences of band positions ( $\nu_C - \nu_D$ ) and  $\nu_B - (\nu_C + \nu_D) / 2$  are assigned factor group splitting and site group splitting respectively. These two spectral characters are concerned with the substitution of ions  $Al^{3+}$ ,  $Cr^{3+}$  and  $Fe^{3+}$  in octahedron, and  $Mg^{2+}$ ,  $Fe^{2+}$  and  $Ca^{2+}$  in dodecahedron. The X-Y diagram drawn by using factor group splitting (ordinate) and site group splitting (abscissa) shows that more than 15% garnets of each diamondiferous kimberlite body with site group splitting larger than  $85cm^{-1}$  because they have subcalcium in dodecahedron and smaller factor group splitting because of their rich chromium contents in octahedron (Fig. 2a-d). However, in all non-diamondiferous rocks, there are no garnet with the above characters (Fig. 2e-h).

IR spectra of most chromites show two strong bands (Fig. 1b). The shift of high-frequency band A is concerned with the distortion of octahedron which is mainly caused by the substitution of  $Al^{3+}$ ,  $Cr^{3+}$  and  $Fe^{3+}$ . Another X-Y diagram drawn by using the positions of band A (abscissa) and band B (ordinate) shows that most chromites from diamondiferous kimberlitic rocks are located at the range of  $635-625cm^{-1}$  for band A, and  $505-495cm^{-1}$  for band B (Fig. 3a-c,h), but those from barren rocks are normally located out of this range (Fig. 3d,e-g).

Part of this work is supported by the Department of Geology, U.W.A. and CRA Exploration Pty Limited. Many thanks to Prof. P.G. Harris, Dr. W.J.Chang, Prof. N.M.S. Rock and Dr. C.Smith.

References:

- (1) Sobolev N.V. et al, 1973, *Contrib. Mineral. Petrol.*, 31, 1-12
- (2) Dawson J.B. and Stephens W.E., 1975, *J. Geol.*, 83, 589-607
- (3) Gurney J.J., 1984, *Univ.W.A. Publ.* 8, 134-166
- (4) Gurney J.J. and Moore R.O., 1989, In: *The Report of Can. Geol. Surv. The Development of Advanced Technology to Distinguish between Diamondiferous and Barren Diatremes*
- (5) Lucase H. et al, 1989, 4th I.K.C., *Kimberlites and Related Rocks*, 2, 809-819, *Geol. Soc. Aust. publ.*, 12
- (6) Sobolev N.V. et al, 1975, *Geologiya i Geofizika*, 16, 11, 7-24
- (7) Gurney J.J., 1989, 4th I.K.C., *Kimberlites and Related Rocks*, 2, 935-965, *Geol. Soc. Aust. publ.*, 14
- (8) Nixon P.H. (ed), 1987, In: *Mantle Xenoliths*, John Wiley Sons, New York
- (9) Gibbs G.V. and Smith J.V., 1965, *Am. Mineral.*, 50, 2023-2039
- (10) Novak G.A. and Gibbs G.V., 1971, *Am. Mineral.*, 56, 791-825
- (11) Hill R.J. et al, 1979, *Phys. Chem. Minerals*, 4, 317-339
- (12) Cahay R. et al, 1981, *Bull. Mineral.*, 104, 193-200
- (13) Preudhomme J. and Tarte P., 1971, *Spectrochem. Acta*, 27A, 845-851
- (14) White W.B. and De Angelis B.A., 1967, *Spectrochem. Acta*, 23A, 985-995
- (15) Wang A., 1987, PhD. Thesis, LASIR. Lille, France, 152-179
- (16) Wang W.Y., 1988, Master Thesis, CAGS, Beijing, China, 39-52
- (17) Guo L.H. et al, 1990, In: *Abstracts of The 15th General Meeting of IMA*, 1, 427-429
- (18) Guo L.H., 1988, Unpublished Report for CRA Exploration Pty Ltd.
- (19) Guo L.H. et al, 1990, In: *Proceedings of The 6th Conf. Mol. Spectro.*, 200-201



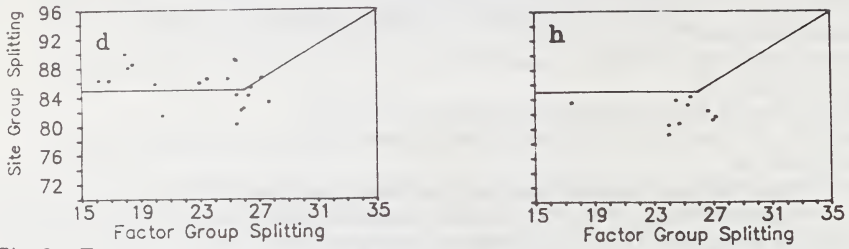


Fig. 2 Factor group splitting vs size group splitting of garnet Diamondiferous kimberlites (a-Liaoning 50, b-Liaoning 42, 3-Shengli 1 and 4-Hongqi 1), Barren kimberlites (c-Shangyu , f-Liuling), Basalt (g-Kuandian), Barren lamproite (h-Jingshan)

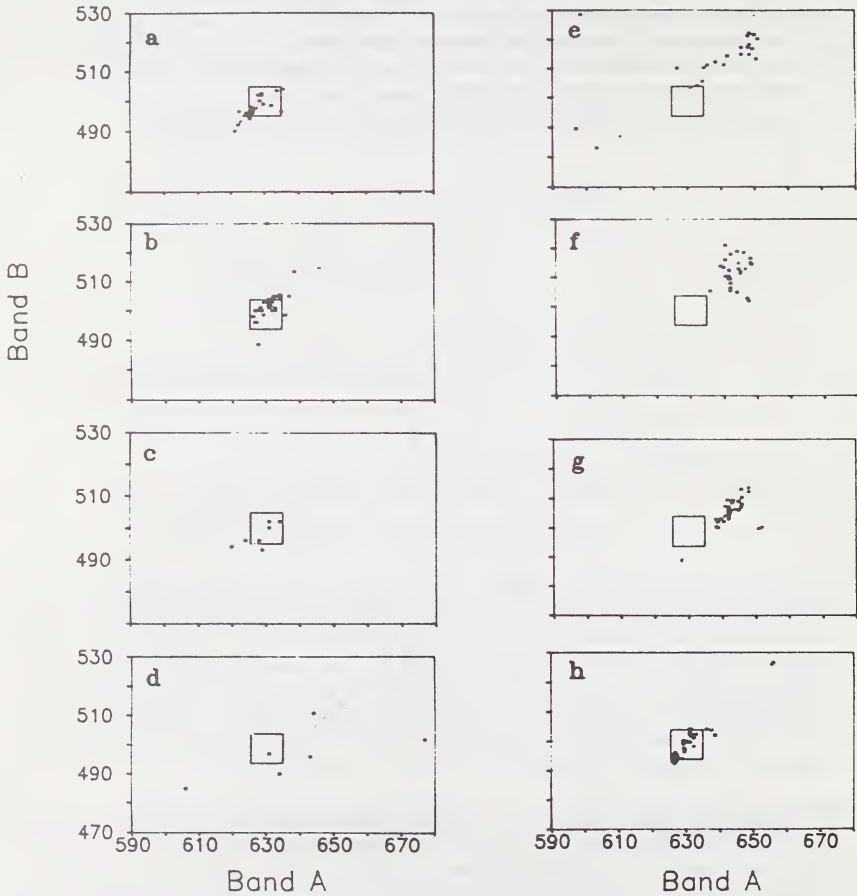


Fig. 3 Relationship of IR band A vs band B of chromite Diamondiferous Kimberlites (a-Shengli 1, b-Liaoning 50, c- Koffiefontein) and lamproite (h-Ellendale 4), Barren kimberlite (d-Rietfontein, e-Shexian), Related rocks (f-Anomaly 19 N.S.W., g-Narracoota Acid volcanics, W.A.)

## EMPLACEMENT AND IMPLICATIONS OF ULTRA-DEEP XENOLITHS AND DIAMONDS FROM THE TRANSITION ZONE.

*Haggerty, Stephen E.*

*Dept. of Geology, Univ. of Massachusetts, Amherst, MA 01003 U.S.A.*

The recognition of high-Si garnet inclusions in diamonds from Monastery (Moore and Gurney, 1985) and Jagersfontein (Tsai et al., 1985; Moore et al., 1991, in press) in South Africa, and from San Luiz in Brazil (Wilding et al., 1989), and of pyroxene exsolved from garnets in xenoliths from Jagersfontein (Haggerty and Sautter, 1990; Sautter et al., 1991; Sautter and Haggerty, this volume), provides a basis for the evaluation of transport mechanisms and the timing of sample entrainment from the transition zone at depths between 400 and 650 km. These ultra-deep samples have significant implications for petrochemical models of the upper mantle, diamond genesis and kimberlite evolution.

There are at least three possible origins for the transition zone: (1) it is isochemical with the upper mantle, but not the lower mantle, and represents a series of phase changes to higher density polymorphs; (2) it is a primordial interface that resulted from fractionation of the core and differentiation of the upper mantle from the lower mantle; or (3) it was created by the buoyancy-equivalent piling up of subducted oceanic slabs. In none of these cases is this zone likely to contain an abundance of heat-producing elements. Therefore, the only viable mechanism for the transport of ultra-deep xenoliths and diamonds from regions in the vicinity of the transition zone (>300 km) is by plume activation arising from instabilities in the D" layer at the core-mantle boundary.

Kimberlites are becoming increasingly accepted as plume-driven melts from the upper mantle. These bodies have been geochemically linked to ocean island basalts and share the distinction with plateau basalts erupted at the onset of continental fragmentation, inasmuch as tectonism and melt generation are both plume-activated (Duncan and Richards, 1991). Major plumes are invoked to account for flood basalts of the Karoo in southern Africa, and plume paths are documented by le Roex (1986). The most prominent plumes on the SE margin of the Kaapvaal Craton that were active at about the time (100 Ma) of the Jagersfontein kimberlite eruptions were the Shona, Bouve and Marion hot spots. We attach particular significance to the location of the Jagersfontein and Monastery kimberlite pipes at the edge of the craton with the association of ultra-deep xenoliths and excess-Si garnets in diamonds. It was at the edge of the craton that the plumes were most vigorous as attested to by the ensuing separation of Madagascar and Antarctica from southern Africa during the Mesozoic. If plumes are indeed generated in the D" layer at the core-mantle boundary (2900 km) then mechanical transport of xenoliths from the region of the relatively shallow transition zone (400 km) would not

appear to be a significant obstacle. The thermal regime and the initial sizes of bodies entrained in the plume may, however, be critical to xenolith survival. Physical entrainment of mantle xenoliths is a new proposal. Plumes are most commonly considered to be only agents of heat transfer, but if melts are produced (e.g., Campbell et al., 1989) and relative viscosities are appropriate to solid media transport, xenolith entrainment is inevitable. Rising plumes on intersection with the transition zone are likely to mushroom because of thermal dissipation. It is critical to sampling of this horizon that temperatures range from liquidus to sub-liquidus, vertically and laterally, throughout the zone. Other barriers and horizons of interference are at the lithosphere-asthenosphere boundary (LAB), and at 75-100 km in the lithosphere in the region of the LILE and HFSE metasomes (LHM). It is either at the LAB or the LHM that garnet-bearing xenoliths equilibrated to form pyroxene lamellae from previously homogeneous high-Si garnets. (Sautter and Haggerty, this volume).

Plumes do not appear to be affected on geological time scales by whole mantle convection (e.g., Olson et al., 1988), thus sustained thermal activity at and within the sub-cratonic lithosphere should be expected. While the volatile content of the transition zone remains unknown, indications from OIBs is that plumes are geochemically enriched. Even with subduction, the transition zone is unlikely to be a source of volatiles because of dehydration and progressive melt extraction of the down-going slab. Therefore, enrichment is very likely derived directly from the D" layer. We propose that this is the main source of volatiles for melt metasomatism of depleted lithosphere. Continued activity might result in extensive metasomatism at the base of the lithospheric keel or tectosphere until some critical threshold is reached in which plumes are transformed to what we now designate as flumes (wet hot spots) and kimberlites are injected. Primary transport of the ultra-deep samples was by plumes, and following equilibration (i.e., exsolution of pyroxene from garnet) by flumes.

Some other possibly important implications for volatiles originating from the D" layer are: (1) a source of C for micro-diamonds, and diamonds in some classes of eclogites; (2) the ubiquitous presence of sulfides as diamond inclusions; (3) erosion at the base of subcratonic lithospheric keel and penetration of diamond-etching and diamond-dissolution fluids and melts; (4) a more rational explanation for the sources of volatiles in LILE and HFSE metasomatizing melts and cube diamond overcoats at higher levels in the lithosphere; (5) a possibly exotic mechanism for carbon isotopic fractionation; and (6) a more viable source for SiC, Fe, and magnesiowüstite-ferropericase inclusions in diamonds. Eclogitic diamonds are of diverse origin, and distinctions in diamond-entrapment ages between some eclogitic and ultramafic diamonds may well be related to a global plume event at ~1.5 Ga, followed by particularly vigorous flume activity and kimberlite eruptions at ~1.0 Ga, and again at 100 Ma. Kimberlite and lamproite eruptions in specific time frames on a global basis can now perhaps be best explained if the timing of eruptions is linked to the geometry of plume instabilities from the D" layer.

The link between and among basalts, OIBs, kimberlites, plumes and plate tectonics is enormously strengthened by the recognition of asthenospherically-derived diamonds and of xenoliths from the transition zone (TZ). If plumes are primarily responsible for diamond eruptives, an inevitable conclusion is that all such eruptives have a high probability of containing transition zone xenoliths (TZX); but this raises an interesting question on the apparent absence of eclogitic or TZX-based diamonds in off-craton kimberlites. One possibility is that off-craton intrusions have a greater opportunity for interaction with oxidizing asthenosphere (Haggerty, 1986): below cratons and in the continental keel model (e.g., Haggerty, 1986), the asthenospheric interval between the base of the keel and the TZ is of the order of 200 km; in the tectosphere model (Jordan, 1975), the interval may be only kilometers thick or may not be present at all; whereas in off-craton regions the interval is about 400 km. Nonetheless, we propose that TZXs are widespread but that because of extensive equilibration, these xenoliths are more generally described as garnet harzburgite, garnet lherzolite, garnet pyroxenite, and eclogite. If the transition zone is to be fully characterized, future studies should concentrate on developing techniques and establishing criteria to unequivocally distinguish between ultra-deep xenoliths and those derived from shallower horizons.

#### REFERENCES

- Campbell, L.H., Griffiths, R.W. and Hill, R.L. (1989) Melting in an Archean mantle plume: heads it's basalts, tails it's komatiites. *Nature* 339, 697-699.
- Duncan, R.A. and Richards, M.A. (1991) Hot spots, mantle plumes, flood basalts and true polar wander. *Rev. Geophys.* 29, 31-50.
- Haggerty, S.E. (1986) Diamond genesis in a multiply constrained model. *Nature* 320, 34-38.
- Haggerty, S.E. and Sautter, V. (1990) Ultra-deep (>300 km) ultramafic, upper mantle xenoliths. *Science*, 248, 993-996.
- Jordan, T.H. (1978) Composition and development of the continental tectosphere. *Nature* 274, 544-548.
- le Roex, A. (1986) Geochemical correlation between southern African kimberlites and South Atlantic hotspots. *Nature* 324, 243-245.
- Moore, R.O. and Guernsey, J.J. (1985) Pyroxene solid solution in garnets included in diamonds. *Nature* 318, 553-555.
- Olson, P., Schubert, G., Anderson, C. and Goldman, P. (1988) Plume formation and lithosphere erosion: A comparison of laboratory and numerical experiments. *J. Geophys. Res.* 93, 15,065-15,084.
- Sautter, V. and Haggerty, S.E. (1991) Ultra-deep (>300 km) ultramafic xenoliths: New petrologic evidence from the transition zone. *Science*, in press.
- Tsai, H., Meyer, H.O.A. Moreau, J. and Milledge, H.J. (1979) Mineral inclusions in diamond: Premier, Jagersfontein and Finsch kimberlites, South Africa, and Williamson Mine, Tanzania: In Boyd and Meyer, eds. *Kimberlites, Diatremes and Diamonds*. 1, 16-26. AGU. Washington, D.C.
- Wilding, M.C., Harte, B. and Harris, J. W. (1989) Evidence of asthenospheric source for diamonds from Brazil. *Extended Abs. IGC*. 3, 359-360.

THE PHYSICAL CHARACTERISTICS AND SYNGENETIC INCLUSION GEOCHEMISTRY OF DIAMONDS FROM PIPE 50, LIAONING PROVINCE, PEOPLE'S REPUBLIC OF CHINA.

Harris, <sup>(1)</sup>J.W.; Duncan, <sup>(2)</sup>D.J.; Zhang, <sup>(3)</sup>F.; Mia, <sup>(3)</sup>Q. and Zhu, <sup>(3)</sup>Y.

(1) Department of Geology and Applied Geology, University of Glasgow, Glasgow, G12, 8QQ, Scotland;

(2) Sino-British Co-operation Brigade, Bureau of Geology and Mineral Resources, Pulandian, Liaoning Province,

PRC; (3) No. 6 Geological Brigade of Liaoning Bureau of Geology and Mineral Resources, Pulandian, Liaoning Province, PRC.

**Introduction:-** Pipe 50 is located in the Toudaogou area, near Fuxian. The kimberlite has an irregular rhomboidal outline, trends east-west with a surface length of 275m and width of 55m, is believed to be of Devonian age (366 to 398Ma), and is intruded into Proterozoic sandstones, (Zhang et al 1989). In this study, the physical characteristics of 13,000 diamonds from this mine covering the whole production are presented, together with data on the nature and chemistry of the syngenetic inclusions, collected over a two-year period.

**Diamond Characteristics:-** Initial shape variations as a function of size, Harris et al (1975) are shown in Figure 1a. The proportion of **primary** diamond shapes is given in Figure 1b, after reassignment of broken diamonds (irregulars) to their sub-shapes. Octahedra (70%) and macles (10%) dominate

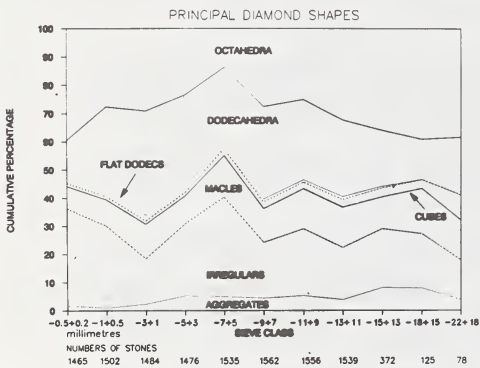


FIGURE 1a

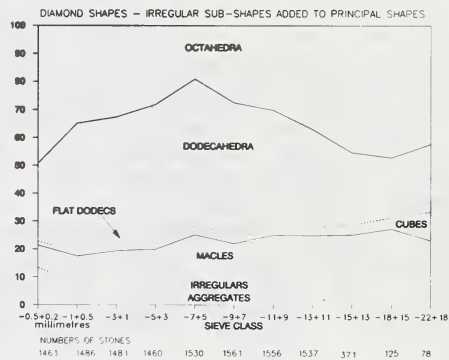


FIGURE 1b

the primary shapes, with about 5% each of cubes and aggregates, there being a small percentage of genuine irregulars. Figure 1b also clearly shows that the proportions of these crystals are independent of diamond size. In addition, from diamond size -7+5 to the very smallest stones, there is a pronounced reversal in the proportion of dodecahedra, (the resorbed form of primary octahedra). This change is also accompanied by a steady and marked increase in the proportion of both sharp-edged octahedra, from 25% to 75% and triangular macles, from 15% to 60%. Octahedral faces of both morphologies consist of triangular growth platelets giving crystal edges a distinct striated appearance.

With diamonds larger than -7+5, colour proportions are also largely independent of size, colourless (55%) and brown (30%) dominating over yellow (8%), the remaining few percent being grey-black or transparent green coated. In sizes smaller than -7+5, the steady increase in colourless stones at the expense of yellow and brown, is probably not real, but reflects the difficulty of determining true body colour in small diamonds.

Apart from the distinctive striated and terraced appearance of the smaller octahedra and macles, a noticeable surface feature on about 10% of dodecahedra are very shallow, irregular bounded, matt etched depressions, which may partially occur over an entire stone, or be confined to a few faces. This surface is considered to be incipient corrosion sculpture, a root zone diamond surface texture, (Robinson et al 1989). More rarely, dodecahedral surfaces exhibit imbrication, or non-alluvial scratch-like markings, the latter, having a very variable surface distribution. In the size range 0.5 to 3.0mm, 45% of diamonds are plastically deformed, but this value falls to 20%, both for the smallest diamonds, where identification is difficult because crystals are sharp-edged and for large diamonds where numbers are small. Plastic deformation is expectedly high among brown diamonds of all sizes (70%), but at Pipe 50, relatively high levels of deformation among colourless (average 30%) and yellows (average 45%), are also recorded.

**Syngenetic Inclusions:-** The diamond paragenesis at Pipe 50 is overwhelmingly peridotitic, only one eclogitic diamond being recovered during the examination period. Olivine and chromite dominate over all other minerals, but chrome diopside has an unusually high and equal occurrence with pyrope garnet, enstatite and sulphides. In all, 59 inclusions were recovered from 55 diamonds. Analysis of individual and co-existing inclusions indicate that the paragenesis is strongly lherzolitic, with a very minor harzburgitic component. Olivines average Fo = 92.40 (n=20), enstatites, En = 93.00, (n=2), and chromites have average Cr2O3 contents of 65.16 wt%, (n=21). Only two of the 5 pyropes are harzburgitic, but the lherzolitic ones have up to 13 wt% Cr2O3). Chrome-rich lherzolitic clinopyroxenes (n=3), (approx. 1.50 wt% Cr2O3) co-exist with the most chrome-rich olivines (0.06wt % Cr2O3), but a fourth clinopyroxene is distinctly chrome-poor (0.40 wt%, when coexisting with pyrope (1.75 wt% Cr2O3). Sulphide inclusions (n=4), are confined only to pyrrhotite with exsolved pentlandite. The single eclogitic diamond turned out to be lherzolitic, containing a pale-orange, relatively high titanium (0.41 wt% TiO<sub>2</sub>) garnet, (4.30 wt% CaO, 1.48 wt% Cr2O3), associated with a pale-green biminerally inclusion of chrome poor (0.64 wt% Cr2O3) clinopyroxene and an orthopyroxene with a Fe/Fe+Mg ratio of 88.60.

**Discussion:-** The constancy in the proportion of **primary** shapes with size for the overwhelmingly peridotitic diamond paragenesis at Pipe 50, implies a very constant nucleation rate and growth for these diamonds. This result may also be a general feature of such diamond populations, as similar graphs have been recorded for the peridotitic diamonds at Finsch and DeBeers Pool mines in Kimberley, (Harris et al 1984).

If upward moving magmas of kimberlite or lamproite release diamonds from disaggregating xenoliths, as proposed by Robinson et al (1989), then evidence from diamond size distribution characteristics, (Deakin and Boxer, 1989), suggests that very large numbers of small diamonds will be released in the final stages of this disaggregation. Whilst many of these diamonds may undergo resorption to extinction, the small proportion that remains is numerically substantial and hence, small sharp-edged crystals are easily recognised in a diamond population. At Pipe 50, diamond size distribution

may play a part in accounting for the unresorbed smaller diamonds, but more probably the unresorbed larger diamonds, are protected either by the xenolith, or if released, because there is insufficient oxygen activity in the magma to cause resorption. Of these two proposals, the second is favoured for Pipe 50, because diamonds of such a wide range of sizes, are unlikely to be released from xenoliths all at once.

The proportional increase in sharp-edged octahedra with decreasing size is not thought to be caused by a new influx of diamonds, as considered by Haggerty (1986). The 30% increase in octahedra at Pipe 50, is not accompanied by any similar increase in the total octahedral content, nor is there any increase in the total macle proportion, both likely consequences if a second diamond population was present. Also, particular attention was paid to the recovery of inclusions from sharp-edged smaller crystals, and no obvious differences in mineralogy or chemistry were noted between them and inclusions recovered from larger more rounded crystals.

Inclusions belonging to the lherzolitic paragenesis, are usually, either rare, or if more substantially present in a specific diamond population, associated with a dominant eclogitic paragenesis, (see e.g. Otter and Gurney, 1989). At Pipe 50, not only are eclogitic inclusions absent, but lherzolitic diamonds constitute the major paragenesis.

## References

- Deakin, A.S. and Boxer, G.L. Argyle AKI diamond size distribution: the use of fine diamonds to predict the occurrence of commercial size diamonds. In J. Ross, Ed., *Kimberlite and Related Rocks*. Vol. 2, p1117-1122. GS Aust. Spec. Publication No. 14.
- Haggerty, S.E. (1986). Diamond genesis in a multiply-constrained model. *Nature*, 320, 34-38.
- Harris, J.W., Hawthorne, J.B., Oosterveld, M.M. and Wehmeyer, E. (1975). A classification scheme for diamond and a comparative study of South African diamond characteristics. In L. Ahrens et al. Eds., *Physics Chemistry of the Earth*, Vol. 9, p765-783. Pergamon Press, Oxford, England.
- Harris, J.W., Hawthorne, J.B. and Oosterveld, M.M. (1984). A comparison of diamond characteristics from the DeBeers pool mines, Kimberley. In J. Kornprobst, Ed., *Annales Scientifique de l'Universit e de Clermond Ferrand II*, 74, 1-13, Elsevier, Amsterdam.
- Robinson, D.N., Scott, J.A., Van Niekerk, A. and Anderson, V.G. (1989). The sequence of events reflected in the diamonds of some southern African kimberlites. In J. Ross, Ed., *Kimberlites and Related Rocks* Vol. 2, p991-1000. GS Aust. Spec. Publication No. 14.
- Otter, M.L. and Gurney, J.J. (1989). Mineral inclusions in diamonds from the Sloan diatremes, Colorado-Wyoming state line kimberlite district, North America. In J. Ross Ed., *Kimberlites and Related Rocks*, Vol. 2, p1042-1053. GS Aust. Spec. Publication No. 14.
- Zhang, P., Hu, S. and Wan, G. (1989). A review of the geology of some kimberlites in China. In J. Ross, Ed., *Kimberlites and Related Rocks*, Vol. 1., p392-400. GS Aust. Spec. Publication No. 14.

## THE TRACE ELEMENT ANALYSIS OF SINGLE DIAMOND CRYSTAL BY NEUTRON ACTIVATION ANALYSIS.

R.J. Hart\*; A. Damanipurshad<sup>(1)\*</sup>; J.P.F. Sellschop<sup>(1)</sup>; H.O. Meyer<sup>(2)</sup>; M.E. McCallum<sup>(3)</sup> and C. Koeberl<sup>(4)</sup>.

(1) Schonland research centre for Nuclear Physics, University of the Witwatersrand, Johannesburg; \*Seconded from the Geological Survey of South Africa; (2) Department of Geoscience, Purdue University, Lafayette, Indiana, 47907;

(3) Department of Earth Resources, Colorado State University, Fort Collins, Colorado, 80523; (4) Institute of Geochemistry of Vienna, Vienna.

### Introduction

The trace element geochemistry of natural diamonds or "diamond and its inclusion" provide valuable information on the environment in which diamonds crystallize. In addition such information may prove to be useful in "fingerprinting" diamonds of different provenience areas.

Existing data on the geochemistry of single diamond crystal are confined mainly to the geochemistry of inclusions in the diamond. ((Meyer and Boyd 1972) The development of the proton microprobe now makes it possible to measure the trace element contents in the diamond matrix itself. However, this technique has the serious drawback that the analysis is confined only to a narrow depth of 50 to 100 microns from the crystal surface and since the trace element content in a diamond may be zoned (Gurney 1991), this technique may not provide a true reflection of the bulk trace element geochemistry in diamond.

Potentially the most powerful technique for determining the bulk trace element content of a diamond is Neutron Activation Analysis (NAA). Previous studies in this field (Fesq et al. 1975, Erasmus et al. 1977) made use of 55 cc intrinsic Ge(Li) detectors (peak to compton ratio of 40:1; efficiency of 10%). The sensitivity of these detectors were not sufficient for the analysis of trace elements in a single diamond crystal and composite samples of between 10 and 20 stones (total 1gm) were analysed. This provided information only on the average chemistry of a group of stones. Improvement in detector technology over the last decade has led to the development of large volume (199cc) Ge(Li) detectors ("Monster" detectors) with an improved peak to compton ratio of 72:1 and an efficiency of 40%. With this detector and improved counting electronics, we have been able to achieve up to a 5 fold increase in sensitivity which now enables us to quantitatively analyse trace elements in small single crystals.

### Sample selection

Thirty-five diamonds both with and without visible inclusions have been selected for trace element analyses by NAA. Ten of the samples are from the George Creek mine in Colorado, nine samples are from a mine near Romaria in Brazil and ten samples are from the Finsch mine in South Africa. The diamonds range in weight from .01 to 0.2 carats and any inclusions are generally less than 10 microns in size. The diamonds also vary considerably in colour and quality, from black to gem quality white.

### Experimental procedure

The diamonds were irradiated in an Oak Ridge type reactor at Pelindaba (South Africa) for ten days, and are then counted 17 hours, 3 days, 12 days, 30 days and 3 months after irradiation. Counting times employed were 6 hours for the first count, and then for 24 hours for each of the subsequent counts. It is important to make sure that the gamma signal counted on the detector comes from the body of the diamond and not from any residual surface contamination, and special care was taken in the cleaning of the diamonds prior to irradiation: the diamonds are boiled individually in a concentrated mixture of HNO<sub>3</sub>, HClO<sub>4</sub> and H<sub>2</sub>SO<sub>4</sub> for 1 hour before encapsulation in a quartz vial and on post irradiation removal, the procedure is repeated. The total neutron flux received by each sample was measured by using a flux monitor in the form of steel wire wrapped around the outside of the vial. Background counts were performed regularly throughout the experiment.

**Quantitative data; precision and accuracy**

Diamonds are particularly well suited to the technique of NAA as the carbon matrix is "transparent" to neutrons and the diamonds have a very low background count. In order to quantify the trace element data in single crystal diamonds it was essential to develop suitable standard material with trace element concentrations and matrix that is comparable to diamond. In this study it was found that a ~ 50:1 mixture of "specpure" graphite with standard rock powders provided us with suitable reference material, although the concentrations of most elements in the standards are still higher than those found in most diamonds. Large volumes of these mixed standards were analysed both at the Schonland Centre, University of the Witwatersrand and at the Institute of Geochemistry, University of Vienna. The interlaboratory comparisons and replica analyses (see Table 1) provide us with a measure of the accuracy and precision of our analyses at ppb levels.

Table 1. A comparison of data for graphite standard from University of Vienna and the Schonland centre. Except where stated values given in ppb

Element	Vienna mean	Schonland mean	n	Std. Dev.
La	60	86	8	30
Na ppm	100	96	8	12
Br	120	68	8	12
As	70	53	8	8.8
Sm	12	15	8	5.9
Au	14	8	8	9.5
U	5	11	4	6.6
Nd	100	110	2	1.4
Ba ppm	6	12	7	11
Lu	5	2	3	2.1
Yb	20	28	5	13
Ce	110	177	4	44
Cr ppm	108	130	9	23
Eu	35	112	4	9.6
Co ppm	2.3	2.9	8	1.4
Fe %	0.17	0.11	7	0.5
Ta	17	18	8	1.4
Sc	460	803	8	11
Ni ppm	55	72	8	17
Tb	20	13	4	8.1
Cs	50	43	6	8.8
Hf	20	25	4	13
Ir	1.4	1.9	6	0.6
W	40	43	7	23
Th	15	20	7	3.4

**Discussion**

All the diamonds thus far analysed contain some trace elements and each individual stone has its own trace element characteristics. This strongly emphasises the need to analyse individual stones rather than composite samples. As expected, clear white diamonds contain only few elements and always at low abundances, whereas stones with inclusions or with deep colour contain relatively high abundances of trace elements. Black diamonds contain almost all the elements listed in Table 1. In all cases, if the diamond contains an identifiable inclusion, the geochemistry reflects that inclusion.

**Trace element geochemistry in relation to environment of crystallization**

In most cases the geochemistry of the diamonds is dominated by siderophile elements and all the indications from this study are that the chemistry of the siderophile elements reflects the environment in which the diamonds crystallized. For example the Au/Ir ratios in two of the diamonds from Finsch (Fig. 1) plot close to the mantle line and are consistent with Au/Ir ratios in diamond obtained by Fesq et al. (1975). It is interesting to note that many of the diamonds thus

far analysed contain Au irrespective of whether or not there is an inclusion such as sulphide which may host Au, suggesting that Au in diamond may exist in the metallic form.

Plots of Fe versus Cr, and Fe versus Sc are shown in Fig. 2 and 3. The data shown in these plots represent diamonds both with and without visible inclusions. Clearly the Finsch diamonds can be separated into the two major parageneses found in diamond inclusions. The samples with high Cr and high Sc content both have visible peridotitic garnet inclusions, whereas the remaining Finsch diamonds (two of which have eglogitic clinopyroxene inclusions) all have lower Cr and Sc contents and plot in separate fields in Fig. 2 and 3. Furthermore, there are indications that both groups of Finsch diamonds have a different signature to the diamonds from North And South America; these have a more restricted geochemistry which is strongly influenced by Fe.

### Trace element Geochemistry in relationship to provenance area

Some diamonds are also relatively enriched in lithophile elements. The chondrite normalized REE patterns for these stones are shown in Fig.4. Clearly the REE patterns for the three suites of diamonds analysed in this study are significantly different. Moreover, the fact that in each case there are two diamonds from each suite with similar patterns provides some measure of confidence in these analyses of REE at ppb levels.

Samples F10 and GC1 are both black diamonds with no visible inclusions or cracks, but the four remaining diamonds range from brown to colourless and are characterised by micro-cracks which contain tiny specks of material. Thus although the REE could be located in the body of the diamond, our interpretation is that these LREE enriched patterns reflect contamination of the diamond by the host kimberlite. In conclusion, we suggest that the lithophile elements (and in particular the REE) tell us more about the kimberlite event rather than about the crystallization environment of diamonds.

### Conclusions

The application of NAA technique to small (<0.2 carats) single crystal diamonds clearly illustrates the ability to analyse trace elements in diamonds down to ppb for some elements. Ultimately such information must prove useful in 1) understanding the origin of diamonds 2) relating diamonds to their source area, and 3) other facets of the diamond industry such as the use of diamonds as semi-conductors.

### References

- Erasmus C.S., Sellschop J.P.F., Bibby D.M., Fesq H.W., Kable E.J.D. Keddy R.J., Hawkins D.M., Mingay S.E., Rasmussen S.E., Renan M.J. and Watterson J.I.W. 1977. *J. Radioanal. Chem.* 38, 133-146.
- Fesq H.W., Bibby D.M., Erasmus C.S., Kable E.J.D., Sellschop J.P.F. 1975. *Phys. Chem. Earth*, 9, 817-836.
- Gurney J.J. 1991. *S. Afr. J. Geol.* 93(3), 424-437.
- Meyer H.O. and Boyd F.R. 1972. *Geochimica et Cosmochimica Acta*, 36, 1255-1273.
- Tredoux M., De Wit M.J., Hart R.J. Lindsay N.M. Verhagen B. and Sellschop J.P.F. *J. Geology*, 97, 589-605.

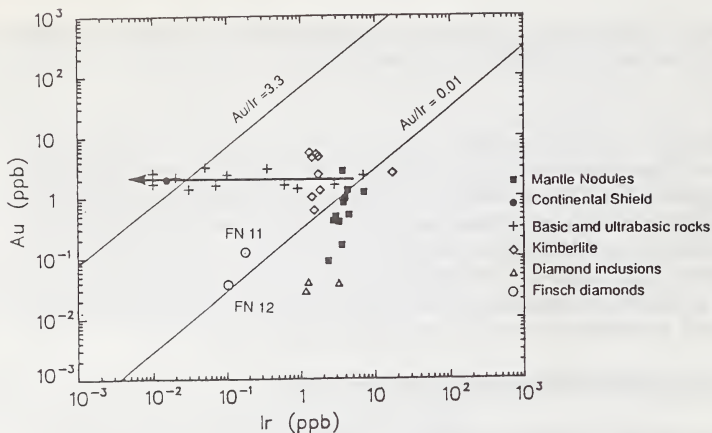


**Fig. 1** A comparison of the Au/Ir ratio for two of the Finsch diamonds to various mantle derived rocks. the arrow shows the mantle (Au/Ir = 0.01) - Crust (Au/Ir = 3.3) differentiation trend. (After Tredoux et. al 1989)

**Fig. 2.3** Plots of Fe versus Cr and Fe versus Sc respectively. The horizontal shading represents the field for the North and South American Diamonds, the vertical shading represents the field for the Finsch peridotitic diamonds and the dotted shading the field for the Finsch eglogitic diamonds.

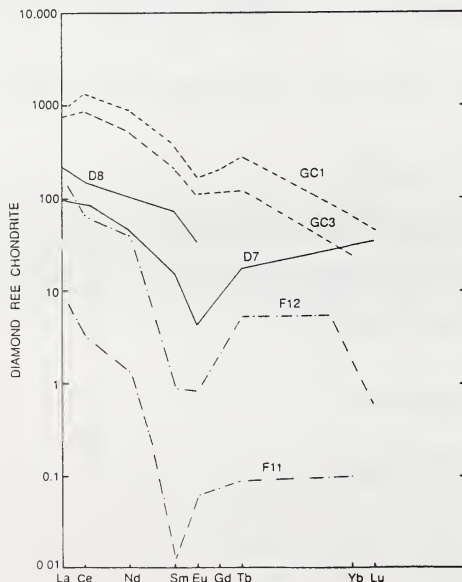
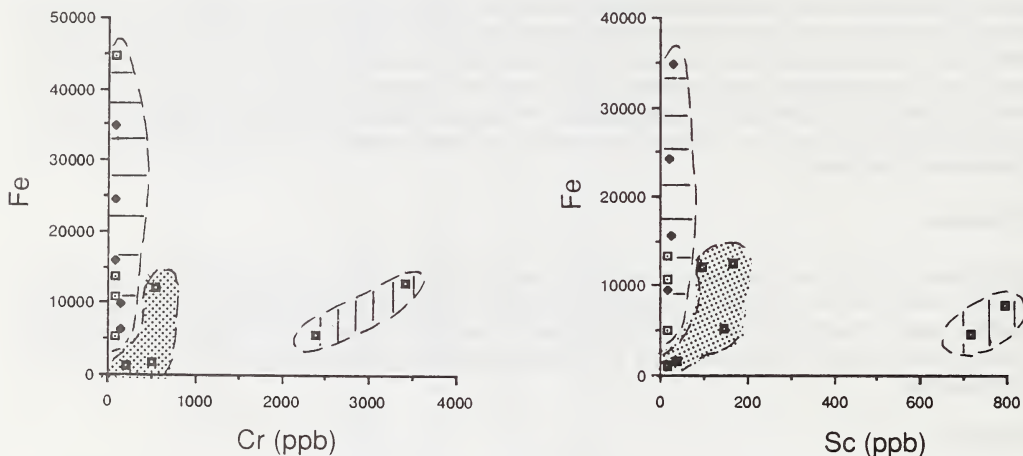


**Fig.4** REE patterns for Finsch (F11 and F12) Brazil (D7 and D8) and Colarado (GC1 and GC3) diamonds.

ASPECTS OF MELT COMPOSITION, CRYSTALLIZATION, METASOMATISM  
AND DISTRIBUTION, SHOWN BY MANTLE XENOLITHS FROM THE  
MATSOKU KIMBERLITE PIPE.

Harte, <sup>(1)</sup>B.; Mathews, <sup>(1)</sup>M.B.; Winterburn, <sup>(2)</sup>P.A.; and Gurney, <sup>(3)</sup>J.J.

(1) Dept. Geology and Geophysics, University of Edinburgh, Edinburgh EH9 3JW, Scotland, U.K.; (2) Anglo-American Research Laboratories, Johannesburg, South Africa; (3) Dept. of Geochemistry, University of Cape Town, Rondebosch 7700, South Africa.

### Introduction

The nature and mobility of mantle melts and their relationships to mantle metasomatism are important topics of extensive recent debate. The garnetiferous peridotite-pyroxenite xenoliths from Matsoku have been of particular interest in this context (e.g. Harte et al., 1975, 1987), and although somewhat unusual for xenoliths from kimberlite, it is evident that they record similar processes of formation to those associated with 'dike' intrusion and metasomatism in many mantle xenoliths from basalts. This paper summarises the most recent work on the Matsoku xenoliths, which has led to clarification of: the chemical character and origin of the melt involved in injection and metasomatism, textural aspects of melt distribution and crystallisation, the production of 'cumulate' chemical compositions, and the relative roles of diffusion and infiltration in metasomatism.

### Trace element evidence of melt compositions

Ion microprobe studies of trace element compositions in the garnets and clinopyroxenes in the pyroxenite sheets ('dikes') and metasomatised rocks have been carried out on a Cameca IMS4f ion microprobe (Edinburgh University/NERC facility). An O<sup>-</sup> primary ion beam was used, and positive secondary ions were measured at high energy (to reduce molecular overlaps) and standardised against NBS glass and natural garnet and clinopyroxene standards. Measurements were made principally for Y, Zr and REE and show considerable similarity between the compositions of Matsoku garnet

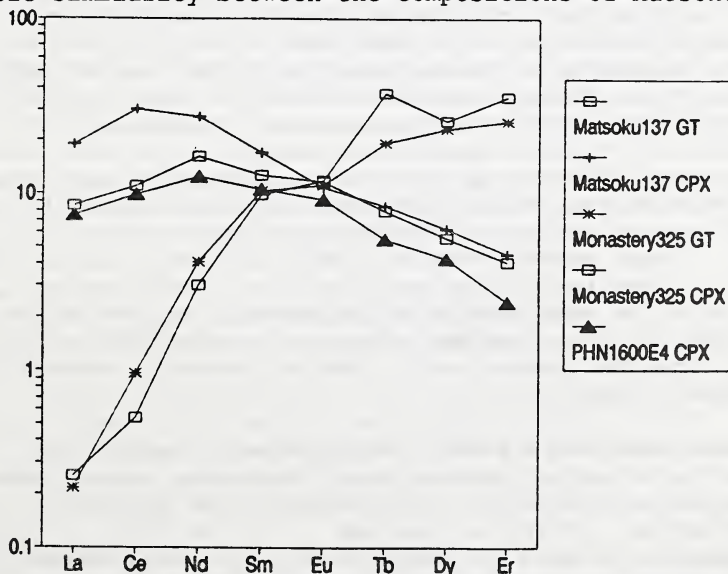


Fig.1 Chondrite normalised REE abundances

and clinopyroxene formed in equilibrium with intruding and infiltrating melt, and those of Cr-poor megacrysts from kimberlites. REE data for a garnetiferous pyroxene-rich 'dike' (specimen LBM 137 documented by Harte et al., 1987) are shown in Fig. 1, where they are compared with Edinburgh ion microprobe data for coexisting garnet and clinopyroxene in a megacryst from the Monastery mine (provided by R. O. Moore), and with cpx megacryst PHN1600E4 (data from Kramers et al., 1981).

Fig. 1 demonstrates the considerable similarity between the trace element contents of the Matsoku 'dike' phases and those of the megacrysts, and thereby suggests that the melt intruding and metasomatising the Matsoku peridotites was of very similar composition to that from which the Cr-poor megacrysts crystallised. Estimation of the Matsoku melt composition using crystal-liquid partition coefficients (Hanson, 1980) yields a melt of OIB-like (primitive basanite) characteristics, as similarly determined for Cr-poor megacrysts (Harte, 1983; Jones 1987). Thus despite the lithospheric P-T estimates (ca. 35 kbs and 1000°C) of the Matsoku xenoliths, there is evidence of intrusion and metasomatism by a melt of asthenospheric origin, similar to that suggested to metasomatise high-temperature deformed peridotites (Harte, 1983).

#### **Melt textures in pyroxenite 'dikes' and modally metasomatised rocks.**

Partially preserved igneous textures involving both euhedral-subhedral and interstitial-xenomorphous pyroxene crystals are found in some of the intrusive pyroxene-rich 'dikes'. These suggest pseudomorphing of the shape of interstitial melt patches by the interstitial-xenomorphous crystals.

Particularly good evidence of melt distribution and melt geometry has been found in the textures of ilmenite concentrations in some modally metasomatised rocks. Irregular and sometimes elongate patches of ilmenite (up to 1.5 cms long) were seen with curious cusped and spiky margins, with suggestions that they might represent melt pseudomorphs. A study of dihedral angles for ilmenite grains between two olivines and between two orthopyroxenes was undertaken, and yielded a very wide spread of values with evidence of bimodal distribution in each case. For olivine the ilmenite dihedral angles were concentrated at 50-60° and 90-100°, while the bimodes for orthopyroxene were at 60-70° and 110-120°. The dihedral angles close 60° were interpreted, following experimental work, as those originally belonging to the melt now pseudomorphed by the ilmenite; whilst the concentration of values around 90-120° were tentatively interpreted as those reflecting the texturally equilibrated value of ilmenite itself (Harte and Matthews, 1989). Experimental work at 1200°C and 5kbs has recently been completed on ilmenite-olivine and ilmenite-orthopyroxene aggregates to check the equilibrium solid dihedral angles of the ilmenite, and this has given values of approximately 100° and 120° for olivine and ilmenite respectively, thereby strongly supporting the above interpretations..

The above features indicate a number of important conclusions:

1) The rate of solid-solid textural equilibration, even at the ambient temperatures of ca. 1000 °C indicated by the Matsoku xenoliths (Harte et al. 1987), is limited.

2) The distribution of melt porosity is clearly non-uniform on the 1-10cms scale at higher melt fractions, and involves 'patches' as well as channels.

3) The low dihedral angles for melt-olivine-olivine show that extremely small amounts of melt should adopt a connected geometry through a olivine-rich matrix (see also Beere, 1975).

4) During crystallisation original melt volumes may be replaced by single minerals, demonstrating mobility of melt components during crystallisation, which would be facilitated by the melt connectivity noted under (3).

5) The migration of melt components during melt crystallisation means that even late stage interstitial melt pools do not preserve their bulk melt composition during crystallisation. These features are similar to those seen in layered cumulate bodies, and partly account for the cumulate chemical composition characteristics of 'dikes' in mantle xenoliths.

6) Features (4) and (5) above provide an explanation of the similarity of textures between some mantle rocks showing modal metasomatism and those of cumulates.

#### **Garnet cracking and metasomatism in petrographically unmodified wallrocks.**

The wallrocks to some pyroxenite 'dikes' show no evidence of modal metasomatism or other change in routine petrographic examination, but are clearly metasomatised to mineral compositions similar to those in the 'dikes'. In view of the apparently unmodified textures, it was originally thought that the metasomatism was largely diffusion controlled. However, the low dihedral angles of the melt noted above, clearly make it possible for melt in low volumes to infiltrate and be drawn into the wallrocks along mineral grain edges, without obvious textural change.

Minerals in these wallrocks have been chemically changed to largely homogeneous compositions, except for garnets, which may show core compositions typical of unmetasomatised peridotite (Harte et al., 1987). Recent extremely detailed electron microprobe analysis and back scattered electron imaging has shown the detailed pattern of the change (principally Fe-Ti enrichment) in garnet composition. Narrow, quite sharply defined zones of chemically modified (Fe-Ti rich) garnet transect regions of little modified garnet. These features imply that during melt infiltration the garnets cracked, and that melt penetrated along the fractures; then, following cracking, garnet growth occurred with Fe-Ti rich compositions controlled by the infiltrated melt, and the fractures were filled with new garnet. These 'healed cracks' are not visible in normal optical examination and are distinct from the visible fractures formed during entrainment and eruption of the xenoliths. The larger healed cracks may show fringes of smaller healed cracks, and it is evident that the cracking and regrowth of the garnet extensively controlled the change in garnet chemistry. The influence of volume diffusion is therefore far less than it originally appeared to be, though probable diffusion-controlled halos of lesser chemical change do occur around the healed cracks and the margins of the garnets.

#### **References**

- Beere, W. (1975) *Acta Metallurgica* 23, 131-138.  
 Hanson, G.N. (1980) *Ann Rev of Earth and Planetary Science* 8, 371-406.  
 Harte, B. (1983) In Hawkesworth, C.J. and Norry, M.J., (eds), *Continental basalts and mantle xenoliths*, Shiva, 46-99.  
 Harte, B., and Matthews, M.B. (1989) 28<sup>th</sup> International Geological Congress Abstracts, volume 2, 32-33.  
 Harte, B., Cox, K.G., and Gurney, J.J. (1975) *Physics and Chemistry of the Earth* 9, 477-508.  
 Harte, B., Winterburn, P.A., and Gurney, J.J. (1987) In Menzies, M.A., and Hawkesworth, C.J., (eds), *Mantle Metasomatism*, 54-220.  
 Jones, R.A. (1987) In Nixon, P.H., (ed), *Mantle Xenoliths*, 711-724.  
 Kramers, J.D., Smith, C.B., Harmon, R.S., and Boyd, F.R. (1981) *Nature* 291, 53-56.

**COMPOSITE MEGACRYSTS AND MEGACRYST AGGREGATES FROM THE WILLIAMS  
KIMBERLITES, MONTANA, USA: MULTIPLE PRODUCTS OF MANTLE MELTS.**

*Hearn, B. Carter, Jr.*

*U.S. Geological Survey, 959 National Center, Reston VA 22092 USA.*

The Williams kimberlites of Eocene age in north-central Montana contain megacrysts (size > 1 cm) of olivine (mostly serpentinized), garnet (gar), phlogopite (phl), clinopyroxene (cpx), and ilmenite (ilm) (in order of decreasing abundance), which are typical of the Cr-poor suite of megacrysts from kimberlites world-wide. Also present are composite megacrysts (megacrysts with inclusions of generally 0.2 to 2 mm size) and rare megacrystalline aggregates (coarse-grained nodules with two or more phases or monomineralic clusters of grain size > 1 cm), in which coexisting phases provide data to calculate temperature (T) and pressure (P) for the Eocene upper mantle.

Composite garnet megacrysts contain grains of one or more of the phases cpx, orthopyroxene (opx), ilm, phl, and calcite, and contain tiny rounded to elongate grains of spinel (sp), rutile (rut), or ilm. Elongate grains are probably exsolved; others could be primary inclusions or annealed exsolution grains. Composite garnet megacrysts have Mg# [= 100Mg/(Mg + Fe)] 74-83, Cr<sub>2</sub>O<sub>3</sub> 0.15-3.39% [% = wt.%], and TiO<sub>2</sub> 0.05-1.35%. These compositional ranges are similar to those for the mono-mineralic garnet megacryst population (McGee, 1986): Mg# 68 to 88 (larger than in any other kimberlite), Cr<sub>2</sub>O<sub>3</sub> 0-2.4 wt%, and TiO<sub>2</sub> 0-1.5%.

Three composite cpx megacrysts contain primary inclusions of gar or phl of > 0.2 mm size. Other cpx megacrysts contain tiny (< 0.1 mm), probably primary inclusions of subrounded, irregular, or euhedral Mg-ilmenite or FeCr sp, and also contain tiny elongate to needle-shaped opx, Mg-ilmenite, Ti-magnetite (Timag), or sp, of probable exsolution origin. Cpx megacrysts have Mg# 84-93, Cr<sub>2</sub>O<sub>3</sub> 0.03-0.57%, and Al<sub>2</sub>O<sub>3</sub> 0.47-3.30%. Cores are generally unzoned, and thin intact rims show higher MgO and lower FeO and Al<sub>2</sub>O<sub>3</sub>. CaO, Na<sub>2</sub>O, and Cr<sub>2</sub>O<sub>3</sub> can be either enriched or depleted in rims, implying that individual megacrysts were exposed to different late-stage fluids.

Six megacryst aggregates consist of gar + cpx, gar + cpx + ol, gar + cpx + ilm, gar + cpx + phl, ilm + gar, and gar + phl + rut. The minerals lack strain features. Several aggregates contain fine-grained veins of Al-rich opx and cpx, Mg-Al sp, and serpentine or chlorite. One contains veins of Al-Ti cpx, Ti-amphibole, and serpentine. Garnet in the gar-phl-rut aggregate has Mg# of 48, suggesting a crustal origin. Garnets in the other five aggregates have Mg# 73-80 and Cr<sub>2</sub>O<sub>3</sub> 0.04-0.81%. Ca-Mg-Fe contents fall in the field of Williams garnet megacrysts (fig. 1), indicating that both could have similar deep source regions. Garnets in ilmenite-bearing assemblages tend to be more Fe-rich than in ilmenite-free assemblages. The megacryst and the aggregate garnet with lower CaO contents both have high TiO<sub>2</sub> contents, similar to CaO-TiO<sub>2</sub> relations in Williams megacryst garnets.

Ilmenites in aggregates and composite megacrysts contain 6.9-13.1% MgO and 0.3-2.0% Cr<sub>2</sub>O<sub>3</sub>, ranges typical of ilmenite megacrysts and xenocrysts in kimberlites. Thus the aggregates may represent upper-mantle sources of ilmenites in kimberlite.

Most of the phlogopites (11.1-15.7% Al<sub>2</sub>O<sub>3</sub>, 0.7-4.7% TiO<sub>2</sub>, 0.1-1.1% Cr<sub>2</sub>O<sub>3</sub>, 0-0.8% BaO, and 0.2-0.7% F) in composite megacrysts and aggregates are similar in composition to primary phlogopites in peridotite xenoliths and to megacryst phlogopites. All are dissimilar to groundmass phlogopites in the host kimberlite, which are more Fe-rich, contain tetra-ferriphlogopite component, lower Al<sub>2</sub>O<sub>3</sub>, and lower Cr<sub>2</sub>O<sub>3</sub>.

Calculated T's of equilibration of composite garnet megacrysts are 940 to 1390 °C by the Ellis and Green (1979) gar-cpx method (EG79) or the Finnerty and Boyd (1986) Mg in cpx method (FB86) (assuming the presence of opx). Calculated

T's for megacryst aggregates are 1045 to 1265 °C by the same methods, and are within the T range of composite garnet megacrysts. For five of the seven analyzed clinopyroxene megacrysts, T is low, 500-660 °C (FB86); T for one is 1130 °C (FB86), and T for one with coexisting garnet is 780 °C (EG79). The lower T clinopyroxenes contain ilm, Ti-mag, or sp inclusions and lack garnet, and thus may be from the more shallow spinel facies in the upper mantle. Calculated P is 55 kb for one composite garnet megacryst by the Nickel and Green (1985) method based on Al in opx, and 45 kb for one aggregate by the Kohler and Brey (1990) method based on CaO in olivine. Projection of T's onto the geotherm estimated from Williams peridotite xenoliths (Fig. 2) implies that many of the aggregates and composite garnet megacrysts are from the 50-60 kb region of high T,P garnet peridotites.

Megacryst aggregates appear to be coarse-grained, pegmatitic products of melts in the lithospheric upper mantle, which crystallized in a range of moderate to high T and P. The chemical similarity of aggregates and megacrysts suggests that the aggregates represent the multi-phase upper-mantle source rocks which were disaggregated to produce at least part of the suite of garnet, clinopyroxene, and ilmenite megacrysts and xenocrysts. The wide range of chemistry and of calculated or inferred T and P indicate that the composite megacrysts and megacryst aggregates crystallized from several separate melts, rather than constituting a related series of products from a single melt. Vein mineralogy in aggregates suggests access of Fe-, Al-, Ti-rich fluids in the gar + sp stability field, just prior to or during ascent of the kimberlite; such fluids or melts must have been somewhat different from the host kimberlite. The geochemical complexity is consistent with the complex history of depletion and enrichment of the Montana lithospheric upper mantle in Montana.

#### References:

- Ellis, D.J., and Green, D.H. (1979) An experimental study of the effect of Ca upon garnet-clinopyroxene Fe-Mg exchange equilibria. *Contributions to Mineralogy and Petrology*, 71, 13-22.
- Finnerty, A.A., and Boyd, F.R. (1987) Thermometry for garnet peridotites: basis for the determination of thermal and compositional structure of the upper mantle. In P.H. Nixon, Ed., *Mantle Xenoliths*, p. 381-402, Wiley and Sons Ltd., London.
- Hearn, B.C., Jr., and McGee, E.S. (1984) Garnet peridotites from Williams kimberlites, north-central Montana, USA. In J. Kornprobst, Ed., *Kimberlites II: The Mantle and Crust-Mantle Relationships*, p. 57-70, Elsevier, Amsterdam.
- Kohler, T.P., and Brey, G.P. (1990) Calcium exchange between olivine and clinopyroxene calibrated as a geothermobarometer for natural peridotites from 2 to 60 kb with applications. *Geochimica et Cosmochimica Acta*, 54, 2375-2388.
- McGee, E.S. (1986) Garnet megacrysts of the Williams diatremes, north-central Montana. *American Mineralogist*, 71, 674-681.
- Nickel, K.G., and Green, D.H. (1985) Empirical geothermobarometry for garnet peridotites and implications for the nature of the lithosphere, kimberlites and diamonds. *Earth and Planetary Science Letters*, 73, 158-170.

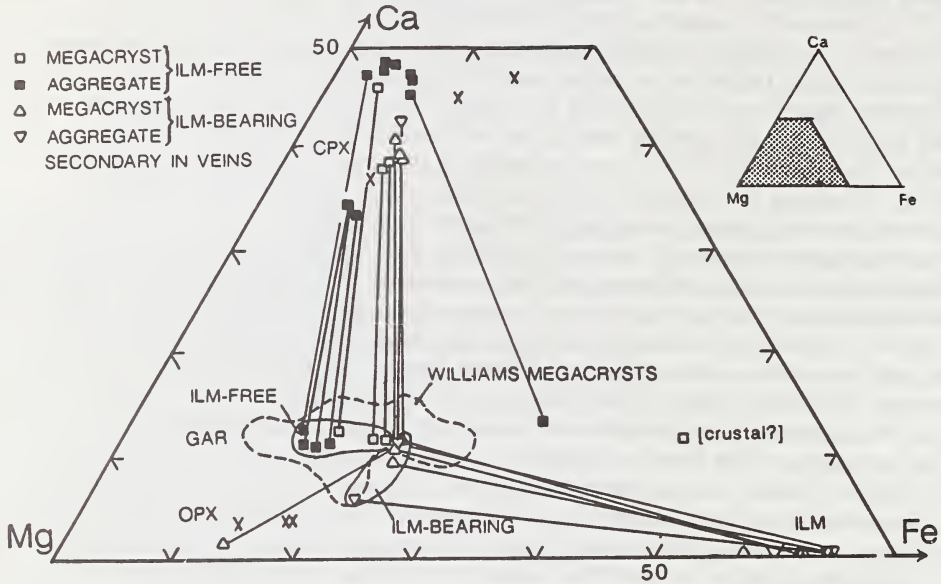


Fig. 1 Ca-Mg-Fe composition (mol %) of gar, cpx, and ilm in composite megacrysts and megacryst aggregates; lines join coexisting phases; dashed-line = field of Williams garnet megacrysts from McGee (1986).

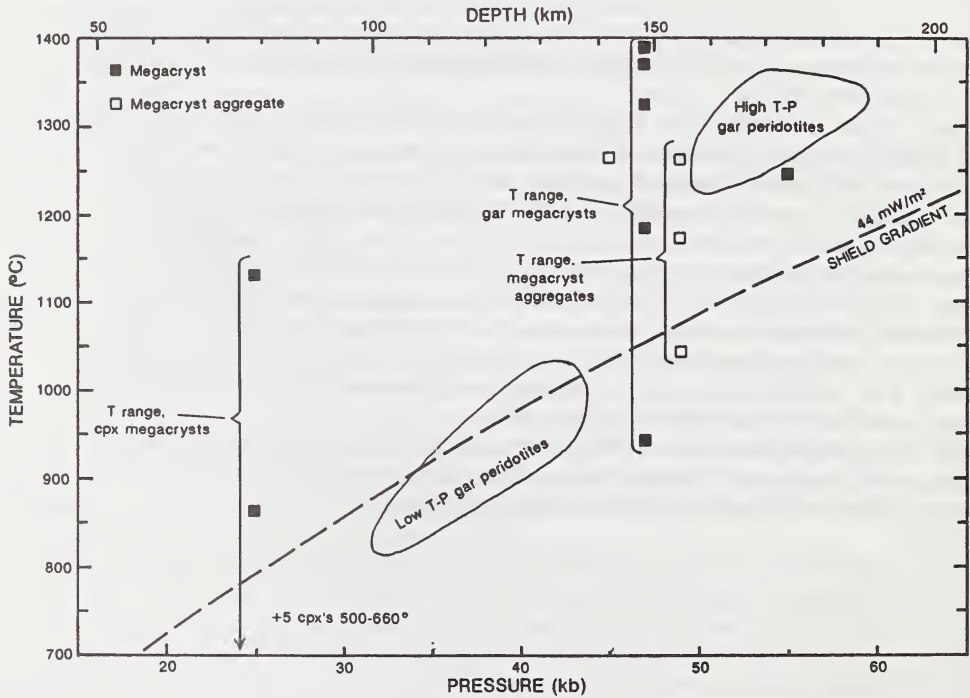


Fig. 2 Calculated T and ranges of T (by EG79 and FB86 methods) for megacryst aggregates and garnet megacrysts (arbitrarily plotted near 48 kb, except two with calculated P), and cpx megacrysts (arbitrarily plotted near 25 kb); fields of Williams garnet peridotites from Hearn and McGee (1984).

## GEOTECTONIC CONTROLS OF DIAMONDS AND KIMBERLITES AND THEIR APPLICATION TO DIAMOND EXPLORATION.

*Helmstaedt, H.H.*

*Department of Geological Sciences, Queen's University, Kingston, Ontario, Canada K7L 3N6.*

Although it is common knowledge that diamond-bearing kimberlites occur primarily on Precambrian cratons, particularly on those underlain by rocks of Archean age, hypotheses explaining this phenomenon have not provided a rigorous theoretical base for area selection in diamond exploration. One of the major problems was the general assumption that exploration for kimberlite diamonds consists of searching for diamondiferous kimberlites and that efforts to establish exploration models need focus only on understanding the larger-scale geotectonic and regional structural controls of kimberlite distribution. Only after it was recognized that most diamonds in kimberlites may represent xenocrysts, has it become clear that understanding the geotectonic environment of diamond formation is an entirely separate, but equally important problem. Realistic diamond exploration models must thus include the following three components:

1. Prediction of regions under which diamonds may have formed.
2. Selection of those areas where diamonds may have survived to be picked up by kimberlites or lamproites.
3. Establishment of regional tectonic and local structural controls of kimberlites, lamproites, or related rocks in the appropriate areas.

The correlation between diamondiferous kimberlites and Archean cratons as well as Archean isotopic dates from southern African diamonds (Kramers, 1979; Richardson et al., 1984) clearly indicate that diamonds formed since early lithosphere development and were able to survive in mantle roots beneath Precambrian shields to be picked up by kimberlites and lamproites ranging in age from the Proterozoic to Late Mesozoic. Judging from mineral inclusions in diamonds and the mineral assemblages of diamond-bearing xenoliths (eclogites and garnet harzburgites), these mantle roots consisted mainly of highly depleted peridotites with lenses of eclogitized mafic rocks. This composition as well as the fact that, in a generally hotter Archean lithosphere, the relatively high P - low T gradient required for diamond formation could only be achieved by tectonic burial of relatively cool material, suggest that the mantle roots were formed by subduction of oceanic lithosphere (e.g., Schulze, 1986; Helmstaedt and Schulze, 1989). Survival of the diamonds is possible only if the refractive, relatively cool and low-density roots stay attached to the craton during subsequent plate motions and remain insulated against later re-heating and excessive tectonic reworking.

Of importance for diamond exploration is the fact that the presence of relatively low-density and low-temperature mantle roots can be detected by their high shear-wave velocities relative to adjacent hotter asthenosphere (e.g., Grand, 1987). Available data indicate that such roots are more common under Archean cratons (as compared to Proterozoic shields and Phanerozoic orogenic belts), though they are not equally developed or present under all Archean crust (e.g., Hoffman, 1990). The key to understanding this secular control on the formation of mantle roots is the Archean tectonic environment, in which a buoyant, shallow mode of subduction was predominant allowing continental nuclei to become tectonically underplated by depleted oceanic lithosphere. Subduction zones became generally steeper in post-Archean times, when the shallow subduction mode was restricted to regions of exceptionally fast plate convergence and/or subduction of young ocean floor (Helmstaedt and Schulze, 1989). Although relatively ancient mantle roots appear to have been a requirement for diamond formation, the distribution of the generally much younger kimberlites may have no correlation with such roots. Large-scale area selection should thus concentrate on regions in which mantle roots have survived at least until kimberlite emplacement. On cratons with geophysically recognizable mantle roots, all kimberlites postdating the establishment of the mantle root should have a relatively high diamond potential. On the other hand, kimberlites on cratons without geophysical evidence of mantle roots would have diamond potential only, if they were emplaced prior to the destruction of an earlier mantle root. In such cases, a careful assessment of the orogenic and magmatic processes that may have destroyed or eroded the roots is necessary.

In North America, mantle roots underlie the Archean southern Slave Province and much of the Superior Province (Hoffman, 1990), suggesting that post-Archean kimberlites in these regions should have diamond potential. On the other hand, if an ancient mantle root had survived the Proterozoic orogenic activity along the margins of the Archean North Atlantic craton (Nain and Greenland), it was destroyed by the Iceland plume that initiated the opening of the Atlantic (Hoffman, 1990). Mesozoic kimberlites on this craton thus have a low diamond potential. Although the Archean Wyoming province has no mantle root at present, the diamond potential of the State Line kimberlites is probably the result of kimberlite emplacement in the Devonian (Naeser and McCallum, 1977), predating the erosion of remnants of an old mantle root by Tertiary shallow subduction (Helmstaedt and Doig, 1975; Bird, 1988) related to the Laramide orogeny.

In southern Africa, on-craton kimberlites of many different ages are diamondiferous, because parts of an ancient mantle root survived under the Kaapvaal craton at least until the end of the Cretaceous. Off-craton kimberlites have a low diamond potential, because mantle roots either never existed in their intrusive paths, or such root were eroded prior to kimberlite emplacement. During area selection on diamondiferous cratons, post-mantle root and pre-kimberlite tectonic and magmatic processes must be considered when evaluating regional or local structural controls that have provided pathways for the kimberlites. Thus mantle-root-friendly features, such as mafic dyke swarms (e.g., Karroo)

must be distinguished from mantle-root-destructive structures, such as larger-scale crustal fractures, hotspots, and plumes, that may control the location of kimberlites, but have a negative effect on the diamond potential of the root. Examples of the latter are crustal-scale fractures in the Brazilian shield, that have controlled the ascent of magmas during the Late Proterozoic Brazilian event and have later served as pathways for Mesozoic kimberlites. An early mantle root under the Brazilian shield, indicated by the occurrence of detrital diamonds in Proterozoic sedimentary rocks, must have been destroyed during Proterozoic orogenic events, for the Mesozoic kimberlites following the Brazilian structures do not contain significant amounts of diamonds.

As shown by the diamond potential of the Kimberley region of Western Australia, post-Archean mantle roots may also be prospective exploration targets, and kimberlites are not the only magmas to tap the roots. The Kimberley region provides an excellent opportunity to test the effects of tectonic and magmatic events on the gradual erosion or destruction of mantle roots, for similar lamproites have sampled the mantle root in the Late Proterozoic (1180 Ma) and the Mid-Tertiary (20-22 Ma) with vastly different economic results (e.g., Jaques, 1989). Here, as in regions of multiple kimberlite events, studies of xenoliths, xenocrysts, diamonds, and diamond inclusions should be more closely integrated with structural and tectonic studies to monitor the status and diamond potential of mantle roots through time, and to establish improved theoretical models for future exploration.

#### References:

- Bird, P. (1988) Formation of the Rocky Mountains, western United States: a continuum computer model. *Science*, 239, 1501-1507.
- Grand, S.P. (1987) Tomographic inversion for shear velocity beneath the North American plate. *Journal of Geophysical Research*, 92, 14065-14090.
- Helmstaedt, H. and Doig, R. (1975) Eclogite nodules from kimberlite pipes of the Colorado Plateau - samples of subducted Franciscan-type oceanic lithosphere. *Physics and Chemistry of the Earth*, 9, 95-111.
- Helmstaedt, H., and Schulze, D.J. (1989) Southern African kimberlites and their mantle sample: implications for Archean tectonics and lithosphere evolution. *Geological Society of Australia Special Publication 14*, 358-368.
- Hoffman, P.F. (1990) Geological constraints on the origin of the mantle root beneath the Canadian shield. *Philosophical Transaction Royal Society London*, A331, 523-532.
- Jaques, A.L. (1989) Lamproite diamonds and their inclusions: New insights from Western Australian deposits. 28th International Geological Congress, Workshop on Diamonds, Extended Abstracts, 36-39.
- Kramers, J. D. (1979) Lead, uranium, strontium, potassium, and rubidium in inclusion-bearing diamonds and mantle-derived xenoliths from Southern Africa. *Earth and Planetary Science Letters*, 42, 58-70.

Naeser, C.W., and McCallum, M.E. (1977) Fission-track dating of kimberlitic zircons. Second International Kimberlite Conference, Santa Fe, Extended Abstracts.

Richardson, S.H., Gurney, J.J., Erlank, A.J., and Harris, J.W. (1984) Origin of diamond in old enriched mantle. *Nature*, 310, 198-202.

Schulze, D.J. (1986) Calcium anomalies in the mantle and a subducted metaserpentinite origin for diamonds. *Nature*, 319, 483-485.

## THE INDIVIDUALITY OF ON- AND OFF-CRATON MEGACRYST SUITES IN SOUTHERN AFRICA.

*Hops, J.J.; Moore, \*R.O.; and Gurney, J.J.*

*Dept. Geochemistry, University of Cape Town, Rondebosch 7700, South Africa. \*Present address: P.O. Box 1372, Wangara, W.A. 6065, Australia.*

Megacrysts (i.e. discrete crystals > 1 cm in diameter) occur at localities both on and off the Kaapvaal craton in southern Africa.

Complications arise from classifications involving field descriptions (size, mineral assemblages) as opposed to those which are based on analytical results (mineral compositions). On the basis of mineral compositions, it is apparent that some megacrysts represent coarse disaggregated minerals from peridotite and eclogite xenoliths; these will not be discussed. Several other suites of compositionally distinct megacrysts can be distinguished on the basis of related mineral compositions and the occasional presence of co-existing phases. These include:

Cr-poor suite (olivine ± orthopyroxene ± clinopyroxene ± garnet ± ilmenite ± phlogopite ± zircon)

Fe-rich suite (olivine ± phlogopite ± zircon ± ilmenite ± clinopyroxene)

Granny Smith suite (clinopyroxene ± phlogopite ± ilmenite)

Group II suite (garnet ± olivine ± clinopyroxene ± rutile)

### The Cr-poor suite

The Cr-poor suite (Nixon and Boyd, 1973; Gurney et al., 1979) is present in both on- and off-craton Group I kimberlites. Major and trace element compositional trends are consistent with fractional crystallization. However, comparison of the megacryst suites from individual Group I localities (cf. Schulze, 1987) indicates differences in mineral compositions and, in some instances, differences in mineral abundances (e.g. abundance of olivine) and mineral assemblages (e.g. absence of ilmenite). Nd and Sr isotopic compositions of clinopyroxenes from the Cr-poor suite are depleted relative to bulk earth and are similar to some ocean island basalts. Differences in isotopic compositions between clinopyroxenes from the same locality are more significant than differences between localities themselves.

The observed differences in mineral compositions, mineral assemblages and mineral abundances attest to the individuality of the Cr-poor suite at each locality and suggest that each must represent a localized feature rather than a continuous horizon in the upper mantle. Thermobarometric evidence suggests that the megacryst suite represents a 'thermal perturbation' of the steady state geotherm consistent with a localized feature. In contrast, certain features particularly the limited variation in mineral compositions and the similarity in isotopic compositions, imply similar Mg-rich asthenospheric source material for all Cr-poor megacryst suites. Differences between localities can be attributed to variable degrees of partial melting, to different

crystallization environments, to differences in the proportions of crystallizing phases and to different degrees of fractional crystallization. The Cr-poor megacrysts are xenocrysts in their host kimberlites.

#### The Fe-rich suite

The Fe-rich suite has been identified at the on-craton Monastery kimberlite (Moore et al., in prep). A tenuous link has been established between the Cr-poor suite and the more evolved Fe-rich suite at Monastery. However, the ilmenite compositions require that assimilation and/or magma recharge has occurred, subsequent to garnet and clinopyroxene crystallization, if the two suites are related. Such processes may have been active late in the fractionation sequence when only relatively small volumes of magma existed, possibly in vein-like isolated intrusions.

#### The Granny Smith suite

The Granny Smith suite has been identified at several on-craton localities near Kimberley and Jagersfontein (Boyd et al., 1984). The clinopyroxenes are found both as discrete and polycrystalline nodules and significant compositional differences are found between localities. The limited range in calcic compositions of the clinopyroxenes corresponds to a small range of temperatures (at approximately 1000°C) if the diopside solvus is applicable, and equilibration to lithospheric conditions is suggested. Nd isotopic ratios of Granny Smith clinopyroxenes are equivalent to those of the Cr-poor clinopyroxenes, but Sr isotopic ratios are higher. These characteristics suggest that the Granny Smith suite might also represent the crystallization products of asthenospheric melts, but in association with assimilation of lithospheric wallrocks, possibly under sub-solidus conditions.

#### The Group II suite

Megacrysts were previously thought to be absent from Group II kimberlites, but recently, Daniels and Gurney (1989) identified Cr-poor garnet megacryst compositions in a study of the heavy mineral concentrate from the Dokolwayo kimberlite in Swaziland. Moore et al. (1990) demonstrated that the major and trace element compositions of the Dokolwayo garnets differ from those of the Cr-poor suite. Directed investigations have since recognised the presence of garnet megacrysts in a large number of Group II kimberlites in South Africa (Moore and Gurney, this volume). The diversity of mineral assemblages in this suite is, however, limited in comparison to the Cr-poor suite.

The Group II kimberlites in the Barkly West dyke swarm host Cr-rich clinopyroxene and garnet megacrysts.

#### Overall

Several megacryst suites might be present at a particular locality. The individuality of the respective suites between the different localities establishes that each must represent a localized feature rather than a continuous horizon in the lithosphere.

#### References

- BOYD, F.R., DAWSON, J.B., and SMITH, J.V. 1984. Granny Smith diopside megacrysts from the kimberlites of the Kimberley area and Jagersfontein, South Africa. *Geochimica et Cosmochimica Acta*, 48, 381-384.

- DANIELS, L.R.M., and GURNEY, J.J. 1989. The chemistry of the garnets, chromites and diamond inclusions from the Dokolwayo kimberlite, Kingdom of Swaziland. 4th International Kimberlite Conference. Geological Society of Australia Special Publication 14, 1012-1021.
- GURNEY, J.J., JAKOB, W.R.O., and DAWSON, J.B. 1979. Megacrysts from the Monastery kimberlite pipe, South Africa. In Boyd F.R. and Meyer H.O.A., Eds., *The Mantle Sample*, p.227-243, A.G.U., Washington.
- MOORE, R.O., DANIELS, L.R.M., and GURNEY, J.J. 1990. Garnet megacrysts in the Group II Dokolwayo kimberlite, Swaziland. *Extended Abstract, Geocongress 90*, 427-430.
- MOORE, R.O., GRIFFIN, W.L., GURNEY, J.J., RYAN, C.G., COUSENS, D.R., SIE, S.H., and SUTER, G.F. (in prep.). Trace element geochemistry of ilmenite megacrysts from the Monastery kimberlite, South Africa.
- NIXON, P.H., and BOYD, F.R., 1973. The discrete nodule association in kimberlites from northern Lesotho. In Nixon, P.H., Ed., *Lesotho Kimberlites*, p.67-76, Lesotho Nat. Dev. Corp., Maseru.
- SCHULZE D.J. 1987. Megacrysts from alkalic volcanic rocks. In Nixon, P.H., Ed., *Mantle Xenoliths*, p.433-452. J. Wiley and Sons.

PETROLOGY, MINERALOGY, AND GEOCHEMISTRY OF THE METTERS BORE NO. 1  
LAMPROITE PIPE, WEST KIMBERLEY PROVINCE, WESTERN AUSTRALIA.

*Hwang, P.; Rock, N.M.S. & Taylor, W.R.*

*Key Centre for Strategic Mineral Deposits, Geology Department, University of Western Australia,  
Nedlands 6009, W. Australia.*

The Metters Bore No. 1 lamproite is a small (2.5 ha) pipe-shaped intrusion, belonging to the Calwinyardah field within the Miocene ( $\approx 20$  Ma) West Kimberley lamproite province (Jaques et al. 1986). It intrudes Permian sediments of the Fitzroy Trough. It is concealed beneath 2 m of red-brown sandy soil and 1.5 m of pisolitic laterite, but is detectable by its strong magnetic signature.

Both magmatic lamproite and fragmental (tuffaceous) material are present. The tuffaceous units occur in the southwest portion of the pipe, and are comprised of at least four types of juvenile lamproite lapilli, supported by a matrix of ash with smaller cognate or accidental particles and occasional veined calcite. The lapilli are typically non-vesiculated, subangular fragments of diopside-olivine-leucite lamproite (up to 3mm across), although fine-grained vitrophyric leucite lamproite, medium-grained diopside-leucite-phlogopite lamproite, and lattice-textured leucite-phlogopite lamproite also occur.

The magmatic rock is dominantly a porphyritic olivine-diopside-leucite-(phlogopite) lamproite (olivine  $\gg$  phlogopite), with an altered glassy groundmass. Olivine phenocrysts and microphenocrysts are almost wholly altered to clays, although one fresh grain with a magnesium number [ $100\text{Mg}/(\text{Mg}+\text{Fe}^{2+})$ ] of 91 was found as an inclusion in a wadeite crystal. Inclusions of chromite up to 20  $\mu\text{m}$  across are common.

*Diopsides* (five compositionally distinct and one indistinct form) describe fields within the pyroxene quadrilateral representing: (1) phenocrysts; (2) groundmass; (3) Ca-rich phenocrysts; (4) heavy mineral concentrate (HMC) fraction; (5) Cr-rich xenocrystic diopsides; (6) broad field of inclusions within amoeboid leucite phenocrysts. They are generally Ti- and Cr-rich, Al-poor diopsides which follow evolutionary trends of Cr-depletion and Fe-enrichment.

*Leucite* phenocrysts are completely altered to analcite and montmorillonite and occur in three different morphologies: (1) singular euhedral phenocrysts; (2) amoeboid-shaped, (3) poorly crystallised glomerocrysts containing abundant pleonaste phenocrysts; poorly crystallised glomerocrysts containing microlites of diopside but no pleonaste.

Three generations of *phlogopite* are present: (1) rare phenocrysts, (2) microphenocrysts and euhedral groundmass flakes, and (3) inclusions. The micas typically have high F contents which range up to 4.13 wt%, BaO contents which average 0.7 wt%, and evolutionary trends of  $\text{TiO}_2$ - and FeO-enrichment and  $\text{Al}_2\text{O}_3$ -depletion.

Compositions of *spinel*s fall into three distinct populations which represent: (1) cognate chrome spinel; (2) heavy mineral concentrate (HMC) spinel; (3) pleonaste. The cognate spinels show evolutionary trends of initial Cr and Ti-enrichment and  $\text{Fe}^{3+}$ -depletion, followed by co-evolving trends of (a) constant Cr and  $\text{Fe}^{3+}$  and (b) Cr depletion and  $\text{Fe}^{3+}$ -enrichment. HMC grains

fractionate towards increasing Ti, Cr, and Fe<sup>3+</sup> compositions with decreasing Al, and pleonastes show the same trends but without Cr-enrichment.

*Amphiboles* are present as K- and Ti-rich richterites and show trends of increasing Ti, Na, and Fe with decreasing Mg.

Accessory phases include *priderite*, *perovskite*, *ilmenite*, *sphene*, *apatite*, *wadeite*, *zircon*, and *barite*. The diopsides, *phlogopites*, *tetraferriphlogopites*, *tetraferribiotites*, and Ti-rich K-richterites have consistent tetrahedral site deficiencies which can be satisfied by tetrahedral Ti<sup>4+</sup>. This is probably a result of the high Ti/Al ratio in lamproite magma.

The groundmass contains abundant needles of *priderite* and *apatite*; less abundant *perovskite*, interstitial potassian titanian richterite, Mn- and Mg- rich *ilmenite*; and rare chrome-spinel, *pleonaste*, and *wadeite*. Heavy mineral concentrates yielded various minerals of mantle origin including Cr-rich diopside (up to 2.5 wt% Cr<sub>2</sub>O<sub>3</sub>), magnesian chrome spinel (up to 16 wt% MgO), and rare *pyrope garnet*.

Geochemically, the Metters Bore No.1 lamproite is an ultrapotassic, perpotassic, and peralkaline rock with high TiO<sub>2</sub> and a magnesium number [100Mg/(Mg+Fe<sup>2+</sup>)] of 62.5. K, Rb, and Ba show considerable mobility due to secondary alteration processes. Incompatible elements are strongly enriched (Fig.1a), at up to 1000 times primitive mantle abundances (370ppm Rb, 1400ppm Sr, 4000ppm Ba, 1100ppm Zr), and Rb/Sr ratios are typically higher than other lamproite suites. Abundances of the compatible elements Ni and Cr are moderate, and average 342 ppm Ni and 367 ppm Cr. These, together with the moderate Mg-numbers, imply evolution of the Metters Bore magma from a more primitive parent. Mantle normalised Sc/V ratios are <1, which is typical for leucite lamproites but different from olivine lamproites in the West Kimberley province. The rare earth elements (REE) are strongly enriched, with 700 times chondrite abundances for light REE and 8 times chondrite for heavy REE (Fig.1b).

Diamond prospectivity diagrams, using chrome-spinel and *pyrope garnet* compositions, imply a low potential for the Metters Bore No.1 lamproite to host economic quantities of diamond.

#### Reference

Jaques, A.L., Smith, C.B. & Lewis, J. (1986) The kimberlites and lamproites of Western Australia. Bulletin of the Geological Survey of Western Australia, 132.

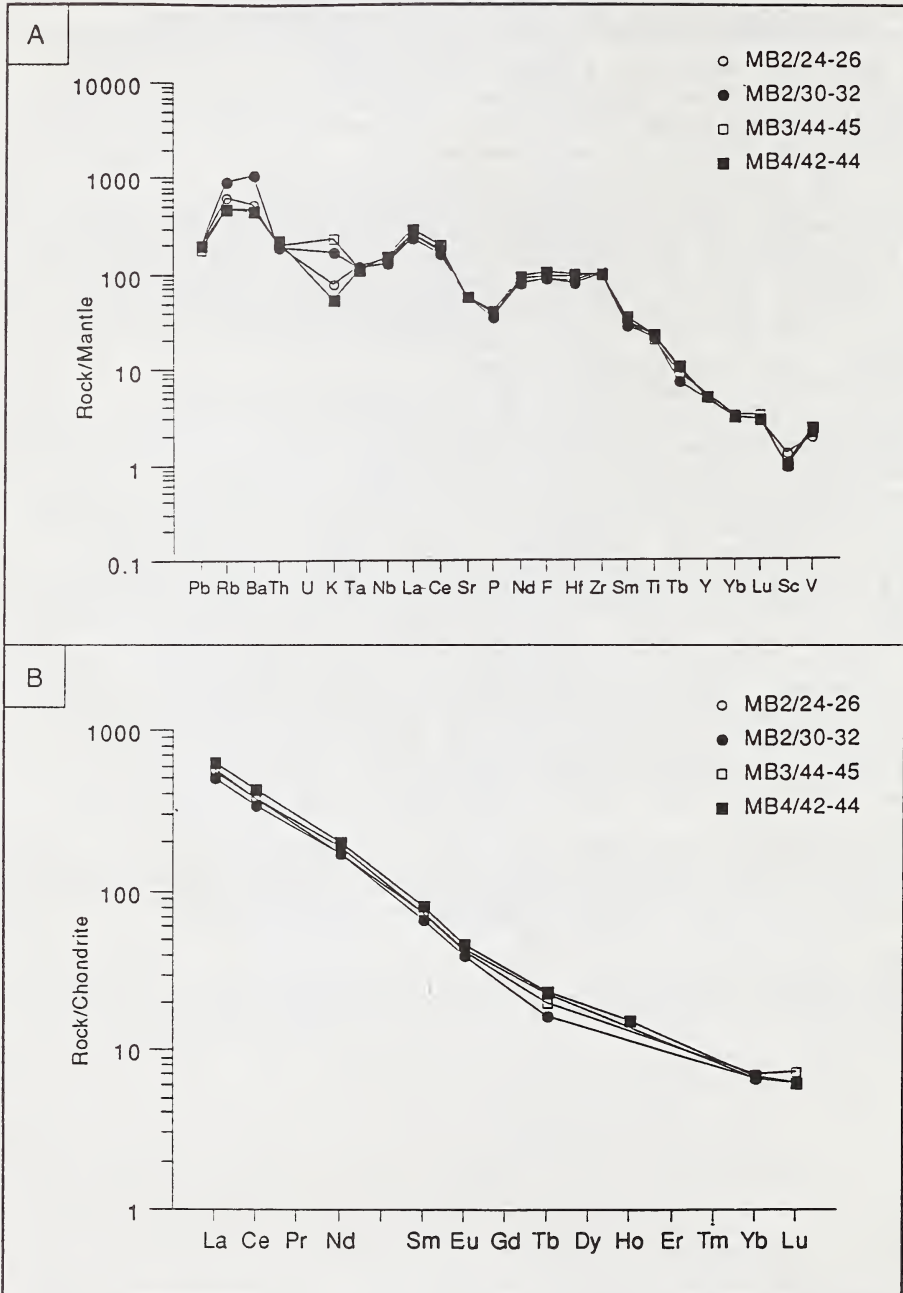


Fig.1. 'Spidergrams' of representative whole-rock samples of the Meters Bore #1 lamproite. (a) Normalized to primitive mantle, (b) normalized to average chondrites.

MANTLE XENOLITHS IN POTASSIC MAGMAS FROM MONTANA: Sr, Nd AND Os  
ISOTOPIC CONSTRAINTS ON THE EVOLUTION OF THE WYOMING  
CRATON LITHOSPHERE.

Irving, <sup>(1)</sup>A.J. and Carlson, <sup>(2)</sup>R.W.

(1) Dept. Geol. Sciences, Univ. of Washington, Seattle, WA 98195 USA; (2) Dept. Terrestrial Magnetism,  
Carnegie Inst. Washington, Washington, DC 20015 USA.

A variety of ultramafic xenoliths occur at several localities within the late Cretaceous to Oligocene volcanics and dikes of the alkalic igneous province of central Montana, U.S.A. In concert with geochemical and isotopic studies of the magmatic rocks (Irving and O'Brien, this volume), similar detailed analysis of the ultramafic xenoliths has been undertaken in an attempt to understand the evolution of the Archean lithosphere and to evaluate its effects on the magmas that percolated through it. Previous work on the magmatic rocks in the Highwood Mountains subprovince (O'Brien et al., 1991) has suggested an important role for Archean lithospheric mantle in providing a small volume component of extreme composition that controlled most of the isotopic and certain trace element features of the erupted magmas.

Two quite distinct suites of ultramafic xenoliths have been studied from Eocene primitive olivine minette dikes from the Highwood Mountains (located near Great Falls) and Eagle Buttes (located 40 km to the northeast). Lithologies at the first locality include peridotites (Cr-spinel harzburgite and spinel lherzolite, with or without mica and amphibole), websterite (one as a band or dike in harzburgite), several types of mica dunite (containing accessory Cr-spinel and clinopyroxene), and glimmerite (as veins cutting harzburgite). The Eagle Buttes suite contains anhydrous, Cr-diopside spinel lherzolites and harzburgites that resemble those found typically in alkalic basalts worldwide. Application of the most reliable thermobarometers for spinel peridotites (Wells, 1977 2-pyroxene solvus; Sack and Ghiorso, 1991 olivine-spinel; Kohler and Brey, 1990 Ca in olivine) is hampered by the very high Ca content of clinopyroxenes and the very low Ca content of olivine (50-160 ppm, using microprobe counting times of 500 sec). Nevertheless, it is evident that the majority of peridotites and dunites from both localities equilibrated at unusually low temperatures (600-700°C). Calculated pressures are 14-20 kbar for the Highwood samples and 12 kbar for those from Eagle Buttes. Two of the mica dunites equilibrated at much higher temperatures (980°C) and apparently at higher pressures than the other Highwood samples. Garnet peridotite xenoliths from the kimberlitic Williams diatreme located about 100 km east of these localities (Hearn and McGee, 1984) must be samples of even deeper lithosphere.

The unique glimmerite vein consists mostly of Ti-rich phlogopitic mica with subordinate orthopyroxene and minor clinopyroxene, plagioclase (An<sub>72</sub>), celsian, zircon and rutile. The pyroxenes give an equilibration temperature of 1020°C, and the presence of calcic plagioclase in this mineral assemblage is not inconsistent with the pressure estimates obtained from other Highwood ultramafic and granulite xenoliths. The presence of zircon and the bulk rock U abundance of 0.8 ppm offer the possibility of precisely dating this vein, particularly if this large xenolith has experienced only transient heating during entrainment and ascent. The vein has a selvage of mica orthopyroxenite adjacent to the surrounding harzburgite.

A striking and unexpected feature of all the Highwood xenoliths is the presence of large negative Eu anomalies (Eu/Eu\* = 0.2-0.4), accompanied by relatively high abundances of trivalent REE (Fig. 1). In contrast, one spinel harzburgite from Eagle Buttes has lower REE abundances with no significant Eu anomaly, yet is relatively light-REE enriched (La<sub>N</sub>/Yb<sub>N</sub> = 16). The peridotites have bulk Mg/(Mg+ΣFe) of 0.87-0.89 with bulk CaO contents of 1.1-2.8 wt.%, whereas the mica dunites are both more and less magnesian (Mg/(Mg+ΣFe) = 0.83-0.91), and have higher Sm/Nd, K, Rb and Ba. The glimmerite is relatively enriched in Ba (1880 ppm), Zr (350 ppm), Th (3 ppm), Cr (930 ppm) and Ni (1280 ppm).

Bulk rock isotopic ratios for several of the Highwood xenoliths range to extreme values ( $^{87}\text{Sr}/^{86}\text{Sr} = 0.715$  to  $0.769$ ,  $\epsilon_{\text{Nd}} = -16$  to  $-40$ ,  $^{187}\text{Os}/^{186}\text{Os} = 0.90$  to  $1.04$ ). Nd model ages relative to depleted mantle range from 2.6 Ga to greater than 4 Ga, and Os model ages ( $T_{\text{RD}}$ , Walker et al., 1989) range from 0.4 to 3.0 Ga (with 3 out of 4 greater than 2.7 Ga). The Os model ages are calculated assuming  $\text{Re}/\text{Os} = 0$  and give the absolute minimum age of Re loss. The samples analyzed so far show an inverse correlation between  $^{187}\text{Os}/^{186}\text{Os}$  and Fo content of olivine, suggesting that Re loss accompanied partial melt removal during formation of the lithosphere in the early Archean (as noted previously by Walker et al. (1989) for xenoliths from southern Africa). In contrast, a 2.5 Ga Sr model age for a mica dunite may imply late Archean/Proterozoic enrichment in Rb by metasomatic addition of mica. The glimmerite vein ( $\epsilon_{\text{Nd}} = -33$ ) is interpreted as an ancient metasome that is probably one example of the material contributing to the wide range of isotopic compositions measured in the younger magmatic rocks.

Ultramafic rocks displaying some similar geochemical features to the Montana xenoliths, including negative Eu anomalies, occur as tectonic inclusions within 3.7 Ga gneisses from Labrador (Collerson et al., 1991). They differ, however, in their isotopic characteristics, and appear to be ancient partial melting residues, without the presumably subsequent but still ancient enrichment signature.

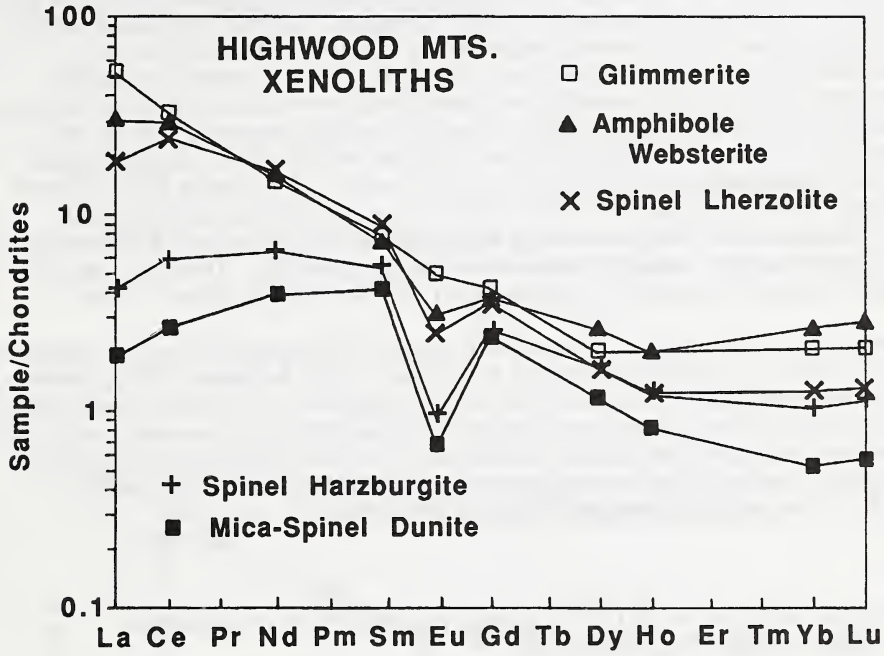
Prior to the metasomatic addition of mica, the olivine-rich rocks from Montana may have been cumulates complementary to ancient feldspathic crust, or possibly residues from partial melting of less ancient asthenospheric mantle. The negative Eu anomalies may be a consequence feldspar removal or perhaps the partitioning behavior of orthopyroxene under highly reducing conditions (McKay et al., 1990). In either case the compositional differences among mantle lithospheric samples throughout central Montana suggest that there is considerable regional variability in equilibration temperature, trace element composition and age (and possibly intrinsic  $f\text{O}_2$ ) as a function of both depth and geographic location. Given this, it is not surprising that there is also wide variation in the isotopic and trace element composition of erupted magmas within this province.

## References

- Collerson, K. D., Campbell, L. M., Weaver, B. L. and Palacz, Z. A. (1991) Evidence for extreme mantle fractionation in early Archean ultramafic rocks from northern Labrador. *Nature*, 349, 209-214.
- Hearn, B. C., Jr. and McGee, E. S. (1984) Garnet peridotites from Williams kimberlites, north-central Montana, U.S.A. In J. Kornprobst, Ed., *Kimberlites II: The mantle and crust relationships*, p. 57-70. Elsevier, Amsterdam.
- Irving, A. J. and O'Brien, H. E. (1991) Isotopic and trace element remote sensing of Montana continental lithosphere from erupted magmas. This volume.
- Kohler, T. P. and Brey, G. P. (1990) Calcium exchange between olivine and clinopyroxene calibrated as a geothermobarometer for natural peridotites from 2 to 60 kb with applications. *Geochimica et Cosmochimica Acta*, 54, 2375-2388.
- McKay, G., Wagstaff, J., and Le, L. (1990) REE distribution coefficients for pigeonite: Constraints on the origin of the mare basalt europium anomaly. In *Lunar and Planetary Science XXI*, 773-774. Lunar and Planetary Institute, Houston.
- O'Brien, H. E., Irving, A. J. and McCallum, I. S. (1991) Eocene potassic magmatism in the Highwood Mountains, Montana: Petrology, geochemistry and tectonic implications. *Journal of Geophysical Research*, in press.
- Sack, R. O. and Ghiorso, M. S. (1991) Chromian spinels as petrogenetic indicators: Thermodynamics and petrological applications. *American Mineralogist*, in press.

Walker, R. J., Carlson, R. W., Shirey, S. B., and Boyd, F. R. (1989) Os, Sr, Nd, and Pb isotope systematics of southern African peridotite xenoliths: Implications for the chemical evolution of subcontinental mantle. *Geochimica et Cosmochimica Acta*, 53, 1583-1595.

Wells, P. R. A. (1977) Pyroxene thermometry in simple and complex systems. *Contributions to Mineralogy and Petrology*, 62, 129-139.



ISOTOPIC EVIDENCE FOR VARIABLY ENRICHED MORB LITHOSPHERIC MANTLE  
IN XENOLITHS FROM NORTH QUEENSLAND, AUSTRALIA.

Irving, <sup>(1)</sup>A.J. and Menzies, <sup>(2)</sup>M.A.

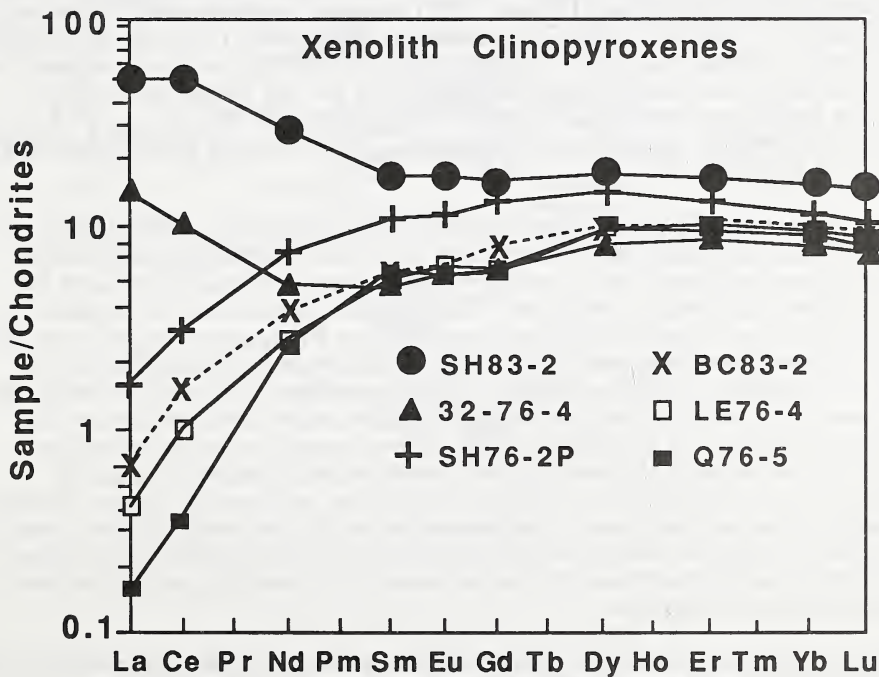
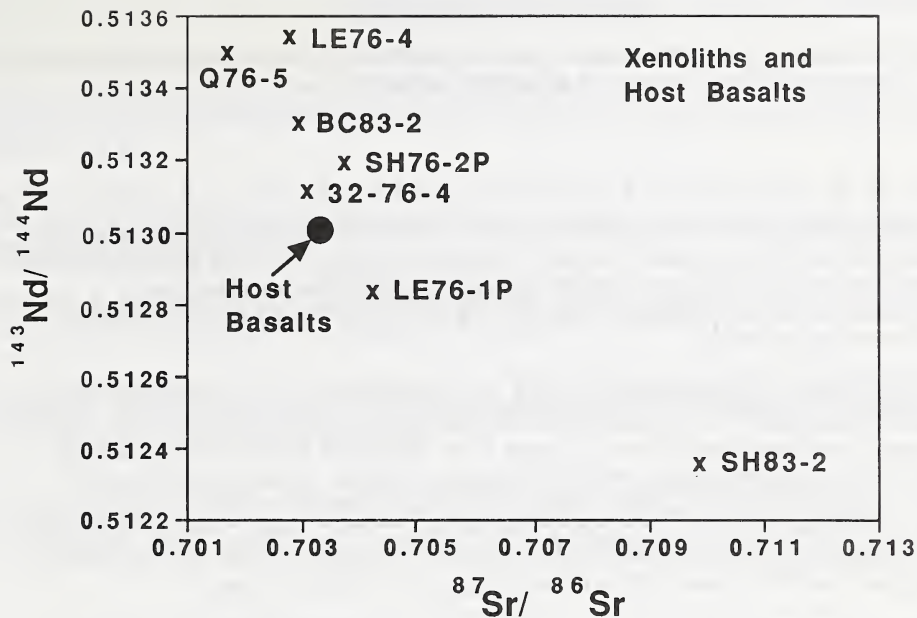
(1) Dept. Geol. Sciences, Univ. of Washington, Seattle, WA 98195 USA; (2) Dept. Geology, Royal Holloway and Bedford New College, Egham, Surrey TW20 0EX ENGLAND.

Accretion of lower Phanerozoic lithosphere in eastern Australia is believed to have involved various intraplate and subduction-related processes. Ultramafic xenoliths from five Recent alkalic basalt eruptive centers in the Atherton, McBride and Chudleigh Provinces of north Queensland provide evidence for variable enrichment of very primitive MORB lithosphere. The samples studied are predominantly Cr-diopside spinel lherzolites and several pyroxenites and amphibole pyroxenites that occur as dikes in large composite samples (Irving, 1980). Nd and Sr isotopic compositions for our samples (not age corrected), along with those reported by O'Reilly et al. (1988), plot mostly within the field of modern MORB (Fig. 1), however, one sample from Sapphire Hill is markedly more enriched ( $^{87}\text{Sr}/^{86}\text{Sr}$  0.70991,  $\epsilon_{\text{Nd}}$  -8). REE abundances for constituent clinopyroxenes range from light REE-depleted to quite light REE-enriched (Fig. 2), and correlate well with the range in isotopic composition. Two host basalts have isotopic compositions typical of continental OIB-like, asthenospheric melts.

The xenolith results are consistent with models of lithospheric mantle based on other xenolith suites (e.g., McDonough and McCulloch, 1987; Menzies, 1990), however, the range in the north Queensland examples is very large over a small area, and implies that the underlying mantle lithosphere is unusually heterogeneous on a small scale. We interpret the results as implying ancient subduction of oceanic lithosphere beneath the eastern margin of Australia, with subsequent metasomatism by fluids, now widely believed to be carbonatitic (Green and Wallace, 1988; Meen et al., 1989).

### References

- Green, D. H. and Wallace, M. E. (1988) Mantle metasomatism by ephemeral carbonatite melts. *Nature*, 336, 459-462.
- Irving, A. J. (1980) Petrology and geochemistry of composite ultramafic xenoliths in alkalic basalts and implications for magmatic processes within the mantle. *American Journal of Science*, 280A, 389-426.
- McDonough, W. F. and McCulloch, M. T. (1987) Isotopic heterogeneity in the southeast Australian subcontinental lithospheric mantle. *Earth and Planetary Science Letters*, 86, 327-340.
- Meen, J. K., Ayers, J. C., and Fregeau, E. J. (1989) A model of mantle metasomatism by carbonated alkaline melts: Trace-element and isotopic compositions of mantle source regions of carbonatite and other continental igneous rocks. In Bell, K., Ed., *Carbonatites: Genesis and Evolution*, p. 464-499. Unwin Hyman, London.
- Menzies, M. A. (1990) Archean, Proterozoic and Phanerozoic lithospheres. In Menzies, M. A., Ed., *Continental Mantle*, 67-86. Clarendon Press, Oxford.
- O'Reilly, S. Y., Griffin, W. L., and Stabel, A. (1988) Evolution of Phanerozoic eastern Australian lithosphere: Isotopic evidence for magmatic and tectonic underplating. *Journal of Petrology, Special Lithosphere Issue*, 89-108.



## ISOTOPIC AND TRACE ELEMENT REMOTE SENSING OF MONTANA CONTINENTAL LITHOSPHERE FROM ERUPTED MAGMAS.

Irving, <sup>(1)</sup>A.J. and O'Brien, <sup>(2)</sup>H.E.*(1) Dept. Geol. Sciences, Univ. of Washington, Seattle, WA 98195 USA; (2) Geol. Survey of Finland, SF-02150 Espoo, FINLAND.*

In a continuing effort to characterize mantle-derived magmas in Montana and the evolution of the subjacent mantle, we have obtained isotopic and trace element data for many late Cretaceous to Oligocene mafic volcanic and shallow intrusive rocks throughout west-central Montana. Most, but not all, of the provinces sampled have been radiometrically dated.

All these rocks are light REE-enriched, and span a range in La abundances from 50-90x chondrites (Adel Mt. Volcanics) to 270x chondrites (Garnet Range). Sr and Nd initial isotopic compositions (Figure 1) range from near Bulk Earth, through slightly enriched to more extreme values, which overlap and extend the fields determined previously for rocks from the Crazy, Highwood and Bearpaw Mountains and Missouri Breaks (e.g., Dudas et al., 1987; Scambos and Farmer, 1988; Dudas, 1991; O'Brien et al., 1991). The more enriched samples have  $\epsilon_{Nd}$  mostly between -10 and -20, but have a wide range in  $^{87}Sr/^{86}Sr$  from 0.7055 (Garnet Range) to 0.7095 (Dillon).

Isotopic composition is partly correlated with eruption age and magma type, but there is considerable variation both in space and time. Most of the Eocene (53-45 Ma) mafic magmas so far analyzed from west-central Montana have  $\epsilon_{Nd} < -10$  and  $^{87}Sr/^{86}Sr > 0.705$ . Exceptions are the kimberlitic and alnoitic magmas from the Missouri Breaks and Haystack Butte (Scambos and Farmer, 1988) that may have ascended explosively because of high CO<sub>2</sub> contents. Mid-Oligocene lavas from Indian Flats (IF, 39 Ma) plot near Bulk Earth, whereas those from Virginia City (VC, 33 Ma) overlap isotopically with rocks from the Highwood and Bearpaw Mountains. In the late Oligocene, isotopic compositions range from near Bulk Earth at Volcano Butte (29 Ma), to  $\epsilon_{Nd}$  of -5 at Black Butte (BB, 24 Ma), to much more negative  $\epsilon_{Nd}$  in the Smoky Butte lamproites (27 Ma) of eastern Montana.

Following our studies in the Highwood Mountains (Irving et al., 1989; O'Brien et al., 1991), we interpret the isotopic array mostly in terms of assimilative interaction between asthenospheric melts (with isotopic compositions near Bulk Earth) and the Wyoming Craton lithospheric mantle keel. This model differs from that proposed by Egger et al. (1988) and Dudas (1991), who contend that the magmas originate entirely within the ancient lithospheric mantle. We believe that mass flux of magma into the lithosphere is required in order to partially melt or assimilate cold, residual peridotite. In either case the geochemistry of the magmas provides indirect information on the nature of the lithosphere (e.g., Menzies, 1989). The observed variation in isotopic composition of the magmas requires that the Precambrian lithospheric mantle is regionally variable in isotopic/trace element composition and possibly in age. However, interpretation of the isotopic data is complicated further by the possibility that rates of magma ascent through the lithosphere may have been spatially variable, and/or that thinning of the ancient lithosphere (by thermal erosion or possibly by extension) was widespread by the mid-Oligocene.

The very radiogenic strontium coupled with the presence of quartz xenocrysts in the lavas from the Dillon area may signify contribution from a crustal component. Nevertheless, we believe that the dominant source of the enriched isotopic characteristics throughout the province is ancient lithospheric mantle, based on the extreme compositions ( $\epsilon_{Nd} = -16$  to  $-40$ ,  $^{87}Sr/^{86}Sr = 0.7149$  to  $0.7693$ ) of mantle xenoliths from minette in the Highwood Mountains (Irving and Carlson, this volume).

## References

Dudas, F. O. (1991). Geochemical features of igneous rocks from the Crazy Mountains, Montana, and tectonic models for the Montana alkalic province. *Journal of Geophysical Research*, in press.

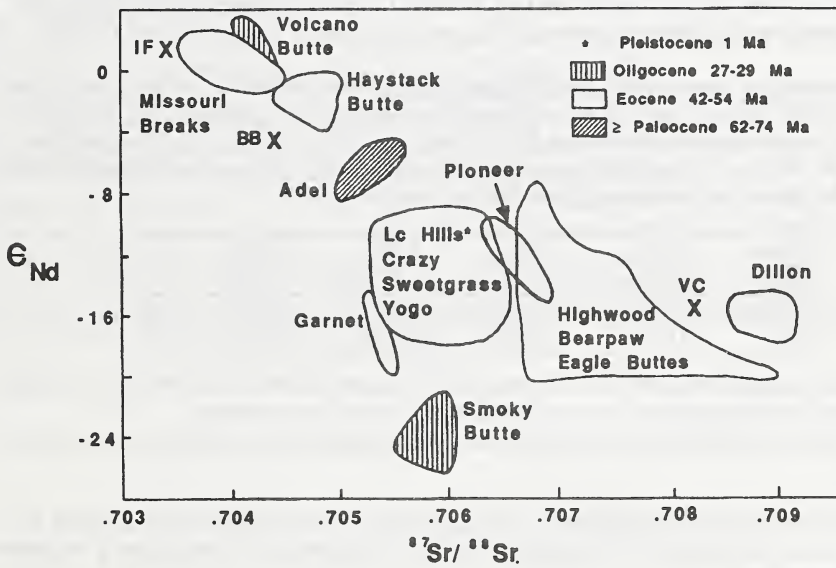
Dudas, F. O., Carlson, R. W., and Egger, D. H. (1987). Regional Middle Proterozoic enrichment of the subcontinental mantle source of igneous rocks from central Montana. *Geology* 15, 22-25.

Egger, D. H., Meen, J. K., Welt, F., Dudas, F. O., Furlong, K. P., McCallum, M. E., and Carlson, R. W. (1988) Tectonomagmatism of the Wyoming Province. *Colorado School of Mines Quarterly*, 33, 25-40.

Menzies, M. A. (1989) Cratonic, circum-cratonic and oceanic mantle domains beneath the western U. S. A.. *Journal of Geophysical Research*, 94, 7899-7915.

O'Brien, H. E., Irving, A. J. and McCallum, I. S. (1991). Eocene potassic magmatism in the Highwood Mountains, Montana: Petrology, geochemistry and tectonic implications. *Journal of Geophysical Research*, in press.

Scambos, T. A. and Farmer, G. L. (1988). Multiple source components for alkalic igneous rocks in the Wyoming Province: Isotopic and trace element evidence from central Montana. *EOS, Transactions of the American Geophysical Union*, 69, 1510.



## A DIAMOND-GRAPHITE BEARING ECLOGITIC XENOLITH FROM ROBERTS VICTOR – INDICATION FOR PETROGENESIS FROM Pb, Nd, AND Sr ISOTOPES.

*Jacob, <sup>(1)</sup>D.; Jagoutz, <sup>(1)</sup>E.; and Sobolev, <sup>(2)</sup>N.V.*

*(1) Max-Planck Institut für Chemie, Abt. Kosmochemie, Saarstrasse 23, 6500 Mainz, F.R.G.; (2) Institute of Mineralogy and Petrology, 630090 Novosibirsk, U.S.S.R.*

The 8.6 kg eclogitic xenolith "Rovic 124" is the largest known diamond-bearing xenolith. It consists of three different zones A1, A3 and A6, which are distinguished in colour as well as in mineral composition and which confirm a complex history of this rock. All zones show subhedral or rounded garnets in an interstitial matrix of cpx and can be classified as Group I according to the classification for Roberts Victor eclogites by Macgregor and Carter (1970) or as Type A according to Jagoutz et al. (1984). Zone A1 and A3 are of normal eclogitic petrography with about equal amounts of cpx and gnt, while zone A6 contains a small amount of graphite. The Graphite is flaky and shows no pseudomorphosis after diamond. Zone A6 consists of more than 90 Vol% garnet and is rich in diamond. Diamond occurs in various shapes and sizes and is only interstitial, sometimes surrounded by phlogopite which occurs along cracks in all three zones (very small amounts in zone A1).

The garnets of Rovic 124 plot in the fields of group B and group A eclogites in the Ca-Mg-Fe plot of Coleman et al. (1965) and show a grosspyritic trend; zone A6 having the highest ( up to 10.2 % CaO) and zone A1 the lowest ( up to 5 % CaO) Calcium-concentrations. Applying the cpx-gnt thermometer by Ellis and Green (1979), zone A1 yields a temperature of 1133°C.

The trace element concentrations in the different sections vary between 1 (A1 gnt) and 5 ppm (A1 cpx) Nd, 0.45 (A6 cpx) and 1.8 ppm (A6 gnt) Sm and 2.5 (A4 gnt) and 137.1 ppm (A1 cpx) Sr. Lead concentrations lie between 49 (A3 cpx ) and 523 (A1 cpx) ppb. The partition coefficients for Nd, Sm, Sr and Pb between clinopyroxene and garnet give a systematic trend, where zone A1 shows the highest and zone A6 the lowest D:

Zone	D <sub>Nd</sub>	D <sub>Sm</sub>	D <sub>Sr</sub>	D <sub>Pb</sub>
A1	5.10	1.45	47.00	2.86
A3/A4	1.06	0.42	43.90	1.10
A6	0.65	0.27	3.34	0.18

The Phlogopite contains 64 ppm Sr, 0.54 ppm Sm, 3.34 ppm Nd and 1076 ppb Pb. It is clearly of metasomatic origin judging by its occurrence along cracks in the nodule. Fe<sup>3+</sup>/Σ Fe ratios as obtained from microprobe analyses of garnet in the different zones seem to be variable.

The Sr isotopic composition are different in clinopyroxenes of the different layers which the Rb content can not account for. It is suggested that the variations in Sr isotopes are a remnant of a layered protolith.

The neodymium isotopes yield young internal mineral ages for the different sections, although the trend of zone A1 being the youngest and zone A6 being the oldest is visible. Zone A1 equilibrated at the time of eruption of the kimberlite (124 Ma, Allsopp and Barret (1975)) and yields an age of 168 Ma ± 52. The small amount of metasomatic phlogopite in this zone in comparison to the much higher amounts in other zones indicates that the phlogopite might have reacted out at the time of the resetting of the minerals in this zone. The Nd internal age is much younger than the one obtained from lead isotopes (363 Ma), but the datapoints lie on or close to the 2.75 Ga isochron which is defined by clean whole rock compositions of diamond-free eclogites from Roberts Victor (Jagoutz et al. (1984)) (Fig.2).

In Lead isotopes (Fig.1), the datapoints of Rovic 124 form a well defined linear array on the left side of the geochron which intersects at μ = 8.3. The range of the ratios observed is large and covers about half of the range observed for several different nodules from Roberts Victor measured by Jagoutz and Zindler (in prep.). The age of the array is 2.98 Ga. Some of the datapoints (A6 gnt, A3 gnt and Phlog.) lie close to or in the field defined for Group II

Kimberlites (Smith et al. (1985)) which is interpreted as influence of the kimberlite on the eclogite during eruption.

There are basically two possible explanations for the observed heterogeneities in Rovic 124:

(i) A likely explanation for the layering is a primary origin:

A layered protolith of basaltic composition and rich in carbon, e.g. oceanic basalt with carbon bearing sediment layer(s), was subducted under the African craton. During subduction all carbon was transformed to diamond. Some part of the diamonds then formed flaky graphite, e.g. due to shearing or uplift along the diamond-graphite stability boundary.

This hypothesis is supported by the Sr isotope composition which account for primary differences in Rb content of the layers prior to subduction.

(ii) The layering could have been produced by metamorphic reactions, induced by a fluid front. This fluid front penetrated zone A1, reduced its trace element content and equilibrated cpx and gnt in their Nd isotopes; any existing diamond would be reacted out. In zone A3 the reaction with the fluid was not complete. This resulted in a partial equilibration of cpx and gnt, yielding an "age" and an amount of trace elements intermediate between the ones for zone A1 and A6, and reducing the carbon content, leaving some graphite behind. Zone A6 was not reached by the fluid front and retains its original mineralogy and chemistry. Against this theory is the fact that the existing graphite does not show pseudomorphosis after diamond. Also the distribution of phlogopite is inverse to the one expected from an entry of the fluid front at zone A1.

Allsopp, H.L., and Barret, D.R. (1975) Rb-Sr determinations on South African kimberlite pipes. *Phys Chem Earth*, 9, 605-617

Coleman, R.G., Lee, D.E., Beatty, L.B., and Brannock, W.W. (1965) Eclogites and Eclogites: Their Differences and Similarities. *Geol Soc Am Bull*, 76, 483-508

Ellis, D.J., and Green, D.H. (1979) An experimental study of the effect of Ca upon garnet-clinopyroxene Fe-Mg exchange equilibria. *Contrib Mineral Petrol*, 71, 13-22

Jagoutz, E., Dawson, J.B., Hoernes, S., Spettel, B., and Wänke, H. (1984) Anorthositic oceanic crust in the archaean mantle (abs.) 15th Lun Planet Sci Conf, 395-396

MacGregor, I.D., and Carter, J.L. (1970) The chemistry of clinopyroxenes and garnets of eclogite and peridotite xenoliths from the Roberts Victor mine, South Africa. *Phys Earth Planet Int*, 3, 391-397

Smith, C.B., Gurney, J.J., Skinner, E.M.W., Clement, C.R. and Ebrahim, N. (1985) Geochemical character of southern African kimberlites: A new approach based on isotopic constraints. *Trans Geol Soc S Afr*, 88, 267-281

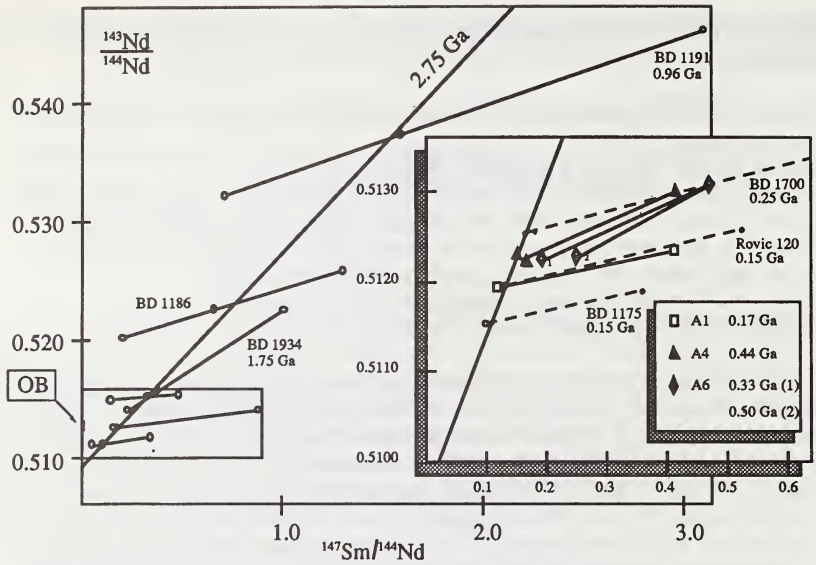


Fig. 1:  $^{147}\text{Sm}/^{144}\text{Nd}$  versus  $^{143}\text{Nd}/^{144}\text{Nd}$  plot shows the 2.75 Ga isochron, defined by "clean whole rocks" of non-diamondiferous xenoliths from Roberts Victor. Open circles are cpx and gnt respectively, closed circles are calculated whole rock compositions. Inset shows isochrons and internal ages for Rovic 124. Age (1) for layer A6 is a clean cpx, age (2) is a ultraclean separate from the same cpx split.

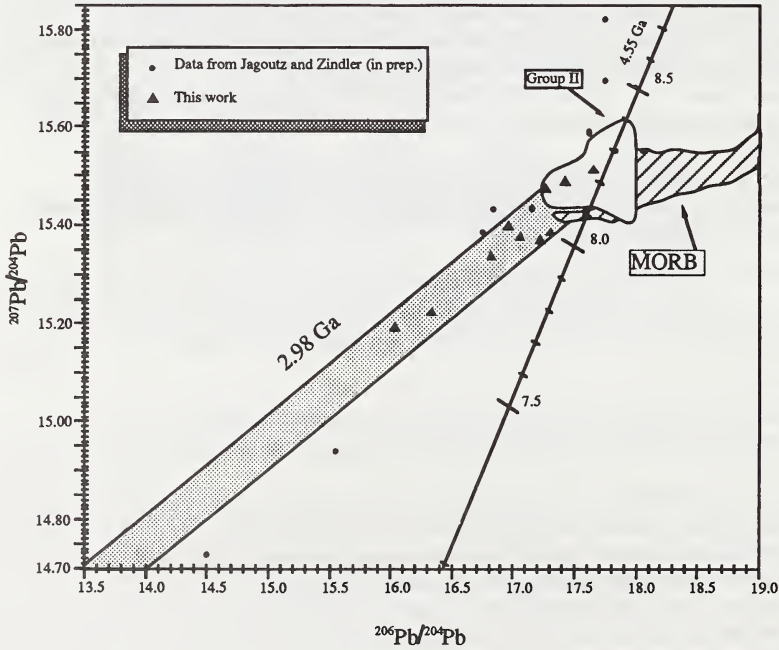


Fig 2: In a  $^{207}\text{Pb}/^{204}\text{Pb}$  versus  $^{206}\text{Pb}/^{204}\text{Pb}$  plot the Rovic 124 data forms a linear array, yielding an age of 2.98 Ga. Geochron and fields for Group II Kimberlites and MORB shown for reference.

## THE ROLE OF FLUORINE IN THE CRYSTALLIZATION OF NIOBIUM AND PHOSPHORUS ORES IN CARBONATITES.

*Bruce C. Jago and John Gittins.*

*Department of Geology, Earth Sciences Centre, University of Toronto, Toronto, Ontario, M5S 3B1, Canada.*

Phase equilibria studies have helped to deduce compositional controls on Nb and P mineralization and paths of fractional crystallization that might be experienced by natural carbonatite melts. High niobium solubilities (5 - 10 wt. % Nb<sub>2</sub>O<sub>5</sub>) in simple, water - saturated calcium carbonate melts (Watkinson 1970) conflict with the generally low Nb<sub>2</sub>O<sub>5</sub> contents (< 0.5 wt. %) of most carbonatites, with the exception of hydrothermally enriched zones in bodies such as Araxa (Mariano 1989). To evaluate this disparity and determine the effect of alkalinity and F content on perovskite and pyrochlore (Pyr) crystallization, experiments were conducted (1 kbar, 550 - 945° C.) in anhydrous, F - bearing Na - Ca carbonate melts [CaCO<sub>3</sub> - Na<sub>2</sub>CO<sub>3</sub> - F (Cc - Nc - F), Jago 1991] with a natural pyrochlore (< 2.1 wt. % F) from Oka (Perrault 1968). The effect of alkalinity and F content on the crystallization history of apatite was determined in the same F - bearing join (1 kbar, 550 - 930° C.) with a natural fluor - apatite (av. 25 anal., 2.8 wt. % F), Jago 1991).

### **Pyrochlore Crystallization in the Quaternary Cc - Nc - F - Pyr**

Figure 1 is a generalized pseudoternary section through the carbonate - rich portion of the quaternary Cc - Nc - Pyr - F (Jago 1991). The plane of the section is dominated by the phase field for pyrochlore owing to the low solubility of pyrochlore (< 0.75 wt. % or < 0.45 wt. % Nb<sub>2</sub>O<sub>5</sub> equiv.) at all binary, ternary and quaternary invariant points which is in agreement with Nb contents of natural systems. A perovskite group mineral occurs as an intermediate compound on the carbonate - pyrochlore binary at Nc<sub>64</sub> Pyr<sub>36</sub> owing to the reaction of pyrochlore with carbonate melt. The perovskite - pyrochlore binary projects into the F - bearing ternary and terminates at a peritectic point with 1 wt. % F (T > 930° C.) at the intersection of the phase fields for carbonate, pyrochlore and perovskite. Under conditions of fractional crystallization, perovskite reacts with the F - bearing melt to form pyrochlore; cotectic crystallization of carbonate and pyrochlore proceeds down temperature to higher F contents and eventual intersection of the phase field for a fluoride mineral at approximately 7 - 8 wt. % F and 590° C. Crystallization of this three phase assemblage enriches the melt in alkalis but proceeds at essentially constant F content to a quaternary eutectic. The location of the peritectic at low F contents and high temperatures explains the general paucity of perovskite + pyrochlore - bearing assemblages in carbonatites, which almost universally experience fractional crystallization, and, the occurrence of pyrochlore reaction rims on perovskite (Oka, Nickel and McAdam 1963; Russian, Kapustin 1980). Alkali - rich hydrothermal fluids must have been F - poor to form lueshite from pyrochlore at Lueshe (Safiannikoff 1959) in Zaire.

### **Apatite Crystallization in the Quaternary Cc - Nc - F - Apatite**

The combined effect of alkalis and fluorine on apatite solubility was examined to extend the range of previous studies to compositions that are relevant to the crystallization of apatite from anhydrous, halogen and alkali - bearing carbonate melts up to extreme compositions of the Oldoinyo Lengai type.

Apatite solubility in Nc - bearing compositions in the ternary Cc - Nc - Ap decreases markedly from 25 wt. % on the Cc - Ap binary to about 4 wt. % on the nyerereite (Ny) - Ap (800° C.) binary. A single ternary eutectic is located on the Cc - rich side of Ny - Ap

at Cc51 Nc 45.5 Ap 3.5 at 787° C. The Nc - rich side of the ternary is dominated by the phase fields for apatite and Na - Ca carbonate - phosphate compounds which results in very restricted phase fields for Ncss and Ny. A ternary eutectic (Nc78 Cc21 Ap1, 700° C.) and ternary peritectic (Nc 40.5 Cc 36.5 Ap3.0, 795° C.) were located on the Nc - rich side of Ny - Ap but phase relations on Nc - Ap were not constrained.

Eutectic temperatures are depressed by approximately 200° C. and apatite solubility by about one half with the addition of 8 wt. % F to ternary compositions. This also establishes the fluorite stability field and extends the compositional range over which alkali - bearing, Cc - rich melts (Nc:Cc < 1) may fractionate to Nc - rich compositions (Nc:Cc > 1) and bypass the thermal barrier imposed by nyerereite in Cc - Nc. Two pseudoternary sections (Figures 2 and 3) illustrate contrasting crystallization schemes in the Cc - rich portion of the quaternary which are a function of apatite solubility and dictated by the form of the apatite liquidus (i.e. convex with T max; gentle negative slope with increasing F content). For melts with bulk Nc:Cc ratios greater than about 1.5 (Figure 2), apatite solubility in F - bearing carbonate melts is insufficient to deplete the melt in F during the course of apatite precipitation. As a result, fractional crystallization invariably proceeds toward the fluorite - apatite cotectic from the carbonate (A--->) or apatite (B--->) stability fields, and melts with low initial F contents can experience two periods of carbonate precipitation. For melts with bulk Nc:Cc ratios less than about 1.5 (Figure 3), apatite precipitation may or may not be sufficient to deplete the melt in F, and the crystallization scheme is largely controlled by the initial F content of the system. For melts with high F contents (> 7 - 8 wt. %), crystal fractionation of apatite (C--->) enriches the melt in F, and crystallization proceeds toward the fluorite - apatite cotectic prior to intersecting the calcite stability field. For melts with less than approximately 7 - 8 wt. % F, apatite precipitation can deplete the melt in F and fluorite precipitation is possible only after cotectic crystallization of apatite and calcite sufficiently enriches the melt in F. Ternary and quaternary phase relations support a trend of alkali - enrichment during magmatic evolution in anhydrous, F - bearing melts and presents viable crystallization paths that can account for fluorite - bearing, calcite - apatite and calcite - bearing, fluorite - apatite vein assemblages.

#### References

- Jago, B. C. (1991) The role of F in the evolution of alkali - bearing carbonatite magmas and the formation of carbonatite-hosted niobium and phosphorus ore deposit. Unpublished Ph.D. thesis, University of Toronto.
- Kapustin, Yu. L. (1980) Mineralogy of carbonatites. Amerind Publishing Co. New Delhi, 259p.
- Mariano, A. N. (1989) Nature of economic mineralization in carbonatites and related rocks. In *Carbonatites: Genesis and Evolution*, K. Bell. (Ed.) 149 - 172.
- Nickel, E. H. and McAdam, R. C. (1963) Niobian perovskite from Oka, Quebec; A new classification for minerals in the perovskite group. *Canadian Mineralogist*, Vol. 7, 683 - 697.
- Safiannikoff, A. (1959) Un nouveau mineral de niobium. *Academic Royale Sceances D'outre-mer, Bulletin*. Vol. 5, in: Kapustin, Y. L. 1980. *Mineralogy of Carbonatites*. Amerind Publishing, New Delhi, 259p.
- Watkinson, D. H. (1970) Experimental studies bearing on the origin of the alkali rock - carbonatite complex and niobium mineralization at Oka, Quebec. In, *Alkaline Rocks: The Montereion Hills*. *Canadian Mineralogist*, Vol. 10, 350 - 361

Figure 1

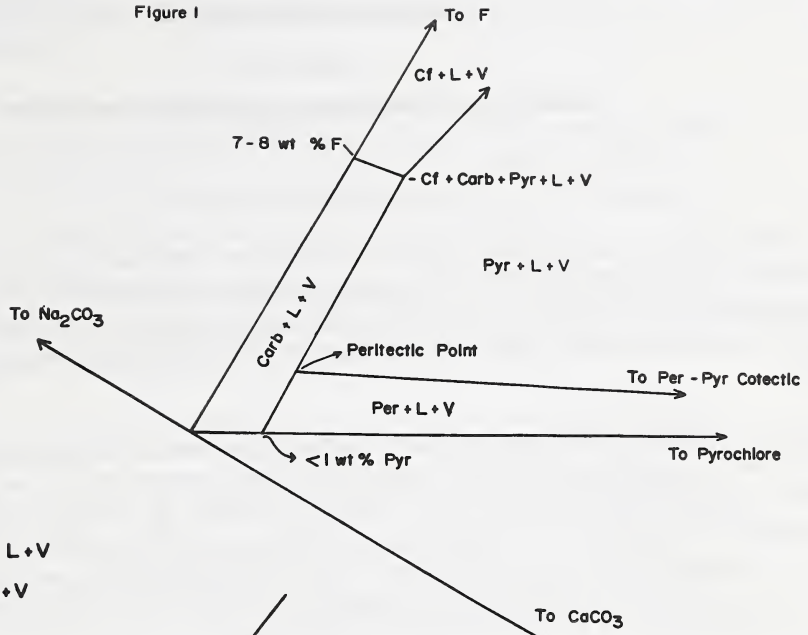


Figure 2

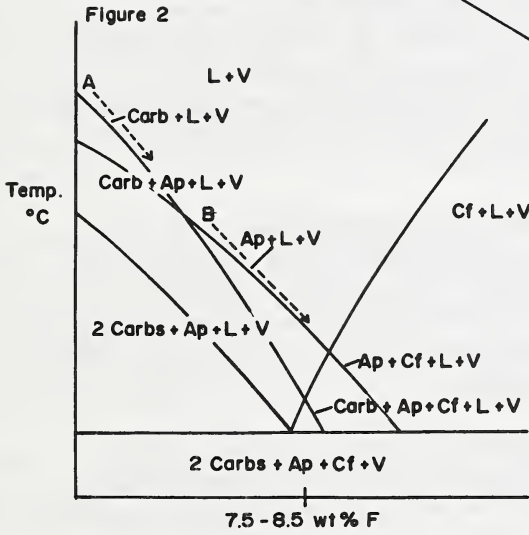
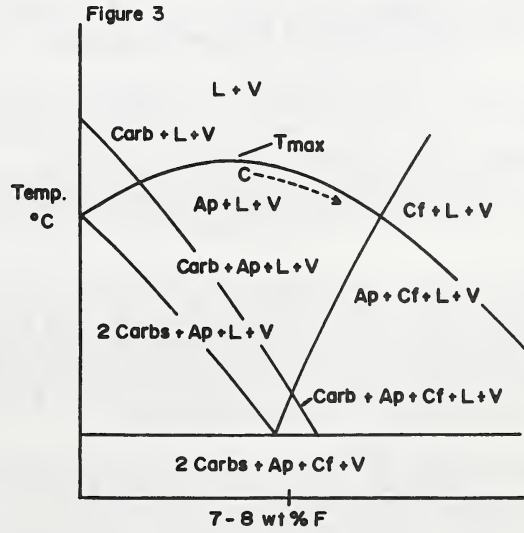


Figure 3



IS CLIFFORD'S RULE STILL VALID? AFFIRMATIVE EXAMPLES FROM  
AROUND THE WORLD.

*Janse, A.J.A.*

*Mintel Pty Ltd, 11 Rowsley Way, Carine, Western Australia 6020.*

In 1966 Clifford published a paper in which he confirmed and re-formulated a concept first stated by W.Q. Kennedy in 1964 that the occurrence of diamondiferous kimberlites is restricted to those parts of the earth's crust which Kennedy called "rigid cratonic nuclei of respectable antiquity,  $\pm 2000$  M.y."

Clifford, following Kennedy, observed that **economically** diamondiferous kimberlites, regardless of their age of intrusion, occur only in areas underlain by basement older than 1600 M.y. which he thought represented Archaean cratonic terrain. His observation was mainly related to occurrences in the African continent, but it appeared to be valid to Siberia as well where since 1955 many economically diamondiferous kimberlites were discovered on the large Siberian Platform.

A certain amount of confusion exists about the interpretation of the term craton. It is often used in a strict time - stratigraphic sense and then it is synonymous with Archaean basement. Hence the question "are these kimberlites on or off craton?", enquires whether or not the kimberlites in question occur in areas underlain by basement rocks of Archaean age. This is considered to have economic consequences.

It is also used in a broader structural-lithological sense in which cratons represent rigid, relatively immobile and generally low grade metamorphic parts of the Earth's crust in contrast to surrounding belts of highly deformed and high grade metamorphic rocks i.e. mobile belts, which can be as young as Palaeozoic in age, although the rocks of the craton are generally understood to be always of Precambrian age.

In this broader sense cratons are coherent blocks in the Earth's crust of any Precambrian age which have become rigid in that they react to surrounding or abutting tectonic forces by faulting, tilting or warping instead of folding. This cratonic condition is attained some time after their latest thermal event when the crustal block has thickened and cooled down.

Thus most cratons *sensu lato* are composed of blocks of Archaean or Early Proterozoic rocks, welded and surrounded by Proterozoic mobile belts. The whole assemblage often carries a bewildering array of local stratigraphic or structural names so that it is confusing for a geologist, not familiar with the area, to understand the tectonic pattern.

In 1984 and again in 1991 the author proposed a simple classification of cratonic blocks into three major divisions, i.e. -

- (i) Archon - in which the basement rocks are of Archaean age;
- (ii) Proton - in which they are of Early to Middle Proterozoic age;
- (iii) Tecton - in which they are of Late Proterozoic age.

The time boundaries between these divisions have been selected as: archons - older than 2500 M.y.; protons - between 2500 and 1600 M.y. and tectons - between 1600 and 800 M.y.

Many cratons, however, are overlain by younger, flat lying, little or undeformed sediments and volcanics (platform cover) so that, in many cases, it is not possible from direct observation to ascertain the nature of the underlying basement. The whole tectonic assemblage of cratonic blocks, mobile belts and cover rocks is often referred to as a Platform.

Furthermore, parts of a craton can be re-activated by a later thermal event and so become rejuvenated from archon to proton or tecton or from proton to tecton and this has consequences for its economic potential.

Close observation shows that all economic kimberlites in Southern Africa occur on the Kalahari Archon and most of them on the Kaapvaal nucleus within the Kalahari Archon. South African geologists go as far as stating that kimberlites occurring outside the boundaries of the Kalahari Archon do not contain any diamonds (Skinner, personal communication). Thus the kimberlites in Namibia, Bushmanland and the southern Cape Province are barren as they are located in the Namaqua-Natal province which is built up by protons and tectons.

Recent research in the USSR has shown that the basement of the Siberian Platform can be divided into several Archaean megablocks (archons) separated by Proterozoic mobile belts. Economic kimberlites (Mir, Aikhal, Udachnaya) occur only on the archons. It is also stated that the basement underneath the platform in the newly discovered kimberlite province 100km north of Arkhangel in Western Russia is Archaean.

In 1979 a primary source rock with a very high content of diamonds was found at Argyle in Western Australia which soon proved to be a very significant economic deposit.

The example of Argyle shows that economically significant, diamondiferous non-kimberlitic primary source rocks can occur "off-craton" (in the sense of Clifford), or off-archon (this paper), but located in an Early Proterozoic mobile belt which surrounds an Archaean craton.

The Argyle rocks, however, are not kimberlite but lamproite and worldwide examples show that other diamondiferous lamproites occur in Proterozoic terrains, i.e. protons.

Economic kimberlites occur in Archaean parts of the North China (Sino-Korean) Archon (Mengyin, Shandong and Fuxian, Liaoning). However, the basement to the Yangtze craton is generally of Proterozoic age, and the only primary source rock for diamond found so far is lamproite (Guizhou).

Diamondiferous, but so far non-economic, kimberlites (Aries, Skerring) occur on the Kimberley Archon, while an economic lamproite (Argyle) occurs in the Halls Creek Proton, close to the edge of the Kimberley Archon.

The Majhgawan pipe in central India, which was long thought to be a kimberlite has recently been classified as a lamproite; it lies right on the edge of the Aravalli Archon.

The alluvial diamonds in Kalimantan occur in areas underlain by highly deformed, medium grade metamorphic basement. Thus their source rocks are very distant or occur in a fragment of old cratonic terrain (Archon or Proton) which has not yet been found or recognised despite considerable exploration efforts by expatriate companies.

Worldwide observation also shows that the most and the largest diamond deposits occur on Archons which have the thickest platform cover and which have been uplifted the most. For example, within the Kalahari Archon, the Kaapvaal nucleus, which has a total thickness of Paleozoic and Mesozoic platform rocks in the order of at least 10,000m and an uplift of at least 3,000m, has the highest regional diamond content, while the Zimbabwe nucleus with a thinner platform cover (now mostly eroded) has the lowest.

Other cratons with high regional diamond potential are the Siberian Platform which has a substantial thickness of platform cover, while in Western Australia the Kimberley craton with its thick cover has proved richer than any other cratons in Australia which have lesser covers.

Perhaps there is a measurable relationship between regional diamond potential and the total thickness of the platform stratigraphic successions and the amount of subsequent uplift. To find this could be the challenge for the next few years.

It is concluded that if Clifford's rule is modified so that his "ancient cratons" represent truly Archaean terrain older than 2500 M.y., then it is still valid. Thus economic kimberlites occur "on-archon" and, in general, more towards the centre of an archon. (This modified Clifford's Rule was called the Clifford-Sinitsyn Rule at the Kimberlite Workshop held in Leningrad in March 1990). Economic lamproites, on the other hand, seem to occur along the periphery of an archon or in surrounding mobile belts preferably close to the edge of an archon. Prospecting methods should be tailored to the type of cratonic basement present to find the most likely primary source rocks.

However, because of the uncertainties in determining the exact petrological nature of the basement in platform areas and in rejuvenated terrain, there is still room for the "inspired" geologist or prospector who goes into the field to find a major diamond deposit in areas condemned by others.

CLIFFORD T.N., 1966. Tectono-metallogenic units and metallogenic provinces of Africa. *Earth and Planetary Science Letters*, 1, 421-434.

JANSE A.J.A., 1984. Kimberlites - where and when? In: J.E. Glover & P.G. Harris (editors) *Kimberlite occurrence and origin: a basis for conceptual models in exploration*, 19-62. University of Western Australia Geology Department and University Extension, Publication No.8.

JANSE A.J.A., 1991. New ideas in subdividing cratonic areas. In: A.V. Sinitsyn et al (editors) *Proceedings of the Kimberlite Workshop held in Leningrad March 1990*. *Sovietskaya Geologiya*.

KENNEDY W.Q., 1964. The structural differentiation of Africa in the Pan-African ( $\pm 500$  m.y.) tectonic episode. *Research Institute of African Geology, Eighth Annual Report of Scientific Results 1962-1963*, 48-49.

## NON-KIMBERLITIC DIAMONDS SOURCE ROCKS.

*Janse, A.J.A.*

*Mintel Pty Ltd, 11 Rowsley Way, Carine, Western Australia 6020.*

Since the discovery of kimberlite as a major primary source rock for diamonds in 1872 various claims have been made for other rocks, which are not kimberlites, to represent a source rock for diamonds. These claims have, at various times, been disputed, ridiculed or proved wrong and in general very little attention was paid to them as the alleged diamond deposits were economically insignificant.

In 1978 and 1979 olivine lamproite was found to be a primary source rock for economically very important diamond deposits. Since then the matter ceased to be of academic interest only and increasing attention has been focussed on assessing the validity of the discoveries of diamonds in various kinds of rock.

In many cases the original discovery could not be repeated by other investigators and it was claimed that the original mineral was misidentified, being a variety of the spinel group instead of diamond. Be that as it may, improved sample processing techniques and modern X-ray equipment have shown that diamonds occur in rocks other than kimberlites and olivine lamproites. Traces of diamond have been reported from related rocks such as less mafic lamproites (leucite lamproites), ultramafic and alkalic lamprophyres (alnoites, aillikites, damkjernites, monchiquites), but there are an increasing number of reports, often quite well substantiated, which state that diamonds were found in dunite/harzburgite or garnet pyroxenite in ophiolite complexes, garnet peridotite in gneiss and in alkaline basalt, eclogite in gneiss, alkaline basalt, dolerite, granite, pegmatite and of course in meteorites and in meteorite impact structures (Table 1).

There are also reports that small diamonds and microdiamonds were found in low grade metamorphic greywacke-turbidite sequences of Lower to Middle Proterozoic age, i.e. Ghana and Northern Territory of Australia, for which no kimberlitic or lamproitic source rock can be found, and in high grade metamorphic paragneiss for which it is claimed that the diamonds have a metamorphic genesis (Kokchetav, Northern Kazakhstan).

Finally there are reports that the isotopic composition of carbonados in Bahia indicates that these may be derived from non-kimberlitic source rocks.

Most of these occurrences are not economically important, except for the alluvial diamond deposits of southeastern Kalimantan (if it is accepted that these are derived from an ophiolitic source rock), for the Popigay impact structure which apparently contains a large resource of small diamonds and which would be economic if it were not located well above the arctic circle, and for the carbonado deposits in Bahia.

Recent research has indicated that diamonds in kimberlites and olivine lamproites are derived from three deep seated sources, i.e. garnet lherzolite, garnet harzburgite and eclogite. It is interesting to note that similar deep seated rocks are brought to the surface by tectonic forces in ophiolite, peridotite and eclogite complexes and that diamonds are claimed to have been found in these rocks in some places.

The content of diamond in these deep seated rocks can be extremely high in places. It can be measured in percentages in eclogite nodules in kimberlites from South Africa or if the octahedral graphites in the Beni Bousera ophiolite are true pseudomorphs after diamond, it can reach 20 per cent. Thus the search is on for an ophiolite in which the diamonds have not been transformed into graphite. Graphite has been found in eclogite and garnet peridotite nodules in kimberlite pipes (Orapa, Jagersfontein, Mir), but also in carbonatites, which gives food for thought and impetus for a wider search.

It is likely that the list in Table 1 is neither complete nor conclusive. Certain occurrences will be or have already been proved wrong (diamonds in alkaline basalt in Kamchatka) or doubtful (metamorphic genesis for diamonds in Kokchetav), but it is certain that other occurrences will be added in future.

**TABLE 1. NON-KIMBERLITIC DIAMOND SOURCE ROCKS CLAIMED BY VARIOUS AUTHORS**

<b>Rock Types</b>	<b>Grade</b>	<b>Indicator Minerals</b>
1. Eclogites in gneissic country rock Kokchetav (Kazakhstan)	high	Py-Alm garnet, Na-Cr pyroxene
2. Garnet-Pyroxenite in Ophiolite complexes Beni Bousera (Morocco)	high?	Py-Alm garnet, chromite
3. Harzburgite/Dunite in Ophiolite complexes Tibet, British Columbia	low	Chromite, platinum minerals
4. Dunites as pipes in country rock Upper Volta	low	Chromite, Mn-ilmenite
5. Alkaline ultrabasic complexes Kotui (Northern Siberia)	low	Chromite, pyrope garnet
6. Ultramafic lamprophyres Western Australia	low	Chromite, Perovskite
7. Alkaline lamprophyres (Monchiquites) Western Australia	low	Chromite
8. Lherzolite nodules in alkaline basalt Mongolia	low	Pyrope, Cr-diopside
9. High grade metamorphics Kokchetav (Kazakhstan)	high?	Py-Alm garnet, pyroxene
10. Garnet Peridotite in gneissic country rock Bohemia	low	Pyrope, Cr-diopside, chromite
11. Olivine Bombs in basalt Ruang Volcano (North Sulawesi)	low	Diamond, olivine
12. Meteorite impact structures Popigay (Northern Siberia)	high?	Hexagonal diamond
13. Dolerite/diabase dykes New South Wales	low	Diamond
14. Xenocrysts in alkaline basalt Kamchatka	low	Diamond
15. Turbidite/greywacke Ghana, Northern Territory	high/med	Diamond
16. Lithified Precambrian Conglomerate Bahia	medium	Carbonado

PERIDOTITIC PARAGENESIS PLANAR OCTAHEDRAL DIAMONDS FROM THE  
ELLENDALE LAMPROITE PIPES, WESTERN AUSTRALIA.

*A.L. Jacques*<sup>(1)</sup>; *A.E. Hall*<sup>(2)</sup>; *J. Sheraton*<sup>(1)</sup>; *C.B. Smith*<sup>(2)</sup> and *Z. Roksandic*<sup>(1)</sup>

(1) Bureau of Mineral Resources, Canberra, ACT, Australia; (2) CRA Exploration Pty Ltd, Perth, Western Australia.

Introduction

The 20 Ma Ellendale lamproite pipes, in the West Kimberley province of Western Australia, are the youngest diamond pipes known. Previous studies (Hall & Smith, 1984; Jaques et al., 1989) have shown that the larger size (> 1 mm) diamonds from these pipes are mostly distinctive lustrous dodecahedra containing equal proportions of peridotitic and eclogitic paragenesis inclusions, and having a wide range of carbon isotopic compositions ( $\delta^{13}\text{C} = -3.4$  to  $-14.4$ ‰). New data show that a distinctive suite of small commercial sized (1.0 - 2.5mm) octahedral diamonds from the Ellendale pipes are of peridotitic paragenesis and similar to small octahedral diamonds found in garnet peridotite (dominantly lherzolite) xenoliths from the Argyle lamproite.

Ellendale planar octahedral diamonds

Amongst the Ellendale diamonds are a distinctive suite of small stones which are typically frosted, step-layered planar octahedra and mostly white to pale brown in colour (Hall and Smith, 1984, fig. 7f). Graphite inclusions are common. Included amongst these stones are hemimorphic forms, half octahedron, half resorbed to dodecahedron (Hall and Smith, 1984, fig. 7e). These are thought to have resulted from partial resorption of diamond protruding from the surface of a xenolith. Subsequent disaggregation of the xenolith released the whole stone with the previously embedded portion retaining its original octahedral form.

The suite contains only peridotitic primary mineral inclusions: olivine, enstatite, olivine + enstatite, Cr-diopside, olivine + Cr-diopside, and olivine + Cr-pyrope. Chrome diopside is abundant ( $\approx 40\%$  of stones with primary silicates), as found in previous studies of the Ellendale stones (21% of peridotitic inclusions), implying a dominantly lherzolite facies derivation.

Olivine ( $\text{Mg}_{90.9-92.4}$ ) and enstatite ( $\text{Mg}_{92.6-92.9}$ , 0.4-0.7%  $\text{Al}_2\text{O}_3$ ) lie within the compositional range previously found for inclusions in Ellendale peridotitic diamonds and, overall, are not as Mg-rich as olivine inclusions in diamond worldwide (mostly  $\text{Mg}_{90.5-92.5}$  cf  $\geq \text{Mg}_{92.5}$ ). Chrome diopside ( $\text{Ca}/(\text{Ca}+\text{Mg}) = 0.43-0.44$ , 1-1.4%  $\text{Cr}_2\text{O}_3$ ), and chrome pyrope ( $\text{Mg}_{84}$ ,  $\approx 9\%$   $\text{Cr}_2\text{O}_3$ ,  $\approx 6\%$   $\text{CaO}$ ) also fall within the compositional range previously established for peridotitic inclusions from Ellendale diamonds. The Ca-saturated nature of the Cr-pyrope is consistent with derivation from a lherzolite assemblage.

Temperature-Pressure Estimates

Equilibration temperatures estimated for inclusions from the Ellendale octahedral diamonds are very similar to those obtained for the Ellendale peridotitic population ( $1125 \pm 50^\circ\text{C}$ ) using a variety of thermometers (Table 1). A nominal pressure

of 5 GPa has been assumed where pressures are unknown which seems a reasonable estimate since very similar pressures were calculated for two of the diamonds.

Diamond	Assemblage	P (GPa)	T (°C)	Method
<u>Ellendale: Jaques et al., 1989</u>				
E4/2	Ol-opx	(5)	1115	Ca in opx
E4/11	Ol-ga	-	1100	Ni in ga
		(5)	1225	Fe-Mg ol-ga
E4/12	Ol-ga	-	1165	Ni in ga
		(5)	1055	Fe-Mg ol-ga
E4/18	Ol-opx-cpx	4.50	1120	Cpx-opx/Ca in ol
		(4.5)	1090	Ca in opx
E4/20	Opx	(5)	1095	Ca in opx
E4/24	Opx	(5)	1145	Ca in opx
Mean			1125	
<u>Ellendale selected octahedra</u>				
E208	Opx	(5)	1135	Ca in opx
E209	Ol-opx	(5)	1020	Ca in opx
E217	Ol-cpx	4.47	(1100)	Ca in ol
E226	Ol-ga	(5)	1150	Fe-Mg ol-ga
Mean			1100	
<u>Argyle: Jaques et al., 1989</u>				
A104	Ol-opx	(5)	1120	Ca in opx
A151	Ol-ga	-	1225	Ni in ga
		(5)	1150	Fe-Mg ol-ga

Note: Thermobarometers given in Brey and Kohler (1990) and Griffin et al. (1989).

These temperatures are slightly higher than those typically obtained for peridotitic inclusions in diamond from kimberlites. Even higher temperatures (1140-1290°C) were obtained from inclusions in diamond and diamondiferous peridotite xenoliths from the Argyle pipe (Jaques et al., 1990). This difference in temperature between Argyle and Ellendale diamonds (especially eclogitic suites) is clearly shown by the much higher level of aggregation of nitrogen in the Argyle diamonds compared to Ellendale stones (Taylor et al., 1990). The mean equilibration temperature for the Ellendale peridotitic diamonds is very similar to that obtained from nitrogen aggregation characteristics for Ellendale 9 peridotitic diamonds for a late Precambrian age of formation (Taylor et al., 1990).

#### Carbon Isotopic composition

The Ellendale planar octahedra have a small range in carbon isotopic compositions ( $\delta^{13}\text{C} = -3.1$  to  $-6.2^{\circ}/\text{oo}$  vs PDB) with a peak of  $\delta^{13}\text{C}$  values at  $-4.8^{\circ}/\text{oo}$ . These fall within the compositional range found previously for peridotitic diamonds from the Ellendale pipes ( $\delta^{13}\text{C} = -3.9$  to  $-6.4^{\circ}/\text{oo}$ , averaging  $-5.2^{\circ}/\text{oo}$ ) and peridotitic suite diamonds from Argyle and elsewhere.

The limited range of the Ellendale peridotitic suite diamonds contrasts with the range of  $\delta^{13}\text{C}$  values observed for Ellendale eclogitic paragenesis diamonds which extend to values more depleted in  $^{13}\text{C}$  ( $\delta^{13}\text{C} = -3.8$  to  $-11.2^{\circ}/\text{oo}$ ). Argyle eclogitic diamonds are even more depleted in  $^{13}\text{C}$  ( $\delta^{13}\text{C}$

mostly -9 to -12<sup>0</sup>/oo) suggesting involvement of significant amounts of recycled crustal carbon (Jaques et al., 1989). Ellendale eclogitic diamonds, by comparison, apparently had a much smaller input of crustal carbon.

### Origin of the diamonds

The recognition of an association of a distinctive diamond morphology, namely step-layered octahedra, with exclusively peridotitic paragenesis inclusions and restricted 'mantle-type' ( $\delta^{13}\text{C} \approx -5^0/\text{oo}$ ) carbon isotopic composition in the Ellendale diamonds mirrors a similar finding in the Argyle diamonds (Jaques et al., 1990). The Argyle lamproite contains distinctive sharp-edged planar octahedral diamonds which have peridotitic inclusions and small negative  $\delta^{13}\text{C}$  values and these have been identified as being derived from diamondiferous peridotite xenoliths of mostly lherzolitic composition.

Microdiamonds at Ellendale, below the size range of the octahedral stones studied in this paper, are of similar planar form and dominant brown or white colour and, may therefore be of similar origin, viz. from primordial mantle carbon in subcontinental peridotitic, mostly lherzolitic, mantle. The less depleted nature (in terms of Mg/Fe) of the inclusions, the relative abundance of chrome diopside inclusions and the Ca-saturated nature of the chrome pyropes suggest a lherzolitic rather than a harzburgitic source for most of the Ellendale peridotitic diamonds.

The preservation and lack of resorption of these diamonds seems likely to be due to shielding in peridotite xenoliths until a comparatively late stage in the eruption of the lamproites. Shielding of eclogitic paragenesis diamonds has been less effective, possibly because of the lower melting temperature of eclogite and earlier disaggregation of the eclogite xenoliths.

### References

- Brey, G.P. and Kohler, T. (1990) *Journal of Petrology*, 31, 1353-1378.
- Griffin, W.L., Cousens, D.R., Ryan, C.G., Sie, S.H., and Suter, G.F. (1989) *Contributions to Mineralogy and Petrology*, 103, 199-202.
- Hall, A.E., and Smith, C.B. (1984) In Glover J.E. and Harris P.G. Eds., *Kimberlite occurrence and origin*, p. 167-212. University of Western Australia Geology Department and Extension, Publication No. 8.
- Jaques, A.L., Hall, A.E., Sheraton, J.D., Smith, C.B., Sun, S-S., Drew, R.M., Foudoulis, C., and Ellingsen, K. (1989) In Ross J. et al. Eds., *Kimberlites and related rocks - volume 2: their mantle/crust setting, diamonds and diamond exploration*, p.966-989. Geological Society of Australia Special Publication No.14.
- Jaques, A.L., O'Neill, H.St.C., Smith, C.B., Moon, J. and Chappell, B.W. (1990) *Contributions to Mineralogy and Petrology*, 104, 255-276.
- Taylor, W., Jaques, A.L., and Ridd, M. (1990) *American Mineralogist*, in press.

## A REVIEW OF THE CARBONATITES OF AUSTRALIA.

A.L. Jacques<sup>(1)</sup>; J. Knutson<sup>(1)</sup>; and R. Duncan<sup>(2)</sup>.*(1) Bureau of Mineral Resources, Geology & Geophysics, Canberra Australia; (2) R.K. Duncan and Associates, Leederville, Western Australia.*

Several major new carbonatite complexes have recently been found in Australia. This paper reviews the geology, mineralogy and geochemistry of carbonatites in Australia and their mineral resources.

**Geology, Age and Setting**

Most of the carbonatites in Australia are of late Proterozoic age and intrude either cratonised Proterozoic mobile belts or the margins of Archaean blocks (Fig.1). The carbonatites all appear to be spatially related to deep-seated faults, and range in form from major circular bodies (some as large as 10km across), with marked magnetic and gravity signatures to small (< 100m) dykes and plugs.

The oldest is the Mount Weld Carbonatite dated at 2.02 Ga which intrudes Archaean greenstones of the Eastern Goldfields Province of the Yilgarn Block (Fig. 1). The Mt Weld carbonatite is a 3 km wide stock or plug buried beneath alluvium and Tertiary lake sediments. The body has a central carbonatite (dominantly sovite) core surrounded by a 500m wide zone of brecciated, biotite-rich wallrock (glimmerite). An earlier generation of cumulate and orbicular textured sovite is intruded by later dolomite-bearing carbonatites typically containing apatite, magnetite, phlogopite and pyrochlore.

The Ponton Creek alkaline complex is a major circular body some 10km across which intrudes Archaean granites and gneisses at the eastern margin of the Yilgarn Block (Fig. 1) and is thought to be of Proterozoic age. The complex, which is covered by some 500m of Permian tillite, has a central core of ultramafic cumulates, dominantly magnetite-bearing olivine clinopyroxenite, cut by narrow veins of apatite-rich carbonatite. Peralkaline syenites are also associated.

The Cummins Range Carbonatite lies at the intersection of the King Leopold and Halls Creek mobile belts at the southern margin of the Kimberley Block (Fig. 1). The carbonatite, which has been dated at 905 Ma, intrudes Precambrian metasediments and gneisses as a zoned vertical stock 1.8 x 1.7 km across. A central carbonatite-rich core is enclosed by an envelope of carbonated and micaceous altered pyroxenite which passes into an outer zone of unaltered pyroxenite. The altered zone is cut by numerous ring dykes and cone sheets of carbonatite and a satellite plug of carbonated mica pyroxenite is also present. Sr and Nd isotopic data suggest that the Cummins Range carbonatite may be related to the Bow Hill lamprophyre further north in the East Kimberley (Fig. 1), which is of comparable age.

The Mundine Well carbonatite is a series of lenses 700m in diameter which intrude a partially assimilated synclinal keel of the Archaean metavolcanic Western Shaw belt of the Pilbara Block of Western Australia (Fig. 1). Rock types include apatite-sovite, altered apatite-magnetite-silicocarbonate, apatite olivine sovite, and alkaline pyroxenite.

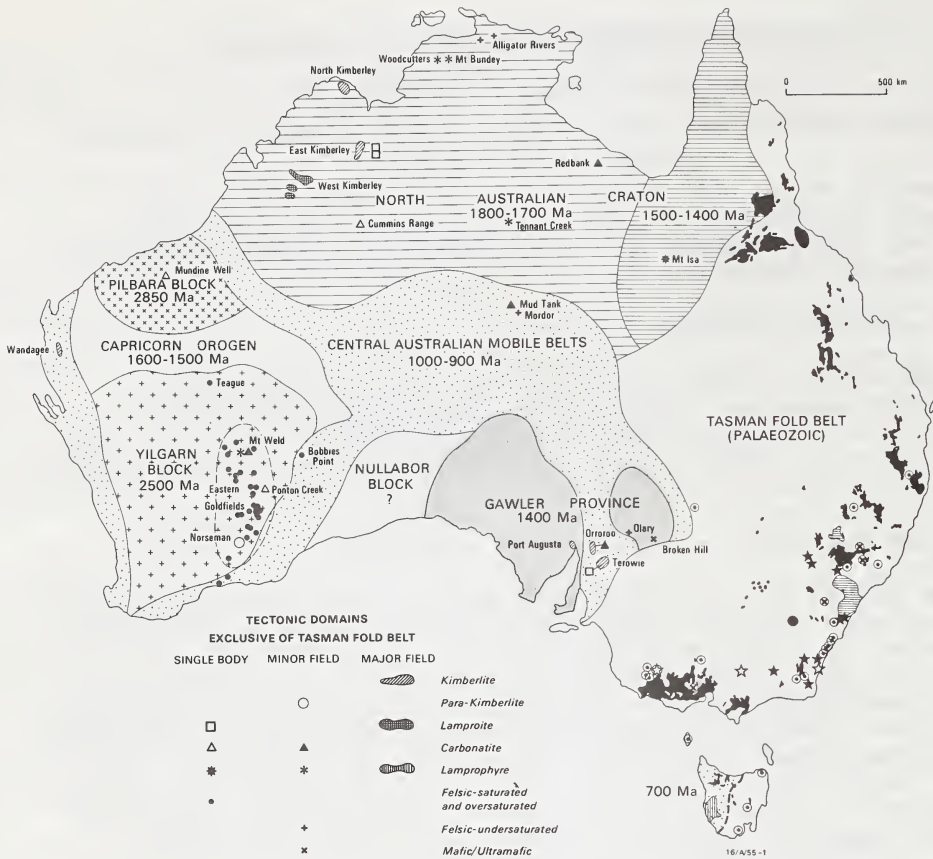


Fig. 1. Distribution of carbonatites and other alkaline rocks in Australia. Details of alkaline rocks in the Tasman Fold Belt are given in Jaques et al., (1985).

The 730 Ma Mud Tank Carbonatite intrudes Early Proterozoic granulites of the Strangways Metamorphic Complex in the southeast part of the Arunta Block in central Australia (Fig.1). The complex consists of a number of carbonate-rich lenses surrounded by mica-rich zones emplaced into poly-metamorphic granulites and granitoid cataclasites. Inclusions of syenite and granulite (some boudinaged) have been pervasively metasomatised and contain albite and alkali pyriboles. Mud Tank Carbonatite appears to have been emplaced at mid-crustal levels ( $\geq 15$  km) possibly during faulting related to the development of the late Proterozoic Amadeus Basin. Mud Tank differs from many other carbonatite complexes in having lower abundances of LREE and other incompatible elements and a slight decoupling of LREE from HREE.

The Redbank breccia pipes are a suite of some 50 carbonate-rich copper-bearing breccia pipes which intrude middle Proterozoic volcanic and dolomitic sedimentary rocks of the Macarthur Basin. Intense K-metasomatism and geochemical enrichments have previously been interpreted as indicating a carbonatitic affinity, viz. a carbonated K-rich trachytic magma. Recently the presence of carbonatitic volcanism has been questioned and the Redbank mineralisation interpreted as resulting from mixing of Cu- and sulphate-rich basal brines with reduced, hydrocarbon-bearing fluids from underlying country rocks with mineralisation occurring in fractures.

The Walloway carbonatite comprises small dykes and plugs of carbonate-rich lamprophyric rocks which intrude late Proterozoic metasediments of the Adelaide Fold Belt. The Walloway intrusions are closely associated with Jurassic (170 Ma) Orroroo kimberlites and isotopic and geochemical data suggest a genetic relationship (Nelson et al., 1988).

### Resources

The Mount Weld Carbonatite hosts a world-class REE deposit together with discrete deposits of Y, Ta, Nb and P developed in a 10-70m thick regolith zone over the carbonatite (Duncan and Willett, 1990). The REE mineralisation is mostly contained in supergene Th-deficient monazite but significant amounts of Y and HREE are contained in secondary churchite. The mineralised zone forms a discrete zone at the centre of the body and contains some 15.4 Mt at 11.2% REO plus yttrium with a cutoff grade of 5%. Included in this resource is a high grade zone of 1.35 Mt with a grade of 23.6% REO and a cutoff grade of 20%. Reserves of other metals include 250 Mt of phosphate at 18% (10% cutoff grade), 145 Mt of tantalum ore at a grade of 0.034% Ta<sub>2</sub>O<sub>5</sub> (0.02% cutoff) and 273 Mt of niobium ore at a grade of 0.9% Nb<sub>2</sub>O<sub>5</sub> (0.5% cutoff).

A REE-enriched regolith zone up to 60m thick is also developed over the Cummins Range Carbonatite and hosts sub-economic LREE, Nb, U and P mineralisation in the form of secondary monazite, and detrital monazite, apatite, pyrochlore and apatite. A resource of 3-4 Mt with a grade of 2-4% REO is inferred (Andrew, 1990).

The Mud Tank Carbonatite yields fine gem quality zircons (alluvial), and degraded mica-rich rocks (hydrobiotite and hydrophlogopite) are currently being evaluated as a vermiculite deposit.

Oxidised high grade ore has been mined from the Redbank copper deposits in the past. A subeconomic resource of 4 Mt with a grade of 2.5% Cu from primary ore bodies has been identified at the two major prospects and the deposits are currently being re-evaluated.

### References

- Andrew, R. (1990) In Hughes, F.E., Ed., *Geology of the mineral deposits of Australia and Papua New Guinea*, p. 711-714. Australasian Institute of Mining and Metallurgy Monograph 14.
- Duncan, R.K. and Willett, G.C. (1990) In Hughes, F.E., Ed., *Geology of the mineral deposits of Australia and Papua New Guinea*, p. 591-597. Australasian Institute of Mining and Metallurgy Monograph 14.
- Jaques, A.L., Creaser, J., Ferguson, J., and Smith, C.B. (1985). *Transactions of the Geological Society of South Africa*, 88, 311-334.
- Nelson, D.R., Chivas, A.R., Chappell, B.W. and McCulloch, M.T. (1988). *Geochimica et Cosmochimica Acta*, 52, 1-17.

## SPINEL – AS INDICATOR FOR DIAMOND.

*Zhou Jianxiong; Zhang Andi; Wang Wuyi; Xie Xilin; Guo Lihe.**Institute of Mineral Deposits, CAGS, 26 Baiwanzhuang Road, Beijing 100037, China*

This extended abstract will concern primarily with macrocryst spinel classification. It is proposed first to discuss the spinel group populations of typical kimberlite and lamproite bodies, to discuss their significance for diamond exploration, and then to discuss their origin. Only the principal points summarized below. Detailed description of the each spinel group and discussion can be found in other papers (Zhang Andi, 1991; Zhou Jianxiong, 1991).

Spinel is one of the most characteristic minerals of kimberlite and lamproite. Although its amount in kimberlite and lamproite varies widely from trace quantities up to about 0.3–0.5% (Sobolev, 1975), it is very resistant to physical and chemical weathering, and it is easily found in the concentration. They are abundant enough to act as indicator for primary source rock. There have been some successful examples in China. One of diamond bearing kimberlite pipe and one of diamond bearing lamproite field were found by tracing spinels.

However, for a long time, as Mitchell said (1987), determining provenance of spinel is still very difficult. It is analogous to the olivine macrocryst problem. And the composition of spinels from kimberlite and lamproite are similar to that of spinels from a wide variety of basic and ultrabasic rocks. Recently the people found the diamond bearing rocks always contain spinels which show similar chemical features to the mineral inclusions in diamond (Gurney, 1989, Dong and Zhou 1980).

In this study the classification of spinel is made by Q-cluster analysis, based upon the predominance of  $\text{Cr}_2\text{O}_3$ ,  $\text{Al}_2\text{O}_3$ ,  $\text{TiO}_2$  and  $\text{MgO}$ . The nearly 5000 analyses from above 68 rock bodies have been studied. Most of quantitative analyses were made by typical EPMA, that is wavelength dispersive spectrometry our lab. Very few came from the reference. The occurrences of spinels include in diamondiferous or barren kimberlites and lamproites, and other relative rocks, such as lamprophyres, basalts, alpine peridotites, layered basic intrusions and meteorite and so on, which are not only from 6 provinces in China, but also from South Africa, Australia, America and USSR. Fig.1 and Table 1 summary the main results obtained by the cluster analysis. These all 12 groups involve almost the all spinels occurred in above mentioned rocks. It is obvious that each group is characterized by different  $\text{TiO}_2$ ,  $\text{Al}_2\text{O}_3$ ,  $\text{Cr}_2\text{O}_3$  and  $\text{MgO}$  contents. And it is easily recognized by computer program based upon the amount of compositions. S1, S2 and S3 groups with very high  $\text{Cr}_2\text{O}_3$  and  $\text{MgO}$  are all direct indicators for diamond. They all contain very low  $\text{Al}_2\text{O}_3$  and  $\text{TiO}_2$ , although they have a little different each other. S1 group almost does not contain  $\text{TiO}_2$ . S2 group contains about 1%  $\text{TiO}_2$ . S3 group contains very high  $\text{Cr}_2\text{O}_3$  and  $\text{MgO}$ , mainly found in meteorite. S4 group can be found in a variety of occurrences, including kimberlite and lamproite. Usually this group were further subdivided according to the  $\text{TiO}_2$  content. S5 group with high  $\text{Al}_2\text{O}_3$  is not typical to kimberlite and lamproite. S6 group with low  $\text{Al}_2\text{O}_3$  and high  $\text{TiO}_2$  is typical for kimberlite, and sometimes found in lamproite. S7 group with high  $\text{Al}_2\text{O}_3$  and  $\text{TiO}_2$  is typical for lamproite, but also found in kimberlite, especially

in mica kimberlite. Other groups are not very important and very easy to discriminate. This classification has been proved very useful for following three fields:

(1) Simplifying the quantitative description for spinel groups in kimberlite, lamproite and other rocks. Fig2 shows the spinel group populations in a few typical kimberlites and lamproites which are characterized for each rock.

(2) Simplifying the description for spinels from nature concentrates. It is very useful to exploration of diamond.

(3) Studing spinel origin.

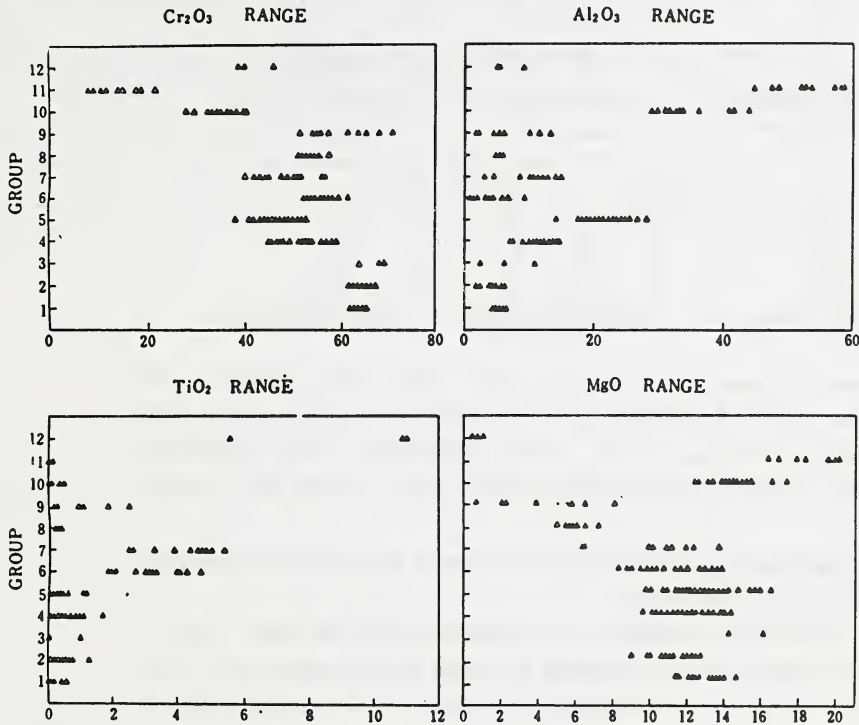


Fig.1. Compositional ranges for 12 group spinels. Obtained by cluster analysis. It shows the different among 12 group spinels.

Table 1. Averaged compositions each group

Group	Name	TiO <sub>2</sub>	Al <sub>2</sub> O <sub>3</sub>	Cr <sub>2</sub> O <sub>3</sub>	MgO	Occurences
S1	poor Ti, Al rich Mg chromite	0.12	5.29	64.00	12.72	Inc KimD LamD
S2	titanian poor Al rich Mg chromite	0.42	4.29	64.63	11.07	Inc KimD LamD
S3	High Mg, Cr chromite	0.36	6.54	67.37	15.43	Met Inc KimD
S4	poor Ti rich Al, Mg chromite	0.48	12.17	52.81	11.69	Lay Chr Lam Kim
S5	poor Ti high Al chromite	0.43	21.67	47.21	13.04	Lap Kim Chr
S6	rich Ti poor Al chromite	3.14	3.87	57.52	10.89	Kim Lam
S7	hith Ti rich Al chromite	4.08	10.25	48.43	10.32	Lam Kim2
S8	poor Al low Mg chromite	0.28	3.35	54.51	5.91	Ler
S9	low Ti rich Fe chromite	0.68	6.17	60.71	3.56	Met Chr
S10	poor Ti rich Cr Mg-Al spinel	0.13	34.14	35.38	14.40	Lap Kim
S11	chrome Mg-Al spinel	0.06	52.50	14.35	18.56	Bas
S12	high Ti rich Fe chromite	9.15	6.49	41.77	0.72	Met

Notes: Inc, inclusion in diamond; KimD, diamondiferous kimberlite; LamD, diamonodiferous lamproite; Kim, Kimberlite; Kim2, mica kimberlite; Lam, lamproite; Lay, layered basic intrusion; Chr, alpine chromite deposits; Lap, lamprophyre; Ler, lherzolite; Met, meteorite; Bas, basalt.

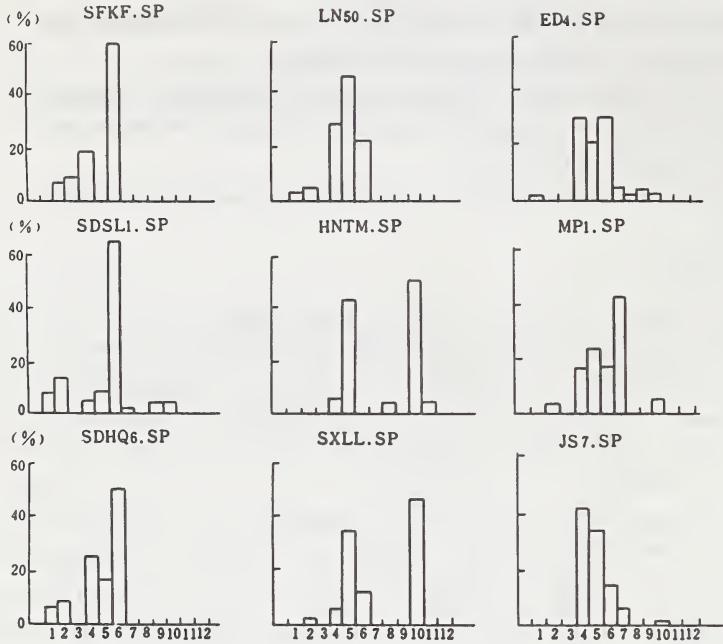


Fig. 2 Histograms of spinel group population from some typical kimberlites and lamproites. Diamondiferous: SFKF, Koffiefontein SA; ED4, Ellendal, WA; SDSL1, Shandong SL1 China; SDHQ6, Shandong HQ6 China; LN50, Liaoning LN50 China; MP1, Guizhou MP1 China, lamproite; Barren: HNTM, Hunan TM China; SXLL, Shanxi LL China; JS7, Hubei JS7 China, lamproite.

The results of present studying show the following criterias which the geologists must consider during the exploration of diamond:

(1) Chemically spinels from kimberlites and lamproites exhibit the widest ranges in  $TiO_2$ ,  $Al_2O_3$ ,  $Cr_2O_3$  and  $MgO$  contents comparing with those of non-kimberlites. This is a very important criteria which we must consider any time. The distribution figers of  $Cr_2O_3-Al_2O_3$ ,  $Cr_2O_3-TiO_2$  and  $Cr_2O_3$  and  $Cr_2O_3-MgO$  are very important for estimating of source rocks.

(2) Macrocryst spinels can be considered to be xenocrysts derived from dunites, harzburgites, lherzolites and pyroxenite which have different P and T physical conditions. In other words, as the paragenesis from dunite to pyroxenite the  $Cr_2O_3$  in spinel decreases with simultaneous increase in amount of  $Al_2O_3$ . That is why that diamondiferous rocks usually contain more groups than barren rocks.

(3) S1 and S2 group spinels directly indicate if the diamond present or not. Diamond bearing kimberlites or lamproites always contain these spinels (see Fig.2). It is possible to use these spinels as semiquantitative criteria. These spinels can be called syngenetic chromite with diamond or diamond phase chromite, and may be used as indicator for finding of new source rocks.

(4) S6 group spinel is very special indicator for kimberlite, S7 group spinel is very special indicator for lamproite. It is very clear to see in the Fig.2. Only in barren rocks S6 and S7 groups were replaced by S5 and S10 groups, for example, the spinels in Hunan and Shanxi kimberlite fildes, China (Fig.2).

(5) According to above mentioned criteria, a comprehensive understand about spinel in a kimberlite or lamproite body can be made based upon at least 50 grain spinel

analyses. It means that more analyses of spinel must be done during the exploration, otherwise it is possible to lose useful information.

(6) Spinels from reletive rocks are different from spinels in kimberlites and lamproites in spinel group population. It is easy to discriminatc each other.

#### Reference

1. Zhang Andi et al., 1991, Database of Indicator Minerals for Diamond (in Chinese with English abstract) .
2. Zhou Jianxiong et al., 1991, Classification of spinel and its significance (in press) .
3. Sobolev N.V. et al., 1975 *Geology and Geophysics* V.16, No.11, P.7-24.
4. Mitchell R. H., 1986, *Kimberlites: Mineralogy, Geochemistry and Petrology*. Plenum Publ. Corp., New York.
5. Gurney J.J., 1989, *Kimberlites and Related Rocks* V.2, P.935-965.
6. Dong Zhenxin. and Zhou Jianxiong, 1980, *Acta Geologica Sinica*, No. 4, P.284-299.

**UNUSUAL SPINEL-GARNET LHERZOLITE XENOLITHS FROM BASALT IN  
EASTERN CHINA: CONSTRAINTS ON THE LATE-TERTIARY THERMAL  
STRUCTURE OF THE UPPER MANTLE.**

*Jin, <sup>(1,2)</sup>Z.-M.; Green II, <sup>(1)</sup>H.W.; Borch, <sup>(1)</sup>R.S. and Tingle, <sup>(1)</sup>T.N.*

*(1) Department of Geology of California, Davis, CA 95616 USA; (2) Department of Geomechanics, University  
China University of Geosciences, Wuhan 430074, PRC.*

Although garnet peridotite xenoliths are common from kimberlite, they are quite rare in basalts. Xenoliths in which coexisting spinel and garnet are found are even more rare. We have identified spinel-garnet lherzolite xenoliths from three localities in Eastern China: A Pliocene alkalic basalt in Nushan County, Anhui Province; a Plio-Pleistocene nephelinite basalt and limburgite in Mingxi County, Fujiang Province; and a Plio-Pleistocene nephelinite tuff in Zhejiang Province. The first locality is in close proximity to the Tangcheng-Lujiang deep fault and the other two are associated with the deep fracture system of the south-east coast of China. The thickness of the crust in these regions is 31-33 km.

These special xenoliths are very similar in both localities. They are 5 - 20 cm in diameter and all are five-phase peridotites (olivine-enstatite-diopside-garnet-spinel) with the following volume proportions: Olivine (55-65%); Orthopyroxene (20-30%); Clinopyroxene (10-15%); Garnet (3-6%); Spinel (2-5%). They have coarse-tabular textures with a distinct foliation defined by elongated olivines and pyroxenes and aligned spinels. The garnets are round and lacking in inclusions; in most cases they have a well-developed thin, fibrous, kelyphitic reaction rim consisting of pale brown translucent spinel and pyroxene. Examination of the dislocation microstructure of the olivines using the oxidation decoration technique also found them to be very similar. In both localities, the olivines of these xenoliths, like the more-abundant spinel peridotites, show evidence of three stages of plastic deformation: (i) Wide, straight, (100) subgrain boundaries induced by low stress deformation; (ii) very narrow (100) boundaries induced by higher stress deformation; (iii) local development of {110} slip bands produced by still higher stresses associated with xenolith extraction from the mantle by the magma (Jin et al., 1989).

All phases of these rocks are homogeneous in chemical composition. Analyses were determined with a Cameca electron microprobe. A representative example from each locality is presented in Table I:

TABLE 1: Composition (wt %) of 5-phase Lherzolite Xenoliths from Eastern China

	MINGXI #M-3					NUSHAN # N-3				
	Ol	Opx	Cpx	Ga	Sp	Ol	Opx	Cpx	Ga	Sp
SiO <sub>2</sub>	40.77	54.39	51.76	41.76	0.11	40.80	53.64	51.03	42.17	0.12
TiO <sub>2</sub>	0.11	0.13	0.43	0.17	0.26	0.01	0.16	0.48	0.16	0.21
Al <sub>2</sub> O <sub>3</sub>	-	3.27	6.14	23.26	49.20	-	5.65	7.53	22.34	56.42
Cr <sub>2</sub> O <sub>3</sub>	0.02	0.50	1.15	1.27	17.09	0.02	0.36	0.69	1.04	9.01
FeO	9.39	6.38	3.15	7.71	11.88	10.49	7.06	3.90	7.69	11.76
MnO	0.13	0.12	0.05	0.36	0.09	0.13	0.16	0.13	0.45	0.08
MgO	49.27	33.77	16.07	20.54	20.22	48.66	32.52	16.33	21.86	21.29
NiO	0.38	-	-	-	-	0.38	-	-	-	-
CaO	0.08	0.79	18.41	5.07	0.33	0.11	0.22	17.97	4.87	0.39
Na <sub>2</sub> O	-	0.17	1.73	-	0.01	-	-	0.70	0.06	0.10
Total	100.05	99.52	99.06	100.16	99.14	100.60	100.82	99.76	100.64	99.38

The chemical compositions of these lherzolites are similar to the few published analyses of other 5-phase peridotites. The correspondence with a xenolith from the Massif Central in France (Berger and Brousse, 1976; Berger, 1977) is particularly striking because of the similarly high Al<sub>2</sub>O<sub>3</sub> and low Cr<sub>2</sub>O<sub>3</sub> contents. A spinel-garnet xenolith from the Pali-Aike volcanic field, Chile (Skewes and Stern, 1979; Stern et al., 1984) and one from a kimberlite in New South Wales, Australia (Ferguson et al., 1977) have significantly more Cr<sub>2</sub>O<sub>3</sub> in the spinels and those from kimberlite in Lesotho, S. Africa (Nixon and Boyd, 1973) are very much richer in Cr<sub>2</sub>O<sub>3</sub> and lower in Al<sub>2</sub>O<sub>3</sub>.

Temperatures and pressures of equilibration were estimated for specimens M-3 and M-4 (Mingxi) and N-3 (Nushan) using the geothermometer of Nickel and Green (1985) and the geobarometer of Bertrand and Mercier (1985). The calculated conditions of equilibration were: #M-3: 1020°C, 1.8 GPa (62 km); #M-4: 1100°C, 2.62 GPa (85 km); #N-3: 1100°C, 1.9 GPa (63 km). These conditions are consistent with stable coexistence of garnet and spinel in chrome-poor peridotite (O'Neill, 1981). To facilitate direct comparison between these xenoliths and those from the literature, we also used the same thermobarometric method to calculate the conditions of equilibration of the 5-phase peridotites from the Massif Central, Lesotho, Pali-Aike, New South Wales, and another garnet-spinel peridotite from Bow Hill, Tasmania for which analysis of the spinel has not been published (Sutherland et al., 1984). The last three of these xenoliths all lie within the range of our temperature and pressure determinations; those from the Massif Central are hotter and deeper (~1270°C; 77 km) and those from Lesotho are much colder and much deeper (~900°C; 115 km). Thus, all of these 5-phase lherzolites except those from South Africa plot on an elevated geotherm whereas those from Lesotho lie on a typical 40 mW/m<sup>2</sup> continental geotherm.

Eastern China has more than 7 localities of garnet peridotite from basalt including at least three localities of spinel-garnet lherzolite. Thus, this area may be a particularly useful region for determination of the structure and composition of this critical depth region of the subcontinental mantle. The opportunity to determine precise temperature and pressure conditions for these unusual xenoliths also will allow us to anchor the geotherm for these regions and thereby assign pressures to spinel lherzolite xenoliths for which only accurate temperatures can be directly determined.

#### REFERENCES

- Berger, E. (1977) Sur la présence d'une lherzolite à grenats en enclave dans le basalte alcalin de la Vestide du Pal (Ardèche): Conditions d'équilibre, implications pétrogénétiques et géotectoniques. *C. R. Acad. Sci. Paris, Fr.*, D. 284, 709-712.
- Berger, E. and Brousse, R. (1976) Une lherzolite à grenats du pipe d'Eglazine (Lozere, France) stabilisée à 1400°C et 30kb. *C. R. Acad. Sci. Paris. Fr.*, D. 282, 1477-1480.
- Bertrand, P. B. and Mercier, J.-C. (1985) The mutual solubility of coexisting ortho- and clinopyroxene: towards an absolute geothermobarometer for the nature system. *Earth Planet. Sci. Lett.* 76, 109-122.
- Ferguson, J., Ellis, D.-J., and England, R. N. (1977) Unique spinel-garnet lherzolite inclusion in kimberlite from Australia. *Geology* 5, 278-280.
- Jin, Z.-M., Green II, H. W. and Borch, R. S. (1989) Microstructures of olivine and stress in the upper mantle beneath eastern China. *Tectonophysics* 169, 23-50.
- Nickel, K. G. and Green, D. H. (1985) Experimental geothermobarometry for garnet peridotites and implications for the nature of the lithosphere, kimberlite and diamonds. *Earth Planet. Sci. Lett.* 73, 158-170.
- Nixon, P. H. and Boyd, F. R. (1973) Petrogenesis of the granular and sheared ultrabasic nodule suite in kimberlites. *Lesotho Kimberlites* by Nixon, P. H. (Editor) 48-56.
- O'Neill, H. St.C (1981) The transition between spinel lherzolite and garnet lherzolite and its use as a geobarometer. *Contrib. Mineral. Petrol.* 77, 185-194.
- Skewes, A. and Stern, C. R. (1979) Petrology and geochemistry of alkali basalt and ultramafic inclusions from the Pali-Aike volcanic field in Southern Chile and the origin of the patagonian plateau Lavas. *J. Volcanol. Geotherm. Res.* 6, 3-25.
- Sutherland, F. L., Hollis, J. D., and Barron, L. M. (1984) Garnet lherzolite and other inclusions from a basalt flow, Bow Hill, Tasmania. *Kimberlites II: The Mantle and Crust - Mantle Relationships*. Kornprobst, J. (Editor), 145-160, Elsevier, Amsterdam.
- Stern, C. R., Saul, S., Skewes, M. A. and Futa, K. (1989) Garnet peridotite xenoliths from the Pali-Aike alkali basalts of southernmost South America. *Kimberlites and Related Rocks*, Volume 2, *Geol. Soc. Australia Spec. Publ.* 14. Ross, J. et al. (Editors). 735-744.

## CARBONADO AND YAKUTITE: PROPERTIES AND POSSIBLE GENESIS.

*Kaminsky, F.V.**Central Research Inst. Geol. Prospecting for Base and Precious Metals, Moscow, 113545 USSR.*

Two types of carbonado are currently known, which are essentially different in composition, properties, the way of formation: it is common carbonado of Brazilian type, and yakutite. The latter was first encountered in the 60-s in placers of the Northern Yakutia and was called by the name of this region. It is represented by grains of flattened hexagonal form, not very large in size. Its main peculiarity is the presence of hexagonal carbon modification - lonsdaleite. It is characterised also by more heavier carbon isotopic composition as compared to carbonado, very low paramagnetic nitrogen content, and other peculiarities, which are generalized in Table:

Grain properties	Carbonado	Yakutite
Shape	irregular, isometric	flattened-hexagonal
Mass, carat	1-40 (up to 3167)	0.01-0.2 (up to 3)
Crystallite size, mkm	0.5-80 (usually 10-40)	0.1-1
Structure	not observed	10-90°
The presence of non-diamond carbon phases	none	lonsdaleite (up to 50%), chaoite also may be present
Photoluminescence spectra	N3, H3, H4, T1 systems	non-structural wide band
Paramagnetic nitrogen impurity (C-center, cm <sup>-1</sup> )	4·10 <sup>18</sup> - 3·10 <sup>19</sup>	absent (less than 10 <sup>15</sup> )
Other paramagnetic centers, cm <sup>-1</sup>	5.5·10 <sup>17</sup> - 4.5·10 <sup>18</sup>	2·10 <sup>18</sup> - 1.2·10 <sup>19</sup>
Carbon isotope composition (δ <sup>13</sup> C, PDB, o/oo)	-23.2 - -30.6	-9.9 - -20.1
Hydrocarbon component impurity, %	up to 0.n	insignificant

A set of structural-compositional peculiarities of carbonado and yakutite allows to consider them as independent mineral varieties, which genetically differ from one another and from diamond.

Primary occurrences of yakutite were encountered in impact metamorphic rocks and also in stone and iron meteorites. Experimental conditions of obtaining of lonsdaleite-bearing

aggregates (momentary impact loading above 150 kb) and cry-stallographic study of yakutite show, that they are para-morphs after graphite, formed as a result of extremely high momentary loading explosive type.

The problem of genesis of carbonado of classical Bra-zilian type is more complicated, because it has been never encountered in primary occurrences. The absence of carbonado findings in kimberlites and lamproites in spite of more than a century of mining of primary deposits in Africa, Siberia, Australia, as well as the peculiarities of carbonado compo-sition permit us to draw a conclusion, that this mineral is associated neither with kimberlites no lamproites, and it is most of all of non-plutonic origin. Based upon studies of carbonado structure L.F.Trueb and W.C.Butterman, and C.Jeynes suggested, that carbonado is an analogue of cera-mics and was formed as a result of high-temperature sintering when adsorbed impurities were eliminated and diamond particles were partially recrystallised. We could consider this mechanism of carbonado formation to be real, taking into account an experimental support for such sintering when producing of artificial carbonado.

Howewer artificial carbonados greatly differ from natu-ral ones by essentially bigger crystallite size, the pre-sence of paramagnetic nitrogen, and other features. The most essential from genetic point of view is high density of dislocations in crystallites of natural carbonado, which have been studied by Y.Moriyoshi et al. Dislocations in cry-stallites are chaotically oriented and do not show polygoni-zation (as it takes place in balas crystallites). As dislo-cations are thermodynamically unstable element of crystalli-te structure and diffuse when heating, preliminary subjected to poligonization, the real pattern contradicts with hypo-thesis of high-temperature sintering with pressure. To ex-plain the genesis of natural carbonado we propose a hypothe-sis of crystallite formation without high pressure under lo-cal heating of carbon substrate. Small crystallite size is a decisive factor in this case.

When studying fine-dispersed metallic and other phases it was established, that surface energy in the smallest (1-100 nm) newly formed crystallites is an independent thermo-dynamic potential, which under certain conditions has an opposite direction as related to chemical potential. Due to this fact the parameters of phase transitions for small cry-stal particles depend on their sizes. This phenomenon was called as "phase dimension effect". If, besides pressure and temperature, we introduce into phase equilibrium calculation the third independent parameter "r", an effective crystalli-te radius, we obtain the following energy condition of sta-bility of crystallite diamond structure:

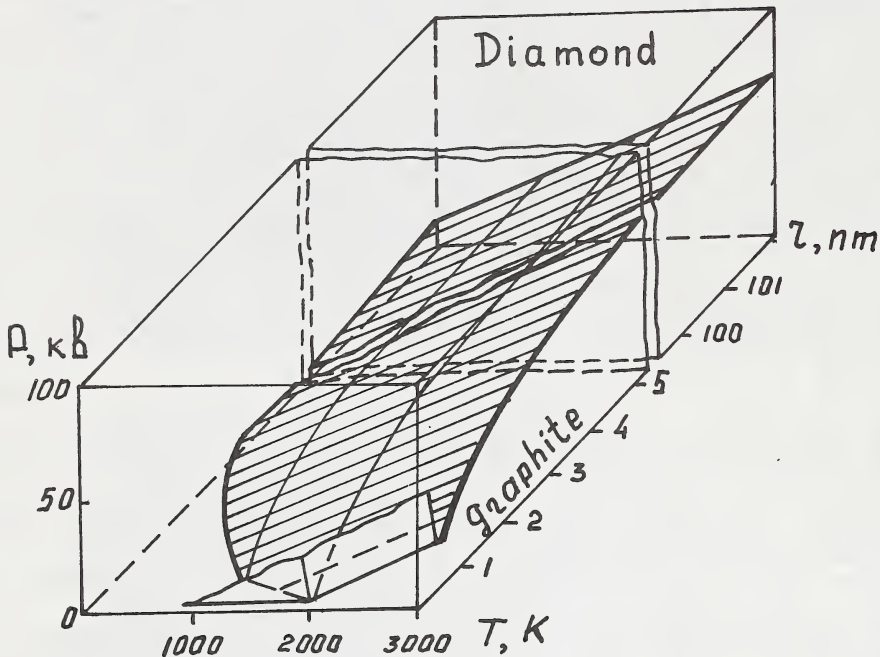
$$\Delta M^V - \left[ (\epsilon_1 \epsilon - \epsilon_2 \frac{d}{a}) \frac{z}{a} - \frac{\epsilon_1 b}{2} \frac{d}{a} \right] \left[ \epsilon \frac{z}{a} \left( \frac{z}{a} + b \right) \right]^{-1} < 0;$$

where  $\Delta M^V$  - difference of volumetric chemical potentials of diamond and graphite,

$\epsilon_1, \epsilon_2$  - difference of energies of  $\sigma$ -bonding and  $\pi$ -bonding in graphite and diamond,

$z, d, a, b, \epsilon$  - geometric parameters of graphite and diamond crystallites.

A diagram of diamond phase equilibrium, calculated from this equation, is described as a surface in space with following coordinates: pressure - temperature - crystallite size:



If the second ("surface") member of the above equation is insignificant ( $r \gg 100$  nm), then the diagram of graphite/diamond equilibrium does not differ from the known one. However as crystallite size decreases ( $r \leq 10$  nm), the surface of phase equilibrium is noticeably deflected to the area of low pressures, while with the " $r$ "  $\sim 1$  nm diamond is stable even in the absence of external pressure in the temperature field up to 2000 K,

Based upon the above constructions we could suggest carbonado formation beyond high pressure field. In this case we could practically explain all the peculiarities of carbonado: degree and nature of dislocations in crystallites; essential impurities of polymerized hydrocarbon compounds; carbon isotopic composition, corresponding to organic matter; and inclusions of mineral phases uncommon for diamond.

# PETROGENETIC CARBONATITE - MELILITTE RELATIONSHIPS IN THE KAISERSTUHL COMPLEX, UPPER RHINEGRABEN.

Keller, Jörg.

Mineralogisch-Petrographisches Institut der Universität Freiburg D-7800 Freiburg, FRG.

In the alkaline rock/carbonatite complex of the Kaiserstuhl, Rhinegraben, the petrogenetic link between calciocarbonatites and silicate melts is represented by highly evolved ultrabasic melilitite-nephelinites. These compositions are traditionally termed *bergalites* (Soellner, 1913). Bergalites are calcite-bearing hauyne-nepheline-melilite-perovskite-apatite-magnetite rocks with SiO<sub>2</sub> contents of 31-37% (Table 1). In several petrological and geochemical aspects bergalites are similar to *turjaites* and *okaites* both being closely associated with carbonatites.

Bergalites occur as dyke rocks in the final stage of magmatic evolution, together with late alvikitic carbonatite dykes (lehnert, 1988). Often both rock types occur together in form of double dyke intrusions.

Sr-, Nd-, and Pb-isotopic evidence groups bergalites of the Kaiserstuhl closely together with carbonatites, and with the olivine nephelinitic and olivine melilititic primary magmas of the Rhinegraben area (Schleicher et al.1990). These three rock types form a petrogenetically coherent association.

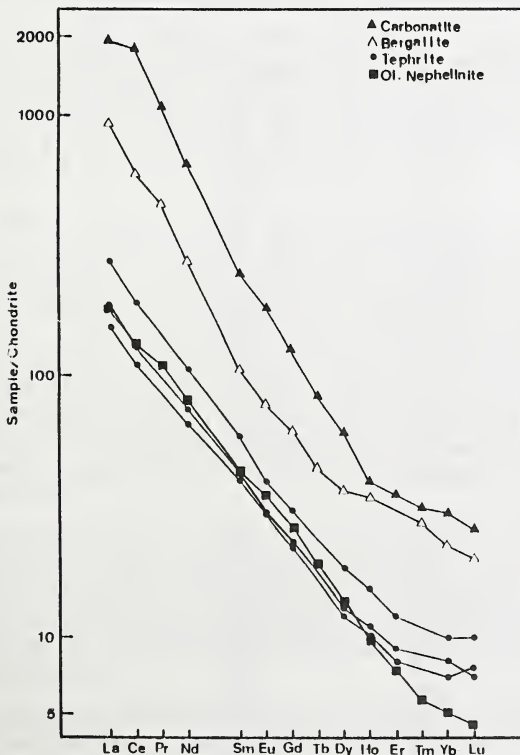


Figure 1: REE contents and patterns of bergalites from the Kaiserstuhl, compared to primary olivine nephelinite, carbonatite and tephrites.

The carbonate content which characterizes bergalites occurs in the form of late stage vugs or interstitial matrix. C/O isotopes have generally acquired a low temperature re-equilibration, however some examples with carbonate isotopic compositions falling in the field of primary igneous carbonatites have been analyzed (Hubberten et al. 1988).

Bergalites are considered transitional between carbonatites and the silicate magmas. Their chemical composition is quite variable (Table 1), but all varieties are highly fractionated with Mg-values of 54 to 38, and low Sc, Ni, Cr, Co contents. Bergalites are distinctly enriched in incompatible elements, especially Sr, Ba, LREE, Nb etc. giving in general a carbonatitic trace element signature. Bergalites are modelled having fractionated from primary olivine-melilite nephelinite at intermediate to high pressure. This extended fractionation is responsible for trace element and CO<sub>2</sub> enrichment. Carbonatite separation occurs at shallow level, but there is no unambiguous petrographic evidence available to decide whether final separation involves liquid immiscibility or residual melt separation. Bergalitic magma compositions (including okaites and turjaites) seem to occur in several carbonatite complexes and their petrogenetic role in the evolution of carbonatites merits focused petrologic attention.

#### References:

- Hubberten HW, Katz-Lehnert K and Keller J (1988) *Chem Geology* 70: 257-274  
 Keller J (1984) *Fortsch Mineral* 62, Beih 2: 2-35  
 Keller J, Brey, G., Lorenz, V. & Sachs, P. (1990) *IAVCEI Int. Volc. Congress Mainz 1990. Field Guide* 60p.  
 Lehnert K (1989) PhD dissertation Univ Freiburg, 290pp.  
 Schleicher H, Keller, J and Kramm U (1990) *Lithos* 26:21-35  
 Soellner J (1913) *Über Bergalith, ein neues melilithreiches Ganggestein aus dem Kaiserstuhl. Mitt Bad geol LA* 7: 415-466

TABLE 1: Chemical compositions of bergalites from Kaiserstuhl Rhinegraben.

SiO <sub>2</sub>	31.96	33.63	35.00	36.15
TiO <sub>2</sub>	1.44	1.73	1.87	1.61
Al <sub>2</sub> O <sub>3</sub>	12.66	13.30	12.58	14.22
Fe <sub>2</sub> O <sub>3</sub>	6.06	5.69	6.82	6.51
FeO	3.79	4.43	3.75	3.98
MnO	.46	.43	.35	.48
MgO	3.00	3.78	4.54	5.71
CaO	16.65	13.79	16.94	11.33
Na <sub>2</sub> O	3.94	6.93	4.40	6.59
K <sub>2</sub> O	2.80	2.04	1.14	2.59
P <sub>2</sub> O <sub>5</sub>	.68	.86	1.13	.81
CO <sub>2</sub>	8.32	6.71	4.75	3.34
SO <sub>2</sub>	.62	.90	.70	2.02
H <sub>2</sub> O	5.84	4.90	4.76	2.11
Total	98.22	99.12	98.38	97.45
V	466	430	510	526
Ni	16	2	15	0
Ba	3337	2320	1882	2909
Sr	3255	3003	3125	2982
Nb	565	548	447	553
La	368	306	263	280
Ce	431	546	479	421
Y	61	73	69	65
Zr	297	420	334	383

## DEVELOPMENTS IN REMOTE SENSING OF CARBONATITES; AIRBORNE IMAGING SPECTROMETRY AT MOUNTAIN PASS, CALIFORNIA AND IRON HILL, COLORADO.

*Kingston, M.J.*

*U.S. Geological Survey, MS 927, Reston, VA 22092 USA.*

Data acquired with the NASA Airborne Visible/Infrared Imaging Spectrometer (AVIRIS) over Mountain Pass in California and Iron Hill in Colorado were analyzed to evaluate the use of narrow-band imaging data for carbonatite exploration as well as for regional geologic mapping. The AVIRIS instrument utilizes a linear array of discrete detectors and 4 spectrometers to collect 224 channels of data over the 400 to 2400 nm wavelength region. The spatial resolution is 20 m for swaths 10.5 km wide.

At Mountain Pass, three flightlines of data were collected over the rugged mountain range which encompasses the carbonatite. A block of Precambrian metamorphic rocks, which are the oldest rocks in the region, is exposed in the eastern flank of the mountains; more resistant Paleozoic sedimentary rocks form the higher western half of the range. The metamorphic complex consists primarily of light-colored granite augen gneiss, biotite granite gneiss and garnet gneiss that are intricately interlayered. These rocks are bounded by normal faults on the northeast and by the extensive north-trending Clark Mountain fault on the west. The carbonatite as well as several bodies of potassium-rich igneous rocks intrude the granite augen gneiss. The carbonatite stock which is the major source of light rare-earth elements (REE) in the United States, was selected several years ago as a test site for evaluating AVIRIS capabilities for detecting REE absorption features.

Dolomite is the most widely distributed lithology in the thick sequence of sedimentary rocks exposed west of the Clark Mountain fault. The area is well suited for remote sensing studies because of the sparse nature of Mohave desert-type vegetation, including Joshua and juniper trees, mesquite, grasses and various cacti.

One flight line of AVIRIS data was acquired over the Iron Hill carbonatite, which also was emplaced in Precambrian metamorphic rock, principally granite gneiss. The dolomitic carbonatite (rauhaugite) appears in plan view as a two-lobed stock. Carbonatite dikes radiate outward from the stock, cutting the associated alkalic rocks which surround the rauhaugite core. The alkalic rocks include pyroxenite, uncomphagrite, ijolite and nephelene syenite. A zone of fenitized rocks, formed by metasomatic alteration of the granite and felsite country rocks, surrounds the carbonatite complex.

Vegetation is considerably more dense in southwestern Colorado than at Mountain Pass. In such areas of moderate to heavy vegetation, a special problem exists in interpreting airborne imagery because mineral spectra may be diluted or masked by spectral features associated with chlorophyll and cellulose.

Various methods can be used to enhance high-resolution airborne data as well as to remove atmospheric and solar

irradiance effects. Two complementary approaches were used at Mountain Pass: (1) the construction of relative absorption band depth (RBD) images and (2) the use of ground-based spectral measurements to calibrate the AVIRIS radiance data to reflectance.

The initial step was to generate the RBD images directly from the data. The resulting images emphasize diagnostic spectral features of minerals, while minimizing reflectance variations due to topographic slope and albedo differences. The specific wavelengths that define the absorption band shoulders and minimum were determined from laboratory spectral reflectance measurements of samples collected in the field area. The absorption bands initially chosen were those positioned at 2200 nm (Al-OH), 2310 nm (dolomite) and 2330 nm (calcite) wavelengths. To construct an RBD image, two or three channels from each absorption band shoulder are summed and then divided by the channels that define the band minimum. Each RBD image is sensitive to a particular absorption feature. Three RBD images may be displayed as a red-green-blue color composite.

Because there are strong atmospheric features in the visible range near the REE spectral bands, RBD images are unsuccessful in defining the presence of REE-bearing rocks. However, such detailed spectral information may be extracted from the AVIRIS radiance data after it has been calibrated to reflectance. An empirical regression calibration was used to achieve this at Mountain Pass. Spectral reflectance measurements were made in the field during the AVIRIS overflight using several targets of different brightness. These reflectance values were regressed against AVIRIS digital numbers and the calculated gain vs. offset correction applied to AVIRIS data over a wide area having similar surface elevation and sky conditions. AVIRIS "spectra" may then be extracted for individual pixels.

Many of the lithologic units were discriminated on the RBD composite images. At Mountain Pass, granite gneiss, dolomite outcrop and the surrounding calcitic alluvial material are clearly separated on a 2200-nm, 2310-nm and 2330-nm RBD color composite image. Granite and quartzite could be separated because the intensity of the 2200-nm absorption feature due to muscovite is directly related to the proportion of that mineral in each rock type. The Clark Mountain fault is delineated on the image both in areas of bedrock and alluvium. Skarn deposits were revealed west of Mountain Pass.

The REE spectral reflectance features of interest to remote sensing are the narrow, sharp absorption bands due to Nd which occur near 580, 740, 800, and 860 nm. It is possible to detect these narrow Nd features only because of the high spectral resolution (AVIRIS channels are only 10 nm apart). At Mountain Pass, spectra which displayed the Nd features were observed in pixels extracted from the mine area. Spectra were extracted which displayed the calcite features at 2330 nm and the 2200 nm feature due to Al-OH-bearing minerals in the granite country rock. Spectra were also extracted from major lithologic units, alluvial fans and areas of hydrothermal alteration and compared with a library of laboratory spectra for mineral identification.

Processing the data at Iron Hill was complicated by the moderately heavy vegetation cover. Various RBD images were

generated but vegetation obscured much of the mineralogical information. The characteristic carbonate feature for rauhaugite, near 2310 nm, coincides with the wavelength region for cellulose absorption. However, vegetation is not so dense at lower elevations, and rauhaugite dikes were located crosscutting the alkalic rocks. The most successful RBD image for spatial definition of the rauhaugite stock represented a broad, but sometimes intense band centered near 1100 nm. This distinct feature, which may occur as a doublet in laboratory spectra, is assigned to ferrous iron that substitutes for magnesium in the dolomite lattice. Results of laboratory spectral measurements of carbonatite samples collected world wide indicate that this absorption feature is common in rauhaugite samples although it is rare in sedimentary or metamorphic dolomites. The distribution of alkalic rocks could also be mapped by the ferrous iron RBD image. The spectral response displayed by rauhaugite is more intense, enabling the separation of the stock and dikes from the alkalic rocks.

A distributed flat field correction was used to remove atmosphere effects from the Iron Hill AVIRIS data so that spectra could be extracted. This technique is an alternative to the empirical regression process used at Mountain Pass and is useful when in situ spectral measurements have not been made. For this calibration, RBD images were first examined to identify pixels having weak or absent mineral and vegetation absorption bands. The average radiance spectrum of these scattered, spectrally flat pixels was then divided through the data set.

Dolomite spectra were extracted from the calibrated Iron Hill data, but there has been limited success in extracting Nd absorption bands. The REE content of Iron Hill carbonatite rocks is low and Nd bands are weak or nonexistent in laboratory and field spectral measurements of these rocks. Also, a chlorophyll absorption band occurs near the Nd feature at 680-nm which will conceal weak Nd features. The next step in future processing of these data is to "unmix" the vegetation, so that the spectral response of underlying rocks and soils may be detected.

High-resolution multispectral imagery is potentially a very effective tool for geologic mapping, both because certain surface minerals can be identified by their spectral-reflectance characteristics and because remote sensing provides a synoptic view of landforms. Imaging spectrometers such as AVIRIS provide sufficient spectral sampling to define diagnostic spectral signatures on a per-pixel basis.

A useful approach to the processing of AVIRIS data is to first construct RBD images, so that the major lithological units may be separated. These images also quickly provide information on the provenance of alluvial material and may show structural details in areas of limited bedrock exposure. For detailed mineralogical characterization, calibration to reflectance units is necessary, so that spectral curves may be extracted and interpreted for selected areas. Because carbonatites display a unique combination of spectral characteristics, including carbonate, Nd, and often ferrous iron absorption features, these methods are useful not only for exploration of carbonatites, but also for the delineation of the surface extent of the carbonatite core, dikes and related alkalic rocks.

## HIGH-RESOLUTION ION-PROBE ANALYSES OF RARE EARTH ELEMENTS IN KIMBERLITIC ZIRCONS.

*Kinny, P.D.*

*Research School of Earth Sciences, Australian National University, GPO Box 4, Canberra, 2601, Australia.*

Certain varieties of kimberlites are known to contain rare accessory zircons which are unusual (although not unique) with respect to typical zircons from upper crustal rocks in that they have large grain-sizes (up to 20mm diameter), and they are relatively depleted in the normally abundant trace-elements U, Th, Hf, Y and the REE. They are widely believed to be xenocrysts of deep-seated origin which nevertheless are interpreted (based on documented age relationships) to have a genetic association with kimberlites and related magmas (Kinny et al., 1989). The results of REE abundance measurements of kimberlitic zircons reported here show that they may also possess a unique REE fractionation pattern with respect to zircons from other rock-types and could thus be of increased value as a diamond-indicator mineral in prospecting.

The REE analyses were made on the SHRIMP ion probe at ANU, Canberra, using high mass-resolution in preference to energy-filtering or peak-deconvolution procedures to avoid spectral interferences. By doing so, lower detection limits and higher precision are achieved for the REE than any other microbeam technique. Further, the small inclusions of different minerals which may contaminate bulk chemical analyses are avoided. The REE analyses are performed on the same 25µm scale as U-Pb isotopic analyses, and all fourteen REE are measured.

Figure 1 shows mean chondrite-normalised REE abundances for kimberlitic zircons from the Jwaneng DK2 pipe in Botswana, in comparison with representative crustal zircons (from a zoned plutonic complex in southeastern Australia). Two ages of zircons are present at Jwaneng (as identified with the ion probe, Kinny et al., 1989), an Archaean suite and a Permian suite ( $244 \pm 4$  Ma), the latter corresponding to the pipe age. The Jwaneng kimberlite zircons share certain characteristics of their REE patterns with the crustal zircons: a rise in the light REE abundances from La to Gd, a positive Ce anomaly and a negative Eu anomaly. However, the principal differences are best illustrated in Figure 2 in which the REE patterns are normalized to that of the granite zircons. Whereas the other crustal zircons have a similar fractionation of the heavy REE with respect to the granite zircons, the kimberlite zircons show significantly less fractionation. This is particularly the case for the young Jwaneng zircons which have a virtually flat chondrite-normalized heavy REE pattern (Fig.1). Figure 2 also illustrates the smaller magnitude of the Ce and Eu anomalies in the kimberlite zircons with respect to the crustal zircons in this instance.

The exact origin of kimberlitic zircons is still unclear, but it appears from the REE data that they are formed from an extremely fractionated and depleted source with respect to typical crustal melts. This may serve in the future as a useful diagnostic tool for kimberlitic zircons.

Reference : P.D. Kinny, W. Compston, J.W. Bristow and I.S. Williams (1989) Archaean mantle xenocrysts in a Permian kimberlite: Two generations of kimberlitic zircon in Jwaneng DK2, southern Botswana. In: Kimberlites and Related Rocks, Geological Society of Australia Special Publication 14, Volume 2, pp 833-842.

Acknowledgment : The Jwaneng zircons were kindly provided by J.W. Bristow, Anglo American Corp. Ltd Research Laboratory, Johannesburg, South Africa.

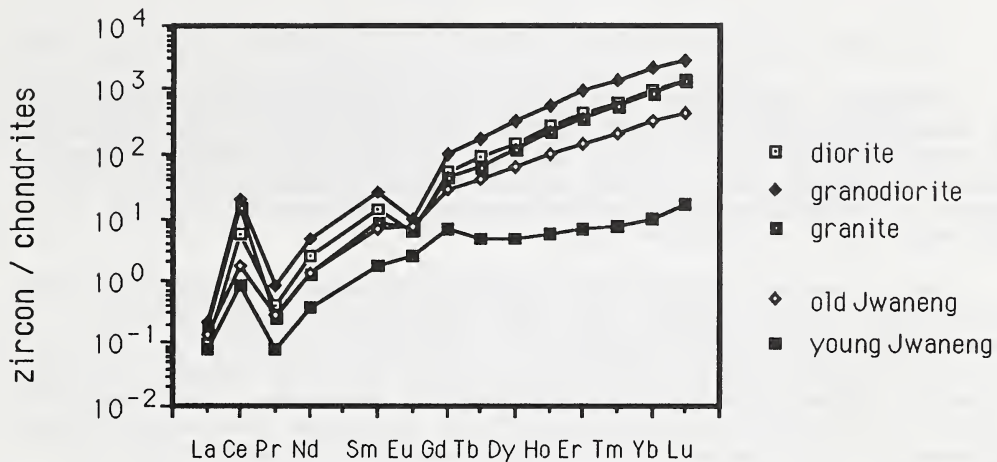


Figure 1

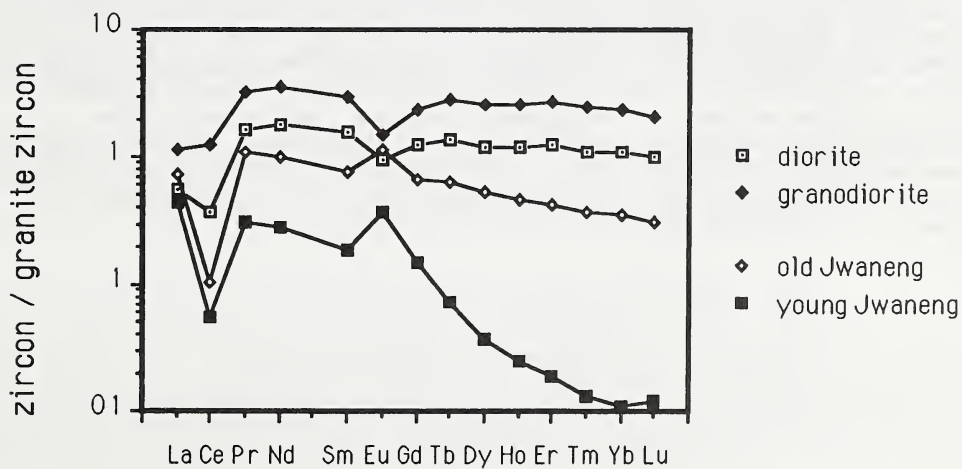


Figure 2

## GEOCHEMICAL CORRELATIONS IN ROBERTS VICTOR EGLOGITES.

Kirkley, <sup>(1)</sup>M.B.; Gurney, <sup>(1)</sup>J.J.; Harte, <sup>(2)</sup>B. and Helmstaedt, <sup>(3)</sup>H.

(1) Dept. of Geochemistry, Univ. Cape Town, Rondebosch 7700, South Africa; (2) Grant Inst. of Geology, Univ. Edinburgh, West Mains Road, Edinburgh, EH9 3JW; (3) Dept. of Geological Sciences, Queen's Univ., Kingston, Ontario, Canada, K7L 3N6.

Eclogite xenoliths in kimberlites may have originated (1) as cumulates from melts of garnet peridotite, (2) as fragments of subducted oceanic crust, and/or (3) through combinations of models 1 and 2, e.g. by the transformation of subcontinental garnet clinopyroxenites by Na-bearing metasomatic fluids derived from a subducted slab.

The strongest geochemical evidence presently available is carbon and oxygen stable isotope data which supports the subduction model.  $\delta^{13}\text{C}$  values of diamonds containing eclogitic inclusions ( $-34\text{‰}$  to  $+2.7\text{‰}$ ) are compatible with crustal (organic and carbonate) carbon sources. Enriched  $\delta^{18}\text{O}$  values in Group I eclogites ( $>6\text{‰}$ ) indicate that they could represent hydrothermally altered basalts, whereas Group II eclogites, with  $\delta^{18}\text{O}$  values  $<6\text{‰}$ , could represent gabbros altered at higher temperatures and lower water/rock ratios. No mantle (high temperature) processes are presently known which can account for the oxygen isotope characteristics of the eclogites.

If the eclogites were originally crustal rocks, it is to be expected that the identity of their protoliths is difficult to prove by geochemical means, considering the wide range of processes which could affect their compositions, e.g. submarine hydrothermal alteration and weathering, low to high grade metamorphism, and mantle metasomatism. On the other hand, if the eclogites represent mantle cumulates, more coherent geochemical trends would be expected. This study examines correlations among major element, trace element, and oxygen isotope compositions in Roberts Victor eclogites in order to further test the proposed models.

## JWANENG FRAMESITES - INCLUSIONS AND CARBON ISOTOPES.

Kirkley, M.B.; Gurney, J.J. and Rickard, R.S.

Geochem. Dept., Univ. Cape Town, Rondebosch 7700, South Africa.

The highly diamondiferous Jwaneng kimberlite diatreme in Botswana, like Orapa, produces numerous examples of polycrystalline diamond aggregate, known as framesite. Carbon isotope compositions have been determined and clinopyroxene, chromite, and garnet have been identified as inclusions in a small sample suite of Jwaneng framesite (Jwf). The inclusions have unusual major element compositions (Table 1) compared to inclusions in single crystal diamonds from Jwaneng and in diamonds worldwide.

Carbon Isotopes The Jwf samples studied exhibit a bimodal distribution of  $\delta^{13}\text{C}_{\text{PDB}}$  values with peaks at approximately -19 and -2‰ (Fig. 1). The framesites appear to be isotopically homogeneous with a maximum difference of 0.5‰ being detected among fragments of individual samples. No  $\delta^{13}\text{C}$  values have yet been found which correspond to the prominent peak in the range -3 to -9‰ developed by peridotitic diamonds worldwide.

Clinopyroxene A clinopyroxene (cpx) inclusion which coexists with chromite in JWF4 contains a high proportion of the ureyite molecule (34%  $\text{NaCrSi}_2\text{O}_6$ ).  $\text{K}_2\text{O}$  content is 0.09 wt%. The cpx is similar in composition (Fig. 2) to cpx in framesites from Orapa (10.24 wt%  $\text{Cr}_2\text{O}_3$ ; Gurney and Boyd, 1982) and from Mir (11.8 wt.%  $\text{Cr}_2\text{O}_3$ ; Sobolev, et al., 1971).

Chromite Jwf chromites are particularly high in  $\text{Cr}_2\text{O}_3$  and low in MgO compared to other chromites closely associated with diamond (Fig. 3). Up to 0.3 wt% ZnO has been detected. The Jwf chromites occur as subhedral crystals embedded in a white alteration product, largely carbonate, which commonly fills vugs and forms coats on Jwf.

Garnet Garnet in JWF11 is intermediate between eclogitic and peridotitic inclusions in Jwaneng single crystal diamonds with respect to  $\text{Cr}_2\text{O}_3$ , CaO and MgO (Fig. 4).  $\text{TiO}_2$  (0.5 wt%) and  $\text{Na}_2\text{O}$  (0.1 wt%) contents are, in contrast, typical of eclogitic diamonds.

$\delta^{13}\text{C}$  values and inclusion compositions indicate that Jwaneng framesites have an eclogitic affinity. That this eclogitic association is a product of subduction of crustal rocks is supported by the presence of ureyitic clinopyroxene (8.4 wt%  $\text{Cr}_2\text{O}_3$ ) in omphacite xenoliths from the Colorado Plateau diatremes which are considered to represent subducted chromite-bearing basalts or clinopyroxenites metasomatized by Na-bearing fluids (Helmstaedt and Schulze, 1988).

REFERENCES

- Gurney, J.J., and Boyd, F.R. (1982) Mineral intergrowths with polycrystalline diamonds from the Orapa Mine, Botswana. Carnegie Institute of Washington Geophysical Laboratory, Annual Report of the Director, 1981-1982, p. 267-273.
- Helmstaedt, H., and Schulze, D.J. (1988) Eclogite-facies ultramafic xenoliths from Colorado Plateau diatreme breccias. In D.C. Smith, Ed., Eclogites and eclogite facies rocks, p. 287-450. Elsevier, Amsterdam.
- Sobolev, N.V., Botkunov, A.I., Lavrent'yev, Yu.G., and Pospelova, L.N. (1971) Peculiarities of the composition of minerals coexisting with diamond from Mir. Zapiski Vsesoyuznyi Mineralogiya Obshchestva, 100, 558-564 (in Russian).

Table 1. Jwaneng framesite inclusion compositions.

	$\delta^{13}\text{C}$ JWF 4 -1.3		$\delta^{13}\text{C}$ JWF 5 -1.3		$\delta^{13}\text{C}$ JWF 11 -18.8	
	CPX	CHR	CHR		GAR	
SiO <sub>2</sub>	54.28	0	0		42.21	
TiO <sub>2</sub>	0.09	0.16	0.15		0.55	
Al <sub>2</sub> O <sub>3</sub>	3.68	3.23	3.43		20.77	
Cr <sub>2</sub> O <sub>3</sub>	11.56	69.51	69.60		3.89	
FeO	1.80	15.95	15.22		7.50	
MnO	0	0.32	0.33		0.37	
MgO	9.78	7.47	8.28		20.84	
CaO	10.63	-	-		3.75	
Na <sub>2</sub> O	7.21	-	-		0.13	
K <sub>2</sub> O	0	-	-		-	
TOTAL	99.02	96.64	97.01		100.01	
OXY	6	4	4		12	
Si	1.997	0	0		3.008	
Ti	0.002	0.004	0.004		0.029	
Al	0.159	0.135	0.142		1.745	
Cr	0.336	1.943	1.927		0.219	
Fe	0.055	0.472	0.446		0.447	
Mn	0	0.010	0.010		0.022	
Mg	0.536	0.394	0.423		2.214	
Ca	0.419	-	-		0.286	
Na	0.514	-	-		0.018	
K	0	-	-		-	
SUM	4.020	2.958	2.961		7.989	

Figure 1. Carbon isotope compositions of Jwaneng framesites.

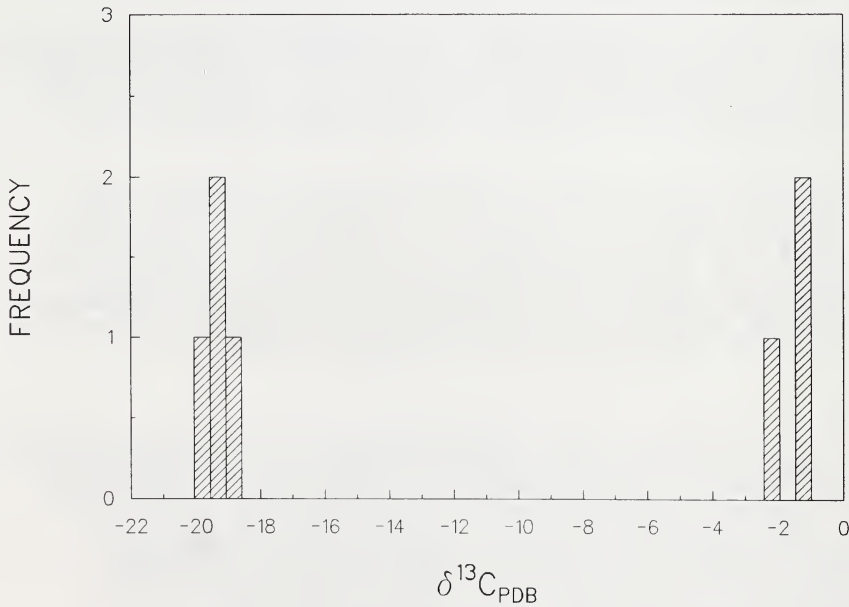


Figure 2. Jwaneng clinopyroxene inclusions.

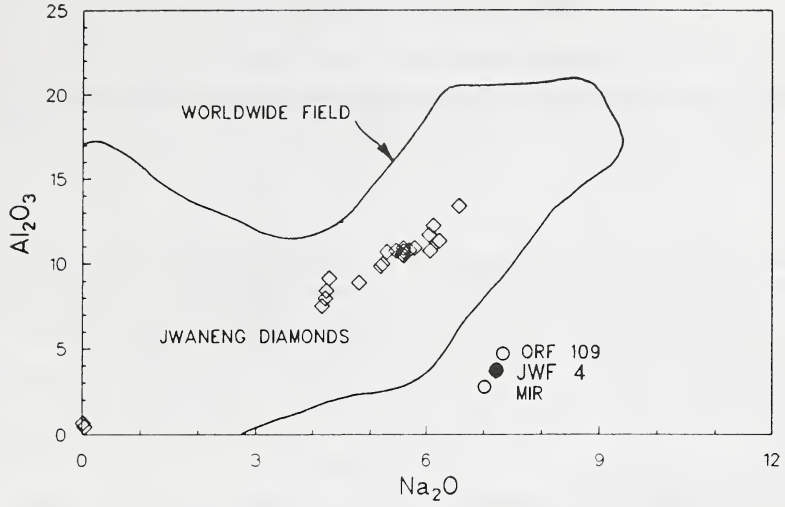


Figure 3. Jwaneng chromite inclusions

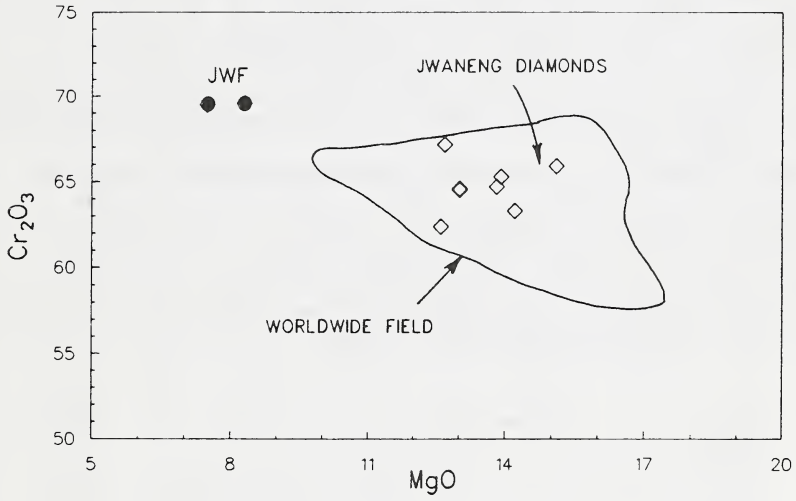
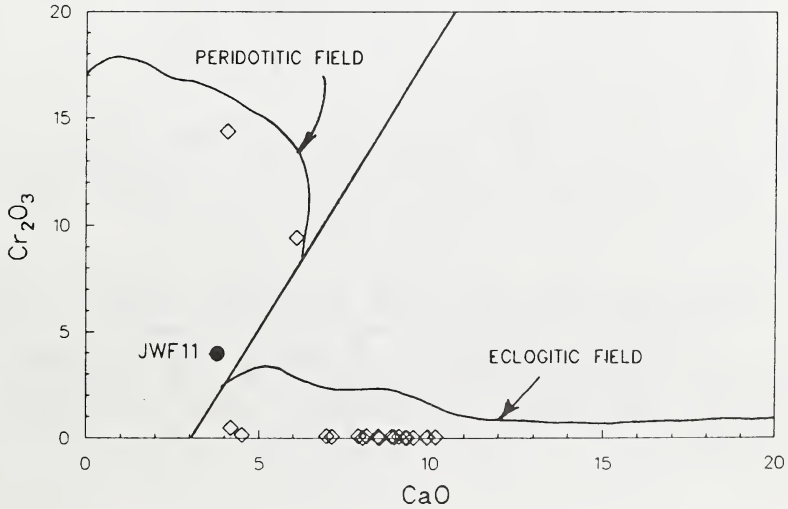


Figure 4. Jwaneng garnet inclusions.



## UNEQUILIBRATED ULTRAMAFIC XENOLITHS FROM UDACHNAYA KIMBERLITE PIPE, WESTERN YAKUTIA.

*Evgenii E. Laz'ko and Victor P. Serenko.*

*Institute of Ore Deposits Geology, Petrography, Mineralogy & Geochemistry, USSR Academy of Sciences, Moscow, USSR.*

Uncommon garnet-bearing ultramafic rocks from kimberlites which contain unequilibrated mineral associations are of great importance for interpretation of mantle petrogenesis and dynamics. Several types of such xenoliths have been found in Udachnaya kimberlite pipe (Sobolev et al., 1984; Laz'ko, 1988). The most interesting samples among them as regards to mantle processes study are: xenoliths with zoned garnets; peridotites with homogeneous minerals (within a single crystal) which composition vary appreciably from grain to grain; "polymict peridotite type" ultramafic rocks containing fragments of unrelated mineral parageneses.

**PERIDOTITES WITH ZONED GARNETS.** These samples are the most common variety of unequilibrated ultramafic xenoliths in Yakutian kimberlites (Serenko et al., 1982; Laz'ko, Serenko, 1983). All of them are typical sheared peridotites with mosaic or fluidal-mosaic textures in which recrystallized olivine, abundant porphyroclasts of pyroxenes and rounded garnet grains are present. A zoning in the latter can be seen sometimes in a hand specimen. Purple transparent core of such garnets are surrounded by orange highly cracked rim.

The proper example of peridotite with zoned garnets is large (10\*6\*6 cm) xenolith TUV-43. The diameter of garnet grains in it reaches up to 6-8 mm. A pronounced concentric symmetrical zoning of the mineral have been detected by a microprobe. Garnet have strong core-to-rim decreases in Cr<sub>2</sub>O<sub>3</sub> and increases in TiO<sub>2</sub> contents. Less prominent rise has been found for Al<sub>2</sub>O<sub>3</sub> and FeO concentrations in the same direction. CaO content slightly decreases and oxidation rate of Fe grows from core to rim:

Oxides	Outer zone1	Intermediate zones					Core 7	Outer zone2
		2	3	4	5	6		
TiO <sub>2</sub>	1.22	1.16	1.13	0.93	0.34	0.02	0.08	1.15
Al <sub>2</sub> O <sub>3</sub>	18.8	18.5	18.9	18.0	17.9	18.1	17.8	19.2
Cr <sub>2</sub> O <sub>3</sub>	3.87	4.30	4.95	6.07	6.67	6.96	7.54	3.78
FeO	9.07	8.80	8.34	8.64	7.82	7.59	7.67	8.27
CaO	5.10	5.07	5.12	5.41	5.62	5.95	6.11	5.07
Fe <sup>3+</sup> /Fe <sub>tot</sub> , %	19.6	20.3	15.5	10.3	10.0	10.6	7.1	17.6

The garnets composition smoothly vary in outer parts of grains only at a distance 0.2-0.7 mm from the edges of crystals. Cores of garnets in TUV-43 peridotite (2-6 mm thick) are homogeneous and have almost identical composition in all examined grains. On the contrary, external parts of the latter have rather different composition even in adjacent grains. In particular the difference in Cr<sub>2</sub>O<sub>3</sub> contents exceeds 1.5 wt.%.

Other minerals of TUV-43 peridotite are homogeneous and chemically equilibrated with outer Ti-rich rim of garnet. Olivine contains 89.1-89.5 of Fo-molecule, orthopyroxene En<sub>90.4-90.7</sub> has low Al<sub>2</sub>O<sub>3</sub> content - 0.55-0.65 wt.%. Subcalcic clinopyroxene composition (mg=0.902, Ca/Ca+Mg= 38.0-38.5%) is indicative of a high-temperature origin of the sample (>1200°C). Bulk rock is strongly exhausted by Al<sub>2</sub>O<sub>3</sub> (0.96 wt.%) and CaO (0.95 wt.%) but despite such depletion it nevertheless contains rare phlogopite plates with "equilibrium" primary-type appearance.

**PERIDOTITE WITH HOMOGENEOUS GARNETS OF DIFFERENT COMPOSITION.** Xenoliths of this variety are rather rare in Udachnaya pipe (Pokhilenko; Sobolev, 1978; Laz'ko et al., 1983). A small (3\*2\*2 cm) nodule TUV-177 from our collection belongs to sheared texture type rocks and contains garnets of different color, from bright purple to dark orange one. A composition of individual garnet porphyroclasts is almost homogeneous except very weak increase of  $TiO_2$  and FeO contents accompanied by decrease in  $Cr_2O_3$  in the outmost parts of few grains. However different porphyroclasts composition varies distinctly from grain to grain ( $Cr_2O_3$  2.26-4.11;  $TiO_2$  0.39-1.17; FeO 7.41-8.96). A clear negative correlation exists between  $Cr_2O_3$  and  $TiO_2$ ,  $Cr_2O_3$  and FeO contents. Besides garnets peridotite contains abundant porphyroclasts of orthopyroxene ( $En_{90}$ ;  $Al_2O_3=0.48$  wt.%) and clinopyroxene ( $mg=0.90$ .  $Ca/(Ca+Mg)=41\%$ ), which are cemented by partly serpentinized fine-grained olivine  $Fo_{89}$ . The composition of separate grains of all constituent minerals except garnet in TUV-177 xenolith is identical. The texture of the rock is fluidal-mosaic with strong foliation. These features are indicative of a particularly intensive deformation of the rock in high-temperature mantle conditions ( $T=1136^\circ C$ ).

**"POLYMICT PERIDOTITE" TYPE ULTRAMAFIC ROCKS.** Xenoliths with fragments of unrelated unequilibrated mineral associations partly resembling "polymict" mantle samples from Bultfontein and De Beers kimberlites (Lawless et al., 1979) are particularly rare in Yakutian diatremes. One xenolith of this type (TUV-29) consists of two quite different (in terms of chemical composition) mineral associations which probably have not been formed at the same time.

The main association is an intensively deformed garnet olivinite with olivine porphyroclasts  $Fo_{84-86}$  and few small scattered grains of violet garnet. The latter belongs to high- $Cr_2O_3$  and low-CaO "diamondiferous peridotites" (Pokhilenko, Sobolev, 1986) variety (table 1). However  $Fe/Fe+Mg$

Table 1. Composition of minerals in TUV-29 nodule.

	1	2	3	4	5	6	7	8	9	10
	Ol	Ol	Gnt	Gnt	Cpx	Cpx	Gnt	Gnt	Ilm	Ilm
$SiO_2$	39.7	38.9	40.0	40.4	55.3	55.1	41.9	41.4	-	-
$TiO_2$	0.00	0.00	0.06	0.11	0.23	0.23	0.70	0.56	47.7	48.7
$Al_2O_3$	0.00	0.00	14.0	13.8	1.73	2.46	20.9	20.8	1.22	0.68
$Cr_2O_3$	0.02	0.00	10.9	11.5	0.16	0.24	0.74	0.66	0.99	0.94
FeO	13.1	15.1	10.7	12.0	4.35	3.69	12.7	13.1	38.8	36.3
MnO	0.13	0.15	0.49	0.58	0.07	0.07	0.27	0.46	0.17	0.25
NiO	0.31	0.18	0.00	0.00	0.03	0.01	0.05	0.07	0.15	0.14
MgO	46.2	44.7	18.6	17.2	16.6	16.4	17.0	17.8	10.9	11.1
CaO	0.05	0.07	3.82	4.35	20.1	19.3	5.53	4.96	-	-
$Na_2O$	-	-	0.00	0.00	1.38	1.84	0.00	0.00	-	-
Total	99.51	99.10	98.57	99.94	99.95	99.34	99.79	99.81	99.93	98.11
mg	86.3	84.1	75.6	71.9	87.2	88.8	70.5	70.8	40.6	42.1

1,2 - coarse grained olivine; 3,4 - violet garnet; 5 - clinopyroxene, large crystal; 6 - clinopyroxene included into orange garnet; 7 - large orange garnet; 8 - orange garnet included into clinopyroxene; 9 - ilmenite, inclusion in garnet; 10 - veined ilmenite in olivine matrix.

of garnets from TUV-29 is almost twice higher than in actual diamond-bearing dunites and harzburgites from Udachnaya pipe (Pokhilenko, Sobolev, 1986).

At the peripheral part of the xenolith large rounded crystals of orange low  $Cr_2O_3$  garnet up to 2 cm in diameter and elongated pale-green FeO-rich clinopyroxene (up to 3 cm) are present. These phases form the main volume of a second mineral association. They strongly resemble the megacrysts of a low-Cr association widely spread in kimberlites both by appearance and in terms

of composition Garnets and clinopyroxenes of "megacrystic" association contain numerous drop-like ilmenite inclusions up to 1 cm in diameter, intergrowths of phlogopite with 1-2 wt.% TiO<sub>2</sub> and tiny Cu-Ni-Fe sulfide globules. Additionally, narrow veins of ilmenite cross the olivine matrix of the main rock. A distribution of minerals in the xenolith and the lack of their compositional equilibrium suggest that "megacrystic" association was formed later than primary garnet olivinite had crystallized and was plastically inserted into the latter rock synchronously with deformation. At the same time in a process of recrystallization the mg-numbers of constituent minerals in olivinite have been partly decreased.

**DISCUSSION.** Unequilibrated high-temperature ultramafic xenoliths from kimberlites are peculiar "snapshots" of subcratonic mantle rocks and conditions just before magma eruption and therefore such nodules are invaluable tool to decipher various mantle processes. Samples like peridotite TUV-177 are suggested to be related to large-scale intensive mixing of hot plastic mantle rocks. In the case under consideration mixing apparently was extremely "dry" process since the indications of melt or fluid presence in the evolved peridotite are negligible. On the contrary, an origin of garnets' zoning similar to one examined in the xenolith TUV-43 are among the best examples of contamination during deformation of depleted peridotites by fluid or highly fluidized melt. The metasomatic agent completely escaped out of the rock after zoning had been formed. The signs of synchronous mixing, melting, deformation and chemical changes of deforming rocks in mantle are even more convincing from TUV-29 xenolith study. We conclude that unequilibrated ultramafic rocks are indicative of an intimate connection of magmatism, fluid mass transfer, and large scale deformation at the regions of kimberlite melt generation in mantle. The total process including kimberlite parental magma origin may be explained by a diapiric ascent of large volume of hot plastic partially melted asthenosphere and its interaction with relatively cold subcratonic lithosphere.

#### REFERENCES

- LAWLESS P.J., GURNEY J.J., DAWSON J.B. 1979. Polymict peridotites from the Bultfontein and De Beers Mines, Kimberley, South Africa. In Boyd F.R. and Meyer H.O.A. eds, *The Mantle Sample*, p.p. 145-155. Amer. Geophys Union, Wash., D.C.
- LAZ'KO E.E. 1988. Ultramafic mantle xenoliths in kimberlites. In Laz'ko E.E. and Sharkov E.V. eds, *Ultramafic rocks*, p.p. 346-379, Nauka Publ. Company, Moscow (in Russian).
- LAZ'KO E.E. and SERENKO V.P. 1983. Peridotites with zoned garnets from Yakutian kimberlites: evidence of high-temperature deep-seated metasomatism and mantle diapirism? *Trans. USSR Acad. Sci., ser. geol.*, No. 12, p.p. 41-53 (in Russian).
- LAZ'KO E.E., SERENKO V.P., MURAVITSKAYA G.N. 1983. Sheared peridotite with a garnet of variable composition from Udachnaya kimberlite pipe (Yakutia). *Rept. USSR Acad. Sci.*, v. 268, No. 6, p.p. 1458-1462 (in Russian).
- POKHILENKO N.P. and SOBOLEV N.V. 1978. Garnets of different composition in sheared lherzolite from Udachnaya kimberlite pipe, Yakutia. XI IMA Meet. Novosibirsk, *Abstr. v. 2*, p. 9 (in Russian).
- POKHILENKO N.P. and SOBOLEV N.V. 1986. Xenoliths of diamondiferous peridotites from Udachnaya kimberlite pipe, Yakutia. *Geol. Soc. Austral. Abstr.*, No. 16, p.p. 309-311.
- SERENKO V.P., NIKISHOV K.N., LAZ'KO E.E. 1982. Zoned garnets in porphyroblastic lherzolites from Mir kimberlite pipe. *Rept. USSR Acad. Sci.*, v. 267, No. 2, p.p. 438-441 (in Russian).
- SOBOLEV N.V., POKHILENKO N.P., RODIONOV A.S. 1984. Inhomogeneities of the deep seated inclusions in kimberlites as an indication of the processes of dynamic evolution in upper mantle substance. 27th IGC sess. Moscow, *Abstr. v. 5*, p.p. 399-400.

## COANJULA DIAMONDS, NORTHERN TERRITORY, AUSTRALIA.

*D.C. Lee<sup>(1)</sup>; S.R. Boyd<sup>(2)</sup>; B.J. Griffin<sup>(3)</sup>; B.W. Griffin<sup>(4)</sup> and T. Reddcliffe<sup>(5)</sup>.*

*(1) Ashton Mining Limited, Jolimont, Western Australia; (2) Department of Earth Sciences, Open University, United Kingdom; (3) Electron Microscopy Centre, University of Western Australia; (4) Division of Exploration Geoscience, C.S.I.R.O., North Ryde, Australia; (5) Ashton Mining Limited, West Perth, Western Australia.*

Two deposits rich in micro-diamonds occur near Coanjula, N.T. The diamonds are typically 0.2mm and rarely exceed 0.5mm in size.

Two diamond bearing kimberlites occur 120km to the north and 24 ultrabasic volcanic pipes occur within a radius of 60km of the microdiamond deposits.

The Coanjula microdiamonds occur in sediments of the Murphy Metamorphics Group which are dated at 2050 Ma. Extensive drilling and sampling has revealed a deposit of microdiamonds which is 12km long and up to 500m wide. A smaller deposit, 2km long and 300m wide is located 5km to the south. The microdiamond content exceeds one per kilogram in some parts of the deposit.

A porphyritic latite - trachyandesite body 3km long and up to 2km wide, with a chilled margin exhibiting spinifex texture, forms a central core to the larger of the microdiamond deposits. The number of microdiamonds in the sediments increases towards the margins of this volcanic intrusive but samples of the trachyandesite have not contained microdiamonds.

More than 70% of the diamonds are opaque cubes with a fibrous structure. A further 4% are colourless, yellow, or green non-fibrous cubes. The remaining 25% of the diamonds are octahedral, dodecahedral or irregular. This unusual suite of microdiamonds is unlike any recorded from kimberlite or lamproite.

The microdiamonds have been analysed by proton micro-probe for trace elements. Nitrogen content and Carbon Isotope ratios have been determined and micro-inclusions have been extracted and analysed. This work was undertaken to determine if the diamonds are of "metamorphic" origin as it has been reported from the Soviet Union (Shatsky, 1989) that fibrous cubic microdiamonds similar to some of the Coanjula diamonds have been found in metamorphic rocks.

Proton micro-probe analysis of 22 Coanjula diamonds showed a large number of elements present in widely varying concentrations. S, K, Ti and Fe are present at levels of 10-100ppm, V, Cr, Cu, Zn, Pb and Zr occur at 0-10 p.p.m. Normalization to constant Fe content greatly reduces the scatter in the data, indicating that most elements are contained in small inclusions of melts, fluids and daughter minerals. Coanjula microdiamonds have trace element patterns broadly similar to microdiamonds from Argyle lamproite but have higher Ti/Fe for the same K/Ca. Ellendale lamproite microdiamonds have much lower K/Ca ratios than either Argyle or Coanjula microdiamonds.

Fe - normalised Cu and Zn show a positive correlation which may be related to micro-inclusions of sulphides. The similarity of Cu/Zn ratios in microdiamonds from Coanjula, Argyle, Ellendale and Zaire (Mabuji Mayi) suggests that they contain similar sulphides and thus have a similar (i.e. mantle derived) origin.

Forty-four of the opaque cube diamonds from Coanjula have been examined for inclusions. Inclusions were exposed by fracturing, ashing and sectioning the stones. Inclusions vary in size but are usually in the 2 to 5 micron range. Many of the cubes are of composite structure with a massive, irregular core overgrown by a fibrous coat to form a cubic stone. When ashed in air at 600°C, the massive core burnt before the fibrous overgrowths.

Chrome-magnetite, diopside, jadeite, garnet and mica inclusions have been analysed in-situ in fractured cubes. These inclusions are compositionally similar to eclogitic (Meyer, 1987) and calc-silicate (Sobolev, 1984) inclusions. Residues after ashing contain both quenched liquid and crystalline phases. Polished sections of the microdiamonds contain primary melt inclusions. A potassic aluminous melt is present as numerous inclusions in the core of one microdiamond (Table 1). The melt data is unlike previously reported compositions (eg Navon et al., 1988) in that titanium is below detection limit.

Twenty seven of the opaque cube diamonds were found to have  $\delta^{13}\text{C}$  values ranging from -10 to -22.5‰. Eleven of the octahedral/resorbed irregular diamonds had  $\delta^{13}\text{C}$  values from -2.5 to -21.5‰ but with a distinct sub-group centred at -4‰. Infra-red spectra were obtained for both opaque cubic and clear irregular diamonds. The spectra indicate a low nitrogen content, the presence of possible type I<sub>b</sub> cubic diamonds and some type IaA diamonds in the irregular group.

It is concluded from the nature of the inclusions, the zoned structure of some of the cubes and the range of isotopic compositions that the Coanjula diamonds are of magmatic origin.

Table 1: Composition of melt inclusions in a microdiamond core

Sample	Inc 1	Inc 2	Inc 3	Inc 4	Inc 5	Inc 6	Inc 7	Mean+S.D.
SiO <sub>2</sub> *	54.66	52.41	53.99	54.13	53.28	55.23	51.54	53.61 + 1.29
TiO <sub>2</sub>	0.00	0.00	0.17	0.00	0.00	0.00	0.28	0.06 + 0.11
Al <sub>2</sub> O <sub>3</sub>	23.46	23.77	23.49	22.74	23.96	22.73	23.49	23.38 + 0.47
Cr <sub>2</sub> O <sub>3</sub>	0.00	0.00	0.00	0.00	0.00	0.00	0.00	-
FeO	4.32	5.61	5.27	4.92	4.32	6.08	5.46	5.14 + 0.66
NiO	0.00	0.00	0.00	0.00	0.00	0.00	0.00	-
MnO	0.00	0.00	0.00	0.00	0.00	0.00	0.00	-
MgO	4.22	3.24	3.03	3.93	3.90	3.96	3.71	3.71 + 0.43
CaO	0.00	0.00	0.00	0.30	0.00	0.00	0.00	-
Na <sub>2</sub> O	3.89	5.64	1.32	3.01	4.72	0.98	4.96	3.50 + 1.81
K <sub>2</sub> O	9.44	9.33	12.60	10.65	9.82	11.02	10.46	10.47 + 1.13
Cl	0.00	0.00	0.13	0.32	0.00	0.00	0.09	0.06 + 0.12
Oxide total**	89.28	73.28	69.95	38.04	68.37	69.88	67.22	

\* Analyses by Link EDS on a JEOL 6400 SEM, data in wt.%.

\*\* total prior to normalisation to 100wt.% oxides

## References:

- Meyer, H.O.A.,(1987) in *Mantle Xenoliths*, Editor P.H. Nixon. pp. 501-522.
- Navon, O., Hutcheon, I.O., Rossman, G.R. and Wasserburg, G.J.,(1988) Mantle-derived fluids in diamond micro-inclusions. *Nature*, 335 (27), 784-789.
- Sobolev, N.V.,(1984) in *Kimberlite Occurrence and Origin*. Editors Glover, J.E. and Harris, P.G. pp. 213-219.
- Shatsky, V.S., Sobolev, N.V., Yefimova, E.S.,(1989). *Extended Abstracts, Workshop on Diamonds*, 28th Int. Geological Congress, Washington, D.C.

## NEW TYPE LAMPROITE OF THE DAHONGSHAN AREA, HUBEI PROVINCE, CHINA.

Liu Guanliang<sup>(1)</sup> and Xu Zhiqiang<sup>(2)</sup>.*(1) Yichang Institute of Geology and Mineral Resources (CAGS); (2) The North Eastern Geology Brigade of Hubei.*

The lamproite of Dahongshan area (31° —31° 44' N, 112° 32' —113° 20' E) lie immediately by the margin of the north part of Yantze craton. About 10 volcanic groups by sea bottom volcanic eruption and 40 hypabyssal intrusives constitute a lamproite belt with 70 km long and 1—6km wide. Their isotope ages range from 490Ma to 352Ma (i.e. from Cambrian to Devonian period).

In previous studies these rocks in this area had been called kimberlite-like, kimberlite, melitite basalts, glass dunite and O1-D1 lamprophyres. Among them four hypabyssal intrusives were identified as lamproite in early eighties. It was found in this work through petrography, geochemistry, mineralogy studies that the rocks mentioned above all belong to lamproites. But some rock bodies of them appear to be transitional between lamproite and kimberlite while other bodies between lamproite and minette.

Our investigation confirms the presence of four distinct rock face assemblages including three volcaniclastic facies and one hypabyssal face. The volcaniclastic facies show variation in occurrence, texture and structure and can be divided into volcanic diatreme; crater breccia; near volcanic crater lapilli, far volcanic sed pyroclastic rocks and tuffite. The hypabyssal intrusive facies occur either separately intrusive body or associated with volcanic eruption rocks and formed lamproite volcanic suite from volcaniclastic rocks (agglomerate, breccia, lapilli and tuff including air-fall) to magma intrusive facies (including lava flow).

According to the suggestions by IUGS (1989) and Scott-Smith, Skinner (1985), Mitchell (1985), the textural and mineral assemblage classification can be recognized as follows. (see table)

The volcaniclastic rocks are mainly composed of olivine-lamproite and magma hypabyssal intrusives are composed of diopside lamproite.

The volcanic diatreme and crater facies consist of breccia (rare agglomerate), lapilli and tuff. The compositions of breccia are mainly autothic breccia of phlogopite-olivine lamproite. The first olivine generation corresponds to the macrocrysts found in kimberlites, but many of olivines are anhedral and show subhedral often with parts of the crystal margin having a complex but euhedral shape. This facies also contain many xenolith of country rocks, rare dunite xenolith, upper mantle xenoliths forming symplectic intergrowths of spinel and crystal fragments. The cement is composed of carbonate, serpenite, etc.

The classification table of Dahongshan lamproite

teatural	mineral
1. Volcaniclastic rock	1. Olivine lamproite
① agglomerate >64mm	① olivine lamproite
② breccia >2mm	② phlogopite-olivine lamproite (including ol-madupitic lamproite)
③ lappilli >—<2mm	③ glass-olivine lamproite
④ tuff <2mm	
2. Magma hypabyssal intrusive	2. Diopside lamproite
⑤ lava flow	④ olivine-diopside lamproite (including ol-Di madupitic lamproite)
⑥ dikes, sills	⑤ leucite-olivine-diopside lamproite
	⑥ sanidine-diopside-madupitic lamproite

Near volcanic crater facies lappilli; this facies are of well-bedding structure which was formed by accumulation of various size lappilli having well-sphericity, roundness and well-smoth. The lappilli materials consist mostly of olivine lamproite or glass olivine lamproite. The crystal fragments are serpentinization olivine, vermiculization phlogopite and ilmenite. The cement is of carbonate, serpente and clay mineral.

Sed pyroclastic rock and tuffite of far volcanic crater facies: The facies were formed by the alternation of pyroclastic sedimentary rock (including air-fall tuff) and dolomitic carbonate of middle Cambrian or early Ordovician system (two period) with well graded beddings. The fragment materials are mainly olivine lamproite but usually been resolved into malmorillonite and ferric material.

Magma hypabyssal intrusive facies: The rocks are with distinct porphyritic texture and are characterised by two generations of olivine (usually serpenization) having euhedral-subhedral and sometimes a complex but euhedral shape. The porphyritic minerals include diopside, leucite. The matrix is composed of phlogopite, sanidine, potassic richterite, apatite, rutile, ilmenite and glassy. Rare peridotite, dunite xenolith are found in some rock bodies.

The whole rock geochemistry about 150 samples from various facies show  $\text{SiO}_2$  35-50%.  $\text{MgO}$  4-26% from basalt to ultrabasic. The  $\text{K}_2\text{O}$  contents are commonly less than that of the West kimberley lamproite. The reason leading to low  $\text{K}_2\text{O}$  may be with relative to particular geological setting of sea-bottom volcanic eruption. As a result, it is not appropriate to judge of ultrapotassic rocks from the  $\text{K}_2\text{O}$  content for the Dahongshan lamproite. However, the  $\text{K}_2\text{O}$  contents of most samples range from 0.5% to 2%, some to 3-5%. The  $\text{K}_2\text{O}/\text{Na}_2\text{O}$  ratios are generally >2, average 6.55. The fresh volcanic

glass are also high in  $K_2O$  ranging from 5.82% to 6.55%. These data show that the lamproites in Dahongshan area belong to ultrapotassic rock suite.

This suite is characterized by higher contents of Ba, Rb, Sr, Pb, Th, U, Ti, Zr, Nb, REE patterns are highly fractionated and enriched in LREE.

The isotopic compositions of the lamproites in Dahongshan area are  $Sr^{87}/Sr^{86} = 0.70380-0.70688$ ,  $Nd^{143}/Nd^{144} = 0.51165-0.51230$ ,  $Pb^{208}/Pb^{204} = 17.737-20.870$ ,  $Pb^{207}/Pb^{204} = 15.330-15.675$ ,  $Pb^{208}/Pb^{204} = 38.656-42.856$ , being in between type II kimberlites and lamproites, and appear a tendency for two direction evolution towards EMI and EMII from PREMA. The isotopic compositions show that the lamproites of Dahongshan area may be relative to old subduction of proterozoic Era.

The minerals commonly present in the lamproites of Dahongshan area as major primary constituent are olivine, diopside, phlogopite, leucite, sanidine, richterite, Accessory phases include apatite, proskite, rutile, ilmenite. The xenocrysts include olivine, spinel, garnet, cr-diopside and ilmenite. For olivine, the compositions of phenocryst of two generations are Fo77-88, of xenocrysts and in mantle xenoliths (dunite, peridotite) are Fo 90-93. Diopside occurs as a phenocryst or groundmass. The compositions of diopside in many of hypabyssal intrusives are variation with two trends: A dominant trend is Ti increasing with Al increasing. Another is of preserving low Ti with Al increasing. The Cr-diopside are high in  $Cr_2O_3$  ranging from 1.72% to 3.08%. The compositions of phlogopite also have two distinct trends of which one is the transitional type (high Al high Ti) towards minette, the other is the characteristics of lamproite. K-richterite is lower in  $K_2O$ , MgO and higher in  $Na_2O$ ,  $Al_2O_3$  than that of the K-richterite of the West Australia lamproites.

The macrocryst compositions of spinel and garnet mostly belong to lherzolite suite and a few parts of them like harzburgite/dunite suite.

The lamproites in Dahongshan area are considered to be derived by partial melting of garnet lherzolite from lithosphere, where the depletion of peridotite source appears to be less strong. The primary magma in metasomation zone of upper mantle had been replaced and enriched in LILE, then uprisen by diapirism and cut through the overlying crust along with sea-bottom volcanic eruption.

THE GENESIS OF PEROVSKITE-BEARING BEBEDOURITE AND THE PROBLEMS  
POSED BY CLINOPYROXENITE-CARBONATITE COMPLEXES.

Lloyd, F.E. and Bailey, D.K.

Dept. Geology, Univ. Bristol, Wills Memorial Building, Queens Rd., Bristol BS8 1RJ, UK.

Bebedourite (Ti-rich, perovskite-titanomagnetite-apatite-phlogopite clinopyroxenite) is an early-formed facies of 91-70 Ma pyroxenite-carbonatite complexes emplaced in a zone of deep-seated faults between the Parana Basin and the Sao Francisco Craton, Brazil. Late-stage carbonatite cores are Nb and REE rich and compare closely with Iron Hill, Colorado, but South African clinopyroxenite-carbonatites, e.g. Phalaborwa, are by contrast poor in these elements.

Type bebedourite from the base of Salitre 1 borehole (114 m) does not show typical cumulus texture. Large (ca. 6 mm across) isolated, coarse aggregates or single grains of diopside are heavily fractured, corroded, fluid-inclusion filled, and "supported" in a coarse matrix. Matrix minerals crystallised in the order: first-generation phlogopite, fluor-apatite, magnetite which both rims and forms inclusions in Ce-perovskite, followed by Ce-perovskite and titanomagnetite. Diopside rims are partly replaced by phlogopite, and typically a narrow band of second generation phlogopite + a carbonated alkali-mafic silicate mineraloid separates diopside from adjacent minerals. Corroded areas and cleavages in diopside are variously filled by phlogopite flakes, apatite, occasional perovskite grains, and veinlets + blebs of the carbonate-silicate mineraloid. Electron microprobe investigation has revealed areas where the mineraloid can be resolved into calcite, K-richterite and a serpentine-like material.

Diopsides are homogeneous, nearly pure (wooll 50, en 44, fs 6), and low in  $\text{Cr}_2\text{O}_3$  (below detection-0.08 wt%),  $\text{TiO}_2$  (0.72-1.06 wt%),  $\text{Al}_2\text{O}_3$  (0.47-0.41 wt%), and  $\text{Na}_2\text{O}$  (0.26-0.35 wt%), characteristics shared by pyroxenes from lamproites (Mitchell, 1979; Hamilton and Rock, 1990) and pyroxenite facies of other pyroxenite-carbonatite complexes e.g. Iron Hill, Colorado. Kimberlite groundmass clinopyroxene (Dawson et al., 1977) has slightly less  $\text{TiO}_2$ , lower MgO/FeO values and higher  $\text{Cr}_2\text{O}_3$ . Petrography indicates that the bebedourite diopside is more primary than the mineral assemblage in which it occurs and is possibly xenocrystic in origin. Such clinopyroxene does not have necessarily any evolutionary relationship with the more Fe- and Na-rich clinopyroxenes of rocks consanguineous with some clino-pyroxenites such as pyroxene sovites, ijolites and syenites.

First-generation phlogopite ( $\text{Mg}/(\text{Mg}+\text{Fe})=0.88$ ) is aluminous. Second-generation phlogopite is peralkaline ( $\text{Mol. K}_2\text{O}+\text{Na}_2\text{O}/\text{Al}_2\text{O}_3$  up to 10.7) and trends towards tetra-ferriphlogopite. In contrast with phlogopites in lamproites  $\text{TiO}_2$  is low in both types. On an  $\text{Al}_2\text{O}_3$  vs  $\text{TiO}_2$  diagram (after Mitchell, 1985) the first generation plots in the field of phlogopites from kimberlites which also overlaps with the

Leucite Hills lamproite field. The second generation defines a kimberlitic ( $\text{TiO}_2$ -poor), as opposed to lamproitic, trend. Low  $\text{Cr}_2\text{O}_3$  in the bebedourite phlogopites, however, is more typical of lamproite than kimberlite phlogopites (Hamilton and Rock, 1990). The suggestion that increasing  $\text{Fe}^{3+}$  in phlogopite relates to increasing  $\text{K}_2\text{O} + \text{Na}_2\text{O} / \text{Al}_2\text{O}_3$  in the liquid (Velde and Yoder, 1977) is consistent with the composition of the interstitial residue (mineraloid + K-richterite).

Perovskites are close to pure composition (average wt%  $\text{TiO}_2 = 56.4$ ;  $\text{CaO} = 39.7$ ) with low  $\text{FeO}$  ( $<1.5$  wt%),  $\text{Na}_2\text{O}$  ( $<0.5$  wt%) and, apart from  $\text{CeO}$  ( $>1\%$ ), relatively low REE and Nb content. In these respects they are typical of perovskites from kimberlites and alkali-mafic lavas and contrast with those from lamproites and carbonatites which show considerable ss towards loparite and leushite end-members (Mitchell, 1985).

In magnetite  $\text{TiO}_2$  is  $<1$  wt%;  $\text{MgO}$  varies from below detection to 2.4 wt%;  $\text{Al}_2\text{O}_3$ ,  $\text{Cr}_2\text{O}_3$  and  $\text{MnO}$  are all  $<0.5$  wt%, a composition that compares closely with an analysis given for magnetite surrounding perovskite in the Premier magnetite-serpentine-carbonate dikes (Mitchell, 1979). Titanomagnetite (average wt%  $\text{TiO}_2 = 26$ ) contains 2.1-4.04 wt%  $\text{MnO}$  which is comparable to carbonatite magnetites (Mitchell, 1979), but the considerable ulvospinel component is much more typical of Mn-bearing magnetites in alkali-mafic lavas, e.g. SW Uganda (Lloyd et al., in press).

The carbonated silicate contains variable  $\text{SiO}_2$  (22-38 wt%),  $\text{MgO}$  (8-13 wt%) and  $\text{CaO}$  (22-33 wt%);  $\text{TiO}_2$  and  $\text{Al}_2\text{O}_3$  are  $<1$  wt%. Apart from high alkalis:  $\text{Na}_2\text{O} \rightleftharpoons \text{K}_2\text{O} = \text{ca. } 3$  wt%, the composition is comparable to calcite kimberlites such as the Premier magnetite-serpentine-calcite dikes. Where blebs of calcite occur the Sr-content of  $>1\%$  implies a primary origin. Associated K-richterite has a composition very close to that found in MARID xenoliths (Dawson and Smith, 1977) with  $\text{Mg}/(\text{Mg} + \text{Fe}) = 90$ ,  $\text{K}_2\text{O} \rightleftharpoons \text{Na}_2\text{O} = \text{ca. } 5$  wt%, and  $\text{TiO}_2$  not  $>0.75$  wt% distinguishing it from Ti-bearing richterites in lamproites and K-mafic lavas (Mitchell, 1985).

On the basis of petrography and mineral chemistry bebedourite may represent clinopyroxene-rich mantle invaded and mobilised by a kimberlite-carbonatite melt. The clinopyroxenite mantle facies could originate as the product of partial melting in the sub-cratonic mantle on a geothermal gradient where clinopyroxene, but not phlogopite and calcite, is stable, i.e., just above the Wendlandt and Egger solidus. Such a melt could accumulate, become gravitationally unstable and slowly rise, crystallising clinopyroxene en-route. In terms of heat balance, however, the P-T path could be expected to remain close to and subsequently reapproach the solidus, (Bailey, 1986) limiting upward movement and causing stagnation. These conditions would encourage the separation of volatile-rich, alkali-mafic silica-calcite fluid/melt. This pegmatitic medium, pervasively injected, could effect the para-contemporaneous auto-remobilisation of part of the clinopyroxenite body as a "mush" of clinopyroxenes with

xenocrystic appearance. A proportion of the clinopyroxenes would be likely true xenocrysts from the products of previous like episodes of diapir stagnation. Eventual emplacement of the crystal mush within the crust would be the consequence of concentrated channeling of the volatile-rich medium beneath a major crustal fault zone.

Phlogopite, apatite and magnetite would precipitate from the pegmatitic medium and late-stage enhanced CO-CO<sub>2</sub> activity would encourage Ti activity and cause precipitation of Ti-minerals in an otherwise Ti-poor assemblage.

The diapiric upward movement of the clinopyroxene "crystal mush" to lower P,T regions could lead to separation and eventual emplacement of an immiscible carbonatite magma.

The bebedourite diopside lacks features that popularly might be expected to imply mantle affinity, i.e. Cr, jadeite, Tschermak's molecule. This raises a question about the nature of the possible mantle source. Another question is the origin of the Nb- and REE-rich signature of the associated carbonatite cores and whether this endorses a kimberlitic connection. Both these questions are being investigated and possible answers will be proposed.

#### References.

- Bailey, D.K. (1986) Fluids, melts, flowage and styles of eruption in alkaline ultramafic magmatism. In *Alkaline and alkaline ultrabasic rocks and their xenoliths. Transactions of the Geological Society of South Africa, Special Issue*, 88, 449-458.
- Dawson, J.B., and Smith, J.V. (1977) The MARID (mica-amphibole-rutile-ilmenite-diopside) suite of xenoliths in kimberlite. *Geochimica Cosmochimica Acta*, 41, 309-323.
- Dawson, J.B., Smith, J.V., and Hervig, R.L. (1977) Late stage diopsides in kimberlite groundmass. *Neues Jahrbuch für Mineralogie Monatsheft*, 12, 529-543.
- Hamilton, R., and Rock, N.M.S. (1990) Geochemistry, mineralogy and petrology of a new find of ultramafic lamprophyres from Bulljah Pool, Nabberu Basin, Yilgarn Craton, Western Australia. *Lithos*, 24, 275-290.
- Lloyd, F.E. (1991) Phanerozoic volcanism of southwest Uganda: a case for regional K and LILE enrichment of the lithosphere beneath a domed and rifted continental plate. In A.B. Kampunzu and R.T. Lubala, Eds., *Phanerozoic extensional magmatism and structural evolution of the African plate*, p. 23-72. Springer-Verlag, Heidelberg, in press.
- Mitchell, R.H. (1979) The alleged kimberlite-carbonatite relationship: additional contrary mineralogical evidence. *American Journal of Science*, 279, 570-589.
- Mitchell, R.H. (1985) A review of the mineralogy of lamprophytes. *Transactions of the Geological Society of South Africa*, 88, 411-437.
- Velde, D., and Yoder, H.S. (1977) Melilite and melilite-bearing igneous rocks. *Carnegie Institution of Washington Yearbook*, 76, 478-485.

## CRYSTALLINE INCLUSIONS IN CHROMITES FROM KIMBERLITES AND LAMPROITES.

*A.M. Logvinova and N.V. Sobolev.**Institute of Mineralogy and Petrography 630090 Novosibirsk, USSR*

A comparative study of inclusions in chrome spinel macrocrysts (more than 0.5 mm) extracted from heavy concentrates of several kimberlite pipes of Yakutia (Udachnaya, Ailkhil, Mir, International) and lamproites of western Australia (Ellendale 4 pipe) have been performed. Out of 1000 spinel grains from kimberlites and 700 grains from lamproites solid inclusions have been identified respectively in 20 % and 10 % of all examined grains. More than 60 % of all inclusions are heavily altered.

Olivines are the most abundant inclusions for both rock types being found in 57 out of 70 chromite grains containing unaltered inclusions. Chrome diopside was fixed in 3 grains, enstatite in 2 grains, pyrope in 5 grains including one of lamproitic chrome spinel.

Kimberlitic spinels with inclusions contain from 0.06 to 3.02 wt %  $\text{TiO}_2$ , from 36.3 to 64.3 wt %  $\text{Cr}_2\text{O}_3$ , from 9.2 to 16.6 wt % MgO. Lamproitic spinels contain from 0.16 to 3.16 wt %  $\text{TiO}_2$ , from 38.3 to 58.5 wt %  $\text{Cr}_2\text{O}_3$ , from 11 to 13 wt % MgO.

Crystalline inclusions from kimberlitic chromites are represented mainly by crystals with well developed octahedral faces, being similar to most inclusions in diamonds by their negative diamond (or chromite) morphology.

Both olivines, pyroxenes and pyrope inclusions from lamproitic spinels are highly resorbed and are rounded.

Olivine included in chrome spinels from kimberlites are containing 89-94 mol% Fo. One chromite grain from Udachnaya pipe with 49.5 wt%  $\text{Cr}_2\text{O}_3$ , 5.3 wt%  $\text{Al}_2\text{O}_3$ , 3.0 wt%  $\text{TiO}_2$  contains two olivine inclusions with 89 and 92 mol% Fo. Olivine included in lamproitic spinel has a narrower range of Fo: from 88 to 90 mol%.

Pyrope presence in one of chromite grains from lamproite (7.3 wt%  $\text{Cr}_2\text{O}_3$ , 6.4 wt% CaO) and in four grains of kimberlitic spinels ( $\text{Cr}_2\text{O}_3$  from 2.0 to 6.9 wt%, CaO from 3.9 to 9.6 wt%) indicates along with some chrome-diopside inclusions lherzolitic and also one wherlitic parageneses of the studied chromite grains.

Temperature estimate for 30 kbar pressure using O'Neill and Wall (1987) approach have shown a range from 790 to 1020°C for all kimberlitic chromites (Av. 914°C for 37 samples) and from 1010 to 1140°C for lamproite spinels (Av. 1062°C for 21 samples). A significant higher equilibration temperature is observed for chromite-olivine pairs from lamproite compared with those of a number of Yakutian kimberlites.

**GEOCHEMICAL SYSTEMATICS IN MANTLE MEGACRYSTS AND THEIR  
HOST BASALTS FROM THE ARCHAEOAN CRATON AND POST-ARCHAEOAN  
MOBILE BELTS OF SCOTLAND.**

*Long<sup>(1)</sup>, A; Thirlwall<sup>(1)</sup>, M.F.; Menzies<sup>(1)</sup>, M.A.; Upton<sup>(2)</sup>, B.G.J. and Aspen<sup>(2)</sup>, P.*

*(1) Department of Geology, University of London (RHBNC), Egham, Surrey TW20 0EX; (2) Department of Geology and Geophysics, Grant Institute, University of Edinburgh, Edinburgh EH9 3JW.*

The origin of megacrysts in alkaline volcanic rocks continues to be a somewhat controversial topic as they can represent (a) polybaric fractionates formed in conduits within the lower lithosphere, or (b) fragments of the peridotite protolith that comprises most of the lower lithosphere, or (c) shallow precipitates formed within crustal magma chambers. In an attempt to address these questions we have studied several on-craton and off-craton xenolith-bearing vents in NW Scotland. In particular mica, clinopyroxene and amphibole megacrysts entrained by Tertiary and Permo-Carboniferous alkaline volcanic rocks on and off the Hebridean craton were analysed for Sr, Nd and Pb isotopes and relative abundances of Sr, Rb, U, Pb and the rare earth elements (REE).

#### ON-CRATON

At present only one xenolith locality at Loch Roag Lewis has been studied within the Hebridean craton.

Micas - Rb/Sr and U/Pb ratios in on-craton mica megacrysts are quite variable (Rb/Sr = 0.538-0.946; U/Pb = 0.068-0.078). Rare earth element abundances in mica megacrysts are characterised by an enrichment in the LREE over the HREE (e.g.  $(\text{Ce/Yb})_{\text{N}} = 38.68-56.35$ ) consistent with what is observed in mica megacryst data from other on-craton and off-craton localities. However no europium anomalies were found as reported by Menzies et al. (1985) for mica megacrysts from off-craton localities in southern Arizona. In the on-craton mica megacrysts  $^{87}\text{Sr}/^{86}\text{Sr} = 0.70505-0.70773$  [ $(^{87}\text{Sr}/^{86}\text{Sr})_{47\text{Ma.}} = 0.70395-0.70628$ ] and extends the reported range for this locality and new  $^{143}\text{Nd}/^{144}\text{Nd}$  data (0.51085-0.51233) overlap with previously published mica analyses (Menzies and Halliday 1988). The Pb isotopic variability is tightly constrained and overlaps with the field of EM1 (i.e. Enriched Mantle 1) apart from one data point which has anomalously low  $^{207}\text{Pb}/^{204}\text{Pb}$  and high  $^{208}\text{Pb}/^{204}\text{Pb}$  ratios. More importantly this mica megacryst has the lowest  $^{143}\text{Nd}/^{144}\text{Nd}$  ratio ( $\epsilon_{\text{Nd}} = -34.2$ ) reported for mica megacrysts from throughout the world.

Clinopyroxenes - Rb/Sr in on-craton clinopyroxenes are similar (Rb/Sr = 0.0031-0.0003) to that reported for other megacrysts but much higher than that reported for peridotite orogenic massifs or xenoliths. U/Pb in clinopyroxenes are similar (U/Pb = 0.065-1.120) to megacrysts from South Africa (on-craton) and the western USA (off-craton) (BenOthman et al, 1990). REE abundances in clinopyroxenes define an inverted U shaped pattern comparable to megacrysts from South Africa and the western U.S.A. (Eggler et al 1989; Shimizu 1975). Overall the chondrite normalised rare earth abundance pattern is enriched in the LREE [e.g. on-craton cpx  $(\text{Ce/Yb})_{\text{N}} = 8.247-8.391$ ].

On-craton clinopyroxene megacrysts have lower  $^{87}\text{Sr}/^{86}\text{Sr}$  ratios than the micas (i.e.  $^{87}\text{Sr}/^{86}\text{Sr} = 0.7046\text{-}0.7049$ ) and Nd isotope data are more radiogenic than the micas ( $^{143}\text{Nd}/^{144}\text{Nd} = 0.512447$ ). Pb isotopic variability ( $^{206}\text{Pb}/^{204}\text{Pb}$ ,  $^{207}\text{Pb}/^{204}\text{Pb}$  and  $^{208}\text{Pb}/^{204}\text{Pb}$ ) is tightly constrained within the EM1 field and as such the clinopyroxene and mica data overlap.

### OFF-CRATON

Within the Proterozoic mobile belt of NW Britain several widespread localities were studied in order to assess the lateral (and vertical) variability of the post-Archaean lithosphere and to compare and contrast the origin of megacrysts within lithosphere of different ages (i.e. Dunaskin Glen, Kiers Hill, Elie Ness, Colonsay).

Micas - Rare earth element abundances in mica megacrysts are characterised by a LREE enriched pattern similar to on-craton micas (e.g.  $\text{Ce}_\text{N}/\text{Yb}_\text{N} = 5.837\text{-}19.041$ ). These data are also similar to what is observed in mica megacrysts from other off-craton localities in eastern Australia and the western USA (Irving and Frey 1984; Menzies et al 1985). Off-craton mica megacrysts have  $^{87}\text{Sr}/^{86}\text{Sr} = 0.74928\text{-}0.70669$  [ $(^{87}\text{Sr}/^{86}\text{Sr})_{280\text{Ma.}} = 0.70540\text{-}0.706290$ ] and the  $^{143}\text{Nd}/^{144}\text{Nd} = 0.51259\text{-}0.51267$  and overlap with previously published mica megacryst analyses for off-craton localities.

Clinopyroxenes - In clinopyroxene megacrysts  $\text{Rb}/\text{Sr} = 0.0004\text{-}0.0158$  and  $\text{U}/\text{Pb}$  ratios =  $0.049\text{-}0.123$ . These ratios are *significantly lower* than that reported for pyroxene megacrysts from off-craton localities within the Proterozoic mobile belts of the western USA ( $\text{U}/\text{Pb} = 0.216\text{-}1.929$ ; BenOthman et al, 1990). REE abundances in clinopyroxenes define an inverted U shaped pattern comparable to megacrysts from on-craton and off-craton localities. Clinopyroxene megacrysts have  $^{87}\text{Sr}/^{86}\text{Sr} = 0.70344\text{-}0.70589$  [ $(^{87}\text{Sr}/^{86}\text{Sr})_{280\text{Ma.}} = 0.70344\text{-}0.70571$ ] and  $^{143}\text{Nd}/^{144}\text{Nd}$  ratios =  $0.51269\text{-}0.51275$ . These data overlap with the range reported for MORB and OIB. Pb isotope data are similar to that reported for other off-craton localities in the western USA and eastern Australia (BenOthman et al 1990, Stolz and Davies 1988).

### MEGACRYST ORIGIN

On-craton megacrysts - Hypothetical liquids that may have co-existed with the megacrysts can be calculated using published partition coefficients and the elemental data outlined above. The calculated melts are very enriched in the LREE [ $(\text{Ce}/\text{Yb})_\text{N} = 50\text{-}70$ ] and are similar to carbonatitic melts (Bell 1989) and pyroxenite xenoliths (Menzies and Halliday 1988). Any suggestion of a relationship between the megacrysts and melts similar to the host basalts can be further tested by comparison of the age corrected isotopic data for the megacrysts with the source characteristics of the host basalts. The on-craton micas and clinopyroxenes have  $(^{87}\text{Sr}/^{86}\text{Sr})_{47\text{Ma.}} = 0.70395\text{-}0.70628$  which is comparable to that observed in ocean island basalts (OIB's) but the range in  $(^{143}\text{Nd}/^{144}\text{Nd})_{47\text{Ma.}} = 0.51082\text{-}0.51241$  is beyond that normally associated with OIB's. As a consequence of this we can conclude that it is rather unlikely that the bulk of the on-craton megacrysts represent

polybaric fractionates from uncontaminated melts whose source region was similar to that of OIB (i.e. asthenosphere or deeper).

Perhaps the on-craton megacrysts are entrained fragments of the peridotite protolith. The Loch Roag Archaean? peridotite protolith appears to be similar to that normally encountered beneath mobile belts and not cratons. This is somewhat anomalous in that an integration of kimberlite-borne and basalt-borne xenolith data from on-craton (Archaean) and off-craton (post-Archaean) localities indicates that the Archaean peridotite protolith is normally highly magnesian and very different from that occurring beneath post-Archaean crust. This has been interpreted to mean that the Archaean protolith is a residue from extraction of komatiitic melts whereas the post-Archaean lithosphere represents a basalt residue. It appears that Loch Roag may be an exception to this rule if we can assume that lateral displacement has not occurred and resulted in the superposition of Archaean upper (crust) and post-Archaean lower (mantle) lithosphere. With regard to the origin of megacrysts we can state that the dominant mineralogy of the peridotite protolith is anhydrous and this makes it a rather unlikely source for hydrous megacrysts. Moreover the REE characteristics of the on-craton clinopyroxene megacrysts differ from that of clinopyroxenes in basalt-borne and kimberlite-borne peridotite xenoliths (Menzies and Hawkesworth 1987 and references therein; Nixon 1987 and references therein).

However one aspect of the megacryst data may link them to present-day enriched lower lithosphere. Pb isotope variations observed in on-craton clinopyroxene and mica megacrysts overlap with that of on-craton enriched spinel lherzolites from Loch Roag (i.e. EM1). This implies a possible co-genetic relationship since the Sr and Nd isotopic data also plot below the mantle array beyond the field occupied by OIB's toward EM1.

The similarity between hypothetical co-existing melts for the on-craton megacrysts and small volume carbonatitic melts and pyroxenite xenoliths from Loch Roag indicates that perhaps the on-craton megacrysts and pyroxenites represent disrupted conduits which formed from the migration and crystallisation of *lithospheric melts*. It is interesting to speculate that perhaps the spread of Sr and Nd isotopic data between OIB and EM1 indicates that a sub-lithospheric component (OIB) in some way triggered melting of the lithosphere (EM1) resulting in hybrid melt products which crystallised within the lithosphere. Eventual disruption and entrainment of this vein/wall rock assemblage would seem to account for the xenolith population, i.e. hydrous and anhydrous megacrysts, hydrous and anhydrous pyroxenites and enriched lherzolites (i.e. reacted wall rock adjacent to veins).

Off-craton megacrysts - Hypothetical melts that may have co-existed with the off-craton megacrysts are less enriched in the LREE ( $[\text{Ce}/\text{Yb}]_{\text{N}} = 7-20$ ) than those calculated for on-craton megacrysts being more similar to alkaline basalts. Moreover the off-craton micas and clinopyroxenes have  $(^{87}\text{Sr}/^{86}\text{Sr})_{280\text{Ma}} = 0.70344-0.70629$  and  $(^{143}\text{Nd}/^{144}\text{Nd})_{47\text{Ma}} = 0.51259-0.51275$  which overlaps with the range observed in OIB's and as such differs from the on-craton megacrysts. We can conclude from these data that the off-craton megacrysts may represent polybaric fractionates of *asthenospheric melts* derived from source(s) similar to that of OIB's.

References.

- Bell, K. (1989) Carbonatites - Genesis and evolution, 618 p. Unwin Hyman, London.
- BenOthman, D., Tilton, G.R., and Menzies, M.A. (1990) Pb, Nd, and Sr isotopic investigations of Kaersutite and clinopyroxene from ultramafic nodules and their host basalts : The nature of the sub-continental mantle. *Geochim. Cosmochim. Acta.* 54, 3449-3460.
- Eggler, D.H., McCallum, M.E., and Smith, C.B. (1979) Megacryst assemblages in kimberlite from northern Colorado and southern Wyoming : Petrology, Geothermometry-Barometry, and Areal Distribution. In Boyd, F.R. and Meyer, H.O.A., Eds., *The Mantle Sample : Inclusions in Kimberlites and other Volcanics*. Proc. Second International Kimberlite Conference. Vol 2, 213-226. AGU Washington D.C.
- Irving, A.J. and Frey, F.A. (1984) Trace element abundances in megacrysts and their host basalts : Constraints on partition coefficients and megacryst genesis. *Geochim. Cosmochim. Acta.* 48, 1201-1221.
- Menzies, M.A. and Halliday, A. (1988) Lithospheric Mantle Domains beneath the Archean and Proterozoic crust of Scotland. *J. Petrol. Special Lithosphere Volume*, 275-302.
- Menzies, M.A., and Hawkesworth, C.J. Upper mantle processes and composition. In Nixon, P.H. ed. *Mantle Xenoliths*, 725-740. J. Wiley and Sons.
- Menzies, M.A., Kempton, P. and Dungan, M. (1985) Interaction of Continental Lithosphere and Asthenospheric Melts below the Geronimo Volcanic Field, Arizona, USA. *J. Petrol.* 26, 663-693.
- Nixon, P.H. (1987) *Mantle Xenoliths*. 844 p. Wiley, England.
- Shimizu, N. (1975) Rare earth elements in garnets and clinopyroxenes from garnet lherzolite nodules in kimberlites. *E.P.S.L.* 25, 26-32.
- Stolz, A.J., and Davies, G.R. (1988) Chemical and isotopic evolution from spinel lherzolite xenoliths for episodic metasomatism of the upper mantle beneath southeastern Australia. *J. Petrol. Special Lithosphere Volume* 303-331.

EXPERIMENTS ON EXPLOSIVE BASIC AND ULTRABASIC, ULTRAMAFIC,  
AND CARBONATITIC VOLCANISM.

Lorenz<sup>(1)</sup>, V.; Zimanowski<sup>(1)</sup>, B. and Fröhlich<sup>(2)</sup>, G.

(1) Institut für Geologie, Universität Würzburg, Pleicherwall 1, D-8700 Würzburg, FRG; (2) IKE, Universität Stuttgart, Pfaffenwaldring 31, D-7000 Stuttgart 81, FRG.

Until recently, explosive volcanism of basic, ultrabasic, ultramafic, and carbonatitic magmas leading to the formation of maars and diatremes has been considered to be the result of near-surface depressurization of the respective magmas and the consequent intensive unmixing of large amounts of volatile phases. During the last twenty years, the study of active and fossil rhyolitic to basaltic volcanoes has shown, however, that phreatomagmatic explosions, i.e. thermal explosions, are much more widespread than previously thought and are the result of a near-surface interaction of rising magma and surface water or groundwater. As the Earth has a hydrosphere consisting of widespread surface water bodies (sea, lakes, rivers) and groundwater (pore or joint water) magma rising to the Earth's surface, with a high probability, has to rise not only through parts of the lithosphere but also into or through the hydrosphere. Thus, there is a high probability that contact with the hydrosphere may result in phreatomagmatic explosions. From the study of maars and diatremes it has also been shown, that every magma type reaching the Earth's surface may get involved in phreatomagmatic explosions if the hydrologic environment is suitable. As long as magma rises to near-surface levels (no matter what its chemistry) and contacts groundwater or surface water in suitable quantities, phreatomagmatic explosions will follow each other rapidly and the respective maar-diatreme volcano will grow in size, i.e. in diameter, depth, and thickness of its tephra-ring.

Many aspects of the tephra deposits and the features of maars and diatremes indicative of a phreatomagmatic origin have been discussed already. Very important aspects are the scarcity or lack of vesicles in the juvenile pyroclasts, the blocky to spherical shapes of these clasts, and their grainsize variation from fine ash to lapilli size. Another important aspect is the large proportion of country rock clasts in the tephra reaching 80 - 90 % and indicating explosive fragmentation in the root zone of the respective diatreme, i.e. in the transition zone between a 1 - 2 m thick feeder-dike and the conical-shaped diatreme.

Maars and diatremes of basic, ultrabasic, ultramafic, and carbonatitic magmas in most aspects do not differ very much between each other neither do they differ in respect to maars and diatremes associated with more silica-rich magmas. Type of alteration and type of country rock clasts including deep seated xenoliths are variables, depending on the particular chemistry and depth of origin of the magma involved and on the particular country rocks surrounding the diatreme. In addition the amount of water involved in the individual explosions is dependant on the local hydrogeological situation.

One particular aspect where there is a difference between most acid to basic magmas and ultrabasic, ultramafic, and carbonatitic magmas concerns the shape of ash grains and lapilli. Only the latter magma types contain a significant amount of spherical ash grains and spherical lapilli indicative of low viscosity and consequent influence of surface tension. So far very little is known about the actual physical processes leading to and causing phreatomagmatic explosions.

Unknown are:

Relative and absolute quantities of magma and water which interact explosively, or participate "passively" in the explosions.

Maximum pressures reached during the explosive process.

Energy balances of the thermal explosion process.

Fragmentation processes of the magma prior, during and after the explosion.  
Fragmentation processes in the surrounding country rocks.

Thermal explosions (including the natural phreatomagmatic explosions) can evolve if a sufficiently hot melt and water mix mechanically and form an ignitable mixture (i.e. coarse fragmentation). The temperature contrast between the hot and the cool liquid results in formation of insulating vapour films ("Leidenfrost effect"). Pressure pulses or other hydrodynamic events in the system can destabilize these vapour films. The consequent collapse of the vapour films (resulting in a so-called direct contact) in combination with an extremely fast enlargement of the heat transferring surface of the melt (i.e. fine fragmentation) results in fast heat transfer from the melt to the water. The water consequently gets superheated and transformed into steam. As the heat transfer happens much faster (about one magnitude) than the vapourization, the water vapourizes "coherently" (i.e. nearly completely and homogeneously), thus resulting in an explosive expansion of highly pressurized steam to ambient pressure.

Numerous experiments were carried out on metal melts and some on thermite melts interacting with water (e.g. Fröhlich, 1987; Wohletz & McQueen, 1984) with only the latter undertaken in respect to phreatomagmatic volcanism. In 1987 an experimental set-up for studies of explosive interaction between water and basic, ultrabasic, ultramafic, carbonate, and carbonatitic melts was constructed by an interdisciplinary research group at the IKE laboratories in Stuttgart. Aim of the project was **not** to build a "mini volcano" but to produce ignitable mixtures of water and hot melt on a small scale in order to investigate basic physical aspects.

The experimental set-up was called TEE-HAUS (Thermal Explosion Experiment House). In this TEE-Haus thermal explosions are generated by the injection of several ml (0.5 to 10 ml) of water into 150 ml of melt. Inductive heating of a crucible (steel or metal ceramics; 5 cm internal diameter, 7.5 cm in depth) to temperatures between 740 - 1800°C is used to melt mixtures of carbonates (Na, K, Ca carbonates) or granulates of volcanic rocks of basic, ultrabasic, or ultramafic composition. Explosions are either triggered by the injection pressure of the water (in case of carbonate melts) or by the impact of a metal object of 0.5 g mass and approx. 8 J kinetic energy (in case of silicate melts). Measurements of explosion intensity, ejection velocity, water mass and water injection velocity, control of melt composition and temperature, adjustment of injection geometry and strength of trigger pulse, video and high speed film documentation of the explosions were performed. The fragments derived from the silicate or carbonate melt of each run were collected and analyzed for their grain size distribution and shape.

In excess of 500 experiments were performed between 1988 and 1991 on carbonate (50/50 %  $\text{Na}_2\text{CO}_3/\text{K}_2\text{CO}_3$ ) and carbonatite (a simplified artificial Lengaitite) melts as well as on Tertiary olivine melilitite (ultramafic) from the Swabian Alb, Tertiary olivine tholeiite (basic) from the Vogelsberg, Quaternary nephelinite and basanite (ultrabasic) from the West Eifel and Permian basaltic andesite from Palatinate (all samples from areas within Germany). During these experiments thermal explosions were observed with all the melts used. The explosions generated inside the crucible exerted repulsion forces to the crucible between several 1000 and 23 000 N. These ranges were found in the carbonate experiments where no external trigger was applied, as well as in the silicate experiments where an external trigger force of approx. 400 N (vertical force component) was applied. One of the most important results of the experimental work is the determination of the magnitude of the trigger pulse for the ignition of phreatomagmatic explosions. Pressure waves of that intensity (8 J) certainly are abundant at active volcanic sites, caused e.g. by volcanic tremor, pressure pulses of the rising magma, or other seismic events. The ejection velocity was found to be in a range between 200 and 400  $\text{m s}^{-1}$ . Explosion energy values up to 500 J were calculated. The maximum explosion pressure was calculated in the range between 10 and 100 MPa.

In case of experiments with vesicular melts irrespective of their chemical composition, the presence of many non-condensable gas bubbles obviously hinders or even prevents the ignition of a thermal explosion (Zimanowski et al., 1991).

A probable explanation for this phenomenon is the damping of the trigger pulse (shock wave) due to the compressibility of the gas bubbles: If the volume ratio of gas bubbles to liquid phase exceeds a yet unknown limit the trigger pulse is damped below the minimum level for destabilizing the vapour films.

Mass ratios of the respective amounts of water and melt which interacted thermally (so-called interactive masses) were determined between 1 : 10 and 1 : 30. Thus, only a small part of the 150 ml of melt interacted thermally with injected water causing the explosion whereas the larger part of the melt was ejected passively from the crucible. Different fragmentation processes result in specific grain size and grain shape populations that can be distinguished from each other. Particles resulting from the fine fragmentation process that precedes and causes the thermal explosion are characterized by angular to subrounded shapes and grain sizes ranging from 20  $\mu\text{m}$  to 180  $\mu\text{m}$ . Due to the mechanism of formation the interactive fragments are characterized by an extremely high cooling rate, therefore, the resulting particles consist of highly unordered glass and have an extremely large surface area. In natural pyroclastic deposits such particles probably will lose their characteristics in short time because of alteration. The majority of the experimentally produced fragments, i.e. the fragments ejected passively, form during the expansion of the generated steam by stimulated Taylor instability wave growth, stripped-off Helmholtz instability waves and free air fragmentation. As the cooling rate of these fragments is distinctly lower than that of the "interactive" fragments, they are still liquid once they formed and, therefore, the shape is characterized by the effects of viscosity and surface tension in respect to the chemical composition of the melt. In natural ultrabasic, ultramafic, and carbonatitic phreatomagmatic volcanism a large proportion of the ash grains and lapilli as well as the bombs show a spherical shape, often display internal layering (lapilli, bombs), contain xenocrysts or xenoliths derived from country rocks (surrounding the diatreme), or contain juvenile clasts which formed penecontemporaneously. Those accretionary features as well as frequent concentrically oriented flow textures demonstrate the liquid state of these fragments after their formation. The results of the experiments suggest, that the pyroclasts described above are related to phreatomagmatic explosions but are not diagnostic to the process of explosive interaction of magma and water itself.

The experimentally produced explosive mixture (igniteable mixture) represents a small geometric element that most probably also occurs during phreatomagmatic events in nature. The behaviour of large scale explosive mixtures of water and magma can be modelled by combination of many small elements, but may require additional scaling factors (e.g. geometric damping or thermal detonation mechanisms). The determined magnitude of energy and pressure pulses in the experiments, however, demonstrates that the mechanism of thermal explosion is suitable to explain large scale fragmentation in diatreme root zones and thus formation of maars and diatremes.

- Fröhlich, G. (1987) Interaction experiments between water and hot melts in entrapment and stratification configurations. *Chem. Geology*, 62, 137-147.
- Lorenz, V. (1985) Maars and diatremes of phreatomagmatic origin, a review. *Trans. Geol. Soc. S. Afr.*, 88, 459-470.
- Lorenz, V. (1986) On the growth of maars and diatremes and its relevance to the formation of tuff-rings. *Bull. volcanol.*, 48, 265-274.
- Lorenz, V. (1987) Phreatomagmatism and its relevance. *Chem. Geol.*, 62, 149-156.
- Wohletz, K.H., and McQueen, R.G. (1984) Experimental studies of hydromagmatic volcanism. *Studies in Geophysics*, N.Acad. Press, Washington, 158-169.
- Zimanowski, B., Lorenz, V. and Fröhlich, G. (1991) Quantitative experiments on phreatomagmatic explosions. *J. volcanol. geotherm. Res.*, in press.

**PALAZOZOIC LITHOSPHERE MANTLE FEATURE BENEATH FUXIAN, LIAONING PROVINCE, CHINA: THE INFORMATION FROM No. 50 KIMBERLITE PIPE.**

*Lu, Fengxiang\**; *Zheng, Jianping\**; *Zhao, Lei\*\**; *Zhang, Hongfu\*\*\**.

*\*China University of Geosciences, Wuhan 430074, P.R. China; \*\* China University of Geosciences, Beijing 100083, P.R. China; \*\*\* Northwest University, Xian 710096, P.R. China.*

### Abstract

#### GEOLOGICAL SETTING

Liaoning diamondiferous district is located in North China Platform. There are two kimberlite fields, Tieling and Fuxian kimberlite field. The former is in north margin of North China Platform, the latter being 340 km south of it. 25 kimberlite bodies are known to occur in Tieling but all of them are barren. 18 kimberlite pipes and 58 dykes are distributed in Fuxian and belong to 3 clusters. Some of these bodies are diamond-rich and have grade type. No. 50 pipe is the best one of diamond-rich kimberlites. It has been eroded to level at the transition from diatreme to root zone.

#### KIMBERLITE AGE OF NO. 50 PIPE

K-Ar datings of kimberlite whole rocks and micas are 422–462 Ma and 398 Ma respectively which may represent the magma emplacement age and crystalline age of mica. But the Rb-Sr isochron age of whole rock is 1109 Ma which may reflect the original age of kimberlite. Most diamonds in No. 50 pipe contain significant amount of nitrogen concentrates to form various type of aggregation which link with age of diamond. This process obeys second order kinetic equations. According to Erans and Harris (1989) method, the two population of the modal age of diamonds in No. 50 were revealed. They are 2200 Ma and 1200–1500 Ma. Obviously, the first group of diamonds were formed older than kimberlite No 50 pipe and the second is near the isochron age.

#### GEOCHEMICAL CONSTRAINS

The mea values of major elements of the kimberlites in No. 50 pipe are as following : SiO<sub>2</sub> 32.63%, MgO 27.68%, TiO<sub>2</sub> 1.2%, K<sub>2</sub>O+Na<sub>2</sub>O 0.79%, P<sub>2</sub>O<sub>5</sub> 0.66%, MgO/(MgO+FeO) 0.88 and the trace elements are Ni 775–1228ppm, Cr 557–606ppm, Ni/Co 9.10–26.24, K/Rb 9.67–17.46, Th/U 9.25, Nb/Ta 19.71–31.95, La 93.71–130.67ppm, La/Yb 205–348, Like all kimberlites in the world, No. 50 pipe kimberlites are characterized by simple linear REE distribution pattern showing extreme light REE enrichment. La and Yb are enriched 150–350 and 1.5–8 times chondritic abundances respectively. The initial <sup>87</sup>Sr/<sup>86</sup>Sr is 0.7074 near the ratios from group-II kimberlites in South Africa; δ<sup>13</sup>C in kimberlites range from -4.4 to -5.4 which are included by the range in δ<sup>13</sup>C of diamonds (from -4 to -8) from No. 50 pipe. Compared with Shandong kimberlites, No. 50 pipe has relative low MgO, Mg/(Mg+Fe), and high TiO<sub>2</sub>, P<sub>2</sub>O<sub>5</sub> and REE. These facts may imply that there is a metasomatic mantle beneath Fuxian showing more enriched with LREE, K, Rb, Sr, Ti, and P, and lesser ultrabasis feature than that beneath Shandong kimberlite feild.

We think that kimberlites are the products of hybridization of three components; they are xenocrysts derived from mantle which are represented by many kinds of macrocrysts, kimberlitic magmas and volatiles. Most of macrocrysts are olivine exhibiting relatively large (>3mm) rounded-anhedral and including octahedon diamonds, Cr-rich garnets and

chromites in No. 50 pipe. They present in considerable (30–40%) quantities in kimberlites. Subtracted those olivines, the approximate composition of bearing-volatile kimberlitic magmas can be obtained. Using least squares method, kimberlitic magmas in No. 50 pipe are roughly fitted for the melting product from phlogopite (10%), magnesite (15%), clinopyroxene (50%), garnet (10%) phases and  $H_2O$ ,  $+CO_2$  (15%). This result of calculation agrees with the high-pressure experiments that kimberlitic magmas may be produced by eutectic-like melting of phlogopite magnesite garnet lherzolite and implies that the source of magmas must include clinopyroxenes to provide CaO to magma.

### MINERALOGICAL CONSTRAINTS

Garnets were found at least 5 types in which three types are considered as mantle-derived. Moderate-Ca chrome pyrope (G9) are more abundant than low-Ca chrome-pyrope (G10) and the concentration of  $Cr_2O_3$  and CaO contents in the formers range from 4.39%–12.77% and 4.55%–8.49% respectively. These garnets increase Ca being correlated with increasing Cr indicating solid solution toward uivrovitic. Green uvarovite-pyropes were also found in No. 50 pipe which are characterized by Ca-rich (14.85%) and Cr-rich (7.67%). All information from mantle-derived garnets show that most of them crystallized in a moderate-high calcium and chrome medium. Orange titanian pyropes are considered megacrystal occurrence. These garnets are typical poor in  $Cr_2O_3$  (<1%). Yellow-green andradites are secondary phases and replaced the globular segregation or as the aggregations set in matrix.

Nature Fe, wustites,  $FeSi_2$  and Ti- $FeSi_2$  have been found in heavy minerals. This mineral assemblage defines low  $f_{O_2}$  environment and close to iron-wustite (IW) buffer. In contrast, according to Sack (1980) and Mo (1982) method, No. 50 pipe kimberlitic magmas are relatively oxidized and approximate to  $f_{O_2}$ 's defined between WM and EMOG buffers. It may be better to explain that the  $f_{O_2}$  of source region of diamond was more reduced than that of magmas. Mantle-derived garnet, orthopyroxene and clinopyroxene from No. 50 pipe give pressure and temperature of 51 kb and 1206°C. Obviously the depth at which the upper mantle melt to form kimberlitic magmas should be deeper than 160km.

### XENOLITH

Three kinds of xenoliths were found in No. 50 pipe kimberlite. They are peridotite series, phlogopitite series and lower crust as well as country rocks materials. Most of peridotite xenoliths are dunite and garnet lherzolite and Cr-rich garnet harzburgite xenoliths are rare. Phlogopitite series including garnet phlogopitite and olivine phlogopitite are relatively coarse-grained and considered to represent autoliths or cumulates of early-generation kimberlite. The REE pattern of garnet lherzolite xenoliths are similar to that of kimberlites,  $La/Yb = 195.2$ , and La is enriched 13 times chondritic abundances. Although a garnet peridotite lithosphere is depleted in basaltic constituents by igneous events, it is subsequently enriched in elements such as REE by a component derived from greater depth.

### CONCLUSION

1. There was a cool, thick and low  $f_{O_2}$  lithosphere beneath Fuxian area at Palaeozoic.
2. It consisted of at least four components, dunites, garnet harzburgites, garnet lherzolites and phlogopitites. No ocean lithosphere material such as eclogite so far has been found and lherzolite played an important role during that time.

3. No: 50 pipe kimberlites are derived from an enriched source with respect to bulk-earth Rb / Sr ratio and slighted enriched than that in Shandong kimberlites.

4. Lithologic and chemical variations observed in mantle xenoliths from other parts of the world have been explained by multiple depletion and enrichment events. But how to explain a relative high calcium enviroment appeared in the upper mantle beneath this area?

First possibility is that lithosphere may consist of Cr-garnet lherzolites with low-Ca Cr-pyropite harzburgite and the dunites lenses. Second possibility is that these lherzolite might represent mixtures of depleted harzburgite or dunite and basaltic melt or Ca-rich fluid.

## MINERALOGY AND GEOCHEMISTRY OF PEROVSKITE-RICH PYROXENITES.

Mariano, <sup>(1)</sup>Anthony N. and Mitchell, <sup>(2)</sup>Roher H.

(1) 48 Page Brook Road, Carlisle, MA 01741; (2) Department of Geology, Lakehead University, Thunder Bay, Ontario, P7B 5E1.

## PEROVSKITE PYROXENITES

Four carbonatite-pyroxenite complexes in the Eastern Periphery of the Paraná Basin, Brazil include units with ore grade accumulations of titanium in the form of anatase. The anatase is derived from the weathering of perovskite pyroxenites.

The circular structures of Catalão I, Serra Negra and Tapira contain perovskite pyroxenites as annuli located between central carbonatite cores and surrounding domed Precambrian sediments which are locally fenitized and silicified. Salitre I and II are satellites of the Serra Negra complex. Salitre I is oval-shaped and consists of pyroxenite and a small apatite carbonatite. Salitre II is a circular plug consisting predominantly of pyroxenite transected by thin carbonatite veins and lamprophyre (olivine phlogopite) dikes.

In some areas of these complexes pyroxenite grades into glimmerite, and the presence of inclusions of apatite, calcite, magnetite and salite in phlogopite indicates the primary nature of the glimmerite. Magnetite and perovskite occur as cumulus aggregates, disseminations and bands that alternate with apatite, calcite and pyroxene layers. Apatite and magmatic calcite are always present.

The object of this study is to demonstrate that perovskite pyroxenites are early-formed members of this type of alkaline complex and to document the transformation of these rocks into supergene anatase ores.

## PYROXENES

Pyroxene compositional variation is of use in assessing the relative degree of evolution of individual rock units within alkaline complexes. The typical evolutionary trend is one of iron enrichment. In all cases the most primitive compositions Similar pyroxene compositional trends are found in undersaturated and oversaturated complexes. Which trend is followed depends more on the peralkalinity and oxygen fugacity than the degree of silica saturation. Pyroxenes from the Brazilian perovskite pyroxenite complexes have diopside-salitic compositions with low aegirine and hedenbergite contents. Many of the pyroxenes are pleochroic in shades of brown-green. Grain margins and areas

adjacent to fractures and cleavages exhibit a stronger green pleochroism and are slightly richer in hedenbergite. Many pyroxenes contain sagenitic-textured magnetite inclusions. Pyroxenes from Salitre I are less evolved than those of Salitre II. Pyroxenes from Tapira and Iron Hill are the most evolved of those examined. All pyroxenes are however relatively unevolved compared to the overall pyroxene compositional trends. This observation demonstrates that perovskite pyroxenites must be early-formed members of this type of alkaline complex. Textural studies suggest that they represent cumulates and are unlikely to be metasomites.

#### PEROVSKITES

Perovskite compositions reflect the degree of evolution of their host magma and the type of magma from which they crystallized. Early-formed perovskites are close to calcium titanate (perovskite end member) in composition. With evolution calcium may be replaced by Na, Sr and REE while Ti is replaced by Nb. Compositional evolution is thus typically from perovskite towards lueshite or loparite. Perovskites in the Brazilian and Afrikander perovskite pyroxenites follow the trend towards loparite. Early-formed perovskites are perovskite with low REE contents. These show textural evidence of reaction with late stage fluids leading to the development of REE enriched rims. In some cases mantles of loparite are developed upon cores of the less-evolved perovskite. Rare earth enrichment is related to the circulation of late-stage hydrothermal fluids. The perovskites in terms of their overall compositions are unevolved, confirming the conclusions derived from the pyroxene compositional trends that perovskite pyroxenites are unevolved members of these complexes. Significant Sr and Na enrichment does not occur in these perovskites and they thus differ from perovskites in carbonatites.

#### ANATASE AND RHABDOPHANE

Perovskite pyroxenites are an important source of Ti where intense lateritic weathering has led to decalcification of perovskite. In the Brazilian complexes anatase is concentrated in the zone of weathering. At deeper levels residual cores of perovskite are found within anatase grains. Below the zone of weathering only fresh perovskite is found. Electron microscopy shows that the anatase displays a platy habit. Aggregations of plates commonly form rosettes. The altered rocks are very porous as all of the components of the pyroxenes and micas originally present are removed during the lateritization process. Solutions percolating through the anatase matrix typically precipitate micaceous crystalline aggregates of rhabdophane, cerianite, monazite and andalite-group minerals. The rare earths are derived primarily from the decomposed perovskite, and the phosphate from apatite.

## MICAS

The compositions of micas parallel those of pyroxenes in showing the relative degree of evolution of the pyroxenites. Rocks from Tapira are the most-evolved and those from Salitre I the least-evolved. Micas within each complex are zoned and exhibit a trend of decreasing alumina from core to margin. This trend represents evolution from phlogopite towards tetraferriphlogopite.

## OLIVINES

Olivines in associated perovskite olivinites are magnesian and unevolved. At Salitre I they contain from 10-12 wt.% FeO and have negligible CaO (< 0.3 wt.%) and MnO contents (< 0.5 wt.%). Salitre II olivines range in FeO content from 8-15 wt.%.

## THE DIAMONDIFEROUS GRAVELS OF THE SOUTHWESTERN TRANSVAAL, SOUTH AFRICA.

*Marshall, T.R.*

*Gold Fields of South Africa Ltd., Luipaardsvlei Geological Centre. P.O. Box 53, Krugersdorp, RSA 1740.*

A detailed analysis of the alluvial diamond gravel deposits of the southwestern Transvaal has indicated that these deposits are far more complex than was previously thought. It is apparent that the gravels consist of a basal alluvial deposit overlain by a calcretized eluvial gravel, a lateritized colluvial deposit and a younger fluvial sequence (Fig. 1). The basal, Primary Older Gravels have recently been discovered to occur below hardpan calcrete in palaeodrainage channels. Where exposed, the sequence consists of up to 2m of clast-supported gravels with angular to sub-rounded clasts of quartzite, vein-quartz, amygdales, lava, banded-ironstone and shale of 1-10cm in size. The -5mm matrix fraction consists of essentially the same components, but with the addition of kimberlitic garnets and ilmenites. The gravels are variously calcretized, with hardpan calcrete usually developed at the surface. Late-stage decomposition of the hardpan calcrete has resulted in the formation of makondos, in which the eluvial gravel component has accumulated. The clasts in the eluvial deposits are composed almost exclusively of chemically resistant, siliceous lithologies.

The colluvial gravels are thin (usually less than 1m thick), aerially extensive deposits that are the result of deflation of the southwestern Transvaal landsurface. They are best developed on deeply-weathered Ventersdorp lava in which pseudokarst solution features have been etched by laterization processes.

Figure 1(a):  
Spatial relationships between the  
Eluvial and Primary Alluvial Gravels  
and the Terrace Gravels.

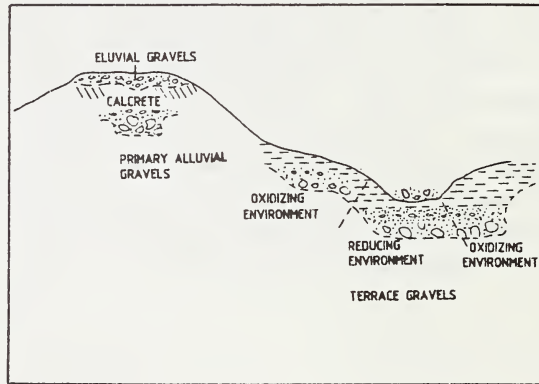
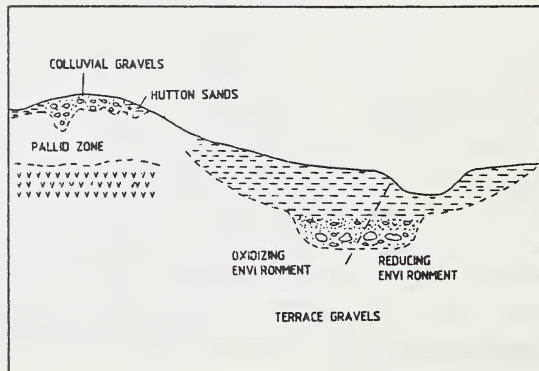


Figure 1(b):  
Spatial relationships between the  
Colluvial and Terrace Gravels.



The younger Terrace Gravels are found everywhere along Plio-Pleistocene drainage lines at depths of 3 to 8m. The deposits consist of an approximately 5m, upward-fining, alluvial, sedimentary sequence deposited on an uneven floor of Ventersdorp lavas. The entire sequence is variably calcretized and the lower portions of the package are either oxidized or reduced, depending on the proximity of the water-table.

It is argued that there is a direct correlation between the gravel stratigraphy of the southwestern Transvaal and that which is developed along the lower Vaal River in the Barkly West district. The (A1) Primary Alluvial Gravels appear to be time correlatives of the Older Gravels (Primary Alluvial Gravels) of Barkly West; the derived older gravels find their equivalent in the colluvial and eluvial components of the southwestern Transvaal; the (A2) Terrace Gravels are most likely equivalent to the Rietput Formation; and the (A3) River Gravels equivalent to the Riverton Formation.

An investigation of the gravels indicates that the clasts have a local origin. By far the majority of the clasts consist of Ventersdorp lithologies. Other clasts can be traced to the Karoo Sequence (both Dwyka and Ecca lithologies), the Amalia, Kraaipan and Zoetlief sequences, and local dyke and vein networks.

In the colluvial and eluvial deposits, many chemically unstable clasts have been totally decomposed by post depositional processes of laterization and calcretization. As a result, these deposits consist almost entirely of siliceous clasts, such as quartz, quartzite, amygdales and agates. This assemblage is non representative of the original gravel and, therefore, cannot be used to infer a source terrane.

Diamonds are found in the alluvial, as well as the colluvial and eluvial gravels. In the latter deposits there does not appear to be any sorting of the diamonds within the gravels. In the alluvial deposits, however, the diamond acts as a heavy mineral and is, therefore, concentrated by sedimentary processes. Economic deposits of diamonds are, thus, to be found in point-bars, downstream confluences, adjacent to dykes, and wherever the hydraulic conditions were optimum for gravel deposition.

Contrary to the findings of previous studies, kimberlitic indicator minerals, such as pyrope garnets, micro-ilmenites, and chrome spinels were recovered from gravels in the southwestern Transvaal. Such indicator minerals were primarily found in the matrix of the alluvial gravels that were extensively calcretized. The eluvial gravels as well as the colluvial gravels contain few, if any, garnets. The bulk of the garnets were likely decomposed by the climatic conditions that promoted the lateritizing conditions prevalent during the African landscape cycle. Analysis of the mineral chemistry of these indicator minerals indicate that many have been derived from a diamondiferous, kimberlite source (Fig. 2).

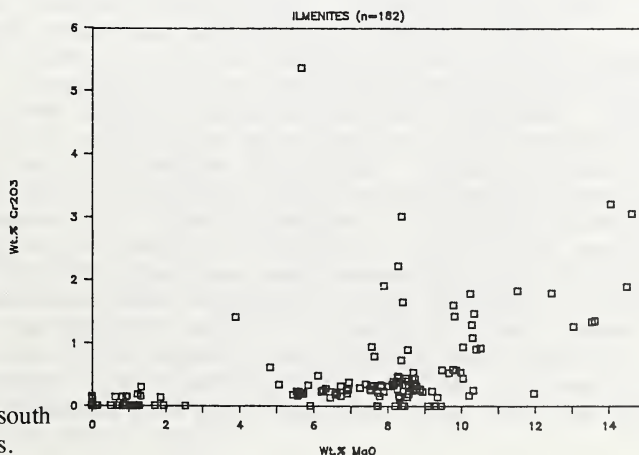


Figure 2(a):  
Cr<sub>2</sub>O<sub>3</sub> vs MgO plot of the southwestern Transvaal Ilmenites.

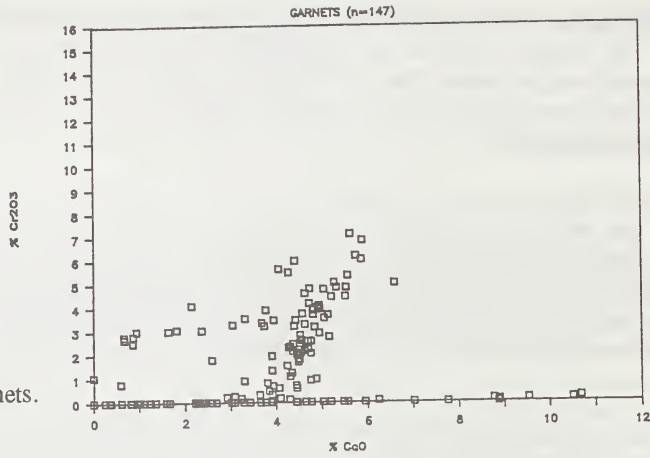


Figure 2(b):  
 $\text{Cr}_2\text{O}_3$  vs  $\text{CaO}$  plot of the  
 southwestern Transvaal garnets.

Evolution of the southwestern Transvaal landscape can be explained within the framework of the accepted geomorphological model for southern Africa. It is envisaged that kimberlites were emplaced in the southwestern Transvaal during the late Cretaceous. Following the rifting of Gondwana, an early Tertiary drainage system developed on the ensuing African surface. As a result of the extremely long period of laterization that followed, the erosion surface was substantially lowered and a residual soil accumulated over the surface. Post African I uplift in the Miocene not only caused piracy and reversal of certain stream segments, but also resulted in the leaching of the African surface and the redistribution and concentration of the colluvial diamondiferous deposits. Subsequent Post African II uplift in the Pliocene resulted in the incision of the A2 drainage-system which reworked portions of the older colluvial gravels. Minor climatic and sea-level oscillations have, further, resulted in the cutting of the present Vaal River terraces.

## LAMPROITIC(?) DIATREMES IN THE GOLDEN AREA OF THE ROCKY MOUNTAIN FOLD AND THRUST BELT, BRITISH COLUMBIA, CANADA.

McCallum, M.E.

*Department of Earth Resources, Colorado State University, Fort Collins, CO 80523, USA.*

During the last 15 years approximately two dozen diatremes have been recognized north of Golden, British Columbia in a northwest trending belt that roughly parallels the B.C.-Alberta province boundary and extends about 55km between the Campbell and Columbia Icefields (Pell, 1987) (Fig. 1). The diatremes are situated within the Rocky Mountain Fold and Thrust Belt and their emplacement relationship to Columbian and Laramide deformation is uncertain. Thirteen discrete "pipes" have been mapped at the Larry, Jack, Mike and Mark localities (McCallum, 1990) and all penetrate a folded and locally faulted sequence of Cambro-Ordovician sedimentary units (Fig. 2). The pipes typically are lensatic, parallel or subparallel locally prominent axial plane cleavage in host rocks, and generally are penetrated by a coincident set of cleavage or foliation planes. One pipe is situated in the core of an anticlinal fold (Fig. 3) and another appears to have been emplaced along a thrust fault, although the latter may be a lensatic, fault emplaced block of diatreme breccia. Tectonic setting suggests that most of these diatremes post-dated folding associated with the Columbian orogeny (younger than 95 ma), and may have been as late as the climax of the Laramide orogeny (60 ma). The well developed cleavage, foliation and local shearing of diatreme breccia indicate at least moderate post intrusion deformation which may have been related to late stage orogenic activity (post folding) or possibly in part in response to post-orogenic relaxation processes. However, several workers (e.g. Pell, 1986, 1987; Ijewliw and Schulze, 1989) postulate a Late Silurian-Early Devonian age for these pipes and preliminary Rb/Sr ratios established from mica separates from the Larry dike complex (Pell, written commun., 1989, Smith, written commun., 1990) support this contention. Apparent inconsistencies between structural relationships and age dates are yet to be resolved.

Diatreme facies tuffisitic breccias predominate and these range from clast to matrix supported, very coarse (block) to fine-grained (lapilli to lapilli-ash) varieties. A locally prominent "sandy" tuffisitic breccia phase is characterized by abundant rounded to subrounded quartz grains (most <0.5mm, commonly comprising >40% of rock) and is texturally similar to sandy tuff phases described at the Argyle and Prairie Creek lamproite pipes in Australia and Arkansas respectively. Breccia clasts are predominantly host rock sediments, but phyllite, schist, gneiss, granitoids, gabbro, diorite, pyroxenite, basalt and lamprophyre fragments are abundant locally. Leucite(?) and or sanidine bearing lamproite(?) clasts are present in some breccia phases at the Jack diatreme. Mineral clasts (other than quartz) and breccia groundmass material generally are difficult to identify due to extensive alteration. However, based on pseudomorphic form, alteration products, and rare unaltered to partially altered grains the presence (or former presence) of variable amounts of olivine, pyroxene, amphibole, sanidine, leucite(?), perovskite, spinel (chromite ?), and devitrified glass has been reasonably well established. Some phases contain abundant fresh phlogopite and/or sanidine. Locally present hypabyssal facies material occurs in irregular zones, narrow crosscutting dikes or xenolithic blocks, and although also generally intensely altered, appears to be mineralogically similar to breccia matrix material. Four small diamonds have been reported; three from the Jack diatreme and one from the Mark 1 pipe.

Preliminary chemical data (Fipke, written commun., 1990) for breccia matrix samples from the Jack diatreme indicate a distinctly ultrapotassic nature (ca. 10wt%  $K_2O$ ), high  $K_2O/Na_2O$  ratios (ca. 67) and moderately high  $SiO_2$  (ca. 52 wt%). These data coupled with the presence of sanidine, high

Ti phlogopite, Sr barite, Sr apatite, glass and pseudomorphs after leucite, olivine, pyroxene and amphibole provide strong evidence to classify the Jack tuffisitic breccia as lamproite although enrichment in incompatible elements (e.g. ca. 200 ppm Zr and 900 ppm Ba) is lower than average for lamproites. Furthermore, whole rock  $Mg/(Mg+Fe)$  ratios of two samples fall well within the lamproite field, low  $Na_2O$  (0.28-1.05 wt%) and high  $MgO + FeO_T$  (0.96-2.35 wt%) contents of sanidine are characteristic of lamproites as are  $Al_2O_3$  levels in phlogopite (1-14 wt%  $Al_2O_3$ ). Limited chemical data for breccia phases from the Larry, Mark and Mike diatremes indicate highly variable compositions and considerably lower levels of alkali enrichment (ca. 2-7wt%  $K_2O$ ) than Jack diatreme material, and concentrations of incompatible elements (e.g., Zr, Nb and Ba) are well below those characteristic of lamproites. However,  $K_2O/Na_2O$  ratios are high (36 to 63), and, although extensively altered, mineral assemblages appear to be fairly similar to those at the Jack pipe. All appear to lack primary plagioclase, melilite, melanite and feldspathoids other than leucite. Allowing for the problems inherent to analyzing diatreme breccias and considering petrographic evidence that suggests a possible lamproitic affinity, the Larry, Mark and Mike tuffisitic breccias are tentatively classified as lamproitic, although an alkaline lamprophyre (sannaite) designation might be appropriate.

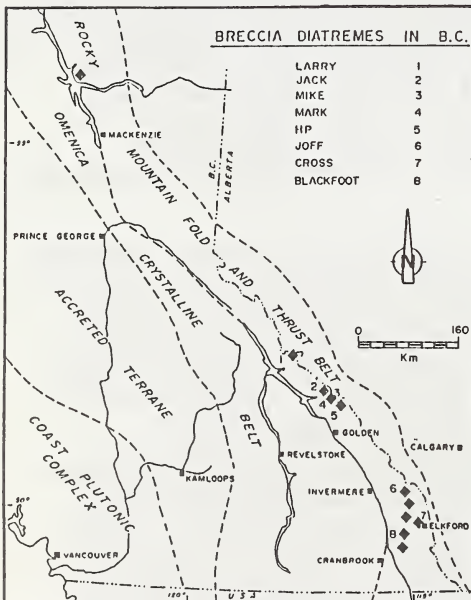


FIGURE 1. Location of the Golden and Elksford area diatremes, southeastern British Columbia. Modified after Pell (1986).

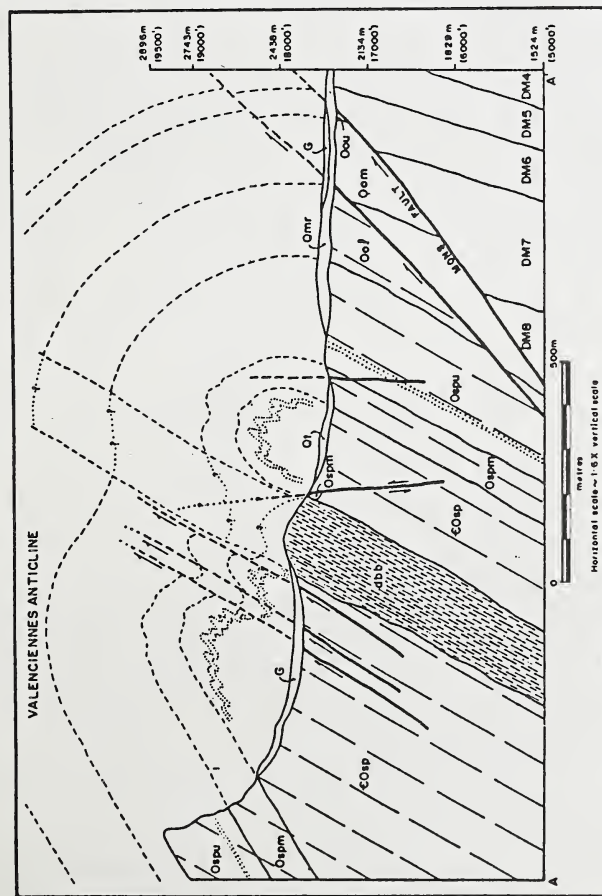


FIGURE 3. Diagrammatic SW-NE structure section across the Mike 1 diatreme which is situated in the core of the Valenciennes anticline and parallels axial plane cleavage in host sedimentary units (McCallum, 1990). G-glaciers and snowbanks; Qt-talus; Qmr-recent moraine; dbb-tuffitic diatreme breccia; DM4 to DM8 - Devonian-Mississippian (?) carbonate sequence; Oou, Oom and Ool-upper, middle and lower members of the Lower Ordovician Ostram Formation (?); Ospu, Ospm and Oosp - upper middle and lower members of the Lower Ordovician-Upper Cambrian Survey Peak Formation (?).

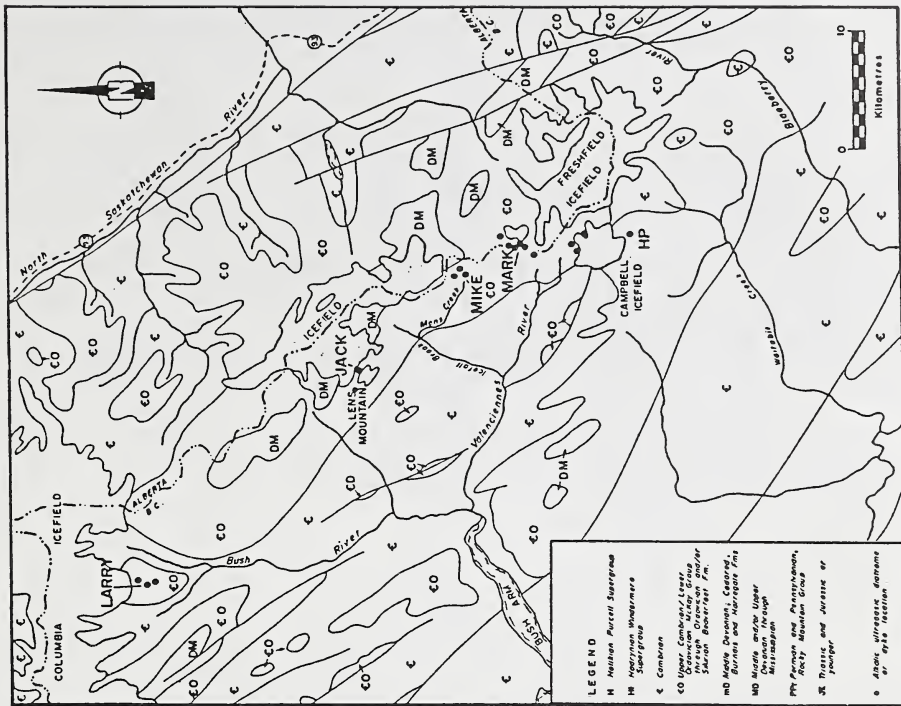


FIGURE 2. General geology of the Golden-Columbia Icefield area and location of the Larry, Jack, Mike, Mark and HP diatremes. Modified after Pell (1987).

## REFERENCES

- Bergman, S.C. (1987) Lamproites and other potassium-rich igneous rocks: a review of their occurrence, mineralogy and geochemistry. In J.G. Filton and B.G.J. Upton eds., *Alkaline igneous rocks*, Special Publication of the Geological Society of London 30, p. 103-190.
- Ijewliw, O.J. and Schulze, D.J. (1989) The Golden cluster of diatremes and dikes. British Columbia Ministry of Energy, Mines and Petroleum Resources, Geological Field work, 1988, Paper 1989-1, p. B39-B46.
- McCallum, M.E. (1990) Geology of the Jack, Larry, Mark and Mike diatremes, Golden Area, British Columbia. In, *The development of advanced technology to distinguish between productive diamondiferous and barren diatremes*, Part II, p. 138-184, 229-321. Canadian Geological Survey Open File Report 2124.
- Pell, J. (1986) Diatreme breccias in British Columbia. British Columbia Ministry of Energy, Mines and Petroleum Resources, Geological Fieldwork, 1985, Paper 1986-1, p. 243-253.
- Pell, J. (1987) Alkalic ultrabasic diatremes in British Columbia. British Columbia Ministry of Energy, Mines and Petroleum Resources, Geological Fieldwork, 1986, Paper 1987-1, p. 259-272.





MORPHOLOGICAL, RESORPTION AND ETCH FEATURE TRENDS OF DIAMONDS FROM  
KIMBERLITES WITHIN THE COLORADO-WYOMING STATE LINE DISTRICT, USA.

*McCallum*<sup>(1), (2)</sup>, *M.E.*; *Huntley*<sup>(1)</sup>, *P.M.*, *Falk*<sup>(1)</sup>, *R.W.* and *Otter*<sup>(2)</sup>, *M.L.*

(1) Dept. of Earth Resources, Colorado State University, Fort Collins, CO 80523, USA; (2) Dept. of Geochemistry, University of Cape Town, Rondebosch 7700, South Africa.

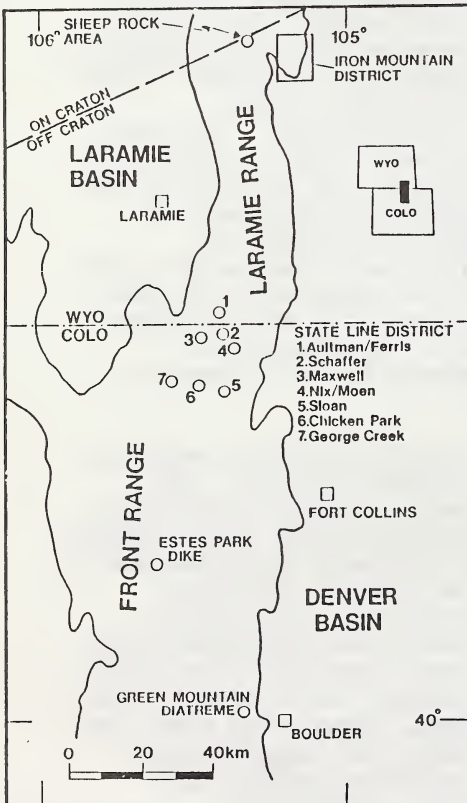
Nearly 1700 carats of diamonds were recovered during company bulk testing of kimberlite occurrences in the State Line District of the Colorado-Wyoming Kimberlite Province. Representative splits of parcels from each locality are being evaluated both physically and chemically along with mineral inclusions, but physical properties are emphasized in this study. Morphological and surface texture characteristics are being described in detail to generate data that may provide insight into the genesis and resorption history of this unique North American diamond suite. Parcels from seven occurrences (Aultman, Maxwell, Schaffer, Chicken Park, George Creek, Sloan 1 & 2, Sloan 5 & 6) (Fig. 1) are included in the evaluation (includes all stones in small parcels and several thousand stones overall). The classification system established by D.N. Robinson (1979) was utilized with modifications.

Degree of stone resorption was established by the method devised by D.N. Robinson to determine the relative percentage of resorption or preservation (Otter and Gurney, 1989). Stones are divided into six classes on the basis of transitional forms between non-resorbed octahedra or cubes (Class 6) and fully developed tetrahexahedra (Class 1) which reflect minimum mass loss of 45% (Robinson, pers. commun., 1984) (Fig. 2, Table 1). Transitional (Class 2-5, 55-99% preserved) and tetrahexahedroid (THH: Class 1, < 55% preserved) forms predominate over octahedra (Class 6, 99-100% preserved) and all occur as single crystals, macles, interpenetrants, and simple and multicrystalline aggregates. Some cubo-octahedra and very rare cubes also were recognized. Single crystal forms dominate all parcels but aggregates and macles are least abundant at the Maxwell and Chicken Park sites and most abundant at George Creek and Sloan. The majority of the diamonds originated as octahedra but differential resorption between kimberlite localities is reflected by the greater proportion of Class 1 and 2 stones (< 70% preservation) at the Maxwell, Aultman, Schaffer, Sloan and Chicken Park sites than at George Creek (> 37% versus ca. 10% in single crystals). Diamonds at all localities exhibit a decrease in degree of resorption with increase in stone size.

A very small proportion of the diamonds district-wide are regularly shaped and more than half of all stones are chipped or broken. Both larger and brown crystals appear to have a greater tendency to breakage, but this property is not exclusive. Although brown crystal color commonly is considered a result of diamond deformation (Robinson, 1979; Robinson et al., 1989), which would favor breakage, many of the best developed deformation textures present in State Line stones occur in colorless crystals that comprise a much smaller proportion of the population (brown > 50% at most localities, colorless < 10%). More than 50% of the Maxwell, Schaffer, Sloan and George Creek diamonds are brown; 70-80% of the Maxwell and Schaffer stones exhibit deformation features, whereas only about 15% of the George Creek stones and 2% of Sloan stones show such features. Strain features in George Creek stones most typically occur as wide deformation lamellae in large colorless crystals. Furthermore, deformation features are present in 75% of the Aultman stones, only 27% of which are brown. Brown colors range from very pale to dark cognac and tend to be more prevalent in smaller stones. Other colors recorded include various shades of gray, amber, yellow and rare pink and green.

In addition to deformation features, more than 40 surface textures are described and these are principally products of resorption and secondary etching (corrosion) processes. Most are rather uniformly represented throughout the diamond parcels, but a few have very restricted distribution. Corrosion sculpture is significant only at the Sloan 2 and Chicken Park sites where it is present on 20% and > 50% of the stones respectively. This apparently is a late phase etch feature that was generated by shallow corrosive root zone activity in a dike and blind diatreme system respectively. However, no corrosion sculpture was observed in diamonds from the George Creek dikes that clearly reflect a root zone environment. The lower degree of resorption (mostly class 4 and 5) thus more limited development of tetraxahexahedroid (THH) surfaces would have retarded development of corrosion sculpture on the George Creek stones. Instead, most George Creek diamonds are characterized by well developed etch sculpture (mosaic of deep trigonal and hexagonal etch pits that generally range from 30 to > 100 microns and cover stone surfaces) which apparently also formed in the dike system. Formation of this feature is favored by larger octahedral surfaces (low resorption) and any minor corrosion sculpture that may have been present would have been obliterated. The etch sculpture probably was initiated in a high T (> 950°C) steam-CO<sub>2</sub> rich melt which was progressively enriched in O<sub>2</sub> with decreasing temperature.

Correlation of mineral inclusion and diamond chemistry data, as they become available, with the physical properties of the respective stones will permit us to interpret the relationships between diamond source and genesis with morphology, resorption and etch features. This should provide information regarding processes that were active deep under North America prior to the late Devonian eruption of the State Line kimberlites.



#### REFERENCES

- Otter, M.L. and Gurney, J.J. (1989) Mineral inclusions in diamonds from the Sloan diatremes, Colorado-Wyoming State Line kimberlite district, North America. In, Kimberlites and related rocks, v. 2, Their mantle/crust setting, diamonds and diamond exploration, Geological Society of Australia Special Publication 14, 1042-1053.
- Robinson, D.N. (1979) Surface textures and other features of diamonds, 221p. Ph.D. thesis, University of Cape Town, Rondebosch, South Africa.
- Robinson, D.N., Scott, J.A., Van Niekerk, A. and Anderson, V.G. (1989) The sequence of events reflected in the diamonds of some southern African kimberlite. In, Kimberlite and related rocks, v. 2, Their mantle/crust setting, diamonds and diamond exploration, Geological Society of Australia Special Publication 14, 980-990.

FIGURE 1. Location map of kimberlite occurrences in the Colorado-Wyoming Kimberlite Province. Front and Laramie Range area underlain by Precambrian crystalline rocks, Basin areas underlain by post-Devonian sedimentary rocks. On craton-off craton line marks boundary between Archean and Proterozoic crustal rocks.

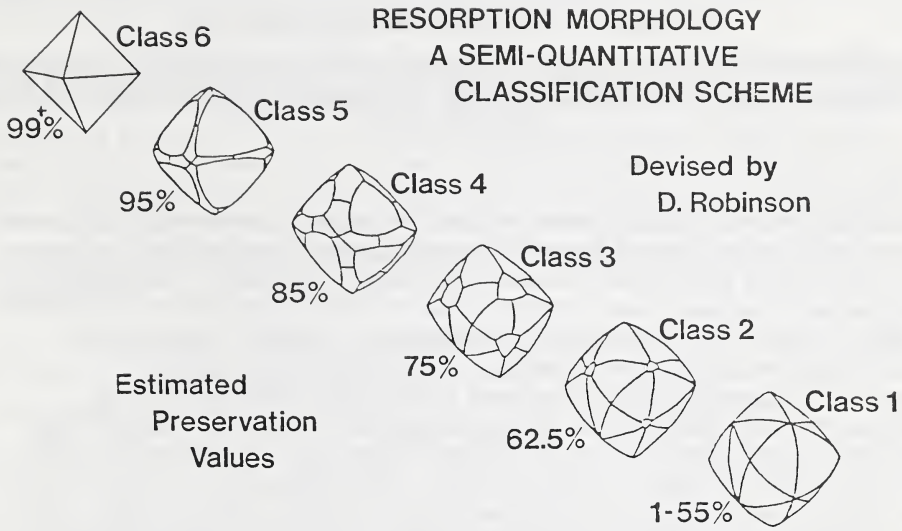


FIGURE 2. Estimated preservation values of progressively more resorbed octahedra (Modified from D.N. Robinson, pers. commun., 1984, and Otter and Gurney, 1989).

TABLE 1. Resorption morphology classification (Modified from D.N. Robinson, pers. commun., 1984, and Otter and Gurney, 1989). Based on relative percentage of preservation of stones converted by resorption from octahedra (or cubes) to tetrahedra.

<u>Class</u>	<u>Percent Preservation</u>	<u>Form</u>
1	1-55	Tetrahexahedra*
2	55-70	"Rounded-dodecahedra"
3	70-80	"Octahedra-dodecahedra"
4	80-90	"Rounded-octahedra"
5	90-99	Octahedra
6	99-100	Planar octahedra

\*May include spheres

## MACRO- AND MICRODIAMONDS FROM ARKANSAS LAMPROITES: MORPHOLOGY, INCLUSIONS AND ISOTOPE GEOCHEMISTRY.

*McCandless*<sup>(1)</sup>, *T.E.*; *Waldman*<sup>(2)</sup>, *M.A.* and *Gurney*<sup>(3)</sup>, *J.J.*

(1) *Dept. of Geosciences, University of Arizona, Tucson, Arizona, 85721, USA;* (2) *Waldman Consulting, 6900 W. Quincy Ave #5E, Littleton, Colorado, 80123, USA;* (3) *Dept. of Geochemistry, University of Cape Town, Rondebosch, 7700, South Africa.*

The lamproites of Arkansas were the first reported occurrences of diamond in igneous rocks in the United States. Diamonds were found at Prairie Creek in 1906, and mining operations commencing shortly thereafter represent the only commercial diamond mine ever operated in the United States (Waldman et al, 1987). In spite of their geological significance, detailed research on diamonds from these localities is lacking. This preliminary study characterizes the morphology, inclusions, and isotope geochemistry of diamonds from these lamproites. Macrodiamonds (>1 mm) for morphology, inclusion and isotopic analysis were obtained from placer operations located on the tailings of the Prairie Creek lamproite. Microdiamonds (<1 mm) were obtained through bulk fusion of ~25 kg samples from the Prairie Creek, Twin Knobs #2, Black Lick, and American lamproites. In total, 63 macrodiamonds and 282 microdiamonds have been examined. Additional color and size information for Prairie Creek diamonds has been tabulated from the Crater of Diamonds State Park records and early mining and historical records covering over 15,000 stones.

For Prairie Creek macrodiamonds, white is the most common colour (62% of total) followed by brown (20%) and yellow (16%; Fig 1). This is in contrast to Australian lamproite diamonds where brown and yellow are predominant (Hall and Smith, 1984). Lamination lines present on both white and coloured stones indicate ductile deformation at mantle conditions (Robinson et al, 1986). The Prairie Creek macrodiamonds are very resorbed- none are octahedra. In the population of 63 stones, 86% are equiform or distorted tetrahedra with irregulars (8%) and fragments (6%) exhibiting only broken or resorbed surfaces. Fine hillocks and low relief surfaces indicate conditions of prolonged and/or intense resorption, similar to diamonds from Ellendale 4 and 9 lamproites in Western Australia (Hall and Smith, 1984). Microdiamond morphology differs dramatically from macrodiamonds. Octahedral twins, aggregates, and fragments are common and tetrahedra are absent. Some tetragonal pitting and crescentic steps occur on otherwise unresorbed crystals. Two microdiamonds exhibit uneven resorption, indicative of a xenocryst origin (Robinson et al, 1989).

Previous studies of inclusions in Arkansas diamonds report inclusions of peridotitic and eclogitic paragenesis, periclase, magnetite, diamond, and sulfides, which were usually retrieved by burning the diamond (Pantaleo et al, 1979). For this study, inclusions were visually located and extracted by cracking the diamond. The translucent surfaces created by resorption made locating and identifying inclusions extremely difficult. Twenty-three inclusions from 10 diamonds were extracted; most are graphite along planes

or in masses as described by Pantaleo and others (1979). Two opaque inclusions which exhibited crystal faces prior to breaking were identified as magnetite and pseudobrookite(?). One olivine inclusion of peridotitic paragenesis was partially liberated from a gem quality white stone.

Twenty-one macrodiamonds from Prairie Creek were analyzed for  $\delta^{13}\text{C}_{\text{PDB}}$ . Eight stones had internal and external portions analyzed. Within-diamond variations are from 0.07-0.54 ‰, with six diamonds slightly lighter inside. Two peaks occur at -3.00 to -6.17 ‰ (ave. -4.67 ‰; 19 stones) and -10.26 to -10.60 ‰ (ave. -10.50 ‰; 2 stones; Fig. 2). There is no correlation between isotopic character and colour or morphology. The diamonds containing the magnetite, pseudobrookite, and olivine inclusions have  $\delta^{13}\text{C}_{\text{PDB}} = -5.13, -4.69, \text{ and } -3.90$  ‰, respectively.

Ten microdiamonds were analyzed, five from Prairie Creek, one each from Twin Knobs #2 and American, and three from Black Lick. Four Prairie Creek microdiamonds are similar to the heavy Prairie Creek macrodiamonds (-0.46, -4.22, -4.45, -6.19 ‰) implying a similar paragenesis (Fig. 2). The American and Twin Knobs #2 microdiamonds are also similar to Prairie Creek (-3.18, -2.20 ‰), as are two of the Black Lick microdiamonds (-3.95, -7.81 ‰). This suggests that the microdiamonds and macrodiamonds share a common carbon reservoir. Light values for one Prairie Creek (-26.06 ‰) and Black Lick (-25.19 ‰) microdiamond preclude a phenocryst origin from a magma with primitive mantle carbon ( $\delta^{13}\text{C} \sim -5.0$  ‰).

In summary, these features indicate that macrodiamonds from the Prairie Creek lamproite experienced intense and/or prolonged resorption similar to macrodiamonds from the Ellendale lamproites of Australia. Lamproite may therefore be a more corrosive agent than kimberlite with respect to diamond. Microdiamonds from the lamproites consist of unresorbed forms which may have been shielded from resorption in small xenolith fragments (McCandless, 1989). Microdiamonds which share common  $\delta^{13}\text{C}$  ratios with macrodiamonds may also be xenocrysts, or could have formed from the same carbon reservoir at the time of pipe emplacement. Two microdiamonds have much lighter  $\delta^{13}\text{C}$  ratios than would be expected for carbon derived from primitive mantle (-5 ‰). Carbon isotopes for both macro- and microdiamonds suggest derivation from peridotitic and/or eclogitic regions in the mantle, which is similar to diamonds from lamproites and kimberlites worldwide.

#### References

- Hall, A.E. and Smith, Chris B. (1984) Lamproite diamonds- are they different? Geology Department and University of Western Australia Publication 8, 167-212.
- Pantaleo, N.S., Newton, M.G., Gogineni, S.V., Melton, C.E., and Giardini, A.A. (1979) Mineral inclusions in four Arkansas diamonds: their nature and significance. *American Mineralogist*, 64, 1059-1062.
- McCandless, T.E. (1989) Microdiamonds from the Sloan 1 and 2 kimberlites, Colorado, USA. 28th International Geological Congress, Extended Abstracts, Workshop on Diamonds, 44-46.

- Robinson, D.N., Scott, J.N., van Niekerk, A., and Anderson, V.G. (1989) The sequence of events reflected in the diamonds of some southern African kimberlites. Geological Society of Australia Special Publication 14, 990-999.
- Waldman, M.A., McCandless, T.E., and Dummett, H.T. (1987) Geology and petrography of the Twin Knobs #2 lamproite, Pike County, Arkansas. Geological Society of America Special Paper 215, 205-216.

Figure 1

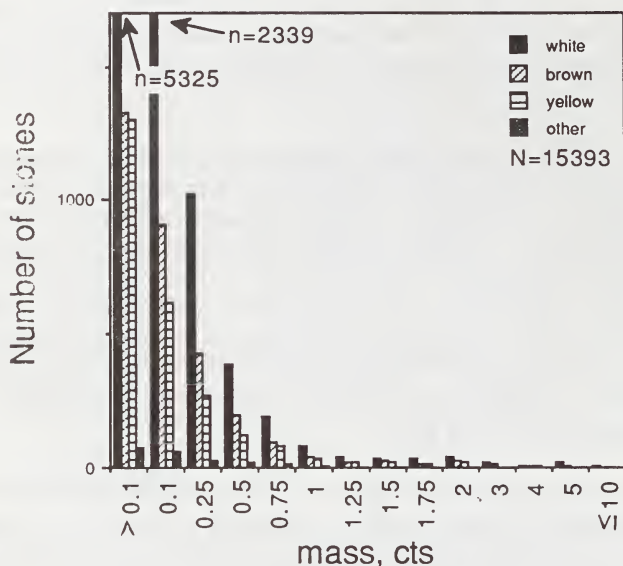
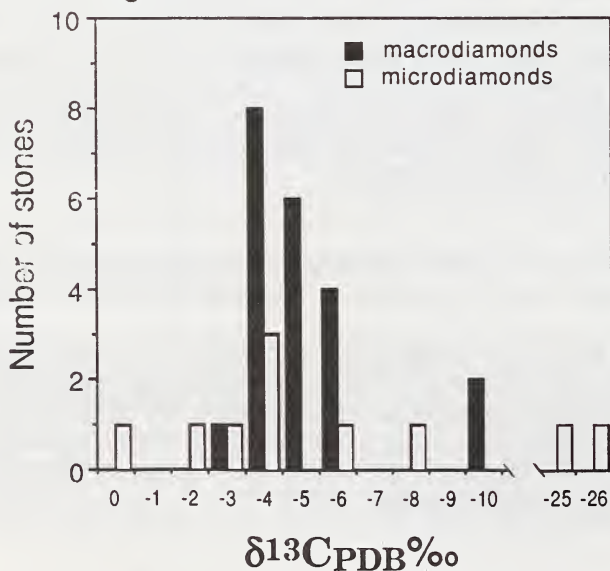


Figure 2



## SECONDARY PHASES IN MANTLE ECLOGITES.

*McCormick, T.C.; Smyth, J.R. and Caporuscio, F.A.*

*Dept. Geological Sciences, Univ. Colorado, Boulder, CO 80309-0250 USA.*

Mantle-derived eclogite xenoliths contain a ubiquitous secondary assemblage located along grain boundaries of the primary phases. Textural and compositional characteristics of these secondary phases have been examined in approximately 60 eclogites from Bellsbank and Roberts Victor kimberlites, South Africa, ranging in composition from Fe- and Mg-rich bimineralic eclogites to grosspydites. The major element chemistry of the primary phases of these samples have been previously described (Smyth and Caporuscio, 1984). The assemblage is much more abundant than, and significantly different from that observed in peridotites at these localities, whereas similar eclogites from different localities show similar secondary assemblages.

Mineralogically, the secondary assemblage appears to be systematically related to the bulk composition of the eclogite. Kyanite eclogites have spinel and secondary clinopyroxene as the dominant secondary phases plus minor Ba-feldspar, barite, and sulfides. In contrast, bimineralic eclogites contain abundant secondary phlogopite and amphibole, in addition to the above minerals, as the secondary assemblage. A few samples also contain rutile that may or may not be secondary. In both secondary phase assemblages, the major- and minor-element contents of these phases (Fe, Al, Mg, Ca, Mn, Ti, and Cr) correlate with the contents of these elements in the primary pyroxene. Analysis of secondary phases in a traverse across a single composite or banded eclogite nodule reveals a continuous, systematic variation in composition (Fig.1). Corresponding major- and minor-element correlations occur amongst the secondary phases, as illustrated by the complete sample suite in Fig. 2. Correlation between secondary phase composition and primary garnet is largely lacking. In a few cases, the infiltration of kimberlite can be ruled out on the basis of trace element studies. However, minor secondary apatite and calcite are observed, particularly in the Cr-rich samples, and may indeed be related to the kimberlite.

Texturally, the assemblage appears to be locally controlled by chemical potential gradients surrounding the primary phases. The assemblage along garnet-pyroxene boundaries in bimineralic eclogites shows a distinct spatial sequence: primary garnet, amphibole + spinel, phlogopite, secondary clinopyroxene, primary pyroxene, such that amphibole always lies between phlogopite and primary garnet. Phlogopite commonly occurs as a necklace of oriented grains along garnet-pyroxene boundaries. Amphibole typically contains euhedral spinel inclusions, and is more common on garnet-garnet boundaries and in cracks in garnet than in association with primary pyroxene. Secondary clinopyroxene occurs along primary pyroxene-pyroxene and pyroxene-garnet boundaries and very seldom on garnet-garnet boundaries. It is typically epitaxial on the primary pyroxene. Spinel is generally small, euhedral grains of green hercynite-spinel solid solutions and occur as inclusions in amphibole in the bimineralic eclogites and as inclusions or symplectic intergrowths with secondary clinopyroxene in kyanite eclogites.

Compositionally, the phlogopites tend to be Al- and Fe-rich compared with micas reported from peridotites (e.g. Delaney et al., 1980; Erlank et al., 1988), although they cover a wide range of compositions. They contain variable amounts of minor elements such as Ba and Ti, with some phlogopites adjacent to rutile containing up to 4 wt% BaO and 9 wt% TiO<sub>2</sub>. The amphibole is pargasite-ferrohastingsite, in contrast to the more Mg- or K-rich amphiboles observed in peridotites (e.g. Erlank et al., 1988). The secondary clinopyroxene is diopside- and Ca-Tschemmakh-rich and strongly depleted in Na relative to the primary pyroxene. The spinel is typically low in Cr (< 7 wt% oxide) except in extremely Cr-rich eclogites where it occurs with up to 50 wt% Cr<sub>2</sub>O<sub>3</sub>.

The presence of phlogopite and spinel rather than feldspars indicates that the secondary assemblage is high-pressure, although lower pressure than the 30-60 kbar of the primary phase equilibrium.

As an alternative to a metasomatic origin, it is possible that the entire secondary assemblage in many samples may be derived from the primary phases plus minor accessory rutile and sulfides. It has long been noted that the pyroxenes in these rocks may contain up to 0.4 wt% K<sub>2</sub>O, and K<sub>2</sub>O contents up to 1.5 wt% have been observed in pyroxene inclusions in diamonds. Having a slightly smaller radius than K, Ba is even more likely to substitute in clinopyroxene in these rocks. A few of the eclogites do contain exsolution lamellae of phlogopite or rutile in the primary pyroxene. Recently, we have observed up to 2000 ppm OH in these pyroxenes and textural evidence suggests that OH contents may have been higher than 5000ppm in the precursor pyroxenes (Smyth et al., 1991). Consistent with a mantle igneous origin for these rocks, exclusion of incompatible elements K, Ba and OH from the pyroxene would likely have occurred on cooling from the solidus temperatures (>1450°C) to the temperature of equilibration of the primary phases (1050 - 1250°C) at pressures of 3 to 6 GPa. The incompatible element-rich assemblage may then have undergone melting and recrystallization on incorporation into the kimberlite with variable amounts of infiltration of the kimberlite fluid.

We observe no conclusive evidence of alteration of the samples by a common metasomatic fluid than can be readily characterized.

#### REFERENCES:

- Delaney, J.S., Smith, J.V., Carswell, D.A., and Dawson, J.B. (1980) Chemistry of micas from kimberlites and xenoliths - II. Primary- and secondary-textured micas from peridotite xenoliths. *Geochimica et Cosmochimica Acta*, 44, 857-872.
- Erlank, A.J., Warters, F.G., Hawkesworth, C.J., Haggerty, S.E., Allsop, H.L., Rickard, R.S., and Menzies, M. (1987) Evidence for mantle metasomatism in peridotite nodules from the Kimberley Pipes, South Africa. In M.A. Menzies and C.J. Hawkesworth, Eds., *Mantle Metasomatism*, p. 221-311. Academic Press, London.
- Smyth, J.R., Bell, D.R., and Rossman, G.R. (1991) Hydrous clinopyroxenes from the upper mantle. Submitted to *Nature*.

Smyth, J.R. and Caporuscio, F.A. (1984) Petrology of a suite of eclogite inclusions from the Bobbejaan kimberlite: II. Primary phase compositions and origin. In J. Kornprobst, Ed., Kimberlites II: The Mantle and Crust-Mantle Relationships, p. 121-131. Elsevier, Amsterdam.

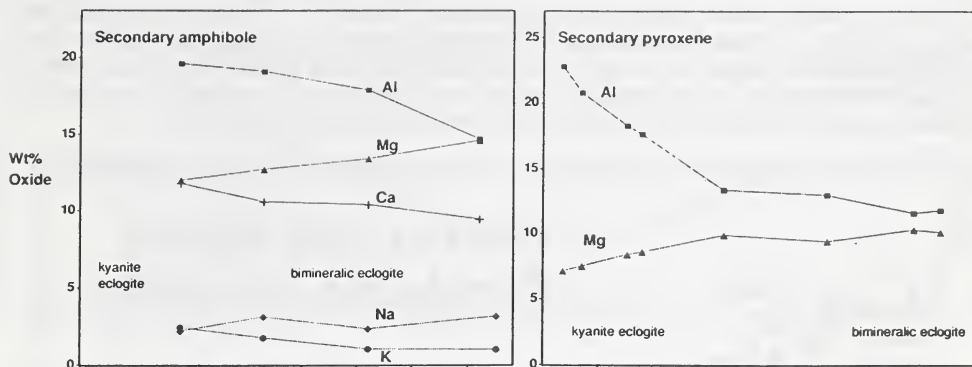


Figure 1. Variation in composition of secondary pyroxene and amphibole in a 30-mm traverse across a composite eclogite, HRV-17 (wt% oxide plotted against distance). No amphibole or phlogopite are observed in the kyanite-bearing region; secondary clinopyroxene and spinel occur throughout.

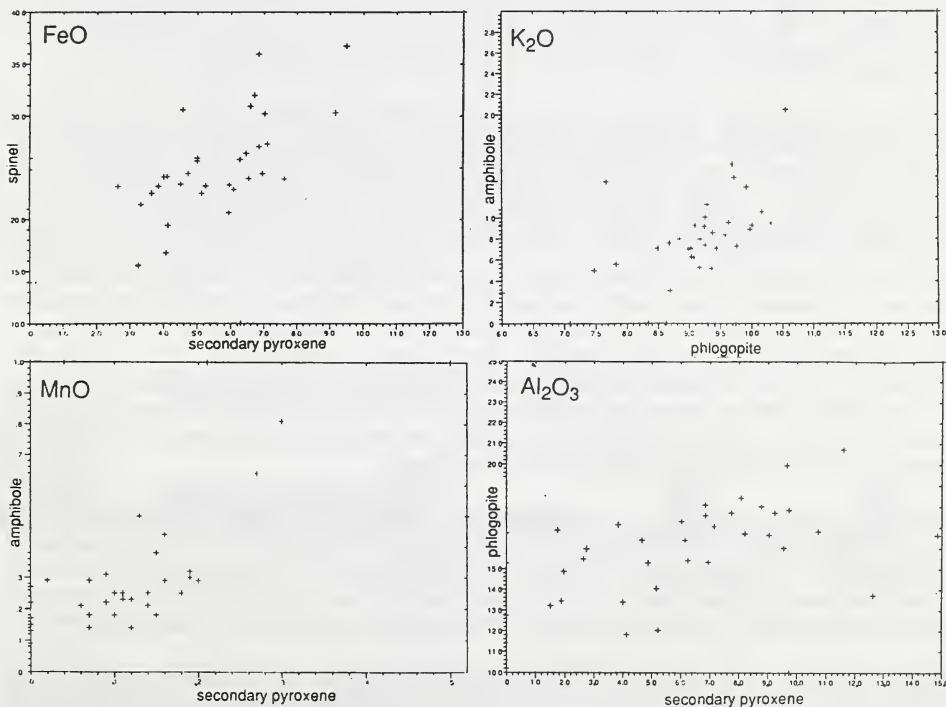


Figure 2. Composition correlation plots of selected major and minor elements amongst secondary phases in mantle eclogites.

## CHEMICAL AND ISOTOPIC SYSTEMATICS OF CONTINENTAL MANTLE.

*W.F. McDonough**Research School of Earth Sciences, Australian National Univ., Canberra, ASCT 2601, Australia.*

Peridotite xenoliths show systematic geochemical trends<sup>1-3</sup>. These systematics are illustrated in Figure 1, where the sequence of elements along the x-axis reflects decreasing incompatible behaviour (from left to right). Patterns displayed by garnet and spinel bearing peridotite xenoliths (Figure 1), are consistent with a two stage history involving the extraction and later reintroduction of melts. These processes control peridotite geochemistry.

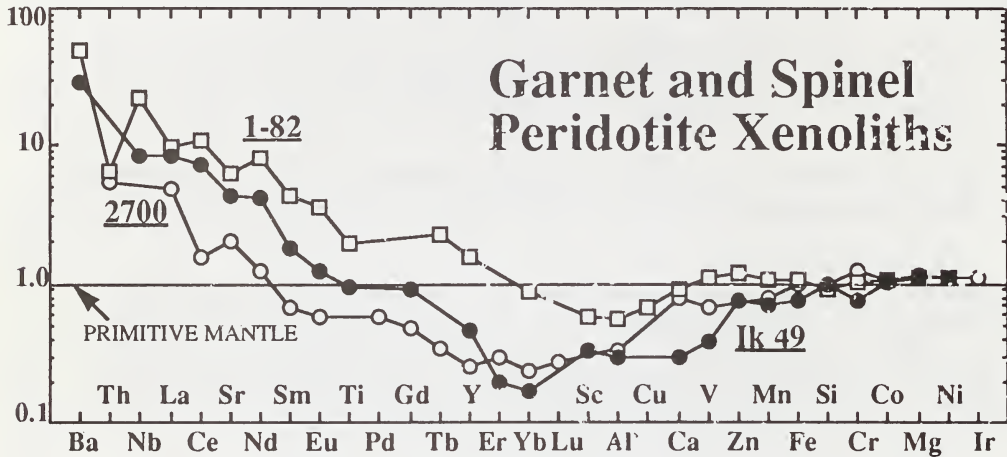


FIGURE 1. Mantle normalized diagram for typical peridotites from continents, including a garnet peridotite<sup>5</sup> (filled symbol) and two spinel peridotites<sup>6, 7</sup> (open symbols). Element abundances normalized to primitive mantle<sup>1, 19, 20</sup>; order of elements is established by the enrichment factors observed in oceanic basalts.

These element systematics are typical of peridotites from non-cratonic and cratonic parts of the continents<sup>1-8</sup> and are schematically illustrated in Figure 2. Here elements are classified into Groups for the sake of further discussion. For most peridotites, the Group V elements (e.g., LREE, P, Sr, Ba, Nb, Ta, Mo, W, Tl, Cs, Rb, K, Th and U) and some of the Group IV elements (e.g., heavy to middle REE, Y, Ti, Na, Zr, Hf, Li, Sb, Sn and Pd) are enriched relative to Primitive Mantle. Members of Group V and IV elements included the highly incompatible and moderately incompatible trace elements, respectively. The Group III elements (e.g., Cu, Zn, Ca, Sc, Al, V, Lu, Yb, Re, Au and Cd), which included the mildly incompatible elements, are generally depleted relative to Primitive Mantle. This behaviour is in contrast to that shown by the Group IV and V elements. The Group I elements (e.g., Co, Cr, Mg, Ni, Rh, Ru, Ir and Os) which include the compatible trace elements and are consistently enriched by about 5% to 50% relative to the Primitive Mantle. Finally, the Group II elements (e.g., Si, Mn, Fe and Ge) show similar abundances in basalts and residual peridotites, indicating that these elements have distribution coefficients close to unity.

Enrichment of Group I elements and depletion of Group III-V elements occurred during an early melt extraction event, probably during the initial stages of lithospheric mantle development and stabilization<sup>3, 7, 9</sup>. The seemingly contradictory enrichments of incompatible elements are due to a later metasomatic enrichment. This enrichment process may have occurred repeatedly, over long time scales and in association with tectonomagmatic reactivation of the lithosphere.

Peridotite xenoliths are samples of the continental mantle, albeit small. Based on a compilation of geochemical data for about a thousand peridotite xenoliths a compositional model for the continental mantle can be developed. The continental mantle in non-cratonic regions possesses a LREE-enriched pattern, with about 1.5 to 4 times the primitive mantle abundance for La, and a relatively flat HREE pattern, with Yb-Lu concentrations about a factor of 2 less than primitive mantle abundances<sup>3</sup>. This two fold decrease in Yb and Lu abundances is consistent with their average major element compositions<sup>3, 10-12</sup>. Peridotite xenoliths (predominantly garnet-bearing) from cratons have on average more depleted major

element compositions<sup>10-12</sup> and likewise have more depleted HREE abundances than the non-cratonic (predominantly spinel-bearing) peridotite xenoliths<sup>3</sup>. This feature is consistent with cratonic peridotites being generated by the extraction of greater degrees of partial melt<sup>11</sup>.

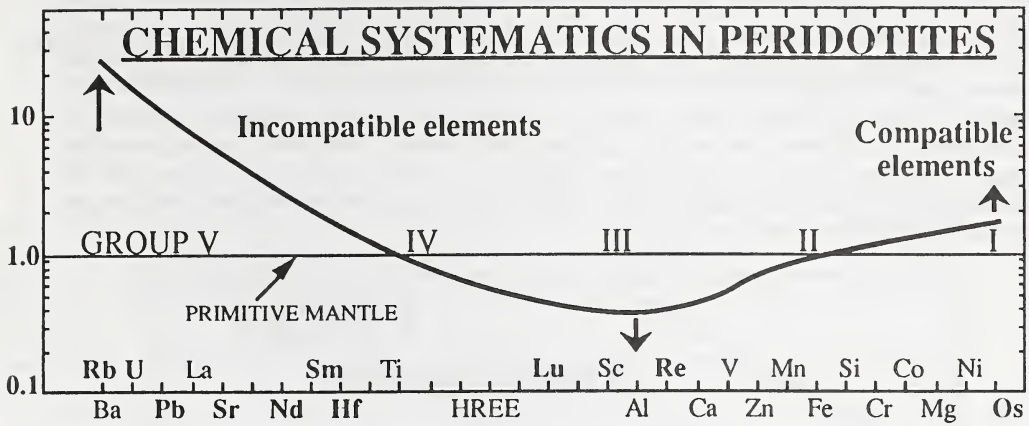


FIGURE 2. A schematic mantle normalized diagram illustrating the systematic geochemical behaviour of elements in garnet and spinel bearing peridotites.

These chemical systematics have important implications for the parent/daughter ratios (i.e., Rb/Sr, Sm/Nd, U(Th)/Pb, Lu/Hf and Re/Os) of the radiogenic isotope systems. Parent and daughter isotopes for the Sr, Nd and Pb isotope systems are incompatible and are therefore more strongly influenced by the early depletion and later enrichment processes. Thus, the age of the melting event, the time difference between this and later enrichment(s) and the composition of the added component will all greatly influence the resultant isotopic characteristics. Consequently, the Sr-Nd-Pb isotope systems are fairly complicated, as is readily shown by the broad spectrum of Sr and Nd isotopic compositions in peridotite xenoliths. In contrast, the parent isotopes <sup>176</sup>Lu and <sup>187</sup>Re are classified with the Group III elements and their daughter isotopes (<sup>176</sup>Hf and <sup>187</sup>Os) are Group IV and Group I elements, respectively. Re/Os data for peridotite xenoliths<sup>13-15</sup> are limited, however, most have subchondritic values (Figure 3). Rhenium tends not to be enriched during metasomatic enrichment events. Likewise, peridotite xenoliths with long term incompatible element enrichments should have low, subchondritic Sm/Nd and Lu/Hf values. Thus, time integrated evolution of these isotope systems in most cratonic and non-cratonic peridotites should be retarded with respect to the bulk earth, leading to distinctive Hf-Os isotopic compositions for the continental mantle (Figure 4). The limited amount of Os and Hf isotope data for continental peridotite xenoliths support this interpretation.

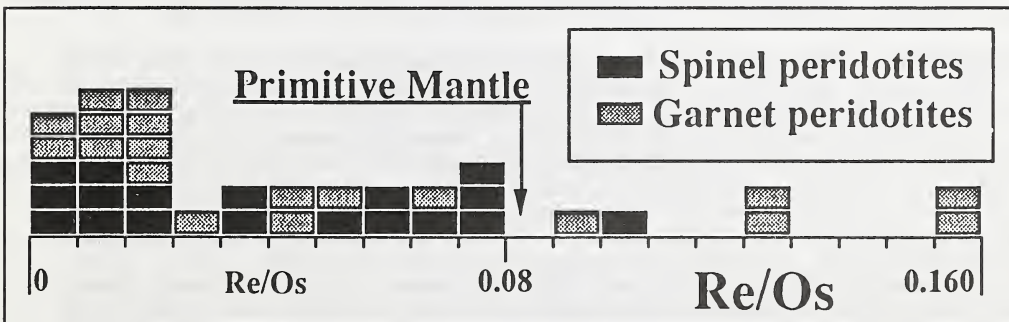


FIGURE 3. A histogram of Re/Os ratios for peridotite xenoliths from continents. Most peridotites have subchondritic (i.e., subprimitive mantle) Re/Os ratios. Samples contaminated by kimberlitic magmas<sup>13</sup> were not included in this histogram. Other garnet peridotites with high Re/Os (shown here) may also have been contaminated.

These chemical and isotopic systematics for the continental mantle can constrain source models for different types of magmas. Sr, Nd, Pb and Os isotope data for southern Africa

kimberlites<sup>13, 16</sup> are consistent with incompatible element-enriched regions of the continental mantle as a source for Group II kimberlites, whereas Group I kimberlites may be derived from similar or deeper mantle sources. The abundant Sr, Nd and Pb isotope data for continental flood basalts are consistent with, but do not require, an incompatible element-enriched source region in the continental mantle. This isotope data in combination with the scant amount of Os and Hf isotope data<sup>17, 18</sup>, however, do not support the hypothesis that continental flood basalts are derived from incompatible element-enriched continental mantle sources. Assuming the bulk composition of the continental mantle possess an incompatible element-enriched composition, then the former should have low Sm/Nd Lu/Hf and Re/Os ratios. Over time this region evolves to negative  $\epsilon_{Nd}$ ,  $\epsilon_{Hf}$  and  $\gamma_{Os}$  compositions (Figure 4). The available Os isotope data for continental flood basalts are similar to the crust ( $+\gamma_{Os}$ )<sup>18</sup> and are inconsistent with source models invoking the continental mantle.

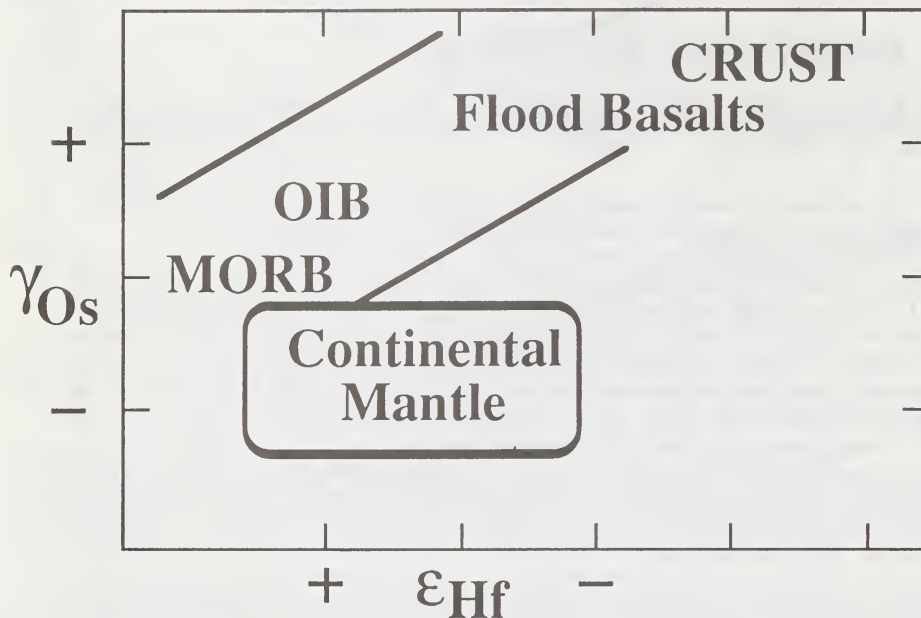


FIGURE 4. Idealized Hf-Os isotope systematics for oceanic basalts (MORB and OIB), flood basalts, continental crust (CRUST) and the continental mantle. This diagram has been constructed from the few available data for Hf and Os isotopes and from predictions on the continental mantle based on the chemical systematics of peridotite xenoliths. The continental mantle is not predicted to be a suitable source for continental flood basalts.  $\epsilon_{Hf}$  and  $\gamma_{Os}$  express differences in parts to the  $10^4$  and  $10^3$ , respectively, from a chondritic value.

- REFERENCES: 1. McDonough, W.F. & Frey, F.A. in *Geochemistry and Mineralogy of Rare Earth Elements* (eds. Lipin, B. & McKay, G.R.) 99-145 (Mineralogical Society of America, Chelsea, Michigan, 1989). 2. Jochum, K.P., McDonough, W.F., Palme, H. & Spettel, B. *Nature* **340**, 548-550 (1989). 3. McDonough, W.F. *Earth Planet. Sci. Lett.* **101**, 1-18 (1990). 4. Nixon, P.H., Rogers, N.W., Gibson, I.L. & Grey, A. *Ann. Rev. Earth Planet. Sci.* **9**, 285-309 (1981). 5. Erlank, A.J., et al. in *Mantle Metasomatism* (eds. Menzies, M.A. & Hawkesworth, C.J.) 221-312 (Academic Press Inc., London, 1987). 6. Menzies, M.A., Rogers, N., Tindle, A. & Hawkesworth, C.J. in *Mantle Metasomatism* (eds. Menzies, M.A. & Hawkesworth, C.J.) 313-361 (Academic Press Inc., London, 1987). 7. Frey, F.A. & Green, D.H. *Geochim. Cosmochim. Acta* **38**, 1023-1059 (1974). 8. Stosch, H.-G. & Seck, H.A. *Geochim. Cosmochim. Acta* **44**, 457-470 (1980). 9. Ringwood, A.E. *J. Geology* **90**, 611-643 (1982). 10. Maaløe, S. & Aoki, K.I. *Contrib. Mineral. Petrol.* **63**, 161-173 (1977). 11. Boyd, F.R. *Earth Planet. Sci. Lett.* **96**, 15-26 (1989). 12. Jordan, T.H. in *The mantle sample: Inclusions in kimberlites and other volcanics* (eds. Boyd, F.R. & Meyer, H.O.A.) 1-14 (AGU, Washington, D.C., 1979). 13. Walker, R.J., Carlson, R.W., Shirey, S.B. & Boyd, F.R. *Geochim. Cosmochim. Acta* **53**, 1583-1595 (1989). 14. BVSP. *Basaltic Volcanism on the Terrestrial Planets* 1-1286 (Pergamon Press Inc., New York, 1981). 15. Nonaka, J. *Über die Häufigkeit von bisher wenig untersuchten Elementen im Erdmantel* (Universität Mainz, 1982). 16. Smith, C.B. *Nature* **304**, 51-54 (1983). 17. Liew, T.C., Cox, K.G., Hawkesworth, C.J. & Hofmann, A.W. *Terra cognita* **6**, 234-235 (1986). 18. Pegrarn, W.J. & Allègre, C.J. *Terra abstracts* **1**, 343 (1989). 19. Sun, S.-s. *Geochim. Cosmochim. Acta* **46**, 179-192 (1982). 20. Sun, S.-s. & McDonough, W.F. in *Magmatism in the ocean basins* (eds. Saunders, A.D. & Norry, M.J.) 313-345 (Geol. Soc. Lond. Spec. Pub., 1989).

## ENHANCEMENT OF GEOPHYSICAL DATA FOR KIMBERLITE EXPLORATION AT IRON MOUNTAIN, WYOMING, USA.

Memmi<sup>(1), (2)</sup>, J.M. and McCallum<sup>(1)</sup>, M.E.

(1) Department of Earth Resources, Colorado State University, Fort Collins, CO 80523 USA; (2) Present address: Department of Geological Sciences, Ohio State University, Columbus, OH 43210 USA.

Composite geophysical data from the Iron Mountain Kimberlite District indicate enhancement of geophysical data may aid in kimberlite exploration by accentuating or revealing subtle anomalies. Surface total magnetic field intensity and conductivity data were processed jointly to assess the utility of their combination for rapid and reliable kimberlite detection. Several anomalies, interpreted to reflect kimberlite, were identified in both geophysical and enhanced data from the Iron Mountain area (Figure 1). Most aberrations generally occur on trend with known kimberlite blows and likely mark the subsurface extension or feeder dikes of these intrusions, or separate bodies emplaced along a common structural trend.

Magnetic and conductivity data were subjected to first through fifth degree complete multinomial regression analysis, with station location and elevation used as predictors. Observations, predictions and residuals from the "best" statistically significant regression equation, chosen on the basis of maximum adjusted  $R^2$  difference, were related to a mutual reference line by ranking and standardization. Subsequently, corresponding components of both the ranked and standardized conductivity and magnetic data were manipulated arithmetically. The best tools for detecting and isolating kimberlite occurrences are magnetic/conductivity ratios.

Data enhancement by combining magnetic and conductivity values is useful where conventional geophysical techniques yield ambiguous and(or) only subtle results. For the Iron Mountain study area, striking composite data deviations commonly correspond to subtle kimberlite-related anomalies in the original data, especially those attributed to kimberlite in the subsurface (compare profiles 1 and 2 with profiles 3 and 4 in Figure 2). Such intrusions generally generate broad wavelength, low amplitude features in total magnetic field intensity and unclear conductivity responses.

Evaluation of conventional and composite geophysical data suggests the subsurface occurrence of a series of east-west trending kimberlite dikes, some of which serve as feeders for both exposed and blind diatremes and(or) blows (Figure 1). Kimberlite emplacement apparently was controlled by abundant east-west faults and joints.

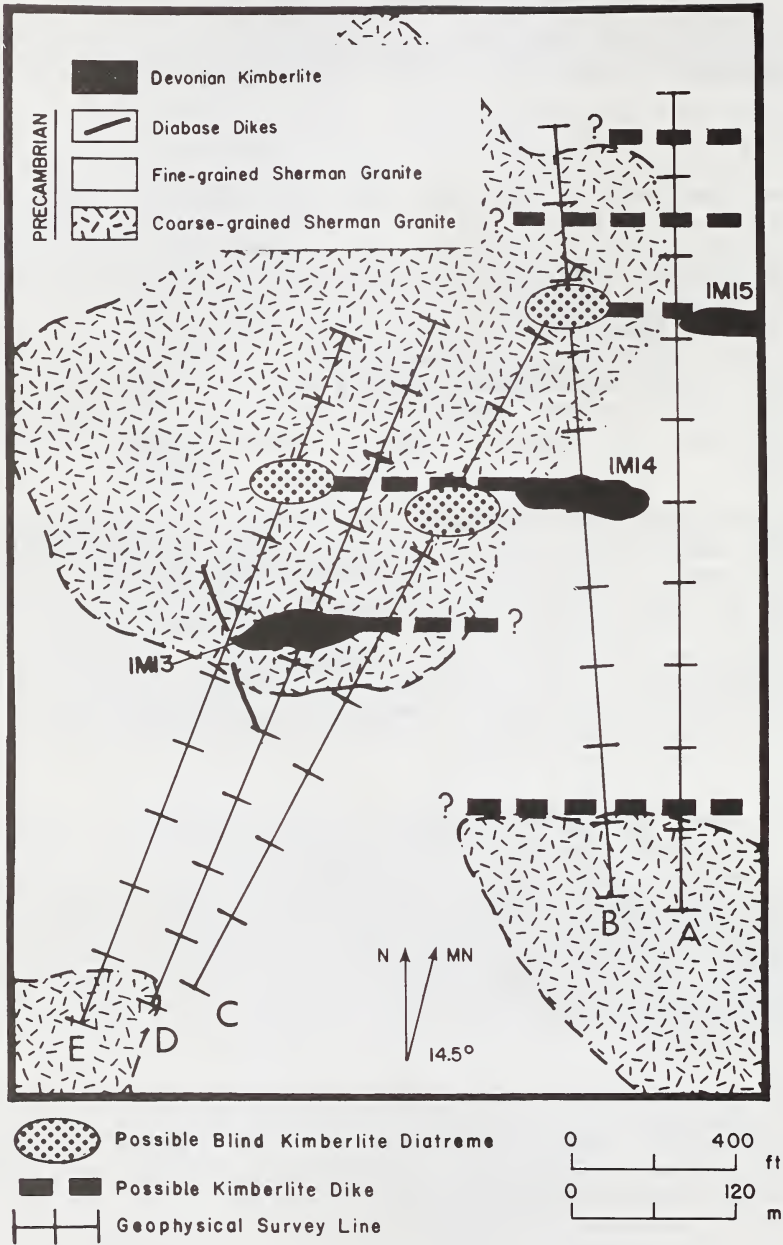


Figure 1. Distribution of hypothesized subsurface kimberlite near kimberlite blows IM13, IM14 and IM15, Iron Mountain Kimberlite District, Wyoming. Suggested subsurface kimberlite occurrences are not to scale.

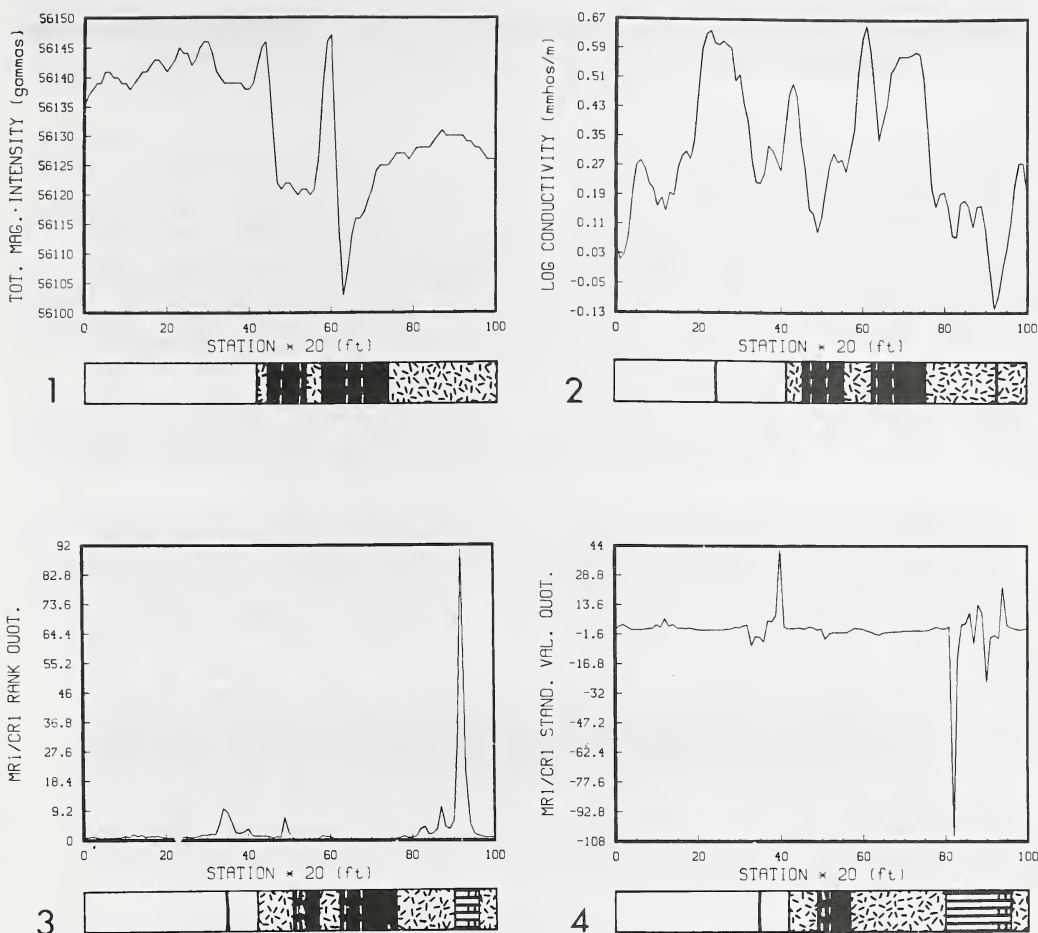


Figure 2. Profiles of conventional and composite geophysical data along Line C, between IM13 and IM14 kimberlite blows, Iron Mountain Kimberlite District, Wyoming (see Figure 1 for location): (1) total magnetic field intensity (2) logarithmic conductivity, (3) residual rank quotient (MR1 = first degree magnetic residual, CR1 = first degree conductivity residual), (4) residual standardized value quotient. Strip beneath each profile indicates subsurface geology inferred from each set of geophysical data.

Interpretive strip explanation: black = probable kimberlite anomaly, striped pattern = possible kimberlite anomaly, stippled pattern = coarse-grained Sherman Granite, blank = fine-grained Sherman Granite, heavy line = fault or major joint, dashed line = proposed kimberlite/granite contact.

## FINITE ELEMENT MODELING OF RESISTIVITY DATA FROM KIMBERLITES IN COLORADO-WYOMING, USA.

*Memmi<sup>(1), (2)</sup>, J.M. and McCallum<sup>(1)</sup>, M.E.*

*(1) Department of Earth Resources, Colorado State University, Fort Collins, CO 80523 USA; (2) Present address:  
Department of Geological Sciences, Ohio State University, Columbus, OH 43210 USA.*

The geoelectric character of three Colorado-Wyoming kimberlite occurrences has been defined via two dimensional finite element intrinsic resistivity inversion. Collinear dipole-dipole resistivity surveys were conducted across the Maxwell 2 pipe, IM36 blow and Sheep Rock 1 (Radichal) diatreme of the State Line, Iron Mountain and Sheep Rock districts respectively, of the Colorado-Wyoming Kimberlite Province. Each of the investigated kimberlite bodies is responsible for a low-high-low "inverted V" pattern in apparent resistivity (Figure 1-A). Such an anomaly typifies a vertical conductor. Colorado-Wyoming kimberlite is 8 to 15 times less resistive than crystalline country rocks (100 - 225 ohm-m for kimberlite versus 1000 - 2500 ohm-m for host rocks).

Following detailed interpretation of the pseudosections of apparent resistivity from each of the three kimberlites, the apparent resistivity data were subjected to finite element modeling to test the efficacy of this technique in producing two dimensional intrinsic resistivity models of kimberlite bodies and country rocks (Figure 1-B). For each pseudosection, the modeling procedure involved (1) centering the kimberlite body as a vertical tabular conductor in the finite element mesh, along with delineating vertical and lateral inhomogeneities in intrinsic resistivity throughout the pseudosection; and, (2) computing models iteratively, varying widths, depths, depth extent, locations and intrinsic resistivities of geologic inhomogeneities and the vertical tabular conductor, until an acceptable fit (average error of 30%) was obtained between the observed pseudosection and the model pseudosection (compare Figure 1-A and Figure 1-C).

The finite element models show that evaluated Colorado-Wyoming kimberlite occurrences are represented adequately by a two layered vertical tabular conductor, with the upper layer corresponding to weathered kimberlite and the lower layer equating to more massive kimberlite (Figure 1-B). Intrinsic resistivity of Colorado-Wyoming kimberlite ranges from 20 to 50 ohm-m compared to values of 1000 to 3000 ohm-m for crystalline host rocks.

Figure 1

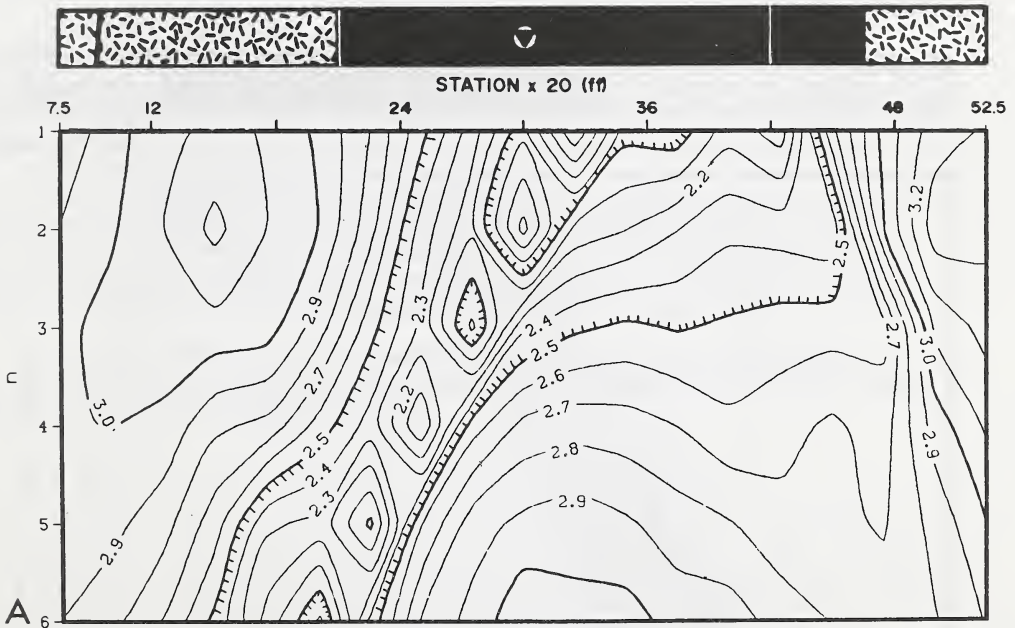
(A) West to east pseudosection of logarithmic apparent resistivity (in ohm-meters) across the Maxwell 2 kimberlite diatreme, State Line Kimberlite District, Colorado. Numbers on vertical axis correspond to inter-dipole or "n" spacing. Strip above profile indicates geology inferred from data compared with mapped contacts.

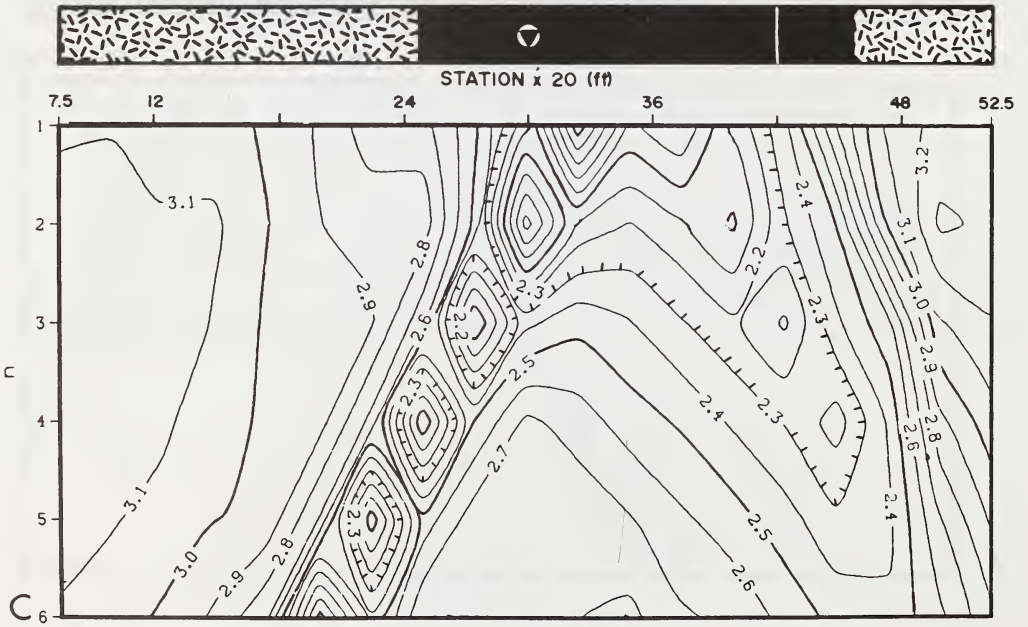
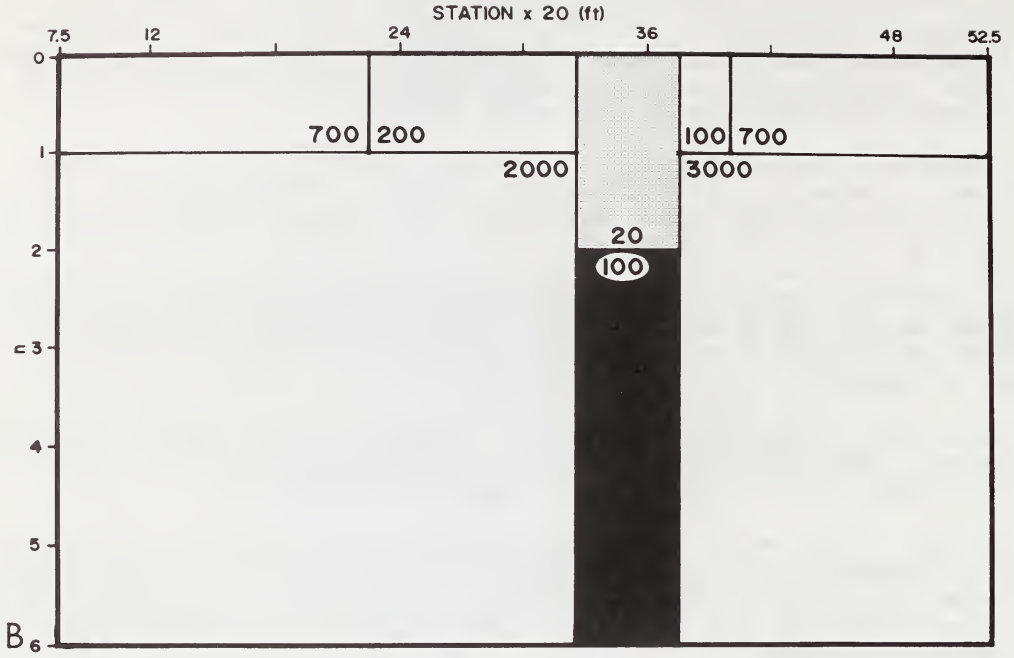
Interpretive strip explanation: triangle = apparent center of diatreme, black = kimberlite anomaly, stippled pattern = Sherman Granite, thick line = fault or major joint, thin white line = mapped kimberlite/granite contact.

(B) West to east two dimensional finite element intrinsic resistivity model across the Maxwell 2 kimberlite diatreme, State Line Kimberlite District, Colorado. Numbers on vertical axis correspond to inter-dipole or "n" spacing.

Media and intrinsic resistivities (in ohm-m) are: 3000 - 2000 = Sherman Granite, 700 = grus, 200 - 100 = grus and weathered kimberlite float, 100 (shaded area) = kimberlite, 20 = weathered kimberlite.

(C) West to east model logarithmic pseudosection of apparent resistivity (in ohm-meters) across the Maxwell 2 kimberlite diatreme, State Line Kimberlite District, Colorado. Numbers on vertical axis correspond to inter-dipole or "n" spacing. (See A above for explanation of interpretive strip).





## INFRARED MICROSPECTROSCOPY OF DIAMOND IN RELATION TO MANTLE PROCESSES.

*Mendelsohn<sup>(1)</sup>, M.J.; Milledge<sup>(1)</sup>, H.J.; Cooper<sup>(1), (2)</sup>, G.I. and Meyer<sup>(3)</sup>, H.O.A.*

*(1) Crystall. & Min. Phys. Unit, Dept. Geol. Sci., University College London, Gower Street, London WC1E 6BT, U.K.;*

*(2) Physics Department, University of York, Heslington, York YO1 1UY, U.K.; (3) Dept. Earth & Atmos. Sci., Purdue University, West Lafayette, IN 47907 USA.*

Infrared spectra of diamond reveal the presence of broad absorption bands in the one-phonon region ( $1332\text{ cm}^{-1}$  to  $900\text{ cm}^{-1}$ ) which vary substantially within and between specimens in both structure and magnitude, although diamond, being centrosymmetric, should not exhibit one-phonon absorption at all. These bands are therefore associated with defects of some kind, generally assumed to consist of nitrogen in various states of aggregation ranging from single nitrogen atoms (Type Ib) present in synthetic diamonds through 2-nitrogen (Type IaA) and 4-nitrogen (Type IaB) aggregates to extend defects of variable size (platelets) associated with a relatively narrow absorption band near  $1368\text{ cm}^{-1}$ . Although this band is outside the 1-phonon region, its development appears to be well correlated with the development of the IaB spectrum in many diamonds, but HP/HT laboratory experiments have shown that it can be reduced or destroyed without affecting the IaB spectrum.

Laboratory experiments have also shown that whereas the activation energy for the Ib -- IaA defect aggregation is low enough for the process to be complete in most natural diamonds, the activation energy for the IaA -- [IaB + Platelet] aggregation is high enough for the process to be incomplete in most natural diamonds. An experimental determination of this activation energy can therefore be used to estimate the residence times and temperatures associated with separate growth horizons in diamonds from different localities or within a particular locality.

Our HP/HT experiments indicate an activation energy of 7 eV, and show conclusively that the aggregation is a second-order process, i.e. it is concentration dependent. However, any given aggregation state is a product of temperature and time, and cannot define either independently, but if the temperature can be established by, for example, inclusion geothermometry, then the infrared spectrum can imply a residence time.

If infrared spectroscopy can provide reliable time/temperature information for individual diamonds, the fact that it is a rapid and non-destructive technique will permit studies of the relative homogeneity or otherwise of diamond populations to be made on statistically significant numbers of specimens more rapidly than is possible from studies of inclusion geochemistry, and importantly, for specimens which do not contain inclusions.

Our results confirm earlier observations that the platelet peak can be destroyed in such HP/HT experiments, but the morphological changes produced by the HP/HT graphitization differ from those reported previously.

Table 1. A comparison between the temperatures calculated using mineral inclusion geothermometers and those calculated using the 'A' → 'B' aggregation state, found from the one phonon region of the diamond infrared spectrum.

DIAMOND	TEMP °C(M.I.)	TEMP °C(I.R.a)	TEMP °C(I.R.b)
RSOV02	1292	1017 → 1043	1161 → 1192
RSOV04	910 → 970	1079 → 1170	1233 → 1337
TP9	1202 → 1295	1066 → 1110	1217 → 1269

M.I. The temperature calculated using inclusion geothermometry.

I.R. The temperature calculated using the infra-red spectrum. A storage time of between 1 and 2 Gy was assumed for the Romaria (Brazil) diamonds (RSOW) and of between 1.5 and 3 Gy for TP9.

a) Using Activation Energy for diamond = 674.8 KJmol<sup>-1</sup> (This work)

b) Using Activation Energy for diamond = 733.0 KJmol<sup>-1</sup> (Evans and Qi 1982)

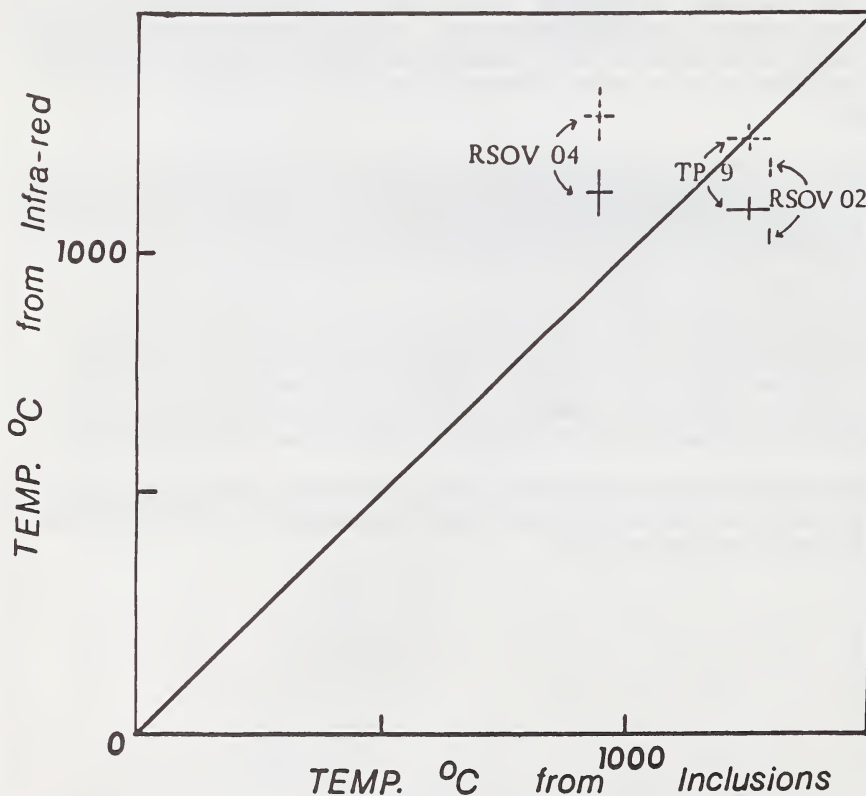


Figure 1. A comparison between the temperatures calculated using mineral inclusion geothermometers and those calculated using the 'A' → 'B' aggregation state found from the one-phonon region of the diamond infra-red spectrum.

— results using Activation Energy for diamond = 674.8 KJmol<sup>-1</sup> (chapter 4)

--- results using Activation Energy for diamond = 733.0 KJmol<sup>-1</sup> (Evans and Qi 1982)

## ASTHENOSPHERE-LITHOSPHERE RELATIONSHIPS WITHIN OROGENIC MASSIFS.

*Martin Adrian Menzies<sup>(1)</sup>; Jean Louis Bodinier<sup>(2)</sup>; Matthew Thirlwall<sup>(1)</sup> and Hilary Downes<sup>(3)</sup>.*

*(1) Department of Geology, Royal Holloway and Bedford New College, University of London, Egham, Surrey TW20 OEX, England; (2) University of Montpellier, Montpellier, France; (3) Department of Geology, Birkbeck College, London, England.*

The existence of small volume melt fractions with MORB/OIB affinity in the asthenosphere has recently received much attention particularly with regard to continual interaction with the base of the overlying lithosphere (MacKenzie 1989). Whilst diamond inclusions, kimberlite-borne and basalt-borne xenoliths provide a vital record of the transformation of continental lower lithosphere of Archaean and Proterozoic age (Menzies and Hawkesworth 1987; Nixon 1987; Menzies 1990), orogenic massifs provide unparalleled "exposure" of upper mantle peridotites of Proterozoic to Phanerozoic age thus facilitating the study of more recent asthenosphere-lithosphere interaction (Bodinier et al 1991; Downes et al 1991; Mukasa et al 1991). Orogenic massifs provide vital information about the temporal and spatial relationships between the peridotite protolith and different generations of melts. Two extreme cases are apparent from recently acquired geochemical data on orogenic massifs from the Mediterranean. At one extreme Phanerozoic asthenosphere-Proterozoic lithosphere is exposed in the Lanzo massif Italy (Bodinier et al 1991) and Proterozoic-Phanerozoic lithosphere in the Lherz massif, France (Downes et al 1991; Mukasa et al 1991). These massifs provide a field laboratory for the study of the formation and segregation of MORB (Lanzo) and transformation of a Proterozoic peridotite protolith by the injection and percolation of small volume melts (some of which are MORB) throughout the Phanerozoic (Lherz).

## LITHOSPHERE-ASTHENOSPHERE TRANSITION.

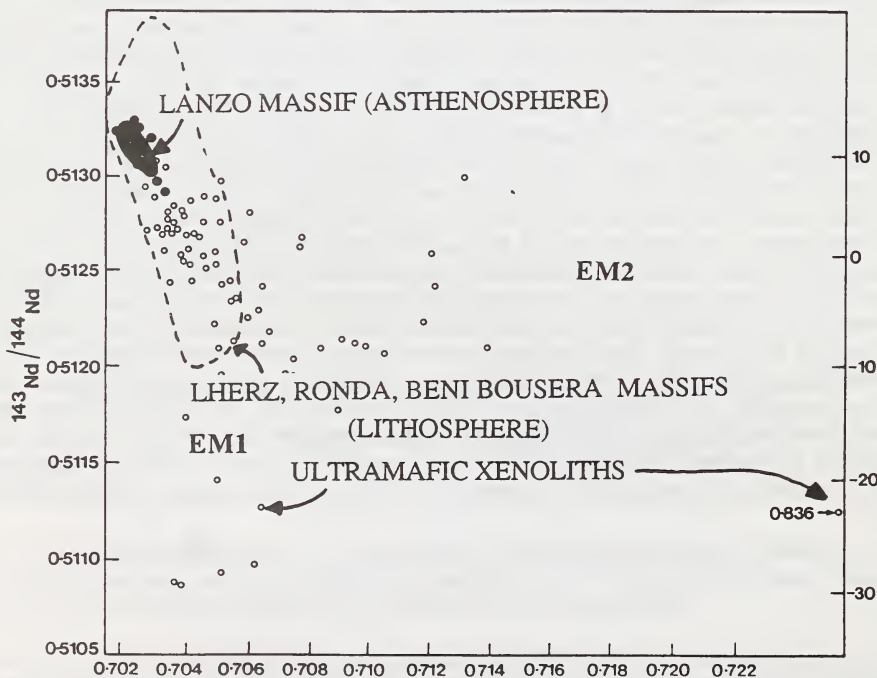
Major, minor and trace element variations within the Lanzo massif, Italy can be used to define chemical provinciality within the massif on the scale of kilometres. While the northern part of the massif is characterised by protogranular textures and fertile lherzolite compositions the southern part of the massif is characterised by sheared textures and more refractory lherzolithic compositions. In terms of partial melting histories, these data indicate that more extensive melt extraction occurred in the south than in the north. In contrast to the major and minor elements, variations in the LREE within the massif are believed to reflect primary mantle heterogeneity in that in the north the lherzolites are only moderately depleted in the LREE whereas in the south they are more markedly depleted in the LREE. When considered in conjunction with Sr, Nd and Pb isotopic geochemistry it is apparent that the northern part has very low  $87\text{Sr}/86\text{Sr}$  ratios and very high  $143\text{Nd}/144\text{Nd}$  ratios - the isotopic characteristics of aged depleted residua similar to (a) the Baldissero massif to the north, and (b) to mantle xenoliths entrained from beneath post-Archaean crust (e.g. Kilbourne Hole, San Carlos). The southern part of the massif is identical to Atlantic MORB asthenosphere with a tightly defined range of Sr and Nd isotopes. Elemental and isotopic data for the southern massif allow us to constrain the composition of the MORB source in particular the Sm/Nd ratio which is found to be similar (0.27) to that calculated from the Nd isotopic evolution of Phanerozoic MORB's from the northern hemisphere. The southern part of the massif is believed to represent deep well mixed convecting upper mantle which rose through the garnet stability field and experienced polybaric melt extraction thus accounting for its more depleted chemistry. The northern part of the massif is considered to be a fragment of sub-continental lithosphere isolated from the convecting upper mantle since the Proterozoic. Between these two extremes there exists a transition zone or hybrid containing components from the lithosphere modified by the ingress of asthenospheric melts. If we consider the north to be part of the **mechanical boundary layer** which underplated Proterozoic crust and the south to be **asthenosphere** then this hybrid zone has all the features of a **thermal boundary layer**. It is apparent from the study of Lanzo that formation of MORB melts began with extraction of < 5% melt in the garnet stability field and

later upwelling into the spinel stability field triggered extraction of larger degrees of melt (5-12%). Moreover the Sm/Nd ratio of the least depleted lherzolite at Lanzo (i.e. analogue of the MORB source) differs from that of MORB melts indicating that during these processes the LREE are fractionated. Indeed consideration of a wider database reveals that throughout the Phanerozoic the MORB source has become more depleted with time.

### HYDROFRACTURING OF PROTEROZOIC LITHOSPHERE.

The possible scale of inhomogeneities in the continental lithosphere can be assessed by consideration of the Lherz massif. The peridotite protolith (mechanical boundary layer) is believed to be a protogranular spinel peridotite that has been deformed thus allowing melt ingress. Melt conduits developed by hydrofracture are now healed with the crystallisation of amphibole-pyroxene veins. A chronology of fluid ingress is apparent at Lherz as (a) LREE enrichment within the protogranular peridotite protolith, (b) hydrofracture systems in porphyroclastic peridotite that helped channel basaltic melt (now crystallised as amphibole pyroxenite); (c) metasomatic and enrichment aureoles in the wall rock adjacent to these veins, and (d) multiple episodes of carbon-dioxide bearing fluid inclusions.

The metasomatic fronts and enrichment fronts that occur adjacent to the melt conduits are defined on the basis of the presence of hydrous minerals and elevated LREE/HREE ratios respectively. Extreme elemental and isotopic heterogeneity exists within the reaction aureole due to melt percolation and reaction with the wall rock (Bodinier et al 1990; Downes et al 1991). The range in Sr and Nd over a 60 cm. section is similar to that of MORB and OIB and greatly exceeds the range for Lanzo. Whilst the Lanzo massif is dominated by depleted mantle domains (MORB source and residue) several chemically discrete enriched mantle domains (i.e. DMM, EM2 and EM1) occur within the tiny massif at Lherz (>200x smaller than Lanzo). This illustrates the isotopic homogeneity of the asthenosphere and the isotopic heterogeneity of the lithosphere - isotopic heterogeneity that could, in some cases, be caused by a time-integrated response to elemental fractionation brought about by the reaction of MORB melt with depleted wall rock. For example a time-integrated response to the elemental fractionation observed within the reacted wall rock sections at Lherz would result in localised development of EM1 domains because of the very low Rb/Sr and Sm/Nd ratios generated in the reaction zone. Clearly concomitant metasomatic and enrichment processes involving MORB melts and depleted or enriched wall rock can be responsible for the development of enriched reservoirs (e.g. EM1) that may be consumed during genesis of small volume alkaline melts within the lithosphere. Where the main hydrous phase to crystallise in the wall rock is amphibole low Rb/Sr ratios and Sm/Nd ratios are observed due to the uptake of Sr and LREE by amphibole and the retention of Rb in the fugitive melt. A time-integrated response to this would produce localised EM1. In contrast where mica dominates in the reaction zone higher Rb/Sr ratios and Sm/Nd ratios are observed resulting in the time-integrated development of localised EM2 domains.



## CONTRASTING CHARACTERISTICS

### Asthenosphere

- (a) porphyroclastic plagioclase and spinel peridotites (=DMM)
- (b) the existence of segregated melts that are compositionally identical to MORB. melts),
- (c) "hot" temperatures : oceanic to geotherm.
- (d) redox state close to or above QFM,
- (e) clinopyroxenes extremely depleted in the LREE (= abyssal/oceanic peridotites),
- (f) no LREE enrichment in the melt-residue system
- (g) isotopic homogeneity (=MORB) and elemental heterogeneity (Figure 1).
- (h) isotopic equilibrium between melt and peridotite

#### Examples :

#### **Orogenic (alpine) massifs.**

Lanzo spinel-plagioclase peridotite Italy,  
 Erro-Tobbio spinel-plagioclase peridotite Italy;  
 Trinity spinel-plagioclase peridotite California;  
 Othris spinel-plagioclase peridotite Greece.

#### **Mantle xenoliths.**

No xenolith analogue.

#### **Oceanic peridotites.**

Segregated plagioclase peridotites;  
 Zabargad Island, Red Sea.

### Lithosphere

- (a) protogranular spinel [and garnet] peridotites(=DMM); development of porphyroclastic & mylonitised peridotites in association with shear zones and magma conduits.
- (b) healed hydrofracture networks (e.g polybaric derivatives of MORB/OIB)
- (c) "cold" temperatures : continental geotherm.
- (d) redox state well below QFM (protolith) or above QFM (metamorphic aureole around hydrofracture systems)
- (e) clinopyroxenes slightly depleted in the LREE (= basalt-borne xenoliths),
- (f) multiple enrichments in the peridotite protolith due to fluid ingress
- (g) isotopic and elemental heterogeneity (=MORB,OIB and crust) (Figure 1).
- (h) isotopic disequilibrium between hydrofractures and adjacent wall rock

#### Examples :

#### **Orogenic (alpine) massifs.**

Lherz spinel peridotite France;  
 Tinaquillo peridotite Venezuela;  
 Baldissero-Balmuccia Italy and many others.

#### **Mantle xenoliths.**

Abundant xenolith analogues :  
 Type IA (LREE depleted) - protolith  
 Type IB (LREE enriched) - protolith+ "fluid"  
 Type II - "fluid" derivative.  
 GP (garnet peridotite) - protolith  
 GPP ( " + mica) - protolith + "fluid"  
 PKP ( " + K-richterite) - protolith  
 "fluid"  
 MARID (mica, amph., rutile, ilmenite, cpx.) - "fluid" derivative.

#### **Oceanic peridotites.**

Abyssal peridotites; St. Paul's rocks Atlantic.

## REFERENCES.

- Bodinier, J.L., Vasseur, G., Vernieres, J., Dupuy, C. and Fabries, J. (1990) Mechanisms of mantle metasomatism : geochemical evidence from the Lherz orogenic peridotite. *J. Petrology*, 31, 597-628.
- Bodinier, J.L., Menzies, M.A., and Thirlwall, M.F. (1991) Transition from sub-continental lithosphere to asthenosphere - REE and Sr-Nd isotopic geochemistry of the Lanzo massif Italy. *Journal of Petrology, Orogenic lherzolites and mantle processes volume* (in press).
- Downes, H., Bodinier, J.L., Thirlwall, M.F., Lorand, J.P., and Fabries J., (1991) REE and Sr-Nd isotopic geochemistry of eastern Pyrenean peridotite massifs : sub-continental lithospheric mantle modified by continental magmatism. *Journal of Petrology, Orogenic lherzolites and mantle processes volume* (in press).
- McKenzie, D. (1989) Some remarks on the movement of small melt fractions in the mantle. *Earth and Planetray Science Letters*, 95, 625-80.
- Menzies, M.A. (1990) *Continental Mantle*. 184p. Oxford University Press, Oxford, England.
- Menzies, M.A., and Hawkesworth, C.J. (1987) *Mantle Metasomatism*. 472 p. Academic Press, England.
- Mukasa, S.B., Wilshire, H.G., Nielson, J., and Shervais, J.W. (1991) Intrinsic Nd, Pb and Sr isotopic heterogeneities exhibited by the Lherz alpine peridotite massif, French Pyrenees. *Journal of Petrology, Orogenic lherzolites and mantle processes volume* (in press).
- Nixon, P.N. (1987) *Mantle Xenoliths*. 844 p. J.Wiley, England.

## COMPREHENSIVE INVESTIGATIONS OF CHINESE DIAMONDS.

Meyer<sup>(1)</sup>, H.O.A.; Andri<sup>(2)</sup>, Z.; Milledge<sup>(3)</sup>, H.J.; Mendelssohn<sup>(3)</sup>, M.J. and Seal<sup>(4)</sup>, M.

(1) Dept. Earth Atmos. Sci., Purdue University, West Lafayette, IN 47907 USA; (2) Inst. Geology, Chinese Acad. Geol. Sci., Beijing, China; (3) Crystall. & Min. Phys. Unit, Dept. Geol. Sci., University College London, Gower Street, London WC1E 6BT, U.K.; (4) Sigillum B.V., Guido Gezellestraat 5, 1077 WN Amsterdam, Holland.

Diamonds from the Shengli kimberlite, near Mengyin, southeastern Shandong Province, and from the No.50 kimberlite, Fuxian group, Liaoning Province have been examined for inclusion type and chemistry, infrared spectra and cathodoluminescence characteristics. Work in progress also includes determination of  $\delta^{13}\text{C}$  and  $\delta^{15}\text{N}$  of selected specimens.

## Inclusions:

In an earlier study (Zhang and Meyer, 1989) the initial results of inclusion chemistry were reported from a sample of approximately 10,000 diamonds (650 ct). Of the 325 diamonds with inclusions eventually selected for further examination the majority of inclusions from both localities, and hence host diamonds, belonged to the ultramafic (peridotitic) suite.

The current sampling was of a much larger population of diamonds (>20,000) and approximately 500 diamonds from Liaoning and 100 from Shandong, all with inclusions, were selected for more detailed examination. From careful visual inspection no eclogitic inclusions were identified, although it must be remembered that omphacitic pyroxene can be misidentified as olivine or enstatite. No orange (eclogitic) garnets were observed (Table 1). Analyses of some inclusions are presented in Table 2.

## Infra-red Microspectroscopy and cathodoluminescence:

*Shandong*

99 diamonds, usually about 1mm in diameter, which were predominantly octahedral in habit, though ranging from sharp-edged specimens with smooth faces to stones with rough surfaces, broken corners, and/or rounded edges were selected which could generally be viewed through a pair of opposed octahedral faces. It was therefore possible to obtain good infrared spectra for most of them, and to take replicate spectra to see whether or not the stones were essentially homogeneous.

Nitrogen concentration varied widely, from specimens containing little enough nitrogen to be classified as Type II diamonds, to concentrations of the order of 2000 ppm. Of the 73 specimens for which replicate spectra were obtained, half (including the Type II specimens) were homogeneous, and half showed some variation in nitrogen concentration.

Almost all those diamonds which contained appreciable amounts of nitrogen also showed the hydrogen peak at 3107  $\text{cm}^{-1}$ , the strength being roughly proportional to the nitrogen concentration in most cases.

For those diamonds which showed appreciable variations of nitrogen concentration within the stone, the extent of defect aggregation increased with the concentration as would be expected if the whole specimen had experienced the same P/T regime after growth i.e. there was no evidence in these small diamonds for more than one stage of growth analogous to the coat and core of coated stones. However, the presence of specimens with high nitrogen content showing little aggregation, together with specimens having low nitrogen content but which show almost complete aggregation indicate that the population itself cannot be homogeneous.

In order to facilitate comparison of inclusion and infrared geothermometry, polished plates are being prepared so that spectra can be obtained in the near vicinity of inclusions which are being microprobed, and inclusion geochemistry may suggest the same result when the polished plates have been studied.

The diamonds did, however, exhibit all degrees of diminution of the platelet peak from completely unaffected to completely destroyed, not only for specimens for which IaB aggregation is virtually complete, but also for intermediate aggregation states.

Cathodoluminescence photographs indicate the presence of light radiation damage on a few specimens, but the general appearance of the group as a whole has no characteristics which would distinguish it from specimens from other kimberlites worldwide.

### Liaoning

Results for the first 84 specimens examined from Liaoning appear similar in every particular, including the range of nitrogen concentrations both within and between specimens, ubiquitous presence of hydrogen, variable degradation of the platelet peak, and the existence of highly-aggregated nitrogen-poor specimens as well as unaggregated nitrogen-rich specimens. The only difference seems to be that there is even less evidence of radiation damage in cathodoluminescence.

Table 1. Visual Examination of Diamonds with Inclusions from Shandong and Liaoning Provinces, China

	Shandong		Liaoning	
	#	%	#	%
*Olivine/Enstatite	65	76	314	83
Diopside	0	0	1	(0.3)
+Garnet	6	7	4	1
Spinel	5	6	21	6
Sulfide	1	1	3	1
Olivine + Garnet	1	1	6	2
Olivine + Spinel	6	7	16	4
Olivine + Sulfide	n.a.	n.a.	12	3
Garnet + Spinel	1	1	0	0
	85	99%	377	100%

\* Colorless inclusions but majority probably olivine.  
+ All purple garnets, presumably Cr-pyrope.

Table 2. Representative Analyses of Inclusions in Diamonds from Shandong and Liaoning Provinces, China.

	OL <sup>1</sup>	EN*	DI*	OMP*	Cr-Py <sup>2</sup>	Py-AR*	CHR <sup>1</sup>
SiO <sub>2</sub>	40.6	57.5	56.0	56.1	41.2	39.6	0.13
TiO <sub>2</sub>	0.00	0.00	0.00	0.00	0.06	0.30	0.31
Al <sub>2</sub> O <sub>3</sub>	0.05	0.56	0.57	16.3	14.3	22.0	3.73
Cr <sub>2</sub> O <sub>3</sub>	0.09	0.28	1.02	0.02	12.3	0.03	66.9
FeO	8.33	4.43	1.86	2.12	6.41	19.8	13.8
MgO	50.0	35.4	19.4	7.38	22.9	9.97	11.9
CaO	0.06	0.78	21.2	11.0	3.00	8.63	0.00
MnO	0.13	0.16	0.10	0.06	0.39	0.39	1.14
NiO	0.31	0.13	0.06	0.00	0.00	0.00	0.11
Na <sub>2</sub> O	0.02	0.14	0.49	6.12	0.00	0.08	0.05
K <sub>2</sub> O	0.00	0.00	0.22	0.00	0.00	0.00	0.00
	99.6	99.4	100.9	99.4	100.6	100.8	98.1

1. Shandong, 2. Liaoning

\* Zhang and Meyer, 1989. All from Shandong.

## MIDDLE JEQUITINHONHA ALLUVIAL DIAMONDS.

Middleton, R.C.

*Geological Clinic Serviços de Mineração Ltda., Rua São José, 46, sala 1001, 20010, Rio de Janeiro, R.J., Brazil.*

The Middle Jequitinhonha Alluvial Diamond deposits are hosted by gravels within the Jequitinhonha Valley between the towns of Peixe Cru and Itira in Northern Minas Gerais in Brazil. The gravels occur within the present river, its floodplains and in palaeo-terraces which are situated 40, 80 and 280 meters above the average water level of the present river. Remnants of the palaeo-terraces, which are characterized by quasi-horizontal topographic features underlain by gravels often, but not invariably, composed of reddened (soil-iron stained) pebbles and cobbles, supported by a sand matrix, which may or may not be overlain by grey floodplain silt. The present Jequitinhonha River is situated at 320 meters above sea level in the central part of the Middle Jequitinhonha Valley near Porto Mandacaru. The Jequitinhonha River has a gradient of 1:138 in the upper reaches of the Middle Jequitinhonha Valley near Peixe Cru and a gradient of 1:420 in the lower reaches around Itira.

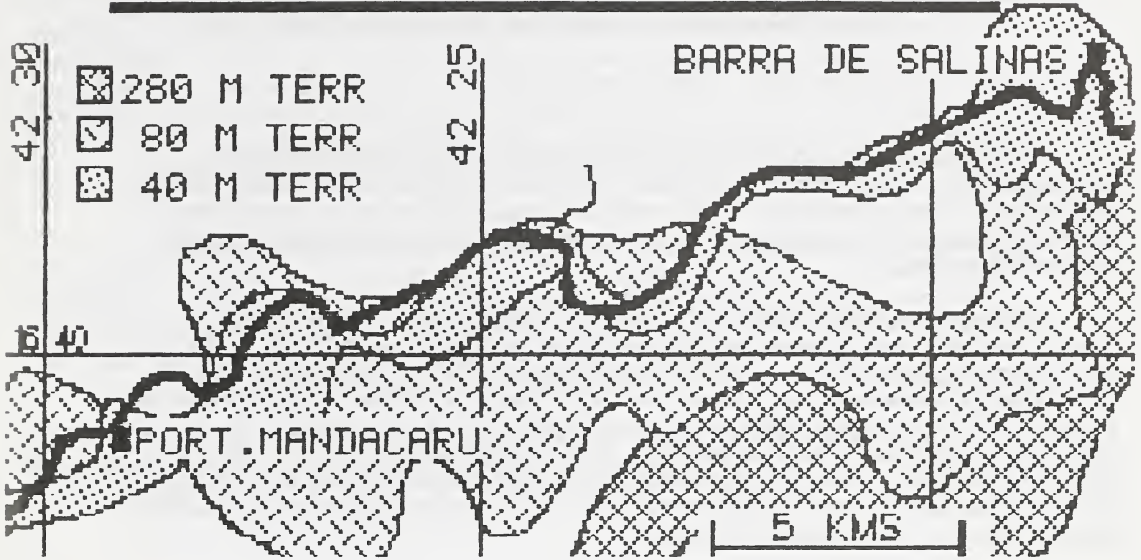
Diamonds are known to occur within the present river gravels, the silt-covered floodplain gravels (generically named the "low terraces") and the 40 meter terrace gravels but no testing has been carried out to date on the 80 and 280 meter terrace gravels. The present river gravels are characterized by the presence of relatively well to poorly sorted coarse-sand matrix-supported highly-rounded quartz cobbles and boulders varying in size up to 20 centimeters across. Rare quartzite (Espinhaço) and carbonaceous quartzite cobbles and pebbles may be present. The heavy mineral content of the matrix sands are comprised of kyanite (>90%), sillimanite, garnet (pyrope and almandine), ilmenite, rutile, zircon, monazite and gold. The low terrace gravels are essentially similar to the present river gravels in composition and distribution. These terraces, which normally only form small remnants adjacent to the present river in the steep-sided valley sections of the river, may be elevated up to 5 meters with respect to the present river gravels or may lie at the same altitude. The low terraces form extensive flats adjacent to the river in the low-energy stretches of the Middle Jequitinhonha Valley around Itira. The bedrock on which the present river and low terraces flow is normally hard, freshly exposed Macaubas and Salinas Formation garnet-kyanite-sillimanite schists. The bedrock is extremely irregular, forming excellent traps for heavy mineral and diamond accumulations. The 40 meter level terrace gravels tend to have the same cobble-pebble and matrix physical and mineralogical composition as the present river gravels but laterite cappings and intercalations may be present. The bedrock schist on which the 40 meter terrace gravels have been deposited is usually unweathered or only slightly weathered, but highly weathered saprolite bedrock sections have been encountered sporadically. The 80 meter level terrace gravel is characterised by very large, highly-rounded quartz cobbles up to 40 centimeters in diameter supported by a matrix of sand and silt. Present indications

are that there is a grain-size gap in the 0.5-3 millimeter fraction which may possibly have been removed during re-deposition of the gravel from a pre-existing site. The heavy mineral fraction is comprised mainly of staurolite, as opposed to kyanite in the lower terrace gravels. This fact may be related to the grain-size gap. The 280 meter terrace has a high percentage of highly-rounded, small, quartz pebbles. Present indications are that there is no grain-size gap and the gravels appear to be largely in-situ. The heavy mineral fraction is comprised mainly of kyanite, garnet, ilmenite and rutile. This terrace can be traced over a wide area in the Middle Jequitinhonha Valley where the Jequitinhonha River apparently meandered in wide, sinuous arcs about 1 million years ago. The widespread preservation of this terrace level is related to the extensive, resistant, quasi-horizontal Limoeiro Pegmatite sills which occur in the central parts of the Middle Jequitinhonha Valley between Buriti and Barra de Salinas. The sills (500 meters above sea level) are more resistant than the enclosing schists and have slowed down hillslope retreat at the cliff-forming outcrops, thus resulting in the preservation of the old river course.

The spectacular preservation of the abovementioned palaeo-terraces at distinct levels in the Middle Jequitinhonha Valley can be explained by sudden breaching of N-S trending resistant barriers that crossed the Jequitinhonha River, past and present. A present example is the resistant N-S striking pegmatite and quartzite barriers that cross the Jequitinhonha River at Barra de Salinas where the river suddenly changes course in a northerly direction as it encounters the pegmatite dyke and then abruptly changes course again southwards, flowing against the quartzite barrier until resuming its ENE course 2 kilometers later where it breaches a fracture in the quartzites. The ENE course of the present Jequitinhonha River in the upper parts of the Middle Jequitinhonha Valley is controlled by a joint set. Deep straight-sided gravel-filled canals result from the action of the river on the joints. On the other hand the ESE course of the river, downstream from Coronel Murta, is controlled by a different joint set related to the granite intrusions in that area.

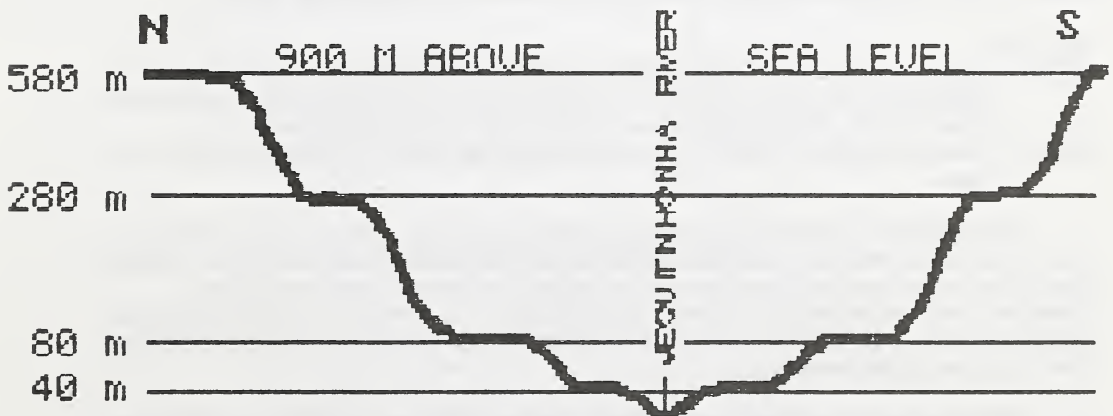
The principle minerals of economic importance in the Middle Jequitinhonha Valley gravels are diamonds, gold, sillimanite, kyanite, ilmenite, rutile and monazite. The diamonds, which are mainly of gem quality, tend to occur mainly in the form of rhombdodecahedra and tend to have a brown to green surface colouration, possibly owing to radiation, which disappears on polishing. The origin of the diamonds is widely considered to be the Sopa Conglomerates which occur in the Grão Mogol area. The gold in the gravels is derived from widespread occurrences of this mineral in the ductile to ductile-brittle shear zones in the area that formed during thrusting (Brasiliano age) against the São Francisco Craton. The sillimanite and kyanite are derived from the schists formed during medium-low pressure metamorphism accompanying the Brasiliano tectono-thermalism in the area. The rutile and monazite are derived from Brasiliano anatexite granites and related hydrothermal action in the host-rocks of the Middle Jequitinhonha Valley.

## MIDDLE JEQUITINHONHA VALLEY



## TYPICAL SECTION ACROSS THE MIDDLE JEQUITINHONHA VALLEY

### SCHEMATIC



## INFRARED AND CATHODOLUMINESCENCE STUDIES OF INCLUSION-BEARING DIAMONDS FROM BRAZIL.

*Milledge<sup>(1)</sup>, H.J.; Mendelssohn<sup>(1)</sup>, M.J. and Meyer<sup>(3)</sup>, H.O.A.*

*(1) Crystall. & Min. Phys. Unit, Dept. Geol. Sci., University College London, Gower Street, London WC1E 6BT, U.K.;*

*(2) Dept. Earth & Atmos. Sci., Purdue Univ., West Lafayette, IN 47907 USA.*

Infrared spectra have been obtained for diamonds from five localities in the Precambrian Sopa conglomerate at Sampaio, Diamantina and Serro, Minas Gerais, and from the equivalent Lavras Formation, 675 km north at Adarai, Bahia as well as from the basal Taua conglomerate of the Cretaceous Bauru Formation at the Agua Suja Mine, Romaria, western Minas Gerais.

Although only small numbers of stones were tested, spectra from all localities showed a range of spectral types, and large variations in nitrogen concentration. Since the IaA - IaB aggregation process is a second-order process (see MJM, HJM, GIC & HOAM, this volume) it is concentration-dependent, so that diamonds which have all experienced the same P/T histories may show different degrees of aggregation if their nitrogen concentrations differ substantially, but in that case the higher degree of aggregation must correspond to higher concentrations. Accurate assessment of such spectra depends on the absolute values of the IaA and IaB absorption coefficients at 1282 cm<sup>-1</sup>, but the effects can be demonstrated generally from the following pairs of spectra.

### DIAMANTINA

HBDT1: Low degree of aggregation for quite a high N concentration, whereas HBAN7 from Adarai shows a similar aggregation state for a much lower nitrogen concentration. Platelet development is normal aggregation.

### SERRO (Minas Gerais)

HBSE8: High N concentration, high degree of aggregation, platelet peak intact.

HBSE11: Aggregation varying with concentration within one stone, platelet peak intact.

### SAMPAIO

HBSP1: More complete aggregation for lower N concentration than HBSP8 but platelet peak intact.

HBSP4: Lower aggregation state for lower N concentration. Platelet peak intact.

### ANDARAI

HBAN1: Shows a very unusual effect, where the platelet peak is absent for an intermediate aggregation state, as in HBSP4. The platelet peak is sometimes absent in specimens where the IaA - IaB aggregation is complete, but seldom at this stage.

HBAN5: Shows a similar N concentration and aggregation state, but with the platelet peak intact.

The existence of these well-aggregated defects in Precambrian diamonds is interesting, because all aggregation must have taken place before emplacement, so that the residence time in the mantle must have been much shorter than for diamonds emplaced in the Cretaceous, and the temperatures correspondingly higher. It is most important therefore to be able to correlate temperatures as implied by infrared spectra with temperatures estimated from inclusion geothermometry.

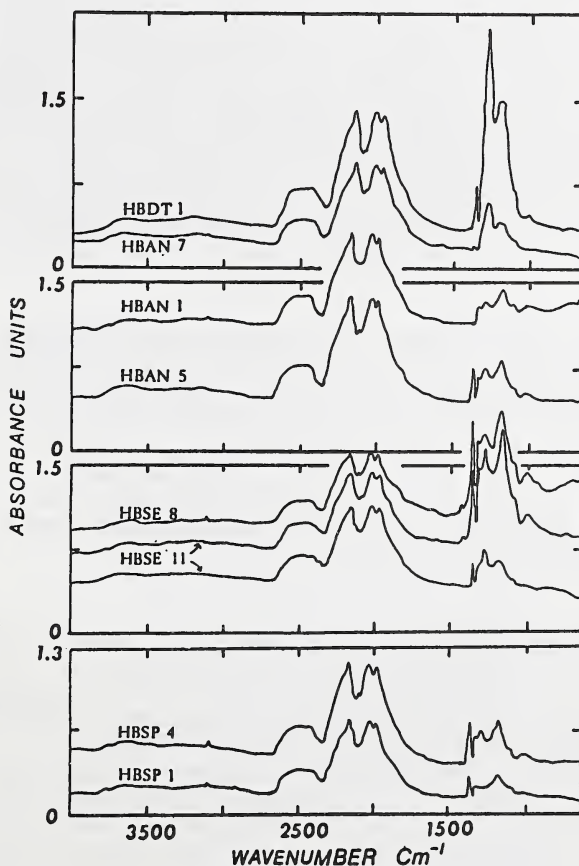
This comparison will only be reliable if diamond plates are polished so as to expose inclusions for microprobe analysis and to make it possible for infrared microspectroscopy to be carried out in the immediate vicinity of the inclusion, because spatial information is frequently lost when the diamond has to be broken to expose the inclusion for probe work. The importance of this spatial correlation was demonstrated for one specimen from Romaria where the spectral and inclusion temperatures were not in agreement, but subsequent spectral measurements on other fragments of the diamond indicated that it was very inhomogeneous.

Rather than fracture these specimens, many of which are inhomogeneous like HBSE11, polished plates are being prepared where possible in order to facilitate comparison of the two methods of estimating temperatures in addition to obtaining the inclusion geochemistry.

Cathodoluminescence studies of Brazilian diamonds have also revealed two interesting facts. As might have been anticipated, there is evidence of alpha-radiation damage of varying degrees of severity, but what is almost unique is the appearance of very well developed red haloes on the surface of a diamond from Romaria. Very slight traces of pink haloes have been detected on one of the Precambrian stones, but extensive and well-defined areas of red luminescence occurred on specimens from Serro and Andarai. In our experience, red cathodoluminescence is comparatively rare, and such discrete patches even more so.

The second observation of interest is that one specimen from Romaria showed very large platelets exposed on an external surface. Relatively large platelets (a few microns in diameter) have now been seen in several diamonds from the Finsch and Argyle mines, but they are usually only detected on polished sections exposing the interior of the stone, and do not extend to the exterior surface, for whatever reason. It is possible, therefore, that this specimen has been substantially resorbed at some stage.

Acknowledgements: We gratefully thank Prof. Darcy P. Svisero for diamonds from Romaria, Western Minas Gerais and Nicolau L.E. Haralyi for those from Eastern Minas Gerais and Bahia.



## ACCESSORY RARE EARTH, STRONTIUM, BARIUM AND ZIRCONIUM MINERALS IN THE BENFONTEIN AND WESSELTON CALCITE KIMBERLITES.

Roger H. Mitchell.

*Department of Geology, Lakehead University, Thunder Bay, Ontario, Canada P7B 5E1.*

Calcite kimberlites are rocks formed from highly differentiated kimberlite magma. As such they might be expected to possess an unusual mineralogy as a consequence of the concentration of incompatible elements in these residual magmas. To examine this possibility, calcite kimberlites from the Benfontein sills Dawson and Hawthorne 1973) and the Wesselton Water Tunnels sills (Mitchell 1984) were investigated by SEM/EDS techniques. The study demonstrated the ubiquitous presence of REE-, Sr- and Ca-Ba-carbonates, Ba-titanates, kinoshitalite, primary Ca-zirconate, Nb-rutile and baddeleyite

### Carbonates

Carbonate diapirs at Benfontein contain five distinct carbonates. The earliest carbonate to form was dolomite. This lines the margins of the diapir and forms euhedral crystals within the core of the structure. Dolomite is included in Mn-bearing ankerite and both minerals are set in a matrix of calcite. Compositional variational, with the exception of Mn in ankerite (2-6 wt.% MnO), is relatively limited (figure 1). Ancylite occurs as euhedral crystals which appear to have crystallized contemporaneously with dolomite. They exhibit a wide range in composition (Table 1, figure 2) with respect to their SrO (8-23 wt%) and REE contents (24-33 wt.% Ce<sub>2</sub>O<sub>3</sub>). Ca-Ba carbonate (benstonite or barytocalcite ?) occurs as rounded-to-irregular exsolution patches in dolomite. Associated phases in the diapir include pyrite and strontio-barite. Sr-free REE-carbonates appear to be absent from the diapirs. A similar Ca-Ba carbonate, also of exsolution origin occurs in calcite, in the Premier Mine calcite kimberlite.

The groundmass of the kimberlite hosting the diapirs consists primarily of calcite with rare dolomite, apatite, spinels, rutile, ilmenite and serpentine. Ancylite and Sr-poor REE-carbonates are common as replacements of rutile and spinel, and as randomly orientated acicular crystals commonly intergrown with ilmenite laths. The Sr-poor carbonates are of relatively constant composition (Table 1, Figure 2) and are considered on the basis of their low CaO (5-6 wt%) contents to be parisite-Ce.

### Hollandite

Euhedral-to subhedral Ba-Fe-titanates are common in the calcite - apatite-rich groundmass of the Benfontein kimberlites and rare in the Wesselton sills. The titanates are K-free, Nb-bearing, Fe-Ba-titanates (Table 2) belonging to the hollandite group of minerals. The titanates represent compositions between the end members BaFe<sub>2</sub>Ti<sub>6</sub>O<sub>16</sub> and BaFe<sub>2</sub>Ti<sub>7</sub>O<sub>16</sub>. Their composition is not similar to priderites found in lamproites or Ba-titanates in group 2 kimberlites. Similar titanates are known from the Arbarastakh carbonatite complex.

### Potassian Kinoshitalite.

The groundmass of zirconolite-bearing Benfontein kimberlite contains poikilitic plates of potassian kinoshitalite (K,Ba)Mg<sub>3</sub>Al<sub>2</sub>Si<sub>2</sub>O<sub>10</sub>(OH)<sub>2</sub> (Table 2). This mineral

has not previously been reported from kimberlites, although it is a common late stage mineral in both sodic and potassic alkaline volcanic rocks e.g. New South Wales leucitites, Bathurst Island nephelinites.

#### Zirconolite/Zirkelite.

Zirconolite, accompanied by baddeleyite, has previously been reported from the Benfontein sills by Raber and Haggerty (1979), as a product of reactions between ilmenite, zircon and residual Ca-rich fluids. In contrast zirconolite/zirkelite found during the course of the current study occurs as isolated 5-30 micron euhedral-to-subhedral single crystals scattered throughout the kimberlite groundmass. The mineral was evidently an early crystallizing phase and many of the crystals now exhibit irregular embayed margins indicative of subsequent resorption. In the Benfontein sills there is an antipathetic relationship between the presence of baddeleyite and zirconolite/zirkelite. In the Wesselton sill, baddeleyite is absent and zirconolite/zirkelite is the principal Zr-bearing phase, together with rare kimzeyitic garnet. Table 2 shows that the Ca zirconate found in the present work is much richer in Zr than typical zirconolites ( $\text{CaZrTi}_2\text{O}_7$ ), including the reaction variety described by Raber and Haggerty (1979). The composition is considered to be closer to that of zirkelite ( $\text{CaTiZr}_3\text{O}_5$ ) than zirconolite.

#### Nb-Rutile

Niobian rutile is common as 10-50 micron euhedral groundmass crystals in the Benfontein sills. Commonly, the crystals are extensively replaced by magnetite, ankeritic carbonate, parisite and ancylite. Mantles of ilmenite are also commonly present. Rutile appears to have been a primary groundmass phase which crystallized contemporaneously with unevolved Cr-bearing spinels. The rutile contains 1.5-3 wt %  $\text{Nb}_2\text{O}_5$  (Table 2).

#### Fersmite

Two euhedral grains of fersmite,  $\text{CaNb}_2\text{O}_6$ , enclosed by calcite were encountered in one sample from Benfontein. The crystals are of uniform composition and contain 69.5 wt.%  $\text{Nb}_2\text{O}_5$ , 16.2 wt.% CaO, 6.8 wt.%  $\text{Ce}_2\text{O}_3$ , 3.5 wt.%  $\text{Fe}_2\text{O}_3$ , and 1.6 wt.% SrO.

Rare earth and strontium rich carbonates have not previously been reported from group 1 kimberlites, although they are common in REE-rich group 2 kimberlites (e.g. bastnesite-Ce in the Frank Smith and Bellsbank occurrences, Mitchell unpub.data). Their presence in the Benfontein sills undoubtedly results from the concentration of REE and Sr in late stage carbonate-rich fluids. However, the absence of similar carbonates in the Wesselton and Premier calcite kimberlites suggests that the Benfontein magmas were of either of unusual composition or underwent extreme differentiation. The presence of REE carbonates does not imply any affinities with carbonatites, as these minerals are now known to form in a variety of late stage hydrocarbothermal parageneses in rocks ranging in composition from nepheline syenite to peralkaline granite.

Dawson, J.B., Hawthorne, B.H. 1973. Magmatic sedimentation and carbonatitic differentiation in kimberlite sills at Benfontein, South Africa. *J.Geol.Soc.London*, 129, 61-85.  
 Mitchell, R.H. 1984. Mineralogy and origin of carbonate

segregations in a composite kimberlite sill. N.Jahrb. Mineral. Abh. 150, 185-197.

Raber, E., Haggerty, S.E. 1979. Zircon-oxide reactions in diamond-bearing kimberlites. Proc. 2nd. Internat. Kimberlite Conf. 1, 229-240.

Table 1. Ancylylite, parisite and Ca-Ba carbonate composition.

Wt. %	1	2	3	4	5	6	7
BaO	-	-	-	-	-	48.8	48.0
CaO	4.0	2.5	4.0	5.1	4.0	19.2	20.0
SrO	22.6	15.3	8.1	1.3	0.5	1.1	-
FeO	-	-	-	3.4	0.3	-	0.6
La <sub>2</sub> O <sub>3</sub>	10.5	15.9	9.7	16.6	12.9	-	-
Ce <sub>2</sub> O <sub>3</sub>	24.1	28.9	33.3	32.8	34.7	-	-
Pr <sub>2</sub> O <sub>3</sub>	2.2	1.4	4.3	3.4	4.4	-	-
Nd <sub>2</sub> O <sub>3</sub>	6.8	6.3	10.5	7.0	12.5	-	-
Sm <sub>2</sub> O <sub>3</sub>	-	-	-	1.1	1.1	-	-
	70.2	70.3	70.9	70.7	70.4	69.1	68.6

1-3 Ancylylite-Ce; 4-5 parisite-Ce; 6-7 Ca-Ba carbonate

Table 2. Kinoshitalite, hollandite and Ca zirconate composition

Wt. %	1	2	3	4	5	6
SiO <sub>2</sub>	24.2	24.8	-	-	-	-
TiO <sub>2</sub>	0.0	0.0	68.4	70.2	2.7	2.0
ZrO <sub>2</sub>	-	-	-	-	85.2	84.1
Nb <sub>2</sub> O <sub>5</sub>	-	-	2.8	1.0	-	-
Al <sub>2</sub> O <sub>3</sub>	21.0	19.2	-	-	-	-
FeO	1.5	2.7	13.7	15.0	0.0	1.6
MgO	22.5	24.2	0.8	0.0	-	-
CaO	-	-	-	-	11.3	10.4
BaO	23.8	23.5	14.1	13.2	-	-
K <sub>2</sub> O	2.2	2.5	0.0	0.0	-	-
	95.2	96.9	99.8	99.4	99.2	98.1

1-2 Kinoshitalite; 3-4 hollandite; 5-6 Ca zirconate

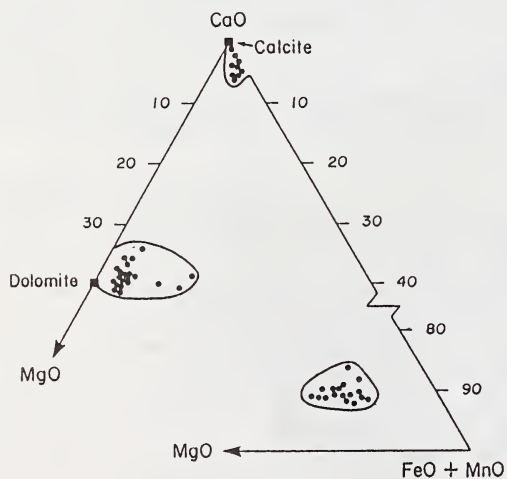


Figure 1

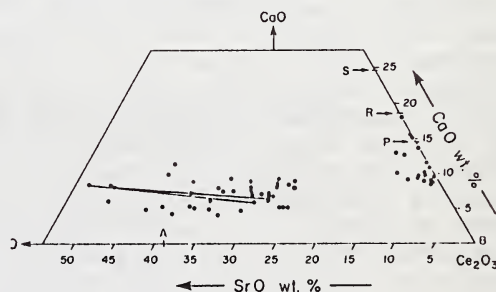


Figure 2.

## WHAT'S IN A NAME? SUGGESTIONS FOR REVISIONS TO THE TERMINOLOGY OF KIMBERLITES AND LAMPROPHYRES FROM A GENETIC VIEWPOINT.

Roger H. Mitchell.

*Department of Geology, Lakehead University, Thunder Bay, Ontario, Canada P7B 5E1.*

Our understanding of the petrogenesis of alkaline rocks has been considerably advanced by the application of modern methods of analysis to the determination of the chemical and isotopic composition of rocks and minerals. Unfortunately, these advances have not been matched by changes in our approach to the terminology of alkaline rocks. Modal classifications have remained essentially unchanged since the nineteenth century. This terminological legacy hinders our understanding of the actual genetic relationships between diverse groups of alkaline rocks and unfortunately leads to inappropriate petrogenetic speculation.

Why do we attempt to classify rocks? One reason is to give a particular assemblage of minerals a name, this being a convenient way of informing other petrologists of the occurrence of this assemblage in some particular geological context. However, a particular assemblage of minerals arises from the operation of petrogenetic processes acting upon a particular magma type and is not a fortuitous random association. Correct classification of rocks is thus vital if the object of the exercise is ultimately to understand petrogenesis. In the past different names have been applied to the same mineral assemblage or the same name is applied to rocks which differ in their mineralogy. Commonly this has led to the "recognition" of incorrect associations and to suggestions of consanguinity where none exists. The proposal that many alkaline rocks may be grouped in a lamprophyre clan is but one example of this approach to terminology.

Existing IUGS-sanctioned non-genetic classifications are unsatisfactory for many alkaline rocks e.g., minettes versus phlogopite sanidine lamproites or carbonatites versus calcite kimberlites. Consequently mineralogical-genetic classifications are proposed in which the name of given alkaline rock is based upon; (1) the total mineral assemblage present, (2) compositional data for these minerals and (3) in some instances the whole rock isotopic composition. The objective of this approach is to identify the parental magma which has given rise to a suite of rocks. Hence, alkaline rocks are assigned to petrological clans. Individual rocks are not considered or named in isolation from other rocks in a given suite. The specific parental magma type is reflected in the nomenclature by a clan name e.g. kimberlite, lamproite, melilitite etc. Modally diverse, but consanguineous, members of a clan are described by modal varietal compound names e.g. olivine phlogopite lamproite, leucite diopside lamproite.

Application of this approach to rocks which contain diamond suggests that there are three genetically-distinct upper mantle-derived magmas which are capable of transporting diamond xenocrysts; kimberlite (formerly group I kimberlite), orangeite (formerly group II kimberlite) and lamproite. Group II kimberlites are renamed as they apparently form a petrological clan that is genetically-

unrelated to group I kimberlites. The rocks now known as group II kimberlites were originally termed (micaceous) kimberlites on the basis of the presence in them of diamond. It is unlikely that if this group of rocks were discovered today they would be termed kimberlites as they have few mineralogical similarities with archetypal group I kimberlites.

The term lamprophyre was introduced as a field term in the nineteenth century to describe hypabyssal rocks that are rich in mica. Usage was confined to describing the macroscopic appearance of the rocks. Subsequently, the term was broadened to include any dike rocks containing mafic phenocrysts (mica, amphibole, pyroxene) set in a felsic groundmass. The term was, and still is, used indiscriminately in this descriptive manner without regard to the nature of the associated rocks and/or tectonic setting of the occurrence. Recently, diverse lamprophyric rocks, kimberlites and lamproites have all been considered to be members of a "lamprophyre clan". However, the P/T conditions of generation and/or source regions of the magmas which formed these rocks are very different and it follows that the rocks cannot be genetically related. Further, as the concept of a petrological clan requires that members of the clan be consanguineous it is evident that the concept of a "lamprophyre clan" is petrologically unsound as there is no universal lamprophyre magma type.

Application of mineralogical-genetic terminology to diverse rocks described as lamprophyres confirms that many varieties are derived from genetically-unrelated magma types. Mica-rich rocks of lamprophyric aspect are commonly found as modal variants of rocks formed from several distinct magma types. They represent rocks that have formed under water-rich or other special conditions relative to other members of the clan. It is proposed here that such rocks be assigned to a "lamprophyre facies". Thus, phlogopite diopside lamproite belongs to the lamprophyre facies of the lamproite clan, whereas sannaite, monchiquite and camptonite are lamprophyric facies of the alkali basalt clan. This concept preserves the original meaning of the term "lamprophyric" and has no genetic connotations.

The lamprophyres facies concept is illustrated by the following examples:

ALKALINE OLIVINE BASALT CLAN

<u>Facies</u>	<u>Rock</u>
Extrusive(lava)	Basalt
Hypabyssal	Diabase
Plutonic	Gabbro

Lamprophyric hypabyssal Sannaite, Camptonite, Monchiquite.

Petrographically different members of the lamprophyre facies result from formation under different volatile, P/T conditions and cooling rates, hence some are heteromorphs. In this clan different facies are easily related to the site and style of crystallization and the lamprophyric facies is entirely hypabyssal. In contrast. in other clans, lava flow or plutonic facies may be of lamprophyric character e.g. the minette lavas of the basanite clan and the phlogopite perovskite pyroxenites of the melilitite clan, respectively.

## GROUP 1 KIMBERLITES

<u>Facies</u>	<u>Rock</u>
Crater	Epiclastic and pyroclastic kimberlite
Diatreme kimberlite	Tuffisitic or volcanoclastic
Hypabyssal	monticellite calcite kimberlite
Lamprophyric hypabyssal	phlogopite apatite kimberlite

In some group I kimberlites simple modal enrichment of phlogopite confers a "lamprophyric aspect" to the rocks. These cases are relatively uncommon and the majority of group I kimberlites have no macroscopic or microscopic lamprophyric character. Note that lamprophyric facies group I kimberlites do not grade in a petrogenetic sense or mineralogical/genetic classification into group II kimberlites or minettes, although the latter may have some gross modal similarities.

## LAMPROITE CLAN

<u>Facies</u>	<u>Rock</u>
Lamprophyric lava	diopside phlogopite lamproite
Hypabyssal	leucite diopside lamproite
Lamprophyric hypabyssal	leucite diopside transitional madupitic lamproite.
Plutonic lamproite.	richterite sanidine

Further examples may be devised with respect to the group II kimberlite, basanite (minettes), melilitite (alnoites, aillikites), nephelinite and "andesitic" (minette, spessartite, kersantite) clans.

Lamprophyres have typically been stigmatized as orphans of dubious and unfathomable antecedents; thus they are consigned by many to the petrological waste basket. Consideration of lamprophyres as a group without regard to their diverse parentage has hindered understanding of their genesis. By adopting the lamprophyre facies concept and using mineralogical/genetic classifications, it is now possible to show that lamprophyres are merely derivatives of common magma types. Using these principles petrologists are hopefully now in a position finally to put this neglected but ubiquitous group of rocks into their correct petrological context.

## GARNET MEGACRYSTS FROM GROUP II KIMBERLITES IN SOUTHERN AFRICA.

*Moore, \*R.O. and Gurney, J.J.**Department of Geochemistry, University of Cape Town, Private Bag, Rondebosch, 7700, South Africa;**\*Present address: P.O. Box 1372, Wangara, W.A. 6065, Australia.*

In a study of the heavy mineral concentrate from the Group II Dokolwayo kimberlite in Swaziland, Daniels & Gurney (1989) identified a suite of garnets which they interpreted to be representative of the Cr-poor suite of megacrysts. This represented a significant find, since it was previously believed that the occurrence of Cr-poor megacrysts was confined to Group I kimberlites. Directed investigations have since recognised the presence of garnet megacrysts in a large number of Group II kimberlites in southern Africa, and this contribution aims at characterising these suites.

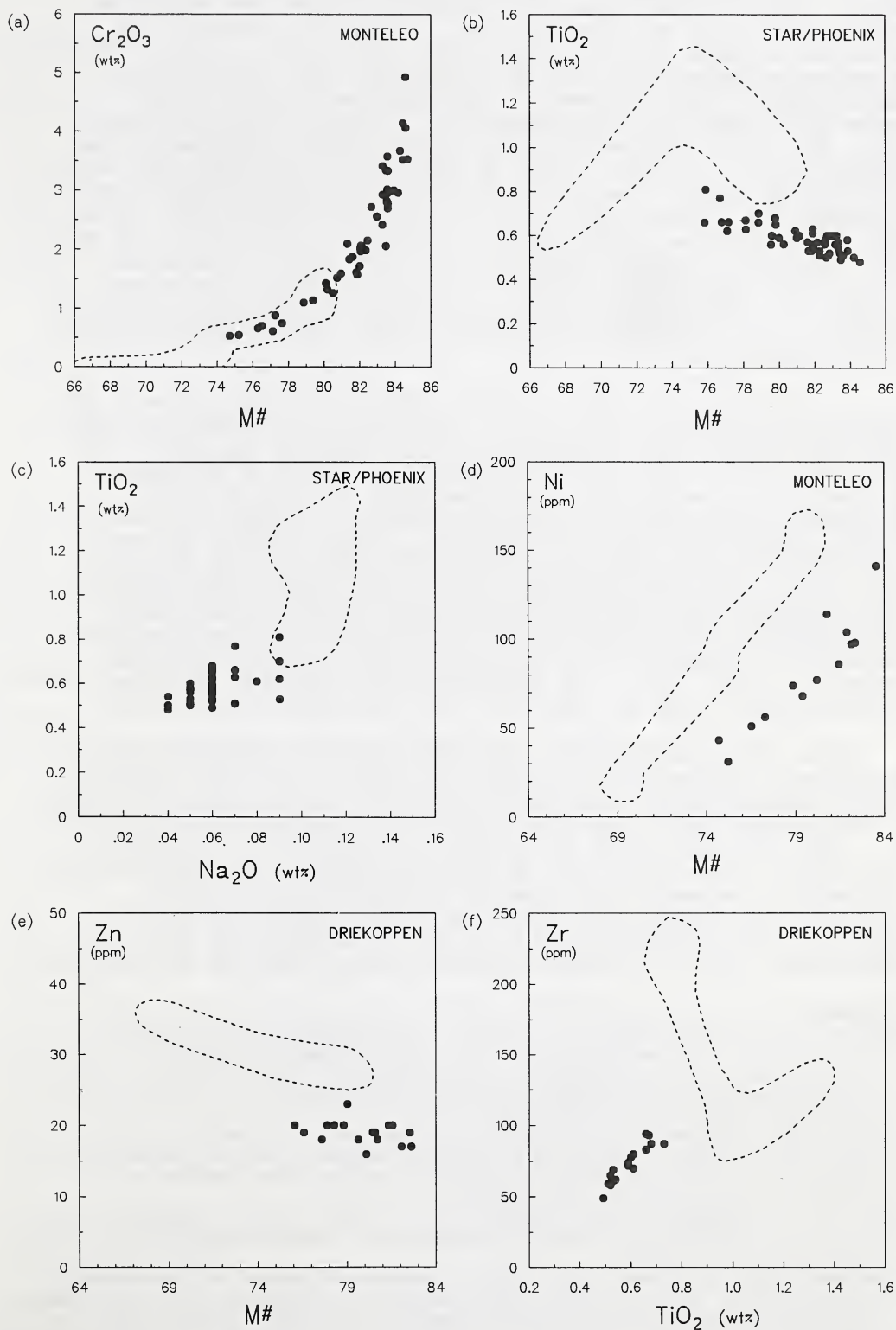
Garnet megacrysts have been recovered from the following Group II kimberlites:- Loxton and Southern Fissures (NE of Kimberley); Excelsior and Newlands (N of Barkly West) and Driekoppen, Monteleo, and the Phoenix Blow (in the vicinity of the Star Mine, O.F.S.). They have also been recovered from the Lace kimberlite in the O.F.S., where olivine and cpx megacrysts are apparently also present (Pers.Comm. D.R. Bell & G. Read). Follow-up work on a suite of garnet megacrysts from Dokolwayo is reported by Moore et al. (1990). Apart from the presence of cpx megacrysts at some of the Barkly West localities (many of which may be from eclogites), none of the other common constituent phases of the Cr-poor megacryst suite have been found at these localities to date.

A random sample of thirty garnets from each locality was selected for study from large collections of garnet megacrysts sampled from the coarse tailings dumps at the mines. Since this material had been processed through a primary crusher, all samples were less than 2 cm in longest dimension. The garnets are deep red in colour, highly fractured and usually have thin kelyphitic rinds developed on grain margins. Major element compositions were determined on a Cameca Camebax microprobe, using routine analytical procedures. Core-rim analyses on a number of test samples revealed no compositional zoning and consequently analyses were undertaken on grain mounts of chips taken from the megacrysts. Fifteen samples from each locality were selected for trace element analysis on the basis of Mg-number ( $M\# = \text{Mg}/(\text{Mg} + \text{Fe})$  atomic). Trace element analyses were undertaken on the proton microprobe at the CSIRO in Sydney, Australia. Details of this instrument and its application to the analysis of geological materials have been described by Griffin et al. (1988).

In assessing the compositional characteristics of the garnets examined in this study, they are compared with a suite of Cr-poor garnet megacrysts from the Monastery kimberlite (Moore, unpublished data). This suite was chosen because it has been well documented and it is considered to be broadly representative of garnet megacrysts in Group I kimberlites.

All seven suites show broadly similar compositional characteristics and a series of representative plots illustrating selected features is presented as Figure 1.

**Figure 1:** A selection of plots illustrating typical compositional trends displayed by garnet megacrysts from Group II kimberlites. Compositional fields for Monastery garnets are included for comparison. Monastery data from Gurney et al. (1979) and Moore (unpublished).



The "Group II" garnet megacrysts are on average more magnesian and chrome-rich compared to the Monastery suite. In general, M# ranges from 86 to 74 and chrome contents from 0.5 to 3.5 wt% Cr<sub>2</sub>O<sub>3</sub>, but at Excelsior, Monteleo and the Phoenix Blow at Star Mine, chrome contents may be as high as 5 wt% Cr<sub>2</sub>O<sub>3</sub>. At all localities Cr<sub>2</sub>O<sub>3</sub> shows an excellent positive correlation with M# (see Fig. 1a). Titanium contents are moderate to high (~0.5-1.2 wt% TiO<sub>2</sub>) and in all cases negatively correlated with M# (e.g. Fig. 1b). The rapid depletion in TiO<sub>2</sub> observed in the Monastery suite which correlates with the commencement of ilmenite precipitation (Fig. 1b) is not evident in any of the suites examined. The garnets show a limited range in calcium (~3.5-5 wt% CaO) which is slightly larger than the even more restricted range commonly observed for garnet megacrysts in Group I kimberlites. They also show elevated trace levels of sodium (~0.03-0.13 wt% Na<sub>2</sub>O) but typically, sodium contents are lower than at Monastery (Fig. 1c). Trace enrichments of Na<sub>2</sub>O in garnet have been correlated with high formation pressures (>45Kb) in eclogitic systems (e.g. McCandless & Gurney, 1989), and we believe this to be applicable here as well.

In general, the trace element contents of the garnets show systematic variation patterns. This is well illustrated in Fig. 1(d) where the Ni content of the Monteleo garnets decreases from ~150 to ~30 ppm over the range of M# present. Similar trends were noted for the other localities and Monastery, although the Monastery trend is offset by lower values of M#. Zn contents typically range between 15 and 30 ppm which is systematically lower than observed at Monastery (Fig. 1e). Zr (~50-100 ppm) and Y (~20-40 ppm) both show a good negative correlations with M# and as such mimic the behaviour of TiO<sub>2</sub>. This is illustrated by the good positive correlation observed between Zr and TiO<sub>2</sub> in the Driekoppen garnets in Fig. 1(f). Ga contents show a general increase with Fe-enrichment, and are typically in the range 10 to 20 ppm.

This preliminary study demonstrates that while the garnet megacrysts recovered from Group II kimberlites show similar basic compositional features to Cr-poor garnet megacrysts (such as restricted CaO & elevated TiO<sub>2</sub>), they differ in detail (Fig. 1). The fact that most elements show systematic variations with M# (in particular Cr, Ti and Ni) appears to indicate that the garnets formed in an igneous fractionation process. Moreover, the behaviour of Ni (Fig. 1d) almost certainly implies that olivine was part of the precipitating megacryst assemblage, while Ti trends indicate that ilmenite was absent.

#### References

- Daniels, L.R.M. and Gurney, J.J. (1989) The chemistry of the garnets, chromites and diamond inclusions from the Dokolwayo kimberlite, Kingdom of Swaziland. In: *Kimberlites and Related Rocks, Vol.2: Their Mantle/Crust Setting, Diamonds and Diamond Exploration*, p. 1012-1021 Blackwell Scientific Publications.
- Griffin, W.L., Jaques, A.L., Sie, S.H., Ryan, C.G., Cousens, D.R. and Suter, G.F. (1988) Conditions of diamond growth: a proton microprobe study of inclusions in West Australian diamonds. *Contributions to Mineralogy and Petrology*, 99, 143-158.
- Moore, R.O., Daniels, L.R.M. & Gurney, J.J. (1990) Garnet megacrysts in the Group II Dokolwayo kimberlite, Swaziland. *Extended Abstract, Geocongress 90*, 427-430.
- McCandless, T.E. & Gurney, J.J. (1989). Sodium in garnet and potassium in clinopyroxene: criteria for classifying mantle eclogites. In: *Kimberlites and Related Rocks, Vol.2: Their Mantle/Crust Setting, Diamonds and Diamond Exploration*, p. 827-832, Blackwell Scientific Publications.

## DISTRIBUTION OF LAMPROITE PATHFINDERS IN SURFACE SOILS.

Muggeridge, Maureen T.

Moonstone Mines N.L., 251-257 Hay Street, East Perth, Western Australia 6004.

## INTRODUCTION

Using data from orientation surveys carried out in the monsoonal Kimberley Region of Western Australia at certain known lamproite localities (Fig.1), the limitations and potential of loam, anthill and geochemical sampling in diamond exploration are considered. Lamproites referred to occur in flat geomorphic settings and are described in detail in Jaques *et al.* (1986). From this limited study, some general conclusions about sampling surface materials can be drawn, but expanded surveys are needed to obtain a thorough understanding of the distribution of diamond pathfinders in the surface environment and establish sound guidelines for exploration practice.

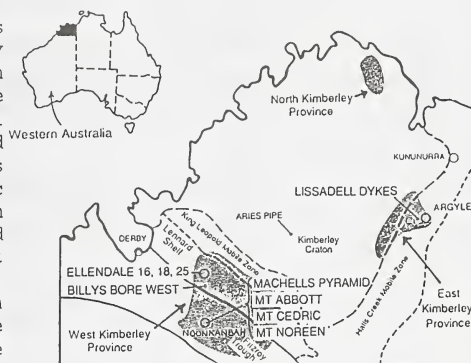


FIGURE 1 Location of Lamproites

## ENVIRONMENTAL VARIABLES

In order to assess the effectiveness of loam and geochemical sampling, various agents that control the environment containing primary host rocks of diamond must be considered. Some of these factors may assist the survival and distribution of kimberlitic (i.e. any potentially diamond-bearing) material at the surface, whilst others have the opposite effect. In general, if degradation is occurring in the host terrain, a kimberlitic body is likely to be disintegrating and shedding debris into the overlying soil and local drainage. If aggradation is taking place, accumulation of alluvium may bury the body in such a fashion as to substantially reduce its surface expression. When burial is relatively rapid and/or particularly deep the kimberlitic intrusive may be totally masked with scant mineralogical or geochemical expression in the upper soil horizon. Ant activity may, in certain cases, assist in maintaining detectable geological indicators at surface levels.

## METHODS

Samples were collected from soil or anthills over lamproite bodies and at varying distances from their perimeters along traverse lines.

## LOAM SAMPLES

The uppermost 1 cm of top-soil was collected for loam samples; where gravel debris was present samples were screened at 2 mm. The size of samples collected varied. Therefore, for comparative purposes, loam sample results in Table 1 have been standardized to "number of indicators per kg of sample screened at minus 2 mm". Where practical, samples were taken at sites with the minimum of obvious disturbance from prior exploratory excavation which may have unnaturally increased the indicator content at surface. Loam samples were reduced to their heavy mineral component by Wilfley Table, heavy liquid and magnetic separation treatment and then examined for kimberlite/ lamproite indicator mineral content.

## ANTHILL SAMPLES

The largest available anthill was selected, assuming a relationship between size and depth of ant excavation. The uppermost, latest built part of the anthill was sampled, as well as some anthill "scree" around its base. Anthill samples were processed in the same manner as for loam samples.

## GEOCHEMICAL SAMPLES

Geochemical analysis was performed on material from many of the loam sample sites (Table 1). Samples were analysed for a range of elements associated with lamproites and kimberlites, including incompatible elements and those of ultramafic affinity. Two samples from the Ellendale area were collected to assess the geochemical background.

## RESULTS

Heavy mineral and geochemical analysis results are given in Table 1.

## HEAVY MINERAL RESULTS

The dominant indicator minerals are chromite and phlogopite, the former having the most frequent occurrence in samples, i.e. the best overall dispersion. Pyrope occurs in some samples from Ellendale No.18, Mount Abbott, Mount Noreen and Mount Cedric. Some samples from Mount Noreen contain potassic richterite, lamproitic diopside and chrome diopside, the latter also occurring in a sample from Mount Abbott.

Where the 0.3-0.4mm size range was analysed in addition to the 0.4-2mm size, the recovery of indicator minerals is at least doubled in all cases where more than one indicator grain is present in the coarser fraction.

Ellendale No.25, with a sandy overburden of 7m, yielded no indicators in either loam or anthill sample. Ellendale No.18, under 6m overburden, yielded some chromite in both samples, but pyrope only in the anthill sample. By comparison to the loam sample, a relatively small proportion of phlogopite is present in the anthill sample from Ellendale No.16, though the chromite content is similar. At Billys Bore West the ants' haul of phlogopite is similarly low by comparison to the loam sample.

Mount Abbott, Mount Noreen and Mount Cedric yielded significant proportions of indicator minerals in central and peripheral zones over the bodies, with a rapid, steady tailing off of indicator content away from the margins. At Mount Noreen, however, there is a sudden increase in indicator levels 250m south of its margin, possibly due to a local concentrating effect or an underlying, undiscovered lamproite body.

Samples from Machells Pyramid and Lissadell Road Dykes yielded only trace quantities of indicators. A further 3 chromites were obtained from one Lissadell sample by examining the 0.1-0.3mm size range.

#### GEOCHEMISTRY RESULTS

Most lamproites in this study show anomalous Mg, P, Ti, Ni, Sr, Zr, Ba and La in the overlying or nearby soils. Elements K, Ca, Cu, Zn, Rb, Nb, Ce and Nd are anomalous at or near some bodies. Values of several times background are obtained for some samples. Li, Co, Sc, V, Cr, Y, Mo and Th give rare or more subtle variance from background. The dispersion halo of anomalous elements around the lamproites sampled is in no case extensive, distances from the periphery not exceeding the breadth of the body, in agreement with findings of Haebig & Jackson (1986). At Mount Noreen, anomalous values for most elements occur around 250m south of the known intrusion, at a point where indicator levels are also exceptionally high. As the extent of dispersion appears abnormal, the case for a concealed lamproite here is considerably strengthened.

#### DISCUSSION AND CONCLUSIONS

Remote sensing and geophysical techniques have serious limitations in that anomalous responses are unqualified. Additionally, the most broadly applied of these methods, magnetics, is relatively insensitive to pyroclastic phases and, when the host environment is strongly magnetic, to kimberlitic rocks in general. Some conclusive indication at surface of the presence of a concealed kimberlitic body is extremely important when prospecting for diamonds. Sampling of surface soils is thus a valuable prospecting tool. For optimum results, however, it must be applied with discrimination and sound understanding of environmental influences.

This limited survey has the following implications, which need substantiation by further investigations:-

1. Indicator mineral yield is increased significantly by examining the grain size range below 0.4mm.
2. Dispersion halos, even for large exposed bodies, and especially where overburden masks the intrusion, may extend only a few hundred metres beyond the margin. Therefore, when planning loam and geochemical sampling programmes, careful consideration should be given to choosing the appropriate sampling interval.
3. Anthill samples, in this study, did not yield higher quantities of indicators than loam samples. Total reliance on anthill samples alone is therefore inadvisable. Ants appear to selectively excavate certain minerals. This may be useful in certain cases and requires investigation.
4. Geochemical analysis of a broad selection of elements should increase the chance of detecting a concealed diamond host rock.

Particular indicators known to survive well in the soil horizon may be relatively uncommon in the host rock. Possible variations in source mineralogy that will have a bearing on the types and concentrations of indicators in associated soils should be considered when planning exploration surveys and assessing loam and geochemical results.

Correct selection of the type, size, spacing and treatment of surface samples for diamond exploration depends upon an understanding of the distribution of diamond pathfinders in regolith. Detailed, broad-based studies involving all known diamond lithologies and a variety of environmental settings are needed to determine reliable sampling methods for diamond exploration.

#### REFERENCES

- Haebig, A.E., and Jackson, D.G. (1986) Geochemical expression of some West Australian kimberlites and lamproites. Fourth International Kimberlite Conference, Perth, Extended Abstracts Volume, Geological Society of Australia 16, 466-468.
- Jaques, A.L., Lewis J.D. and Smith, C.B. (1986) The kimberlitic and lamproitic rocks of Western Australia. Bulletin of the Geological Survey of Western Australia 132, 268p.



PRESSURE - TEMPERATURE - VOLUME PATH OF  
MICRO-INCLUSION-BEARING DIAMONDS.*Oded Navon.**Institute of Earth Sciences, The Hebrew University, Jerusalem 91904, Israel.*

Bulk composition, mineralogy, and internal morphology of micro-inclusions in cubic and coated diamonds, suggest that they represent an  $\text{H}_2\text{O}-\text{CO}_2-\text{SiO}_2-\text{K}_2\text{O}$ -rich fluid, trapped by the diamonds during their growth. However, the depth and temperature of their formation have remained unclear. Some authors suggested that micro-inclusion-bearing (MIB) diamonds grew as phenocrysts from their host kimberlite, or from a fluid phase that separated from it. Others preferred a more complex evolution at depth.

P-T conditions of diamond formation are commonly constrained using mineral equilibria between primary crystalline inclusions. Unfortunately, no such inclusions have been found in cubic diamonds, except for one report of a sanidine inclusion in the coat of a coated diamond (Novgorodov et al., 1990). The micro-inclusions themselves contain crystalline quartz, apatite, carbonates and phyllosilicates (Guthrie et al. 1989), but these are probably secondary phases that grew from the trapped fluid at a later stage.

Infrared spectroscopy of inclusion-rich zones in the diamonds did not reveal the characteristic quartz absorption bands at 779 and 798  $\text{cm}^{-1}$  (Navon et al., 1988). Following the identification of quartz by TEM, the infrared spectra were re-examined and it is proposed here that the bands at ca. 784 and 811  $\text{cm}^{-1}$  (Figure 1) are quartz absorption bands that were shifted to higher energies as the result of high internal pressure currently existing in the inclusions.

Using a diamond anvil cell, Velde and Couty (1987) calibrated the shift of the 779 and 798  $\text{cm}^{-1}$ , and other bands of powdered quartz as a function of pressure. The MIB diamonds also contain small grains of quartz inside a diamond matrix and are a very close analog of the diamond cell experiment. The recorded positions of the quartz bands in 25 diamonds was recorded using the Nicolet SX60 FTIR in Prof. G.R. Rossman's laboratory at Caltech. Figure 1. presents the result together with the pressure calibration of Velde and Couty. The energy shift of both bands correspond to pressures of 1.6-2.1 GPa (16-21 kbar).

Such high internal pressures should effect other bands as well. The broader bands at ca. 475 and 525  $\text{cm}^{-1}$  are consistent with about 2 GPa pressure shift of the 464 and 515  $\text{cm}^{-1}$  bands of quartz (Velde and Couty, 1987). It must be noted, however, that many silicates absorb in this region and the bands may be related to the presence of other phases. Carbonates are also present in the micro-inclusions. EDS analyses by both TEM (Guthrie et al. 1989) and electron probe (Navon, this volume) show that they contain Ca, Mg, and Fe. Since no IR data exist for complex carbonates at high pressure, it is impossible to uniquely identify the carbonate phases, or to use them as a barometer. No high pressure IR data has been found for apatite.

The high pressure within the micro-inclusions is, to the best of my knowledge, the highest pressure ever recorded in any fluid inclusion. The preservation of this high internal pressure was probably enabled by the small sizes of the inclusions combined with the high strength of the diamond. Larger inclusions would probably lead to decrepitation of the diamond matrix (Taylor, 1985). Extrapolating Taylor's decrepitation model to sub-micrometer size inclusions, it seems likely that the stress applied by the micro-inclusions can be accommodated elastically by the diamond.

Guthrie et al. (1989) found euhedral crystals within the inclusions. In no case the crystals filled the entire volume of the inclusions. These observations and the detection of water by IR strongly suggest that the pressure within the inclusions is hydrostatic exerted by water. If so, and if the inclusion volume is conserved, a pressure - temperature path may be calculated along a water isochore. The isochore assumption is reasonable as diamond compressibility is small and its high Young's modulus ensures small elastic response to removal of confining pressure during eruption. Both are almost fully compensated by thermal expansion. Rough calculations predict volume changes of less than a few permilles. A less founded assumption is that precipitation of the crystalline phases do not introduce significant volume changes.

At 1.8 GPa, 23 C, water freezes to ice VI with specific volume of  $0.71 \text{ cm}^3/\text{gr}$ . The shape of the IR water band does not resemble that of ice VI. It looks similar to that of liquid water. This is probably because the large surface/volume ratio of the micro-inclusions and their high solute content prevent freezing. In that case a specific volume of  $0.77 \text{ cm}^3/\text{gr}$  is estimated from the metastable extension of liquid water compression data (Liu, 1982). This volume may now be used with a suitable equation of state to predict pressures at high temperatures.

The MRK equation of Holloway (1981) cannot be extrapolated to such small volumes. That of Kerrick and Jacobs (1981) yields unreasonably high pressures. Both were fitted only to low-P data (<8 kbar). Taylor (1985) suggested a new modification for use at high pressures. Saxena and Fei (1987) used shock wave and low-P data to fit a virial equation of state. The resultant P-T paths are presented in Figure 2. When heated to reasonable temperatures (1000-1200 C) the internal pressure in the inclusions falls very close to pressure estimates for South-African diamonds (Boyd and Gurney, 1986, Meyer, 1987).

Based on the shift of the IR absorption of quartz, an internal pressure of 1.6-2.1 GPa is estimated for micro-inclusions in diamonds at room temperature. The inclusion volume is similar to their volume at high P and T. Neglecting volume changes due to precipitation of solid phases from the initial fluid, the water isochore intersects the geotherm at a pressure range that is typical of most diamonds. This is in agreement with additional observations that strongly suggest that MIB diamonds were formed within the diamond stability field in the upper mantle and not as a metastable phase. The high internal pressure is also a clear indication that most inclusions remained sealed, preserving the original, unaltered fluid from which the MIB diamonds grew.

- Boyd, F.R., and Gurney, J.J. (1986) Diamonds and the African lithosphere. *Science*, 232, 472-477.
- Guthrie, G.D., Navon, O., Veblen, D.R. (1989) Analytical and transmission electron microscopy of turbid coated diamonds. (abst) *EOS*, 70, 510.
- Holloway, J.R. (1977) Fugacity and activity of molecular species in supercritical fluids. In D.G. Fraser, Ed., *Thermodynamics in Geology*, p.161-181. Reidel, Boston.
- Kerrick, D.M., and Jacobs, G.K. (1981) A modified Redlich-Kwong equation for  $H_2O$ ,  $CO_2$ , and  $H_2O-CO_2$  mixtures at elevated pressures and temperatures. *Amer. J. Sci.*, 281, 735-767.
- Liu, L. (1982) Compression of ice VII to 500 kbar. *Earth Planet. Sci. Lett.* 61, 359-364.
- Meyer, H.O.A. (1987) Inclusions in diamonds. In P.H. Nixon, Ed., *Mantle xenoliths*, Wiley, London.
- Navon, O., Hutcheon, I.D., Rossman, G.R., and Wasserburg, G.J. (1988) Mantle-derived fluids in diamond micro-inclusions. *Nature*, 335, 784-789.
- Novgorodov, P.G. et al. (1990) Inclusions of K-rich phase, coesite and omphacite in a coated diamond crystal from the Mir pipe. *Doklady Acad. Nauk. USSR*, 310(2), 439-445.
- Saxena, S.K., and Fei, Y. (1987) High pressure and high temperature fluid fugacities. *Geochim. Cosmochim. Acta*, 51, 783-791.
- Taylor, W.R. (1986) A reappraisal of the nature of fluids included by diamond - a window to deep-seated mantle fluids and redox conditions. *Geol. Soc. Aust. Special Publ. No. 12*,
- Velde, B., and Couty, R. (1987) High-pressure infrared spectra of silica glass and quartz. *J. Non-Crystal. Solids*, 94, 238-250.

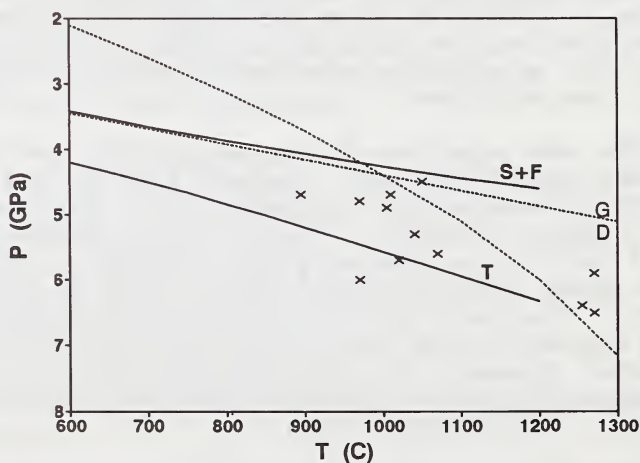
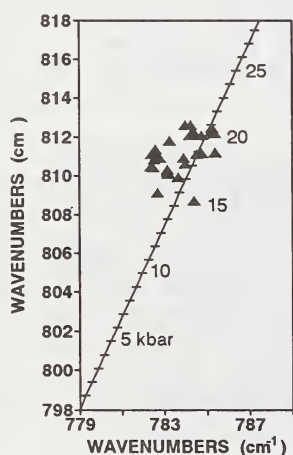


Figure 1. Peak wavenumbers of two IR absorption bands of quartz in micro-inclusions in diamonds. The scaled line indicates the pressure shift of the two bands, determined experimentally by Velde and Couty (1987). The quartz in the inclusions is under 15-21 kbar.

Figure 2. P-T path of MIB diamonds. Solid lines - isochores for water with specific volume of  $0.77 \text{ cm}^3/\text{gr}$ . S+F - Saxena and Fei, 1987; T - Taylor, 1985. Dotted line - Graphite-diamond transformation, dashed line - the  $40 \text{ mW/m}^2$  geotherm. Crosses - P-T condition of diamonds with crystalline silicate inclusions (Meyer, 1987).

## RADIAL VARIATION IN THE COMPOSITION OF MICRO-INCLUSIONS AND THE CHEMICAL EVOLUTION OF FLUIDS TRAPPED IN DIAMONDS.

Oded Navon.

*Institute of Earth Sciences, The Hebrew University, Jerusalem 91904, Israel.*

Many coated and cubic diamonds from Zaire, Botswana, and other localities carry multitudes of sub-micrometer inclusions that contain H<sub>2</sub>O-CO<sub>2</sub>-SiO<sub>2</sub>-K<sub>2</sub>O-rich fluids. The complex internal structure, and the high internal pressure within the inclusions (Navon, this volume) strongly suggest that the inclusions are primary and that the diamonds grew from the same fluid. If so, the chemical evolution of the trapped fluid may be followed by studying the chemical variation of the micro-inclusions along a radial profile.

More than hundred individual inclusions were analyzed along an approximate radial direction in a diamond from Jwaneng, Botswana. ON-JWN-87 is a 5.6 carat (1121 mg), grey cubic diamond. A 1 mm thick wafer cut parallel to (100) reveals internal radial zonation. The center of the diamond is free of inclusions. It is surrounded by a 1.8 mm wide opaque zone where most inclusions are found. The next 0.16 mm wide zone is inclusion-free, and is followed by a 0.45 mm wide translucent band with lower density of inclusions. The outer 0.5 mm is again free of micro-inclusions.

Analyses were performed using a JEOL JXA 8600 electron-microprobe. A focused, 15 KV, 50 nA beam scanned a 0.5x0.5 μm area (large enough to cover the whole inclusion). Data were collected for 100 seconds using an EDS and four WDS spectrometers, and reduced using a full ZAF correction. Total oxide content varied between 1-33 wt% (average: 5%). Compositions were finally normalized to total oxide content of 100%. The X-Y coordination of each analysis spot was recorded and was later projected to calculate the radial position of the micro-inclusion.

Most analyses yielded an average composition which is broadly similar to that obtained in previous ion-probe analyses (Navon *et al.*, 1989). Twelve inclusions deviate significantly from the average composition. Ten of them have very high oxide content (12-33%), and their composition seems to represent discrete mineral phases. Three are rich in CaO, MgO, and FeO (>85%) with Ca>Mg+Fe, and Mg>Fe. They are interpreted as ferroan dolomites. One is rich in FeO and MgO and is probably a magnesian siderite. Three Si-Fe-Mg-Ca-rich inclusions have an approximate formula of (Fe, Mg, Ca)Si<sub>2</sub>O<sub>5</sub> and are probably a mixture of carbonate and quartz, phases that have been previously identified by TEM in the coat of a coated diamond (Guthrie *et al.*, 1989). The composition of two Si-Mg-Fe-K-Al-rich inclusions is close to that of phlogopite. One Si-Ti-rich inclusion was also found.

The composition of all other micro-inclusions was plotted against their radial position (Figure 1). SiO<sub>2</sub> and CaO exhibit clear, opposing trends. CaO content increases outward in the internal, inclusion-rich part of the diamond and decreases sharply in outer band. SiO<sub>2</sub> decreases in the inner zone, and then increases in the outer zone. FeO, MgO and to a lesser degree Na<sub>2</sub>O follow the CaO trend (with Mg/(Mg+Fe) almost constant at 0.52±0.05). TiO<sub>2</sub>, Al<sub>2</sub>O<sub>3</sub>, and to a lesser extent K<sub>2</sub>O follow the trend of SiO<sub>2</sub>. The trends are

better defined in the outer band. The distinction between the two groups of elements was also recognized in a cursory profile done in another diamond.

The chemical evolution of the fluid may be the result of melting, crystallization, or phase separation in a system that may include silicic, carbonatitic, and hydrous fluids. I believe that the complex growth history of micro-inclusion-bearing diamonds, the extreme enrichment in incompatible elements, the low Mg/Fe ratio of the fluid, and, as shown below, the chemical evolution of the trapped fluid can be best explained by fractional crystallization of melt at depth. If so, the nature of the crystallizing phases may be deduced from the compositional evolution of the trapped fluid, as recorded in the micro-inclusions.

The increase in CaO and decrease in SiO<sub>2</sub> content in the inner zone suggest the crystallization of a Ca poor silicic phase. Extrapolation of the linear regression fits of Figure 1 to CaO=0 yields the following approximate composition for the crystallizing phase(s): SiO<sub>2</sub>, 50%; TiO<sub>2</sub>, 10%; K<sub>2</sub>O, 10%; Al<sub>2</sub>O<sub>3</sub>, 10%; MgO, 9%; FeO, 6%; and no Na<sub>2</sub>O. This composition is broadly similar to that of phlogopite, except for the low MgO content. It is suggested that removal of phlogopite, coupled with dissolution of a MgO-rich phase controlled the evolution of the fluid during the stage in which the inner, inclusion-rich zone grew.

The chemistry of the outer zone calls for the crystallization of a CaO-rich, silica poor phase. Similar extrapolation to SiO<sub>2</sub>=0 suggests the removal of a phase(s) with the following composition: CaO, 38%; FeO, 21%; MgO, 15%; K<sub>2</sub>O, 15%; and small quantities of TiO<sub>2</sub>, Al<sub>2</sub>O<sub>3</sub>, and Na<sub>2</sub>O (<3%). Except for the high K<sub>2</sub>O, the composition is that of a ferroan dolomite, with Ca:Mg:Fe equals 100:56:44. At present, I can offer no explanation for the almost constant K<sub>2</sub>O concentration along the profile.

It is suggested that the fluid trapped in the micro-inclusions during the growth of the diamond represents a water-carbonate-rich melt. This melt cooled and evolved under pressures and temperatures of the diamond stability field in the upper mantle. The primary melt was rich in incompatible elements and was probably similar to kimberlites and lamproites. In the final stages, the residual melt was extremely enriched in water, carbonate and incompatible elements, and acquired a very low Mg/Fe ratio. Diamond precipitation commenced during these late stages. It was then accompanied by phlogopite, and later by carbonates. In a few rare cases, these solid phases were also included in the growing diamond. As shown in Figure 2, there exists a good correlation between the chemical trends revealed by the fluid and the composition of the solid trapped phases.

CaO, MgO and FeO make about 45% of the total weight of oxides in the inclusions. This, and the high concentration of carbonate detected by IR suggest that the residual fluid was carbonatitic in nature, and that at high pressure, carbonatitic fluids with high content of water and K<sub>2</sub>O may dissolve appreciable quantities of silica (cf. Baker and Wyllie, 1990). The coexistence of carbonate and diamond buffers the oxygen fugacity close to the QFM buffer (Blundy *et al.*, 1991) suggesting that micro-inclusion-bearing diamonds were formed under relatively oxidizing conditions.

Acknowledgements. I thank J.W. Harris and DeBeers for the diamond, D. Szafranek for EPMA, and N. Summer for review.

Baker, M.B., and Wyllie, P.J. (1990) Liquid immiscibility in a nepheline-carbonate system at 25 kbar. *Nature*, 346, 168-170.

Blundy, J.D., Brodholt, J.P., Wood, B.J. (1991) Carbon fluid equilibria and the oxidation state of the mantle. *Nature*, 349, 321-324.

Guthrie, G.D., Navon, O., Veblen, D.R., (1989) Analytical and transmission electron microscopy of turbid coated diamonds (abst). *EOS*, 70, 510.

Navon, O., Spettel, B., Hutcheon, I.H., Rossman, G.R., Wasserburg, G.J. (1989) Micro-inclusions in diamond from Zaire and Botswana. *Extended Abstracts, Workshop on Diamonds, 28 International Geological Congress, July 15-16, Washington, DC.*

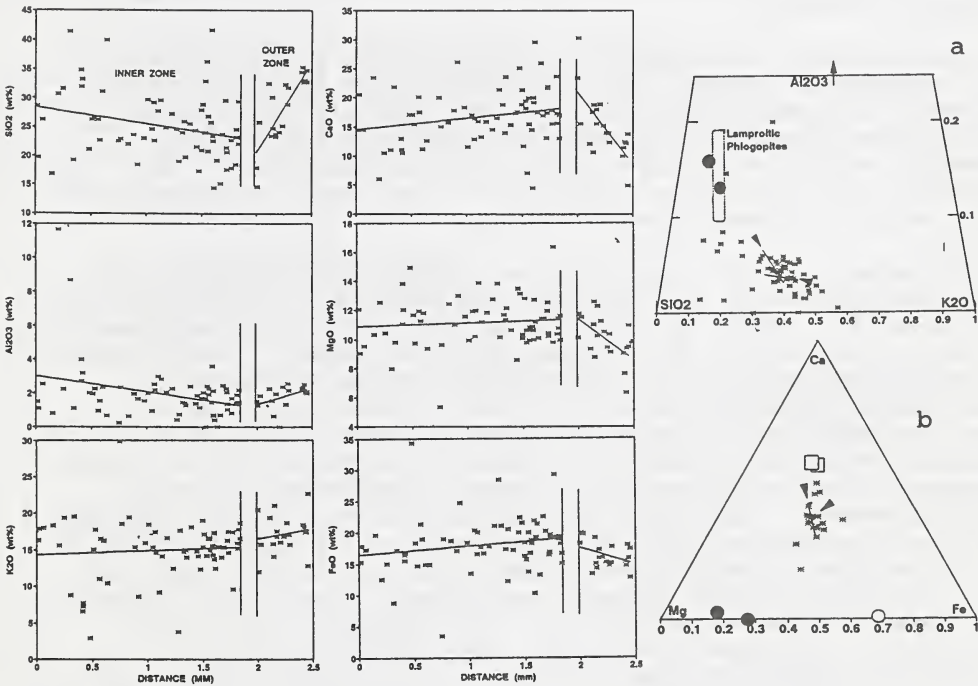


Figure 1. Normalized oxide concentrations vs. radial distance (measured from the boundary between the central zone and the inclusion-bearing inner zone). Lines - Linear regressions of the data in each zone.

Figure 2. a.  $Al_2O_3$ - $SiO_2$ - $K_2O$  of inclusions in the inner zone (horizontal scale expended). Diagonal line -  $Al_2O_3$ - $SiO_2$ - $K_2O$  along the regression line of Fig. 1.; the direction of compositional evolution with time/radius is indicated by the arrow. Sub-horizontal line - the trend in the outer zone. Solid circles: phlogopitic micro-inclusions in the diamond. Rectangle: phlogopites in Western Australian lamproites (Jaques *et al.*, 1986). b. Ca-Mg-Fe molar proportions in outer zone inclusions (asterics and vertical line and arrow). The right arrow indicates the location and direction of the line representing the trend in the inner zone. Composition and direction of the outer zone inclusions may be produced by dolomite removal. Squares-dolomitic inclusions, open circle-sideritic inclusion, filled circles-phlogopitic inclusions.

## Cr GARNET – DIAMOND RELATIONSHIPS IN VENEZUELA KIMBERLITES.

Nixon<sup>(1)</sup>, P.H.; Griffin<sup>(2)</sup>, W.L.; Davies<sup>(3)</sup>, G.R. and Condliffe<sup>(1)</sup>, E.

(1) *Department of Earth Sciences, University of Leeds, Leeds LS2 9JT*; (2) *CSIRO, Division of Exploration Geoscience, PO Box 136, North Ryde, Australia 2113*; (3) *Department of Geological Sciences, University of Michigan, Ann Arbor, MI48109-1063, USA.*

A swarm of NNW-trending kimberlite dykes and sills in the Guaniamo area of Bolivar Province occupy the NW portion of the Guyana Craton. They are the oldest kimberlites so far recorded (ca. 1.9 Ga) and have petrographic features and chemistry (taking into account tropical weathering) of Group 1 macrocrystic olivine monticellite kimberlite. Overlying alluvials contain diamonds derived wholly or in part from these kimberlites and not from the Roraima sedimentary Group as previously believed.

Heavy mineral concentrates contain high proportions of coarse octahedral spinel (up to 66.6% Cr<sub>2</sub>O<sub>3</sub>) and a few show alteration to yimengite, K(Cr, Ti, Fe, Mg, Al)<sub>12</sub>O<sub>9</sub> (second recorded occurrence) attributed to metasomatism within harzburgitic rocks near the base of the lithosphere. No peridotite xenoliths were found other than small aggregates of Cr pyrope and serpentinised olivine.

Chromium garnets (red, purple; green) are abundant and include harzburgitic, lherzolitic and wehrlitic varieties (CaO = < 2-24 wt %; Cr<sub>2</sub>O<sub>3</sub> up to 14 wt %, Fig 1) i.e. an extremely wide range from only a few kimberlite specimens. Model Sm/Nd isotope ages determined on two single grains of subcalcic (harzburgitic) pyrope are ca. 2.6 Ga. These grains show chondrite normalised humped REE patterns with peaks at Nd (6 x chondrite) which are similar to those reported by Shimizu and Richardson (1987) for subcalcic garnet inclusions in South African diamonds. The subcalcic nature of the garnet implies formation in a harzburgite that had suffered a large degree of melt extraction. The REE enrichment and 2.6 Ga Nd model age record an ancient trace element enrichment event that preceded or accompanied diamond formation. In contrast, two calcic (lherzolitic) garnets show smooth LREE depleted patterns signifying a different involvement in the evolutionary events of the craton notwithstanding a similar model Sm/Nd isotope age (2.6 Ga).

A single diamond inclusion was notable in being a calcic pyrope (CaO = 5.17; Cr<sub>2</sub>O<sub>3</sub> = 5.18 wt %). Two others (courtesy of H.O.A. Meyer) from unspecified Venezuela localities are normal subcalcic (G10) varieties. Application of Ni thermometry to all three grains gave temperatures of c. 1300°C which are considerably above those of concentrate garnets (maximum 1050°, Fig 2).

The twin peaks shown in Figure 2 represent a group of low temperature (750-900°C) i.e., shallow, predominantly low Cr calcic lherzolitic garnets and a group of higher temperature (900-1050°C) high Cr lower Ca lherzolite-harzburgite garnets. Within the latter group there is some evidence that lherzolites may be interspersed with more depleted harzburgites within the lithosphere (cf. Boyd and Nixon, 1988), a situation reflected by the limited diamond inclusion data above. Four subcalcic garnets close to G10 composition fall within the temperature range 900-1000°C compared with the normal South African range of 1000-1150°C.

Assuming a Kaapvaal-type geotherm, the proportion of garnets derived from the basal lithosphere diamond zone (950-1250°C range) is low considering the observed high diamond grades. One possibility is that the ambient geothermal gradient in this part of the Guyana Craton was shallower (cooler) at the time of kimberlite eruption compared with that in the Kaapvaal Craton.

The difference in temperatures indicated by the garnet inclusions in diamond (closed system) and those from the concentrates (open system harzburgites, lherzolites etc) could represent the degree of cooling between the time of diamond formation (garnet encapsulation) at 2.6 Ga and eruption at ca. 1.9 Ga.

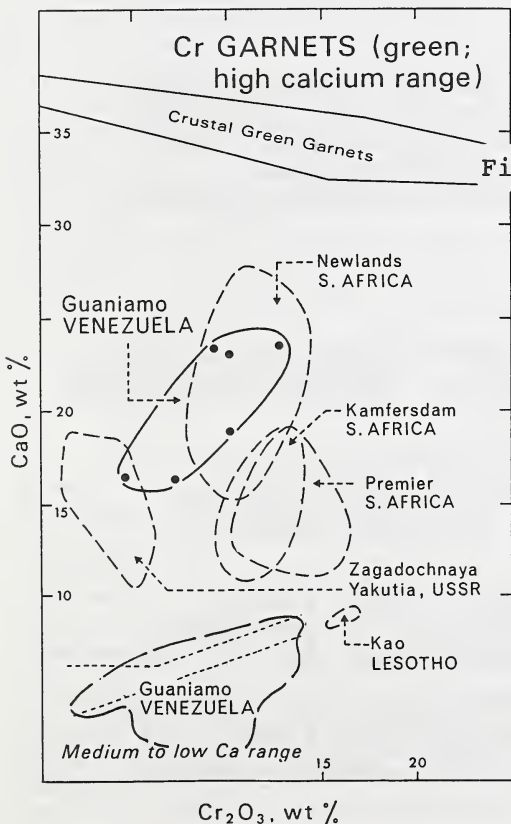


Figure 1 CaO-Cr<sub>2</sub>O<sub>3</sub> composition fields of chromium garnets in Guaniamo kimberlites, Venezuela. The medium to low Ca field is represented by 123 garnet analyses. Traversing this field the sloping dotted lines embrace the field of lherzolite garnets, with that of wehrlites above and dunite-harzburgites below (Sobolev et al. 1973). Non Venezuela data after Schulze, 1989.

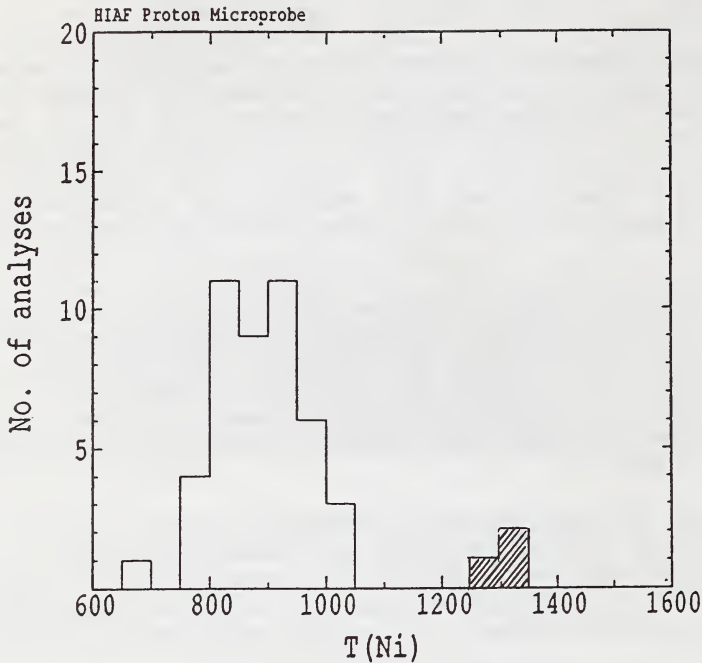


Figure 2 Composite histogram of  $T_{Ni}$  for 48 Cr pyropes from Guaniamo kimberlites. The "twin peaks" represent lherzolitic and lherzolitic + harzburgitic type garnets (low and higher temperature ranges respectively); the three high temperature garnets are diamond inclusions.

#### References

- Boyd, F.R. and Nixon, P.H. (1988). Low-Ca garnet harzburgites: origin and role in craton structure. Carnegie Institution of Washington. Ann. Report, 8-13.
- Schulze, D.J. (1989). Green garnets from South African kimberlites and their relationship to wehrlites and crustal uvarovites. Geol. Soc. Australia. Spec. Publication. No. 14, 820-826.
- Shimizu, N. and Richardson, S.H. (1987). Trace element abundance patterns of garnet inclusions in peridotite-suite diamonds. Geochim. Cosmochim. Acta. 51, 755-758.
- Sobolev, N.V., Lavrent'yev, Yu.G., Pokhilenko, N.P. and Usova, L.V. (1973). Chrome-rich garnets from the kimberlites of Yakutia and their paragenesis. Contr. Mineral. Petrol., 40, 39-52.

## THE COMPOSITION OF PARTIAL MELTS IN A VOLATILE BEARING, REDUCED MANTLE.

*Odling<sup>(1)</sup>, N.W.A.; Green<sup>(2)</sup>, D.H. and Harte<sup>(1)</sup>, B.*

*(1) Dept. of Geology and Geophysics, University of Edinburgh, West Mains Rd., Edinburgh, Scotland EH9 3JW, U.K.;*

*(2) Dept. of Geology, University of Tasmania, G.P.O. Box 252C Hobart, Tasmania, Australia.*

The migration and reaction of partial melts (PM) and/or volatile dominated fluids have been commonly invoked to explain chemical enrichments apparent in many upper mantle xenoliths, and such processes are inferred to be important in generating different melt compositions and types of magmatism. In considering these processes it is crucial to understand the relationship between the intensive variables pressure (P), temperature (T) and  $fO_2$ , and the character of the melts/fluids produced. The determination of the chemical character of PM by direct melting of peridotite in experiments is difficult because crystal growth during quenching severely modifies the composition of the interstitial melt. Thus, despite their perceived importance very little is known about the composition of PM as a function of P, T,  $fO_2$  and percentage volatile present.

### ***Determination of partial melt compositions***

In partial melting experiments crystal growth during quenching renders the resultant glasses unrepresentative of partial melts present at high pressure and temperature (Green, 1976). In an attempt to circumvent this problem, and so achieve representative partial melt compositions, Stolper (1980) devised the 'sandwich technique' in which a layer of basalt is placed next to the peridotite to increase the modal proportion of partial melt (basalt) within the charge. During quenching the melt composition is modified only adjacent to crystals and so large areas of glass separated from crystal rich areas will preserve the equilibrium melt composition. This approach, however, suffers from two limitations:

- (1) the peridotite and the melt composition used in the basalt layer must be genetically related;
- (2) a particular basalt composition can only be used over a restricted temperature range before crystallization results in amounts of melt too small to preserve the equilibrium melt composition.

Where such compositional pairs are available this technique has been employed to examine the position of 'dry' cotectics in P/T/compositional space (e.g. Falloon et al., 1988). In contrast, the compositions of melts generated by the melting of 'wet' peridotite (either fluid saturated or fluid undersaturated) are poorly constrained. The use of the sandwich technique to determine the character of partial melts of 'wet' peridotite requires knowledge of not only the oxide composition of a suitable partial melt but also both the nature and amount of volatile species held in solution. As these are poorly constrained the sandwich technique presents significant problems in its application to the study of partial melting of peridotite in the presence of volatiles.

### ***Determination of EPM by Melt inclusion Synthesis: A New Technique.***

In order to examine the compositions of equilibrium partial melts (EPM) of volatile bearing peridotite we have devised a technique in which EPM are isolated from the bulk of the charge as inclusions in olivine. Olivine plugs were cut from

San Carlos olivine ( $\text{Fo}_{90}$ ), fractured by thermal stressing and placed adjacent to peridotite mix within a carbon capsule. This was then sealed in an outer Pt capsule along with a buffer assemblage of WC,  $\text{WO}_2$ ,  $\text{WS}_2$  and C and a stearate fluid source. This arrangement maintains the  $\text{fO}_2$  at approximately one log unit above the buffer reaction iron-wustite and the  $\text{fS}_2$  one log unit above the reaction of iron to troilite. The volatile fraction of the fluid consists of a  $\text{H}_2\text{O}-\text{CH}_4$  mixture and under fluid saturated conditions is maintained at a constant species ratio by the buffer assemblage. Any melt and/or fluid generated migrates into the fractures in the olivine plug where become entrapped as inclusions up to  $100\mu\text{m}$  in diameter generally of negative euhedral form.

#### **Run conditions and Results.**

Experiments were performed in a piston-cylinder apparatus at 20 kbar/1175°C. The charges consisted of Hawaiian pyrolite 'fertile' peridotite minus 40% olivine component ( $\text{Fe}/(\text{Fe}+\text{Mg})=0.87$ ) combined with bulk volatile contents of 1, 5 and 20 wt.% (runs ED63, ED58 and ED65 respectively). In each case the experiments resulted in charges consisting of melt plus crystals all including olivine as an equilibrium phase. The host olivine plug showed in each case a single population of inclusions containing melt only. Analysis of the inclusion glasses (open symbols off figure 1.) shows that they have been modified to varying extents by inward growth of the walls of the inclusion. Assuming that the the Fe/Mg partitioning relationship between volatile bearing melt and olivine is the same as that between dry melt and olivine (Roeder and Emslie, 1970) it is possible to restore the inclusion melt compositions by the addition of olivine until equilibrium with the primary olivine of the charge is reached. The calculated compositions are given in Table 1. and are plotted in figure 1. (closed symbols). Given here are the results of three experiments in which the melts co-exist with a residual mineralogies of amphibole lherzolite (ED63, estimated 5% melt), lherzolite (ED58, estimated 20% melt) and harzburgite (ED65, estimated 40% melt). The melt compositions calculated vary with percentage fluid added to the charge as follows: 1% fluid - nepheline normative picrite ( $\text{Fe}/(\text{Fe}+\text{Mg})=0.74$ ); 5% fluid - mildly hypersthene normative ( $\text{Fe}/(\text{Fe}+\text{Mg})=0.75$ ); 20% fluid - mildly quartz normative ( $\text{Fe}/(\text{Fe}+\text{Mg})=0.76$ ). The variety in melt composition is clearly the result of the migration of the cotectic positions as the phase field of olivine expands with increasing volatile content. Both the nepheline and hypersthene normative melt compositions lie between the 20 and 25 kbar cotectics and their extensions defined for 'dry' hawaiian pyrolite by Falloon et al. (1988) (Figure 1.). The small implied shift of the cotectic positions for these fluid contents towards higher normative olivine contents is probably due to pressure uncertainties as Taylor and Green (1987) have detailed a depolymerizing effect for  $\text{CH}_4$  similar but subordinate to  $\text{H}_2\text{O}$ . The quartz normative composition obtained by melting with 20% added volatile is consistent with a large expansion of the olivine phase field as might be expected from the addition of a large amount of depolymerizing mixed volatile.

The results presented here are preliminary but clearly demonstrate that under constant temperature, pressure and  $\text{fO}_2$  the liquids generated by partial melting of peridotite can vary from substantially nepheline normative through hypersthene to quartz normative compositions. It follows that in addition to temperature, pressure and  $\text{fO}_2$  it is important

to consider the amount of volatile present in determining the genesis of any magma for which there is evidence for a role for volatiles.

**References:**

Falloon, T.J., Green, D.H., Hatton, C.J. and Harris, K.L. (1988) Anhydrous partial melting of Fertile and Depleted peridotite from 2 to 30 kbar and application to basalt petrogenesis. *Journal of Petrology*, 29, 1257-1282.

Green, D.H. (1976) Experimental testing of equilibrium partial melting of peridotite under water saturated, high pressure conditions. *Canadian Mineralogist*, 14, 255-268.

Roeder, P.L. and Emslie, R.F. (1970) Olivine-liquid equilibrium. *Contributions to Mineralogy and Petrology*, 29, 275-289.

Stolper, E. (1980) A phase diagram for Mid Ocean Ridge Basalts: preliminary results and implications for petrogenesis. *Contributions to Mineralogy and Petrology* 74, 7-12.

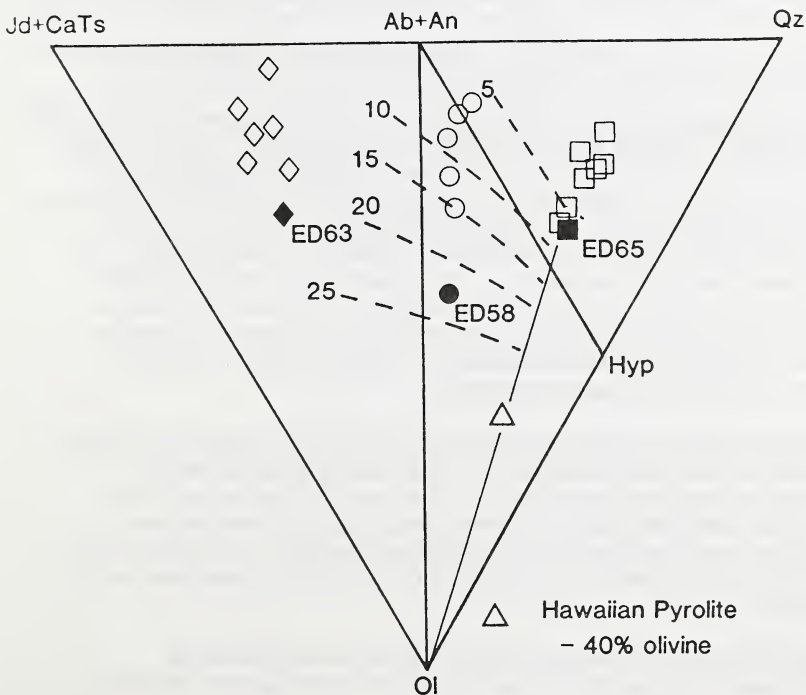
Taylor, W.R. and Green, D.H. (1987) The petrogenetic Role of Methane and the effect on liquidus phase and the solubility mechanism of reduced C-H volatiles. In: B.O. Mysen, Ed. *The Geochemical Society Special Publication 1*, 139-154.

**Table 1.** Calculated partial melt compositions.

	SiO <sub>2</sub>	TiO <sub>2</sub>	Al <sub>2</sub> O <sub>3</sub>	Cr <sub>2</sub> O <sub>3</sub>	FeO	MgO	CaO	Na <sub>2</sub> O	K <sub>2</sub> O	MnO	Total
ED63	46.45	5.92	17.93	0.10	6.00	9.06	8.11	4.06	1.94	0.19	99.76
ED58	47.53	3.16	12.76	0.14	8.48	14.32	10.72	1.95	0.67	0.04	99.77
ED65	50.98	1.77	13.35	0.36	7.46	12.60	12.38	0.50	0.34	0.18	99.92

**Figure 1.**

CIPW Normative projection from diopside onto the plane Jd+CaTs-Qz-Ol. Dashed lines indicate the position of Olivine+orthopyroxene+clinopyroxene cotectics for 2-25 kbar (after Falloon et al., 1988). Open symbols: melt inclusion analyses. Closed symbols: Calculated average liquid compositions of Table 1.



## GEOCHEMICAL AND GEOPHYSICAL MANTLE DOMAINS.

O'Reilly, <sup>(1)</sup>Suzanne Y.; Griffin, <sup>(2)</sup>W.L. and Chen, <sup>(1)</sup>Y.D.<sup>(1)</sup> School of Earth Sciences, Macquarie University, Sydney, NSW 2109, Australia;<sup>(2)</sup> CSIRO Div. of Exploration Geoscience, Box 136, N. Ryde, NSW 2113, Australia.***Geochemical Domains******Geochemical Characteristics***

Four mantle domains within the spinel lherzolite stability field have been characterized geochemically using a large sampling base of xenoliths entrained in basaltic rocks. Regions sampled are from eastern Australia and eastern China; xenoliths analysed range from spinel lherzolite (metasomatized to varying degrees) to granulites and pyroxenites (frozen basaltic magmas and cumulates thereof).

Three regions of eastern Australia define isotopically distinct domains in  $\epsilon\text{Nd}/^{87}\text{Sr}/^{86}\text{Sr}$  space. The most comprehensive data set, from western Victoria, shows a wide spread of values from around  $\epsilon\text{Nd}=6.5$ ,  $^{87}\text{Sr}/^{86}\text{Sr}= .703$  extending in a mixing hyperbola to extremely "enriched" values ( $\epsilon\text{Nd}= -8$ ,  $^{87}\text{Sr}/^{86}\text{Sr}= .716$ ). The NSW and Qld domains trend off the mantle array towards high  $^{87}\text{Sr}/^{86}\text{Sr}$  values but define separate fields. Additional constraints for models of geochemical evolution are provided by the isotopic characteristics of suites of granulites and pyroxenites. Many of these formed within the mantle by crystallization of melts with a crustal isotopic signature. These melts formed within a mantle volume already metasomatized and imprinted with "subduction-type" isotopic signatures. This ties in with eastern Australia's tectonic history which has involved multiple rifting and collision episodes during the Phanerozoic.

Xenoliths from the Nushan (China) region show a high degree of modal metasomatism. However, these xenoliths shows no pronounced  $^{87}\text{Sr}/^{86}\text{Sr}$  enrichment; this must reflect the addition of fluids with a primordial or, at least, mantle-array isotopic signature.

***Metasomatic processes***

To assess the significance of the geochemical characteristics of continental lithospheric mantle, we have carried out a detailed study on a suite of spinel lherzolite xenoliths from the western Victoria domain, southeastern Australia (O'Reilly et al, 1991). These xenoliths are samples of the lithospheric mantle, showing varying degrees of metasomatism. Forty carefully selected whole rock spinel lherzolites have been analyzed (using a variety of techniques) for major and trace elements and over thirty for Nd and Sr isotopic composition. Twelve of these were chosen for proton-microprobe analysis to establish the distribution of trace elements in coexisting phases of cryptically and modally metasomatized lherzolites. To assess mass balance, the modes of the spinel lherzolites analyzed by proton-microprobe were calculated using the whole-rock composition and electron-microprobe analyses of constituent minerals. Mass balance was established within error limits for all rocks where interstitial glass was not present. This indicates that few of the LIL elements reside in "interstitial sites" or as grain-boundary coatings, but are contained in metasomatic phases.

(i) This work demonstrates that the trace-element abundances and patterns of mantle rocks are controlled primarily by the crystal chemistry of metasomatic phases (cryptically-metasomatized clinopyroxene + amphibole, mica, apatite). The variable distribution of these volatile-bearing phases in space and time results in a decoupling of major, minor and trace elements during metasomatism, mainly reflecting crystal/fluid partitioning. For example, Nb is restricted to amphibole or mica-bearing rocks and Sr, REE, Pb, U and Th are most enriched in rocks containing modal apatite.

(ii) Open-system crystallization has taken place, with the mode of the rock determining the bulk KD between rock and fluid. If no volatile-bearing phases are formed

(amphibole, mica or apatite), uptake of LIL and HFS elements is limited by the capacity of clinopyroxene to accept these elements.

(iii) The trace element characteristics of some of the mantle rocks are similar to those typically ascribed to "crustal contamination" of melts. This applies to LREE, Zr and Ba abundances, and even isotopic signatures, for the western Victorian mantle.

These results have important implications for contamination of small-volume, apparently primitive or primary magmas, including most continental alkali basaltic types. The LIL and HFSE trace elements in modally metasomatized mantle rocks are concentrated in phases which are less refractory and more easily broken down in heating events (e.g. along magma conduits). When these phases break down, the trace elements cannot be accepted into the residual lherzolite phases and are therefore partitioned into melt, providing very easy contamination of ascending or infiltrating magmas. Therefore, the heterogeneity observed in the trace element patterns of sequences of continental basaltic rocks does not necessarily reflect source heterogeneity. It may merely be the cumulative imprint of varying degrees of contamination by different types of metasomatized lithospheric mantle.

### *Geophysical Domains*

Data from xenoliths are also crucial in interpreting remotely-sensed (geophysical) information on the lithospheric mantle including thermal, magnetic, seismic, gravity, electromagnetic properties. Measurements of acoustic velocities of mantle xenoliths (O'Reilly et al., 1990) and characterization of thermal states have allowed realistic modelling of seismic profiles to define the fine structure of the crust-mantle boundary and lower crust/upper mantle stratigraphies in cratonic and non-cratonic lithosphere sections.

Results show that the thermal profiles of lithospheric sections must be known to model Vp profiles realistically. In addition, the conventional use (by seismologists) of dunite as a generalized mantle wall-rock results in overestimates of mantle Vp. The variable anisotropy (up to 10%) in acoustic velocities measured in moderately foliated mantle rocks may account for enigmatic seismic reflectors in mantle regions, especially at boundaries of large-scale tectonic blocks.

Integration of petrologic, geochemical and geophysical data can provide a holistic models for the structure and evolution of different lithospheric domains. Many significant mantle events appear to be coupled to tectonic episodes observed in crustal layers. This methodology can be used to identify large continental blocks with contrasting chemical and physical properties relevant to the formation and preservation of diamonds.

### *References*

- O'REILLY, S. Y., JACKSON, I., and BEZANT, C., 1990. Seismic and thermal parameters of upper mantle rocks from eastern Australia: implications for seismic modelling. *Tectonophysics*, 185, 67-82.
- O'REILLY, S. Y., GRIFFIN W. L., and RYAN, C., 1991. Residence of trace elements in metasomatized spinel lherzolite xenoliths: a proton-microprobe study. *Contrib. Miner. Petrol.* in press.

## DIAMOND GROWTH HISTORIES REVEALED BY CATHODOLUMINESCENCE AND CARBON ISOTOPE STUDIES.

Otter<sup>(1)</sup>, M.L.; Gemeke<sup>(2)</sup>, D.A.; Harte<sup>(3)</sup>, B.; Gurney<sup>(1)</sup>, J.J.; Harris<sup>(4)</sup>, J.W. and Wilding<sup>(3)</sup>, M.C.

(1) Dept. of Geochemistry, University of Cape Town, Rondebosch, 7700 South Africa; (2) Electron Microscope Unit, University of Cape Town, Rondebosch, 7700 South Africa; (3) Dept. of Geology and Geophysics, University of Edinburgh, Edinburgh, EH9 3JW Scotland; (4) Dept. of Geology and Applied Geology, University of Glasgow, Glasgow G12 8QQ, Scotland.

The internal macro-structures of large (>2 carats) diamond crystals from four southern African kimberlites have been characterized using cathodoluminescence (CL) techniques, and the variation of carbon isotope composition within some of the crystals has been determined using the Edinburgh University/NERC ion microprobe.

Eclogitic and peridotitic inclusion suite diamonds from the Premier mine and peridotitic diamonds from Bultfontein, Finsch and Koffiefontein mines were investigated. The diamonds were halved along the cubic plane {100} and polished. The CL characteristics of the polished faces were investigated using both Technosyn and Nuclide optical cathodoluminescence systems as well as a Cambridge S180 SEM with a CL detector. Most of the diamonds are zoned with respect to CL. The zones presumably reflect variations in impurity content and distribution (e.g. nitrogen, see Davies, 1979), but the nature of the variation is unknown in detail.

The CL zoning indicates complicated histories of periodic growth with some phases of resorption. Alternations of cuboid and octahedral growth occur (Lang, 1974) in some crystals. In some cases, the cuboid growth orientation appears to result from simultaneous growth on two small octahedral faces. The three-dimensional manifestation of such growth would be an average growth surface roughly parallel to a rhombic-dodecahedral face. Well defined CL zones sometimes truncate one another. Some truncations suggest resorption as shown by rounding-off of the corners of inner CL growth zones by an unrounded, continuous CL zone formed outside them. Other truncations do not involve rounding, but show sharply angular cross-cutting CL zones and may involve a change from cuboid to octahedral growth. This second type of truncation is partly related to differences in growth rate in different crystallographic directions, but resorption may be involved in some cases.

Five diamonds, representing the peridotitic and/or eclogitic diamond groups at all four localities, were chosen for single-point carbon isotope analysis using the Cameca IMS 4F Ion Microprobe at the University of Edinburgh. A primary  $\text{Cs}^+$  ion beam, with a beam spot diameter of  $\sim 5 \mu\text{m}$ , allowed variations of the carbon isotope composition within and between CL zones to be determined. The analyses are believed to be precise to  $\pm 1 \text{ ‰}$   $\delta^{13}\text{C}$  (versus PDB) based on replicate analyses of a synthetic diamond standard.

Significant (i.e.  $> 1 \text{ ‰}$ ) carbon isotope variation was found between the zones defined by CL in some of the crystals, but other crystals showing conspicuous CL zones appeared to be homogeneous throughout. Where carbon isotope variation occurred, as much as  $4 \text{ ‰}$  change was found between zones, but no systematic variation in  $\delta^{13}\text{C}$  from centre to edge was observed. This is similar to the observations of Wilding et al. (1990) and suggests that the diamonds did not crystallize in a single isotope fractionation sequence from a closed system carbon reservoir. Thus, open system behavior with variations in oxygen fugacity and/or source  $\delta^{13}\text{C}$  are indicated.

#### REFERENCES

- Davies, G. (1979) Cathodoluminescence. In J.E. Field, Ed., *Properties of Diamond*, p. 165-181. Academic Press, London.
- Lang, A.R. (1974) On growth sectorial dependence of defects in natural diamonds. *Proceedings of the Royal Society of London*, A340, 233-248.
- Wilding, M.C., Harte, B., and Harris, J.W. (1990) Carbon isotope variation in a zoned Bultfontein diamond, determined by S.I.M.S., Geological Society of Australia, Abstracts, 27, 112.

## A PHYSICAL CHARACTERIZATION OF THE SLOAN DIAMONDS.

*Otter<sup>(1)</sup>, M.L.; Gurney<sup>(1)</sup>, J.J. and McCallum<sup>(2)</sup>, M.E.**(1) Dept. of Geochemistry, University of Cape Town, Rondebosch, 7700, South Africa;**(2) Dept. of Earth Resources, Colorado State University, Fort Collins, CO 80523, USA.*

The physical characteristics of diamonds from six kimberlite phases of the Sloan 1 & 2 kimberlite complex of the Colorado-Wyoming State Line kimberlite district have been investigated. Both primary and secondary features were described including crystal state (breakage), primary morphology, resorption morphology, primary and secondary mass/size, colour and surface features.

Approximately 50% of the Sloan diamonds are broken crystals. Considering primary morphology, three-quarters of the Sloan diamonds are inferred to have crystallized as single crystal octahedra, whereas a quarter crystallized as macle twins or simple aggregate crystals. Cubo-octahedral, cube and polycrystalline aggregate forms occur only in trace quantities. Resorption morphology is classified according to a method devised by D.N. Robinson (see Otter and Gurney, 1989) which allows a semi-quantitative calculation of the proportion of individual diamonds lost to resorption. According to the data, approximately 25% of the bulk Sloan diamond mass/volume was lost during resorption. The Sloan diamonds define a log-normal distribution with respect to secondary mass/size with 85 % of the stones weighing less than 0.03 carat. The largest diamond reported from Sloan weighs 1.24 carats (Shaver, 1988). A semi-quantitative calculation of primary mass for individual diamonds (whole crystals only) suggests that, before resorption, very few of the Sloan diamonds exceeded two carats in mass. With respect to colour, 70% of the Sloan diamonds are brown, 25% are grey and 5% are colourless. Pristine yellow, amber, pink and green diamonds occur only in trace quantities. A quarter of the Sloan diamonds display xenolithic surface features (e.g. knob-like asperities, surficial graphite, and non-uniform resorption) which suggests that a significant proportion (if not all) of the diamonds were derived by the disaggregation of xenolithic host rock materials. Only 2% of the diamonds exhibit lamination lines which are attributed to deformation. Resorption features (e.g. trigons, shield-shaped laminae, elongate hillocks) are common on the Sloan diamonds and late-stage features (resorbed breakage surfaces, frosting and corrosion sculpture) are also documented.

Relationships between physical characteristics are observed. For instance, diamonds exhibiting the brown coloration were apparently more susceptible to breakage relative to diamonds of other colours. Finally, variation in

diamond characteristics between kimberlite phases also is documented. For example, corrosion sculpture is extremely common on diamonds from the Sloan 2 kimberlite phase, but rare on diamonds from other kimberlite phases in the diatreme.

The significance of these data will be discussed with respect to the diamond crystallization environment(s) sampled by the Sloan kimberlite magma as well as environments encountered by the diamonds subsequent to growth, especially in the kimberlite itself.

#### REFERENCES

- Otter, M.L., and Gurney, J.J. (1989) Mineral inclusions in diamonds from the Sloan diatremes, Colorado-Wyoming State Line kimberlite district, North America. 4th International Kimberlite Conference, Kimberlites and Related Rocks Vol. 2, Geological Society of Australia Special Publication No. 14, 1042-1053.
- Shaver, K. (1988) Exploration of the Sloan Range complex: a diamondiferous kimberlite prospect in northern Colorado. Mining Engineering, January, 1988, 45-48..

## PRIMARY DIAMOND SUBPOPULATIONS AT INDIVIDUAL LOCALITIES.

*Otter, M.L. and Gurney, J.J.**Dept. of Geochemistry, University of Cape Town, Rondebosch, 7700, South Africa.*

"Primary diamond subpopulations" occurring within individual kimberlite and lamproite localities are defined based on diamond and mineral inclusion data. It is suggested that each of the defined subpopulations represents a distinct diamond crystallization environment which was present in the upper mantle and available for sampling at the time of kimberlite or lamproite emplacement.

Localities are considered separately. Individual diamonds from each locality are assigned to a particular subpopulation based on correlations between all available data, including mineral inclusion composition, host diamond carbon isotope composition and, when available, other diamond characteristics such as primary diamond morphology and size.

This multivariate approach is possible because a large database for relatively large numbers of diamonds from a number of individual localities is now available. The subpopulations defined conform generally to previous paragenetic classifications, which are based solely on inclusion composition. However, at many localities, diamonds, previously classified into the same paragenetic group are subdivided and, in a few cases, paragenetic groups are combined. Another result of this approach is that many diamonds which, in previous studies, could not be classified with respect to paragenesis because they lacked the appropriate mineral phases, can now be assigned to a group based on other data. This allows a better assessment of the proportions of each diamond type at each locality and affords a better definition of the paragenetic environments represented by the various diamond subpopulations.

Once each subpopulation has been defined, the potential source and petrogenesis are inferred. Thermobarometric data for the various subgroups at each locality allow inferences on their spatial relationships within the Earth's mantle and, in some cases, isotopic age information places constraints on their temporal relationships. Ultimately, comparisons of the subpopulations found at the various localities allows a stratigraphy of the upper mantle to be constructed which, when considered along with the tectonic setting of their kimberlite host, can provide new insights which are relevant to diamond genesis and to defining the structure and evolution of the lithosphere.

GRAPHITE-BEARING PERIDOTITES FROM THE KAAPVAAL CRATON:  
THEIR CARBON ISOTOPIC COMPOSITIONS AND IMPLICATIONS FOR  
PERIDOTITE THERMOBAROMETRY.

D.G. Pearson<sup>(1)</sup>; F.R. Boyd<sup>(2)</sup>; S.W. Field<sup>(3)</sup>; J.D. Pasteris<sup>(4)</sup>; S.E. Haggerty<sup>(5)</sup> and P.H. Nixon<sup>(6)</sup>.

(1) Dept. of Terrestrial Magnetism, Carnegie Institution of Washington, Washington D.C. 20015, U.S.A.; (2) Geophysical Laboratory, Carnegie Institution of Washington; (3) Dept. of Geology, Stockton State College, Pomona, NJ 08240, U.S.A.; (4) Dept. of Earth & Planetary Sciences, Washington University, St. Louis, MO 63130; (5) Dept. of Geology & Geography, University of Massachusetts, Amherst, MA 01003, U.S.A.; (6) Dept. of Earth Sciences, Univ. of Leeds, Leeds LS29JT, U.K.

The graphite-bearing ultramafic xenoliths studied in this investigation are predominantly coarse, low-temperature peridotites derived from the Kaapvaal lithosphere. Two specimens, however, are exsolved megacrysts, probably derived from low-temperature pyroxenites. The peridotites include garnet harzburgites exhibiting variable depletion in Ca, garnet lherzolites, a spinel-facies peridotite and pargasite (amphibole) peridotites. These xenoliths have come from kimberlites erupted along the southern margin of the Kaapvaal craton (Kimberley, Jagersfontein and northern Lesotho) as well as the Premier pipe in the central part of the craton. To our knowledge, no graphite-bearing peridotites have been found in xenolith suites from off-craton kimberlites in East-Griqualand and Namibia.

Graphite most commonly occurs as dispersed, subhedral to euhedral flakes and multicrystalline stacks of flakes with a grain size ranging up to 3mm. In many specimens the graphite is interstitial, but in some the graphite flakes are enclosed in primary grains, particularly garnet and enstatite. Multiple flakes of graphite in a single xenolith are the rule, some xenoliths contain as many as several tens or more. Aggregates of graphite crystals have a vein-like planar distribution in two specimens from Jagersfontein. In pargasite-bearing garnet peridotite PHN5633, the flakes of graphite are concentrated on a flat face of the xenolith, suggestive of an origin on a vein wall. In garnet lherzolite JAG 500 the graphite is concentrated in two diffuse bands, one coincident with a zone of garnet and diopside. The second graphite band is parallel but transects coarse olivine and enstatite. An orthopyroxenite xenolith from Premier (FRB1399) contains polycrystalline blebs of graphite as well as graphite inclusions in enstatite, together forming 10-20% of the xenolith.

The graphites from the peridotites give Raman spectra comparable to those from well ordered, highly crystalline graphite from granulite-facies terranes (Pasteris & Wopenka, 1991) with well defined first- and second-order peaks, at or close to the the normal peak positions. The spectra indicate that the graphite is of high-temperature origin and distinct from the fine-grained graphite found in serpentinised kimberlitic olivine (Pasteris, 1988). However, numerous graphites from an exsolved megacryst, JX-23, show deviation from the above spectra, with downshifting of the first- and second-order peaks that is not presently understood.

Estimates of equilibration temperature and pressure for the graphite peridotites range widely from those characteristic of the shallow mantle to those corresponding to the diamond-graphite transition. A graphite-bearing spinel-facies peridotite from Letseng (PHN4258) has equilibrated near the top of the mantle. Greater temperatures and depths calculated for the garnet-bearing peridotites, using a variety of thermobarometer combinations, are consistently less than those calculated for diamond-bearing peridotites (Fig. 1). This consistent relationship is evidence that the graphite and diamond in these rocks have crystallised within their respective stability fields. A point for a graphite peridotite overlaps a point for a diamond peridotite in only one plot (Fig. 1D). This may be interpreted as either an exception to the consistency or a minor failure of the thermobarometer in application to natural samples.

The transition in temperature and depth from graphite to diamond peridotites that is illustrated by the plots in Fig. 1 approximates the

graphite-diamond equilibrium boundary determined by experiment. This relationship represents a success for peridotite thermobarometry and it appears that the calculation used for Fig. 1A is the most successful. A lesser number of points appear in plots for which temperature was calculated from the pyroxene solvus (Fig. 1A & C) because many of the graphite peridotites lack diopside.

Graphites from the peridotite xenoliths show a range in  $\delta^{13}\text{C}$  from -3.8‰ to -12.3‰ (Table 1) with a mode between -5 and -7‰ (Fig.2). The range encompasses the -10.0‰ value for graphite from a Kimberley garnet harzburgite found by Schulze and Valley (submitted). Graphite from the two exsolved megacrysts fall within this range (Table 1). Graphite has up to 1.6‰ variation between individual flakes in the amphibole-bearing specimen PHN5633 and a 1.4‰ variation in the the "vein" graphite from JAG500. This variation could be due to progressive carbon isotope fractionation in a gas phase that deposited the graphite. The occurrence of multiple flakes of graphite in vein-like form in several Jagersfontein peridotites suggests a metasomatic origin (Field and Haggerty, 1990). All the graphites from peridotites fall within the range of  $\delta^{13}\text{C}$  values of peridotite suite diamonds and are also within a few ‰ of the range of carbon extracted from MORB glasses. This indicates that the graphite in the lithospheric peridotites crystallised from a similar reservoir to peridotite suite diamonds. The isotopic similarity between this reservoir and carbon from the asthenospheric mantle, as characterised by MORB glasses, is consistent with the crystallisation of both diamonds and graphite in the lithospheric mantle from asthenosphere-derived fluids.

Table 1. Carbon Isotope Composition of Graphite from Kaapvaal Peridotites

Sample	Locality	Lithology	$\delta^{13}\text{C}$ ‰
<u>PERIDOTITES</u>			
E-8	Thaba Putsoa	Gt harzburgite	-9.8
PHN 1555a	Mothae	Harzburgite	-12.3
PHN 1569	Thaba Putsoa	Gt lherzolite	-6.7
PHN 2492	Kao No.2	Low-Ca	-5.8
		Gt harzburgite	
PHN4258	Letseng-la-Terai	Sp.harzburgite	-7.1
PHN 5633 (a)	Jagersfontein	Pargasite	-6.9
PHN 5633 (c)	"	bearing	-6.3
PHN 5633 (d)	"	Gt harzburgite	-7.9
JAG 84-500 (a)	Jagersfontein	Graphite	-5.4
JAG 84-500 (b)	"	associated with	-4.8
		Gt-Cpx veins	
JAG 84-500 (A)	Jagersfontein	in Gt	-4.0
JAG 84-500 (B)	"	harzburgite	-5.2
JAG 89-5	Jagersfontein	Gt harzburgite	-3.8
FRB 888	Bulfontein	Gt harzburgite	-5.0
<u>EXSOLVED MEGACRYSTS</u>			
JX-23	Jagersfontein		-6.8
JAG 89-10	Jagersfontein	Opx ex Cpx ,Gt	-7.2

#### References

- Brey, G.P, Kohler, T.P., and Nickel, K.G. (1990) Geothermobarometry in natural four phase lherzolites, part I: Experimental results from 10-60 kb. *Journal of Petrology*, 31,1313-1352.
- Deines, P, Harris, J.W. and Gurney, J.J. (1987) Carbon isotopic composition, nitrogen content and inclusion composition of diamonds from the Roberts Victor kimberlite, South Africa. *Geochimica Cosmochimica Acta*, 51,1227-1243.
- Field, S.W. and Haggerty, S.E. (1990) Graphitic xenoliths from the Jagersfontein kimberlite, South Africa: Evidence for dominantly anhydrous melting and carbon deposition. *EOS*, 71,658.
- Kropotova and Fedorenko, B.V. (1970) Carbon isotopic composition of diamond and graphite from eclogite. *Geokhimiya*, 10, 1279 (in Russian).
- Pasteris, J.D. (1988) Secondary graphitisation in mantle-derived rocks. *Geology*, 16, 804-807.
- Pasteris, J.D. and Wopenka, B. (1991) Raman spectra of "graphite" as indicators of degree of metamorphism. *Canadian Mineralogist* (in press)

Pearson, D.G., Boyd, F.R. and Nixon, P.H. (1990) Graphite-bearing mantle xenoliths from the Kaapvaal craton: Implications for graphite and diamond genesis. *Carnegie Inst. Yearbook 1989-1990*, 11-19.

Schulze, D.J. and Valley, J.W. (submitted) Carbon isotopic composition and equilibration conditions of graphite-bearing eclogite and garnet peridotite xenoliths from kimberlite: Anomalously light carbon subducted into the shallow lithospheric mantle. *American Mineralogist*.

Sobolev, N.V., Gailmov, E.M., Ivanovskaya, I.N. and Yefimova, E.S. (1979) The carbon isotope compositions of diamonds containing crystallographic inclusions. *Doklady Akademii Nauk SSSR*, 249, 1217-1220.

Taylor, B.E. (1986) Magmatic volatiles: Isotopic variations of C, H and S, In J.W. Valley, H.P. Taylor Jr and J.R. O'Neill, Eds., *Stable Isotopes in High Temperature Geological Processes*, p185-219, Min.Soc.Am.

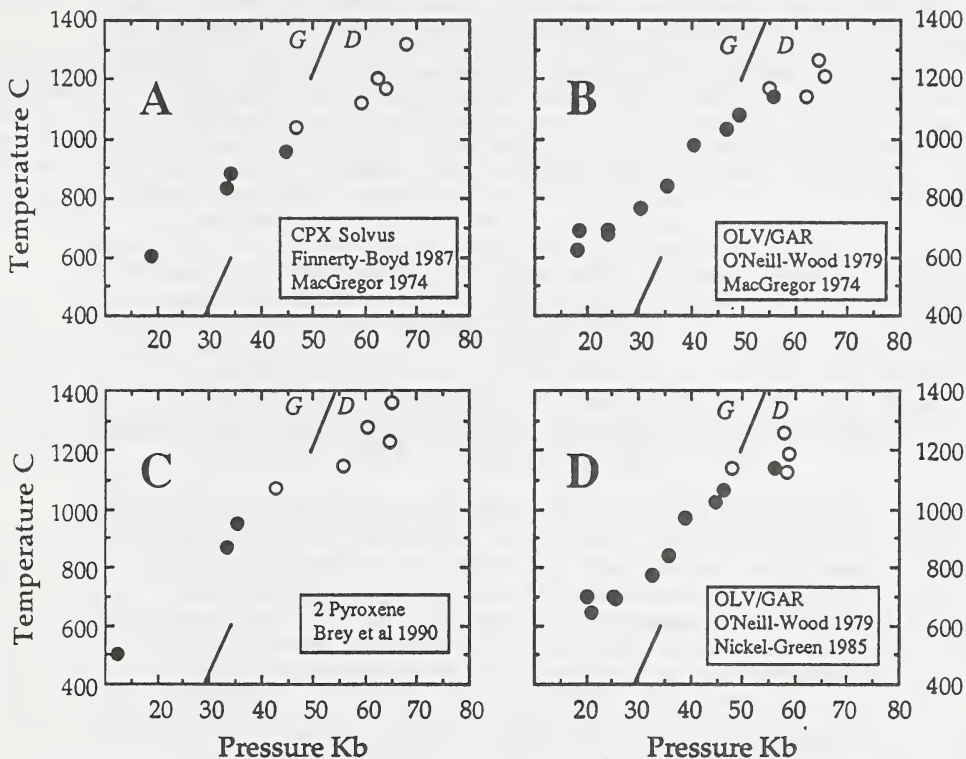


Fig.1: Temperature and pressure of equilibration for graphite-peridotites (solid circles) and diamond-bearing peridotites (solid circles) estimated with a variety of thermobarometers. Specimens include lherzolites, harzburgites and amphibole-bearing peridotites. [A]: T by the Finnerty & Boyd, 1987, pyroxene solvus thermometer (FB86), P by the MacGregor, 1974, (MC74) barometer. [B]: T by Fe/Mg olivine-garnet, O'Neill & Wood, 1979, P by MC74 as in A. [C]: T (2-pyroxene solvus) & P (BKN) Brey et al, 1990. [D]: T by olivine-garnet as in B, P by Al in OPX, Nickel & Green, 1985 (NG85). For references see Pearson et al (1990).

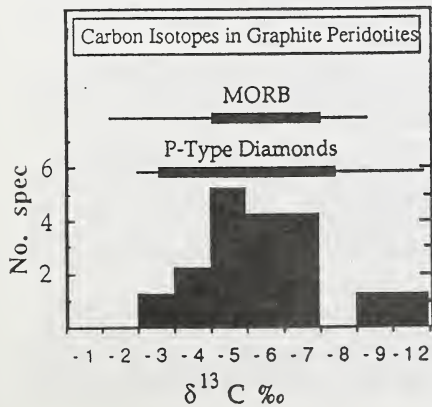


Fig. 2: Histogram of carbon isotope data from graphite peridotites (this report & Kropotova & Fedorenko, 1970) compared to P-Type diamonds (Sobolev et al, 1979; Deines et al, 1987) and carbon in MORB glasses (Taylor, 1986). Thick bars represent 90% of analyses.

## DIAMOND FACIES PYROXENITES FROM THE BENI BOUSERA PERIDOTITE MASSIF AND IMPLICATIONS FOR THE ORIGIN OF ECLOGITE XENOLITHS.

*D.G. Pearson<sup>(1)</sup>; G.R. Davies<sup>(2)</sup> and P.H. Nixon<sup>(3)</sup>.*

*(1) Department of Terrestrial Magnetism, Carnegie Institution of Washington, Washington D.C. 20015, U.S.A.; (2) Dept. of Geological Sciences, University of Michigan, Ann Arbor, Michigan, U.S.A.; (3) Dept. of Earth Sciences, University of Leeds, Leeds LS29JT, U.K.*

The Beni Bousera peridotite massif contains mineralogically diverse pyroxenite layers, many of which are lithologically analogous to xenoliths erupted by deeply-derived kimberlite/alkali basalt magmatism. Two garnet clinopyroxenites have been found to contain graphite as octahedral aggregates and other forms of cubic symmetry which are interpreted as graphitized diamonds (Pearson *et al.*, 1989). This interpretation is supported by the occurrence of cubo-octahedral faceted CPX and GT inclusions within the octahedra. The pyroxenite suite shows major and compatible trace element fractionation trends indicating crystallisation from magmatic liquids fractionating OPX, CPX, GT. Combined with the mineralogical zonation observed in many of the layers the chemical variation indicates pyroxenite crystallisation as wall-rock cumulates from magma flowing through the peridotites. However, incompatible elements vary widely in abundance and show no correlation with major element fractionation indices. The majority of pyroxenites are more LREE-depleted than the peridotites, the former having  $(Ce/Sm)_n$  ranging from 0.016 to 0.91. These data preclude derivation of the pyroxenites from either the host peridotites or a single mantle-derived magma and require a chemically heterogeneous source. Positive and negative Eu anomalies in the pyroxenites ( $Eu/Eu^* = 0.7$  to 2.4) indicate the parent liquids were derived from low pressure precursors which had experienced plagioclase fractionation.

Oxygen isotope analyses of CPX from the pyroxenite suite show a wide variation in  $\delta^{18}O$  values (+4.9 to +9.3‰), in contrast with the restricted range shown by the host peridotites ( $\delta^{18}O_{CPX} = +5.3$  to +6.0‰). Coexisting CPX-GT and CPX-OPX mineral pairs from the pyroxenites are in high temperature isotopic equilibrium suggesting that the O-isotope variation is not the result of recent disequilibrium/metasomatic processes. There is no correlation between  $\delta^{18}O$  and fractionation indices such as mg no. implying that the oxygen isotope variation is not due to high temperature igneous processes and that the pyroxenites are not derived from normal mantle peridotite sources. The oxygen isotope data indicates derivation of the pyroxenites from precursors that have experienced crustal, low temperature hydrothermal alteration at high water rock ratios (Pearson *et al.*, 1991).

Acid-washed CPX separates from the pyroxenites show extreme Nd and Sr isotopic diversity ( $^{143}Nd/^{144}Nd = 0.5139-0.5122$ ,  $^{87}Sr/^{86}Sr = 0.7023-0.7110$ , Fig. 1) but many show decoupled parent/daughter ratios implying they have suffered a recent partial melting event (<200Ma). Mixing of the pyroxenites with late stage, crustal fluids/melts during the emplacement of the massif cannot explain the diverse scatter of the pyroxenite CPX on an Sr-Nd isotope diagram (Figure 1). The data may be explained by crystallisation of the pyroxenites from melts of subducted oceanic crustal precursors which experienced variable degrees hydrothermal alteration (which acted to increase  $^{87}Sr/^{86}Sr$ ) and incorporated variable amounts of sediment during subduction. Incorporation of the sediment produced unradiogenic  $^{143}Nd/^{144}Nd$  and more radiogenic  $^{87}Sr/^{86}Sr$ . Pyroxenite CPX show scattered trends of  $\delta^{18}O$  vs  $^{87}Sr/^{86}Sr$  (which ranges up to 0.7110). Samples with the highest  $\delta^{18}O$  values also have high  $^{87}Sr/^{86}Sr$  (0.7078-0.7085). The relatively diffuse Sr-O isotope correlation is to be expected if the pyroxenites are derived from

melts of different portions of subducted oceanic crust that experienced alteration at different water/rock ratios.

The high  $^{207}\text{Pb}/^{206}\text{Pb}$  of some of the pyroxenite CPX are consistent with subducted sediment incorporation in some of the parental magmas. Furthermore, the Pb data constrain some of the pyroxenites to be relatively young (<200 Ma) which is consistent with the relatively unradiogenic  $^{143}\text{Nd}/^{144}\text{Nd}$  of the graphite-bearing pyroxenites despite their very high  $^{147}\text{Sm}/^{144}\text{Nd}$  (up to 1.7). Some pyroxenites with unradiogenic initial  $^{87}\text{Sr}/^{86}\text{Sr}$  (0.7025) and very radiogenic  $^{143}\text{Nd}/^{144}\text{Nd}$  (0.5139) may be up to 1 Ga old; this age is consistent with Os isotope data for the Beni Bousera pyroxenites (Luck and Allègre, 1990).

Derivation of the pyroxenites from hydrothermally altered, subducted oceanic crust over a period of possibly 1 Ga is capable explaining their diverse radiogenic and stable isotope systematics and their incompatible element heterogeneity. Recent, small degree melting of some of the more "evolved" pyroxenites due to diapiric upwelling during emplacement of the peridotite massif from the diamond stability field enhanced their LREE depletion and disrupted isotope-trace element relationships.

Graphite from the garnet clinopyroxenites has low  $\delta^{13}\text{C}$  values (-16 to -27.6%).  $\text{CO}_2$  released by high temperature step-heating of a CPX separate also yielded significant amounts of isotopically light carbon ( $\delta^{13}\text{C} = -22\%$ ) indicating, along with field relationships, that the isotopically light carbon in the graphitic pyroxenites is inherited from the precursor diamonds and may have originated from subduction of either kerogenous carbon or isotopically light hydrothermal carbonate veins in altered oceanic crust.

The Beni Bousera garnet pyroxenites are mineralogically and chemically comparable to eclogite xenoliths from kimberlites, some showing evidence of having contained the high diamond contents found in several diamondiferous eclogites (eg. Robinson et al., 1984). The current dispute whether some eclogites from kimberlites represent subducted metamorphosed oceanic crust or high pressure, mantle derived cumulates may be resolved if some eclogites crystallised from melts (producing igneous textures) derived from subducted oceanic lithosphere (giving crustal isotopic signatures). The subducted crustal signature of the Beni Bousera pyroxenites and the isotopically light  $\delta^{13}\text{C}$  values of the diamond pseudomorphs they contain is further support for a subducted origin for some E-type diamonds.

#### References

- Luck, J.M. and Allègre, C.J. (1990) Osmium isotopes and mantle processes. *Terra Abstracts*, 2, 134-135.
- Pearson, D.G., Davies, G.R., Nixon, P.H. and Milledge, H.J. (1989) Graphitised diamonds from a peridotite massif in Morocco and implications for anomalous diamond occurrences. *Nature*, 338, 60-62.
- Pearson, D.G., Davies, G.R., Nixon, P.H., Greenwood, P.B. and Mathey, D.P. (1991) Oxygen isotope evidence for the origin of pyroxenites in the Beni Bousera peridotite massif, North Morocco: Derivation from subducted oceanic lithosphere. *Earth and Planetary Science Letters*, 102, 289-301.
- Robinson, D.N., Gurney, J.J. and Shee, S.R. (1984) Diamond eclogite and graphite eclogite xenoliths from Orapa, Botswana. In J. Kornprobst, Ed., *Kimberlites II: The mantle and crust-mantle relationships*, p11-24, Elsevier, Amsterdam.

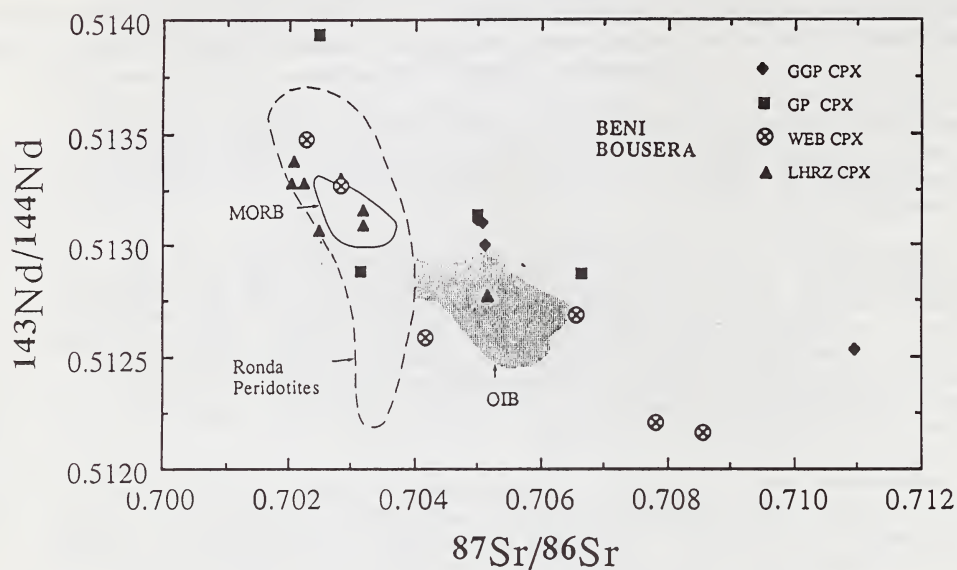


Figure 1: Sr-Nd isotope plot of CPX from Beni Bousera pyroxenites and peridotites compared to MORB, OIB and Ronda peridotites. GGP =graphite garnet clinopyroxenites, GP = garnet clinopyroxenites, WEB = websterites, LHRZ = spinel lherzolites.

RHENIUM-OSMIUM ISOTOPE SYSTEMATICS IN SOUTHERN AFRICAN AND SIBERIAN  
PERIDOTITE XENOLITHS AND THE EVOLUTION OF SUBCONTINENTAL  
LITHOSPHERIC MANTLE.

D.G. Pearson<sup>(1)</sup>; S.B. Shirey<sup>(1)</sup>; R.W. Carlson<sup>(1)</sup>; F.R. Boyd<sup>(2)</sup>; P.H. Nixon<sup>(3)</sup>; N.P. Pokhilenko<sup>(4)</sup> and L. Brown<sup>(1)</sup>.

(1) Department of Terrestrial Magnetism, Carnegie Institution of Washington, 5241 Broad Branch Rd N.W., Washington, D.C. 20015; 2) Geophysical Laboratory, Carnegie Institution of Washington, 5251 Broad Branch Rd N.W. Washington, DC 20015; (3) Dept. Earth Sciences, Leeds University, U.K.; (4) Institute of Geology & Geophysics, Siberian Branch, USSR Academy of Sciences, Novosibirsk, USSR.

The Re/Os isotope system provides a powerful tool for constraining models for the formation of cratonic mantle "roots" by relating Re/Os model depletion ages in peridotitic mantle residues to chemical changes resulting from basaltic/komatiitic melt extraction and temperature/pressure estimates from mineral thermobarometry. High Os concentrations in the xenoliths relative to the host kimberlite magma means that the Re-Os system is much less susceptible to the effects of xenolith infiltration by the kimberlite (Walker et al., 1989). The Siberian and Kaapvaal cratons both have roots extending into the diamond stability field and contain crustal rocks over 3.5 Ga old. The abundant kimberlites erupted through these cratons frequently entrain xenoliths from varying depth allowing analysis of rocks from the whole lithospheric section. Osmium isotope ratios in whole rock peridotite xenoliths of various lithologies have been determined by the N-TIMS (negative thermal ionization mass spectrometry) technique.

Peridotite xenoliths from the lithosphere beneath the Archean Kaapvaal craton analysed in this study and data from the study by Walker et al. (1989) show a range of  $^{187}\text{Os}/^{186}\text{Os}$  from 0.880 to 1.070. Many of these xenoliths have extremely unradiogenic  $^{187}\text{Os}/^{186}\text{Os}$  compared to xenoliths from alkaline magmas intruding Proterozoic lithosphere, 1.002 to 1.095 (R. Walker, unpublished data), and dredged oceanic abyssal peridotites, 1.003 to 1.099 (Martin in press; Fig. 1). The distinct Os isotope characteristics of peridotite xenoliths from Archean cratons indicate the peridotites have resided in the ancient lithospheric "root" to the craton for very long time periods (> 2 Ga), where they have been chemically and physically isolated from the convecting asthenosphere.

Os concentrations in the Kaapvaal xenoliths range from 1.47 to 9.60 ppb and  $^{187}\text{Os}/^{186}\text{Os}$  is negatively correlated with degree of major element depletion (eg. mg# of olivine). A low-Ca garnet harzburgite, PHN2825 (mg# 0.96), from Liqhobong, S.E.Kaapvaal margin, gives a  $^{187}\text{Os}/^{186}\text{Os}$  of  $0.880 \pm 0.002$  and a minimum Re-Os model depletion age ( $T_{\text{RD}}$ ) of 3.3 Ga (Fig.1) assuming the rock lost all its Re at this time. Incomplete removal of Re during melting would lead to a higher model age. The 3.3 Ga Re depletion age for PHN2825 is significant in that low Ca-garnet harzburgites are thought to be one of the dominant source lithologies for P-Type diamonds (eg. Nixon et al., 1987) and the Re depletion age is within error of the Sm/Nd model ages determined by Richardson et al (1984) on garnet inclusions in diamond. A coarse garnet harzburgite, also from Liqhobong, has a  $^{187}\text{Os}/^{186}\text{Os}$  of  $0.915 \pm 0.001$  and a minimum Re-Os model age of 2.8 Ga. These ages are comparable to a 2.8 Ga Re-Os model age

obtained by Walker et al. (1989) from a Letseng peridotite, also near the S.E. margin of the craton, and indicate ancient stabilization of the margins of the sub-continental Kaapvaal lithosphere.

The lowest Os abundance in the suite occurs in the ultra-depleted low Ca-garnet harzburgite. Although Os is a compatible element in mantle residues at moderate amounts of melting, high degrees of melting (>30%), perhaps associated with komatiite extraction, may result in the break down of Os hosting phases in the residue, eg. sulphides or native metals and hence cause low Os abundances in ultra-depleted residues such as low Ca-garnet harzburgites

Two spinel facies peridotites of shallow origin, from the Premier pipe, have  $^{187}\text{Os}/^{186}\text{Os}$  of  $0.940 \pm 0.003$  and  $0.962 \pm 0.005$ , yielding Proterozoic minimum Re-Os model ages (Fig. 1). Proterozoic Re-Os model ages were also obtained from high temperature garnet peridotites from Premier by Walker et al. (1989). This result is surprising in that the Premier kimberlite intrudes a more central area of the craton compared to the N. Lesotho pipes and therefore may be expected to be older. The present data set shows no geographical correlation with Re depletion age of the lithosphere and no apparent correlation between depletion age and depth of equilibration in the lithospheric mantle as determined by mineral thermobarometry. These findings may indicate significant age heterogeneity in the nuclei that accrete to form cratonic lithosphere but further detailed investigation is required of depth/age relationships of xenoliths from individual pipes.

#### References

- Martin, C.E. (in press) Osmium isotopic characteristics of mantle derived rocks. *Geochimica et Cosmochimica Acta*, vol 55.
- Nixon, P.H., van Calsteren, P.W.C, Boyd, F.R. and Hawkesworth, C.J. (1987) Harzburgites with garnets of diamond facies from southern African kimberlites. In P.H. Nixon, Ed., *Mantle Xenoliths*, 523-533, Wiley, New York.
- Richardson, S.H., Gurney, J.J, Erlank, A.J, and Harris, J.W. (1984) Origin of diamonds in old enriched mantle. *Nature*, 310, 198-202.
- Walker, R.J., Carlson, R.W., Shirey, S.B. and Boyd, F.R. (1989) Os, Sr, Nd and Pb isotope systematics of southern African peridotite xenoliths: Implications for the chemical evolution of subcontinental mantle. *Geochimica et Cosmochimica Acta*, 53, 1583-1595.

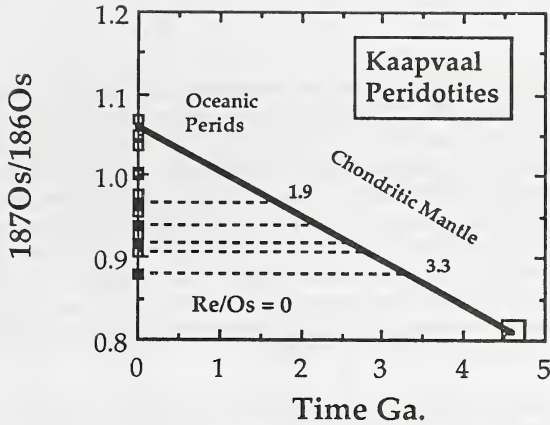


Figure 1. Osmium isotope evolution diagram for Kaapvaal peridotite xenoliths. Present day isotopic compositions are projected back to the Chondritic Mantle Evolution Curve ( $^{187}\text{Re}/^{186}\text{Os} = 3.3$ ) given by Walker et al. (1989) assuming a  $^{187}\text{Re}/^{186}\text{Os}$  of zero to yield minimum Re model depletion ages ( $T_{\text{RD}}$ ); age indicated in Ga. Additional data are Kaapvaal peridotite xenoliths analysed by Walker et al (1989), open squares, and the range for oceanic abyssal peridotites from Martin (in press), shaded region.

THE THERMAL EVOLUTION OF CRATONIC LOWER CRUST/UPPER MANTLE:  
EXAMPLES FROM EASTERN AUSTRALIA AND SOUTHERN AFRICA.

*N.J. Pearson*<sup>(1)</sup>; *S.Y. O'Reilly*<sup>(1)</sup> and *W.L. Griffin*<sup>(2)</sup>.

(1) *School of Earth Sciences, Macquarie University, Sydney NSW 2109, Australia;* (2) *Div. Expl. Geosciences, CSIRO, North Ryde NSW 2113, Australia.*

Xenolith suites of inferred lower crustal origin occur in kimberlites and basaltic rocks near the eastern margin of the Australian craton (EMAC) and in kimberlites marginal to or off the southern margin of the Kaapvaal craton, southern Africa (SAF). Mafic rock types are dominant and include garnet websterites (garnet+clinopyroxene+orthopyroxene±spinel), mafic granulites (garnet+clinopyroxene+plagioclase±orthopyroxene±amphibole±quartz±scapolite±rutile), kyanite-bearing mafic granulites (garnet+clinopyroxene+kyanite+plagioclase±orthopyroxene±quartz±scapolite±rutile) and eclogites (garnet+clinopyroxene+rutile±quartz±kyanite). Both xenolith suites preserve reaction microstructures and mineral chemistry evidence for the transformation of igneous assemblages and microstructures to granulite and eclogite: these features are interpreted as reflecting progressive cooling (Griffin *et al.*, 1990; Pearson *et al.*, 1991; Pearson & O'Reilly, 1991).

Geothermobarometry on these xenoliths yields the ambient temperature at each depth at the time of entrainment in the magma and can be used to construct a paleogeotherm. P-T data obtained from the EMAC mafic xenoliths define a curve stretching from 800 °C at 10 kbar to 1020 °C at 22 kbar (Fig. 1). This curve is displaced c. 150 °C below the xenolith-derived geotherm for the lower crust/upper mantle beneath the Phanerozoic Tasman Fold Belt, eastern Australia (O'Reilly & Griffin, 1985) and indicates a distinct thermal variation away from the craton boundary. Despite preserving evidence of cooling toward a conductive steady state geotherm, the shape of the EMAC geotherm retains an advective heat flow signature.

The geotherm constructed from the southern Africa mafic xenoliths is less tightly constrained with a greater scatter in P-T data (Fig. 1). The data are distributed in a band from 650 to 750 °C at 10 kbar to c. 1000 °C at 20 kbar, with a range in temperature of up to 150 °C at a given pressure. The lower limits of the P-T band overlap with the P-T field derived from the Lesotho xenolith suite (Griffin *et al.*, 1990), but are still well above the cratonic geotherm defined by garnet peridotites (e.g. Finnerty & Boyd, 1987).

These large lateral variations in temperature at the base of the crust and the definition of distinct thermal regimes related to tectonic environment are significant to the relative stability of eclogite and granulite mineral assemblages. The restriction of lower-crustal eclogite suites to craton or craton-margins, and their apparent absence from younger terranes with elevated geotherms (e.g., south-east Australia) is a consequence of this temperature difference.

A stratigraphy based on the P-T data from the EMAC and SAF mafic xenoliths indicates the interlayering or coexistence of eclogite and granulite over a depth range of 30 - 70 km in both cratons. Thermal relaxation toward a steady-state conductive geotherm should result in the progressive re-equilibration of mafic igneous intrusions around the crust/mantle boundary, under granulite facies conditions. As cooling proceeds, an increasing proportion of mafic compositions will react to produce eclogite facies assemblages. Reactions progress is dependent not only on P-T conditions but on bulk compositional constraints and reaction kinetics. The wide range in bulk compositions from both the EMAC and SAF xenolith suites is a major factor in controlling the proportions of granulite to eclogite. The role of kinetic factors in the granulite to eclogite transition is emphasized by the preservation of reaction microstructures, chemical zoning and the greater scatter of P-T data points with decreasing temperature, due to increasingly sluggish reaction rates.

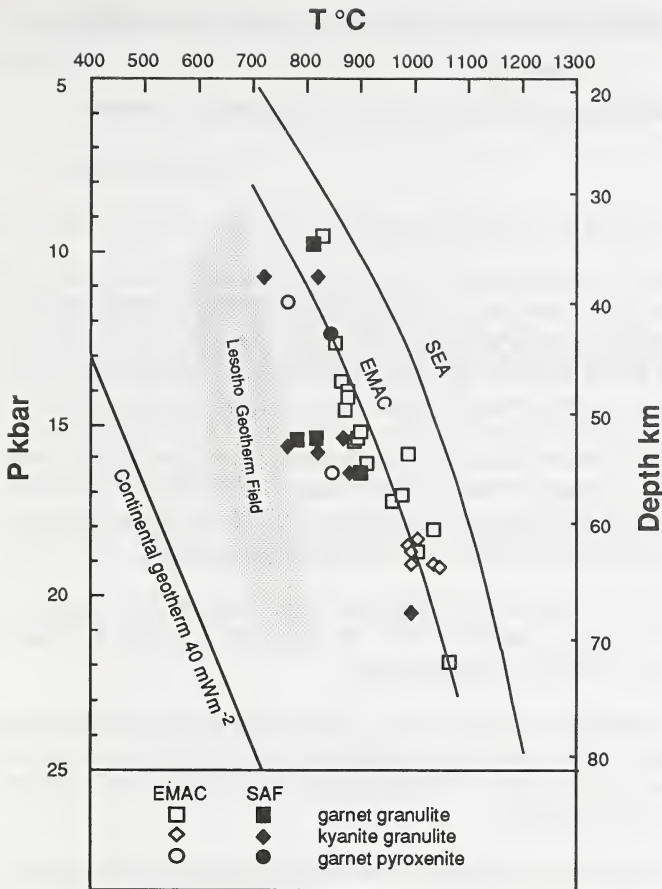


Fig.1: Pressure (P) - temperature (T) - depth profile for xenoliths from the eastern margin of the Australian craton (EMAC) and southern Africa (SAF). Also shown are the xenolith-derived geotherm for south eastern Australia (SEA; O'Reilly & Griffin, 1985) and the Lesotho Geotherm Field (Griffin *et al.*, 1990). The continental geotherm ( $40\text{mWm}^{-2}$ ) is taken from Pollack & Chapman (1977). Details of the thermobarometric methods used are presented in Pearson *et al.*, (1991).

## REFERENCES

- Finnerty, A.A. & Boyd, F.R., 1987. Thermobarometry for garnet peridotites: basis for the determination of thermal and compositional structure of the upper mantle. in: Nixon, P.H., Ed., *Mantle Xenoliths*, Wiley, London, p.381-402.
- Griffin, W.L., O'Reilly, S.Y. and Pearson, N.J., 1990. Eclogite stability near the crust-mantle boundary. in: Carswell, D.A., Ed, *Eclogite Facies Rocks*, Blackie, Glasgow, p.291-314.
- O'Reilly, S.Y. and Griffin, W.L., 1985. A xenolith-derived geotherm for southeastern Australia and its geophysical implications. *Tectonophysics*, 111, 41-63.
- Pearson, N.J. and O'Reilly, S.Y., 1991. Thermobarometry and P-T-t paths: the granulite to eclogite transition *J. Metamorphic Geology*, in press.
- Pearson, N.J., O'Reilly, S.Y. and Griffin, W.L., 1991. The granulite to eclogite transition beneath the eastern margin of the Australian craton. *European Journal of Mineralogy*, in press.
- Pollack, H.N. & Chapman, D.S., 1977. On the regional variation of heat flow, geotherms and lithospheric thickness. *Tectonophysics*, 38, 279-296.

## CHARACTERIZATION OF LAMPROITES FROM PARAGUAY (SOUTH AMERICA).

*Preser, I.B.**Dep. Geologia, Facultad de Ciencias Exactas y Naturales, U.N.A.C.C, 1039, Assunción-Paraguay.*

Lamproites were found in the ultrapotassic Guairá-Paraguari Province, 80 km SE from the capital city of Asunción (south Central Paraguay). This region constitutes the western portion of the intracratonic Paraná Basin and was affected by potassic to ultrapotassic magmatism of mesozoic age (~ 133 My), occurring mainly within the so-called Asunción rift.

The recognized lamproite bodies are plugs, dikes and pipe-like, and associated with other volcanic rocks such as basanites (leucite-bearing alkalibasalts), damkjernites, ouachitites, sannaites, peridotites microxenolith-bearing monchiquites and cocites, as well as intrusive rocks as ijolites, peridotites microxenolith-bearing shonkinites and carbonatites.

The "Ñande Yara gracia" (ÑYgr) plug is about 200 m diameter lamproitic in character pipe-like and intruded into leucite-bearing basaltic rocks. Its exposure is masked by soil, vegetation and blocks of neighbouring volcanic alkaline rocks.

The ÑYgr rocks in hand specimen, is dark gray in colour and porphyritic due the presence of abundant leucite crystals with a glomeroporphyritic structure (up to 10 mm in diameter), some diopside prisms, serpentine (after olivine) crystals (up to 1 mm in diameter); occasional minute vesicle are filled with zeolites.

LEUCITE is present as octogonal or rounded twinned phenocrysts with pleochroic inclusions (purple to lemon canario), zoned and elongated K,Ti-richterite (with margins altered to a light green-yellow secondary phase, similar to that described by Mitchell and Lewis, 1983 in the Prairie Creek olivine-lamproite) and also diopside, serpentine (after olivine), rectangular opaques, prismatic lance-like opaque (jeppeite) associated with priderite, and devitrified glass. Other phenocrysts are pale yellow-green zoned and twinned DIOPSIDE laths; idiomorphic serpentine (after OLIVINE); and rectangular to allotriomorphic OPAQUES (up to 1 mm) the groundmass consists of colourless diopside prisms, rectangular opaques idiomorphic shchervakovite, some K,Ti-richterite, phlogopite, apatite, priderite, wadeite and lucasite; plus interstitial sanidine and devitrified glass.

The rock can be classified as a OLIVINE-BEARING LEUCITE LAMPROITE (according to Scott-Smith and Skinner, 1984) or as a LEUCITE DIOPSIDE LAMPROITE = CEDRICITE (following Wade and Prider, 1940 ; Mitchell, 1984). This lamproite is similar to the "West Kimberley" lamproites and also Kapamba lamproites (cf. Scott-Smith and others, 1988).

Orange to deep red and red-wine to lilac garnets, Cr-diopside, ilmenite, Cr-spinels and diamonds (dodecahedrons to rounded, irregular, macles and aggregates) were obtained from the ÑYgr pipe and overlying soil.

The ÑYgr rock chemistry shows high TiO<sub>2</sub>, MgO and high ratios of K<sub>2</sub>O/Na<sub>2</sub>O, K<sub>2</sub>O/Al<sub>2</sub>O<sub>3</sub>. The CaO, Al<sub>2</sub>O<sub>3</sub> and Na<sub>2</sub>O are low, LREE/HREE and LILE/HFSE enrichment is similar to the "West Kimberley" ultrapotassic rock type.

Thus, the Guairá-Paraguarí Ultrapotassic Province is another potential diamondiferous province.

## REFERENCES

- MITCHELL,R.H. 1985. A review of the mineralogy of lamproites. *Trans. Geol. Soc. S. Afr.*, **88**: 411-437.
- MITCHELL,R.H. and LEWIS,R.D. 1983. Priderite-bearing xenoliths from the Prairie Creek mica peridotite, Arkansas. *Canadian Mineralogist*, **21**: 59-64.
- SCOTT-SMITH,B.H. and SKINNER,E.M.W. 1984. Diamondiferous lamproites. *Journal of Geology*, **92**: 433-438.
- SCOTT-SMITH,B.H.; SKINNER,E.M.W.; LONEY,P.E. 1988. The Kapamba lamproites of Luangwa Valley, eastern Zambia. In *Kimberlites and related rocks: their mineralogy, petrology and chemistry*. Geol. Soc. Aust. Spec. Publ. 14,p. 189-205.
- WADE,A. and PRIDER,R.T. 1940. The leucite-bearing rocks of the west kimberley area, Western Australia. *Quart. J. Geol.Soc. London*, **96**: 39-98.

## MINERAL INCLUSIONS IN DIAMONDS FROM JAGERSFONTEIN MINE.

*Rickard, R.S.<sup>(1)</sup>; Gurney, J.J.<sup>(1)</sup> and Harris, J.W.<sup>(2)</sup>.*

*(1) Dept. of Geochemistry, University of Cape Town, S.A.;*

*(2) Dept. of Applied Geology, University of Strathclyde, Glasgow, U.K.*

A total of 33 inclusions have been recovered from 28 diamonds from the now defunct Jagersfontein mine. Despite the small suite of minerals studied, the results are noteworthy because of the high proportion of unusual features exhibited within the standard world-wide framework that both eclogitic and peridotitic diamond inclusions have been found.

The peridotitic suite is represented by chromites, garnets and olivines. The eclogitic suite minerals found were garnets, clinopyroxenes and coesite, whilst orthopyroxene was also recorded in a websteritic association geochemically linked to the eclogitic parageneses as previously described at Monastery and Orapa.

In the peridotitic suite, 4 chromites have Cr<sub>2</sub>O<sub>3</sub> contents ranging from 61 to 64.2 wt%, 3 sub-calcic garnets fit in the G10 field. One of these (J6a) is unusual in having only 2.51 wt% Cr<sub>2</sub>O<sub>3</sub>. Completing the suite are 3 olivines with Fo contents in the range 91-92. They are unusual in having high Cr and Ca contents. A fourth olivine (J15a) has a Fo content of 78.8, outside the peridotitic range and is only matched in mantle rocks by olivines in garnet websterites, such as those reported from Matsoku, Lesotho. J15a also has Fo equivalents in megacryst suite olivines. A websterite association is also proved by two orthopyroxene inclusions (J14a, J22a) which occur in two three phase polymineralic inclusions together with garnet and clinopyroxene. Both orthopyroxenes are enriched in FeO and CaO and have low Mg/Mg+Fe. The Clinopyroxenes are low in Al<sub>2</sub>O<sub>3</sub> and Na<sub>2</sub>O compared to those from the eclogitic suite. A third clinopyroxene inclusion (J10a) has a similar composition and is also included in the websteritic association. The garnets have TiO<sub>2</sub> levels of .6 wt%, Cr<sub>2</sub>O<sub>3</sub> of 1.4 wt% and 1.08 wt%, and Na<sub>2</sub>O levels of .08 wt% and .14 wt%, making them more enriched in these elements than similar inclusions from Monastery and Orapa.

The pyroxene solid solution in garnet first noted at Monastery Mine (Moore 1986) and interpreted to reflect a particularly high crystallisation pressure, has been found to be common in Jagersfontein diamonds, certainly occurring in garnets in seven diamonds in the suite studied. One of these diamonds, (J22) contains a websteritic assemblage gar-cpx-opx in addition to (gar-px)<sub>SS</sub>. The websteritic assemblage gives calculated equilibration conditions of 1272°C at 49.5kb. (using Lindsley and Dixon 1976 and Nickel and Green 1985), whilst the (gar-px)<sub>SS</sub> indicates pressures > 145kb. The other six garnet/clinopyroxene solid solutions give a pressure range of 100 to 145kb which suggests that at least some of the diamonds from Jagersfontein have formed in the depth interval from 150km to in excess of 450km. The same range was implied at Monastery (Moore 1986) and Brazil (Wilding and Harte, 1989). A second websteritic assemblage in (J14) gives similar calculated equilibration conditions, whilst an eclogitic gar-cpx pair in diamond (J37) equilibrated at 1295°C at an assumed pressure of 50kb according to the method of Ellis and Green (1979). These are within the diamond stability field.

The remaining minerals coesite (J13a) which co-existed with a garnet (J13b), and a garnet clinopyroxene co-existing pair (J37) are clearly eclogitic. The calculated equilibration temperature for J37 is 1295°C using the method of Ellis and Green (1979), and assuming all iron is present as Fe<sup>2+</sup>, and a pressure of 50Kb. Again this is within the diamond stability field and in reasonable agreement with the calculated temperatures of the websteritic association, which suggest that they were formed under similar temperature/pressure conditions.

It is inferred from this small suite of mineral inclusions from Jagersfontein diamonds that a probably incomplete inventory of diamond source rocks includes garnet and or chromite harzburgite, iron-rich eclogite, garnet websterite, majorite and rare coesite eclogite. Eclogite xenoliths with diamond have been reported from Jagersfontein previously. Majorite could be the protolith for rare mantle assemblages recently described by Haggerty and Sautter (1990). Sub-calcic peridotitic (G10) garnets and high Cr<sub>2</sub>O<sub>3</sub> chromites, presumably derived from disaggregated diamond harzburgite are present as macrocrysts in the Jagersfontein kimberlite. The websterites and coesite eclogite have not been reported as xenoliths.

The overwhelming majority of peridotitic xenoliths described by others from the Jagersfontein kimberlite are not suitable diamond source rocks and have distinctly different mineral compositions compared to the inclusions in the diamonds. This situation pertains to all other similarly studied localities in southern Africa.

The low proportion of peridotitic inclusions in Jagersfontein diamonds contrasts with their abundance at Koffiefontein, 55km to the NNW.

## References

- Ellis, D.J., and Green, D.H. (1979) An experimental study of the effect of Ca upon garnet-clinopyroxene Fe-Mg exchange equilibria. *Contrib. Mineral. Petrol.* 71, 13-22.
- Haggerty, S.E., and Sautter, V. (1990) Ultradeep (Greater than 300 Kilometers), Ultramafic Upper Mantle Xenoliths. *Science* Vol. 248, 993-996.
- Lindsley, D.H., and Dixon, S.A. (1976) Diopside-enstatite equilibria at 850 to 1400°C, 5 to 35 Kbars. *Am. J. Sci.* 276, 1285-1301.
- Moore, R.O. (1986) A study of the kimberlites, diamonds and associated rocks and minerals from Monastery Mine, South Africa. PhD thesis (unpublished), University of Cape Town, South Africa.
- Nickel, K.G., and Green, D.H. (1985) Empirical geothermobarometry for garnet peridotites and implications for the nature of the lithosphere, kimberlites and diamonds. *Earth Planet. Sci. Lett.* 73, 158-170.
- Wilding, M.C., and Harte, B. (1989) Evidence of Asthenospheric source for Diamonds from Brazil. 28<sup>th</sup> I.G.C. Abstracts. Vol.3, 359-360.

TABLE 1: Inclusions in Jagersfontein Mine Diamonds.

	J1a Chr	J2a Chr	J3a Chr	J4a Chr	J6a Gar	J7a Gar	J8a Gar	J10a Cpx	J11a Gar	J12a Olv
SiO <sub>2</sub>	n.d.	n.d.	n.d.	n.d.	42.43	41.83	41.56	55.16	41.32	40.78
TiO <sub>2</sub>	n.d.	.14	.07	.02	n.d.	.02	.03	.11	.13	n.d.
Al <sub>2</sub> O <sub>3</sub>	7.08	7.40	9.50	4.20	22.37	15.36	18.07	1.15	22.76	.02
Cr <sub>2</sub> O <sub>3</sub>	63.27	62.35	60.96	64.18	2.51	11.98	8.03	.15	.17	.06
FeO	13.78	14.61	13.46	17.90	5.57	4.59	6.11	5.53	12.80	7.14
MnO	.79	.82	.79	.90	.24	.36	.34	.04	.41	.11
MgO	14.36	13.70	14.93	11.93	23.23	24.85	22.72	19.37	15.78	51.08
CaO					3.08	.98	2.31	16.74	6.36	.06
Na <sub>2</sub> O								1.06	.10	
K <sub>2</sub> O								.03		
NiO										.43
Total	99.29	99.02	99.13	99.13	99.43	99.97	99.17	99.34	99.83	99.68
	J13a Coes	J13b Gar	J14a Gar	J14a Cpx	J14a Opx	J15a Olv	J17a Cpx	J19a Olv	J21a Olv	J22a Gar
SiO <sub>2</sub>	98.78	42.14	41.47	54.41	56.32	38.52	55.45	40.39	41.07	40.92
TiO <sub>2</sub>	.05	.16	.60	.14	.11	.02	n.d.	n.d.	n.d.	.57
Al <sub>2</sub> O <sub>3</sub>	.09	20.90	21.10	1.36	.76	.02	.66	n.d.	.03	20.40
Cr <sub>2</sub> O <sub>3</sub>		.26	1.40	.24	.10	.02	.08	.06	.08	1.08
FeO	.20	13.37	13.03	6.82	10.88	19.48	3.62	8.25	8.03	13.75
MnO		.39	.41	.20	.17	.19	.08	.10	.09	.39
MgO		16.07	17.15	18.84	30.77	40.68	18.32	49.64	50.05	17.37
CaO	.11	6.07	5.04	17.14	1.31	.11	20.85	.07	.09	4.71
Na <sub>2</sub> O		.25	.07	.90	.15		1.04			.14
K <sub>2</sub> O							n.d.			
NiO								.35	.38	
Total	99.23	99.61	100.26	100.03	100.56	99.04	100.10	98.86	99.82	99.33
	J22a Cpx	J22a Opx	J22b (Gar-px) <sub>in</sub>	J23a (Gar-px) <sub>in</sub>	J24a Gar	J25a (Gar-px) <sub>in</sub>	J26a Gar	J26b Gar	J27a (Gar-px) <sub>in</sub>	J28a Gar
SiO <sub>2</sub>	54.16	55.95	47.94	46.17	41.15	42.96	40.49	40.19	44.79	41.52
TiO <sub>2</sub>	.12	.08	.67	.23	.90	.19	.42	.44	.23	.56
Al <sub>2</sub> O <sub>3</sub>	1.65	.71	8.82	15.95	19.83	19.34	22.47	21.99	16.69	21.84
Cr <sub>2</sub> O <sub>3</sub>	.27	.06	.55	.28	2.23	.20	.08	.08	.22	.53
FeO	7.08	10.29	13.75	11.05	13.22	13.00	15.25	15.45	12.82	11.91
MnO	.15	.17	.30	.27	.42	.43	.30	.31	.35	.26
MgO	18.35	31.28	22.08	19.25	16.94	15.91	12.41	13.09	18.86	18.95
CaO	16.37	1.17	5.52	5.91	5.43	7.94	8.28	8.48	6.05	3.79
Na <sub>2</sub> O	1.43	.29	.33	.69	.04	.26	.14	.14	.29	.08
K <sub>2</sub> O	n.d.	n.d.								
NiO										
Total	99.58	99.99	99.96	99.80	100.16	100.23	99.84	100.17	100.30	99.44
	J29a (Gar-px) <sub>in</sub>	J31a (Gar-px) <sub>in</sub>	J32a (Gar-px) <sub>in</sub>	J34a Cpx	J35a Cpx	J37a Cpx	J37b Gar			
SiO <sub>2</sub>	45.89	42.84	47.29	54.06	54.27	54.81	40.99			
TiO <sub>2</sub>	.22	.10	.19	.61	.55	.60	.70			
Al <sub>2</sub> O <sub>3</sub>	17.27	21.46	14.09	6.52	8.67	6.84	22.94			
Cr <sub>2</sub> O <sub>3</sub>	.41	.11	.21	n.d.	.02	.18	.18			
FeO	10.26	13.49	11.00	13.47	9.16	5.52	13.03			
MnO	.25	.33	.29	.12	.09	.11	.31			
MgO	19.60	15.90	19.35	8.09	8.62	13.82	16.62			
CaO	5.24	6.10	7.03	13.77	13.91	13.94	4.71			
Na <sub>2</sub> O	.44	.12	.54	3.77	4.54	4.00	.24			
K <sub>2</sub> O				.05	.04	.24				
NiO										
Total	99.58	100.45	99.99	100.46	99.87	100.06	99.72			

n.d. = not detected

Mineral compositions obtained on a Cameca Camebax Microbeam electron microprobe, using close standards and a ZAF correction procedure.

J14a & J22a are single inclusions of Gar-Cpx-Opx minerals touching each other.

**ILMENITE-BEARING PERIDOTITES AND MEGACRYSTS FROM  
DALNAYA KIMBERLITE PIPE, YAKUTIA.**

*Rodionov<sup>(1)</sup>, A.S.; Sobolev<sup>(1)</sup>, N.V.; Pokhilenko<sup>(1)</sup>, N.P.; Suddaby<sup>(2)</sup>, P. and Amshinsky<sup>(1)</sup>, A.N.*

*(1) Institute of Geology and Geophysics, Novosibirsk, URSS;*

*(2) Imperial College of Science and Technology, London. UK.*

Dalnaya kimberlite pipe is outstanding among Yakutian kimberlites in terms of abundance of ilmenite peridotite xenoliths and megacrysts.

Our collection consists of about 200 megacrysts of Ilm, Cpx, Gar, Opx, and Ol and their intergrowths and inclusions in different combinations. Ilmenite-pyrope peridotite compose about about 10% of all ultramafic xenoliths population and exceed 100 samples.

**Ilmenite-pyrope lherzolite (IL)**

All samples are altered to different extent. Therefore, in many cases we could not analyse Opx, but its presence in most samples is proved by typical bastitic pseudomorphs and (or) by Gar composition.

The majority of ilmenite peridotites xenoliths belong to a lherzolite paragenesis type (Ol + Cpx + Opx + Gar + Ilm + Phl).

Several points should be underlined summarising this group petrography.

1) some xenoliths have a sheared structure, many - a mosaic one and most part - transitional from mosaic to granular structure. Just small part of these xenoliths reveals typical granular structure.

2) Gar grains are zoned in many samples, what one can see either under binocular or from profile analysis (Rodionov, 1988). For sample D-60/79 difference in concentrations reaches for Cr<sub>2</sub>O<sub>3</sub> (core-rim, wt%): 6.77-1.05; CaO: 6.27-4.78; Al<sub>2</sub>O<sub>3</sub>: 16.8-21.4; MgO: 17.9-19.5; for FeO, MnO and TiO<sub>2</sub> no significant variations were fixed. In some samples with zoned garnets (normally about 6-10 mm in size) small grains (0.2-1 mm) of second generation Gar are present. Composition of GarII grains corresponds to outer zones of GarI. Core of GarI normally is free of ilmenite inclusions, that appear in the rim. Ilmenite inclusions from the inner part of the rim sometimes differ in composition from grains in matrix (in D-60/79: TiO<sub>2</sub> - 54.3-52.7, Al<sub>2</sub>O<sub>3</sub> - 1.55-0.73, MgO - 15.9-12.5 wt%). For Cpx, Opx or Ol no signs of zoning were fixed.

3) Practically all samples contain "pools" of greenish-black highly altered aggregates, that develop along grain boundaries or form rounded "bays" along fractures in all minerals. Serpophite, mica, ore minerals and ochre material composed these pools. We considere these aggregates as products of alteration of partial (residual?) melt.

P-T parameters of equilibria are lower than ones for South Africa analogs (900-1120<sup>0</sup>C at 30-35 kb).

### Megacryst suite (M)

Abundance of megacrysts permits to compare Dalnaya pipe with Monastery pipe (South Africa). General features of their appearance are similar to megacryst suites described in other localities. So we will concentrate here on peculiarities of Dalnaya pipe megacrysts.

1) They are a bit less in average size than African ones. According after P.H.Nixon and F.R.Boyd (1973) the lowest dimension of 1 cm it is 2.5 cm with maximum (cm): Gar - 4.0, Ilm - 5.9, Cpx - 6, Opx - 3, Ilm-Cpx intergrowths - 9.5.

No one typical graphic intergrowth of Ilm and silicate was found. On the other hand several megacrysts of high chromium type were recorded similar to Sloan pipe (USA, Eggler, MacCallum, 1976).

The majority of Ilm megacrysts are recrystallized either totally or more common partly. Gar megacrysts often bear traces of partial melting.

Compositions of megacrysts do not reveal "crystallization" trends like South African suites. There is only general tendency appearing in enrichment of all minerals in Fe, Al and Ca contents in association with Ilm. Like and for (IL) equilibria parameters are lower in comparison to South Africa (900-1050<sup>0</sup>C and P < 30 kb). For several discrete Cpx nodules T reaches 1200-1250<sup>0</sup>C.

### Ilmenite-pyrope wehrlites (IW)

The most interesting Ilm-bearing assemblage is a first time established in Dalnaya paragenetically proved xenoliths and megacrysts of ilmenite-pyrope wehrlite (Rodionov et. al., 1977; Rodionov, Pokhilenko, Amshinsky, 1989).

All reported earlier xenoliths of this type were either not accompanied with mineral analysis or Gar analysis corresponded to two-pyroxene types of paragenesis and therefore such samples were called according to composing minerals proportions.

Xenoliths have unusual structure and are composed of big (up to 2.5 cm) crystals of Gar + Cpx + Ilm + Ol + Phl (the two last fases can be not presented). Ol is practically totally serpentinized. There is a small grained (0.2 mm) aggregate of the same minerals + Amph + Spln in interstices and along fractures in the big crystals. We consider this material as product of quenching of partial melt what is confirmed by very strong zoning of small euhedral spinels in sample D-100/81 and euhedral form of Cpx.

Megacrysts of the same paragenesis look very much alike "normal" lherzolitic type and can be distinguished only on the basis of their chemistry (Gar first of all).

As we have only four xenoliths and their both structure and composition of big crystals strongly corresponds to megacrysts of the same type their compositions were combined in following discussion.

Temperature range of equilibria is estimated as 800-880<sup>0</sup>C (assuming pressure 25 kb).

### Discussion and summary

It is reasonable to compare compositional variations of minerals from all considered groups as they are presented in the same kimberlite body. Another point is that in xenoliths

of Ilm lherzolites occasionally mineral grains reaching 1 cm occur. And disintegration of such xenoliths can be one of the sources of megacrysts in kimberlite matrix.

Comparison of all corresponding minerals between groups show:

1. Inside no one group crystallization trend can be reconstructed on the basis of major elements chemistry.
2. As could be suggested range of composition of discrete nodules overlaps variations for each individual group.
3. If to compare average composition for each group (for association with Ilm) a certain tendency appears quite evident. In the range IL-M-IW of all minerals regularly increases while Cr-contents is decreasing; for Cpx ratio Ca/Ca + Mg increases also that reflects decreasing of equilibria temperature.

The fact that IW - end member of this trend is established both as megacrysts and consolidated rock xenoliths can be a basis for conclusion that more refractory megacrysts of ilmenite-pyropite lherzolite paragenesis also passed a stage of consolidation. In our opinion it excludes a possibility of M crystallization from kimberlite melt. Abundant traces of cataclasis in these megacrysts confirm this conclusion.

Our results permit to interpret established range as a product of deep-seated metasomatic processing of normal mantle peridotite (first of all sheared) by fluids enriched in Ti, Fe, Ca, K and other non-coherent elements. Process took place in uplifting mantle diapir, that is reflected in Gar zone. Partial melting in the upper part of the diapir in combination with collecting re-crystallization led to forming of coarse-mega-crystalline rocks. Disintegration of these rocks (due to presence of residual melt) during kimberlite emplacement produce megacrysts.

Absence of crystallization trend in comparison to South Africa is due to general comparatively "cool" mantle conditions producing less scale of melting. In other words Dalnaya ilmenite assemblages were derived from several isolated chambers. At the same time our data approve general tendencies in evolution of titanium branch associations.

## References

- NIXON, P.H. & BOYD, F.R. 1973. The discrete nodule association in kimberlites from northern Lesotho. In NIXON, P.H. (ed.) *Lesotho kimberlites*, Lesotho Nat. Dev. Corp., 67-75.
- EGGLER, D.H. & MacCALLUM, M.E. 1976. A geotherm from megacrysts in the Sloan kimberlite pipes, Colorado. *Carn. Inst. Wash. Yearbook* 75, p. 538-541.
- RODIONOV, A.S. 1988. Ilmenite peridotite xenoliths with zoned garnet from Dalnaya kimberlite pipe (Yakutia). In *Ultramafic paragenesis minerals from kimberlites and conditions of their genesis*, Novosibirski, 86-94 (in Russian).
- RODIONOV, A.S.; AMSHINSKY, A.N.; POKHILENKO, N.P.; SOBOLEV, N.V. 1984. Xenoliths of ilmenite-pyropite wehrlites and the problem of kimberlite megacrysts suite genesis. In 10<sup>th</sup> Seminar "Geochemistry of magmatic rocks", (abst.), Moscow, GEOCHI, 153-154 (in Russian).
- RODIONOV, A.S.; POKHILENKO, N.P.; AMSHINSKY, A.N. 1989. Megacryst suite in Yakutian kimberlites: new data. In *Problems of kimberlite magmatism*, Novosibirski, Nauka, Siberian Div., 120-126 (in Russian).

## STATISTICAL DISTRIBUTIONS FOR DIAMONDS.

*Rombouts, L.**Terraconsult bvba, Jan Van Rijswijcklaan 84, B-2018 Antwerpen, Belgium.*

Models for the sizes and spatial distribution of diamonds are necessary to sample and evaluate diamond deposits in a rational and economic way. The distribution models can be interpreted as the result of physical processes acting on discrete particles. For instance, size distributions could be diagnostic for constraints during crystallisation of the diamonds.

If the growth of diamonds in the mantle was subject to the proportional effect, diamond sizes will be well approximated by two-parameter lognormal distributions. If we assume, on the other hand, a size-invariant growth, fractal models will be applicable, with the size distribution obeying a power law. Lognormal distributions fit very well the size distributions of macrodiamonds in kimberlites, lamproites and sediments. The size distributions of microdiamonds (e.g. in the Argyle lamproite), however, seem to follow a power law. The difference between the lognormal and fractal distribution can be illustrated with the theory of fragmentation. If fragmentation is explosive - or sudden and pervasive -, the resulting fragments will follow a fractal size distribution. This has for instance been studied in coal mines, where the sizes of coal fragments from the broken mine face follow a power law. On the other hand, if breakage is slow, say in a mill, at every stage in the process the fragments created are a random fraction of a previous larger fragment. This proportional effect will result in a lognormal size distribution for the fragments. The model of stable growth proportional to size seems plausible for macrodiamonds in the mantle. Kimberlites tap these macrodiamonds as xenocrysts. The power law of the microdiamonds seem to point to a sudden random growth, possibly at the time of kimberlite explosion.

Deviations or variants on these ideal cases will often create distributions intermediate between Pearson III and Pearson V type curves. Within this family are gamma distributions, inverse gaussian distributions, three- and four-parameter lognormal distributions and log-hyperbolic distributions. The latter two are especially useful in an alluvial environment, where due to alluvial sorting a linear relationship could exist between the average stone size and the standard deviation.

During diamond crystallisation in the mantle, carbon molecules will diffuse by random walk to the nearest nucleation seed. If the nucleation seeds appear at random but at a constant rate in time and per unit volume, the distribution of the volumes of influence of each seed

will have a coefficient of variation of 1.066. The latter is very similar to the coefficient of variation of diamond sizes in the Banankoro kimberlite pipes in Guinea, where diamonds are large, clear and well-crystallised.

Diamonds are brought to the earth's surface during kimberlite volcanism and are spread in secondary deposits by rivers, wind and sea. Sichel's compound Poisson distribution is a very useful model to describe the distribution of diamonds as particles in space. The compound Poisson distribution is obtained by mixing a simple Poisson distribution with a distribution intermediate between the Pearson III and V curve. The model can be visualized as a random distribution of clusters. The compound Poisson distribution is flexible with parameter  $\theta$  (between 0 and 1) indicating the degree of clustering. If  $\theta$  is zero, the distribution becomes a simple Poisson distribution, with particles distributed at random without clustering. If  $\theta$  approaches one, the clustering effect becomes stronger. This allows the clustering of diamonds in favourable trapsites to be modelled.

If samples of diamond deposits are large enough to contain several tens of stones, the resulting grade distribution will lose its discrete character and tends to be lognormal. In kimberlites or lamproites, the grade contains a spatial structure, which can be modelled in a spherical variogram. A random distribution of points will create a spherical variogram if the number of points are counted in successively overlapping spheres. The range of the variogram is then equal to the degree of overlapping of two successive spheres.

The value distribution of diamonds is well approximated by lognormal distributions. The value distribution will show a high logarithmic variance in deposits with a high gem content. The t-estimator is in such a case more efficient than the arithmetic mean for estimating the average carat price of the diamonds.

## CRATONIC AND OCEANIC LITHOSPHERIC MANTLE BENEATH NORTHERN TANZANIA.

*Roberta L. Rudnick<sup>(1)</sup>; William F. McDonough<sup>(1)</sup> and Bruce W. Chappell<sup>(2)</sup>.*

*(1) Research School of Earth Sciences, Australian Nat. Univ., Canberra, A.C.T. 2601 Australia;*

*(2) Dept. of Geology, Australian Nat. Univ., Canberra, A.C.T. 2601 Australia.*

Cratonic peridotite xenoliths from kimberlites in southern Africa have compositions distinct from those carried in alkali basalts which erupt through post-Archean crust. Off-craton, or "oceanic" peridotite xenoliths show increasingly forsteritic olivines with increasing modal olivine content, similar to trends observed in oceanic peridotites and consistent with progressive extraction of basaltic magma. In contrast, cratonic peridotites have high Fo contents over a wide range of modal olivine contents and generally contain high modal enstatite (Boyd, 1989). These mineralogical differences are reflected in higher SiO<sub>2</sub> and lower FeO contents (Hawkesworth et al., 1990, McDonough, 1990) in cratonic xenoliths. Cratonic xenoliths also possess lower concentrations of HREE, Sc, Mn, V (McDonough, 1990), suggesting severe depletion by partial melting. The differences between cratonic and non-cratonic peridotites have been attributed to fundamentally different growth processes of the lithospheric mantle in Archean and post-Archean times (Boyd, 1989, Hawkesworth et al., 1990). In particular, generation of komatiitic magmas in the Archean may have produced a highly depleted, SiO<sub>2</sub>-enriched residue that was buoyant in comparison to the surrounding (fertile) mantle. An alternative explanation is that the melt-depleted character and SiO<sub>2</sub>-enriched nature of Kaapvaal peridotites may reflect addition of SiO<sub>2</sub> to highly depleted (komatiitic) residues by slab-derived fluids (Kesson and Ringwood, 1989). In this abstract we examine new and published data for garnet and spinel peridotite xenoliths from the Lashaine and Olmani ankaramite volcanoes in northern Tanzania that place constraints on the mode of growth of lithospheric mantle.

The Quaternary Lashaine and Olmani volcanoes lie approximately 30 km from one another near Arusha in northern Tanzania. They lie within the southern extension of the East African Rift and occur in a Proterozoic (ca. 2 Ga) mobile belt in an area of extensive pan-African crustal reworking (Nixon, 1987). The age of crust formation is unknown. The Archean Tanzanian craton lies ~150 km to the west but Archean rocks are unknown in the Arusha area. The Lashaine xenolith suite was extensively described by Dawson and co-workers in the early 1970's (Dawson et al., 1970, Dawson and Smith, 1973, Reid and Dawson, 1972, Reid et al., 1975, Rhodes and Dawson, 1975, Ridley and Dawson, 1975). Their studies document the remarkable freshness of both garnet and spinel peridotite xenoliths from Lashaine in comparison to kimberlite-hosted xenoliths from the Kaapvaal craton. Relatively little published data exist for Olmani xenoliths (Jones et al., 1983), which are typically ultra-refractory (F<sub>93-94</sub>) clinopyroxene-bearing dunites or wehrlites.

### *Main Features*

Both garnet- and spinel-bearing peridotites occur at Lashaine. The garnet peridotites are strikingly similar to low temperature garnet peridotites from the Kaapvaal craton, whereas the spinel peridotites are generally more refractory than typical spinel peridotites from non-cratonic regions. Estimated equilibration pressures and temperatures for the Lashaine garnet-bearing xenoliths are similar to those from Kaapvaal, falling on the ~44 mW/m<sup>2</sup> geotherm. Moreover, the enstatite-rich and refractory character of low temperature Kaapvaal peridotites is also found in the Lashaine garnet peridotites, which have Fo = 90-93, modal olivine = 65-89% (Fig. 1a) and SiO<sub>2</sub> contents higher than spinel peridotites from Lashaine or elsewhere. REE patterns of the Lashaine garnet peridotites mimic those of the coarse granular Kaapvaal peridotites: they are LREE enriched ((La/Yb)<sub>n</sub> = 4-67) with harzburgites having lower HREE contents than lherzolites (e.g., McDonough and Frey (1989)).

Spinel peridotites from Lashaine have equilibration temperatures overlapping those of garnet peridotites, but are chemically different from both Kaapvaal and Lashaine garnet peridotites. These spinel peridotites have higher modal olivine contents for the same range of Fo contents and lie at the terminus of Boyd's "oceanic trend" (Fig. 1b); they also have lower SiO<sub>2</sub> and higher MgO contents than the garnet peridotites but exhibit similar overall REE contents and patterns. Compared with spinel peridotite xenoliths world-wide they have lower SiO<sub>2</sub> and higher MgO and Ni contents, suggesting that they are more refractory. In this respect they are most similar to spinel peridotites xenoliths from Olmani.

assemblages. Texturally, at least some of the clinopyroxenes are secondary: they rim spinels and are observed as veins cross-cutting the olivine matrix (see next section and Jones et al (1983)). The peridotites exhibit a range of modal olivine contents, although most contain >80% modal olivine, similar to but at higher Fo-contents than Lashaine spinel peridotites (Fig. 1b). None of these samples contain garnet, but the spinels have extremely Cr-rich compositions (Cr/(Cr+Al) up to 89). This feature, coupled with equilibration temperatures similar to the Lashaine peridotites and "fingerprint" intergrowths of pyroxene and chromite, suggests that some of the Olmani samples may have contained garnet that broke down due to rising temperature or falling pressure. The Olmani peridotites are more refractory than any hitherto reported in the literature, however despite their high MgO and Ni contents, Cr contents are highly variable (500-2500 ppm). These unusually refractory compositions may be the result of partial melting and cumulate processes; partial melting proceeded to where garnet was consumed ( $\geq 50\%$  melting), leaving behind an olivine ( $\pm$ pyroxene +minor chromite) residue, while ascending magmas may have precipitated forsteritic olivine cumulates at or near their source. These samples may thus be prime candidates for residues and cumulates that have equilibrated with komatiitic magma.

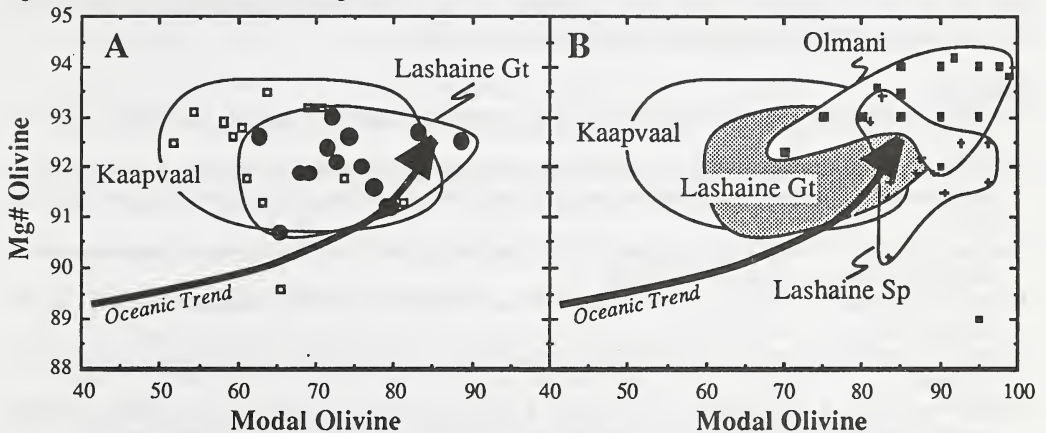


Fig. 1 Modal olivine versus Mg# of olivine (Fo content), after Boyd (1989). A. Garnet peridotites: open squares are low temperature Kaapvaal peridotites, filled circles are garnet peridotites from Lashaine. B. Spinel peridotites: crosses are Lashaine spinel peridotites and small closed squares are Olmani spinel peridotites. Kaapvaal data are from Boyd and Mertzman (1988), Lashaine and Olmani data are from Rhodes and Dawson (1975), Jones et al. (1983) and our unpublished results.

### Secondary enrichments

Both Lashaine and Olmani xenoliths exhibit evidence for elemental enrichments following partial melt depletion. At Lashaine this enrichment is manifested by the presence of phlogopite whereas at Olmani the enrichment is associated with growth of secondary clinopyroxene. Anhydrous Lashaine xenoliths exhibit incompatible trace element enrichments comparable to those of some Kaapvaal low temperature garnet peridotites, whereas all phlogopite-bearing xenoliths from Lashaine are enriched in the high field strength elements (HFSE: Nb, Zr, Hf, Ti) relative to REE of similar compatibility, i.e. they have high Nb/La, Hf/Sm, Zr/Sm and Ti/Eu. These fractionations are uncommon in anhydrous peridotites and the converse of that observed in hydrous spinel peridotites from non-cratonic regions (McDonough, 1990). In addition to HFSE enrichments, the phlogopite-forming event also enriched the peridotite in FeO, CaO, and Al<sub>2</sub>O<sub>3</sub>. These features suggest introduction of phlogopite into depleted mantle peridotite in an open system, probably by interaction with a basaltic melt.

The secondary clinopyroxenes in the Olmani peridotites grew after partial melt depletion, possibly by interaction of the residual orthopyroxene with a carbonatite melt. Such interaction has the potential of adding CaO without Al<sub>2</sub>O<sub>3</sub> and FeO (Green and Wallace, 1988, Meen, 1987) and can explain the very high CaO/Al<sub>2</sub>O<sub>3</sub> ratios (1.3-8.0) observed in these samples. All Olmani samples are LREE enriched, and two samples exhibit unusual enrichments of LREE. These LREE enrichments occur without comparable enrichments in HFSE, giving the whole rock a strongly HFSE depleted pattern and (La/Yb)<sub>n</sub> up to 600. Although HFSE depletions are characteristic of island arc basalts (IAB), such magmas generally do not show fractionated Hf/Sm and Zr/Sm ratios (White and Patchett, 1984), which is in stark contrast to the Olmani samples. The cause of these fractionations are as of yet unknown, however similar

*Discussion*

The cratonic geochemical characteristics of the Lashaine garnet peridotites suggest that this portion of the mantle is Archean in age, consistent with the very low  $\epsilon_{Nd}$  (-24) found in at least one of the garnet peridotites (Cohen et al., 1984) (this is the lowest  $\epsilon_{Nd}$  recorded in any peridotite xenolith, including those from southern Africa). We infer that both ancient cratonic and "oceanic" type mantle exist beneath northern Tanzania. In addition, these data imply that the two mantle lithologies bear a close spatial relationship: the lower portion of the lithosphere is refractory garnet peridotite similar to that of the root of the Kaapvaal craton, whereas the shallower levels are also refractory, but contain a large proportion of modal olivine and may represent refractory residues formed in an oceanic environment. This mantle stratigraphy may have formed in one of the following scenarios: (1) the earliest crust may have developed on pre-existing, depleted oceanic lithosphere which was subsequently thickened by underplating buoyant peridotite, refractory after komatiite extraction, (2) an extremely depleted (i.e. dunitic) lithosphere may have been enriched in  $SiO_2$  by addition from below (possibly from fluids off a subducting slab), however these fluids did not interact at shallow levels, or (3) Archean and post-Archean lithospheric mantle may have been juxtaposed through collisional tectonics, with the Archean portion thrust below the post-Archean portion.

References

- Boyd, F. R. (1989) Compositional distinction between oceanic and cratonic lithosphere. *Earth Planet. Sci. Lett.*, 96, 15-26.
- Cohen, R. S., R. K. O'Nions and J. B. Dawson (1984) Isotope geochemistry of xenoliths from East Africa: implications for development of mantle reservoirs and their interaction. *Earth Planet. Sci. Lett.*, 68, 209-220.
- Dawson, J. B., D. G. Powell and A. M. Reid (1970) Ultrabasic xenoliths and lava from the Lashaine volcano, northern Tanzania. *J. Petrol.*, 11, 519-548.
- Dawson, J. B. and J. V. Smith (1973) Alkalic pyroxenite xenoliths from the Lashaine volcano, northern Tanzania. *J. Petrol.*, 14, 113-131.
- Green, D. H. and M. E. Wallace (1988) Mantle metasomatism by ephemeral carbonatite melts. *Nature*, 336, 459-462.
- Hawkesworth, C. J., P. D. Kempton, N. W. Rogers, R. M. Ellam and P. W. van Calsteren (1990) Continental mantle lithosphere, and shallow level enrichment processes in the Earth's mantle. *Earth Planet. Sci. Lett.*, 96, 256-268.
- Jones, A. P., J. V. Smith and J. B. Dawson (1983) Glasses in mantle xenoliths from Olmani, Tanzania. *J. Geol.*, 91, 167-178.
- Kesson, S. E. and A. E. Ringwood (1989) Slab-mantle interactions 2. The formation of diamonds. *Chem. Geol.*, 78, 97-118.
- McDonough, W. F. (1990) Constraints on the composition of the continental lithospheric mantle. *Earth Planet. Sci. Lett.*, 101, 1-18.
- McDonough, W. F. and F. A. Frey (1989) Rare earth elements in upper mantle rocks. In B. R. Lipin and G. A. McKay, Eds., *Geochemistry and Mineralogy of Rare Earth Elements*, p. 99-145. Mineralogical Society of America, Washington, D.C.
- Meen, J. K. (1987) Mantle metasomatism and carbonatites; an experimental study of a complex relationship. *Geol. Soc. Am. Spec. Paper*, 215, 91-100.
- Nixon, P. H. (1987) Kimberlitic xenoliths and their cratonic setting. In P. H. Nixon, Eds., *Mantle Xenoliths*, p. 215-240. John Wiley & Sons, New York.
- Reid, A. M. and J. B. Dawson (1972) Olivine-garnet reaction in peridotites from Tanzania. *Lithos*, 5, 115-124.
- Reid, A. M., C. H. Donaldson, R. W. Brown, W. I. Ridley and J. B. Dawson (1975) Mineral chemistry of peridotite xenoliths from the Lashaine volcano, Tanzania. In L. H. Ahrens, J. B. Dawson, A. R. Duncan and A. J. Erlank, Eds., *Physics and Chemistry of the Earth*, p. 525-543. Pergamon Press, New York.
- Rhodes, J. M. and J. B. Dawson (1975) Major and trace element chemistry of peridotite inclusion from the Lashaine volcano, Tanzania. In L. H. Ahrens, J. B. Dawson, A. R. Duncan and A. J. Erlank, Eds., *Physics and Chemistry of the Earth*, p. 545-557. Pergamon Press, New York.
- Ridley, W. I. and J. B. Dawson (1975) Lithophile trace element data bearing on the origin of peridotite xenoliths, ankaramite and carbonatite from Lashaine volcano, N. Tanzania. In L. H. Ahrens, J. B. Dawson, A. R. Duncan and A. J. Erlank, Eds., *Physics Chem. Earth*, p. 559-569. Pergamon Press, New York.
- White, W. M. and P. J. Patchett (1984) Hf-Nd-Sr isotopes and incompatible element abundances in island arcs: implications for magma origins and crust-mantle evolution. *Earth Planet. Sci. Lett.*, 67, 167-185.

ULTRA-DEEP (> 300km), ULTRAMAFIC XENOLITHS:  
DIRECT PETROLOGICAL EVIDENCE FOR THE TRANSITION ZONE.

Sautter<sup>(1)</sup>, V.; Haggerty<sup>(2)</sup>, S.E.

(1) Lab. Geophysique, Bat. 510, Université Paris XI, 91405 Orsay, France;

(2) Dept. Geology, University of Massachusetts, 01003 Amherst, USA.

The seismologically delineated transition zone from 400 to 670 km depth is a fundamental discontinuity in the bulk Earth between the upper and the lower mantle. The mineralogy and chemistry of this inaccessible zone is of enormous interest but its petrology is highly controversial, mainly because of two competing models (pyrolite versus piclogite), but compounded by the uncertainty of whether the transition zone is the lower limit of ocean slab subduction (Anderson, 1989 ; Ringwood, 1975), or whether slabs continue to the core-mantle boundary. High pressure experiments predict that both pyroxene to garnet and olivine to  $\beta$ -spinel transformation occur at the 400 km seismic discontinuity. Natural analogs of pyroxene-garnet solid solution have recently been recognized in diamond inclusions from South Africa (Moore and Gurney 1985) and Brazil (Wilding et al. 1989) and represent the first mineralogical evidence from the transition zone. We present here the first petrological evidence from the 400 km discontinuity (Haggerty and Sautter, 1990 ; Sautter et al. 1991).

The xenoliths (24 samples) are from the Jagersfontein kimberlite pipe in South Africa. The biggest xenolith (9 x 5 cms) is a four phase garnet lherzolite (garnet, olivine, clinopyroxene, orthopyroxene). The rock is heterogeneous because garnet (15 to 10 % by volume) forms a 1 to 1.5 cm thick band throughout a matrix dominated by olivine (40 to 50 %) and orthopyroxene (30-40 %) and 5 to 10 % clinopyroxene. Other samples range from garnet-clinopyroxene-orthopyroxene associations to discrete garnet ; these specimens are less than 3 cm in diameter. A common feature of the entire set of samples is pyroxene exsolution rods within single garnet crystals that are parallel to apparent  $\langle 111 \rangle$  directions of the cubic host. Based on the crystal chemistry of pyroxene exsolution, the xenoliths are divided into two groups. The first group is

composed of purple garnet (1 to 2 % wt Cr<sub>2</sub>O<sub>3</sub>, Pyr<sub>69-73</sub>Alm<sub>15-20</sub>Gross<sub>11-12</sub>) with clinopyroxene exsolution (Jd<sub>13-20</sub>Wo<sub>36-43</sub>Hyp<sub>43</sub>) and attached single crystals of apple green clinopyroxene of similar composition ; the garnet lherzolite sample falls into this group. The second group is defined by discrete pink garnet crystals (up to 80 % mole of pyrope) with orthopyroxene exsolution (Mg/Mg + Fe = 0.95). In both groups, the garnet is of ultramafic affinity. Modal proportions, however, are higher for Cpx exsolution (between 85Gt:15Cpx and 70Gt:30Cpx) than for Opx exsolution (90Gt : 10Opx).

Primary garnet compositions are calculated by recombining the estimated quantity of pyroxene rods within the garnet host. This calculation rests on the interpretation of the present textures as conclusive evidence that the pyroxene exsolved from a homogeneous Ca-Na majorite. Exsolution induced by a disproportionation of a solid solution implies rigorous orientation of the crystalline precipitate within the host. Preliminary TEM observations indicate that the  $\langle 001 \rangle$  direction in the pyroxene rods is parallel to the  $\langle 111 \rangle$  direction in garnet. Such a relationship would minimize Si and Al diffusion paths as it matches the tetrahedral chains of Si in pyroxenes with the octahedral sites of garnet that contain both Si and Al under very high pressures (> 80 kbar). The relative orientation of the two phases is further described by (110) garnet parallel to (010) clinopyroxene.

Reconstitution of pyroxene in garnet in the MAS, CMAS, NCMAS systems and natural analogs require P of at least 100 kb (Fig.1). A conservative estimate is 130 kb, placing the xenoliths at or close to the 400 km seismic discontinuity. The seismic discontinuity thus appears to be due to the olivine to  $\beta$ -spinel transition as well as pyroxene dissolution in garnet. From these xenoliths and the high Si garnet inclusions in diamonds we infer that there is a mixture of eclogite and lherzolite at the discontinuity. Such data (on centimeter scale samples) do not permit, however, evaluation of the degree of chemical heterogeneity at those depths. Consequently a homogeneous pyrolitic mantle with centimeter wide eclogitic layers due to stretching of

oceanic slabs by convection, or a heterogeneous mantle with a chemical change from lherzolite to piclogite at the 400 km discontinuity due to piling up of oceanic slabs in the transition zone, are both valid petrological models. As presently constituted, the xenoliths have reequilibrated at 900-1000°C and 45 kb in the lithosphere prior to crustal emplacement. Upward transport at the head of a plume is proposed (Haggerty and Sautter, this volume).

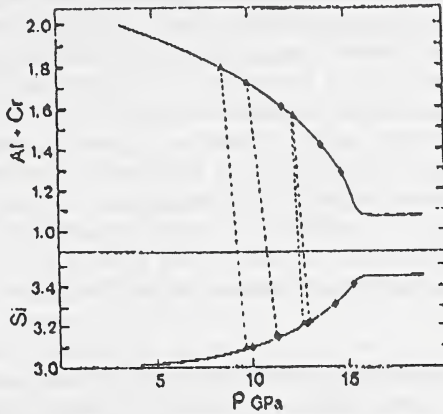


Figure 1 Geobarometer from Irifune (1987) and Akaogi and Akimoto (1979) : excess Si in garnet as a function of pressure. Solid triangles are the reconstructed garnet from Jagersfontein. The diamond symbols corresponds to garnet inclusions in diamonds.

- Anderson, D. L. (1989) *Theory of the Earth*, 366 p., Blackwell Scientific.
- Ringwood, A. E. (1975) *Composition and petrology of the Earth's Mantle*, 618 p. McGraw-Hill, New York.
- Moore, R.O. and Gurney, J.J. (1985) Pyroxene solid solution in garnets included in diamond. *Nature*, 318, 553-555.
- Wilding, M.C., Harte, B., and Harris, J.W. (1989) Evidence of asthenospheric source for diamonds from Brazil. *Extnd. Abstr. 23rd IGC*, 3, 359-360.
- Haggerty, S.E. and Sautter, V. (1990) Ultradeep (greater than 300 kilometres), ultramafic upper mantle xenoliths. *Science*, 248, 993-996.
- Sautter, V., Haggerty, S.E. and Field, S. (1991) Ultradeep (>300 km), ultramafic xenoliths : new petrologica evidence from the transition zone. *Science*, In press.

LOW-Ca GARNET HARZBURGITE XENOLITHS FROM SOUTHERN AFRICA:  
ABUNDANCE, COMPOSITION, AND BEARING ON THE STRUCTURE AND EVOLUTION  
OF THE SUBCRATONIC LITHOSPHERE.

*Daniel J. Schulze.*

*Department of Geology, University of Toronto, Erindale College, Mississauga, Ontario, Canada L5L 1C6.*

Most natural diamonds probably exist in the upper mantle as members of a low-Ca garnet harzburgite assemblage. Xenoliths of low-Ca garnet harzburgites (with or without diamonds) are purported to be rare, although xenocrysts of low-Ca Cr-pyrope derived from such rocks have been shown to exist in virtually all kimberlites on the Kaapvaal Craton in southern Africa (e.g., Boyd and Gurney, 1982; Gurney, 1985). This has led to suggestions that, relative to other types of mantle xenoliths, low-Ca garnet harzburgites disaggregate more readily upon eruption, yielding xenocrysts of diamond and low-Ca garnet, with few intact low-Ca garnet harzburgite xenoliths surviving (e.g., Boyd and Gurney, 1982; Gurney, 1985). In the present study, xenoliths of low-Ca garnet harzburgite were sought in the Kimberley dumps, and their abundance compared with estimates from garnet xenocryst populations of the Kimberley mines. Investigation of garnet xenocrysts was extended to include 11 additional kimberlites across the Kaapvaal Craton. Note that in similar, earlier studies only Cr-rich purple garnets were analyzed, and thus the data cannot be used to estimate the abundance of low-Ca garnet harzburgites in the upper mantle.

Garnet harzburgites constitute approximately 9% of the mantle xenolith population at Kimberley, (945 nodules studied by Schulze, 1986). As 11 of 45 garnet harzburgites analyzed contain Cr-pyropes with CaO contents lower than those from the Kimberley lherzolite field, approximately 2% of the Kimberley xenolith population is low-Ca garnet harzburgite. If only garnet-bearing xenoliths are considered (41% of the nodule suite), low-Ca garnet harzburgites constitute approximately 5% of the suite. Analysis of 469 garnets from the Wesselton, Du Toit's Pan, and Bultfontein mines yielded an average value of about 5% for low-Ca garnets among the entire garnet population (Table 1). If 41% of Kimberley ultramafic xenoliths are garnet-bearing, the garnet xenocryst data yield a value of 2% low-Ca garnet harzburgite for the mantle sampled by the Kimberley kimberlites.

At the Finsch Mine, low-Ca garnets constitute approximately 6% of the garnet xenocryst population (Table 1). Three low-Ca garnet harzburgites (one diamond-bearing) have been identified in a suite of 104 garnet peridotites at Finsch, approximately 3% of the peridotite population (Gurney, 1985; Skinner, 1986; Viljoen et al., ms in preparation). At both Kimberley and Finsch, therefore, low-Ca garnet harzburgites are present in the xenolith suites in abundances that approximately agree with estimates from the garnet xenocryst population. There is no need to invoke the presence of interstitial magnesite or liquid to cause preferential disaggregation of this type of nodule (e.g., Boyd and Gurney, 1982).

Elsewhere on the Kaapvaal Craton, garnet xenocryst populations yield similarly low values for low-Ca garnet harzburgites, with locally significant exceptions (Table 1). High values for volume abundance of low-Ca garnet harzburgite (as calculated for peridotite-eclogite ratios by Schulze, 1989) exist in the Boshof kimberlite cluster (13% at Blaauwbosch, 21% at Roberts Victor, 34% at New Elands) and at Eendrag (23%) and

Star (27%). At Bobbejaan, Kaalvallei, Lace and Premier values are 3-8%, with an apparently smaller, but uncertain, quantity at Balmoral. In contrast to the present estimate for low-Ca garnet harzburgite abundance at Premier (6%), 19% of the garnet peridotite nodules studied by Danchin (1979) are low-Ca garnet harzburgites. The reason for this difference is unknown. A similarly high abundance (25%) was reported for the xenolith suite at the Zero kimberlite (Shee et al., 1989).

Many of the Kimberley low-Ca garnet harzburgites have zoned garnets, with rims typically enriched in Ca and either enriched or depleted in Cr, relative to cores. Changes are in the direction of garnets in the lherzolite field. All other minerals are homogeneous and magnesian (e.g.,  $Mg/(Mg+Fe) = 0.929 - 0.949$  in olivine).

Both Kimberley and Finsch low-Ca garnet harzburgite equilibrated on a steady-state subcontinental geothermal gradient. At Kimberley they are within the range of equilibration of the majority of garnet lherzolites (1000°C, 42 kb to 1150°C, 56 kb), whereas the Finsch low-Ca garnet harzburgites overlap with, but are mostly shallower than, Finsch garnet lherzolites (Skinner, 1986; Viljoen et al., ms in preparation). Similarly, low-Ca garnet harzburgites studied by Boyd and Nixon (1988) apparently equilibrated throughout the subcratonic lithosphere, and not at any specific depth, and all of the examples from the Zero pipe equilibrated in the graphite stability field (Shee et al., 1989). There is thus no evidence for low-Ca garnet harzburgites being concentrated in a "root" to the lithosphere.

Late Ca-metasomatism, similar to that inferred to be the cause of zoning in the Kimberley low-Ca garnet harzburgites, can also be inferred for other localities. Though zoning has not been recognized in the Finsch low-Ca garnet harzburgites, they, and many Finsch garnet xenocrysts (e.g., Group B of Gurney, 1985), are intermediate in composition between garnet lherzolites (>4% CaO) and most garnets in diamonds at Finsch (<2% CaO). Furthermore, at Liphobong, Dawson et al. (1978) documented a low-Ca garnet harzburgite in which garnet rims are Ca-enriched relative to cores.

In conclusion, low-Ca garnet harzburgites are thought to exist beneath the Kaapvaal craton as small, isolated bodies scattered vertically and horizontally throughout a lherzolite-dominated lithosphere, generally in low volume (3-6%), though locally abundant (to 35%). Subsequent to acquiring their low-Ca signature (and diamonds), Ca was reintroduced into the low-Ca garnet harzburgites on a wide scale, perhaps through diffusive exchange with surrounding garnet lherzolite. Uniformly low-Ti argues against involvement of a silicate melt.

#### REFERENCES

- Boyd, F.R., and Gurney, J.J. (1982) Low-calcium garnets: Keys to craton structure and diamond crystallization, Carnegie Inst. Wash. Year Book, 81, pp. 261-266.
- Boyd, F.R., and Nixon, P.H. (1988) Low-Ca garnet harzburgites: Origin and role in craton structure, Ann. Rept. Dir. Geophys. Lab., 1987-1988, pp. 8-13.
- Dawson, J.B., Smith, J.V., and Delaney, J.S. (1978) Multiple spinel-garnet peridotite transitions in the upper mantle: Evidence from a harzburgite xenolith, *Nature*, 273, pp. 741-743.
- Danchin, R.V. (1979) Mineral and bulk chemistry of garnet lherzolite and garnet harzburgite xenoliths from the Premier Mine, South Africa, in *The Mantle Sample: Inclusions in Kimberlites, and Other Volcanics*, F.R. Boyd and H.O.A. Meyer, eds., AGU, Washington, D.C., 104-126.

- Gurney, J.J. (1985) A correlation between garnets and diamonds in kimberlites, in *Kimberlite Occurrence and Origin: A Basis for Conceptual Models in exploration*, J.E. Glover and P.G. Harris, eds., Univ. W. Australia Pub. 8, pp. 143-166.
- Schulze, D.J. (1986) Quantitative estimation of relative xenolith abundances of ultramafic xenoliths, Kimberley, South Africa, *Geol. Soc. Amer. Abstr. Prog.*, 18, p. 742.
- Schulze, D.J. (1989) Constraints on the abundance of eclogite in the upper mantle, *Journal of Geophysical Research*, 94, 4205-4212.
- Shee, S.R., Bristow, J.W., Bell, D.R., Smith, C.B., Allsopp, H.L., and Shee, P.B. (1989) The petrology of kimberlites, related rocks, and associated mantle xenoliths from the Kuruman Province, South Africa, in *Kimberlites and Related Rocks Volume I: Their composition, occurrence, origin and emplacement*, J. Ross, ed., Blackwell, Carlton, Australia, pp. 61-82.
- Skinner, C. (1986) A study of peridotites from Finsch, B.Sc. thesis, Univ. Cape Town.

Table 1. Relative abundances of rock types sampled by kimberlites on the Kaapvaal Craton, in volume percent, as determined from garnet xenocryst populations.

Kimberlite	Rock Type*			
	L	H	W	E
Finsch	94	6	0 <sup>+</sup>	tr <sup>+</sup>
Bultfontein	93	6	1	tr
Du Toit's Pan	94	6	0	tr
Wesselton	96	3	0	1
Balmoral	99	? <sup>#</sup>	0	tr
Eendrag	72	23	4	1
Bobbejaan	95	3	0	3
Blaauwbosch	81	13	3	3
New Elands	62	34	0	4
Roberts Victor	61	21	3	16
Star	71	27	0	2
Kaalvallei	89	3	0	8
Lace	83	8	0	10
Premier	91	6	3	0

\* Rock type abbreviations: L = lherzolite, H = harzburgite, W = wehrlite, E = eclogite.

<sup>+</sup> A value of 0 indicates that garnets from this rock type were not found in the garnet population, tr indicates garnets from this rock type are present in the garnet population, but represent less than one percent by volume.

<sup>#</sup> Balmoral garnets include some that are marginally, but not clearly, lower in CaO than most of those in the lherzolite field, which is not well defined at this pipe.

## CARBON ISOTOPE COMPOSITION OF GRAPHITE IN MANTLE ECLOGITES.

Schulze<sup>(1)</sup>, D.J.; Valley<sup>(2)</sup>, J.W.; Viljoen<sup>(3)</sup>, K.S. and Spicuzza<sup>(2)</sup>, M.

(1) Department of Geology, University of Toronto, Erindale College, Mississauga, Ontario, Canada; (2) Department of Geology and Geophysics, University of Wisconsin, Madison, Wisconsin, USA; (3) Anglo American Research Laboratories, Johannesburg, South Africa.

The carbon isotopic composition of diamond is reasonably well-known from measurements on hundreds of diamonds of known paragenesis. With very few exceptions,  $\delta^{13}\text{C}$  values of peridotite-suite diamonds are in the restricted range -2 to -9‰<sub>PDB</sub>, whereas  $\delta^{13}\text{C}$  for eclogitic diamonds ranges from approximately +2 to -34‰<sub>PDB</sub> (e.g., Sobolev et al., 1979; Deines, 1980; Harris, 1987). In contrast to this large data set, few isotopic data have been published for either eclogitic or peridotitic mantle-derived graphite. Values of  $\delta^{13}\text{C}$  for primary graphites from peridotite xenoliths (-4.8 to -10.04‰; Kropotova and Fedorenko, 1970; Pearson et al., 1990; Schulze and Valley, in press) are similar to those from peridotitic diamonds. Existing carbon isotope data for graphite in mantle eclogites from Mir (Kropotova and Fedorenko, 1970), Roberts Victor (Deines et al., 1987), and Orapa (Deines et al., 1991) are, with one exception, in the "typical mantle range" (-3.98 to -8.7‰<sub>PDB</sub>). Graphite from a Schaffer, Wyoming kyanite eclogite (Schulze and Valley, in press) is unusually light, with  $\delta^{13}\text{C} = -14.31\text{‰}$ . An additional anomalous graphite analysis ( $\delta^{13}\text{C}$  of -20.3‰) was reported by Deines et al. (1991) for a corundum-garnet-spinel assemblage of uncertain affinity, also from Orapa. To enlarge the data base for mantle-derived graphites, we present carbon isotope data for graphites from 23 eclogite xenoliths, from the Bellsbank and Jagersfontein kimberlites in South Africa and the Orapa and Letlhakane kimberlites in Botswana.

Most of our new data (Table 1) are normally distributed about a  $\delta^{13}\text{C}$  value near -5 to -6‰. Interesting features in this new data set include a very light value of -12.50‰ for an eclogite from Letlhakane, and the fact that 3 of the 8 Bellsbank samples have a  $\delta^{13}\text{C}$  value near -2.9‰. These latter values are unusually heavy, relative to the strong peaks for both eclogitic and peridotitic diamonds at approximately -6‰, but are similar to many of the  $\delta^{13}\text{C}$  values for loose diamonds of unknown affinity from Bellsbank. One third of the diamonds from the Dan Carl Mine at Bellsbank reported by Deines (1980) have  $\delta^{13}\text{C}$  values in the range -2 to -3‰.

Graphites from mantle eclogites thus appear to have an overall  $\delta^{13}\text{C}$  distribution similar to eclogite-suite diamonds. In both suites there is a strong peak near -6‰, with a significant number of samples at lower and higher values, although the relatively few graphites do not define as wide a range of  $\delta^{13}\text{C}$  values as does the larger eclogitic diamond population.

The origin of the isotopically light and heavy eclogitic diamonds is controversial. Considered in isolation, the range of  $\delta^{13}\text{C}$  values for both eclogitic diamonds and graphites could be explained by several different processes. These include precipitation of native carbon from  $\text{CO}_2$  and  $\text{CH}_4$  vapours through Rayleigh fractionation, isotopic inhomogeneity in the mantle remaining since the accretion of the Earth, and subduction

of oceanic basalt containing crustal biogenic and carbonate carbon (e.g., Deines, 1980; Kirkley and Gurney, 1989). Only the subduction hypothesis, however, adequately accounts for many of the other characteristics of mantle eclogites, characteristics such as positive Eu anomalies and anomalously high and low  $\delta^{18}\text{O}$  and  $\delta^{34}\text{S}$  values, that defy explanation in terms of mantle igneous processes.

We suggest that the anomalous  $\delta^{13}\text{C}$  values for graphite in mantle eclogites support the subduction hypothesis. Furthermore, the model of Helmstaedt and Schulze (1989) of the formation of the subcratonic lithosphere by tectonic emplacement of ocean-floor material beneath the cratons can be extended to include even the shallow portion of the lithosphere represented by rocks from the graphite stability field.

Table 1. Carbon isotope composition of graphite from mantle eclogites, analyzed at the University of Wisconsin.

Location	Sample	$\delta^{13}\text{C}_{\text{PDB}}$	
Lethakane	JSL-200	-5.54	
	JSL-201	-5.69	
	JSL-202	-5.37	
	JSL-204	-7.68	
	JSL-206	-12.50	
	JSL-207	-5.68,	-5.75
	JSL-208	-5.98	
Jagersfontein	K7/555	-5.90	
Bellsbank	K64/124	-2.94	
	K64/128	-5.69	
	K64/129	-7.04	
	K64/133	-2.95	
	K64/134	-2.84	
	K64/147	-5.38	
	K64/149	-4.96	
K64/169	-5.47		
Orapa	K1/399	-6.55	
	K1/400	-6.19	
	K1/401	-6.23	
	K1/402	-4.64,	-4.71
	K1/403	-5.67	
	K1/404	-6.29	
	K1/406	-6.00	

## REFERENCES

- Deines, P., Harris, J.W., Robinson, D.N., Gurney, J.J., and Shee, S.R. (1991) Carbon and oxygen isotope variations in diamond and graphite eclogites from Orapa, Botswana, and the nitrogen content of their diamonds. *Geochimica et Cosmochimica Acta*, 55, 515-524.
- Deines, P., Harris, J.W., and Gurney, J.J. (1987) Carbon isotopic composition, nitrogen content and inclusion composition of diamonds from the Roberts Victor kimberlite, South Africa. *Geochimica et Cosmochimica Acta*, 51, 1227-1243.
- Deines, P. (1980) The isotopic composition of diamonds: Relationship to diamond shape, color, occurrence and vapor composition. *Geochimica et Cosmochimica Acta*, 44, 943-961.
- Harris, J.W. (1987) Recent physical, chemical, and isotopic research of diamond. In P.H. Nixon, Ed., *Mantle xenoliths*, p.477-500. Wiley, London.
- Helmstaedt, H., and Schulze, D.J. (1989) South African kimberlites and their mantle sample - Implications for Archean tectonics and lithosphere evolution. In J.Ross, Ed., *Kimberlites and related rocks Volume II: Their composition, occurrence, origin and emplacement*, p.358-368. Blackwell, Carlton, Australia.
- Kirkley, M.B., and Gurney, J.J. (1989) Carbon isotope modelling of biogenic origins for carbon in eclogitic diamonds. 28th International Geological Congress, Workshop on Diamonds, Extended Abstracts, 40-43.
- Kropotova, O.I., and Fedorenko, B.V. (1970) Carbon isotope composition of diamond and graphite from eclogite. *Geokhimiya*, 10, 1279 (in Russian).
- Pearson, D.G., Boyd, F.R., and Nixon, P.H. (1990) Graphite-bearing mantle xenoliths from the Kaapvaal Craton: Implications for graphite and diamond genesis. Annual Report of the Director of the Geophysical Laboratory, 1989-1990, 11-19.
- Schulze, D.J., and Valley, J.W. (in press) Carbon isotope composition of mantle graphite: Anomalously light carbon subducted into the shallow subcontinental lithosphere (abs.) Geological Association of Canada/Mineralogical Association of Canada Annual Meeting, Toronto, May, 1991.
- Sobolev, N.V., Galimov, E.M., Ivanovskaya, I.N., and Yefimova, E.S. (1979) The carbon isotope compositions of diamonds containing crystallographic inclusions. *Doklady Akademii Nauk SSSR*, 249, 1217-1220.
- Valley, J.W., and O'Neil, J.R. (1981)  $^{13}\text{C}/^{12}\text{C}$  exchange between calcite and graphite: A possible thermometer in Grenville marbles. *Geochimica et Cosmochimica Acta*, 45, 411-419.

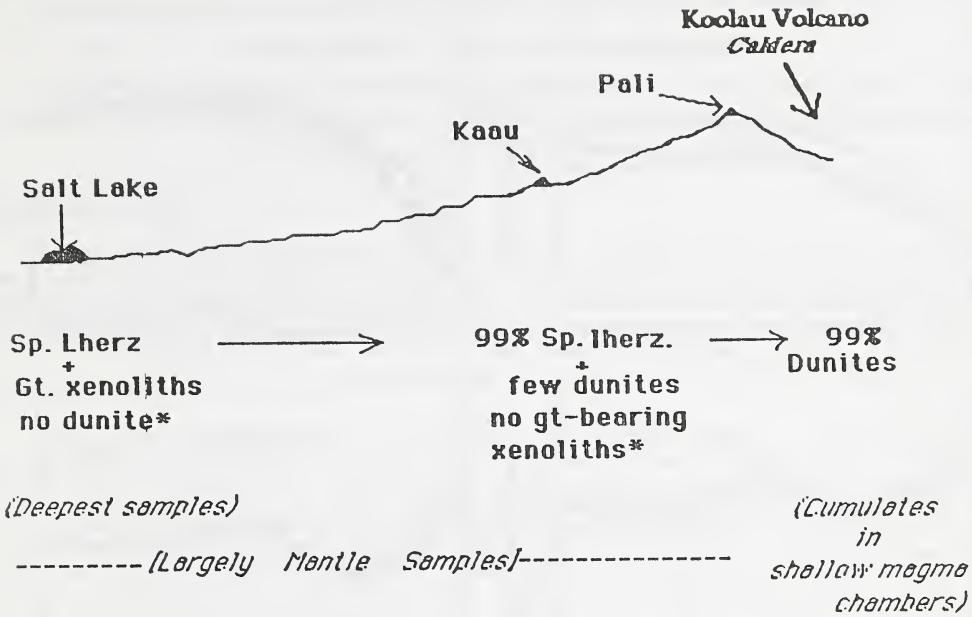
ON THE SCALE OF HETEROGENEITIES IN CLINOPYROXENES OF SPINEL LHERZOLITE  
XENOLITHS FROM OAHU, HAWAII: IMPLICATIONS FOR NON-MODAL  
ADVECTION-DIFFUSION CONTROLLED TRACE ELEMENT ENRICHMENT.

*G. Sen*

*Department of Geology, Florida International University, Miami, Florida 33199.*

Ion and electron microprobe investigation of clinopyroxenes of Hawaiian spinel lherzolite xenoliths was undertaken to examine the scale of major, minor, and trace element variabilities in the Hawaiian upper mantle. A total of about 50 xenoliths were examined, and these come from Kaau, Pali, Kalihi and Salt Lake vents of the post-erosional Honolulu Volcanics (Fig. 1). Kalihi, Kaau and Pali vents occur close to the caldera area of the Koolau shield volcano, and Salt Lake is situated on the apron of the volcano. Thus, the premise of this study was also to document 3-D variations in the spinel lherzolitic lithosphere on a km-scale beneath an extinct hot spot generated volcano that had also suffered post-erosional magmatism. Whereas opxs are LREE-depleted in all xenoliths, cpxs show a large range:  $[Ce/Sm]_{c.n.} = 0.2-2.7$  (Fig. 2). Salt Lake cpxs mostly exhibit LREE-enriched to convex upward REE patterns and only one xenolith shows slightly depleted pattern (Fig. 2). Kaau and Pali xenoliths vary from depleted to enriched types. Transitional "Spoon"-shaped (concave upwards between La and Eu) patterns also occur in all the xenoliths close to the Koolau caldera, but are notably absent in the Salt Lake suite. In individual xenoliths strong intergrain and intragrain REE variation exists. A cpx grain with a spoon-shaped pattern and lower absolute REE contents occurs in the same rock containing another grain with strongly LREE-enriched pattern. Cores are commonly LREE-depleted or spoon-shaped whereas the rims are strongly LREE-enriched or spoon-shaped with higher REE abundance. In composite xenoliths from Salt Lake, cpxs in the pyroxenite (vein) and lherzolite (wall) both have convex-upward REE pattern, and the absolute abundances increase in the wall rock cpx as the vein is approached. It is clear that the starting (protolith) cpx was strongly depleted in LREE (as would be expected of a N-MORB depleted residue. Later non-modal enrichment was caused by fluids related to two periods of magmatic activity - Koolau (tholeiitic) and Honolulu (post-erosional alkalic). The nature of the variations (collectively & individual cpxs) suggests that selective and differential enrichment of LREEs (but no enrichment Eu-to-Yb) occurred, and it is proposed that the process was an advection-diffusion controlled mechanism. Overall, origin of these heterogeneities is attributed to a combination of the following processes: First, fusion and heterogeneous extraction of northern Pacific MORBs depleted the lithosphere. Second, internal deformation (matrix deformation during melt extraction) and metamorphic segregation processes resulted in the development of porphyroclastic texture and mineral foliation. Third, migrating fluid leaving the asthenosphere cracked and reacted with the lithosphere. Fourth, heating of the lithosphere largely by transient Hawaiian magmas while moving over the hot spot caused the lithosphere to thin, resulting in the conversion of the lower garnet lherzolite layer into a spinel+pyroxene cluster bearing lherzolite (LREE-depleted) of the type found in Pali. Passing Koolau magmas may have further depleted the spinel lherzolite lithosphere in incompatible elements while enriching it in Fe. Finally, significant coarsening of grain size, veining, stoping, Fe, LREE, and Na-enrichment and hydrous mineral precipitation along cracks within the lithosphere occurred during interaction of the lithosphere with parental magmas of the post-shield Honolulu magmas derived from the asthenosphere.

### Summary Diagram



### Spinel lherzolite Clinopyroxene Characteristics

Salt Lake	Kaau	Pali	Ulupou/Kalihi
Na,Cr content higher than in other vents; & these values are not correlated with [Fo]ol	Na,Cr contents lower; & Na increases with increasing [Fo]ol		Similar Na,Cr as in Kaau & Pali

Fig. 1 Distribution of xenoliths in Honolulu Volcanics

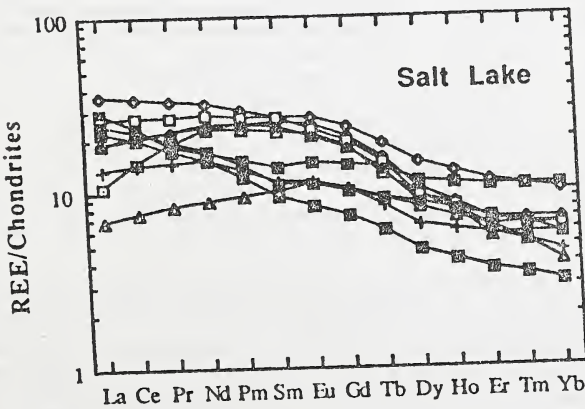


Fig. 2 REE/Chondrite plots for cpx in spinel lherzolites from Oahu. Elements analyzed are: La, Ce, Nd, Sm, Eu, Dy, Er, Yb. Others are interpolated.

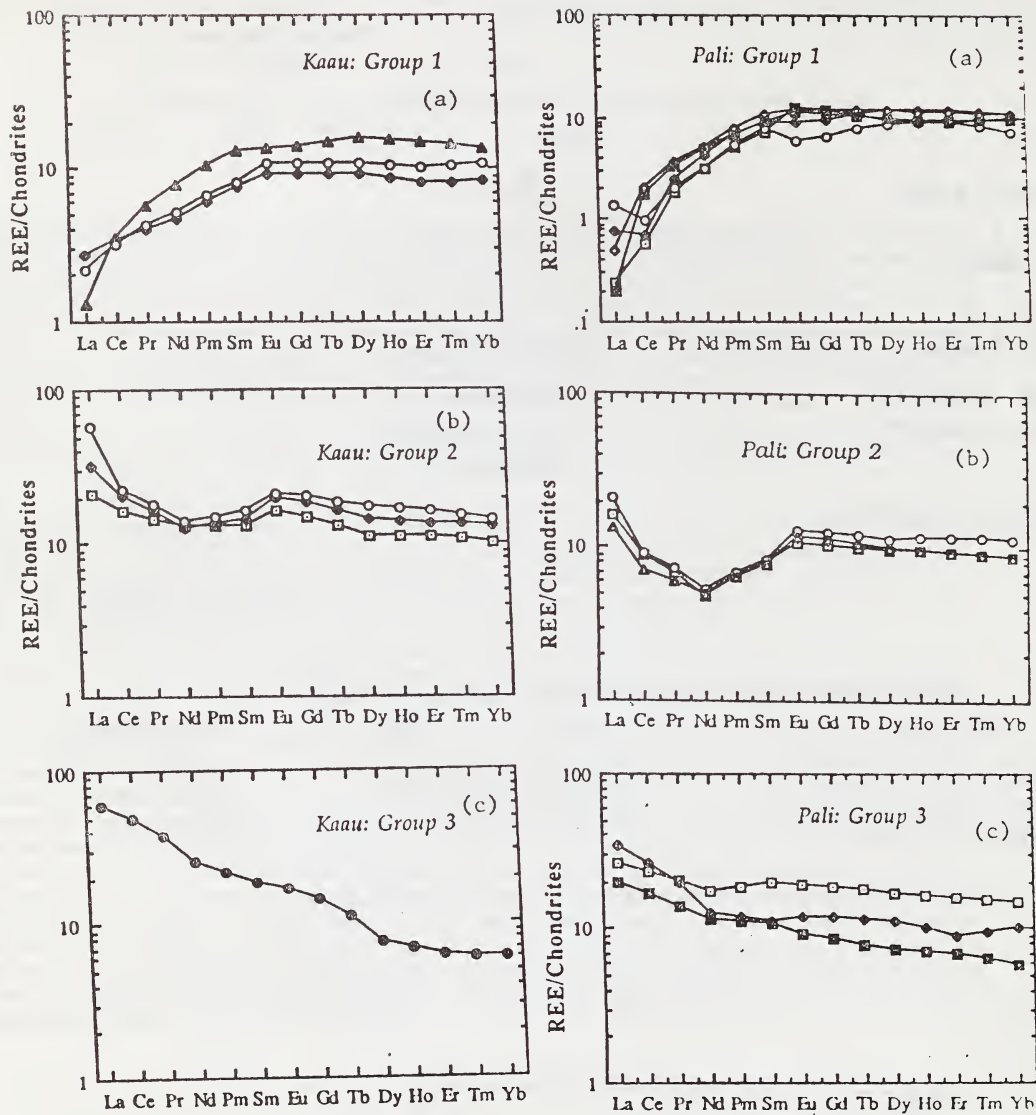


Fig.2 .... Continued.

PETROGRAPHY AND GENERAL CHEMICAL FEATURES OF POTASSIC MAFIC TO  
ULTRAMAFIC ALKALINE VOLCANIC ROCKS OF MATA DA CORDA FORMATION,  
MINAS GERAIS STATE, BRAZIL.

Sgarbi<sup>(1)</sup>, P.B.A. and Valença<sup>(2)</sup>, J.G.

(1) Instituto de Geociências, Universidade Federal de Minas Gerais. Av. Antonio Carlos, 6627 - 31270 Belo Horizonte - MG; (2) Instituto de Geociências, Universidade Federal do Rio de Janeiro. Cidade Universitária - Ilha do Fundão - CEP 21910. Rio de Janeiro - RJ, Brazil.

## INTRODUCTION

This abstract focuses on relevant petrographic and chemical features of kamafugitic lavas of the Mata da Corda formation, cropping out near the town of Carmo do Paranaíba (western Minas Gerais state). The studied area (approximately, 450 km<sup>2</sup>) constitutes part of the Cretaceous Sanfranciscan basin.

## GEOLOGY

The rock succession in the Sanfranciscan basin represented by the Areado (hereafter called AR) and Mata da Corda (hereafter called MT) formations, is 500 m thick and unconformably overlies folded metapelites of the Upper Proterozoic Bambuí group. The AR formation (Lower Cretaceous) consists of fluvial polymictic conglomerates (Abaete member), lacustrine shales, sandstones, limestones and marls (Quirico member), and aeolian and fluvio-deltaic sandstones (Tres Barras member). The MT formation (Upper Cretaceous) overlies the latter formation, from which is separated by local erosive unconformities. It comprises a 40 to 60 m thick pile of K-rich mafic to ultramafic alkaline lavas (Patos facies), volcanic conglomerates and sandstones (Capacete facies) and clayey sandstones with little volcanic contribution (Urucuaia facies). The lavas and non-volcanoclastic rocks have a larger spatial distribution and are volumetrically more significant than the volcanoclastic rocks. The lavas form small exposures (frequently, very weathered) of massive, thin horizontal and subhorizontal, poorly-vesiculated flows (in places, individually, not exceeding 0.5 m thick). In some outcrops, the extrapolated thickness of a sequence of flows may reach 10 m.

## PETROGRAPHY

Under the IUGS scheme (Streckeisen, 1980) the MT lavas are ultramafitites, mafitites, leucitites and kalsilitites (hereafter, called, respectively ULT, MAF, LEU and KAL). These ULT and MAF have unidentified felsic phase(s) and estimated values (vol. %) of mafic index from 80 to 70 and 60 to 70, respectively; whereas the LEU and KAL contain leucite (pseudomorphs) and kalsilite (pseudomorphs and fresh and clear grains), and get their names from that felsic phase present in larger amount. In addition, the lavas are all feldspar-free, with abundant clinopyroxene (mostly, diopside), perovskite and Ti-magnetite, and very fine to medium-grained porphyritic to seriated textures. An interstitial material is always present and often intensely altered to zeolites and clay minerals. In some rocks it has been determined as kalsilite based on electron microprobe analysis; but in other rocks this material could not be accurately identified and it has been modally considered as an unidentified felsic phase.

The ULT and MAF are porphyritic to seriated rocks. The porphyritic types show phenocrysts (up to 20 vol.%, and 0.2 to 2.0 mm in size) of olivine (Fo<sub>91-85</sub>), clinopyroxene (diopside), perovskite, Ti-magnetite, melilite (euhedral and subhedral pseudomorphs), apatite and phlogopite (rarely, as 3.0 mm large plates). The very fine to fine-grained groundmass has clinopyroxene (diopside, up to 50%), Ti-magnetite, perovskite, unidentified interstitial material, and may also contain minor amounts of phlogopite and apatite. The seriated types have coarser grains but are modally and mineralogically akin to the previous types.

The LEU and KAL are very similar fine to medium-grained rocks, very frequently, with a typical seriated texture. Some of them, however, may develop textures which resemble those of the ULT and MAF Mineralogically. The LEU and KAL are similar to the latter groups of rock, with the exception that they contain leucite (subhedral pseudomorphs) and kalsilite (euhedral pseudomorphs and/or anhedral fresh grains). Both feldspathoids occur as essential phases in the seriated LEU and KAL or in the very fine-grained intergranular groundmass of the porphyritic LEU. In these porphyritic rocks, the feldspathoids, in spite of being found in the groundmass, are absent from the phenocrysts and microphenocrysts, which consist of clinopyroxene (diopside to salite), Ti-magnetite, apatite and perovskite.

The above mentioned rocks (usually, the fine-grained types) may contain scarce and small (mostly, < 20 mm across) cognate inclusions of fine to medium-grained cumulate rocks, consisting of diopside, perovskite, Ti-magnetite, phlogopite and kalsilite. Most commonly, the inclusions are of kalsilite pyroxenites, but more rarely, perovskite modally dominates and they become kalsilite "perovskitites". In both cases, kalsilite is an interstitial phase.

## CHEMISTRY

Twenty-three samples of the MT lavas have been chemically analysed (results not fully given). These data indicate that: (1) the lavas are all ultrabasic and the majority falls into two distinct groups (GI and GII), according to the  $K_2O/Na_2O$  and  $K_2O$  values. GI is potassic and has (WT%)  $SiO_2=38-42$ ,  $TiO_2=5-7$ ,  $Al_2O_3=5-8$ ,  $Fe_2O_3>4<5$ ,  $FeO=8-9$ ,  $MgO=8-14$ ,  $CaO=11-17$ ,  $K_2O=1-3$ , and  $Na_2O>0-2$ ; whereas GII is ultrapotassic, with (WT%)  $SiO_2=43-45$ ,  $TiO_2=5-6$ ,  $Al_2O_3=7-9$ ,  $Fe_2O_3>3<4$ ,  $FeO=7-9$ ,  $MgO=6-9$ ,  $CaO=8-12$ ,  $K_2O=4-7$  and  $Na_2O>0-2$ . (2) In the  $Na_2O+K_2O$  versus  $SiO_2$  plot, the compositions delineate a broad trend from moderately (GI) to strongly (GII) alkaline. (3) The compositional spectrum of the lavas shows mainly non-linear variation trends of increasing  $SiO_2$ ,  $Al_2O_3$ ,  $K_2O$ ,  $Na_2O$ , Nb, Zr and Y, and decreasing FeO, CaO, Cr and Co, with decreasing MgO. (4) Discrimination diagrams using  $SiO_2$ , CaO, MgO, and FeO (total iron) exhibit most lava compositions in fields of kamafugitic affinity.

## SUMMARY AND CONCLUSIONS

The evidence on the Mata da Corda (MT) lavas in this work suggests that: (1) Because of the uncertainties in the mineralogy and modal analysis it is difficult to establish a clear correspondance between petrographic and chemical (potassic and ultrapotassic) groups for these lavas. (2) The observed chemical compositional variations of the lavas are consistent with an evolutionary general trend from potassic, Mg-richer and moderately alkaline to ultrapotassic, Mg-poorer and strongly alkaline members. Low-pressure crystal fractionation of clinopyroxene, olivine, perovskite and magnetite, probably controlled this trend. (3) Cretaceous "lamproites" (Leonardos *et al.*, 1990) and kimberlites and lamprophyres (Svisero *et al.*, 1979) have been reported in the general region, but the available petrography, mineralogy and chemistry of the Cretaceous K-rich MT lavas, in the area, are more compatible with a kamafugitic affinity.

## REFERENCES

- Leonardos, O.H., Ulbrich, M. & Gierth, E. (1990). "Lamproitos": uma fonte alternativa para os diamantes do Alto Paranaíba. XXXVI<sup>o</sup> Congresso Brasileiro de Geologia, Bol. de Resumos, 120.
- Streckeisen, A. (1980). Classification and nomenclature of volcanic rocks, carbonatites and melilitic rocks. IUGS subcommission on the systematics of igneous rocks. Geologische Rundschau 69, 194-207.
- Svisero, D.P., Hasui, Y. & Drumond, D., (1979). Geologia de Kimberlitos do Alto Paranaíba, Minas Gerais (Geology of kimberlites of the Upper Paranaíba, Minas Gerais). Min. Metall. 42 34-38.

THE PETROLOGY OF THE WESSELTON KIMBERLITE SILLS,  
KIMBERLEY, CAPE PROVINCE, SOUTH AFRICA.

*Shee<sup>(1)</sup>, S.R. and Clement<sup>(2)</sup>, C.R.*

*(1) Stockdale Prospecting Limited, South Yarra, Australia;*

*(2) Geology Dept. (Diamond Division), AAC, Johannesburg, RSA.*

A major complex of kimberlite sills and associated dykes are exposed in water drainage galleries developed in country rocks at the 40 metre level surrounding the Wesselton Mine. They were discovered in 1976 by C.R. Clement, E.M.W. Skinner and L. Kleinjan of the Geology Department, DBCM Ltd.

The sills intrude the contact zone between the upper Dwyka shales (upper Carboniferous, 310 - 280 my) and a Karoo dolerite sill (195 - 135 my). It is apparent that the competent nature of the dolerite sills prevented the breakthrough of the kimberlite magma and promoted the formation of kimberlite sills (Hawthorne, 1968). The sill and dyke complex predates the pipe (88.6 + 0.8 my; Smith, 1983a) and is cut by it. The sills are extensive and Clement (1982) has estimated that prior to the emplacement of the pipe they extended over an area of 70 hectares. The sills have a maximum thickness of 5 metres but are generally <1 metre thick (Hill, 1977). Individual sills range between a few centimetres and 0.5 metres in thickness and extend over horizontal distances of several hundred metres. Such features indicate the original presence of a highly mobile magma and baking of the adjacent shales testify to relatively high intrusion temperatures (Clement, 1982). The Wesselton sills display many of the structures recorded from the Benfontein complex by Dawson and Hawthorne (1973). These include prominent layering and magmatic sedimentation features.

Hill (1977) mapped two different types of hypabyssal facies kimberlites in the sill complex. The first variety is an altered aphanitic kimberlite containing rare macrocrysts. Serpentinised olivine phenocrysts are set in a fine grained matrix of calcite, phlogopite, spinel, ilmenite, perovskite, serpentine and apatite. Carbonate-rich segregations or diapirs in this kimberlite sill type have been described by Mitchell (1984). The second variety of kimberlite occurring in the sills is an unaltered macrocrystic kimberlite which contains small, scattered mantle derived harzburgite xenoliths, anhedral olivine macrocrysts and smaller, euhedral olivine phenocrysts set in a fine grained base. The matrix contains variable amounts of calcite, monticellite, phlogopite, spinel, ilmenite, perovskite, apatite and serpentine (Shee, 1985). The sills are Group 1 kimberlites (Smith, 1983 a and b). Most of the dykes associated with the sill complex are altered, aphanitic varieties and can be correlated with the first type of sill kimberlite. Only a few of the dykes are fresh, macrocrystic kimberlites and correspond to the second type of sill kimberlite. The latter kimberlite type forms the subject of this study.

Whole rock geochemical analyses reveal that the macrocrystic sill kimberlites are less MgO-rich (18.9 - 20.3 wt %) than the macrocrystic main pipe kimberlites (27.1 - 33.4 wt %) at Wesselton. This is mainly a function of the relative paucity of anhedral olivine macrocrysts in the sills (8 - 11 vol %) compared to the main pipe intrusions (26 - 33 vol %). The relatively high CaO contents of the sill kimberlites (13.8 - 15 wt %) compared to the main pipe kimberlites (6.40 - 9.50 wt %) is reflected in the high modal abundance of groundmass monticellite (22 - 32 vol %) in the former compared to the latter (4 - 9 vol %) (Shee, 1985). Olivine phenocryst cores in the sills have bimodal compositions but the rims have a common composition. Average compositions of the two core populations and rims are :

1 : Fo 92.9, 0.38 wt % NiO, 0.10 wt % MnO, CaO not detected.  
 2 : Fo 86.5, 0.25 wt % NiO, 0.17 wt % MnO, 0.11 wt % CaO.  
 Rims : Fo 86.9, 0.17 wt % NiO, 0.21 wt % MnO, 0.17 wt % CaO.

Groundmass phlogopites in the sill kimberlites have higher mean TiO<sub>2</sub> and lower mean MgO (2.29 wt % and 23.7 wt % respectively) than groundmass phlogopites from the main pipe intrusions (means 1.27 wt % TiO<sub>2</sub> and 24.8 wt % MgO). The sill phlogopites have higher BaO contents (0.05 - 5.55, mean 1.37 wt %) than the main pipe groundmass phlogopites (nd - 1.97, mean 0.30 wt %). These features indicate that the sill phlogopites have crystallised from a relatively more evolved magma. The sill phlogopites have bimodal compositions with respect to Al<sub>2</sub>O<sub>3</sub> contents (9 - 10 and 14 - 18 wt %) indicating two periods of phlogopite growth.

Orange, anhedral aluminous chromites with low TiO<sub>2</sub> contents have similar compositions to orange fingerprint chromites in harzburgite xenoliths in the sill kimberlites and are thought to be xenocrysts derived from the disaggregation of such xenoliths. These xenocrysts are not in equilibrium with the kimberlite magma and have been mantled by opaque titanomagnetites which have similar compositions to those occurring as discrete euhedral crystals in the groundmass. Euhedral chromites and titanomagnetites occur as inclusions within olivine phenocrysts in the sill kimberlite, a feature which is not seen in the main pipe intrusions. The sill groundmass spinels show a normal kimberlite magmatic trend with a decrease in chromium and a progressive increase in TiO<sub>2</sub>, MgO, total FeO and Fe<sup>3+</sup>/Fe<sup>2+</sup> as crystallisation proceeds. The Fe<sup>2+</sup>/Fe<sup>3+</sup> ratios and Al<sub>2</sub>O<sub>3</sub> contents remain nearly constant. The sill groundmass spinels evolve to more FeO, Fe<sub>2</sub>O<sub>3</sub> and TiO<sub>2</sub>-rich compositions than those in the main pipe bodies. Heavy mineral concentrates of the sill kimberlite are mainly magnetites with minor titanomagnetites and a single chromite (Shee, 1985).

Ilmenite inclusions in olivine phenocrysts and groundmass ilmenites are less abundant in the sill kimberlites than in the main pipe intrusions. The sill ilmenites have high MgO (10.94 - 12.55, mean 11.87 wt %) and Cr<sub>2</sub>O<sub>3</sub> (3.25 - 5.65, mean 4.58 wt %) contents. Ilmenites from heavy mineral concentrates of the sill kimberlites have similar compositions suggesting that the concentrate ilmenites are derived from the groundmass. The relatively MgO-poor compositions of the sill groundmass ilmenites compared to those in the main pipe intrusions can be attributed to crystallisation from a more fractionated magma.

The CaO contents of olivines is controlled by pressure (Simkin and Smith, 1970; Stomer, 1973), temperature (Finnerty and Boyd, 1978) and the CaO content of the magma (Watson, 1979). It is postulated that the first olivine phenocrysts crystallised under high pressure (within the upper mantle) and are magnesian (Fo 93) and do not contain detectable CaO in their cores. The kimberlite magma moved diapirically upwards and a second generation of olivine phenocrysts began to crystallise under relatively low pressures - perhaps during near surface intrusion. These phenocrysts are less magnesian (Fo 86) compared to the early phenocrysts and contain detectable CaO in their cores. The relatively FeO-rich compositions of these phenocrysts is attributed to crystallisation from a relatively fractionated kimberlite magma and/or to contemporaneous crystallisation of olivine and monticellite under low pressure. The CaO enrichment trend shown by the phenocryst rims is thought to be caused by reaction with residual magma that is progressively becoming more CaO-rich and/or by pressure release during magma emplacement. The whole rock compositions and the chemistry of olivine phenocrysts and groundmass phlogopite, ilmenite and spinel are all consistent with derivation from a fractionated kimberlite magma.

Clement (1982) suggested that precursor kimberlite dykes and sills play an important role in the subsequent development of kimberlite pipes. The early

dykes and sills are intruded along near surface joints and fractures and upon crystallisation effectively "seal" the area. This "sealing" process is thought to be responsible for subsurface pressure build-up, for providing time for the development of precursor vapour phases to accumulate and, consequently, for the initiation of subsurface embryonic pipe-forming processes.

#### References.

- Clement, C.R. (1982) A comparative geological study of some major kimberlite pipes in the Northern Cape and Orange Free State. Ph.D. thesis, University of Cape Town, South Africa.
- Dawson, J.B. and Hawthorne, J.B. (1973) Magmatic sedimentation and carbonatitic differentiation in kimberlite sills at Benfontein, South Africa. *Journal of the Geological Society*, London, 129, 61-85.
- Finnerty, T.A. and Boyd, F.R. (1978) Pressure dependent solubility of calcium in forsterite coexisting with diopside and enstatite. *Carnegie Institute of Washington Yearbook*, 77, 713-717.
- Hawthorne, J.B. (1968) Kimberlite sills. *Transactions of the Geological Society of South Africa*, 71, 291-311.
- Hill, D.R.H. (1977) Field relationships and petrography of the kimberlite sills and associated dykes at the 40 metre level of the Wesselton Mine, Kimberley, South Africa. B.Sc. Hons. thesis, University of Cape Town, South Africa.
- Mitchell, R.H. (1984) Mineralogy and origin of carbonate-rich segregations in a composite kimberlite sill. *Neues Jahrbuch Miner. Abh.*, 150, 2, 185-197.
- Shee, S.R. (1985) The petrogenesis of the Wesselton Mine kimberlites, Kimberley, Cape Province, R.S.A. Ph.D. thesis, University of Cape Town, South Africa.
- Simkin, T. and Smith, J.V. Minor element distribution in olivine. *Journal of Geology*, 78, 304-325.
- Smith, C.B. (1983a) Pb, Sr, and Nd isotopic evidence for sources of southern African Cretaceous kimberlites. *Nature*, 304, 51-54.
- Smith, C.B. (1983b) Rubidium-strontium, uranium-lead and samarium-neodymium isotopic studies of kimberlite and selected mantle derived xenoliths. Ph.D. thesis, University of the Witwatersrand, Johannesburg, R.S.A.
- Stormer, J.C. (1973) Calcium zoning in olivine and its relationship to silica activity and pressure. *Geochimica and Cosmochimica Acta*, 37, 1815-1821.

**BARIUM-RICH, OLIVINE-MICA LAMPROPHYRES WITH AFFINITIES TO  
LAMPROITES, FROM THE MT BUNDEY AREA, NORTHERN TERRITORY, AUSTRALIA.**

*Sheppard, S.; Taylor, W.R. and Rock, N.M.S.*

*Key Centre for Strategic Mineral Deposits, University of Western Australia, Nedlands, W.A. 6009, Australia.*

Potassic igneous rocks, transitional between lamproites of continental intra-plate settings and shoshonitic volcanic and lamprophyric rocks (e.g. minettes) of active continental margins, are known from several localities world-wide but their petrogenesis, tectonic setting and relationship to Ti-rich lamproites are poorly understood. Lack of detailed mineralogical and geochemical documentation of such 'transitional lamproites' has contributed to difficulties in distinguishing them from true lamproites. In this abstract we describe an occurrence of unusual olivine-mica lamprophyre dykes which intrude Early Proterozoic, low-grade metasediments and granitoids of the Mt Bunday area, Pine Creek Inlier, northern Australia. Their mineral assemblages and mineral chemistry are typical of shoshonitic (calc-alkaline) lamprophyres, but their whole-rock chemistry more closely resembles lamproites.

The Mt Bunday lamprophyres are spatially and probably genetically associated with a post-tectonic, composite syenite-granite pluton. Numerous dykes of 0.5-3.0 m thickness intrude the granite and syenite; contacts with the pluton are sharp and margins of the dykes may be chilled. Rb-Sr isotopic data shows that the lamprophyres, syenite and granite fall on the same isochron defining an age of  $1810 \pm 32$  Ma with an initial  $^{87}\text{Sr}/^{86}\text{Sr}$  ratio of 0.7038. A U/Pb age on zircons from the granite define a more precise age for the pluton, and thus for the lamprophyres, of  $1832 \pm 6$  Ma (R.W. Page, written communication, 1990). The lamprophyres are composed of 1-5 mm phenocrysts of altered, euhedral olivine (5-30%) and minor clinopyroxene, and up to 10% mica phenocrysts set in a groundmass of  $\leq 0.5$  mm orthoclase, mica, amphibole, clinopyroxene, minor magnetite, apatite and sphene, with accessory zircon and (?) monazite. Felsic globular structures composed of plagioclase, calcite and mica are a minor (<3%) but widespread component of the dykes.

*Olivine* phenocrysts are completely replaced by chlorite, quartz and magnetite, and are surrounded by green-brown mica. Phenocryst and groundmass mica compositions mainly fall in the biotite field ( $mg\# = 54-72$ ). The most common type of biotite is dark green with abundant acicular inclusions of (?) Ti-oxide usually zoned to pale rims free of inclusions. The other type of biotite is pale orange-brown, with dark rims reflecting a slight decrease in Mg/Fe ratios. The two types have similar compositions and appear to be distinguishable from each other only on the basis of the higher  $\text{Fe}^{3+}/\text{Fe}^{2+}$  ratio of the green biotite. Biotite compositions (2-8wt%  $\text{TiO}_2$  and 12.0-13.5wt%  $\text{Al}_2\text{O}_3$ ) fall within the calc-alkaline lamprophyre field on  $\text{Al}_2\text{O}_3$ - $\text{TiO}_2$  and  $\text{Al}_2\text{O}_3/\text{TiO}_2$ -MgO/FeO<sup>(T)</sup> diagrams but are generally displaced toward the lamproite field.

*Feldspar* is orthoclase (Or<sub>70-90</sub>) and its low iron content ( $\leq 0.5$ wt%  $\text{Fe}_2\text{O}_3$ ) clearly distinguishes it from lamproitic feldspars (1-5wt%  $\text{Fe}_2\text{O}_3$ ). *Clinopyroxenes* are diopsides (Mg<sub>80-86</sub>, 0.7wt%  $\text{TiO}_2$ , 1.2-3.3wt%  $\text{Al}_2\text{O}_3$ ) which fall within the calc-alkaline lamprophyre field, but toward lamproitic compositions on  $\text{SiO}_2/\text{TiO}_2$ -MgO/FeO<sup>(T)</sup> and  $\text{TiO}_2$ - $\text{Al}_2\text{O}_3$  diagrams. Crystals commonly display oscillatory zoning superimposed on gradational zoning toward more  $\text{TiO}_2$ -rich, MgO-poor rims. *Amphiboles* are tremolites (52-57wt%  $\text{SiO}_2$ , <0.8wt%  $\text{TiO}_2$  and  $\Sigma$ alkalis <2 wt%, commonly  $\leq 1$  wt%) with

minor edenite substitution. They plot within the field of "mainly secondary amphiboles" on a  $\text{TiO}_2$ - $\text{SiO}_2$  diagram (Fig. 4.4; Rock, 1990), an origin supported by rare cores of diopside to the tremolite. The only oxide phase present in most dykes is a  $\text{TiO}_2$ - and  $\text{Cr}_2\text{O}_3$ -poor (<0.2 wt%  $\text{TiO}_2$  and <0.1 wt%  $\text{Cr}_2\text{O}_3$ ) magnetite, although chromian magnetite (13-15 wt%  $\text{Cr}_2\text{O}_3$ ) is a rare mineral in some samples. The above mineral compositions together with the absence of richterite, leucite, groundmass tetraferriphlogopite and the minor titanate minerals that characterize lamproites, demonstrate that the Mt Bunday dykes have closest mineralogical affinity with shoshonitic mica lamprophyres (minettes).

No mantle or crustal xenoliths have been found in the dykes, but some contain xenocrysts of partly resorbed perthite and quartz derived from the granite-syenite pluton. Many of the dykes contain (?) cognate xenoliths, 0.5-1.0 mm in diameter, composed of amphibole and minor biotite and magnetite. These observations are consistent with Pb isotope data which indicate negligible upper crustal contamination of the lamprophyres.

The Mt Bunday lamprophyres have ~46-49 wt%  $\text{SiO}_2$ , ~1.5-2 wt%  $\text{TiO}_2$ , ~8-12 wt%  $\text{MgO}$ , ~2 wt%  $\text{Na}_2\text{O}$  and ~5-7.5 wt%  $\text{K}_2\text{O}$ . Magnesium numbers (*mg#*) lie in the range 65 to 75 (assuming atomic  $\text{Fe}^{3+}/\text{Fe}^{2+} = 0.3$ ). Those lamprophyres with the highest *mg#*s contain >350 ppm Ni and >600 ppm Cr and are therefore candidates for primary melts of mantle peridotite. Minor olivine  $\pm$  clinopyroxene fractionation may be important in generating the less magnesian lamprophyres. Relative to typical minettes the Mt Bunday lamprophyres are more strongly enriched in Ta, Nb, Th, U, Ba, P, Zr and REE but have comparable Sr, F, Sc, V and Cr contents. The dykes contain similar levels of Zr (650-930 ppm), Sr (1600-3700 ppm), La (165-260 ppm), F (3500-4900 ppm) and Ba (4600-10000 ppm) to lamproites (see Rock, 1990) but they are not peralkaline (molar  $[\text{K}_2\text{O}+\text{Na}_2\text{O}]/\text{Al}_2\text{O}_3 = 0.8-1.0$ ). The closest analogues to the Mt Bunday lamprophyres are jumillites from SE Spain and cocites from northern Vietnam.

On mantle-normalized abundance diagrams (Fig.1), the Mt Bunday dykes show negative Ta-Nb and Ti anomalies - a feature characteristic of subduction-related magmas. The magnitude of the Ta-Nb anomaly is, however, intermediate between typical subduction-related minettes, which have much larger negative anomalies, and Ti-rich lamproites, which either lack such anomalies or have slight Ta-Nb anomalies (see Fig.1 and also Foley and Wheller, 1990). The intermediate nature of the Mt Bunday dykes is further illustrated on a Zr-Nb plot (Fig. 2). Both the Mt Bunday lamprophyres and the jumillites plot in a field intermediate between minettes associated with subduction or post-collisional settings and West Kimberley leucite-lamproites of continental intra-plate origin.

Current petrogenetic models for the transitional lamproites suggest they may be either (1) generated by partial melting above a 'fossil' subduction zone (e.g. Venturelli et al., 1984) or (2) generated in enriched sub-continental mantle in which the enrichment event has no relationship to subduction processes but carries a subduction-type signature due to the stability of residual titanate minerals (e.g. Foley and Wheller, 1990). For the Mt Bunday lamprophyres, modelling of the Sr isotope data is consistent with enrichment of the source area ~150-350 Ma before partial melting, suggesting that model (1) may be appropriate if evidence can be found for a ~1.9-2.0 Ga calc-alkaline magmatic event in the Pine Creek Inlier. However, the detailed magmatic history of this region is not well known.

The presence of subduction-related (model 1) or residual-titanate-related (model 2) Ta-Nb-Ti anomalies in transitional lamproite magmas implies an oxidized mantle source region at depth ( $f_{\text{O}_2} > \text{FMQ}$ ) (Foley and Wheller, 1990). Irrespective of the depth of generation, diamond or

graphite will not be stable under these conditions and unless oxidation of the subcontinental mantle is only of very local extent, a transitional lamproite province is unlikely to be highly prospective for diamond.

REFERENCES

Foley, S.F. and Wheller, G.E. (1990) Parallels in the origin of the geochemical signatures of island arc volcanics and continental potassic igneous rocks: the role of residual titanates. *Chemical Geology*, 85, 1-18.  
 Rock, N.M.S. (1990) *Lamprophyres*. Blackie & Sons Ltd, Glasgow.  
 Venturelli, G., Capedri, S., Di Battistini, G., Crawford, A., Kogarko, L.N., and Celestini, S. (1984) The ultrapotassic rocks from southeastern Spain, *Lithos*, 17, 37-54.

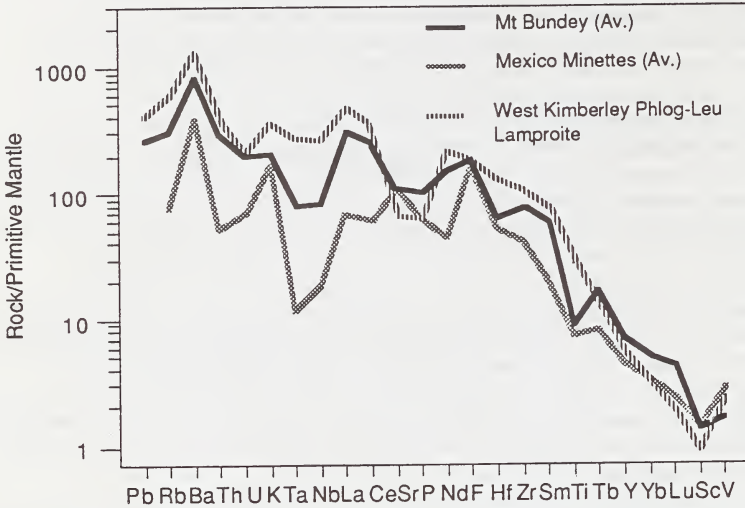


FIG. 1. Mantle normalised plot showing the intermediate nature of the Mt Bunday dykes relative to subduction-related minettes and a lamproite from the West Kimberley Province, Western Australia.

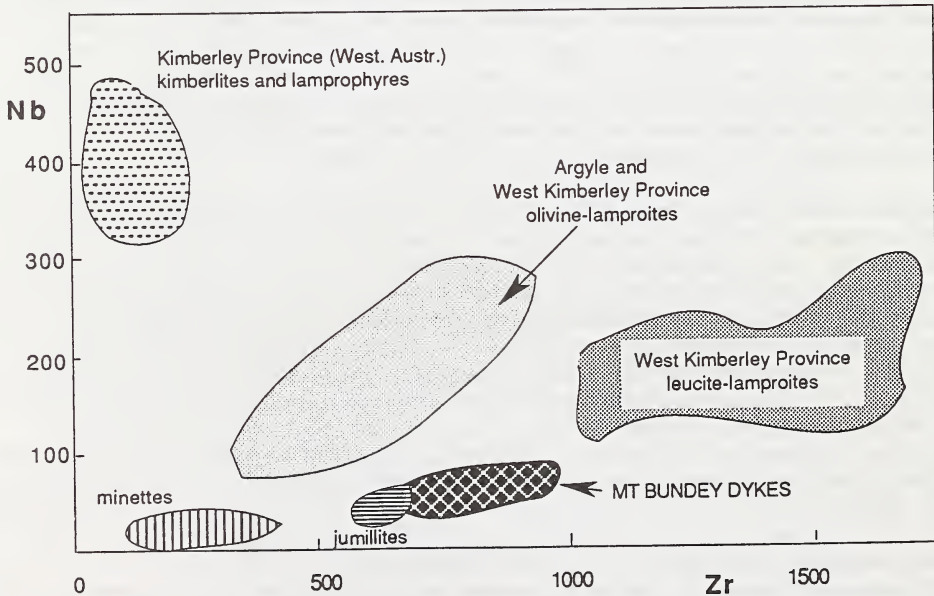


FIG. 2. Nb versus Zr plot (ppm) showing the intermediate nature of the Mt Bunday rocks and Spanish jumillites relative to minettes and West Kimberley Province (Western Australia) lamproites.

## THE ARKHANGELSK DIAMOND-KIMBERLITE PROVINCE - A RECENT DISCOVERY IN THE NORTH OF THE EAST-EUROPEAN PLATFORM.

Sinitsyn<sup>(1)</sup>, A.V.; Ermolaeva<sup>(1)</sup>, L.A. and Grib<sup>(2)</sup>, V.P.

(1) Research Institute "Horizon", Leningrad State Univ. Petrodvorets. 198904, U.S.S.R.; (2) Geological Enterprise "Arkhangelskgeologia", Arkhangelsk, 163001, U.S.S.R.

The discovery, in 1970-1980, of kimberlites in the north part of the East-European platform might have happened earlier had prospecting followed promptly upon correct data interpretation. In 1936, in the vicinity of Nenoksa, on the Onezhsky Peninsula on the White Sea coast, instead of the expected Paleozoic sediments, a random hydrogeological borehole intersected exotic breccia. It was interpreted by different geologists as variously greywacke, basic tuff, agglomeratic breccia, etc. The nature of this breccia remained doubtful until 1968 when a routine ground magnetic survey around Nenoksa revealed local magnetic anomalies of 400-2000 gammas intensity, one of which coincided with the old Nenoksa borehole. Boreholes drilled to check the anomalies disclosed a group of explosive pipes filled by eruptive breccia. Petrographic investigations of the pipe rocks determined picrite-porphyrites and nondiamondiferous kimberlites (Sinitsyn et al., 1973) and, later on melilitic picrites. The red colour of the pipe rocks, due to country rock contamination, was unusual, and served as a psychological barrier to their recognition at first. It was discovered later, that the pipes usually become dark green at depth. The discovery of the Nenoksa pipes led to the recognition of a significant new magmatic complex in the region and the initiation of prospecting for diamond-bearing kimberlites (Sinitsyn et al., 1973; Stankovsky et al., 1973).

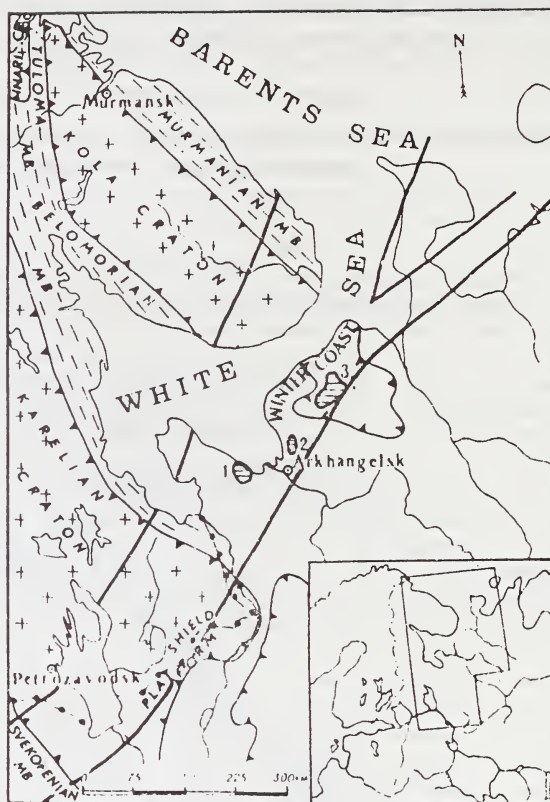
The Nenoksa pipes comprise a field on the northeastern border of the Onezhsky Riphean (ca. 1800 Ma) buried rift and are situated in the zone of the diagonal Verkhovsky fracture. They are represented by vertical vents oval to subround in plan, up to 425 m in diameter. At the time of writing, about 30 pipes have been discovered, but the total number may be much higher. They intrude argillites of the Upper Proterozoic Redkinsky formation and are covered by Quaternary moraine. Xenoliths of fossil wood indicate a maximum age of Devonian-Middle Carboniferous.

Investigators noted the world-wide trend of kimberlitic magmatism to localise in the border zones of interplatform synclines or broad crustal downwarps, therefore included tectonic analyses of the northern part of the East-European platform in the next stage of investigation. The 1000 km-long Arkhangelsk trend of Late Proterozoic-Early Paleozoic tectonic activity was readily detected on satellite images (Sinitsyn et al., 1982) from Omega Lake northeastward to Kanin Nos Peninsula.

The entire zone was regarded as prospective for kimberlite occurrence (Sinitsyn et al., 1982). The first step included high precision airborne magnetic survey followed by geological mapping inside the zone adjacent to the Nenoksa area of the Winter coast of the White Sea. Simultaneously radar airborne mapping was initiated for the entire Arkhangelsk tectonic activation trend of about 204 000 km<sup>2</sup> aiming for photoanomalies of the pipe type. Geological mapping resulted in 1976 in the discovery of small kimberlite sills, cropping out along the bank of the Mela River.

Checking of the pipe-type magnetic anomalies started in 1980, and the first borehole drilled on the Winter Coast intersected the Pomorskaya kimberlite pipe. The debates whether pink-reddish breccias are kimberlites or not ceased after economic diamonds were assayed in them. The subsequent prospecting search resulted in the discovery of about 50 pipes on the Winter Coast, 15 of which were proven to be diamondiferous. Several neighbouring fields or clusters are distinguished - Zolotitsa, Verkhotinskaya, Kepino, Mela, Izhmozero and Poltozero.

The general geological setting of the Winter Coast pipes is much the same as that of the Nenoksa field - the pipes intrude the Upper Proterozoic (Vendian) strata and are transgressively covered by Carboniferous, Permian and Quaternary rocks. They contain xenoliths of carbonized wood and Ordovician rocks, suggesting Devonian age. SHRIMP analyses of perovskite from Pionerskaya pipe performed by Anglo-American Research Laboratories yielded 462 mln.y., which is Ordovician. Porphyritic and autolithic kimberlites (TKB) are predominant, with monophase and polyphase pipes being equally abundant. Some of the pipes retained the crater facies - the so called "sedimentary kimberlites" up to 250 m thick. The area of individual pipes ranges from 6000 m<sup>2</sup> - 2.5 km<sup>2</sup>.



Pipe fields: 1 - Nenoksa, 2 - Izhmozero, 3 - Zolotitsa clusters

The Winter Coast pipes are classified according to their composition into four groups: (1) high magnesium kimberlites (Zolotitsa group and two pipes of Kepino group), (2) high iron kimberlites (Verkhotinskaya group, several pipes of the Kepino group and Mela sill), (3) alkaline picrites, including alnoite-type melilite picrites (most pipes of the Kepino group and adjoining Izhmozero field), and (4) fresh basaltic pipes of tholeiitic affinity (Poltozero group). Only kimberlite pipes have proven to be diamondiferous.

The boundaries of the buried Kuloi craton, Karelian and Kola Archæan cratons, and the surrounding Proterozoic mobile belts are shown on the Fig. It is obvious that all diamondiferous kimberlite pipes are confined to the Kuloi cratonic area.

Several kimberlite fields form a vast zone about 1000 km long within Arkhangelsk tectonic trend, predicted from radar mapping data. A problem of selecting promising target areas resulted. Under these circumstances, the South African prospecting experience as presented by T. Clifford's rule (Clifford, 1966) assumed special importance, i.e. all economic diamond-bearing kimberlite pipes are found inside Archæan cratonic areas.

Structural analyses of the Arkhangelsk province from Clifford's point of view was feasible only by interpreting the tectonic framework of the East-European platform according to the South African model of Archaean cratons and Proterozoic mobile belts. At first, the model appeared discordant with Soviet geology, but, considering the possible prospecting return, tempting enough to try.

The main conclusions resulting from this exercise follow; 1. The Arkhangelsk activation trend is a border tectonic zone along the western rim of the Vendian-Paleozoic basin of the Russian plate. It obliquely transects the heterogenous Precambrian basement.

2. The known kimberlite fields of the Arkhangelsk province reveal two different structural settings: a) the Zolotitsa (productive) group of fields has an intercratonic setting, and b) the Nenoksa and Izhmzero (nonproductive) fields are within the Belomorian mobile belt.

Hence, Clifford's rule specifying intercratonic setting for diamondiferous pipes has been proven to be valid.

In summary, it must be conceded that the tectonic controls proposed for the Arkhangelsk province, including structural directions and trends of tectonic activation can be validly applied only to the northern part of the platform. Furthermore, reported recent occurrences in the Ukraine, Belorussia, Novgorod district, Estonia, Sweden and Kola Peninsula reveal a different structural pattern and were subjected to different tectonic controls. Each occurrence requires individual study.

The Arkhangelsk discovery puts the East European platform in a row with the South African and the East Siberian provinces eventually might be of comparable diamond potentials.

## KIMBERLITIC OLIVINE.

*Skinner*<sup>(1)</sup>, *E.M.W.*; *Hatton*<sup>(1)</sup>, *C.J.*; *Stock*<sup>(1)</sup>, *C.F.* and *Shee*<sup>(2)</sup>, *S.R.*

(1) *Anglo American Research Laboratories, P.O. Box 106, Crown Mines 2025, RSA;*

(2) *Stockdale Prospecting Ltd., 60 Wilson Str., South Yarra, Victoria 3141, Australia.*

1. INTRODUCTION

This study is based on analyses from more than 1000 occurrences. In fresh hypabyssal-facies, macrocrystic Group I and Group II kimberlites (*sensu stricto*) olivine commonly represents 50 volume per cent of the rock. In rare cases, e.g. parts of sill and dyke complexes olivine accounts for up to 80 volume per cent. Several varieties of olivine occur (Skinner, 1989).

- (1) Anhedral xenocrysts with a modal size of 2mm (size range <0.5mm to >20mm) derived from various sources, including disaggregated mantle peridotite, failed proto-kimberlites, LIHN megacryst suites and HILN megacryst suites; making up about 25 vol %.
- (2) Subhedral to euhedral phenocrysts with a modal size of 0.3mm (size range <0.1mm to >5mm) representing early forming (within mantle) discrete crystals, crystal overgrowths (only in some kimberlites) and late forming (surficial) discrete crystals; making up about 25 vol %.
- (3) Olivine as a constituent mineral of peridotite xenoliths.
- (4) Olivine inclusions within peridotitic diamonds.

Distinction between anhedral xenocrysts and subhedral / euhedral phenocrysts is facilitated by several factors, such as; differences in morphology, grain size, internal textures (e.g. undulose extinction, kink-banding, etc.) inclusions of other minerals (large and very small) as well as differences in major and trace element compositions.

2. KIMBERLITE GENESIS

Since olivine crystallises throughout the history of the kimberlite magma, both in the upper mantle and at surface, the differences in the olivine populations provide valuable clues to interpretation of processes operating during the genesis at kimberlite in the upper mantle, during ascent and during emplacement of the kimberlite magma at surface.

- 2.1. Hotspot Magmas. It is assumed that kimberlites are initiated by hotspot activity and that hotspot magma originates by reheating of basalt which has accumulated at the core-mantle boundary (Hofmann and White, 1982). The basalt becomes bouyant, rises, and is trapped at the base of the lithosphere. Olivine

of the HILN variety crystallises from this magma.

In the next stage of kimberlite genesis mantle peridotite is assimilated as a result of heat released by crystallisation of the basalt. Two sites of assimilation are distinguished; in the reduced, diamond-bearing lithosphere (RL) and in the underlying, oxidised, volatile-enriched lithosphere (VEL).

- 2.2. Assimilation of reduced mantle peridotite. Assimilation of reduced peridotite results in a simultaneous increase in the magnesium and nickel contents of the melt. Olivines that crystallise from this melt are thus relatively Mg and Ni-rich (LIHN) and are related to the Cr-poor megacryst suite. More extensive assimilation produces magmas which crystallise the Cr-rich megacryst suite. As yet olivines associated with this suite are unknown.
- 2.3. Proto Kimberlite Melts. True kimberlite melts form when the hotspot basalt assimilates VEL formed as a consequence of earlier subduction processes. Assimilation of volatiles produces a low viscosity proto kimberlite magma (PKM) which easily penetrates the lithosphere. Volatile-poor megacryst magmas are trapped in the lithosphere but may be incorporated by the ascending proto kimberlite.
- 2.4. Early Ascent. Rising batches of PKM cool and crystallise early phenocrysts of olivine. Some of these may fail and be sampled by later PKM's incorporating earlier olivine crystals of differing Mg-numbers.
- 2.5. Peridotite Disaggregation. After heat loss during early ascent, kimberlite can no longer entirely digest peridotite and partial assimilation (of opx, cpx and garnet) takes place leaving xenocrysts of olivine. These constitute the majority of the anhedral olivine xenocryst population.
- 2.6. Magma Coalescence. Ascending kimberlite magmas may pond at resistive interfaces within the lithosphere (e.g. at the base of the assumed Roberts Victor eclogite complex). At this level the final, successful kimberlite gathers together earlier failed kimberlite and/or megacryst magmas, disrupts and samples (as xenoliths) the resistive layer and ascends rapidly to surface.

The successful kimberlite will always be more oxidised and volatile-rich than failed kimberlite or megacryst magmas, since ascent requires a high volatile content; and the more volatile rich, the more oxidised a magma will be that interacts with VEL. Kimberlites sampling earlier PKM's will thus oxidise that magma. Olivine overgrowths with zoned Ni (Skinner, 1989) may grow in response to the change in oxygen fugacity.

- 2.7. Mantle Ascent. As the successful kimberlite ascends rapidly little olivine crystallisation takes place.
- 2.8. Ascent through the Crust. As the magma ascends

through the upper crust (at 1.5 kbar =  $\pm$  5km) there is a dramatic change in the position of the CCO buffer relative to other oxygen fugacity buffers. This change may cause substantial degassing and result in rapid slowing of the rate of ascent of the magma and renewed crystallisation of olivine. Crystal growth will vary substantially depending essentially on the magma temperature. In some kimberlites (e.g. Bellsbank, Bobbejaan Fissure) very little early (mantle) olivine phenocrysts occur and the late (near-surface) phenocrysts are all fine grained (<0.1mm) due to rapid cooling.

- 2.9. Post Emplacement Effects. After emplacement and final crystallisation of olivine the residual magma cools and fractionates further. The residue becomes reactive towards olivine resulting in zoned reaction mantles on all grains.

### 3. GROUP 1 AND GROUP 2 KIMBERLITES

The different character of Group 1 and Group 2 kimberlites may be explained by differences in the proportions of reduced and oxidised lithosphere assimilated by their antecedent hotspot basalts.

Group 1 hotspot basalt is considered to be voluminous relative to Group 2 hotspot basalt, with the former penetrating the RL and producing many failed megacryst magmas while the latter assimilate proportionately more of the VEL. The lower proportion of megacryst magma in Group 2 kimberlites ensures that their magnesium number is higher than Group 1 kimberlites.

### 4. CONCLUSION

Even though olivine is the most abundant constituent of kimberlite (s.s.), it is possibly the least researched and understood mineral relative to other mantle - derived constituents. This is due to several factors, such as; its commonly altered state, difficulty in classification and limited use as an indicator mineral in diamond prospecting. Because of this the debate as to whether olivine macrocrysts are xenocrysts, phenocrysts or megacrysts continues. This study assists in resolving this dispute and also contributes to the understanding of the processes involved in kimberlite genesis.

### REFERENCES

Hofmann, A.W. and White, W.M. (1982). Mantle plumes from ancient oceanic crust, *Earth Planet. Sci. Lett.* 57, 421-436.

Skinner, E.M.W. (1989) Contrasting Group I and Group II kimberlite petrology: towards a genetic model for kimberlites. In J. Ross, Man. ed., *Kimberlites and Related Rocks, Their Composition, Occurrence, Origin and Emplacement*, Geol. Soc. Australia Spec. Publ. 14, p. 528-544.

THE PETROGRAPHY, TECTONIC SETTING AND EMPLACEMENT AGES OF  
KIMBERLITES IN THE SOUTH WESTERN BORDER REGION OF THE KAAPVAAL  
CRATON, PRIESKA AREA, RSA.

Skinner<sup>(1)</sup>, E.M.W.; Viljoen<sup>(1)</sup>, K.S.; Clark<sup>(2)</sup>, T.C. and Smith<sup>(2)</sup>, C.B.

(1) Anglo American Research Labs., PO Box 106, Crown Mines, 2025, South Africa. (2) Bernard Price Institute of Geophysical Research, University of the Witwatersrand, Johannesburg, 2050.

### 1) Introduction

Approximately 130 kimberlite bodies are known to occur in the south western border region of the Kaapvaal craton (Figure 1). Based on tectonic/geologic settings as well as petrological groupings five separate domains are recognised.

### 2) Setting and Petrographic variation

**Domain I** - The region north of the Doornberg Fault, underlain by unambiguous Archaean, Kaapvaal Basement. The kimberlites are predominantly Group 2 varieties (8). Three Group 1 varieties also occur.

**Domain II** - The region to the east of the southward extension of the Doornberg Fault, also underlain by Archaean, Kaapvaal Basement. The kimberlites (20) are predominantly Group 1 varieties (eg Britstown pipe). One of the Group 2 varieties namely Sweetput-Soutput is transitional with respect to both petrography and radiometric isotope ratios (re. Clark et al., this volume).

**Domain III** - The region more or less wedged between the Doornberg and Brakbos faults, and underlain by Marydale Group basement rocks considered to be largely Marydale of Archaean age (Cornell et al. 1986). All the kimberlites (45) are Group 2 varieties, but most display petrographic tendencies towards Group 1 varieties (e.g. the presence of significant numbers of ilmenite xenocrysts). All fall well within or close to the isotopically enriched field of Group 2 kimberlites on the Nd/Sr diagram (Clark et al., this volume) but some have significantly lower initial Nd ratios.

**Domain IV** - The region south of Domains II and III but north of Domain V, underlain by mid-Proterozoic rocks forming part of the Namaqua Mobile Belt. Most of the kimberlites are Group 1 varieties (26) but two Group 2 kimberlites also occur. Mixed radiometric ages have been recorded and one kimberlite (Pampoenpoort) has a slightly enriched Nd-Sr signature.

**Domain V** - The region south of latitude 31°30'S underlain by Basement of uncertain nature. All the kimberlites (7) are barren Group 2 varieties exhibiting transitional characteristics both with respect to

petrography and isotope geochemistry (Skinner, 1989). Petrographically they are closer to Group 1 varieties than the kimberlites occurring in Domain II. The types, size and abundance of specific matrix minerals vary widely even on a thin section scale.

Examination of heavy mineral concentrates from the kimberlites reveal that many of the Group 2 kimberlites in this region contain ilmenite as well as chrome-poor garnet and clinopyroxene megacrysts.

**3) Emplacement Ages**

Seventeen kimberlites have been dated by a variety of techniques and by different analysts (re. Table 1 and Figure 1). The wide diversity of ages (ranging between 67 and 167 Ma) in this comparatively restricted area, is somewhat unusual and contrasts sharply with many other areas of kimberlite emplacement. One exception is the field of kimberlitic rocks in East Griqualand, also located close to the Kaapvaal craton boundary (SE border region). Here emplacement ages, ranging between 63 and 194 Ma have been recorded (e.g. Nixon et al., 1983).

Domain	Kimberlite	Group	Age	Method
I	Witberg Pipe	1	114	1
I	Sanddrift	2	126±2	2
II	Sweetput-Soutput	2/1	114±1 & 90±14 to 117±13	2 & 4
II	Britstown	1	74±1	2
III	Welgevonden	2	122±3	2
III	Kalkput	2	114.1, 116.4 & 117±0.4	3 & 5
III	Markt	2	127±3	2
III	Jonkerwater	2	119±2	2
III	Middelwater	2	118±3	2
IV	Pampoenspoort	1/2	103±1	2
IV	Hartebeesfontein	1	74±1	2
IV	Lushof	1	67.7 & 78.3	3
IV	Uintjiesberg	1	101±1	2
IV	Beyersfontein	1	81.5±1.5	5
V	Droogfontein	2/1	100±25 to 143±24	4
V	Skietkop	2/1	136±9 to 167±8	4
V	Melton Wold	2/1	138±14 to 145±13	4

Methods - 1.Rb-Sr model mica ages 2.Rb-Sr isochron mica and whole rock ages 3.Zircon U-Pb ages (Davis, 1977 & 1978) 4.Perovskite ion-probe ages (Barton unpubl. data) 5.Zircon U-Pb ages (Pidgeon unpubl. data)

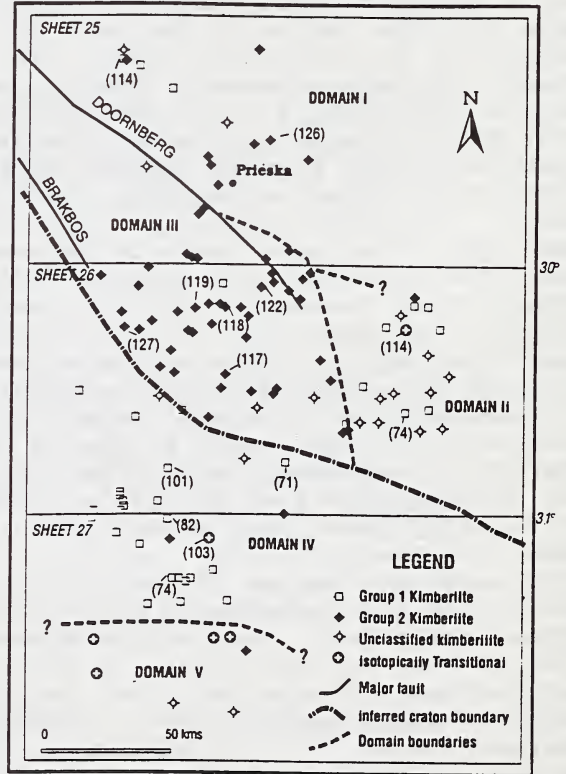


Fig 1. Distribution of kimberlites in the vicinity of Prieska - south western marginal zone of the Kaapvaal Craton

Although the ages and age distribution patterns might appear to be complex and may represent random events, some order can be applied to this data by relating ages to petrographic type, location within specific domains and relative position of these bodies within the overall distribution patterns of all Jurassic/Cretaceous kimberlites in South Africa. In terms of the latter, Group 2 kimberlites in this region could be expected to be around 115 Ma, assuming generation from a simple hotspot system active below a NE moving plate. On a similar basis the expected age of Group 1 kimberlites in this area would be around 75 Ma.

Most of the Group 2 kimberlites (7/10) range between 114 and 127 Ma, whereas most of the Group 1 bodies (4/7) range between 73 and 82 Ma. In both Groups, average ages (120 and 75 Ma respectively) are close to the expected hotspot age. Group 2 kimberlites with anomalous older ages are all transitional types and all occur within Domain V. Of the anomalous older Group 1 kimberlites, 2 bodies (both in Domain IV) are around 102 Ma and one (in Domain I) has a model age of 114 Ma. The latter is similar to the lower age of the Group 2 kimberlites and is in fact located in close proximity to Group 2 bodies. The two 102 Ma old Group 1 kimberlites have intermediate ages (between the common Group 1 and Group 2 ages) and can easily be explained in terms of simple hot spot generative mechanisms.

#### 4) Conclusion

The kimberlites in this comparatively restricted region exhibit variations in petrographic character, tectonic setting, emplacement age as well as isotopic and geochemical signatures. Study of this unique geological setting has led to a better understanding of kimberlite genesis and upper mantle processes.

#### References

- Cornell, D.H., Hawkesworth, C.J., Van Calsteren, P. and Scott, W. (1986) Sm-Nd study of precambrian crustal development in the Prieska-Copperton region, Cape Province. *Trans. geol. Soc. S. Afr.*, 89, 17-28.
- Davis, G.L. (1977) The ages and uranium contents of zircons from kimberlites and associated rocks. *Second Int. Kimberlite Conf. Extended Abstracts* (Carnegie Inst., Washington, D.C.).
- Davis, G.L. (1978) Zircons from the mantle. *United States Geol. Surv. Open-File Report 78-701*. ed. by R.E. Zartman, 86-88.
- Nixon, P.H., Boyd, F.R. and Boctor, N.Z. (1983) East Griqualand kimberlites. *Trans. Geol. Soc. S. Afr.*, 86, 221-236.
- Skinner, E.M.W. (1989) Contrasting Group I and Group II kimberlite petrology. *GSA Special Publication No. 14* pp528-544.

## PATTERNS OF DIAMOND AND KIMBERLITE INDICATOR MINERAL DISPERSAL IN THE KIMBERLEY REGION, WESTERN AUSTRALIA.

*Smith, Chris. B.; Haebig, A.E. and Hall, A.E.*

*CRA Exploration Pty. Ltd., 21 Wynyard St., Belmont, Western Australia 6104.*

Heavy mineral sampling of stream sediments and soils (loam) for diamonds and for kimberlite indicator minerals has been the most successful method for diamond pipe discovery in the twentieth century, being responsible for the discovery of the major pipe mines in Siberia, Botswana, and Australia. Yet few case histories have been documented of how the method works, or have described how its effectiveness changes with varying terrain conditions. This paper integrates a number of such cases to view them in the context of variations in the climate, geomorphology and geology of the Kimberley Region.

Kimberlites and lamproites within this Region (Jaques et al., 1986) have been emplaced at 1200 Ma, 800 Ma, and 20 Ma, providing opportunity for liberation and widespread dispersion of diamonds and kimberlitic indicator minerals in the geological past as well as the present day. The Kimberley Region covers an area of some 300,000 km<sup>2</sup> of tropical woodland savannah in northern Australia between latitudes 14° and 18° S. It consists of a high peneplain, the Kimberley Plateau, mostly of 300-800 m elevation, carved out of Proterozoic sediments and volcanics and sloping gently north eastwards towards the sea. The peneplain surface dates from the Cretaceous, perhaps even from the Proterozoic, and carries a good stream drainage network but one of only moderate energy. The Plateau is bounded by deeply dissected ranges (King Leopold Ranges in the south west, Durack Ranges and dissected ground of the Halls Creek Mobile Zone to the east), rising to over 900 metres elevation and characterised by rivers with high energy and erosive power. In the south west the ranges give way southwards to the arid lowland plains of the Great Sandy Desert, underlain by Phanerozoic sediments of the Canning Basin, with elevations typically less than 200 metres. The drainage regime here is poorly developed and of low energy.

The climate during the Cretaceous and early Tertiary was hotter and wetter than today. Most of Australia was covered by rain forest in which southern beeches (*Notofagus* sp.) were prominent. Drainage on the peneplains would have been dominated by sluggish streams of low energy, moving a sandy bed load (Wyrwohl, pers. comm.). A deep weathering profile was developed with formation of laterite, bauxite and silcrete where local geological bedrock conditions were appropriate; the silicification of the Pteropus kimberlite and lateritisation of the Skerring pipe may date from this time. As much of the Kimberley Region is underlain by quartz-rich sandstone, ferruginous laterites are not as well developed as in other parts of Australia and the weathering profile is dominated by thin sand. By the late-Miocene to early-Pliocene, conditions became more arid and the Kimberley rain forest gave way to the more open woodland savannah of today. With less dense vegetation erosion rates increased, and the removal of the top 30-100 m of the lamproite crater volcanic sequence (and former

tuff ring?) at Ellendale would date from this time. Likewise, the oldest ferruginous "A Terrace" diamondiferous gravels at Smoke Creek, downstream from the Argyle lamproite, are late-Miocene and testify to high-energy poorly-sorted conditions in this mountainous region (Deakin et al., 1989). Desertification took place during arid phases in the later Tertiary, with extensive dune development in the Great Sandy Desert, now vegetated over in the southern Kimberley. On the Kimberley Plateau fine red aeolian sand infilled the valleys and remnants are still preserved today. During the Quaternary, arid phases have oscillated with more pluvial inter-glacial times such as at the present day. Annual rainfall today varies from 1500 to 500 mm, decreasing southwards towards the Great Sandy Desert. The rainfall is seasonal, most of it falling within the 4 month period from November to February. Furthermore most of that rain falls in short, sharp, heavy thunder storms. Consequently stream flow is subject to sudden flash floods, but for much of the year the smaller streams are dry. Sediment transport is therefore governed by the high energy flood events, and probably has been since the late-Miocene (e.g. Argyle alluvials).

Low grade regional metamorphism has affected the 1200 Ma lamproites of Argyle and Lissadell Road. Extensive alteration has taken place during ascent and emplacement of lamproite and subsequently, with secondary replacement of virtually all primary minerals except diamond and chrome spinel. Argyle today is being actively eroded and any former weathering profile has been removed. In this arid but high energy environment, diamonds and indicators in colluvium and proximal drainage have not been concentrated to grades above the primary content of the pipe. Chromite is about 6 times as common as diamond; pyrope, picroilmenite and chrome diopside are exceedingly rare. Numbers of chromite  $+0.4$  mm rapidly decrease downstream from a few hundred grains per 40 kg sample to a few tens by 5 km to sporadic occasional grains thereafter. Commercial-sized diamond extends downstream from Argyle for 150 km (Jaques et al, 1986), but economic quantities appear restricted to the first 30 km above the confluence of Smoke and Limestone Creeks with the very large Ord River (Lake Argyle). Coarse diamond decreases from 40 stones per tonne near source to some 2 stones per tonne by 15 km downstream. The occurrence and retention of Smoke and Limestone Creek alluvial diamond deposits proximal to the pipe is due to good trapping by boulder gravel in the stream load, combined with favourable geomorphological trap sites.

Argyle-style diamonds (as identified by characteristic morphology, C isotopic content and mineral inclusion composition, Sobolev et al, 1989) are widely dispersed over 70,000 km<sup>2</sup> of the Kimberley Plateau as a result of extensive earlier postulated Precambrian palaeo-dispersion. Erosion of the Argyle Pipe has been variously estimated from a few tens to less than 200 m and took place during the middle Proterozoic and Tertiary. However, several thousand metres of erosion of the nearby diamondiferous Lissadell Road Dyke and conceivably of other dykes and former pipes intruding the crystalline basement in this Field could have contributed to palaeo-dispersion of Argyle-style diamonds. Similar broad alluvial dispersion of other diamond styles across the central-north Kimberley Plateau has resulted in confusing trails for explorationists (Sobolev et al., 1989). The local 800 Ma Pteropus and Aries Pipes have contributed some of these stones, but most are not directly sourced from any known pipe and the secondary distribution is

thought to result from paleo-dispersion and reworking. Although humid tropical weathering caused extensive Mesozoic to early Tertiary lateritisation and silicification of kimberlites in the Kimberley Plateau, resulting in selective destruction of many indicator mineral species, clear trails of the more resistate minerals lead back to those kimberlites being eroded today. The most resistate mineral species have been diamond, followed by zircon and chromite. Ilmenite survives better than garnet and dominates the concentrates (Atkinson, 1989) but still suffers extensive oxidation in the laterite profile. Chrome diopside, orthopyroxene and olivine are rarely found even in soil overlying these kimberlites. Dispersal of indicators in loam is caused by soil creep, sheet wash, and wind action and generally does not exceed 400 m from a kimberlite, but trains of the more resistate chromite and zircon in the moderate energy stream drainage of up to 36 km are recorded by Atkinson (1989).

The Miocene lamproites of the West Kimberley are little eroded (less than 100 m). Due to the low relief and aridity, characteristic of this area for most of post-emplacement time, the dispersion of indicators and diamonds has been dominantly aeolian and is restricted typically to within 200 m of pipes. Some lateritisation has taken place but has not been sufficiently extensive for widespread destruction of indicator minerals at surface. A loam sample on an olivine lamproite may contain a few thousand chromite, but only some 10 garnets and perhaps 2 or 3 diamonds. Minerals characteristic of lamproite, e.g. potassic richterite and priderite, can be used as indicators close to source. However, the amphibole is not resistate to weathering, and its presence in this tropical environment, like chrome diopside, is restricted to loams virtually on top of pipes. Priderite, a groundmass mineral usually <0.4 mm size, is generally too fine grained to be sought in dispersal trains. Poorly developed, low energy drainage, shows a 10-fold enrichment in indicator mineral concentrations close to a pipe, but downstream results fall off exponentially, diamond and garnet persisting for some 2 km and chromite for 10 km in 50 kg samples. Only very limited diamondiferous palaeo-gravel channels have been located to date, and none have appreciable grade or proven economic significance. Any major eluvial/alluvial diamond concentrations formed in the Miocene have been eroded and transported away; local country rock sheds little gravel and bedrock trapping mechanisms are poor.

In summary, variations within the Kimberley Region show how chemical destruction of the least durable indicator minerals occurred under early Tertiary humid tropical weathering, with concentration of the resistates diamond, chromite and zircon, whereas arid environments gave lesser weathering effects. Concentration is promoted by low energy drainage, not by high energy erosive regimes, and aided by trapping features such as gravel and favourable physiography. Dispersal in loam by soil creep, sheet wash and wind generally does not exceed a few hundred metres. Dispersal trains are longest in streams with moderate to high energy and can extend for a few tens of km.

## REFERENCES

- Atkinson, W.J., (1989). Geological Society of Australia Special Publication No. 14, Blackwell, Melbourne, p. 1075-1107.
- Deakin, A.S., Boxer, G.L., Meakins, A.E., Haebig, A.E., and Lew, J.H. (1989). Geological Society of Australia Special Publication No. 14, Blackwell, Melbourne, p. 1108-1116.
- Jaques, A.L, Lewis, J.D., and Smith, C.B., (1986) Geol. Surv. Western Australia, Bull. 132, 268 p.
- Sobolev. N.N., Galimov, E.M., Smith, C.B., Yefimova, E.S., Hall, A.E., and Usova, L.V., (1989) Geologiya i Geofizika, N.12

DIAMOND PROSPECTIVITY FROM INDICATOR MINERALOGY:  
A WESTERN AUSTRALIAN PERSPECTIVE.

*Smith*<sup>(1)</sup>, *Chris. B.*; *Lucas*<sup>(1)</sup>, *H.*; *Hall*<sup>(1)</sup>, *A.E.* and *Ramsey*<sup>(2)</sup>, *R.R.*

(1) *CRA Exploration Pty. Ltd., 21 Wynyard St., Belmont, Western Australia 6104;*

(2) *University of Western Australia, Hackett Drive, Crawley, Western Australia.*

Since the first discovery of kimberlite in South Africa, over 100 years ago, it has been the desire of explorationists to devise a rapid scheme for establishing whether a particular find was diamond bearing or not, without recourse to costly bulk sampling.

The recognition of distinctive compositions of resistate minerals associated with diamond such as sub-calcic (G10) garnets by Gurney and Switzer (1973) and Sobolev (1974) was one of the first steps in establishing such an appraisal system. Various workers have correlated the presence and abundance of diamond with the chemistry of ilmenite (Fesq et al, 1976) and chromite (Sobolev, 1974), and the methods were further developed by Gurney (1984) and by Moore and Gurney (1989) whose outline represents the sophisticated state of diamond grade prediction today. The latter authors use the soda content of eclogitic garnets as a predictor of eclogitic diamond grade and the chemistry of sub-calcic chrome pyropes along with high chrome chromite to emphasise the importance of the harzburgitic paragenesis for peridotitic diamond formation. High-chrome magnesian ilmenites are empirically correlated with high diamond grade, a relationship speculated by the authors as reflecting low oxygen fugacities within the kimberlite magma during upward transportation from the mantle source. Low oxygen fugacity should favour retention of unresorbed diamond, and therefore the ilmenite composition can be used as a diamond preservation predictor for both styles of diamond paragenesis.

Concentrates from kimberlites of the North and East Kimberley of Western Australia (Jaques et al., 1986; Lucas et al., 1989) are characterized by an abundance of megacrystal ilmenite and subordinate garnet, which ranges in composition from titanium pyrope of megacrystal or sheared lherzolite paragenesis to peridotitic chrome pyrope. Sub-calcic garnets are present in small quantities, indicating a depleted component in the mantle and hence a potential for peridotitic diamond paragenesis. Eclogitic garnet is present but in such low numbers as to limit its usefulness in predicting grade. As only a few of the kimberlites carry magnesio-chromites with Cr<sub>2</sub>O<sub>3</sub> values typical of diamond inclusions, the diamond contribution from the spinel harzburgite paragenesis in these kimberlites is thought to be insignificant.

Many North Kimberley kimberlites, e.g. Hadfields and Pteropus, carry ilmenites with high Cr<sub>2</sub>O<sub>3</sub> and MgO which indicate good potential for diamond preservation, but the general lack of associated G10 garnets or high chrome chromites implies an insignificant diamond contribution from the harzburgitic parageneses so the overall predicted grade is poor. In general there is good agreement between actual and predicted grade.

Most lamproites from the West Kimberley and Argyle contain little mantle derived garnet and are practically devoid of megacrystal magnesian ilmenite (Jaques et al., 1986; Lucas et al., 1989; Moore and Gurney, 1989). Most concentrate ilmenites recovered are Mg-poor Mn-bearing groundmass types which cannot be used in diamond grade predictions. The poor representation of eclogitic minerals in concentrates restricts their use in predicting grade and belies the importance of the eclogitic diamond paragenesis at Ellendale and especially at Argyle. Carbon isotope and diamond inclusion work by Jaques et al. (1989) show that roughly 96% of the Argyle stones and nearly half of those from Ellendale come from eclogites.

The lherzolitic mineral suite is prominent within the peridotite diamond paragenesis in Australian lamproites, unlike the African and Siberian situation where the harzburgitic suite is pre-eminent. This is shown by frequent chrome diopside inclusions within diamond (Jaques et al., 1989) and indirectly confirmed by concentrate mineralogy which, while containing lherzolitic garnets, commonly lacks the sub-calcic varieties. Interestingly, amongst the Ellendale pipes, the most diamondiferous does not contain the most sub-calcic garnets. As yet, no sub-calcic garnets have been found in Argyle concentrate (Lucas et al., 1989), the richest diamond bearing lamproite of all. High-chrome chromites with  $\text{Cr}_2\text{O}_3 > 60\%$  and  $\text{MgO} > 12\%$  are present in both the diamondiferous and weakly diamondiferous pipes and may represent a chromite harzburgite diamond paragenesis as suggested by Moore and Gurney (1989).

In conclusion, Moore and Gurney's rules so successfully used in Africa and north America are effective for the Western Australian kimberlites where the dominant source of diamond paragenesis appears to be depleted harzburgite from the diamond stability field. As these authors themselves warn, the appraisal scheme meets with less success in estimating the diamond bearing potential of lamproites. One problem with lamproites is the paucity of eclogitic minerals in the concentrates which prevents proper assessment of the contribution from the dominant eclogitic paragenesis of the Australian lamproite diamonds.

Three other shortcomings of the scheme have become apparent on applying it to the Australian situation. Firstly the assumption that the dominant peridotitic diamond paragenesis is harzburgitic is not necessarily true. It is not the case at Argyle or at Ellendale where the lherzolitic paragenesis is as important, if not more so. Secondly G10 garnets, indicative of depleted harzburgitic upper mantle, need not necessarily come from the diamond stability field (Boyd and Nixon, 1989; Shee et al., 1989) and hence may be unreliable diamond predictors. This is shown by the presence of G10 garnets at the barren North Kimberley occurrence of Skerring. The development and use by Griffin (1990) of a garnet-Ni thermometer, which suggests Skerring peridotitic garnets (G10s included - Griffin, pers. comm.) are either too cold or too hot to be associated with a lithospheric source of diamond, may be the next refinement to the scheme for predicting diamond grade from indicator mineral chemistry. Thirdly, the role of ilmenite chemistry in predicting diamond preservation is not clear. This certainly seems to be the case at Skerring where ilmenite chemistry is invoked to remove "non-existent" diamonds. Also at Argyle the diamonds are highly resorbed yet the high chrome-bearing magnesian ilmenite chemistry predicts little resorption.

## REFERENCES:

- Boyd, F.R., and Nixon, P.H., 1988. Low-Ca garnet harzburgites: origin and role in craton structure. Geophysical Laboratory, Carnegie Institute of Washington, Annual Rept., 1987-88, p. 8-13.
- Fesq, H.W., Kable, E.J.D., & Gurney, J.J., (1976) The geochemistry of some selected South African kimberlites and associated heavy minerals. National Institute for Metallurgy. South Africa. Report No. 1703.
- Griffin, W.L. (1990) The nickel thermometer: A new tool for diamond exploration. CSIRO Division of Exploration Geoscience, Exploration Research News 4, p. 3-4.
- Gurney, J.J., and Switzer, G.S., (1973) The discovery of garnets closely related to diamonds in the Finsch Pipe, South Africa. Contrib. Mineral. Petrol., vol.39, p. 103-116.
- Gurney, J.J., (1984) A correlation between garnets and diamonds in kimberlites. In J.E. Glover and P.G. Harris, Eds., Kimberlite Occurrence & Origin, University of Western Australia, Geology Dept. Publ. 8, p. 143-166
- Jaques, A.L, Lewis, J.D., and Smith, C.B., (1986) The kimberlites and lamproites of Western Australia. Geol. Surv. Western Australia, Bull. 132, 268 p.
- Jaques, A.L., Hall, A.E., Sheraton, J.W., Smith, C.B., Sun, S-S., Drew, R.M., Foudoulis, C., and Ellingsen, K., (1989) Composition of crystalline inclusions and C-isotopic composition of Argyle and Ellendale diamonds. In J. Ross, Ed., Kimberlites and Related Rocks, Volume 2, Their Mantle/Crust Setting, Diamonds and Diamond Exploration. Geological Society of Australia Special Publication No. 14, Blackwell, Melbourne, p. 966-989.
- Lucas, H., Ramsay, R.R., Hall, A.E., Smith, Chris B., and Sobolev, N.V., (1989) Garnets from Western Australian kimberlites and related rocks, In J. Ross, Ed., Kimberlites and Related Rocks, Volume 2, Their Mantle/Crust Setting, Diamonds and Diamond Exploration. Geological Society of Australia Special Publication No. 14, Blackwell, Melbourne, p. 809-819.
- Moore, R.O., and Gurney, J.J., (1989) The development of advanced technology to distinguish between diamondiferous and barren diatremes. Geol. Surv. of Canada Open File Report 2124, part 1, p. 1-90.
- Shee, S.R., Bristow, J.W., Bell, D.R., Smith, C.B., Allsopp, H.L., and Shee, P.B., (1989) The petrology of kimberlites, related rocks and associated mantle xenoliths from the Kuruman Province, South Africa, In J. Ross, Ed., Kimberlites and Related Rocks, Volume 1, Their Composition, Occurrence, Origin and Emplacement. Geological Society of Australia Special Publication No. 14, Blackwell, Melbourne, p. 60-82.
- Sobolev, N.V., (1974) Deep seated inclusions in kimberlites and the problem of the composition of the upper mantle. Translated by D.A. Brown, 1977, AGU, Washington, 279 p.

ECLOGITE XENOLITH WITH EXSOLVED SANIDINE FROM THE PROTEROZOIC  
KURUMAN KIMBERLITE PROVINCE, NORTHERN CAPE, R.S.A.

Smith<sup>(1)</sup>, C.B.; Ramos<sup>(2)</sup>, Z.N.; Hatton<sup>(2)</sup>, C.J.; Horsch<sup>(2)</sup>, H. and Damarapurshad<sup>(3)</sup>, A.

(1) Bernard Price Institute for Geophysical Research, U. Witwatersrand, Johannesburg 2050, R.S.A.; (2) Anglo American Research Laboratories, Box 106, Crown Mines 2025, R.S.A.; (3) Schonland Research Centre for Nuclear Sciences, U. Witwatersrand, Johannesburg 2050, R.S.A. and Geological Survey of South Africa, Silverton 0001, R.S.A.

The zero kimberlite is one of twelve known occurrences of kimberlites and related rocks of the Kuruman Province, northwest Cape, South Africa. Radiometric dating has demonstrated that these bodies are 1600 to 1700 Ma in age (Shee et al., 1989), and are thus amongst the oldest known kimberlites. They occur as small eroded pipes or dykes located on the western edge of the Kaapvaal Craton (greater than 2500 Ma) adjacent to the younger Kheis belt (about 1800 Ma) of the northern Cape Province. Zero is an oval-shaped pipe, 300m by 200m, intrusive into the early Proterozoic Campbell Rand dolomite of the Transvaal Supergroup. Texturally the kimberlite is a macrocrystic hypabyssal type, and is mineralogically classified as an opaque mineral-rich phlogopite calcite group I kimberlite.

The kimberlite is notable for the high mantle-derived xenolith content, but the pipe is capped by extensive calcrete, and preserved material is available only from drill core. The xenolith suite comprises equal proportions of eclogite and peridotite, the latter rocks having been studied by Shee et al. (1989) who documented evidence for a hot, perturbed geotherm. The eclogite nodules have not been studied previously in any detail. For this study a single eclogite xenolith was extracted from the Zero drill core for petrologic study, the sample being one of two initially chosen for their uncommonly large size, unusual degree of freshness, and unusual textural relations between garnet and clinopyroxene. Careful petrographic study of the specimen indicates that it is essentially a large clinopyroxene megacryst that has exsolved garnet and sanidine. Sanidine has only rarely been described as occurring in mantle eclogite (Smyth and Hatton, 1977; Smith, 1977; Ater et al., 1984), and this is the first known case where sanidine is a clear exsolution product, occurring both as discrete grains at clinopyroxene and garnet grain boundaries and as crystallographically controlled exsolution blebs within clinopyroxene. Prior to exsolution the megacryst must have contained substantial potassium in solid solution, implying a very high pressure origin.

Average major elements analysis and standard deviations of the mineral phases (Table 1) demonstrate that they are relatively homogeneous. Garnet is relatively magnesian and calcium-poor, and in this regard is distinctive compared to previously documented sanidine-bearing samples from kimberlite. The example described by Smyth and Hatton (1977) and Wohletz and Smyth (1984) is a grosspyrite with considerably greater Ca. Of twelve samples noted by Ater et al. (1984) from the Colorado-Wyoming kimberlites, nine are kyanite- and/or corundum-bearing and the other three are significantly more Fe- and Ca-rich than the Kuruman example. Clinopyroxene in the Kuruman sample has low to moderate Na<sub>2</sub>O of 1.7%. Na<sub>2</sub>O in garnet (0.05%) and K<sub>2</sub>O in clinopyroxene (0.03%) are low compared to type 1 diamond-bearing assemblages (McCandless and Gurney, 1989), and Cr<sub>2</sub>O<sub>3</sub> is relatively high in both minerals. All of these chemical features indicate a type 2 association for the sample, as is the case for most other documented sanidine-bearing eclogites. The K<sub>f</sub> value is 3.24, and

for an assumed pressure of 50 Kb the equilibration temperature is 1000<sup>0</sup>C. This falls slightly below the peridotitic geotherm calculated by Shee et al. (1989).

Clinopyroxene and garnet are both enriched in Ce (20.2 and 9.5 ppm, respectively), and relative to La and Nd the clinopyroxene has a distinct negative Ce anomaly with overall LREE enrichment (La/Eu = 4.54). High Ce in garnet also gives a LREE enriched pattern, with HREE enrichment from Gd to Lu. Further isotopic and trace elements analysis are in progress.

Given the setting and age of the Kuruman kimberlites, data from this xenoliths and as yet unstudied additional members of the eclogite assemblage could have important bearing on the understanding of the origins and evolution of lithospheric mantle beneath the Kheis belt and marginal to the craton for which various subduction-type models have been postulated.

## REFERENCES

- ATER, P.C., EGGLER, D.H. and McCALLUM, M.E. (1984) Petrology and geochemistry of mantle eclogite xenoliths from Colorado-Wyoming kimberlites: recycled ocean crust? In J. Kornprobst, ed., *Kimberlites II: The Mantle and Crust-Mantle Relationships*, Elsevier Science Publishers, Amsterdam, 309-318.
- McCANDLESS, T.E. and GURNEY, J.J. (1989) Sodium in garnet and potassium in clinopyroxene: criteria for classifying mantle eclogites. In J. Ross, Man. ed., *Kimberlites and Related Rocks, Their Mantle/Crust Setting, Diamonds and Diamond Exploration*, v.2, Geol. Soc. Australia Spec. Publ. 14, p. 827-832.
- SHEE, S.R., BRISTOW, J.W., BELL, B.R. SMITH, C.B., ALLSOPP, H.L. and SHEE, P.B. (1989) The petrology of kimberlites, related rocks and associated mantle xenoliths from the Kuruman Province, South Africa. In J. Ross, Man. ed., *Kimberlites and Related Rocks, Their Composition, Occurrence, Origin and Emplacement*, v.1., Geol. Soc. Australia Spec. Publ. 14, p. 60-82.
- SMITH, C.B. (1977) Kimberlite and mantle-derived xenoliths at Iron Mountain, Wyoming. MS thesis, Colorado State University.
- SMYTH, J.R. and HATTON, C.J. (1977) A coesite-sanidine grosspyrite from the Roberts Victor kimberlite. *Earth Planet. Sci. Lett.* 34: 284-290.
- WOHLETZ, K.H. and SMYTH, J.R. (1984) Origin of a Roberts Victor sanidine-coesite grosspyrite: thermodynamic considerations. In J. Kornprobst, ed., *Kimberlites II: The Mantle and Crust-Mantle Relationships*, Elsevier Science Publishers, Amsterdam, 33-42.

**Table 1.** Electron Microprobe Analysis of Garnet, Clinopyroxene and standard deviations for N analysis.

N	GAR	CPX	SAN
	6	10	3
SiO <sub>2</sub>	40.9 +/- .3	54.8 +/- .03	62.2 +/- .3
TiO <sub>2</sub>	0.06 +/- .02	0.10 +/- .02	-
Al <sub>2</sub> O <sub>3</sub>	22.8 +/- .2	2.94 +/- .09	18.4 +/- .3
Cr <sub>2</sub> O <sub>3</sub>	0.25 +/- .03	0.15 +/- .02	-
FeO	16.2 +/- .1	4.88 +/- .12	0.77 +/- .05
MnO	0.45 +/- .02	0.07 +/- .02	-
MgO	14.9 +/- .2	14.5 +/- .2	-
CaO	4.59 +/- .12	20.3 +/- .1	-
Na <sub>2</sub> O	0.05 +/- .02	1.71 +/- .06	0.37 +/- .10
K <sub>2</sub> O		0.03 +/- .01	15.6 +/- .3

## PYROXENE CRYSTAL CHEMISTRY AND THE EVOLUTION OF ECLOGITES IN THE MANTLE.

*Smyth, J.R.; McCormick, T.C. and Caporuscio, F.A.*

*Department of Geological Sciences. University of Colorado, Boulder, CO 80309-0250 USA.*

Mantle eclogites as represented in inclusions in South African kimberlites show a wide variation in major element composition from coesite- or corundum-bearing grosopydites to kyanite eclogites to Fe- and Mg-rich bimineralec eclogites. In major element composition, the bimineralec samples resemble MORB; the coesite grosopydites resemble anorthosite; and the corundum grosopydites do not resemble any crustal rock type. In rare earth elements, the bimineralec samples also resemble MORB, having concentrations of 2 to 20 times chondritic values with flat to slightly LREE-depleted patterns. The grosopydites (both coesite and corundum-bearing) show characteristic depletions in both light and heavy REE and slight enrichments in the middle REE with maxima at Eu (Caporuscio and Smyth, 1990). Oxygen isotope values range from about +2 to +10‰, a much greater range than exhibited by other mantle samples, but do not appear to vary systematically with major-element compositions.

In many samples, particularly the grosopydites, there is abundant evidence of garnet and garnet-plus-kyanite exsolution from the clinopyroxene. We have also observed epitaxial rutile and phlogopite that have apparently exsolved from clinopyroxene. Re-assembling the clinopyroxene from exsolved phases we see an unexpectedly complex crystal chemistry. Textures in two corundum grosopydites suggest that most of the garnet and clinopyroxene in the rock had exsolved from a single precursor pyroxene that could not have existed at pressures less than about 3 GPa. These observations strongly support the hypothesis of Lappin (1978) that the grosopydites may be the result of an accumulation of hyperaluminous pyroxene at pressures greater than 3 GPa (Smyth et al., 1984, 1989).

Alternatively, other recent studies have favored an origin for the grosopydites as subducted feldspathic cumulates (MacGregor and Manton, 1986; Shervais et al., 1988, Taylor and Neal, 1989, Neal et al., 1990). This hypothesis accounts for the large variation in oxygen isotopic values in these rocks, although not in any consistent or systematic way. However, it fails to account for corundum-normative grosopydites; and it fails to account for the extreme values of radiogenic isotope ratios observed in these rocks (Shervais et al., 1988; Caporuscio, 1988; Neal et al., 1990).

The key to understanding these rocks, however, appears to lie in understanding the crystal chemistry of the pyroxenes. Smyth (1980) reported microprobe data indicating up to 9 mole percent vacancy in the M cation sites. McCormick (1986) located the cation vacancy in the M2 site by means of electron channeling and X-ray single crystal diffraction. The reconstructed exsolved pyroxene reported by Smyth et al. (1984) would have had about 17% M2 vacancy. Smyth et al. (1991) report IR spectra indicating up to 1800 ppm by weight OH in one

sample and a linear correlation of cation deficiency (vacancy) with H content. Extrapolating this relationship, we would infer that the most vacancy-rich pyroxene analyzed would have about 2600 ppm by weight OH and the reconstructed precursor pyroxene about 0.5 wt% OH. We are currently pursuing X-ray and neutron single crystal diffraction studies of this pyroxene to structurally locate the hydrogen.

This is much more H than any other nominally anhydrous phase common in the eclogite or peridotite suite of rocks, with the possible exception of rutile (Rossman and Smyth, 1990). It is two to three orders of magnitude more than co-existing garnet. In the eclogite-rich mantle suggested by Anderson (1984), clinopyroxene could be the dominant hydrous phase. Further, the H released from the pyroxene on cooling from solidus temperatures provides a source of H for auto-metasomatism of the eclogites. This would account for at least part of the ubiquitous secondary assemblage observed on nearly every grain boundary in the eclogites.

The REE composition of the grospydites is also consistent with an origin by high pressure igneous accumulation of clinopyroxene. In particular, the MREE enrichments and much lower total REE contents of the grospydites are typical of clinopyroxene-liquid fractionations, and inconsistent with plagioclase-liquid fractionations.

The great range of oxygen isotope values observed for these rocks suggests a low-temperature process. However, we have observed mineral-mineral fractionations up to 3.0% for a garnet-coesite pair indicating that significant fractionation can indeed occur at mantle temperatures. Further, we observe a correlation of garnet-clinopyroxene fractionation of oxygen isotopes with vacancy (and presumably OH) content. This suggests that oxygen isotopes might be disturbed or affected by the H-content or evolution of hydrous fluid from the pyroxene. However, these observations do not preclude the involvement of a low temperature process in that the silicate liquids may be the result of partial melting of subducted material.

In summary, it appears that clinopyroxene crystal chemistry may control much of the chemical evolution of eclogites in the mantle. The major and trace element whole-rock compositions seem to be the result of igneous accumulation of a liquidus pyroxene at pressures above 3 GPa, and exsolution textures seem to require that some of these rocks were almost single-phase pyroxenes. Hydrogen contents of eclogitic clinopyroxene are the largest of any pyroxene and correlate with M2 cation vacancies. The large amounts of structurally-bound OH may allow clinopyroxene to be the dominant hydrous phase in some possible mantle compositions. Further, evolution of H and other incompatible elements from clinopyroxene may account for some of the ubiquitous secondary phases observed on grain boundaries in mantle eclogites.

#### REFERENCES

- Anderson, D.L. (1984) Kimberlite and evolution of the mantle. In J. Kornprobst, Ed., *Kimberlites II: The Mantle and Crust-Mantle Relationships*, p. 309-318. Elsevier, Amsterdam.

- Caporuscio, F.A. (1988) Petrogenesis of mantle eclogites from South Africa, PhD Dissertation. Univ. of Colorado, Boulder, CO, USA. 134pp.
- Caporuscio, F.A. and J. R. Smyth (1990) Trace element crystal chemistry of mantle eclogites. *Contributions to Mineralogy and Petrology*, 105, 550-561.
- Lappin, M.A. (1978) The evolution of grosspydite from the Roberts Victor Mine, South Africa. *Contributions to Mineralogy and Petrology*, 66, 229-241.
- MacGregor, I.D. and Manton, W.I. (1986) The Roberts Victor eclogites: ancient ocean crust? *Journal of Geophysical Research*, 91, 14063-14079.
- McCormick, T.C. (1986) Crystal-chemical aspects of non-stoichiometric pyroxenes. *American Mineralogist*, 71, 1434-1440.
- Neal, C.R., Taylor, L.A., Davidson, J.P., Holden, P., Halliday, A.N., Nixon, P.H., Paces, J.B., Clayton, R.N., and Mayeda, T.K. (1990) Eclogites with oceanic crustal and mantle signatures from the Bellsbank kimberlite, South Africa, Part 2. Sr, Nd, and O isotope chemistry. *Earth and Planetary Science Letters*, 99, 362-379.
- Rossmann, G.R. and Smyth, J.R. (1990) Hydroxyl contents of accessory minerals in mantle eclogites and related rocks. *American Mineralogist*, 75, 775-780.
- Shervais, J.W., L.A. Taylor, G.W. Lugmair, R.N. Clayton, T. Mayeda, and R.L. Korotev. (1988) Early Proterozoic oceanic crust and the evolution of subcontinental mantle: eclogites and related rocks from southern Africa. *Geological Society of America Bulletin*, 100, 411-420.
- Smyth, J.R. (1980) Cation vacancies and the crystal chemistry of breakdown reactions in kimberlitic omphacites. *American Mineralogist* 65, 1257-1264.
- Smyth, J.R., McCormick, T.C. and Caporuscio, F.A. (1984) Petrology of a suite of eclogite inclusions from the Bobbejaan kimberlite I. Two unusual corundum-bearing kyanite eclogites. In J. Kornprobst, Ed., *Kimberlites II: The Mantle and Crust-Mantle Relationships*, p. 109-119. Elsevier, Amsterdam.
- Smyth, J.R., Caporuscio, F.A. and McCormick, T.C. (1989) Mantle eclogites: evidence for igneous fractionation. *Earth and Planetary Science Letters*, 93, 133-141.
- Smyth, J.R., Bell, D.R., and Rossmann, G.R. (1991) Hydrous clinopyroxenes from the upper mantle. Submitted to *Nature*.
- Taylor, L.A. and Neal, C.R. (1989) Eclogites with oceanic crustal and mantle signatures from the Bellsbank kimberlite, South Africa, Part 1. Mineralogy, petrography, and whole rock chemistry. *Journal of Geology*, 97, 551-567.

## THE IMPURITY CENTERS AND SOME PROBLEMS OF DIAMOND GENESIS.

*Sobolev, E.V.**Institute of Inorganic Chemistry S.D.Ac.Sc. USSR, Novosibirsk, USSR.*

The initiation of discussions dealing with the impurity centers in diamonds originates to the classical contributions of 1934 (Robertson, Fox & Martin), who have subdivided the natural crystals into two types (I and II) with postulating the problem of the nature of differences available. The later great interest to this problem had arisen in 1959 in the classical experiments by Kaiser & Bond, also by Smith, Sorokin, Galles & Lasher, who had identified two structural states of impurity nitrogen - single substituting atoms (by ESR) and the non-paramagnetic associations of the substituting atoms, so-called A-centers (mass-spectrometric analysis, lattice parameter, density as compared with IR & UV-absorption spectra). But starting with 1960 this discussion has followed a wrong trend, the idea of impurity polymorphism being refused with the wrong identification of the associative A nitrogen form as the platelets parallel to the cubic planes.

In our experiments carried out as early as 1962, also in our publications (the first published in 1964) we have chosen the trend of impurity polymorphism by proving the existence of single substituting atoms in all crystals of natural diamond (N-centers, 1964), also of A-centers being the pairs of substituting atoms (1967), nitrogen platelets - B2 centers (1965), as well as some others then unidentified nitrogen forms (1968). As late as 1971 this concept of ours was formulated by the author in a structural form which does exist at present time with some small corrections (see our review 1989). Methods applied by the author in a search of correlation between various properties of the same crystal (ESR, optical, X-ray, el. mycr., etching analysis, etc) with the quantitative basis, such as several band systems in the IR absorption spectra with the decomposition of A & B1 bands. The principal condition of the proposed structural model of each of the centers is the lack of contradictions with none of the properties of each of the centers. Coverage of a great number of crystals (hundreds & thousands), among them selected carefully of much greater number has ensured high reliability of the experimental results. At present, we are familiar with over 10 nitrogen centers of various structure, five of which are thought to be the principal for natural crystals both by their occurrence and by the average and maximum nitrogen content in the specimen under study. One of the principal ones is the A-form, with nitrogen content in some cases reaching  $10^{21}$  at/cm<sup>3</sup>, but the minimum recorded A nitrogen content of our specimen was  $2 \cdot 10^{17}$ . The structure of this form as a pair of substituting nitrogen atoms in the neighbouring carbon positions follows from the over-all set of properties as well as from the nature of arbitrary paramagnetic centers formed of A-centers during particle irradiation followed by annealing or dislocational processes with a hyperfine splitting on the two nitrogen nuclei. The results obtained by Davis (1976) dealing with the symmetry fixing of A-centers using uniaxial compression methods proposed by A.A. Kaplyansky do not contradict to these data.

We have studied abundant crystals of natural diamonds from various regions (apart from the fields of USSR, we have studied those from South Africa, Australia, India, Brazil, etc) in which we have fixed N-form, but as of secondary importance compared with the A-form. Nevertheless the correlation between them may be constant for some of the fields. By the correlation value we have separated two types of fields: Yakutian & Uralian with crystals from North Yakutia belonging to Uralian type whose mean content of N-centers is twice as high. Some of octahedra from African fields do belong to this type. Meanwhile, among the crystals of Archangelskaya Province one has fixed the mixture of two types. It is to be stressed

that the concept that is very popular in special literature saying that the N-centers are lacking in most of the colourless crystal of natural diamonds of highest quality is wrong; it is a consequence of the peculiarities of the apparatus applied in the experiments.

Of more complex associations of the nitrogen atoms we have separated to main group  $N_3V$  paramagnetic assemblage that are active both for absorption & luminescence 415 nm. The optical analogue of paramagnetic centers was identified by the author in 1969, while the modern model was published first in 1972. For a majority of natural diamond crystals the higher content of 415 nm centers results in increase of N-centers versus to that of A-centers. The nitrogen contents in this form is not very high. It is much higher for B1 form (N9), that may belong according to our assumption to nitrogen segregations in octahedra planes with the three-valent substituting nitrogen atom of amino-type as a main structural element, quite like to hypothetical  $N_4V$  assemblage, a popular structural model for B1 but not N9 centers. The B1 (N9) centers are also active at X-rays excited blue & cathode-luminescence with indications of concentrational saturation. This type of luminescence as well as other ones may be quenched by the A-centers, so when combined with saturation effects the X-ray ex. & cathode luminescence of most of the natural crystals reflect at the cross-sections the quantitative distribution of A-centers. We note that the trend fixed in vast literature to assign the IR-system of BI & UV system N9 to different centers is absolutely wrong.

Finally, the last of the principal nitrogen centers are those well known ones as early as in 60-ties, nitrogen platelets in cubic planes. Their IR-system B2 (not A) has some peculiarities connected with platelets dimension for example the maximum position of the main band etc. This experimental fact was checked many times and by many methods (for example by etching, etc.) and we must realize that Lang model of platelets but with some real structure elements such as benching from the center to periphery with the individuality of the marginal domain as a band of  $1432\text{ cm}^{-1}$  etc, is quite convenient for the understanding the large family of facts.

The impurity hydrogen can be also fixed by IR-spectra of natural diamond crystals; we hold here also the concept of impurity polymorphism as early as 1966. The model of the main  $C_2H_2$ -center was proposed by the author in 1971; at present it has been confirmed by the recent results for the Raman spectra with indications of SERS effects etc. (see review 1989), justifying in favour of surficial localization of centers. As based on the date obtained by the authors & those referred in literature, these centers are most probably located at the inner surfaces of octahedral submicrocavities (voids).

The problems of nitrogen center genesis in diamond crystals have been discussed by the author in initial contributions. We think that the viewpoint popular in special literature dealing with the origin of A-centers in the process of high-T long-time annealing from N-centers is not correct, as it contradicts the well known of type Ib and Ia combination with type Ib included in type Ia. So the  $N_2$  centers has the growth nature, their structure is caused by the form of supply of nitrogen from the mineral-forming environment. We also regard the hydrogen  $C_2H_2$  centers to be growth nature as they also are due to the main form of hydrogen supply. The nitrogen pairs may, in principal, be formed by only of molecular  $N_2$ , but also of chemically bonded nitrogen, for example, to  $CN_2$ , though when combined with a acetylene  $C_2H_2$  the molecular nitrogen becomes to be the preferential form. As for some others (principal) nitrogen & hydrogen centers, they may be, in principal, both growth (such as  $C_2H$ ) & secondary (B1, B2) but the date obtained for natural crystals indicate that the possibility of their generation was laid probably as a nucleus in the process of growth of each of the zones with an abrupt reduction of activation barrier for diffusion, perhaps, by the mechanism of deformational stimulation.

Thus analysis of the structure of impurity centers in diamonds permit one to identify the two components of the mineral forming environments, such as nitrogen & acetylene. The source of nitrogen seemed to be degassing of the Earth's Mantle, while acetylene would rather be formed by the reaction  $\text{CaC}_2 + \text{H}_2\text{O}$ ;  $\text{CaC}_2$  could be the product of the reaction of  $\text{CaCO}_3$  with metal sulphides (for diamonds these inclusions belong to the most common ones) or oth. It is quite likely that  $\text{C}_2\text{H}_2$  was the source of diamond carbon, though this version may be obstructed by IIa type crystals. Presence of acetylene in the natural diamond crystals permits one to understand numerous traces of dynamic processes of explosion type with crushing of crystals fixed repeatedly in the inner zoning. Fluid diffusion whose components were  $\text{N}_2$  and  $\text{C}_2\text{H}_2$  through the environment may be highly inhomogeneous which may be responsible for the exceptionally inhomogeneous distribution of crystals in the source rocks.

The essential role of inhomogeneity in the processes of nitrogen diffusion was postulated by the author in 1966 in a joint paper with V.S. Sobolev.

We also believe the role of acetylene & its products to be most probable in formation of explosion pipes at  $500^\circ\text{C}$  followed by a subduction of the cooled ( $400\text{-}500^\circ\text{C}$ ) kimberlite magma into the formed emptiness. Such concepts aid in understanding numerous experimental evidence dealing with the pipes and diamonds of the principal fields, such as high preservation of crystals, often preservation of their green radiational coat, essential diamond differentiation over the pipe cross-section, but high reproducibility both quantitatively and qualitatively by the depth and many others very common and hardly explainable at present versions of hot kimberlite magmatism. As for the time interval between the termination of crystal growth in the upper mantle & subduction of the quite cool kimberlite magma into the explosion pipe, the period that may be very long is to be fixed not by the impurity centers of the diamonds and included minerals but proceeding from some different experimental evidence.

ROBERTSON, R.; FOX, J.J.; MARTIN, A.E. (1934) The two types of diamond. *Phil. Trans. Roy. Soc.*, **232**: 463-535.

KAISER, W. & BOND, W.L. (1959) Nitrogen, a major impurity in common type I diamond. *Phys. Rev.*, **115**: 857-863.

SMITH, W.V.; SOROKIN, T.P.; GALLES, I.L.; LASHER, G.J. (1959) Electron spin resonance of nitrogen donors in diamond. *Phys. Rev.*, **115**: 1546-1552.

DAVIES, G. (1976) The A nitrogen aggregate in diamond - its symmetry and possible structure. *J. Phys. "C", Sol. St. Phys.* **9**: L537-L542.

SOBOLEV, E.V. (1989) *Harder than Diamond* (sec. edit.) 190pp, Novosibirsk, Nauka (Russian).

## ECLOGITE PAREGENESIS OF DIAMONDS FROM UDACHNAYA AND MIR PIPES, YAKUTIA.

*N.V. Sobolev*<sup>(1)</sup>; *V.M. Zuev*<sup>(2)</sup>; *S.M. Bezborodov*<sup>(2)</sup>; *A.I. Ponomarenko*<sup>(1)</sup>; *Z.V. Spetsius*<sup>(2)</sup>; *S. Kuligin*<sup>(1)</sup>; *E.S. Yefimova*<sup>(1)</sup>; *V.P. Afanasiev*<sup>(1)</sup>; *V.I. Koptil*<sup>(3)</sup> and *A.I. Botkunov*<sup>(2)</sup>.

(1) *Institute of Mineralogy and Petrography, 630090, Novosibirsk, USSR;* (2) *Yakutalmaz, 678170, Mirny, USSR;*  
(3) *Yakutskgeologiya, 677892, Yakutsk, USSR.*

An unique collection of xenoliths of diamondiferous eclogites from Udachnaya pipe, collected by the authors over a long period of time and consisting of more than 120 samples of different sizes (principally 2-5 cm in longest dimension) is compared with data (Sobolev et al., 1983) on more than 40 diamondiferous eclogite xenoliths collected for years from the Mir pipe. Most eclogites have been collected at processing plants where samples of kimberlite with diamonds exposed at the surface are checked.

In most samples euhedral garnets are embedded in the pyroxene matrix but in a number of cases garnet-pyroxene occur in banded structures. Modal proportion of garnet varies from almost pure garnetite down to samples with about 35-40 % of modal garnet. Kyanite eclogites containing up to 10 % of kyanite are typical mostly for Udachnaya pipe. Only one sample of this type was collected in Mir pipe. A few corundum eclogites have been found in both pipes.

Diamonds in the studied samples vary widely both in size and number in each specimen. The largest diamonds exposed at the surface have a size up to 8-9 mm across, smallest diamonds extracted from some dissolved specimens have a size up to 40-50 microns. Diamonds usually have a variable morphology but octahedral crystals predominate. Within single samples in most cases the diamond morphology is similar. In several samples of eclogite, diamonds contain inclusions of garnet, omphacite and sulfides.

Comparison of major and minor elements abundances in garnets from diamondiferous eclogites and inclusions in diamonds from the same pipe shows that both types of garnets contain similar CaO and Na<sub>2</sub>O within each pipe, but with higher CaO for both inclusions and eclogites from Udachnaya pipe. TiO<sub>2</sub> content is almost double for included garnets compared to eclogitic ones. All Mir pipe garnets are richer in iron in comparison to Udachnaya eclogite and inclusion garnets.

Omphacites from eclogites are more sodic than omphacites from diamonds both for Udachnaya and Mir pipes, but in general Mir pipe omphacites contain more Na<sub>2</sub>O. Very systematic differences are noted in K<sub>2</sub>O contents between omphacites from diamonds and diamondiferous eclogites. In spite of detectable K<sub>2</sub>O content for all studied omphacites, pyroxenes included in diamonds for both pipes contain up to 2-2,5 times more K<sub>2</sub>O on average than pyroxenes from diamondiferous eclogites. As was previously shown for Mir pipe (V.S. Sobolev et al., 1972) this might be related to the loss of a major part of K<sub>2</sub>O by pyroxenes during reequilibration at subsolidus temperatures.

The temperature estimates, using Ellis and Green (1979) approach, show that the inclusions have been equilibrated at temperatures up to 1220-1230°C on average for both pipes compared with average equilibration temperatures of 1100-1150°C for diamondiferous eclogites.

VOLCANOLOGY AND GEOCHEMISTRY OF THE ELLENDALE LAMPROITE FIELD  
(WESTERN AUSTRALIA).

*Stachel*<sup>(1)</sup>, *T.*; *Lorenz*<sup>(1)</sup>, *V.*; *Smith*<sup>(2)</sup>, *C.B.* and *Jaques*<sup>(3)</sup>, *A.L.*

*(1) Inst. für Geologie, Pleicherwall 1, 8700 Würzburg, Germany; (2) CRA - Exploration Pty. Ltd., P.O. Box 175, Belmont, W.A. 6104, Australia; (3) Bureau of Mineral Resources, GPO Box 378, Canberra, ACT, Australia.*

**INTRODUCTION**

The Miocene (20-22 Ma) Ellendale Volcanic Field (Western Australia) is located on the Phanerozoic Lennard Shelf, adjacent to the SW margin of the Precambrian Kimberley Block. The field consists of about 50 ultrapotassic volcanic bodies, subdivided into two main groups: ultrabasic olivine lamproites and more silica-rich leucite lamproites (JAQUES et al. 1986). Most of the Ellendale Field lamproites carry diamond: two olivine lamproite pipes contain subeconomic diamond grades and 3 other olivine lamproite pipes have average grades of 1 carat/100 tonnes or more whereas the leucite lamproites are either barren or contain only traces of diamond. This paper reports results of detailed geological, petrological and geochemical investigations of two olivine lamproites (Ellendale 4 and 9) for which extensive drill core material is available and two well exposed leucite lamproites bodies (Mt North and 81-Mile Vent). Detailed field mapping of the two leucite lamproites was carried out, with recording of flow banding attitudes in magmatic phases and cross and planar bedding dips in volcanogenetic sedimentary units.

**VOLCANOLOGY**

The detailed mapping and geological investigations support the general outline of SMITH & LORENZ (1989) who described the formation of maars at Ellendale in response to phreatomagmatic activity which probably started when lamproite magma, rising in a zone of structural weakness (feeder dike), reached the interface between relatively impermeable shales and siltstones of the Fairfield Group and the overlying sandstones of the Permian Grant Group which formed a high yielding aquifer. On eruption large amounts of detrital quartz grains from the then poorly consolidated Grant Group sandstones were ejected in addition to juvenile lamproite clasts. This induced repeated collapse of the wallrocks and the overlaying pyroclastic deposits. A small diatreme formed above which the maar crater rapidly grew laterally because of the low slope stability of the Grant Group sandstones. Whilst the diatreme continued to grow in depth, the maar crater increased in size due to further landslides and simultaneously sand-rich tuffs were deposited inside and outside of the crater. Massflow and landslide units with intercalated surge and fall, originally deposited on the crater floor, became part of the diatreme due to its subsidence.

In all four pipes investigated the stratigraphically higher tuff deposits have lower contents of accidental quartz grains than underlying units. This is attributed to the progressive drawing downward of the groundwater table within the Grant Group sandstones towards the more impermeable shales and siltstones of the Fairfield Group eventually resulting in the eruption of almost quartz-free tuffs when the diatreme root zone lay within the Fairfield Group. Deposits formed within the maar crater at this point are similar to earlier deposits - mainly mass-flow deposits with intercalated surge and fall

deposits - apart from a lower quartz content and a marked decrease in the number of landslide deposits of Grant Group sandstone which are rare or even absent (as in Mt North and 81-Mile Vent) in the upper tuff horizons. Thin intercalated scoria horizons observed in drill core imply that even during the main phreatomagmatic phase of maar formation groundwater access to the root zone was restricted several times. Eventually the root zone penetrated deeply into the Fairfield Group shales, supply of groundwater ceased, and explosive activity finally terminated.

Following a period of lava fountain activity magma rose within the diatreme and eventually filled the maar crater as either a lava lake (olivine lamproites) or lava dome (leucite lamproites), depending on the viscosity of the melt. At the pipes investigated in outcrop, the transition from phreatomagmatic to extrusive magmatic activity is marked by a phase of intense redeposition i.e. mass flow deposits. Simultaneous with, or immediately following emplacement of the magmatic core, the tuffs, especially those adjacent to the magmatic phase, were intruded by numerous small sills and dikes. Late-stage dikes and sills are most common in the leucite lamproite pipes where the intrusive rocks commonly are a composite of medium-grained lamproite and schlieren of fine-grained lamproite. Sills and dikes in the olivine lamproite pipes appear to be comparatively rare perhaps because of their different viscosity; alternatively, they may not have been recognized in the poorly preserved drill core material.

#### PETROGENESIS OF OLIVINE LAMPROITES

Petrographic differences within the investigated olivine lamproite pipes (Ellendale 4 and 9) are mainly restricted to in-situ cooling phenomena (e.g. crystallization of poikilitic phlogopite and K-richterite). However, small phlogopite phenocrysts, which are present in the tuffs of both pipes, became completely resorbed in the magma batches which subsequently formed the lava lakes, thus indicating low pressure reequilibration. Geothermometry and oxygen fugacity calculations based on olivine-spinel equilibria indicate crystallization of the tuffs and fine grained magmatic lamproites at temperatures (at 1 atmosphere) of 1050-1250°C under relatively reducing conditions ( $f_{O_2}$  at or slightly below the FMQ buffer). Inverse zoned olivines<sup>2</sup> (forsterite rich rims) indicate an increase in oxygen fugacity during ascent, as predicted by FOLEY et al. (1986) as a consequence of dissociation of small amounts of  $H_2O$ , driven by  $H_2$  loss. Spinel zoning, however, indicates oxidation only for the slowly cooled lava lake centers, where  $f_{O_2}$  became increased by 2-3 log units relative to the FMQ buffer. Much of the geochemical variation in Ellendale 4 appears to be due to significant (up to 25%) olivine fractionation (xenocrysts and phenocrysts) in the later magmatic phases. In contrast, Ellendale 9 shows much less variation in major element chemistry but significant variations in incompatible trace element abundances. The trace element abundances are not consistent with olivine fractionation but suggest an origin either by derivation of Ellendale 9 magmas by differing degrees of partial melting and/or small scale heterogeneities in their mantle source regions. Diamond distribution within Ellendale 4 and 9 pipes is not controlled by combustion or dissolution. The observed variation in diamond grade with specific units within each pipe is inferred to result primarily from fractionation (Ellendale 4) and a decreasing efficiency in sampling of the mantle source region by successive magma batches (Ellendale 9).

*PETROGENESIS OF THE LEUCITE LAMPROITES*

Petrographic differences within the lava domes of the investigated leucite lamproites are mainly attributed to intratelluric crystallization, since lithological boundaries (differences in phenocryst content and size) were found to be razor sharp (81-Mile Vent) or connected by a thin (about 1m) transition zone (Mt North). However, within the medium-grained part of the lava dome of Mt North in-situ crystallization produced small petrographic differences which are crossed by the magmatic flow banding.

The various petrographic units of Mt North and 81-Mile Vent are characterized by significant differences in their chemical composition, with the early formed units being richer in Si, Al, and K and poorer in Ti, Mg and Fe, relative to later units. Volcanological and petrographic evidence suggest production from a layered magma reservoir, where crystal fractionation, mainly of olivine, diopside, and an iron-titanium oxide phase but including small amounts of phlogopite and apatite, took place. However, in the case of Mt North the observed trace element pattern does not fit the model derived from the major elements. A decoupling of major and trace elements (including MgO and Ni) suggests operation of additional processes including entrainment of phlogopite and mixing of magmas with different trace element abundance and abundance ratios and possibly derived by different degrees of melting over different depth intervals.

The magma reservoirs for Mt North and 81-Mile Vent are inferred to have been located within the crust because the mineral compositions reflect formation at low pressures and the low pressure mineral assemblage is dominated by olivine with only minor phlogopite. Experiments on leucite lamproites (FOLEY 1989) show that olivine is a liquidus phase below 10 kbar above which it is replaced by phlogopite. Leucite, hercynite-pleonaste and corundum-bearing xenoliths are interpreted as partially molten crustal xenoliths incorporated in the melt within the magma reservoir. Olivine compositions and zoning together with olivine/melt equilibria, suggest that the magma chamber, at least for Mt North, was characterized by oxidizing conditions. This oxidizing environment in the magma chamber might explain the complete absence of diamonds at Mt North which is uncommon in the Ellendale Field.

- Atkinson, W.J., Hughes, F.E., and Smith, C.B. (1984): A review of the kimberlitic rocks of Western Australia. In J. Kornprobst, Ed., *Kimberlites 1: kimberlites and related rocks*, p. 195-223, Elsevier, Amsterdam
- Foley, S. (1989): The genesis of lamproitic magmas in a reduced fluorine-rich mantle. *GSA S.P. No 14*, 616-631
- , Taylor, W.R., and Green, D.H. (1986): The role of fluorine and the oxygen fugacity in the genesis of the ultrapotassic rocks. *Contrib. Mineral. Petrol.*, 94, 183-192
- Jaques, A.L., Lewis, J.D., and Smith, C.B. (1986): The kimberlitic and lamproitic rocks of Western Australia. *Geol. Surv. W.A. Bull.*, 132, 268 p.
- Smith, C.B. and Lorenz, V. (1989): Volcanology of the Ellendale lamproite pipes. *GSA S.P. No 14*, 505-519
- Stachel, T. (1990): The Ellendale Volcanic Field - Volcanology, petrography, and geochemistry of 4 pipes. *Diss. Univ. Würzburg, Germany*, 359 p.

MANTLE XENOLITHS FROM THE QUATERNARY PALI-AIKE VOLCANIC FIELD OF SOUTHERNMOST SOUTH AMERICA: IMPLICATIONS FOR THE ACCRETION OF PHANEROZOIC CONTINENTAL LITHOSPHERE.

*Stern, Charles R.*

*Department of Geological Sciences, University of Colorado, Boulder, Colorado 80309, USA.*

The Quaternary alkali basalts of the Pali-Aike volcanic field occur within the region of southernmost Patagonia that has been interpreted as Phanerozoic accretionary continental lithosphere (de Wit, 1977; Ramos, 1988; Stern et al., 1989 and 1990). The ultramafic xenoliths they contain are thus samples of mantle significantly younger, and perhaps formed by different processes, than the cratonic Archean and early Proterozoic mantle sampled by kimberlites. The presence of garnet-bearing peridotites among the Pali-Aike ultramafic xenoliths provides a rare window to the deeper portions of this accretionary subcontinental mantle lithosphere.

Important petrochemical features of the Pali-Aike xenoliths include:

(1) A significant proportion (>15%) of the Pali-Aike xenoliths are fertile, Fe-rich, coarse-grained garnet-lherzolites (modal garnet + clinopyroxene >20%), although infertile Mg-rich harzburgites are the dominant type among the Pali-Aike xenoliths as in many other alkali basalt and kimberlite xenolith suites. Mineral geothermometry and geobarometry suggest that while the upper part (30-60 km depth) of the subcontinental mantle lithosphere below Pali-Aike is composed almost exclusively of infertile Mg-rich harzburgite (Figure 1), the deeper portion (>60 km depth) consists dominantly of fertile garnet-lherzolite. This implies a significant chemical and density gradient within the mantle section represented by the xenoliths.

(2) Mineral geothermometry and geobarometry indicate that temperatures of the lithosphere approach the basalt solidus (>1150°C) at 80 km depth (Figure 1). This suggests a relatively thin lithosphere below Pali-Aike, perhaps thinned and heated by the back-arc processes that produced the Pali-Aike basalts (Douglas et al., 1987; Stern et al., 1990).

(3) Fertile garnet-lherzolites have isotopic composition that fall within the mantle array defined by oceanic basalts, with the isotopic composition of some xenoliths approaching that of mid-ocean ridge basalts ( $\epsilon_{Nd} > +7$  and  $\epsilon_{Sr} < -30$ ). No radiogenic phases ( $\epsilon_{Nd} < 0$  or  $\epsilon_{Sr} > 0$ ), formed by ancient enrichment events such as are well documented within many kimberlite xenolith suites, have been observed within the Pali-Aike xenoliths.

(4) Some xenoliths have light-rare-earth-element depletion, with high Sm/Nd ratios (normalized Sm/Nd >>1). However, in general Sm/Nd ratios do not correlate with  $\epsilon_{Nd}$ , suggesting non-modal metasomatism has affected many of the Pali-Aike xenoliths as has been demonstrated for many other xenolith suites. Modal metasomatism, consisting of

phlogopite ± amphibole veins, is also a prominent feature within some of the Pali-Aike garnet-lherzolites. The Nd-isotopic composition of these veins are similar to those of

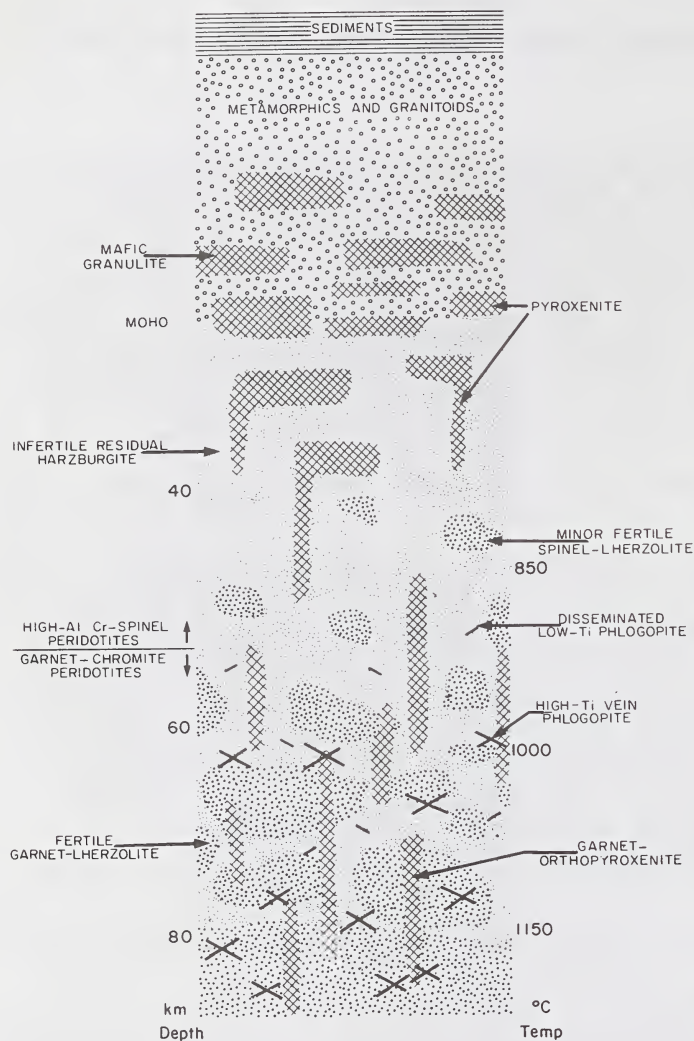


**Figure 1.** Schematic cross section through the portion of the continental lithosphere of southernmost South America represented by the xenoliths in the Pali-Aike basalts.

the Pali-Aike basalts, and given the high Rb/Sr of the veins, the small difference in their Sr-isotopic composition with the host basalts can be accounted for by an age correction of less than 1 m.y. Thus these modal metasomatic features are interpreted as being caused by intrusion into the lithosphere of melts and/or fluids genetically related to the host Pali-Aike alkali basalts.

The Phanerozoic accretionary subcontinental mantle lithosphere below southernmost South America, as represented by the Pali-Aike xenoliths, is distinct in many obvious ways compared to the Archean and early Proterozoic subcontinental

lithosphere represented by xenolith suites within kimberlites: it is thinner, its geothermal gradient is higher, it lacks significant quantities of eclogite as well as diamonds or other phases formed by ancient lithospheric enrichment events, and most significantly it is chemically and density stratified over a relatively short vertical distance of a few tens of kilometers such that the deeper portion consists of fertile Fe-rich lherzolites which occur, but are uncommon, within the kimberlite suite of coarse grained, undeformed peridotite xenoliths.

The inferred vertical chemical zonation of the subcontinental mantle lithosphere represented by the Pali-Aike xenoliths, with infertile Mg-rich harzburgites grading downward into fertile Fe-rich lherzolites, is similar to the vertical chemical zonation expected for oceanic lithosphere formed by melt extraction below a mid-oceanic spreading center. Also, the isotopic and trace-element composition of some xenoliths approach what would be expected for MORB-source mantle. Accordingly the subcontinental mantle lithosphere below Pali-Aike is interpreted to have formed by tectonic capture, during the early Paleozoic, of a segment of what previously had been oceanic lithosphere formed at a late-Proterozoic mid-ocean spreading center. Lithospheric underplating and non-modal metasomatism within this subcontinental lithosphere may have occurred in association with subsequent tectonic events such as the opening of the South Atlantic during the Mesozoic or the subduction of the Chile Rise in the Cenozoic, but the most recent phase of modal metasomatism is associated with the generation of the Pali-Aike host basalts which has caused heating and thinning of the subcontinental mantle.

De Wit, M.J. (1977) The evolution of the Scotia Arc as a key to the reconstruction of Gondwanaland. *Tectonophysics*, 37, 53-81.

Douglas, B.J., Saul, S.L., and Stern, C.R. (1987) Rheology of the upper mantle beneath southernmost South America inferred from peridotite xenoliths. *Journal of Geology*, 95, 241-253.

Ramos, V.A. (1988) Late Proterozoic-Early Paleozoic of South America - a collisional history. *Episodes*, 11, 168-174.

Stern, C.R., Futa, K., Saul, S., and Skewes, M.A. (1989) Garnet peridotite xenoliths from the Pali-Aike basalts of southernmost South America. In *Kimberlites and Related Rocks 2*, Geological Society of Australia Special Publication 14, 735-744.

Stern, C.R., Frey, F.A., Futa, K., Zartman, R.E., Peng, Z., and Kyser, T.K. (1990) Trace element and Sr, Nd, Pb, and O isotopic composition of Pliocene and Quaternary alkali basalts of the Patagonian Plateau lavas of southernmost South America. *Contributions to Mineralogy and Petrology*, 104, 294-308.

## ANOMALOUS HOSTS, UNUSUAL CHARACTERS AND THE ROLE OF HOT AND COOL GEOTHERMS FOR EAST AUSTRALIAN DIAMOND SOURCES.

*Sutherland*<sup>(1)</sup>, *F.L.*; *Temby*<sup>(2)</sup>, *P.*; *Hollis*<sup>(1)</sup>, *J.D.* and *Raynor*<sup>(3)</sup>, *L.R.*

(1) *Australian Museum 6-8 College Street, Sydney, NSW, 2000*; (2) *Clutha Ltd., 40 Pacific Highway, St. Leonards, NSW 2065*; (3) *Deceased.*

Eastern Australia is an enigmatic diamondiferous region. Unlike the southern and western Australian cratonic provinces, it lacks obvious kimberlitic or lamproitic sources. Mining has largely recovered diamonds from alluvial deposits, usually from leads under basalts. There are separate diamond provinces in which stones show different morphological, inclusion, carbon isotope and nitrogen aggregation characteristics. Some alluvial diamonds show so little abrasion that nearby sources are indicated. Known volcanic hosts are basaltic rocks not normally associated with diamonds. The abundant diamond type (Copeton, NSW) is distinct from most other diamond suites.

The concentration in northern NSW (Copeton, Bingara, Walcha) mostly shows rounded, resorbed multiply twinned crystals. Inclusions are notably coesite and an unusual calc-silicate suite. The  $\delta^{13}\text{C}$  values are dominantly heavy (-3.3 to +2.4‰) and N contents (up to 1200ppm) commonly aggregate to show relatively high % of A defects. The data points to a parent of sedimentary or sea water modified character, which entered diamond facies conditions in the lithosphere probably before the early Palaeozoic. Six diamonds came from tholeiitic dolerite forming dykes in late Carboniferous granite and are probably a contaminant, being accompanied by accessories typical of granite contact suites. They could come from older deep leads or late Carboniferous basal beds below the granite contact. Late Cretaceous (c.70Ma) tholeiites and laterites occur in New England and diamonds under lateritised basalt (Inverell) suggest pre-Cainozoic sources. Diamonds related to a 36Ma alkaline dyke in Silurian (?) metamorphics at Walcha suggest underlying sources within the fold belt.

Diamonds in Airly Mt. deep leads (pre-41Ma) are octahedra and rounded forms. They contain coesite and have  $\delta^{13}\text{C}$  values (-3.8 to -9.8‰; N.V. Sobolev, comm.) typical of the range for both peridotitic and eclogitic paragenesis. Diamonds from Rocky River, between Walcha and Copeton, are octahedra.

Pale zircons found with diamonds at Airly Mt., Bingara and nearby breccia pipes range in uranium contents (50-600 ppm U) and yield Jurassic to Triassic ages (130-240Ma). Elsewhere (Tolmie, Gundagai, New England, Brigooda, central Queensland gemfields, Cooktown) large zircons with low U contents typical of kimberlitic zircons (<30ppm) are found with breccia pipes or in gem alluvial deposits (some diamondiferous). These zircons range from late Tertiary to Cretaceous ages (3-107Ma).

Studies of mantle xenoliths from Mesozoic-Tertiary volcanics using new thermobarometry (Brey & Kohler) show 'hot' geotherms, some as hot as any recorded, existed in eastern Australia at various times. However variations in the thermal gradients suggest that lower gradients were linked to limited deep melts in the Mesozoic. The high Cainozoic gradients may represent restricted perturbations caused by magma ponding and need not affect the diamond graphite transition at depth.

Analysis of the Mesozoic-Cainozoic intraplate volcanism suggests episodic surges related to rifting and subsequent hot spot activity. A new concept of 'boomerang' volcanism proposes migratory flare ups from incipient deep undersaturated melting develops into major silicic crustal magmatism then dwindles back to minor amounts of deep melting. The 'boomerang' tips and beyond have potential for leucititic and nephelinitic melts, approaching lamproitic and kimberlitic activity, to tap any existing diamond zone. Even during thermal rifting, flood basalt or hot spot activity (Tasman Cretaceous margin, Tasmanian Jurassic dolerites, Cainozoic central volcano migration) the thermal effects were probably laterally localised or intermittent so that cooler geotherms could co-exist elsewhere. An example from southern Australia is Jurassic tholeiite on Kangaroo Island contemporaneous with diamond-bearing kimberlites 350km away at Terowie.

Cooler geotherms were probably most widespread in interior east Australia in the Cretaceous interval between the major hot spot episodes, linking into ages of some low-U zircons and apparent initial exposures of sources of alluvial diamonds. Diamonds appearing at basaltic centres which only carry mantle xenoliths from PT regions lying well above the normal diamond stability zone can be explained by:

- (1) blasts of degassing from the diamond zone; or
- (2) intersection of diamond sources already emplaced at higher levels (older kimberlites or peridotite bodies).

Diamonds can survive greenschist metamorphism and the unusual Copeton diamonds are located in a tectonically complex fold belt, which includes ophiolitic bodies. An older lithospheric source for these diamonds may be related to widespread subduction events of Cambrian or earlier age suggested by various lines of isotopic evidence on Tasmanian, Victorian and New South Wales igneous and xenolith suites.

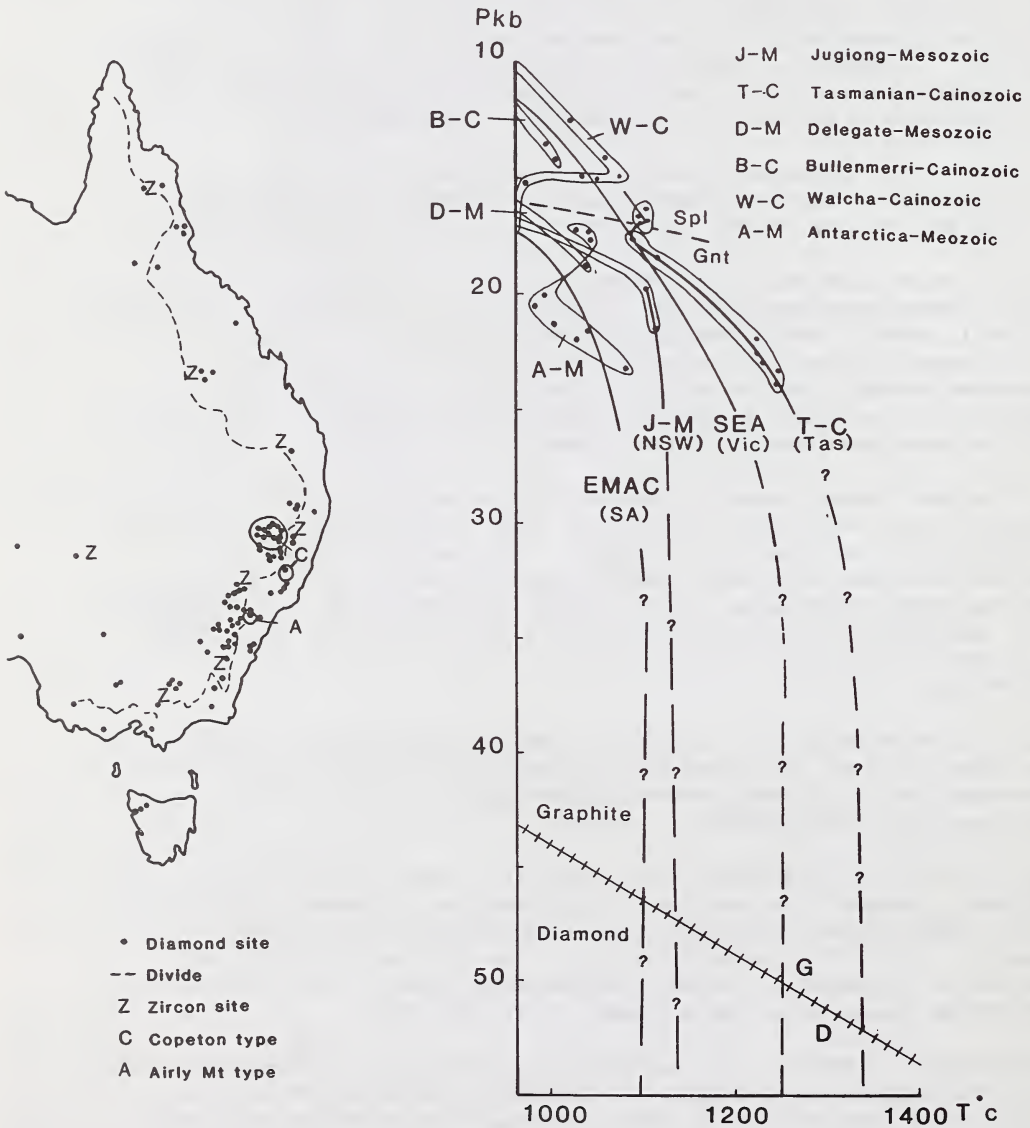
The east Australian diamond province is unusual and its detailed study provides scope for some interesting solutions for locating its diamond sources. The mantle isotopic characteristics, and high geotherms recorded from Tasmania suggests that this area is the least prospective for diamonds within eastern Australia in post Triassic igneous provinces.

#### REFERENCES:

- Brey, G.P. & Kohler, T. (1990). Geothermobarometry in four phase lherzolites II. New thermobarometers and the practical assessment of existing thermobarometers. *Journal of Petrology*, 31, 1353-1378.
- O'Reilly, S.Y. & Griffin, W.L. (1990). Geophysical and petrologic properties of the crust/mantle boundary region, eastern Australia: Relevance to the Eromanga-Brisbane Transect. In D.M. Finlayson, Ed., *The Eromanga-Brisbane Geoscience Transect*. Bureau of Mineral Resources Geology & Geophysics, Australia, Bulletin, 232, 203-212.
- Sobolev, N.V. (1984). Crystalline inclusions in diamonds from New South Wales, Australia. In *Kimberlite occurrence and origin*, J.E. Glover & P.G. Harris eds. Publications Geology Department & University Extension, University of Western Australia, 8, 213-219.

FIGURE CAPTIONS: (a) Distribution of reported alluvial diamonds and diamond-bearing pipes and dykes, eastern Australia, shown in relation to the main topographic divide. The distribution of the unusual Copeton diamond type (Sobolev, 1984) is shown in relation to the more usual Airly Mt. diamonds. Low U zircon finds are also indicated.

(b) Pressure-temperature section, east Australia-Antarctica showing PT fields derived from lower crust-upper mantle xenolith suites in Mesozoic-Cainozoic basaltic rocks, based on Brey & Kohler (1990) geothermometer barometer estimates on garnet - 2 pyroxene analyses in the literature and authors unpublished data. The position of the spinel/garnet lherzolite transition (Spl/Gnt) is shown. The Southeast Australian (SEA) and Eastern Margin Australian Craton (EMAC) geotherm curves (after D'Reilly & Griffin 1990) are steepened downwards to give minimum depths of intersection of the graphite/diamond transition (G/D).



MANTLE XENOLITHS FROM ALKALI BASALTS IN THE NOGRAD-GOMOR  
REGION OF HUNGARY AND CZECHOSLOVAKIA.

Szabó, <sup>(1), (2)</sup>Csaba and Taylor, <sup>(1)</sup>Lawrence A.

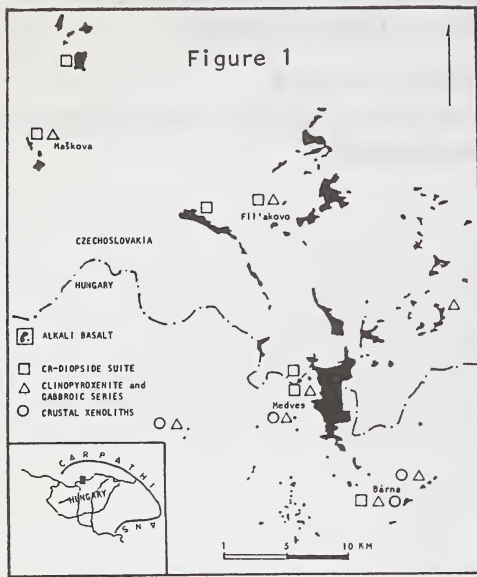
(1) Dept. of Geological Sci., Univ. of Tennessee, Knoxville, TN 37996 USA; (2) Dept. of Petrol. & Geochem., Eotvos  
Lorand University, Budapest, Hungary.

**INTRODUCTION:** Neogene to Quaternary alkali basalts are widely distributed within the Carpathian-Pannonian region of eastern Europe. These basalts contain abundant ultramafic and mafic nodules, as well as a large variety of mafic and salic megacrysts. The present study focuses on the great variety of ultramafic xenoliths from the Nograd-Gomor Region (NGR). We have collected more than 100 ultramafic xenoliths from 4 of the most important localities in the NGR (Fig. 1), and 43 samples were selected for detailed study. These have been studied in thin section, and numerous electron microprobe analyses have been performed on the various phases. These petrographic and chemical data form the basis for characterization of these xenoliths and provide insight into their petrogenetic evolution and metasomatic histories. Trace element and isotopic studies are in progress.

**GEOLOGIC SETTING:** In the NGR, numerous volcanic vents have produced extensive flows and dikes and thereby formed a wide plateau. Volcanic activity started at 2.8 Ma and continued to 1.0 Ma (Balogh et al., 1986). The early stage of development of the Pannonian Basin involved upwelling of a mantle diapir (Stegena et al, 1975; Adam, 1976). This is thought to have initiated the thermal regime from which the volcanic rocks were later derived.

**Host Rocks** - The NGR basalts range in texture from aphanitic to porphyritic. Mainly olivine, but also clinopyroxene, and plagioclase, occur as phenocrysts within a groundmass of clinopyroxene, plagioclase, apatite, oxide phases, - glass, - nepheline, - trace amounts of K-feldspar and phlogopite. The basalts possess low silica contents (46.6-49.7%), high alumina (16.3-18.6%), high total alkalis (5.9-7.2%), and low Mg# (53.3-65.7). When compared to typical xenolith-bearing alkali basalts from other world-wide locales, they are notably lower in Mg# basalts (67-74). This factor, in addition to their high differentiation indices (39-51) and high normative nepheline contents (up to 10.7%), may indicate that the original magma was modified by fractional crystallization and assimilation at depth.

**Xenoliths** - The xenoliths from NGR can be divided into three texturally and genetically distinct groups: 1) Cr-Diopside Suite (cf, Wilshire and Shervais 1975); 2) Clinopyroxenite and Gabboic Series, which may be representative of cumulates of the Al-augite suite of Wilshire and Shervais (1975); and 3) accidental upper crustal xenoliths.

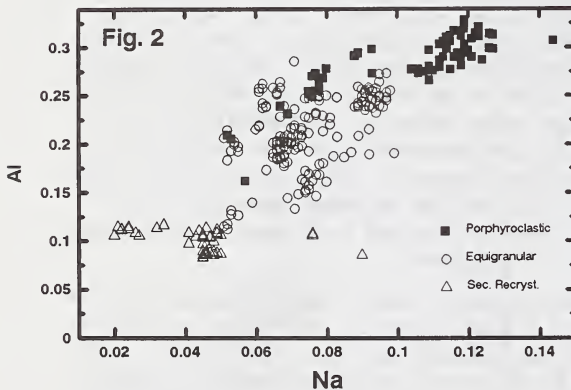


### XENOLITH PETROGRAPHY AND CHEMISTRY:

The xenoliths which are the object of this present study are from the Cr-Diopside Suite. These xenoliths have been grouped on the basis of mineralogy and texture into three types:

1) Spinel Lherzolites and Harzburgites - These are modally dominated by olivine with small amounts of amphibole locally present. Most of the lherzolites, which now appear to be "dry", possess sites where a hydrous phase was present but is now occupied by a secondary assemblage consisting of clinopyroxene, spinel, feldspar, phlogopite, amphibole, olivine, and glass. The overall texture of this type of xenolith is classified (after Mercier & Nicolas, 1975) as porphyroclastic and equigranular, with some transitional.

2) Dunite and Wehrlite - Olivine makes up 85 to 90 modal % of these xenoliths. Phlogopite with distinct



lineation is characteristic.

The textures show signatures of secondary recrystallization. Based upon the lineation of the mica within these xenoliths, it would appear that the phlogopite predates the deformation event.

3) Olivine Hornblendite - The original olivine is largely replaced by amphibole which now constitutes more than 70% of the xenolith. Triple junctions, slight deformation, and twinning of the remaining olivine suggest an equigranular texture for the pre-alteration xenolith.

Cr-diopside-rich veinlets (2-7 mm) within the lherzolites and wehrlite have undergone the same overall deformation as the host xenoliths. It is obvious that the emplacement of this veinlet preceded the deformational event.

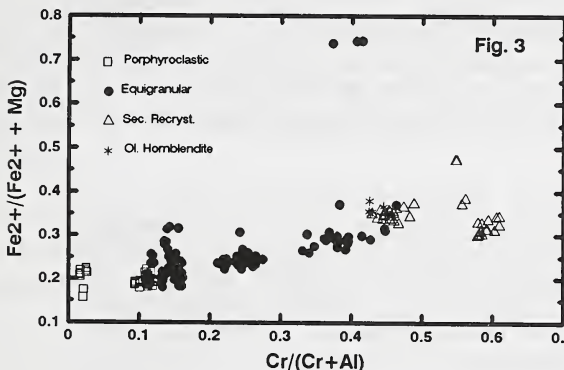
Mineral Chemistry - We have attempted to correlate mineral compositions with texture since it appears that the textures are representative of particular petrogenetic conditions. The ranges of mineral compositions of the spinel lherzolites and harzburgites are similar to many other occurrences (e.g., Basaltic Volcanism Vol., 1981; Nixon, 1987). Olivine and orthopyroxene have Mg# in the range of 0.87-0.91 and 0.88-0.91, respectively. The compositions of these phases are independent of textural type except for a small increase in  $Al_2O_3$  in the orthopyroxene from porphyroclastic xenoliths. Clinopyroxene and spinel compositions vary with texture. In porphyroclastic and transitional xenoliths, clinopyroxenes are enriched in Al and Na compared to equigranular xenoliths (Fig. 2). The variation in Mg# of the clinopyroxene is directly correlated with those of olivine and orthopyroxene. The spinels in porphyroclastic xenoliths are high in  $Al_2O_3$  and have low Fe# values [ $Fe^{2+} / (Fe^{2+} + Mg)$ ] (Fig. 3).

Recrystallized xenoliths have distinctive compositions of clinopyroxene and spinel. Compared to compositions in other textures and as shown in Fig. 2, clinopyroxenes are low in  $Al_2O_3$ ,  $Na_2O$ , and  $FeO$  and high in  $SiO_2$  and  $Mg\#$  (0.91-0.93). As shown in Fig. 3, spinels have the highest  $Cr\#$  [ $Cr/(Cr+Al)$ ],  $Fe\#$ . These compositions seem to indicate the possibility of a depletion process having acted upon these mantle samples. The olivine of the highly metasomatized olivine hornblendite is characterized by enriched compositions of Fe and Mn; the orthopyroxene is enriched in Fe, Mn, and Ca. The spinel is depleted in Mg and Al (Fig. 3), which may be related to the formation of hornblende. The amphibole which occurs in all these xenoliths is Ti- and Cr-rich pargasitic, with higher  $Al_2O_3$  than similar xenoliths from other world-wide localities. It is typically associated with remobilized spinel. Indeed, the interstitial setting of amphibole as a replacement phase and unstrained habit indicate formation after the deformation of the xenoliths.

In the recrystallized xenoliths, phlogopites occur with high contents of  $TiO_2$  (1.2-2.6 %),  $Cr_2O_3$  (1.3-2.3 %), and  $Na_2O$  (0.7-1.1 %). This chemistry is typical for secondary phlogopites of the upper mantle (Delaney et al.,

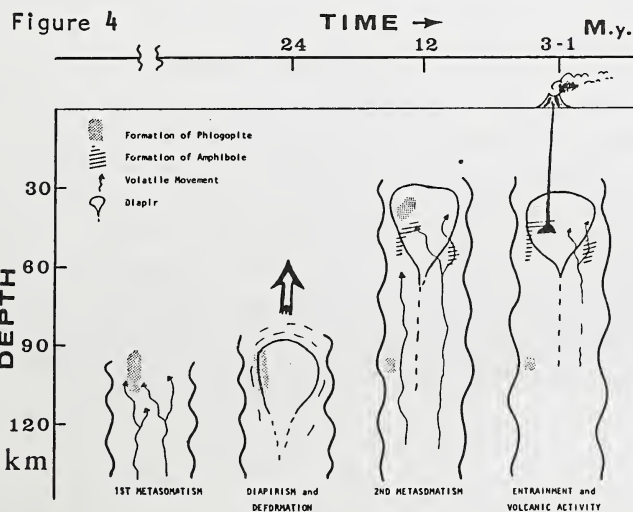
1980). The high  $Mg\#$  (0.91) is in accordance with those of the other silicates, implying equilibration within the xenoliths. However, extremely high fluorine contents, up to 3.5 %, are uncommon in phlogopites in ultramafic xenoliths from the alkali basaltic series.

**DISCUSSION:** The textures of the xenoliths and mineral chemistry can be integrated into an overall scenario of mantle events within the NGR portion of the Carpathian-Pannonian area of eastern Europe. These stages are depicted schematically in Figure 4 and are discussed below in chronologic order: 1) 1st



2) Diapirism and Deformation; 3) 2nd Metasomatism; and 4) Entrainment and Volcanic Activity.

**Stage 1. 1st Metasomatism** Within the xenoliths, it would appear that there was an ancient metasomatism which resulted in the local formation of phlogopite. The upward migrating, metasomatizing fluids was rich in water, but also contained appreciable fluorine and potassium, as evidenced by the high Fluorine contents of the phlogopite. Although no garnet was found in these xenoliths, we cannot exclude that garnet was not completely replaced by this hydrous alteration. The phlogopite is distinctly linedated, indicating its formation before the deformation event.



**Stage 2. Diapirism & Deformation** All of the xenoliths display evidence for strong deformational event. The most intense deformation, as revealed from the xenolith textures, was in the Southeast region of the NGR. The textures are mostly porphyroclastic to the Northeast & progress to equigranular, to transitional and to secondary recrystallized as the region of most intense deformation is approached. We postulate that this deformation was associated with deep-seated diapiric movement, which began after the

termination of subduction in the Carpathian belt at about 24 M.a. (Stegena et al., 1975). This diapiric upwelling continued until about 12 M.a. when it reached its highest position at about 30 km depth. This is based upon heat-flow calculations and estimation of the amount of crustal thinning (Dovenyi & Horvath, 1988).

**Stage 3. 2nd Metasomatism** Possibly associated with or as a direct consequence of the asthenospheric upwelling, another period of metasomatism affected the xenoliths. This is evidenced by the pervasive presence of undeformed amphibole superimposed upon the deformed texture of the mantle xenoliths. The presence of this parasitic hornblende limits the depth of this metasomatism to less than about 70 km.

**Stage 4. Entrainment and Volcanic Activity** Alkaline basaltic volcanism occurred within the last few million years. This entrained the mantle xenoliths and brought them to the surface. Geothermobarometric estimates of the xenoliths show last equilibration at 950-110 °C and 8-18 kbars. These conditions correspond to the depth of entrainment at 27-60 km. Interaction with the basaltic melt resulted in breakdown of some of the amphibole, as well as small amounts of spinel and clinopyroxene. A new selvage of phases is present in place of these decomposed minerals and consists of secondary clinopyroxene, spinel, feldspar, phlogopite, amphibole, olivine, and glass. The presence of enriched contents of K and Ti in some of the product crystals indicate that their formation was the result of metasomatic fluid from the basaltic melt.

**REFERENCES:** Adam (1982) *Geosci. Mining Bull. Hungarian Acad. Sci.* 15, 221-236; Balogh et al. (1986) *Acta Miner.-Petro. Szeged* 28, 75-93; **Basaltic Volcanism Study Project** (1981) p. 282-310. Pergamon; Delaney et al. (1986) *Geochim. Cosmochim. Acta* 44, 857-872; Dovenyi & Horvath (1988) *AAGP Mem.* 45, 195-235; Mercier & Nicolas (1975) *Jour. Petrol.* 16, 454-487; Nixon (1987) Wiley & Sons, 844 p; Stegena et al. (1975) *Tectonophysics* 26, 71-90; Wilshire & Shervais (1975) *Phys. Chem. Earth* 9, 257-272.

THE GROUP-2-KIMBERLITE – LAMPROITE CONNECTION: SOME CONSTRAINTS FROM THE BARKLY-WEST DISTRICT, NORTHERN CAPE PROVINCE, SOUTH AFRICA.

*Kenneth M. Tainton and Paul Browning.*

*Dept. of Earth Sciences, University of Cambridge, Downing Street, Cambridge, CB2 3EQ, UK.*

Group-2 (micaceous) kimberlites and lamproites are derived from enriched source regions within the sub-continental lithosphere. Comparison of the petrogenesis of these rock types has, however, been complicated by the fact that they have not previously been described from the same cratonic block. The Sover-Doornkloof and Sover-North intrusions lie within the Barkly-West Group-2 kimberlite cluster in the northern Cape Province, South Africa. The bodies intrude andesites of the Ventersdorp Supergroup. Sover-Doornkloof and Sover-North would be described on petrographic grounds as having kimberlitic and lamproitic affinities respectively. These bodies therefore allow comparison of the petrogenesis of kimberlite and lamproitic intrusions from a common cratonic setting.

Sover-Doornkloof is a 6.5km long bifurcating, en echelon dyke set striking NNE-SSW. The dyke consists of diamondiferous, macrocrystic phlogopite kimberlite (Group-2), and shows evidence for multiple intrusion. The individual magma pulses are indistinguishable in terms of mineral chemistry and whole-rock geochemistry. Flow differentiation has resulted in an inhomogeneous distribution of olivine macrocrysts through the kimberlite. The whole-rock composition of the kimberlite is correlated with the modal proportion of olivine macrocrysts. Mixing between entrained mantle peridotite and the host kimberlite magma is the primary cause of whole-rock geochemical variation within the intrusion.

The Sover-North intrusion, lying 1.5 km W of Sover-Doornkloof, is an elliptical plug having a surface area of approximately 600m<sup>2</sup>. Sover-North is a composite intrusion, consisting of an early, xenolith-rich phase (SN1), and a later, auto-intrusive plug (SN2). The SN1 intrusion contains rare macrocrysts and abundant phenocrysts of olivine, poikilitic phlogopite, diopside microlites and pseudomorphs after leucite set in a base of altered sanidine and glass. Potassic-richterite is also present in the groundmass of the SN2 intrusion. Both the poikilitic (madupitic) phlogopite of SN1 and the euhedral groundmass plates in SN2 are strongly zoned to Al<sub>2</sub>O<sub>3</sub>-poor, TiO<sub>2</sub>-rich rims. This zoning scheme has been described by Mitchell (1985) from numerous lamproite occurrences and is regarded as atypical of kimberlite micas. In addition, the groundmass of the SN1 intrusion contains an accessory hollandite mineral compositionally similar to priderite. On the basis of the classification schemes of Scott-Smith and Skinner (1984) and Mitchell (1985), SN1 is described as an olivine-leucite-phlogopite lamproite, and SN2 as an olivine-potassic richterite-phlogopite lamproite. Despite marked differences in the petrography and groundmass mineral chemistry of the SN1 and SN2 intrusions, they are geochemically identical.

In terms of major and compatible trace element compositions, the Sover-North intrusions are intermediate between those of the Kaapvaal Craton Group-2 kimberlites and olivine lamproites from Western Australia and North America. However, mixing with entrained mantle peridotite and surface alteration processes have disturbed these geochemical systems, obscuring the major element compositions of the initial magmas.

Both the Sover-North lamproites and the Sover-Doornkloof kimberlite show extreme enrichment in the incompatible trace elements. However, the kimberlite shows a greater degree of enrichment in the highly incompatible elements (Th, Ta, Nb) than the lamproite, allowing discrimination between the respective intrusions (Fig. 1). This relationship is also demonstrated by the rare-earth elements (Fig. 2). Although chondrite normalised rare-earth element profiles of Sover-North lamproite samples show complete overlap with the compositional range of Sover-Doornkloof kimberlite samples, the fractionation of LREE relative to HREE is greater for the kimberlite (mean La/Yb = 179) than for the lamproite (mean La/Yb = 129). This relationship would argue against generation of the lamproites by fractional crystallisation from the (more primitive) kimberlite magma.

The intrusions have radiogenic strontium ( $^{87}\text{Sr}/^{86}\text{Sr} = 0.7071\text{-}0.7076$ ) and unradiogenic lead ( $^{206}\text{Pb}/^{204}\text{Pb} = 17.062\text{-}17.428$ ,  $^{207}\text{Pb}/^{204}\text{Pb} = 15.441\text{-}15.529$ , and  $^{208}\text{Pb}/^{204}\text{Pb} = 37.440\text{-}37.716$ ) isotopic compositions. The Sover-North lamproite has, on average, slightly less radiogenic Sr and Pb than the Sover-Doornkloof kimberlite. This would not be consistent with generation of the compositional differences between these bodies by crustal contamination, as the observed contaminants of the Sover-North lamproitic magma have higher  $^{87}\text{Sr}/^{86}\text{Sr}$  than the kimberlite.

The isotopic compositions of the intrusions indicates that the magmas were derived from source reservoirs that had been isolated from the convecting mantle for at least 1Ga. The similarity in isotopic ratios indicate that the enrichment histories and incompatible trace element compositions of the respective source regions were similar. The observed geochemical differences between the intrusions suggest that, for the Kaapvaal Craton at least, Group-2 kimberlite and lamproite magmas may be derived by variable degrees of partial melting of similar, enriched source reservoirs.

#### References:

- Jaques, A.L., Sun, S.-S., and Chappell, B.W. (1989) Geochemistry of the Argyle (AK1) lamproite pipe, Western Australia. In *Kimberlites and related rocks*, Vol. 1, p. 170-188. Blackwell, Victoria.
- Mitchell, R.H. (1985) A review of the mineralogy of lamproites. *Trans. geol. Soc. S. Afr.*, 88, 411-437.
- Scott-Smith, B.H., and Skinner, E.M.W. (1984) A new look at Prairie Creek, Arkansas. In Kornprobst, J., Ed., *Kimberlites 1: Kimberlites and related rocks*, p. 255-283. Elsevier, Amsterdam.

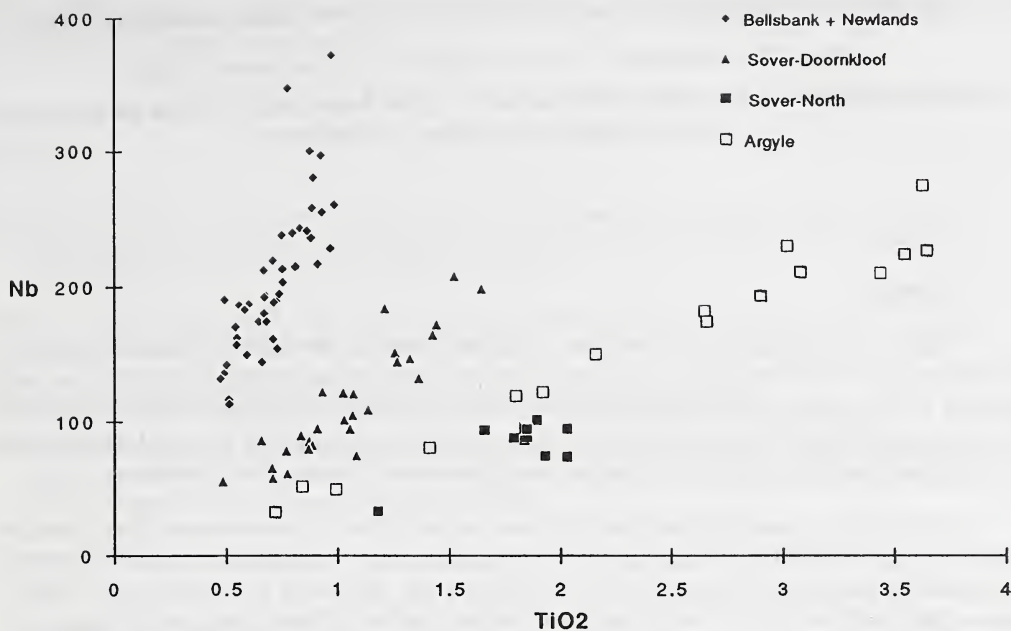


Fig.1: Plot of Nb (ppm) versus TiO<sub>2</sub> (wt. % oxide) for samples of the Bellsbank, Newlands and Sover-Doornkloof kimberlites, Sover-North and other lamproitic intrusions from South Africa, and the Argyle lamproite (Jaques et al, 1989).

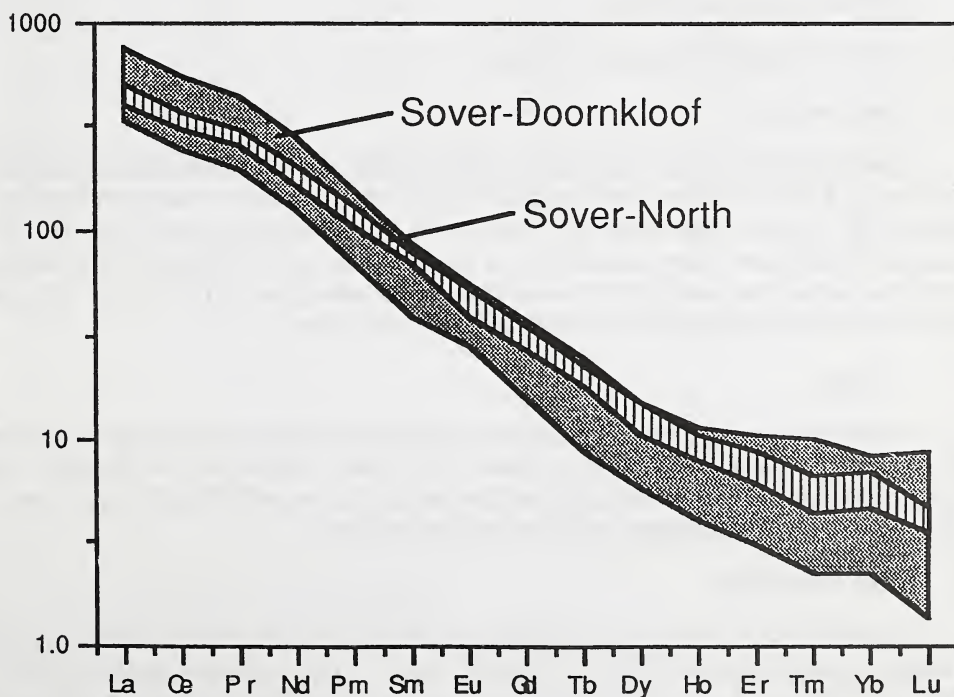


Fig. 2: Chondrite normalised rare-earth element spidergram for samples from the Sover-Doornkloof kimberlite and Sover-North lamproite.

## THE MATA DO LENÇO MICA-RICH KIMBERLITE, WESTERN MINAS GERAIS.

Tallarico <sup>(1)</sup>, F.H.B.; Souza <sup>(1)</sup>, J.C.F.; Leonardos <sup>(1)</sup>, O.H. and Mayer <sup>(2)</sup>, H.O.A.

(1) Instituto de Geociências, Dept. GRM, Univ. Brasília, CP. 153044. Brasília, Brasil. (2) Dept. Earth Atmos. Sci., Purdue University, West Lafayette, IN 47907, USA.

### General

Many Cretaceous kimberlite-like intrusions occur in the Monte Carmelo region in the vicinity of the Alto Paranaíba arch. The Mata do Lenço intrusion (MLI) intrusion is a new discovery of this type but is distinguished from the others for by being extremely rich in mica. Fresh outcrops of the MLI can be observed in the roadside near the gate to the Mata do Lenço farm, 3 km northwest of Morro Vermelho, near the town of Abadia dos Dourados.

The MLI is a small ellipsoidal intrusion, about 50 m in diameter and has intruded mica-schists and banded iron formations of the Araxá Group - a highly deformed Proterozoic meta-volcanic/sedimentary sequence of the Brasília belt. The rock constituting the MLI is massive dark and porphyritic with a trachytic texture and local flow structures. It consists of macrocrysts of olivine, phlogopite and enstatite set in a fine grained matrix of olivine, phlogopite, diopside, perovskite, richterite spinel and glass. Possible leucite need to be confirmed.

Xenoliths recognized in the MLI are:

- a) Glimmerites, including a possible MARID rocks.
- b) Harzburgites and dunite .
- c) Local Araxá Group country rocks.

### Macrocrysts

Macrocrysts of olivine, phlogopite and enstatite occur. The phlogopites reach a maximum size of 5 mm and show wavy extinction, kink bands, opaque exsolution lamellae and reaction rims. Olivine xenocrysts and phenocrysts, reach maximum grain size of 2.0 mm. Xenocrysts usually show wavy extinction and xenomorphic habit. Phlogopite and serpentine are common alteration products of olivine. Enstatite macrocrysts up to 0.5 mm, are strongly fractured and show deformation lamellae and wavy extinction.

### Matrix

The fine grained matrix displays an inequigranular texture with some areas showing poikilitic features as well as trachytic texture. It consists of thin laths of diopside, olivine microphenocrysts, phlogopite associated with minor richterite, poikilitic phlogopite, perovskite, spinel, and possibly analcime replacing leucite and glass.

### Bulk Chemistry

The MLI when compared to ultrabasic, ultramafic rocks, and kimberlites (Table 1), has a high concentration of K<sub>2</sub>O, CaO, Al<sub>2</sub>O<sub>3</sub>, Fe<sub>2</sub>O<sub>3</sub>, P<sub>2</sub>O<sub>5</sub> and low SiO<sub>2</sub>. It has a high K<sub>2</sub>O/Na<sub>2</sub>O (4.64) and Fe<sub>2</sub>O<sub>3</sub>/FeO (7.95) values and low MgO/(FeO + Fe<sub>2</sub>O<sub>3</sub>) (1.62) ratio. The overall chemistry matches well the average values for Group II Kimberlites, except for very

TiO<sub>2</sub> in MLI. However, the presence of richterite, leucite and glass, if substantiated, will preclude the MLI being a kimberlite.

## References

- BERGMAN, S.C. 1987. Lamproites and other potassium-rich igneous rocks: A review of their occurrence, mineralogy and geochemistry. Proceedings of the Conference on Alkaline Igneous Rocks, Edinburgh. Geological Society of London Special Publication, in press.
- DAWSON, J.B., SMITH, J.V. 1977. The MARID (mica-amphibole-rutile-ilmenite-diopside) suite of xenoliths in kimberlite. *Geochim Cosmochim Acta* 41: 309-323.
- DAWSON, J.B. 1980. *Kimberlites and their xenoliths*. Berlin, Springer-Verlag. 252p.
- SMITH, C.B., GURNEY, J.J., SKINNER, E.M.W., CLEMENT, C.R. & EBRAHIM, N. 1985. Geochemical character of southern african kimberlites: a new approach based upon isotopic constraints. Transactions of the Geological Society of South Africa, 88, 267-280.

Table 1. Comparative data of MLI and ultrabasic, ultramafic, and kimberlites averages.

	(1)	(2)	(3)	(4)	(5)	
	SiO <sub>2</sub>	40.60	43.20	37.31	35.20	31.10
	TiO <sub>2</sub>	0.50	0.13	5.86	2.32	2.03
	Al <sub>2</sub> O <sub>3</sub>	0.85	2.70	6.90	4.40	4.90
	Fe <sub>2</sub> O <sub>3</sub>	-	-	10.26	-	-
(wt%)	FeO	12.60 *	8.34 *	1.29	9.80	10.50
	MgO	42.90	41.10	18.73	27.90	23.90
	MnO	0.19	0.13	0.15	0.11	0.10
	CaO	1.00	3.80	8.51	7.60	10.60
	Na <sub>2</sub> O	0.77	0.30	0.73	0.32	0.31
	K <sub>2</sub> O	0.04	0.03	3.39	0.98	2.10
	P <sub>2</sub> O <sub>5</sub>	0.04	0.05	0.59	0.70	0.70
	Ignition loss	0.04	-	5.49	10.70	13.00
	TOTAL	99.08	99.98	99.17	100.03	99.64
	Cu			78	52	30
	Ni			723	420	1400
	Cr			1821	580	1800
	Zn			89	84	60
	Y			13	27	16
(ppm)	Zr			456	922	290
	Pb			100	44	30
	Be			4	-	-
	Ba			1252	5120	3000
	Sr			800	1530	1140
	Co			107	87	85
	V			170	123	85
	Bi			-	-	-
	Sn			41	-	-

(\*) FeO + Fe<sub>2</sub>O<sub>3</sub>.

(1) Average for ultrabasic rocks (Vinogradov, 1962 in Dawson, 1980).

(2) Average for ultramafic rocks (Wedepohl, 1962, in Dawson, 1980).

(3) MLI (analyzed for ICP).

(4) Kimberlite average (Dawson, 1980; Bergman, 1987).

(5) Average for Group II Kimberlites (Dawson, 1980; Smith et al., 1985).

## CRUSTAL SIGNATURES IN MANTLE ECLOGITES: REE PATTERNS OF CLINOPYROXENE AND GARNET BY SIMS AND INAA.

Taylor, <sup>(1)</sup>Lawrence A.; Eckert, <sup>(1)</sup>James. O.; Neal, <sup>(1)</sup>, <sup>(2)</sup>Clive R. and Crozaz, <sup>(2)</sup>G.

(1) Dept. of Geological Sciences, Univ. of Tennessee, Knoxville, TN 37996; (2) Dept. of Earth Science, Univ. of Notre Dame, Notre Dame, IN 46556; (3) McDonnell Center for Space Sci, Washington Univ., St. Louis, MO 63130.

**INTRODUCTION** The origin of eclogite xenoliths in kimberlites and alkali basalts is at present the subject of much controversy. There are three contrasting petrogeneses proposed for these "mantle-derived" eclogites: 1) as high-pressure igneous cumulates (garnet pyroxenites) within the upper mantle [e.g., McGregor & Carter, 1970; Smyth et al., 1989; Caporuscio & Smyth, 1990]; 2) as relicts of the Earth's primary differentiation shortly after accretion [e.g., Anderson, 1981; McCulloch, 1989], and 3) as metamorphic products of a subducted oceanic crustal protolith [e.g., Jagoutz et al., 1984; MacGregor & Manton, 1986; Shervais et al., 1988; Taylor & Neal, 1989; Neal et al., 1990]. Basically, it is the last-named genesis which stands in direct opposition to the others. And it has been the premise of our studies that crustal progenitors of some of these eclogites will impart distinctive chemical characteristics upon these rocks and that these signatures remain even after metamorphism, metasomatism, and melting.

### CHARACTERISTICS OF BELLSBANK ECLOGITES

	GROUP A	GROUP B	GROUP C
	MANTLE CUMULATE	SUBDUCTED OCEANIC CRUST MORB	CUMULATE
Clinopyroxene			
Na <sub>2</sub> O	0.6-2.8	3.7-5.7	7.6-8.7
Al <sub>2</sub> O <sub>3</sub>	0.9-3.5	5.5-8.6	14.8-17.0
Cr <sub>2</sub> O <sub>3</sub>	0.1-1.3	< 0.1	< 0.1
Garnet			
Comps.	Mg-rich	Fe-rich	Ca-rich
Cr <sub>2</sub> O <sub>3</sub>	1.0-2.2	< 0.1	< 0.1
Mineral MG#'s			
Garnet	78-93	57-59	67-73
Cpx	90-96	86-89	90-93
Opx	89-93	—	—
Whole-Rock MG#	82-89	61-67	72-78
REE's	LREE-enriched HREE-depleted	LREE-depleted HREE-enriched	LREE-depleted HREE-depleted
Eu Anomaly	No	No	YES
Isotopic Comps.			
$\delta^{18}O$	+5.1 to +5.6	+2.9 to +4.0	+3.4 to +4.7
$\epsilon^{Nd}$	-19 to -16	+39 to +241	+46 to +112
87Sr/86Sr	0.7042-0.7046	0.7086-0.7100	0.7083-0.7101

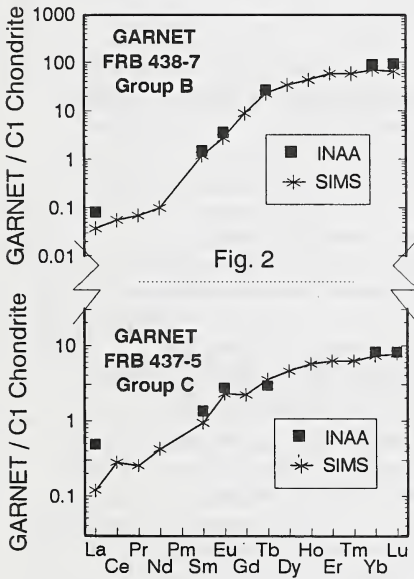
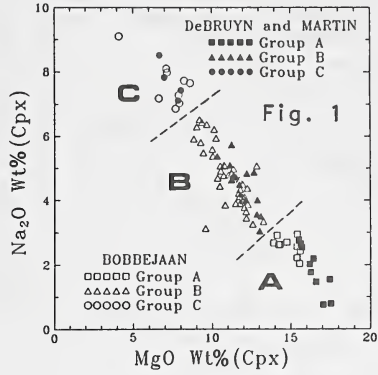
Table 1. Compiled from Taylor & Neal (1989) and Neal et al. (1990).

### SOUTH AFRICAN ECLOGITES

We have determined the mineral chemistry from 28 eclogite samples from the Bellsbank kimberlite DeBryun and Martin Mine, So. Africa. All eclogites have experienced metasomatism, witnessed by interstitial phlogopite, amphibole, K-feldspar, and celsian. Nine of the freshest samples were chosen for "ultrapure" mineral separation and whole rock (INAA and XRF) analysis. Isotope (Sr, Nd, O) and INA analyses were performed on these separates. These data have allowed a three-fold classification of eclo-

gites to be constructed, i.e., Groups A, B, and C. [The chemistry of these groups are based upon the classification of Coleman et al. (1965).] From these data, petrogeneses of these eclogites can be approximated [Taylor & Neal, 1989; Neal et al., 1990; Table 1].

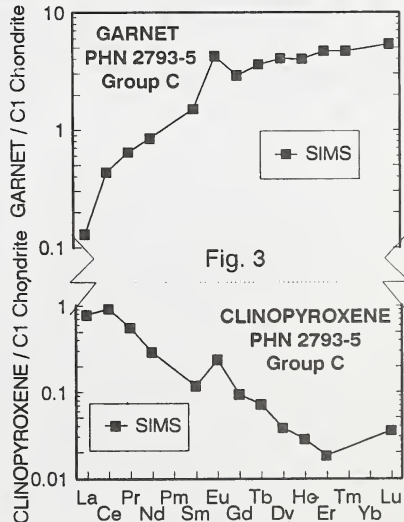
The mineral chemistry of the three eclogite groups suggests a petrogenesis by fractionation from an evolving magma. Smyth and Caporuscio (1984) have performed an extensive mineralogical investigation of the pyroxenes and garnets in eclogites from the Bobbejaan kimberlite (a different fissure of the Bellsbank kimberlite). Figure 1 shows the compositions of the Bobbejaan pyroxenes (after Smyth & Caporuscio, 1984), along with 28 from our DeBruyn and Martin eclogites. Although three groups are shown after Taylor and Neal (1989), Smyth et al. (1989) insist that the entire trend is attributed to simple fractionation. However, we have maintained that REE, in addition to whole-rock, mineral, and isotopic compositions are not consistent with such a petrogenesis [Taylor & Neal, 1989; Neal et al., 1990; Neal & Taylor, 1990].

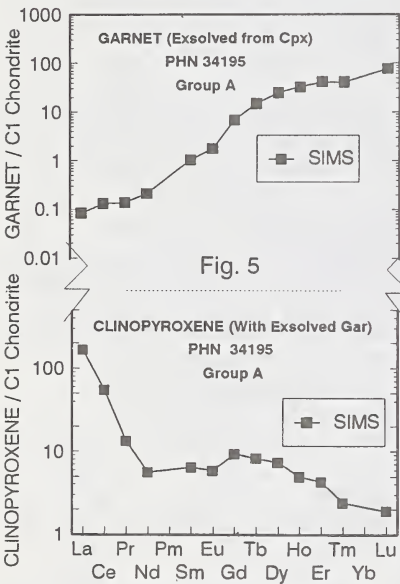
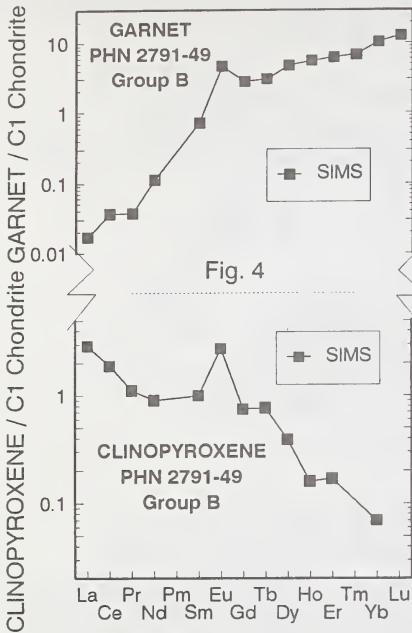


**SYNOPSIS OF GEOCHEMICAL DATA** Group B and C eclogites have low  $\delta^{18}O$  values of 2.9-4.7 ‰, high  $^{87}Sr/^{86}Sr$  of 0.7083-0.7101, and extreme  $\epsilon_{Nd}$  values +39 to +241. Group C minerals and eclogites possess positive Eu anomalies. Group A eclogites exhibit  $\delta^{18}O$  of 5.1-5.6 ‰, near the mantle value of 5.7, lower Sr of 0.7042 - 0.7046, and  $\epsilon_{Nd}$  values of -19 to -16. Major-element, whole-rock chemistries of Group B and C eclogites are similar to MORB and high-alumina basalt or gabbro, and the  $\delta^{18}O$  values are consistent with high-temperature hydrothermal alteration of an oceanic crustal component (e.g., basalt and anorthositic gabbro). Also, this sea-water interaction could have been the source of the high radiogenic Sr. The extreme  $\epsilon_{Nd}$  values could represent the effects of volatilization and metamorphism associated with the basalt/eclogite transition of the down-going plate. Thus, our eclogite investigations tend to support an

oceanic crustal origin for Group B and C eclogites (Shervais, 1988; Taylor & Neal, 1989; Neal & Taylor, 1990; Neal et al., 1990), but Group A eclogites are probably high-pressure mantle cumulates (e.g., high  $Mg\#$ 's, high Cr contents of minerals, and  $\delta^{18}O \approx$  mantle values).

**DIFFERENCE OF INTERPRETATION** Smyth et al. (1989) and Caporuscio and Smyth (1990) contended that these same eclogites are the products of accumulation of hyper-aluminous clinopyroxene -- i.e., mantle origin. Herein lies a controversy! At the center of this dilemma lies the nature of the REE patterns. We claim to observe a positive Eu anomaly, whereas Caporuscio and Smyth (1990) stated that the REE pattern is simply a function of MREE enrichment. Such an enrichment implies both a LREE and HREE depletion, resulting in a convex upward profile to the garnet and





clinopyroxene patterns. Which interpretation of the patterns is correct??

**SIMS ANALYSES** In an attempt to establish the credibility of the INA analyses on ultrapure mineral separates, several clinopyroxene and garnet grains were analyzed by SIMS at Washington University. Fig. 2 shows excellent agreement between previous INAA results and the SIMS analyses. Notice that the pattern for Group B garnet is smooth, whereas the Group C garnet displays a positive Eu anomaly, albeit small. To us, this does not look like simple MREE enrichment.

Fig. 3 shows interesting REE patterns from a "new" eclogite. The group designation is placed upon the eclogites by the mineral compositions, after Taylor and Neal (1989). Figure 3 depicts the patterns for another Group C eclogite, wherein a positive Eu anomaly is apparent for both the Cpx and garnet. Figure 4 shows some unexpected results, with REE patterns for a Group B eclogite containing Cpx and garnet with positive Eu anomalies. The positive Eu anomaly is present and distinct in each of these coexisting minerals from a Group B eclogite. This finding adds some additional complications to the petrogenesis in that there was apparent plagioclase involvement in a progenitor where the final eclogite is not extremely aluminous. In other words, does the presence of a positive Eu anomaly always signify involvement of plagioclase??

**GARNET EXSOLUTION FROM CPX** Several of the eclogites from Bellsbank contain Cpx which has evolved garnet + minor amounts of corundum and/or kyanite. Based upon our data and compositions for exsolved garnet/Cpx pairs reported by Smyth and Caporuscio (1984), it would seem that this exsolution occurs in all three eclogite groups (i.e., A, B, & C). The  $\text{Na}_2\text{O}$  and  $\text{Al}_2\text{O}_3$  contents of Cpx vary across the whole gamut of eclogite compositions. Garnet occurs in two distinct

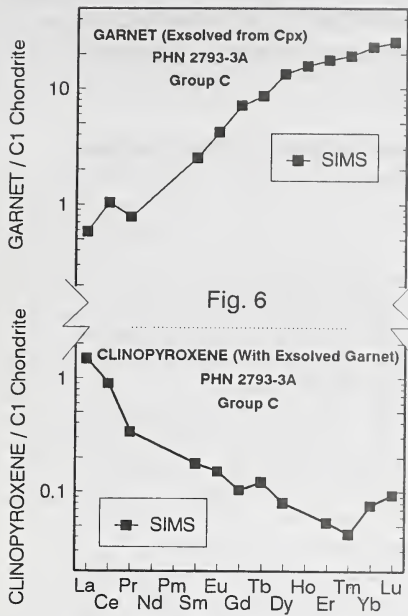


Fig. 6

textures: 1) as elongate, discontinuous blebs and lamellae; and 2) as xenomorphic crystals, both as inclusions in matrix Cpx and between Cpx grains. Locally, garnet lamellae tend to merge into larger, xenomorphic inclusions. Garnet and Cpx exhibit inter- and intra-granular homogeneity, including exsolved lamellae & matrix grains, & imply thorough subsolidus reequilibration. These relations contrast with the inhomogeneity reported from exsolution intergrowths in Roberts-Victor grosspydites (Harte & Gurney, 1975).

SIMS analyses were performed on both the Cpx and the exsolved garnets from several samples. Figures 5 & 6 show the REE patterns for garnet and Cpx in a Group A and a Group C eclogite. In all samples, Cpx and garnet show relative enrichment of LREE and HREE, resp. This is identical to eclogites which show no evidence of exsolution. As shown by Figure 6, these SIMS analyses complicate the interpretations.

**REE patterns from Cpx/garnet exsolution in Group C eclogites show no Eu anomaly.**

These inconsistent Eu anomalies are puzzling and may be related to the exsolution process. But, this does not explain the Group B eclogite with the positive Eu anomaly (Fig. 4). As Group B eclogites are thought to derive from altered oceanic basalt (Taylor & Neal, 1989), perhaps some protoliths were high-Al basalts in which part of the plagioclase was of cumulate origin.

**CONCLUSIONS**

- o The Eu anomaly in REE patterns of mantle eclogites and their minerals is real and is not simply a MREE enrichment; it is a crustal signature;
- o A positive Eu anomaly is indicative of a plag-bearing crustal progenitor;
- o Exsolution of garnet from Cpx occurs in all three eclogite Groups;
- o Group B eclogites can have positive Eu anomalies; some Group C eclogites do not - it appears that a continuum exists between Groups B and C.

**REFERENCES:** Anderson [1981] *Science* 213, 82-89. Caporuscio & Smyth [1990] *Contrib. Min. Pet.* 105, 550-561. Coleman et al. [1965] *Geol. Soc. Amer. Bull.* 76, 483-508. Jagoutz et al. [1984] *Lunar Planet. Sci.* XV, 395-396. MacGregor & Carter [1970] *Phys. Earth Inter.* 3, 391-397. MacGregor & Manton [1986] *J. Geophys. Res.* 91, 14063-14079. McCulloch [1989] in *Kimberlites and Related Rocks II: Their Mantle/Crust Setting, Diamonds, and Diamond Exploration*, 864-876. Neal & Taylor [1990] *Earth Planet. Sci. Lett.* 101, 112-119. Neal et al. [1990] *Earth Planet. Sci. Lett.* 99, 362-379. Shervais et al. [1988] *Geol. Soc. Amer. Bull.* 100, 411-423. Smyth & Caporuscio [1984] in *Kimberlites II: The Mantle and Crust-Mantle Relationships*, 121-132. Smyth et al. [1989] *Earth Planet. Sci. Lett.* 93, 133-141. Taylor & Neal [1989] *J. Geol.* 97, 551-567.

MAJOR ELEMENT SYSTEMATICS OF ALKALINE VOLCANIC AND LAMPROPHYRIC  
ROCKS – TOWARD A GEOCHEMICAL AND PETROGENETIC CLASSIFICATION  
SCHEME FOR THE POTENTIALLY DIAMONDIFEROUS ALKALINE ROCKS.

*Taylor, W.R. and Rock, N.M.S.*

*Key Centre for Strategic Mineral Deposits, Department of Geology, University of Western Australia,  
Nedlands, W.A., 6009, Australia.*

Understanding the petrogenesis of the alkaline volcanic and lamprophyric rocks has frequently been clouded by nomenclatural problems arising from their mineralogical and compositional diversity. Lamprophyric rocks of essentially identical bulk chemical composition, for example, may have very different phenocryst and groundmass mineralogies due to differences in their low pressure crystallization and degassing histories. These problems have tended to obscure petrogenetic relationships and have led to contentious type-locality or mineralogically-based classification schemes. Major and trace element whole-rock geochemistry provides information essential for correct rock classification and in practice, some combination of mineralogy and petrochemistry is required to classify lamprophyric rocks. While many useful discriminant diagrams are available for assessing mineral chemistry, rock geochemical classifications have received less attention. In this study our aim is to remedy this situation by extending the geochemically-oriented classification scheme of Foley et al. (1987) for ultrapotassic rocks to include the continuum of sodic to potassic alkaline rocks. Our approach differs from that of Foley et al. in that: (1) chemical analyses included in our database have been restricted to relatively primitive compositions to cover rocks most likely to be of direct mantle derivation i.e. to include the potentially diamondiferous rocks; and (2) more rigorous statistical procedures (multigroup discriminant analysis) have been applied to confirm the validity of assigned groups.

The database, which contains more than 1800 major and trace element analyses of alkaline volcanic and lamprophyric rocks, was assembled by combining the relevant parts of the LAMPDA database of Rock (1990) and ultrapotassic rock database of Foley et al. (1987) with a significant number of new analyses from the literature. The database, which originally contained >3000 analyses, was screened to eliminate non-primitive and altered compositions. Analyses that met the following criteria were retained: (1)  $FeO^*/MgO < 1.25$ ; (2)  $Al_2O_3 < 15wt\%$ ; (3)  $MgO > 5 wt\%$ ; (4) LOI (exclusive of  $CO_2$  for some rock types)  $< 12wt\%$ . Using  $CaO-Al_2O_3$ ,  $TiO_2-K_2O$ , and  $SiO_2-MgO$  bivariate diagrams, major element (10 oxide) compositions were assigned to one of six geochemical groupings. The first four groups correspond broadly to Groups I-IV of Foley et al. (1987): Group I (lamproites), Group II (kamaufugites), Group III (shoshonites), Group IV (transitional lamproites). The new groups are: Group V (kimberlites) and Group VI (basanites, nephelinites and mellilitites). Further within-group subdivisions were made on the basis of compositional similarity. As also shown by Foley et al. (1987) for the ultrapotassic rocks, the  $CaO-Al_2O_3$  plot effects maximum separation of the groups although considerable overlap exists. The  $CaO-Al_2O_3$  plot is additionally useful in a petrogenetic sense since the fields occupied by Groups I-VI can be correlated with differences in the chemical nature of their mantle source regions, depths of origin and activity of volatile species such as  $CO_2$ . Based on experimental evidence, the low CaO contents of Group I and some Group V rocks imply depleted,  $CO_2$  and clinopyroxene-poor, phlogopite-bearing peridotite sources whereas more fertile garnet lherzolitic to pyroxenitic sources are implied for Groups II and VI. Experimental and xenolith studies show that rocks of highest pressure origin will be found in Groups I, II and V and rocks outside these

groups should probably be regarded as having low diamond-bearing potential. Group III (shoshonitic) rocks are typically found in convergent continental margin tectonic settings and their origin is most probably related to subduction zone processes - an environment not normally regarded as conducive to diamond stability at depth.

Because no one simple oxide plot can fully separate the various groups and their subdivisions, multigroup discriminant analysis using the SYSTAT® package was applied to confirm the validity of the assignments. High percentages (>90% and mostly >95%) of inter-group correct classifications were achieved, confirming the statistical validity of our six-fold classification scheme. Within-group correct classifications were also high, and mostly exceeded 85%. Figures 1 and 2 show graphically the results of 10-oxide multigroup discriminant analysis for kimberlites and related rocks i.e. the rocks most likely to contain diamond (Group V, II and olivine lamproites from Group I) and for lamproites and related rocks (Groups I and IV). In both figures, factors (1) and (2) include a large component of CaO and Al<sub>2</sub>O<sub>3</sub>, respectively, so that they resemble bivariate CaO-Al<sub>2</sub>O<sub>3</sub> plots, however, only multidimensional treatment can achieve optimal separation into groups and sub-groups.

For the Group I, II and V rocks (Fig. 1) it is clear that chemical variation on the basis of major oxides is gradational between groups and subgroups, e.g. gradation exists between micaceous kimberlites and olivine lamproites; and between calcic kimberlites, carbonatitic kimberlites and aillikites. Some Group II rocks have been shown to host traces of diamond and those Group II compositions taken to be of highest pressure origin, e.g. those plotting near the Group I boundary, are of particular interest as further rock-types that might be candidates for hosting economic quantities of diamond. The discriminant plot for lamproites and transitional lamproites (Fig. 2) shows that the different lamproite sub-groups tend to cluster, emphasizing distinct, largely regionally controlled, compositional differences. Minor overlap is evident between Mediterranean-type lamproites and the cocite sub-group, and between Holsteinsborg-type lamproites and New South Wales-type leucitites. An important feature of the diagram is the separation of lamproites and transitional lamproites into two types either side of the dashed line in Fig. 2. The line divides high-TiO<sub>2</sub> compositions, to the left, from low-TiO<sub>2</sub> composition to the right. This division has important petrogenetic significance, since rocks in the low-TiO<sub>2</sub> group are largely associated with continental margin collisional belts where there has been some previous record of subduction, whereas rocks in the high TiO<sub>2</sub> group are found in continental intra-plate settings. The diamond potential of a province containing high TiO<sub>2</sub> lamproites (e.g. the West Kimberley region, N.W. Australia) appears to be significantly greater than a province containing low-TiO<sub>2</sub> lamproites such as the southern Mediterranean region. It is worth noting that the low-TiO<sub>2</sub> "olivine lamproites" of the Aldan Shield do not classify within Group I, and they are probably picritic variants of Group IV or Group III (shoshonitic) rocks. The very few calcic lamproite (madupite) compositions that meet the criteria for relatively primitive melts, plot in a separate field in Fig. 2. This field also includes the kalsilite-bearing lavas from San Venanzo and Cuppello which have closest bulk compositional affinity with calcic lamproites, rather than with kamafugites with which they have previously been placed on mineralogical grounds.

#### References

- Foley, S.F., Venturelli, G., Green, D.H., Toscani, L. (1987) The ultrapotassic rocks: characteristics, classification, and constraints for petrogenetic models. *Earth Science Reviews*, 24, 81-134.
- Rock, N.M.S. (1990) *Lamprophyres*. Blackie & Sons Ltd, Glasgow.

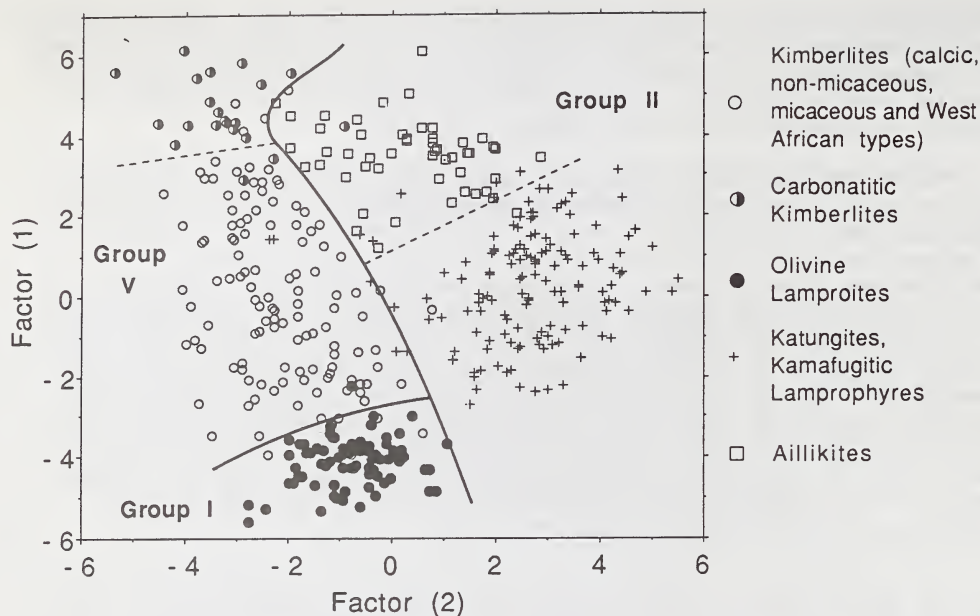


Fig.1 Discriminant analysis factor plot for Group V rocks (kimberlites), olivine lamproites from Group I, and Group II rocks (kamafugites).

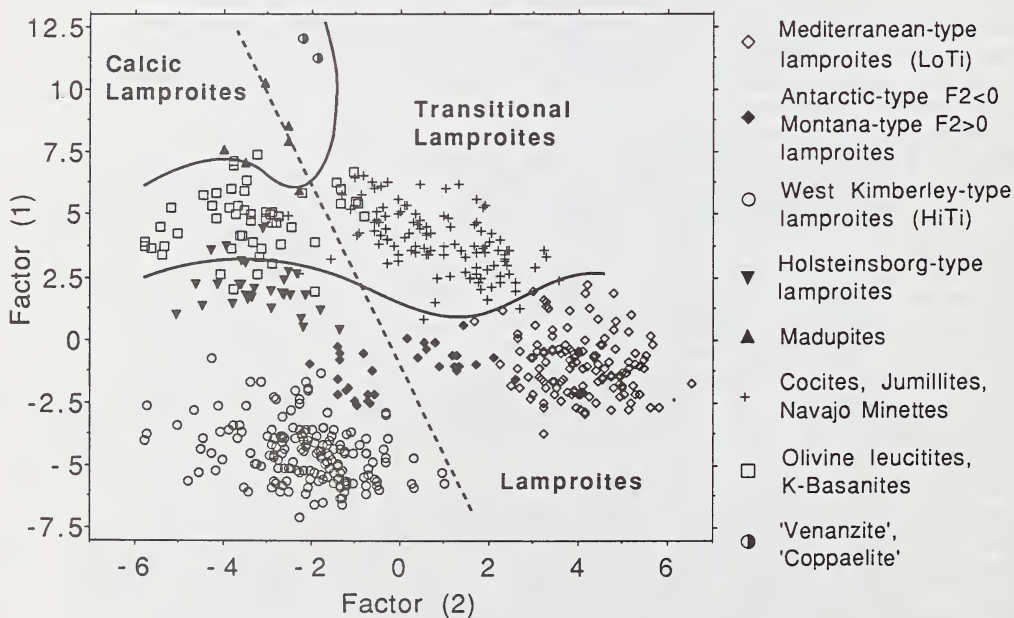


Fig. 2 Discriminant analysis factor plot for Group I rocks (lamproites, excluding olivine lamproites) and Group IV rocks (transitional lamproites). Dotted line separates high-TiO<sub>2</sub> (left) from low-TiO<sub>2</sub> (right) compositions.

MINERAL CHEMISTRY OF SILICATE AND OXIDE PHASES FROM FERTILE PERIDOTITE  
EQUILIBRATED WITH A C-O-H FLUID PHASE – A LOW  $f_{O_2}$  DATA SET FOR THE  
EVALUATION OF MINERAL BAROMETERS, THERMOMETERS AND OXYGEN SENSORS.

Taylor, W.R.<sup>(1)</sup> and Green, D.H.<sup>(2)</sup>

(1) Key Centre for Strategic Mineral Deposits, Department of Geology, University of Western Australia, Nedlands, W.A. 6009, Australia. (2) Geology Department, University of Tasmania, G.P.O. Box 252C, Hobart, Tasmania 7001, Australia.

To determine which particular mineral thermometer and barometer formulations provide the most accurate calibrations for natural spinel or garnet peridotite assemblages, one method is to test them against independent experimental data from multicomponent (natural-system) compositions (e.g. Carswell and Gibb, 1987a). Oxygen sensor formulations, involving ilmenite- or spinel-olivine-orthopyroxene equilibria, may be tested in a similar fashion (e.g. Ballhaus et al., 1990). This approach, however, is limited by the quality of the experimental data. In some older experimental studies, mineral chemical data is of questionable quality because of problems with Fe-loss to noble metal capsules, and unknown or variable  $Fe^{3+}$  contents of phases due to uncontrolled  $f_{O_2}$ . Knowledge of  $Fe^{3+}$  levels, in particular, is important in evaluating thermometers based on Mg-Fe exchange equilibria.

In this paper we present new mineral compositional data from thirty-five  $f_{O_2}$ -controlled experiments on fertile peridotite (mg# 87, Hawaiian pyrolite composition) that can be used to evaluate geothermometers, geobarometers and oxygen sensors. [Original references for all of the thermometers and barometers quoted below can be found in either Carswell and Gibb (1987a) or Finnerty and Boyd (1987)]. All experiments were C-O-H fluid saturated and were run under conditions of  $P = 0.9$  to 3.5 GPa,  $T = 1050$  to 1260°C and  $f_{O_2} \sim IW+1$  log units (see Taylor and Green, 1988). Improvements to experimental techniques, such as the use of graphite inner capsules, have eliminated Fe-loss problems allowing longer runs times (~50 hours at 1050°C to ~10 hours at 1200°C) and hence better approach to equilibrium. Microprobe analyses of mineral phases were carefully screened on compositional criteria to exclude overlapped and non-stoichiometric analyses. Subsolidus phase assemblages are  $TiO_2$ -saturated and consist of olivine, orthopyroxene, clinopyroxene, garnet or spinel, ilmenite, chromian rutile, amphibole and/or phlogopite. Amphibole and phlogopite persist to ~20°C above the solidus, but ilmenite and rutile are absent in above-solidus assemblages. Because  $f_{O_2}$ s are controlled to very low levels, just above the IW buffer, silicate phases contain negligible  $Fe^{3+}$  contents, and spinel and ilmenite have  $Fe^{3+}/\Sigma Fe$  ratios that are similar to those of spinels and ilmenites associated with diamond. Pyroxenes have unusually high  $TiO_2$  levels compared with those of mantle origin: an average of 0.5 wt% in orthopyroxenes (with positive temperature dependence in the subsolidus) and an average of 1.3 wt% in clinopyroxene.

For the pressure range investigated (i.e. to 3.5 GPa), we found that the Wells (1977) orthopyroxene-clinopyroxene solvus thermometer gives the most accurate (to within  $\pm 50^\circ C$ ) and precise (i.e. least scatter) temperature estimates as shown in the  $T_{calc}-T_{expt}$  plot in Fig. 1. The absence of a pressure correction term, however, is believed to reduce the accuracy of the Wells thermometer at pressures greater than ~3.5 GPa (Carswell and Gibb, 1987a). The Harley (1984) garnet-orthopyroxene thermometer also yields satisfactory temperature estimates but slightly more scatter is evident in the  $T_{calc}-T_{expt}$  plot compared with the Wells thermometer. Other orthopyroxene-clinopyroxene thermometers such as those

of Lindsley and Dixon (1974), Finnerty and Boyd (1987) or Bertrand and Mercier (1985) yield temperature underestimates for pyroxenes equilibrated at <2.0 GPa and overestimates for >2.0 GPa pyroxenes. The O'Neill and Wood (1979) garnet-olivine and Powell (1985) garnet-clinopyroxene thermometers yield consistent temperature overestimates of ~100°C and ~50°C, respectively. Although these two thermometers were recommended by Carswell and Gibb (1987b), it is also evident from their xenolith data that these thermometers have a tendency to overestimate temperatures by some 50-100°C relative to the Harley (1984) thermometer, particularly at T>1100°C. We therefore cannot recommend the O'Neill and Wood (1979) or Powell (1985) thermometers for garnet peridotites xenoliths equilibrated at T>1100°C.

Of the garnet-orthopyroxene geobarometers, we recommend a modified version of the Nickel and Green (1985) formulation. Because our orthopyroxene compositions are rich in TiO<sub>2</sub>, with up to 0.2 Ti atoms per Al atom, large pressure overestimates result when the proportion of Al in the M1 site is calculated with the equation suggested by Nickel and Green (1985) i.e.  $X_{Al}(M1) = (Al-Cr-2Ti+Na)/2$ . This equation implies Ti substitution in orthopyroxene via MgTiAl<sub>2</sub>O<sub>6</sub>-type molecules. We instead recommend calculation of Al in M1 by the equation  $X_{Al}(M1) = (Al-Cr+Ti+Na)/2$  which implies a different Ti substitution mechanism, possibly with Ti present in the tetrahedral site; there is no stoichiometric evidence for the presence of Ti<sup>3+</sup> in these pyroxenes as is a possibility at low experimental fO<sub>2</sub>s, although existence of Ti<sup>3+</sup> cannot be ruled out. The modified Nickel and Green (1985) barometer yields P estimates all within ±0.5 GPa. The Perkins and Newton (1980) and Wood (1974) modification 'C' barometers also yield satisfactory pressure estimates (within ±0.6 GPa). The Harley (1982) barometer tends to consistently underestimate pressure by 0.2-0.3 GPa while the MacGregor (1974) barometer consistently overestimates pressure by 0.5 GPa. The Bertrand (1986) barometer is more erratic but there is a tendency to underestimate pressure by ~0.4 GPa.

Because our experiments were controlled within the fO<sub>2</sub> range IW+0.5 to IW+1.5 log units by the WCWO buffer (Taylor and Foley, 1989), spinel and ilmenite compositions may be used to evaluate oxygen sensor formulations. Despite the low Fe<sup>3+</sup> contents in our experimental spinels (which must be calculated from stoichiometry and are therefore subject to relatively large errors), we find that both the O'Neill and Wall (1987) and the Ballhaus et al. (1990) formulations of the spinel oxygen sensor yield fO<sub>2</sub>s within 1 log unit of the experimentally predicted values. At high spinel Cr/Cr+Al ratios (>0.6), however, there is a tendency for the Ballhaus et al. sensor to overestimate fO<sub>2</sub> by ~0.5-1.0 log units and for the O'Neill and Wall sensor to underestimate fO<sub>2</sub> by a similar amount. Since Cr-rich spinels are potentially important indicators of fO<sub>2</sub> in the diamond source region, recalibration of these sensor formulations for high Cr compositions may be necessary. The Ballhaus et al. (1990) spinel-olivine Mg-Fe thermometer yields very satisfactory temperature estimates except for very high Cr/Cr+Al spinels. The Mattioli and Wood (1988) oxygen sensor formulation yields erratic fO<sub>2</sub> over- and underestimates. The ilmenite oxygen sensor of Egglar (1983) overestimates experimental fO<sub>2</sub>s by ~1.5 log units and is not recommended.

#### References

- Ballhaus, C, Berry, R.F., and Green, D.H. (1990) Oxygen fugacity controls on the Earth's upper mantle, *Nature*, 348, 437-440.
- Carswell, D.A. and Gibb, F.G.F. (1987a) Evaluation of mineral thermometers and barometers applicable to garnet lherzolite assemblages. *Contributions to Mineralogy and Petrology*, 95, 499-511.
- Carswell, D.A. and Gibb, F.G.F. (1987b) Garnet lherzolite xenoliths in the kimberlites of northern Lesotho: revised P-T equilibration conditions and

- upper mantle palaeogeotherm. *Contributions to Mineralogy and Petrology*, 97, 473-487.
- Eggler, D.H. (1983) Upper mantle oxidation state: evidence from olivine-orthopyroxene-ilmenite assemblages, *Geophysical Research Letters*, 10, 365-368.
- Finnerty, A.A. and Boyd, F.R. (1984) Evaluation of thermobarometers for garnet peridotites, *Geochimica et Cosmochimica Acta*, 48, 15-27.
- Finnerty, A.A. and Boyd, F.R. (1987) Thermobarometry for garnet peridotites: basis for the determination of thermal and compositional structure of the upper mantle. In P.H.Nixon, Ed., *Mantle Xenoliths*, p.381-402, John Wiley.
- Mattioli, G.S. and Wood, B.J. (1988) Magnetite activities across the  $MgAl_2O_4$ - $Fe_3O_4$  spinel join, with application to thermobarometric estimates of upper mantle oxygen fugacity. *Contributions to Mineralogy and Petrology*, 98, 148-162.
- O'Neill, H. and Wall, V.J. (1987) The olivine-orthopyroxene-spinel oxygen geobarometer, the nickel precipitation curve, and the oxygen fugacity of the Earth's upper mantle. *Journal of Petrology*, 28, 1069-1102.
- Taylor, W.R. and Green, D.H. (1988) Measurement of reduced peridotite-C-O-H solidus and implications for redox melting of the mantle. *Nature*, 332, 349-352.
- Taylor, W.R. and Foley, S.F. (1989) Improved oxygen-buffering techniques for C-O-H fluid-saturated experiments at high pressure. *Journal of Geophysical Research*, 94, 4146-4158.

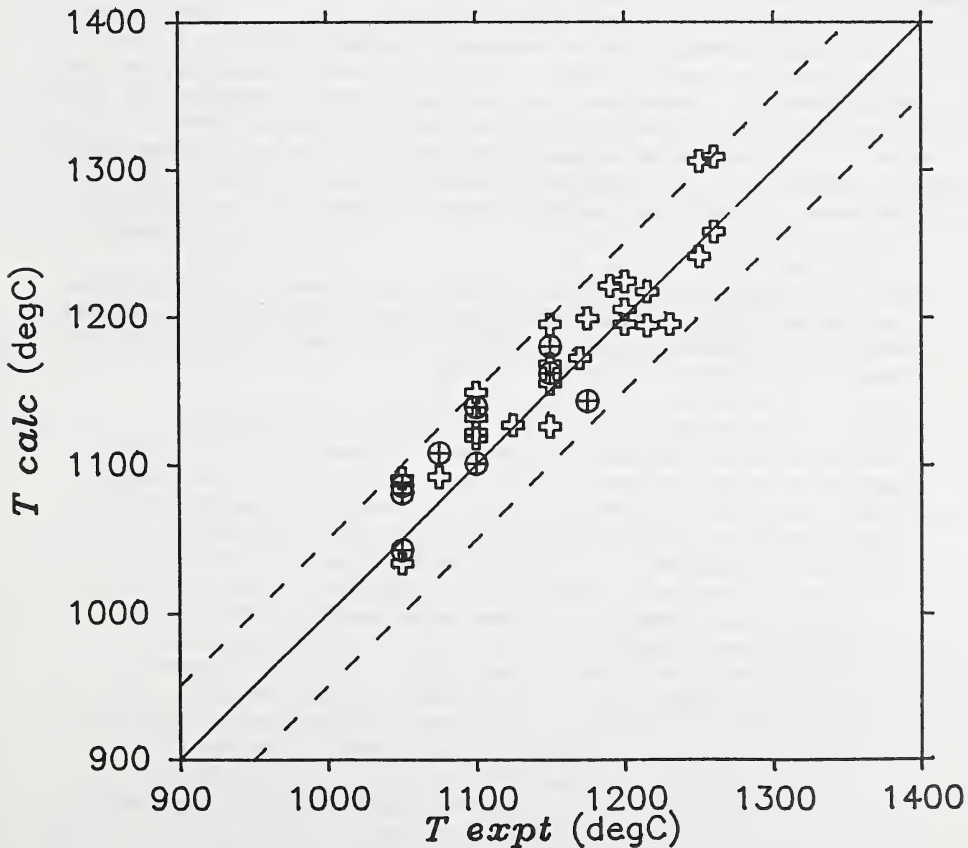


Figure 1.  $T_{calc} - T_{expt}$  plot for the Wells (1977) thermometer. Cross symbols =  $P > 2$  GPa experiments; Circles with cross =  $P < 2$  GPa experiments.

OVERT AND CRYPTIC STRONGLY POTASSIC MAFIC LIQUIDS IN THE  
NEOGENE MAGMATISM OF THE NORTHERNMOST PART OF THE  
RIO GRANDE RIFT, U.S.A.: A LITHOSPHERIC DRIP-FEED INTO A  
ASTHENOSPHERIC-SOURCE MAGMAS?

Thompson, <sup>(1)</sup>R.N.; Gibson<sup>(1)</sup>, S.A. and Leat, <sup>(2)</sup>P.T.

(1) *Dept. of Geological Sciences, University of Durham, South Road, Durham, DH1 3LE, U.K.*;

(2) *British Antarctic Survey, High Cross, Madingley Road, Cambridge, CB3 0ET, U.K.*

At present the Rio Grande rift extends as a physiographic feature for about 700km from near the Mexico/USA border to a northern terminus near Leadville, Colorado. From the time of its initiation, at about 25 Ma, until as recently as 5 Ma there was a northward prolongation of the rift between approximately Aspen, NW Colorado, and the Colorado/Wyoming border. The extension in this northernmost rift segment was distributed amongst several sub-parallel graben, as in the southernmost part of the rift. As elsewhere within both the rift and other parts of the Basin and Range structural province, the extension and related magmatism in NW Colorado was mostly concentrated into two phases: between about 25 and 20 Ma, and between about 13 and 5 Ma. Whilst the second tectonomagmatic phase continues to the present in the southern Rio Grande rift, the northernmost segment was uplifted substantially and ceased to extend at about 5 Ma. At that time the Yellowstone mantle plume is thought first to have approached this area, although still hundreds of km to the NW, and a component of this abrupt uplift may have been dynamic elevation above the plume head. Extension began only a few Ma after the initiation of the San Andreas fault system and it is generally supposed that NW Colorado was underlain by subducted fragments of the Farallon lithospheric plate until at least as recently as 10 Ma. Between about 25 and 10 Ma the predominant magmas extruded in this area were basalts with elemental characteristics resembling those of oceanic subduction-related melts; mostly calcalkaline, with subordinate absarokites and shoshonites. The first liquids to appear with the elemental and isotopic characteristics of ocean-island magmatism (OIB) were basanites at Yampa, at about 5.5 Ma.

Very sparse strongly potassic lavas and hypabyssal plutons accompanied the basalts throughout this region. These are: (1) Minette (~24 Ma) at Middle Park; (2) Minette dykes and sills (~10 Ma) throughout the Elkhead Mts; (3) Minette dykes (~5.5 Ma) at Yampa; (4) Lamproite lavas (~1 Ma) at Leucite Hills, ~150km NW of the Elkhead Mts. The Leucite Hills magmatism is logically regarded as part of the NW Colorado province; it is little further from the centre of that region than the Grand Mesa basalts to the south. Incompatible element abundances in examples from each of these four occurrences are summarised in Fig. 1. It is clear that, although they were all erupted or emplaced within a relatively small area, these strongly potassic magmas were very variable in composition. The Middle Park minette and Leucite Hills lavas have similar compositions but they are both different from the Elkhead Mts and Yampa minettes. Isotopically, these rocks all show the combination of relatively low  $^{87}\text{Sr}/^{86}\text{Sr}$  and very low  $\epsilon_{\text{Nd}}$  that characterises magmas thought to originate from EM1 lithospheric mantle, or at least to contain a large fraction from such a source. Nevertheless, judging from the surface geology, most of the NW Colorado igneous province is definitely not sited on the Archaean Wyoming craton. Its southern boundary, the Cheyenne belt, passes just north of the Elkhead Mts and the oldest radiometric ages throughout NW Colorado are ~1.8 Ga.

In addition to the overt strongly potassic magmatism listed above, there are other occurrences in NW Colorado where a good case can be made that a strongly potassic mafic liquid was a sporadic major additive to predominantly basaltic liquids. The best examples for showing this phenomenon are the dykes and volcanic necks at Yampa, and flow-by-flow chemical studies of lava successions at Yarmony Mt. and Flat Tops. The contrasting incompatible element abundances and ratios of the extreme compositions amongst the Yampa alkalic rocks, a minette and a basanite resembling those of ocean islands (with OIB-like radiogenic isotope ratios), are shown on Fig. 2. Once corrected for fractional crystallisation, the compositions of the other Yampa samples fall between these extremes. On Yarmony Mt. a succession of 11 basaltic lavas (~24 Ma) is preserved. Flow number 7 from the base has similar major elements to the others, apart from slightly higher  $\text{SiO}_2$ . But it is dramatically relatively enriched in such incompatible elements as K, Ba, Th, La and Zr. Both the elemental and isotopic differences between this and the other flows fit a model in which this particular magma batch was contaminated by 10-20% of strongly potassic mafic melt from an old lithospheric mantle source. The Flander section of the contemporaneous Flat Tops lavas provides two more examples of this phenomenon, showing subtle differences from the Yarmony Mt case. Thirty consecutive (24-20 Ma) flows at Flander can be divided into several groups with secular geochemical variations that are consistent with models of open-system fractional crystallisation, together with a small concomitant input from assimilated Proterozoic upper crust. In addition, two anomalous K-rich flows occur (one low and one high in the section) which have incompatible abundances and ratios that cannot be attributed to any plausible crustal contaminant. A strong case can be made from elemental evidence that these two magma batches contain substantial fractions of strongly potassic mafic melt. The very unusual feature of the Flander K-rich lavas is they have somewhat lower  $^{87}\text{Sr}/^{86}\text{Sr}$  and higher  $^{143}\text{Nd}/^{144}\text{Nd}$  than other flows in the section. Therefore, if the strongly potassic component was present in the form of local incompatible-element enrichment in the lithospheric mantle, before Lower Miocene stretching and heating, it can only have existed for a geologically short period of time.

Taken as a whole, these studies give a consistent picture of the magmatic response of a region with relatively thick lithosphere to stretching and heating from below. Detailed geophysical data on the lithosphere thickness in NW Colorado are lacking but the nearby State Line area, along the Front Range in northern Colorado, yielded diamondiferous kimberlites in the Devonian. The very close associations of strongly potassic mafic melts with basalts throughout the area (except the Leucite Hills) suggest that heat advected into the sub-continental lithospheric mantle by basic magmas originating deeper may have caused local melting of the most-easily-fusible parts of the lithosphere. The elemental and isotopic compositions of the strongly potassic mafic liquids - both those forming separate magma batches and those occurring as components of mixtures - show substantial variability in the composition of this fraction of the lithospheric upper mantle beneath NW Colorado and SW Wyoming, on a scale of tens of km. The age of the process that gave rise to the sources of the strongly potassic magmas also appears to have varied between the age of the lithosphere (~1.8 Ga) and as little as Mesozoic. Turning to the predominant basalts of the region, the only ones that can be ascribed to asthenospheric sources without reservations are the OIB-like Yampa basanites. The broadly calcalkaline "subduction-related" geochemical features of the older basalts are most simply explained by postulating that they originated in asthenospheric mantle that was chemically modified by melts and/or fluids released from underlying slabs of subducted Farallon plate. Nevertheless, the distinctive chemical features of these basalts are far from unique and it is difficult to determine with complete certainty the relative amounts of components with lithospheric and asthenospheric sources in them.

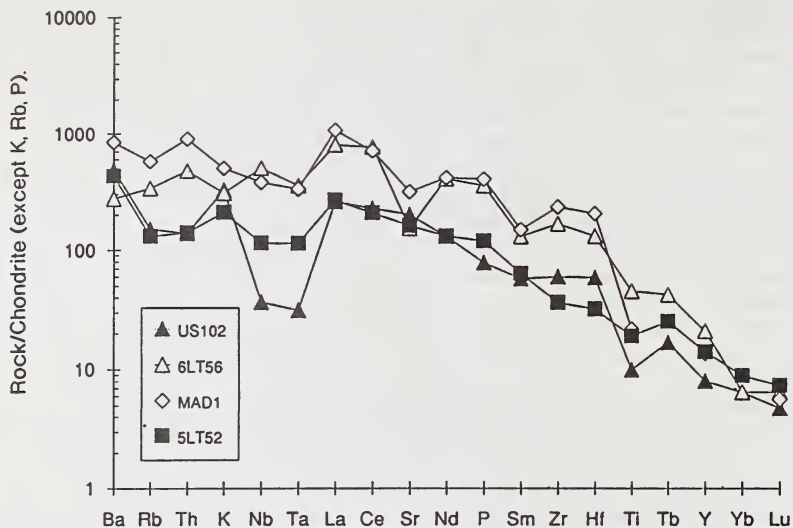


Fig. 1. Comparison of incompatible trace element abundances and ratios in four Neogene occurrences of strongly potassic mafic magmatism in NW Colorado and southern Wyoming. Localities are: US102, Elkhead Mts; 6LT56, Middle Park; MAD1, Leucite Hills; 5LT52, Yampa. See text for details.

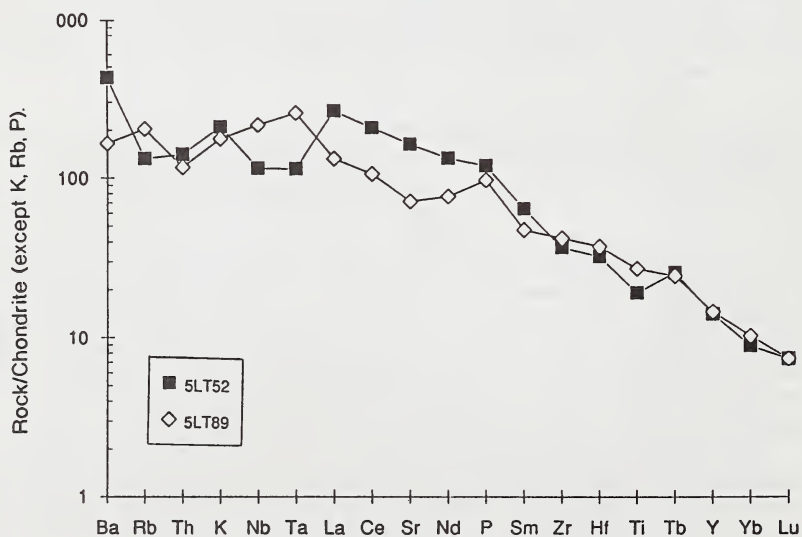


Fig. 2. Comparison of incompatible trace element abundances and ratios in the extreme mafic magma compositions of the Yampa igneous field, NW Colorado. 5LT52, minette; 5LT89, OIB-like basanite.

**HOT, COLD, WET, AND DRY HUTAYMAH ULTRAMAFIC INCLUSIONS:  
A RECORD OF MANTLE MAGMATISM BENEATH THE ARABIAN SHIELD  
AND FLANKING THE RED SEA RIFT.**

*Thomber, C.R.*

*U.S. Geological Survey, MS 903, DFC, Denver, CO 80225 USA.*

Harrat Hutaymah is the youngest, smallest and most isolated of the Cenozoic mafic alkaline volcanic fields (harrats) of Arabia. Situated farthest off the flank of the Red Sea rift at the northeastern margin of the uplifted and exposed Arabian Shield (lat27°N., long42°E.), Hutaymah is unique among Arabian harrats in that it is diatreme dominated and xenolith rich. Inclusions sample a variety of ultramafic rock types that occur deep within and beneath the ~40-km-thick Proterozoic crust. A comprehensive suite of 713 Hutaymah ultramafic xenoliths and megacrysts comprises 31% spinel peridotite; 57% pyroxenite and 12% amphibolite, and includes 2% peridotite in contact with either pyroxenite or amphibolite. Petrographic study of 430 polished thin sections, 985 microprobe analyses of minerals in 193 samples, and 68 whole rock analyses allow subdivision of the traditional Cr-diopside (Type I) and Al-augite (Type II) groups of ultramafic xenoliths into three broad categories of anhydrous inclusions ("dry" rocks): (1) Al-Fe-Ti-rich to Mg-Cr-rich igneous pyroxenite; (2) Al-Fe-Ti-rich to Mg-Cr-rich metamorphic pyroxenite; and (3) Mg-Cr rich peridotite ( $\pm$  partial melt). Less abundant hydrous equivalents of these groups ("wet" rocks) include kaersutite-bearing Al-Fe-Ti-rich igneous pyroxenite and amphibolite, and pargasite- and phlogopite-bearing Mg-Cr-rich peridotite and metamorphic pyroxenite. Among the main categories of anhydrous and hydrous inclusions, 26 ultramafic rock types were identified (Table 1). In general terms, the variety of ultramafic rocks reflects the heterogeneity within the approximate depth range of spinel lherzolite stability and in the path of ascending Quaternary/Tertiary mafic alkaline magmas.

As used herein, "hot" inclusions have relatively high pyroxene equilibration temperatures (1000-1150°C) (Wells, 1977) and textures, modal mineralogy, and mineral compositions that reflect primary igneous crystallization, high temperature deformation, or partial melting. These samples illustrate the effects of injection and dynamic crystallization of host-related mafic alkaline magma and the complementary effects of heating, fluid infiltration and partial melting of surrounding mantle lherzolite. "Cold" inclusions have relatively low pyroxene equilibration temperatures (<950°C), and textures, modal mineralogy and mineral chemistry, that reflect metamorphic annealing, recrystallization and deformation during cooling. Similar bulk rock and mineral compositional trends and gradational textural and modal characteristics between "hot" rocks of igneous origin and their "cold" metamorphic counterparts reflect either Proterozoic or precursory Cenozoic episodes of deep alkaline magmatism. The ratio of Al+Na+Fe+Ti/Mg+Cr in pyroxenes (plotted vs Ca content of clinopyroxene in figure 1) is used here as an index of alkali basaltic components relative to the refractory (or residual) components of mantle peridotite.

#### ANHYDROUS IGNEOUS PYROXENITES

"Hot" and "dry" pyroxenites comprise 36% of the Hutaymah suite and exhibit a continuous compositional array from rare Fe-rich clinopyroxenite (khaki green), through common Al-Fe-Ti-rich varieties (black), to less abundant Mg-Cr-rich clinopyroxenite (dark green). This entire group is distinguished by clinopyroxene (cpx) having a low Ca content (Figure 1). Where present, orthopyroxene (opx) has a complementary high-Ca content and yields high two-pyroxene equilibration temperatures (1000-1150°C).

**Al-Fe-Ti-rich** cumulus clinopyroxenite (including cpx megacrysts), websterite and wehrlite are compositionally similar to the magmatic cpx, cpx-opx or cpx-olivine assemblages crystallized experimentally from alkali basaltic liquids over a pressure range equivalent to a depth interval of ~70 - ~30 km, which also corresponds to that of spinel lherzolite stability. Igneous crystallization over this entire depth range is indicated by composite clinopyroxenite and spinel lherzolite xenoliths; however, because there is no primary (igneous) garnet (>70 km) and there are numerous samples containing only cpx (70-50 km), it is possible that the entire Al-Fe-Ti-rich magmatic suite was sampled from within  $\pm$  10 km of the base of the 40-km-thick crust.

**Mg-Cr-rich** igneous clinopyroxenites, except for rare megacrysts, are all composed of allotriomorphic- to hypidiomorphic granular cpx, which is frequently twinned and (in some samples) encloses olivine to produce heteradcumulus textures. A striking feature of coarse-grained samples is symplectitic to poikilitic cpx-opx intergrowth. This high-temperature recrystallization process reflects near-solidus (synmagmatic?) deformation in the presence of a fluid phase (Boland and Otten, 1985). The Al+Na+Fe+Ti/Mg+Cr and

low-Ca clinopyroxene signature of "hot" Mg-Cr-rich pyroxenites is transitional between that of partial-melt-bearing Mg-Cr-rich peridotite and Al-Fe-Ti-rich cumulates (Figure 1), and suggests primary crystallization from mixtures of alkali basaltic magma and melted lherzolitic wall-rock. This interpretation is supported by the association of these three varieties of "hot" inclusions within sample suites from individual localities.

#### ANHYDROUS METAMORPHIC PYROXENITES

"Cold" and "dry" metamorphic pyroxenites comprise 21% of the Hutaymah suite and, similar to "hot" pyroxenites, exhibit a continuous compositional range from Al-Fe-Ti-rich pyroxenites (black) to Mg-Cr-rich pyroxenites (emerald green). Petrogenesis of this group is attributed to processes of *in situ* annealing, subsolidus recrystallization and deformation during cooling of igneous pyroxenite at variable depths. These metamorphic rocks all have Ca-rich cpx and Ca-poor opx and corresponding low temperatures of equilibration (<950°C) relative to their igneous counterparts (Figure 1, Table 1). The range in Al+Na+Fe+Ti/Mg+Cr of pyroxene is generally consistent with that of bulk-rock chemistry in this group and is comparable to the range observed in igneous pyroxenites (Figure 1).

Among the Al-Fe-Ti-rich metamorphic samples there is complete textural gradation between equigranular to granular spinel-free orthopyroxenite and websterite, green-spinel websterite ( $\pm$  plagioclase, olivine, sapphirine, and garnet), and porphyroblastic-granular garnet pyroxenite. Less deformed variants within this group provide textural hints of an igneous origin including centimeter-scale igneous layering, annealed (relict) cumulus textures and intrusive veining of peridotite. Some websterites of the Al-Fe-Ti-rich group ( $\pm$  olivine and including some veins in peridotite) have higher Mg/Fe pyroxene compositions, relative to their igneous counterparts that indicate pre-metamorphic crystallization from either primitive alkaline basalt or a magma mixed with melted lherzolite. Pyroxene Al+Ti concentrations in this group are all higher than in Mg-Cr-rich metamorphic pyroxenites and differ from igneous equivalents in a manner consistent with pyroxene subsolidus exsolution and intergranular garnet-forming reactions. Thermobarometry of garnet bearing samples (Wells, 1977; Wood, 1974), and available experimental evidence (e.g., Irving, 1974) indicate isobaric cooling and recrystallization of alkali-basalt fractionates over a depth range of 33-40 km, and provide evidence for pre-host-volcanic (and possibly Proterozoic) magmatic underplating of the crust.

Mg-Cr-rich metamorphic pyroxenites include clinopyroxenite, websterite, olivine websterite and orthopyroxenite. Coarsely exsolved Cr-Mg-rich cpx megacrysts exhibit compositional and textural gradation with equigranular varieties of websterite and olivine websterite (one large websterite sample has a megacrystic core). Websterite ( $\pm$  olivine) also occurs as discrete samples, as concordant layers in foliated peridotite or as intrusive veinlets in porphyroclastic peridotite. Mg-Cr-rich metamorphic pyroxenites have higher Al+Na+Fe+Ti/Mg+Cr pyroxene than similar high-Ca cpx and low-Ca opx of "cold" porphyroclastic lherzolite and overlapping those of "cold" foliated and equigranular lherzolite (Figure 1). This signature of enrichment in alkali basaltic components is comparable to that of "hot" (partial-melt-bearing) peridotite and Mg-Cr-rich igneous pyroxenite. Mg-Cr-rich metamorphic pyroxenites are interpreted to have crystallized from either mixed melts, generated within lherzolite adjacent to basaltic magma, or *in situ* melting of enriched (hydrous?) lherzolite mantle. In either case, the relic igneous origin is masked by subsequent cooling and textural and chemical equilibration with surrounding peridotite.

#### ANHYDROUS PERIDOTITES

"Hot" and "cold" Mg-Cr-rich "dry" peridotites are characterized by the presence or absence of intra- and inter-granular partial melt. There are two categories of anhydrous non-melted lherzolites, protogranular to porphyroclastic and foliated to equigranular (Table 1). Both have low-temperature pyroxene chemistry (800-900°C) and non-reacted grain boundary interfaces, and there is complete textural gradation within and between them. The latter category of deformed and recrystallized lherzolite has a higher modal abundance of pyroxene having higher Al+Na+Fe+Ti/Mg+Cr, overlapping that of Mg-Cr-rich metamorphic pyroxenite (Figure 1). Some relict porphyroclastic samples include neoblastic zones in gradational contact with concordant layers of Mg-Cr-rich metamorphic pyroxenite. These samples are the "frozen" record of a process involving melting, internal mobilization and recrystallization of preexisting lherzolite. Partial-melt-bearing peridotites provide "hot" examples of this process in the "active" magma/mantle system.

"Hot" peridotites are porphyroclastic to foliated, disruptive and fluoidal. This group ranges to relatively high temperature (<950-1100°C), and low-Ca cpx, high Ca-opx and has Al+Na+Fe+Ti/Mg+Cr enriched pyroxene compositions that overlap those of Mg-Cr-rich igneous pyroxenites (collected at the same localities) (Figure 1). An interpretation of melting and component exchange between peridotitic wall-rock and adjacent alkaline magma is best exemplified by Mg-Cr-rich wehrlites, which are composed of lherzolitic olivine porphyroclasts amidst igneous clinopyroxene.

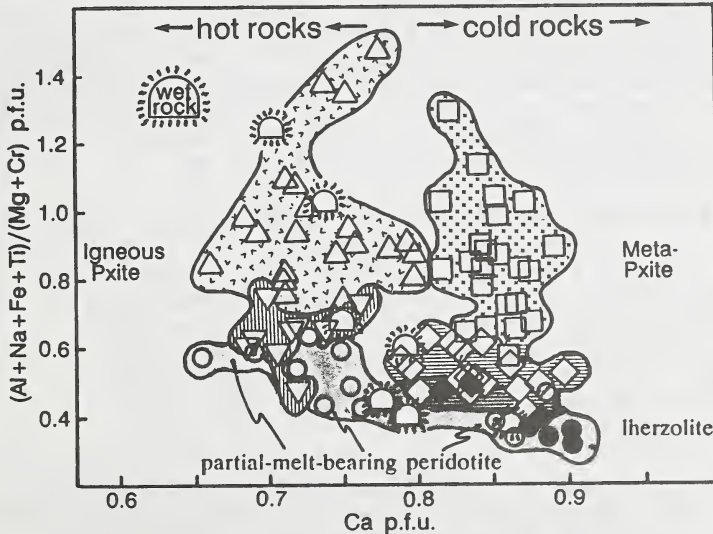
**HYDROUS INCLUSIONS**

By analogy with their "dry" equivalents, "wet" inclusions range from "hot" to "cold" varieties. Pyroxenes, where present, exhibit a similar range in chemistry (Figure 1). Pargasite- or phlogopite-bearing Mg-Cr rich pyroxenite and peridotite are found only at localities with abundant kaersutitic megacrysts or amphibolites (including kaersutite in contact with peridotite) and are thus correlated with primary hydrous alkaline magmatism. Discrete and composite association of hydrous inclusions and partial-melt-bearing peridotite suggests solidus depression within "cold" and "dry" spinel lherzolite mantle affected by metasomatism involving H<sub>2</sub>O-rich magmatic fluids. The extent to which such fluids may have been generated by magmatic interaction with preexisting amphibole-spinel-lherzolite remains enigmatic.

Table 1: Mg-Cr-rich and Al-Fe-Ti-rich Hutaymah ultramafic rock types (symbols shown are used in Figure 1).

<p><b>ANHYDROUS IGNEOUS PYROXENITES</b></p> <p>Al-Fe-Ti-rich Fe-rich clinopyroxenite (incl. cpx megacryst) Websterite (1000-1100°C) △ Wehrlite and olivine clinopyroxenite Clinopyroxenite Clinopyroxene megacryst</p> <p>Mg-Cr-rich ▽ Orthopyroxene-clinopyroxenite (± olivine), (incl. cpx megacryst)(1000-1150°C)</p> <p><b>HYDROUS INCLUSIONS</b></p> <p>Al-Ti-Fe-rich ☀ Kaersutite clinopyroxenite and websterite ☀ Kaersutite megacryst ☀ Kaersutite-amphibolite</p> <p>Mg-Cr-rich ☀ Pargasite-spinel-peridotite (± partial melt) ☀ Pargasite- or phlogopite-pyroxenite</p>	<p><b>ANHYDROUS METAMORPHIC PYROXENITES</b></p> <p>Al-Fe-Ti-rich □ Websterite (spinel free) (800-850°C) Orthopyroxenite (spinel free) (800-850°C) Green-spinel websterite (± sapphire) (750-850°C) Green-spinel olivine websterite (840-940°C) Green-spinel plagioclase websterite (800°C) Green-spinel garnet pyroxenite (700-850°C) Garnet pyroxenite (spinel free)(700-850°C)</p> <p>Mg-Cr-rich ◇ Orthopyroxenite (incl. opx megacryst) (770-950°C) Olivine websterite (850-950°C) Websterite and clinopyroxenite (750-950°C) Clinopyroxene megacryst (exsolved-relict) (900°C)</p> <p><b>ANHYDROUS PERIDOTITE</b></p> <p>Mg-Cr-rich ● Protogranular-porphroclastic lherzolite (800-870oC) ◆ Foliated-equigranular lherzolite (870-900oC)</p> <p>Partial-melt-bearing peridotite: ○ Lherzolite and harzburgite (950-1100°C) ○ Wehrlite</p>
---	---

Figure 1: Average clinopyroxene core compositions from different samples; grouped as listed in Table 1 (p.f.u. = pyroxene formulae units).



**REFERENCES**

Boland and Otten (1985) Symplectitic augite, evidence for discontinuous precipitation as an exsolution mechanism in Ca-rich clinopyroxene, *Journal of Metamorphic Geology*, 3, 13-20.

Irving, A.J. (1974) Geochemical and high pressure experimental studies of garnet pyroxenite and pyroxene granulite xenoliths from the Delegate basaltic pipes, Australia, *Journal of Petrology*, 15, 1-40.

Wells, P.R.A. (1977) Pyroxene thermometry in simple and complex systems, *Contributions to Mineralogy and Petrology*, 62, 129-139.

Wood, B.J.(1974) The solubility of alumina in orthopyroxene coexisting with garnet, *Contributions to Mineralogy and Petrology*, 46, 1-15.

## KIMBERLITE STRUCTURAL ENVIRONMENTS AND DIAMONDS IN BRAZIL.

*Linda A. Tompkins.**Key Centre for Strategic Mineral Deposits, University of Western Australia, Nedlands,  
Perth, 6009, Western Australia.*

Diamond-bearing source rocks worldwide are recognized as occurring within cratonic areas stabilized by 1,500 Ma (Clifford, 1966; Atkinson, 1989). In most cases these areas coincide with ancient (>2.5 Ga) Archean nuclei (eg. South Africa, USSR; Mitchell, 1986) but in others with younger (~1.5Ga) Proterozoic mobile belts (eg. North Western Australia; Atkinson, 1989). Diamond-bearing primary sources within ancient Archean nuclei appear to be confined to kimberlite source rocks, and lamproites to Proterozoic mobile belts. Exceptions do exist, for example at Eurelia (Scott-Smith et al., 1984), where diamondiferous kimberlite dikes occur within a late Proterozoic mobile belt.

Four cratonic blocks are recognized in Brazil (Fig. 1) and are defined as areas not affected by the Pan-African age Brasiliano event (Schobbenhaus and Campos, 1984). South of the São Francisco craton of Schobbenhaus and Campos (1984) occurs a larger area referred to by Almeida (1981) as the Paramirim craton. The boundaries of the Paramirim craton are defined by a zone of crustal thickening as determined from regional Bouguer anomaly profiles (Haralyi and Hasui, 1982). The São Francisco craton is not defined by regional gravimetrics.

Brazil is the world's eighth largest diamond producer but currently has no mines based on a primary source. Fourteen kimberlite/"lamproite" provinces are now known and all occur along one of three principal lineaments (Fig. 1): the NE-SW trending Transbrasileano lineament; the NW-SE striking lineament 125°AZ, and the Blumenau lineament. The principal diamond productivity in Brazil is confined to Lower Proterozoic to recent age, sediment-hosted deposits (Tompkins and Gonzaga, 1989) either on the Amazônico Craton, or on and to the west of, the São Francisco Craton; often both in regions where kimberlite and related rocks occur.

Known kimberlites on the Amazônico Craton (locations 1-4; Fig. 1) occur in the Rio Negro-Juruena Mobile Belt, in a zone that was cratonized by 1.5 Ga (Teixeira et al., 1989). Kimberlites, "lamproites", and related rocks to the west of the São Francisco craton all occur within the limits of the reworked Paramirim craton (Fig. 1), in a zone that was consolidated in the Jequí event (2.7 Ga), and partially reworked during the Uruaçuano (1,300 - 1,000 Ma), and Brasiliano (450-700 Ma) events.

The economic potential of the kimberlites and related rocks is unknown, but, diamonds are reported from kimberlites on the Amazônico and Paramirim craton areas. Preliminary mineral chemical data of garnet inclusions in diamonds from the Juina kimberlite field (Locality 4; Fig. 1) suggest magma sampling from deep (>200km) upper mantle, possibly asthenospheric, source regions (Wilding et al., 1989) at this locality. Shallower level xenolith signatures are recorded from the area to the southwest of the São Francisco craton (locations 8,9 of Fig. 1; Svisero et al., 1984; and location 7 of Fig. 1; Tompkins, 1987). Analyses of heavy mineral concentrates from two pipes near the edge of the São Francisco

craton (location 10; Fig. 1) indicates that these magmas sampled garnet peridotite (Tompkins and Ramsay, 1991).

It would appear that Clifford's (1966) rule for kimberlites is applicable to Brasil. The potential for non-kimberlite diamond source rocks in Brasil may possibly be extended to include areas within the larger, partially reworked, Paramirim craton. However, considerably more data are required to better define the tectonic settings, the distribution of various alkaline rock types present, the relative timing of emplacement of these intrusions, and the types of mantle sources sampled by these rising magmas. This data, coupled with diamond inclusion mineralogy, should enable better geochemical and tectonic modeling of the regions in question.

#### ACKNOWLEDGEMENTS

Special thanks are extended to Andrei Sinityn for the invitation to attend the Kimberlite Workshop in Leningrad, 1990, where an earlier version of this paper was given. Review and critical comments by A.J.A. Janse, H.O.A. Meyer, C.B. Smith, N.M.S. Rock, R.R. Ramsay, W. Taylor, and Z. Andi on various versions of this work are acknowledged. David Robinson provided considerable help and expertise on GIS compilation of diagrams. All are gratefully acknowledged.

#### REFERENCES

- Almeida, F.F.M. de (1981) O craton do Paramirim e suas relações com o do São Francisco. Anais do Simposio sobre o craton do São Francisco e suas faixas marginais, Coordenação da Produção Mineral, Salvador, Bahia, 1-10.
- Atkinson, W.J. (1989) Diamond exploration philosophy, practice and promises: a review. In: Kimberlites and Related Rocks, Volume 2, Geological Society of Australia Special Publication no. 14, Blackwell Scientific Publications, 1075-1107.
- Clifford, T.N. (1966) Tectono-metallogenetic units and metallogenic provinces of Africa. Earth and Planetary Science Letters, 1, 421-434.
- Haralyi, N.L.E. and Hasui, Y. (1982) The gravimetric information and the Archean-Proterozoic structural framework of eastern Brazil. Revista Brasileira de Geociências, 12, 160-166.
- Mitchell, R.H. (1986) Kimberlites, mineralogy, geochemistry, and petrology, Plenum Press, New York, 442p.
- Scobbenhaus, C. and Campos, D. de A. (1984) A evolução da plataforma Sul-Americana no Brasil e suas principais concentrações minerais. In: C. Schobbenhaus, D.de A. Campos, G.R. Derze, and H.E. Asmus; editors. Geologia do Brasil, Departamento Nacional de Produção Mineral, Brasília, 9-53.
- Schobbenhaus, C.; Campos, D.de A.; Derze, G.R. and Asmus, H.E. (1981) Mapa geológico do Brasil e da area oceânica adjacente incluindo depósitos minerais. Escala 1:2,500,000. Departamento Nacional da Produção Mineral, Brasília.
- Scott-Smith; Danchin, R.V.; Harris, J.W. and Stracke, K.J. (1984) Kimberlites near Orroroo, South Australia. In: J. Kornprobst, editor. Kimberlites I: Kimberlites and related rocks. Developments in Petrology, 11A, Elsevier, New York, 121-142.
- Svisero, D.P.; Meyer, H.O.A.; Haralyi, N.L.E. and Hasui, Y. (1984) A note on the geology of some Brazilian kimberlites. Journal of Geology, 92, 331-338.
- Teixeira, W.; Colombo, C.G.T.; Cordani, U.G.C. and Kawashita, K. (1989) A review of the geochronology of the Amazonian Craton; Tectonic implications. Precambrian Research, 27, 213-227.
- Tompkins, L.A. (1987) Exploration for kimberlites in the SW-

Goias region, Brazil: Mineral chemistry of stream sediment samples. Journal of Geochemical Exploration, 27, 1-28.

Tompkins, L.A. and Gonzaga, G.M. (1989) Diamonds in Brazil and a proposed model for the origin and distribution of diamonds in the Coromandel region, Minas Gerais, Brazil. Economic Geology, 84, 591-602.

Tompkins, L.A. and Ramsay, R.R. (1991) The Boa Esperança and Cana Verde pipes; Corrego D'anta, Minas Gerais, Brasil. (Extended Abstract) Fifth International Kimberlite Conference, Minas Gerais, Brasil, this volume.

Wilding, M.C.; Harte, B. and Harris, J.W. (1989) Evidence of asthenospheric source for diamonds from Brazil (abstract). 28th International Geological Congress, Washington, D.C., 3, 359-360.

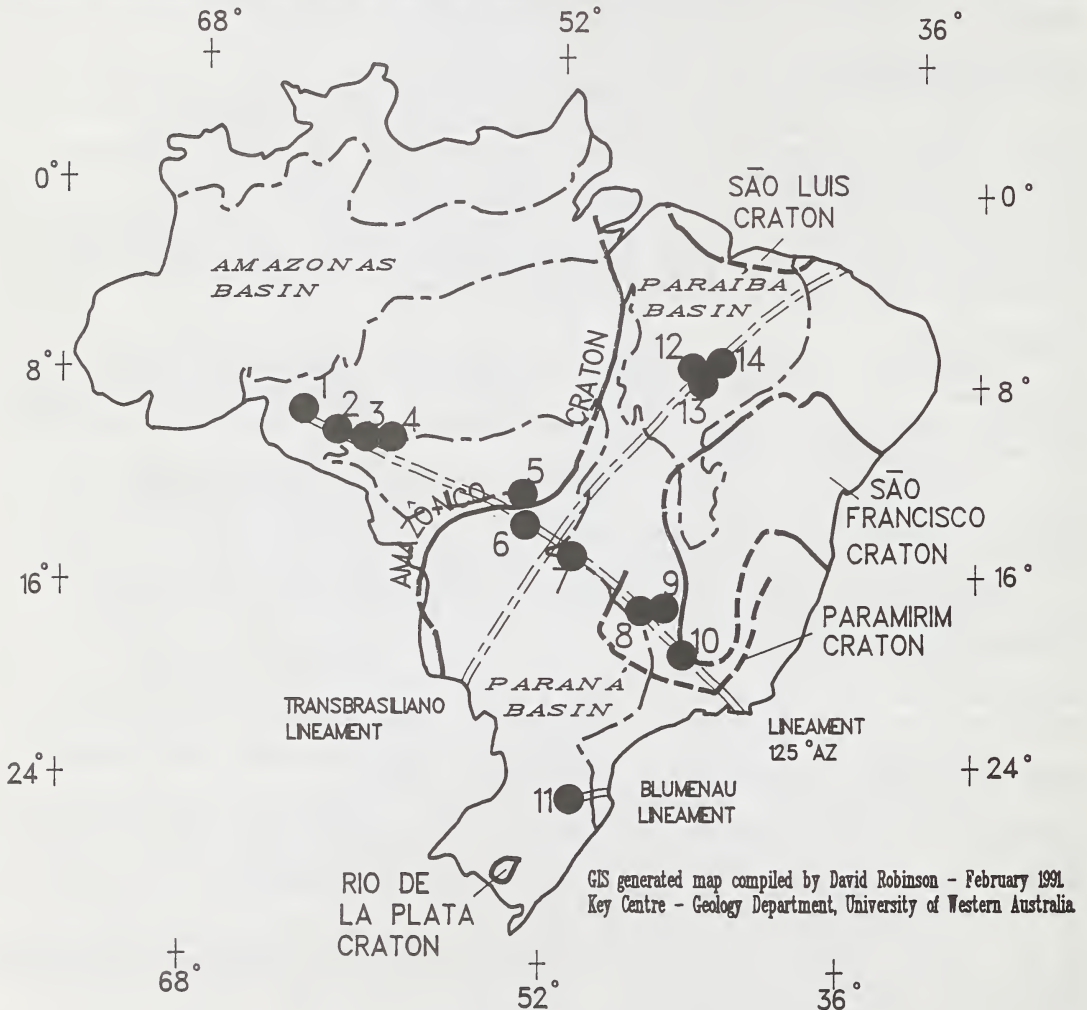


Figure 1. Principal structural environments in Brasil from Schobbenhaus and Campos (1984) and Almeida (1981). The solid circles refer to kimberlite/lamproite provinces from Tompkins and Gonzaga (1989) and A.J.A. Janse (pers. comm., 1990) and, are identified as follows: 1=Arquemes; 2=Pimenta Bueno; 3=Vilheno; 4=Aripuãna (Juina); 5=Paranatinga (Batovi); 6=Poxereu; 7=Amorinópolis; 8=Alto Paraníba; 9=Presidente Olegário; 10=Bambui; 11=Lajes; 12=Redondão; 13=Santa Filomena-Bom Jesus (Gilbues); 14=Picos.

## THE BOA ESPERANÇA AND CANA VERDE PIPES; CÓRREGO D'ANTA, MINAS GERAIS, BRAZIL.

*Linda A. Tompkins and Robert R. Ramsay.*

*Key Centre for Strategic Mineral Deposits, University of Western Australia, Nedlands, Perth 6009, Western Australia.*

### INTRODUCTION

The Corrego D'anta region, located 200km northwest of Belo Horizonte, Minas Gerais state, was originally prospected for kimberlites by small private Brazilian companies in the late 1970's. Five "kimberlites": Boa Esperança; Inga, Quartel, Almeida and Cana Verde, are known to occur within a larger area referred to as the Bambuí province (Barbosa, 1983; Location 10 of Fig. 1, Tompkins, 1991, this volume). This paper describes the geology, bulk rock geochemistry and, mineralogy of -2mm, +0.25mm heavy mineral concentrates (HMC) from the Boa Esperança and Cana Verde pipes.

Both pipes are situated along a major NW-SE trending lineament (lineament. 125° AZ; Bardet, 1977) that extends from the Amazônico craton in the NW, to Rio de Janeiro in the SE. In the region of Minas Gerais, it is referred to as the Alto Paranaíba Arch. The two pipes are separated by a distance of 22km, with the Cana Verde pipe located closer to the cratonic nucleus of the São Francisco craton. They intrude the southwestern edge of the São Francisco craton, but within the boundaries of the larger Paramirim craton as defined by Almeida (1981). This area was consolidated during the Jequií event (2,700my), but partially reworked during the Transamazônico (2,000 my) and Brasiliano (450-700 my) events. The pipes post-date a period of Jurassic rifting along lineament 125° AZ and throughout Brazil. In Brazil, magmatic rocks intruded during this period include kimberlites, carbonatites, "lamproites", and other related rocks. Cana Verde and Boa Esperança are, therefore, considered to be Lower Cretaceous in age, or younger.

### BOA ESPERANÇA

The Boa Esperança pipe is intruded into fine-grained laminated siltstones of the Upper Proterozoic Bambuí Group. It crops out within a dry drainage basin that is only seasonally active. Field mapping of the intrusion has shown it to have an elongated configuration of at least 220m in length, with an average width of 55m, or about 1.2 hectares in area.

Exposure of the intrusion in an old excavation pit identifies the rock as a dark-green micaceous breccia. It contains abundant country rock clasts, as well as altered pyropic garnet-bearing ultramafic xenoliths. Due to the altered nature of the rock petrographic studies are not informative.

Bulk rock analysis of altered breccia at the surface shows it to be an ultramafic rock with MgO=16.71 wt%, Ni=950ppm, and fairly rich in incompatible trace elements such as Ba (742ppm), and Sr (892ppm). Apart from SiO<sub>2</sub> and Al<sub>2</sub>O<sub>3</sub>, which are possibly affected by country rock contamination, the analyses fall within the range of average kimberlite (Mitchell, 1986).

Diamond indicator minerals (DIM) in HMC include: relatively common, red-purple chrome-pyrope; emerald-green chrome-diopside; a few chrome-rich spinels and, rare Mg-Cr-ilmenites. Other minerals include: almandine; pale-green Cr-poor diopside; Ti-magnetite and, rare apatite. No micro-diamonds were recovered, but insufficient material was processed to view this as a reliable indication of diamond potential.

Cr-pyrope compositions are lherzolitic to wehrlitic (Sobolev et al., 1973) with up to 10 wt% Cr<sub>2</sub>O<sub>3</sub>. Cr-rich spinels vary from 0.70-0.85 molar Cr/(Cr+Al) and 0.40-0.60 molar Fe<sup>2+</sup>/(Mg+Fe<sup>2+</sup>), with generally high TiO<sub>2</sub> values up to 6 wt%. Iron oxidation ratios (Fe<sup>3+</sup>/Fe<sup>2+</sup>) suggest fO<sub>2</sub> conditions between WM to IW. Ilmenites have MgO values up to 10 wt% and Cr<sub>2</sub>O<sub>3</sub> up to 3 wt%.

#### CANA VERDE

The Cana Verde intrusion is intruded into fine-grained well laminated slates and siltstones of the Upper Proterozoic Bambuí Group. The intrusion consists of fine-medium grained light-green colored micaceous tuffs and tuff-breccias. A large dark-green serpentinized xenolith has also been observed. The exact surface dimensions are not known.

Bulk rock analysis of the tuff-breccia yield moderate values of SiO<sub>2</sub> (48-49 wt%), and Al<sub>2</sub>O<sub>3</sub> (6.32-8.40 wt%), with low MgO (3.77-4.09 wt%) values suggestive of country rock contamination. However, high K<sub>2</sub>O (5.54-10.72 wt%), and TiO<sub>2</sub> (8.44-10.05 wt%) values coupled with high Ba (874-2,571 ppm) and Sr (1,224 ppm) are suggestive of a lamproitic composition. Bulk rock analysis of the serpentinized xenolith yielded high MgO (19.50 wt%) and Ni (730 ppm) values and together with the presence of Cr-diopside and garnet suggest that it is an altered garnet lherzolite.

DIM in the HMC include: relatively common red-purple Cr-pyrope; emerald-green Cr-diopside and a few Cr-rich spinels. Also present are: rare Mg-Cr-ilmenites, including some with coarse-grained spinel exsolution lamellae, and Cr-Nb-rutile intergrown with Mg-Cr-ilmenite. Other minerals include: almandine; rare sphene; and amorphous Ca-Nd-La-phosphates. No micro-diamonds were recovered, but insufficient material was processed to use this as a reliable assessment of diamond potential.

Cr-pyrope compositions are lherzolitic with up to 6 wt% Cr<sub>2</sub>O<sub>3</sub>. Cr-rich spinels vary from 0.65-0.95 molar Cr/(Cr+Al) and 0.35-0.80 molar Fe<sup>2+</sup>/(Mg+Fe<sup>2+</sup>), with generally high TiO<sub>2</sub> values up to 8 wt%. Iron oxidation ratios suggest fO<sub>2</sub> conditions between WM to IW. Ilmenites have MgO values up to 10 wt% and Cr<sub>2</sub>O<sub>3</sub> up to 6 wt%.

#### CONCLUSIONS

Initial data suggest that the Boa Esperança pipe may be a kimberlite, while the Cana Verde pipe has bulk compositions more typical of lamproites. HMC chemistry shows that garnet peridotite was sampled, as represented by lherzolitic garnet, clinopyroxene and, Cr-rich spinel. Ti-metasomatism, is pervasive at both localities as indicated by the presence of Ti-rich chrome spinels, Mg-Cr ilmenites and, Cr-Nb-rutile-ilmenite intergrowths.

Although no micro-diamonds were recovered from either pipe, the land owners at Cana Verde report the recovery of macro-diamonds (Barbosa, 1983). DIM compositions do not indicate the presence of harzburgite which is regarded as the dominant source of peridotitic diamond (Gurney, 1984). However, diamond-bearing kimberlites containing only garnet lherzolite are described elsewhere (Scott-Smith et al., 1984). Thus the presence of garnet lherzolite DIM's supports deep mantle sampling, but indications of Ti-metasomatism may have decreased the diamond potential of the source rocks.

#### ACKNOWLEDGEMENTS

Research was supported by an Australian Overseas Postgraduate Research Scholarship (OPRS) to LAT, and University of Western Australia Scholarships to LAT and RRR. Access to the intrusions and permission to publish is granted by Capa Ltda., Rio de Janeiro, Brasil. Laboratory support was provided by CRA for heavy mineral separation, Ashton Mining for micro-diamond separation, and the University Western Australia, Electron Microscopy Center for mineral analyses. All are gratefully acknowledged.

#### REFERENCES

Almedia, F.F.M. de (1981) O craton do Paramirim e suas relações com o do São Francisco. Anais do Simpósio sobre o craton do São Francisco e suas faixas marginais. Coordenação da Produção Mineral, Salvador, Bahia, 1-10.

Barbosa, O. (1983) Diamante no Brasil, Ocorrências, Prospecção, e Lavra. Companhia de Pesquisa de Recursos Minerais, Série Diamante no. 1, Rio de Janeiro, 68p.

Bardet, M.G. (1977) Geologie du Diamant. Troisieme partie gisements de diamants d'Asia, d'Amerique, d'Europe et d'Australasie. Bureau Recherches Géol. Min., Memoire 83, 169p.

Gurney, J.J. (1984) A correlation between garnets and diamonds in kimberlites. In: J.E. Glover and P.G. Harris, editors. Kimberlite Occurrence and Origin: A basis for conceptual models in exploration. The Geology Department and University Extension, The University of Western Australia, Publication no. 8, 143-166.

Mitchell, R.H. (1986) Kimberlites; Mineralogy, Geochemistry, and Petrology. Plenum Press, New York, 442p.

Scott-Smith, B.; Danchin, R.V.; Harris, J.W. and Stracke, K.J. (1984) Kimberlites near Orroroo, South Australia. In: J. Kornprobst, editor. Kimberlites I: Kimberlites and Related Rocks. Developments in Petrology, 11A, Elsevier Publishing, New York, 121-142.

Sobolev, N.V.; Laurent'yev, Yu. G.; Pokhilenko, N.P. and Usova, L.V. (1973) Chrome-rich garnets from the kimberlites of Yakutia and their paragenesis. Contributions to Mineralogy and Petrology, 40, 39-52.

Tompkins, L.A. (1991) Kimberlite structural environments and diamonds in Brasil. (Extended abstract) Fifth International Kimberlite Conference, Minas Gerais, Brasil, this volume.

## REDUCED CARBONACEOUS MATTER IN BASALTS AND MANTLE XENOLITHS.

*Tracy N. Tingle\* and Michael F. Hochella, Jr.*

*Department of Geology, Stanford University, Stanford, CA 94305 USA; \*now at Department of Geology, University of California, Davis, CA 95616 USA.*

Crack surfaces and grain boundaries in many basalts and mantle xenoliths display a peculiar bluish purple discoloration or iridescence that suggests the presence of a thin film. C x-ray mapping and x-ray photoelectron spectroscopy (XPS) indicate that such iridescent surfaces possess a thin film of amorphous C a few nm thick (Mathez and Delaney, 1981; Mathez, 1987; Tingle et al., 1990; 1991). C in the films is predominantly C-C and/or C-H bonded species with smaller amounts of various C-O bonded species. Less commonly, carbonaceous particles up to 20  $\mu\text{m}$  across are present on crack surfaces in some xenoliths. Carbonaceous matter (films and particles) contains minor quantities of Si, Al, alkalis, halogens, transition metals, N, O and sometimes organic compounds (mostly hydrocarbons). With the exception of organics, these are components expected to be present in volcanic gas, and the crack surfaces on which carbonaceous films occur probably are produced by thermal stresses during eruption and cooling of the basaltic lava and attendant xenoliths. Mathez (1987) and Tingle et al. (1990; 1991) have postulated that carbonaceous films are produced by heterogeneous surface reactions involving volcanic gas and fresh, chemically active crack surfaces. Indeed, we have produced carbonaceous films, similar in thickness and C speciation to those observed in natural rocks, in laboratory experiments simulating the volcanic environment.

Carbonaceous matter on crack surfaces has been observed in a variety of samples from different geologic environments. These include basalts and peridotite xenoliths from the 1801 AD flow of Hualalai Volcano, Hawaii, San Carlos and Kilbourne Hole, Arizona, basalts from the Kilauea east rift and the Mid-Atlantic Ridge, megacrysts (garnet and diopside) from the Jagersfontein kimberlite, and gabbros from the Pt-group element mineralized zones of the Bushveld and Stillwater layered igneous complexes. The chemistry of this carbonaceous matter shows considerable variation among samples from different localities and even among samples from the same locality.

Organic compounds associated with carbonaceous films have been detected by very sensitive thermal desorption photoionization mass spectrometry in some samples (Tingle et al., 1990; 1991). They are desorbed at temperatures of 300-700°C and consist principally of compounds with molecular weights less than 150 amu (mostly alkanes, alkenes and aromatics with lesser amounts of N- and O-bearing compounds and sulfur species). That temperatures in excess of 300°C are required to desorb organic material suggests that the observed species are pyrolysis products of more complex compounds or that the low molecular weight species must be physically or chemically bound in the carbonaceous material. It has been shown that organic matter, when present, is not laboratory or instrument contamination, environmental biogenic matter incorporated during residence at the Earth's surface, or pyrolyzed biogenic matter incorporated by the lava advancing over vegetation during eruption. Not all samples with carbonaceous films contain organics. For example, organics were detected in only 3 of 5 xenoliths analyzed from Hualalai, and organic compounds were not detected in any of the Stillwater and Bushveld samples. Tingle et al. (1990) have suggested that 10-50% of the total C in the San Carlos olivine films may be organic, although estimates of the organic abundance or even relative amounts of organic versus amorphous C are subject to some uncertainties.

The organic matter associated with carbonaceous films has two possible sources. Organic compounds may have been produced by Fisher-Tropsch-like catalytic reactions at the mineral-gas interface. Alternatively, organic compounds may have been assimilated into the volcanic gas prior to eruption and then deposited on crack surfaces during C film formation. The small amount of organic matter generally present is not sufficient to determine its origin. As pointed out by Tingle et al. (1990, and references contained therein), on the one hand, biogenic matter (low molecular weight hydrocarbons and biomolecules, steranes and terpanes) has been identified in volcanic emanations, hydrothermal fluids, and steam from geothermal fields. On the other hand, abiogenic

synthesis of a diverse suite of organic compounds has been achieved in meteorites (carbonaceous chondrites) in the solar nebula and in laboratory experiments, although silicates are not generally regarded as the substrates on which organic synthesis reactions occurred. Also, methane and light hydrocarbons in hydrothermal fluids of the East Pacific Rise and Mid-Atlantic Ridge are abiogenic, although the mechanisms by which they are produced are not well understood. Also, hydrocarbons in fluid inclusions in rocks of the Khibiny and Ilimaussaq alkaline intrusions are demonstrably abiogenic. We believe the present data favor an abiogenic synthesis, although a biogenic origin cannot be dismissed at this time.

The isotopic composition ( $\delta^{13}\text{C}$ ) of C in films on iridescent crack surfaces in San Carlos olivine was determined by stepped combustion techniques to be  $-32\text{‰}$  (D. P. Matthey and T. N. Tingle, 1991, manuscript in preparation), suggesting that there is a strong fractionation of C isotopes during C film formation. Even if 50% of the crack-situated C in the San Carlos olivine is assimilated biogenic matter with  $\delta^{13}\text{C} = -50\text{‰}$ , the  $\delta^{13}\text{C}$  of C films deposited by the volcanic gas on fresh crack surfaces would be  $-14\text{‰}$ , which is considerably more depleted than the  $-5$  to  $-8\text{‰}$  typically observed for  $\text{CO}_2$  in basaltic gases.

To further investigate the formation of carbonaceous films and the possible abiogenic synthesis of organic matter during eruption and cooling of basaltic magma, we have exposed freshly cleaved {010} surfaces of San Carlos olivine to C-O-H gases at  $400\text{--}800^\circ\text{C}$ . Two gas compositions were employed:  $2\text{CO}_2 + 2\text{H}_2\text{O} + \text{H}_2$  and  $2\text{CO}_2 + \text{H}_2$  derived from decomposition of oxalic acid dihydrate and oxalic acid, respectively. In one set of experiments, gem-quality single crystals were loaded in air with a small amount of oxalic acid and welded shut; the samples were heated to  $800^\circ\text{C}$  and quenched in liquid nitrogen to produce cracks. In a second set of experiments, large single crystals were cleaved in an argon glove bag and loaded into Au tubes with oxalic acid, hermetically sealed and then welded shut. Samples were then heated to  $400\text{--}800^\circ\text{C}$  for 2-30 min to allow for heterogeneous reactions between the mineral surface and gas phase to occur.

Carbonaceous films were produced in all samples, but none of them contained any detectable organic material. Films attained thicknesses comparable to those observed in natural samples. The speciation of C in films was dependent on the gas composition and  $f(\text{O}_2)$ . Films produced at relatively oxidizing conditions resembled those observed in natural samples, in that the prominent species observed were C-C/C-H with lesser amounts of C-O bonding; films produced at the more reduced conditions consisted of roughly equal amounts of carbide, C-C/C-H, and C-O species. Scanning electron microscopy has not revealed any crystallites or particles on these surfaces. It is important to note that thermodynamic calculations for these two sets of experiments do not predict graphite, carbides, carbonates, or hydrocarbons to be stable phases. Similarly for natural samples, the chemical environment during eruption is much too oxidizing for graphite (and presumably amorphous C) and hydrocarbons to be stable phases. These experiments suggest that the nature of fresh crack surfaces is such that they can stabilize amorphous C and hydrocarbons in a cooling lava.

The study of carbonaceous matter has several implications. First, the low-temperature ( $400\text{--}700^\circ\text{C}$ ) isotopically light ( $-26\text{‰}$ ) C released by stepped heating techniques from basalts and xenoliths (Matthey, 1988) is not all contamination as was previously thought; part of the low-temperature C is due to carbonaceous films on crack surfaces, grain boundaries, and vesicle and fluid inclusion walls. In their measurement of the  $\delta^{13}\text{C}$  of carbonaceous films in San Carlos olivine, Matthey and Tingle (1991, manuscript in preparation) found that approximately 50% of the C analyzed below  $800^\circ\text{C}$  was due to C films, 10% was due to adventitious C contamination of olivine surfaces, and 40% was instrument contamination.

Second, the apparent fractionation of C isotopes between  $\text{CO}_2$  vapor and  $\text{CO}_2$  dissolved in basalt melt indicated by the "popping rocks" of the Mid-Atlantic ridge (Pineau et al., 1976) and the later experiments of Javoy et al. (1978) may be explained by the presence of isotopically depleted C films on vesicle walls and cracks in the popping rocks and experimental glasses. The vapor-melt C isotopic fractionation is expected to be close to that of  $\text{CO}_2$ -calcite (because C dissolves in basalt melt as  $\text{CO}_3^{2-}$  species) at magmatic temperatures ( $1\text{--}2\text{‰}$ ), and the recent experimental results of Matthey et al. (1990) support this. The mantle C flux of  $0.6\text{--}7.2 \times 10^{14}$  g/yr calculated assuming a  $4\text{‰}$  fractionation (Javoy et al., 1982) must be reconsidered, and with it the hypothesis that C must be subducted in order to explain the modern mantle C flux.

There are several lines of evidence to suggest that C is indeed subducted, but most of that will be carbonates in pelagic sediment and altered oceanic crust with  $\delta^{13}\text{C} \approx 0\text{‰}$ , and a much smaller amount will be kerogen with very depleted  $\delta^{13}\text{C}$ . Thermal models of subduction zones and carbonate phase equilibria predict that carbonates, in general, will not decompose during subduction. However, the vast majority of  $\text{CO}_2$  coming out of the Earth today has a very uniform  $\delta^{13}\text{C} = -5$  to  $-8\text{‰}$ . It seems to us that the  $-5\text{‰}$   $\delta^{13}\text{C}$  of the modern mantle is best explained by a primordial C source (of approximately the same isotopic composition) that was stable during accretion and differentiation. That such a C reservoir might exist in a planetary core is suggested by the presence of graphite in iron meteorites, and  $\delta^{13}\text{C}$  of such graphite is  $-5$  to  $-8\text{‰}$  (Deines and Wickman, 1975). At present, the best evidence of C recycled by subduction appears to be diamonds of eclogitic paragenesis with depleted  $\delta^{13}\text{C}$  (Kirkley and Gurney, 1989).

## REFERENCES

- Deines, P. and Wickman, F. E. (1975) A contribution to the stable carbon isotope geochemistry of iron meteorites. *Geochimica Cosmochimica Acta*, 39, 547-557.
- Javoy, M., Pineau, F., and Iiyama, I. (1978) Experimental determination of the isotopic fractionation between gaseous  $\text{CO}_2$  and carbon dissolved in tholeiitic magma: A preliminary study. *Contributions to Mineralogy and Petrology*, 67, 35-39.
- Kirkley, M. B., and Gurney, J. J. (1989) Carbon isotope modelling of biogenic origins for carbon in eclogitic diamonds. Workshop on Diamonds, 28th Int. Geol. Congress, Washington, D. C.
- Mathez, E. A. (1987) Carbonaceous matter in mantle xenoliths: Composition and relevance to the isotopes. *Geochimica Cosmochimica Acta*, 51, 2339-2347.
- Mathez, E. A., and Delaney, J. R. (1981) The nature and distribution of carbon in submarine basalts and peridotite nodules. *Earth and Planetary Science Letters*, 56, 217-232.
- Matthey, D. P. (1988) Carbon isotopes in the mantle. *Terra Cognita*, 7, 31-37.
- Matthey, D. P., Taylor, W. R., Green, D. H., and Pilinger, C. T. (1990) Carbon isotopic fractionation between  $\text{CO}_2$  vapour, silicate and carbonate melts: An experimental study to 30 kbar. *Contributions to Mineralogy and Petrology*, 104, 492-501.
- Pineau, F., Javoy M., and Bottinga, Y. (1976)  $^{13}\text{C}/^{12}\text{C}$  ratios of rocks and inclusions in popping rocks of the Mid-Atlantic Ridge: Their bearing on the problem of isotopic composition of deep-seated carbon. *Earth and Planetary Science Letters*, 29, 413-421.
- Tingle, T. N., Hochella, M. F., Becker, C. H., and Malhotra R. (1990) Organic compounds on crack surfaces in olivine from San Carlos, Arizona and Hualalai Volcano, Hawaii. *Geochimica Cosmochimica Acta*, 54, 477-485.
- Tingle, T. N., Hochella, M. F. and Mathez, E. A. (1991) Carbonaceous matter in peridotites and basalts studied by XPS, SALI and LEED. *Geochimica Cosmochimica Acta*, 55, (in press).

THE ARIES DIAMONDIFEROUS KIMBERLITE PIPE CENTRAL KIMBERLEY BLOCK,  
WESTERN AUSTRALIA.

Towie, <sup>(1)</sup>N.J.; Marx, <sup>(2)</sup>M.R.; Bush, <sup>(1)</sup>M.D. and Manning <sup>(2)</sup>E.R.

(1) Triad Minerals N.L., Melbourne, Victoria, Australia; (2) Poseidon Exploration Ltd., Adelaide, SA, Australia.

The Aries kimberlite pipe is situated in the Kimberley Region of Western Australia, 270 km east-north-east of the coastal town of Derby and 250 km west of the Argyle diamond mine.

The pipe is intruded into the Proterozoic sediments and basalts comprising the Kimberley Basin which is thought to be underlain by an Archean cratonic basement.

The pipe has been dated by the Rb-Sr phlogopite method at about 820 Ma (C.B. Smith 1989) Nearby tillites provide evidence of subsequent glaciation at 700ma.

## II. EXPLORATION

Systematic diamond exploration of the Kimberley Region commenced in 1971 and this led to the discovery of numerous kimberlites and lamproites including the Argyle pipe in the period from 1975 to 1980.

Traditional drainage sampling by the Triad/Freeport partners confirmed the presence of kimberlitic chrome spinels which led to the Aries pipe discovery in 1985.

Three depressions up to 20m deep form the surface expression of the kimberlite within the sandstone country rock and are easily visible on aerial photographs.

The 40 Nanoteslar aeromagnetic response is distinctive but not dipolar.

The VLF magnetic and electric field signatures fairly consistently but not invariably define the pipe contact zones.

The surface spectral signature as detected by the Geoscan MKII multispectral scanner indicates a clear anomaly in band ratios typical of montmorillonite.

## III. THE ARIES PIPE

### A. Structural

The size of the pipe is 20 hectares based on contacts primarily inferred from sandstone outcrop. Limited drilling to a maximum depth of 100m has shown that the wallrock contacts dip at 60-80°. There are four distinct lobes.

The northern extension appears to either contain massive reefs of basalt and sandstone, or else it has a small central core with radiating dykes and sills.

A 1m thick sill has been confirmed approximately 100m from the centre of this lobe.

The northern lobe is mostly xenolithic breccia with 95% basalt xenoliths and <5% kimberlite matrix.

The central lobe contains two large basalt reefs and in the vicinity of these the predominant rock type is xenolithic breccia as above. Kimberlite, micaceous kimberlite and kimberlite breccia with little xenolithic dilution are found in the southeast portion of the lobe.

The southern lobe is mostly kimberlite breccia with a high dolerite and sandstone content as well as basalt. It degenerates into a zone of brecciated quartzite country rock with kimberlite dykes in the southern tail.

The top 20m of the kimberlite is heavily oxidized to clay with a sharp transition to silicified kimberlite separated by a thin laterite layer. In the central lobe there are 1-4m of overlying ferruginous gravels with a marked depletion of -2mm diamonds compared to the underlying kimberlite. This indicates a fossil drainage no longer visible. Clayey silt overlies the gravel ranging from several centimetres to 6m depth.

#### B. Geochemistry

A loam sample taken from the central lobe in the surficial clayey silt gave no anomalous geochemical signature compared to the nearby basaltic soils apart from enhancement of Cr and Zr (0.4% on Kimberlite). Compared to proximal doleritic soils Cr, Ni and La have been shown to be enhanced. A kimberlite soil analysis is given in table 1.

The yellow ground analysis shows a surprising similarity to the soil sample from above. This sample of yellow ground was taken from weathered kimberlite breccia with <20% Xenolithic dilution.

TABLE 1 (Values in ppm)

ELEMENT :	Nb	Nd	Ce	La	V	Cr	Ni	Sr	Ba
Surface Soil	11	<20	NA	17	23	415	14	8	56
Yellow ground (6m depth)	10	<2	70	20	100	NA	<5	50	210

#### IV. ALLUVIALS

The extensive alluvial deposits downstream of the Aries pipe were initially detected and outlined by the surface chromite distribution pattern within the Harris Creek valley system.

At least three gravel horizons west were uncovered, the ages of which are thought to date from Miocene to present times. The two main channel deposits are weakly diamondiferous.

THE ULTRABASIC POTASSIC ROCKS OF PRESIDENTE OLEGARIO, SERRA DA  
MATA DA CORDA, MINAS GERAIS, BRAZIL.

Ulbrich, <sup>(1)</sup>M.N.C. and Leonardos, <sup>(2)</sup>O.H.

(1) *Inst. Geociências, Univ. São Paulo, CP 20899 São Paulo-SP, Brazil;* (2) *Inst. Geociências, Univ. Brasília, CEP 153044 Brasília-DF, Brazil.*

Ultrabasic potassic-ultrapotassic rocks are generally included in one of three groups: kimberlites, lamproites and kamafugites. Petrographically, the distinction between these groups seems relatively simple. The fragmental texture of kimberlites contrasts with the volcanic features found in lamproites and kamafugites. The latter two can be further identified by the presence (or absence) of some typical minerals.

This straightforward scheme, however, is blurred by examples of mineralogical and chemical convergence, as shown by similarities between micaceous kimberlites and lamproites, or by cases in which mineralogy seems to point to one of the rock groups while chemistry points to another.

Such a situation was found during studies on the rocks of the Presidente Olegário pipe.

Ultrabasic potassic rocks -tuffs, lavas and small intrusions, mapped as the Patos facies of the Mata da Corda Group- occur as isolated outcrops on dissected plateaus in the Serra da Mata da Corda, western Minas Gerais State. They invade Late Cretaceous sandstones over an area of about 4500 Km<sup>2</sup>. Outcrops are generally poor, largely because of agriculture. Fertile clays, derived from the Patos tuffs and lavas, cover the plateaus and are frequently capped by a 1- to 5-m-thick iron crust formed by weathering.

The Presidente Olegário pipe, observed along a newer road-cut near the city of the same name, also belongs to this ultrabasic volcanic province. It is composed of a sequence of massive and amygdaloidal lavas and tuffs, cut by centimetric altered dikes and tuffisitic breccias.

The lapilli and ash tuffs contain cogenetic and accidental material. Some pyroclastic horizons also present rounded fragments of variable size of two different types: a) volcanic rocks with abundant phenocrysts of altered melilite(?) (Suite I); b) fresh, medium to coarse-grained, banded clinopyroxenites (Suite II) with diopside, perovskite, titanomagnetite, apatite, schorlomite, titanite, Ba-rich K-feldspar (BaO=3%) and wadeite.

The lavas are porphyritic with subidiomorphic pheno- and microphenocrysts of olivine (Fo=90) in a matrix of diopside, perovskite, Mg-ilmenite (MgO=5.0-8.6%), titanomagnetite, apatite, poikilitic Ti-phlogopite (TiO<sub>2</sub>=4.6-6.0%) and Ti-K richterite (K<sub>2</sub>O=5.0, TiO<sub>2</sub>=3.4%) within a glassy base containing Mg, Ca, K and Ba.

Chemical analyses of the massive lavas indicate an ultrabasic potassic composition (Table 1). The rocks are also metaluminous, rich in Ti and with rather low mg values. They present high amounts of incompatible elements, mainly Ba. REE are abundant (Table 1) and show a steep distribution pattern (Fig. 1): La/Yb ratios are high and the Eu anomaly is absent.

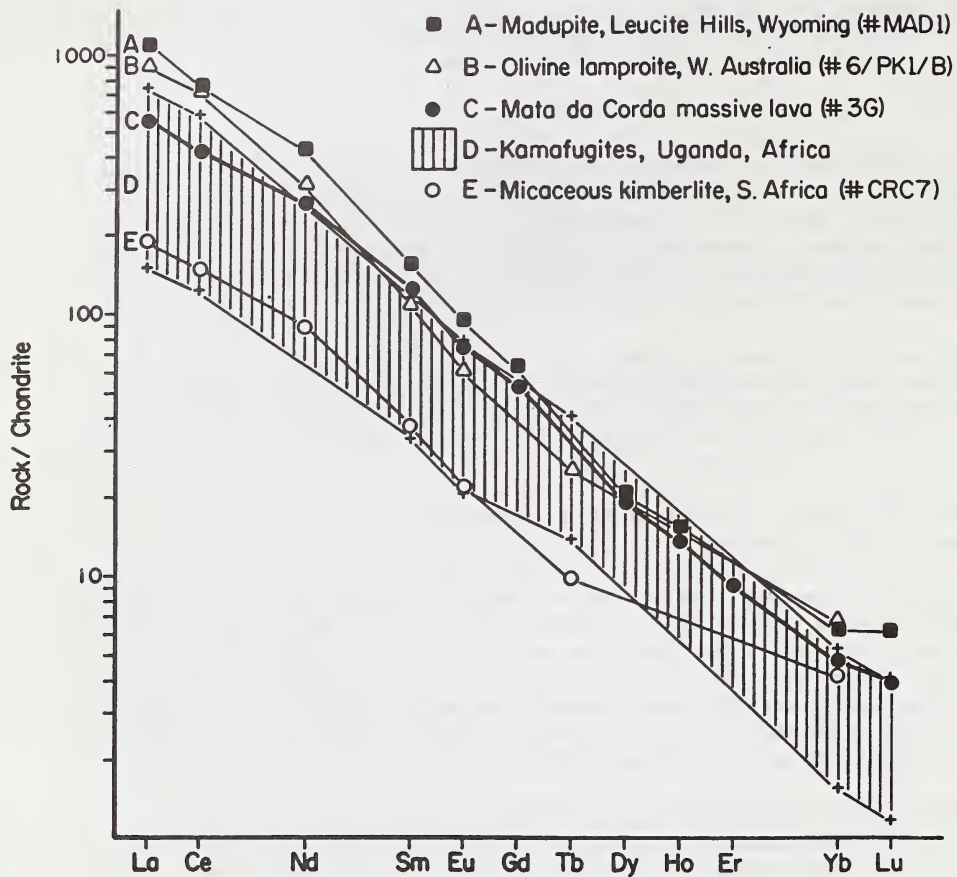


Fig. 1. Chondrite normalized REE diagram showing REE abundance in an ultrabasic potassic rock from Presidente Olegário, Serra da Mata da Corda compared to basic-ultrabasic lamproïtes, a micaceous kimberlite and kamafugites. The kamafugitic field includes data for katungites and mafurites (higher REE contents) and ugandites (lower REE contents). Sources: A-Thompson, R.N. et al. 1984. *Phil.Trans.R.Soc.Lond.* A310, 549-590. B, E-Fraser, K.J. et al. 1985/86. *Earth planet.Sci.Lett.* 76, 57-70. C-this work. D-Mitchell, R.H. & Bell, K. 1976. *Contr.Mineral.Petrol.* 58, 293-303

*Acknowledgements* - Support for field and laboratory work came from the Brazilian agencies CNPq and FINEP (FINEP-USP. Proc. 42.86.0491.00).

The mineralogy and texture of these lavas resemble those of ultrabasic lamproites, a resemblance enhanced by their high Ba content and the coexistence with fragments containing wadeite (Suite II). Major element chemistry, however, indicates a kamafugitic affinity. Also, the possible presence of melilite in the Suite I fragments, whose emplacement was certainly related to the eruption of the lavas, may point to a kamafugitic association; it is unknown in lamproitic occurrences. Contents of REE in ultrabasic potassic rocks are usually high, but they show a regional variability that seems to be related to differences in mantle source material and/or petrogenetic behavior; they share a somewhat steep and continuous distribution pattern (high La/Yb values, Fig.1). The distribution pattern for the Presidente Olegário lava (curve C, Fig.1) is similar both in profile and abundance to some kamafugites (mafurites and katungites) and olivine lamproites (Fig.1); it also is, as generally observed elsewhere, enriched in REE when compared to kimberlites.

The lavas thus present features that straddle the supposedly clear-cut characteristics defined in the literature as being "typical" of kamafugites and ultrabasic lamproites

Table I: Chemical analyses of Presidente Olegário, Serra da Mata da Corda massive lavas

Sample	3G	3G1	87-04		3G	3G1	87-04
wt%				ppm			
SiO <sub>2</sub>	39.1	37.2	38.9	Ba	10748	11644	11656
TiO <sub>2</sub>	6.0	6.6	6.5	Rb	150	150	160
Al <sub>2</sub> O <sub>3</sub>	5.6	5.3	5.0	Cs	n.a.	<10	<10
Fe <sub>2</sub> O <sub>3</sub>	8.6	5.9	6.1	Sr	1250	1310	1650
FeO	4.67	6.8	7.0	Zr	710	790	800
MnO	0.19	0.18	0.17	Nb	200	192	33
MgO	17.1	18.4	15.0	Y	30	38	62
CaO	10.1	10.6	11.6	V	200	n.a.	n.a.
Na <sub>2</sub> O	0.75	0.81	0.56	Cr	752	570	650
K <sub>2</sub> O	2.3	2.2	1.7	Co	n.a.	80	66
P <sub>2</sub> O <sub>5</sub>	0.47	0.5	0.49	Ni	338	440	270
H <sub>2</sub> O <sup>+</sup>	3.05	3.73	4.67	Cl	<20	110	93
CO <sub>2</sub>	0.6	0.3	0.45	La	173	153	183
S	0.07	0.08	0.05	Ce	348	294	340
F	0.24	0.21	0.19	Nd	159	147	168
rest	1.73	1.83	1.86	Sm	23.4	19.2	28.86
less O=F,S	0.14	0.13	0.10	Eu	5.5	4.24	5.15
sum	100.43	100.21	100.14	Gd	13.4	10.98	13.46
# mg <sup>1</sup>	0.74	0.76	0.72	Dy	6.2	4.8	6.05
(Na+K)/Al	0.66	0.70	0.55	Ho	1.0	0.7	1.01
K <sub>2</sub> O/Na <sub>2</sub> O <sup>2</sup>	2.0	1.80	2.0	Er	2.0	1.58	2.40
				Yb	1.0	0.91	1.09
				Lu	0.13	0.10	0.18

1: # mg=Mg/(Mg+Fe<sup>2+</sup>) calculated with Fe<sub>2</sub>O<sub>3</sub>/FeO ratio of 0.2;

2: molar ratio; n.a.=not analysed.

Analyst: C. Dutra, GEOLAB, Belo Horizonte, Minas Gerais, Brazil.

## DIAMOND- AND GRAPHITE-PERIDOTITE XENOLITHS FROM THE ROBERTS VICTOR MINE.

*Viljoen, K.S.; Robinson, D.N and Swash, P.M.*

*Anglo American Research Labs., Kimberlite Res. and Serv. Lab., PO Box 106, Crown Lines, 2025, South Africa.*

### INTRODUCTION

The Roberts Victor kimberlite is situated in the Orange Free State, South Africa. This is within the central part of the Kaapvaal craton. It is a Group 2 kimberlite which has been dated at 128 My.

It is well known for the high proportion of eclogite xenoliths present, particularly in relation to the more usual dominance of peridotite xenoliths at most other kimberlites. MacGregor and Carter (1970) estimated that eclogites constituted over 95% of the xenolith population, and Hatton (1978) found that 98% of 700 nodules examined were of eclogitic, rather than peridotitic affinity. Recently, an attempt was made to characterise the peridotite suite more fully. A one day visit to the mine resulted in the collection of 20 specimens. Each xenolith was first sawn in two with a boron nitride impregnated saw. One half was carefully cleaned of adhering kimberlite matrix, crushed and digested in hydrofluoric acid. Examination of the acid residue proved that six of the xenoliths contain diamond, two contain both diamond and graphite while another four contain only graphite.

### PETROGRAPHY

The peridotites are rounded and range in size from 10 cm to 30 cm in diameter. They are all extremely altered to serpentine, calcite and quartz. Olivine and orthopyroxene have been completely destroyed, clinopyroxenes are partially altered and garnets and spinels are fresh. All the xenoliths show coarse (undeformed) relict textures.

### MINERAL CHEMISTRY

Olivine and orthopyroxene are too altered to analyse. The clinopyroxenes are calcic diopsides. They have moderate to high  $\text{Cr}_2\text{O}_3$  (0.57% to 4.9%) and low  $\text{Al}_2\text{O}_3$  (1.3% to 2.8%) and  $\text{Na}_2\text{O}$  (0.87% to 2.11%). Garnets are represented by both calcium saturated (lherzolitic) and low-calcium (harzburgitic) varieties.  $\text{TiO}_2$  concentrations are all low (generally < 0.2%). Using the garnet chemistry as a guide, the six diamond-bearing xenoliths are represented by three lherzolites and three harzburgites (figure 1). One of the two graphite/diamond peridotites is a harzburgite while the other is a lherzolite. Of the four graphite peridotites one is a lherzolite while the rest (3) are harzburgites. Primary spinel was found in thirteen

xenoliths. They are chromites ( $Cr/Cr+Al >.75$ ) with low  $TiO_2$  (<1%).

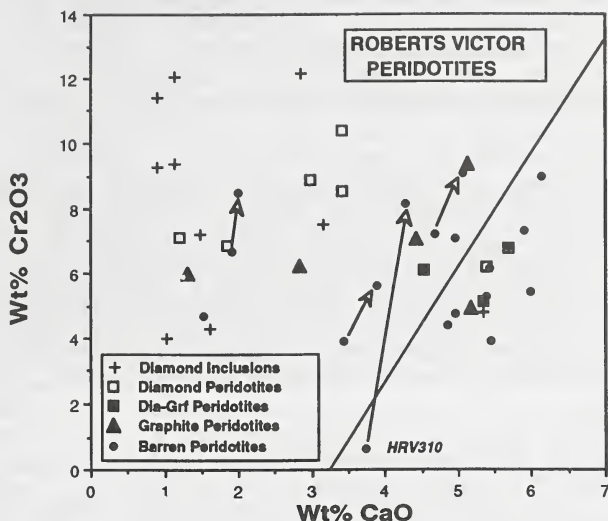


Fig. 1.  $CaO-Cr_2O_3$  trends in garnets from peridotites (this study; Hatton 1978) and diamond inclusions (Gurney et al, 1984). Arrows indicate the range found in garnet compositions for each xenolith. Sample HRV310 is a peridotite with a websterite vein (Hatton, 1978).

#### GEO-THERMOBAROMETRY

The altered nature of the xenoliths makes it impossible to apply any geobarometer, or to obtain any temperature estimate for clinopyroxene-free xenoliths. Temperature estimates for clinopyroxene-bearing lherzolites can be obtained from the garnet-clinopyroxene thermometer. Calculation at 50kbar shows that the diamond peridotites (2 samples) equilibrated at approximately 1000 °C. Barren lherzolites define a temperature range from 1050 °C to 1200 °C. This equilibration temperature for the two diamondiferous lherzolites is similar to the range found in most diamondiferous eclogites (1000 to 1100 °C) from Roberts Victor (Gurney et al, 1984), suggesting that eclogitic diamonds and lherzolitic diamonds at this locality might have formed in the same region of the mantle.

#### DIAMONDS

The numbers of diamond crystals recovered from individual xenoliths range up to 19. Two xenoliths produced substantially greater numbers of diamond which, however, are bounded largely by breakage surfaces and must represent pieces of one or a small number of crystals. Diamond crystal sizes range from 0.3 to 0.5mm in four of the xenoliths, between 1 and 1.5mm in one case and from 2.5 to 3mm in another. The pieces mentioned in two other xenoliths range up to 2mm in diameter. Octahedral crystals

predominate. These range from sharp-edged individuals with no or few trigonal etch pits to examples with partly bevelled edges and relatively numerous and large trigonal pits. In most cases, the bevelling at octahedral edges is by surfaces that are approximately dodecahedral, rather than tetrahedra for most diamonds in the mine production. Graphite commonly veneers the bevelled portions as well as octahedral areas where flat-bottomed, trigonal pits have coalesced to leave residual, serrate laminae. Breakage surfaces to the fragmental grains in two of the xenoliths are either frosted or exhibit trigonal etch pits. These features indicate that the breakage is due to natural causes. The relatively small diamonds in four of the xenoliths are virtually colourless. In another case, brown diamonds occur together with yellow diamonds in the same xenolith. In two other xenoliths the diamonds are grey to black on account of microscopic inclusions, presumably graphite.

The abundances and masses of diamonds in the xenoliths are thousands of times those in the host kimberlite. Therefore, it is possible for at least most of the diamonds in the kimberlite to be accounted for by the disaggregation of xenoliths such as those described. The predominantly octahedral morphology amongst the xenolith diamonds, versus tetrahedra morphology for the kimberlite diamonds, can be explained by the much more limited exposure of the xenolith diamonds to oxidising, kimberlitic magmatic fluids. The occurrence of brown with yellow diamonds in a single xenolith suggests that at least one of the diamond colours is secondary in origin.

#### REFERENCES

- Gurney, J.J., Harris, J.W. and Rickard, R.S. (1984). Minerals associated with diamonds from the Roberts Victor mine. In Kornprobst, J., ed., *Kimberlites. II: The Mantle and Crust-Mantle relationships*, pp. 25-33. Elsevier, Amsterdam.
- Hatton, C.J. (1978). The geochemistry and origin of xenoliths from the Roberts Victor mine. Unpubl. Ph.D. thesis, Univ. Cape Town.
- MacGregor, I.D. and Carter, J.L. (1970). The chemistry of clinopyroxenes and garnets of eclogite and peridotite xenoliths from the Roberts Victor mine, South Africa. *Phys. Earth Planet. Interiors*, 3, 391-397.

APPLICATION OF SIMPLE PARAMAGNETIC SUSCEPTIBILITY TO RAPID  
DISCRIMINATION OF ILMENITE COMPOSITIONS IN EXPLORATION FOR KIMBERLITE  
IN THE COLORADO - WYOMING PROVINCE, USA.

*Vos, W.P. and McCallum, M.E.*

*Dept. of Earth Resources, Colorado State University, Fort Collins, CO 80523 USA.*

Magnesium-rich ilmenite (picroilmenite) is one of the most characteristic minerals of kimberlite rocks, but its recognition in concentrates recovered during exploration programs may be complicated by the presence of significant quantities of non-kimberlitic ilmenite (e.g. ferroilmenite from gabbro-anorthosite, manganoilmenite from granitic rocks or carbonatite). The possibility of separation based on natural variations in the magnetic behavior of different types of ilmenites was tested on sample material from throughout the Colorado-Wyoming Kimberlite Province (Fig. 1). A rod type self-releasing electromagnet tapered to a point to create a "point source" magnetic field was utilized. Sample populations were separated electromagnetically in a series of runs in which amperage and resulting point source magnetic field strength (measured in oersted) were incrementally and progressively increased (Table 1). Each category (A-J) corresponds to a standardized range of approximately 150 oersted in magnetic field strength as measured at the tip of the rod.

Initial testing was conducted on three suites of samples exhibiting maximum variation in chemistry in an attempt to quantify characteristic simple paramagnetic susceptibility (SPMS) behavior patterns (Vos, 1989). A picroilmenite suite was obtained from megacrysts from Colorado-Wyoming kimberlite occurrences, ferroilmenite (both groundmass and ore varieties) was collected from the Laramie Anorthosite Complex and associated titaniferous magnetite-ferroilmenite ore bodies in Wyoming, and a manganian ilmenite suite from stream sediment concentrate from the Guaiamo region of Venezuela was used. The picroilmenite suite was eventually expanded to include 3,600 grains from 19 Colorado-Wyoming kimberlite occurrences. Four SPMS pattern groups evolved from this suite, and these relate to different kimberlite occurrences: Group 1 - Schaffer, Aultman and Ferris; Group 2 - Sloan, Moen, Nix and Chicken Park; Group 3 - Iron Mountain District; and Group 4 - Estes Dike and Green Mountain (Fig. 1).

Cumulative SPMS histogram patterns are presented as 100 total count normalized data, thereby effectively ratioing each of the categorical values (A-J) into relative percentages. Although significant overlap may exist in SPMS patterns, variable paramagnetic behavior generally reflects differences in bulk chemistry, valence states of major cations ( $\text{Fe}^{2+}$ ,  $\text{Fe}^{3+}$ ,  $\text{Ti}^{4+}$ ,  $\text{Al}^{3+}$ ,  $\text{Mn}^{2+}$ , and  $\text{Mg}^{2+}$ ), and structural position of those cations within the ilmenite structural-chemical lattice (Lindsley, 1976). Ferroilmenites are characterized by higher FeO and lower MgO and  $\text{Cr}_2\text{O}_3$  than kimberlitic picroilmenites and have distinct SPMS behavior patterns. Their magnetic field strengths generally are greater than 1,000 to 1,100 oersted (category D) whereas picroilmenites typically have much lower field strengths (Fig. 2). Manganoilmenites also generally are less magnetic than ferroilmenites, but tend to be more magnetic than picroilmenites.

Differences in SPMS behavior within the four recognized Colorado-Wyoming picroilmenite groups reflect variations in primary chemistry or subsequent alteration chemistry (Vos, 1989). Group 1 and 2 ilmenites generally contain higher amounts of MgO,  $\text{Cr}_2\text{O}_3$  and  $\text{Fe}_2\text{O}_3$  than Group 3 ilmenites, and Group 2 ilmenites show maximum enrichment in  $\text{Cr}_2\text{O}_3$ ,  $\text{TiO}_2$  and MgO which accounts for their generally low SPMS values. Group 3

ilmenites contain the highest total iron contents, which are reflected in their overall higher relative SPMS values. Group 1 ilmenites tend to have magnetic values similar to Group 2 ilmenites, which are lower than anticipated. A weaker magnetic susceptibility in these ilmenites probably is a function of pervasive severe alteration which produced nonmagnetic secondary products such as rutile, goethite and leucosene, and likely was accompanied by selective leaching of  $\text{Fe}^{2+}$  and/or oxidation of  $\text{Fe}^{2+}$  to  $\text{Fe}^{3+}$ . Some Group 2 ilmenites, especially from Chicken Park, exhibit a strong magnetic character due to the presence of abundant "exsolved" titanomagnetite lamellae. Group 4 ilmenites have SPMS values intermediate between Group 3 and Groups 1 and 2, and are characterized by high  $\text{TiO}_2$  and  $\text{MgO}$  and very low  $\text{Fe}_2\text{O}_3$ .

Picroilmenite Groups 1, 2 and 4 show relatively good magnetic discrimination from ferroilmenite (Group 5) and effective separation can be achieved at about 1,100, 1,400, and 1,200 oersted magnetic field strengths respectively (Fig. 3 a,b,d). Group 3 picroilmenite, with a broader range of SPMS values, can be less effectively separated from ferroilmenite, but a reasonable separation can be achieved at about 900 oersted magnetic field strengths (Fig. 3c). Separation would be considerably less effective if manganoilmenite were present (Fig. 2).

Based on these preliminary observations on Colorado-Wyoming kimberlite concentrate, it appears that the SPMS properties of ilmenites may be exploited in separating ferro- from picroilmenites in kimberlite exploration surveys, especially where concentrates are saturated with ferroilmenite. This technique could substantially reduce the amount of opaque oxide chemical analyses needed for effective detection of kimberlitic picroilmenite. However, care should be taken to carefully investigate the SPMS behavior of regionally indigenous ferro; mangan- and picroilmenites prior to determining the most effective applied magnetic-separation field strength.

## REFERENCES

- Lindsley, D.H. (1976) The crystal chemistry and structure of oxide minerals as exemplified by the Fe-Ti oxides. In D. Rumble III, Ed., *Oxide Minerals*, Mineralogical Society of America, Short Course Notes, v. 3, p. L1-L60.
- Vos, W.P. (1989) Kimberlite exploration, S. Laramie Range, Wyo. and magnetism, textures, and chemistry of Mg-ilmenite, 326p. M.S. thesis, Colorado State University, Fort Collins, Colorado.

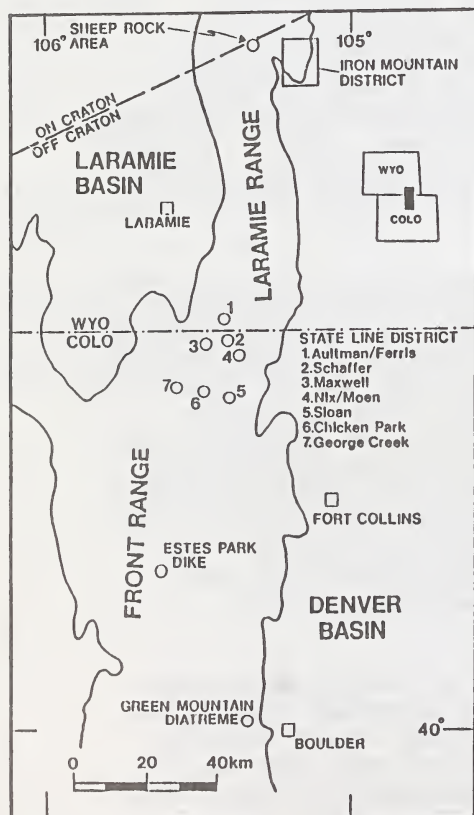


FIGURE 1. Location map of kimberlite occurrences in the Colorado-Wyoming Kimberlite Province. Front and Laramie Range area underlain by Precambrian crystalline rocks, Basin areas underlain by post-Devonian sedimentary rocks. On craton-off craton line marks boundary between Archean and Proterozoic crustal rocks.

TABLE 1. Magnetic field strength measured in oersted at probe tip of self-releasing electromagnet (current in amperes).

Current In amps	Field In Oersted	Current In amps	Field In Oersted	Average Current	SPMS <sup>a</sup> Category
0.139	330	0.127	320	0.133	A
0.202	617	0.201	645	0.202	B
0.369	825	0.369	765	0.369	C
0.478	1000	0.479	1019	0.475	D
0.559	1150	0.561	1227	0.560	E
0.674	1360	0.669	1373	0.672	F
0.765	1450	0.770	1440	0.768	G
0.878	1535	0.872	1560	0.875	H
0.937	1600	0.965	1625	0.951	I
10.937	1600	10.965	1625	n/a	J <sup>b</sup>

<sup>a</sup> Category J represented by grains left behind after run at strongest magnetic field strength (1610 average oersted, or for this study, essentially nonmagnetic)

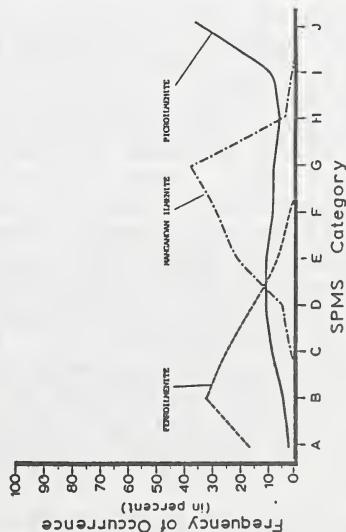


FIGURE 2. Total normalized SPMS histogram data representing the three major sample subpopulations of ilmenite. Solid line is ilmenite, dashed line is manganese ilmenite, and dot-dash line is magnetite. Note a mutual intersection at Category D (ca. 1,000-1,100 oersted).

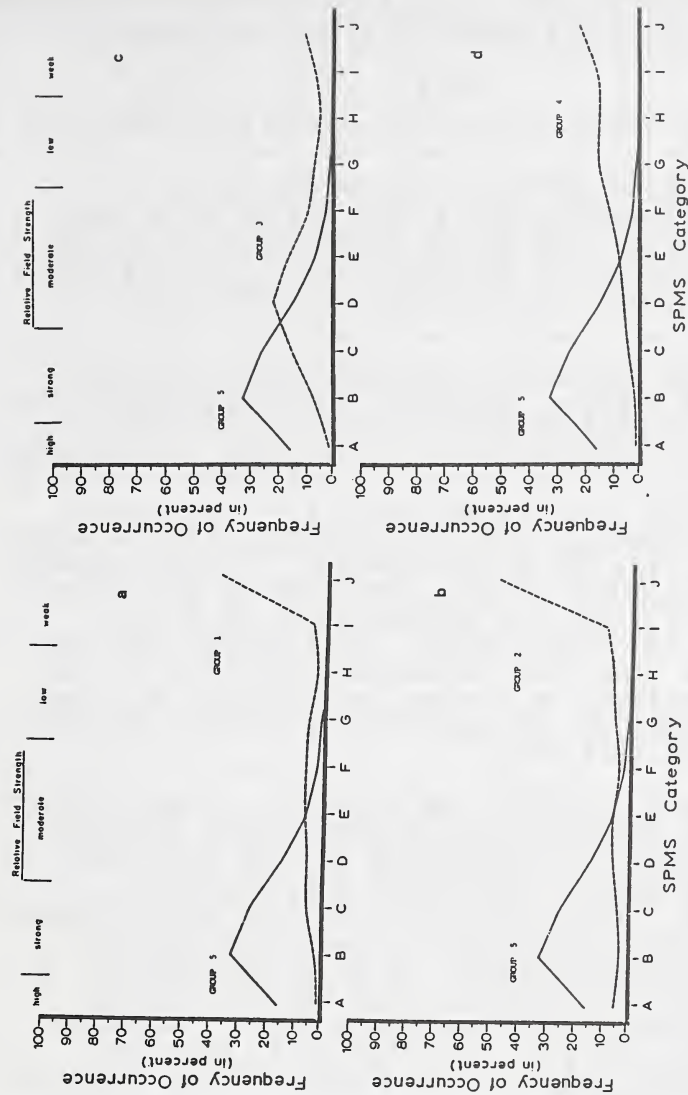


FIGURE 3. a. Normalized SPMS histogram comparing paramagnetic behavior patterns of Group 1 ferroilmenites (Aulaman, Ferris and Schaffer; dashed line) with Group 5 ferroilmenites (solid line). b. Normalized SPMS histogram comparing paramagnetic behavior patterns of Group 2 ferroilmenites (Sloan, Mix and Tucker; dashed line) with Group 5 ferroilmenites (solid line). c. Normalized SPMS histogram comparing paramagnetic behavior patterns of Group 3 ferroilmenites (Iron Mountain; dashed line) with Group 5 ferroilmenites (solid line). d. Normalized SPMS histogram comparing paramagnetic behavior patterns of Group 4 ferroilmenites (Estes Park and Green Mountain; dashed line) with Group 5 ferroilmenites (solid line).

## COMPARISON OF ELEMENT DISTRIBUTION IN RARE EARTH-RICH ROCKS FROM THE KANGANKUNDE AND KNOMBWA CARBONATITE COMPLEXES.

*Wall, F.**Department of Mineralogy, British Museum (Natural History), Cromwell Road, London, SW7 5BD, UK.*

Rare earth (REE) minerals are often important constituents of carbonatites where they may be of primary igneous origin, such as some of the fluocarbonates in the Sulfide Queen carbonatite at Mountain Pass, or be the result of late stage metasomatic, hydrothermal or supergene processes.

The Kangankunde carbonatite complex, Malawi and the Nkombwa carbonatite complex, northern Zambia are similar in that they consist of predominantly magnesium and iron-rich carbonatites, have no associated silicate rocks, have caused extensive fenitization to the surrounding basement rocks, and contain high concentrations of REE which are particularly concentrated in an unusual "epidote coloured" green monazite associated with Ba, Sr, REE mineralization. The petrography of the Kangankunde complex is well described by Garson and Campbell-Smith (1965) and the Nkombwa carbonatite is described by Reeve and Deans (1954). It is hoped that an electron microprobe study and subsequent comparison of the chemistry of the minerals in the two carbonatites will help to find common factors in the element distribution in REE-rich carbonatites of this kind.

Abundant monazite, baryte, and quartz are common to both carbonatites. Some degree of REE mineralization pervades most of the carbonatite at Kangankunde but the main REE mineral assemblages are: (1) monazite, quartz, baryte, florencite/goyazite, limonitic iron oxide, and minor apatite intergrown with the florencite and (2) ankerite and/or dolomite, monazite, strontianite, and minor bastnäsite. At Nkombwa the assemblage is different and much of the REE mineralization is concentrated in quartz rocks, including (1) monazite, quartz, baryte, iron oxides (2) monazite, daqingshanite, baryte, quartz, iron oxides and (3) monazite, isokite, quartz, dolomite.

A comparison of the monazite from the two carbonatites shows that it's chemistry is broadly similar in being Th-poor (less than 1 wt% ThO<sub>2</sub>) and in containing Sr but there are some compositional differences and texturally the monazites are quite different. Kangankunde monazite forms aggregates of euhedral crystals whereas the Nkombwa monazite occurs as chains of spherulites. Both monazites can show replacement textures: at Kangankunde monazite and strontianite can be pseudomorphous after an unknown hexagonal mineral and at Nkombwa the monazites sometimes appear to define relic rhombohedral cleavage directions in quartz suggesting replacement of carbonate. The Nkombwa monazite is more Sr-rich than that at Kangankunde (2 - 5 wt% SrO rather than 1 - 3 %) and, unlike the Kangankunde monazite, it usually contains small amounts of Ca and Ba. There is also a Ca-rich variant with 5 wt% CaO and low totals although analysis by x-ray diffraction and infrared spectroscopy has not confirmed the presence of a hydrated phase such as rhabdophane.

The baryte in both carbonatites is always Sr-poor, even though it must have formed in a strontium-rich environment

and is known to be able to accommodate several per cent strontium. The Sr must have partitioned preferentially into minerals such as strontianite, Sr-containing monazite, daqingshanite, isokite and goyazite.

Bastnäsite at Kangankunde always occurs as sheaves of needles, a habit that Mariano (1989) observes to be indicative of a hydrothermal origin, and does not selectively partition any of the light REE with respect to the monazite. The florencite/goyazite series minerals show more variation: the, often euhedral rhombic, crystals are highly concentrically zoned Sr versus REE and can contain inclusions of bastnäsite as well as intergrown REE-poor apatite. Chondrite normalized signatures are light REE-enriched but more variable than those of the monazite. Like the bastnäsite at Kangankunde, the daqingshanite has a light REE chondrite-normalized distribution which is very similar to that of associated monazite.

The most different distribution of REE in either complex is seen in occasional Kangankunde quartz-apatite-iron oxide rocks which are interpreted as of late hydrothermal origin. The apatite consists of turbid cores with overgrowths which are strongly zoned with mid-REE enriched patterns quite different from that of the main carbonatite.

Although the monazite mineralization in the two carbonatite complexes is similar, each has its own distinctive suite of associated minerals and range of monazite compositions. This latter comparison is useful because it is noted that within each carbonatite complex the monazite compositions from both carbonate and quartz rocks plot together indicating that the within each complex both the quartz and carbonate rocks have been subject to the same phases of mineralization. The mineralization in both carbonatites is believed to be of secondary, probably low temperature, hydrothermal origin. Under these conditions, monazite is Th-poor but can accommodate some Sr and possibly, at Nkombwa, Ca and Ba. Baryte appears not to be able to accommodate strontium and there is little differential partition of REE between monazite and coexisting REE minerals such as bastnäsite.

Tiny blebs of the sodium-containing mineral, burbankite which are found occasionally in carbonates in both carbonatites may be evidence of a primary crystallising REE mineral and apatites seen being altered by incipient REE mineralization in some dolomite carbonatites at Kangankunde may be a source of phosphate.

#### REFERENCES

- Garson, M.S. and Campbell-Smith W. (1965) Carbonatite and agglomeratic vents in the Western Shire Valley. Memoir No. 3, Malawi Government Geological Survey Department, 171 p. Government Printer, Zomba, Malawi.
- Mariano, A.N. (1989) Economic Geology of Rare Earth Elements. In B.R. Lipin and G.A. McKay, Ed., Geochemistry and Mineralogy of Rare Earth Elements. Mineralogical Society of America Reviews in Mineralogy, 21 p308-337.
- Reeve, W.H. and Deans, T.D. (1955) An occurrence of carbonatite in the Isoka District of Northern Rhodesia. Colonial Geology and Mineral Resources, 4, 271-281.

## MICRO-STRUCTURAL VARIATIONS IN MANTLE DERIVED GARNETS.

Alian <sup>(1)</sup>Wang; <sup>(2)</sup>P. Dhamelincourt; Lihe <sup>(1)</sup>Guo; Wuyi <sup>(1)</sup>Wang and Andi <sup>(1)</sup>Zhang.<sup>(1)</sup>Chinese Academy of Geological Sciences, 100037 Beijing, China; <sup>(2)</sup>Laboratoire de Spectrochimie Infrarouge et Raman, CNRS, 59655 Lille, France.

As the most deeply sourced rock, kimberlite carries a large number of mantle derived crystals, as well as diamonds with their mineral inclusions, up to the Earth's surface. It makes the possibility to obtain the information on the mantle environment from the compositional and structural characters of these crystals.

There were many comprehensive studies on the compositional characters of these mantle derived crystals [1,2]. But to date, very few studies on their structural features were reported. In this work, the capability of undestructive, "in situ", micro-zone analysis of Raman "structural microprobe" technique has been used to distinguish some micro-structural variations in the mantle derived garnets, as well as in the pyrope inclusions of diamonds.

The Raman spectra of over sixty pyrope grains had been obtained: 24 from the kimberlites of China; 8 from lamproites of China and Australia; 3 are the pyrope inclusions taken out by cracking their host diamonds; the others were selected from pierite-porphyrite, serpentine, alkaline basalt, lumburgite, ultrabasic beccia etc.. Figure 1 shows the typical Raman spectra of these pyropes. The spectrum of mantle derived pyrope demonstrates the degeneration of long-range ordering in its structure, which means that its translational symmetry in three dimensions was interrupted or distorted by some micro-structural defects and variations [3].

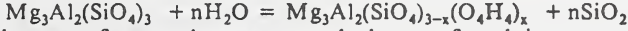
The first type of micro-structural variation is the polyhedral distortions due to the substitutions of cations at  $S_6$  and  $D_2$  sites [4]. These distortions are exhibited by the frequency shifts of three main Raman bands, and by the increase of site-group splitting [ $\bar{\nu}_B - (\bar{\nu}_C + \bar{\nu}_D) / 2$ ] as well as the decrease of factor-group splitting [ $\bar{\nu}_C - \bar{\nu}_D$ ] in the Infrared spectra of the mantle derived pyropes (Fig.2). This structural character has begun to be used to discriminate the diamondiferous rocks in Chinese exploration works.

The second type of micro-structural variation is the formation of amorphous structural elements through the irregular polymerization of  $(SiO_4)$  tetrahedra [5]. The Raman spectroscopic evidences for the appearance of these elements are the enlargement of bandwidths, the rise of spectral background, and the appearance of some distinguishable distortions in bandwings. In addition, the polymerization of  $(SiO_4)$  tetrahedra was demonstrated by the obvious changes in relative intensities of three main Raman bands, especially by the strong decrease of  $\sim 920\text{cm}^{-1}$  band which representing the symmetric stretching vibration of "isolated"  $SiO_4$  tetrahedra (Fig.1). The appearance of amorphous structural elements in mantle derived crystals suggests a possible mechanism of phase-transition under the special environment in the Earth's mantle, i.e. from a crystal phase to an amorphous phase [6]. It could be considered that at a very high pressure but relative low temperature conditions, such as in certain deep region of the upper mantle beneath an old craton, where some crystals can not get enough energy to overcome a potential threshold of transforming to another crystal phase, so had to take the amorphous status, which is more compressible, to adapt their high-pressure environment.

The third type of anomalous structural element found in some mantle derived pyropes is the structural hydrous component. It was distinguished by three Raman bands and two overlapped Infrared bands in  $3500-3800\text{cm}^{-1}$  region (Fig.3). These spectra also verify that the hydrous component enter pyrope structure by substituting  $(SiO_4)$  tetrahedron at  $S_4$  site in forms of  $(O_4H_4)^{4-}$  [7]. According to the model of Solomon [8], at "low asthenosphere

(160km—300/400km)<sup>u</sup>, some mantle water began to enter the structures of magnesium-silicates in forms of substituting the oxygen anion as (OH)<sup>-</sup> group when free-fluid phase of water with very high density still exist. At the depth > 300/400km, the free-fluid phase will disappear, almost all mantle water will be dissolved in the crystal structures of mantle minerals. Therefore the existence, and the quantity of the structural hydrous component found in a mantle derived crystal might offer the information of its forming depth.

The second and third anomalous elements were found coexisting in the structure of a pyrope inclusion (100x250 μm) which was taken out from a diamond grain (3x2.1mm). This experimental result approve the possible genetic correlation of these two micro-structural variances in the special environment of the upper mantle where diamond forms:



The fourth type of anomalous structural element found in some mantle derived pyropes is the elements of Majorite phase [9]. It was distinguished by an extra band near ~ 930cm<sup>-1</sup> in the Raman spectra, and an extra set of diffraction points in the electron diffraction patterns of these pyropes (Fig.4). As we know, the solid-solution of Majorite and pyrope is one of the major phases in the bottom of the upper mantle and in the transition zone. So the existence, and the quantity of Majorite phase element in a pyrope grain will mark the T-V conditions and the depth where the pyrope was formed.

In conclusion, some micro-structural variations in the mantle derived garnets have been distinguished mainly by micro-Raman spectroscopic investigation. To study further the inducing conditions of these variations, will be helpful to advance our understanding of the mantle environment and the related geological processes.

## REFERENCES

- (1) Gurney JJ (1985) In: Kimberlite occurrence and origin, ed by Glover JE, Harris PG. Uni. W. Australia Pub. No.8.
- (2) Meyer HOA (1987) In: Mantle xenoliths, ed by Nixon PH. John Wiley sons Ltd.
- (3) Brawer S (1975) Phys. Rev. B11:3173-3194.
- (4) Novak GA et al (1971) Am. Mineral. 56:791-825.
- (5) McMillan P (1984) Am. Mineral. 69:622-644.
- (6) Hemley RJ et al (1988) Nature 334:52-54.
- (7) Lager GA et al (1989) Am. Mineral. 74:840-851.
- (8) Solomon SC (1972) J. Geophys. Res. 77:1483-1502.
- (9) McMillan P et al (1989) Phys. Chem. Minerals 16:428-435.

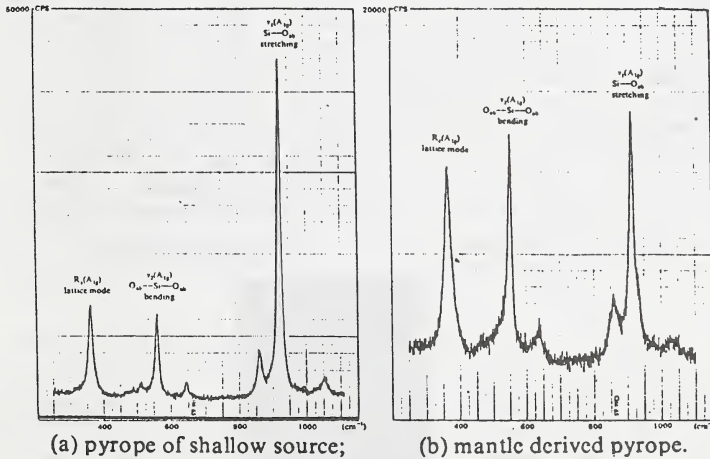
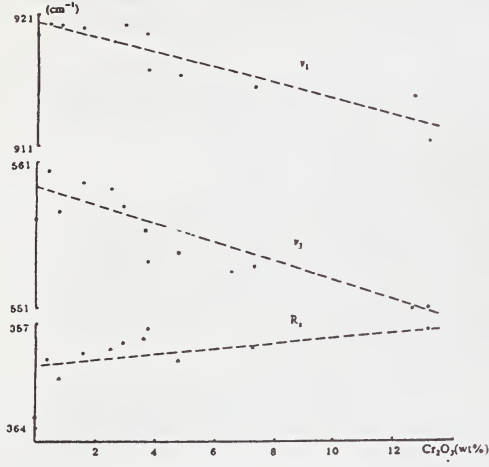
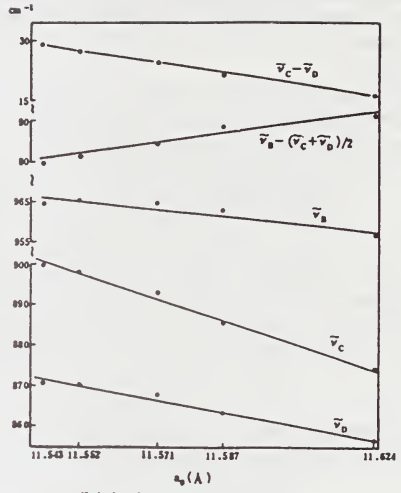


Figure 1 Typical Raman spectra of megacryst pyropes:

Figure 2 The characters of frequency shifts:

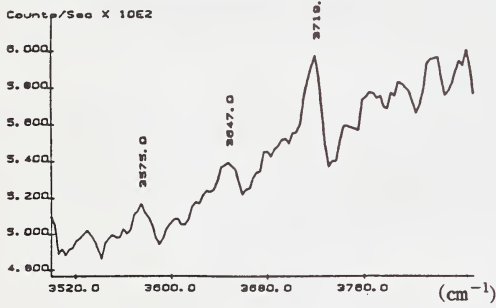


(a) in Raman spectra;



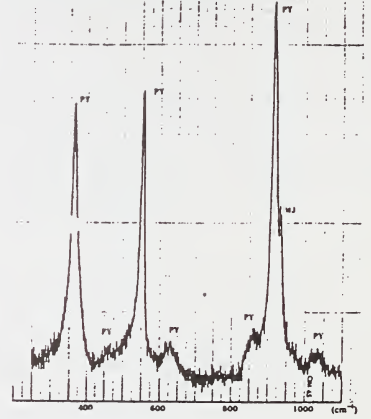
(b) in Infrared spectra.

Figure 3 Stretching vibration bands of  $(O_4H_4)^{4+}$  in mantle derived pyrope:

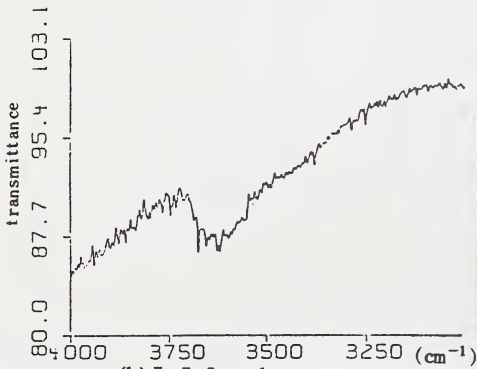


(a) In Raman spectrum;

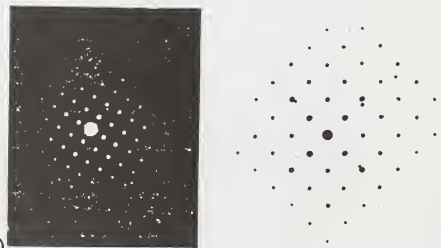
Figure 4 Experimental evidences for the existing of Majorite structural elements in mantle derived pyropes:



(a) Raman spectrum;



(b) In Infrared spectrum.



(b) Electron diffraction pattern.

## THE COMPOSITION OF THE PRIMITIVE UPPER EARTH'S MANTLE.

Wedepohl, K.H.

*Geochemical Institute, University Goettingen, W-3400, Goettingen, Germany.*

The primitive mantle contains the silicate portion of the Earth after core and before crust formation. The upper convecting mantle is probably separated from the lower mantle convection by a density barrier observable in a seismic discontinuity at about 670 km depth. Ringwood and Irifune (1988) assume that the transformation of the  $Mg_2SiO_4$  spinel into a perovskite structure of  $MgSiO_3$  (plus MgO) in harzburgite-like rocks is responsible for this discontinuity. The upper mantle has a mass of  $1.07 \times 10^{21}t$  (about 25 % of the bulk mantle) and the crust represents a mass of  $0.03 \times 10^{21} t$ .

Several approaches have been used by different authors to constrain the composition of the primitive mantle. They were mainly based on comparison with primitive chondritic matter (for refractory elements), extrapolations from depleted to fertile peridotite and komatiite compositions, element correlations in primitive and fractionated rock species such as oceanic basalts, global heat flow balances and radioactive/ radiogenic isotope transport between major units of the Earth. The largest sets of primitive mantle values were published by Jagoutz et al. (1979) and by Hofmann (1988). We will use these data as reference for our evaluation (Column E of Table 1).

Our two approaches to get additional information on primitive mantle concentrations of about 40 elements are related to a detailed investigation of the two spinel lherzolite containing tectonites of Balmuccia and Baldissero in the Ivrea-Verbanò Complex of northern Italy. These rocks are very fresh and probably represent typical materials of the moderately depleted sub-lithospheric mantle which convects and produces MORB-type melts. We have analyzed 32 large samples by various instrumental methods (RFA, ICP, AAS, INA etc.) (Hartmann and Wedepohl, 1991). Both peridotite masses contain mainly lherzolite with an average modal composition of 56 % olivine, 28 % orthopyroxen, 14 % clinopyroxene and 1.5 % spinel. They have lost on average 6 % MORB by earlier partial melting. The heterogeneity inside the two masses can be characterized by the variation of  $Al_2O_3$  from 2.0 to 5.0 %.

In our first approach we have used the correlations of the elements Li, Na, Sc, Ti, V, Ga, Sr, Y, Zr, Nb, REE, Hf, Ta to the  $Al_2O_3$ -content of the samples which partly reflects the crystal chemical behavior of these elements in the clinopyroxene structure. The lines of regression in these correlations can be used to define the element concentrations at 4.0 %  $Al_2O_3$  which is the Al concentration of the primitive mantle reported by Hofmann (1988) and other authors. These interpolated primitive mantle values are listed in Column C of Table 1 beside concentrations of 94 % of the Balmuccia average plus 6 % MORB (the latter values are from Hofmann, 1988 and Wedepohl, 1981).

For our second model we have calculated primitive mantle compositions from the sum of 97.2 % Balmuccia mantle plus 2.8 % bulk crust concentrations of the various elements. The bulk crust consists of about 75 % continental and 25 % oceanic crust. The composition of the continental crust has recently been estimated by the present author on the

basis of large data sets of upper crustal rocks as well as granulites and petrologic information on crustal layering. It is less mafic and has higher concentrations of highly incompatible elements (including heat producing isotopes) than the estimate by Taylor and McLennan (1985). The difference between the two crustal estimates which are listed in Column D of Table 1, has only influence on "primitive mantle" values of the highly incompatible elements K, Rb, Ba, Pb, U and LREE.

The balance based on our data indicates that the crust consists of almost half of all partial melting products of the convecting upper mantle. The continental part of the crust has on average a tonalitic composition and the oceanic part represents MORB. The other more refractory half of the partial melting products was either retained in the mantle or returned into it during Earth's history. The composition of the moderately depleted upper mantle (including the highly depleted lithospheric part) is in balance with the composition of the crust with the exception of the elements U (Th,Cs), Rb, Pb, K (and Tl). The primitive mantle has contained these elements in unidentified K-rich minerals which have not survived. A part of the crustal content of these elements was probably supplied from the lower mantle. Both of our models confirm that the average spinel lherzolite from Balmuccia is a perfect representative of the typical upper mantle composition. They also confirm that the upper mantle has its separate convecting system which does not allow major material exchange with the lower mantle. About 30 of our new "primitive mantle" values are close to those published by Jagoutz et al. (1979), Hart and Zindler (1986) and Hofmann (1988) on the basis of different methods. Discrepancies to be mentioned occur in case of (F,Na,P, S), Ti, Cr, Fe and Cu. Our differences in Na might be caused by the selection of the Balmuccia peridotite as model material. This point requires additional research. We claim that at least our "primitive mantle" values on F, P, S, Cr, Fe and Cu are superior to those in the reported literature.

- Hart, S.R. and Zindler, A. (1986) In search of a bulk-earth composition. *Chem. Geol.*, 57, 247-267.
- Hartmann, G. and Wedepohl, K.H. (1991) The composition of peridotite tectonites from the Ivrea-Verbano Complex (N-Italy) representing various stages of mantle depletion. (in preparation)
- Hofmann, A.W. (1988) Chemical differentiation of the Earth: the relationship between mantle, continental crust and oceanic crust. *Chem. Geol.*, 90, 297-314.
- Jagoutz, E., Palme, H., Baddenhausen, H., Blum, K., Cendales, M., Dreibus, G., Spettel, B., Lorenz, V. and Wänke, H. (1979) The abundances of major, minor, and trace elements in the earth's mantle as derived from primitive ultramafic nodules. *Lunar Planetary Science X*, 610-612.
- Ringwood, A.E. and Irifune, T. (1988) Nature of the 650 km discontinuity: implications for mantle dynamics. *Nature*, 331, 131-136.
- Taylor, S.R. and McLennan, S.M. (1985) The continental crust: its composition and evolution. 312 p. Blackwell Scientific Publications.
- Wedepohl, K.H. (1981) Tholeiitic basalts from spreading ocean ridges. The growth of the oceanic crust. *Naturwissenschaften* 68, 110-119.
- Wedepohl, K.H. (1991) Chemical composition and fractionation of the continental crust. *Geolog. Rundschau*, 80 (in press).

Table 1

Balances for calculation of primitive mantle concentrations based on moderately depleted mantle rocks from Ivrea (N. Italy)

	A Spinel lherzo- lite Balmuccia $\bar{x}_{18} \pm s$	B Spinel lherzo- lite Baldissero $\bar{x}_{14} \pm s$	C Primitive mantle values from element- Al relations/from 94 % Balmuccia + 6 % MORB	D Primitive mantle values from 97.2 % Balmuccia + 2.8 % bulk crust (Wedepohl, 1991/ Taylor, McLennan, 1985)	E Primitive mantle values Jagoutz et al. (1979) Hart and Zindler (1986) Hofmann (1988)
Li	2.4 ± 0.4	2.0	2.6 / 2.8	2.7 / 2.7	2.4 J
F	6 ± 2	5 ± 2	/ 15	19 /	13.5 J
Na	1187 ± 336	1329 ± 114	1610 / 2190	1770 / 1760	2460 H 2730 J
Mg	234600 ± 10300	239400 ± 4820	/ 223680	229060 / 229235	228000 H 225000 J
Al	16880 ± 4230	16300 ± 1320	/ 20840	18670 / 18750	21500 H 21700 J
Si	209400 ± 930	208500 ± 1400	/ 209600	210000 / 209680	214800 H 214000 J
P	39 ± 10	26 ± 12	/ 67	58 /	83 H & Z
S	232 ± 114	144 ± 27	/ 272	251 /	
K	23 ± 5	26 ± 4	/ 124	450 / 223	258 H 260 J
Ca	22300 ± 6070	19440 ± 1860	26800 / 25800	23110 / 23380	22940 H 26600 J
Sc	15.9 ± 3.1	14.4 ± 0.9	18.0 / 17.4	16.1 / 16.4	14.9 H 16 J
Ti	623 ± 273	498 ± 53	860 / 1006	743 / 768	1085 H 1300 J
V	83 ± 20	72 ± 5	100 / 93	85 / 87	83 J
Cr	2568 ± 176	2628 ± 38	/ 2440	2500 / 2500	3465 J
Mn	1053 ± 39	1046 ± 40	/ 1062	1048 / 1061	1000 J
Fe	64500 ± 4120	63400 ± 3650	/ 64850	64150 / 64670	58600 H 58700 J
Co	106 ± 3	100 ± 30	/ 102	104 / 104	100 J
Ni	2040 ± 117	2071 ± 72	/ 1930	1990 / 1990	2080 H 1950 J
Cu	35 ± 17	27 ± 5	/ 37	35 / 36	6.4 J
Zn	51 ± 3	50 ± 2	/ 53	51 / 52	59 J
Ga	3 ± 0.8	2.6 ± 0.4	3.7 / 3.8	3.4 / 3.4	3.9 J
Rb	(0.05)	(0.05)	/ 0.34	1.5 / 0.73	0.54 H 0.73 J
Sr	7.5 ± 3	6.1 ± 1	10.2 / 15.0	15.3 / 13.7	18.2 H 19.6 H & Z 25 J
Y	2.9 ± 1.1	2.7 ± 0.3	4.2 / 4.9	3.6 / 3.5	3.9 H 4.6 J
Zr	4.8 ± 1.6	3.9 ± 0.8	6.0 / 10.8	10.0 / 7.5	9.7 H 11 J
Nb	(0.5)		0.6 / 0.68	(0.88)/(0.74)	0.62 H 0.9 J
Ba	1.1 ± 0.7	≤ 0.5	/ 3.9	17.9 / 6.7	6.0 H 6.9 J
La	0.12 ± 0.13	0.04 ± 0.02	0.20 / 0.35	0.76 / 0.48	0.61 H 0.70 J
Ce	0.40 ± 0.45	0.17 ± 0.10	0.80 / 1.1	1.4 / 1.2	1.6 H
Nd	0.45 ± 0.49	0.22 ± 0.07	0.75 / 1.1	1.1 / 0.85	1.19 H 1.17 H & Z
Sm	0.19 ± 0.16	0.13 ± 0.02	0.44 / 0.40	0.32 / 0.28	0.39 H 0.42 J
Eu	0.092 ± 0.065	0.064 ± 0.008	0.14 / 0.16	0.13 / 0.09	0.14 H 0.17 J
Gd	0.33 ± 0.21	0.26 ± 0.03	0.50 / 0.61	0.44 / 0.32	0.51 H
Tb	0.08 ± 0.04	0.06 ± 0.01	0.10 / 0.13	0.093 / 0.078	0.094 H
Dy	0.45 ± 0.22	0.39 ± 0.04	0.57 / 0.80	0.56 / 0.56	0.64 H
Yb	0.31 ± 0.12	0.30 ± 0.02	0.43 / 0.53	0.37 / 0.37	0.41 H 0.46 J
Lu	0.052 ± 0.021	0.051 ± 0.003	0.066 / 0.08	0.063 / 0.061	0.064 H 0.069 J
Hf	0.13 ± 0.04	0.10	0.20 / 0.30	0.26 / 0.21	0.27 H 0.34 J
Ta	0.03 ± 0.01	0.04 ± 0.01	0.035 / 0.041	0.050 / 0.051	0.035 H 0.03 J
Pb	(0.035)	(0.016)	/ (0.08)	(0.28) / 0.20	0.18 H
U	(0.004)	(0.002)	/ (0.008)	(0.036) / 0.023	0.020 H 0.026 J

THE CHARACTERISTICS AND ORIGINS OF ULTRABASIC VOLCANIC ROCKS AND THEIR XENOLITHS FROM LIXIAN AREA, GANSU PROVINCE, P.R. OF CHINA.

Ye, <sup>(1)</sup>Weikun and Lu, <sup>(2)</sup>Fengxiang.

(1) *Fujian Institute of Geosciences, Fuzhou 350011, P.R. of China;* (2) *China University of Geosciences, Wuhan 430074, P.R. of China.*

Many of small Cenozoic ultrabasic volcanic rocks and their ultramafic xenoliths from Lixian area, Gansu Province, China, are found. These volcanic rocks are belong to foidite group with lower SiO<sub>2</sub> (38-41, wt% ) and Al<sub>2</sub>O<sub>3</sub> (7-8), higher MgO (11-18), CaO (12-16), Na<sub>2</sub>O+K<sub>2</sub>O (3-8), and TiO<sub>2</sub> (3-4). They are divided into 1) olivine nephelinite: olivine + clinopyroxene + nepheline; 2) sub-mafurite: olivine + clinopyroxene + kalsite, and contains phlogopite, Ti-K-richierite and melilite. Their transitional element distribution patterns all are strongly depletion in Cr and Ni, enrichment in Ti. Their REE distribution patterns are high total REE contents (340-570 ppm ), enrichment in LREE and depletion in HREE ( $La_n/Yb_n=34-56$ ).

Most of the ultramafic xenoliths in the volcanic rocks are spinel lherzolites belong to peridotite series, a few of them are harzburgite, dunite and pyroxenite. Moreover a rare kind of calcite pyroxenite was found. These spinel lherzolites are richer in Al<sub>2</sub>O<sub>3</sub> (2.6-3.3, wt% ), CaO (3.0-4.6), and Na<sub>2</sub>O+K<sub>2</sub>O (0.4-0.9), lower in SiO<sub>2</sub> (43-45) and MgO (38.3-38.5) on the chemistry with slightly depletion feature. There are fine corresponding relationship between xenoliths and the host rocks on major elements. Petrogenesisly they are considered to be related to the host magma and to be residual materials after the upper mantle underwent partial melting by 3-4%. By estimated, this kind of ultramafic xenoliths formed at 23-26 kbar pressure and 1060-1100 °C temperature, and from 76-86 km depth.

Compared with the same kind of rocks from other areas in the world and estimated, it is suggested that the kind of magma in this area was originated under the conditions: 1260-1300 °C temperature, 26-28 kbar pressure and 85-90 km depth. These host rocks widely contain calcites and some calcite pyroxenite xenoliths are found, these are also suggested that the host magma originated under the enviroment of richer CO<sub>2</sub> or CO<sub>2</sub> makes main rule among volatile components, and begin to cryst.

On the aspects of geology, petrology, chemistry and origied conditions from these volcanic rocks, there are obvious regular transitional relationships correspond to their geographic distributions, and the extreme direction distinct features of compositions; moreover the distributions of these rocks bodies are controlled obviously by both NNE blind fractures and NWW fractures. These characters reflect the possible machanism of the ultrabasic magma in this area is that the subduction of Shongpan-Ganzhi ocean crust forward northern direction in Mesozoicera lead to cau cause the enviroment of richer  $H_2O$  and  $CO_2$ , deeper depth from south to north, then activity of Cenozoic NNE within-plate tension deep fractures cause to happen small degree partial melting of wedge-shaped upper mantle, thus formed the magma in this area.

Furthermore, the paper has studied the clinopyroxene complex zones in the host rocks.

Keywords: Gansu China, Cenozoiea, ultrabasic volcanic rock, foidite, nephelinite, sub-mafurite, xenolith, petrogenesis, Ti-K-richerite, clinopyroxene zone.

## EVIDENCE FOR A DEEP ORIGIN FOR SÃO LUIZ DIAMONDS.

*Wilding<sup>(1)</sup>, M.C.; Harte<sup>(1)</sup>, B. and Harris<sup>(2)</sup>, J.W.**(1) Dept. of Geology and Geophysics, University of Edinburgh. Edinburgh EH9 3JW, Scotland, U.K.; (2) Dept. of Geology and Applied Geology, University of Glasgow, Glasgow, G12 8QQ, Scotland, U.K.***Introduction**

The diamonds recovered from the Sao Luiz river in northern Mato Grosso state, in Brazil, are believed to be derived from nearby kimberlites related to the Cretaceous Aripuena Kimberlite province. These kimberlites are intruded into the Rio Negro-Juruena belt, a possible island arc terrane, which yields Proterozoic metamorphic ages and lies between partly remobilised Archaean belts of the Guyana-Guapore craton. The particular importance of the Sao Luiz diamonds lies in the unusual characteristics of the diamonds themselves, and, as outlined in this study, their syngenetic inclusion content, which extensively shows mineralogical and geochemical features indicative of deep (sub-lithospheric) origins. The majority of inclusions fall into two groups, one containing garnet-rich inclusions and the other consisting largely of oxide, colourless silicate and rare carbide inclusions.

**The Garnet-rich Inclusions Suite.**

Petrographically most of these inclusions have the appearance of orange to pale orange garnets of eclogitic inclusion paragenesis. Back scattered electron (BSE) images and electron microprobe analysis shows that in detail, whilst some inclusions consist of garnet alone, most inclusions contain a minor phase of clinopyroxene chemical composition in addition to a garnet-like phase. Rarely, other uncertain phases and possible alteration products are also present.

Two groups of these apparently garnetiferous inclusions have been established on the basis of their silicon content. The first group is indistinguishable in major-minor element chemistry from typical garnets of eclogite paragenesis and shows normal silicon contents. In the second group the silicon values are higher than the three cations (per 12 oxygens) expected in a normal garnet structure and range up to 3.3. The aluminium concentrations in the high-silicon garnets are lower than those of normal garnets presumably partly because the excess silicon atoms occupy octahedral sites in the garnet structure. However, the decrease in Al is greater than that equivalent to the increase in Si, and there is no further compensation by increase in typical octahedral site cations such as Ti and Cr (Fig. 1a). However, the high-silicon garnets commonly show divalent cations + Na in excess of the 3 (per 12 oxygens) needed to fill the cubic site (Fig. 1b). Thus some divalent cation substitution in the octahedral site is suggested, which would also help to maintain charge balance as a result of the Si for Al substitution. Na contents up to 0.08 cations in the high-silicon garnets also adjust charge balance.

The cation substitutions shown by the high-silicon garnets suggest high-pressure pyroxene solid solution in the garnet structure (Moore & Gurney, 1985; Irifune et al., 1989). Overall the Sao Luis garnets suggest depths of formation from around 180 km, near the expected base of the lithosphere, to around 400 km. Temperature estimates for coexisting garnet-clinopyroxene pairs with normal-silicon garnet range from 1281 to 1665°. For the high-silicon garnet parageneses, temperature estimates are even higher and are considered unreliable because of the unusual garnet-chemistry and, in some cases, a lack of equilibrium as shown by variable mineral chemical compositions.

Textural relationships between garnet and clinopyroxene vary considerably, though the clinopyroxene is usually concentrated at the margins of the inclusions. In association with the normal-silicon garnets, clinopyroxene is usually in a small number of grains with clear indications of faceted boundaries. The clinopyroxene associated with high-silicon garnets has more irregular, often curving, boundaries and may occur as numerous scattered small 'blebs' as well as larger and more discrete clinopyroxene grains. In one instance the clinopyroxene has the form of possible exsolution lamellae within the garnet. However, the chemical compositions show that the clinopyroxenes commonly seen, could not be produced along with normal-silicon garnets as a result of decomposition of the high-silicon garnets. The textures and the occasional variability of mineral compositions in the case of the high-silicon garnets, suggest a frozen reaction history, perhaps involving melt.

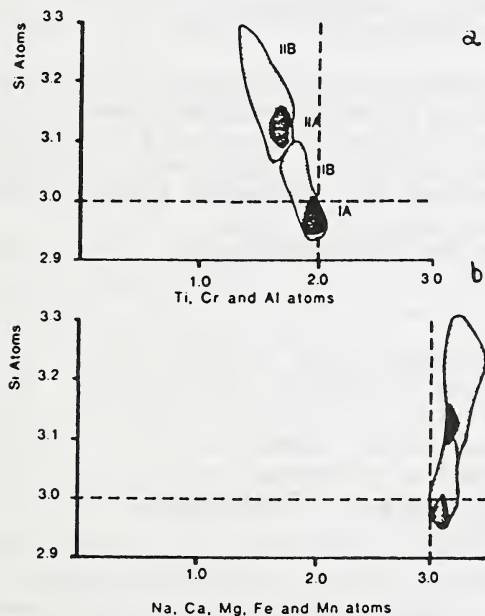


Fig. 1 Plots of normal Octahedral site cations and Cubic site cations against Si Content. Increasing Si is associated with decreasing Al+Ti+Cr and increasing Na+Ca+Mg+Fe+Mn, as one goes through the sequence from normal-silicon garnet without clinopyroxene (IA), to normal silicon garnet with clinopyroxene (IB), to high-silicon garnet without clinopyroxene (IA), to high-silicon garnet with clinopyroxene (IIB).

Ion microprobe analyses of the garnets also show evidence of complex relationships, particularly for the more incompatible elements. Each garnet analysed shows moderately constant relative abundance of Y and the HREE (Sm to Lu). Between garnets these HREE concentrations vary largely from 8x to 60x chondrite, with a tendency for the high-silicon garnets to be in the lower part of this range. The LREE are progressively depleted with decreasing mass relative to HREE, but variations in concentrations are very large and such variations are seen in garnets of normal and high-silicon content. La varies from 5x

to  $<0.01x$  chondrite. A similar range of variations is seen in Nb, and concentrations up to  $15x$  chondrite show that garnet may carry substantial Nb. Melts in equilibrium with the inclusions could vary from OIB-like to MORB-like. The commoner trace element compositions are similar to those of normal eclogitic inclusions in diamonds and thus do not preclude an original sublithosphere origin for these normal eclogitic inclusions.

**The oxide, colourless silicate and carbide inclusions suite.**

The non-garnetiferous inclusions from Sao Luiz diamonds are varied, but many show distinctive features indicating a very high pressure origin. The oxides are MgO-FeO (periclase-wustite) solid solutions, which show a range of Fe/Fe+Mg values from 0.16 to iron-rich values of 0.61. In addition to Fe and Mg there are variable small amounts (usually  $<1$  wt%) of Cr, Al and Ni in the oxide phases. Some of the Ni may be present as metal rather than oxide and there are also small inclusions ( $<2\mu\text{m}$ ) of iron-nickel alloy, with a composition Fe:Ni = 70:30, in many of the oxides.

The colourless group of inclusions includes silicates with the compositions of wollastonite, silica ( $\text{SiO}_2$ ), and diopside, all of exceptional purity. The remaining two silicates are an unidentified alumino-silicate phase close to  $\text{Ca}_2\text{Al}_2\text{SiO}_7$  and an olivine (Fo=85). In one case  $\text{SiO}_2$  co-exists with a ferripericlase of Fe/Fe+Mg 0.30. In addition to the silicates, two colourless to pale blue crystals of SiC composition (moissanite) have been recovered from 2 diamonds.

Experimental evidence shows that below 650 km in the mantle, olivine and pyroxene should be represented by ferripericlase and perovskite-structured pyroxene (including a possible phase of wollastonite composition and perovskite structure).  $\text{SiO}_2$  may occur as stishovite. The Sao Luiz inclusions may represent this sub-650km mineralogy. The position of moissanite in this mineralogy is uncertain, but it implies reduced conditions.

**References.**

- Moore, R. O. & Gurney, J. J. (1985) "Pyroxene solid solution in garnets included in diamond." *Nature*, 318, 553-555
- Irifune, T., Hibberson, W. O. & Ringwood, A. E. (1986) "Eclogite-garnet transformations in basaltic and pyrolite compositions at high pressure and temperature." *Geological Society of Australia Abstracts*, 16, 259-263.

## INCLUSION CHEMISTRY, CARBON ISOTOPES AND NITROGEN DISTRIBUTION IN BULTFONTEIN DIAMONDS.

*Wilding<sup>(1)</sup>, M.C.; Harte<sup>(1)</sup>, B. and Harris<sup>(2)</sup>, J.W.*

*(1) Dept. of Geology and Geophysics, University of Edinburgh. Edinburgh EH9 3JW, Scotland, U.K.; (2) Dept. of Geology and Applied Geology, University of Glasgow, G12 8QQ, Scotland, U.K.*

Inclusion-bearing diamonds from the Bultfontein Kimberlite, Kimberley, South Africa have been examined for their inclusion chemistry, nitrogen characteristics and carbon isotope composition (Wilding, 1990). The results have been compared with existing data from other Southern African kimberlites.

Nearly all of the inclusions from the Bultfontein diamonds are of peridotite paragenesis and have an inclusion chemistry similar to other peridotite diamonds. The Bultfontein diamonds have a high abundance of chromite inclusions, a feature shared with other mines in the De Beers Pool (De Beers, Dutoitspan and Wesselton). There is a change in the chemistry of chromite inclusions across the Bultfontein diamonds, chromites located at the centre of the diamond are more magnesian and chrome-rich than the peripheral chromites which are relatively iron-rich. Pressure and temperature estimates for the Bultfontein diamonds suggest a range of pressures of origin of 41 to 55Kbar and temperatures of formation of 930 to 955° C.

Infrared studies of the Bultfontein diamonds show a range of nitrogen contents from 0 to 1457ppm. Most of this nitrogen occurs as a combination of the Type IaA (two adjacent nitrogens) and Type IaB (four nitrogens) aggregates, with Type IaA dominant.

The carbon isotope composition of the Bultfontein diamonds have a mean  $\delta^{13}\text{C}$  value of  $-4.66\text{‰}$ , a value which is slightly heavier than the mean values for Premier ( $-4.84\text{‰}$ ), Roberts Victor ( $-6.40\text{‰}$ ) and Finsch ( $-5.98\text{‰}$ ). The  $\delta^{13}\text{C}$  value for the chromite-bearing diamonds is  $-3.76\text{‰}$ , and the high abundance of chromites at this mine might account for the slight differences in  $\delta^{13}\text{C}$  distribution. Ion microprobe studies of a single diamond show a variation of  $\delta^{13}\text{C}$  across the diamond of  $5.1\text{‰}$  and this variation was found to be related to growth zones identified by cathodoluminescence (Wilding and Harte, 1990). The  $\delta^{13}\text{C}$  variation in the single diamond suggests that diamond formation occurred in an open system with a variation in redox conditions controlling both growth and  $\delta^{13}\text{C}$ .

### References.

Wilding, M. C. (1990), "A study of diamonds with syngenetic inclusions." Unpubl. PhD. Thesis, University of Edinburgh.

Wilding, M. C. and Harte, B. (1990) "Carbon isotope variation in a zoned Bultfontein diamond determined by SIMS." **Geological Society of Australia abstracts**, 27, 112

THE MOANA-TINGUINS MELILITITE PROVINCE, PIAUI STATE,  
NORTHEASTERN BRAZIL.

*P.A. Williamson*<sup>(2)</sup>; *N.B. da Silva*<sup>(1)</sup>; *P. Valle*<sup>(2)</sup> and *J.V. Robey*<sup>(1)</sup>.

*(1) Geology Department (Diamond Division), Anglo American Corporation of South Africa, Johannesburg, South Africa; (2) Sopemi - Pesquisa e Exploração de Minérios S.A. CP 04-0087, CEP 71200 - Brasília - DF, Brazil.*

## INTRODUCTION

Diamond prospecting by Sopemi S.A. during early 1980's led to the discovery of 40 intrusives of melilititic character in the Picos area of Piauí State, northeast Brazil.

The intrusions occur along a SW-NE trend between 6° 30' and 7° 10' latitudes and 41° and 42° W longitudes. The bodies have been named Moana-1 to 20 in the southwest and Tinguins-01 to 20 towards the northeast (figure 1).

One of the intrusives have been dated at  $216 \pm 11$  Ma (mid-Triassic zircon fission track age) while U/Pb dating produced an age of 235 Ma (Upper Permian). Further dating is in progress.

## GEOLOGICAL SETTING

The melilitites intrude the Devonian Cabeças Formation which is composed of arenites and siltites in the eastern part of Maranhão Basin.

## TECTONIC SETTING

The Maranhão Basin formed in basement which was affected by the Brasiliano Orogeny (450-700 Ma). Inferences drawn as to the nature of the underlying basement through exposures along basin margins and from limited borehole information suggest a maximum basement age of 693 Ma (Brito Neves et al., 1984).

The intrusives are located along a southwest - northeast structural trend, suggesting an influence of the underlying basement structures. The most notable is the Transbrasiliano Lineament which seems to have controlled the emplacement of the bodies (figure 2).

## DESCRIPTION OF THE INTRUSIVES

The intrusions are often oval in shape and range in size between 1 to 130 hectares.

The bodies are classified texturally as crater facies olivine melilitites. Drilling of the Moana-01 body indicates a thickness of approximately 175 meters for the crater facies sediments. The crater infill consists of well to poorly sorted volcanoclastics showing planar structures. Rounded to angular country rock fragments composed of arenites and siltites occur in varying proportion, together with occasional basement fragments of schist and quartzite. Pelletal juvenile lapilli of olivine melilitite, interpreted as the host igneous source, are also present. Mantle derived peridotitic xenoliths are present.

The juvenile lapilli show relict textures typical of macroporphyrific hypabyssal facies melilitite. They consist of abundant olivine macrocrysts and phenocrysts set in a matrix dominated by melilitite laths, some phlogopite, minor opaques, apatite and perovskite. Occasional clinopyroxene microlites in or around lapilli are found set in an-~~altered~~ fine grained matrix. Olivine commonly shows the complex shapes and parallel growth aggregates typical of melilitites.

#### XENOCRYST MINERAL CHEMISTRY

Garnet xenocrysts are predominantly Ti-poor, low to moderate Cr types which are similar to the garnets from garnet lherzolites. Subordinate amounts of Ti-rich, megacrystic and eclogitic garnets also occur.

Ilmenites have low to moderate Mg and range to high Cr and Ti compositions.

Spinel is predominantly high Mg, moderate Cr varieties, typical of lherzolites. A few grains are high Ti varieties.

Clinopyroxenes show variations in the composition between individual intrusions but are predominantly low-temperature calcic types. Some relatively Fe-rich MARID varieties and a few high-temperature subcalcic clinopyroxenes are present.

#### CONCLUSION

The Moana-Tinguins province constitutes crater facies olivine melilitite intrusive into sediments of the Maranhão basin. The basement age is of a maximum of 693 Ma while the bodies intruded during the mid-Triassic to Upper Permian.

Mineral chemistry of xenocrystic minerals suggest sampling of relatively shallow regions of the upper mantle.

#### References:

Brito Neves et al.(1984). Journal Geodynamics 1, 495-510.

Figure 1: Moana-Tinguins Province Location Map

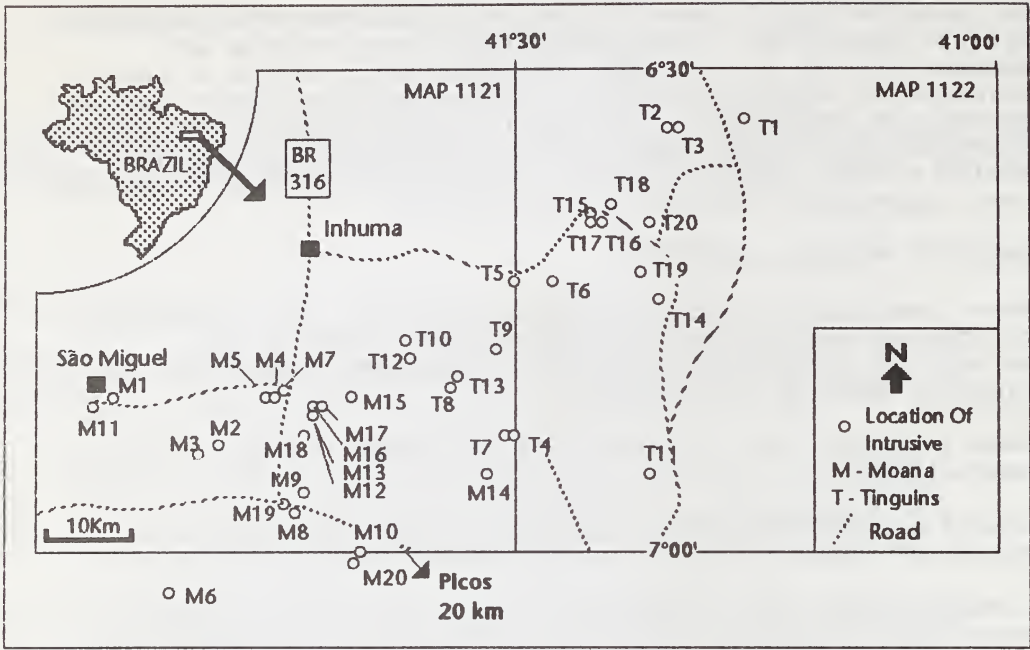
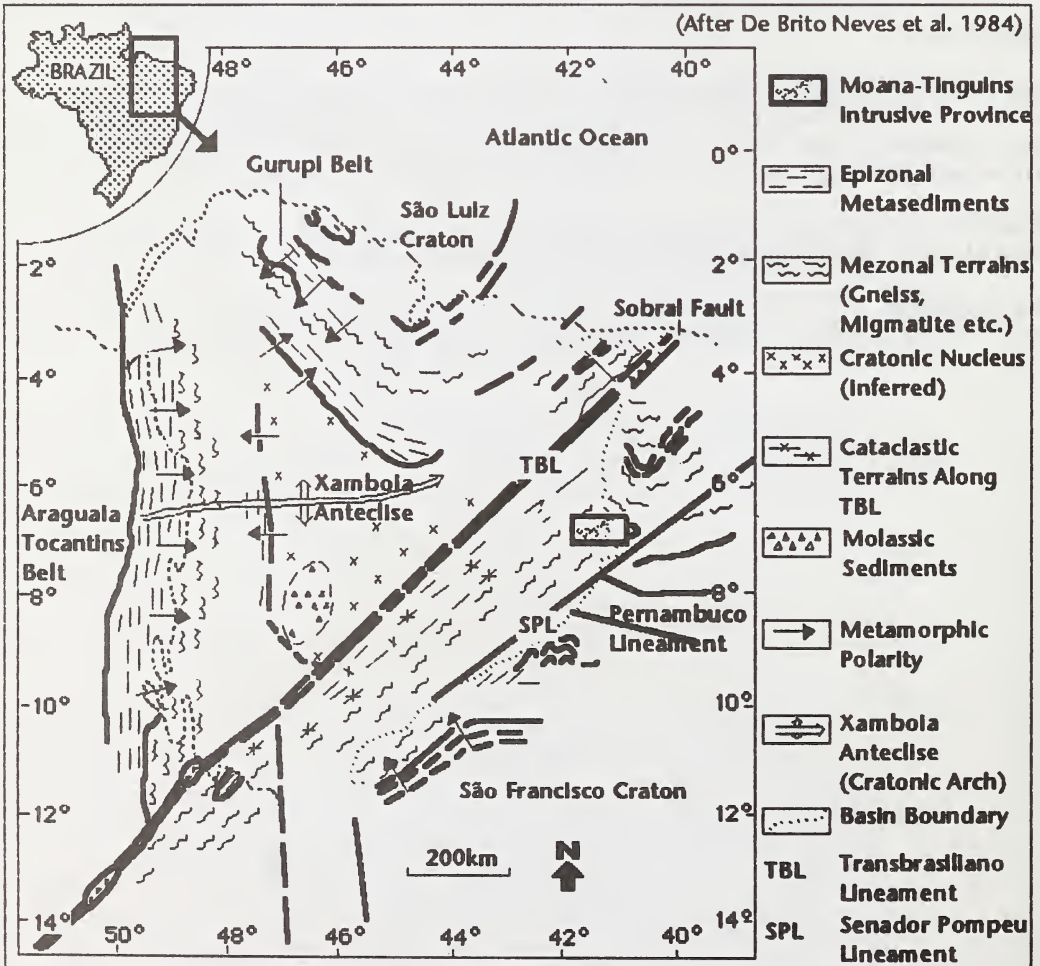


Figure 2: Geological Sketch Map Of The Maranhão Basin Basement

(After De Brito Neves et al. 1984)



## THE PETROLOGY OF THE CLEVE KIMBERLITE, EYRE PENINSULA, SOUTH AUSTRALIA.

*Wyatt<sup>(1)</sup>, B.A.; Shee<sup>(1)</sup>, S.R.; Griffin<sup>(2)</sup>, W.L.; Zweistra<sup>(3)</sup>, P. and Robison<sup>(1)</sup>, H.R.*

*(1) Stockdale Prospecting Ltd., 60 Wilson Street South Yarra Vic 3141 Australia; (2) CSIRO, Div. Exploration Geoscience, PO Box 136, North Ryde NSW 2113 Australia; (3) Anglo American Res. Labs., PO Box 106, Crown Mines, 2025 South Africa.*

### INTRODUCTION

The Jurassic Cleve-01 kimberlite is situated some 10kms north of the town of Cleve on the Eyre Peninsula. It occurs as a small dyke and blow complex, having a width of 20m and strike length of a few hundred metres, and has been dated at  $180 \pm 3$  Ma on U-Pb in groundmass perovskite (Bristow, unpublished data).

The Eyre Peninsula forms part of the Archaen Gawler Craton which has undergone 3 cycles of protracted orogenic development during the early to mid-Proterozoic, but has essentially remained stable since ca.1450 Ma (see Fanning et. al. 1988). Cleve-01 intrudes the Mangalo schists of the Proterozoic Hutchison formation. To the west, a thick sequence of younger Palaeozoic and Mesozoic sediments occur in the nearby Poldia Trough, an intra cratonic half graben with which the emplacement of Cleve-01 may be associated.

### Petrography

The petrographic terminology used in this paper is based on Skinner and Clement, (1979). Cleve-01 consists of both diatrema and hypabyssal facies kimberlite suggesting derivation from the lower levels of a diatrema. Mineralogically it can be described as an opaque-bearing phlogopite-monticellite kimberlite of Group 1 type (Smith, 1983). Three varieties of kimberlite are present; porphyritic, porphyritic breccia and pelletal-tuffisitic kimberlite.

The porphyritic variety contains abundant euhedral, serpentinised olivine phenocrysts (mean = 0.5mm, up to 1.2mm in size), scarce ilmenite microcrysts (0.3 to 0.6mm in size) and occasional baked country rock xenoliths (up to 6mm in length) set in a matrix consisting of granular serpentinised monticellite (0.025 to 0.060mm, mean = 0.04mm) and lesser phlogopite. Extremely rare, rounded macrocrystic grains of serpentinised olivine up to 4mm are also present. The phlogopite occurs as small (0.01 to 0.02mm) laths and platelets interstitial to the monticellite. Possible melilite is also present. Scarce, small (0.5mm) irregular segregations of calcite and serpentine occur in the matrix. Coarse (0.025 to 0.08mm) groundmass spinel and perovskite are abundant (10%) and occur as subhedral to euhedral grains or in clusters up to 0.25mm across. Subhedral to euhedral pyrite up to 0.02mm is also fairly common. Rare groundmass ilmenite up to 0.03mm is also present. Texturally, this variety is classified as a hypabyssal facies, weakly segregationary and porphyritic kimberlite. Mineralogically, it is an opaque-bearing phlogopite-monticellite kimberlite.

In some instances country rock xenoliths exceed 15 volume per cent. In such cases, the rock is classified texturally, as a hypabyssal facies, porphyritic breccia and, mineralogically as a richterite and opaque-bearing phlogopite-diopside-monticellite kimberlite. Petrographic relationships clearly indicate that the richterite and diopside have formed by reaction between the country rock xenoliths and the kimberlite magma.

The pelletal-tuffisitic kimberlite consists of irregular to rounded pelletal lapilli and country rock fragments of biotite-quartz-feldspar gneiss up to 10mm in size, set in a serpentinised matrix. The lapilli average 0.6mm across with a few reaching 2mm in diameter. The lapilli are cored by subhedral to euhedral olivine phenocrysts (no macrocrysts were observed) up to 1.3mm in size and fragments (usually plagioclase or lesser quartz) of country rock xenoliths. The matrix of the lapilli consist of euhedral olivine microphenocrysts, euhedral and atoll textured spinels up to 0.1mm, subhedral perovskite, subhedral to euhedral pyrite (0.015mm), granular serpentine probably after monticellite, fine phlogopite, secondary clays and fine diopside microlites. The diopside occurs mainly toward the outer margins of the lapilli matrix. The interpelletal matrix consists predominantly of fine grained serpentine, abundant diopside microlites and rare phlogopite. This variety is classified texturally as a diatrema facies pelletal-tuffisitic kimberlite. Mineralogically, it is an altered (clay mineralised), phlogopite-monticellite kimberlite.

#### Mineral Chemistry of Concentrate Minerals.

Cleve-01 is dominated by macrocrysts of ilmenite with lesser amounts of chromian spinels, garnets and rare clinopyroxene. The size distribution of the ilmenites are very strongly biased towards the finer 0.3-0.5mm fractions compared to the coarser 1.0-2.0mm fractions, with the compositions varying distinctly with size (Figure 1). MgO varies from a mode of 8 wt% in the coarse fraction to 11 wt% in the fine fraction. Cr<sub>2</sub>O<sub>3</sub> and Al<sub>2</sub>O<sub>3</sub> is mostly less than 0.3 wt% for all fractions. Proton probe trace element data for ilmenites show a reasonably well defined positive Nb-Zr relationship (ca 800-2000 ppm Nb, 400-800ppm Zr) but poorly defined Nb-Ni (ca 0-700 ppm Ni) and Ni-Mg relationships when compared to the well constrained megacrystic suite from Monastery (Moore et al, in press).

The Cleve-01 ilmenites therefore probably derive from sampling of multi-batch magmas, of which at least the fine high-MgO fraction may correspond to coarse grained microphenocrysts crystallising as an early groundmass phase in the kimberlite magma.

The majority of the chromian spinels have 55-65 wt% Cr<sub>2</sub>O<sub>3</sub> and less than 1 wt% TiO<sub>2</sub>. Two populations are defined by MgO contents; 8-12 wt% and 13-15 wt% respectively. A significant minority of grains have TiO<sub>2</sub> 1-6 wt%, some of which may derive from coarse groundmass spinels. The trace element contents of the spinels are more or less in keeping with Group 1 kimberlites with respect to Zn (400-700ppm) and Ga (10-60 ppm), but are high in Ni (1000 ppm compared to 600-700 ppm for other Group 1 kimberlites. They therefore do not have any obvious association with spinels from harzburgites or lherzolites (Griffin et al, this vol.). The high Ni may suggest a high temperature origin.

The Cleve-01 garnets are distinctly bi-modal, with low and high Cr<sub>2</sub>O<sub>3</sub> populations being present (1-3 wt% and 5-9 wt% Cr<sub>2</sub>O<sub>3</sub>), and the vast majority belonging to the lherzolic paragenesis (Sobolev, et al. 1973). Virtually all the garnets are low TiO<sub>2</sub> varieties (less than 0.4 wt% TiO<sub>2</sub>), and typical high TiO<sub>2</sub> megacrystic garnets are not present. Using the Ni garnet geothermometer (Griffin et al, 1989) essentially two temperature populations are defined; one at ca 650-800°C (Y/Ga>2) and the other, 1000°-1250°C (Y/Ca<<1) corresponding to the low and high Cr<sub>2</sub>O<sub>3</sub> groups respectively (Figure 2). Although the high temperature garnets fall into the diamond stability field assuming a normal continental geotherm, the very low Y/Ga ratios are atypical of most African and Siberian kimberlites (Griffin and Ryan, unpublished data). This population in fact may be related to a separate high-Cr<sub>2</sub>O<sub>3</sub> suite formed at relatively low pressures as defined by the low temperature garnet population.



## METALLOGENIC MODEL OF KIMBERLITE IN NORTH CHINA CRATON, CHINA.

P. Zhang<sup>(1)</sup> and S. Hu<sup>(2)</sup>.*(1) Ministry of Geology and Mineral Resources, Beijing, China; (2) 7th Geological Brigade, Linyi, Shandong, China.*

## 1. Temporal and Spatial Distribution of Kimberlites in North China Craton.

There are many kimberlites in the North China craton (abbreviated to "NCC"). They are Mengyin, Fuxian, Tieling, Huanren-Tonghua, Hebi, Shexian, Liulin, Yingxian, Datong kimberlite fields.

The Mengyin kimberlite field consists of 11 pipes and 47 dikes. Most kimberlites wall rock is Archean gneiss, just very few kimberlites have c-o limestone wall rock. Most of pipes and all dikes have root-zone hypabyssal facies kimberlite, only a few pipes have a little diatreme-facies tuffisitic kimberlite breccia. All of them are diamondiferous kimberlites but only several pipes and one dike are economically diamondiferous. Radiometric dating of Mengyin kimberlite gave an age range of 450 to 500 Ma, but the best datum is 457 +/- 7 Ma. The field is located about 60 Kms of westside of Tanlu fault.

The Fuxian kimberlite field consists of 18 pipes and 58 dikes. The wall rock of kimberlites are Proterozoic sandstone and limestone. The basement age is older than 2500 Ma. Most of pipes and all dikes have root-zone hypabyssal facies kimberlite, but two pipes have diatreme-facies tuffisitic kimberlite breccia. The best one of isotopic age of Fuxian kimberlite is 462.7 +/- 4.8 Ma. Most of Fuxian kimberlite are diamondiferous kimberlite and only a few pipes are economically diamondiferous. The diamond quality of Fuxian kimberlite is the best one of all over the world. They contain 60 % of gem stone and most of gem stones are colourless and transparent.

The kimberlites of Tieling, Huanren-Tonghua, Hebi, Shexian, Liulin, Yingxian and Datong do not contain diamond or contain diamond very very poor and did not do any radiometric dating. All of these kimberlites are root-zone hypabyssal facies kimberlite. The basements of Tieling, Yingxian and Datong kimberlites have an age of Archean and the basements of Huanren-Tonghua, Hebi, Shexian and Liulin kimberlites have an age of Proterozoic. The Tieling kimberlite field is located near the Tanlu fault. The Hebi and Shexian kimberlite fields are located near the Taihangshan fault. The Datong, Yingxian and Liulin kimberlite fields are located near the Fenwei fault (see the sketch map).

## 2 Basic Features of North China Craton

## 2.1 Position and area of North China Craton

NCC is located in northern part area of China, including the whole area of Shanxi, Hebei, Shandong and Liaoning four provinces and Beijing, Tianjin two cities and part of Inner Mongolia, Ningxia Autonomous Region, Jilin, Henan, Anhui, Shaanxi and Jiangsu provinces, forming a northern wider and southern narrower reversed triangle in China. The area is about 1.46 million km<sup>2</sup>.

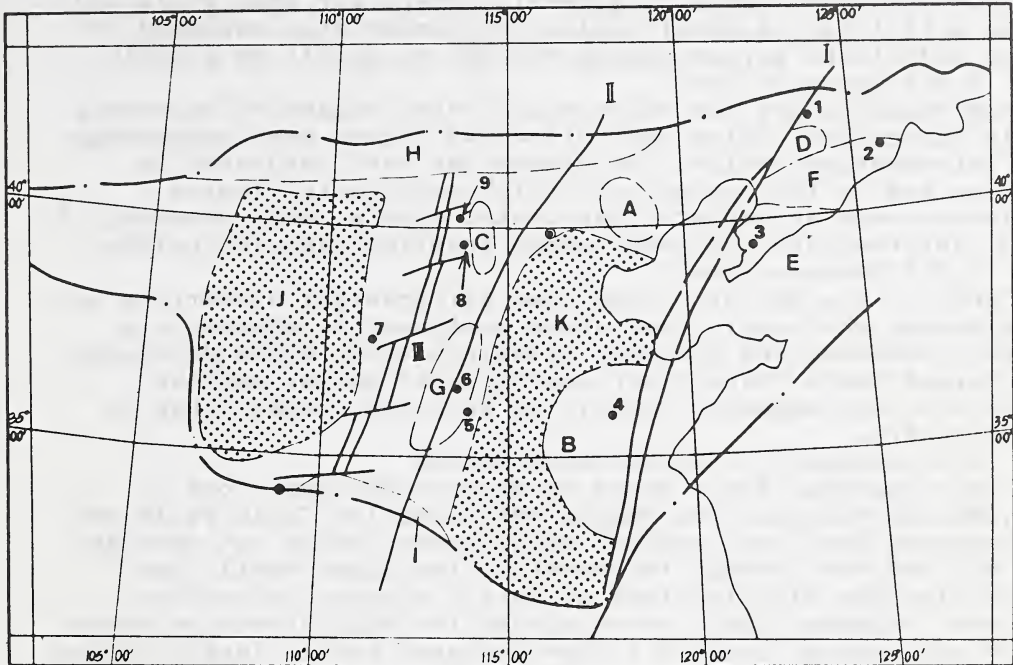
## 2.2 Brief history of development of North China Craton.

## 2.2.1 Archeozoic Era

Archean was the period of geosyncline developing period, but the time of geosyncline development were different with different areas. Some older nuclear areas could have been outlined as follows:

- A. Jidong area (Eastern Hebei) with Archean age of 3500-3700 Ma.  
 B. Luxi area (Western Shandong) with Archean age of 2500-3300 Ma.  
 C. From Wutaishan-Henshan (Northern Shanxi) to Jining (Inner

## KIMBERLITES SKETCH MAP OF NORTH CHINA CRATON



- |  |                                      |
|--|--------------------------------------|
| 1. Tieling kimberlite field.                       | 2. Huanren-Tonghua kimberlite field. |
| 3. Fuxian kimberlite field.                        | 4. Mengyin kimberlite field.         |
| 5. Hebi kimberlite field.                          | 6. Shexian kimberlite field.         |
| 7. Liulin kimberlite field.                        | 8. Yingxian kimberlite field.        |
| 9. Datong kimberlite field.                        | I. Tanlu fault.                      |
| II. Taihangshan fault.                             | III. Fenwei fault.                   |
| A. Jidong old nuclear.                             | B. Luxi old nuclear.                 |
| C. Wutaishan old nuclear.                          | D. Anshan old nuclear.               |
| E. Liaonan old nuclear.                            |                                      |
| F. Hunjiang-Taizihe Proterozoic mobile zone.       |                                      |
| G. Taihangshan Proterozoic mobile zone.            |                                      |
| H. North margin of craton Proterozoic mobile zone. |                                      |
| I. South margin of craton Proterozoic mobile zone. |                                      |
| J. Rerduosi Mz-Kz basin.                           | K. North China Mz-Kz basin.          |

Monggoia) area with Archean age of 2500-3200 Ma.  
 D. Anshan area (Northern Liaoning) with Archean age of 3100 Ma.  
 E. Liaonan area (southern Liaoning) with Archean age of 2500-3000 Ma. The other areas of NCC evolved to geosyncline developing stage in different period of time in Archean. By the end of Archean the areas stated above folded back and formed the NCC Archean crystalline basement.

## 2.2.2 Proterozoic Era

The areas where sediments occurred in Archean were relatively stable. Some of them subsided and accepted the sediment in Proterozoic Era and others were stable at above the sea level, where the Proterozoic sediments were missing. During the time some mobile belts developed, e.g. Hunjiang-Taizihe and Taihangshan Proterozoic mobile belts and the Proterozoic mobile belt at south margin and north margin of NCC. All these mobile

belts show that in Proterozoic Era many faults activities occurred forming many fault depressions where very thick fiysch sediments, a large quantity of volcanic rocks and a series of magma intrusions occurred. By the end of Proterozoic Era whole NCC consolidated and formed unitary basement of NCC.

#### 2.2.3 Palaeozoic Era

In Palaeozoic Era whole NCC was very stable, a typical craton developing stage. There was a sedimentary gap between Middle Ordovician and middle Carboniferous period, which was parallel unconformity not angular unconformity, suggesting in Palaeozoic Era NCC was very stable in general, except for some fault and magma activities in small scale. The kimberlites emplaced in Upper Ordovician period during the NCC to uplift as a whole.

#### 2.2.4 Mesozoic Era

During Mesozoic Era the NCC was activated suggested by strong fault acticities, which controlled and formed many upwarings and intermontane basins, the upwarings were subjected to erosion and in the basins very thick continental facies sediments were accumulated associated with a large quantity of acid, intermediate and basic magma eruptions and intrusions.

#### 2.2.5 Cenozoic Era

In Cenozoic Era NCC still had some differential elevations and subsidences obviously. Some areas continued to elevate, e.g. Western Shandong and Southern Liaoning, other areas depressed and formed North China Plain and Eerduosi Basin, but the structural and magmatic activities were much weaker than in Mesozoic Era.

#### 2.3 Lineament in North China Craton

The main regional fault zones in NCC are NNE and close to EW (NEE) directions. The famous NNE direction Tanlu Fault and Taihangshan Fault are reginal fault zones, which cut through the NCC and cut through the crust to the upper mantle and controlled the distributions of mantle sourece intrusions. The next biggerst fault zones are EW (or NEE) direction zones, which are several hundred to one thousand kms in length. These two directions fault zones cut the NCC into many rhombic blocks.

### 3 Regional Metallogenic Model of Kimberlite in North China Craton

3.1 All diamondiferous kimberlites and economic kimberlites emplaced in Archean basement areas, e.g. Fuxian and Mengyin kimberlite fields. The kimberlites emplaced at the margin of the craton have no diamonds or very poor, e.g. Tieling kimberlite field. All the kimberlites emplaced in Proterozoic mobile belts have no diamond, e.g. Hebi, Shexian and Hunjiang-Taizihe kimberlite fields.

3.2 The kimberlites dominantly emplaced in both sides of huge regional fault zones, e.g. Tieling, Fuxian and Mengyin kimberlite fields emplaced on both sides of Tanlu fault, Shexian and Hebi kimberlite fields emplaced on one side of Taihangshan fault, Daton, Yingxian and Liulin kimberlite fields emplaced on both sides of Fenwei fault.

3.3 The shapes of pipes and trending directions of dikes are controlled by surface faults.

3.4 The pipes emplaced in Archean and Protorezoic system have been eroded to root zone at present. It is impossible to find kimberlites which occurred in upper Palaeozoic Era or Mesozic Era because the kimberlites emplaced in upper Ordovician Period. Therefore, to search for preserved crater or diatrema facies kimberlite must work in lower palaeozoic formation (especially in Ordovician) areas.

Accordance with the model stated above, it can be forecasted:

1. kimberlitic type primary sources of diamonds shall be looked for dominately in NCC, and should work in the areas which surround the older nuclear or itself, where the NNE or EW directions regional fault zones occurred and lower Palaeozoic formations preserved, and
2. in NCC lamproites might have emplaced, which should be looked for in the Proterozoic mobile belts stated above especially in the Proterozoic mobile belts in both south and north margin of NCC. Because the former was subducted by Qinling block from south and the later was subducted by Siberian block from north in Proterozoic Era. The block subducting activities might have been advantageous to the emplacement of lamproite.

## MICAS IN KIMBERLITES FROM CHINA.

*Dong Zhenxin.**Geological Museum of China, Beijing, 100034.*Occurrence:

Micas, the common minerals of kimberlites from China, have seven modes of occurrence: (1) megacryst (1-10cm); (2) macrocryst (5mm-1cm); (3) microphenocryst and groundmass mica (0.005-1mm); (4) reaction and replacement product micas as rims upon olivine or garnet; (5) mica intergrowths with Cr-spinel, ilmenite and magnetite; (6) mica as epigenetic inclusion in diamond; (7) mica in deep seated xenoliths from kimberlite.

Content:

The abundance of micas in kimberlites varies widely from 2 to 50%, but often 5-20%. Free- and poor- diamond kimberlites (Northern Liaoning, Guizhou, Hubei, Henan, Hebei and Shanxi) richer in micas than those of rich-diamond kimberlites (Shandong and Southern Liaoning).

Variety:

The micas in kimberlites of China mainly belong to phlogopites, Mg-biotite and Fe-biotite are rare according to Guidotti's (1975) classification method (Fig.1). The varieties of micas of different occurrences are not alike, such as, major megacryst and macrocryst micas belong to phlogopite. Groundmass micas fall into phlogopite-Fe-biotite field, but most of them are phlogopite-Mg-biotite. The tetraferriphlogopites are phlogopite. Mica intergrowths with Cr-spinel, ilmenite and magnetite, and epigenetic inclusion in diamond are phlogopite - Mg-biotite.

The lamproite micas belong to Mg-biotite.

Color, pleochroism and morphology:

The megacryst and macrocryst micas occur as silvery yellow. Most megacryst and some macrocryst micas are rounded, broken, distorted or kink banded and show undulose extinction. Some macrocryst micas occur as sieve texture, showing several olivines (Pseudomorph) have been included in same mica. Groundmass micas are yellow-brown in color. Based on the optical property, micas in kimberlites can be divided into two groups: normal and reversed pleochroism. Reversed pleochroism micas are not present in the deep seated xenoliths that contain micas. Generally macrocryst micas with normal pleochroism have been replaced by reversed pleochroism micas along cleavage planes and margins.

Zoning:

Macrocryst micas exhibit complex  $TiO_2$ - $Cr_2O_3$  zonation, showing disorderly variations from cores to rims, reflecting changes of the complex formation conditions.

Mineral chemistry:

Megacryst and macrocryst micas are rich in  $Cr_2O_3$  (up to 0.44%), poor in FeO (1.75-6.34%). Primary groundmass micas occur as tetraferriphlogopites and titanian phlogopites, most of them are high FeO, low  $Cr_2O_3$  (<0.30%). There exist significant differences between groundmass micas of diamond-rich and -poor or -free kimberlites, the former (e.g. No.50 kimberlite pipe in Liaoning)

contains lower in FeO (2.84%) and TiO<sub>2</sub> (1.59%) than the latter (such as Shanxi and Hebei kimberlites, FeO up to 21.07%, TiO<sub>2</sub> 4.98-6.39%). The micas showing reversed pleochroism are characterized by Fe<sup>3+</sup>-rich, Al<sub>2</sub>O<sub>3</sub>-deficient at tetrahedral sites. Most megacryst and some macrocryst micas are probably xenocrysts which have compositions similar to primary micas in deep seated xenoliths, but other that differ from xenolith phases are phenocrysts which formed during the early stages of crystallization. Micas in lamproites from Guizhou and Hubei are higher in TiO<sub>2</sub> (8.48-15.72%) and FeO (9.78-14.89%), and lower in Cr<sub>2</sub>O<sub>3</sub> (<0.11%), NiO (<0.20%), Mg/(Mg+Fe) (63.50-75.46%) than those of kimberlites.

Micas in kimberlites contain 0.10-0.11% Rb<sub>2</sub>O, 0.005-0.041% Li<sub>2</sub>O, 0.06-0.07% Ba, 0.008-0.010% Sr, 0.003-0.004% Zn, 0.003-0.004% Ga, 5-9 ppm Cs<sub>2</sub>O, 8.8-10.9 ppm B and 1-3 ppm Be, respectively.

Megacryst mica from Shandong kimberlite contains 34.67 ppm total REE, 0.25-27 times chondritic abundance, which is not principal carrier of REE in kimberlites. REE distribution pattern for kimberlite mica is similar to that of minette (Shanxi), but the latter contains more total REE (63,94 ppm).

#### Transformation of heating mica:

The study of transformation for the heating mica has been undertaken by chemical analyses, x-ray analyses, infrared absorption spectra and Mossbauer spectra. The heating micas at 1100 °C have been transformed into olivines and leucites (Fig.2).

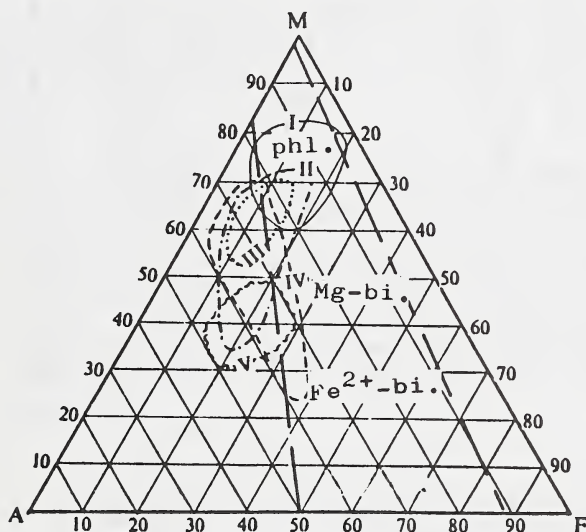


Fig.1 Classification diagram of micas for different occurrences

I-tetraferriphlogopite with reversed pleochroism ; II-epigenetic inclusion in diamonds; III- megacryst and macrocryst micas in kimberlites; IV-groundmass micas in kimberlites; V-lamproites (Guizhou and Hubei). (compositional field by Guidotti et al. 1975)

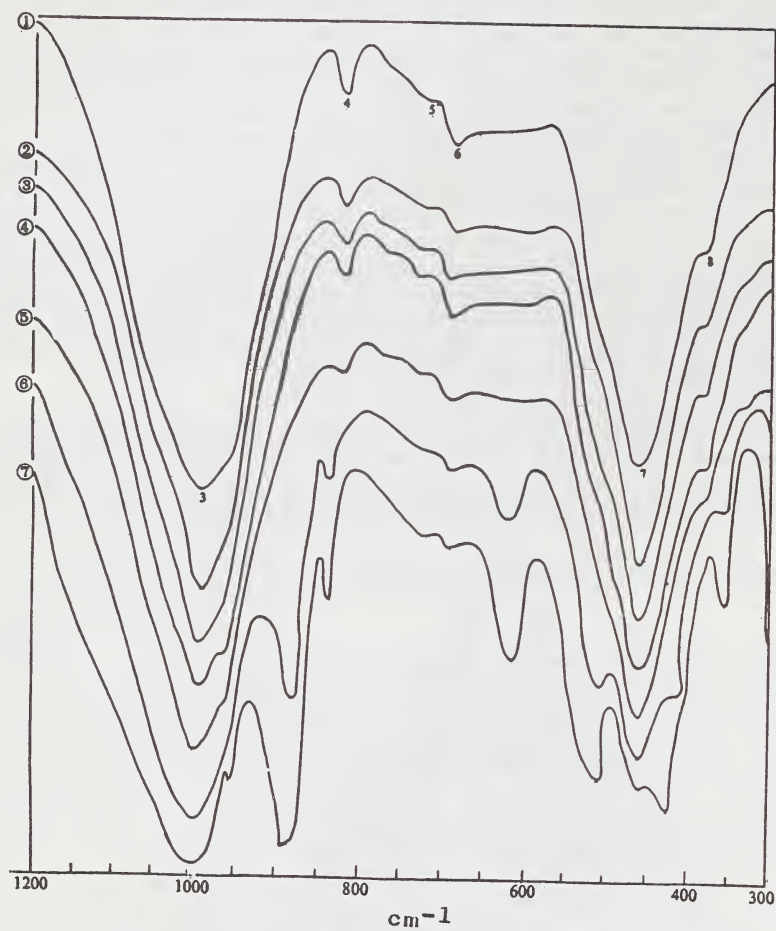


Fig.2 Infrared absorption spectrum diagram of a heating phlogopite

① heatless sample; ② heating 700 °C; ③ heating 800 °C; ④ heating 900 °C; ⑤ heating 1000 °C; ⑥ heating 1100 °C; ⑦ heating 1200 °C

## OLIVINES IN SHANDONG KIMBERLITES.

Dong Zhenxin.

Geological Museum of China, Beijing, 100034.

Occurrences:

Generally, olivines in the kimberlites from Shandong have been recognized to have six main modes of occurrences: (1) megacryst (>10mm) (pseudomorph); (2) coarse grained (macrocryst) olivine (5-10mm); (3) medium grained olivine (2-5mm); (4) microrgranular or groundmass olivine (0.005-0.5mm); (5) olivine as inclusion in diamond; (6) olivine (pseudomorph) of deep seated xenolith in kimberlite.

Content and morphology:

Content of the olivine together with its alteration product ranges widely from 20 to 80%, but usually 25-50%.

Morphologically, olivines of different size may be distinguished. Large olivines are anhedral, rounded to elliptical grain, but small olivines occur as subhedral to euhedral crystals.

Color:

Colors of olivines in Shandong kimberlites range from colorless to greenish and green. Relationship between colors and sizes of olivines has been known, the large crystals are colorless and greenish, but the small crystals (groundmass olivines) are green.

Zoning:

The olivines in Shandong kimberlites show complex zoning patterns. Three compositional variation trends have been observed from core to rim in the olivine: (1) iron-rich trend; (2) magnesian-rich trend; (3) iron-rich and magnesian-rich trends are present in the same olivine. Although the zoning patterns are complex, the major-element zoning is, however, very limited, usually causing less than 0.5%  $F_0$  variation between core and rim (Fig.1). NiO and CaO variations are weak and complex.

Mineral chemistry:

The olivines in kimberlites from Shandong are highly magnesian,  $F_0$  content being 90.2-92.5%.

The olivine compositional variation is correlated with their colors. Colors range from colorless and greenish to green with increase of Fe content.

Early generation olivines contain richer in  $F_0$  (90.9-92.5) than the late generation olivines ( $F_0$  90.2-91.5) (Fig.2).

The differences in composition of the olivines exist between the individual kimberlites with different diamond contents, such as olivines of Shengli-1 pipe have more  $F_0$  contents than the Hongqi-6 pipe with decrease of diamond contents in the kimberlites.

Olivines as inclusions in diamonds are extremely rich in  $F_0$  and have relatively restricted within 93.06-100.

CaO (<0.14%), NiO (<0.74%),  $Cr_2O_3$  (<0.17%) and  $TiO_2$  (<0.17%) contents of the olivines are extremely low. Increases in CaO contents of the olivines are correlated with increases in  $F_0$ . The general trend of increasing  $Ni_2SiO_4$  (Ni-olivine) with increasing  $F_0$  is observed.

Olivines as inclusions in diamonds are high in  $Cr_2O_3$  (up to 1.29%).

The olivines of late generation contain more  $TiO_2$  (up to 0.17%) than those of early generation (<0.11%).

Infrared absorption spectrum:

There are 10 strong absorption bands (982, 948, 880, 837, 606, 510, 465, 420, 380, 363  $\text{cm}^{-1}$ ) within 350-1200  $\text{cm}^{-1}$  of infrared absorption spectra of olivines from Shengli-1 pipe. The presence of 420 and 606  $\text{cm}^{-1}$  shows that the olivine studied belongs to forsterite.

Origin:

All the groundmass olivines are true phenocrysts. Coarse and medium grained olivines predominantly are phenocrysts except a little sources of fragmented megacryst and dunite-lherzolite xenoliths.

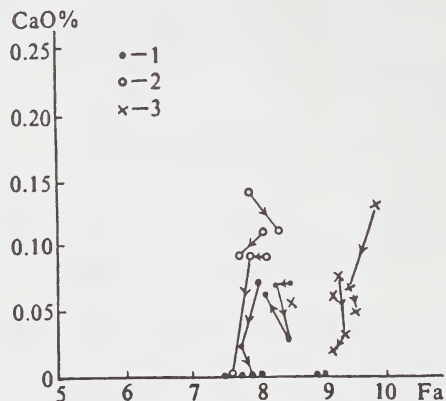


Fig.1 CaO versus Fa for olivines in Shengli-1 pipe from Shandong Province

1-coarse grained olivine; 2-medium grained olivine; 3-microgranular(groundmass) olivine

(The arrow shows zonation variation trend from core to rim)

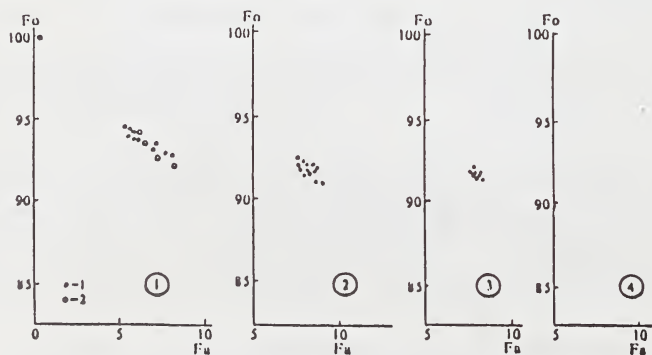


Fig.2  $F_o$  versus  $F_a$  for olivines of different occurrences

- ① 1-olivine as inclusion in Shandong diamonds;  
2-olivine as inclusion in diamond ( Meyer 1987);  
② coarse grained olivine; ③ medium grained olivine;  
④ microgranular(groundmass) olivine

## GEOCHEMISTRY OF INDICATOR MINERALS FROM CHINESE KIMBERLITES AND LAMPROITES.

Jianxiong Zhou<sup>(1)</sup>, W.L. Griffin<sup>(2)</sup>, A.L. Jaques<sup>(3)</sup>, C.G. Ryan<sup>(2)</sup> and T.T. Win<sup>(2)</sup>.

(1) Institute of Mineral Deposits, CAGS, Beijing 100037, China; (2) SCIRO Div. of Exploration Geoscience, North Ryde 2113, Australia; (3) Bureau of Mineral Resources, Canberra, 2601, Australia.

Over 900 grains of indicator minerals, including pyrope, chromite, ilmenite, LIMA and yimengite have been analyzed by EMP and proton microprobe. The bodies studied come from seven different provinces and include both diamondiferous and barren intrusives. The data show consistent patterns that can be used in exploration and evaluation of prospects within each area.

Kimberlites and lamproites have been found only in the Sino-Korean craton and the Yangzi craton, while similar bodies in the Talimu craton (Xinjiang Autonomous Region) have proven to be lamprophyres. Most studied bodies in the Sino-Korean craton are Group I kimberlites; some contain economic deposits of diamonds, while others are barren. The Yangzi craton contains both lamproites and possible Group II kimberlites; some contain low grades of diamonds. Among the indicator minerals, pyrope and chromite are very common, while ilmenite is rare, being restricted to kimberlites in Shandong and Liaoning. LIMA and yimengite are found in Shandong kimberlites, especially Hongqi No. 27.

The diamondiferous kimberlites of Liaoning and Shandong provinces contain abundant G9 garnets with Cr<sub>2</sub>O<sub>3</sub> up to 11 wt.%, and a significant number of moderately subcalcic pyropes. Barren kimberlites have, in general, higher proportions of low-Cr pyropes. Subcalcic garnets are rare in the lamproites, and the average Cr content of lamproite pyropes is lower than those from diamondiferous kimberlites. Garnets from the diamondiferous Liaoning kimberlites show a broad bimodal distribution of T<sub>Ni</sub> (Griffin et al., 1989a), with peaks centered on 950°C and 1150°C (Fig. 1a). There is a minor high-T group (>1300°C) which is interpreted as megacryst-related, and is present mainly in the lower-grade pipes of the district. Most of the lower-T garnets are depleted, with Y<10ppm, Zr<40 ppm and Zr/Y~2-3. Many grains have higher Zr (to 200 ppm) and high Zr/Y, without corresponding Ti enrichment. This pattern is interpreted as the effect of hydrous metasomatism. The Shandong garnets are characterized by much higher temperatures, with major peaks at 1150-1300°C and 1400-1550°C (Fig. 1b). The high-T peak is dominated by low-Cr, high-Zr,Y garnets, which are interpreted as megacryst-related. Many lherzolite garnets in the Shandong pipes are depleted, like those from Liaoning, but many others have elevated Zr and Y, strongly correlated with Ti; this is interpreted as the effect of melt-related metasomatism (Griffin et al, 1989b; Smith et al, 1991), associated with the observed megacryst population. The diamondiferous Maping No. 1 lamproite of Guizhou Province shows a broad T distribution from 1150-1300°C; the higher-T part of the range is represented by megacryst-type garnets. The lherzolitic garnets from Guizhou are depleted, like those from Shandong and Liaoning.

Garnets from barren pipes in all districts are characterized by low-T garnets (T<1000°C), with a minor high-T population and a small proportion in the "diamond window" (950-1250°C) (Fig. 1c). Even where temperatures above 950°C are recorded, the garnets retain the low-Zr (Zr<40 ppm), high-Y (Y>20ppm) signature typical of low-T, low-P garnets; the relatively high temperatures may reflect short-lived heating events, rather than the ambient geotherm (Smith et al., 1991). A plot of Zr/Y vs. Y/Ga (Fig. 2) clearly separates the garnets of the barren and diamondiferous pipes: nearly all garnets from barren pipes have Zr/Y <1 and Y/Ga>2.

The kimberlites of the Sino-Korean craton contain abundant high-Cr chromite macrocrysts; these can be divided into two populations (P1 and P2) on the basis of major- and trace-element composition (Figs.3,4). P1 has high Cr# (100Cr/Cr+Al >80) and moderate Mg#, and some grains are similar in major-element composition to diamond-inclusion spinels. TiO<sub>2</sub> ranges from 0-4%, and is positively correlated with Ni. P1 is typical of spinel macrocrysts in South African Group 1 kimberlites, and is derived largely from harzburgite and lherzolite wall

rocks (Griffin et al., 1991). P2 has lower Cr# and higher Mg#; Ti and Ni contents are low, and Zn contents are high (>1000 ppm). This population is probably derived from disaggregated lherzolites, in the graphite stability field (op. cit.). Diamondiferous kimberlites in the Sino-Korean craton contain both populations; barren kimberlites contain only P2. The P1 population in the Shandong kimberlites has generally higher Zn and lower Ni than that in Liaoning province, suggesting that a higher proportion of the material in these pipes comes from the graphite stability field. Chromites from the barren Henan and Hebei kimberlites contain 50-60% Cr<sub>2</sub>O<sub>3</sub>, and have low Ti contents. However, only a few grains have the major-element/trace element relations of a typical kimberlitic population. Their low Ni and high Zn contents (Fig. 4) indicate that most grains have come from shallow, low-T lherzolites, in the graphite stability field.

Chromites from the Guizhou and Hubei lamproites are generally lower in Cr and Zn, and higher in Ni than those from the kimberlites, regardless of their diamond content (Fig. 4). They are dominated by a population common to lamproites worldwide, and inferred to be magmatic (op. cit.); very few grains can be identified as being derived from lherzolite or harzburgite wall-rock. It is not possible to separate these diamondiferous and barren lamproites on the basis of chromite chemistry.

Ilmenites are clearly divided into two groups, one with low MgO and high MnO (>1%), and one with high Cr<sub>2</sub>O<sub>3</sub> (1-7%) and MgO (up to 16%). The first type is found in eg. the Shengli No. 1 mine; it has low Nb, Zr and Ni, and is clearly of crustal origin. The second type has been studied at the Hongqi No. 27 pipe; it does not show the smooth covariation of Nb, Ni, Zr etc. that characterizes most African and Siberian ilmenite megacryst populations. This, and the unusually high Cr contents, suggest a link to the LIMA association, rather than to fractionation of a megacryst-type magma.

This orientation study demonstrates that trace-element studies of garnets and chromites can be used in the Chinese cratons to improve diamond exploration by early discrimination of barren and potentially diamond-bearing sources. Barren sources sampled thus far all contain garnets and spinels derived from shallow levels of the mantle, rather than from the diamond stability field. The data also suggest significant differences in the thermal state of the lithosphere on either side of the major Tanlu suture. These differences may have broader implications for exploration strategies.

Griffin, W.L., Cousens, D.R., Ryan, C.G., Sie, S.H. and Suter, G.F. 1989a. *Contrib. Mineral. Petrol.* 103, 199-202.

Griffin, W.L., Smith, D., Boyd, F.R., Cousens, D.R., Ryan, C.G., Sie, S.H. and Suter, G.F. 1989b. *Geochim. Cosmochim. Acta* 53, 561-567.

Griffin, W.L., Ryan, C.G., Gurney, J.J., Sobolev, N.V. and Win, T.T., 1991. (this vol.)  
Smith, D., Griffin, W.L., Ryan, C.G. and Sie, S. 1991. *Contr. Mineral. Petrol.*, in press.

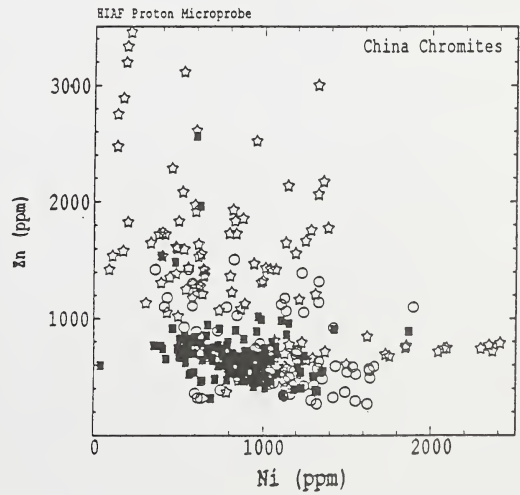
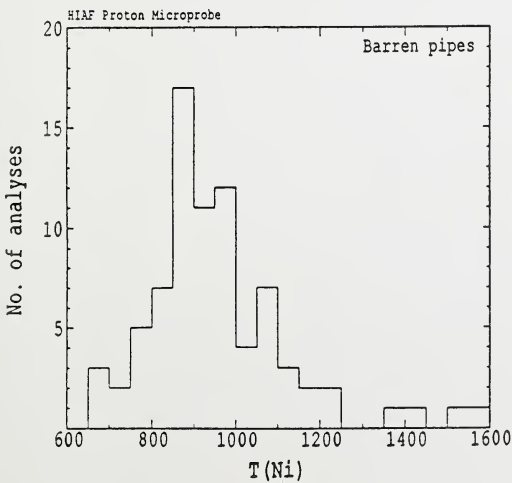
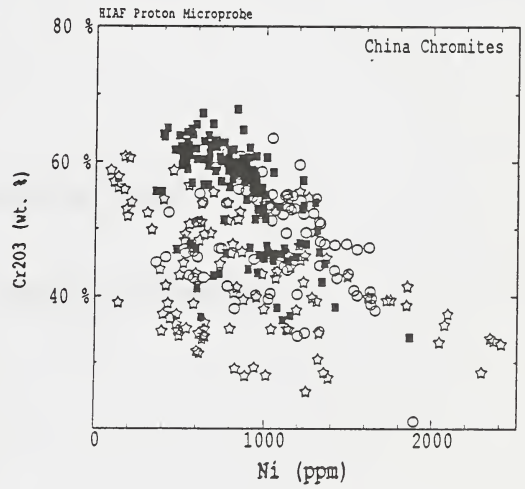
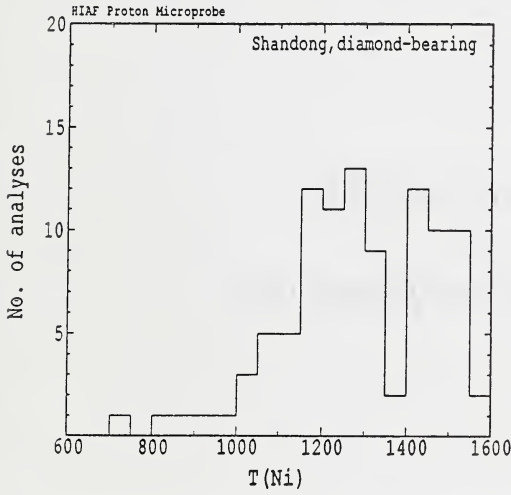
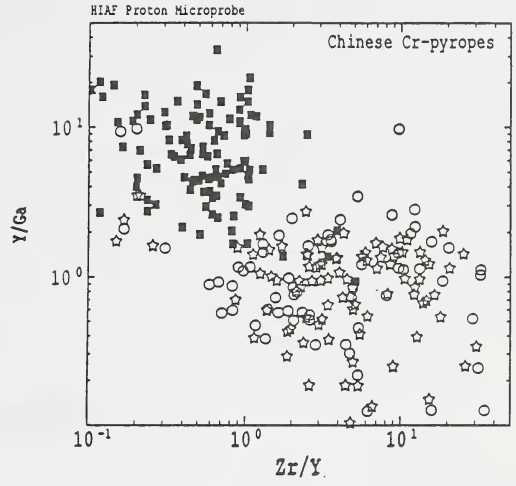
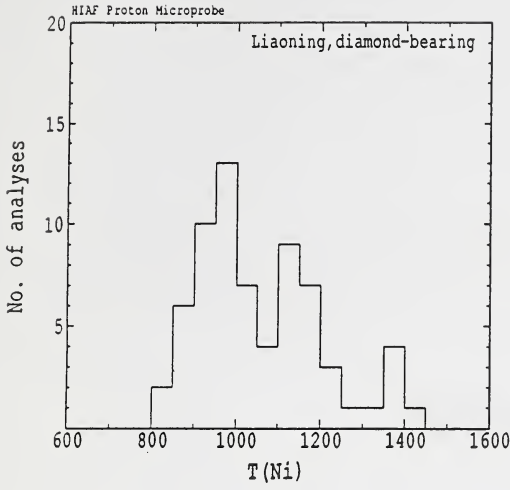
#### FIGURES (next page)

Fig. 1 (left). TNi histograms for diamondiferous kimberlites of Liaoning and Shandong provinces, and for barren kimberlites from Liaoning, Shanxi, Henan and Hebei provinces.

Fig. 2 (top right). Zr/Y - Y/Ga plot for garnets. Squares, barren kimberlites; circles, Liaoning diamondiferous kimberlites; stars, Shandong diamondiferous kimberlites.

Fig. 3 (middle right). Cr-Ni relations in chromites. Squares, diamondiferous kimberlites; circles, lamproites; stars, barren kimberlites.

Fig. 4 (lower right). Zn-Ni relations in chromites. Symbols as in Fig. 3.





# *Appendix*

*Abstracts received from  
non-participant russian scientists*



## THE PECULIARITIES OF THE MINERAL COMPOSITION OF THE DIAMOND BEARING ECLOGITES FROM THE UDACHNAJA KIMBERLITE PIPE.

*Bezborodov*<sup>(1)</sup>, *S.M.*; *Garanin*<sup>(2)</sup>, *V.K.*; *Kudrjavitseva*<sup>(2)</sup>, *G.P.* and *Schepina*<sup>(2)</sup>, *N.A.*

(1) SPC "Jakutalmaz", 678189, Udachni, Jakutskaja ASSR, USSR; (2) Geological Department of Moscow State University, 119899, Lenin's Hills, Moscow, USSR.

The complex study of the mineralogical composition of the diamond bearing eclogites, 67 xenoliths from the Udachnaja kimberlite pipe, including 15 nodules of orange garnets, is carried out by the method of optical and scanning electron microscopy, coloured cathodoluminescence (CL), electron-probe analysis, optical spectroscopy and colorimetry. All the samples of the investigated eclogites have the traces of cataclasis and recurrent metasomatic influence of fluids, causing the intensive replacement of garnet by hydrogarnet and by complicated mineral association (diopside - amphibole - green spinel) and decomposition of clinopyroxene and plagioklase, considerably calcium pyroxene and serpentine.

The diamond crystals in the studied collection of eclogites are of octahedral shape with the microrelief of dissolving and, very seldom, with poorly developed edges of rhombododecahedron. The diamond crystals of the cubic habitus are discovered in one of the studied samples. The sizes of crystals vary from 20  $\mu$  to 6 mm and, in this case, several diamond crystal of different sizes are discovered in numerous xenoliths. About 30 diamond crystals on the surface of eclogites are studied by the method of coloured cathodoluminescence on the basis of optical microscopy. Most of them have the blue colour of the cathodoluminescence (with high concentration of nitrogen, type I), with the exception of several samples, where together with the crystals of blue CL-colour, the ones of clearly marked yellow colour (type IIa and type IIb) are discovered. The discoveries like these one may have proved the different genetic nature of the diamond crystal in one xenolith.

The rock forming garnet and clinopyroxene are the "conservatives" of the diamond crystals included into them and they provide the conservation of even small crystals of diamond (size of several microns) when they are brought up to the surface of the kimberlite magma.

In the optical absorption spectra of the garnets, the observed lines of absorption are facilitated by the chromophormic centres  $Fe^{2+}$ ,  $Fe^{3+}$ , and  $Cr^{3+}$  and are also connected with the availability of complicated chromophormic centres  $Fe^{2+}+Ti^{4+}$  as was discovered by the method of optical spectroscopy and colorimetry. Their correlation and concentration facilitate the different shades of colour of garnets from the investigated eclogites, from dark yellow-orange to light yellow-orange. On the modified diagram of colour in the colorimetric coordinates  $p_c$  and  $\lambda_c$ , the points of colour of the investigated garnets are in the field of the diamond bearing magnesian-ferrous, disthene and corundum eclogites.

In all the investigated samples, garnet refers to pyrope-almandine-grossular row with wide range of pyrope (29.3-75.5 mol.%), almandine (13.3-46.4 mol.%) and grossular (0.7-52.0 mol.%) minerals. The practically full absence of chrome and increased content of titanium (to 0.67 wt.%  $TiO_2$ ) and sodium (to

0.63 wt.% Na<sub>2</sub>O) are characteristic for garnets. With the increase of grossular mineral in garnet and decrease of pyrope one, the regular change of colorimetric garnet parameters takes place: the value P<sub>c</sub> decreases and dark-yellow-orange colour is changed into light-yellow-orange. According to J.Dawson and W.Stephens (1975) classification all garnets refer to four groups: titanium pyrope, calcium pyrope-almandine, titanium and calcium magnesian almandine, pyrope-grossular almandine.

As a result of usage of the data base on garnet from eclogites and the application of discriminant analysis (Garanin et al., 1990), garnets were considered as a mineral from ilmenite-rutile diamond bearing magnesian-ferrous eclogites, biminerall diamond bearing magnesian-ferrous eclogites, aluminous (corundum and disthene) eclogites, magnesian ilmenite-rutile diamond bearing eclogites. The group magnesian-ferrous of eclogites is also marked out where garnets is sharply different from the known ones by the analysis by high contents of iron (to 1.51-1.95 wt.% Fe<sub>2</sub>O<sub>3</sub> and 12.16-14.35 wt.% FeO), magnesium (17.4-19.57 wt.% MgO) and low content of calcium (2.47-3.06 wt.% CaO).

Not only the typomorphism of the garnet composition but also that of clinopyroxene is studied. According to the classification of W.Stephens and J.Dawson (1977) the studied clinopyroxenes are referred to diopside, jadeitic diopside and omphacite. The studied pyroxenes are referred to the group of pyroxenites, disthene and corundum diamond bearing eclogites and biminerall diamond bearing eclogites by using the data base on clinopyroxene from eclogites and their chemico-genetical classification and methods of discriminant analysis (Garanin et al., 1990). All of them refer to isomorphic row diopside-jadeite-ferrosilite (+clinoenstatite). In this case diopside and jadeite minerals constitute together more than 80 mol.%. The ratio Ca/(Ca+Mg) constitute 41-56. The evaluation of crystallization temperatures of eclogites is carried out for all the samples, in which clinopyroxene is analysed.

The variation of temperatures, using the geothermometer of Ellis-Green (1979), are about 1024-1137°C under the pressure of 40 kbar. The composition of the accessory minerals in all the varieties of eclogites was also studied: corundum (sapphire), disthene, ilmenite, rutile, sulfide pyrrhotine-pentlandite-chalcopyrite (+jerphisherite) association. The wide spreading of ilmenite-rutile intergrowths in magnesian eclogites should be noted.

Two main evolution trends have been established for eclogites: magnesian - magnesian-calcium and magnesian - magnesian-ferrous. They are clearly shown in the regular change of compositions and different schemes of isomorphic replacement in garnets: Mg ↔ Ca and Mg ↔ Fe<sup>2+</sup>.

The differences in the composition of garnets and pyroxenes - inclusions in diamond, on the one hand, and rock forming garnets and pyroxenes of eclogites, containing diamond, on the other hand, were established. The new criteria for the searching of the kimberlite rocks on the basis of the typomorphism of the rock forming garnets and pyroxenes from the diamond bearing eclogites are offered and different genetic models of the diamond bearing eclogites and their role in the general evolution of the both mantle and crustal rocks are discussed.

#### References :

1. Dawson, J.B., and Stephens, W.E. (1975) Statistical analysis of garnets from kimberlites and associated xenoliths. *J.Geol.*, 83, 589-607

2. Ellis, D.J., and Green, D.H. (1979) An experimental study of the effect of Ca upon garnet-clinopyroxene exchange equilibria. *Contrib. Miner. & Petrol.*, 71, 13-22
3. Garanin, V.K., Kudrjavitseva, G.P., Mikhailichenko, O.A., and Marfunin, A.S. (1990) The inclusions in diamond and diamond bearing rocks, 272 p., Moscow University, Moscow
4. Stephens, W.E., and Dawson, J.B. (1977) Statistical comparison between pyroxenes from kimberlites and their associated xenoliths. *J. Geol.*, 85, 433-449

## ORE MINERALS FROM THE LAMPROITE GROUND MASS.

*Bogatikov*<sup>(1)</sup>, *O.A.*; *Garanin*<sup>(2)</sup>, *V.K.*; *Kononova*<sup>(1)</sup>, *K.A.*; *Kudrjavitseva*<sup>(2)</sup>, *G.P.*;  
*Makhotkin*<sup>(1)</sup>, *I.L.* and *Mikhailichenko*<sup>(2)</sup>, *O.A.*

(1) *Institute of Geology, Geochemistry and Mineralogy Ore Deposits, Academy Sciences of USSR, 109017, Staromonetni per., 35, Moscow, USSR;* (2) *Geological Department of Moscow State University, 119899, Lenin's Hills, Moscow, USSR.*

The study of mineralogy of oxides from the lamproite ground mass of different regions (Australia, Spain, USSR) and magnetic properties of these rocks has allowed to define their typomorphism at the level of provinces, types of lamproite rocks (ultrabasic, basic) and their facies belonging (tuffs, tuffbreccia, intrusive lamproites, dyke facies). It is shown that the typomorphism of the composition of minerals from the ground mass of lamproites and their spreading correlates to the lamproite diamond bearing. The spreading of microcrystal oxides ("density" of ore mineralization), the set of different mineral phases and their correlation, the size of the extracts and their chemical and phase composition refer to the typomorphic features of oxides from the ground mass of lamproites.

In a nutshell, the essence of the discovered typomorphism is the following. As far as its details at the province level are concerned - this is a wide occurrence of rutile, perovskite and K-Ba containing titanates in the ground mass of lamproites of Australia; apatite and ilmenite for dyke rocks of Spain and titanomagnetite (magnetite) specification of Aldan Shield lamproites. It should be also noted that there is the decrease of chrome and magnesian content of the microcrystalline mineralization during the transition from ultrabasic to basic and medium (from olivine to phlogopite, leucite, diopside and etc. lamproites) and the increase in the same direction of its titanium and, especially, iron content. Speaking about the facies belonging of lamproites it should be noted that there is a wide spreading (to one order and more) of microcrystalline oxides in the rocks of dyke facies as compared with the diatreme one and, parallelly to it, its structure is more coarse grained. The similar difference is observed between intrusive and tuff (or breccia) facies, but at somewhat lower level.

Taking into account the importance of microcrystalline extractions in the ground mass of spinels as more sensitive indicators of the surroundings of origin and evolution of the lamproite magma, we'll consider in more details the analysis of the typomorphic peculiarities of spinels. The most characteristic one is the following: the prevailing (or wide) development, among microcrystalline oxides, of high magnesian type of chromite in the ground mass of rich and diamond bearing rocks and their mainly homogeneous form of extractions. With the decrease of the rock diamond bearing, the homogeneous grains of chrome spinellides are changed into zonal extractions with chrome magnetite borders.

The range of spinellide of non-diamond bearing rocks is characterised by the clearly marked domination of the zonal chromite-chrome magnetite extractions over homogeneous chromite one and domination of homogeneous chrome magnetite and titanomagnetite differences. This tendency unanimously illustrates the direct link between the depth and oxide potential of the

developing lamproite system, on the one hand, and its diamond bearing, on the other hand.

On the basis of the magnetic data some peculiarities of ferrimagnetics reflecting the conditions of their formation can be discovered. In particular, for lamproites, containing zonal grains of chrome spinels, the curves  $I_m(T)$  in the heating cooling cycle are irreversible. Depending on the composition of the zones both the increase magnetization of  $I_m$  saturation and Curie  $T_c$  temperature (olivine - chrome spinellide) and the decrease of these parameters (chrome spinellide - magnetite) can take place. Chrome spinellides with the high content of chrome on the  $I_m(T)$  curve in the  $T < T_c$  field have a sharp decrease of  $I_s$  while  $T$  is increased. The  $I_m$  increasing in result of the thermo treating indicates the formation of ferrimagnetic phase with the high content of magnetite mineral (transformations pyrrhotine - magnetite, titanomagnetite - magnetite and ilmenite lamellae and others). In its turn, zonality and the titanomagnetization process show the conditions for less probable preservation of diamond. The availability of high chrome content, vice versa, proves the depth conditions of the lamproite formation. High content of titanomagnetite and magnetite proving the oxidation processes shows the unfavourable conditions for the diamond formation. It is reflected in high values of magnetic susceptibility  $\chi_o$ , magnetizations  $I_n$ ,  $I_m$ ,  $I_{ms}$  and the values of temperatures Curie  $T_c \approx 580^\circ\text{C}$ .

Thus, the study of oxides from the ground mass is the effective way to carry out the passportization of the lamproite bodies and their diamond bearing evaluation.

## NATURAL DIAMONDS GROWTH CONDITIONS ACCORDING TO THE MINERAL INCLUSIONS STUDY.

*Bulanova, G.P.*

*Yakutian Institute of Geological Sciences.*

The method of diamond cutting and polishing we used allows to study syngenetic inclusions in diamonds "in situ". The inclusions investigation is provided in close connection with diamond internal structure and its physical properties. The new approach to the diamond genesis reconstruction is founded on the idea of 3 heterogeneous areas existence in diamond crystals: central (yellow luminescence), intermediate (blue luminescence) and periferal one (no luminescence) (Bescrovanov, 1986). Accordingly, in diamond growth history there were three stages differing in physical-chemical conditions. The above areas particularly well seen if the growth form change is observed in crystal: cube (cubo-octahedral or rounded form) octahedren. This sequence of areas in diamonds reflectes the main line of diamond growth evolution, sometimes it may differ.

Inclusion confinement to this quazihomogeneous on physical properties area permit comparing of the chemical alteration in inclusions of the same name both in one diamond and in different ones. Thus it makes possible to identify the evolution of environment chemistry and PT-regime in diamond genesis. Only such confinement or location we consider to be genetic. Accordingly, only those syngenetic inclusions which belong to the same area of diamond are considered to be in true mineral equilibrium. Because the above zonal structure is thin it is evident that dramatic alteration in inclusion chemistry is unlike. We identified the differences in olivine and chromite composition. For inclusions of eclogite association they are fixed in the composition of omphocite and pyrope-almandine. Besides, the order of ultrabasic silicate inclusions crystallisation for the time of diamond growth was established:  $Ol \rightarrow Ol + En + Gr \rightarrow Ol + En + Gr + Cpx$ . This order is intirèly the same as the silicate crystallization order in ultrabasic melt (fluid). Thefore one can conclude that these diamonds grow as the first phase from carbon solution in silicate melt.

Our investigation didn't show any difference in internal structure of diamonds with ultrabasic and eclogitic inclusions suite. So we conclude that these diamonds grew in liquid environment too.

Besides zonal structure octahedren diamonds have zonal-sectoral and sectoral ones. It seems that macroinclusions (more than 20 mk) are located only in octahedren pyramids of growth in suth diamonds. Microinclusions (less than 20 mk) and particules were located in its cubic growth pyramides only.

It is a vary rare event when octahedren diamonds have no zonal structure. Our study shows that inclusions in them have no differences in composition.

Lately we began to study such morphological varieties of diamond as cubes and coated diamonds. Coated diamonds represent in contrast with thin zonality the rough one. The identity of the coat material and cubic diamonds (the II-Orlo's variety) is confirmed by their physical properties. It seems that cubic diamonds contain only microinclusions, like those in cubic sectors of octahedren diamonds. We identified rutile, sanidine, apatite, mica and carbonate microinclusions in cubic diamonds. Similar in composition microinclusions were founded in coated diamonds. They are presented by mixture of sanidine, rutile, apatite and

coesite (+/- Bt). Unfortunately, we failed to identify exactly their nature. Are they melt, partly crystalline or crystalline ones still unknown. But what is very important is the fact that they belong to eclogite association.

Within the ontogenetic approach to diamond investigation we began together with Matsyuk and Platonov (IGFM, Kiev) to study optical spectra of Gr, Ol, Cpx, and chromite. The results of the investigation shows that these minerals from diamonds have some crystal-chemical features which distinguish them from the minerals of mantle xenoliths. The main distinction is the lowest concentration of optically active centres of  $\text{Fe}^{3+}$  ions in mineral inclusions. It indicates a very low redox condition of their crystallization. The presence of  $\text{Cr}^{2+}$  ions in spinels confirm such conclusions. The ions of  $\text{Cr}^{3+}$  are in other mineral structures, including olivine. In enstatite structure Cr enters according jadeite isomorph scheme as Sobolev believed earlier. We plan to extend these investigations for inclusions from different areas of the same diamond crystal.

We consider that the ontogenetic approach to diamond and its syngenetic inclusions study is the most up-to-date and perspective method of investigation. Using it we hope to create diamond genesis model, based on the most objective available information given by diamonds themselves.

## THE EVOLUTION OF NATURAL DIAMOND GROWTH CONDITIONS.

*G.P. Bulanova and L.A. Pavlova.**Yakutsk Institute of Geosciences, Siberian Branch, Academy of Sciences, Yakutsk, USSR.*

A comprehensive study of whole diamonds from three Yakutian kimberlite pipes as well as plane-parallel plates cut out of them was carried out. From birefringence (BF), and photoluminescence (PL) patterns, the internal stratigraphy and change in luminescence colour were studied and the location of syngenetic inclusions in growth zones and areas was determined. The composition of inclusions were determined using the electron microprobe.

The purpose of the present study was to trace the evolution of growth conditions of natural diamond monocrystals from Yakutian kimberlite pipes.

Octahedral monocrystals show an inhomogeneous structure and a complicated growth history. Study of diamond anatomy by BR-patterns has established their growth characteristics: fine zoning, zoned-sectorial structure, dislocations, the presence of seeds, and the distribution of macro- and micro-inclusions. PL-patterns give a more general idea of the growth history of the crystals: change in growth morphology, alternation of physically homogeneous areas in various stones. Three heterogeneous areas that reflect the main trend of their growth history: central (yellow-luminescent) → intermediate (blue-luminescent) → peripheral (no luminescence) (Beskrovanov, 1986) are the most widespread in diamonds from the Mir pipe (ca. two-thirds). Such crystals also exhibit a change in growth morphology: cube, cubo-octahedron or rounded form → coarse layered octahedron → fine layered octahedron. Such diamonds constitute only one-third at Udachnaya and 23d Party Congress pipes. The greater part of octahedral diamond experience no change of growth form.

The zoned-sectorial distribution of syngenetic inclusions in diamonds was studied. For inclusions of the ultrabasic paragenesis, the following crystallization sequence of silicates was found:  $Ol \leftarrow Ol + Gr + Enst \leftarrow Ol + Gr + Enst + Cpx$ . This is similar to the crystallization sequence of silicates from ultrabasic melt (Mysen, Kushiro, 1977), suggesting that diamonds containing ultrabasic inclusions grew from carbon solution in a silicate melt (fluid).

A change in composition was found from chromite and olivine inclusions located in different zones in the same diamond crystal. For chromites, this change can be expressed as  $MgAl \leftarrow FeCr$  or  $Mg, Fe \leftarrow Fe(Cr, Al)$ . For diamond inclusion olivines, normal and inverse zoning is observed. This indicates different sources for mantle rocks from which the olivines and chromites were entrapped in diamonds.

Diamonds with the eclogitic suite of inclusions are similar in internal structure to diamonds with the ultrabasic inclusion suite. This indicates that they also grew in a liquid. A change in composition is shown by omphacites and pyrope-almandines from different growth zones in the same diamond. Coexisting pairs of these minerals become somewhat richer in Mg and Fe from central zone to peripheral.

"Coated" diamonds, which exemplify coarse zoning, were found to belong to the eclogitic paragenesis. Besides pyrope-almandine, omphacite, coesite and rutile, typical for this paragenesis, they also contain sanidine, biotite, apatite and micro-inclusions compositionally similar to melt inclusions. The same kinds of microinclusions were found by Naivon et. al. (1989). It appears that coated diamond forms at the final, subsolidus evolutionary stage of eclogite melts, whereas the coat itself forms from a fluid phase. Probably this fluid predated the appearance of kimberlite melt.

The results of the present study lead to several important conclusions about the growth history of natural diamond. Changes in the composition of mineral inclusions located in different growth zones of the same octahedral diamond are smooth and small, and are probably due to liquid (fluid) differentiation during the diamond growth. The temperature range of single diamond crystallization is 50 to 200°C, the  $fO_2$  value can vary from IW buffer to WM.

Different types of mantle rocks of ultrabasic and basic composition, formed in Archean time in the regions of stable cratons, are the sources of diamonds in kimberlite rocks. It appears that diamonds from each different source are characterized by their own evolution path.

## CHEMICO-GENETIC CLASSIFICATION OF THE MOST IMPORTANT MINERALS-SATELLITES OF THE DIAMOND.

*Bushueva, E.B.; Varlamov, D.A.; Garanin, V.K.; Kudrjavitseva, G.P.; Laverova, T.N. and Schepina, N.A.*

*Geological Department of Moscow State University, 119899, Lenin's Hills, Moscow, USSR.*

Typomorphic peculiarities of the chemical composition and physical properties of the main minerals-satellites of the diamond (garnet, clinopyroxene, orthopyroxene, chrome spinellide, ilmenite, rutile) are of great importance during the searching for the diamond deposits (kimberlites, lamproites and others) and estimation of their productivity. These minerals occur in the kimberlites as megacrystals, inclusions in diamond and in the diamond bearing peridotites and eclogites. A lot of works, including generalizing ones (Sobolev, 1974; Gurney, Moore, 1989; Garanin et al, 1990) are devoted to the application of the indirect mineralogical criteria during the estimation of the kimberlite diamond bearing. Chemico-genetical classifications of the diamond minerals-satellites represent the basis for the improvement of the known criteria of diamond bearing and for the development of the new ones.

The data banks and chemico-genetic classification of the most important minerals from all the inclusions in the diamond and from the aggregations with it, from the diamond bearing and nondiamond bearing xenolithes, peridotites, and eclogites as well as from megacrystals from the kimberlite rocks. The created data bank is based on more than 4000 electron-probe analyses of both original minerals and the ones borrowed from numerous literature sources.

The software used during the work with data base on the chemistry of minerals-satellites of the diamond includes statistical methods (cluster analysis and others), which are applied during the creation of chemico-genetic classifications. The method of the discriminant analysis is used to compare newly input electron-probe analyses with ones which already in the data bank and to refer them to the corresponding chemico-genetic group according to the coefficients values of the graphed discriminant functions.

The software ensures the definition of the correlations of diamond bearing and nondiamond bearing paragenesis in the analysed samples of minerals with the graphing of linear (column) and circle diagrams. Besides the packet of the applied programmes has been developed to carry out traditional re-calculation of MS analyses (the calculation of minals, crystallochemical coefficients and indicator relation), graphreflection of analytical results (printing of diagrams and histograms) and statistical processing within the range of every one from the separated cluster and chemico-genetic groups (calculation of average contents, root-mean-square deviation, carrying out of the correlation analysis and so on.).

The software allows to evaluate the rocks productivity with the application of all known by now indirect mineralogical methods and to improve the latter in the future.

The developed chemico-genetic classifications of minerals-satellites are the basis for the usage of the automatised systems to obtain the objective information about the diamond bea-

ring of the tested object in the relation of minerals-satellites of diamond bearing and nondiamond bearing paragenesis, about the contribution of the rocks of ultra basic or eclogite paragenesis into the diamond bearing of the tested object.

References:

1. Garanin, V.K., Kudrjavitseva, G.P., Mikhailichenko, O.A., and Marfunin, A.S. (1990) The inclusions in diamond and diamond bearing rocks, 272 p., Moscow University, Moscow
2. Gurney, J.J., and Moore, R.O. (1989) Geochemical correlations between kimberlitic indicator minerals and diamonds. The development of advanced technology to distinguish between diamondiferous and barren diatremes. Can.Geol.Survey, p.1-15
3. Sobolev, N.V.(1974) Deep seated inclusions in kimberlites and the problem of the composition of the upper mantle. English Translation by Brown, D.A., 1977, A.G.U., Washington D.C.

MINERALOGICAL-ISOTOPIC DYNAMICS, PHYSICO-CHEMICAL CONDITIONS AND STAGES OF SERPENTINIZATION PROCESS OF KIMBERLITES FROM YAKUTIA.

*K.N. Egorov; G.V. Bogdanov*

*Institute of Earth's Crust, 664033 - Irkutsk, USSR.*

Petrology of the serpentinization of kimberlites based on the analysis of samples of more than 20 pipes from various kimberlite fields in Yakutia, is discussed. Petrographic, thermal, X-ray diffraction and spectral methods coupled with electron-scanning and transmission microscopy were applied to study kimberlites and serpentine minerals. Some zones of metasomatic transformation of kimberlites depending on the degree of serpentinization, abundance ratio and mode of formation of different serpentine types together with associated secondary minerals are distinguished. A sequence of development of secondary mineral assemblages in these zones is as follows: 1) lizardite+chrysotile+magnetite; 2) lizardite+chrysotile+magnetite (up to 5-10%); 3) lizardite+chrysotile+calcite+magnetite+sulfides; 4) chrysotile+calcite+lizardite+magnetite+sulfides; 5) chrysotile+calcite+magnetite+sulfides. The chemical composition of secondary minerals depends on the sequential succession of zones. Microprobe analyses of lizardites (100 analyses) show appreciable CaO and Cl contents (0,29-1,04 wt.% and 0,98-1,07 wt.%, respectively). Lizardites of the intermediate zones are characterised by the highest Fe content (20-25%). Serpentes of such a composition represent the first occurrence in Yakutian kimberlites. During serpentinization Fe/Fe+Mg ratios and MgO, CaO contents gradually increase from the first zones to the last ones. The composition of chrysotiles (> 200 analyses) of all studied zones of secondary transformation of kimberlites strongly differs from that of lizardites. A higher Mg/Mg+Fe ratio, high Al<sub>2</sub>O<sub>3</sub> and low CaO, Cl

and MnO contents are characteristic of chrysotiles. With increasing degree of serpentinization the Mg/Mg+Fe ratio and Al<sub>2</sub>O<sub>3</sub> content of chrysotiles increase.

O, C, and Sr isotopic data indicate that chloride-calcic meteoric-hydrothermal waters derived from sedimentary rocks of the cover are responsible for the serpentine-carbonate mineralization of kimberlites. C and O isotopic compositions regularly change from light to more hard during serpentinization.

Analysis of mineral-petrographic, isotopic-geochemical data coupled with thermodynamical computing permits estimation of the physico-chemical conditions of kimberlite serpentinization. Acidity-alkalinity of the system varies from subacid reaction of solutions through alkaline and to neutral or acid one during the metasomatic transformation of kimberlites. At the first stages of kimberlite serpentinization the solutions are characterized by a high partial CO<sub>2</sub> pressure and higher activity of calcium chloride, which result in intensive dissolution and following Mg accumulation in solutions. The low chemical activity of silicon is characteristic of kimberlite serpentinization. The late episodes of magnesian metasomatism are characterized by low  $f_{\text{CO}_2}$  and high  $f_{\text{O}_2}$  and/or  $f_{\text{S}_2}$  values.

Kimberlite serpentinization displays a well defined allochemical character. Behaviour of components such as Mg, Si, Al, Fe completely depends on the type and degree of serpentinization. The increasing role of Mg removal with proliferation of kimberlite serpentinization is the main chemical feature of the process. The total chrysotilization of kimberlites proceeds with an increase in the Si and Al chemical potential under high alkalinity of solutions. The Fe migration during kimberlite serpentinization is regulated by the composition of fluid phase ( $f_{\text{O}_2}$  or

$f_{S_2}$ ) and by pH of the solution. The similarity and differences in serpentine mineralogy and physico-chemical conditions of the serpentinization of ultra-basic kimberlite inclusions are considered in details. Comparative characteristics of the kimberlite serpentinization and various genetic types of hyperbasites from the folded regions are presented.

EVIDENCE OF MAGMATISM, MATASOMATISM AND DEFORMATION PROCESSES  
OBTAINED FROM THE STUDY OF THE UNIQUE COMPOSITIONALLY COMPLEX  
NODULE FROM THE UDACHNAYA KIMBERLITE PIPE (YAKUTIA).

*K.N. Egorov; G.V. Bogdanov; L.V. Solovjeva; V.G. Barankevich and V.I. Lipskaya.*

*Institute of Earth's Crust, 664033 - Irkutsk, USSR.*

35x20 cm nodule of sheared peridotite is characterized by disturbed and laminar subtypes of mosaic porphyroclastic texture. Rock matrix consists of monomineral aggregate of olivine neoblasts, containing rare porphyroclasts of red-orange garnet, grass-green diopside, enstatite and olivine. Garnet and pyroxenes occur as large separate porphyroclasts or bimineral intergrowths (garnet-diopside, diopside-enstatite). 3x5 mm very jointy olivine porphyroclasts of lenticular or curved flattened shapes are gradually recrystallized at periphery into fine-grained neoblast matrix. 5x3 cm large enstatite crystals with irregular boundaries are broken into fragments which are pulled apart by olivine matrix. Fracture bands and cleavage crack curving leading to formation of cleavage microtexture, are observed in enstatite. Marginal parts of separate enstatite blocks are recrystallized into fine-grained aggregate of isometric crystals. Morphologically diverse diopside porphyroclasts vary from 3-5 mm up to 6-7 cm. Usually diopside porphyroclasts are recrystallized and are transformed into lens or lenticular intercalations of fine-grained porphyroblast matrix. Diopside displays a obvious evidence of plastic flow resulting in filling of fissures and interblock spaces as well as in partial rimming the garnet porphyroclasts and enstatite. A striking feature of the studied sheared peridotite is the intensive garnet deformation. 6x3 cm garnet porphyroclast are broken into separate fragments elongated in line. Configuration of garnet porphyroclasts are quaint. Minerals of sheared peridotite are che-

mically similar to megacrysts of titanium assemblage from kimberlites. Ferruginous olivine ( $\text{FeO} > 13 \text{ wt.}\%$ ) has the noticeable Ti and Ca contents. Enstatite enriched in Fe, Ti, Ca and Na is classified as high-titaniferous bronzite. Diopside porphyroclasts are a subcalcic variety ( $\text{Ca}/\text{Ca}+\text{Mg} \ 50\%$ ) containing  $0,3-0,4 \text{ wt.}\% \text{TiO}_2$ ,  $1,4-1,9 \text{ wt.}\% \text{Na}_2\text{O}$ ,  $1,8-2,0 \text{ wt.}\% \text{Al}_2\text{O}_3$  and  $0,3-0,5 \text{ wt.}\% \text{Cr}_2\text{O}_3$ . A high Ca/Ca+Mg ratio ( $> 50\%$ ) as well as low contents of  $\text{Al}_2\text{O}_3$  ( $0,4-0,8 \text{ wt.}\%$ ), FeO ( $2,5-3,5 \text{ wt.}\%$ ) and  $\text{Na}_2\text{O}$  ( $0,3-0,6 \text{ wt.}\%$ ) are characteristic of diopside neoblasts. Garnet is identified as titaniferous pyrope; it has  $1,3 \text{ wt.}\% \text{Cr}_2\text{O}_3$ ,  $4,5 \text{ wt.}\% \text{CaO}$  and  $0,15 \text{ wt.}\% \text{Na}_2\text{O}$ .

The deformation of garnet lherzolite was accompanied by an intensive metasomatism with separate minerals affected by melting. The melting process affects first of all marginal and weak inner zones of garnet. Microportions of melt are transformed into brown amorphous material saturated by the smallest chromite inclusions or they are crystallized into composite mineral aggregates. Interstices within garnet are composed of Al-orthopyroxene, Al-clinopyroxene, olivine, amphibole of pargasite series, Al-spinel, ilmenite, Ti-phlogopite, carbonate and sodalite. The mantle fluid components as  $\text{H}_2\text{O}$ ,  $\text{CO}_2$ , Cl, F, S as well as alkalis and Ti participated in partial melting of garnet lherzolite. Besides of the above-mentioned mineral parageneses thread veinlets of jouravskite and afwillite are observed in garnet. Clinopyroxene porphyroclasts are surrounded by an aggregate of calcic diopside neoblasts associated with Ti-phlogopite and spinel. Reactional olivine replacement by monticellite leading to homoaxial pseudomorphs formation is an unusual phenomenon. Ti-phlogopite and magnetite are developed between the monticellite grains and the olivine relicts. Monti-

cellite and signs of replacement of olivine by monticellite are absent in kimberlite including the nodule.

On the basis of the available data processes of textural and chemical transformation of garnet lherzolite and its genesis, are discussed.

GEOLOGY, PETROLOGY AND MINERAL COMPOSITION OF THE UDACHNAYA  
KIMBERLITE ORE COMPLEX (YAKUTIA).*K.N. Egorov; B.M. Vladimirov and G.V. Bogdanov.**Institute of Earth's Crust, 664033 - Irkutsk, USSR.*

The Udachnaya kimberlite ore complex consists of two large conjugate pipes, an eastern pipe, Udachnaya-Vostochnaya (UV) and a western pipe, Udachnaya-Zapadnaya (UZ), as well of three satellite pipe bodies and eight kimberlite veined bodies. The Mesozoic veins composed of potassic trachites and dykes of dolerite and trachidolerites are spatially associated with kimberlites. All kimberlite veins are intruded by satellite bodies and the UV and UZ pipes. A part of veined kimberlite bodies do not outcrop and occur only as fragments in the UZ and UV pipes. Satellite pipes are the "blind" bodies and do not contact with the UV and UZ pipes. The main UV and UZ pipes are characterized by a composite geological structure. Four phases of kimberlite emplacement are distinguished for the UZ pipe and five phases for the UV pipe. Intrusive contact relationships allowed to establish the sequence of formation for each pipes.

The history of formation of the Udachnaya kimberlite ore complex comprises four stages. Geological and radiological data show a significant (> 50m.y.) time interval between separate episodes of kimberlite magmatism. The first stage is characterized by the formation of kimberlite veins. The "blind" veined bodies are composed of mica kimberlite with pyroxene matrix, containing sometimes an abundant amount of sphene (10-20%). Mineral and chemical compositions of this kimberlite type are similar to those of olivine lamproites of Australia and lamprophyres of Swartruggens. The outcropped veins are composed of calcite kimberlite with a varying phlogopite content. Sr, C and O iso-

topic compositions together with Sr and Ba distribution in calcites from veins indicate that two sources (mantle and sedimentary) are responsible for carbonate formation. At the second stage stock-like bodies composed of monticellite kimberlite intruded the UV and UZ pipes. This kimberlite type (I phase) is characterized by a pronounced zoned olivine with higher Fe/Fe+Mg ratio and CaO content. Low mg and high content of impurities of Al, Ti and Na are characteristic of monticellite. A rare assemblage of sodium minerals (sodalite, zemkorite, shortite) occurs in matrix of monticellite kimberlite from the UV pipe. At the second stage another two phases are formed in UZ pipe: 1) massive kimberlite with phlogopite-carbonate matrix (II phase), 2) kimberlite breccia (III phase). Micaceous kimberlite composing a large intrusive body with vertical contacts in the UZ pipe, is mineralogically similar to veined carbonate kimberlite. The third stage is characterized by the greatest volume of kimberlite material represented in the form of: 1) kimberlite breccia of IV phase in the UZ pipe and 2) kimberlite breccias of II, III and IV phases in the UV pipe. At this stage three satellite pipes, composed of intensively carbonatized breccias are probably formed. The kimberlite breccia of the UZ pipe contains a lot of fragments of the early phases (up to 50-70%) and crust inclusions. In kimberlite breccias of the UV pipe an amount of xenoliths of country rock already comprising many mantle inclusions increases progressively from II to IV phase.

At the fourth stage of formation of the Udachnaya kimberlite complex a suite of veined bodies (V phase) is intruded into the UV pipe. The bodies are composed of massive kimberlite with olivine-monticellite matrix. This kimberlite type differs from monticellite kimberlite of stock-like bodies of I phase of the UV and UZ pipes in olivine, monticellite, spinel and other minerals contents.

Comparison of kimberlites of different ages within the complex shows the distinct differences in mineral, petrochemical and isotope-geochemical compositions. Kimberlites of each stage are characterized by its own composition and evolutionary trends of crystallization of silicate and particularly of ore minerals of phenocrysts as well as of matrix. Variations in mineral composition of kimberlites depend on distribution of petrogenetic oxides and rare elements in rocks.

Variety of comagmatic kimberlite rocks from the Udachnaya complex indicates that two initial magmas are derived from different (saturated and slightly depleted) mantle sources. In addition, evolution trend and degree of differentiation of each magma were different.

TREND OF SiO<sub>2</sub> IN GARNETS FROM KIMBERLITE PIPES.

G.D. Feoktistov and B.M. Vladimirov.

Institute of Earth's Crust, 664033 – Irkutsk, USSR.

Abstract. The trend of SiO<sub>2</sub> content in garnets from kimberlite pipes is studied statistically. The trend is established for garnets from kimberlite pipes of the Yakutian kimberlite province (Siberian platform) whose paragenetic associations have been previously described by N.V. Sobolev (1), from eclogites of metamorphic complexes (0,001–0,05% of Na<sub>2</sub>O) and from diamonds of the Mir pipe. The trend is established for garnets from kimberlite pipes of the Yakutian kimberlite province (Siberian platform) whose paragenetic associations have been previously described by N.V. Sobolev (1), from eclogites of metamorphic complexes (0,001–0,05% of Na<sub>2</sub>O) and from diamonds of the Mir pipe.

Chemical compositions of garnets from the Yakutian kimberlite province (Siberian platform) whose paragenetic associations have been previously described by N.V. Sobolev (1), were studied statistically. To this aim 122 chemical analyses of garnets from kimberlite concentrates, eclogite xenoliths, grosspyrites and disthen eclogites, from diamondiferous eclogites, from inclusions in diamonds, intergrowths with diamonds and associated with diamonds from Sobolev's work (1), were selected.

Regular surface trend of SiO<sub>2</sub> of second order in garnets in MgO-Al<sub>2</sub>O<sub>3</sub> and Cr<sub>2</sub>O<sub>3</sub>-CaO coordinates is established. Garnets enriched in Al<sub>2</sub>O<sub>3</sub> and MgO contain abundant SiO<sub>2</sub> in respect to total amount of RO and R<sub>2</sub>O<sub>3</sub>. MgO and CaO, Al<sub>2</sub>O<sub>3</sub> and Cr<sub>2</sub>O<sub>3</sub> pairs of oxides display the strongest negative correlations. SiO<sub>2</sub> have strong correlations: positive with MgO and negative with CaO. Moreover, SiO<sub>2</sub> shows a significant positive correlation with Al<sub>2</sub>O<sub>3</sub>, whereas its correlation with Cr<sub>2</sub>O<sub>3</sub> is negative, below the level of significance of correlation coefficient. The above correlations influence variation trend of SiO<sub>2</sub> content: in garnets it generally increases with increasing of MgO (less for Al<sub>2</sub>O<sub>3</sub>) and with decreasing of CaO (less for Cr<sub>2</sub>O<sub>3</sub>).

A stable increased admixture of Na<sub>2</sub>O (0,1–0,22%) compared to garnets from eclogites of metamorphic complexes (0,001–0,05% of Na<sub>2</sub>O) is established in garnets from diamondiferous eclogites (2). High contents of Na<sub>2</sub>O admixture are also observed in garnets enclosed in diamond (1).

Increased admixture of Na<sub>2</sub>O in garnets testifies (1) their belonging to high-pressure diamond-pyrope facies, with isomorphous replacement  $\text{CaAl} \rightleftharpoons \text{NaSi}$  taking place in such garnets. Possibility of this isomorphism is proved by experimental crystallization of garnet of Na<sub>2</sub>CaSi<sub>5</sub>O<sub>12</sub> composition at pressure up to 18 GPa (3). When synthesizing garnet phase at high pressure (10–20 GPa). A.E. Ringwood and A. Major (4) demonstrated the possibility of crystallization of pyroxene solid solution with garnet in which an excess of silica due to the entrance into the garnet composition of the mineral Mg<sub>3</sub>(MgSi)Si<sub>3</sub>O<sub>12</sub> appears, i.e. during isomorphous replacement  $\text{MgSi} \rightleftharpoons \text{AlAl}$ .

We found that variation trend of SiO<sub>2</sub> content in garnet evidences increase of SiO<sub>2</sub> content in garnet groups whose paragenesis obviously corresponds to diamond-pyrope facies (pyropes from intergrowths with diamonds of the Mir pipe and magnesian garnets included in diamond) and also in garnet groups extracted from rocks and possibly belonging to diamond-pyrope facies (garnets associated with diamonds, garnets of diamondiferous eclogites and chrome-pyropes poor in Ca, from kimberlite concentrate).

The presented data suggest that abundant silica content in garnet composition may indicate their formation under pressure corresponding to conditions of diamond-pyrope depth facies. Its appearance is possibly conditioned by the entrance into the garnet composition either of the mineral Na<sub>2</sub>CaSi<sub>5</sub>O<sub>12</sub> with simultaneous increase (>0,1%) of Na<sub>2</sub>O content, or of the mineral Mg<sub>3</sub>(MgSi)Si<sub>3</sub>O<sub>12</sub> with small admixture of Na<sub>2</sub>O in garnets.

## REFERENCES:

1. Sobolev, N.V. Deep-seated inclusions in kimberlites and the problem of the composition of the upper mantle. – Novosibirsk, Nauka, 1964, 264 p.
2. Sobolev, N.V., Lavrent'ev Yu. – Contrib. Miner. Petrol., 1971, vol. 37, p. 7-12.
3. Ringwood A.E., Major A. – Earth and Planet. Sci. Lett., 1971, vol. 12, n<sup>o</sup>. 4.
4. Ringwood A.E., Major A. In: Petrology of the upper mantle. – M.: Mir, 1968, p. 203-273.

## ISOTOPE FRACTIONATION RELATED TO KIMBERLITE MAGMATISM AND DIAMOND FORMATION.

*Galimov, E.M.*

*V.I. Vernskii Institute of Geochemistry and Analytical Chemistry, Academy of Sciences of the USSR,  
Kosygin str. 19, B-334 Moscow, USSR.*

Experimental data on carbon isotope composition of diamond, carbonate component of kimberlite, graphite, and organic carbon related to kimberlite minerals obtained during study of diamond bearing sources of East Siberia and some other regions show that  $\delta^{13}\text{C}$  values of different forms of carbon related to kimberlite magmatism vary widely: from -35 to +35 ‰.

The median value of  $\delta^{13}\text{C}$ -distribution for about 2000 diamonds studied in our laboratory is -4.54 ‰. More than 90% of diamonds from kimberlites have  $\delta^{13}\text{C}$  which fall into the narrow range: +4‰ of this value. However the whole range of variation of carbon isotope composition of natural diamonds is from -34 to +2.8‰. On the basis of analysis of more than 600 diamonds, containing mineral inclusions, it has been established, that diamonds of ultrabasic paragenesis have  $\delta^{13}\text{C}$  values almost entirely within the narrow range of  $\delta^{13}\text{C}$  variations: -4.5+4, whereas  $\delta^{13}\text{C}$  of diamonds of the basic (eclogitic) paragenesis cover the whole range of the isotope variations for diamonds. When a diamond consists of several sequential generations of growth (coated diamonds, diamond-in-diamond),  $\delta^{13}\text{C}$  values of the early generation varies widely whereas the isotopic composition of the later is more uniform. The  $\delta^{13}\text{C}$ -distribution for diamonds is specific for a particular occurrence (different kimberlite pipes, different regions etc.).

Carbonates of magmatic origin in kimberlites from pipe Udachnaya are characterized by  $\delta^{13}\text{C}$  values similar to those for diamonds of the ultrabasic paragenesis from the same pipe. However some autholiths are extremely enriched in  $^{13}\text{C}$  as high as +35‰. Organic compounds in kimberlites, including that occurring in fluid inclusions of magmatic minerals (olivine and pyrope) are depleted in  $^{13}\text{C}$  down to -30‰.

One of the possible causes of the observed isotope variations is believed to be the incorporation of the crustal carbon into the mantle. However this idea is inconsistent with some of the regularities observed, e.g. existence of the isotope heterogeneity within the same crystal, difference between internal and external parts of coated diamonds, peculiarities of isotope distribution for diamonds from different kimberlite bodies and of different paragenesis. Also, the range of the isotope variations of magmatic carbon in kimberlites is comparable or even exceeds that of sedimentary carbon of the oceanic crust, including both of its carbonate and organic form. It is unlikely that the subducted carbon would retain the isotope heterogeneity in full scale.

The alternative explanation of the isotope variations is based on the possibility of significant isotope fractionation in the mantle. Isotopic fractionation under equilibrium conditions at high temperature is small and may have been responsible for a maximum fractionation of 3-5%, depending on temperature and composition of C-H-O system. However, even small isotope effects between two components may provide large isotopic fractionation, if these components have different distribution coefficients between phases of a system, and these phases may spatially be separated. This situation may occur if a reduced subasthenospheric fluid interacts with the relatively oxidized lithosphere. As fluid ascends isotope fractionation between reduced and oxidized carbon in conjugation with the Rayleigh distillation mechanism may result in high enrichment of the residual carbon of the fluid in the light isotope.

On other hand, the same process, supposed, which leads to the isotope fractionation of carbon in the fluid may bring about formation of a basic melt. This might explain why the isotopically light diamonds are associated with the basic assemblage of the mineral inclusions.

The oxidized lithosphere could appear not from the beginning of the Earth history. If the ancient mantle was completely reduced, the mechanism of the isotope fractionation could not operate and isotopically light diamonds could not occur at that time. Moreover, if appearance of the eclogite assemblage related to the same process, diamonds of eclogite paragenesis could not occur among the most ancient diamonds. In the extreme case, which cannot be ruled out, the ancient diamonds could be predominantly (if not entirely) of ultrabasic paragenesis while the younger diamonds are predominantly (if not entirely) of eclogitic paragenesis. The boundary between "the ancient" and "the younger" depends on the actual history of the evolution of the redox state of the mantle. It might be elucidated by the carbon isotope study of diamonds combined with geochronology study of their mineral inclusions.

The same approach may be applied to consideration of isotope fractionation related to the carbonate component. The  $\delta^{13}\text{C}$ -value of about -5 ‰ is initial for the  $\text{CO}_2$  component of the mantle as well. Under high pressure mantle rocks contain  $\text{CO}_2$  in carbonate form. When the carbonate bearing rocks or melts get the shallower depths which correspond to the boundary of stability of carbonate (at the pressure less than 25 kbar under  $T > 1100^\circ\text{C}$ ) carbonate decomposes and  $\text{CO}_2$ -gas is released. Expansion of the gas must have brought

about propagation of a fracture, through which the fluidizing magma could rush to the surface. This process must also be resulted in adiabatic drop of temperature. When temperature decreases to about  $700\text{--}800^\circ\text{C}$  carbonates again become stable and  $\text{CO}_2$  reacts with the silicates (even in a low pressure). Experimental study showed that reaction of  $\text{CO}_2$  with  $\text{CaO}$  was accompanied by kinetic isotope effect up to 10,5 ‰. With an isotope effect of this magnitude the Rayleigh distillation process may result in enrichment of the residual  $\text{CO}_2$  greater than +40%, when less than 1% of the  $\text{CO}_2$  remains unbound.

Hence one can explain occurrence of the  $^{13}\text{C}$ -enriched calcite in kimberlite, in particular, in the form of autoliths. The mineralogical peculiarities of the latter, which are believed to indicate that they crystallized from a turbulent flow of a fluidizing magma, are in agreement with the mechanism of their enrichment in  $^{13}\text{C}$  isotope suggested here.

The adiabatic cooling also provides a possible explanation for several other curious features of kimberlite magmatism. It is known that kimberlite magma, despite the fact that it moves rapidly from a high-temperature zone, is relatively cool. The walls of kimberlite pipes and xenolites do not bear any evidence of strong thermal alteration. Besides, since kimberlites are rich in a  $\text{CO}_2$ -component, many believe that a kimberlite magma is essentially degassed during formation of a kimberlite pipe and consequently loses a large amount of  $\text{CO}_2$ . However there exists an almost stoichiometric correspondence between  $\text{CO}_2$  and  $\text{CaO}$  content in different kimberlites, that indicates that kimberlite magma loses little (if any) its  $\text{CO}_2$  component. This is in agreement with the model suggested.

## NEW TECHNOLOGY OF THE SEARCHING OF THE DIAMOND BEARING KIMBERLITES METHODOLOGICAL BASIS AND FIELDS OF APPLICATIONS.

*Garanin, V.K. and Kudrjavitseva, G.P.*

*Geological Department of Moscow State University, 119899, Lenin's Hills, Moscow, USSR.*

The development of diamond deposits and searching for the new ones in Archangelsk and Jakutian kimberlite provinces, industrial development of the deep horizons on the working pit as well as retesting of the numerous kimberlite bodies in the Jakutian diamond bearing province facilitate the need for the development and active usage of the mineralogical methods of the evaluation of the kimberlite diamond bearing. New mineralogical criteria for the searching of the diamond deposits have been offered by the laboratory working on the problems of the diamond deposits of the Geological Department of Moscow University. These methods together with remote sensing methods form the basis of the new technology of the diamond deposits searching.

The complex methodology of diamond bearing evaluation is based on the two groups of the mineralogical criteria.

The first group of criteria allows to evaluate the potential diamond bearing of the object. They are based on the typomorphism of the mantle minerals from the inclusions in the diamond, intergrowths with it, from the diamond bearing peridotites, pyroxenites and eclogites as well as on the typomorphic peculiarities of the chrome spinels composition and picroilmenite from the ground mass of the kimberlite rocks. The criteria of this group are necessary but not sufficient to define the tested object as a diamond bearing one.

The second group of the mineralogical criteria defines the degree of the diamond crystals preservation during their delivery to the surface by the kimberlite system. The slow rate of xenogenous material raise, including diamond in the conditions of the increasing influence of the oxidation potential and alkaline-carbonate melt in the conditions of the increased temperatures facilitates the "burning" of the diamond and leads to the decrease of the kimberlite diamond bearing. The same conditions effect the chemical and phase composition of minerals-sattelites of the diamond (MSD) and microcrystalline spinels and ilmenite from the ground mass of kimberlites.

The most contrast changes are connected with the formation of the kelyphite rims on the garnets and rims of replacement on the grains of olivine, chromediopside, ilmenite, chrome spinel and other minerals by the formation of the resorbed surfaces on the MSD grains with the characteristic shapes of the microrelief, with the wide development of the decomposition solid solution structures in the MSD grains, with the formation of the different set of minerals in the kimberlite cement as a result of replacement and of fractioning of the kimberlite magma (chrome spinels of varying composition, titanomagnetite, manganese picroilmenite, rutile and perovskite).

The mass crystallization of perovskite shows the high alkalinity of mineral formation surroundings and directly defines the poor diamond bearing of the tested object.

The priority of the mineralogical criteria of the diamond bearing deposits searching developed in this laboratory is protected legally by a series of the authors certificates and their efficiency is tested on the several objects of the Archangelsk and Jakutian diamond bearing provinces.

The complex methodology is realised on the basis of the analytical complex, including the automated systems for the analysis, processing, storage and accumulation of the newly input information (Fig.1). The technological process provides the highly efficient express and local analysis of morphology, physical properties, chemical and phase composition of minerals. The data bank for all the most important MSD has been set up and realised to develop the chemico-geological MSD classification both from the xenolithes of the depth rocks and from the ground mass of kimberlites, to define the typomorphism of minerals from the diamond paragenesis and the usage of this information to solve different search-evaluation problems.

The results of cluster analysis together with the available mineralogical information allowed set up chemico-genetical classifications for MSD with the extraction of typochemical features of the diamond paragenesis. The defining laws for sorting out (according to the types) the mineral paragenesis of newly incoming mineral analysis were calculated on the basis of discriminant analysis. The whole package of programmes with graphical supplement for the statistical processing of the results of the MSD investigation on the personal computers was set up.

The chemico-genetical MSD classifications are the basis for the effective work of the complex methodology with the application of the automated systems. The essence of the methodology, which has been realized on the new chemico-genetical classification of MSD with usage of the MSD data base in the combination with mighty analytical complex, lies in the complex study of diamond minerals-sattelites by different methods on the basis of the complex of mineralogical criteria of diamond bearing with the purpose to show the preservation of mineral parageneses, statistical spreading along the deposit, extraction among them the diamond bearing parageneses. The advantage of the methodology is achieved by the increase of evaluation reliability of the kimberlite ore bearing as a result of the complex approach, i.e. not only on one, but on the complex of signs considering not only the possibilities of the diamond crystal formation but also its preservation in the process of delivery to the surface.

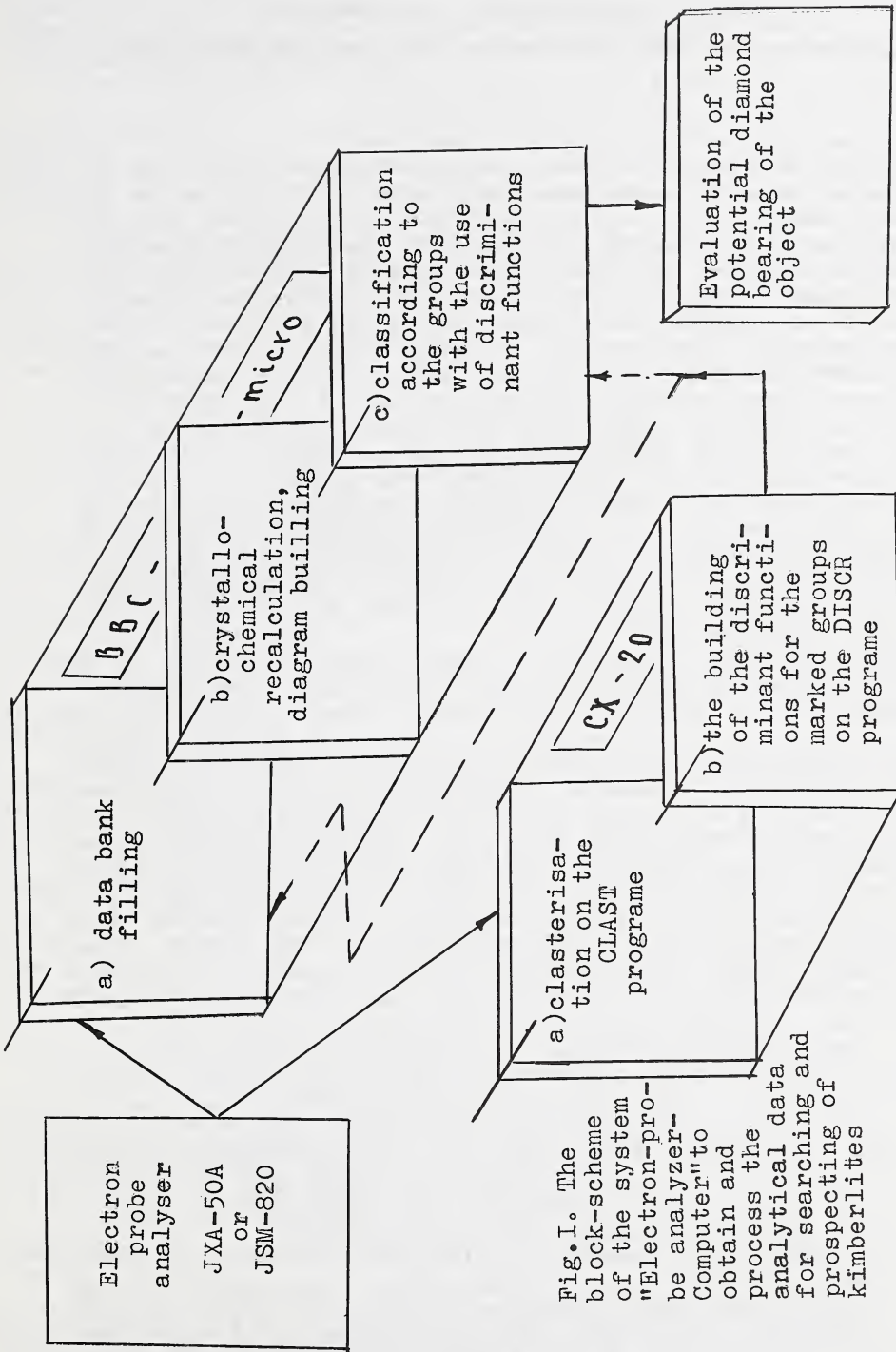


Fig. 1. The block-scheme of the system "Electron-probe analyzer" to obtain and process the analytical data for searching and prospecting of kimberlites

## THE COMPARATIVE CHARACTERISTICS OF ILMENITE FROM THE KIMBERLITE PROVINCES OF THE USSR.

*Garanin, V.K., Kudrjavitseva, G.P. and Laverova, T.N.*

*Geological Department of Moscow State University, 119899, Lenin's Hills, Moscow, USSR.*

Ilmenite is a widely spread mineral in the kimberlite pipes of the Jakutian diamond bearing province. It occurs as inclusions in the diamonds, impregnations in the ground mass of kimberlite, in xenoliths of the mantle rocks (peridotites, pyroxenites, eclogites), including the diamond bearing ones. It is the accessory mineral of the kimberlite rocks. Two genetic sources of this mineral are discovered in the Jakutian kimberlites: a) ilmenite - the product of disintegration of the abyssal rocks of ultrabasic and basic composition and metasomatized rocks; b) ilmenite from the ground mass of kimberlites.

Ilmenite from the deep rocks is characterized by the considerable range of the composition. Several stages of the ilmenite rock formation are established. The genesis of this mineral is connected with the evolution of magnesian-ferrous mantle melt, enriched by titanium. Crystallization differentiation in combination with liquation leads to the crystallization of the mottled series of the ilmenite rocks: peridotites, pyroxenites and eclogites. The earliest of them are crystallized in the diamond stability field.

Ilmenite from the ultrabasic rocks is characterized by the high content of magnesium (more than 6 wt.% MgO), increased - of aluminium (0.4 wt.%  $Al_2O_3$ ) and chromium (more than 0.4 wt.%  $Cr_2O_3$  to 10 wt.%); from eclogites - low content of magnesium (less than 4 wt.% MgO), aluminium (0.3 wt.%  $Al_2O_3$ ), chromium (0.2 wt.%  $Cr_2O_3$ ) and somewhat increased content of manganese (more than 0.5 wt.% MnO). The trend of the ilmenite rocks evolution is finished by the formation of original high-ferrous garnet-ilmenite intergrowths; the ilmenite in them is characterized by high content of hematite mineral (>20 mol.%  $Fe_2O_3$ ) and low one of geikielite (<25 mol.%  $MgTiO_3$ ) and possesses the ferrimagnetic properties at room temperature. The similar ilmenite is widely spread in the central part of Jakutian province (Malo-Botuobinskoje field), the bodies there are characterized by the highest diamond bearing. In this case, the presence of ilmenite influences considerably the magnetization over the kimberlite pipes of this region. The regular change of the composition of ilmenite from the ultrabasic rocks, is observed in the northern direction during the transition from the central field to the periphery of the province: its contents of magnesium and chromium in the ilmenite are increased and the degree of the change of rocks as a result of the occurrence of the processes of the mantle metasomatism is increased.

In some kimberlite bodies, in ilmenite nodules, the lamellas of decomposition of the solid solution, represented by the chrome spinels of the varying composition are widely observed. The regular connection between the wide spreading of the similar ilmenite and decrease of the kimberlite bodies diamond bearing is discovered. The mineralogical criterion of the evaluation of the kimberlite bodies diamond bearing has been developed on the basis on the phase heterogeneity of ilmenite.

The ilmenite composition from the ground mass of kimberlites is being regularly changed from high magnesian (MgO >

5 wt.%) of chrome ilmenite in the productive pipes and low magnesian ( $\text{MgO} < 5 \text{ wt.}\%$ ) manganese in poor productive pipes. The differences in the ilmenite composition from the kimberlite rocks of different phases of intrusion are observed. In this case, the rocks of later phases (less deep ones) contain ilmenite enriched by manganese.

The sequence of crystallization of the mineral of the kimberlite ground mass during the decrease of PT-parameters of the surroundings is established: high magnesian olivine ( $\text{Fo} > 90\%$ ) + high titanium chrome spinel  $\rightarrow$  magnesian olivine ( $\text{Fo}$  from 90 to 92 %) + high magnesian ilmenite  $\rightarrow$  chrome containing titanium magnetite  $\rightarrow$  perovskite + rutile  $\rightarrow$  magnetite.

Ilmenite in the diatremes of the Arkhangelsk diamond bearing province is spread only in the two out of five fields in its eastern border. The diamond bearing of these kimberlite bodies is rather poor. The pipes are characterized by the high content of ilmenite nodules at the non-considerable presence of the chrome spinels grains. Xenoliths of ilmenite ultrabasites also occur. The size of the ilmenite nodules is usually less than 5 mm, i.e. considerably less than the size of ilmenite nodules in the Jakutian and South African kimberlites (to 10 cm). The impurities of aluminium (less than 0.7 wt.%  $\text{Al}_2\text{O}_3$ ), chromium (to 7 wt.%  $\text{Cr}_2\text{O}_3$ ), manganese (to 0.5 wt.%  $\text{MnO}$ ) are characteristic of ilmenite. In a whole, the increased content of magnesian (from 10 to 17 wt.%  $\text{MgO}$ , in average - 13 wt.%) and decreased - of the  $\text{Fe}^{3+}$  (less than 14 mol.%  $\text{Fe}_2\text{O}_3$ ) are noticed for ilmenite. The ilmenite composition in general is stable, independent on the diatreme location and it is located on the diagrams in the coordinates  $\text{MgTiO}_3$ - $\text{FeTiO}_3$ - $\text{Fe}_2\text{O}_3$  and  $\text{MnO}$ - $\text{Al}_2\text{O}_3$ - $\text{Cr}_2\text{O}_3$  in the same field. It is close to the ilmenite composition from the pipes of Daldino-Alakitski and more northern fields of the Jakutian kimberlite province.

Among xenoliths of the deep rocks in the Arkhangelsk diatremes, only ilmenite hercynites with orange-red low chrome and ferrous garnets are discovered and it shows the genetic affinity of the ilmenite nodules mainly to these rocks. The grains of ilmenite of the eclogite paragenesis occur very seldom and they are characterized by low magnesian content (less than 3.0 wt.%  $\text{MgO}$ ), chromium (less than 0.01 wt.%  $\text{Cr}_2\text{O}_3$ ) and are typical for xenoliths of magnesian-ferrous eclogites. Thus, in the Arkhangelsk diamond bearing province, the diatremes with extreme ilmenite specialization and extremely low diamond bearing poor represented mineral-satellites of diamond, and xenoliths of the magnesian series of ultrabasic rocks, occur.

It should be noted, that ilmenite in the kimberlite cement occur in the same diatremes, though it is not the most abundant mineral. Low magnesianity (less than 1 wt.%  $\text{MgO}$ ), increased manganeseanity (1-5 wt.%  $\text{MnO}$ ), low aluminium content (less than 0.6 wt.%  $\text{Al}_2\text{O}_3$ ) and chromium (less than 0.8 wt.%  $\text{Cr}_2\text{O}_3$ ) are characteristic for ilmenite.

In general, ilmenite is similar to the mineral from the non-productive pipes of the northern fields of the Jakutian province.

The following sequence of crystallization of minerals of the kimberlite ground mass from the Arkhangelsk province is established: Al-Ti-containing chrome spinel  $\rightarrow$  chrome ulvospinel  $\rightarrow$  rutile  $\rightarrow$  ilmenite  $\rightarrow$  titanomagnetite.

Thus, the definite mineralogical and geochemical specialization of the two biggest diamond bearing provinces of the USSR, showing completely different conditions of the evolution not only of the minerals of magnesian-ferrous series of the mantle rock, but also kimberlite melts, is observed.

## MINERALOGY OF OXIDES FROM THE GROUND MASS OF KIMBERLITES OF JAKUTIJA AND NORTHERN EUROPEAN PART OF THE USSR.

*Garanin, V.K., Kudrjavitseva, G.P. and Michailichenko, O.A.*

*Geological Department of Moscow State University, 119899, Lenin's Hills, Moscow, USSR.*

The complex approach towards kimberlite studies taking into account their geologico-structural position in the combination with the detailed mineralogical investigations is thought to be the most reasonable approach during the search for the deposits of diamonds and the evaluation of their productivity on the basis of the indirect mineralogical criteria and with the substantial shortage of the expensive drilling. During the fulfillment of the complex approach to the kimberlite studies a series of the laws of the kimberlite formation is being discovered and it provides the scientifically based methods for the purposeful mineralogical search for the diamond bearing evaluation with ones available now ( on the chrome content of garnets and chrome spinels - N.V.Sobolev with co-authors ; on the IR-spectra of chrome spinels - I.J.Nekrasov and others) has set up the basis for the introduction of the methodology of the forestalling testing of the kimberlite bodies with small volume of drilling. It is reasonable to introduce this methodology at the preliminary stage of the kimberlite testing to find out the first priority objects for their further detailed geological survey and evaluation of the perspectives of the diamond bearing of a region in general.

Many theoretical problems of the kimberlite formation and some practical tasks call for fundamental research of ilmenite and spinels from the kimberlite ground mass. The authors have carried out a considerable volume of the analytical work widely using the electron-probe analysis method and image analysis for ilmenite and spinels in the association with olivine, rutile, perovskite and other minerals from the ground mass of the kimberlite rocks.

The representative data have been chosen from the kimberlite pipes of the central regions (Malo-Botuobinski, Daldyno-Alakitski) and peripheral regions ( Kuonamskoje, Kharamaiskoje) of the Jakutian diamond bearing provinces and from the central field (Zolotizkoje) and frontier fields (Verkhotinskoje, Kepinskoje, Sojanskoje) of the Arkhangelsk kimberlite province. The carried out investigations allowed to define the position of spinels and in the process of the kimberlite formation evolution. The peculiarities of the space distribution and oxides composition in the kimberlite bodies of the Jakutian and Arkhangelsk diamond bearing provinces have been defined.

In the Jakutian diamond bearing province :

1. Spinels from the kimberlite ground mass show typomorphism of the composition. The peculiarities of the chemical and phase composition of these minerals are sensitive indicators of the changes of the conditions of the mineral formation surroundings.
2. The increase of the share of magnetite mineral in the spinel composition from the kimberlite ground mass is definitely accompanied by the decrease of the original productivity of the kimberlite pipes.

3. The highly productive central regions are characterised by the prevailing role of ilmenite in the cement composition, including the zonal separation of this mineral with the borders of titanomagnetite; the similar zonal structures are not practically marked for the peripheral regions of the province where titanomagnetite is most widely spread among oxides.
4. Typomorphism of the composition of the investigated minerals in the kimberlite bodies of the central and frontier parts, emphasizing the zoning of the Jakutian diamond bearing province and conforming the poor productivity of kimberlites along the periphery has been established.

In the Arkhangelsk kimberlite province:

1. In the heavy fraction of the Zolotizkoje field diatremes spinels prevail sharply in amount over the other minerals-satellites of diamond. Picroilmenite occurs only in single signs.

Only magnesian Al-Ti containing chrome spinels are spread in the kimberlite ground mass. Chrome ulvospinel (as a rule on the upper horizons of diatremes) is formed in the borders round the nuclei of Al-Ti containing chrome spinels for some diatremes.

2. In the diatremes of the northern ground of bodies the minerals of the heavy fraction are represented by spinels, garnets, chrome diopside. The content of the heavy fraction minerals is considerably less than in the central field. Picroilmenite is absent.

Cr-Al-containing titanomagnetite with clearly subordinate (single extractions of Al-Ti containing chrome spinels is the prevailing ore mineral of the kimberlite ground mass. The diatremes are poor diamond bearing.

3. In the diatremes of the south-eastern group among the heavy fraction minerals picroilmenite, sometimes, picroilmenite and garnet (mainly red-orange, typical representative of ilmenite hyperbasites and sheared lherzolites) prevail. Chrome spinels are considerably less spread.

There's a rather wide set of ore minerals in cement (as compared with central and northern fields); there are single grains of magnesian Al-Ti containing chrome spinels and magnesian ulvospinel. Titanomagnetite and picroilmenite with the increased manganese content are spread to a greater extent. Rutile is the prevailing ore mineral. Diatremes are very poor diamond bearing.

4. Recently non diamond bearing diatremes of effusive appearance, represented by basaltoids have been discovered in the Arkhangelsk province on the eastern frontier of the craton (east-northern-east).

The single signs of the minerals-satellites of diamond are discovered in the heavy fraction of these bodies (garnet and chrome spinels). Al-Mg-containing titanomagnetites with complete absence of magnesian Al-Ti-containing chrome spinels are widely spread in cement.

As the result of the carried out investigations the general scheme of the kimberlite fluid evolution of the basis of the crystallised sequence of oxide separation has been offered, the new mineralogical criteria of the diamond bearing evaluation of the kimberlite bodies have been developed according to the peculiarities of ilmenite composition (determination of MgO and MnO) and spinels (determination of magnetite  $\text{FeFe}_{\approx 0.4}$  and ulvospinel  $(\text{Mg,Fe})_{\approx 2}\text{TiO}_4$  components) from the kimberlite

ground mass effective for usage in combination with other indirect mineralogical methods (on xenocrystals of olivine, garnet, clino- and orthopyroxene, chrome spinels and others minerals), especially when the "outcome" of the core is very small and the content of the mineral-satellites in the concentrations of the enrichment of kimberlites is not representative enough.

High information capacity of ilmenite and spinels from the kimberlite ground mass has been established in genetic and applied aspects. It proves some disadvantage of narrow investigations (only spinels, only ilmenite, only phenocrysts, only nodulars, etc.) and this narrow investigation is opposed by the complex one (the most complete one) for studying different mineral phases in kimberlites.

The discovered mineralogical specialization of the fields is correlated with the diamond bearing and allows to region the provinces and to sort out the new bodies with the high degree of reliability and to define the most perspective ones for diamonds among them.

PETROGENESIS OF PRAIRIE CREEK LAMPROITES: CONSTRAINTS FROM MELT INCLUSIONS AND HIGH-PRESSURE EXPERIMENTS.

*A. Gimis; I. Solovova; I. Ryabchikov and L. Kogarko.*

Crystalline, fluid and melt microinclusions in minerals of Prairie Creek (USA, Arkansas) lamproites have been studied in order to obtain information about composition and crystallization conditions of melts. It was shown that shallow-level crystallization proceeded at temperatures 1050-1150°C, while olivine, clinopyroxene and Cr-spinel were liquidus minerals. At this stage liquid was saturated by predominantly CO<sub>2</sub>-H<sub>2</sub>O fluid with CO<sub>2</sub> pressure being more than 4 kb. Silicate melts contain up to 14 wt.% of K<sub>2</sub>O at about 7-9 wt.% MgO. Also typical are high concentrations of P, Ti, Ba, F and very high K/Al ratio. Based on the chemistry of homogenized melt inclusions the composition of the least evolved liquid have been calculated - (wt.%) SiO<sub>2</sub> 44.1, TiO<sub>2</sub> 4.4, Al<sub>2</sub>O<sub>3</sub> 4.5, FeO(t) 9.3, MgO 17.8, CaO 3.8, BaO 1.5, K<sub>2</sub>O 9.9, Na<sub>2</sub>O 2.4, P<sub>2</sub>O<sub>5</sub> 2.4. Similar liquid must have been in equilibrium with mantle residual assemblage. Synthetic material of such composition have been prepared and used in melting experiments conducted at 5-20 kb total pressure with pure H<sub>2</sub>O, H<sub>2</sub>O-CO<sub>2</sub> fluid as well as at fluid absent conditions. At all parameters the first crystalline phase is olivine. Further crystallization sequence depends critically on fluid regime:

dry	OL - OL+CPX
H <sub>2</sub> O	OL - OL+PHL - OL+PHL+CPX
H <sub>2</sub> O-CO <sub>2</sub>	OL - OL+OPX - OL+OPX+PHL

Assuming that natural fluid was predominantly a mixture of CO<sub>2</sub> and H<sub>2</sub>O, we conclude that initial lamproitic melts were in equilibrium with phlogopite-bearing harzburgitic residua. A little amount of garnet probably was also retained in solid residua. Extrapolating phase equilibrium data the conditions of primary melt generation have been assessed - about 40 kb and 1400°C.

# AL-SOLUBILITY IN ORTHOPYROXENE IN EQUILIBRIUM WITH GARNET: A REINTERPRETATION OF EXISTING EXPERIMENTAL DATA AND THE PETROGENETIC IMPLICATIONS IN GARNET PERIDOTITE XENOLITH.

Yu. N. Kolesnik.

Institute of Geochemistry and Physics of Minerals Acad. Sci. of Ukrainian USSR. Palladin Prospekt,  
34. 252068 Kiev 68, USSR.

Finnerty and Boyd (1984) discovered that the application of available correction schemes for solution of other components (concerning MAS) in pyroxenes and garnet decreased both accuracy and precision of P,T estimates. The discrepancies are likely to be a result of imprecision in activity models for silicates. The proposed orthopyroxene - garnet geobarometer is recalibrated incorporating the determination of the high temperature equilibrium fractionation of elements between different sites in orthopyroxene structure, based on the statistical thermodynamic principles. We took into account the experiments in MAS, CMAS, FMAS, CFMAS systems and obtained a close agreement with thermochemical properties of minerals. Only three empirical constants are used ( $\Delta S^\circ$  and  $\Delta H^\circ$  of the reaction  $Mg_2Si_2O_6 + MgAl_2SiO_6 = Mg_3Al_2Si_3O_{12}$  and  $V^c$  - Function of Mg-Tschermak component).

The results of isopleth calculations and of estimated stability fields in P,T space of some garnet peridotite xenolith in CFMAS (and partly Cr) system are shown on Fig.1,2.

The remarkable feature of the new P,T determinations is that the equilibrium field of diamond - bearing peridotite and inclusions in diamond (vertical bars on Fig.2) are drawn along the line of conductive geotherm for surface heat flow  $40 \text{ mW/m}^2$  calculated by Pollack et al (1977) (fat solid line on Fig.2). The T estimates were made with two-pyroxene (Wells, 1977 and Lindsley, 1983) and garnet-olivine (O'Neill, Wood, 1979) geothermometers. The field of diamond-bearing peridotite covers a temperature range  $T > 1000^\circ \text{C}$  which satisfies the diamond-graphite constraint. Temperature of other garnet peridotite xenoliths (dotted area on Fig.2) are higher in relation to "cool" shield geotherm. The estimated boundary between this field and the field of P,T distributions for suits of garnet lherzolite from southeast Australia, Solomon Islands (Malaite), Canada (Ile Bizard) as well as from alkali basalts, lamprophyres and some carbonatites (dashed area on Fig.2) - lies near the ledge on the solidus for peridotite- $\text{CO}_2$ - $\text{H}_2\text{O}$  after Wyllie, 1979 (broken fat line on Fig.2).

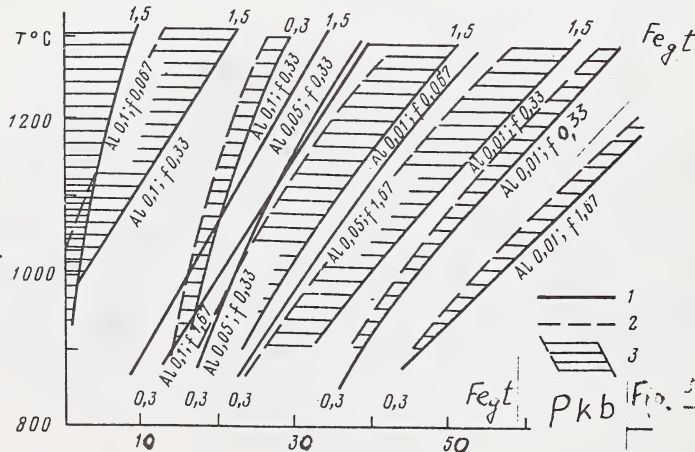


FIGURE CAPTIONS

Fig.1 Calculated data on the alumina solubility in orthopyroxene in equilibrium with garnet in the CFMAS system.

1.  $Al/2 = Al(VI)$  - isopleth in orthopyroxene as well as isopleth of iron fractionation "f" between coexisting garnet and orthopyroxene:

$$f = Fe_{opx} / Fe_{gt}$$

, where  $Fe_{opx}$  - the iron amount in  $(Fe, Mg, Al)_2(Si, Al)_2O_6$ .

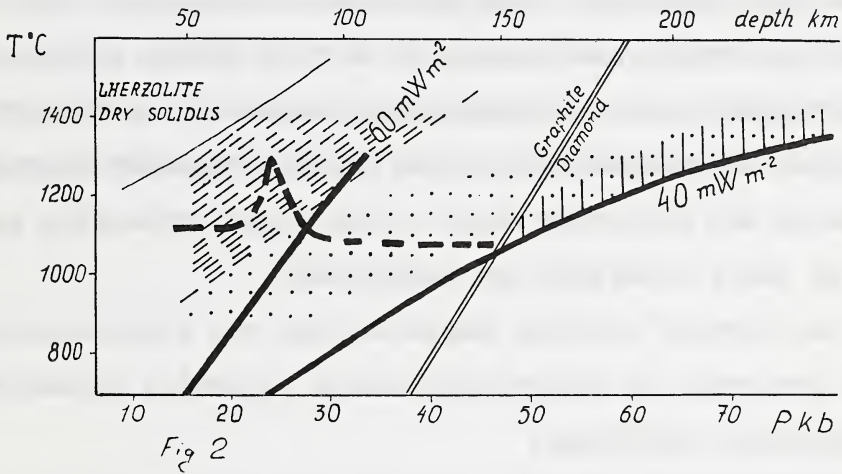
$Fe_{gt}$  - the iron amount in  $Ca_{0.3}(Fe, Mg)_{2.4}Al_2Si_3O_{12}$ .

All Fe is assumed to be divalent.

2. The garnet composition  $Ca_{0.6}(Fe, Mg)_{2.4}Al_2Si_3O_{12}$  at other same compositions of opx. and gt.
3. A Ca content shift in garnet.

Fig.2 Fields of P,T estimates for garnet lherzolite nodules.

(diamond-graphite equilibrium - after Kennedy, 1976 ; other explanations are in text).



## GENETIC TYPES OF KIMBERLITE PIPE CRATERS OF A NEW DIAMOND-BEARING PROVINCE OF THE USSR AND SOME ASPECTS OF THEIR DEVELOPMENT.

*Kolod'ko A.A.; Levin V.I.; Frantsesson E.V. and Kisel' S.I.*

*Central Research Institute of Geological Prospecting for Base and Precious Metals (TsNIGRI), Moscow; North Department of Complex Investigation, TsNIGRI, Arkhangelsk.*

1. Shallow erosion of some newly-revealed kimberlite pipes and, as a result, well-preserved craters filled with specific volcanic and volcano-sedimentary rocks are distinctive features of the new diamond-bearing province situated in the north of the USSR European part.

2. Texturally, structurally and compositionally the crater fill consists of tuffs, tuffites, tuffstones as well as sandstones, siltstones, and claystones with pyroclastic admixture. The former three make up a tuffaceous member 20 to 40 m thick, and the latter three compose a volcano-sedimentary member 30 to 40 m thick.

3. Based on the position of and the relationship between these members the following major crater types reflecting specific features of their formation are recognised:

I - one-layered craters. Deposits form one volcano-sedimentary member dominated by sandy-argillaceous varieties accumulated under lakustrine conditions;

II - two-layered craters. Deposits are composed of the upper volcano-sedimentary member which is analogous to the member of the first type and the lower tuffaceous one derived from the explosion products either as direct fallout onto the crater bottom or as outwash from the area laying outside the crater;

III - three-layered craters. Deposits consist of three members of which the lower and upper members are volcano-sedimentary, while the middle unit is tuffaceous. The lower member is chiefly composed of sandy rocks similar to host rocks. It was

formed in the environment of the prevalent gravity rockfall. The middle (tuffaceous) member was developed simultaneously with the lower unit by gravity rockfall and volcanic ejecta outwash from the area lying outside the crater. The upper member is analogous to that of the first type.

4. The defined types of the crater structure from the kimberlite field record a general pattern in the periodic development of kimberlite volcanism featured by a regular series, from composite long-operating pipes—"leaders" to underdeveloped objects (with one-layered craters) marking the attenuation of volcanic activity within the territory in question.

5. Variety of volcanic structure types and different depths of postore erosion determine a multifactor distribution pattern of indicator components in the overlying deposits. It is due to this reason that there take place various prospecting situations requiring development of prognostic-prospecting models and a corresponding package of methods for their realisation.

## TRADITIONAL AND NEW TYPES OF DIAMOND-BEARING ROCKS AND METHODS FOR THEIR ESTIMATION.

*I.L. Komov.**Institute of Geochemistry and Physics of Minerals, Ukr. SSR Academy of Sciences, Kiev.*

Diamond-bearing rocks comprise the following types: kimberlites, lamproites, impactites, eclogite-amphibolites and eclogite-gneiss metamorphic complexes, ultrabasic (ultrabasites) and basic (basaltoids) rocks.

Diamond in kimberlites is a polygenetic mineral and is genetically related to ultrabasic and basic mantle rocks. Kimberlitic magma transported diamond and other minerals of deep seated rocks (products of the mantle substratum disintegration). These conclusions are substantiated by radiological and mineralogical data, by crystal inclusions with octahedral cut (negative crystals) available in diamonds, whose deformation proceeded in the course of a long period of geological time (billion years and even more), by diamond presence in deep-rock xenoliths of diverse composition. Peculiarities of the kimberlite composition are governed, as a rule, by the crystalline basement structure.

Natural geothermometers, the character of the dislocation structure of crystals, forms of nitrogen show that crystallization of diamonds occurred at a temperature of 1200-1500°C, the depth of formation being 200 km as much. These data necessitate important conclusions:

- the main techniques applied in search for diamond-bearing kimberlites are mineralogical and geophysical methods based on revealing structure-compositional and physical inhomogeneities of the kimberlite fields; the division of kimberlites into productive and perspectiveless cannot

be realized by petrochemical and geochemical methods.

Urgent seems to be the problem of complex estimation of kimberlites and following extraction of gold, platinum and precious coloured stones - pyrope, chrysolite, chrome-diopside. The preservation of diamonds during rock processing can be done on the base of blending.

Large and rich diamond deposits abroad are associated with lamproites. Characteristic features of lamproites are their Mg, K, Ti, Zr, Ba enrichment by light rare-earth elements, availability of olivine, phlogopite, richterite in rocks and presence of such potassium minerals as leucite, wadeite, jappeite, shcherbakovite as well as zircon, barite, garnet (of the pyrope series with low titanium contents), chrome-diopside, chromite. Geological mapping of lamproites and identification of proper olivine varieties among tuffs are required for predictive work. The latter may be carried out in such a succession: geophysical research (magnetic prospecting, ondometric methods), geological mapping, geochemical work (detection of potassium, barium aureoles), drilling, mining sinking, large-scale bulk sampling with a view to produce a required quantity of diamonds, evaluation of their content and qualities. Large diameter wells are drilled with bulk sampling of the material (sample mass - 40kg).

In assessing the diamond content in metamorphous rocks the following characters are taken into account as their productivity criteria:

- wide variations in the mineral and chemical composition of rocks, frequent alternation of very contrasting Precambrian geological formations metamorphosed under conditions of the amphibolitic facies of metamorphism;

- the development of complex and variegated paragenesis of minerals in the zones of potassium metasomatism:  
graphite, quartz, feldspar, forsterite, biotite, phlogopite, muscovite, spinel, clinohumite, tourmalin, pyroxene (diopside, omphacite), garnet (pyrope-almandine, pyrope-grossular), dolomite, calcite.

Diamonds contained in metamorphous formations are usually fine, green-yellow. Mineralogical (typomorphic signs of garnet, pyroxene) and geochemical features (by potassium aureoles) are used in search for diamonds.

COMPOSITION OF GROUNDMASS MINERALS FROM PETROGRAPHICALLY  
DISTINCT TYPES OF KIMBERLITES.*V.P. Kornilova.**Institute of Geological Sciences. Lenin avenue, 39. Yakutsk, 677982, USSR.*

There are several classifications of kimberlite rocks based on their quantitative - mineralogical composition wherein kimberlite rocks are grouped in terms of the quantity of olivine, phlogopite, carbonate (Mitchell, 1970) or diopside, phlogopite, monticellite and other minerals (Scinner, Clement, 1979). Studies of kimberlites have shown that the rocks that differ in structural-textural characteristics and hence petrogenesis can have a similar mineralogical composition. We believe that massive, microporphyritic kimberlite rocks, which fill dykes and stocks, are related to intrusive facies of kimberlite magmatism, whereas brecciated, medium- and macroporphyritic kimberlites, which fill veins and pipes, are related to subexplosive facies (Kovalsky, 1963; Kovalsky et al., 1969; Kornilova et al., 1983). Study of groundmass and phenocryst minerals from compositionally similar kimberlite rocks of different facies has revealed certain differences in the compositions of minerals depending on the facies.

Groundmass monticellite and diopside from monticellite- and diopside-bearing intrusive kimberlites, respectively, are richer in Fe compared to those from similar varieties of kimberlite breccias. Besides kimberlite diopside is characterized by higher  $TiO_2$  and  $Al_2O_3$  compared to almost pure diopside of the groundmass of kimberlite breccias. Phenocryst olivines, and especially their margins, from monticellite- and diopside-bearing

kimberlites are on the average richer in Fe in comparison with olivines from kimberlite breccias.

Mineralogically similar kimberlites of different facies have groundmass ore minerals of similar compositions. However, mineralogically different kimberlites exhibit, irrespective of their facies, substantial differences in titanium, chromium, iron and particularly aluminium contents. Aluminium content of spinel in non-micaceous kimberlites is higher than that of micaceous kimberlites.

Moreover, some intrusive kimberlites are similar in mineralogical composition to alnoite-series rocks associated with alkalic-ultrabasic massifs. Study of the rock-forming minerals of alnoitic rocks from the Tomtor and Chadobetz fields has revealed insignificant differences from intrusive kimberlites.

Our studies show that with mineralogical classification kimberlites which belong to different petrogenetic types and have different quantities of indicator minerals and diamonds fall in one group. No diamonds have so far been found in intrusive kimberlites

THE REGULARITIES OF VARIABILITY OF KIMBERLITE  
COMPOSITIONS IN MULTI-PHASE PIPES.

*Kostrovitsky S.I.*

*Institute of Geochemistry, Siberian Branch, USSR Academy of Sciences, Irkutsk, USSR.*

The majority of well studied great kimberlite pipes belong to multi-phase formations. About five kimberlite varieties fill such pipes as Mir, Udachnaya-Zapadnaya, Udachnaya-Vostochnaya, Aykhal. The kimberlites of different phases of intrusion form individual independent bodies within pipes. The contact relationships between them display the sequence of their intrusion. It turned out that in a number of observed pipes the initial phases of intrusions are associated with kimberlites of the massive texture and the final phases relate to autolith-bearing breccias.

The study of petrochemical and microelement compositions showed that kimberlites of separate phases of intrusion possess a distinct composition feature. As the factor analysis indicates, the main trend of petrochemical variability of kimberlites is due to variations of carbonate and silicate components of rocks. This shows different intensity of superimposed carbonatization and to lesser extent magmatic differentiation. The next distinct trend is derived for multi-phase pipes from the so-called "significant" oxides, which are mostly stable in the secondary processes. The tendency for diminishing  $TiO_2$ ,  $FeO$ ,  $K_2O$  and  $P_2O_5$  contents is well defined from initial phases of intrusion towards final ones; kimberlite becomes more magnesian. The mineralogical particularities of kimberlites are related to the behaviour of oxides. This is a gradual decrease of microilmenite content and a relative amount of high-Fe olivine to final stages of intrusion.

It should be emphasized that on the diagram of a factor analysis with total geochemical data on kimberlites of two pipe bodies of the Udachnaya, the fields of kimberlite varieties are mainly located in a sequence of their intrusion. The kimberlites of initial phases of intrusion, in contrast to final ones, seem to be more rich in Th, Zr, Nb and V. This regularity of distribution of microadmixtures agrees well with that given above for petrogenic oxides. The maximum concentrations of  $TiO_2$  and  $P_2O_5$  are observed in the pre-pipe veins which accompany most of large pipes. It indicates that the observed trend of variability of kimberlite composition is of general character.

The kimberlite pipes are usually grouped as linear extended chains - clusters of pipes. The tendency for a decrease of  $TiO_2$  and FeO in kimberlites in one direction is evident within linear chains of pipes. The regular change of microilmnite composition is observed on the limited data (within one chain of pipes of Daldyn field).

Similar to formation of multi-phase pipes, the formation of linear clusters of pipes is considered as successively forming multi-channel system connected with the common mantle chamber, but isolated spatially within sedimentary cover.

The evolution of kimberlite composition is due to different factors:

- 1) relatively more intensive interaction of initial phases (versus subsequent one) of kimberlite intrusion with deep-seated rocks of the mantle;
- 2) thermal-diffusion mechanism of differentiation which is responsible for enrichment of the upper part of the rising magmatic column with easily fusible elements.

CHROME TITANATE INCLUSIONS OF UNUSUAL COMPOSITION IN PYROPES FROM  
LAMPROPHYRES AND KIMBERLITES.

*Kostrovitsky S.I. and Garanin V.K.*

Some accessory minerals of lamprophyric rocks, which make up the pipe and dyke bodies of the Chompoloo field, located within the Aldan alkali province can be referred to kimberlite associations. Pyrope, Mg-Al chromite, chrome-diopside, pycroilmenite produce typical spectrum of mineral phenocrysts, common for these rocks. The study of crystalline inclusions in phenocrysts turned out to be informative. High-Cr ultra-basic associations with inclusions of chromite ( $\text{Cr}_2\text{O}_3$  - up to 58,6% ), pycroilmenite ( $\text{MgO}$  - up to 14,7% ,  $\text{Cr}_2\text{O}_3$  - up to 2,4%), chromous rutile ( $\text{Cr}_2\text{O}_3$  - up to 8,4%) and chrome titanates of unique composition is mostly remarkable amongst the associations, observed in garnets.

The high-Cr associations of mineral inclusions is found in red-violet pyropes of lherzolite paragenesis. The main peculiarity of their composition is the presence of knorringite mineral. The chrome titanates are small crystalline ingrowths of 0.001 - 0.3 mm, which are marked by a high degree of idiomorphism. Two groups of chrome titanates are distinguished. The first group is characterized by the following composition:  $\text{TiO}_2$  - 56.9 ÷ 59.7%,  $\text{Al}_2\text{O}_3$  - 1.8 ÷ 2.1%,  $\text{Cr}_2\text{O}_3$  - 21.3 ÷ 22.7%,  $\text{FeO}$  - 8.4 ÷ 9.3%,  $\text{MgO}$  - 3.3 ÷ 3.7%,  $\text{CaO}$  - 0.2 ÷ 0.9%,  $\text{Na}_2\text{O}$  - 0 - 0.2%,  $\text{K}_2\text{O}$  - 0 ÷ 0.4%,  $\text{ZrO}_2$  - 3.2 ÷ 3.7%. The second group has close but markedly different composition:  $\text{TiO}_2$  - 60.9 - 68.3%,  $\text{Al}_2\text{O}_3$  - 0.8 ÷ 1.9%,  $\text{Cr}_2\text{O}_3$  - 11.4 ÷ 19.4%,  $\text{FeO}$  - 8.8 ÷ 11.7%,  $\text{MgO}$  - 3.2 ÷ 4.6%,  $\text{CaO}$  - 1.4 ÷ 1.9%,  $\text{Na}_2\text{O}$  - 0.2 ÷ 0.4%,  $\text{K}_2\text{O}$  - 0.2 ÷ 0.6% ,  $\text{ZrO}_2$  - 0.9 ÷ 4.0%.

Identification of chrome titanates is a complicated problem. The X-ray analysis did not provide any reliable results because of small inclusions. The comparison with the data from literature sources (Haggerty, 1983) indicated, that the chrome titanates are close in composition to the minerals of crichtonite group (loverengite) and pseudo-brookite group (armalcolite). But there are some peculiarities in the composition of the studied minerals which do not surely permit their classification.

The high-Cr titanates of the first group, which are close to the minerals of the crichtonite group are different from the latter in the deficit of large-ionic cations (Ca, Na, C, et al). Their total (Ca, Na, K) should be 1, but virtually it varies within the interval 0.07-0.37 (when recalculated for atom amount). The chrome titanates of the second group are close on  $TiO_2$  content to armalcolite and on  $Cr_2O_3$  content as well as large-ionic cations, to loverengite.

It is quite possible, that the studied chrome titanates refer to the same continuous series of chrome titanate minerals. The correlation analysis showed the close relationship between oxides, which reflect wide developed isomorphic replacement in these minerals. Two groups of oxides are distinguished:

1)  $TiO_2$ , FeO, MgO, CaO,  $Na_2O$ ,  $K_2O$  and

2)  $Al_2O_3$ ,  $Cr_2O_3$ ,  $ZrO_2$

The negative evident relationship is observed between these two groups. Oxides positively correlate within each group. The highest negative correlation is found for  $TiO_2$  and  $Cr_2O_3$ , the figurative points on the plot lie on the straight line.

The chrome titanates of the second group are found in pyropes with knorringite mineral from typical kimberlites. It indicates that the high-Cr titanates refer to the high-P association.

SR, C, O ISOTOPE COMPOSITION IN KIMBERLITES OF THE  
NORTH-RUSSIAN PROVINCE (USSR).

*Kostrovitsky S.I.*<sup>(1)</sup>; *Skripnichenko V.A.*<sup>(2)</sup>; *Plusnin G.S.*<sup>(1)</sup> and *Bodrov V.A.*<sup>(3)</sup>

(1) *Institute of Geochemistry, Acad. Sci. USSR. 664033, Irkutsk, P.B. 4019, USSR;*

(2) *Archangelsk Geol. Surv., Archangelsk, USSR;* (3) *Institute CNIGRI, 113545, Moscow, USSR.*

As compared with the Yakutian kimberlites which intruded in the crust of carbonate composition, the kimberlites of the North-Russian Province intruded into the Vendian terrigenous sequence mainly consisting of quartz sandstones, argillites and siltstones. The sedimentary cover is nearly 1 km thick. The new kimberlite province is located in the tectonic mobile zone (within the Zimnegorsk aulacogen) in the marginal part of the platform. This specific occurrence is responsible for morphological as well as compositional features; (i) existence of sills along with pipes; (ii) a wide composition variation in kimberlites including appearance of picrites; (iii) development of such secondary minerals as sepiolite and saponite along with serpentine; (iv) low concentration of a carbonate component in the rock of pipes.

The denudation of pipes from the North-Russian Province is small and amounts to several tens of meters. The upper parts of the pipes are filled up by the rocks of the crater facies (breccias and xenotuff breccias). In the pipe bodies the massive varieties are fairly rarely observed. The autoliths in breccias consist of massive fine-porphyrific kimberlites. The sills are also composed of the same type of massive kimberlites with a high concentration of carbonate component.

The isotope composition of Sr was determined at the Institute of Geochemistry in Irkutsk, and compositions of C and O were measured at CNIGRI Institute in Moscow. The table shows these results as well as calcite contents in the rocks and Sr in calcite. It should be noted that Sr in the carbonate phase was determined from acid extracts. This could lead to overestimating the values of Sr contents in calcite. The isotope Sr composition of silicate phase of kimberlites as well as picrites in pipe bodies has stable values and varies within a narrow range ( $^{87}\text{Sr}/^{86}\text{Sr}$ )<sub>norm</sub> = 0.7050–0.7057. The close isotopic characteristics indicate a common magmatic source for kimberlites and picrites of the North-Russian Province. The carbonate phase of the pipe kimberlites and picrites has  $^{87}\text{Sr}/^{86}\text{Sr}$  ratios ranging from 0.7047 to 0.7111. The low values, similar to those of the silicate phase, are estimated for autoliths. Similar low ratios (0.7036–0.7050) are found for a carbonate component of kimberlite sill Mela that suggests its magmatic nature. The Sr isotope composition of hydrothermal calcite (0.7095) is intermediate between the values which characterize the host rocks (0.711–0.713) and the mantle carbonate phase of kimberlite (0.704–0.705).

Together with the study of Sr isotope composition  $\delta\text{O}^{18}$  and  $\delta\text{C}^{13}$  were measured for the same samples in the carbonate component. As compared with the Yakutian kimberlites (for which the correlation between the isotope characteristics of Sr and O has been revealed (Kostrovitsky, 1986)), in kimberlites of the North-Russian Province the correlation between Sr and C and between C and O is more distinctive.

Table of Sr, C, O isotope composition in kimberlites of the North-Russian Province

No	Rock	CaCO <sub>3</sub> Pipe, in rock sill in wt%	Sr, in wt%	87Sr/86Sr	δC13, in ‰	δO18, in ‰	
Kimberlites (carbonate phase)							
1c	xenotuff- breccia	Karpin- skaya	1.2	0.99	0.7095	-3.1	+25.7
2	- " - carbonated	Koltsov- skaya	11.0	0.07	0.7111	-1.6	+22.7
3c	breccia	Lomonosov	1.5	1.01	0.7092	-5.1	+22.1
4c	autolith	Karpin- skaya	1.3	1.49	0.7057		
5	- " -	Lomonosov	11.0	0.52	0.7047	-6.8	+12.8
6c	porphyric massive	Anomaly- 695	45.0	0.035	0.7079	-8.1	+20.2
7c	porphyric massive	Mela sill	80.0	0.16	0.7036	-4.7	+22.1
8c	- " -	- " -	88.0	0.22	0.7050	-5.4	+21.7
9c	hydro- thermal veined calcite	Lomonosov	44.0	0.013	0.7095	-1.5	+22.6
Kimberlites (silicate phase)							
3s		Lomonosov		0.015	0.7057		
6s		Anomaly-695		0.023	0.7051		
7s		Mela sill		0.05	0.7052		
Picrites (carbonate phase)							
10c	porphyric massive	Dike Igmo- Ozersk	2.0	0.49	0.7098	-1.1	+26.8
11c	xenotuff breccia	Yuras- skaya	13.8	0.077	0.7085	-3.9	+24.3
12c	breccia	Nenok	1.5	0.17	0.7101	-6.6	+21.4
Picrites (silicate phase)							
10s		Dike		0.023	0.7050		
13s	massive	Krutiha		0.03	0.7052		
Host rocks (carbonate phase)							
14c	dolomite (xenolith)		80.0	0.046	0.7108	-0.6	+26.0
15c	sandstone		14.5	0.021	0.7131	-2.8	+20.2

$\delta^{13}\text{C}$  value of magmatic calcite varies from -4.7% to -7.6%, of hydrothermal calcite and carbonized kimberlites from -1.5% to -1.6%, of host rocks of the sedimentary cover from -0.6% to -2.8% in the PDB system. Oxygen from the carbonate component of kimberlite is marked by a heavy isotope composition, as a rule  $\delta^{18}\text{O} > +20\%$  in the SMOW system. The value  $\delta^{18}\text{O}$  (+12.8%) is similar to the mantle value only in a single sample of autolith.

Discussion. The main features of Sr, C and O isotope systematics in the kimberlites from the North-Russian platform are similar to those described elsewhere for kimberlites from the other provinces. The endogenic melt component in the kimberlites and picrites is characterized by low  $^{87}\text{Sr}/^{86}\text{Sr}$  (0.704 to 0.706) ratio, typical range of  $\delta^{13}\text{C}$  (-5% to -8%). The relatively high  $\delta^{18}\text{O}$  values result from profound changes of the kimberlites by the secondary hydrothermal-metasomatic processes. On the whole, the isotope compositions of Sr, C and O indicate a significant influence of the host rocks on kimberlites. The carbonate component of kimberlites in the pipe bodies was mainly formed due to this influence. The mantle carbonate is preserved in the massive porphyritic varieties of kimberlites and picrites only.

Kostrovitsky S.I. (1986) Geochemical features of the kimberlite minerals. Publ. House "Nauka", Novosibirsk, 263 p. (in Russian).

## GEOLOGICAL STRUCTURE AND MINERALOGY OF THE KIMBERLITES OF THE ARCHANGELSK KIMBERLITE PROVINCE.

*Kudrjavitseva*<sup>(1)</sup>, *G.P.*; *Bushueva*<sup>(1)</sup>, *E.B.*; *Vasiljeva*<sup>(1)</sup>, *E.R.*; *Verichev*<sup>(2)</sup>, *E.M.*; *Garanin*<sup>(1)</sup>, *V.K.*; *Grib*<sup>(1)</sup>, *V.P.*;  
*Laverova*<sup>(1)</sup>, *T.N.*; *Mikhailichenko*<sup>(2)</sup>, *O.A.*; *Posukhova*<sup>(1)</sup>, *T.V.* and *Schepina*<sup>(1)</sup>, *N.A.*

(1) *Geological Department of Moscow State University, 119899, Lenin's Hills, Moscow, USSR;*

(2) *PGO "Arkhangel'skgeologia", 163001, P. Vinogradova str., 168, Arkhangel'sk, USSR.*

New kimberlite diamond bearing province had been discovered on the Northern European part of the USSR at the end of 70-s. The main features of the craton geological structure are defined by its location in the zone of joint of the largest blocks of the Eastern European platform: Baltic Shield and Russian platform. Several kimberlite fields (Fig.1), in which the bodies are represented by pipes and sills, were discovered in the region. The formation time of the craton kimberlite pipes is Late Devon - Middle Carbon.

The kimberlite pipes of Arkhangel'sk kimberlite province are represented by tuffs, tuffites, tuffobreccias, autolithic breccias. The low degree of erosion of the presence of the clearly marked crater facie. All types of ore bearing rocks are practically completely composed of the minerals of light fraction, represented by serpentine, saponite, carbonates, hydromicas, minerals of palygorskite-sepiolite group. The quantity relation of minerals within the range of different bodies and parts vary considerably. The content of diamond minerals-satellites in the heavy fraction is considerably lower than in the kimberlite bodies of Jakutian and South African diamond bearing provinces. Chrome spinelides are the most widely spread. The minerals of high-aluminous eclogites and grosspyrites are completely absent.

The relation between the space position of diatremes and fields and between the peculiarities of the heavy fraction composition of the kimberlite rocks emphasizing the zonality of the kimberlite province had been revealed.

The rocks composing the diatremes can be divided into several groups according to the mineralogical peculiarities of these rocks.

The diatremes of the central (Zolotizkoje) field are characterized by the industrial diamond bearing. The sharp predomination of the chrome spinelides is characteristic for the heavy fraction of the kimberlites. Garnet, diopside occur in the subordinate amount, microilmenite was found in rare cases. The minerals of the diamond bearing paragenesis are widely spread: pyrope and chromite from dunite-harzburgites and high chromium lherzolites, pyrope-almandine from predominantly magnesian-iron eclogites. Magnesian Al-Ti-containing chrome spinelides ( $> 55 \text{ wt.} \% \text{ Cr}_2\text{O}_3$ ) predominate in the ground mass of the kimberlite rocks. Sometimes the borders of the chrome ulvospinel are observed around the nuclei of this mineral; usually such formation are observed in the rocks of the lower horizons of the kimberlite pipes.

The series of signs, showing the resemblance of the composing pipes rocks with lamproites, were established. The most important of these signs are the morphological types of diamond (usually complex crystals of dodecahedron habitus, and considerably rarer of cubic and octahedron), the predomination of chrome spinelides in the heavy fraction; the wide spreading of Fe-Ti-oxides and barium mineralization in the ground

mass; small amount of xenolithes of the depth rocks; and practically complete absence of picroilmenite.

Diatremes of the north-eastern (Verkhotinskoje field) and eastern (Shochinskoje field) groups of bodies are distinguished by low and poor diamond bearing. Minerals of heavy fraction are represented by chrome spinelides, pyrope, chrome diopside with complete absence of picroilmenite. The content of the mentioned minerals is considerably less than in the kimberlite of Zolotizkoje field.

The main ore mineral of the ground mass of the kimberlites is Cr-Al-containing titanomagnetite at the clearly marked subordinate spreading of magnesian Al-Ti-containing chrome spinelide.

The diatremes of eastern (Sojanskoje field) and south-eastern (Kepinskoje field) group of bodies among minerals of heavy fraction picroilmenite and red-orange garnet predominate; chrome spinelides are considerably less spread. Ilmenite and sheared lherzolites are the most widely spread parageneses of the depth rocks. The diamond bearing of the rocks of the diatremes of these fields is very poor.

Rutile predominates in the ground mass of the kimberlites; titanomagnetite and picroilmenite with the increased content of manganese are widely represented. The grains of Al-Ti containing chrome spinelides and magnesian ulvospinel occur in the sharply subordinate amount.

The zonality of the new diamond bearing kimberlite province is emphasized by the development of the pipes of the non-diamond bearing basaltoids on the periphery of the eastern border of the province. In these pipes only isolated signs of the diamond minerals-satellites are revealed.

The mineralogical specialization of the kimberlite fields is facilitated by their geologico-tectonical position and correlates with the diamond bearing of the diatremes. The revealed geological and mineralogical peculiarities allow to carry out the regioning of the Archangelsk diamond bearing province, defining at the same time new diamond prospecting areas.

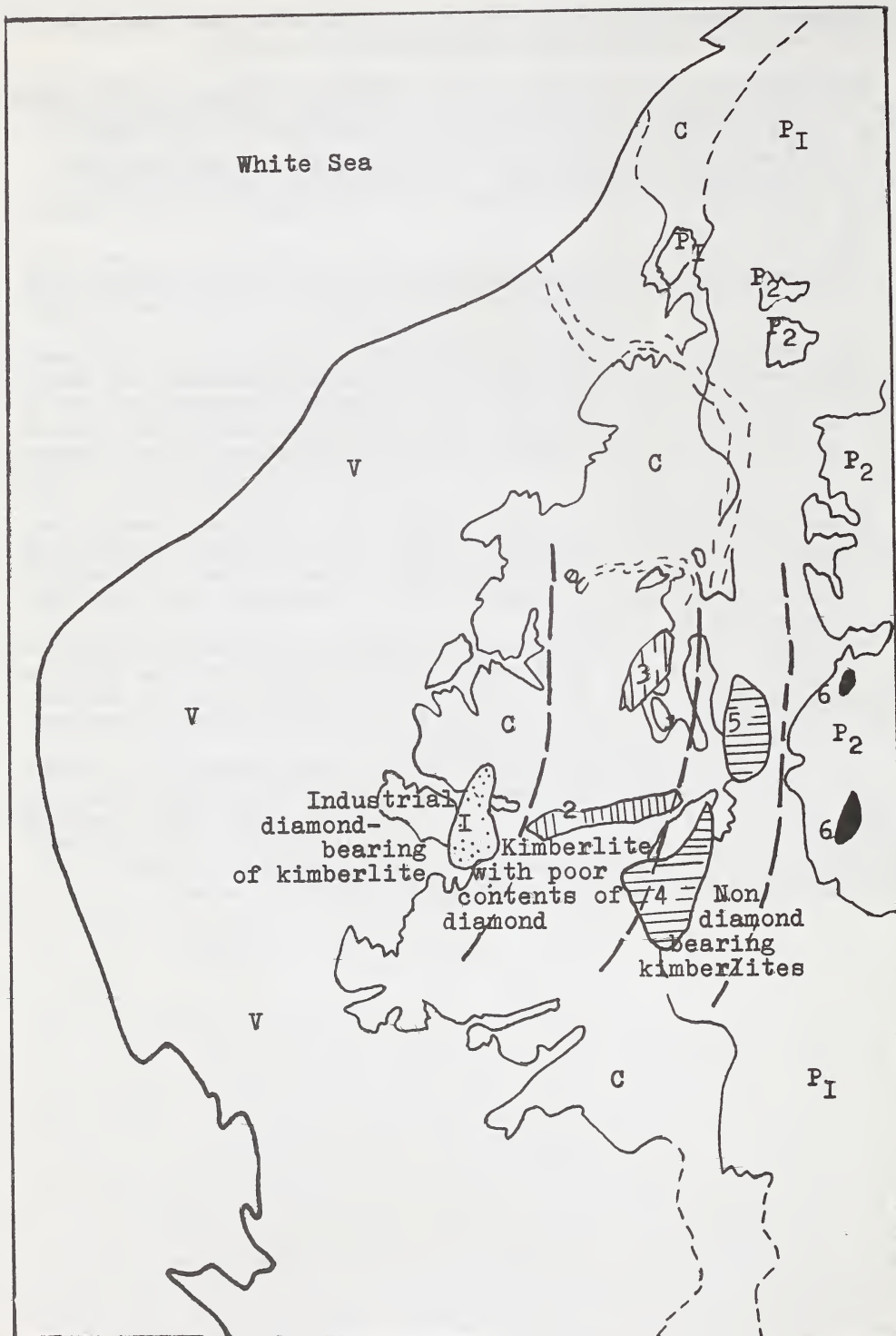


Fig. I. Distribution of kimberlite fields in Arhangelsk kimberlite province. Kimberlite field: 1-Zolotitskoe, 2-Shochinskoe, 3-Verhotinskoe, 4-Kepinskoe, 5-Soenskoe, 6-Turinskoe field of basaltoid pipes

THE FORMATION KIMBERLITE DIAMONDS THROUGH CHEMICAL SYNTHESIS  
IN OPEN CATALYTIC SYSTEM.

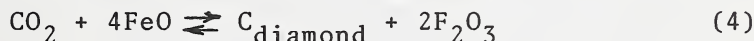
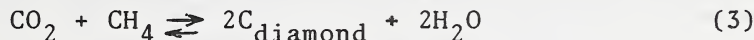
*Kulakova, I.I.; Rudenko, A.P. and Skvortsova, V.L.*

*Chemical Department, Moscow State University, 119899, USSR.*

The existence of natural diamond of various genetic types and successful synthesis of diamond show the possibility of various mechanisms of diamond formation. All possible processes of diamond formation may be divided into two groups: crystallization processes during polymorphic transformation of graphite to diamond under high P,T-conditions and processes of chemical synthesis of diamond from low carbon-containing molecules under relatively mild P,T-conditions.

We consider the problem of kimberlite diamonds formation in the context of general laws of chemistry, thermodynamics and catalysis taking into account the theory of open catalytic systems and geochemical features of diamond occurrence in kimberlites.

Hereby we suggest a model in which the formation of kimberlite diamonds result from catalytic polycondensation of simple carbon-containing substances in non-stationary open catalytic systems, such as in the following reactions:



Each of these processes has an aromatic polycondensation analogue that eventually produces under the same P,T-conditions: graphite, bitumens and others products. Thermodynamic conditions and catalysts for diamond and graphite formation are similar, but the oxidizing medium potential and the rates of these processes are different.

According to the model one can distinguish two stages the macroscopic diamond crystals formation. The first one formation of diamond ("germs") can proceed either in a static system (up to the equilibrium) or in the open system in non-equilibrium conditions. And diamond "germ" forms as a result of polycondensation of carbon-containing substances in the form of epitaxial films on planes of some minerals, containing catalytically active ions for diamond polycondensation (Cr, Mn, Fe and others) and having crystallostructural correspondence with the diamond lattice. This is in good accordance with the "central" inclusi-

ons in diamond crystals and with the regularities of their orientation.

The second stage (up to the formation of macroscopic crystals) is possible only in open non-equilibrium systems when the initial substances (CO, CO+H<sub>2</sub> and others) cause gradual growth of crystal and the movable products (CO<sub>2</sub>, H<sub>2</sub>O) are gone, the equilibrium of the above-mentioned reactions<sup>2</sup> being shifted to the right.

The main components of such an open system are growing crystals and the surrounding mineral coat, containing ions-catalysts of diamond growth/oxidation (Cr, Fe, Mn, Ni and others). Increasing size of diamonds or their oxidation are determined by the medium redox potential and temperature.

The following facts support this model:

- decrease in the content of diamonds in kimberlite tubes with depth;
- difference in the content and morphology of diamond in different zones of the same tube;
- existence of tubes either continuous diamonds or lacking them within one and the same region;
- catalytic activity of kimberlites in the oxidation-growth processes of diamonds;
- present of mineral coats on the diamond crystals and their physico-chemical and mineralogical peculiarities;
- correspondence between diamond contents of kimberlites and their catalytic activities, chemical composition and contents bitumens.

## DIAMONDS IN METAMORPHIC ROCKS.

*E. Nadejdina and T. Shalashilina.**Central Research Institute of Geological Prospecting for Base and Precious Metals, 113545, Moscow, USSR.*

Diamonds of a new type were found in metamorphic rocks. Small sizes (in average 20-50 mkm, maximal - up to 1,2 mm), dominating hexahedral (cubic) habit and yellow-green color differ them from kimberlite diamonds. Absence of lonsdalite aparts them from impact ones.

The crystals are usually semi-transparent, roughly-shaped without brilliant brightness. The only exclusions are sharp-edged plane-faced octahedra with smooth planes {111}. Since the features of epigenetic dissolution are absent a set of shape sculptures-hilly, bud-like, tiled-together with unfilled sectors of the crystals are accounted for the growth conditions only.

Along with prevailing yellow-green such colors of the crystals as greenish-grey, grey, dark and rare milk-white occur. All they could have different tints. Intensity of yellow-green color is defined by enrichment with the structural impurity of nitrogen in paramagnetic state, dark color - by syngenetic inclusions of graphite. Almost all varieties of diamonds display abnormal birefringence.

Based on crystallographic analysis with application of REM-technique main habit varieties were educed: cubic, octahedral, skeletal, spheroidal. One more group includes plane-faced with sharp edges or plane-curve-faced crystals combining simple forms: cube-octahedra, cube-octahedra-rhombododecahedra, etc. Single varieties of cubic and skeletal crystals have no analogous among natural and artificial diamonds.

Complex instrumental studies of diamonds have been carried out. Thus, isotope analysis shows enrichment in light carbon with  $\delta^{13}\text{C}$  ranging from -1.75 to -1.71 ‰ for diamonds and from -1.84 to -1.74 ‰ for host rocks graphite. This fact indicates a common source of diamonds and graphite and, hence, their genetic closeness. The assumption is consistent with apparent similarity of the trace elements sets for the diamonds and graphite. On JNAA data content of such trace elements as Na, Al, Sb, As, Au is an order higher while amount of K, Cr, Mn, REE is two orders higher for studied diamonds than respective average values for kimberlite diamonds.

The excess of Cr, REE, and sometimes Co suggests in particular their probable catalytic role in crystallisation of diamonds. Optical properties of the crystals are defined by the content and distribution of major impurity of nitrogen and to less extent, by structural hydrogen. For the diamonds absence of X-ray luminescence and weak greenish, in single cases-bluish laser induced luminescence with nitrogen centers SI, H3, (N3) are typical.

IR-spectra show the presence of nitrogen in N - (absorption band at  $1282\text{ cm}^{-1}$ ) and in A-form (absorption band at  $1238\text{ cm}^{-1}$ ), in single "bulk" samples in - BI-form ( $1175\text{ cm}^{-1}$  and  $1010\text{ cm}^{-1}$ ) and structural hydrogen with absorption band at  $3107\text{ cm}^{-1}$  on data of H. Blinova.

With application of EPR - method contents of single and exchange - connected pairs and threes of nitrogen paramagnetic atoms were measured. They exceed respective values for kimberlite diamonds at least as two orders of magnitude.

X-ray section topography studies display internal structure of diamonds being zonal-sectoral, non-homogeneous, fine-crystalline or comprising different blocks. The blocks differ in degree of perfection and, hence, in crystal lattice parameters values. Maximal deflection of the value is noted for the most imperfect cubic crystals:  $a=3.557$  in comparison with  $a=3.567$  for variety III kimberlite diamonds using the terminology of Orlov (1977).

Diamonds with zonal-sectoral internal structure have weakly diversified lattice parameters in inner and outer zones of the crystal space. Two types of misorientation are measured: from 10 to 20 angle minutes between sectors and from 3 to 5 minutes between microcrystallites inside every sector. Microcrystallite sizes are estimated as up to ones of microns.

Unlike kimberlite diamonds growth in  $\langle 111 \rangle$ ,  $\langle 100 \rangle$  and  $\langle 110 \rangle$  directions, metamorphic diamonds show unfilled sectors of crystal space corresponding to those directions. Thus, absence of tangential growth features, the set of habit varieties typical for normal (fibrous) growth mechanism, absence of oxidation dissolution features; excess of trace elements, enrichment in non-transformed paramagnetic nitrogen and other structure dependent properties suggest that crystallisation of metamorphic diamonds proceeded in short period of time. It had impulse character in highly disbalanced environment supersaturated with carbon and enriched by strange impurities under relatively low temperatures and pressures.

PRIMARY MELT INCLUSIONS IN ECLOGITE DIAMONDS AND THEIR  
GENETIC IMPLICATION.

*P.G. Novgorodov.*

Study of primary melt microinclusions in diamonds from the Mir pipe (Bulanova et al., 1988; Novgorodov, Bulanova, 1988; Novgorodov et al., 1990) is very important for understanding petrological and geochemical aspects of mantle processes. These works, together with other published data, permit the following main conclusions regarding genesis.

1. Melt inclusions of andesite composition in diamonds are thought to represent a fragment of initial melting of diamondiferous mantle eclogites (Green, Ringwood, 1968; Sobolev, Sobolev, 1975). From data available, all calculated temperatures for the association garnet/omphacite (Ellis, Green, 1979, P=50 kb) of inclusions in diamonds from the Mir, Roberts Victor, Premier, Orapa, Sloan kimberlites and Argyle lamproites fall in the interval between the wet and dry solidus for eclogites on P-T diagrams. Diamondiferous eclogites probably experienced partial melting if they initially contained some volatiles (H<sub>2</sub>O, CO<sub>2</sub>).

2. It appears that a high-potassium melt represents a fragment of the final evolutionary stage of mantle eclogites. Its disproportionation might occur as follows:  $mK_2O \cdot nNa_2O \cdot Al_2O_3 \cdot 6SiO_2 \cdot V^I \rightarrow 2mSa + 2nJd_{ss} + [I - (m+n)] Ky + 5[I - (m + 0.6n)] Cs + V^{II}$ , where V<sup>I</sup> = dissolved volatiles, V<sup>II</sup> = fluid phase. The fluid phase should be in equilibrium with the association Gar + Omph + Sa + Ky + Cs + Rut + FeS. Xenoliths containing such a suite of minerals from Roberts Victor (Smith, Hatton, 1977) and Udachnaya (Spetsius et al., 1984) are likely to represent relics of similar processes that occurred in the upper mantle. The above reaction may explain transition from rutile eclogites into kyanite ones.

3. Fluid microinclusions in coated and cubic diamonds from Zaire and Botswana (Navon et al., 1988, 1989), which are enriched in SiO<sub>2</sub>, K<sub>2</sub>O, TiO<sub>2</sub>, FeO and trace elements, probably characterize the subsolidus evolutionary stage. Data on melt and fluid microinclusions, although they are available only

for several samples from the Yakutian and African diamondiferous provinces, seem to reflect a single geochemical trend of mantle eclogite evolution.

4. It appears that a clear core of eclogite diamonds crystallized from melt whereas rims from a fluid phase supersaturated with carbonaceous matter relative to diamond. The core-rim interface is a phase boundary whereat the solidus temperature of the system is attained. The medium evolved with decreasing P and T, which was probably consistent with a rising mantle diapir represented by heterogeneous eclogite material.

5. High  $K_2O$  content of omphacite inclusions in diamonds from various parts of the world may indicate their crystallization in the presence of a substantially high-potassium melt or fluid.

6. Recently, preliminary data on the U content of coated diamonds were obtained using f-radiography (L.L.Kashkarov, unpubl. data). The U content is  $0.6 \pm 0.1$  ppm in clear cores of diamond,  $>3 - 7$  ppm in melt inclusions,  $50 - 100$  ppm in local cracks. The medium from which diamonds crystallized seems to have been rich in U.

7. Methodologically, the studied melt microinclusions represent a new type of inclusions. A local crack and a disordered graphite film which are related to such inclusions may be the result of partial degassing during kimberlite magmatism in the crust where  $P_{fl} > P_{tot}$  was attained at the inclusion-matrix interface. These features can be used as visual indicators in choosing diamond crystals that are likely to contain primary melt inclusions.

## NATIVE METALS IN KIMBERLITES OF YAKYTIA AND THEIR GENESIS.

O.B. Oleinikov.

*Institute of Geological Sciences, Lenin avenue, 39, Yakutsk, 677891, USSR.*

Study of accessory minerals in rocks of the kimberlite formation and mantle xenoliths has revealed the presence of various native metals and associated oxygen-free compounds in them. Of minerals of the native element classes, iron, nickel, copper, gold, zinc, aluminium, lead, tin, chromium and antimony were found. A manganese variety (more than 1 wt.% Mn) has been established for iron; zinc, tin and tin - zinc varieties for copper; a ferrous variety for zinc; copper, magnesium, magnesium - copper and manganese - zinc varieties for aluminium; and a tin variety for lead. Seven intermetallic compounds:  $\text{CuZn}$ ,  $(\text{Cu, Fe, Mn})\text{Al}_2$ ,  $(\text{Fe, Mn})\text{Al}_2$ ,  $\text{CuAl}_2$ ,  $\text{Cu}_6\text{Sn}_5$ ,  $(\text{Cu, Zn})_{14}(\text{Sn, Sb})$ ,  $(\text{CuZn})_5(\text{Sn, Sb})$ ; two antimonides:  $\text{Cu}_2\text{Sb}$  (cuprostibite),  $\text{SnSb}$  (stistaite); and moissanite were found in association with the native metals and their chemical varieties.

The species and compositions of the studied minerals are similar in both rocks of the kimberlite formation and xenoliths of unaltered and serpentized rocks. However, most favourable for the appearance and for preservation of native metals among kimberlite magmatites are autolith - bearing kimberlite breccias with a high proportion of groundmass, alneites, and phlogopite - rich and for highly carbonatized varieties of kimberlite. Comparison of the data obtained for rocks with unaltered, partly and completely serpentized olivine revealed no relationship between the degree of serpentization and the number of grains and species of native metals.

Minerals of the native element classes were formed in two stages. The first (mantle) stage was related to evolution of upper mantle material. The second (mantle - crust) stage was related to processes that took place in the kimberlite system proper. P-T parameters varied within 3,5 - 65 kb and 700-1300°C during the first stage and from near - surface conditions to 65 kb and 200 - 1200°C during the second stage.

Two mechanisms are suggested for the formation of native metals. The first one involves reduction of rock - forming elements of a silicate - oxide substrate due to a change in redox conditions. The second envisages crystallization of the metals by gas condensation of elements of an intratelluric fluid. The reduction mechanism is restricted by a buffering effect on reduction reactions of a silicate - oxide substrate: even with excess  $CH_4$  and  $H_2$  the  $H_2O$  that forms during reaction prevents  $fO_2$  from reaching the value at which native iron is produced (Persikov, 1985). Rare finds of native iron attest to a lack of wide - scale reduction.

A wide occurrence of methane in a gaseous phase of mantle and kimberlite rocks suggests the appearance of organometallic compounds as agents of elements migration in fluids. Desintegration of such complexes can explain the formation of native metals and moissanite.

From the above said, the similarity between mineral associations produced during the two stages of native mineral forming processes becomes understandable.

## KIMBERLITE-CONTROLLING ZONES IN THE CRUST AND UPPERMOST MANTLE OF THE WEST YAKUTIA: THEIR COMPOSITION AND EVOLUTION.

*A.F. Safronov; V.D. Suvorov; A.I. Zaitsev; N.I. Nenashev and I.P. Shcherbakova.*

*Institute of Geological Sciences, Lenin avenue 39, Yakutsk, 677007, USSR.*

Seismic studies of the uppermost mantle in the southern part of the Yakutian kimberlite province (YKP), Western Yakutia, have established a narrow, linear zone of anomalously high velocities (up to 8,5 - 9,0 km/s) along the Moho. All known kimberlite fields of the southern YKP are located within this zone. Rb - Sr and K - Ar age determinations of kimberlite rocks crustal and upper mantle rocks xenoliths and samples of the buried basement from within the zone gave the following age intervals: 1000 - 1290, 600 - 900, 340 - 390, 210 - 230 Ma. Ages of crustal and upper mantle xenoliths and buried basement rocks fall in all the four intervals, whereas those of kimberlite rocks correspond to the last two younger intervals. The spatial confinement of the dated samples to the above mentioned zone permits us to consider it as a kimberlite-controlling zone (KCZ).

Along the Moho, the KCZ is expressed by the predominance of eclogites over peridotites. Geophysical characteristics of the crust suggest it is saturated with small peridotite bodies.

The formation of the KCZ began no later than 1200 Ma ago and proceeded in several episodes corresponding to the above age intervals. Each of the episodes could be consisted with an epoch of kimberlite magmatism.

It appears that KCZ in the crust and uppermost mantle as well as exposed kimberlites indicate the beginning of destruction of the continental lithosphere. The destruction

process can proceed as follows: 1)Initiation of KCZ and eruption of kimberlites. 2)Further development of KCZ is expressed by pre-rift surface upwarping and eruption of kimberlites and picrites. 3)The onset of continental rifting and manifestation of rift magmatism.

The confinement of some kimberlite provinces to passive continental margins is an indirect evidence for such a scenario of KCZ evolution.

PRE-CAMBRIAN DIAMOND-BEARING VEINED BODIES FROM SOUTH-WEST  
OF THE SIBERIAN PLATFORM.

*A.P. Sekerin; Yu. V. Menshagin; B.M. Vladimirov and V.A. Lashchenov.*

*Institute of the Earth's Crust, 664033 - Irkutsk, USSR.*

The structural position and mineral composition of diamond-bearing veins which have previously been classified as mica kimberlites from South-West of the Siberian Platform are discussed.

The veined bodies are localized within the limits of the Early Proterozoic intracratonal mobile zone cratonized at the Upper Riphean-Vend. Picrites, basalts, trachybasalts, ultrapotassic trachytes, alkaline-ultrabasic rocks and carbonatites, and ultrapotassic basaltic picrites were intruded. The late two rock types contain some high-pressure minerals.

The diamond-bearing bodies occur as veins, which length is up to 1 km and the thickness varies from some cm up to 1 m. The country rock matrix is texturally porphyric and structurally fluidal. Porphyric phenocrysts are represented by serpentine and talc pseudomorphs after olivine and by phlogopite. The oriented microclites of phlogopite enclosed in the apoglassy matrix predominate in the ground mass. Carbonate is found as a rock-forming mineral in one vein in which limestone interbedded the country rocks. The available data coupled with isotopic studies allow the secondary assimilation origin of carbonate to be assumed.

Inclusions of ultrabasic rocks and eclogitized gabbro are observed in veins.

The studied rocks are petrochemically different from kimberlites and they are similar to olivine lamproites from the Argyle pipe. They also differ from kimberlites in concentrations and ratios of coherent and non-coherent elements and correspond to lamproites from West Australia.

The rocks are dated by Rb-Sr age determination of  $1268 \pm 12$  m.y. Age of the alkaline-ultrabasic rocks of carbonatitic complex from the same region is 640-740 m.y.

A characteristic mineralogical feature is the predominance of chrome-spinellids in ore minerals and the orange almandine-pyropes of eclogitic paragenesis in garnets (Pyr=38%, Alm=34%, Gross=24%). Picroilmenites and low manganese ilmenites are absent. Ilmenites are characterised by a higher (up to 4%) Mg content. Three amphibole types are distinguished: potassic magnesioarfvedsonite, titanopargasite and unidentified chrome-bearing ultra-potassic amphibole. The higher  $TiO_2$  content is common to phlogopite (f=10-25%). The mineral compositions of olivine, orthopyroxene, chrome-diopside and chrome-spinellids are studied. Zircons, Nb-rutile, anatase, moissanite, spinel, apatite, sphene, turmaline, epidote, armalcolite, priderite and diamonds occur in these rocks.

The analysis of the available data suggests a lamproitic origin of rocks studied.

## GEODINAMIC REGIME OF KIMBERLITE MAGMATISM MANIFESTATIONS ON THE SIBERIAN PLATFORM.

*Shpount, B.R.*

*Central Research Institute of Geological Prospecting for Base and Precious Metals, TsNIGRI,  
Varshavskoye Shosse, 129B, Moscow 113545, USSR.*

During the Neogene time, the Siberian platform witnessed numerous recurrent stages of magmatic reactivation manifested both by basic magmatism and kimberlite formation. The typical property of these reactivation stages was that basic magmatism in each cycle was 15-20 m.y. younger as compared to the kimberlite formation flare-ups.

The riftogenic basic magmatism was manifested to different scale in the Riphean, Vendian, Middle and Late Paleozoic time. In the Late Paleozoic-Early Mesozoic, it occurred in the geodynamic environments of dispersed spreading resulting in the formation of trap synclises. In the Middle and Late Mesozoic and in Early Cenozoic, the magmatism was confined to zones of incomplete rifting. The kimberlite magmatism manifestations "echoed" each flare-up of basic activity, while the kimberlite formation was associated both with the inverse development stages in paleorift systems and epochs of regional gaps in the platform cover accumulation.

Reconstruction of paleorift systems of different age has shown that riftogenic structures frequently inherit each other's trend. The trend of the longest and deepest Late Precambrian and Middle Paleozoic riftogenic depressions was inherited from the protorift troughs originated in the Late Archean and Early Proterozoic time.

Paleorift systems are fringed by linear collision zones /ramps/- the peculiar small-scale subduction areas compensating the paleorift tension. During their short-term impulse opening due to decompression these zones were injected by small amounts of magma generated in the deepest upper mantle layers. A striking feature of the ramp magma-controlling zones was that their small areas accommodated numerous kimberlite bodies of different age.

Both the paleorift systems and their fringing ramp zones have different characteristics of the deep structure. The paleorift systems correspond to dome-like uplifts in the Moho discontinuity (with an amplitude up to 8 km) and reduction in crustal thickness up to 32-34 km due to wedging out of the upper velocity layers. Seismic sounding also reveals a high degree of layering of the lower velocity level (6.8-7.0 km/s) and the upper mantle. This may be interpreted as relics of ancient destruction resulting from riftogenic tension and mantle degassing.

Absence of correlation between the gravimagnetic field anomalies has been reported for the collision /ramp/ zones located as far as 150-200 km away from the paleorift axes.

Detailed seismic studies conducted by V.D. Suvorov allowed to identify the ramp zones in the lowermost crustal layers by the dramatic increase in the boundary velocities (up to 9.1 km/s), the appearance of 8-12 km deep trenches in the Moho discontinuity, the anticlinal uplifts at the intracrustal K-reflection boundary, higher Poisson's ratio and higher absorption of resilient waves due to increased compression and significant growth of mass exchange.

The paleorift areas usually correspond to the platform cover; synclises while the ramp zones are associated with reduction in the cover thickness and numerous sedimentation gaps.

The classical kimberlite fields tend to be associated with areas of intercrossing of ramp zones and Late Precambrian - Middle Paleozoic dyke belts. It is noteworthy that the long axes and dyke root bodies of kimberlite pipes run parallel to the trend of ramp zones. This also confirms the magma-controlling role of those regional dislocations.

Another genetic group of diamondiferous rocks has been recognized on the Siberian platform. It is represented by specific picrite - lamproite complexes of subvolcanic rocks and volcanic formations. These are confined to the intersection areas of paleorift structures and to strike slip faults of the transform type. These complexes formed synchronously with the classical kimberlites during the Middle Paleozoic, Early and Middle Mesozoic time.

However, the conditions of melt generation in transform zones differed from those of kimberlite melt generation in ramp structures primarily by their fluid regime ( $H_0$  )  $C_0$  ) and by the depth of mantle sources of magma generation. This resulted in the formation of specific mineral associations chiefly of the eclogitic and lherzolitic parageneses and of specific round - shaped diamonds. The latter are designated as the "Ebelyakh" and "Uraltan" ones and occur over extensive dispersion areas of the northern Siberian platform.

Hence the extension and compression regimes have been shown to combine in the considered tectonic environments. The difference lies in the fact that the classical kimberlite magmatism is characterized by the superimposition of riftogenic branches with basic dyke belts on the collision (ramp) zones while the picrite-lamproite complexes feature the reverse picture, i.e. the riftogenic "shafts" resulting from extension are crossed by strike slip fault zones of transform type.

## THE CATALYTIC FUNCTION OF KIMBERLITE ELEMENTS IN THE FORMATION OF NATURAL DIAMONDS.

*Skvortsova, V.L.; Kulakova, I.I. and Rudenko, A.P.*

*Chemical Department, Moscow State University, 119899, USSR.*

Taking into consideration the laws of catalytic transformation of diamond /1/ and also taking into account data of catalytic polycondensation of simple carbon-containing substances we propose a model of kimberlite diamonds formation from simple carbon-containing substances (for example,  $\text{CO} + \text{H}_2 \rightleftharpoons \text{C}_{\text{diamond}} + \text{H}_2\text{O}$ ). The most important parameter of this model is the catalytic activity of medium which determines both the growth rate and oxidation-dissolution rate of diamond.

We obtain data about the catalytic nature of diamond oxidation-growth processes, role of surface chemical state in these processes and catalytic activity of certain elements in diamond oxidation by water and carbon dioxide which are natural oxidizing agents of diamond.

Our investigations show that the catalytic activity of ions is determined by their chemical nature, valence state and structural accordance of ionic radius to crystalline chemical parameters of diamond planes.

The latter factor is responsible for the differences in rates of catalytic oxidation of different planes and for variation of habitus of crystals in this process. So, the diamond oxidation by water vapor (900°C) in the presence of the Fe(III) ions leads to gradual transformation of octahedral crystals into dodekahedral ones.

It is shown that catalytic activities of a number of natural minerals are similar to those of corresponding oxide mixtures. This makes it possible to model catalytic activities of natural objects. Alkaline melts of kimberlites are also catalytically active in diamond oxidation, the mean catalytic activities of kimberlites from various deposits being different.

The fact that all etched pictures on natural diamonds including the rare ones were reproduced in laboratory proves the possibility of catalytic oxidation of diamond crystals during the formation of kimberlite tubes.

In our opinion the existence of mineral coats on the diamond crystal, their mineral, chemical, isotopic composition and morphological peculiarities confirm the catalytic function of kimberlites in the formation of natural diamonds.

The suggested model of the formation of diamonds is fur-

ther supported by the established connection between the diamond content of kimberlites and their chemical composition and catalytic activities in diamond oxidation and by irregularity of distribution of diamonds along the tube.

This has enabled us to suggest a physico-chemical criterion for valuation of diamond content in kimberlites.

---

<sup>1/1</sup> Rudenko, A.P., Kulakova, I.I., and Shturman (Skvortsova) V.L. 1978. The oxidation of natural diamonds. New data about minerals of the USSR, 28, 105-125.

## MINERAL INCLUSIONS IN BORT FROM THE MIR PIPE, YAKUTIA.

G.B. Smelova.

Yakutsk Institute of Geosciences, Siberian Branch. Academy of Sciences. Yakutsk, USSR.

This paper presents the results of studying mineral and chemical compositions of crystal inclusions in bort.

The inclusions were studied in a sample that measured 7x5x3 mm and consisted of two varieties of bort: fine- and coarse-grained. The fine-grained aggregate makes up the central part of the sample and consists of opaque, up to 0.2 mm sized individuals lacking well-defined crystallographic form. The coarse-grained bort grows over the fine-grained one as a porous crust with cavities and consists of large (up to 1 mm), transparent individuals which also lack well-defined crystallographic form. In one of the cavities there is a druse of well-shaped octahedral diamonds measuring 0.8 - 1 mm.

The sample was cut in two across the druse. Under a microscope, the two polished surfaces of the cut showed numerous transparent and opaque inclusions. The latter are mostly concentrated in the central, fine-grained part of the sample and are 5x15  $\mu$  or less in size. In the outer, coarse-grained part, inclusions are fewer but larger (up to 45x135  $\mu$ ). The compositions of the inclusions were determined using a "Camebax-Micro" microanalyzer.

Only opaque inclusions were found in fine-grained bort. Of them, magnetite (*Mt*) and sulphide (*M<sub>SS</sub>*) inclusions are considered to be syngenetic. They have no accompanying cracks and have a hexagonal shape in cross-section. There are also two-phase inclusions which represent *Mt* - sulphide intergrowths. They also have a hexagonal shape but cannot be considered as syngenetic because they are accompanied by cracks that extend to the surfaces of diamond grains.

*M<sub>SS</sub>* inclusions contain (in wt.%) 28.15-30.05 - Ni, 28.21-30.69 - Fe, 0.18-6.82 - Cu, 0.09-0.36 - Co, and 34.44- 38.04 - S. Syngenetic *Mt* inclusions are practically free of TiO<sub>2</sub> (0-0.71 wt. %) and rich in NiO (up to 3.39 wt.%). In the two-phase inclusions, *Mt* is similar in composition to syngenetic *Mt*, whereas sulphide has the composition 8.54 -

Fe, 55.46 - Ni, 0.28 - Co, 1.19 - Cu 31.65 - S (in wt.%) and corresponds in stoichiometry to NiS (probably millerite).

Coarse-grained bort contains syngenetic garnet, pyroxene and magnesite inclusions in addition to  $M_{SS}$  and two-phase inclusions that are much fewer than in the fine-grained variety of bort

Elongated inclusions of garnet correspond in  $Cr_2O_3$  and CaO contents (3.33-3.64, 3.45-5.69 wt.% respectively) to pyrope of the lherzolitic paragenesis. A pyroxene inclusion, in the form of a parallelogram in cross-section, corresponds in composition to chrome-diopside (1.93 wt.  $Cr_2O_3$ ).

Magnesite inclusions which are found in the coarse-grained bort (six inclusions) and the druse (one inclusion) measure  $5 \times 10 \mu$  and have a hexagonal form in cross-section. Magnesite from the druse is higher in Fe (9.24 wt.% FeO) than that from the coarse-grained bort (4.06 - 4.79 wt.% FeO).

The results lead to the following conclusions:

(1). Based on the chemistry of garnets (Sobolev, 1974) and  $M_{SS}$  inclusions (Yefimova et al., 1983), the studied inclusion suite belongs to the lherzolitic paragenesis of the ultrabasic association. The crystallization temperature is about  $1150^\circ C$  at 45 kbar using the Ellis-Green's geothermometer (1979).

(2). Magnetite is similar in composition to that crystallized from sulphide melt (Skinner, Peck, 1979; Al'mukhammedov, 1982). This suggests that during the early stage of the formation of bort an unmixable sulphide melt existed from which magnetite,  $M_{SS}$  and probably magnetite-sulphide intergrowths were crystallized. In the latter, the sulphide was represented by pentlandite or  $M_{SS}$  later replaced by millerite.

(3). The presence of magnesite and magnetite indicates more oxidized conditions (consistent with OFM buffer) for the formation of bort compared to diamond monocrystals.

(4). A lesser number of magnetite inclusions in coarse-grained bort compared to fine-grained bort indicates a higher oxygen fugacity during the formation of the fine-grained variety of bort.

ON THE PROBLEM OF VERTICAL ZONING OF KIMBERLITE BODIES.  
(ON THE EXAMPLE OF LESOTHO).

*Smimov G.I.; Kharkiv A.D and Zinchuk, N.N.*

The problem of diamond content and composition change with the depth in kimberlite bodies remains extremely the matter of current interest up to the present. For its decision data of prospecting well and exploring openings and also data of directly operation work are used, but interpretation of results obtained quite often are in the contradictory nature. Kimberlite bodies - pipes, dykes and swells, related to dykes of Lesotho, which, owing to peculiarity of geologic development of the region, were turned out to be stripped on different hypsometric levels with drops of heights to 1,5-1,6km in comparatively small distances (130-150km) are unique in this respect. This creates favourable possibility to trace vertical kimberlite changeability within indicated interval without boring of expensive wells.

The authors undertook an attempt to trace changes in relation of pipes, dykes and swells, their dimensions and morphology, composition and peculiarities of diamondiferousness of 4 groups of Lesotho kimberlite bodies, located on different altitudes (about 3,2; 2,6; 1,8; 1,5km) above sea level. The carried out investigations established predominance of dyke facies (with a number of which swells are connected) over pipe facies in all areas. Appreciable differences in size and morphology of dykes have not been registered; at the same time, considerable reduction of pipe formation areas in the direction from mountainous sections to relatively low sections is observed. The bonding mass of dyke swells and some pipes contains increased amounts of perovskite, ilmenite of second generation, and, in a number of cases, phlogopite and monticellite, that is reflected on increased content of  $TiO_2$ ,  $K_2O$  and  $P_2O_5$  in these rocks. Xenoliths of plutonic rocks are characteristic of decreased PT-conditions of formation. Xenoliths of pyroxene-spinel facies prevail among them, and varieties of diamond facies do not practically occur. In spite of appreciable variations of composition in each group and even inside one of a specific body, the increased content of microilmenite, moderately chromous pyrope and

clinopyroxene is registered for majority of dykes and pipes. From secondary minerals, the development of saponite (sometimes to complete substitution of rocks of some dykes by corresponding argillaceous formations) is extremely characteristic one. The study of all garnet selections from kimberlite concentrates of all 4 groups shows either presence of literally single grains of this mineral of diamondferrous facies (Litseng la Terae, Kao, etc.), or their complete absence (majority of non-diamondferrous bodies), that confirms reliability of N.B. Sobolev's mineralogical criteria of kimberlite diamondferrousness.

Thus, the carried out investigations of Lesotho kimberlites have not revealed just a little differences in vertical, almost 1,5-km-sequence, except dimensions of pipe areas. These data are quite in conformity with results of study of a number of Yakutiya kimberlite bodies, traced by prospecting wells up to the depth of 1,0 - 1,2 km.

THE PROBLEM OF PRIMARY SOURCE OF BRAZIL-TYPE DIAMONDS  
(THE CASE-HISTORY OF DISCOVERY OF DIAMOND DEPOSITS  
IN THE ARKHANGELSK REGION).

*V.K. Sobolyev.*

*TsNIGRI (Central Research Institute of Geological Prospecting for Base and Precious Metals)  
North Department, Arkhangelsk, USSR.*

The problem of primary source of spheroidal (rounded) diamonds of the Brazil type has for many years been the most controversial issue of diamond geology. The idea of their origin has mostly been based on data from placers. In the USSR the relation of these diamonds to peridotites of orogenic stage in geosyncline development used to be considered as most trustworthy (A.A.Kukhareenko, 1955). Later on, an idea was advocated that spheroidal diamonds of the Brazil type were associated with common kimberlites (Yu.L.Orlov, 1973). One period the suggestion was in the go that they were exclusively related to Precambrian sources of kimberlite and problematic origin (M.P.Metelkina et al., 1970). The deeper insight into understanding the primary sources of spheroidal diamonds (PSSD) at the theoretical level was gained in the early 1970s when a revision programme on diamonds started in the Arkhangelsk Region. Based on the analysis of data on mineralogy of diamonds, chrome spinellides and individual grains of chrome pyropes co-occurring in a terrigenous complex of the Northern Timan, the PSSDs of the area were attributed to kimberlites differing, at the mineralogical level, from known diamond-bearing varieties of Yakutiya and Africa. The PSSDs appear to be featured by low contents of chrome pyropes, and especially pyroilmenites, and by relatively high contents of chrome spinellides (V.K.Sobolyev, 1979).

2. The major argument in favour of setting-up the concentrating prospecting programme for kimberlites on the White-Sea Winter Coast was the similarity of its heavy-concentrate-mineralogical situation with that of the North Timan area and the discovery of a sheet-like body (sill) of ultrabasic fine-crystalline porphyritic magmatites initially defined as picritic porphyrites and redefined, in light of the idea of the PSSD, as kimberlites two years after the finding (1977). Three years later, a pipe-like body containing lean concentration of spheroidal diamonds of the Brazil type was revealed in the area. That was followed by discovery of similar bodies with commercial concentrations of spheroidal diamonds.

3. The combined indications established in the course of the investigation (summary content of indicator-minerals, their spectra, morphology, typochemism, etc.) allowed us to attribute them to the kimberlites which differ, at mineralogical level, from classical Yakutiyan and African kimberlites with commercial diamonds (V.K.Sobolyev et al., 1983, 1988).

4. The correlation between the PSSD of the SE Belomoriye area and the kimberlites from other provinces was based on comparison between association of deep-seated magmatites of the area in question with known series of magmatites containing kimberlites. They have been assigned to a previously unknown variety of kimberlites within so-called alneite-kimberlite-karbonatite series of deeply-originated volcanites in terms of V.I.Vaganov (1978). Mineralogically, they are the closest to

olivine lamproites of Australia but associated with sodium rather than with ultrapotassium mantle differentiates.

5. The problem of the PSSD placement within the global framework of kimberlite provinces was correctly tackled by M.A. Gnevishnev (1972). According to this author, spheroidal diamonds are confined to the peripheral parts of diamond-bearing provinces, while their central parts host the deposits dominated chiefly by flat-sided crystals. In 1970s the idea prevailed in the USSR that peripheral parts of platforms had no diamond potential. However, after discovery of the PSSD in SE Belomoriye area the diamond potential of the peripheral parts of platforms developed on the ancient basements (cratons) and adjoining zones of Proterozoic mobile belts are hardly in need for additional proof.

6. In prospecting for the PSSD under conditions of the North of the Russian Plate, the heavy-concentrate mineralogical method retains its priority as a tool for prognostication and selection of areas to be involved into concentrating prospecting programme.

METASOMATIC PROCESSES IN SUBCONTINENTAL LITHOSPHERIC MANTLE  
BENEATH THE SIBERIAN PLATFORM.*L.V. Solovjeva; V.G. Barankevich and L.L. Lipskaya.**Institute of the Earth's Crust, 664033 - Yakutsk, USSR. IRGIREDMET, Irkutsk.*

Metasomatic alterations of substance of deep-seated xenoliths from the Udachnaya kimberlite pipe, based on textural and petrographic evidence may be attributed to two episodes of different age. A characteristic mineral association represented by phlogopite, Cr-rich spinel, sulfides and more rare graphite and apatite appears to belong to the earlier episode of metasomatism. Phlogopite forms relatively large plates (0,5-5 mm) which are homogenous within the limits of one grain and specimen except for very narrow rims (50-150 mkm) belonging to the later process.  $TiO_2$  and  $Cr_2O_3$  in phlogopites from a part of specimens are < 1% and correspond to primary micas reported by Carswell (1975) and its contents in other specimens are higher. Graphite occurs in two websterite specimens containing large (1-2 cm) exsolved pyroxenes healed by fine grained granoblastic aggregate of phlogopite, garnet, pyroxenes, sulfides and graphite. Grains of graphite are a part of granoblastic fabric and exhibit intergrowths with garnet and phlogopite on grain margins.

Isotopic composition of carbon in metasomatic graphite yield  $\delta^{13}C$  values equal to -7,83 and -10,82‰ (Galimov et al., 1987). This carbon which is lighter than the carbon used for the mantle datum (2-7‰), is nevertheless of obvious mantle origin deriving from greater depths than those of websterite equilibrium (~25 kbar).

The lighter isotopic composition of carbon may be explained by removal of heavy carbon during carbonatization of the mantle

environment (Galimov et al., 1987), or by making the carbon lighter at expense of a successive graphite precipitation within rising reduced fluid ( $\text{CH}_4$ , H). The latter mechanism is confirmed by  $f_{\text{O}_2}$  values corresponding to position between buffer curves MW-IW (for Ol-Opx-Sp equilibrium). Temperatures estimates obtained from En-Di solvus indicate the decrease in following order: calculated homogenized pyroxenes in large relict crystals, calculated homogenized pyroxenes in matrix, compositions of pyroxenes without exsolved intergrowths in matrix. Apatite occurs in one specimen of orthopyroxenite where, together with small crystals of phlogopite, pyroxenes and sulfides, it heals large exsolved grains of orthopyroxene.

Textural evidences suggest that the early metasomatism developed prior to rock deformation. This process appears to take place at the Early Archean and is related to evacuation of reduced fluids and crust granitization.

The late metasomatic process is pervasive in xenoliths of various lithology and is manifested in reaction rims on minerals of primary paragenesis. This type of metasomatism is abundantly developed in deep-seated xenoliths of kimberlites and lamproites from many areas of the world. It occurs in the form of polymineral rims on garnet: Al-orthopyroxenes, Al-clinopyroxenes, chemically heterogeneous spinel, phlogopite, rare amphibole of pargasite type. Orthopyroxene is replaced by acicular amphibole, Al-clinopyroxene, spinel. Sulfides are totally or partially substituted by djerfisherite. This process is responsible for melting patches in xenoliths.

$f_{\text{O}_2}$  value calculated from ilmenite-spinel equilibrium in reaction rims of eclogite xenolith and melting patches into megacrust of Cr-low garnet is slightly below HM (hematite-magnetite) curve. Such a metasomatic type is characteristic of the prekimberlite episode and is probably related to oxidized asthenospheric fluids.

O, C AND Sr ISOTOPIC COMPOSITION OF CALCITES IN GARNET MEGACRYSTS  
AND CARBONATIZED GRANULITIC XENOLITHS FROM THE UDACHNAYA  
KIMBERLITE PIPE, YAKUTIA.

*L.V. Solovjeva; L.V. Dneprovskaya; M.N. Maslovskaya and S.B. Brandt.*

*Institute of the Earth's Crust, 664033 - Yakutsk, USSR.*

Calcite in megacrysts of Cr-low garnet ( $TiO_2=1-2\%$ ,  $Cr_2O_3=0,6-3,15\%$ ,  $mg=0,73-0,81$ ) from the Udachnaya and the Mir kimberlite pipes occurs within particular fine-grained polymineral inclusions. The latter consist of red-brown phlogopite (20-30%), dotted spinel (3-7%), amphibole (0-30%) and serpentine (10-40%). In some cases small grains of ilmenite and a dotted perovskite are observed. Inclusions fill the rounded cavities which dimensions vary from 0,5 up to 3 mm. Their texture is a typical microporphyric in which small euhedral and subhedral crystals of phlogopite, amphibole and calcite are enclosed in the interstitial material composed of serpentine, probably replaced the former glass. Crystals of amphibole and phlogopite rim the deeply corroded garnet boundary replaced by an ultrafine-grained dark-brown material typical of kelyphite rimming the garnets. Shulze (1985), Hops (1986) assume similar polymineral inclusions to be due <sup>to</sup> crystallization of kimberlite-related melts entrapped by megacrysts. The initial  $^{87}Sr/^{86}Sr$  ratios in calcites of similar polymineral inclusions from the Udachnaya pipe are higher than 0.706.

O, C and Sr isotopic studies of totally or partially carbonatized xenoliths representing almost monomineral medium- or coarse-grained rocks consisting of semi-transparent grains of calcite as well as of a small amount of bluish serpentine have been carried out. In contrast to calcite, serpentine exhibits a zoned distribution thus increasing its content in xenolith rims. Relict minerals in different samples are represented by garnet, biotite

and pyroxene. The isotopic-geochemical characteristics of the core carbonate component for three xenoliths are as follows:  $\delta^{18}\text{O}=27,1\pm 20,4^\circ/\text{oo}$ ;  $\delta^{13}\text{C}=-4\pm 5^\circ/\text{oo}$  and  $\text{Sr}=9500\pm 10000$  ppm. The carbonate constituent of the kimberlite which includes one xenolith shows  $\delta^{18}\text{O}=15,2^\circ/\text{oo}$  and  $\delta^{13}\text{C}=-4,2^\circ/\text{oo}$ ; that of seven kimberlite samples from the Udachnaya pipe shows the following variations:  $\delta^{18}\text{O}=17,9\pm 22,6^\circ/\text{oo}$  and  $\delta^{13}\text{C}=-2,9\pm 7,2^\circ/\text{oo}$ . The carbonate extract from the Precambrian fine-grained marble with magnetite shows the  $\delta^{18}\text{O}$  and  $\delta^{13}\text{C}$  values to be  $25,1^\circ/\text{oo}$  and  $1,37^\circ/\text{oo}$ , respectively. Carbonates from the Paleozoic terrigenous-sedimentary rocks containing kimberlites yield the mean values of  $\delta^{18}\text{O}=25,3\%$  and of  $\delta^{13}\text{C}=-1,5^\circ/\text{oo}$ .

The authors suggest the metasomatic replacement of crust granulites by calcite to be due to gas-fluid phases related to kimberlite systems. These fluids appear to be the main source of carbon and strontium. The oxygen source in carbonatized granulites is probably of more complex origin and it seems to be related to ancient metacarbonate rocks.

COGNATE SUITE OF GARNET CLINOPYROXENITE-OLIVINE WEBSTERITE-  
LHERZOLITE FROM THE UDACHNAYA KIMBERLITE PIPE, YAKUTIA.*L.V. Solovjeva and B.M. Vladimirov.**Institute of the Earth's Crust, 664033 - Yakutsk, USSR.*

A suite of garnet clinopyroxenite-olivine websterite-lherzolite (CWL) according to quite a number of petrographic and mineralogical properties determining its cognate character differ from the other granular xenoliths from the Udachnaya kimberlite pipe.

Lherzolites, harzburgites, more rarely dunites of spinel, spinel-garnet and garnet abyssal facies (HL) represented probably metamorphosed restites, which are remnants after extraction of basaltoid and komatiitic melts strongly predominate in the granular deep-seated xenoliths from the Udachnaya pipe. Rocks of the CWL suite make up not more than 3% in granular population. In contrast to the HL suite they are characterised by a wide variation of garnet, pyroxenes, olivine and are classified as garnet lherzolites, garnet-olivine websterites and garnet clinopyroxenites. The presence of phlogopites and sulfides, developed in the form of globules in garnet and clinopyroxene and in the form of dispersed impregnation are characteristic of lherzolites and olivine websterites of the CWL suite. Small inclusions of ilmenite and Ti-spinel are observed in phlogopite plates. Ti-spinel does not exhibit reactional relationships with garnet. Thin exsolved intergrowths of ilmenite and rutile are common for garnet and pyroxenes. Rock texture suggests a paragenetic character of phlogopite plates. Phlogopite, ilmenite, Ti-spinel and impregnated sulfides appear to be crystallized at the late stage of formation of the main paragenesis. Reactional mineral assemblage is manifested in the form of polymineral kelyphite rims on garnet, orthopyroxene and in the form of reactional djerfisherite zones on sulfides.

Minerals of the CWL suite essentially differ from corresponding minerals of the HL suite in lower Mg/Mg+Fe ratio of silicates, higher  $\text{TiO}_2$  contents in garnet and clinopyroxene and lower  $\text{Cr}_2\text{O}_3$  contents in garnet, and higher  $\text{Na}_2\text{O}$  and  $\text{Al}_2\text{O}_3$  contents in clinopyroxenes. Direct correlations between Mg content in olivine, garnet, clinopyroxene and phlogopite as well as between  $\text{TiO}_2$  and  $\text{Cr}_2\text{O}_3$  contents in garnet and clinopyroxene, are observed. These correlations are probably expected to be the evidence of the total equilibration of the chemistry of minerals at the late stage of rock formation at a moment when phlogopite, sulfides, ilmenite and Ti-spinel were crystallized. On the basis of Fe and Mg distribution (Ellis, Green, 1979) between small regular clinopyroxene crystals in garnet and host-garnet and for large grains of these minerals in rock, the higher temperatures of the beginning of crystallization are obtained. The position of five samples of the CWL suite on geotherm for the Udachnaya pipe corresponds to two levels, 60-70 km and 120 km, respectively. Bulk chemical composition of two samples is the most consistent with komatiites of peridotite type. All the above data do not contradict a hypothesis of magmatic origin of the CWL suite. Its intrusion and fractional crystallization appear to have taken place after the main episode of cooling and metamorphism of the mantle lithosphere but prior to development of prekimberlite metasomatism.

LAYERED STRUCTURE OF THE UPPER MANTLE BENEATH THE SIBERIAN  
PLATFORM: PETROLOGICAL AND GEOPHYSICAL DATA.*L.V. Solovjeva and L.L. Zavjalova.**Institute of the Earth Crust, 664033 - Yakutsk, USSR.*

P-T data for deep-seated xenoliths from kimberlites in Yakutia, obtained by thermobarometric methods, reveal layered stratified structure of the mantle in the Udachnaya pipe area (the central part of the platform) to the depth of 220 km and in the Obnazhennaya pipe area (Olenek uplift) down to 120 km. The mantle in the central part of the platform to the depth of 180 km is recognized to be largely composed of restite spinel, spinel-garnet and garnet lherzolites and harzburgites, and by horizons of pyroxenites, websterites, olivine websterites occurring between 60-78 km, 90-96 km and 141-171 km depths.

These three horizons are affined in their depth and thickness to low velocity layers recorded beneath the Siberian platform according to the deep seismic sounding data (Egorkin et al., 1984). Two layers of rocks of pyroxenite-websterite series approximately corresponding to the upper layers in the mantle lithosphere under the central part of the platform, are distinguished under the crust in the Obnazhennaya pipe area. A detailed study of petrography, petrochemistry and mineralogy of rocks from pyroxenite-websterite series indicate that they are commonly cumulates of the former ultramafic melts of komatiitic type and more seldom are products of total crystallization of such melts, which existed in the ancient mantle lithosphere at corresponding depths in the form of large intrusive sheets.

The roof of the lower low velocity layer on the seismic profile under the central part of the platform (depth of 190 km) conforms to the upper part of the zone corresponding, according to P-T data, to sheared peridotites whose origin is more often related

to the asthenosphere. There is some vertical displacement of the four layers revealed by petrological methods, relative to the low velocity layers determined by geophysical data.

The geotherm constructed on the samples from the Udachnaya pipe is close to that with the heat flow of  $40 \text{ mW/m}^2$  and to an empiric geotherm by F.R.Boyd (1984) for the same pipe. The pristine geotherm is also reconstructed after the relict exsolution orthopyroxenes in harzburgites and lherzolites of restitè type, which is  $200\text{--}300^\circ\text{C}$  higher than that of the last chemical equilibrium in samples. This temperature difference as well as a probable presence of large intrusive sheets of komatiite melts in the ancient mantle lithosphere suggest the continuous hot stage in the life of the upper mantle followed by the stage of long term cooling. The latter is quite distinctly determined by unidirectional reaction of replacement of spinel paragenesises by garnet ones, recorded everywhere in deep-seated xenoliths from kimberlites in different regions of the world. The ancient stage of metasomatism was manifested in already cooled rigid and brittle lithosphere in the form of mineral products. The estimation of the bulk composition of the mantle lithosphere in the Udachnaya pipe area according to the balance of pyroxenite-websterite and harzburgite-lherzolite layers, show that the mantle was sufficiently depleted in basaltoid components ( $\text{TiO}_2$ ,  $\text{Al}_2\text{O}_3$ ,  $\text{FeO}$ ,  $\text{CaO}$ ,  $\text{Na}_2\text{O}$ ) already during the hot stage of its existence.

## A STUDY OF MICROINCLUSIONS IN MINERALS OF SPANISH LAMPROITES.

*I. Solovova; A. Gimis; L. Kogarko and I. Ryabchikov.*

In order to estimate thermodynamic conditions and melt compositions of Spanish lamproites, microinclusions in olivine, clinopyroxene, sanidine, apatite, phlogopite, and calcite have been studied. Among daughter minerals in melt inclusions Ol, Phl, San and F-Ap were determined. Unusual compositions of daughter minerals correspond to unusual chemistry of lamproitic lavas: i.e. San contains large quantities of both Mg and Fe, Phl contains up to 8 wt.% TiO<sub>2</sub> and more than 1 wt.% F.

Homogenization temperature of melt inclusions in the most magnesian olivine is 1250°C and decreases with increasing of X<sub>Fe</sub> of Ol to 1050°C. Average composition of homogenized melt inclusions in the earliest olivine studied (X<sub>Fe</sub>=0.08) is following: (wt.%) SiO<sub>2</sub> 52.1, TiO<sub>2</sub> 0.2, Al<sub>2</sub>O<sub>3</sub> 11.6, FeO(t) 3.9, MgO 5.4, CaO 0.1, BaO 0.3, Na<sub>2</sub>O 0.9, K<sub>2</sub>O 13.5, P<sub>2</sub>O<sub>5</sub> 3.4, F 0.9, Cl 0.3. The composition of the late-stage melts is represented by primary melt inclusion in calcite: SiO<sub>2</sub> 64.7, TiO<sub>2</sub> 0.8, Al<sub>2</sub>O<sub>3</sub> 17.8, FeO(t) 1.1, MgO 0.2, CaO 2.5, Na<sub>2</sub>O 0.3, K<sub>2</sub>O 4.6. Water content of this evolved melt is about 8 wt.%. For more primitive melts a value 4 wt.% have been estimated.

Fluid inclusions are mostly partially decrepitated low-dense CO<sub>2</sub>. Sometimes salt crystals on the walls of fluid inclusions are visible, proving high halogen concentrations in the fluid.

Daughter sanidine in melt inclusions contains appreciable amount of Fe<sup>3+</sup> which is characteristic of high oxygen fugacity. On the other hand liquid immiscibility detected in residual glasses is possible only under relatively reduced conditions. Thus our data confirm highly variable oxygen fugacity during lamproite crystallization which was advocated by Venturelli et al. (1988).

On the basis of our data we propose a model of primary melt formation by the melting of Phl-bearing lherzolite at relatively low pressures.

## STUDY OF GASEOUS PHASE IN DIAMONDS WITH ECLOGITIC AND ULTRABASIC INCLUSIONS FROM YAKUTIAN KIMBERLITE PIPES.

*S.B. Tal'nikova; Yu. P. Barashkov and I.M. Svoren'*

*Yakutsk Institute of Geosciences (USSR).*

The reproducibility of the results obtained by various degassing methods for diamonds from different deposits suggests that the liberated gases are relicts of a fluid of the diamond crystallization medium.

To get additional information and to test a possible relationship of gas composition of diamonds to their inclusions paragenesis and to the presence of solid inclusions, we studied diamonds whose paragenesis was in most cases known from the composition of solid inclusions.

Gases which are sorbed in dislocations, vacancies, microcracks and other lattice defects of diamond were liberated by heating a sample in an inert atmosphere using special device connected with an MX-1303 mass-spectrometer. Diamond crystals were thoroughly cleaned immediately prior to analysis using a specially developed scheme. Before each analysis, the device was degassed by heating to 423...473 K. Cooling was performed at a constant evacuation value ( $10^{-7}$  Torr). The cleaned crystal was placed in a glass capsule. After the device was mounted and connected with mass-spectrometer, the system was evacuated up to  $1 \times 10^{-7}$  Torr. Due to minimum weight of the sample, heating was carried out at  $T=693$  and  $1593$  K. The gases thus obtained were fed to the mass-spectrometer.

We analyzed six diamond crystals from Udachnaya pipe (samples 3165, 3027, 3038, 3689, 3207, 3037) one (sample 1169) from Mir and one (sample 2086) from Aykhal. Crystals 3689, 3207, 2086, and 1169 were colourless, flat-faceted octahedra, 3027 was a

yellow cube, 3038 was a grey opaque cube, 3037 was a macle of a coated diamond, and 3165 was a crystal of indefinite shape. Octahedral crystals 3689 and 1169 contained olivine and pyrope-almandine inclusions respectively. These crystals were sawn in such a manner that one half contained inclusions and the other had no visible inclusions. Crystal 3037 was preliminarily crushed and its yellow coat separated from the transparent core. The studied samples varied in weight from 4.4 to 194.3 mg. The concentration and composition of liberated gases vary from crystal to crystal. All samples contain  $H_2$ ,  $N_2$  and  $CO_2$ . Other gases are present in only some of the crystals:  $CO$  in 1169, 3689, 3037;  $H_2O$  in 2086, 3165, 3038, 1169, 3207, 3037;  $CH_4$  in 3038, 1169, 3207, 3037;  $C_2H_6$  in 3038. Both halves of 3689 have gases of similar composition but the half with olivine inclusions is somewhat higher in  $CO_2$ ,  $CO$  and  $N_2$ . The situation is different in crystal 1169.  $N_2$ ,  $CO_2$  and  $CH_4$  contents are several times higher in the half with pyrope-almandines compared to the half free of visible inclusions. The latter half also contains  $CO$  and  $H_2O$ . In 3037, gas content of the transparent core is much higher than that of the yellow coat. Gases in the grey cube 3038 differ in composition not only from the yellow cube 3027 but also from the rest of the studied samples. It was the only crystal which contained the  $C_2H_6$  homologue. The yield of gases (in g/g of crystal) varies widely, from  $47.699 \times 10^{-6}$  to  $684.974 \times 10^{-6}$ , in eclogitic diamonds and in a narrower interval, from  $4.221 \times 10^{-6}$  to  $5.247 \times 10^{-6}$ , in ultrabasic diamonds.

This, the present study has revealed that gas composition is dependent on the presence of solid inclusions in diamond. Higher gas contents of the diamond halves containing mineral inclusions are probably due to sorption of volatiles at the diamond-inclusion interface. Gas contents of eclogitic diamonds are an order of magnitude higher than those of ultrabasic diamonds.

## UPPER MANTLE COMPOSITION BENEATH YAKUTIAN KIMBERLITE PROVINCE.

A.V. Ukhanov<sup>(1)</sup> and A.D. Kharkiv<sup>(2)</sup>.*(1) Vernadsky Institute of Geochemistry and Analytical Chemistry, Moscow; (2) Central Research Institute of Geological Prospecting for Non-ferrous and Precious Metals, Moscow.*

Mineralogical studies in Yakutian province have shown that "sampling" by kimberlitic magma seems to be rather selective. There are a lot of gaps and misrepresentations even in the most complete and informative upper mantle "sections" drafted on the basis of P-T "records" in mantle mineral assemblages.

On the P-T plots (Ukhanov, Ryabchikov, Kharkiv, 1988) the points are scattered along smooth curvilinear trajectories what are thought to be paleo-geotherms. They are consistent with continental geotherms by Clark and Ringwood (1964) for "Obnazhennaya" and "Udachnaya", but "Mir" geotherm is shifted 100-150 C to lower temperatures. In contrast to Lesotho geotherm by Boyd (1976) no inflexions or breaks have been revealed in Yakutian ones. That implies more stable thermal regime in Yakutia in the period of kimberlitic magmatism. The reconstructed upper mantle "sections" for the north (Obnazhennaya), middle (Udachnaya) and south (Mir) of the province are grossly drafted. In general the upper mantle of the region is characterized: 1) by wide extended spinel or partly granitized peridotites of "barren" type directly below Mocho; 2) by prevalence of "fertile" garnet peridotite, sheared or unsheared, at deeper levels; 3) by the presence of various garnet-pyroxene rocks - Mg-rich pyroxenites at more shallow levels and eclogites at depth; 4) by spreading of ilmenite-bearing rocks through the whole sections and amphibole-flogopite metasomatite in their upper parts.

In this paper emphasis is placed on the origin of some garnet-pyroxene rocks. More than ten subgroups of them can be distinguished within the investigated xenolith suites but at present only for the largest ones reliable petrogenetic interpretations can be proposed. The geologically spectacular xenoliths of the coarse garnet pyroxenites, which are so abundant in "Obnazhennaya", have visible banding and are composed of 3 to 5 minerals enriched in MgO and Cr (Cpx+Gar+Opx+Ol+CrSp). Taken as a whole the xenoliths resemble fragments of a layered intrusive body. If it is more than appearance and the rocks are fundamentally magmatic the garnet cannot be a magmatic mineral in any case since

it seems to replace the chromium spinel and partly pyroxene. Before the replacement the layers had consist of Opx, or Cpx , or both and at least locally of plagioclase that has been pointed to by the positive Eu anomalies on REE patterns revealed for some nodules. At the same time the negative Eu anomalies for orthopyroxene and chromium spinel indicate that these two minerals had been crystallized together with plagioclase like in basic-ultrabasic magmas.

A portion of the magma is thought to be intruded in the top of the mantle sequence to form a vast layered massif with chromite horizons and zones enriched in sulfides. In that connection it is worth to mention extremely high gold abundances (up to 6 ppm) in rare xenoliths and chromite ore nodules in some pipes. The following garnet development in layered pyroxenites was caused by pressure increasing under some fluid influx. The ultramafic basis of massif was transformed to the garnet lherzolite which appears to be depleted in less degree than the more shallow harzburgite.

## THE GENETIC TYPES OF NATURAL DIAMONDS.

*A.A. Valter and V.N. Kvasnitsa.**Inst. of Geochem. and Phys. of Minerals, Ukr. SSR, Kiev.*

Diamond is a polygenetic mineral, which is generated not only in the Earth interiors but also during the high velocity impact of cosmic bodies and by the vapor condensation of interstellar matter. Probably the diamonds distribution correlate in a hole with the carbon abundance. The atomic ratio C/Si can be evaluated in the Earth crust as  $1.8 \cdot 10^{-3}$ , in the mantle 0.1 and in the Space 125. Now it is possible to distinguish the mantle magmatic, crust magmatic, shock metamorphic and condensational types of the diamond origin.

The mantle diamonds still is known only in the Earth, but its existence is quite possible in the interiors of the Lunar and greater cosmic bodies. It can be realized because in the initial matter of the Planets, if it is of the carbonaceous chondrite type, is the sufficient content of C.

At the Earth mantle the diamond was formed by the high P-T parameters in the static conditions. It represents by the ultrabasic (peridotite) diamond, basic (eclogite) diamond and by the diamond of the rocks with intermediate composition (garnet pyroxenite). These diamonds were intruded in the Earth crust by the kimberlitic and lamproitic magmas. The most possible parameters of its crystallisation are  $P \approx 4.5-6$  GPa;  $T \approx 1000-1500^\circ\text{C}$ . The crystal growth of diamond is diffusional and is the result of chemical reactions with hydrocarbons participation and by the graphite-diamond transition.

The diamond of metamorphic rocks quite differ from the mantle diamond and forms small ( $n-10 \cdot n$  microns) cubic and skeletal crystals and aggregates. One will suggest that this diamond was formed by the lower parameters, probably at the expense of disperse organics. The forms of diamonds bring in evidence the supersaturation by the

carbon and high speed of crystal growth and cooling. As N.V. Sobolev and others suppose this type of diamond was formed in the crust.

The shock metamorphic diamond of meteorites and impactites was formed by the graphite-diamond transition in the shock waves. The "compulsory" diffusion and the other ways and also geometric models of graphite-diamond transition, which ensure the approximate coherence between the initial and new phases, are discussed. The existence of the lonsdaleite in the impact diamond is possible only in a form of very small crystallites. With the extension of its dimensions the cubic diamond phase become more advantageous energetically. In the case of shock metamorphism of poor graphitised organics the weakly crystallized cubic diamond is appeared. The optimum parameters of shock graphite-diamond transition and its chilling is estimated for the Earth rocks as 50-70 GPa and 1000-2000°C for existence of residual temperature duration in melts at the  $T \geq 1500^\circ\text{C}$  for the time of order of one day. The positive factor of diamond preserving is the reduce conditions of impact exposure.

The graphite-diamond shock transition is realised in the Earth crust (impactites) and in the iron meteorites at the moment of its impact against the Earth (Canyon Diablo meteorite) and by the shock in the Space (Antarctic meteorite ALHA-77283).

The most high diamond content among the natural materials exist in ureilites - up to 1%. In this case the mixture of poor crystallized graphite and small diamond crystals probably are subjected to the influence of shock metamorphism. That reflected in the higher dimensions of the diamond crystallites and in the absense or relatively low content of lonsdaleite.

The colloidal (with 28 Å of middle dimension)<sup>diamond</sup> was discovered during the last years in carbonaceous and ordinary chondrites. The most probably this diamond is formed by interstellar gas condensation. The problems of its origin is still discussed.

## KELYPHITES ON GARNETS IN MANTLE XENOLITHS AND KIMBERLITES: COMPOSITION, GENESIS, PETROLOGICAL IMPLICATION.

*Vishnevsky Alexei A.*

*USSR, 252142, Kiev, Palladina av. 34, Institute of Geochemistry and Physics of Minerals Ukr. Acad. of Sci.*

### COMPOSITION.

Today in kelyphites identified more than fifteen minerals, the most common of which are phlogopite, clinopyroxene, orthopyroxene, amphibole, chlorite, serpentine, carbonates, minerals of spinel group. On garnets in mantle xenoliths mainly developed two pyroxene - spinel rims, while in kimberlites, in most cases, kelyphites have phlogopite-spinel composition.

Chemical composition of minerals from kelyphites highly specific and variable:

orthopyroxene -  $Mg/Mg+Fe=0.76-0.97$ ,  $Al_2O_3=5-13$  wt.%, CaO - up to 2.5wt.%;  
clinopyroxene -  $Ca/Ca+Mg=0.31-0.57$ ,  $Mg/Mg+Fe=0.72-0.91$ ,  $Al_2O_3=4-14$  wt.%;  
phlogopite -  $Mg/Mg+Fe=0.78-0.94$ ,  $Cr_2O_3$  - up to 8.9 wt.%;  
spinel -  $Mg/Mg+Fe=0.09-0.86$ ,  $Cr/Cr+Al=0.01-0.90$ , etc.

Established positive correlation between content of Cr, Ti, Fe in minerals from rims and its content in replacing garnets.

### GENESIS.

I. PT-conditions of formation. Process of formation of kelyphitic mineral aggregates, realized in several stages, in general outline could be conceived in a such way:

first stage -  $10 < P < 40$  kbar,  $800 < T < 1300^\circ C$  - reaction replacement of garnets by high-temperature mineral assemblages, i.e.: Phl+Spl, Phl+Cpx+Spl, Opx+Cpx+Spl, Phl+Opx+Cpx+Spl, Amf+Opx+Cpx+Spl;  
second stage -  $P < 5-10$  kbar,  $T < 800^\circ C$  - amphibolization and chloritization of silicate minerals of high-temperature assemblages;  
third stage -  $T < 400^\circ C$  - serpentinization and carbonatization of earlier formed mineral aggregates.

2. Chemical regime. During the process of kelyphitization the most mobile components are Si, Ca, K, Na,  $H_2O$ , less mobile - Mg, Al, Fe and inert - Ti and Cr. In all cases take place considerable introduction of  $H_2O$ , K, Na and insignificant amounts of Fe into forming coronas. Negative balance shows Si and often Al. Other components (Ca, Mg, Mn) have both - positive and negative balance.

3. Causes, speed and possible mechanism of formation. One of the main factors, which stipulated the process of kelyphitization, was sharp decrease of pressure at  $T \approx \text{const}$ ; the last is a result of rapid ascent of kimberlite magma from mantle to the surface. Other significant cause - action of rich in alkalies and  $H_2O$  kimberlitic magma (fluid) on garnets.

On the base of published experimental data we suppose that replacement of garnets by high-temperature assemblages is a transient process, that finished in the majority of cases during a few hours.

Kelyphitization of garnets in mantle xenoliths and kimberlites conceived us as a process of metasomatic replacement of them in the upper mantle. Evidence of that - morphological features of kelyphites, established regularities of migration of components and PT-conditions of process.

#### PETROLOGICAL IMPLICATION.

Developed notions about nature and conditions of formation of kelyphites allows to discuss a number of questions regards the genesis of kimberlitic rocks. For example, proposed two-stepped scheme of changing of PT-conditions during the ascent of kimberlitic magma to the surface, estimated speed of its ascent, suggested considerations about its chemical evolution during transportation from the mantle, etc.

BASALTIC AND MICA KIMBERLITES OF THE SIBERIAN PLATFORM AND THEIR  
TIME-SPACE AND GENETIC RELATIONSHIPS.

*B.M. Vladimirov; K.N. Egorov; M.N. Maslovskaya; L.V. Dneprovskaya and A.V. Boltentkov.*

*Institute of the Earth's Crust, 664033 - Irkutsk, USSR.*

Four age groups of kimberlites are distinguished in East-Siberia, namely: Riphean (1260 m.y.), Middle Paleozoic (344-409 m.y.), Lower Mesozoic (217 m.y.) and Upper Mesozoic (149-159 m.y.). Most of contemporaneous bodies form isolated fields and zones. A number of fields comprising bodies of similar ages, are classified as complexes.

In all Phanerozoic complexes both basaltic and mica kimberlite types are present. Their spatial relationships are very diverse. Usually basaltic and mica kimberlites form their own bodies and rarely they coexist in twinned and multiphase pipes and also in veined bodies of different phases. Pockety segregations, autoliths and xenoliths of mica kimberlite are found in many pipes composed of basaltic kimberlites. Abundance ratios of bodies consisted of basaltic and mica kimberlites from different complexes are not similar. All Pre-Cambrian and most of Upper Mesozoic bodies are mica kimberlites. In the Lower Mesozoic complex both rock types occur in equal number of bodies and in the Middle Paleozoic basaltic kimberlites predominate.

Based on detailed study of some Paleozoic bodies stripped in the Udachny mine time-space relationships and isotopic-geochemical features of different kimberlite types, are given. Here at the south-western and eastern edges of quarry two parallel veins (~~№№~~ 2,4) of mica kimberlites intruded by the Udachnaya-Zapadnaya and Udachnaya-Vostochnaya multiphase pipes, are

exposed. The Udachnaya-Zapadnaya and Udachnaya-Vostochnaya pipes are composed of mica and basaltic kimberlites, respectively. Two "blind" isometric bodies consisted of basaltic kimberlites are stripped along the strike of the vein № 2. Four veins of basaltic kimberlites, which have no contacts with the pipe are exposed at north-western and western edges of the quarry.

Three varieties of mica kimberlite are distinguished at the Udachny mine: 1) massive clinopyroxene-phlogopites, 2) phlogopite breccia and 3) fluidal phlogopites. The first variety composes veined bodies of early phases of emplacement (veins №№ 2,3,4). Phlogopite and clinopyroxene (30-35 and 15% of rock volume, respectively) occur as tabular and prismatic microlites only in groundmass. The second variety is abundant in the Udachnaya-Zapadnaya pipe. Phlogopite consists 15-20% of rock and occurs as deformed tabular xenocrysts and undeformed phenocrysts. The third variety occurs in autoliths from the Udachnaya-Zapadnaya pipe. Bulk phlogopite (up to 30% of rock) is represented by plates in groundmass. Ore minerals of all varieties are spinel, perovskite and ilmenite. Pyropes, picroilmenite and chromite are present as accessory minerals.

Basaltic kimberlites from the Udachny mine consist mostly of olivine-monticellites. Phlogopite is sporadically present as xeno- and phenocrysts. Ore minerals are spinel, perovskite, and ilmenite. Pyrope, picroilmenite, chrome diopside, orthopyroxene and chromite occur as accessory minerals.

Sr and O isotopic studies of basaltic kimberlites gave low  $^{87}\text{Sr}/^{86}\text{Sr}$  ratios (0.7042-0.7047), which are typical of those from other kimberlite localities and of primitive or slightly depleted mantle. Clinopyroxene-phlogopite kimberlites

are similar to basaltic type in Sr isotopy. Their Rb-Sr ages are 352 m.y. Structurally brecciated and fluidal phlogopite kimberlites have higher  $^{87}\text{Sr}/^{86}\text{Sr}$  ratios (0.7054-0.7090) with  $\delta^{18}\text{O}$  values ranging from 16.2 to 22.6‰. Rb-Sr ages of the former are  $345 \pm 5$  m.y.

Phlogopite phenocrysts occurring in both basaltic and phlogopite kimberlites show low initial  $^{87}\text{Sr}/^{86}\text{Sr}$  ratios (0.7040-0.7050) and variable Rb/Sr ratios (50, 200), which suggest their crystallization from isotopically homogeneous melt under different physico-chemical conditions.

Phlogopite xenocrysts do not form their own isochrone. At the moment of kimberlite body formation they had  $^{87}\text{Sr}/^{86}\text{Sr}$  ratios  $> 0.8$ , characteristic for alkaline rocks of the platform basement.

The obtained data indicate the initially common mantle source for all kimberlite varieties from the Udachny mine and mixed mantle-crust origin of phlogopite kimberlites from the Udachnaya-Zapadnaya pipe.

CARBONATITES OF K-ALKALINE COMPLEXES OF THE ALDAN,  
NORTH PAMIR AND SOUTH MONGOLIA.*Vladykin N.V.**Institute of Geochemistry, Irkutsk, USSR.*

The calcite, calcite-fluorite and Ba-Sr carbonatites are found in the complicated laminated complexes of K-alkaline rocks. The carbonatites of the South Mongolia, Aldan (Murun, Khani, Arbarastakh, Intili massifs) as well as of North Pamir (Darai-Pioz) were studied. The complexes are composed of K-ultramafic rocks (Bt-pyroxenites, K-ijolites, melanephelinite) leucite and alkaline syenites, alkaline granites.

In the Murun and Darai-Pioz massifs the carbonatites are intruded after the alkaline granites, they possess the unique mineral composition. Among the rare minerals, charoite, tinansite, pectolites, mizerite, agrellite, ekanite, dalyite are available here. The marked variations of the chemical and rare-element composition is typical of carbonatites. Nb, TR, Ba, Sr, P occurrences are known. The studied carbonatites were formed from the residual melt. It is confirmed by the presence of the molten inclusions and Ba-Sr carbonatite disintegration.

CHEMICAL COMPOSITION AND GEOCHEMICAL FEATURES OF MICAS FROM  
LAMPROITES OF THE ALDAN SCHIELD, USSR.

*Vladykin, N.V.*

*Institute of Geochemistry, Irkutsk, USSR.*

The chemical composition and the concentrations of 25 rare elements were studied in 60 mica samples from the Aldan lamproites. They refer to Mg-biotite Fe-phlogopite tetraferri-phlogopite type according to the chemical composition. Al deficiency and the heightened Ti, Ba, Cr concentrations are typical of them.  $T e^{3+}$  occur in the tetrahedral coordination instead of Al. The natural change of rare element concentrations is observed in micas from the early olivine lamproites to the later leucite and sanidine varieties. The low concentrations of lithophile elements and high ones of siderophile elements are common to the micas of lamproites. It indicates their deep mantle genesis.

GEOLOGICAL POSITION, PETROLOGY AND GEOCHEMISTRY OF LAMPROITES  
(ALDAN SCHIELD, SIBERIA).*Vladykin, N.V.**Institute of Geochemistry, Irkutsk, USSR.*

15 occurrences of lamproites are found in the Western, Central and Eastern Aldan at present. They form sills, necks, eruptive breccias, dykes, stocks and individual layers in the laminated intrusions of K-alkaline rocks. The Khani olivine lamproites are the Proterozoic age, the rest lamproites are the Mz-age. The olivine-micaceous, leucite-micaceous and sanidine-K-richterite-micaceous varieties are distinguished according to mineral composition. The characteristic accessory minerals (chromite, wadeite, K-richterite, K-batisite, priderite) are available.

The heightened K, Mg, Ba, Sr, Cr, Ni, Cu concentrations and the decreased concentrations of Nb, TR are typical of the Aldan lamproites. Eu-anomalies are absent in the TR spectrum. The Aldan lamproites are genetically connected with volcanic-plutonic complexes of K-alkaline rocks.

## INCLUSIONS OF PLUTONIC MINERALS IN DIAMONDS FROM KIMBERLITE ROCKS OF THE NORTHERN EAST-EUROPEAN PLATFORM.

*Zarharchenko O.D.; Khar'kiv A.D.; Botova M.M.; Makhin A.I. and Pavlenko, T.A.*

According to data of visual diagnosis it has been revealed, that diamonds with plutonic minerals inclusions from kimberlite pipes of the East-European platform (EEP) amount to 0,6 - 2% from the whole quantity of crystals. Inclusions of olivine and coesite are observed in diamonds of all pipes the most often; the quantity of inclusions of chrome-spinellid is also increased, garnets and pyroxenes occur more seldom.

The most minerals-inclusions are characteristic of a crystallographic cut as polyhedrons, that imparted them a rounded shape.

Inclusions have been analysed with X-ray scanning spectral microanalyser "Kamebax-Microbeam", Cameca (acceleration voltage 15 kW, 15mA).

Minerals of ultrabasic paragenesis. The composition of chromous garnet, chrome-spinellid, olivine, clinopyroxene and orthopyroxene have been studied.

Among five analysed grains of chromous garnet four grains belong to high-chromous knorringite-bearing variety, in which the content of  $\text{Cr}_2\text{O}_3$  ranges from 10 to 13%, CaO - from 2,4 to 5,4%, ferruginousness of garnets is low and ranges from 11,9 to 15,3%. Besides recorded pyropes, garnet with low content of  $\text{Cr}_2\text{O}_3$  - 3% and CaO - 2,9% and low ferruginousness ( $f \approx 12\%$ ) has been established.

As for known chrome-spinellid - inclusions, once more analysed 14 grains are characteristic of low ferruginousness from 23 to 38 and of high chromousness from 83 to 90%. Their content of  $\text{Cr}_2\text{O}_3$  ranges from 64 to 90%, moreover, in about half of chromites the amount of  $\text{Cr}_2\text{O}_3$  is higher, than 67%, that in inclusions of chromites from Yakutiya diamonds occurs very seldom and it is a regional typomorphic feature. The content of  $\text{TiO}_2$  in chrome-spinellids ranges from hundredth parts of percent to 0,26%.

All five analysed olivine grains have similar composition and are characteristic of low ferruginousness of 6,6 to 7,9%.

Impurity of  $\text{Cr}_2\text{O}_3$  was found in three olivine inclusions, moreover, in olivine, in its turn, was included in chrome-spinellid, the content of  $\text{Cr}_2\text{O}_3$  is extremely high -0,45%. In two olivines the impurity of NiO is registered.

The aggregate of chrome-diopside and enstatite, found in one of diamonds, is of essential interest. Chrome-diopside is characteristic of increased magnesia content  $\text{Ca}/\text{Ca}+\text{Mg} = 43,2$ , that in paragenesis with enstatite affirms high temperature of equilibrium.

Inclusion of chromous pyroxene, having emerald-green colour, is characteristic of increased content of  $\text{Cr}_2\text{O}_3$  -7,8% simultaneously with anomalously high  $\text{Na}_2\text{O}$  - 5,9%. Combination of chrome and sodium in clinopyroxenes leads to arising of rare component  $\text{NaCr}_2\text{O}_6$  - ureyite, which in pure state occurs only in meteorites. The content 8% of  $\text{Cr}_2\text{O}_3$  corresponds to 15% of ureyite component. Pyroxenes with such composition as inclusions in diamonds have not been fixed earlier.

Eclogitic paragenesis. From minerals of a given paragenesis garnet, clinopyroxene and coesite have been analysed.

Garnet (11 analyses) is represented by pyrope-almandine variety, which ferruginousness is 42 - 55%. The content of Ca-component is 20 - 32%, and in two samples value of Ca-component is particularly high -37 and 39%, respectively. In two diamonds, together with orange-coloured garnets, colourless inclusions of coesite were distinguished and analysed.

The compositions of two omphacite inclusions are identical. Their content of jadeitic mineral is high (about 50%), impurity of  $\text{K}_2\text{O}$  is 0,80%. According to peculiarities of chemical composition they belong to the most rich in jadeite pyroxenes, known among inclusions in diamonds. Both by content of jadeite component and content of impurity  $\text{K}_2\text{O}$ , the studied pyroxenes approach pyroxenes from diamonds of Argail lamproitic pipe in the Western Australia.

Thus, the cited data show, that on a level with typomorphic features, common for a given complex of minerals of all regions, inclusions in diamonds of EEP are characterized by a series of regional features.

ANCIENT DEPLETED SUBCONTINENTAL LITHOSPHERE UNDER SIBERIAN  
PLATFORM: Nd-Sr ISOTOPIC AND REE EVIDENCE FROM GARNET  
PERIDOTITE XENOLITHS OF MIR PIPE (WESTERN YAKUTIA).

A.Z. Zhuravlev; E.E. Laz'ko and A.I. Ponomarenko.

*Instit. of the Ore Deposits Geology, Petrography, Mineralogy & Geochemistry, USSR Academy of Sci., Moscow, USSR.*

A combined petrological and geochemical study of two garnet peridotite xenoliths (A-246 and A-339) from Mir kimberlite pipe has been accomplished. Both fragments are typical partly serpentinized appreciably depleted lherzolites (containing  $Al_2O_3$  1.79 and 2.86; CaO 2.50 and 3.37 wt.% respectively). The textures of the rocks are protogranular with some manifestations of deformation. Equilibrium P-T conditions of peridotites suggest they are fragments of thermally unperturbed "normal" (cold) palaeolithosphere.

Besides microprobe and bulk chemical analyses the concentrations of ten REE in coexisting minerals of peridotites have been measured by isotope dilution technique, and the isotope composition of Sr and Nd has been determined. The distributions of REE in minerals are similar to other garnet peridotites from kimberlites (Shimizu, 1975): the main phases concentrating lanthanoids are garnet and clinopyroxene which strongly LREE depleted (low Ce/Yb) and LREE enriched (high Ce/Yb) respectively. Olivine and orthopyroxene contain the extremely low concentrations of REE in comparison with the concentrators of the latter and render to be appreciably contaminated with a small portions of a kimberlite matter in spite of careful cleaning procedure of analysed minerals separates.

The garnet-clinopyroxene pair for A-339 peridotite define the mineral Sm-Nd age of  $1.7 \pm 0.1$  b.y (Fig. 1). The calculated model Sm-Nd age  $T_{CHUR}$  of this rock is much older - 3.0 b.y. This value is in appreciable disagreement with the 2.1 b.y. model Rb-Sr age defined by clinopyroxene Rb-Sr systematics. In any case however the age of A-339 peridotite is significantly older than the intrusion age of the host kimberlite from Mir pipe (360 Ma). The calculated  $\epsilon_{Nd}^T$  value for a parental rock A-339 is exceedingly high ( $+23.0 \pm 1.6$ ) and indicative of a long-term extreme REE depletion of an upper mantle region from which the examined xenolith have been excavated by a kimberlite melt.

The Sm-Nd age of A-246 peridotite (also defined by garnet-clinopyroxene pair) is  $0.91 \pm 0.01$  b.y (Fig. 1). Therefore this rock is almost twice younger than the other one, but it is still significantly older in comparison with the including kimberlite. However the calculated  $\epsilon_{Nd}^T$  value for a parental A-246 rock is  $+22.5 \pm 0.5$ , i.e. actually equal to the other fragment.

The unexpected and impressive result of Sm-Nd dating is the old isotopic ages of both xenoliths studied. Nevertheless these ages are *minimum* value. Such conclusion can be easily drawn when considering the factors which could distort the data obtained (contamination of analyzed mineral separates by small portions of kimberlite, isotopic exchange between coexisting garnet and

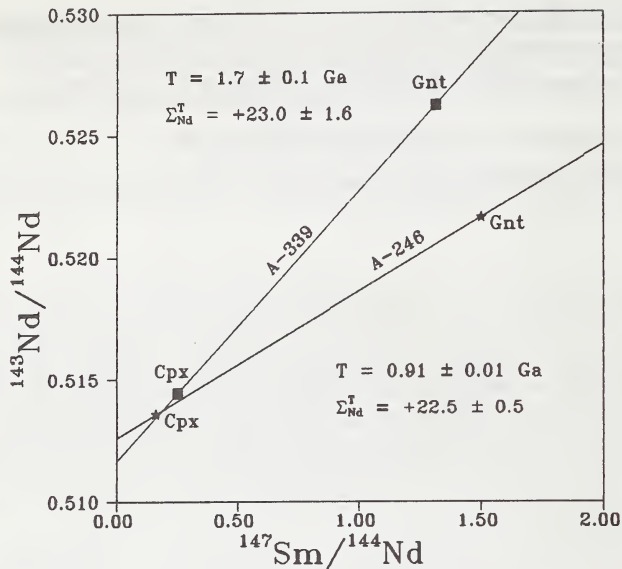


Figure. Sm-Nd age diagram for coexisting garnet and clinopyroxene from A-339 and A-246 peridotites.

clinopyroxene in mantle, etc.). Therefore peridotite examined do actually have much older age than kimberlite from Mir pipe.

The large time interval between the age of mantle samples and including volcanic rocks is rather unusual. We are aware of the only such example among mantle peridotites - sample M-602 also originating from Mir pipe (McCulloch, 1986). Our new data unequivocally confirm a possibility of ancient isotopic marks conservation in ultramafic rock xenoliths from kimberlites. Petrologic implications of these old Sm-Nd ages are that they correspond either to the time of crystallization of parental rocks of xenoliths or to the moment of their final reequilibration which has been accompanied by perfect isotope homogenization. In other words, after the stabilization of garnets' and clinopyroxenes' isotopic systems (1.7 and 0.91 b.y. for nodules A-339 and A-246 respectively) the rocks examined did not survive a significant thermal event including their transport in a kimberlite melt.

The other striking feature of rocks studied is their abnormally high  $\epsilon_{\text{Nd}}^T$  values. The latter strongly exceed  $\epsilon_{\text{Nd}}$  values usually detected in majority of mantle volcanics and their xenoliths. Assuming that both rocks have developed as practically closed systems (on a xenolith-size scale), their highly positive  $\epsilon_{\text{Nd}}^T$  marks require long-lived strongly REE depleted source. Since in a convective mantle (i.e. contemporary asthenosphere) such values are much less, the only realistic source of discussed xenoliths could be seen in a subcontinental lithosphere under Siberian craton. Similar anomalously REE depleted mantle rocks have been detected in some other

localities in Central and East Asia - Transbaikal Lake region, Mongolia, and Eastern China. We suggest that a definite layer of the lithospheric mantle under the eastern part of Asia continent may have an anomalous Nd isotope composition. This layer may correspond to a presumed highly depleted mantle reservoir (Zindler, Hart, 1986).

The difference between Sm-Nd and Rb-Sr model age of both peridotites does not allow to develop a simple one-stage model explaining the evolution of their parental sources. The history of development of the corresponding mantle region under Siberian craton has been long and complex. There is hardly possible to reconstruct it unequivocally using the data obtained. It is quite evidently however that the mantle evolution of both rocks have included a protolith depletion and enrichment by some main oxides and incompatible elements, recrystallization processes, cooling and other events. Two most realistic alternative petrogenetic models are considered. The early partial melting episode is most important event in both of them. Probably it documents the initial development and stabilization of the subcontinental lithosphere. Later incompatible element enrichment event postulated by the first scenario, documents reactivation episode which have occurred in stable lithosphere. Such process is problematic in the second model. Sm-Nd ages of peridotites mark the time of their final isotopic "closing".

#### REFERENCES

- McCULLOCH M.T. 1986. Sm-Nd systematics in eclogite and garnet peridotite nodules from kimberlites: implications for the early differentiation of the Earth. *Geol. Soc. Austral.*, Abstr., no.16, p.p. 285-287.
- SHIMIZU N. 1975. Rare earth elements in garnets and clinopyroxenes from garnet lherzolite nodules in kimberlites. *Earth and Planetary Science Letters*, v. 25, no.1, p.p. 26-32.
- ZINDLER A. and HART S.R. 1986. *Chemical Geodynamics. Annual Reviews of Earth and Planetary Sciences*, v 14, p.p. 493-571.





